

*Carnegie  
Institution*

OF WASHINGTON

*Year Book 64*

*1964-1965*







~~A.D. SINGER~~  
DIRECTOR'S OFFICE







*Carnegie  
Institution*

OF WASHINGTON

*Year Book 64*

*1964-1965*



Library of Congress Catalog Card Number 3-16716  
Garamond/Pridemark Press, Baltimore, Maryland



# Contents

	<i>Page</i>
Officers and Staff	iv
Report of the President	1
Reports of Departments and Special Studies	1
Mount Wilson and Palomar Observatories	3
Geophysical Laboratory	59
Department of Terrestrial Magnetism	251
Committee on Image Tubes for Telescopes	353
Department of Plant Biology	363
Department of Embryology	439
Genetics Research Unit	517
Cytogenetics Laboratory	537
Bibliography	553
Report of the Executive Committee	555
Report of Auditors	557
Abstract of Minutes of Sixty-Seventh Meeting of the Board of Trustees	575
Articles of Incorporation	577
By-Laws of the Institution	581
Index	587



# *President and Trustees*

## PRESIDENT

Caryl P. Haskins

## BOARD OF TRUSTEES

James N. White

*Chairman*

Henry S. Morgan

*Vice-Chairman*

Garrison Norton

*Secretary*

Amory H. Bradford

Omar N. Bradley

Vannevar Bush

Walter S. Gifford

Carl J. Gilbert

Crawford H. Greenewalt

Caryl P. Haskins

Barklie McKee Henry

Alfred L. Loomis

Robert A. Lovett

Keith S. McHugh

Margaret Carnegie Miller

Henry S. Morgan

Seeley G. Mudd

William I. Myers

Garrison Norton

Richard S. Perkins

Elihu Root, Jr.

William W. Rubey

Frank Stanton

Charles P. Taft

Charles H. Townes

Juan T. Trippe

James N. White



## *Trustees continued*

### AUDITING COMMITTEE

Keith S. McHugh, *Chairman*  
Alfred L. Loomis  
Juan T. Trippe

### EXECUTIVE COMMITTEE

Henry S. Morgan, *Chairman*  
Amory H. Bradford  
Walter S. Gifford  
Carl J. Gilbert  
Crawford H. Greenewalt  
Caryl P. Haskins  
Robert A. Lovett  
William I. Myers  
Garrison Norton  
Richard S. Perkins  
James N. White

### RETIREMENT COMMITTEE

Omar N. Bradley, *Chairman*  
Garrison Norton  
Richard S. Perkins  
Frank Stanton

### COMMITTEE ON ASTRONOMY

Seeley G. Mudd, *Chairman*  
Amory H. Bradford  
Crawford H. Greenewalt  
Elihu Root, Jr.

### FINANCE COMMITTEE

Richard S. Perkins, *Chairman*  
Walter S. Gifford  
Crawford H. Greenewalt  
Alfred L. Loomis  
Henry S. Morgan  
Elihu Root, Jr.

### COMMITTEE ON BIOLOGICAL SCIENCES

Alfred L. Loomis, *Chairman*  
Margaret Carnegie Miller  
William I. Myers  
Charles P. Taft

### NOMINATING COMMITTEE

Keith S. McHugh, *Chairman*  
Barklie McKee Henry  
Garrison Norton  
James N. White

### COMMITTEE ON TERRESTRIAL SCIENCES

Juan T. Trippe, *Chairman*  
Barklie McKee Henry  
Richard S. Perkins



# Staff

## MOUNT WILSON AND PALOMAR OBSERVATORIES

*813 Santa Barbara Street  
Pasadena, California 91106*

Horace W. Babcock, *Director*  
Halton C. Arp  
William A. Baum  
Ira S. Bowen, *Distinguished  
Service Staff Member*  
Edwin W. Dennison  
Armin J. Deutsch  
Jesse L. Greenstein  
Robert F. Howard  
Robert P. Kraft  
Robert B. Leighton  
Guido Münch  
J. Beverley Oke  
Allan R. Sandage  
Maarten Schmidt  
Olin C. Wilson  
Harold Zirin  
Fritz Zwicky

## GEOPHYSICAL LABORATORY

*2801 Upton Street, N. W.  
Washington, D. C. 20008*

Philip H. Abelson, *Director*  
Peter M. Bell<sup>1</sup>  
Francis R. Boyd, Jr.  
Charles W. Burnham  
Felix Chayes  
Gordon L. Davis  
Gabrielle Donnay  
Joseph L. England  
P. Edgar Hare  
Thomas C. Hoering  
Gunnar Kullerud  
Donald H. Lindsley  
J. Frank Schairer  
George R. Tilton  
Hatten S. Yoder, Jr.

<sup>1</sup> Appointed August 1, 1964.

## DEPARTMENT OF TERRESTRIAL MAGNETISM

*5241 Broad Branch Road, N. W.  
Washington, D. C. 20015*

Merle A. Tuve, *Director*  
Ellis T. Bolton, *Associate Director*  
L. Thomas Aldrich  
Roy J. Britten  
Louis Brown  
Bernard F. Burke  
Dean B. Cowie  
Scott E. Forbush  
W. Kent Ford, Jr.  
Stanley R. Hart  
Olaf Hartmann  
Cinna Lomnitz<sup>2</sup>  
Alois Th. Purgathofer<sup>3</sup>  
Richard B. Roberts  
Vera C. Rubin<sup>4</sup>  
I. Selwyn Sacks  
Ulrich Schmucker<sup>5</sup>  
T. Jefferson Smith  
John S. Steinhart  
Kenneth C. Turner<sup>6</sup>

<sup>2</sup> Resigned July 15, 1964

<sup>3</sup> Resigned May 15, 1965

<sup>4</sup> From April 1, 1965

<sup>5</sup> On leave of absence from March 16, 1965

<sup>6</sup> From July 1, 1964



*Staff continued*

DEPARTMENT OF PLANT BIOLOGY

*Stanford, California 94305*

C. Stacy French, *Director*

Jeanette S. Brown

David C. Fork

William M. Hiesey

Harold W. Milner<sup>1</sup>

Malcolm A. Nobs

DEPARTMENT OF EMBRYOLOGY

*115 West University Parkway*

*Baltimore, Maryland 21210*

James D. Ebert, *Director*

David W. Bishop

Bent G. Böving

Donald D. Brown

Robert L. DeHaan

Irwin R. Konigsberg

Elizabeth M. Ramsey

Mary E. Rawles

GENETICS RESEARCH UNIT

*Cold Spring Harbor*

*New York 11724*

Alfred D. Hershey, *Director*

Elizabeth Burgi

Barbara McClintock

*Cytogenetics Laboratory*

*Ann Arbor, Michigan*

Helen Gay

<sup>1</sup>Died July 13, 1965



## *Staff continued*

### OFFICE OF ADMINISTRATION

*1530 P Street, N.W., Washington, D.C. 20005*

Caryl P. Haskins	<i>President</i>
Edward A. Ackerman	<i>Executive Officer</i>
Marjorie H. Walburn	<i>Assistant to the President</i>
Donald J. Patton	<i>Acting Director of Publications</i>
Joan D. Galbraith	<i>Editor</i>
Eleanor F. Peck	<i>Associate Editor</i>
James W. Boise	<i>Bursar; Secretary-Treasurer Retirement Trust</i>
Kenneth R. Henard	<i>Assistant Bursar; Assistant Treasurer Retirement Trust</i>
Richard F. F. Nichols	<i>Executive Secretary to the Finance Committee</i>
Marshall Hornblower	<i>Counsel</i>

---

### *Staff Members in Special Subject Areas*

Tatiana Proskouriakoff

Anna O. Shepard

*Staff continued*

RESEARCH ASSOCIATES

*Carnegie Research Associate*

J. D. McGee  
*Imperial College of Science and Technology, University of London*

*Research Associates of the Carnegie Institution*

Louis B. Flexner  
*University of Pennsylvania*

Harry E. D. Pollock  
*Carnegie Institution*

C. E. Tilley  
*Cambridge University*





# Former Presidents and Trustees

## PRESIDENTS

Daniel Coit Gilman, 1902–1904

Robert Simpson Woodward, 1904–1920

Vannevar Bush, 1939–1955

John Campbell Merriam, 1921–1938;

*President Emeritus 1939–1945*

## TRUSTEES

Alexander Agassiz	1904–05	Seth Low	1902–16
George J. Baldwin	1925–27	Wayne MacVeagh	1902–07
Thomas Barbour	1934–46	Andrew W. Mellon	1924–37
James F. Bell	1935–61	Roswell Miller	1933–55
John S. Billings	1902–13	Darius O. Mills	1902–09
Robert Woods Bliss	1936–62	S. Weir Mitchell	1902–14
Lindsay Bradford	1940–58	Andrew J. Montague	1907–35
Robert S. Brookings	1910–29	William W. Morrow	1902–29
John L. Cadwalader	1903–14	William Church Osborn	1927–34
William W. Campbell	1929–38	James Parmelee	1917–31
John J. Carty	1916–32	Wm. Barclay Parsons	1907–32
Whitefoord R. Cole	1925–34	Stewart Paton	1916–42
Frederic A. Delano	1927–49	George W. Pepper	1914–19
Cleveland H. Dodge	1903–23	John J. Pershing	1930–43
William E. Dodge	1902–03	Henning W. Prentis, Jr.	1942–59
Charles P. Fenner	1914–24	Henry S. Pritchett	1906–36
Homer L. Ferguson	1927–52	Gordon S. Rentschler	1946–48
Simon Flexner	1910–14	David Rockefeller	1952–56
W. Cameron Forbes	1920–55	Elihu Root	1902–37
James Forrestal	1948–49	Julius Rosenwald	1929–31
William N. Frew	1902–15	Martin A. Ryerson	1908–28
Lyman J. Gage	1902–12	Henry R. Shepley	1937–62
Cass Gilbert	1924–34	Theobald Smith	1914–34
Frederick H. Gillett	1924–35	John C. Spooner	1902–07
Daniel C. Gilman	1902–08	William Benson Storey	1924–39
John Hay	1902–05	Richard P. Strong	1934–48
Myron T. Herrick	1915–29	William H. Taft	1906–15
Abram S. Hewitt	1902–03	William S. Thayer	1929–32
Henry L. Higginson	1902–19	James W. Wadsworth	1932–52
Ethan A. Hitchcock	1902–09	Charles D. Walcott	1902–27
Henry Hitchcock	1902	Frederic C. Walcott	1931–48
Herbert Hoover	1920–49	Henry P. Walcott	1910–24
William Wirt Howe	1903–09	Lewis H. Weed	1935–52
Charles L. Hutchinson	1902–04	William H. Welch	1906–34
Walter A. Jessup	1938–44	Andrew D. White	1902–03
Frank B. Jewett	1933–49	Edward D. White	1902–03
Samuel P. Langley	1904–06	Henry White	1913–27
Ernest O. Lawrence	1944–58	George W. Wickersham	1909–36
Charles A. Lindbergh	1934–39	Robert E. Wilson	1953–64
William Lindsay	1902–09	Robert S. Woodward	1905–24
Henry Cabot Lodge	1914–24	Carroll D. Wright	1902–08

Under the original charter, from the date of organization until April 28, 1904, the following were ex officio members of the Board of Trustees: the President of the United States, the President of the Senate, the Speaker of the House of Representatives, the Secretary of the Smithsonian Institution, and the President of the National Academy of Sciences.





*Report* OF  
THE *President*



*This current which goes on its way and which is not so different from the blood of men,  
from the eyes of men when they look straight ahead without fear in their hearts,  
without the daily tremor for trivialities or even for greater things;  
when they look straight ahead like the traveller who is used to gauging his road by  
the stars . . .*

EDMUND KEELEY AND PHILIP SHERRARD—*Six Poets of Modern Greece*

*Let us consider how three hundred years from now our present fearful falterings will be regarded. Will it be said that with the advancement of knowledge well under way and man's horizons just beginning to clear, the human race became so pre-occupied with material ills that it succumbed to terror and, in the interests of security, curiosity was confined? Or will it be said that, frightened as they were and bowed down by much trouble and suffering, nevertheless in one country—the traditional home of freedom—men still retained confidence in the importance of the great intellectual adventure?*

*The next twenty-five years will probably answer these questions, although those who are alive may not understand the full significance of what transpires. To my mind a fair indication of the way the tide is running will be afforded by noting to what extent we are still interested in finding and supporting Andrew Carnegie's "exceptional man."*

JAMES BRYANT CONANT—*Andrew Carnegie as Patron of Learning*

*Man was not made for leisure and he will go on accepting these challenges in the future, as he has done in the past. The spirit of man will continue to shape the path of human destiny "borne on the swiftly beating wings of great desire."*

HAROLD HARTLEY—"Man and Nature," *the Romanes Lecture*

*I have never thought it an accident of history that the age of reason was concerned equally with the sciences and with society. It was David Hume, whose thought in many ways epitomized his times, who pronounced the scientists of all ages inseparable from the societies that bred them. In words which must be no less flattering, even if a little more disconcerting, to you today than to his Edinburgh contemporaries, he said: "Though the persons who cultivate the sciences with such astonishing success as to attract the admiration of posterity be always few in all nations and all ages—the mass cannot be altogether insipid from which such refined spirits are extracted."*

FRANK STANTON—*Commencement Address at the California Institute of Technology, June 11, 1965*

WHAT WILL BE THE ASPECT of the root and branch of American science a decade or two decades hence? Where will its most dynamic growth be found? What will be the quality of its evolution in the major visions of our universe and of ourselves that it may disclose? Again, what will be its place in our society 20 years from now? As a whole people, how will we visualize it then? What rank will it take among our deepest values? In coming years, will it continue to fulfill to best advantage the extraordinary potential that it surely bears, not only for deepening and ennobling our national culture, but for enriching the lives of countless individual men and women who in the future may have more leisure to experience the intellectual excitement and the spiritual haven that it offers?

How will science in its least practical reaches fare in the public understanding and esteem of a society that throughout its history has been strongly oriented technically, and which, perhaps in large part for this very reason, tends to merge its ideas of the nature and the purpose of science with those of technology, and to demand importunately from both



the magic of novel products and material power? In an era when both science and technology have been so widely and so vividly associated with their immense contributions to defense, what may be the effect on our public attitudes to the deeply uncommitted areas of science if we are able to enter on a period comparatively free of major world conflict?

These are difficult questions to address to the future of the scientific way. On two planes of concern—the evolution of the substance of science in the years to come, and the relations of science to our larger society—the demands upon prophetic vision that such questions make appear presumptuous. In any explicit sense, of course, such demands are in fact impossible to meet in either context. The evolution of the substance of science is of its very nature free and untrammelled and not to be confined within the bounds of detailed forecast. The unknown cannot be predicted, and it is of the essence of science that it deals with the unknown. Not even the mode of attack upon the unknown can be foretold far into the future for any particular discipline. For the strategy of tomorrow must be, as it has always been, highly pragmatic, determined by a multitude of relevant conditions. The methods of probing nature have historically been quite different—indeed, sometimes quite opposite—among different branches of science, as Stephen Toulmin has wisely observed. Even within a single discipline, often enough, the philosophy of approach has undergone drastic change as the field evolved. And on the plane of the social milieu of science in the future, and of its relation to that milieu, neither scientist nor philosopher, nor student of society, can put into meaningful terms questions that have not, in part at least, been lived by his society, let alone formulate detailed answers for which there are no antecedent guides. It is tempting to brush aside such queries as unrealistic and troublesome, and distracting to our efforts to cope with a present already challenging enough.

Yet these presumptuous questions are not only troublesome and difficult. They are also extremely important. Upon the answers that we find to them, couched though they must be in terms far more general, perhaps far more inchoate, than we might wish, a great deal of the quality of American science over the coming decades could well depend. And in the wider if also more coarsely structured vein to which such questions are inevitably addressed, a broad design of the evolution of science can surely be discerned. On such a scale, moreover, it displays an impressive continuity. Its elements were shaped at least as early in our culture as that dramatic Greek period when science may literally have been born—the years between the work of Parmenides and Heraclitus and the death of Aristotle, when the philosophy of making the objective analysis of nature an overriding concern of the intellect quite literally turned the consciousness of the West to that scientific mode of assessing the environment that ever since has been its hallmark. In the larger aspect, no later scientific revolution has stood

apart from the source-stream of that epoch, nor deviated from its basic ethic. In substance as in philosophy, each later burst of scientific growth has been deeply nourished by its heritage of earlier discovery and concept, transmitted in a continuous, if often tortuous, flow. Each, moreover, has been closely linked with the existing technology of its time, and sensitive to the technical needs and demands of its society, profoundly influenced by them, and profoundly affecting them in turn. However fragmented the course of science may appear when closely viewed in any of its detailed reaches, in deeper and more general features it has indeed preserved a striking unity over the centuries. In this sense, the past of science may surely be considered prologue.

There could hardly be a more appropriate vantage point from which to view the landscape of some of the great concerns of science, both past and future, than the immediate present. For the past, last year and this signalize two anniversaries of major significance in all of scientific development. Last year was the 400th anniversary of the birth at Pisa, on February 15, 1564, of Galileo Galilei. This year marks the hundredth anniversary of that cold and snowy night in February 1865 when Gregor Johann Mendel read the first part of a paper embodying 11 years of work in the breeding of peas before a small and apparently indifferent audience at the Modern School of Brunn. For the future, both the great disciplines for which these anniversaries commemorate major turning points are once again so transforming our visions both of our outer universe and of our inner worlds as to constitute in our time what may be reckoned, in a truly historical sense, a contemporary scientific revolution fully comparable with earlier ones that now are classic. This revolution is not completed. In both sectors, advances are obviously at flood tide today, with the richest promise for the future. It is interesting, too, and it may be of more than passing significance, that the first anniversary marks the passage of four centuries, the second of but one.

In 1609, during a visit from Padua to his native Pisa, Galileo intercepted a rumor that, as he put it, "a certain Fleming"—perhaps the Dutch optometrist Hans Lippershey—had applied for a patent on a system of combined lenses that made distant objects seem larger and nearer. Within 10 months Galileo had built an instrument of this kind. In rapid succession, as he relates in *The Starry Messenger*, there followed a telescope that enlarged the image more than 60 times, then one that magnified more than a thousand. With such an instrument he was quickly able to ascertain that the moon had a rough surface instead of a smooth and uniform one, to detect



spots on the sun, to determine that Jupiter had satellite moons, and to resolve the Milky Way, until then considered a homogeneous mass, into myriad individual stars.

The telescope that Galileo described was roughly the equivalent of a modern opera glass. Sixty-two years later, in 1671, Newton was to present to the Royal Society a model of his reflecting telescope. It was of  $6\frac{1}{3}$ -inch focal length, and it magnified 38 diameters. A century and a half later, in 1820, Sir John Frederick William Herschel, aided by his father, had completed the design for a reflecting telescope of 20-foot focal length, with a mirror 18 inches in diameter. Those few landmarks provide a fair estimate of the gain in instrumental power that had been brought to astronomy in approximately 200 years.

Consider now the gain that was to accrue over the short century and a quarter to follow. When the Hale telescope on Palomar Mountain was dedicated on June 3, 1948, an instrument was brought to the service of astronomy of focal length more than 20 times that of Herschel's instrument, furnished with a mirror of more than 10 times the diameter and of more than 100 times the light-gathering power—a power so great that it could detect the flame of a single candle at 40,000 miles. In less than three generations the magnitude, the complexity, and the capacity of this one class of astronomical instruments has increased far more, both absolutely and in rate of growth, than during almost three and one-half centuries following the appearance of Galileo's first model.

Such changes in the power and complexity of one instrument, of course, tell but a fraction of the story of the burgeoning richness and diversity of the observational resources that have been brought to the service of astronomy over the same period. Diffraction gratings of new powers of resolution, photographic emulsions of new orders of sensitivity in the infrared and ultraviolet, electronic aids of new dimensions of versatility and complexity have become the tools of astronomers. During the last decade the image tube has been developed to the point where it promises to add extremely significant gains to the powers for information collection of existing telescopes. And the evolution over the past few years of the great modern radio telescopes has provided astronomy with perhaps the most powerful aid it has ever had, short of the optical telescope itself.

But if the purely instrumental advances achieved during the three and a half centuries since Galileo—and especially in the last half-century of our own time—are breathtaking in their power and complexity, the changes they have helped to bring to our concepts of the nature and scale of the universe are yet more spectacular. In 1572 and again in 1577 comets of exceptional brilliance appeared over Denmark. Each was carefully observed by Tycho Brahe, who concluded that they lay beyond the moon and thus at a vast celestial distance. How far away was the moon? In *The Starry*

*Messenger* Galileo quoted a figure that was probably older than his time—it may well have been Tycho's own calculation—a figure of about 60 earthly diameters. So the farthest objects of the universe, as marked by Tycho's comets, lay about 475,000 miles from the earth.

A little over 200 years later that figure had grown considerably. A textbook of astronomy written by an American student at the Paris Observatory and published in America in 1841 contained the statement, "Professor F. W. Bessel, of the Königsberg Observatory, in October, 1838, communicated to the publick that he had been able to obtain an annual parallax upon the double 61 of the Swan. . . This places that star at the distance of 657,000 times ninety-five millions of miles from the earth, and light, which moves with a known velocity, employs ten years and three-tenths years to traverse this distance." The farthest observed object had moved out to 10% light-years. And the same textbook added, "It is probable that the great stratum, called the Milky Way, is that in which the sun is placed, though perhaps not in the very center of its thickness. We gather this from the appearance of this galaxy, which seems to encompass the whole heavens, as it certainly must do if the sun is within the same." As late as 1920 it was still widely believed that the Milky Way really comprehended our entire universe. Only within the last 20 years have we become fully aware that this galaxy of ours is in fact but one among millions or perhaps billions of such galaxies, lacing the heavens, stretching to distances of which the world of 1920 or even of 1950 could have had little conception, each galaxy, like the individual stars that make it up, involved in an evolutionary history peculiarly its own. Within the range of the Hale telescope on Palomar Mountain lie perhaps a thousand million such galaxies.

A decade ago, in 1955, the Mount Wilson and Palomar Observatories were able to report redshift measurements of clusters of celestial objects with velocities of recession as high as 60,000 kilometers per second, and anticipated finding redshifts implying velocities over 100,000 kilometers per second, corresponding to calculated distances as great as a billion light-years. Four years later Rudolph Minkowski photographed through the Hale telescope a cluster of galaxies that appeared, from redshift values of their spectra, to be receding at the rate of 138,000 kilometers per second, almost half the speed of light, and to lie at an estimated distance from the earth of much more than a billion light-years. This discovery, too, underlined spectacularly the significance of the growing partnership of radio with optical telescopes in the exploration of the heavens. For the objects measured by Minkowski were first located, to an accuracy of a few seconds of arc in the sky, by radio astronomers at the Cavendish Laboratory in Cambridge, England, and at the Owens Valley Radio Observatory of the California Institute of Technology.

Now, a scant six years later, vast new reaches of the universe have be-



come observable in the dramatic findings of Allan Sandage and Maarten Schmidt and their colleagues, which clearly herald only the beginning of further immense advances in our concepts of the universe—the chapter of the quasi-stellar radio sources. It is a chapter that is still in good part unwritten. But surely it could signal a revolution in our vision fully comparable with that initiated more than three centuries ago when Kepler, in the very year of Galileo's dramatic observational discoveries, published his *Astronomia Nova* with its data demonstrating that the planetary orbits are ellipses. Recently, quasi-stellar radio source 3C9 was found by Schmidt to have a redshift corresponding to a velocity of recession of approximately 238,000 kilometers per second—in the neighborhood of 80 per cent of the speed of light—and it is estimated to lie several billions of light-years away. It may be that we are looking backward to a time only a few billion years after expansion of the universe began. One quasi-stellar radio source identified somewhat over a year ago was reckoned to be about two and a half trillion times as luminous as our own sun. It has been calculated that, to keep such an object at its current luminosity for even so short a time, astronomically speaking, as a million years, matter equivalent to that contained in 100,000 suns might have to be converted into radiant energy. In the quasi-stellar source, whence comes this vast supply?

Such findings and the concepts they engender have altered our ideas of the nature and extent of our universe more radically in the 400 years since the birth of Galileo than in all the preceding history of the western world. But in that time the rate of discovery itself has so accelerated that now insights achieved within only three years have illumined and expanded and welded together individual and partial visions that required many earlier decades to win. As these insights stand today, they promise a future view that not only may affect the scientific concepts of man at the very deepest levels but may well profoundly influence his view of himself and of his place in nature, and above all of that future kind of society that John R. Platt has so vividly imagined and described. This is the panorama of the past and the present and the prospect for the future that the advance of knowledge and understanding in that particular area of investigation of the universe that we identify with Galileo Galilei presents to us as we look forward to the coming years.

When Gregor Johann Mendel had finished reading the second—the mathematical—half of his paper to the audience in the Modern School of Brunn, the concept of unit factors of inheritance, the genes, persisting in diverse crosses, recoverable from them, sometimes more enduring than mountain chains yet on occasion altering rapidly in an instant, had been established for all time. Today these “atoms” of genetics are as familiar

to us as the physical atoms of Dalton. But, like the atoms of Dalton, they were neither familiar nor palatable to the audience that first heard about them, or read about them in the published paper, nor indeed to a whole generation to follow. By 1900 the concept of Mendelian genes was little further advanced than it had been in 1865. Had this been the only channel open to conceptual growth in the science of heredity, genetics might indeed have stagnated.

But there were other channels, more accessible to chemists than to plant breeders. Mendel had scarcely finished his work when a young biochemist named Miescher, working at Strasbourg, undertook some analyses of the living cell. In the course of the work he treated cells with a digestive enzyme, and was interested to find that though the enzyme broke down the protein of the cytoplasm it left the contents of the nucleus largely intact. Miescher named this resistant substance, so distinct from the protein, "nuclein." In later years he obtained rich supplies of nuclein from the sperm of the salmon which still in that day ascended the Rhine as far as his home in Basel, and with it greatly extended his investigations. Eventually it was determined that the substance reacted as an acid, that its molecule had a threadlike structure and was, relatively speaking, enormous, and that when disintegrated chemically it broke into a great number of apparently similar subunits held together by phosphate bonds. When isolated it formed a gummy white powder, which ultimately became a dusty staple on the back shelves of biochemical laboratories. It received a name—deoxyribonucleic acid—and even the sobriquet that in years yet distant was to become a staple of our vocabulary—DNA. The German biochemist Robert Feulgen chanced to treat it with acid fuchsin, and it turned a brilliant purple—fuchsia. When Feulgen tried the same stain on some living cells their chromosomes stood forth in that same brilliant purple. So the chromosomes were apparently largely composed of DNA.

That was almost the extent of our recognition of the role of DNA in heredity when, midway in the fifth decade of this century, Linus Pauling and Robert Corey suggested that the molecule of DNA might consist in effect of long, helically wound strands to which were attached the four characteristic bases, two purine and two pyrimidine. They fully understood that a linear order of the bases had somehow to match the linear order of amino acids in a protein. Probably in order to make such matching possible, they envisioned the bases as being attached to the outside of the molecular chain. But it was difficult to understand how a substance with an acid reaction could carry projecting bases on its molecule. A few years later, the work of Crick and Watson and Wilkins and their co-workers had solved the basic puzzle, had shown that the bases do not project outward but instead link the two helically wound strands much like the treads of a spiral staircase and that their vital role is that of encoding by their order our own



hereditary traits and those of all other living things. The reasoning that made that huge step possible rested on concepts far removed from those of Mendelian genetics or even from conventional biochemistry. Those concepts rested in part on a contemporary version of the insight so dramatically revealed by Louis Pasteur when he demonstrated in 1848 that two substances, tartaric acid and paratartaric acid, extracted from the same wine vat, of the same gross chemical composition, could yet differ profoundly in their properties because of minute differences in the patterns of their crystal lattices. That same insight was reinforced a decade later by August Kekule in his famous paper on the structural chemistry of carbon compounds. In submicroscopic nature, as in art, *structural pattern* may matter a great deal more than gross composition. That insight, in its modern context, was to come especially easily to an age widely concerned with information theory, punch-tape recording, coded storage and retrieval, and computers. It may well be, in fact, that such reasoning could not have been achieved in another time or by other than geneticists and chemists as sensitive to these currents of the age as to their own specific disciplines.

It required just short of a century for the concepts of genetics to advance from the stage attained by a Mendel and a Miescher to that envisioned by Pauling and Corey and their contemporaries. It took little more than a decade to bring to their present state the concepts of Watson and Crick and Wilkins, and to give intimations of more distant and equally breathtaking horizons. We recognize now that the richness and the fineness of detail and the comprehensiveness of genetic information coding and of the mechanisms that control its expression are such as to stagger the imagination. There is clearly ample capacity for variety in the modes of genetic coding to encompass the whole range of living nature in the world, and to provide for its entire evolutionary history over the last two and a half billion years, with much, much to spare. Most important of all, the last decades have brought home, finally and for all time, the crucial perception that infinitely delicate coordination and control and precisely structured, submicroscopic agents by which the information governing that coordination and control is preserved and modulated and disseminated, lie at the very roots of the process of life. We are already beginning to uncover a rich store of specific illustrations of that principle in nature. Examples will multiply over the coming years.

These, of course, are but two vignettes, but two conspicuous illustrations lightly sketched, of the scientific past and present, at the level of ideas, from which, in some measure, we may try to gain some insights for the future. The practical consequences of our broader scientific past, of course, form the very fabric of our daily lives, so comprehensive and so tightly



woven that unless we stop to separate the individual threads we are unlikely even to be aware of them. In our day it is hard to remember that in Benjamin Franklin's time some 90 per cent of our people lived on the land, engaged in an agriculture which with some precariousness supported a population of perhaps three million souls. That population, now grown to nearly 200 million, is far better nourished today by the technically supported efforts of some seven per cent of its numbers. The effort to reconstruct the scientific and technical America of even a half-century ago, indeed, is vividly reminiscent of a view through the clouded windows of some archaic mansion, standing vacant since the days of Commodore Perry. When Henry Adams stood awed before an electric dynamo at the Paris Exposition of 1900 and saw in it "a symbol of infinity," he was viewing it from a personal background where less than two per cent of the power used in his country was electrically generated. The United States of 1910 knew wireless telegraphy from the experiments of Marconi at the turn of the century, but as recently as 40 years ago eloquent suggestions of the possibilities of radio broadcasting fell largely on deaf ears. Although in 1903 the epochal 12-second flight of Orville Wright had been accomplished at Kitty Hawk, followed by the 59-second flight of his brother Wilbur, and the first movie to tell a connected story had been produced, there was little hint of either a motion-picture industry or an aircraft industry and little more of a telephone or an automobile industry. Even the basic discoveries that would soon underlie a gigantic television industry were all but unknown.

It is striking indeed to recall the list of instruments and products that now are embedded so securely at the center of our civilization that we have almost ceased to think about them. The "wonder" drugs, including the nerve drugs, the new vaccines, and the newer antibiotics, are all far younger than we commonly remember. It is astonishing to recall that hardly a half-century has passed since the national death rate in the United States from influenza and pneumonia was reckoned at more than 180 persons in each 100,000 of population, a rate that was to fall to 39 only 48 years later. In the field of materials a wide range of plastics, synthetic rubber, the synthetic gems that now occupy so central a position in technology and industry, are but of yesterday. So are the materials of highest purity that can be prepared today and find such wide industrial uses—zirconium, tantalum, titanium. In the field of instruments many of the developments that we reckon as staples, and many more with major applications that must reach far into the future—masers and lasers, transistors, computer technology, the technology of communications satellites—lie in the immediate past, or actually in the present. And a world's anticipation of the potentials of nuclear power is patent.

The social impact of such all-pervading products of science needs no underlining. Here, of course, the past and present merge imperceptibly



with the future. Many of the new tools developed in this decade have as yet hardly indicated their possible ranges of service to society in the years to come. But we can begin to discern some of these future ranges, though only in the most preliminary and probably fragmentary fashion. Consider, for example, the laser. Since lasers were invented scarcely five years ago one of the principal goals of development has been to maximize their yield of energy. For the operation of lasers is still incompletely understood, and the outputs of which they are theoretically capable have certainly not yet been fully attained. But some of the manifold practical applications of the enormous energies already achieved can be fairly readily visualized even now: in industry in melting, welding, and cutting refractory materials, in range-finding, in communication, in planetary astronomy, in a variety of military contexts promising unconventional possibilities. With the appearance little more than a year ago of the continuous argon laser, the attainable yields of gas lasers have been increased probably by several orders of magnitude over older helium-neon types. Indeed, the beam from the new type even when unfocused carries sufficient energy to ignite inflammable materials placed across its path.

It surely requires no great imagination to predict the magnitude or the importance of such potential applications in the future. But we may be in for some real surprises too. Who, for instance, could have guessed a few years ago that the laser might offer to medicine and surgery their most effective weapon in the treatment of that disastrous disorder, relatively so common and so frequently fatal to sight, the detached retina? Yet the ruby laser ophthalmoscope, operated at appropriate levels of energy, is capable of so "spot-welding" the detaching retina to the underlying choroid that in dramatic instances the detachment has been arrested or even prevented, and vision saved.

Similar predictions of future practical impacts of science, fraught no doubt with similar surprises, can be made in fields that in years to come could massively affect our terrestrial environment. The oceans, for example, occupy nearly 70 per cent of the globe's area. Their treasures are becoming constantly more evident: locked in the hidden ores along the continental shelves—gold, magnetite, diamonds—held in the minerals lying as nodules on their floors or buried within their beds—nickel, cobalt, vanadium, zinc, copper, manganese—or contained in the nutritional wealth of their various planktons, plant and animal, free-floating and fixed within the corals and in the mantles of great bivalve molluscs of the reefs. They will surely be detected and exploited in the coming years with ever-growing ingenuity and power. It is clear that water will become an increasingly scarce and precious commodity in the years ahead, and its reclamation as well as its conservation will be a gathering concern. We shall surely see increasingly effective techniques applied to the complex problems of desalination. We shall come to

depend more and more importantly upon communications satellites. One specific forecast in this area may be inherent in the contemporary concept of a satellite equipped with a very-high-frequency capability allowing experimental exchange of messages in both directions between ground facilities and commercial airplanes flying the Atlantic routes, perhaps presaging regular ground-to-air and air-to-ground communications services. Only a bit further on may be satellites with individual capacities of at least 1,000 two-way telephone circuits, satellites that could be launched multiply from single rocket boosters. And in the relatively near future we may see the placing of an Early Bird satellite over the Pacific Ocean to link the United States and Western Europe with Hawaii and Japan. We shall become increasingly effective in the prediction of weather, and it is by no means impossible that we shall succeed in modifying it in significant ways.

There is surely much that is generally and rather confidently predictable in such views of the future. But the visions by far the most easily projected are those concerning technology and scientific application. Less susceptible to clear prediction, in general, are the conquests that will lie closer to the heart of science. Yet even here some of the most striking general directions can readily be discerned. It is abundantly evident, for instance, that the dramatic explorations of the quasi-stellar radio sources must indeed lead on—as they are doing already—to more comprehensive and profound ideas of the nature of our universe and our place within it, and of our own fate, than we have ever achieved. If, as now seems possible, the evidence ultimately proves to favor the picture of a closed, pulsating universe, periodically expanding, recontracting, and once again expanding, that vision will dramatically link the future with the past. For such a possibility is wholly consistent with Hubble's original formulation and observational verification of the idea that our universe is indeed expanding. It marks the further logical extension of 40 years or more in the continuous development and elaboration of an idea basic to all astronomy. In a different context, perhaps we can already foresee that one of the immensely challenging areas for the future of cosmology must lie in the search for gravitational radiation, analogous to the older search for and study of electromagnetic radiation. How important could a comprehension of gravitational radiation prove in understanding the energy balance of space?

In the life sciences, too, some of the great vistas for the future are unequivocally indicated today, though the answers to a multitude of the questions they will bring, and even the nature of the questions themselves, lie at present beyond our ken. A projection of the Mendelian and Darwinian revolutions to new facets of the kingdom of life may bring some extraordinary widening of view. One specific contemporary insight at molecular



level into the detailed processes by which the unit of heredity in the chromosome impresses its message on the final protein through which the design of the body is itself expressed may be typical and illustrative here. Many geneticists now believe that the message in the hereditary material specifically codes only the sequence of amino acids in a protein, not its three-dimensional structure. The ultimate folded shape that the polypeptide chain of the protein takes may well be a secondary function of the amino acid sequences. But that final molecular shape is no accident. Indeed it is becoming clear that, in some cases at least, the final form of the molecule is as specific and as closely adapted to its particular biological function as the wing of a bird.

At the Laboratory for Molecular Biology of the British Medical Research Council at Cambridge the brilliant and exhaustive analysis of the detailed configuration of the oxygen-storing protein myoglobin has now been pushed forward from the 2.0-angstrom resolution achieved several years ago, itself a stupendous accomplishment, to 1.4 angstroms. In a model resolved to such a degree of fineness most of the 1,260 nonhydrogen atoms of myoglobin can be distinguished, and the positions of 1,200 or more have already been determined. Such a picture allows assessment in detail of the shape of the whole molecule. It is now evident that the protein chains are folded in such a manner as to bring into close proximity amino acid groups which in the unfolded structure would lie relatively distant. It seems a reasonable guess that such portions of neighboring chains of amino acids, brought together by folding, may constitute specific sites of enzyme activity. In contrast, other portions may represent inactive regions, possibly designed for straightforward mechanical support. If this is true, how, in the case of myoglobin and the more complex haemoglobin, are these specific sites related to the function of oxygen transport itself? And what insights can this finding provide concerning the nature of the active sites of yet other enzymes, equally important in the functioning of our bodies?

Hard upon this revealing analysis of the highly specific relation of function to form in a molecule of critical biological importance has come another—the determination, by the same essential method, of the three-dimensional structure of the molecule of the enzymatic protein lysozyme to a resolution of 2.0 angstroms, recently achieved at the British Royal Institution. Here again specific active sites have been located on the enzyme molecule, through ingenious methods of blocking their action with suitable compounds, as an industrial catalyst might be poisoned, and then determining the locations of attachment to sensitive regions. Interestingly enough, a potent inhibitor of the bactericidal property of lysozyme is that equally powerful—and differently acting—bactericide penicillin. There can hardly longer be doubt, not only that the folding of protein molecules is far from random, but that we shall come to see in this precise shaping new examples of the

evolution of biological fitness, illustrating principles at the submicroscopic level vividly reminiscent of those set forth by Darwin and Wallace at the level of entire plants and animals. And we shall surely come to think of this evolution of molecules in the general frame of dynamic operating systems, in terms of feedback and reinforcement. Already we have the suggestion of a class of biochemical reactions, called "allosteric," in which the end product of a biosynthetic pathway prevents its own overproduction by binding to specific inhibition sites on an enzyme critical in its synthesis, thus regulating the rate of its manufacture at a level optimal for the welfare of the organism as a whole.

Our traditional ideas of the shape assumed by the strands of hereditary material itself within cell or virus may be due for change and enlargement too. We have conventionally envisioned the machinery of heredity, elucidated by Watson and Crick, as essentially linear, doubled, helically wound strands of DNA, which may replicate by a separation of those strands and the synthesis of new complementary partners, with each original strand acting as a template. It has always been difficult to understand, however, precisely how this was accomplished, and it may well differ in different organisms. Now we have the discovery from work of the last two years at the California Institute of Technology that the threads of DNA in the polyoma virus, at least at certain times, are not in the form of linear strands. Nor do they have the shape of the ring of two-stranded DNA already found in certain other viruses and in bacteria. Rather they may form an apparently untidy, twisted loop. Untidy it surely appears. But its geometry, and experiments with models, suggest that when one strand of the DNA is broken the contorted loop will assume the circular form already familiar. When both strands are severed the conventional linear alignment of strands should result. The twisted form may be the consequence of a peculiar set of time relations at replication of the genetic material—the result of the closure of the molecular ring *before* the helix of the double-stranded DNA composing it is completely wound. Thus there may be regions of the molecule where the last portions are added in the process of replication, after the ring itself is formed. There is a real chance that further study of the topology of this twisted form of DNA may yield highly suggestive and detailed evidence about the time-course of its doubling and about its state during replication.

Equally suggestive of the future are contemporary studies concerned with discovering exactly how specific genes transmit their information to the messenger ribonucleic acid that in turn will govern the building of a protein. In a certain bacteriophage, evidence is accumulating to suggest that the transcription of the whole message contained in a given particle of DNA does not occur simultaneously, but, like replication, may be sequential, beginning in the case investigated in the right-hand half of the



molecule. In work recently reported from Cornell University, the detailed structure of a molecule of "transfer" ribonucleic acid, responsible for transporting the amino acid alanine to the precise site where it is built into a protein molecule, has been elucidated. Will the next decade bring a clear and detailed understanding of exactly how the encoded hereditary message makes itself felt in the structure of the whole organism? And if so, what implications will such knowledge carry for all of biology, and indeed of medicine?

Such are a very few of the specific challenges for tomorrow in the great fields so deeply affected by the revolutions of Darwin and Mendel, chosen almost at random as illustrations from among a myriad of possibilities. But more general questions for the future crowd in apace upon the sciences of life. What, for instance, are the processes that bring about the exquisitely regulated and coordinated differentiation of the cells in a growing embryo? What of the great frontier defined by the challenge to understand the processes enabling nerve cells to discharge their wonderful functions, singly and collectively, in nervous systems and in cerebra? Through increasingly profound and insightful researches in sensory physiology we shall be winning knowledge no doubt directly relevant to the treatment of nervous disorders. We shall also be adopting an approach that would have pleased Galileo when he wrote, "I cannot find any bounds for my admiration how reason was able, in Aristarchus and Copernicus, to commit such rape upon their senses as, in spite of them, to make itself master of their belief." And in thus going effectively behind and beyond the senses, we shall be doing more. In studies of the nature of perception and of cognition in future years we may well indeed forge approaches to that grandest and most profound concern of all—the modes of evolution of human consciousness itself.

What hints of the general character of the sweep of science in years to come can be drawn from such panoramas, viewed at the intersection of past and future where we stand? A rather specific hint further emphasizes the contrast mentioned earlier between the unpredictability of the detailed contours of advance or even of specific strategies of attack in any particular branch of science and the greater uniformity and consistency of some of the broader features of the moving scientific front. In many important respects the development of strategy and indeed of detailed philosophy has surely been almost opposite in the physical as against the life sciences. Concepts and approaches that have historically proved unsuitable in one area have on occasion served as important evocators in the other. Furthermore, strategies of investigation and foci of interest have often shifted radically during the evolution of a single science. Before the phlogiston theory was

set aside great effort was devoted to the study of the colors of flames in violent chemical reactions. It was a worthy investigation, and carefully conducted. Yet it became utterly irrelevant and was discarded when the theory to which it was addressed was set aside. Mendel's study of the genetics of peas was of profound significance when it was achieved; the study of the same material today is relevant mainly to rather special areas of botany and agronomy. These specific aids to the building of a science are characteristically adopted and discarded as need and circumstance dictate. As P. B. Medawar has pointed out, contrary to a widespread impression the sheer factual content of specific scientific fields is likely to diminish with their growth rather than pile up to greater and ever more unassimilable masses with the years. For as any science matures the scaffolding of its facts, hitherto diverse and sometimes apparently almost unrelated, is constantly being reduced by and included into theories of growing comprehensiveness. Or presumed facts are shown not to accord with those theories and are discarded. Or the theories themselves may be rejected, carrying with them the facts marshaled in their support. But the great frames of investigation, like astronomy and the life sciences, have continued to build steadily over the centuries. Today they are frontiers as vital as they have ever been. It is almost inconceivable that they will not maintain that vitality as far into the future as can be imagined.

A somewhat broader insight, brought home vividly both by past and present, concerns the character of those critical periods of history when the whole world view of man suffers fundamental change in consequence of great new orientations achieved by science. The first of such revolutions in view, during that tremendous period of Greek thought when, if in any single time and place, the scientific mode originated, was not only poignantly intense. It was also remarkably brief. William Barrett has pointed out that the emergence of the mode of conscious reason that marked this turning point in Greek thought, and indeed in the whole evolution of thought in the West, took place within little more than the single generation of Plato himself. The same intense dynamism dominated the revolution in our view of the universe and our own place within it heralded by the work of Copernicus and Kepler and Galileo. The Newtonian revolution was characterized by similar intensity and brevity. During the 40 years between the restoration of Charles II and the end of the seventeenth century it is clear that the world outlook of the leaders of a nation suffered changes more profound than any that wars or drastic political changes could have wrought. That transformation reached far into the society, far beyond its leaders, to thoroughly mold the universal attitude of the age. Manifestly the same qualities characterized the Age of Darwin.

So perhaps one of the greater lessons of the past is that the eras of major change characteristically ran swift and deep, and were incredibly dynamic.



In this aspect the general profile of scientific evolution in the past frequently resembled that of the strand of an abacus, periods of intense change tending, on the whole, to alternate with quieter periods of consolidation. Why should this have been so? In part, it is possible that a kind of fatigue with dynamism, a kind of eschewing of the novel, even a kind of rejection of change as threatening and inimical, may have succeeded some particularly brilliant and radical period of advance, producing temporary stagnation. This seems to have happened in later Athenian times, and certainly was reflected in the tenor of the Royal Society for a period following the Age of Newton. But perhaps a more important factor was the real need, following a time of truly violent change, to pause and consolidate, to reweave the torn fabric of universal ideas. If this factor was and continues to be really significant, then, as the pace and the variety of scientific advance increase yet further in the future, as the circle of change widens and begets more change, we may well look for important shifts of pattern. Perhaps the intervals between the beads on the evolutionary strands will simply become shorter and shorter. But now, in fact, there are a multitude of strands tightly entwined, and the beads of swift change may not be placed synchronously among them. Major sweeps in our ideas about the nature of the universe may not coincide precisely with periods of major growth in our ideas, for example, about the nature of life. And so the general profile of change to which we were adjusted in the past may be obliterated altogether. We may well come to live almost continually, not only with technical change itself, on however broad a scale, but also with a plethora of revolutionary new ideas. This, indeed, may almost be our present situation. It carries its own psychological hazards, of which we should be sensitively aware.

In any event there can be no shadow of doubt that mankind is once again in the midst of an era of change in total outlook fully comparable with that of the classic scientific revolutions. In trying to envision its future course, yet another quality of the earlier revolutions may be significant. This is the extraordinary degree to which both their substantive content and the character of their development reflected the predominant social and technical environments and the social and technical demands of their times—reflected and responded to them. Surely it was no accident that the society where Galileo worked on his first telescopes, and which acclaimed his work so warmly, was also a society of dynamic and expanding oceanic trade, with deep interests in the arts of navigation and the use of heavenly bodies for navigational guidance. Nor can it have been accidental that those too were the years when studies of hydraulics proceeded apace, or when, amidst the lifting and hauling of the new commerce of the city-states, considerations of the nature of forces became a preoccupation of physics. It was the abundant vintage of 1613 that drew Kepler's attention to the

defective means then in use for estimating the capacities of wine jugs and in 1615 provoked his classic essay *Nova Stereometria Doliorum*, which, in helping to measure the cubic contents of those jugs, also helped to lay the foundations for the discovery of the infinitesimal calculus. It can have been no accident that the mathematics of insurance and of interest underwent such an extraordinary expansion in the latter half of the Renaissance, precisely when it was badly needed in the burgeoning transactions of the society. It was surely no coincidence that the heyday of mechanical notions about the working of the body and mind, in the time of Descartes, both followed and fed a peak of interest in the construction of clockwork mechanisms; or, as earlier remarked, that our modern ideas of the mechanisms of heredity developed in an era dominated by the new ideas of coding and communication. Always science seems to have flourished best, to have made its richest contributions, in an atmosphere that almost paradoxically combined the elements of a maximum freedom of inquiry with those of a lively—though often inchoate—stimulus of social demand and need. We may well inquire of the contemporary scientific revolution: what will be the nature of the predominant claims made upon it, and of the stimuli given to it, by our own environment in the years ahead?

Few questions, of course, could be more complex; few more difficult to answer. The immense intricacy of the social milieu of our day—the fact that for both science and technology it is in many respects a world society, poses dimensions so numerous and diverse that they are extremely hard to characterize even generally. But one dimension for the future is surely unmistakable. It is provided by the very substance of society, dictated by the overarching circumstance, already so vividly apparent, that in the future it will be the environment created by humanity itself, the environment of human social forms, of individual human needs, that must take high place in all our reckoning, and that will equal or surpass more traditional concerns in its consuming relevance and import.

It is hard to imagine that this newly predominant feature of our world, bringing as it must intensified demand for ever fuller understanding of ourselves, will not exert a profound influence in defining new sectors to command scientific attention. Indeed that influence is already evident. What previous era has displayed so sophisticated an interest in the dynamics and the structure and the evolution of populations? What previous era has entertained a concern of anything like the degree of penetration or objectivity for such novel and difficult areas of inquiry as those presented by patterns of individual evolution in the context of the population or the society of which that individual is a part? What previous era has been explicitly concerned with conceptual aspects of the evolution of altruism? This is not only the hundredth anniversary of the reading of Mendel's paper



at Brünn. It is also the year when the work of J. B. S. Haldane closed. Perhaps in future decades we shall look on this as a scientific milestone of equal significance, and yet more prophetic for the future.

So much for some elements of the internal growth of science over the years ahead. What now of that second aspect, made trebly important in our time by the dynamic growth of our civilization and its changing concerns and character—the “external” development of science in its relations to the society which it serves, and of which it forms so integral and decisive a part? What of our deepest attitudes, as a people, toward science in the future?

These far-reaching and highly practical issues could well concern us urgently in a decade or even less, and could equally well undergo important transformations within that short span. For, as Adolf Berle has pointed out, if our total national productivity should double, as predicted in some quarters, by 1980, if the total income annually received by private individuals should reach the staggering figure of one trillion dollars, as seems entirely possible, it is difficult to imagine that the whole quality of American life, the whole direction of individual preoccupation and aspiration, will remain unchanged. A computer today can turn a rough engineering sketch not only into an accurate drawing, but into appropriate instructions for machining. In the course of a few minutes it can compare and optimize a vast range of possible designs for a manufactured product. When automation of this sort becomes general throughout American industry, what happens to the occupations and the concerns of a great number of trained and specialized professional men and women? Where do they turn for personal satisfaction? Perhaps special measures will be necessary to help fulfill the needs of numbers of people who will surely wish to take advantage of a renewed opportunity for intellectual growth and inspiration, rather than face an inactivity enervating and damaging to self-respect. Is it not possible under these circumstances that the scientist, the philosopher, the poet will come in greater measure than today to mold the quality of our society? Is it not possible that the widespread opportunity to participate in, or even simply to observe, the new reaches of science as they unfold may be reckoned one of the great contributions of the scientific way to our society in the future?

But if this contribution is to become effectively available, a far wider and deeper understanding of the nature and purpose of science is required than we have yet achieved. There are some particular hazards here to which we should give serious attention. A critical one is the real danger of a popular misconception about the nature of the scientific way which could prove damaging through the loss of a sense of ethical purposiveness to which

it might contribute. That misconception finds its basis in the widespread impression already alluded to that during our century particularly, despite the creation of numerous border disciplines, despite the widespread and frequent transplanting of the powerful intellectual and practical tools of one branch of science into the service of a newer one, the general approaches of the various sciences, not only their detailed strategies, have become more and more sundered. The evolution of science at its working level seems popularly to have been in the direction of ever-increasing fragmentation.

Now the working scientist, of course, has long taken for granted this diversity in the tools and methods by which various aspects of nature must be explored. It is as though each branch of science encompassed an independently evolving system of practical detail, with an individuality peculiarly its own, transferable to another discipline only to a relatively limited extent. It is a long time since the working scientist has seriously sought the goal of a universal, unitary core of methodology applicable to science as a whole. But unless the distinction between method and goal in science is fully comprehended, outside as well as inside the scientific profession, this obvious picture of fragmentation in the *modes* of the search for scientific knowledge could harbor a genuine social peril. For the hope that the delvings of the mind may ultimately achieve a single coherent vision of reality is one of the oldest, the most natural, and the most widely and deeply cherished of our dreams. We have long entrusted this search in our society to the world of the intellect and more and more in recent decades to the world of the scientific intellect. What might happen to hope, and to our sense of intellectual purpose and direction, if at some future time we as a people were to conclude that the whole scientific search for truth points, not toward a comprehending vision, but only to the elaboration of an endless series of fragmented localized areas of detailed information, never to be related in any meaningful way? The dangers that such a conception, if widely held, could pose to the estimation of science in our society in the future—and not only of science but of the rational exercise of the intellect in any context—are as notable as the conceptual limitations and fallacies of the view.

It is correspondingly urgent that the postulate itself be critically assessed. In one aspect, of course, the matter involves the profound and challenging issue, already touched on in another context, of the relatedness of the various sciences at a substantive level far beyond the tools and strategies by which new information is secured. But apart from that basically technical matter lies a far deeper one. The common objective of all scientific effort is manifestly the search for truth. Very early in its history science defined “truth” as the sensory impression, verifiable by many men, of some feature of that world of natural phenomena conceived to be away from, outside of, unaffected by the observer. Perhaps it was roughly the equivalent of “knowl-



edge'' as understood by the empiricist contemporaries of Locke. But that stage had already been outgrown by seventeenth-century science. Already notions of truth and falsity had been extended beyond observations to the theories built to contain and relate them. A prime requisite of the concepts of the science that followed the Newtonian revolution was that a structure of cause and effect be defined that should, as Newton himself emphasized, "be kept free of occult influences."

But the revolutionary developments of our own day have made even such a definition of truth too limiting. There is no doubt that a more widely relevant vision is needed, both of the quality of truth itself in science and of the consequent nature of the task of science in seeking out that truth. Perhaps we may find a definition suggested several years ago by Martin Johnson, a definition compelling the most sober reflection, both more meaningful in our world and more closely related to the philosophical challenges of science today. Perhaps we may come to think of scientific truth as, above all else, a measure of the coherence of systems of thought and of the communicability among them; as a property primarily of interchangeability both among observers and among scientific propositions relating to differing situations in nature. If the primary task of science remains today the search for truth in such a definition, we may well conclude that the highest aim of scientific inquiry is to make knowledge communicable in all possible situations; and that a measure of the validity of such knowledge may be the degree of its coherence among such situations. In striving toward such an objective the fragmenting of efforts made and the diversity of directions taken, both so essential to the winning of specific information at the practical level, stand out clearly as only necessary means, quite distinct from ends. Correspondingly, the fear of loss of overriding purpose, such a prevailing source of anxiety in our society, loses its reality in a scientific context.

Possibly there is another considerable hazard for the relation of science to the changing society of our future to which we should be sensitive. It may be introduced in a question, by no means trivial in itself. What will happen to the public understanding and valuing of the scientific way in a future society that is not only materially opulent, not only a generous provider of individual leisure and individual wealth for its citizens, as we may not unrealistically imagine that ours will be, but also, as we may hope, a nation free from major military conflict? For a quarter of a century now, we have been exposed to great wars, or the imminent threat of great wars. There can be no doubt that we literally owe our national existence and our individual lives to the powerful weapons that a vigorous technology, drawing upon stores of scientific knowledge accumulated over many years,

was able to devise and produce in time to turn the tide, a technology culminating in that of the atomic bomb. The evidence is overwhelming, and the belief nearly universal, that it is such weapons and the threat of them, serving as our shield, that have earned us surcease over the last few years from major holocausts, and that promise to preserve such immunity in the future.

Partly as a consequence of this, and partly as a consequence of our long and spectacularly conducted battle with disease, there is a widespread disposition in our society to equate science and its purposes primarily with the two great technical areas of defense: protection against military conquest, and protection against bodily ills. Inevitably the public evaluation of the scientific way is strongly colored by those identifications. It has often been remarked that the public esteem in which a new vaccine or antibiotic is held, and the enthusiastic support and acclaim for the particular labors through which it was produced, tend to fade when the target disease itself is brought under control. Will public concern for the military aspect of technology, which is so often reckoned as the other side of the scientific coin, wane also one day in long years of freedom from major conflict to which we may properly aspire? If so, how will this affect popular concern with science itself? The event will offer a test not only to the public judgment and understanding of science. At a very deep level it will be a test of the real values of scientists themselves. And in the last analysis, it must be their own evaluations of their task and of its proper objectives that will condition the final public view of science.

This question involves another matter, broader and yet more serious. It is the tendency, too prevalent among us, to confuse the objectives of technology in general with those of science. It is a most natural misconception. Since the very beginning of our nation, technology and science have historically served in the closest partnership, each indispensable to the other. Throughout the modern world, indeed, wherever technology is strong and well developed, there also is science; where either is weak, in the world of today, the other partner cannot be strong. Our whole experience as a nation has comprehended their ever increasing interdependence, until now they are so close-knit as to form a well-nigh homogeneous fabric. It is not easy, often enough it is not possible, to distinguish where the purposes of one partner end and those of the other begin. Furthermore, in all our history as a technically adept people, we have never had much practical incentive to make the distinction. It is no wonder that we equate their objectives so widely and so generally. And yet in fact they are far from identical. They differ importantly in some basic ways. The perception of these distinctions is not an academic matter. It is fundamental to a genuine public understanding of science.

Modern research has amply demonstrated the great age of technology



in the history of civilization, and archeological findings leave no doubt that the technological revolution antedated the Greek scientific revolution by several thousand years. During the period in ancient China when so many striking technological innovations were achieved it would seem, on the surface, that virtually every condition prevailed for the achievement of a scientific revolution too. Skilled craftsmen were available in abundance; there was a lasting period of peace and order; there was a wealthy and cultured segment of society with ample leisure for contemplation, as the religious and philosophical developments of the period vividly testify. Yet it was actually far away in medieval Europe, superficially so much less promising soil, that the scientific revolution flowered.

Why this odd twist of history, to all appearance so improbable? It is surely one of the great enigmas in the whole development of culture, and perhaps it will never be answered satisfactorily. But a penetrating suggestion of Barrett is most challenging and emphasizes how far apart the primitive roots of science and technology may have lain in the earlier histories of civilizations, however closely entwined and tightly knit they have become in modern times. Barrett has emphasized that it was probably in Greece alone, in approximately that critical time of Plato, that man took the tremendous and fateful intellectual step of deliberately separating the realm of rational consciousness from its enveloping background of the subconsciously sensed, the wider but mistier realm of intuition. Out of India and China, where already brilliant advances in technology had been made, came, instead of the developments leading to a scientific evolution, the rich but very different philosophies of the great Oriental sages, Lao-tse and Confucius and their contemporaries. They did not antedate Socrates by more than a century or so. But their philosophies were cast in the very opposite mold, striving to achieve, not a clear distinction between the intuitive and the rational aspects of man but, on the contrary, their harmonious fusion. A well-developed technology could and did flourish in that climate. A scientific evolution was not possible in it, despite a wealth of other favorable circumstances. Few vistas of cultural history could illustrate with greater clarity one essential difference between science and technology.

That difference remains today. It is epitomized by the widely divergent objectives of each. At one extreme of the spectrum from science through technology, the essential purpose of science is the broadening of knowledge, the deepening of understanding. That is its end, its total obligation. If that is well fulfilled, so is its destiny. At the other extreme of the spectrum, the ultimate merit for technology is the effectiveness with which it can bend the knowledge won by science to effective social use. In this comparison, its attitudes and goals, its procedures, and its practical scale of values may more closely resemble the generalized daily working philosophy of society as a whole than those of science itself. Indeed, the characteristic

processes and goals of technology are commonly far more visible to a society than are those of its science. That visibility is greatly enhanced by the circumstance that technology, unlike science, normally produces conspicuous and useful products which, devised as they ordinarily are with the aid of the knowledge that science provides, are more than likely to be popularly attributed to science itself. It follows that there are peculiar dangers for science in a society as technologically polarized as our own—dangers that will be with us for a long time. We shall need to exercise special vigilance on this score in the years ahead, as both the magnitude and the proportion of the support of science from federal sources, often conjoined almost indistinguishably with support for technology, and in effect ultimately apportioned according to the public will, increase yet further. In this climate public misunderstanding of the nature of science and the requirements for healthy scientific growth could in the long run seriously jeopardize the quality of science itself. One of the truly damaging things that could happen to scientific scholarship—and indeed to the very spirit of science—under these conditions would be for its approaches and goals to be publicly equated with those of technology, and for it to be consequently subjected, however gently or subtly, to assessments and demands formulated primarily in those terms.

We should never deceive ourselves about how serious such effects really could be, in the worst imaginable circumstances. In such circumstances it would be entirely possible for the fabric of American science to be subtly distorted over the long term by public support unwisely or improperly administered—by the lavish granting of funds for this and the withholding of funds for that, on the judgment of an insufficiently knowledgeable collective patron. Equally serious would be the real danger that such a situation long continued could threaten a subtle but menacing corrosion of the inner structure of science itself. For it could present to science a strong and persistent temptation to be less than wholly scholarly in its approaches—to dazzle its public patron with arresting technical prospects and thereby reap added material means for conducting some of the science to support it, or even, so the argument might go, for adding a whole sector of undirected scientific research that could not otherwise have been accomplished. We are not without contemporary examples of this situation, and it can be serious indeed. For not only can it threaten the very essence of the scientific way itself. Not only can it favor in practice the effective promoter whose primary value may be the conventional and tired goal of operation for its own sake over the investigator whose efforts and attention are more deeply committed to the winning of new knowledge. Even worse, possibly, is the fact that it can further compromise the future by playing upon and thus deepening the confusion between scientific and technical processes and goals.



So as the prospects of science over the coming decades are passed in review, not only its substantive potentialities appear vitally exciting. Given a climate of public concern and belief—and understanding—there is every evidence that its future in a context of broad service to society can also be one of extraordinary brilliance, that science as a whole can and will continue to furnish one of the most fruitful and powerful sectors of our national culture. But there is no doubt that we must be extremely vigilant about the climate. It is worth repeated emphasis and continuing reflection that science in our nation today is materially endowed at a level unique in all the history of man—at a level so high, indeed, that it is literally coming to tax severely the human resources of our country to maintain the pace. And it is also constantly to be recalled that only a small part of the support of American science comes today from the kinds of patrons to whom it had become adjusted over its long formative centuries, and who also had become adjusted in considerable degree to its demands and needs: wealthy individuals, generalized scientific societies, foundations, industry endowed with unusual vision. In 1943, in the midst of war, the United States Government paid for approximately 40 per cent of all research and development performed in industry. Last year, in the full tide of peace at home, that figure was about 60 per cent, while 70 per cent of the total research and development in the country was government supported. And total annual expenses for research and development in the United States, estimated at \$5.6 billion in 1954, had increased to \$18.7 billion in 1964. In the coming decade the figure may well double again. Further, it is particularly to be noticed that as much as 90 per cent of the research supported in universities by government is supported by primarily mission-oriented agencies.

The potential of that kind of support is incredibly great. But so also is the challenge. Even in the days when a minuscule science found only individual or occasionally corporate support it was not always easy to establish optimal working relations and an optimal working climate. Galileo was unusually fortunate in his patrons, both individual and academic, and yet at times even he felt compelled to change his milieu. Some of his contemporaries were far less comfortable and far more peripatetic. In Newton's day, harsh clashes between science and its patrons, individual or institutional, were not uncommon. Even as late as the second World War the proportion of technically based industries in the United States that really understood how to support science effectively and how to create appropriate working environments for it was extremely small.

In recent years, however, there has been dynamic change. Over the mere last three decades the advances in understanding of the nature, the requirements, the objectives of science by its older classes of supporters have been impressive. Now the same demand is extended to us all, on an

infinitely greater scale, and on a plane far more difficult and powerful. The means of meeting this demand, of course, like the means of meeting so many other challenges of the day that involve the roots of our national culture, lie massively with the forces of education and of communication, themselves in the midst of such vast change. How well those means are marshaled, how well our pressing obligations on this front are met over the coming years, will surely determine in great degree the future of science as a dynamic cultural force in our society.

*There is no culture without legacy, and we cannot and must not reject anything of ours, the legacy of the West. Whatever the works of the future may be, they will bear the same secret, made up of courage and freedom, nourished by the daring of thousands of artists of all times and all nations.*

ALBERT CAMUS—*Resistance, Rebellion, and Death*



## *The Year in Review*

*Science is not primarily concerned with the uniqueness of events but with what they have in common with other events*—WILLIAM RUSSELL BRAIN, *Science*, 148, 1965, 198.

A report on the year's work of the Institution in its context of the Nation's great scientific programs must indicate what the Institution does not do, as well as what it does. Having made its choices of method, where does its work fit among the great streams of United States and international "science" as they were revealed during the year?

As a glance at the reports of the National Science Foundation, the National Institutes of Health, the Atomic Energy Commission, and the large private granting foundations will show, research work on an extremely wide range of scientific subjects is now supported most generously in the United States. The lines of such work have often been viewed as "streams" of activity. But taken together the streams in fact resemble a flood, with some currents moving more rapidly or in greater volume than the whole. The cross-connections among the currents are many and often unpredictable, and they occur with ever accelerating frequency. The currents of large volume are often more easily identifiable to the lay observer than the more tenuous ones of greater velocity. Often streams of high potential significance may at the moment be among the most obscure. Thus it would be misleading to attempt to rank the many currents in gradations of potential importance. But we can note those that are especially attractive either to imaginative scientists or to supporters of fundamental science.

A list of the fields widely considered intriguing in the mid-1960s would certainly include high-energy nuclear physics, solid-earth geophysics and geochemistry, organic geochemistry, organic and physical chemistry, planetary physics, planetary geology and space biology, the atmospheric sciences and solar physics, stellar and cosmological astrophysics and astronomy, applied physics, oceanic geology and hydrography, pure and applied mathematics, marine biology, developmental biology, genetics and evolutionary biology, neurophysiology, research on behavioral systems including human and animal populations, and investigations of photosynthesis.

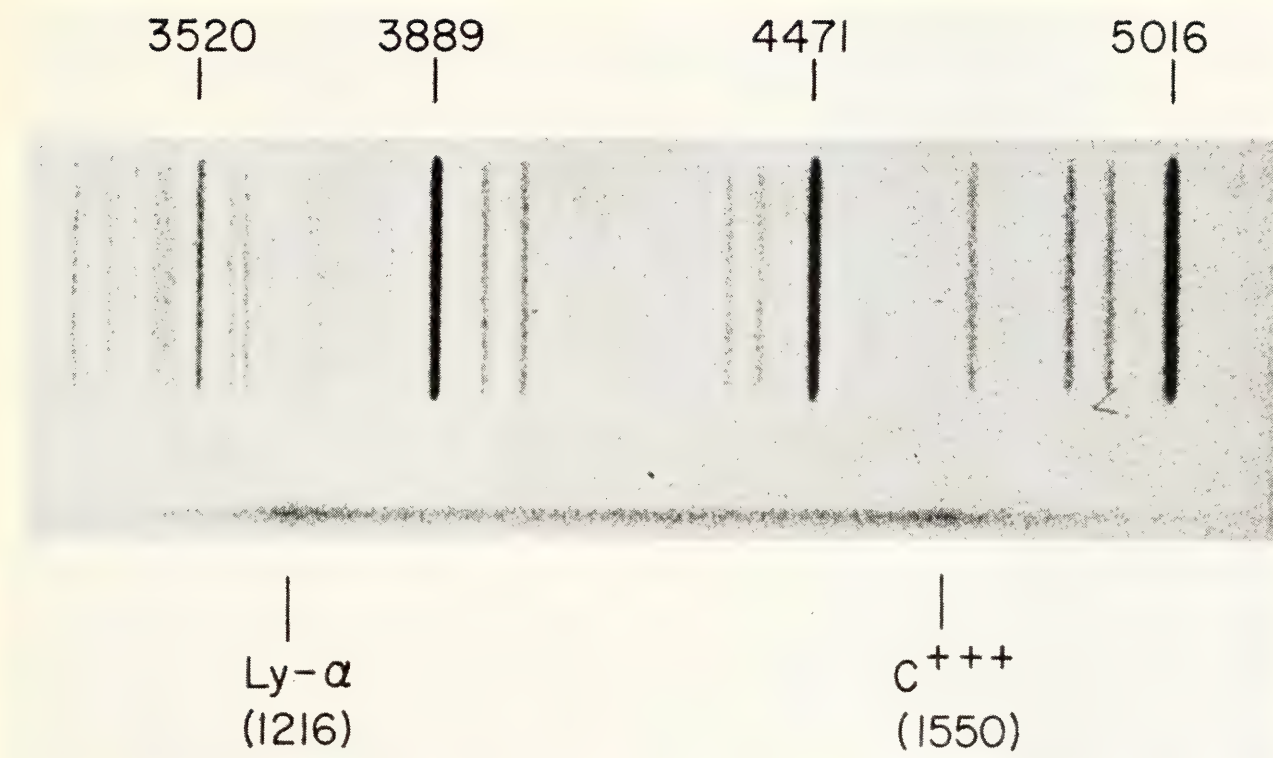


Plate 1. Spectrogram of 3C9 redshift  $\Delta\lambda/\lambda_0 = 2.012$ . Spectrum of the quasi-stellar radio source 3C9. The source spectrum, at bottom, shows two broad emission lines. The Lyman line of hydrogen, with a wavelength at rest of 1,216 Å, is observed at a wavelength of 3,666 Å, measured relative to the standard wavelength given at top. The emission line observed at 4,668 Å is from triply ionized carbon (C<sup>+++</sup>), which has a wavelength at rest of 1,550 Å. (Reproduced from a spectrum taken at the prime focus of the Hale telescope, Palomar Mountain.)





Plate 2. Four quasi-stellar radio sources obtained with the Hale telescope. Each of the four objects has a pointlike image on all but the most heavily exposed plates. The large image of 3C273 is a photographic effect due to image spreading in the emulsion. The print of 3C273 was derived from three plates superposed in order to show more clearly the jet extending outward from the quasi-stellar source.

The Institution's research interests of the past year touched upon more than half these fields. Among them are developmental biology, investigations of photosynthesis, genetics and evolutionary biology, the physiology of nervous systems, solid-earth geophysics and geochemistry, planetary and solar physics, planetary geology, and stellar and cosmological astrophysics and astronomy. These fields include several in which it is commonly assumed that large teams and heavy annual costs for equipment are necessities. Yet neither characteristic applies to the Institution's research work. The most expensive fixed investments of the Institution, in telescopes and other astronomical equipment, have low annual costs because of their long, useful lives, and team research at the Institution never involves more than a few staff members, voluntarily associated. The Institution's work thus illustrates the important role to be played today in a great number of scientific research fields by programs of relatively low cost built around the work of the gifted individual investigator. The Institution, of course, is not alone in this approach. A particularly striking recent illustration of highly significant results that have flowed from such economically modest origins was reported during the year in *Science*. H. Alfvén called attention to the significance of H. Gerstenkorn's recalculation of the history of orbital distances of the moon from the earth. Gerstenkorn's calculations, which suggest that the moon did not break off from the earth, as previously hypothesized, were made, as Alfvén says, "by a high school teacher having no other assets than his interest and his free time."<sup>1</sup>

Even though the Institution's pattern of support must seem a very liberal one by comparison with Gerstenkorn's, the members of its staff generally believe in their intellectual kinship with Gerstenkorn's methods, rather than with those of large group efforts. The Institution, too, interests itself vitally in the scientist's "free time," as M. A. Tuve has observed, "buying it, and then giving it back to him."

It seems appropriate to turn first to the year's activities in those fields where group effort is most evident—in the planetary sciences, astrophysics, and astronomy. Two general problems of astronomical interest were especially prominent during the year in international scientific activity: solar and planetary physics, and evolutionary cosmology.

### *Cosmological Problems*

Cosmology has probably fascinated men as long as they have sought an interpretation of existence. But it is only within recent years that enough solid evidence has accumulated to permit tenable inferences about the history of the universe and some predictions about its future state. Since the opening of the window on the universe provided by radio observation,

<sup>1</sup> H. Alfvén, Origin of the moon, *Science*, 148, 1965, 476-477.



optical study of radio objects has become of special importance to cosmology. Because of its still unrivaled reach into space, the 200-inch Hale telescope has provided unique opportunities to the staff of the Observatories year after year in securing ever more interesting evidence for cosmological interpretation. The year 1964–1965, brought, if anything, yet further acceleration in discoveries of importance to cosmology.

Before 1960 the most distant galaxy for which a measurable spectrum had been obtained gave a redshift of  $\Delta\lambda/\lambda_0 = 0.20$ ,<sup>2</sup> and the most distant cluster of galaxies observed photoelectrically had a redshift of  $\Delta\lambda/\lambda_0 = 0.35$ . In that year, just before his retirement from the Observatories, Rudolph Minkowski obtained two spectrograms of a peculiar galaxy identified with the radio source 3C295, and found for it a redshift of  $\Delta\lambda/\lambda_0 = 0.4616$ .

During this year even more spectacular redshifts were observed for some of the quasi-stellar radio sources<sup>3</sup> first catalogued by radio astronomers. Using the Hale telescope, M. Schmidt of the Observatories obtained spectra and redshifts for five quasi-stellar sources that lie startlingly farther away than any other known object in the universe. The most distant of the five, 3C9, is so remote that its redshift is  $\Delta\lambda/\lambda_0 = 2.012$ ; the others, in decreasing order, are 1.055, 1.037, 1.029, and 0.734. For 3C9, Lyman  $\alpha$ , the strongest line in the spectrum of the hydrogen atom, is observed to be shifted from its normal position at 1,212 Å up to 3,666 Å. This is considered a cosmological redshift. In viewing the light of the 3C9 spectrogram one is looking back to a time only a few billion years after the expansion of the universe began.

Much progress toward the optical identification of radio sources was also made by A. R. Sandage, P. Veron, T. A. Matthews, and J. D. Wyndham. They analyzed most of the 328 listings of the revised *Third Cambridge Catalogue*, using new, precise radio positions from several radio observatories and checked by three-color photometry. They found that 29 of these sources are in the Galaxy. Ninety-five definitely can be identified with radio galaxies; and 35 are considered as certain quasi-stellar sources.

An analysis by Sandage of the new data suggested that we may be on the verge of conclusive evidence about the validity of important hypotheses concerning the dynamic structure of the universe. The two most important hypotheses are the “steady state,” in which it is postulated that the universe is continuously regenerating itself, and the “big bang” hypothesis, which traces all cosmological attributes to a single primeval explosion.

When Sandage plotted redshifts for 40 radio galaxies against corresponding magnitude determinations he found them to fit a straight line to the limit of the redshift determination at  $\Delta\lambda/\lambda_0 = 0.26$ . Photometry of the nine quasi-stellar sources for which Schmidt has measured redshifts up to

<sup>2</sup> Here  $\lambda$  = the normal wavelength of an observed spectral line, and  $\Delta\lambda$  is the extent of displacement toward the red of the observed line as viewed in a receding source.

<sup>3</sup> A quasi-stellar source (QSS) is a radiation source of small dimension (a light-year or less) and extraordinary intensity (probably 100 times that of a normal galaxy).

$\Delta\lambda/\lambda_0 = 2$  showed that, within the accuracy of the data, these also are consistent with a linear relationship between magnitude and redshift.

Such a linear relationship gives some basis for comparing the cosmological models, corresponding to a value of  $+1$  for the deceleration parameter<sup>4</sup>  $q_0$ . An object at the enormous distance of 3C9, in a  $q_0 = +1$  model universe, differs in apparent luminosity by a factor of about 10 when it is compared with such an object in the steady-state model of the universe, for which  $q_0 = -1$ . The data currently available are not consistent with the steady-state model. However, the present data sample is small. If redshifts and accurate photometry can be obtained for three times as many quasi-stellar sources, it should be possible to determine the value of  $q_0$  with confidence and thereby open a new chapter in describing the history of the universe. If further results like those obtained by Sandage and Schmidt during the year 1964–1965 are brought out in the completed analysis, an expanding but decelerating model of a universe (one version of the big-bang hypothesis) would seem to be favored.

An interesting theoretical study was completed during the year by Sandage and G. A. Tammann on background cosmic light from galaxies. It has been suggested in the past that background cosmic light might be used to discriminate among different cosmological models and provide an observational test of various cosmologies. Such observations could be part of the national space program, so Sandage and Tammann calculated the expected light levels for the principal cosmological models thus far proposed. The conclusion is that the level of the cosmic light is very low in comparison with other sources of continuous light. The study indicated that the combined light of the zodiac and the Galaxy would be more than 100 times stronger than the cosmic signal. Furthermore, even if the cosmic component in the total light were detectable, the differences among the models are very small. Sandage concluded that no test of cosmological models will be possible from cosmic light observations.

### *Development of Astronomical Observing Facilities and Equipment*

The greatly heightened interest in extraterrestrial observation during recent years has spurred efforts to increase the now highly limited capacity of the world's astronomers to observe objects of the greatest cosmological significance. Although the 48-inch schmidt telescope at Palomar was most useful in Sandage's study of quasi-stellar objects, the final word at the Observatories on the nature of new objects always falls to the great Hale telescope. Its uniqueness is a source of concern to the Observatories. Although the Hale instrument's observing time is allotted with the utmost regard for scientific promise, it has long been obvious to the Institution

<sup>4</sup> The deceleration parameter is  $q_0$  determined by velocity and acceleration as a function of distance in the universe.



that astronomy and human knowledge would benefit enormously from the addition of other giant telescopes to the available equipment of the international astronomical community.<sup>5</sup> The Observatories' staff therefore have cooperated in the planning of other large instruments the world over. Their counsel has been sought and given on all except one or two of the major optical telescopes planned in recent years. I. S. Bowen, Distinguished Service Staff Member and former Director of the Observatories, and B. H. Rule, Chief Engineer of the Observatories, have been particularly active in this cause. It was therefore gratifying to find that there are now 10 projects in the world for the construction of telescopes of 120 inches or larger.

These projects were considered sufficiently promising to warrant the organization of an international symposium on the construction of large telescopes, held at Tucson, Arizona, and Pasadena, California, between April 5 and April 12, 1965. Dr. Bowen was chairman of the organizing committee, and the Observatories acted as co-hosts with the Kitt Peak National Observatory and Lick Observatory. A group of astronomers, optical designers, and telescope engineers exchanged ideas and information and discussed the problems of design, construction, and operation. A visit for detailed inspection of the Hale telescope was included in the program of the symposium.

The Observatories also were actively concerned during the year with site investigations for a possible new major observatory in the southern hemisphere. Continuing a study started in the year 1962–1963, observations of the quality of seeing were made on three coastal mountains in Coquimbo province, Chile, and at the Siding Spring Observatory in New South Wales, Australia. The results to date show a clear superiority for observing conditions in Chile, where testing is continuing on Cerro Morado and on Cerro Pachon. The mean amplitude of image tremor as measured by the astronomical seeing monitors in Chile has averaged, for the summer months, slightly better than 0.7 second of arc, and 70 per cent of all the nights there can be classed as photometric. These prospective sites, at about 30°S latitude and at elevations between 7,000 and 9,000 feet above sea level, thus appear to be extraordinary, in that they offer superlatively good observing conditions.

It is hoped that the superb physical qualities of one of these sites ultimately can be exploited in the construction of a new observatory of the Palomar class. An instrument of 200-inch mirror size is considered the most effective possible addition to ground-based equipment, promising the shortest lead time to actual observing. The Institution is prepared to cooperate in the establishment of such an observatory under appropriate sponsorship.

<sup>5</sup> Discussed also in the *Report of the Panel on Astronomical Facilities*, Committee on Science and Public Policy, National Academy of Sciences, 1964.

Another approach to improvement of the world's astronomical observing facilities has been through electronics. For the past 11 years Institution staff have provided leadership for the development of photoelectric image tubes for telescopes. The Committee on Image Tubes for Telescopes, under the general direction of M. A. Tuve of the Department of Terrestrial Magnetism, is a cooperative project of the Department, the Mount Wilson and Palomar Observatories, the Lowell Observatory, the National Bureau of Standards, and the U. S. Naval Observatory. A large measure of the financial support needed by the Committee has been contributed by the National Science Foundation.

Image tubes derive their potential importance for observational astronomy from their photon efficiency. Fewer photons are required to cause the ejection of an electron from a good photoelectric surface than are required to produce a developable grain in a photographic emulsion, hitherto the standard recording surface for astronomical observation. The task of the Committee and its industrial contractors, however, has been an exacting one. The sought-for device not only had to exploit photoelectric sensitivity, but also had to have resolution at least comparable to the photographic plate now customarily used, no spurious background of significance, and few fluctuations in the image produced; and to present an image-producing surface of reasonable size. These rather stringent requirements have been met in large measure by a "cascaded" image tube developed by the Electron Tube Division of the Radio Corporation of America (RCA) for the Committee. (See Plate 3, facing p. 44.)

Twenty of the tubes were delivered during the year. The Committee and its collaborators thereby reached a point where they could apply the tubes to definite research problems. Special optical systems have had to be developed for efficiently presenting the optical image from a telescope to the tube and for projecting its output onto a photographic plate for final recording. Five different systems, applying to differing research problems, were designed and made available to five observatories. A system for spectral classification was put into operation at Yerkes Observatory, one for high-dispersion stellar spectra at Kitt Peak National Observatory, coudé spectrograph systems at Lick and Mount Wilson observatories, and a Cassegrain spectrograph system at Lowell Observatory. Gains of  $\times 10$  or  $\times 12$  in exposure time for equal resolution are achieved for the tube systems over that for the best blue-sensitive photographic plates.

### *Geophysics and the Earth as a Planet*

As mastery of that startling new scientific tool, the rocket and its auxiliary instruments, has progressed, scientific interest in the study of the planets has heightened and activity in the field has increased substantially. This was particularly evident in the years from 1963 to 1965 as the lunar and



planetary probes were prepared and executed. The interest and activity related to the extraterrestrial probes has been paralleled by a rise in ground-based research. For many years investigations of the planets have had a place, at times a prominent one, in the observational program of the Mount Wilson and Palomar Observatories. They continued during the year, with studies of the spectra of Mars, Venus, Jupiter, and the Galilean satellites, the asteroid Vesta, and the moon, by six observers. The construction of model atmospheres for each of the major planets also was undertaken in a theoretical study.

The mounting general interest in planetary study has brought with it a growing awareness of the earth as a planet—indeed, the most accessible of all planets for the detailed study of planetary physical attributes. Thus geologists have used the equipment of the observatories for the observation of other planets, and the findings of geophysics are now seen to have broader significance as they are scanned for their inferences about the conditions and the history of other planets. The Institution, with major commitments to the field of solid-earth geophysics, has its most extended relation to the planetary sciences through geophysical research. The program of mineralogical analysis of meteorites carried on at the Geophysical Laboratory in recent years is a good example of this relation. As in other years, research of this type was undertaken both at the Geophysical Laboratory and at the Department of Terrestrial Magnetism.

M. A. Tuve, Director of the Department of Terrestrial Magnetism, has noted that there are very few extremely costly experiments in solid-earth geophysics. Instead, such research in the United States is generally supported by a large number of relatively small expenditures. He describes the situation as “not necessarily a virtue of solid-earth geophysics, but . . . a reality.”<sup>6</sup> It is a reality that has suited the Institution in part because of the continued adaptability of geophysical research to individual attention, but also because of the long tradition for such research here, dating back more than six decades.

In the Introduction to his report this year P. H. Abelson, Director of the Geophysical Laboratory, observes that geophysicists of the Institution are “at home in two laboratories. One is in Washington. The second encompasses the earth and part of the solar system.” As Abelson says further, a “broad connection with the whole earth” is sought for those studies concerned with the earth’s crust or its mantle. For others, observations that reveal relations to the solar system are desired. These interests were illustrated during the year by studies of the earth’s magnetic properties, of meteorite minerals, of the organic components of ancient rocks, and by several studies seeking to interpret general and specific properties of the

<sup>6</sup> M. A. Tuve, Solid-Earth Geophysics, *Transactions of the American Geophysical Union*, 46, 1965, 203–204.

earth's crust. A large number of the known special fields in geophysics were represented; the most notable exception was the study of the atmosphere.

The Equatorial Ring Current, a system of electric currents high above the earth's surface, has long been an object of study by S. E. Forbush of the Department of Terrestrial Magnetism. When the sun is in an active period the earth is surrounded by solar plasma. Protons and electrons are deflected into various paths and orbits by the earth's magnetic field, giving a resultant "ring current" several earth's radii out from the earth at the equator. A possibility existed that these "drift" currents, which cause compass variations, were continuously present. However, Forbush's studies of magnetic variation coefficients for disturbed and quiet days during periods of diminishing solar activity show that the ring current drops to zero for a few of the days during periods of solar quiescence, one of which now prevails.

Two interesting inferences about the conditions attending meteorites arriving at the earth's surface can be derived from two sets of experiments conducted at the Geophysical Laboratory on the phase equilibria of minerals. In one the complex polymorphism of enstatite ( $\text{MgSiO}_3$ ) was examined by F. R. Boyd, Jr., and J. L. England. There are two principal crystal forms, the rhombic and the monoclinic.<sup>7</sup> Nearly all the terrestrial enstatites taken from a wide variety of rocks are rhombic. On the other hand, both rhombic and monoclinic forms occur in meteorites, sometimes intergrown in the same meteorite. A third crystal form, protoenstatite, has been observed only in the laboratory. The lack of natural terrestrial clinoenstatite is puzzling because it is the equilibrium form in temperatures in the lower range of enstatite formation and at all pressures. On the other hand, both clinoenstatite and rhombic enstatite are found in meteorites. The phase studies by Boyd and England, of the Geophysical Laboratory, on enstatite are also applicable to minerals from extraterrestrial sources. The studies suggest that the mineral assemblage in the meteorites where the two types of enstatite occur was formed at temperatures above  $1,000^\circ$  and pressures below 8 kilobars (kb).<sup>8</sup> Although the enstatites might also have been formed at much lower temperatures, the presence of glass in the same meteorites implies the higher magmatic temperatures.

Petrologic interest in a form of silica known as coesite has been stimulated by discoveries at the Meteor Crater in Arizona and in other geologic situations. At the Geophysical Laboratory P. M. Bell, G. Simmons, and J. Hay have studied the quartz-coesite phase equilibrium<sup>9</sup> and have found that coesite can be synthesized at room temperatures. This was done by

<sup>7</sup> The terms "rhombic" and "monoclinic" refer to the geometric relation of the three axes of the crystal.

<sup>8</sup> One kb is equivalent to 987 atmospheres, or approximately 14,500 pounds per square inch.

<sup>9</sup> The relation between different minerals with the same or similar elemental composition; usually refers to temperature and pressure at time of formation.



applying pressure to silica gel within an apparatus known as a shearing squeezer. The device, first described by P. W. Bridgman of Harvard, uses two opposed tapered piston anvils, to one of which torque is applied. The results suggest that coesite is formed under conditions of high pressure, like those of a meteorite impact, but that high temperatures are not necessary to its formation.

*Geologic Events Underlying Certain Catastrophes.* In the search for generalizations about the earth's properties, few events have been of more absorbing interest than those that cause the great natural catastrophes of volcanic eruptions and earthquakes. The destructive force of earthquakes has been experienced many times in settled parts of the world, most recently in Chile and in Alaska. Volcanic eruptions, when they occur, are even more impressive. H. S. Yoder, Jr., notes in this *Year Book* that the total energy release from such an explosion has been estimated to equal from 1 to 100 megatons of TNT. A single explosion in the East Indies in 1815 moved 36 cubic miles of solid material. The 1883 explosion at Krakatoa, also in the East Indies, killed 36,000 people and threw ash into the stratosphere, where it affected world weather for several years. Both for the fundamental information that it provides about the behavior of the earth's crust and mantle and to assist in the development of methods of prediction to alert people whose lives are vitally affected, investigation of these phenomena is important.

An understanding of the physical chemistry of the volcanic explosion process may ultimately provide a basis for assaying potential hazards by suitable geophysical techniques. During the year Yoder studied the influence of water on the melting behavior of simple silicate systems as a contribution to the understanding of volcanic eruptions. Some of the first experiments bearing on this problem were conducted at the Laboratory by G. W. Morey about 40 years ago. Morey studied potassium silicate and water at pressures up to 1 kb, and found that gas pressure increased rapidly under special conditions when a melt, saturated with crystals and gas, cooled. This model, however, was considered not generally applicable to natural systems. Yoder has now devised a simple system that will represent those magmas of greatest geological importance. His system includes the pyroxene mineral diopside and the feldspar anorthite plus water in pressures (10 kb or less) now considered typical of the mantle region in which magmas are generated. Yoder's experiments showed that gas (mainly water vapor) can be expelled from both saturated and undersaturated magmas when the containing pressure is decreased. The conclusion is that the water content of magmas at depth, where they are under pressure, provides an adequate propellant for volcanic explosions. As a concluding note to the report on his experiments, Yoder says, "It is perhaps not unwarranted to have some concern over the potentially explosive character of the stratovolcanoes of the

western areas of the United States. There is a clear need to establish observatories near Mount Rainier and Lassen Peak, for example.”

An inference of at least equal interest on earthquakes has resulted from studies by S. Suyehiro. Suyehiro is a Carnegie Corporation Fellow on leave of absence from his post in Japan, where the study of seismology has long been important because of the great seismic activity observable on the Japanese islands. Participating in the Andes program of the Department of Terrestrial Magnetism, Suyehiro has observed that the size-frequency-of-occurrence pattern of foreshocks preceding the large Chilean earthquake of 1960 differs remarkably from the pattern of aftershocks for the same

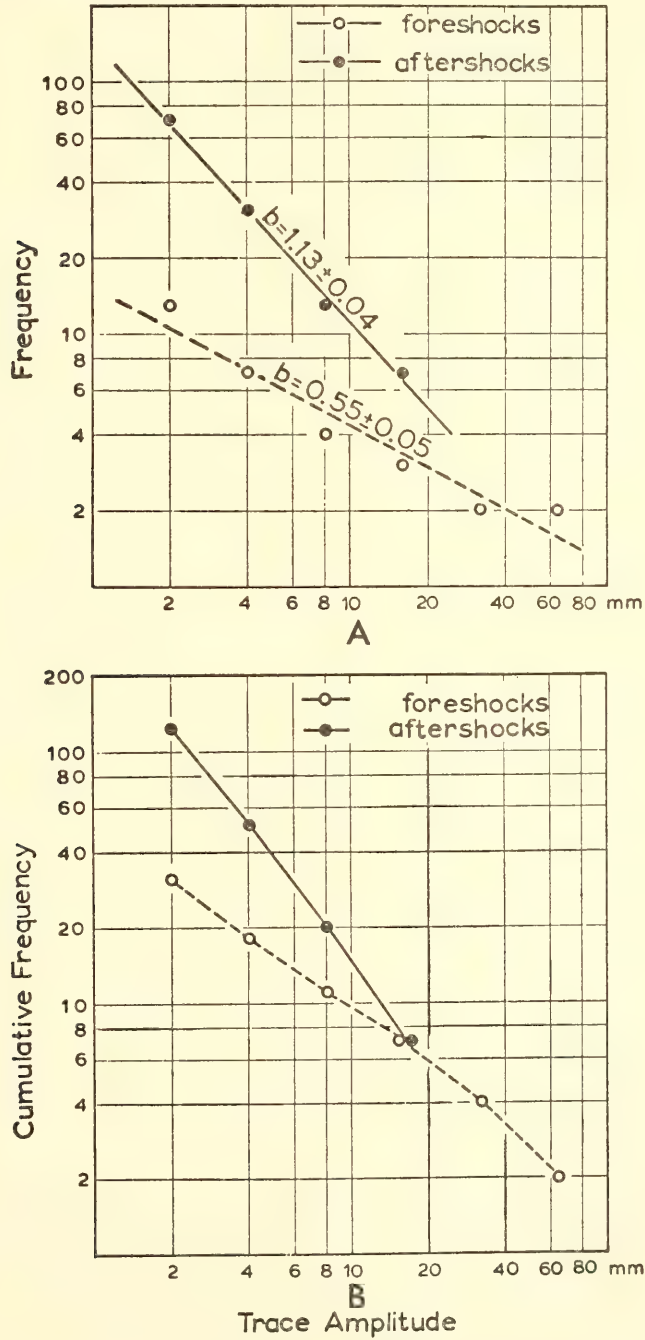


Fig. 1. Pattern differences of foreshocks and aftershocks, great Chilean earthquake of 1960.



region. Suyehiro had previously discovered a similar difference between foreshocks and aftershocks in a Japanese earthquake. Apparently each seismically active region has a characteristic "normal" ratio of small shocks to those of moderate intensity. These normal ratios, furthermore, seem to be about the same for much of the world. Suyehiro has found that in the period of a day or two before a large earthquake the normal pattern of shocks is replaced by one with relatively few shocks of smaller size as compared with those of moderate intensities. After the large earthquake the sequence of minor shocks again resumes the normal ratio of small to moderate shocks. The Department of Terrestrial Magnetism considers that this newly discovered characteristic of foreshocks may be significant in the search for warning signals that may be used in "earthquake prediction."

*Ore Minerals.* Another property of the earth's crust—but a noncatastrophic one—that has held intense interest for human society since prehistory has been the geographical and stratigraphic location of economically usable minerals. G. Kullerud and his associates at the Geophysical Laboratory have continued studies pursued for some years past of minerals associated with ore bodies or found in the vicinity. During the year A. J. Naldrett and Kullerud commenced a detailed study of ore formation at the recently developed Strathcona Mine at Sudbury, Ontario. The Strathcona Mine contains copper-iron-nickel sulfide ore. Intensive studies of certain minerals in the noritic<sup>10</sup> country rock vary with distance from the ore bodies. For example, biotite mica distant from the body is of a normal green variety, but as the ore body is approached a brown oxy-biotite becomes increasingly more common. The ore is surrounded by an envelope extending many hundred feet where the biotite is exclusively of the brown oxy type. The composition of the feldspar in the country rock also changes gradually, becoming increasingly more sodic (albitic<sup>11</sup>) as the ore is approached. The Strathcona ore body thus is surrounded by reaction zones extending considerable distances from the ore. Since similar reaction zones have been shown for other ore bodies it is reasonable to infer that knowledge of mineral characteristics in the reaction zones may be used advantageously in exploration for ores as yet undiscovered.

*Methods of Geophysical Research.* Two other examples of improved methods of interpreting and measuring the attributes of the earth's crust are worth noting for the light they throw on the way of the individual investigator. As the result of their investigations of heat flow and thermal properties of the bottom of Lake Superior and the bottom of Seneca Lake, New York, J. S. Steinhart and S. R. Hart of the Department of Terrestrial Magnetism have suggested a possible new method of measuring the outward

<sup>10</sup> Norite is a gabbro in which more than half of the pyroxene is orthorhombic. A gabbro is an igneous rock of granitoid texture containing feldspar and pyroxene minerals.

<sup>11</sup> Albite =  $\text{NaAlSi}_3\text{O}_8$ .

flow of heat from the inside of the earth's crust that avoids the costly drilling of large numbers of very deep holes. The measurement of heat flow in the earth is highly important in geophysics because thermal energy is needed to drive the processes by which mountain ranges are built, oceanic trenches created, and other major alterations to the face of the earth effected over geologic time. Accurate heat-flow data are vital to sound theory about these processes. Steinhart and Hart state in their report this year that "it is the temperature differences and their history within the earth that could provide the basic understanding of the orogenic history of the earth."

Average values of the heat flow from the surface of the earth have been obtained, but knowledge of regional variations is essential to discover the thermal imbalances now shaping the earth's surface. These are obtained with relative ease from the bottom sediments of oceans, where atmospheric temperature effects are negligible. However, measurements on land may require access to mines or boreholes some hundreds of meters deep. Since the bottom water of deep lakes in temperate or cold regions is nearly isothermal, Steinhart and Hart believe that ocean-bottom techniques may be successfully applied to the measurement of heat flow in a shallow stratum of sediments at lake bottoms. Their measurements of thermal conditions and sediments at the bottom of Seneca Lake suggest that this new procedure may have general applicability for investigation of regional heat inequalities in the earth.

Experience with orbiting satellites and other probes of the stratosphere, mesosphere, and exosphere in recent years has shown that the assimilation, retrieval, and interpretation of information are at least as difficult as its collection. As Abelson has observed, if information cannot be used its collection is little more than an academic extravagance. This problem is not a new one. For the Institution it is at least as old as the 25-year program of collecting data on terrestrial magnetism that commenced in 1905. More recently the Geophysical Laboratory has shown that it is also a problem for petrographic and petrologic data. The Laboratory's punch-card library contains more than 7,500 entries for Cenozoic volcanic rocks alone; there are probably at least 1,500 more published analyses of the rocks not yet included in the library. Abelson states that the number of published analyses of igneous rocks of all kinds may be as large as 35,000. This is a vast body of information whose correct interpretation is critical to generalizations about the composition and history of the lithosphere.

F. Chayes has been studying machine methods of storing these data in such fashion that subsets, based on varying combinations of geographic, chemical, normative, taxonomic, and other properties, can be readily retrieved for display or statistical processing. Recent *Year Books* have reported his earlier descriptions of the basalt-trachyte association of the oceanic islands and of the chemical contrast between circumoceanic basalts



and those found on oceanic islands. They were obtained from analysis of sample frequency distributions, and showed that the lavas of the oceanic island environment are much richer in titania ( $\text{TiO}_2$ ) than lavas found on the continental margins of the oceans. During this year Chayes extended his studies to andesite, the most common volcanic rock type on the continental margins of oceans. His study of data from more than 1,500 samples shows that there is a remarkable inconsistency between the "norms"<sup>12</sup> of andesite specimens described by petrographers and the definitions of andesite provided by textbooks and petrographic systematists. Despite the accepted systematic definitions of andesite, which indicate that these rocks are silica-saturated, a considerable excess of normative silica is typical of the andesite group. Chayes notes that andesites that "satisfy systematic definitions . . . are evidently in short supply."

The few tests of new techniques thus far made indicate that modern methods will permit efficient exploitation of petrochemical data and possibly lead ultimately to important new generalizations about the character of igneous rocks in the earth's crust.

### *Comparative Biochemistry of Fossil and Contemporary Organisms*

For several years Abelson and his colleagues at the Geophysical Laboratory have conducted a program of biogeochemical studies that are giving new views of life on earth and new conceptions of the biogeologic time scale. With the aid of new and more versatile gas-chromatographic techniques, T. C. Hoering and Abelson made further contributions during the year to understanding the occurrence of fatty acids in rocks. Two types of compounds are of interest for analysis in this connection—the free fatty acids and the straight-chain aliphatic groups found in the insoluble organic matter of rocks. Fatty acids are major components of living organisms and may be expected to be abundant in recent and old rocks. The dominant saturated fatty acids in cells are palmitic (16 carbon atoms per molecule) and stearic acid (18 carbon atoms). Both are found in rocks. On the other hand, though unsaturated fatty acids containing 18 carbon atoms are also abundant in cells, no trace of them has ever been found in sediments older than a few years. Yet rocks contain relatively large amounts of acids with odd numbers of carbons and with more than 20 carbon atoms in the chain. Hoering and Abelson state that profound changes in the concentration and molecular weight distribution of fatty acids must occur rapidly in geological environments.

Like the free fatty acids, the aliphatic groups present in the insoluble

<sup>12</sup> A petrographic norm is a hypothetical mineral composition of a given rock, calculated according to certain rules, and intended to indicate typicality.

organic matter of rocks can be found in sedimentary rocks of all known ages. It is significant that these groups have been identified in rocks as old as 1,600 million years, since they are very characteristic products from the transformation of organic matter. As Abelson and Hoering note, they "provide a suitable record of some facets of very ancient life on earth." The research undertaken thus far has raised several interesting questions for future research. What is the chemical reaction that binds fatty acids into the organic matter of sediments? By what chemical reactions are the acids with an odd number of carbon atoms formed? How are acids of long-chain length synthesized in the sediments?

One of the most intriguing of these questions involves the relation between the soluble-free fatty acids and the aliphatic groups of the insoluble organic matter in them. Noting that soluble hydrocarbons had been isolated from sedimentary rocks as old as the 3,000-million-year Fig Tree shale of South Africa, Hoering examined the question during the year. Hypothesizing that the soluble materials might be migrants into the rock and that the insoluble part must be indigenous, Hoering examined the isotopic composition (carbon<sup>13</sup>/carbon<sup>12</sup> ratio) of the two. In young rocks where the soluble matter is thought to be in place the ratios agreed, but in several of the most ancient rocks the ratios did not agree. Hoering concluded that the presence of soluble aliphatic hydrocarbons in an ancient rock are not necessarily clues to biological activity in the era of the rock. They may be "contaminants" from a more recent geologic period.

The techniques of biogeochemistry also have been applied by P. E. Hare and Abelson to a clarification of the fossil record of life on earth. With some rare and recently discovered exceptions the fossil record commences with the relicts from Cambrian times (about 700 million or more years ago). Some paleontologists have suggested that this sudden appearance of the record of multicellular life in the Cambrian in reality represented only a transition from unpreservable organic hard parts to mineralized skeletons of calcium phosphate, calcium carbonate, or silica. Hare and Abelson have found evidence for just this pattern of evolution in the phylum *Mollusca*. Their study of widely distributed specimens of primitive and highly evolved animals shows that the hard parts of primitive mollusks contain 100 or more times the organic matter found in hard parts of highly evolved animals. Variation in the content of glucosamine is even more striking. Glucosamine is an indicator of chitin, which is a polymer of acetyl glucosamine. Chitin is a major constituent of the hard parts of many phyla, most notably among insects. Primitive forms appear to contain as much as 10,000 times more glucosamine of this chemical than do highly evolved types.

These data add to the accumulating evidence that life did not suddenly "emerge" in Cambrian times. Instead, nature's facilities for record-keeping appear to have passed a threshold at that time.



### *Further Research on Biological Problems*

It has often been observed that the age of biological research has now commenced. Indeed, some of the most intellectually fascinating and socially important problems for scientific research confront biology today. As talents from neighboring fields like physics and chemistry are increasingly applied, with a great new storehouse of sensitive instruments to draw upon, and extensive financial support, the biological sciences are entering the finest period in their history. Not only is the number of scientists entering biology burgeoning, but the list of "fields," or specialized points of view also increases almost yearly. The entire front of biological problems is under attack in varying degrees of intensity, from the physics of energy exchange to the most esoteric aspect of ecology. It is only by stretching the imagination that we can consider biology a unified "field" or a "subject" in this day. It is really a massive agglomeration of fields of the highest complexity, with some of the most difficult objectives and refractory materials ever to be attacked by the rational procedures of science. It is the area par excellence in which the individual investigator of today can exercise his talent and ingenuity. The staff of the Institution thus continues to be attracted to it, extending a tradition of more than 60 years.

The Institution's research in the biological area is spread through the activities of five departments. It includes the studies in developmental biology at the Department of Embryology, work in the biochemical and biophysical aspects of genetics and evolutionary biology at the Genetics Research Unit and the Department of Terrestrial Magnetism, and the study of photosynthesis and experimental taxonomy at the Department of Plant Biology, as well as the study of biogeochemistry at the Geophysical Laboratory, described above.

*Research on Photosynthesis.* The complexity of a research problem in biology is well illustrated by the challenge to analysis posed by the photosynthetic process. M. D. Kamen, in his helpful volume, *Primary Processes in Photosynthesis*,<sup>13</sup> has described skillfully the general dimensions of the problem of photosynthetic investigation. Setting a scale of elapsed time in the photosynthetic process that begins with the incidence of light on a cell and ends with cell growth and division (Plate 4), he goes on to describe "eras" of interest to several specific research approaches. Thus there are the eras of radiation physics, photochemistry, biochemistry, and physiology, which presumably also lead into the era of ecology. The eras overlap and knowledge about them varies, as Kamen illustrates in his accompanying "spectrum of ignorance." Similar diagrams might be constructed for other fields of biological research interest, some of them displaying even greater complexity, as in developmental biology.

<sup>13</sup> M. D. Kamen, *Primary Processes in Photosynthesis*, Academic Press, New York, 1963, pp. 4-6.

The photosynthetic research program of the Institution at the Department of Plant Biology falls into the eras of photochemistry and biochemistry as delineated by Kamen. The Department pioneered research on photosynthesis in the United States, its first interest dating from the arrival of H. A. Spoeher at the Desert Laboratory, the predecessor of the Department, at Tucson, Arizona. Spoeher, a carbohydrate chemist trained in Berlin, first mentions photosynthesis in his report of 1917. When the Department was established at Stanford in 1929, photosynthesis research became one of its important activities. Between 1930 and 1940 it was joined by a number of other research centers on photosynthesis, particularly at universities, leading to the extraordinarily diversified interest of today.

One of the most useful measures of photosynthetic activity is the observation of change in the absorption of light by certain pigments when they are activated by light of specific wavelengths. The absorption changes caused by illumination of living cells by light of appropriate wavelengths reflects the oxidation and reduction of various intermediate "electron-carrying" substances closely associated with the use of light in photosynthesis. The oxidation or reduction of several of these carriers can be studied separately by choosing wavelengths corresponding to the absorption peaks of the carriers. By extension, the absorption changes can also be used to investigate the activity of the different pigment systems that are at the heart of photosynthesis.

Two separate systems of pigments are now believed to act in the photosynthesis of green plants. These two systems (temporarily called system I and system II)<sup>14</sup> apparently drive two associated but very different photochemical reactions, both essential to photosynthesis. In 1963-1964 the Department of Plant Biology, by measuring absorption changes, found that the copper-protein plastocyanin formed a link between the two systems, being capable of both oxidation and reduction. Other compounds known as cytochrome *f* and cytochrome *b* had previously been located as probable intermediaries between the two systems. Continuing the Laboratory's interest in the nature and sequence of components in the electron pathway linking the two photochemical systems, D. C. Fork and W. Urbach in 1964-1965 localized the action of plastocyanin more specifically than ever before. It was found to act prior to cytochrome *f* in the chain of intermediates transporting electrons, thus fitting another hitherto unknown detail into the slowly developing conceptual model of the photosynthetic process.

Knowing of the probable existence of two pigment systems through

<sup>14</sup> System I is composed mainly of a long-wavelength form of chlorophyll *a* absorbing red wavelengths of light. System II is composed mainly of a group of pigments known as accessory pigments, including chlorophyll, that absorb light at shorter wavelengths than the pigments of system I. The two systems operating together show an "enhancement" effect; i.e., joint operation results in a greater output than the sum of outputs of the individual systems operating alone.



photochemical effects, biochemists are presented with the tantalizing problem of attempting to separate the two systems without alteration of their photochemical activity. Experimentation on this separation at the Laboratory was intensified during the year by J. Brown and C. Bril. The major task in the experiments was to break apart the chloroplast units containing the two pigment systems. After many exploratory experiments with differing materials and methods, the detergent deoxycholate, acting on the alga *Euglena*, yielded two fractions, a lighter one containing chlorophyll *a* 670 and a heavier one greatly enriched in chlorophyll *a* 695. Fractionation of the pigment complexes also was obtained from the green algae *Dunaliella* and *Ulva*, by a process of repeated freezing and thawing.

The *Euglena* fractions were tested for photo-induced absorbance changes. It was found that the two fractions responded differently to actinic light, in a manner correlated with light absorption by the different forms of chlorophyll *a*. Indication of a partial separation of parts of the electron-transport mechanism of photosynthesis was thus obtained.

In addition to the two principal photochemical systems in plants, already referred to, there are others. A possible clue to the operation of a third system was given through experiments conducted during the year by A. Ried. Exposing the alga *Chlorella* to flashes of light of different wavelengths, Ried observed the transient increases and decreases in the respiration rate of the cells. He found that these transient effects appear at various times, from a few seconds to 10 minutes after exposure to light, some of them lasting for many minutes. He concluded that several types of linkage existed between the photosynthetic and the respiratory mechanisms of plant cells. A particularly interesting effect was obtained with certain wavelengths of blue light. These exposures caused a very large increase in the respiration rate of *Chlorella* cells, coming to a peak eight minutes after a one-second light exposure. The amount of oxygen absorbed as a result of this blue-light exposure was more than 500 times the amount of oxygen evolved by the cells during the one-second exposure. There is a clear implication that the blue-light effect is not a part of the two principal pigment systems, but instead may activate an enzyme in the mechanism for cellular respiration, and may be part of another photochemical system.

Kamen's descriptive diagram (Plate 4) might well be modified to include an "era" of ecology overlapping one or more of the other eras. Following a tradition of more than 40 years' interest in experiments on the evolution of ecological races and species, O. Björkman at the Department of Plant Biology combined ecology and photochemistry to study the modification of climatic races of higher plants as they adapt their photosynthetic systems to particular environments. He found that climatic races of goldenrod (*Solidago virgaurea*) from shaded and exposed habitats differ strikingly in their response to light intensity during leaf development, and that these



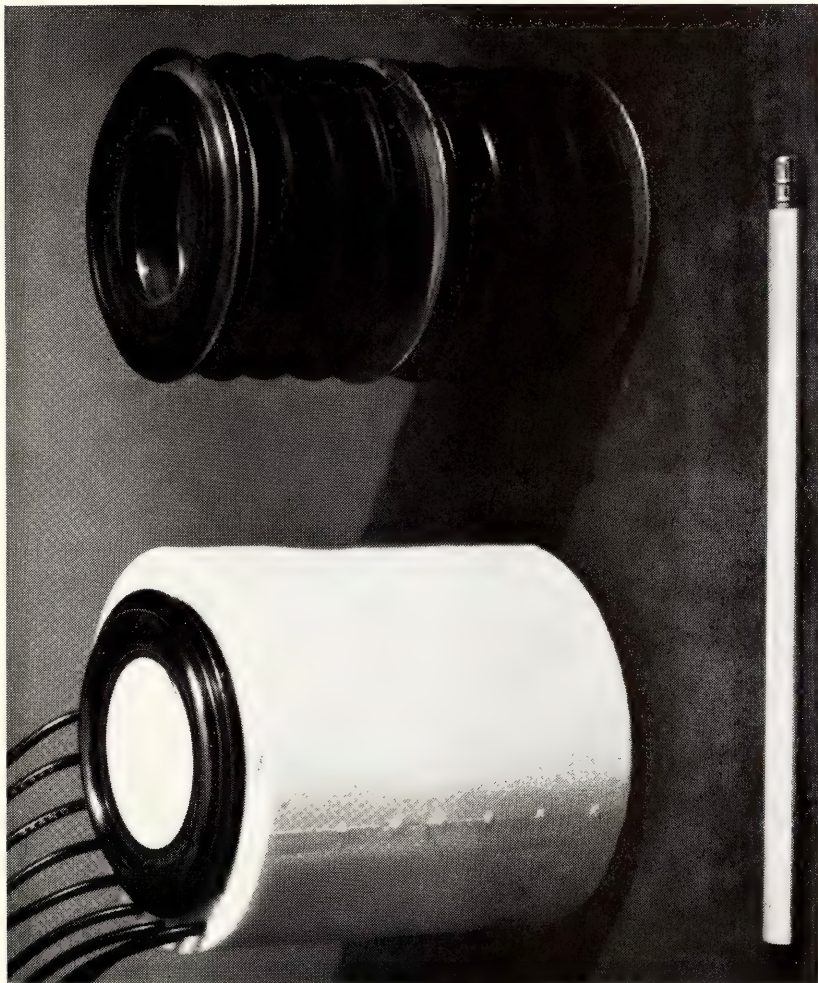
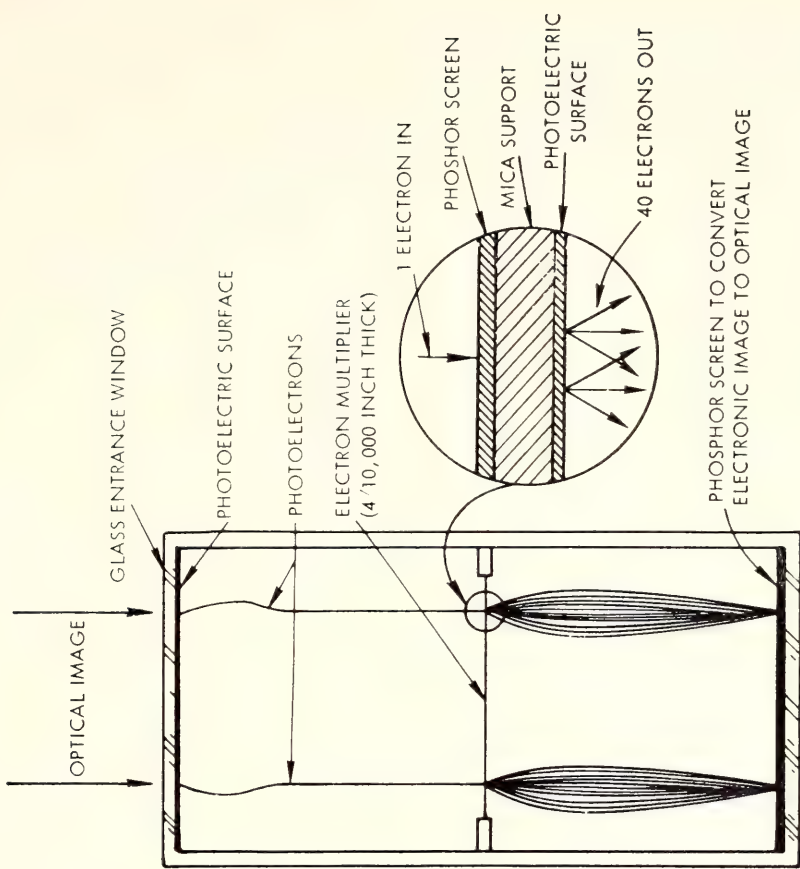


Plate 3. RCA cascaded image intensifiers. The tube at left in the photograph is encapsulated in rubber ready for use. It is standing with the photocathode down, phosphor up. The wires are leads to the accelerating electrodes. The tube with the phosphor down at right in the photograph, before encapsulation, shows the accelerating electrode structure. The electron multiplying "sandwich" is midway down the tube. Cross section at right of the photograph.



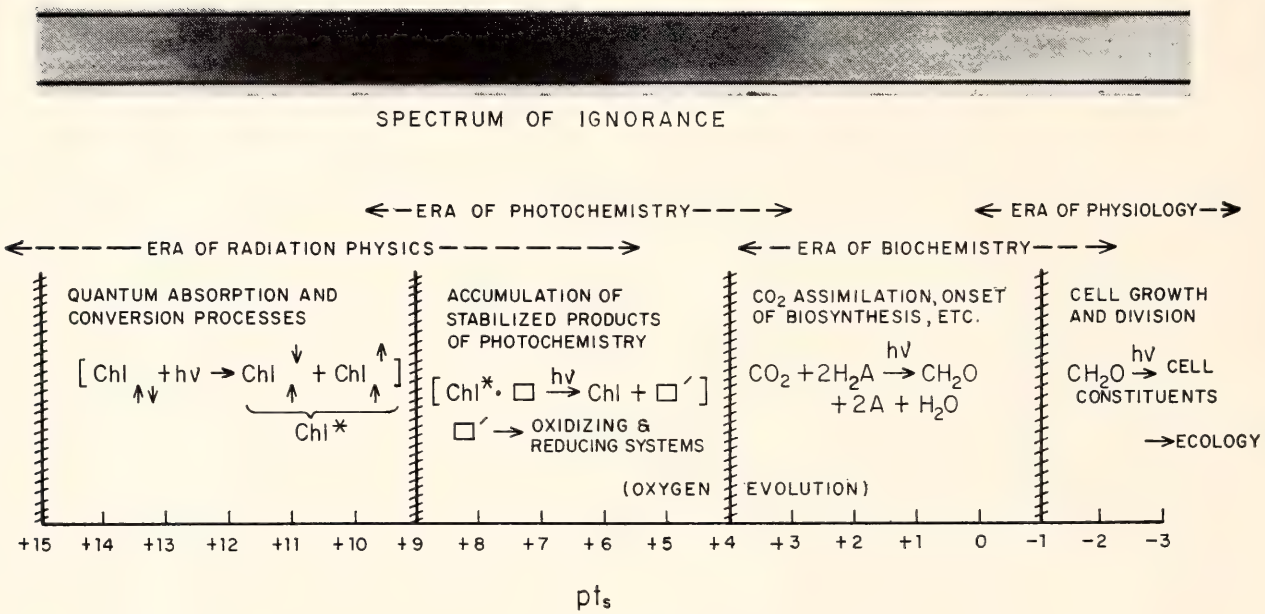


Plate 4. The eras of photosynthesis. The lower numerical scale *pt* is in terms of the “logarithm of the reciprocal of time, expressed in seconds.” The first era begins with “the absorption of the radiant energy as a quantum of visible or infrared light.” The total elapsed time of the scale is 16 2/3 minutes (10<sup>3</sup> seconds). (Courtesy M. D. Kamen.)

responses have a connection with photosynthetic system II. Leaves from a shade-adapted plant show a large "enhancement" effect when exposed to light beams of low intensity at two appropriate colors. Leaves of the same clone show only a small enhancement effect when grown at high-intensity light. Björkman also found that there were differences in light absorption under the same two conditions. He concluded from this evidence that the functioning of system II was impaired in plants native to shaded environments when grown at too high a light intensity. The opposite was true of leaves from plants native to a high light-intensity habitat. They were shown to have a more active system II when grown at high light intensity than when grown at low light intensity. The shade-adapted plants thus use weak light more efficiently than those in a sunny habitat, whereas the sunny habitat plants use the high-intensity light more efficiently. Although it is plain that system II is involved in the effects observed, other observations suggest that enzyme-controlled reactions also are concerned. The results seem to confirm an hypothesis held by Björkman that plants have evolved biochemical modifying devices to overcome major limiting external factors in a particular climatic environment. However, the exact nature of the device is still undetermined for *Solidago*. Similar differences also have been observed by Björkman and other Staff Members of the Department in genetically distinct races of the monkey flower *Mimulus*.

*Studies of Plant DNAs.* Björkman's experiments at the Department of Plant Biology in one sense might be considered contributions to evolutionary biology, a composite field in which there is widely ramifying activity among scientists interested in biological problems. Another and exciting episode in the study of evolutionary biology was experienced during the year at the Biophysics Section of the Department of Terrestrial Magnetism.

Displaying again the versatility of the techniques developed by the Biophysics Section in recent years and the wide reach of their interest, members of the Section<sup>15</sup> turned to the analysis of plant DNAs. The DNA-agar technique, which was used in 1963–1964 to demonstrate homologies among different animal species, was used this year to demonstrate similar DNA homologies among families of plants. Following the development by E. T. Bolton of a successful, simple method of extracting purified plant DNA, members of the Section applied the DNA-agar method to the study of homologies among the DNAs of representative ferns, gymnosperms (conifers), and angiosperms (flowering plants). Homologies among the legumes and among the cereals in particular were studied.

The homology experiments showed that about one half of the nucleotide sequences of vetch (*Vicia villosa*) DNA are similar to those in the common garden pea, while only about one fifth of the sequences are common to both

<sup>15</sup> In 1964–1965, E. T. Bolton, R. J. Britten, D. B. Cowie, R. B. Roberts, and the Carnegie Institution Fellows P. Szafranski and M. J. Waring.



beans and peas. A small amount of homology, amounting to about five per cent of the DNA sequences, was detectable between tobacco (*Nicotiana glauca*), another dicotyledon<sup>16</sup> of a different family, and peas. No homology was found between a representative of the monocotyledon subclass, rye, and the dicotyledonous peas. On the other hand, the homologies between barley (57 per cent) and rye, and wheat (75 per cent) and rye were striking (Figs. 2 and 3). Some observations of very general interest have been made by the Section from the first results.

First, the genetic diversity among plants, as measured by these first DNA interaction experiments, is at least as great as that between the distantly related man and mouse in last year's homology experiments. It is suggested that cultivated plants, subject to human intervention in their genetic composition, may have been submitted to a "forced draft" evolution. A series of future experiments on homologies should give insights on evolutionary processes in botanical forms never before obtained.

Second, the lack of interaction between the DNAs of rye (monocotyledons) and peas (dicotyledons) may indicate a relatively rapid evolutionary change among classes of plants. The ancestral stock that gave rise to both the monocotyledons and the dicotyledons is thought to have existed as recently as 135 million years ago. On the other hand, DNA similarities among vertebrate animals can be detected whose common ancestors existed probably 450 million years ago.

Third, quantitative comparisons of DNA homologies may possibly serve as indicators of interfertility among plants. For example, the DNAs of rye and barley have a 60 per cent similarity and are not interfertile, but rye and wheat, which are interfertile, show an 80 per cent homology between their DNAs. It may be possible from data on homologies to chart the possibilities for successful crosses of plants that would be of great use to the plant breeder. Experiments to test the possibilities are being conducted by the Section in cooperation with the Bureau of Plant Industry of the U. S. Department of Agriculture.

*Animal DNAs and Evolutionary Biology.* The DNA-agar method was also used by the Biophysics Section during the year in a series of extensive measurements of the renaturation<sup>17</sup> of DNAs from the cells of higher organisms. The measurements showed a considerable amount of nucleotide-sequence homology *within* the DNA of individuals of a given species. This result indicates that repetitive nucleotide sequences contribute to a fundamental structural plan for the DNA present in higher organisms.

The Section's experiments during the year showed that repeated sequences able to pair with each other in tests for complementarity need not

<sup>16</sup> Dicotyledons and monocotyledons are subclasses of the botanical class angiosperms.

<sup>17</sup> Recombination of previously disassociated or separated single strands of DNA, or nucleotide sequences from such strands.

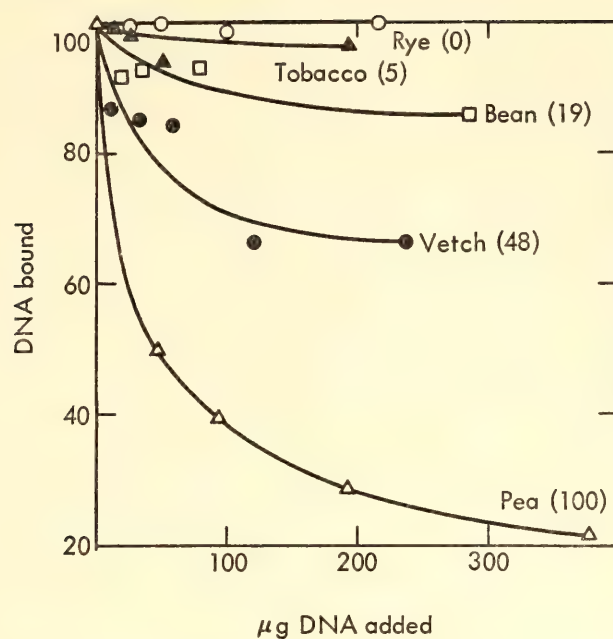


Fig. 2. Legume DNA homologies (plus the dicotyledon, tobacco) as shown by DNA-agar column measurements.

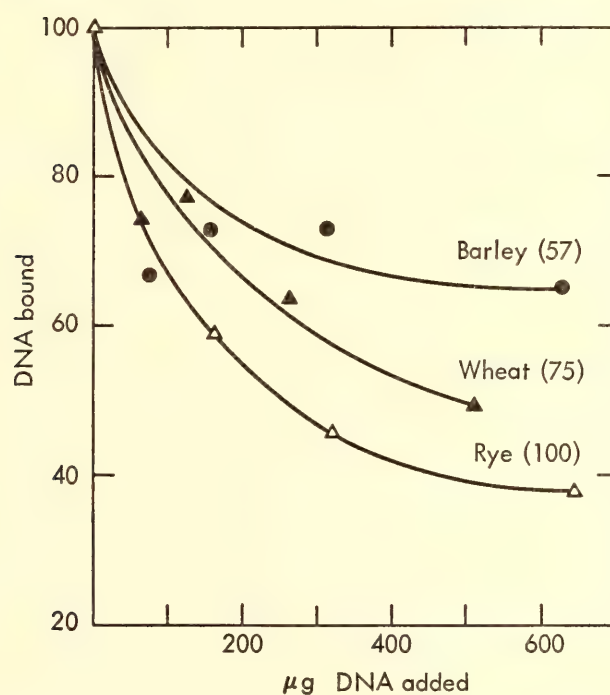


Fig. 3. Cereal DNA homologies, as shown by DNA-agar column measurements.

be strictly identical. The nucleotide sequence of one gene may be made up of fragments that show complementarity with sequences in several other genes. Section staff suggest that the pattern of repetitions of nucleotides in the genome of a particular animal result from a "balance" of processes over time that have included duplication, translocation, point mutation, and deletion of nucleotide sequences (Fig. 4). These studies imply that DNA



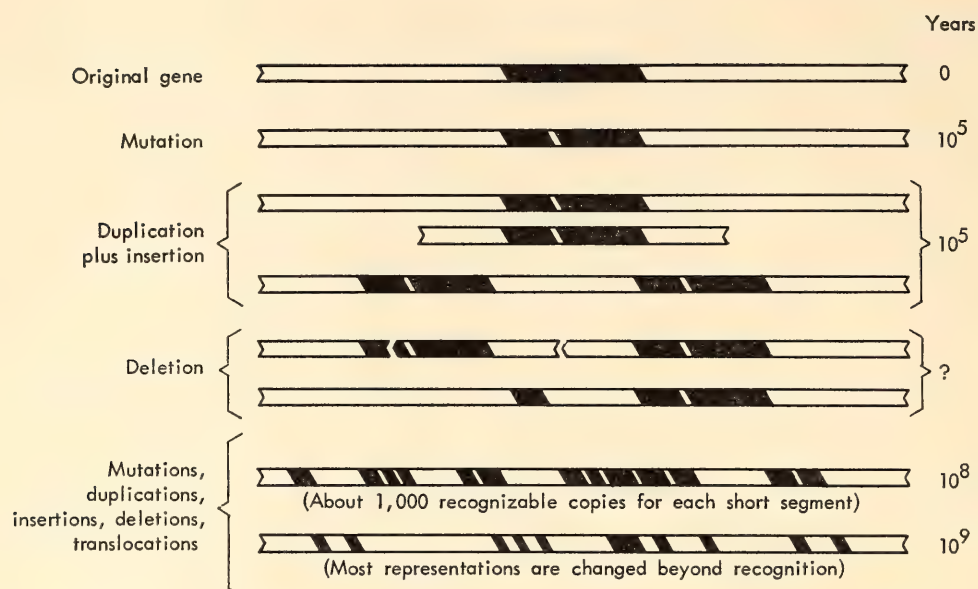


Fig. 4. A diagram of the possible origin and history of a family of repeating sequences in the DNA of a vertebrate. The DNA of an arbitrarily chosen gene has been indicated in black, in order to show its contribution to nucleotide sequences in the descendants. Two regions of sufficient length that derive from the same part of the original gene can form complementary strand pairs which are stable in a standard DNA-agar experiment. Time is indicated as a general guide. Number of years is not intended to represent rate of occurrence of the events themselves but approximate times of appearance of resulting DNA sequences in the population of animals.

nucleotide sequence duplication is a very general phenomenon and that there is, as the Section's report says, "an enormous amount of internal relationship" among nucleotide sequences in the genome of higher organisms.

The Section staff conclude that the existence of a large amount of nucleotide sequence repetition in the DNA of higher organisms "must deeply influence the processes of evolution." They caution against premature conclusions from experiments undertaken on only two organisms (mouse and calf), but one can well agree with their final statement that it is "abundantly evident that a new area has been opened to exploration."

*Biochemical Genetics.* Evolutionary biology, of course, is a broad subject to which many other fields besides biophysics have contributed. The methods of morphological taxonomy, comparative physiology, paleontology, and still others are important. But the one subject without which evolutionary biology in the 20th Century cannot be mentioned is genetics. The merging interests exhibited today on the broadly advancing front of biological research are well illustrated in some experiments conducted in the Genetics Research Unit. The work of A. D. Hershey and his associates, reflecting a long-held interest, also was directed during the year toward a description of the properties of DNA particles. In a series of elegant experiments employing a number of bacteriophages they made several significant contributions to the study of structure and function of nucleic acids in phage particles. Such experiments have produced evidence concerning gene

location within the DNA molecule and concerning the order of transcription of the genetic code to RNA.

About two years ago Gisela Mosig found a class of particles from a bacteriophage known as T4 that contain uniform DNA fragments two thirds the normal length of the DNA molecule in that phage. Subsequent genetic experiments suggested that the missing one third of the DNA molecule represents a single segment of the genome, constant in length but random in position on the circular "map" of the genome. Mosig's experiments during the year confirmed this hypothesis quantitatively. She showed a given gene to be present in two thirds of the defective particles and absent from one third. The ratio of one third to two thirds was shown to be constant for other single genes. Other experiments showed that two defective particles may form cooperating pairs that can initiate phage growth in one third of the bacteria infected with two particles. Three particles form functional triplets in two thirds of the bacteria infected with them. These are the exact probabilities, statistically determined, to be expected from the hypothesis as to randomness in position of the missing one third suggested by the earlier experiments.

This series of experiments led Mosig and Hershey to the following conclusions: (1) The DNA fragments in the defective T4 particles terminate at random points in the genome of the phage. (2) The DNA molecule and the genome are colinear. This is demonstrated by the fact that a two-thirds length fragment contains two thirds of the chromosomal genes. (3) Genes can cooperate to produce a normal organism with equal efficiency when present either as a single intact chromosome or as the presence of two or three incomplete fragments.

A step was also taken during the year toward the completely accurate physical mapping of phage genes. E. Goldberg of the Genetics Research Unit found that a DNA fragment probably not much larger than the length of a gene will recombine genetically with intact, replicating chromosomes of phage T4. Goldberg's method permits the physical mapping of genes that lie close together. A previously developed analogous method was valid only for genes lying far apart.

One of the major unsolved problems of present-day genetics and molecular biology is the control of transcription of genetic messages from the chromosomal DNA to messenger RNA and then to protein synthesis. Experimenting with lambda phage, A. Skalka has given the first physical description of sequence in the activity of different parts of the phage genome. Lambda phage has a "hybrid" chromosome of two parts whose DNA differs in base composition as much as the DNAs from separate species usually differ. Skalka found that the "right" half of the lambda molecule, characteristically high in adenine and thymine content, contained the first gene or genes to be transcribed into DNA. Another interesting feature of her



observations was the demonstration of an increased rate of DNA-RNA transcription from both halves of the DNA molecule when measured at late times in the process of replication. The data are of special interest for the information they provide on the "operator" theory in regulation of gene action, proposed by Jacob and Monod, or the somewhat different controlling systems described earlier by Barbara McClintock of the Genetics Research Unit. Skalka's data suggest that not only may there be operator control of individual genes, but also a broader type of control that regulates simultaneously many or all of the genes in the same half of the lambda DNA molecule. Especially they suggest that further inquiry into mechanisms controlling transcription of the DNA message in lambda phage is justified.

*Experiments in Developmental Biology.* Among other matters, the Department of Embryology shared an interest in a question of genetics and evolutionary biology that is receiving increasing attention—the role in cell growth of nonnuclear or cytoplasmic DNA. The question lies close to one of the major problems of developmental biology to which the Department is committed. The general problem is the nature of interaction between genes and cytoplasm.<sup>18</sup> Indeed, a fascinating question which first arose nearly 60 years ago is still with us: Are there nonchromosomal genes?<sup>19</sup> There is perhaps an even more fundamental question of concern today: Among the many ordered sequences of reactions in an organism, how many and what are directly dependent on genetic action and how many are initiated or primed thereby, thereafter proceeding independently of the nucleus?<sup>20</sup> It is now known that extranuclear DNA in cells is localized in chloroplasts and mitochondria.<sup>21</sup> It is also known that mitochondria are the seat of several enzyme systems associated with protein synthesis. Nevertheless, J. D. Ebert notes in his Introduction to the Department's report that the role of the extranuclear DNA, in the mitochondria and elsewhere, is not known. Ebert adds, "It cannot yet be stated with certainty that the DNA found in mitochondria is responsible for any of the information required for the synthesis and development of mitochondrial structure."

One of the most intriguing aspects of this question has been the function of the "cytoplasmic" or "egg" DNA in the eggs and early embryos of several animals, especially certain species of frog. The Department reported in *Year Book 63* (p. 515) that the eggs of the South American clawed toad, *Xenopus laevis*, and the frog, *Rana pipiens*, contain 100 to 300 times the amount of DNA present in the diploid body cells of the same species.

<sup>18</sup> J. Ebert, *Interacting Systems in Development*, Holt, Rinehart and Winston, New York, 1965, p. 90.

<sup>19</sup> Ruth Sager, Genes Outside the Chromosomes, *Scientific American*, 212, 1965, 70–79, provides a current semipopular description of some observations and hypotheses.

<sup>20</sup> Ebert, *op. cit.*, p. 108.

<sup>21</sup> Mitochondria are tiny bodies (0.2 to 5.0  $\mu$ ) of varying shapes occurring in the cytoplasm of every cell (bacteria, blue-green algae, and mammalian red blood cells excepted) and known to have certain energy conversion functions.

In the previous year I. B. Dawid of the Department isolated these DNAs and found them to be double stranded. His experiments further suggested that this "preformed" DNA is not used directly in the formation of chromosomal DNA in early embryonic stages, as had been thought. During 1963-1964 Dawid continued to study the relation of the egg DNAs to the somatic DNAs of *Xenopus* and *Rana*. Using the DNA-agar technique in a series of "competition" experiments Dawid studied the homologies of egg DNA from *Xenopus* to liver DNA from the same species. His findings show that the fraction of liver DNA homologous to egg DNA lies between 0.1 and 5.0 per cent. The implication thus is clear that egg DNA is specialized and is something more than a store of materials for the first cell divisions. Furthermore, the evidence from these experiments strongly suggests a mitochondrial location for the egg DNA. What its specific function may be is a problem left for future investigation.

Although a substantial amount of information about the structure and general functions of mitochondria have accumulated in recent years, there are other aspects of their structure and function that have so far defied analysis. In addition to being sites of protein synthesis, the mitochondria are known to act as the "powerhouses" of the cell, being the sites of the process known as oxidative phosphorylation that ends in the production of the energy compound ATP (adenosine triphosphate). During the year M. C. Reporter and Ebert obtained experimental results that may be helpful in relating the now familiar fine structure of mitochondria to their enzymatic roles. Experimenting further with the antibiotic antimycin A, and a previously isolated mitochondrial factor that affords protection against antimycin A (*Year Book* 62, p. 424), they believe that they have obtained a marker that can be used in studying the development of mitochondrial structure, as well as relating a specific structural site to enzyme function. They now believe that mitochondrial factor to be a protein containing nonheme iron. They have suggested that the factor represents the extracted mitochondrial site of action of antimycin A. If their hypothesis is correct a step will have been taken toward correlating specific site and function in these important cell elements.

*Experiments Giving Information on Tumor Cells.* One of the most continuously active and best supported areas of biological research in recent years has centered around the "cancer problem," that is, the abnormal localized multiplication of some type of cell in the higher animals, and particularly man. Again following a thread of interest at the Department from other years, Ebert, M. E. Kaighn, and Pauline Stott have made further studies of the effects of the Rous sarcoma virus. Their attention was directed particularly toward understanding what types of cells a tumor virus will infect and transform, a problem they consider to be receiving relatively little attention elsewhere, although the effects of viruses



on cell replicative mechanisms are being very thoroughly studied. Their experiments during the year gave the first convincing evidence that the Rous sarcoma virus could infect a cell capable of differentiation. More than four fifths of a set of cultured muscle colonies proved to be susceptible to Rous virus infection. Partially or totally transformed muscle-cell colonies were obtained from single myoblasts (embryonic muscle cells) infected by the virus at the time of plating. Thus it is now known that the virus can transform one type of differentiating cell, in addition to fibroblasts<sup>22</sup> and mesenchymal cells.

These experiments, and others now being carried out at several laboratories in the United States and abroad, were made possible by the past development of techniques for cloning<sup>23</sup> differentiating cells, pioneered by I. R. Konigsberg of the Department. Ebert notes in his Introduction to the Department's report that with these techniques "it now appears possible to determine how such viruses interact with cells at precise times in their life histories," and "to determine how the 'state of differentiation' of a cell influences its susceptibility to viruses." The leads given in last year's experiments are now being followed up in other experiments to determine the amount and rate of viral syntheses in muscle at each major point in its development. The susceptibility to infection of muscle clones will also be compared with clones of cartilage cells and fibroblast cells. Ebert considers the comparison of these types of cells especially meaningful because of their common origin in the early embryo.

Other evidence of even more direct interest concerning the cancer problem was provided in experiments conducted by the Biophysics Section of the Department of Terrestrial Magnetism. Perhaps more than any other activity of the Institution during the year they reflect the results that come from what members of the Section have referred to as "personal expression in the choice of . . . research and in the means by which it is conducted." Commencing with the discovery last year that there was a striking parallel between lysogenic<sup>24</sup> systems in bacteria and virus-induced transformation of normal to cancer cells in tissue cultures of higher organisms, R. B. Roberts and his colleagues in the Section have been probing for information that would lead to a rational foundation for cancer chemotherapy.

The problem attacked particularly by Roberts and his colleagues was that of releasing virus from the genome of lysogenic bacteria, on the assumption that this might give information about the possible release of tumor-inducing viruses in the cells of higher organisms. Their experiments indicated

<sup>22</sup> Fibroblast—a type of cell that lays down the connective tissue framework in muscles.

<sup>23</sup> Cloning—the development of cell colonies in culture from single cells.

<sup>24</sup> A lysogenic system in bacteria is one where the genic material of an infective phage may be carried latent on the genome of the bacterium, reproduced from generation to generation in latent form, but still capable of eventual infectivity.

that two stages exist in the release of the virus from lysogenic bacteria. The first is the introduction of a "defect" into the viral and bacterial DNA. A number of different agents can cause such a defect. The antibiotic mitomycin C and ultraviolet light are examples. Bringing about the defect, however, is not alone sufficient to guarantee subsequent release of the virus. Repair mechanisms may appear and remove the defect before the virus is released. Therefore, the second stage is the use of agents that presumably inhibit repair. Such agents enhance the effectiveness of virus-releasing agents. The combination of a defect-inducing agent and a repair-preventing agent thus is much more effective in releasing the virus from the bacterial genome than either one used alone. The Section report states that this general principle seems to apply to the more complicated mammalian systems in which tumor viruses act as well as to the bacterial system.

The Section staff conclude that selective repression of lysogenic cells among susceptible bacteria can be effectively obtained by the following procedures: (1) introduction of defects into the DNA by radiation or radiomimetic drugs such as mitomycin; (2) the inhibition of repair mechanisms in the DNA by agents like hydroxyurea or phenethyl alcohol inhibiting the DNA synthesis; (3) inhibition of protein synthesis by drugs like chloramphenicol, puromycin, or amino acid analogues; and (4) addition of the chelators<sup>25</sup> such as EDT (ethylene diamine sodium tetraacetate) to amplify the effectiveness of the initial radiation or radiomimetic agent.

After the initial experiments with bacteria gave a general guide to procedure, a parallel set of experiments with tumor-bearing mice was carried out at the National Institutes of Health by T. L. Lincoln of the Johns Hopkins University, and A. Gelderman of the Institutes. These experiments strongly suggest that the same logic followed to bring about the release of lysogenic virus in bacteria also applies to the release of ascites tumor-causing virus in mice. In every case, the Section reports, the chemotherapeutic combinations suggested by the bacterial work have been much more effective than any of the drugs used singly. For example, a combination of mitomycin C, puromycin, and EDT produced a prolonged inhibition of ascites tumor growth in the mice even though none of the agents had any effect when used singly (Fig. 5).

The Section notes finally that it remains to be seen whether or not this combination chemotherapy can be effective in inhibiting solid tumors of animals and man. The ascites tumors are fluid, and there is no problem of having drugs reach the tumor cells. The report ends with the hope that

<sup>25</sup> A chelator is a chemical compound causing formation of chelate groups or rings, "cyclic" compounds wherein a central metallic atom is surrounded by a ring of other elements that has been closed by coordination with an unshared pair of electrons.



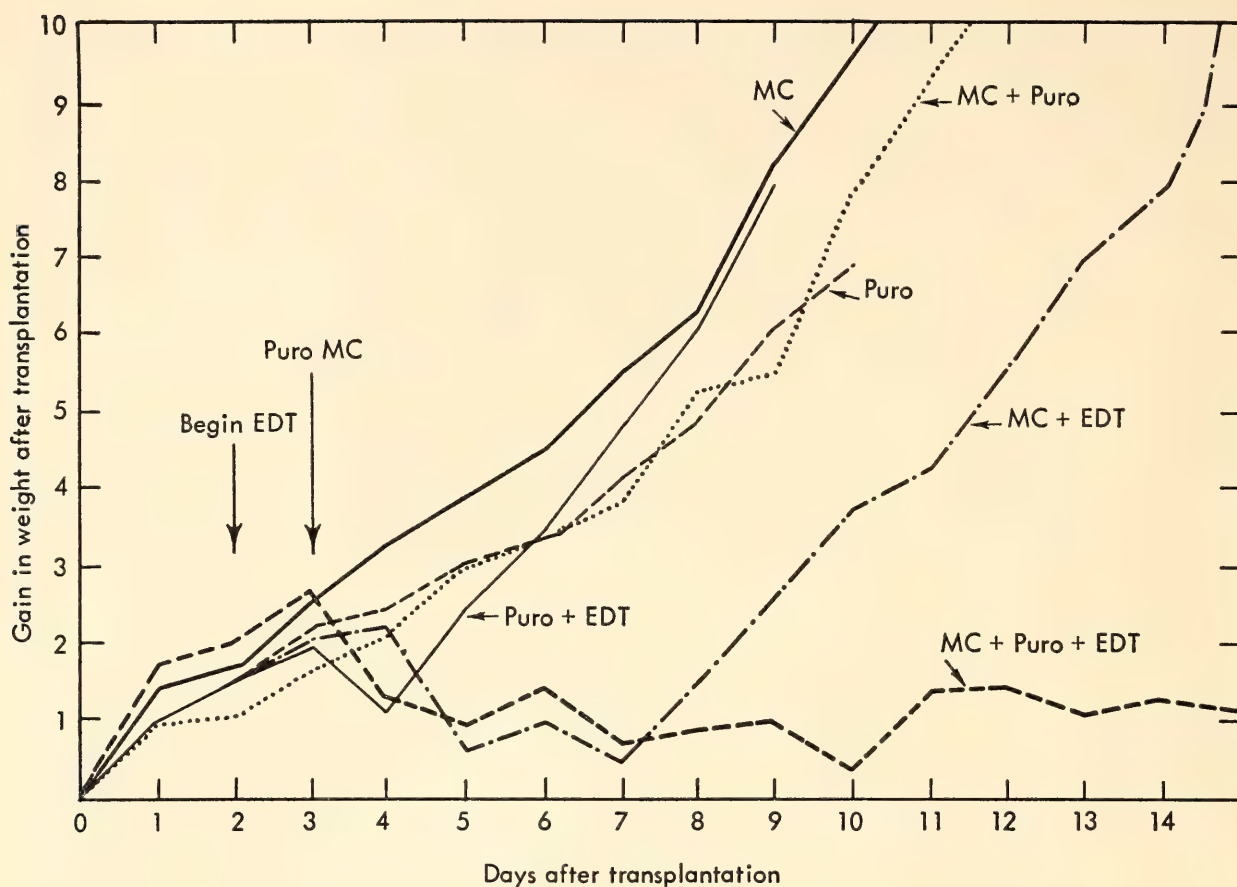


Fig. 5. Average weights of mice with transplanted ascites tumors, as subjected to treatment by MC (mitomycin), Puro (puromycin), and EDT, singly and in combination. The lowest curve (dashed line) shows the inhibitory effects of a "rational" drug combination.

"the rationale of using one drug to introduce defects in the DNA and other drugs to inhibit the repair of the defects may be a useful guide in cancer chemotherapy."

### *Visitors and Fellows—the Place of the Scientific Pilgrims*

The activities reported in this review are in the main the product of the thought and investigation of Institution Staff Members. But they also represent significant contributions by the Institution's Fellows and visiting scientists.

J. B. Adams has observed that one of the attributes of our present culture is the pilgrim scientist whose movements in some ways parallel those of the pilgrims of medieval times. He notes, "just as it was customary for the medieval pilgrim to be fed, housed, and looked after by the monasteries, so the modern research laboratory must set aside funds to pay foreign pilgrim scientists and to send its own on tour."<sup>26</sup> One may place in this group a wide variety of men and women, from the promising postdoctoral Fellows to *Emeriti* of international fame. The Institution continues to be impressed

<sup>26</sup> *Science*, 148, 1965, 1562.

with the contributions that the pilgrim scientist can and does make to its work. Just as important, its own staff have benefited greatly from the pilgrimages that members occasionally make in the United States and abroad. The environment that nourishes the individual investigator almost by definition nourishes also the pilgrim scientist.

Every one of the Institution's departments has been a home for at least several of these scholars during the year. The strength of these temporary additions to the staff of the Institution and their meaning to communication in science can be judged from their numbers and origins. During the year the Institution was host to 61 Fellows who stayed for periods varying from a few months to the entire year. Some have been in residence, or will remain in the laboratories, for more than one year. These visitors were drawn from 40 universities and 11 other research institutions in the United States and 16 foreign countries.

The other side of the picture is shown in the travel of Institution staff, whose visits elsewhere keep them abreast of their colleagues' work in the informal interinstitutional cooperation that is so characteristic of science today. Ninety-four scientific Staff Members of the Institution were on travel status within the United States or abroad for varying periods at some time during the year. Some of the travel was for attendance at national and international conferences; other travel was for field study, or for delivering special lectures; but it was particularly useful in affording periods of residence at laboratories that conduct research in fields akin to those of the Staff Members. Some of these visits may be renewed over a period of years, as in the development of the South American program of seismic studies of the Institution, or in connection with the new La Plata radio astronomy observatory in Argentina, whose establishment the Institution is at present aiding.

An excellent illustration of staff relations with other institutions is presented by B. McClintock's participation in developing inter-American cooperation to study races of maize. These activities, first sponsored by the National Academy of Sciences-National Research Council, were later assisted by the Rockefeller Foundation.

Commencing in 1957 with a training program in Peru for analysis of the chromosome constitutions of maize races, McClintock's work was broadened the following year to studies of the chromosome constitution of varieties of maize indigenous to Ecuador, Bolivia, and Chile. These studies showed that detailed cytological information about chromosome morphology could help to determine the geographic centers of origin of cultivated maize and to trace migrations of its races from such centers over past centuries. In 1959 the research was extended to Mexico and Central America.

The Mexican and Central American studies further suggested that chromosome analyses could be very useful for breeding purposes, because



the degree of genetic divergence of various races could be estimated from knowledge of the chromosome constitutions.

The training of Latin American students in these techniques of analysis at the University of North Carolina between 1962 and 1964 was the next step, aided by Rockefeller Foundation fellowships. Several interesting advances in knowledge of chromosomal behavior came from the research conducted by students in this advanced training program, in which McClintock cooperated. One of the discoveries is of definite interest in study of a problem mentioned earlier in this review, that of the form, location, and function of the different DNAs within cells. W. Monteiro, of the University of Minas Gerais, Brazil, found one type of cell in the anther<sup>27</sup> of maize where the DNA is loosely diffused within the cell nucleus. This contrasts with the normal form, where it is organized within distinctive bodies surrounded by membranes in nuclei. McClintock states that it illustrates an aspect of DNA hitherto not considered in genetic theory.

The participants in the graduate training program for maize genetics research have now returned to South America, where their work will be conducted in close collaboration. A new tool for investigating the genetic and historical background and characteristics of this very important crop plant, indigenous to Latin America, thus has been established.

Widely ramifying sets of relations in modern science, like these, based on the interest, skills, and personal inclinations of individual investigators, go far toward maintaining the element of novelty for all scientists. As Hershey observes in the Introduction to his Genetics Research Unit report, without novelty "nature and art cannot charm." He adds, "except for the element of novelty, ritual could take the place of research." He suggests also that one reason for the costliness of contemporary research is that the threshold of human surprise is rising. However, the experience of the Institution during the past year, as in previous ones, continues to demonstrate that the independent scientific investigator, free to choose or abandon professional associations at will, can preserve novelty for himself even if his equipment is not of the most costly. Such novelty, achieved or promised, further attracts the pilgrims who, in turn, help to maintain that climate of unorthodoxy where there is no fear, to use a phrase of Ebert's, of "large ideas that turn out to be wrong."<sup>28</sup>

An institution that fosters the self-committed investigator raises the probability of encountering the novel, as compared with the "mission-oriented," or the "practical" approach. In so doing, we believe that the threshold of the possible is also raised, to the advantage of all research.

<sup>27</sup> Anther is the pollen-bearing segment at the end of the stamen of flowers.

<sup>28</sup> J. D. Ebert, *Interacting Systems in Development*, Holt, Rinehart and Winston, New York, 1965, p. 21.

### *Losses . . .*

With the death of Herbert Hoover on October 20, 1964, the Institution lost a friend who had served as a Trustee for 29 years, from 1920 to 1949. The honors he received for his contributions to human welfare and his public activities over his long and full career are well known. Perhaps it would be most fitting for me to record his deep and lasting interest in science, which resulted in his long association with the Institution.

No other President of the United States has held so many scientific honors as Herbert Hoover, and probably no President before him had taken such an interest in the development of science. He was a member of the American Association for the Advancement of Science, the National Academy of Sciences, and many other eminent scientific bodies. Early in his mining career he advanced the flotation process, and devised a means of profitably recovering metal zinc from low-grade silver ore. Many of his awards were given for scientific and technical distinction, as, for instance, the John Fritz Gold Medal awarded him jointly by several mining and engineering societies in 1929.

He remained on the Board of Trustees during his Presidency, and throughout the years of his Trusteeship contributed greatly to the development of the Institution. He helped to plan the longest voyage of the *Carnegie*, and was instrumental in developing a close relationship between the Department of Plant Biology and Stanford, his mother University. From first to last he was an advocate of scientific research. "Would it not be a practical thing to do to give adequate organized financial support to pure science?" he asked in 1925. "If, by chance, we develop a little contribution to abstract learning and knowledge, our nation will be immensely greater for it."

Mr. Hoover thus pioneered a point of view that is now in full tide as national policy. The Institution is honored to have shared some of the days of pioneering with him.

It is with great sadness that I report the death of Harold W. Milner, Staff Member at the Department of Plant Biology since 1928. Mr. Milner, who died on July 13, 1965, at the age of 62, was in the full tide of activity in his work at the Department.

A most versatile investigator, Milner had divided his time between laboratory work in biochemistry and in editorial duties. In the laboratory, he was in the midst of studying environmental effects, such as light intensity and temperature, on photosynthesis. In earlier years he had worked with Dr. Spoehr on the chemical composition of algae and had developed a method for deliberately producing algae with unusually high protein or fat content. He was highly skilled in the techniques of microanalytical chem-



istry. As an editor he was precise and consistently exacting. At the time of his death he had just completed editing the Department's Annual Report for this *Year Book*. He was the author of many journal and magazine articles and was coauthor of several Carnegie Institution publications.

Milner undertook the massive task of translating over 300 Russian articles on several aspects of photosynthesis of special interest to his colleagues in the Department of Plant Biology. He later became interested in distributing these articles to scientists in other laboratories in this country and abroad. Toward this end he signed over all rights for his work to the John Crerar Library in Chicago with the assurance that the articles would be made available to all interested scientists.

His cheerful good humor, his willing cooperation, and his valuable work will be sorely missed by his friends at the Department of Plant Biology and everywhere in the Institution by those who had the good fortune to know him.

With the passing of George W. Morey on October 3, 1965, the Institution lost an enduring and valuable friend.

Dr. Morey joined the staff of the Geophysical Laboratory in 1912, just five years after its inception. In 1957 he retired, after a long and fruitful career. A deeply sensitive man, Dr. Morey was a remarkable combination of pure scientist and practical technologist. He worked in both worlds, to the benefit of each.

In the research laboratory he began his career with experimentation on silicates and other minerals under extreme conditions of temperature and pressure. His initial work provided the basis for most of his subsequent research and led to insights into mineral formation, ore deposition, and the chemical processes of magmatic differentiation. These investigations also led him to propose a new theory of volcanic eruption based on phase equilibria relations.

In the area of technology, Dr. Morey was world-renowned for his contributions to the chemistry and constitution of glass. During both world wars he took leave from the Laboratory to put his knowledge and practical experience to work in the manufacture of strategic optical glass. During World War I, he was general manager of the Spencer Lens Company; in World War II, he was responsible for the design, construction, and operation of the largest optical glass plant ever built, a division of the Corning Glass Works. He invented a new family of glasses with high refractive indexes and wide dispersion, having great advantages for photographic lenses, especially when used in aerial photography. The annealing process that he perfected was applied to the manufacture of the Pyrex disk for the 200-inch Hale telescope on Palomar Mountain.

After serving as a Staff Member in the Geophysical Laboratory for 45 years, during one of which he was its Acting Director, Dr. Morey formally retired on June 30, 1957. On July 1, 1957, he joined the staff of the U. S. Geological Survey where he remained until his death.

Recognition came to Dr. Morey from many directions. In 1927 the Chemical Society of Washington awarded him its Hillebrand Prize; in 1948 he was specially honored to be the first recipient of the Arthur L. Day Medal of the Geophysical Society of America; and in 1959 he was chosen to receive the Potts Medal of the Franklin Institute.

Such honors form but the tangible indications of the high esteem in which he was held by all his friends in the Institution, and most especially by those at the Geophysical Laboratory, where he held an honored position for nearly half a century.

With deep regret I must also record the deaths this year of four former Staff Members: Chester H. Heuser of the Department of Embryology; Samuel Kirkland Lothrop of the Division of Historical Research; and Henry Freeborn Johnston and Wilfred C. Parkinson, both of the Department of Terrestrial Magnetism.

Dr. Heuser, who was a Staff Member at the Department of Embryology from 1921 until 1950, and a Research Associate from 1951 until his death, died on January 1, 1965, at the age of 79.

Dr. Heuser joined the Carnegie staff in 1921 after holding appointments at the Harvard Medical School, at the Wistar Institute of Anatomy and Biology in Philadelphia, and at the Johns Hopkins School of Medicine. At the Department of Embryology, he was Curator of the Embryological Collection. His research was devoted to a study of early human embryos, but he also held interests in other branches of mammalian embryology, especially of the rhesus monkey and the pig. He was known to embryologists throughout the world for the remarkable skill with which he prepared the fragile and valuable specimens that were entrusted to him. He was one of the first great American embryologists, combining technical acumen and a vast fund of specialized knowledge with imagination and complete devotion.

Dr. Lothrop, one of the Institution's most distinguished archaeologists, died at the age of 73 in Belmont, Massachusetts.

An authority on Latin American cultures and on pre-Columbian art, Dr. Lothrop was associated with the Division of Historical Research in 1922 and 1923 and again in 1932 and 1933. He conducted expeditions in Guatemala, Panama, and Mexico, and one of his most exciting finds was at the Río Grande in Coclé, Panama, where he and his associates discovered a large assortment of gold ornaments at a burial site. The site, they found, was once occupied by a previously unknown but highly civilized people. Dr.



Lothrop's discoveries in Panama won him the Loubat Prize from Columbia University in 1938.

At the time of his death, Dr. Lothrop was the only living recipient of the three most coveted awards in archaeology: the Alfred Vincent Kidder Award of the American Anthropological Association; the Viking Fund Medal of the Wenner-Gren Foundation; and the Huxley Memorial Lecture Medal of the Royal Anthropological Institute of Great Britain.

Dr. Johnston, a Staff Member of the Department of Terrestrial Magnetism from 1910 to 1946, save for a period of service with the British Navy in World War I, died in Bethesda, Maryland, on April 25, 1965.

Dr. Johnston was born in Hay, Ontario, Canada, in 1888, and, on taking a degree in physics at the University of Toronto in 1910, joined the staff of the Department of Terrestrial Magnetism. During his earlier years of service with the Institution Johnston undertook extensive magnetic observations in the course of several cruises with the *Carnegie*. He also carried out rigorous field work in Africa and Latin America to collect magnetic data, and from 1923 to 1929 he was Observer-in-Chief of the Department's Watheroo Observatory in Western Australia. After his return to Washington he was Chief of the Section of Observatory-Work from 1931 to 1946. In 1946, when illness compelled Johnston's early retirement, Dr. Vannevar Bush praised his "long period of effective and faithful service to the Institution."

Mr. Parkinson, a member of the Department of Terrestrial Magnetism for 37 years, died in Sydney, Australia, at the age of 80. He was British by birth, and had studied at the Royal Naval College, Greenwich, England.

Mr. Parkinson's name is associated in particular with the Watheroo Observatory in Western Australia, constructed by the Department of Terrestrial Magnetism in the year 1917-1918 in order to augment the number of southern hemisphere observatories where terrestrial-magnetic, electrical, and ionospheric phenomena could be observed. Parkinson helped to locate the final site chosen in 1916, and he was its Observer-in-Chief in 1921 and for most of the period between 1930 and 1946. During the 1920s he also undertook magnetic observations in many parts of the world, and was in charge of the Huancayo, Peru, magnetic observatory of the Department from 1923 to 1925. Following his retirement in 1950, he accepted an appointment to a UNESCO Technical Assistance Mission to Brazil to supervise the installation of magnetic equipment near Belém. Earlier, during his residence in Australia, he had been one of the founding members of the Royal Society of Australia. His life was one of singular devotion to the painstaking collection and interpretation of data on terrestrial magnetism, one of the major initial scientific undertakings of the Carnegie Institution.

Several retirements have brought deep losses to the Institution.

Ailene J. Bauer had been a pivotal member of the Institution for so long that it is difficult to apprehend what her loss will mean to us.

Mrs. Bauer came to the Institution in October of 1939 as Secretary to the Director of Publications. Within a few years she was made Assistant to the Director, and from 1951 until her retirement she served as Director of Publications. From the beginning her keen sense of organization and her comprehensive grasp of detail combined to make her contributions invaluable.

Most important of all, in her post she embodied the very spirit of the Institution. A grateful recipient once wrote: "It is difficult to thank the anonymous dear sir or madam who runs the department, or the person who uses red ink on bills, or the inhabitant of dusty stacks or warehouses who searches for books. I feel that all contribute to the atmosphere of kindness that prevails in the department—I know that all merit my gratitude." Such an atmosphere was inspired and perpetuated by Mrs. Bauer throughout her 26 years with the Office of Publications, and similar sentiments were expressed by countless others in this country and abroad in tribute to her warmth, her enthusiasm, and her unflagging interest.

Lucile Stryker, the Institution's Editor, retired on June 30th of this year. Mrs. Stryker came to the Carnegie Institution in 1956, after 24 years as Editor-in-Chief for the scientific publishing house of John Wiley & Sons. Few people could have been so excellently prepared for the task they were to undertake. During her first seven years with Wiley & Sons, she had single-handedly edited some 350 books in various technical fields. After she came to the Institution she continued personally to meet with authors, printers, and engravers, and to cope with the many unpredictable problems that arise in the course of publishing each Institution book.

Mrs. Stryker has great experience and administrative skills, and in addition she is one of those rare editors who combine a technical knowledge of what a publisher can do with an erudite understanding of what an author is trying to do. Not surprisingly, her advice and her assistance were—and continue to be—widely sought in the editing of various scientific journals. She will be profoundly missed at the Institution.

With the retirement of Mrs. Anne M. McConnell on January 31, 1965, the Mount Wilson Observatory lost a devoted member of its administrative



staff, who had a long record of faithful service to the Department. Mrs. McConnell first came to the Mount Wilson Observatory in 1930, and since 1952 she had served as Administrative Assistant. Her capable handling of administrative problems greatly facilitated the smooth functioning and the scientific work of the Department. She will be greatly missed at the Observatory.

*. . . And Gains*

It gives me particular pleasure to welcome Dr. Charles Hard Townes as a Trustee of the Institution, elected on May 7, 1965.

In a world increasingly committed to specialization, men who can combine gifts in many fields are increasingly rare. Charles Townes is such a man.

Now provost and professor of physics at the Massachusetts Institute of Technology, Dr. Townes has had both an extraordinarily brilliant and a widely varied career since 1939, when he received his doctorate from the California Institute of Technology.

For several years Dr. Townes pursued research as a member of the technical staff at the Bell Telephone Laboratories. At the outbreak of World War II, however, he was immediately assigned to the task of developing radar bombing, a system by which it became possible to bomb through heavy clouds and at night. After the war, he turned his attention to microwave spectroscopy, a new field growing out of the wartime contact of physics and electronics. In 1948 he went to Columbia University as an associate professor, where he continued his research in microwaves, and ultimately became chairman of the Department of Physics. It was during this period that he first conceived the idea of the maser—the production of short microwaves by controlled molecular or atomic activity. Since that time, the maser, and the subsequent laser, have provided science with novel and highly flexible basic tools and new technologies harboring a myriad of possibilities. After two years in Washington as vice-president and director of research of the Institute for Defense Analyses, Dr. Townes assumed his present position at the Massachusetts Institute of Technology in 1961.

Dr. Townes has been the recipient of many honors and awards. In addition to 12 honorary degrees, he has received the Research Corporation Annual Award (1958), the Comstock Award from the National Academy of Sciences (1959), and the Stuart Ballantine Medal from the Franklin Institute (1962), to mention but a few. In 1964 he shared the Nobel Prize in Physics with two Russian scientists for his part in the invention of the maser and the laser.

In speaking of the role of basic scientific research, Dr. Townes once said: “We must constantly remind ourselves that the most important practical

results often come from the human drive towards goals and ideals which may seem far from practical." The Carnegie Institution of Washington was founded upon just such a conviction.

It gives me special pleasure to record a number of honors that have come to Staff Members of the Institution over the past year.

The National Academy of Sciences at its Annual Meeting on April 28, 1965, presented its Kimber Genetics Medal to Dr. Alfred D. Hershey. This is one of the highest honors in the nation in the field of genetics.

Dr. Barbara McClintock was one of the seven scholars named Andrew D. White Professor-at-Large of Cornell University on April 30, 1965. Dr. McClintock received the award for international distinction in her field of scholarship.

Dr. Elizabeth M. Ramsey received the honorary degree of Doctor of Medical Sciences from the Woman's Medical College of Pennsylvania on June 8, 1965, in recognition of her accomplishments in the field of anatomy. In addition, an exhibit of Dr. Ramsey's on the primate placenta was awarded a prize at the thirteenth annual clinical meeting of the American College of Obstetricians and Gynecologists held in San Francisco, April 5-8, 1965. Dr. Ramsey also received a citation at the 60th anniversary luncheon meeting of the District of Columbia Young Women's Christian Association for her services as President of the Women's Committee of the National Symphony Orchestra and as a Research Associate and Pathologist with the Carnegie Institution of Washington.

Dr. C. Stacy French was elected a member of the Deutsche Akademie der Naturforscher Leopoldina.

Dr. James D. Ebert, Director of the Department of Embryology, was elected a Trustee of the Marine Biological Laboratory, Woods Hole, Massachusetts, on August 14, 1964, and to membership in the American Academy of Arts and Sciences on May 12, 1965.

Dr. Fritz Zwicky, Staff Member of the Mount Wilson and Palomar Observatories, was elected vice-president of the International Academy of Astronautics.

Dr. Edward A. Ackerman, Executive Officer, was elected Chairman of the Board, Washington Center for Metropolitan Studies, on November 24, 1964. Dr. Ackerman also served on the White House Task Force on Natural Resources from September 3 to November 10, 1964.





# *Reports of Departments and Special Studies*

Mount Wilson and Palomar Observatories

Geophysical Laboratory

Department of Terrestrial Magnetism

Committee on Image Tubes for Telescopes

Department of Plant Biology

Department of Embryology

Genetics Research Unit

Cytogenetics Laboratory





# *Mount Wilson and Palomar Observatories*

Operated by Carnegie Institution of Washington  
and California Institute of Technology

*Pasadena, California*

Horace W. Babcock  
*Director*

## OBSERVATORY COMMITTEE

Horace W. Babcock  
*Chairman*

Carl D. Anderson

Jesse L. Greenstein

Robert B. Leighton

Allan R. Sandage

Olin C. Wilson



# Contents

Introduction . . . . .	5	Spectroscopic observations of quasi-stellar sources . . . . .	27
Observing Conditions . . . . .	6	Absolute energy distribution . . . . .	27
Solar Observations . . . . .	6	Variability of quasi-stellar sources . . . . .	28
Large-scale magnetic fields . . . . .	6	Interpretation . . . . .	28
Development of solar flares . . . . .	7	Photometry . . . . .	28
Features of the chromosphere and corona . . . . .	8	Radio-Quiet Quasi-Stellar Galaxies . . . . .	29
Eclipse observations . . . . .	8	Galaxies . . . . .	30
Planets and the Moon . . . . .	9	Energy measurements . . . . .	30
Mars . . . . .	9	Magnitudes and redshifts . . . . .	30
Venus . . . . .	9	Redshift-diameter relation . . . . .	31
Major planets . . . . .	9	Investigations of individual galaxies . . . . .	31
Moon . . . . .	10	Compact galaxies and compact parts of galaxies . . . . .	32
Stellar Spectroscopy and Photometry . . . . .	10	Posteruptive galaxies . . . . .	33
White-dwarf spectra . . . . .	10	Peculiar galaxies, multiple galaxies, and clusters of galaxies . . . . .	34
Subdwarfs . . . . .	11	Catalogue of galaxies and clusters of galaxies . . . . .	34
Spectra of magnetic stars . . . . .	11	Supernovae . . . . .	35
Globular-cluster stars . . . . .	11	Miscellaneous stars . . . . .	35
Molecular spectra . . . . .	12	Theoretical Studies . . . . .	35
Carbon isotope determinations . . . . .	12	Background cosmic light from galaxies, integrated to the observable horizon . . . . .	35
Standard spectrophotometry of spectral lines . . . . .	13	Statistics of galaxies . . . . .	37
Chemical composition of stellar atmospheres . . . . .	13	Gravitational scattering of light from distant objects . . . . .	37
Lithium in main-sequence visual binaries . . . . .	15	Density of neutral hydrogen in intergalactic space . . . . .	37
Chromospheres and stellar rotation . . . . .	15	Stellar interiors . . . . .	37
Spectroscopic observations of dK and dM stars . . . . .	16	Infrared spectrum of the solar corona . . . . .	38
Color-magnitude and chemical-composition relations . . . . .	16	Guest Investigators . . . . .	38
Studies in stellar rotation . . . . .	17	Image Tubes . . . . .	45
U Geminorum stars . . . . .	18	Instrumentation . . . . .	47
Wolf-Rayet stars . . . . .	18	Optical systems . . . . .	47
T Tauri stars . . . . .	19	Solar instruments . . . . .	47
M stars . . . . .	19	Instrumentation for the large reflectors . . . . .	48
Pulsating variables . . . . .	20	Sixty-inch photometric telescope . . . . .	50
Absolute energy distribution . . . . .	20	Other projects . . . . .	50
Eclipsing binaries . . . . .	21	Plans for the Carnegie Southern Observatory . . . . .	50
Peculiar A-type stars . . . . .	21	Site testing in Chile . . . . .	50
Infrared Stellar Spectroscopy . . . . .	22	Site testing in Australia . . . . .	52
Star Clusters . . . . .	22	Large telescope mirrors . . . . .	52
M92 . . . . .	22	References Cited . . . . .	53
M15 . . . . .	23	Bibliography . . . . .	53
NGC 1866 . . . . .	23	Staff and Organization . . . . .	56
Interstellar Gas and Gaseous Nebulae . . . . .	24		
Infrared Sky Survey . . . . .	25		
Radio Sources . . . . .	26		
Identification . . . . .	26		

## INTRODUCTION

Before 1960, the most distant galaxy for which a measurable spectrum had been obtained gave a redshift of  $\Delta\lambda/\lambda_0 = 0.20$ , and the most distant cluster observed photoelectrically had a redshift of  $\Delta\lambda/\lambda_0 = 0.35$ . In that year, just before his retirement from the Observatories, Rudolph Minkowski obtained two spectrograms of a peculiar galaxy identified with the radio source 3C295 and found a redshift of  $\Delta\lambda/\lambda_0 = 0.4616$ .

Even more spectacular redshifts have been found recently for some of the quasi-stellar radio sources originally catalogued by radio astronomers. Using the 200-inch Hale telescope, Maarten Schmidt has now obtained spectra and redshifts for five quasi-stellar sources that are farther away than any other known object in the universe. The most distant of the five, 3C9, is so remote that its redshift is  $\Delta\lambda/\lambda_0 = 2.012$ ; the others, in decreasing order, are 1.055, 1.037, 1.029, and 0.734. For 3C9, Lyman  $\alpha$ , the strongest line in the spectrum of the hydrogen atom, is observed to be shifted from its normal position at 1,216 Å up to 3,660 Å. The only generally acceptable interpretation is that this is a cosmological redshift and that we are therefore looking back to a time only a few billion years after the expansion of the universe began.

Much progress toward the optical identification of radio sources has been made by Allan Sandage, Philippe Veron, John D. Wyndham, and T. A. Matthews, who have analyzed during the report year most of the 328 listings of the revised *Third Cambridge Catalogue* using new, precise radio positions from various radio observatories. They find that 29 of the sources are in the Galaxy, and that 95 can definitely be identified with radio galaxies, while 35 certain and 18 possible identifications relate to quasi-stellar sources, all checked by three-color photometry.

A discussion by Sandage has shown that the magnitude-redshift data for 40 radio galaxies fit a straight line to the limit of the redshift determination at  $\Delta\lambda/\lambda_0 \simeq 0.26$ . Photometry of the nine quasi-stellar sources for which Schmidt has measured redshifts reaching  $\Delta\lambda/\lambda_0 = 2$  shows that, within the accuracy of the data, these also are consistent with a linear relation between magnitude and redshift.

In considering cosmological models, the foregoing linear relation corresponds to a value  $+1$  for the deceleration parameter  $q_0$ . Sandage points out, however, that the derivation of a firm value for  $q_0$  must wait until a larger sample of data has been obtained. At the enormous distance of 3C9, a difference in apparent luminosity by a factor of about 10 occurs when the  $q_0 = +1$  model is compared to the original steady-state model of the universe, for which  $q_0 = -1$ . It can be said that the data currently available are not consistent with the steady-state model, and that if redshifts and accurate photometry can be obtained for three times as many quasi-stellar sources, it may be possible to specify the value of  $q_0$  with confidence.

From April 5 through 12 the Mount Wilson and Palomar Observatories were co-hosts with the Kitt Peak and Lick Observatories to an international symposium on the construction of large telescopes. The symposium was held under the auspices of the International Astronomical Union and was supported financially by the National Science Foundation, with I. S. Bowen as chairman of the organizing committee. At present there are 10 projects for the construction of telescopes of 120-inch aperture or larger. The symposium was planned primarily to permit an exchange of ideas among the astronomers and engineers responsible for these projects. In addition to four days of discussion



held in Tucson and Pasadena, visits were made to Kitt Peak, Palomar Mountain, and Mount Hamilton, making possible a detailed inspection of the only two telescopes in the size range under discussion that are now in operation. Approximately 60 astronomers, optical designers, and engineers, including representatives from nine of the projects, attended.

Observatory-site testing progressed in the southern hemisphere, where observations on the quality of the seeing have been made on three coastal mountains in Chile and at the Siding Spring Observatory in New South Wales, Australia. The results to date show the clear superiority of sites in Chile, where testing is con-

tinuing on Morado and on Pachon. The mean amplitude of image tremor as measured by the astronomical seeing monitors in Chile has averaged for the summer months slightly better than 0".7, and 70 per cent of all the nights there can be classed as photometric. There is no doubt that these prospective sites, at about 30°S latitude and at elevations between 7,000 and 9,000 feet above sea level, offer superlatively good observing conditions.

Scientific results reported here are for the 11-month interval from July 1, 1964, to May 31, 1965; the bibliography and observing conditions relate to the full year ending on June 30, 1965.

## OBSERVING CONDITIONS

Total rainfall at Mount Wilson for the year was 31.85 inches. Most of this precipitation occurred as a result of two major storms, one in the middle of November 1964, when 15 inches of snow fell; the other between March 31 and April 13, 1965, which brought altogether 70 inches of snow. The deepest snow on the ground at any one time was 46 inches. The snows of early April halted observations with the solar towers for two weeks, the longest interruption since the ice storm in January 1933.

At Palomar Mountain 41 inches of snow fell and the total precipitation was 27.3 inches. Observations made with the major telescopes are represented in Table 1.

TABLE 1. Observations

Telescope	Complete Nights, number	Partial Nights, number	Total Hours Worked
60-inch	187	77	2,071
100-inch	250	41	2,498
200-inch	220	70	2,464

## SOLAR OBSERVATIONS

Routine solar observations were made by Thomas Cragg, Merwyn Utter, and Robert Howard on 315 days. The numbers of records of the various kinds made between July 1, 1964, and June 30, 1965, were as follows:

Direct photographs	300
H $\alpha$ spectroheliograms, 30-foot focus	310
K2 spectroheliograms, 30-foot focus	300
Magnetograms	214

Magnetic classifications of sunspot groups were made visually on 138 days during the year.

### *Large-Scale Magnetic Fields*

Robert Leighton has continued his study of solar magnetic fields and velocity fields. The principal effort has been on further testing of a theory of transport of magnetic fields by the large-scale current flows on the solar surface and on an attempt to devise a model of the solar cycle. The latter effort has not yet been successful, but shows some promise.

Dr. V. Bumba of the Astronomical Institute of the Czechoslovak Academy of Sciences, Ondrejov Observatory, R. F.

Howard, and Sara F. Smith of the Lockheed Solar Observatory continued their study of the distribution of large-scale magnetic fields. The principal observational data used have been the daily magnetograms obtained at Mount Wilson with improved angular resolution ( $23''$ ) since the summer of 1959. Synoptic (rotation) charts were drawn for this interval, and a study was made of the distribution of weak magnetic fields over the solar surface. It was found that in the neighborhood of the sunspot latitudes the weak magnetic fields (the remnants of old active regions) are distributed in a rather regular pattern, which is coherent across the entire surface of the sun. Although active regions continuously add magnetic flux to this background field pattern, the lifetime of the pattern is many months. A frequent characteristic feature of the pattern is a unipolar magnetic region (UMR), a large region of weak magnetic fields — with magnetic polarity that of the “following” spots for the hemisphere in which the UMR occurs. The strongest fields of a UMR are characteristically in the leading portion, which may extend down to the equator. Following the leading portion, the weak extended tail stretches poleward. The total extent in longitude of a UMR may exceed  $180^\circ$ .

The magnetic fields of UMRs were observed to drift toward the poles. Thus it is apparent that, as H. W. Babcock predicted (1961), the UMRs provide magnetic flux to the polar fields, which is responsible for the polar field reversal about the time of sunspot maximum. Preceding the UMRs are weak extended regions of opposite magnetic polarity (leading for that hemisphere) named “ghost unipolar magnetic regions” that evidently represent the return to the sun of some of the lines of force originating in the UMR, but not all of the lines, since their flux is much lower than that of the UMR. The rest of the UMR lines of force probably return to the sun at lower latitudes. During the period August 1959 to August 1964, eight UMRs were counted. Some of these

may somehow have been connected with other UMRs or a renewal of previous UMRs. There is a good correlation between these UMRs and 27-day recurrent magnetic storms in that the leading portion of the UMR crosses the central meridian of the sun two to four days after the commencement of the magnetic storm. It is likely that the source of the storm particles can be associated with the “ghost” UMR or with the background fields that precede the UMR.

Some preliminary analyses have been made of the average magnetic field of the sun (averaged over the visible solar disk) as measured for several periods during the last activity cycle. The relation between this average field and solar activity and the background fields will be studied. First results indicate that the average field, although it varies somewhat from day to day, remains almost always positive. This can be explained by the fact that most of the activity was in the northern hemisphere, which means that the northern polar field was stronger than that in the south—at least during the last half of the cycle—placing an excess of negative fields in the polar regions. The fields in the equatorial regions were predominantly positive, and they affect the measured average field more than do the polar fields.

#### *Development of Solar Flares*

Drs. Bumba and Howard have studied the development of solar flares as seen on the K-line flare patrol films from Mount Wilson. The purpose of using the calcium flare patrol pictures was to determine the relationship of the development of solar flares to the small-scale distribution of magnetic fields on the solar surface. It can safely be assumed that the magnetic lines of force exist where emission is seen in the calcium line. Of the 200 flares examined, all showed the same characteristic behavior in the development stage. The first brightening occurred at the point where several network cells intersect—that is, the “corner”



of a network cell. The development from that stage was along the small emission regions that delineate the network cells. In the case of the largest flares, whole network cells were filled in with the brightening of the flare. The importance of the preexisting network structure in the development stages of a flare is very great.

Harold Zirin has begun a morphological classification of flares, distinguishing five types according to their position and shape.

#### *Features of the Chromosphere and Corona*

Dr. Bumba, Dr. J. Kleczek of the Ondrejov Observatory, and Dr. Howard studied the relation of photospheric magnetic fields to coronal features. Mount Wilson magnetograms and Sacramento Peak Observatory green-line coronal filtergrams were used. Coronal loops or arches connect regions of opposite magnetic polarity in the photosphere and evidently represent the location of lines of force. In general, older magnetic features have larger and fainter arches associated with them. The youngest magnetic regions have generally amorphous coronal features associated with them. The brightest coronal features are usually associated with the highest photospheric magnetic gradients.

Zirin has been working on a new model of the chromosphere-corona transition zone, extending that published by Zirin and Dietz (1963). In the new model, the quiet solar corona consists of long plumes localized above the spicule "bushes" at the edges of the chromospheric network cells. Over the interior of network cells there is no reversal of temperature, but the density falls off sharply with a scale height of 100 km. The problem of the

stability of the plumes is not yet solved. The plumes are seen only near the poles because they are masked by the corona over active regions. Christopher Anderson, a graduate student, has been studying the K-line reversal in the chromospheres along with Zirin. They have found the K reversal to be an integration effect, with only individual peaks on the red or violet side of the line, and sometimes none whatever at any given point. The broadening of the central absorption near the limb appears to be due to the greater effect of the spicule forest near the limb. The spicules have broader profiles than the other chromospheric material, and hence broaden the central absorption. A number of step-scan spectrograms have been obtained with the spectrograph of the 60-foot tower.

#### *Eclipse Observations*

In collaboration with Dr. G. Righini of the Arcetri Observatory and R. M. Cameron and his associates of the Douglas Aircraft Co., Armin Deutsch again adapted a two-prism stellar spectrograph for observation of the coronal spectrum during total eclipse. Four spectrograms were obtained on May 30, 1965, from a NASA jet aircraft flying with the umbra over the Pacific Ocean near the Marquesas Islands. What would seem to be coronal emission lines appear at the wavelengths of H and K on at least two of the plates. The angular resolution was decidedly better than that achieved on the spectrogram obtained during the eclipse flight over Canada in 1963. However, all the 1965 plates are underexposed, and it remains to be seen how much useful data can be obtained from them. The reductions are proceeding at Florence under the supervision of Dr. Righini.

## PLANETS AND THE MOON

*Mars*

The intensity distribution in the rotational lines of the  $4\nu_2 + \nu_3$  band of  $\text{CO}_2$  at  $2.06\ \mu$  in the spectrum of Mars has been studied by Guido Münch and G. Neugebauer with the coudé spectrograph of the 100-inch Mount Wilson reflector. A 300-groove/mm replica grating provides in the focal plane of the 114-inch camera a dispersion of  $11.3\ \text{\AA}/\text{mm}$  in the first order. By using exit multislits with spacing equal to that between the rotational lines to be studied and widths at least half as large, effective resolving powers of 7,000 and more have been reached. With a PbS detector cooled at liquid nitrogen temperature, signal-to-noise ratios of the order of 20 are reached for the moon and Mars with time constants of 0.4 and 25 sec, respectively. As a measure of the product of the pressure and the amount of absorber, the intensity ratio between the maxima and the minima in the rotational structure has been used. For an Elsässer band model and a slit transmission function varying in wavelength  $\lambda$  as  $\cos^2(2\pi\lambda/\delta)$ , where  $\delta$  is the line spacing, analysis has shown that the intensity ratio between maxima and minima is asymptotically linear with the product of the pressure and amount of absorber as the band becomes increasingly saturated. The linear dependence of this ratio observed in the moon as a function of air mass has been verified and accounted for in terms of laboratory data and the known amount of telluric  $\text{CO}_2$ . Observations of Mars have been made in the R-branch of the  $4\nu_2 + \nu_3$  band with a 3-unit exit multislit and in the P-branch of the same band with a 10-unit multislit. Calculations are now under way to interpret these data as a part of the general problem of redetermining the pressure in the Martian atmosphere.

The weak  $5\nu_3$  band of  $\text{CO}_2$  at  $\lambda 8,660\ \text{\AA}$ , needed for determination of the total amount of  $\text{CO}_2$  independent of the pres-

sure, has been repeatedly observed photographically under a dispersion of  $3.5\ \text{\AA}/\text{mm}$ , thus increasing considerably the precision of the equivalent widths of the weak lines. A preliminary discussion of the data has suggested that the value for the surface pressure in the atmosphere of Mars, as indicated by the new data, is about 20 millibars.

*Venus*

High-resolution observations of the  $\nu_1 + \nu_2 + 3\nu_3$  band of  $\text{CO}_2$  at  $\lambda 10,490\ \text{\AA}$  have been made by Münch with the photoelectric scanner of the 100-inch coudé spectrometer at various phases of the planet. His observations have the ultimate purpose of verifying the variation with phase of the rotational temperatures that have been reported for other  $\text{CO}_2$  bands; they will be continued during the forthcoming eastern elongation of the planet.

*Major Planets*

Model atmospheres for the major planets have been constructed by Laurence Trafton as part of his doctoral dissertation. On the basis of the pressure-induced rotational and translational absorption of  $\text{H}_2$ , pure and in mixtures with helium, nongray models in radiative equilibrium have been constructed. The opacity of  $\text{NH}_3$  has been included in the case of Jupiter. It has been found that models for which only the thermal opacity of pure  $\text{H}_2$  is included are incompatible with the observations, and the presence of helium is strongly indicated. For Jupiter, a rather large value of the helium to hydrogen ratio is implied if there is not an internal heat source. However, the observations are more nearly compatible with a helium to hydrogen ratio of about 2, for an internal heat source small in comparison with the incident solar flux.

Robert Wildey, using the 200-inch telescope, made observations in the



8–14  $\mu$  infrared of the regions of the disk of Jupiter shadowed by the Galilean satellites for all eclipses occurring during Palomar twilight. The “hot shadow” phenomenon observed on the planet in 1962 was not present during observations in late 1964 and early 1965. Murray and Wildey, however, consider the earlier observations unambiguous and conclude that the presence or absence of the phenomenon is the result of temporal variations that characterize Jupiter’s atmosphere.

Observations of the brightness of the Galilean satellites themselves, and of the asteroid Vesta, were obtained by Murray, also in the 8–14  $\mu$  region.

### *Moon*

Spectrophotometric observations of various regions on the moon were acquired

by Murray with the Cassegrain photoelectric spectrum scanner on the 60-inch telescope. In a search for luminescence in the H and K lines of Ca II, Thomas McCord and Dennis Matson made an analysis of these spectrophotometric observations, as a graduate-student research project. No definite evidence for luminescence was found. An upper limit was 0.5 per cent of the background radiation. A parallel but less conclusive project was carried out with the Snow telescope by the same group.

Wildey collaborated with Murray and Westphal in mapping the 8–14  $\mu$  brightness temperature of the moon’s dark side, using their 24-inch telescope on White Mountain in the summer of 1964. Many hot spots were detected, and it was noted that the lunar maria are slightly warmer than the uplands well into the lunar night.

## STELLAR SPECTROSCOPY AND PHOTOMETRY

### *White-Dwarf Spectra*

As a result of the major investigation completed by Eggen and Greenstein, colors and spectra of 166 white dwarfs were recorded. With the continued discovery of white dwarfs from proper-motion surveys, 30 additional objects have been entered in new lists made by Greenstein. Most of these are conventional white dwarfs of type DA. In particular, a very large fraction of the new Lowell proper-motion survey of blue stars of small proper motion, averaging 0.2 sec of arc or less, proves to be the DA type. Apparently a good number of white dwarfs belong to the very low-velocity population, with mean tangential velocities under 20 km/sec. However, one very exciting new white dwarf of appreciable proper motion, Giclas 47-18, has been found. A photoelectric color by Sandage showed that it is quite blue with a  $U - B$  of

– 1.0 magnitude. Its spectrum has broad lines of neutral carbon, and relatively sharp bands of  $C_2$ . It is related in some ways to the  $\lambda 4,670$  stars, but is outstanding in sharpness of carbon bands and the presence of neutral carbon. Its temperature is high enough to show neutral helium had any been present in substantial amounts. No hydrogen lines are seen. Apparently G47-18 contains only carbon or heavier elements, and is an excellent proof of the formation of carbon in the interior of evolved stars. The source of opacity is unknown, since carbon at 15,000°K surface temperature has not yet been studied theoretically or spectroscopically at high pressures.

Attempts to measure low-dispersion plates of white dwarfs for the Einstein gravitational redshift have been started with the new Grant oscilloscope-presentation measuring machine recently purchased on the U. S. Air Force contract.

The mean error per plate from three lines seems to be about  $\pm 20$  km/sec. A group of 12 plates of members of the Hyades cluster gives a statistical value of the redshift of about  $+50$  km/sec. Measurable spectra are available for nearly 20 white dwarfs in wide visual binaries.

J. B. Oke, using the photoelectric scanner, has begun measuring absolute energy distributions in the spectra of white dwarfs, and has made observations of 10 stars. The stars have been selected to cover the whole range of temperatures observed by Greenstein. The energy distributions will be compared with model-atmosphere fluxes, now becoming available, from which it will be possible to obtain a more accurate temperature scale.

### *Subdwarfs*

In the course of surveys of suspected proper-motion blue stars for which only rough photographic estimates of color were available, it has been found that for all but the bluer stars there is an appreciable admixture of stars that are not white dwarfs. Greenstein and Eggen have recently completed a list of 50 such stars, with spectra, and some with colors. It is found that the Lowell stars of suspected photographic color index  $-1$  are essentially all white dwarfs, and about three quarters of those of color estimate 0 are white dwarfs. Very few white dwarfs are found among field stars of color index estimated  $+1$ , except in a few cases where common proper-motion pairs have shown a red primary with a bluer secondary of color  $+1$ . Thus the rough photographic colors are at least a useful finding guide for stars of 0 and  $-1$  estimated color.

### *Spectra of Magnetic Stars*

A large joint observational program has been carried through by Greenstein, Conti, Danziger, and Deutsch, with photometric observations by Oke. The goal was to obtain highly accurate spectroscopic photometric information

on the variations of the spectrum, temperature, color, brightness, and Balmer discontinuity of  $\alpha^2$  Canum Venaticorum and two other magnetic variables. Such data for the periodic magnetic variables are extremely important for interpretation of the physical processes of magnetic variation, as well as for the abundance anomalies and their changes around the cycle. Spectra have been obtained from  $\lambda 3,300$  to  $\lambda 6,800$  every night in one cycle (5.469 days) of this star, and from  $\lambda 6,800$  to  $\lambda 8,800$  in a slightly more scattered interval over two cycles. Consequently, a line list can be prepared for the entire photographable spectrum, together with identifications and radial velocity variations. Quantitative analysis of this material has been started, first to provide blanketing corrections to the photometric scans for temperature and surface gravity estimates, and subsequently for the composition determinations. To provide higher accuracy than has been hitherto available, three plates per night were taken in the  $\lambda 5,000$ -to- $\lambda 6,800$  region, with a more modest coverage of one to two plates per night in the other spectral regions.

### *Globular-Cluster Stars*

Robert Stoeckly has analyzed new observations of the B<sub>pec</sub> star Barnard No. 29 in the globular cluster M13. This is a star that is far above the horizontal branch of the H-R diagram and whose mass has been estimated spectroscopically to be  $0.2 M_{\odot}$ . Spectrograms at  $18 \text{ \AA/mm}$  give ratios of abundance fractions of elements relative to the sun ranging from 0.1 for nitrogen and silicon to  $<0.007$  for carbon. The radial velocity appears to have varied by about 20 km/sec during 10 years, so that the presence of a second component is inferred. Photoelectric observations of the continuum and Balmer decrement are abnormal, and two possible explanations are being investigated: (1) The star is cool and extremely hydrogen deficient ( $T_e =$



12,000°K,  $n_{\text{H}}/n_{\text{He}} \approx 10^{-4}$ ), or (2) the star has a hot, low-gravity component ( $T_e = 21,000^\circ\text{K}$ ,  $\log g \approx 2.5$ ) and a giant companion.

Greenstein and Oke are extending their study of horizontal-branch field stars to the stars in globular clusters. Both slit spectra and scans are being obtained. Observations have been confined so far to stars in M15 and M92, both very metal-deficient clusters. Preliminary reductions suggest that the masses may be significantly less than one solar mass, and variable.

### *Molecular Spectra*

It is clear that the wide variety of possible evolutionary situations for red giants requires a study of these cool, complicated spectra. Because molecular spectroscopy has so far yielded isotope ratios only for carbon, Greenstein and his collaborators have begun a program to study molecules of astrophysical interest. In the S stars, the possible isotope abundance variations from normal stars can be studied on plates of R Andromedae and R Cygni. Mrs. Dorothy Locanthi has been measuring accurate wavelengths for the zirconium-oxide features from violet to infrared in these two stars, and some regions of the blue spectrum of V Cancri. With isotopic wavelengths available from unpublished measurements in Stockholm, it seems probable that appreciable progress can be made on the isotope ratios for zirconium in S stars. Mrs. Locanthi suggests the possible identification of a band at  $\lambda 6,495$  as niobium-oxide.

Another very important isotope ratio is that of  $\text{Si}^{30}/\text{Si}^{28}$ , which can be studied in late K giants and early M giants. Greenstein has obtained a set of very high-resolution spectra at Palomar which show approximately 50 fairly unblended lines of SiH.

The isotope shifts have been computed by Mrs. V. Peterson, and an attempt will be made to obtain laboratory spectra as well for the rare isotope. In a possible slow neutron capture cycle in red giants,

suggested by Fowler and Hoyle, the  $\text{Si}^{30}$  could be enhanced. It would not be expected to appear in ordinary red giants. The plates available of S stars that have other evidences of heavy-element slow neutron processing are of marginal quality for this investigation, and further spectra will be obtained for the S stars. However, the silicon isotope ratios in normal stars are almost immediately available. Greenstein presented an extensive review of the elemental abundance problem, with emphasis on isotope determinations, at the symposium sponsored by the Utrecht International Astronomical Union on stellar atmospheres and abundance determinations.

### *Carbon Isotope Determinations*

Wyller completed his study of the  $\text{C}^{12}\text{N}^{14}$  and  $\text{C}^{13}\text{N}^{14}$  bands in late-type carbon stars, based on the electrodeless discharge production of spectra with the Mount Wilson coude of the normal and enriched isotopic spectra at the same dispersion as the stellar spectra. His results will provide a basis for lower-resolution analysis of the isotope ratios. He has been able to provide individual rotational line lists and, in addition, lists of some 25 indicators of  $\text{C}^{12}$  or  $\text{C}^{13}$ .

The lines are largely in the  $\lambda 7,900$  to  $\lambda 8,100$  region and can be used quantitatively at 20 Å/mm in stars with moderate saturation. The average separation of the features runs from 2 Å to 4 Å. For the detection of  $\text{C}^{13}$ , dispersions as low as 50–100 Å/mm could be used. As for the individual rotational lines, Dr. Wyller finds that it is necessary to produce laboratory spectra because of the perturbations of some of the levels, or the incorrectness of the analysis of some of the bands. The infrared cyanogen bands are now well mapped and analyzed for normal and isotopic molecules.

Wyller finds a very wide range in the  $\text{C}^{12}/\text{C}^{13}$  ratio. With correction possibly not quite complete for saturation of the bands, it seems possible that  $\text{C}^{13}$  is more abundant than predicted in equilibrium



in the carbon-nitrogen-oxygen cycle; values as high as 2.4 : 1 are indicated, whereas the carbon cycle gives 4.3 as the minimum ratio. Wyller suggests several possibilities for the origin of excessive  $C^{13}$ , one of which is by neutron irradiation in the envelopes of carbon-rich Wolf-Rayet stars.

### *Standard Spectrophotometry of Spectral Lines*

For some years there has been an outstanding discrepancy in the reliability of photographically determined equivalent widths in comparison with the possible photoelectric accuracy. This discrepancy, the variety of stellar spectrographs used around the world, and the importance of having line intensity standards, led the International Astronomical Union to establish a subcommission on spectrophotometric standards for line intensities. Greenstein and, later, Dr. K. O. Wright of the Dominion Astrophysical Observatory, have been active in this subcommission. The first results appeared in a joint paper by Wright, Lee, Jacobson, and Greenstein in the *Publications of the Dominion Astrophysical Observatory*; 110 spectrograms of varying dispersions were obtained at Dominion and 22 at Mount Wilson and Palomar Observatories. Lines were measured in a systematically consistent way for 12 representative stars of spectral types B to G. The publication gives the recommended means, standard hydrogen-line profiles, photographs, and tables, as well as some tracings. It is certain that the original diffraction gratings at Mount Wilson and at Palomar are free from serious scattered light, and that the calibration devices are reliable (wedge spectrograph and step-slit device at Mount Wilson, and wedge spectrograph at Palomar). The results of the comparisons are, however, not yet quite satisfactory. The Mount Wilson coude spectrograph gives on the average six per cent lower equivalent widths, and the high-resolution photoelectric scanner, one

per cent smaller equivalent widths, than the average adopted—which is largely weighted by the Victoria 72-inch results. The Palomar equivalent widths run about 12 per cent less than the average. In general it has been found that the dispersions lower than 10 Å/mm give very low accuracy, especially for the weak lines, and cannot be used for abundance determinations except with extreme care. The fact remains that higher dispersion spectra give lower equivalent widths; a plausible explanation of this was given some years ago by Deutsch (1954).

### *Chemical Composition of Stellar Atmospheres*

Oke and Greenstein have studied a very interesting star, BD+39°4926, which has the largest known Balmer discontinuity. It was originally thought to be like the horizontal-branch stars. Spectra at 9 Å/mm taken by Greenstein at Palomar show that this star has extremely weak metallic lines for its temperature, near 7,000°K, and is of high luminosity. In addition, the spectrum has weak but numerous lines of C I and O I. Helium is also suspected. The composition is extraordinary in being extremely metal poor, but at the same time having nearly the normal (i.e., solar) abundances of carbon and nitrogen. Before a model atmosphere can be prepared, a detailed study is needed because of the high excitation potential of these lines and the low stellar temperature. However, preliminary analysis gives carbon and nitrogen abundances so different from the metallic abundances as to suggest, if the star is very old, that the synthesis of carbon and oxygen in the interstellar gas was essentially completed to its present value when the star was formed. Judging from the low metal abundance, it was in a very early stage of galactic evolution. Alternate explanations that would involve the synthesis of carbon and oxygen in the star itself do not seem acceptable.

Danziger has completed an abundance



determination of the elements in the subdwarfs  $\gamma$  Pavonis and  $\zeta^1$  Reticuli. Some of these data combined with previously determined results for Ba II, CH, and one Am star have been used to support the theory of the *s*-process production of the relevant heavy elements.

An abundance analysis of the chemical elements in the F subdwarf  $\sigma$  Boötis relative to Procyon by Danziger, using previously published data, reveals an almost uniform underabundance of all elements, including the heavy ones, by a factor of 0.6 in the logarithm. Effective temperatures determined from  $H\gamma$  profiles of these stars are in good agreement with effective temperatures from continuum scans obtained by other observers, lending weight to the abundance results.

Conti and Danziger have completed a survey of early F stars mainly on the main sequence but including subgiants and supergiants. There is a wide range of lithium content in these stars of the order of a factor of 100. More detailed analysis of the data is in progress.

A combined spectroscopic and spectrophotometric study of the short-period variable VZ Cancri has been carried out by Danziger and Oke. The temperature variation over the cycle determined from continuum scans and  $H\gamma$  profiles are in good agreement. An abundance analysis relative to Procyon reveals a metal deficiency of a factor of 2 to 3. It seems likely that VZ Cnc is a cluster-type variable. With the use of the most probable intrinsic luminosity under this assumption, the gravity obtained from fitting the continuum scans to model atmosphere fluxes predicts a mass of  $0.2 M_{\odot}$ . A more complete analysis throughout a cycle is being undertaken.

Conti, with George Wallerstein and Robert Wing of the University of California at Berkeley, have completed a study of abundances in 10 main-sequence stars of the Hyades cluster, including one A-type star from Praesepe, a cluster that shares the motion of the Hyades. Using model atmospheres and

a curve-of-growth technique, they find that all these stars have the same abundances with the exception of 68 Tauri, the bluest star in the Hyades, which is similar to a metallic-line star. Both 68 Tau and HD 73666 in Praesepe are located near their cluster turnoff points, but the latter star is normal in every respect. For the coolest stars it is necessary to modify the model atmospheres to take account of blanketing. There is evidence for nonlocal thermodynamic-equilibrium effects in the stars studied, but there seems to be little change in deviations from thermodynamic equilibrium along the main sequence.

Conti has made a high-dispersion spectroscopic survey of the sharp-line early A stars brighter than  $5^m.5$  and accessible from Mount Wilson. He finds that the number of these stars is in excess of what would be expected from the average  $V \sin i$  at this spectral type. All the stars had been classified as normal on lower-dispersion spectra, but Conti finds that nearly one half of them show anomalously weakened scandium lines and strengthened strontium. This is precisely the property of metallic-line (Am) stars that previously have been identified only as early A5. Because the hydrogen lines are relatively insensitive to temperature in the early A spectral type, an excessive strength of metallic lines is not obvious until a detailed analysis is completed. For this reason the Am characteristics of Sirius and 68 Tau have only recently been recognized. Conti argues that, by analogy, many other Am stars exist among the early A stars, identifying them with his anomalous stars. Most of his anomalous stars are spectroscopic binaries, in agreement with the better known later Am stars.

Conti has obtained the plates for a spectroscopic study of seven sharp-line early A stars in the Pleiades cluster. A preliminary result indicates that three of these stars show anomalous scandium and strontium and are probably Am stars. A detailed analysis is presently



under way. Am stars have not previously been identified in clusters with B stars, or as companions to them, and this has had some influence on the theories of the origin of metallicism. A later type Am star has tentatively been identified in the cluster, but it is a "mild" type.

Conti and Danziger have completed a study of lithium and beryllium abundances in several early F stars and two K giants. They find lithium abundances from nearly 100 times solar to upper limits slightly above the solar value. The beryllium abundances range from slightly above to slightly below the solar value, but no lithium or beryllium has been detected in Procyon or Arcturus. The upper limit for beryllium in the former star is nearly 100 times below the solar value, suggesting strongly that Procyon, unlike all other F stars studied, has had a drastic depletion of beryllium. The Li/Be ratios in the other F stars range from approximately 10 to unity. The predicted spallation production ratio for these elements is about 2. The high ratio observed for several stars could mean that lithium has been produced by other processes. In Pollux, both lithium and beryllium are present in about the same ratio as in the sun, but with somewhat less abundance. This K giant has presumably destroyed some lithium but has not appreciably depleted beryllium.

#### *Lithium in Main-Sequence Visual Binaries*

Spectrograms covering the region of the lithium line at  $\lambda 6,707$  have been taken by O. C. Wilson for the members of 27 main-sequence visual binaries, mostly in the spectral range F3 to G0. All but three of the pairs were observed by means of an RCA image tube attached to the 114-inch camera of the coude spectrograph of the 100-inch telescope. Baum collaborated with W. K. Ford, Jr., and A. Purgathofer of the Committee on Image Tubes for Telescopes. In some of these visual binaries the lithium line is

stronger in the brighter member, in some in the fainter member, and in still others it is about equally strong in both members. In the remaining pairs no lithium is seen in either component. This diversity can be seen to form a consistent picture if it is supposed that the lithium concentration in the members of a pair is about the same when the stars are first formed, at which time the Li I line will appear stronger in the fainter and cooler component because of the low ionization potential of lithium. Then, if it is assumed that the depletion of lithium is more rapid in the fainter member because of the transport of surface material by the convection zone, it is evident that after some time the lines will be equal in the two components, after which the line will appear stronger in the brighter component. Finally, the lines will pass below the level of detectability for both stars. To this extent the observed Li I intensities in the visual pairs are consistent with the current view of the production and destruction of lithium.

#### *Chromospheres and Stellar Rotation*

Last year Wilson and Dr. Andrew Skumanich of the High Altitude Observatory reported on spectroscopic observations of a considerable number of main-sequence stars lying below  $b-y = 0.325$  in the color system of Strömgren and Perry. A number of these stars exhibit H and K emission and are restricted to the vicinity of the zero-age edge of the distribution in the  $c_1 - (b-y)$  diagram. In addition, several stars showing considerable rotational line widening were found just above the main body of the plotted points. It seemed worth while to extend the observations further up the main sequence for two reasons: (1) to find where, on the zero-age edge, the rotating stars originated, and (2) to see how far up the zero-age edge chromospheres, as evidenced by H and K emission, could be traced.

For these purposes Wilson has made spectroscopic observations of nearly 100



stars with  $0.240 < b - y < 0.325$  during the year. The work is not yet complete, but the results so far are interesting. It is found that rapid rotation sets in quite abruptly on the zero-age edge near  $b - y = 0.27$ . The rotating stars mentioned above presumably originated here, and have been moved by evolution to their present locations in the  $c_1 - (b - y)$  diagram. If this is correct, the boundary between rotating and nonrotating stars in the diagram must correspond closely to the evolutionary track of stars starting near  $b - y = 0.27$  on the zero-age edge of the main sequence.

Only two more stars with H and K emission have been found, one of them at  $b - y = 0.304$ , and both on the zero-age edge. Hence chromospheres, and thus presumably active hydrogen convection zones, are now known to exist not far from the abrupt onset of rotation.

#### *Spectroscopic Observations of dK and dM Stars*

Wilson has continued observations of dK and dM stars from Vyssotsky's catalogue for the purpose of obtaining the frequency distribution of H and K emission intensities. From this material it is hoped that knowledge of the rate of star formation in the Galaxy can be derived. Nearly 300 stars have now been observed spectroscopically, and two spectrograms have been obtained for more than 180 of them. The observational part of the program is drawing to a close and it is expected that the work of measuring the emission intensities will get under way shortly.

#### *Color-Magnitude and Chemical-Composition Relations*

Deutsch and Conti have found that in the passbands of Strömgren's  $u, v, b, y$  photometric system about half the line absorption occurs in lines that fall on the "flat" part of the curve of growth for stars of solar type. These lines are very insensitive to changes in the metal abundance; however, their strength is

directly proportional to the velocity parameter  $V$  of the curve of growth. Strömgren's index  $m_1$ , which is defined in terms of the colors  $(v - b)$  and  $(b - y)$  in order to provide a measure of the strength of the metallic lines, therefore responds directly to changes in turbulence much more sensitively than to changes in metal abundance. In particular, a simple calculation shows that the whole range of  $m_1$  values observed in G0 dwarfs of the disk population will occur if these stars are of identical composition and structure, but differ among themselves only by about  $\pm 0.15$  in  $\log V$ . This corresponds to a range of turbulent velocities from zero to approximately 2.6 km/sec, which is twice the value found in the solar atmosphere. On the other hand, if the G0 dwarfs of the disk population all had the same turbulence and atmospheric structure as the sun but differed only in metal abundance, this would have to range over an order of magnitude to produce the values of  $m_1$  that Strömgren has observed.

Deutsch and Conti do not disclaim the occurrence of metal-poor and metal-rich stars in the disk population. When taken with the results of abundance analyses by Wallerstein and others, however, their calculations do establish that the weak-line and strong-line characteristics observed in these stars result principally and directly from differences in turbulence. If the abundance analyses are correct, turbulence correlates with metal abundance. But the determination of the latter quantity is the more precarious, for it depends on the accurate measurement of a relatively small number of weak lines, and on a precise determination of the temperature. In any case it is clear that turbulence blanketing alone can produce  $U - B$  color excesses up to 0.06 magnitude relative to the Hyades, and that this effect probably dominates the line blanketing and determines the weak-line or strong-line characteristic of the yellow dwarfs with  $U - B$  color excesses that are less than 0.12 mag-



nitude. The metal abundance directly affects the blanketing in these objects only as a relatively small additional perturbation.

It remains necessary to find an explanation for the variation of turbulence from star to star. It is already known from the work of Eggen and others that line strength correlates loosely with age. The sense of the correlation is that in main-sequence stars turbulence tends to decay with advancing age. O. C. Wilson has recently given evidence that in these objects chromospheric activity also tends to decay with age. But to judge from what is seen in the sun, and from the theoretical work of Lighthill and Proudman, de Jager, and many others, both chromospheric activity and microturbulence are manifestations of the same mechanical flux that originates in the (invisible) hydrogen convective zone; both could well decay together if this flux diminishes with advancing age.

Although the data are not available to permit a detailed calculation, the results of Deutsch and Conti for solar-type stars are probably also applicable to some of the A and F stars. In particular, it would seem probable that the high  $m_1$  indices so often found in metallic-line stars are a direct result of the high turbulent velocities that have been found from curve-of-growth studies of a number of these stars. Deutsch and Conti have also shown that the close companions which, according to Abt, these objects usually have, are probably luminous enough in some of the systems to reduce  $m_1$  to the relatively moderate values that Strömgren has observed in some metallic-line stars.

#### *Studies in Stellar Rotation*

An extensive study of the mean apparent rotational velocity  $\langle V \sin i \rangle$  as a function of  $M_V$  for the stars of galactic clusters is under way by Robert Kraft. A comparison of this quantity in the Hyades and in Coma has been completed and these conclusions are reached:

(1) The frequency of binaries and of Am stars is approximately the same in the two clusters. (2) The function  $\langle V \sin i \rangle$  is the same for both clusters when the two Ap stars of Coma are omitted. (3) When allowance is made for evolutionary and abundance effects,  $\langle V \sin i \rangle$  for the Hyades and Coma does not differ significantly from the field.

The study also shows that (1) it is very unlikely that the rotational axes of stars in clusters show any preferential direction; (2) the frequency distribution of  $V$  (about  $\langle V \rangle$ ) is Maxwell-Boltzmann. The dependence of average angular momentum per gram as a function of stellar mass is also discussed.

A redetermination of rotational velocities for stars in the Pleiades has been carried out by Kraft, Christopher Anderson, and Robert Stoeckly. It is shown that Smith and Struve originally underestimated the rotational velocities of the Pleiades stars between A0 and F5 by about 50 km/sec on the average; also that  $\langle V \sin i \rangle$  for the Pleiades is larger than its value in the field for  $M_V$  down to +3.0. An extension to still fainter absolute magnitudes is planned by Kraft. On the basis of this work and the work of Abt and Hunter, it is proposed that even after stars arrive on the main sequence after gravitational contraction there is still some slowing down of apparent rotation.

A study of rotational velocities for Praesepe stars is under way by Baum, James McGee, and Kraft. An interesting feature is the use of an electronographic image tube to obtain those spectra of Praesepe stars that are fainter than  $M_V \sim +3$ . Preliminary results indicate that, while Treanor's estimates of  $V \sin i$  are essentially correct on the average, individual values may be considerably in error.

Kraft has obtained spectra at 18 Å/mm of all stars of the very young I Persei ( $\alpha$  Per) group down to about F5 V to study  $\langle V \sin i \rangle$ . Preliminary indica-



tions are that the rotational velocities are rather high. An interesting by-product of this work is the discovery of an Ap star in I Per with strong lines of Y II. There is little doubt that the star is a member of I Per. This result, together with the presence of an Ap star in the Pleiades-like  $\sigma$  Velorum cluster, indicates that Ap stars occur in young groups and are not confined to the older Coma-like clusters, as thought earlier. This in turn makes extremely doubtful the view that Ap stars are stars in a post-red-giant stage of evolution.

#### *U Geminorum Stars*

Kraft, and Dr. W. J. Luyten of the University of Minnesota completed a study of the absolute magnitude of U Geminorum variables. The solar motion is derived as  $A_{\odot} = 263^{\circ}$ ,  $D_{\odot} = +19^{\circ}$ ,  $S_{\odot} \cong 30$  km/sec, and  $\langle M_V (\text{min}) \rangle = +7.5 \pm 0.7$ . It is suggested that the red components of U Gem stars lie on the main sequence and satisfy the  $\mathfrak{M} - L$  relation. Such group members as RU Pegasi, SS Cygni, and AE Aquarii, which have the longest orbital periods, are thought to be in fact intrinsically brighter than the average U Gem stars. Thus the contradiction between the spectroscopic and motion-derived parallaxes can be resolved, since the stars with the longest orbital periods are those that also show the spectrum of the late-type components, and are those from which the spectroscopic absolute magnitudes were originally derived.

Kraft reconsidered the space distributions and solar motion parameters of U Gem stars and variables of the W Ursae Majoris class. Distances were computed to all objects of these two types lying in a cylinder of radius 450 pc and height 900 pc, with axis at right angles to the galactic plane. It was shown that the  $z = r \sin b$  distributions of the two kinds of stars are identical. Further, the kinematical parameters are the same within the errors. There is, therefore, no objec-

tion on these grounds to the hypothesis that the U Gem variables are evolutionary descendants of the W UMa stars.

New orbits were obtained for HV 8002 and SS Aurigae. The periods are  $3^{\text{h}}50^{\text{m}}$  and  $4^{\text{h}}20^{\text{m}}$ , respectively. Both are single-line binaries of type sdBe.

#### *Wolf-Rayet Stars*

Observations of binary and single Wolf-Rayet stars brighter than 11th magnitude have been continued by Kuhl with the Cassegrain photoelectric scanner. The intensities of emission lines and continua have been measured in the wavelength range  $\lambda 3,200$  to  $\lambda 11,000$ , with the scanner used as a narrow-band photometer. In the near infrared,  $\lambda 6,000$  to  $\lambda 11,000$ , several of the brighter stars have been scanned with a  $20 \text{ \AA}$  exit slit so that the emission features could be identified. The strongest lines in the WN sequence are He II +  $H\alpha$   $\lambda 6,562$ , N IV  $\lambda 7,116$ , He II  $\lambda 10,124$ , and He I  $\lambda 10,830$ ; and in the WC sequence, He II +  $H\alpha$   $\lambda 6,562$ , C III  $\lambda \lambda 6,730, 8,196, 9,705$ , C IV  $\lambda \lambda 7,050, 7,726$ , He II  $\lambda 10,124$ , and He I  $\lambda 10,830$ . There are also intrinsic variations of emission-line intensity in most of the stars observed. The star HD 50896 mentioned in *Year Book 63* (p. 21) as showing excessively large variations has been observed in detail to detect any possible systematic trends. Preliminary results do not show any evidence for such behavior.

The continuous energy distribution of Wolf-Rayet stars has been studied in detail. Because of the discrepancies in previous temperature estimates and, in particular, the low color temperatures derived by various observers, it was hoped that the greater inherent accuracy of the photoelectric method would resolve the difficulty. On a two-color diagram ( $\lambda 3,636 - \lambda 4,786$  versus  $\lambda 4,786 - \lambda 5,556$ ), the Wolf-Rayet stars fell along two separate sequences, which indicated that the WC stars are cooler than the WNs. A similar effect was found by Dr. Feinstein. How-



ever, a careful look at the wavelength regions observed indicates that even in 50-Å bands some emission-line contamination can be expected, especially in the WCs. After appropriate corrections the effect essentially disappeared; Dr. Feinstein's results must be similarly in error because of the much larger bandpasses of the *U*, *B*, *V* system.

The corrected two-color diagram was then used to obtain reddening corrections by assuming that the Wolf-Rayet stars unreddened to a  $B - V = -0.33$ , as indicated by the standard reddening law. The unreddened continuous energy distribution curves fall into two groups (with a few intermediate cases) distinguished by their slope and curvature. The binary stars have curves resembling those of O stars (as expected because of the presence of the brighter O-type companion), whereas those of the single stars are much steeper in the blue and less steep in the near infrared. There is no essential difference between the WCs and the WNs, nor is there any marked correlation with spectral type, which implies that the emission-line spectrum must be determined by the far-ultraviolet energy distribution. However, the energy distribution curves of the single stars are definitely peculiar and certainly *not* those of blackbodies. The color temperatures derived at  $\lambda\lambda 3,500, 5,000, 6,750$ , and  $9,500$  show a marked decrease with wavelength, being  $\sim 100,000^\circ$  at  $\lambda 3,500$  and decreasing to  $\sim 15,000^\circ$  at  $\lambda 9,500$ . The peculiar distribution makes it extremely difficult to define a unique temperature for the Wolf-Rayet stars. The lack of a Balmer discontinuity and the steep slope of the energy curve in the ultraviolet imply a high effective temperature; an approximate fit of models in the blue indicates  $T_{\text{eff}} \gtrsim 50,000^\circ\text{K}$ . However, this leaves an excess of observed radiation in the ultraviolet and in the near infrared. The explanation most likely will result from the theory of radiative transfer in extended envelopes, whereby the emitted

radiation is considerably modified by the atmosphere.

### *T Tauri Stars*

Continuous energy distribution curves are being obtained for the brighter T Tauri stars in order to derive better effective temperature estimates and thus to locate them more precisely in the HR diagram. The curves will also permit quantitative comparisons of various hypotheses concerning the origin of the excess ultraviolet continuous emission.

The Ca II K line widths as measured from coudé spectra indicate that the Wilson-Bappu effect does not apply to T Tauri stars. It leads to absolute magnitudes many times larger than those normally estimated by other means. The discrepancy must arise from the more violent atmospheric conditions (e.g., mass ejection) encountered in T Tauri stars in comparison with normal stars.

### *M Stars*

A preliminary program to examine the feasibility of a narrow-band near-infrared classification system for late M stars was carried out by Kuhi. MK standards were observed with the photoelectric scanner using a 40-Å bandpass at about 20 wavelengths, for which sensitivity to spectral type and luminosity class had been determined from scans taken with a 10-Å exit slit or from previously published luminosity criteria. No difficulty was encountered in finding indicators of spectral type; the ratio of continuum  $\lambda 7,530$  to TiO  $\lambda 7,134$  changes by two magnitudes from M0 to M7; other TiO bands,  $\lambda\lambda 6,720, 7,940$ , and  $8,880$ , are more or less sensitive. Vanadium-oxide bands become more useful for types later than M6 to M7. However, most of the photographic luminosity criteria, such as line ratios of iron and titanium (Fe I  $\lambda 8,514$ /Ti  $\lambda 8,435$ ), or individual lines such as K I  $\lambda 7,699$  or Na I  $\lambda\lambda 8,183$  and  $8,195$ , are not sensitive enough when measured in a 40-Å bandpass. The ratio of two



continuum wavelengths,  $\lambda 9,700/\lambda 6,122$ , shows very good luminosity separation when plotted against spectral type; e.g., 0.3 magnitude between I and II, 0.2 magnitude between II and III, and 0.3 magnitude between III and V for spectral type M2. Thus in principle the spectral type and luminosity class are readily determinable. In practice, however, interstellar reddening would destroy the effectiveness of the continuum as a luminosity criterion and hence the usefulness of the system for classification of very faint stars. It is therefore hoped that some additional luminosity criterion can be found.

### *Pulsating Variables*

Simultaneous coudé and photoelectric-scanner observations of several stars of the  $\delta$  Scuti and  $\beta$  Canis Majoris star types are being carried out by Danziger and Kuhi. The changes in the effective temperature and surface gravity, and hence the radius, can be determined from the  $H\gamma$  profiles, the Balmer discontinuity, and the continuous energy distribution. Preliminary results for  $\rho$  Puppis suggest that the variation in temperature is small and that the light variation is mainly due to the radius variation of the star.

### *Absolute Energy Distribution*

Conti and Oke have completed a study of 24 stars in the Hyades. Both photoelectric scans for  $\lambda 3,390$ – $\lambda 10,800$  and slit spectra were used to determine absolute energy distributions of the continuum. These were compared with fluxes computed from Mihalas' model atmosphere to determine effective temperatures. The derived effective temperature-color relation for the main sequence passes through Vega ( $T_e = 9,350^\circ\text{K}$ ). The sun also falls on this same relation, indicating that the absolute flux system now being employed for stars is very nearly correct. Using this new temperature scale and bolometric corrections, one finds that the initial main sequence fits the one computed theoretically by

Iben, provided a mixing length parameter  $(\ell/H_d) \approx 1$ .

Whiteoak completed observations for a study of late-type dwarf stars which show considerable variations of the color  $P - V$  within each spectral type. About 50 stars with spectral types between G5 and K7 were observed at 17 discrete wavelengths between 4,956 Å and 10,500 Å with the Cassegrain scanner attached either to the 60-inch or the 100-inch reflector at Mount Wilson. The adopted resolution was 50 Å. The photomultiplier employed was an RCA 7102. Reduction to intrinsic fluxes was carried out by the observation of several stars that have been calibrated by Oke. Preliminary results suggest that, for stars of a particular spectral type, there is a considerable range of temperatures as defined by the slopes of the red continua. In general, the temperature variations seem to be correlated with the  $P - V$  colors.

The observations were completed by Whiteoak for an investigation of the wavelength dependence of interstellar reddening in five regions of the Milky Way, namely, in Perseus, Orion, Monoceros, Cygnus, and Cepheus. For 38 stars of early spectral type, continuum intensities were obtained at 30 wavelength settings between  $\lambda 3,448$  and  $\lambda 10,500$  with the Cassegrain photoelectric scanner attached to either the 60-inch or the 100-inch reflector at Mount Wilson. Observations at blue wavelengths were effected with the use of an RCA 1P21 photomultiplier; an RCA 7102 tube was employed for the red spectral region. The observations were reduced to intrinsic relative fluxes by the additional observations of stars that had been calibrated previously by Oke. The calibration was slightly modified below the Balmer limit and above the Paschen limit in order to yield a virtually continuous energy distribution for the observed stars of the earliest spectral types. Stellar reddening was derived by adopting theoretical models for unreddened energy distributions. The models for individual



stars were chosen by matching observed and theoretical Balmer discontinuities. The results confirm the variation of the galactic reddening law with longitude. Instead of being correlated with galactic structure, the law appears to be abnormal in regions containing  $H\alpha$  emission. In Orion, the law for stars outside the nebula is different from the law for stars within it.

### *Eclipsing Binaries*

Eggen completed his program of photometric observations of eclipsing binaries (mostly of the contact type). Among the systems chosen from the *Variable Star Catalogue*, two (AU Serpentis and XY Boötis) probably have incorrect periods, one (V449 Orionis) may be a T Tauri star, three (AC Leonis, V954 Ophiuchi, V803 Aquilae) showed no variation, and two (SZ Lyncis, BP Pegasi), or possibly four (V960 Ophiuchi, CV Cygni), are short-period RR Lyrae variables. Light curves in  $U$ ,  $B$ ,  $V$  were obtained for a contact binary in M67 and in  $R,I$  for VW Cephei. Photometry of early-type stars in the fields of several variables was obtained to aid in estimating the interstellar reddening. Photometry was also obtained for the physical companions to AM Leonis, AK Herculis, +30°2163, BX Andromedae, RZ Draconis, ZZ Cephei, CD Tauri, YZ Cassiopeiae, AD Herculis, MM Herculis, and ZZ Cygni, and for the newly identified proper-motion companions to VW Cep, V700 Cygni (Luyten), and W Ursae Majoris. AH Virginis is identified as a possible member of the Wolf 630 group, and several members of galactic clusters include EM Cephei, V701 Scorpii, TX Cancri, LW and BH Centauri, SZ Camelopardalis, and AH Cephei.

The members of clusters and wide physical pairs indicate that (1) the contact systems have a total luminosity and mass equivalent to two equal stars of the observed color, and (2) the observed  $U$ ,  $B$ ,  $V$  colors are not seriously affected by distortion of the components. The

short-period contact systems occupy a well-defined region in the color-period diagram with the position in this diagram affected by the evolutionary age. The available data for the short-period binaries among the U Geminorum stars and old novae, supplemented with new  $U$ ,  $B$ ,  $V$  observations of WZ Sagittae and  $R,I$  observations of RU Pegasi and AE Aquarii, suggest that those with periods in the same range as the contact binaries, i.e., V Sagittae, SS Cygni, RU Peg, and AE Aqr, may represent a later development of the contact systems; but, unless drastic period changes are acceptable, the shorter-period systems, i.e., WZ Sge, VV Puppis, UX Ursae Majoris, may represent the alternative development of stars that could not form (or if formed could not long exist) as contact binaries with periods less than 0<sup>d</sup>25. Both  $R,I$  and  $U$ ,  $B$ ,  $V$  photometry of RU Peg and its common proper-motion companions show that the red component of the close system is a main-sequence star with  $M_V$  near +6<sup>m</sup>.

### *Peculiar A-Type Stars*

Eggen has discussed the colors, luminosities, and motions of the 112 Ap stars brighter than visual magnitude 7.0 for which accurate apparent motions are available. He concludes that (1) these objects show little or no differential line-blanketing in comparison with normal objects in the same part of the ( $M_V$ ,  $B - V$ ) plane; (2) the Hg, Mn, and Si stars populate the Pleiades main sequence and most of the Eu, Sr, Cr stars lie above this sequence in a region contiguous to that occupied by the Am stars; (3) the Hg, Mn, and Si stars are kinematically related to the early B-type stars; (4) on the main sequence, the peculiar stars are slow rotators, but (a) there are stars seen pole-on that do not have a coherent magnetic field, (b) some Ap stars deviate considerably from pole-on, and (c) slow rotators are not necessarily Ap stars; (5) with the possible exception of two or three Eu stars, the deviations of the



observed colors from the ( $U - B$ ,  $B - V$ ) relation for main-sequence stars can be interpreted as resulting from reddening and gravity effects alone; (6) the only available mass for an Ap star (ADS 9352 Aa) places it on the mass-luminosity

relation; (7) at least 20 per cent of the Ap stars are spectroscopic binaries with the distribution of known periods similar to those for the Am stars; and (8) the weak-lined “ $\lambda$  Boötis” stars do not lie below the Pleiades’ main sequence.

## INFRARED STELLAR SPECTROSCOPY

The 100-inch coudé spectrograph, in the form arranged for the infrared observations of Mars, has been used by Münch and G. Neugebauer to explore the spectra of bright stars in the region  $\lambda\lambda 2.3\text{--}2.5\ \mu$ , with a resolving power of about 2,000. Actually, the signal-to-noise ratios obtained for a star as bright as  $\alpha$  Orionis, with a short time constant, are large enough that a resolution more than three times as high would be practicable. Stellar observations with such high resolving powers require, however, the introduction of a seeing-compensation system because of the necessary narrow entrance slits; such a system is now under development.

The extremely red objects in Taurus and Cygnus discovered by Neugebauer, Martz, and Leighton have been photoelectrically measured in the region  $0.8\text{--}1.1\ \mu$  by Jeffrey Scargle with the Cassegrain scanner of the 60-inch Mount Wilson telescope. Photographic spectroscopy of the Taurus object, obtained by Münch at Palomar, has shown the characteristic of a far-advanced M-type spectrum, the most prominent absorption features of which are the vanadium-oxide band systems of about  $0.74\ \mu$  and  $0.79\ \mu$ .

The quadrupole lines in the (2, 0) band of  $H_2$  at  $\lambda\lambda 1.16\ \mu$ ,  $1.14\ \mu$ , and  $1.12\ \mu$  are being observed in various low-tem-

perature stars, with the use of the photoelectric scanner of the 100-inch coudé spectrometer, with the ultimate purpose of determining the concentration of  $H_2$  as a function of temperature and gravity.

A search for He I  $\lambda 10,830$  absorption of possible chromospheric origin in selected stars of late spectral type brighter than fourth magnitude is being made by Vaughan and Zirin with the coudé scanner of the 100-inch telescope. In preliminary observations (fast scans) of 10 giant stars of spectral types F8–M3, having both strong and weak Ca II K-emission intensities, no He I line has been found, so that an upper limit of  $W_\lambda < 30\ \text{m}\text{\AA}$  can apparently be set for the equivalent width of the line in these stars. Interferometric techniques will later be used to extend the detection sensitivity to about  $2.5\ \text{m}\text{\AA}$ . Several stars with spectral types B7–A2 have also been observed. It is of interest that the peculiar A0 star  $\alpha^2$  Canum Venaticorum shows an absorption feature of about the expected strength ( $W_\lambda \sim 160\ \text{m}\text{\AA}$ ), agreeing in wavelength to within  $0.1\ \text{\AA}$  with the center of gravity of the transitions  $\text{He}^4\ \text{I}\ (2^3\text{S}_1 - 2^3\text{P}_{1,2})$ ; more detailed observations are being planned to determine whether the feature is variable and to provide a possible test for the presence of the isotope  $\text{He}^3$ .

## STAR CLUSTERS

### *M92*

Analysis of three-color photometry of stars brighter than  $V = 17^m0$  in the globular cluster M92 was completed by

Sandage, and Dr. M. F. Walker of the Lick Observatory. The program was started in 1954 to obtain ultraviolet excess values for giant stars in many globular clusters to confirm and extend



the discovery of the metal-abundance deficiencies in the old halo objects made by these authors in NGC 4147 in 1953. The M92 data, unpublished when confirmation of the large  $\delta(U - B)$  excess was obtained in 1956, has been augmented sporadically in the past eight years, and the number of photoelectrically observed stars brighter than  $V = 17^m$  is now about 75.

Analysis of the material has shown that, in addition to the large  $\delta(U - B)$  excess for the giants, a new and unexpected feature exists in the color distribution for stars on the subgiant- and asymptotic-giant branch of the color-magnitude diagram of M92. Stars of equal  $B - V$  on the two branches differ by as much as  $0^m.25$  in  $U - B$ . Differences of surface gravity for stars on the two branches cannot be the explanation because the observed difference in the emergent ultraviolet flux is 30 times too great. An unknown source of continuous opacity or abnormal line strengths for stars on one branch compared with the other could explain the difference. It is possible that differences in metal abundance caused by nucleosynthesis in the postevolution of the asymptotic branch stars could be involved.

Similar results have been found in an analysis of three-color data for M3. Although the effect is at present unexplained, its existence points to possible new phenomena in the evolution of globular-cluster giant stars.

#### M15

Sandage and Basil Katem are attempting to determine the intrinsic width of the main sequence in the color-magnitude diagrams of several globular clusters. Measurements and reduction have been completed for 350 stars in M15 fainter than  $V = 19$  on seven plates in each color of the  $B, V$  system taken with the 200-inch telescope. Calibration was obtained from the faint photoelectric sequence determined previously in M15 by Sandage; see *Year Book 63* (p. 22).

The statistical analysis for an answer

on the intrinsic width of the main sequence has not yet been finished, but a new feature of the color-magnitude diagram is suggested by the available data. A gap appears on the main sequence about one magnitude fainter than the break-off point, similar to the gap reported last year in the old disk clusters M67 and NGC 188. The absence of stars in the gap of M67 and NGC 188 was thought to be due to the fast time scale of collapse. The reason globular clusters were not expected to have a gap is that the deficiency of the metals in the member stars suggests that the carbon-nitrogen cycle does not operate for stars near one solar mass, but rather that the energy is produced by the proton-proton chain, which is more widely spread throughout the interior of the stars. The convective core would then be absent in these stars and hydrogen exhaustion would not occur simultaneously throughout the core; therefore no rapid core collapse would take place. Hence, the suggested observation of a gap in the M15 main sequence is surprising. If the gap is real, then either (1) the explanation of the gap in M67 and NGC 188 may not be correct, or (2) the supposition that globular-cluster stars do not contain convective cores may be wrong.

An effort to check the results is in progress by measurements of nearly 500 stars in the globular cluster M92 on 14 plates (7 in each color of  $B$  and  $V$ ) taken with the 200-inch telescope. Measurement and reduction of the  $V$  plates are complete, but the results from the  $B$  plates are not yet known. Although the photometric accuracy required is near the limit that can be achieved because the gap appears at a faint level ( $V \simeq 20^m$ ) and is only  $\Delta V = \pm 0^m.10$  wide, the large number of plates being measured should produce a definite answer within the year.

#### NGC 1866

In 1957 Arp established photoelectric standards near NGC 1866, the spherical blue star cluster on the outskirts of the



Large Magellanic Cloud. Now he and Frank Brueckel have reduced the photographic records of the variable stars in NGC 1866 that A. D. Thackeray accumulated over the years. High-accuracy light curves for seven of the eight cepheids known to belong to the cluster have been obtained in both blue and visual colors. The cepheids at mean color all lie together on the red side of the Hertzsprung gap and just at the beginning of a well-defined giant branch. Period-luminosity and period-color properties are identical with cepheids in the Small Magellanic Cloud. But the period-amplitude behavior of the cepheids and the color-magnitude diagram of the cluster both show NGC 1866 to be intermediate in properties between the SMC and the Galaxy. In particular, the giant branches become progressively redder at the same age in the

SMC-NGC 1866-Galaxy sequence. Such a progression would be expected if the metal content became progressively stronger in the direction SMC-NGC 1866-Galaxy. If this is the correct explanation, the frequencies of cepheid periods, inferred mass densities, and other properties of these three galaxies can also be explained in a natural way.

A chapter dealing with all the globular clusters in our own Galaxy has been prepared by Arp for Vol. V of *Stars and Stellar Systems* (edited by Kuiper and Middlehurst). It deals with the distribution of different kinds of globular clusters and properties of the system of globular clusters. Best distances, reddening, and intrinsic properties are given for all globular clusters in a definitive master table. A distance to the center of our own Galaxy of 9.9 kpc is derived.

## INTERSTELLAR GAS AND GASEOUS NEBULAE

Danziger and Conti have obtained IIaF plates of distant B stars in whose spectra the interstellar sodium D lines are strong, with a view to lowering the upper limit of interstellar lithium set by Spitzer in 1949. No positive identification of the interstellar lithium lines has been made, but the upper limit will be at least a factor of 5 lower than the previous limit.

The installation of pulse-counting equipment in the 100-inch coudé scanner and the adaptation of Fabry-Perot interferometers to the system have made possible the observation of interstellar absorption lines under high resolution with photoelectric techniques. Münch and Vaughan, using an FW 130 photomultiplier with S20 response (without the interferometer), found that a direct scan of one of the Na D lines in  $\alpha$  Cygni can be made with a resolving power of  $10^5$  in about one hour with a 5 per cent uncertainty, under good seeing conditions. With the Fabry-Perot etalon, the sensitivity to seeing is much less, and one can reach twice as high resolution in about half as long a time.

Oke has used the scanner to measure the absolute flux from the central non-filamentary part of the Crab Nebula. The energy distribution agrees moderately well with that published by O'Dell; a rather abrupt change in the slope of the energy distribution occurs at  $\lambda 4,300$ .

Vaughan is making interferometric observations to provide profiles of the He I  $\lambda 10,830$  metastable resonance emission line in bright, compact planetary nebulae covering a range of expansion velocities at a resolution of about  $\frac{1}{3}$  Å at the 60- and 100-inch telescopes. The nebulae thus far observed are IC 418, NGC 6572, and NGC 6826, all having relatively low expansion velocities. The shapes and widths of the  $\lambda 10,830$  line are essentially identical in these nebulae. The intrinsic line structure of the line is partly blended because of thermal broadening and differential motions within the nebulae. Some slight asymmetry of the lines, but no kinematical structure, is observed in the integrated light from the nebulae as a whole. Differences can be seen in the intensity ratios of the



intrinsic fine-structure components, which may show some correlation with Lyman- $\alpha$  radiation intensities inferred from He I  $\lambda 10,830/\lambda 5,876$  line intensity ratios provided by O'Dell (private communication). Note that in all cases the  $\lambda 10,830$  line is displaced by about  $+13$  km/sec, or about one half the line width, with respect to the heliocentric nebular velocities reported from spectroscopic studies by O. C. Wilson. Vaughan had previously reported (in 1964) a velocity shift of nearly the same magnitude and the same sign between  $\lambda 10,830$  and [O III]  $\lambda 5,007$  in the Orion Nebula.

There are compelling reasons for believing that the observed shifts cannot be attributed to a calibration error. While they have not been explained, their possible origin as the result of redistribution in frequency caused by resonance scattering in the nebulae is being studied. Such a possibility would be of interest in connection with more general problems concerning the diffusion and escape of resonance-line radiation in optically thick nebulae.

Arp found that the galactic nebula NGC 1999 in Orion shows strong polarization all around its rim, with the electric vector parallel to the rim.

H. van Woerden has continued his

study of the kinematics and cloud structure of the interstellar medium, combining data on Ca II from high-dispersion spectra taken at the 100-inch coudé with 21-cm hydrogen-line profiles observed at Dwingeloo Radio Observatory in the Netherlands. He finds, both in Orion and in a general survey of hydrogen at intermediate galactic latitudes, that the internal motions within hydrogen clouds closely follow Gaussian distributions, with radial-velocity dispersions ranging from 1 to 5 km/sec. This result is in good agreement with studies by Muller, and by Clark, Radhakrishnan, and Wilson, of hydrogen in the absorption spectra of point sources, and with Mrs. Dieter's investigation of the 21-cm emission in the region of the north galactic pole. Clouds with velocity dispersions smaller than 1 km/sec appear to be rare. The major limitation of the hydrogen studies is in their resolution on the sky; this limitation is removed in the optical spectra. Analysis of the latter indicates that the calcium ions, too, have velocity dispersions ranging upward from 1 km/sec. Caution is required here since the narrowest components found are only a little wider than the instrumental profile; the optical studies might therefore be limited by velocity resolution.

## INFRARED SKY SURVEY

As one part of a program of infrared astronomy sponsored by the National Aeronautics and Space Administration, a survey of the sky in two infrared spectral ranges,  $0.68\text{--}0.92\ \mu$  and  $2.01\text{--}2.41\ \mu$ , is being carried out by R. B. Leighton, G. Neugebauer, and B. Ulrich. D. E. Martz was associated with the project during its initial stages. The motivation for such a survey is to obtain an unbiased census of objects that radiate in the  $2.0\text{--}2.5\ \mu$  atmospheric window; this will, of course, include many ordinary stars, but might also reveal many potentially interesting objects that would not be included in an

a priori selection of objects to be measured.

The survey instrument is located on Mount Wilson and consists essentially of a 62-inch  $f/1$  aluminized plastic mirror capable of  $2'$  resolution. The entire mirror is vibrated sinusoidally at 20 cps to move images across a detector system composed of a liquid-nitrogen-cooled, eight-element array of PbS detectors, arranged in a north-south line of four "push-pull" pairs, and a silicon photo-detector. Each pair of PbS detectors spans a declination (Dec) range of  $10'$  so that  $40'$  are spanned by the entire



array. The Si detector spans a 20' Dec range coinciding with that of the central two pairs of PbS detectors, and is located about 15' west of the PbS array. The telescope is normally swept in right ascension (RA) at 15 or 30 times sidereal rate in a raster pattern one hour of RA in "length" with 15' Dec steps. In this way a strip of sky 3° or 6° wide in Dec is covered each night, with each point of sky being covered at least twice.

The sensitivity is such that minimum detectable sources have infrared apparent magnitudes of approximately  $I(0.8 \mu) \approx 9$  and  $K(2.2 \mu) \approx 5$ . From results obtained to date, it is estimated that ultimately several thousand objects bright enough at 2.0–2.5  $\mu$  to be measured within  $\pm 0.2$  magnitude will be detected. Positions can be measured within about 1' in Dec and 0<sup>m</sup>.1 in RA. Although the system is preferentially sensitive to "point" sources, it is calculated that a 450°K blackbody radiator with a 10" radius would give a signal-to-noise ratio of about 10:1.

Data from the survey are being reduced with the use of the California Institute of Technology computing

facility. The complete survey may require about two years. A number of strikingly red stars have already been found. Since most of these "super-red" stars occur in the Milky Way, interstellar reddening may be of some consequence, but in at least a few cases the stars seem to be intrinsically extremely red. The color index  $I - K$  of about 20 stars has been as large as 7–8, which indicates blackbody temperatures as low as 1,000°K. The brightest of the super-red stars so far found has a  $K$  magnitude of about 0.

As another part of the program of infrared astronomy, Dowell Martz, a senior research engineer, and Eric Becklin, a graduate student, constructed a multichannel photometer for use in the wavelength regions between 1  $\mu$  and 15  $\mu$ . With this photometer, Becklin has made broadband measures of several stellar objects, especially the extremely cool stars found in the survey carried out on Mount Wilson, at several wavelengths between 2  $\mu$  and 4  $\mu$ . In addition, he has made an extensive spatial survey of the distribution of 2.2- $\mu$  radiation emitted from the Orion Nebula.

## RADIO SOURCES

### *Identification*

Sandage, with P. Veron and, independently, John D. Wyndham and T. A. Matthews of the Owens Valley Radio Observatory staff, continued the program of identifying quasi-stellar radio sources. During the year most of the revised *Third Cambridge Catalogue* of radio sources was analyzed, with the use of very precise radio positions from Wade, Toth, and Heeschen at the National Radio Astronomy Observatory, from Adgie at the Royal Radar Establishment, England, and from the California Institute of Technology (CIT) observers. Near the end of the report year a cooperative agreement for joint identification work

was made between Sandage, Veron, and Wyndham.

It appears that most of the revised *3C Catalogue* will be identified with optical objects. The catalogue contains 328 sources, of which one is probably spurious (3C129.1); 29 are galactic or probably galactic; 40 of the presumed extragalactic sources are in highly obscured regions near the galactic plane. The 258 remaining identifiable sources can be divided into four groups, according to progress toward final identification as of June 1965:

1. There are 95 certain and 32 possible identifications with radio galaxies. They are nearly all elliptical galaxies or compact galaxies of Morgan's class N.



About 50 per cent are in groups or clusters.

2. There are 35 certain and 18 possible identifications with quasi-stellar radio sources (QSSs). Three-color photoelectric photometry has confirmed that all 35 have the abnormal color indices that distinguish the member of the class. The percentage of QSSs to the total list is  $53/258 = 20$  per cent. This is a minimum value because there will be many QSSs in groups 3 and 4.

3. There are 18 sources in empty optical fields to the limit of the 48-inch schmidt plates. Photography of these fields has begun with the 200-inch telescope.

4. There are 60 sources remaining which lack accurate radio positions, and no positive identification can yet be made.

#### *Spectroscopic Observations of Quasi-Stellar Sources*

Immediately after the discovery of the redshifts of the quasi-stellar radio sources 3C273 and 3C48, it became clear that the quasi-stellar sources should be observable to very large redshifts. It was expected, however, that their detection would be difficult because there was considerable uncertainty about the far ultraviolet emission spectrum that these objects might exhibit. Also, the detection of the emission lines was hampered by their large width (around 40 Å) and their low intensity relative to the continuum (perhaps about 20 per cent). The first source in which the emission lines could not at once be identified was 3C245. Dr. Schmidt, who observed this object starting in 1963 at the suggestion of Dr. C. Hazard, then of the University of Sydney, found two weak emission lines. The source 3C287, observed early in 1964, showed two emission lines with the same ratio of wavelengths (about 1.47) as those in 3C245. This ratio fitted well with that of C III ( $\lambda 1,909$ ) and of Mg II ( $\lambda 2,798$ ).

In October 1964, Schmidt observed

CTA 102, which again showed two lines with wavelength ratio about 1.47. However, the source 3C9 yielded two lines with wavelength ratio about 1.27. This ratio suggested identification with Ly  $\alpha$  ( $\lambda 1,261$ ) and C IV ( $\lambda 1,550$ ), but obviously confirmation of all these line identifications was greatly needed. This might have been obtained from a search in the infrared for lines that normally are seen in the visual part of the spectrum. The long exposure times that would have been required (more than 25 hours) made such a search rather impracticable.

Confirmatory evidence was finally obtained in February 1965. First, spectra of the QSS 3C254 showed not only the line pair with ratio 1.47, but also three other lines that could be identified with familiar lines of [Ne V], [O II], and [Ne III]. This confirmed the identification of the two former lines as Mg II ( $\lambda 2,798$ ) and C III ( $\lambda 1,909$ ). Second, further observations of 3C287 showed a line in the far ultraviolet at 3,192 Å, which, with the above evidence, was immediately identified as C IV ( $\lambda 1,550$ ). The finding of this line confirmed its earlier suggested identification in 3C9.

The resulting redshifts  $z = (\lambda - \lambda_0)/\lambda_0$  are 0.734 for 3C254, 1.029 for 3C245, 1.037 for CTA 102, 1.055 for 3C287, and 2.012 for 3C9. If they are cosmological redshifts, we are looking back in time, in the case of 3C9, to a few billion years after the expansion of the universe started. Redshifts of this magnitude should play an important role in the further study of cosmological models. Observations aimed at further redshift determinations are being continued by Schmidt.

#### *Absolute Energy Distribution*

Oke has continued to measure absolute energy distributions in the spectra of QSSs. Observations have been made of 3C48, 3C245, and 3C286. The energy distribution in 3C48 is moderately red and in agreement with the broadband results of Matthews and Sandage. In the



infrared,  $H\beta$  and  $\lambda 5,007$  of [O III] have been measured, with  $\lambda 5,007$  found to be approximately three times stronger than  $H\beta$ . The line  $H\alpha$  has also been found at  $\lambda 8,970$ . The absolute intensity is high, but quantitative results have not yet been obtained because the line is in a region of serious atmospheric absorption. There is some evidence for very broad unidentified features in the spectrum. In 3C286, a recent series of photoelectric-scanner measurements has indicated the presence of an emission line near  $\lambda 3,528$ . If this emission line is combined with the one found by Schmidt at  $\lambda 5,170$ , it is evident that  $\lambda 5,170$  is the Mg II line  $\lambda 2,798$ , and  $\lambda 3,528$  is the  $\lambda 1,909$  of C III. The value of  $z$  is 0.848.

#### *Variability of Quasi-Stellar Sources*

A study has been started of the optical variability of the visually quasi-stellar nuclei of extragalactic radio sources, with the use of the films and plates taken by Zwicky and his collaborators from 1934 until 1964. Photographic magnitudes were derived by Zwicky and Mrs. Karpowicz from 66 plates taken between May 8, 1934, and April 1961. Preliminary results show that the maximum amplitude of the variations amounts to about 0.6 photographic magnitudes and that there is a suggestion of an overall periodicity of four years with a second harmonic of two years.

#### *Interpretation*

A reappraisal of the nature of the redshifts found in the QSSs is being carried out by Schmidt. The cosmological interpretation of the redshifts leads to an energy flux of around 100 times that of giant galaxies. Since the light variations demand a small size of the optical source, of perhaps a light-year or less, one has to face the problem of producing an enormous amount of energy in a very small volume. It may be well, at this stage, to reinvestigate the nature of the redshifts. The spectra of the brighter

QSSs allow estimates of the electron density to be made, as mentioned in *Year Book 63* (p. 28), which play an important role in these discussions.

The first alternative explanation of the redshifts is that they might be gravitational. Schmidt has revised an earlier discussion of 3C48 that he and Greenstein had published and finds that a lower limit for the mass is  $2 \times 10^{13} M_{\odot}$  and a lower limit to the distance is 2 Mpc. These revised limits are based on the requirement that the total mass in the Local Group of galaxies cannot exceed  $2 \times 10^{12} M_{\odot}$  from the virial theorem. On the basis of gravitational redshifts, the observed redshift-magnitude relation cannot be understood.

The second alternative explanation is offered by Terrell, who suggests that the QSSs might have been ejected from the nucleus of our Galaxy. The distance to 3C273 would then have to be at least 200 kpc to explain the absence of observed proper motion. The redshift-magnitude relation would imply that all QSSs were ejected in one explosion. Study of the spectra allows a lower limit of  $10^5 M_{\odot}$  to be placed on the mass of 3C273. The assumption that it is typical of the 1,000 or more QSSs that must exist gives a lower limit to their total mass of  $10^8 M_{\odot}$ . Since most of them travel at a speed little less than that of light, the total kinetic energy would be  $10^{62}$  ergs. It appears, then, from this and the previous explanation, the noncosmological interpretations of the redshifts would lead to results that are less probable and more spectacular than the cosmological interpretation.

#### *Photometry*

Sandage began three-color photometry of all radio sources with known values of the redshift to obtain absolute luminosities and the Hubble expansion diagram. Data for 40 radio galaxies and all known QSSs were obtained.

Corrections for finite photometric measuring apertures and for the redshift

K term were applied to all data. A new table of the K correction was computed from Oke and Code's energy distribution curve of the giant elliptical NGC 4374.

The Hubble diagram in both  $V$  and  $B$  magnitudes shows very little dispersion ( $\sigma \text{ mag} \simeq 0^m.5$ ) for radio galaxies whose  $L$  (radio)  $\geq 2 \times 10^{40}$  ergs/sec. Furthermore, the correlation line of  $m$  on  $z$  is indistinguishable from the line for the first brightest nonradio galaxies in the great clusters such as Coma, Coronae Borealis, and Ursae Majoris II. Because these are the brightest galaxies known, it appears that a necessary condition for a galaxy to become a strong radio source is that it be a giant elliptical or N-type galaxy near the top end of the mass and luminosity functions.

The data fit a straight line ( $q_0$  apparent

$= +1$ ) to the limit of the redshift determination (almost all by M. Schmidt) at  $\Delta\lambda/\lambda_0 \simeq 0.26$ . This redshift is not large enough to lead to a decision among cosmological models. However, photometry of the nine QSSs for which Schmidt has redshifts reaching  $\Delta\lambda/\lambda_0 = 2$  also lie on a linear relation ( $q_0 = +1$ ) to the accuracy of the data. At these enormous redshifts, the difference between the steady-state model and the  $q_0 = +1$  model is  $\Delta m = 2^m.4$ , which is a factor of nearly 10 in intensity. It is too early to give a definitive value of  $q_0$  from only nine objects, but at the moment the present sample does violate the  $[m, z]$  prediction of the original steady-state theory of the universe. A sample of 30 QSSs will probably be necessary to give a firm conclusion.

## RADIO-QUIET QUASI-STELLAR GALAXIES

During the search for QSSs by the two-color method, Sandage noticed that many ultraviolet starlike objects appeared on the plates far from the radio positions. Photoelectric photometry of the first four of these objects, initially called interlopers, showed that they imitated the QSSs in their peculiar color distribution and could not be distinguished from the true QSSs by their optical properties alone.

A special survey for more interlopers was made of two fields with the 48-inch schmidt by Veron. Photometry by Sandage showed that 15 of 21 objects measured had QSS colors, but were radio quiet to  $10^{-25}$  W/ $m^2$  cps at 178 MHz. The distribution of interlopers found in this way was similar to that of blue "stars" found by Haro and Luyten in high galactic latitudes, and Sandage concluded that many of the fainter Haro-Luyten objects and the interlopers were identical.

Counts in the Haro-Luyten *Catalogue* showed that  $N(m)$  underwent a sharp change of slope near  $B \simeq 15^m$ , which is the magnitude at which the color distribution

radically changes in the  $U - B$ ,  $B - V$  diagram for the blue objects. The  $N(m)$  and two-color diagrams could be understood if, instead of being stars, the objects were highly redshifted, radio-quiet blue stellar galaxies. The slope  $dN(m)/dm$  of the count distribution was observed by Haro and Luyten to be 0.38, which was the predicted value on cosmological theory if the redshift-apparent magnitude relation for these interlopers was the same as for the QSS.

Sandage therefore predicted that many objects of the Haro-Luyten class should have redshifts. Observations by Sandage with the 200-inch prime-focus spectrograph showed that blue objects Tonantzintla 256 and 730 had redshifts of  $\Delta\lambda/\lambda_0 = 0.1307$  and  $0.0877$ , respectively, while one of the interlopers found by Veron had  $\Delta\lambda/\lambda_0 = 1.241$ , as determined by Schmidt.

The conclusion, therefore, is that at least some of the Haro-Luyten halo "stars" are not stars at all but distant, radio-quiet objects similar to the QSSs in optical properties. These objects have



been named quasi-stellar galaxies (QSGs). It is important to emphasize that, unlike the Morgan N-type compact galaxies, most of them appear starlike on plates, with no hint of nebulosity.

The spatial density of QSGs to QSSs is estimated to be 500:1, but only if most of the Haro-Luyten objects fainter than  $B \simeq 16$  prove to be extragalactic. If the QSGs are a later stage of evolution of QSSs, the ratio of lifetimes in these two phases would then be 500:1. Adopting  $10^6$  years as the radio life of QSSs would give  $5 \times 10^8$  years as the lifetime of the blue "star" phase of QSGs. It is too early to understand the mechanism of formation, but one attractive hypothesis appears to

be that these are galaxies just forming, and what is observed is the collapse phase—a process believed to have occurred in our own Galaxy at its time of formation. The collapse of our Galaxy was discussed by Eggen, Lynden-Bell, and Sandage in *Year Book 61* (pp. 25–26).

The QSGs, if more numerous than QSSs, should be of great significance in the study of the cosmological problem. But it must be emphasized that it is not yet clear how many of the Haro-Luyten objects fainter than  $B = 16$  are actually extragalactic. Determining this percentage will be an important problem in this subject for the next few years.

## GALAXIES

### *Energy Measurements*

Oke has used the scanner to make further measurements of the absolute energy distribution in the spectra of galaxies. A careful comparison is being made between M31 and M32 to determine the cause of the marked difference in color. Most of the new observations have been made in the red and infrared from  $\lambda 5,000$  to  $\lambda 11,000$ . Douglas A. Keeley and Oke are trying to determine the stellar content required to produce the observed energy distributions. K corrections are being computed with the use of complete energy distributions.

Oke and Wallace L. W. Sargent have obtained both slit spectra and photoelectric spectrophotometric measures of the Seyfert galaxy NGC 4151. Absolute intensities of most of the emission lines have been determined. The electron temperature is approximately  $40,000^\circ\text{K}$  and the density appears to be high, although the various density criteria do not agree. The continuum is very red and apparently without features, indicating that it is not produced by cool stars. Bound-free and free-free radiation from hydrogen also cannot be responsible for

the continuum. The most likely explanation is that the continuum is synchrotron radiation. Similar photoelectric measurements of the continuum have been made for NGC 1068 and 1275. In both of these cases the continuum may be largely synchrotron radiation.

### *Magnitudes and Redshifts*

Schmidt has published redshifts and qualitative descriptions of the spectra of 31 radio galaxies. Only 3 radio galaxies show no emission lines, while 9 show only  $\lambda 3,727$  of [O III]; the remaining 23 radio galaxies exhibit other forbidden lines and the Balmer lines of hydrogen in emission. Thus almost all radio galaxies show emission, whereas less than 10 per cent of comparable nonradio D galaxies do so. Absorption lines are seen only if the emission lines are few and weak. In the few cases where the size of the emission region has been established, analysis of the spectrum yields the density and mass of ionized hydrogen. In 3C33 the size of the H II region is 3 kpc, the electron density is about  $5\text{ cm}^{-3}$  (if uniform) and the mass of ionized gas is  $2 \times 10^9 M_\odot$ . The recombination time of the ionized gas ( $2 \times 10^4$  years) is only one tenth of



the minimum lifetime of the radio source as computed from the separation of the two radio components (200 kpc). This, together with the high incidence of emission lines in radio galaxies, suggests that there is a continuing source of excitation in the optical galaxy long after the formation of the radio source.

### *Redshift-Diameter Relation*

During 1964–1965, Baum made some successful observations at Palomar with a new instrument mentioned in *Year Book 63* (p. 40). It is called a “galaxy image synthesizer,” and its purpose is to provide data on the angular diameters of galaxies belonging to clusters. The more distant the cluster, the smaller and fainter the member galaxies appear to be. Angular diameter is therefore an observable parameter to be used, together with redshift and magnitude, in testing various cosmological models. The new diameter data will be interpreted in conjunction with the photoelectric redshifts and magnitudes that Baum has been collecting during recent years.

The galaxy image synthesizer is a photographic device for comparing the images of real galaxies with synthetic ones. Two plates are exposed simultaneously, one to a cluster of galaxies and the other to an adjacent field of stars. The synthetic galaxies are generated by moving the star-field plate during exposure in such a way that an ideal point image would be spread out into the intensity profile of an E0 galaxy. The amplitude of motion can be changed from one pair of plates to the next so that a graded sequence of sizes is synthesized for comparison with the real galaxies on the nonmoving plates. The method is immune to all the usual disturbing effects, such as atmospheric “seeing,” night-sky radiation, emulsion turbidity, and instrumental scattering. This cancellation of disturbing effects is essential, because the program has to include clusters so distant that the images of member galaxies can barely be dis-

tinguished from those of faint stars under good observing conditions.

Owing to the large uncertainties with every test of world models, it is extremely important to observe all possible parameters and take them into account. For this reason, the redshift-diameter relation, even if only rough, will be a crucial input. It is perhaps less vulnerable to age effects than galaxy magnitudes and counts of QSSs. Although the accuracy of Baum’s diameter-measuring method may be marginal, no practical alternative seems to be available with today’s techniques. To date, 17 pairs of plates have been obtained with the galaxy image synthesizer, and about a dozen more are needed to attempt a first assessment of the results.

### *Investigations of Individual Galaxies*

Miss Swope has worked on the color-magnitude diagram of the Leo II System, another dwarf galaxy like the Draco System. She has measured over 2,000 stars on two photographic and two photovisual plates; other plates, that Baade had taken, can be used to transfer the photographic magnitude of S.A. 57 to the Leo II System, but as yet no standards are available for the photovisual system. The horizontal branch of the C-M diagram is at  $22^m0$ . There are some 200 variables in Leo II that were discovered by Baade. Most are RR Lyrae-type variables; a few are red giants.

Arp, using special photographic techniques, has discovered a faint luminous ring around the prototype spiral galaxy M81. The ring has been explained in terms of the synchrotron action of electrons with energy  $\geq 1,000$  Bev exploded from the neighboring M82 companion galaxy. This interpretation offers the first demonstration of the existence of an overall magnetic field around a galaxy. Moreover, because the brightness and duration of the ring are very sensitive to the strength of the M81 magnetic field, the strength of the magnetic field around this normal Sb



spiral can be accurately computed as a few microgauss at approximately 20 kpc from its center. A recent private communication from De Jong at the National Radio Observatory shows that the isophotes of radio emission flare out just over the position of the ring, particularly at 1,410 Mc/sec. Spectroscopic and photographic work with the 200-inch and polarization with the 200-inch and 48-inch will continue. Studies of this very faint ring, both optically and in radio wavelengths, hold promise of yielding information both on the behavior of plasmas under galactic and intergalactic conditions and on the magnetic and plasma properties of galaxies themselves. According to Arp, present results permit one to compute a corrected time interval of about  $4 \times 10^5$  years since the explosion in M82 (cf. Lynds and Sandage, 1963; and Burbidge, Burbidge, and Rubin, 1964).

#### *Compact Galaxies and Compact Parts of Galaxies*

Three lists have been compiled by Zwicky containing the positions of about 700 compact galaxies and compact parts of galaxies. Direct photographs and spectra of more than 100 of these objects have been obtained by Zwicky with the 200-inch telescope. Among them are a dozen that are blue and that have emission-type spectra, described below.

While the average surface brightness,  $\sigma$  (photographic magnitudes per square second of arc), of ordinary galaxies such as listed and described in the NGC and the *Shapley-Ames Catalogues* lies in the range  $21.0 < \sigma < 26.0$ , the luminous compact galaxies that are resolvable with the 200-inch telescope and that have been investigated so far are characterized by average values of the surface brightness which lie in the range  $15.0 < \sigma < 21.0$ . Those compact extragalactic objects that cannot as yet be resolved with the largest telescopes, such as the QSSs and the compact nuclei of some of the radio-

quiescent galaxies, have values of  $\sigma < 15.0$ .

Among the compact galaxies, as characterized by their spectra, representatives of three subclasses are of particular interest: (1) Compact galaxies with emission spectra (Table 2); the symbolic velocities of recession for the last four systems lie in the range from 778 km/sec to 11,470 km/sec. (2) Compact galaxies with pure absorption spectra (Table 2). (3) Compact galaxies with mixed spectra. Among the systems investigated, these are the most frequent. One example is the object containing two very compact nuclei within a less luminous compact matrix at RA  $1^h20^m6^s$ , Dec  $+34^\circ19'$  (1950), whose spectrum shows the Balmer lines as well as H and K in absorption and  $\lambda 3727$  bright.

In addition to all possible combinations of  $U - B$ ,  $B - V$  encountered in the study of ordinary stars, white dwarfs and QSSs, some even stranger colors, such as  $U - B = -2.0$  and  $B - V = 0$  are found for compact galaxies whose spectra show a very weak continuum with one very bright emission line,  $\lambda 3,727$ , dominating the whole spectrum.

According to prepublication information made available by Dr. J. D. Wyndham of the Radio Astronomy group of the California Institute of Technology, not more than five per cent of the 700 compact objects contained in the lists mentioned above are radio sources with a flux greater than 9 flux units at 178 MHz [1 flux unit =  $10^{-26}$  W/m<sup>2</sup> (cps)<sup>-1</sup>]. Since radio-emitting compact galaxies (of type N, for instance) have the same spectral characteristics as some of the compact galaxies investigated, Zwicky concludes that, among compact galaxies of a given set of characteristics, both structurally and spectrally, some are strong radio emitters while others are not. Among the radio-quiescent quasi-stellar compact galaxies of the subclass just discussed, objects were found whose spectra are identical with those of the QSSs and all

TABLE 2. Compact Galaxies with Emission and Absorption Spectra

1950 Position		
Right Ascension	Declination	Type of Spectrum
<i>Emission Spectra</i>		
17 <sup>h</sup> 27 <sup>m</sup> 1	+50°15'	Featureless continuum; blue
01 19.5	−1 18	Blue continuum with broad width of ~ 100 Å emission bands superposed
16 22.1	+41 12	Intense blue continuum with permitted and forbidden emission lines of H, He II, [O II], [O III], [Ne III], [Ne V], [S II] superposed
14 39.2	+53 44	Continuum of moderate intensity with emission lines of H, He II, C III, C IV, [O II], [O III], [Ne III], [Ne V], [S II] superposed
9 30.5	+55 27	Double system. Both spectra showing moderate and weak continuum, respectively, with emission lines of H, He II, [O II], [O III], [Ne III]
11 08.5	+28 57	Weak continuum with only λ3727 or [O II] very intense in emission
<i>Absorption Spectra</i>		
12 28.0	+12 46	K0, with broad absorption lines corresponding to an internal radial velocity dispersion of 370 km/sec
1 01.2	+29 52	Spectrum of type A7, $V_s = 24,360$ km/sec, radial velocity dispersion greater than 700 km/sec

of which, if moved to a few times their present distance, could not be distinguished from stars with any of the present-day optical telescopes.

Changes in apparent brightness of some very compact galaxies seem to occur. In particular, marked variability has been observed in the case of an object at RA 0<sup>h</sup>38<sup>m</sup>33<sup>s</sup>, Dec +40°03' (1950), but it could not yet be ascertained what the real nature of the object is or if some variable foreground star lies in its line of sight.

*Posteruptive Galaxies*

A few dozen probable cases of posteruptive galaxies have been singled out for more detailed analysis with the 200-inch telescope. Direct photographs and spectra of these outstanding systems have been obtained:

1. Galaxy at RA 14<sup>h</sup>49<sup>m</sup>18<sup>s</sup>, Dec +35°45' (1950). The galaxy shows conical jets to both sides, which, to judge from tests with the 48-inch schmidt, appear

polarized. (This system also bears the Vorontsov-Velyaminov designation VV 324a.)

2. Galaxy at RA 14<sup>h</sup>48<sup>m</sup>58<sup>s</sup>, Dec +35°47' (1950). This galaxy shows a beautiful emission-line spectrum, indicating a symbolic velocity of recession of  $V_s = 1,140$  km/sec.

3. Double galaxy NGC 5394-5395 at RA 13<sup>h</sup>56<sup>m</sup>36<sup>s</sup>, Dec +37°40' (1950). NGC 5394 has a very compact core, a halo, and extensions, resulting in a most remarkable spectrum.

4. Galaxy at RA 15<sup>h</sup>14<sup>m</sup>06<sup>s</sup>, Dec +43°21' (1950). At right angles to an edge-on spiral, this galaxy shows two faint but uniform, symmetrical conical extensions, the distance from tip to tip being several times that of the main body of the galaxy (*Proc. Padua Symp. Giornate Galileiane*, 1964).

5. System at RA 11<sup>h</sup>22<sup>m</sup>42<sup>s</sup>, Dec +54°40' (1950). Massive disk with long narrow plume in which there is a starlike condensation. Both the compact disk and



the starlike condensation are blue, showing broad emission lines. Line widths are about 100 Å for H $\beta$  and H $\gamma$ . The object is also identical with VV 144 and with Luyten's blue "star," LB 2012. Symbolic velocity of recession  $V_r \cong 6,500$  km/sec.

*Peculiar Galaxies, Multiple Galaxies,  
and Clusters of Galaxies*

Direct investigations of the structure, the spectra, and the polarization of peculiar galaxies have been continued by Zwicky, Arp, Herzog, and Kowal. Herzog has carried out some interesting studies on the possible three-dimensional structures of double systems of galaxies. He has also found some remarkable cases of the absorption of light through intergalactic bridges (see *Publ. Astron. Soc. Pacific*, 77, 94, 1965, and 77, 119, 1965). C. T. Kowal found one of the first probable cases of an intergalactic obscuring cloud (*Astron. J.*, 69, 757, 1964). A second possible case of this type is being investigated by Zwicky. Kowal has also pointed out the probability that NGC 3314 in the Hydra I cluster of galaxies is a postmerger galaxy of the type of M82, with a polarized lateral jet. Zwicky and Mrs. M. Karpowicz have completed the statistical analysis of "Areas in the Sky Covered by Clusters of Galaxies," listed in Vols. III and V of the *Catalogue of Galaxies and Clusters of Galaxies* prepared by Zwicky with the cooperation of Herzog, Wild, Kowal, and Mrs. Karpowicz.

The *Atlas of Peculiar and Interacting Galaxies* has been in preparation by Arp for more than four years. It consists of 338 photographs, mostly taken with the 200-inch telescope under good seeing conditions, arranged on 57 pages in groups of objects that are empirically similar. The photographic printing was done by William B. Miller, Observatory Photographer. The *Atlas* will be submitted soon for publication as a supplement to the *Astrophysical Journal* and will also be available in the form of 11- by 14-inch photographic copies. In the compilation, Arp has begun to obtain spectra of objects

whose radial velocities have not yet been measured.

The set of limiting plates obtained with the 200-inch telescope during the process of making the *Atlas* has revealed many interesting stellar, semistellar, and diffuse objects that are now being studied spectroscopically. One object which appeared to be like a slightly fuzzy double star turned out to be a tiny double galaxy. For each component  $M_{pg} \approx -13$ , and the diameter is only 70 psc. With an appropriate plate and filter combination, the 48-inch telescope revealed a slightly larger object which, like the other, had [O III] lines in emission, about  $2\frac{1}{2}^\circ$  away from the first object. More objects will be searched for with the 48-inch in the coming year with this method.

These observations confirm that there are many extragalactic objects with highly unusual diameters. Those discovered by Arp and now being investigated by him are undoubtedly related to the blue galaxies first discovered by Haro (1956), the compact galaxies later discussed by Zwicky, and the blue extragalactic objects recently encountered by Sandage in his and Veron's photographic search for QSSs.

Arp, in collaboration with Eugene Haslan of the Lick Observatory, made composite photographs of the Coma and Virgo clusters of galaxies with the  $f/1$  schmidt camera in a search for faint nebulous material within. No such nebulosity was revealed in preliminary evaluation.

*Catalogue of Galaxies and  
Clusters of Galaxies*

Since the publication of Vols. I and II of the *Catalogue*, attention has been concentrated on the completion of Vols. III and V, while the necessary observational material is being secured for Vols. IV and VI. The work on Vol. V, which covers 99 fields of the National Geographic Society Sky Survey with the 48-inch schmidt, has now been completed by



Zwicky with the cooperation of Mrs. M. Karpowicz and C. T. Kowal. The results of the survey of 2,679 clusters of galaxies have been readied by Zwicky for Vol. III, and Herzog expects to finish his work on the photographic magnitudes of the individual galaxies to be included by the end of 1965. The construction of the *Catalogue* has been supported in large part by the National Science Foundation.

For Vol. IV, Herzog has taken 40 per cent of the direct films and 15 per cent of the "Schraffur" films. For Vol. VI, 75 per cent of all necessary photographs have been obtained with the 18-inch schmidt, and the work of reduction and evaluation has been started.

### *Supernovae*

In the period from May 31, 1964, to May 31, 1965, the search for supernovae has been carried out by H. S. Gates, C. T. Kowal, G. Reeves, and F. Zwicky with the aid of a grant from the National Science Foundation. Eleven supernovae have been discovered in the period mentioned—one by Gates, four by Kowal, and six by Zwicky. An additional supernova was identified by Arp in a galaxy at RA  $11^{\text{h}}8^{\text{m}}5$  and Dec  $+28^{\circ}58'$  (1950), just one minute of arc north of NGC 3561

on a 200-inch plate obtained by Zwicky on April 15, 1953. With weather conditions unfavorable and telescope time scarce, only a few among the fainter objects could be investigated with the prime-focus spectrograph of the 200-inch telescope. However, informative spectra of the bright supernovae in NGC 3631, 3938, 4303, and 4666 were secured.

Light curves were constructed by Zwicky and Mrs. Karpowicz for the supernova 1956a of type I in NGC 3992 and SN 1957a of type II in NGC 2841. SN 1957a seems to have been a hybrid object of only moderate luminosity between the regular types I and II.

### *Miscellaneous Stars*

Rosino's star near M88, which he found bright in November and December 1961, and which for some years hovered between the apparent photographic magnitudes 19–22, was found to have brightened up again to the 13th magnitude on March 26, 1965. Afterward it faded again by seven magnitudes.

A number of repeat plates of the Palomar Sky Survey have been blinked against the original plates and a number of faint variables and fast-motion stars have been found.

## THEORETICAL STUDIES

### *Background Cosmic Light from Galaxies, Integrated to the Observable Horizon*

From time to time it has been suggested that measurements of the surface brightness of the background cosmic light caused by galaxies observable to the horizon might be used to discriminate between different world models, thereby providing an observational test of various cosmologies. In view of the probability that such observations will be made as part of the national space program, calculations of the expected light levels using the theoretical  $N(m)$  curves for galaxies predicted by cosmological theory have

been made by Sandage and Tammann.

The calculation was made in two stages of varying complexity. First, the galaxies were all assumed to have the same absolute luminosity  $\bar{M}$  consistent with the constant  $C$  of the redshift–apparent magnitude relation used in the original derivation of the  $N(m)$  curves in 1961 (Sandage, 1961, Equations 34 and 35). This first step is therefore idealized because the effect on  $N(m)$  of the spread of  $M$  by the luminosity function is neglected. In the second stage, this spread is taken into account by a procedure that provided differential corrections to the first calculations. Three



TABLE 3. The Cosmic Light for Different World Models\*

$q_0/\lambda$	5,545 Å	6,333 Å	10,300 Å	30,000 Å
-1	{ 28.17	27.65	26.17	24.40
	{ 1.87	1.97	1.82	0.23
0	{ 27.84	27.25	25.64	23.29
	{ 2.52	2.86	2.97	0.64
+1	{ 28.00	27.44	25.89	23.81
	{ 2.18	2.40	2.35	0.39
+2.5	{ 28.14	27.60	26.09	24.10
	{ 1.91	2.06	1.96	0.30

\* The units are magnitudes/ $\square''$  and  $10^{-20}$  erg  $\text{cm}^{-2}$   $\text{sec}^{-1}$  Å $^{-1}$  ( $\square''$ ) $^{-1}$ .

assumed luminosity functions were used. They were Holmberg's function going from  $M_B = -22^m25$  to  $M_B = -12^m25$ , Kiang's function with limits  $M_B = -22^m63$  and  $M_B = -14^m63$ , and Zwicky's hypothetical exponential function cutoff at  $M_B = -22^m25$  and  $M_B = -12^m0$ . (The cutoffs in the last function do not affect the answers.) The corrections due to the spread of  $M$  and in differences in the mean  $M$  were found by analytical methods of stellar statistics and were checked by a numerical calculation of  $N(m)$  using the Holmberg  $\phi(M)$ .

All calculations were carried out for four model universes ( $q_0 = -1, 0, +1, +2.5$ ), which include the steady-state case ( $q_0 = -1$ ). For each model the expected light was calculated at four wavelengths (5,545 Å; 6,333 Å; 10,300 Å; and 30,000 Å). The effect of redshift was included by adopting a mean  $I(\lambda)$  curve for field galaxies derived from photoelectric data by Stebbins and Whitford, Code, Oke, and Tifft, and shifting the curve by the  $\Delta\lambda/\lambda_0$  appropriate to each apparent magnitude. Table 3 gives the results in magnitudes per square second of arc and in absolute units of  $10^{-20}$  erg  $\text{cm}^{-2}$   $\text{sec}^{-1}$  Å $^{-1}$  ( $\square''$ ) $^{-1}$  for the first simplified calculation assuming constant  $M$  with no dispersion. (The magnitude zero points for the three longer wavelengths are normalized so that the color indices are all zero for an A0 star.)

The corrections to these values due to

the three luminosity functions are given in Table 4. The conclusion is that the level of the cosmic light is exceedingly low in comparison with other sources of continuous light flooding in. The average surface brightness of stars in our own Galaxy in the galactic poles is of the order of  $V = 23.5$  mag/ $\square''$ . Moreover, the zodiacal light near the ecliptic poles is of comparable strength. Therefore, even if the observation of the cosmic light were to be undertaken by satellite above the airglow, which is itself about 22 mag/ $\square''$ , the combined light of the zodiac and of our own Galaxy would overpower the cosmic signal by a factor of more than 100. In view of these difficulties, it would seem that the experiment will not be simple, if even possible.

Sandage points out that, even if the cosmic component of the total signal were

TABLE 4. Sky Brightness Corrections for Luminosity Functions

Limits	Magnitude Correction
Holmberg -22.25 { -12.25 }	+0.39
Kiang -22.62 { -14.62 }	+0.16
Zwicky -22.25 { -12.00 }	+0.67

to be detected, the differences among the models would be very small, amounting at most to a factor of about 2.5 at  $\lambda 30,000 \text{ \AA}$  between the steady-state ( $q_0 = -1$ ) and the  $q_0 = 0$  model. In view of the inherent difficulties, it appears that no test of cosmological models is possible via this route.

Interest of cosmic-ray physicists is in the energy density of the cosmic light in intergalactic space. The absolute flux in Table 3, integrated over all wavelengths, corresponds to a thermal energy density between  $4 \times 10^{-3}$  and  $6 \times 10^{-3}$  electron volt  $\text{cm}^{-3}$ , depending on the value of  $q_0$ . This corresponds to an equivalent intergalactic blackbody temperature due to the optical radiation of galaxies of  $1^\circ\text{K}$  in all world models considered.

#### *Statistics of Galaxies*

The study begun last year by Gunn on applications of spectral-theoretic statistical techniques to the problem of the statistical distribution of galaxies in space is nearing completion. Various cosmological tests based on the theory involving both higher moments of the number counts and the background light from galaxies too faint to be observed directly are being investigated. Recomputations of theoretical count-magnitude relations and  $k$  corrections are also being made.

#### *Gravitational Scattering of Light from Distant Objects*

The statistical scattering of light from very distant objects and its effect on the observed angular-diameter-proper-diameter relation in cosmology has been investigated by Gunn. It is found that an uncertainty of a small percentage in the angular diameter of small objects can be expected from this source, with corresponding errors in the measured fluxes. The effect increases roughly as the three-halves power of the redshift, and the details depend on knowledge of the statistical distribution of galaxies in space.

#### *Density of Neutral Hydrogen in Intergalactic Space*

The observations by Schmidt of the QSS 3C9 with a redshift of 2.01, have been used by Gunn and Peterson to arrive at a new and very low value for the density of neutral hydrogen in intergalactic space; the value obtained is about  $10^7$  times lower than the density predicted on the basis of the Einstein-de Sitter ( $q_0 = 1/2$ ) model. They have shown that an ionization level close to this can be maintained by bremsstrahlung radiation from the intergalactic gas itself, if the present temperature is between  $10,000^\circ$  and  $500,000^\circ$  and the expansion has not deviated too far from adiabacy. Thus there is no real contradiction with the usual cosmological models. One consequence of such a high ionization level is that the optical depth in Thomson scattering becomes appreciable at large redshifts; the flux of 3C9 can be expected to be reduced by about 30 per cent if  $q_0 = 1/2$ , and by more for larger values.

#### *Stellar Interiors*

T. Neil Divine has completed a study of the evolution of stars composed only of helium and small amounts of heavy elements. In these models the equation of state for partially degenerate gas has been treated as carefully as possible. The energy source is the triple- $\alpha$  reaction and the  $\alpha$  reactions that produce oxygen and neon. The stars evolve off the helium main sequence, which is located well to the left of the normal main sequence in the Hertzsprung-Russell diagram, toward cooler and more luminous objects. For helium stars with masses somewhat less than one solar mass, the central temperature never becomes high enough for carbon or oxygen burning to occur. In these cases the evolutionary models go to higher effective temperatures and, if carried beyond the present studies, might lead directly to white dwarfs. The more



massive helium-star models resemble Wolf-Rayet stars in many respects.

### *Infrared Spectrum of the Solar Corona*

The line spectrum of the solar corona in the instrumental infrared has been studied theoretically by Münch. The existence of forbidden lines of Mg VIII, Si IX, and Si X at  $\lambda\lambda 3.03 \mu$ ,  $3.86 \mu$ , and  $1.43 \mu$ , respectively, has been predicted and their strengths estimated. Disregarding a small probability for the lines to be totally absorbed in the atmosphere, it

appears that these coronal lines should be as strong, in absolute units, as the strongest in the photographic region. Their detection would, therefore, be within easy range of modern photoconductive detectors were it not for the uncertainty in the atmospheric absorption. The very low value of the daylight sky brightness in this spectral region makes these lines promising for coronagraphic work. Plans are now being made to attempt a detection of the lines during the November 1966 total solar eclipse.

## GUEST INVESTIGATORS

Dr. Frank J. Low of the National Radio Astronomy Observatory obtained observations at a wavelength of 1 mm with a thermal detection radiometer at the prime focus of the 200-inch Hale telescope. The radiometer utilizes a combination of infrared and microwave techniques to couple the 1-mm wavelength energy into a germanium bolometer cooled in a helium cryostat to  $2^\circ\text{K}$ . The performance of the 200-inch, viewed as a radio telescope, was better than expected: the half-power beamwidth was  $60''$ , and the sidelobe level was quite acceptable. An absolute calibration in terms of brightness temperature or flux density was made possible by previous observations with a small telescope. The brightness temperature at the center of the moon had been measured as a function of phase.

In addition to lunar scans, which provided the calibration, measures were obtained for Jupiter, Mars, the QSS 3C273, and the Crab Nebula. For Jupiter and Mars the brightness temperatures at 1 mm are, respectively,  $155 \pm 15^\circ\text{K}$  and  $196 \pm 40^\circ\text{K}$ . A flux density of  $300 \pm 100 \times 10^{-26} \text{ W m}^{-2}(\text{cps})^{-1}$  was obtained for 3C273. More than 100 individual measures were made during the single night of observations. From a statistical treatment of these data, it can be seen that the probability is only 2 per cent that

the flux is less than  $100 \times 10^{-26} \text{ W m}^{-2}(\text{cps})^{-1}$ . The maximum flux measured at microwave frequencies for this QSS is  $30 \times 10^{-26} \text{ W m}^{-2}(\text{cps})^{-1}$  and in the near infrared,  $5 \times 10^{-26} \text{ W m}^{-2}(\text{cps})^{-1}$ . A similar number of measures was made of the Crab Nebula. The  $60''$  beam of the 200-inch was centered on the radio position; an upper limit of  $100 \times 10^{-26} \text{ W m}^{-2}(\text{cps})^{-1}$  was obtained. This value is consistent with an extrapolation of the microwave spectrum. No evidence was found for a neighboring source with a positive spectral index.

Dr. William M. Sinton and Dr. Peter B. Boyce of the Lowell Observatory obtained infrared interferometric spectra of stars and the planet Mars during twilight in March and April with the 200-inch Hale reflector. Many of the stars observed were carbon stars. In spectra of carbon stars, Sinton and Boyce had earlier found that the carbon monoxide absorptions at  $2.3\text{--}2.4 \mu$  were abnormally weak. Only one interferogram was obtained of Mars because of losing much of the scheduled time owing to poor weather. The observed objects besides Mars were EU Delphini,  $\alpha$  Ursae Majoris, RS Cygni, U Cygni,  $\sigma$  Canis Majoris, BL Orionis, T Lyrae, and  $\alpha$  Lyrae.

Dr. Philip C. Keenan of the Perkins Observatory obtained 21 coudé spectrograms of Mira variables (11 in the blue



region and 10 in the red) with the 200-inch telescope at Palomar, primarily as part of a joint study with Deutsch of the spectra of variables near maximum light. On the red plates the intensity of the  $\lambda 6,132$  band of yttrium oxide could be estimated for all 10 stars. One of the variables, RV Cassiopeiae, had a sufficiently large radial velocity to allow the interstellar D lines to be well resolved on the spectrogram. The Se variable R Andromedae was observed to have an unusual maximum in that a number of emission lines in the red region appeared for the first time. This spectrogram was turned over to Dr. Greenstein and Mrs. Locanthi for inclusion in their detailed study of this star.

Professor L. Gratton, Director of the Laboratory of Astrophysics of the Astronomical Observatory of Rome, undertook two observational programs with the 100-inch telescope. Some plates were obtained for a spectrophotometric investigation of G dwarfs and K giants, directed to the determination of the relative abundance of elements. For the other program—an investigation of atmospheric motions in cepheids—a number of spectrograms were borrowed from the Observatory files. All these plates will be measured with an automatic machine at the laboratory in Frascati, Rome.

Dr. George Wallerstein of the University of California spent part of the year in Pasadena during a sabbatical leave from Berkeley. On three nights on the 100-inch, he obtained high dispersion spectra of 10 K-type giants in the violet in order to get absolute magnitudes by the Wilson-Bappu method. These stars and nine others being analyzed in cooperation with Dr. H. L. Helfer of the University of Rochester for chemical abundances; the absolute magnitudes will facilitate a discussion of correlations between chemical composition and space motions.

Dr. Kenneth M. Yoss of the University of Illinois Observatory obtained spectrograms of seven K-type giants in the

galactic clusters NGC 752 and NGC 2264 at 40 Å/mm with the 60-inch reflector. These calibrated plates are to be combined with several hundred plates of nearby standard stars previously obtained with the same instrument, and for which absolute magnitudes are known, in order to establish a relation between spectrographic criteria and luminosity, with composition as the independent variable. Using the 32-inch camera of the 100-inch reflector, coudé plates were obtained of six K giants, two with exceptionally strong and four with very weak CN absorption, as well as three standard stars for which abundance analyses have been made. Both IIa-O and IIa-D plates were used at dispersions of 10 and 15 Å/mm, respectively. Relative abundances of the strong and weak CN stars will be determined.

Investigations into galactic star clusters have been made with the 48-inch schmidt and the 60-inch reflector by Dr. Robert J. Chambers of Pomona College. With the 48-inch schmidt, tests were made of photographic transfer capabilities between clusters having photoelectric sequences to unequally faint magnitudes, in order to use the fainter sequence to extend the other while avoiding the zero level problem common to usual transfers. Iris photometry of these plates is in progress. A test was made of a random-hole "image spoiler" mask mounted in front of the 48-inch corrector plate. The resulting images are larger and softer because of diffraction. (A report of this test was published in the June 1965 *Astronomical Journal*.) Sixty-inch Xf-spectra of non-main-sequence stars within the boundaries of clusters NGC 2422 and NGC 2437 have been taken to determine membership via radial velocities. Examination of main-sequence cluster stars (to the limits of the 4-inch camera) has revealed no peculiar A or metallic line stars, although BD — 14°2000 is a Be star, appearing within the boundary of NGC 2422. It is probably not a cluster member.



Dr. Robert H. Koch of Amherst College used the photoelectric scanner on the 60-inch reflector during July 1964. Observations were made to isolate the seven 50-Å-wide intervals in the radiation curve of U Ophiuchi that were originally observed in the summer of 1963. With the light curve now sufficiently delineated, the orbital analysis may permit the evaluation of the limb-darkening coefficient in the continuum and within the Balmer and helium lines. The reduction of the data is complete, but analysis is in only a preliminary stage.

Dr. Koch also made direct scans of  $\beta$  Lyrae from 3,500 Å to 6,000 Å. From these scans monochromatic magnitudes have been measured at the standard wavelengths, emission line strengths have been determined, and limits on the light contributed by the emission features have been evaluated for both *V* and *B* light curves. The limits appear to be permitted by both the spectroscopic and photometric characteristics of the system, and they provide the initial rectification parameters to be applied to the light curves.

Dr. G. Tammann continued the observations for the Basel Observatory program concerning *RGU* photometry in star fields with different galactic latitudes and longitudes. Enough 48-inch plates were obtained for two fields, that of SA 71 and a Puppis field containing three open clusters. Faint standards were measured with the 60- and 100-inch telescopes near the clusters M37, NGC 6883, and NGC 7510. With the 100-inch telescope Tammann has also measured *UBV* magnitudes of the *W Ursae* Majoris-type variables AC Leonis, AM Leonis, and XY Leonis. A program to measure *UBV* magnitudes of extremely compact galaxies with the 100-inch telescope could not be carried out owing to very unfavorable weather conditions. For Sandage's identification program of objects in the revised *Third Cambridge Catalogue*, Tammann obtained a number of 48-inch plates.

Dr. D. E. Osterbrock and Mr. J. L'Ecuyer of the University of Wisconsin obtained spectrograms with the 100-inch coude spectrograph for a study of line profiles in planetary nebulae. The plates were taken with the 32-inch camera and the high-dispersion grating, giving a dispersion of approximately 4.5 Å/mm for  $\lambda 4,686$ ,  $H\beta$ , and  $[O\ III]\ \lambda\lambda 4,959, 5,007$ ; and approximately 6.7 Å/mm for  $\lambda 5,876$ ,  $H\alpha$ , and  $[N\ II]\ \lambda\lambda 6,548, 6,583$ . The exposure times ranged up to 7½ hours, and 31 plates (each including blue and red spectral regions) of seven nebulae were obtained. Strip calibration exposures for spectrophotometry were taken on each spectrogram. Reduction of these plates has been started by Dr. Osterbrock and J. S. Miller, using the Yerkes microphotometer. To date, 17 individual line profiles of NGC 7662 have been reduced and averaged to give the profiles of  $H\alpha$ ,  $H\beta$ ,  $\lambda\lambda 4,686, 4,959$ , and  $5,007$  in the center of the nebula. These profiles are fairly symmetric, showing the well-known doubling studied by O. C. Wilson. The  $[O\ III]$  profiles drop to zero intensity in their centers, showing that there is no  $O^{++}$  with zero expansion velocity near the center of this nebula. The He II profile drops at its center to approximately 20 per cent of peak intensity, and the  $H\alpha$  and  $H\beta$  profiles drop at their centers to approximately 35 per cent of their full intensities. The individual halves of the double profiles have widths, in this nebula, of approximately 25 km/sec for H, 20 km/sec for He II, and 15 km/sec for O III. The ultimate goal of the program is to compare the observationally determined line profiles with synthetic profiles calculated from theoretical models of expanding planetary nebulae, to test and to choose among the synthetic profiles.

Dr. L. H. Aller of the University of California at Los Angeles and Dr. Stanley Czyzak of the Wright-Patterson Air Force Base obtained observations of the following planetary nebulae with the *f/1* schmidt camera and nebular spectro-



graph at the Newtonian focus of the 60-inch telescope: NGC 2371-72, IC 1747, J 320, IC 351, IC 2165, NGC 6445, NGC 6751, NGC 6778, NGC 6818, NGC 6885, NGC 6894, NGC 6905, NGC 7008, NGC 7026, and IC 4997.

Spectrograms of suitable comparison stars were also obtained so that line intensities could be derived for the stronger emission features in these objects. Unfortunately, for some of the objects it was possible to secure only one plate apiece because of unfavorable weather conditions. Aller and Czyzak also observed on three nights at the 100-inch coudé, where they obtained high-dispersion spectrograms of the bright planetaries NGC 6803, IC 4593, and NGC 6825. In February and May they used the photoelectric spectrum scanner at the Cassegrain focus of the 60-inch to obtain data for these planetaries: J 900, IC 3568, NGC 3242, NGC 4361, IC 4593, II 4634, NGC 7026, NGC 6884, NGC 6058, and NGC 6891. Measurements on NGC 3242 and NGC 4361 were confined to the ultraviolet where both tracing and charge-integration techniques were employed. Because of the high background sky brightness, especially for southern objects, and because most emissions in planetary nebulae are very faint, it is possible to measure only the strongest lines in the spectra of these objects, notably the green nebular lines,  $\lambda 4,861$ ,  $\lambda 4,340$  (which is strongly contaminated with the Hg sky glare at  $4,359$ ),  $\lambda 4,101$ ,  $3,970$ ,  $3,868$ , and  $3,727$ . In the brighter objects, a few additional lines such as  $\lambda 4,471$  of He I are measurable; while in the fainter objects, it is possible to measure only the green nebular lines,  $\lambda 4,861$ , and sometimes  $\lambda 3,727$ . By combining photoelectric and photographic measurements, it is possible to obtain improved line-intensity data over a greater range in intensity than would be possible otherwise.

Because of its high intrinsic interest as a nonthermal source, Aller and Czyzak devoted much attention to NGC 3242 and

are preparing a paper on it for publication. Reductions are nearly completed for NGC 6543 and for IC 3568. It has been necessary to observe NGC 3242 for three observing seasons in order to obtain minimum data for this object.

With the Cassegrain photoelectric scanner at the 60-inch, Aller and Czyzak have also observed monochromatic magnitudes of a number of stars, of which coudé spectra were secured at the Lick Observatory. These are mostly A and B stars of particular interest because of their abnormal spectra. Some are magnetic stars; others contain lines of manganese, gallium, and other elements with unusual strength. To interpret the line-intensity data by model atmosphere methods, it is necessary to have accurate temperatures which can be obtained from energy distribution measurements, interpreted with the aid of a model atmosphere. The following stars have been observed in this program: 53 Tauri, 15 Cancri,  $\alpha$  Leonis,  $\eta$  Virginis,  $\pi$  Boötis,  $\iota$  Coronae Borealis,  $\iota$  Herculis,  $\phi$  Herculis,  $\nu$  Herculis, 112 Herculis,  $\tau$  Capricorni, HR 4072, 7664, 8349.

The line-intensity data are needed in connection with theoretical studies of gaseous nebulae. The data analysis is assisted with a grant from the U. S. Air Force Office of Scientific Research; much of the reduction of the nebulae data is carried out by Czyzak at Wright-Patterson Air Force Base.

Dr. Robert Parker of the Washburn Observatory, University of Wisconsin, continued his investigations of the physical conditions in the Cygnus Loop, obtaining spectra of five individual filaments and using the spectra of planetary nebulae as calibration sources. The spectra were obtained with the B spectrograph on the 60-inch; they include the spectral regions  $\lambda\lambda 3,700-5,000$  and  $\lambda\lambda 5,500-6,750$ . The observations extend those previously published in three ways: (1) They encompass several fainter lines, including  $\lambda\lambda 4,068$ ,  $4,071$ ,  $4,101$ ,  $4,686$ ,  $5,577$ ,  $5,876$ , and  $6,300$ ; (2) they should en-



able the problem of the Balmer decrement to be resolved; and (3) they provide, for at least one filament, a measure of the optical continuum. Measures were also made with the Cassegrain scanner on the 100-inch to obtain the total flux in  $H\alpha$  and N1 from a few of the brighter filaments. These data will allow comparison of the optical intensities with the observations of the radio flux. The blue and ultraviolet continuum of NGC 1068 was also measured with the Cassegrain scanner to permit comparison with the radio data (Osterbrock and Parker, 1965).

Dr. W. J. Luyten of the University of Minnesota observed with the 48-inch schmidt telescope on two nights in November and April and took 23 plates repeating the earlier Survey plates. These were used for proper-motion work, and on them, as well as on others taken earlier, a large number of proper-motion stars were found, including some 300 new stars with absolute magnitudes fainter than +16.5 (photographic); before this survey began, only 12 such stars were known.

The plates required for the completion of a further extension of the Palomar Sky Survey to declinations  $-36^\circ$  and  $-42^\circ$  have been obtained by Dr. John Whiteoak of California Institute of Technology Owens Valley Radio Observatory. The entire extension consists of 100 fourteen-inch plates of fields photographed with the Palomar 48-inch schmidt telescope. Exposure times were limited to 20 minutes to minimize the image deterioration due to relative refraction effects across a plate field. Since refraction increases rapidly at the zenith angles corresponding to these declinations, exposures were centered about the meridian. With 20-minute exposures, the field centers are sufficiently spaced in right ascension to permit the observation of a continuous strip of sky at one declination. An amber plexiglass filter was employed with a 103a-E emulsion. The filter yields a gain of about 50 per cent over the light transmitted by the conventional red Survey filter within the spectral range of the emulsion.

Dr. T. Gehrels of the University of Arizona, using the 48-inch schmidt at Palomar, obtained 14 plates of Trojan asteroids and of Geographos. The plates will be measured and reduced at the Leiden Observatory by Dr. and Mrs. C. J. van Houten. The purpose is to obtain the magnitude-frequency relation of the Trojan asteroids down to the 20th magnitude, and to compare it with that of the common asteroids.

Dr. Pierre Connes, on leave from the Centre National de la Recherche Scientifique, Paris, France, tested with the Snow telescope a Fourier spectrometer built at the Jet Propulsion Laboratory in Pasadena. This instrument, consisting of a Michelson interferometer with servo-controlled drive, had previously given accurate laboratory emission and absorption spectra in the near infrared ( $1-2.5 \mu$ ) with resolutions down to  $0.1 \text{ cm}^{-1}$ . With the Snow telescope the Fourier spectrometer produced solar spectra in good agreement with those of the McMath-Hulbert *Atlas* and with about twice as much resolving power. On Venus, the instrument produced spectra with about the same resolution ( $4 \text{ cm}^{-1}$ ) as those of Kuiper (obtained with the 82-inch telescope at the MacDonald Observatory). However, the signal-to-noise ratio in the spectrum remains mainly limited by seeing effects, and not by receiver noise, which means that the instrument requires further development before full use can be made of a larger telescope.

Dr. Barry M. Lasker, a Fellow of the National Science Foundation, has in progress a program of photoelectric photometry of galaxies in eight bands of intermediate width located between  $3,400 \text{ \AA}$  and  $8,000 \text{ \AA}$ . Wavelengths have been chosen that are relatively free of major absorption-line features for redshifts up to about  $5,000 \text{ km/sec}$ .

The magnitudes and the spectral energy distributions of E and S0 galaxies in clusters of predominately elliptical galaxies and in the general field are sought for several reasons: The question of homogeneity of the spectral energy



distributions is important when the magnitudes of redshifted galaxies are to be corrected to zero velocity, and is relevant to theories concerning the formation of galaxies. Color-magnitude relations among members of clusters of galaxies will also be obtained. Furthermore, it is planned to supplement these data with spectra of moderate dispersion in order to study the stellar content of a few selected galaxies. Standards have been established and compared to absolutely calibrated stars, and a few galaxies have been measured. Preparations are also in progress for the narrow-band photography, in emission lines, of some small, dense, density-limited H II regions.

Dr. A. G. Wilson and Dr. G. E. Kocher of the Rand Corporation have continued their investigations of the diameters of galaxies in nearby clusters. A process of iterative photographic copying of cluster plates on high-contrast emulsions is used to "stellarize" the galaxy profiles. (This is in effect the inverse of the method adopted by Baum in his galaxy-image synthesizer.) The diameters of stellarized galaxy images may be measured with good internal consistency by conventional micrometric techniques. Provisional results show that the distributions of the sizes of major axes of elliptical galaxies are multimodal. While the distributions are suggestive of those theoretically predicted by Edelen, the present results cannot be sharpened to an observational confirmation of the theoretical  $[n(n+1)]^{1/2}$  diameter distribution.

Wilson has begun a program of securing redshifts of the brightest galaxies in the nearby previously unobserved clusters, using the B spectrograph or the 100-inch. Distances to these clusters are required not only for galaxy diameter studies, but also for investigation of the structure in the spatial distribution of clusters.

As part of the continuing Rand-University of California at Los Angeles study of the effectiveness of schmidt telescopes in observing distant space

vehicles, Kocher succeeded in photographing the Soviet Mars probe ZOND II at a distance of 300,000 km, using the 48-inch telescope under conditions of good seeing and dark sky. Two 103a-O plates showing the faint trail of the spacecraft in Hydra were obtained on December 1, 1964.

The existing Palomar Sky Survey plates do not allow many galaxies to be differentiated from stars for objects fainter than about magnitude 18.5, a serious limitation in Dr. T. A. Matthews' program to identify the optical objects that produce radio sources. To improve the information content of the faint images and to study some of the brighter identifications, Matthews, of Caltech's Owens Valley Radio Observatory, has obtained plates of 65 identifications using the 48-inch schmidt telescope and fine-grained IIa-D and IIa-E plates. These show a significant improvement in the amount of information available over the 103a-O and 103a-E plates used in the Sky Survey, especially when the seeing is better than 2. Also, plates of 26 brighter identified sources have been taken with the 100-inch telescope, again using the fine-grained plates. This plate material has been invaluable in classifying the fainter identified radio galaxies in an extension of the work begun by Matthews, Morgan, and Schmidt. The results will be incorporated in a paper on the identification of the 3C revised sources, in collaboration with Wyndham, Fomalont, and Veron.

In examining the plates already taken, it was noted that 75 per cent of the radio galaxies show peculiarities, such as jets (7 per cent), diffuse plumes outside the galaxy (9 per cent), absorption features (10 per cent), structure in the nuclear region (17 per cent), structure in the envelope (9 per cent), nonsymmetry in the surface brightness or extent of the envelope (47 per cent). The percentage (in parentheses) of each group showing the peculiarity is only a lower limit since large-scale plates are not available for many of the objects.



Some details for a few of the more interesting objects are given here. The D galaxy identified with 3C293 has the most absorption of any of the radio identifications, the nuclear region being almost completely obliterated. The quasi-stellar object identified with 3C138 is not stellar in appearance on a 48-inch IIa-D plate taken in good seeing. The identifications for Hercules A, 3C444, and 3C346 are featureless diffuse objects with no nucleus, but each has a starlike image in the outer envelope.

It is planned to study more nonradio-source D galaxies to find out how common such peculiarities are in this type of galaxy, but at first sight these peculiar features are probably caused by or associated with the violent explosion that produced the radio source.

Dr. H. J. Rood, a Stockwell Fellow from the University of Michigan, studied NGC 4486-B, the Virgo Cluster E0 galaxy 7.3 north preceding M87. The surface brightness distribution in the range of radial distances  $2'' \lesssim r \lesssim 13''$ , derived from plates loaned by Sandage and by Baum, does not satisfy de Vaucouleurs' formula, but fits the relation advanced by King for globular star clusters. The mass-to-light ratio, deduced using the virial theorem, is  $M/L_{pg} = 80$  (solar units). It is likely that NGC 4486-B is a tidally limited satellite of M87.

Baum and Rood have undertaken an investigation of galaxies located in several selected fields near the center of the Coma cluster. For this program, surface brightness distributions of selected galaxies have been determined photoelectrically and a series of long- and short-exposure 200-inch plates have been obtained in yellow light. The material, supplemented by additional observations by Sandage, is being used to derive the distributions of surface brightness along the major and minor axes of all galaxies with  $V \leq 17$  in the selected fields. The integrated luminosities, morphological types, and position angles of the major axes of

the galaxies are also being determined.

Dr. Walter E. Mitchell, Jr., of Perkins Observatory, with the assistance of R. R. Wright, used the Snow telescope to obtain high dispersion spectra in integrated sunlight for the following regions, totalling 960 Å:  $\lambda\lambda 3,903-4,393$ ,  $5,037-5,214$ ,  $5,811-5,900$ ,  $6,199-6,300$ , and  $6,497-6,600$ . A new mosaic of 12 six-inch aluminized flats was assembled for this program. Grating 91B was used in a double-pass arrangement. Observation of the ultraviolet solar spectrum at the center of the disk was completed, from  $\lambda 3,333$  down to  $\lambda 3,000$ . The detector was an RCA 7265 multiplier phototube. In a program being conducted with Howard, the profiles of 11 solar lines of moderate strength and different Zeeman splitting were observed.

Dr. Bruce Murray of the Division of the Geological Sciences, Caltech, used the 200-inch Hale telescope in December 1964 to obtain observations across the 7" diameter disk of Mars in the 8-14  $\mu$  region.

Robert L. Younkin of the Caltech Propulsion Laboratory has continued spectrophotometric measurements of the moon and planets from 3,200 Å to 1.1  $\mu$  with the Mount Wilson 60-inch reflector. During the past year the primary emphasis has been on the planet Mars. The monochromatic color of the planet has been measured at several phase angles to determine the wavelength dependence of the phase coefficient. Although the 1965 opposition was an unfavorable one from the standpoint of planetary image size, a successful comparison was made of the intensity ratio of maria to continents, as a function of wavelength. It has been established that the 8,000-8,500 Å absorption band of limonite is absent from the reflection spectrum of the continents, contradicting the assumption of several authors, based upon polarimetric and visual photometric observations, that limonite is the surface material of these regions. In addition, monochromatic limb darkening curves were obtained in both polar and equatorial directions. During this op-



position, Mars exhibited a pronounced limb brightening in the ultraviolet.

The monochromatic reflectivity of Mars in the near infrared has been determined from measurements made at the 1963 opposition. This has permitted the first accurate determination of the radiometric albedo of the planet.

Mr. Younkin continued measurements of Saturn to determine the ratio of the radiance of the ring to that of the planet as a function of ring opening at various wavelengths. It has been previously reported by Younkin and Münch that the radiance of Saturn shows an ultraviolet minimum near  $\lambda 3,800$ . This result is dependent upon absolute measurements by other observers of the intensity of  $\alpha$  Lyrae short of the Balmer limit. This ultraviolet minimum has been independently confirmed by the ratio of the

planet-ring intensities, which shows a similar minimum.

The 20-inch telescope at Palomar was used by Dr. D. H. McNamara of Brigham Young University on five nights in an attempt to detect luminescence from portions of the moon's surface. Narrow-band interference filters were utilized in an attempt to detect weak emissions filling in the bottom of the strong H and K absorption lines. The results of this test proved to be entirely negative.

Howard A. Pohn of the U. S. Geological Survey, Flagstaff, Arizona, had planned to use the 60-inch telescope to take photoelectric calibration measurements of the moon in April to complement those taken by Ranger VII and Ranger VIII spacecraft. Because of unfavorable weather, however, the measurements could not be made.

## IMAGE TUBES

Photoelectric image tubes were put to more significant astronomical use during the present report year than in any previous year. In the image-tube work at the Observatories there has been a shift of emphasis from the testing of techniques toward obtaining of astronomical results. Altogether, there were three observing sessions with McGee's Lenard window tube and one session with an RCA cascaded converter. All these observations were made on Mount Wilson at the focus of the 114-inch coudé camera of the 100-inch telescope, where previous efforts of this kind have been made in recent years. The tubes were mounted in much the same manner as earlier, but various modifications have been made by Baum to facilitate this kind of work.

In December 1964, W. Kent Ford, Jr., of the Carnegie Institution's Department of Terrestrial Magnetism, Baum, and A. Th. Purgathofer of Lowell Observatory ran tests of an RCA cascaded converter with the Mount Wilson equipment. This tube was one of the 20 cascaded con-

verters being procured under rigid specifications by the Carnegie Image Tube Committee with National Science Foundation support. When a front-to-front pair of  $f/2$  Burke-James lenses was used to transfer the output image of the tube from the phosphor screen to baked IIa-O plates, the rate of blackening of the plates was 80 times that for unaided baked IIa-O plates exposed to the same  $\lambda 3,500$  optical input as the photocathode. Under these conditions about three grains were being blackened for each primary photoelectron ejected from the photocathode. The net information gain of the system over unaided baked IIa-O plates was, therefore, by a factor of about 25 before a discount was made for the lower resolution of the tube.

The limiting resolution of the tube alone was about 40 line pairs/mm. This, however, was degraded both by the transfer lenses and by the photographic emulsion on which the final output image was recorded, so that the overall resolution of the system was less than 20



lp/mm. A study of the transfer functions of the components of the system showed that resolutions tend to combine in series more nearly as  $[\Sigma(1/R_i)]^{-1}$  than as the commonly assumed formula  $[\Sigma(1/R_i^2)]^{-1/2}$ . Experiments were made with a 0.4-magnification schmidt camera in place of the pair of Burke-James lenses; the result with the schmidt camera was poorer because the degradation due to the compression of the image on the emulsion more than offset the superior performance of the schmidt camera.

The RCA cascaded converter is a cylinder about four inches in diameter and about five inches long. It has a tri-alkali photocathode at the input end, an intensifying membrane in the middle, and a P-11 phosphor screen at the output end. The diameter of the image is 40 mm. The magnetic focusing field of 250 gauss was produced by a shaped array of Alnico V bar magnets surrounding the tube, and an accelerating potential of 11 kv per stage was applied.

Astronomical observations with the RCA cascaded converter in December were made jointly by Wilson, Baum, Ford, and Purgathofer. They were concerned with the strength of the  $\lambda 6,707$  Li I line in the components of binaries, and the astronomical results are discussed elsewhere in this report. The speed gain of the tube over unaided photographic emulsions was a little greater at  $\lambda 6,070$  than at  $\lambda 3,950$ . The photocathode has somewhat lower quantum efficiency at  $\lambda 6,707$ , but so also do photographic emulsions. Exposures with the tube at  $2.8 \text{ \AA/mm}$  required about an hour for eighth-magnitude stars.

In January 1965, Professor J. D. McGee and Dr. Baum ran tests of some Lenard window tubes that McGee brought to Mount Wilson from his laboratory in London. The Lenard window tube is a cylinder about  $3\frac{1}{2}$  inches in diameter and 12 inches in length. It has an antimony-cesium photocathode at the input end and a thin aluminized mica window at the output end. There is no internal intensifying membrane. The

primary photoelectrons are accelerated along the full length of the tube. They are given enough energy to pass through the mica window and impinge directly onto an electronographic emulsion pressed against the outside of the window. If the tube is operated with an applied potential of 40 kv, a typical photoelectron loses about half that energy in passing through the mica, and it triggers several grains in the emulsion. Although there is some statistical variation in this process, most of the photoelectrons make recorded impacts; a Lenard window tube therefore has about the same fundamental efficiency as a cascaded converter system with an equally sensitive cathode. The Lenard window tube, however, has a much higher resolution than a cascaded converter system (including transfer optics) and it is able to deliver its superior efficiency with fine-grained emulsions having an extensive information capacity as well as with coarser-grained emulsions that have high rates of blackening. Operationally it has the advantage of requiring no transfer optics at the output end, but the disadvantages of a higher accelerating potential, a physically larger focusing magnet array, and a greater vulnerability to ambient magnetic disturbances. The Lenard window tube is also somewhat more delicate than a cascaded converter, but Baum has devised a film-handling mechanism that is relatively free of hazard to the tube.

At  $\lambda 4,480$  the best of the Lenard window tubes tested at Mount Wilson was found to blacken Ilford XM emulsion about 30 times faster than an unaided baked Ila-O plate placed at the same optical focus as the cathode. Ilford G5 emulsion was found to be about 3.5 times slower. The XM emulsion is slightly coarser grained than Ila-O, whereas G5 is somewhat finer grained. The resolution on XM was about 45 lp/mm.

In January astronomical observations with the Lenard window tube were made jointly by Kraft, McGee, and Baum. Two subsequent sessions in March were conducted by Kraft and Baum after



McGee's return to London. The observations were concerned with stellar rotations in the Praesepe cluster and are reported elsewhere in this report. The Carnegie Institution and the Observatories are much indebted to Professor McGee of the Imperial College of Science and Technology, University of London, for his interest and collaboration in the work.

Future image-tube programs are now planned for the 73-inch coudé camera at Mount Wilson, the 72-inch coudé camera at Palomar, and the newly designed Cassegrain image-tube spectrograph for the 200-inch Hale telescope. The installation has already been prepared by Baum and Ribbens for operation of a cascaded converter at the 73-inch Mount Wilson camera.

## INSTRUMENTATION

An instrument committee of six staff members under the chairmanship of Oke was appointed during the year to recommend priorities and to improve coordination of the Observatories' instrumentation program. Instrument design and construction have been under the general supervision of B. H. Rule, Chief Engineer. E. W. Dennison, as head of the Electronics Laboratory, bears the main responsibility for design, construction, and maintenance of the increasingly complex electronic instruments, and R. Ribbens has been in charge of mechanical design and machine shop for the Mount Wilson section.

### *Optical Systems*

The investigation of optical systems for use with image-intensifier tubes, reported in *Year Book 63* (p. 39), has been continued by Bowen. Special attention has been given to the optical parts of a low-dispersion spectrograph for nebular and galactic studies.

A reexamination of the concentric mirror systems for re-imaging the phosphor on the photographic plate at magnifications of unity or greater (Cases II and III described in *Year Book 63*, pp. 39-40) has shown that it is possible to reduce very greatly the spherical aberration by a slight adjustment of the magnification and the ratio of the radii of the mirrors. This eliminates the corrector plate and removes the large off-axis aberrations that are introduced by such a plate in the rapidly diverging beam

coming from the phosphor in these cases.

Like the schmidt camera, the concentric mirror systems in general yield a curved field. Because of the thickness of the windows of the image tube, required to withstand atmospheric pressure, any field flattener must be placed at some distance from the focus. This renders the design of such a flattener much more critical than in the case of a schmidt camera. However, by using a two-element design, it has been possible to achieve a satisfactorily flat field without the introduction of objectionable aberrations.

### *Solar Instruments*

The new data system for the 150-foot solar tower, consisting of a solar image guider, a raster-scan control and coordinate digitizer, and a data processor and recorder, was placed in limited service in early June 1965.

The solar image guider consists of two pairs of optical pickup heads which are connected by fiber-optic "light pipes" past a mechanical chopper to two photomultipliers. The average anode current of the photomultipliers is kept essentially constant by means of a feedback circuit that controls the multiplier supply voltage. This provides automatic compensation for variations in light that occur as a result of changing sky conditions. The a-c components of the anode signals are fed to two servoamplifiers and motors that micrometrically tilt the second flat mirror of the telescope. Tests indicate that the final performance will meet the design



specifications of positioning the solar image to better than a second of arc. Provision has been made to "lock out" the servocontrol if passing clouds obscure the solar image. Reacquisition of the image will occur if any one of the four optical heads is illuminated.

The raster scan and coordinate digitizer were designed and constructed by the Datex Corporation. A digital encoder is attached to each of the two orthogonal drive screws that determine the position of the optical servodetector heads. Scan rates may be set from approximately 135" per second of time to 4,000 seconds of time per 1", this range being required for high-speed magnetograph scans at one extreme and compensation for solar rotation for single point measurements on the solar disk at the other. Between scans, the second coordinate will advance incrementally by an amount ranging from approximately 0.27" to 270". These characteristics permit rectangular raster scans to be made ranging from the entire solar image down to the smallest active regions with an accuracy essentially the same as the telescope lens resolving power.

The third section of the instrument consists of a data acquisition and recording system. The data are recorded in groups of 30 characters or digits. Each "file" or set of data groups is preceded by an identification group containing the date, provision for computer instructions, the file number, and 20 characters that may be set to any arbitrary number to indicate seeing, wavelength, observer, and so forth. Each data group now contains universal time to 0.1 sec, the X and Y coordinate of the scanning frame, the intensity, the magnetic field strength, a relative measure of the radial velocity, and provision for two additional three-digit quantities. The measurements for the magnetic and intensity values are obtained by means of integrating digital voltmeters with integrating times adjustable from 0.1 to 20.0 sec in a 1, 2, 4, 10 sequence. The final recording is done

on magnetic tape directly compatible with the IBM tape readers at the Caltech computing center.

A project proposal and preliminary design study were made on a combination optical system for a new equatorial solar telescope, following ideas developed by Zirin. The design provides for a 10-inch coronagraph, guiding optics, 15-inch Cassegrain system with vertical coudé, and multiple Cassegrain foci. The proposal calls for mounting on a 50-foot concrete tower in a clamshell-type dome.

A 40-foot tower for evaluating the quality of the solar seeing has been erected on Mount Wilson by Leighton with support from the U. S. Office of Naval Research. It is the first of about five that are planned for as many sites in the southern California area to test the dependence of the solar image quality upon various factors, such as altitude, proximity to the ocean, and character of the surrounding vegetation.

A rapid-sequence 35-mm camera has been modified to take short exposures (about 1/500 sec) every 10 seconds. It is hoped that this camera may be used for cinematography of the solar granulation. A simpler 35-mm camera has been modified for use with the spectroheliograph of the 60-foot tower. It is intended for taking lapse-time movies in several spectral lines to study the chromospheric oscillation.

#### *Instrumentation for the Large Reflectors*

A pressure-scanning Fabry-Perot interferometer for use in series with the two-channel photoelectric spectrum scanner in the 100-inch coudé has been constructed and tested by Vaughan and Münch. The instrument is designed to accommodate interchangeable 1/2-inch interferometer etalons and is intended for specialized investigations to provide resolving powers higher than can be achieved with available grating spectrographs. Quantitative observations of interstellar absorption lines are now being made.



The possibilities of constructing an efficient high-resolution magnetically scanned monochromator and analyzer for polarization of resonance radiation are being experimentally studied by Stuart Ridgway and G. Münch.

The resonance chamber thus far used is a Pyrex cell filled with metallic sodium, which, together with its heaters, is placed between the poles of four-inch electromagnet with a one-inch gap. The resonance radiation scattered in the cell is photoelectrically observed in a direction transverse to the magnetic field. Further developments in this project being considered are the use of atomic beams instead of sealed cells, and the longitudinal observation of the scattered radiation through Zeeman-effect pole pieces.

A two-channel pulse-counting photometer for the 100-inch was designed and built to use as a spectrophotometer with the coudé spectrograph. One channel is connected to a photomultiplier that scans incrementally along the spectrum, while the second channel monitors a broad band on either side of the scanned portion of the spectrum. The monitor uses a counter that continues to count until a preset value is reached. At this time both counters are shut off and the result is encoded and recorded before the scanning slit is advanced by a stepping motor to the next position. The digital ratio recorder compensates exactly for variations in seeing and in atmospheric extinction. The counters are of a reversing type, which permits complete dark-count compensation by means of a synchronous chopper in front of the spectrograph slit.

In addition to presentation on visual digital indicators, the data are recorded on a printed paper tape and summary punch cards. This repetition provides increased reliability in case of mechanical failure of either recorder. An analogue output is also available for the observer to monitor the output of the main counter as the observations proceed.

This two-channel data acquisition

system has been used at the Newtonian focus with a broad-band photometer and at the Cassegrain focus with the spectrum scanner. In all cases, electrical interference from the summary punch, telescope relays, and the nearby television transmitters has been eliminated for all positions of the dome and telescope. Portions of this system were experimentally used on the 60-inch telescope with the spectrum scanner. Again, no interference was encountered at any telescope position.

The Electronics Laboratory is also completing, for use with photometers at the 200-inch telescope, a two-channel data acquisition system, that can be considerably expanded in the future. A "data room" has been provided adjacent to the observing floor of the dome.

Plans are well advanced for increased utilization of the Cassegrain focus of the Hale telescope. Nearing completion is design of a precision offset guider and instrument adapter frame, which will accommodate spectrographs, scanners, and photometers. A special Cassegrain observer's cage and chair are under construction.

Instrument development mostly under sponsorship by the National Aeronautics and Space Administration included completion of the 200-inch Cassegrain  $f/9$  lens system, with guiding optics and plate holders. A photoelectric spectrum scanner for the 200-inch prime focus was started originally by the Observatories and completed with NASA funds. Modifications were made to digitize the grating drive and to provide additional cooled photomultiplier detectors.

Proposal studies and preliminary designs have been completed for a new 200-inch Cassegrain nebular image-tube spectrograph, which is ready for detailing and fabrication.

Preliminary proposals and designs were prepared by Oke, Rule, and Dennison for a dual 20-channel photoelectric spectrometer, with associated data system, to be used at the Cassegrain focus of the 200-



inch; this instrument is being funded by the Advanced Research Projects Agency.

### *Sixty-Inch Photometric Telescope*

Design studies and preliminary details were completed by Rule for a 60-inch photometric telescope proposed for installation on Palomar Mountain. The instrument, intended for rapid and efficient observation of objects not faint enough to require the 200-inch, is to have a Ritchey-Chrétien optical system with wide-field Cassegrain and five-mirror coudé foci. Layouts have been prepared for the 45-foot two-story dome, structural details of which will be similar to those of the dome of the 48-inch schmidt.

The 60-inch-diameter fused-silica mirror blank (funded by NASA) is already on hand. A new optical grinding and polishing machine with a capacity of 72 inches has been built and assembled in the Mount Wilson optical shop. Equipped with a diamond-wheel cutting head, it is now ready to start work on the 60-inch disk.

### *Other Projects*

A design study for modernization of the Mount Wilson 60-inch reflector, in use since 1908, has been made. A number of improvements are contemplated, including a flip ring for Cassegrain-coudé changes, reactivation of the coudé focus, and installation of improved drives and setting devices. It is expected that in the future a greater part of the time of the 60-inch may be devoted to planetary and lunar observations.

The Mount Wilson 10-inch astrographic telescope, which accommodated the five-inch Ross lens, has been retired after some 50 years of service. In its dome is now installed a 24-inch fork-mounted Cassegrain reflector built at Caltech in 1963 for Dr. Bruce Murray's far-infrared photometric program. The instrument is also adaptable to conventional photoelectric photometry.

Smaller projects completed or under way include improvement of two microphotometers, an exposure meter for the 100-inch coudé spectrograph, and Baum's galaxian image synthesizer.

## PLANS FOR THE CARNEGIE SOUTHERN OBSERVATORY

### *Site Testing in Chile*

Three peaks on the AURA property of the Cerro Tololo Inter-American Observatory have been investigated for seeing with two astronomical seeing monitors (ASMs) under the direction of Irwin and with the assistance of Manfred Wagner. The continued cooperation and assistance of the CTIO personnel are gratefully acknowledged. Observations on 105 nights were made on Cerro Morado (7,151-foot altitude), 50 nights on Cerro Pachon (8,939-foot altitude), and 105 nights on Cerro Tololo (7,241-foot altitude).

Table 5 gives the number of nights and the median zenith seeing for all ASM observations in Chile to date.

Two ASMs were operated side by side

on Tololo for 30 nights and, when carefully focused and adjusted, gave similar results to a high degree of accuracy. Observations were started on Morado in late October, and simultaneous observations on Tololo and Morado on 27 nights gave a median zenith seeing that was identical for the two sites. The second ASM was moved from Tololo to Pachon in late December. A comparison between Morado and Pachon, using only simultaneous observations (normally made every half hour), gave the results shown in Table 6.

The comparison between the two sites is being continued. Pachon is somewhat windier than Morado and is about 10°F colder on the average at night. However, Pachon is normally above the

TABLE 5. ASM Observatories in Chile

Observation Dates	Median Zenith Seeing					
	Tololo		Morado		Pachon	
	No. of Nights	Sec of Arc	No. of Nights	Sec of Arc	No. of Nights	Sec of Arc
1963 Dec.	12	0.60				
1964 Jan.-Feb.						
Mar.-Apr.						
May-June						
July-Aug.						
Sept.-Oct.						
Nov.-Dec.	33	0.65	28	0.67		
1965 Jan.-Feb.			33	0.68	27	0.68
Mar.-Apr.			24	0.64	8	0.80
May			16	0.83	13	0.84

summer haze level, which sometimes rises above the Tololo and Morado summits.

It is highly gratifying that the best seeing apparently comes in the spring and summer when the Magellanic Clouds are best placed for observing; this is also a time of minimum cloudiness.

All ASM observations have been corrected to the zenith by multiplying by  $(\cos z)^{1/2}$ . Inasmuch as the Magellanic Clouds are observed from the Tololo area at zenith distances of 40° or more, the validity of this correction factor required testing, and this was done in two ways. Four months of Morado observations were first used, and observations made at zenith distances less than

40° compared with those made at larger zenith distances. The latter group comprised about one fourth of the total number of observations. The two groups gave zenith answers identical to the nearest 0.01. Second, three observational runs were made on Canopus to air masses greater than 4. When the log of the observed seeing was plotted against the log of the air mass, the slopes for the three runs were 0.4, 0.4, and 0.5, respectively, with an uncertainty of  $\pm 0.1$  for each slope determination. These results are in good agreement with the theoretical value of the slope of 0.5.

A 2.5-mile-long, 3-meter-wide dirt road from Lonely Cactus Pass to the CARSO camp near the Morado summit was completed in January. The distance by road between the Morado and Tololo summits is 6.5 miles. A corral for horses and mules was built at La Mollaca Springs, about 1.5 miles below Lonely Cactus Pass. This was used first to supply the Morado ASM camp and the Morado road crew, and is now used to supply the Pachon ASM camp over three miles of road and seven miles of improved trail. The mud hut belonging to the

TABLE 6. Morado and Pachon Observations

1965	No. of Observations	Median Zenith Seeing, seconds of arc	
		Morado	Pachon
Jan.-Feb.	149	0.61	0.63
Mar.-Apr.	63	0.51	0.63
May	116	0.82	0.87



Association of Universities for Research in Astronomy was refurbished and two new prefabricated cabins built alongside it. A 40-foot anemometer mast has been erected on the Morado summit rock. A cabin for the ASM observers was built on Pachon near a small spring (El Bonito) 0.3 mile from the summit rock on which is located a 20-foot anemometer mast.

Visits were made to the Chile sites by Dr. Caryl P. Haskins, President of the Carnegie Institution, in October 1964, and by Dr. William A. Baum of the Mount Wilson Observatory staff in April 1965.

#### *Site Testing in Australia*

Daniel Crotty set up and operated an ASM at the Siding Spring Observatory (elevation 3,823 feet), beginning in December 1964. This site is in New South Wales some 300 miles north of Canberra in the Warrumbungle Range. Operation of the instrument was frequently hampered by wind, which for 50 per cent of the clear night hours had a speed in excess of 23 mph. The mean image tremor, as determined on 16 nights selected for the low wind speed in January, February, and March, was 0".9. For the period of observation, 44 per cent of the nights were photometric. At the end of the report year, New South Wales was experiencing one of the worst droughts on record.

Comparisons, which in general were quite consistent, were made between the ASM records and visual estimates of the seeing by observers using the 40-inch reflector of the Siding Spring Observatory. Through a cooperative arrangement with the Mount Stromlo Observatory, the Carnegie Institution is helping to support further operation of the ASM at Siding Spring.

While in Australia, Crotty visited sites in the Stirling Range in the extreme southwestern corner of the continent, and arranged for nighttime cloud obser-

vations by a local resident. The data for five months preceding March 1965 indicated that 30 per cent of the nights were clear at 9:00 p.m. and 6:00 a.m. For March, April, and May only 21 per cent of the nights were clear. This unfavorable information confirmed earlier reports regarding the sky conditions in that area. Recent meteorological reports on Mount Singleton, also in Western Australia at latitude 29°S and with an elevation of 2,290 feet, have also been unfavorable. Crotty visited Mount Serle and Mount McKinley in the Northern Flinders Range, some 300 to 400 miles north of the city of Adelaide. The Mount Stromlo Observatory was operating a site-testing station on the former peak, while an expedition from the University of California was testing Mount McKinley with an ASM. The possible advantage of a site on the northwest edge of a geological feature known as Wilpena Pound was pointed out. Crotty concluded that, while more quantitative data are greatly to be desired, there is probably no potential observatory site in Australia superior to Siding Spring Mountain.

#### *Large Telescope Mirrors*

Specifications for a 200-inch fused silica mirror blank were prepared by Rule following discussions with representatives of the Corning Glass Works and of the Quartz Division, General Electric Co.

To acquire quantitative information on the surface deformation to be expected for a solid 200-inch mirror of fused silica in various attitudes with different types of edge support, the consulting services of Professor H. H. Bleich, Director of the Institute of Flight Structures, Columbia University, were obtained. He made semianalytical investigations of mirror deformation for a number of different cases. The results promise to be quite valuable in the selection of an optimum design for the support system.

## REFERENCES CITED

- Babcock, H. W., *Astrophys. J.*, 133, 572, 1961.  
 Burbidge, E. M., G. R. Burbidge, and V. Rubin, *Astrophys. J.*, 140, 942, 1964.  
 Deutsch, A. J., *J. Opt. Soc. Am.*, 44, 492, 1954.  
 Haro, G. *Bull. Obs. Tonantzintla*, 8, No. 14, 1956.  
 Lynds, C. R., and A. Sandage, *Astrophys. J.*, 137, 1005, 1963.  
 Osterbrock, D. E., and R. A. R. Parker, *Astrophys. J.*, 141, 892, 1965.  
 Sandage, A., *Astrophys. J.*, 133, 369, 1961.  
 Vaughan, A. H., *Astron. J.*, 68, 151, 1964.  
 Zirin, H., and R. D. Dietz, *Astrophys. J.*, 138, 664, 1963.

## BIBLIOGRAPHY

- Aller, Lawrence H., *see* Kaler, James B.  
 Arp, Halton C., Properties of the galactic nucleus in the direction of NGC 6522, *Astrophys. J.*, 141, 43-72, 1965.  
 Arp, Halton C., Ring around a galaxy, *Engineering and Science*, 28, 13, 1965.  
 Arp, Halton C., Galaxy M31, *Science*, 145, 952, 1964.  
 Arp, Halton C., Faint ring around the spiral galaxy M81, *ibid.*, 148, 363-364, 1965.  
 Arpigny, Claude, Detailed study of the CN violet (0, 0) band in cometary spectra, *Ann. Astrophys.*, 27, 393-405, 1964.  
 Arpigny, Claude, The resonance-fluorescence excitation of the CO<sup>+</sup> comet-tail bands in Comet Humason (1961e), *ibid.*, 406-416, 1964.  
 Arpigny, Claude, Spectra of Comet Humason (1961e), *Observatory*, 84, 118-121, 1964.  
 Baade, Walter, and Henrietta H. Swope, Variables in the Andromeda Galaxy—Fields I and III, *Astron. J.*, 70, 212-268, 1965.  
 Baschek, Bodo, Häufigkeiten von Na und Mg in Metalllinien- und Ap-Sternen, *Z. Astrophys.*, 60, 76-86, 1964.  
 Baschek, Bodo, and J. Beverley Oke, Effective temperatures and gravities of Ap, Am, and normal A-type stars, *Astrophys. J.*, 141, 1404-1410, 1965.  
 Basler, Roy P., Leif Owren, Robert Howard, and Sara F. Smith, New evidence on the nature of solar M-regions (abstract), *Am. Geophys. Union Trans.*, 45, 2, 1964.  
 Baum, William A., Photosensitive detectors, *Annual Review of Astronomy and Astrophysics*, Vol. 2, 165-184, Annual Reviews, Inc., Palo Alto, Calif., 1964.  
 Baum, William A., Facts and myths concerning image tubes (abstract), *Astron. J.*, 69, 532, 1964.  
 Baum, William A., Review of *The Galaxy and the Magellanic Clouds*, Intern. Astron. Union Symp., 20th, edited by F. J. Kerr and A. W. Rodgers, Australian Academy of Science, Canberra, 1964, *Publ. Astron. Soc. Pacific*, 77, 226, 1965.  
 Berger, Jeanne, *see* Zwicky, Fritz.  
 Bowen, Ira S., Telescopes, *Astron. J.*, 69, 816-825, 1964.  
 Bowen, Ira S., Informal discussion, Le Choix de Sites d'Observatoires Astronomiques (Site Testing), *Intern. Astron. Union Symp.*, 19th, Gauthier-Villars et Cie., Paris, 1964.  
 Bowen, Ira S., Explorations with the Hale telescope, *Science*, 145, 1391-1393, 1964; condensed version, *Astron. Soc. Pacific Leaflet* 429, 8 pp., March 1965.  
 Bowen, Ira S., *see also* Kaler, James B.  
 Bumba, V., and Robert Howard, Large-scale distribution of solar magnetic fields, *Astrophys. J.*, 141, 1502-1512, 1965.  
 Bumba, V., and Robert Howard, A study of the development of active regions, *ibid.*, 1492-1501, 1965.  
 Bumba, V., R. Howard, and J. Kleczek, Association of green-line coronal features with photospheric magnetic fields, *Publ. Astron. Soc. Pacific*, 77, 55-57, 1965.  
 Bumba, V., Robert Howard, and Sara F. Smith, Large-scale patterns of the solar magnetic field (abstract), *Astron. J.*, 69, 535, 1964.  
 Capriotti, Eugene R., The effect of self-absorption of Balmer-line radiation in gaseous nebulae due to hydrogen atoms in the 2s state, *Astrophys. J.*, 140, 632-637, 1964.  
 Conti, Peter S., The presence of lithium in  $\delta$  Eridani, *Observatory*, 84, 122-123, 1964.  
 Conti, Peter S., and G. Wallerstein, Abundances in 68 Tauri (Hyades) and HD 73666 (Praesepe) (abstract), *Astron. J.*, 69, 537, 1964.  
 Deutsch, Armin J., Participant in informal discussion, Additional Meeting of the Royal Astron. Soc. on "Stellar Evolution," *Observatory*, 84, 245-257, 1964.  
 Deutsch, Armin J., and G. Righini, An airborne observation of coronal spectrum at the eclipse of July 20, 1963, *Astrophys. J.*, 140, 313-318, 1964.



- Eggen, Olin J., Colors, luminosities, and motions of the nearer G-type stars, *Astron. J.*, 69, 570–609, 1964.
- Eggen, Olin J., New double stars of small separation, *Publ. Astron. Soc. Pacific*, 76, 357, 1964.
- Eggen, Olin J., Masses, luminosities, colors, and space motions of 228 visual binaries, *Astron. J.*, 70, 19–93, 1965.
- Eggen, Olin J., and Jesse L. Greenstein, Spectra, colors, luminosities, and motions of the white dwarfs, *Astrophys. J.*, 141, 83–108, 1965.
- Eggen, Olin J., and Allan Sandage, New photoelectric observations of stars in the old galactic cluster M67, *ibid.*, 140, 130–143, 1964.
- Eggen, Olin J., and Allan Sandage, The colors of some high-latitude blue stars, *ibid.*, 141, 821–826, 1965.
- Greenstein, Jesse L., The history of stars and galaxies, *Proc. Nat. Acad. Sci. U.S.*, 52, 549–565, 1964.
- Greenstein, Jesse L., The quasi-stellar radio sources, *McGraw-Hill 1965 Yr. Book of Science and Technol.*, pp. 19–25, McGraw-Hill Publishing Co., New York, 1965.
- Greenstein, Jesse L., Some implications of the alteration of the composition of magnetic stars, *Stellar and Solar Magnetic Fields, Intern. Astron. Union Symp.*, 22nd, pp. 78–80, edited by R. Lüst, North-Holland Publishing Co., Amsterdam, 1965.
- Greenstein, Jesse L., Stellar magnetic fields, *ibid.*, pp. 437–448.
- Greenstein, Jesse L., and Philip C. Keenan, A spectroscopic study of NGC 188, *Astrophys. J.*, 140, 673–680, 1964.
- Greenstein, Jesse L., and Rudolph Minkowski, The central stars of planetary nebulae of low surface brightness, *ibid.*, 1601–1603, 1964.
- Greenstein, Jesse L., and Maarten Schmidt, The quasi-stellar radio sources 3C48 and 3C273, *ibid.*, 1–34, 1964; *Quasi-Stellar Sources and Gravitational Collapse*, Chap. 13, pp. 175–211, edited by Robinson, Schild, and Schücking, University of Chicago Press, Chicago, 1965.
- Greenstein, Jesse L., *see also* Eggen, Olin J.; Stawikowski, Antoni; Wright, K. O.
- Herzog, E., Three-dimensional structures in double systems of galaxies, *Publ. Astron. Soc. Pacific*, 77, 94–96, 1965.
- Herzog, E., Absorption in intergalactic bridges, *ibid.*, 119–120, 1965.
- Howard, Robert, Magnetic observations relating to solar flares, *AAS–NASA Symposium on the Physics of Solar Flares, NASA SP-50*, pp. 89–93, edited by Wilmot N. Hess, Scientific and Technical Information Division, Washington, D.C., 1964.
- Howard, Robert, Large-scale solar magnetic fields, *Stellar and Solar Magnetic Fields, Intern. Astron. Union Symp.*, 22nd, pp. 129–136, edited by R. Lüst, North-Holland Publishing Company, Amsterdam, 1965.
- Howard, Robert, Robert Leighton, and Harold Zirin, Solar astronomy neglected, *Science*, 147, 1087–1088, 1965.
- Howard, Robert, *see also* Basler, R. P.; Bumba, V.
- Irwin, John B., Review of *Astronomy*, edited by Samuel Rapport and Helen Wright, New York University Press, New York, 1964; *Science*, 148, 794, 1964.
- Irwin, John B., Serendipity in astronomy, *Sky and Telescope*, 28, 192–195, 1964.
- Irwin, John B., The significance to astronomy of Southern Hemisphere observatories, *Texas Quart.*, 7, 161–172, 1964.
- Jacobson, T. V., *see* Wright, K. O.
- Joy, A. H., Seventy-five years of the Astronomical Society of the Pacific, *Publ. Astron. Soc. Pacific*, 77, 81–88, 1965.
- Kaler, James B., Lawrence H. Aller, and Ira S. Bowen, Spectrophotometric studies of gaseous nebulae, IV, The Orion Nebula, *Astrophys. J.*, 141, 912–922, 1965.
- Karpowicz, Maria, *see* Zwicky, Fritz.
- Kearns, Charles E., and Konrad Rudnicki, Motions in the tail of Comet Humason (1961e), *Acta Astron.*, 15, 1–10, 1965.
- Keenan, Philip C., *see* Greenstein, Jesse L.
- Kleczek, J., *see* Bumba, V.
- Kowal, Charles T., An intergalactic obscuring cloud? *Astron. J.*, 69, 757–758, 1964.
- Kraft, Robert P., and Olin C. Wilson, The strength of the Li I line in the spectra of main-sequence F- and G-type stars, *Astrophys. J.*, 141, 828–832, 1965.
- Kraft, Robert P., George W. Preston, and Sidney Carne Wolff, The width of H $\alpha$  as the discriminant of luminosity in the spectra of late-type stars, *ibid.*, 140, 235–249, 1964.
- Kraft, Robert P., *see also* Krzeminski, W.
- Krzeminski, W., and Robert P. Kraft, Binary stars among cataclysmic variables, V, Photoelectric and spectroscopic observations of the ultra-short period binary Nova WZ Sagittae, *Astrophys. J.*, 140, 921–935, 1964.
- Kuhi, Leonard V., A possible flare of W Ursae Majoris, *Publ. Astron. Soc. Pacific*, 76, 430–432, 1964.
- Lee, E. K., *see* Wright, K. O.
- Leighton, Robert, *see* Howard, Robert.
- Matthews, Thomas A., William W. Morgan, and Maarten Schmidt, A discussion of galaxies



- identified with radio sources, *Astrophys. J.*, 140, 35-49, 1964; *Quasi-Stellar Sources and Gravitational Collapse*, Chap. 10, pp. 105-134, edited by Robinson, Schild, and Schücking, University of Chicago Press, Chicago, 1965.
- Mihalas, Dimitri, A spectroscopic estimate of the atmospheric properties of O stars, *Astrophys. J.*, 140, 885-901, 1964.
- Mihalas, Dimitri, Model atmospheres and line profiles for early-type stars, *Astrophys. J., Suppl. Ser.* 92, 321-438, 1965.
- Miller, William C., Application of pre-exposure to astronomical photography, *Publ. Astron. Soc. Pacific*, 76, 328-349, 1964.
- Miller, William C., A pre-flasher for photographic plates, *ibid.*, 433-434, 1964.
- Minkowski, Rudolph, *see* Greenstein, Jesse L.
- Morgan, William W., *see* Matthews, Thomas A.
- Münch, Guido, An interstellar cloud with a high concentration of CN molecules, *Astrophys. J.*, 140, 107-111, 1964.
- Münch, Guido, and Luis Münch, Radial velocities of distant OB stars, *ibid.*, 162-166, 1964.
- Münch, Guido, and Robert L. Younkin, Molecular absorptions and color distributions over Jupiter's disk (abstract), *Astron. J.*, 69, 553, 1964.
- Münch, Guido, *see also* Younkin, Robert L.
- Münch, Luis, *see* Münch, Guido.
- Murray, Bruce C., James A. Westphal, and Robert L. Wildey, The eclipse cooling of Ganymede, *Astrophys. J.*, 141, 1590-1592, 1965.
- Oke, J. Beverley, Photoelectric spectrophotometry of stars suitable for standards, *ibid.*, 140, 689-693, 1964.
- Oke, J. Beverley, The optical spectrum of 3C273, *ibid.*, 141, 6-18, 1965.
- Oke, J. Beverley, *see also* Baschek, Bodo.
- Owren, Leif, *see* Basler, Roy P.
- Pohn, Howard A., *see* Wildey, Robert L.
- Preston, George W., *see* Kraft, Robert P.
- Righini, G., *see* Deutsch, Armin J.
- Rudnicki, Konrad, *see* Kearns, Charles E.
- Sandage, Allan, Participant in informal discussion, Additional Meeting of the Royal Astron. Soc. on "Stellar Evolution," *Observatory*, 84, 245-257, 1964.
- Sandage, Allan, Exploding galaxies, *Sci. Am.*, 211, 38-47, 1964.
- Sandage, Allan, The existence of a major new constituent of the universe: The quasi-stellar galaxies, *Astrophys. J.*, 141, 1560-1578, 1965.
- Sandage, Allan, and John D. Wyndham, On the optical identification of eleven new quasi-stellar sources, *ibid.*, 141, 328-331, 1965.
- Sandage, Allan, *see also* Eggen, Olin J.
- Schmidt, Maarten, Optical spectra and redshifts of 31 radio galaxies, *Astrophys. J.*, 141, 1-5, 1965.
- Schmidt, Maarten, Large redshifts of five quasi-stellar sources, *ibid.*, 1295-1300, 1965.
- Schmidt, Maarten, *see also* Greenstein, Jesse L.; Matthews, Thomas A.
- Skumanich, Andrew, *see* Wilson, Olin C.
- Smith, Sara F., *see* Basler, Roy P.; Bumba, V.
- Stawikowski, Antoni, and Jesse L. Greenstein, The isotope ratio  $C^{12}/C^{13}$  in a comet, *Astrophys. J.*, 140, 1280-1291, 1964.
- Suess, Hans E., *see* Tammann, Gustav Andreas.
- Swope, Henrietta H., *see* Baade, Walter.
- Tammann, Gustav Andreas, Zum neunzigsten Geburtstag von Ejnar Hertzsprung, *Orion*, 9, 1, 1964.
- Tammann, Gustav Andreas, Quasistellare Radioquellen, *Bild der Wissenschaften*, 2, 221, 1965.
- Tammann, Gustav Andreas, and Hans E. Suess, Neuere Untersuchungen über die Atmosphären von Mars, Venus, Merkur, und der Roten Riesen, *Umschau*, 64, 556, 1964.
- Trafton, Laurence M., The thermal opacity in the major planets, *Astrophys. J.*, 140, 1340-1341, 1964.
- Utter, Merwyn G., The heavens in 1965, *Astron. Soc. Pacific, Ann. Ser.*, 8 pp., January 1965.
- Veron, P., Optical positions of eight quasi-stellar objects associated with radio sources, *Astrophys. J.*, 141, 332, 1965.
- Veron, P., On the optical position of the stellar object associated with the radio source MSH, 14-121, *ibid.*, 1284-1285, 1965.
- Wallerstein, G., *see* Conti, Peter S.
- Westphal, James A., *see* Murray, Bruce C.
- Wildey, Robert L., The Moon's photometric function, *Nature*, 200, 1056-1058, 1963.
- Wildey, Robert L., Temperature measurements in the solar system, *Astron. Soc. Pacific Leaflet* 425, 8 pp., November 1964.
- Wildey, Robert L., A computer program for the transformation of lunar observations from celestial to selenographic coordinates, *Icarus*, 3, 136-150, 1964.
- Wildey, Robert L., Photometry of the earth from Mariner 2, *J. Geophys. Res.*, 69, 4461-4472, 1964.
- Wildey, Robert L., On line-blanketing normalization of subdwarf photometry, *Astrophys. J.*, 141, 943-948, 1965.
- Wildey, Robert L., A quasi-traditional spectroscopic radial velocity technique applied to the rotation of Venus, *Nature*, 206, 1238-1239, 1965.



- Willey, Robert L., The hot shadows of Jupiter, *Science*, 147, 1035-1036, 1965.
- Willey, Robert L., and Howard A. Pohn, Detailed photoelectric photometry of the Moon, *Astron. J.*, 69, 619-634, 1964.
- Willey, Robert L., *see also* Murray, Bruce C.
- Wilson, Olin C., Chromospheric activity and lithium, *Publ. Astron. Soc. Pacific*, 76, 238-240, 1964.
- Wilson, Olin C., and Andrew Skumanich, Dependence of chromospheric activity upon age in main-sequence stars: Additional evidence, *Astrophys. J.*, 140, 1401-1408, 1964.
- Wilson, Olin C., *see also* Kraft, Robert P.
- Woerden, Hugo van, Rapport over het 14E Congress van de Union Radio-Scientifique Internationale, *Rapporten Kon. Nederl. Akad. Wetensch. Amsterdam*, XVI, 53-54, 1964.
- Wolff, Sidney Carne, *see* Kraft, Robert P.
- Wright, K. O., E. K. Lee, T. V. Jacobson, and J. L. Greenstein, Line intensities in the spectra of representative stars of spectral types B to G, *Publ. Dominion Astrophys. Obs.*, 12, 173-291, 1964.
- Wyller, Arne A., Identification of the (2, 0)  $C^{13}N^{14}$  band in the spectra of carbon (abstract), *Astron. J.*, 69, 565, 1964.
- Wyndham, John D., *see* Sandage, Allan.
- Younkin, Robert L., and Guido Münch, Wavelength dependence of the band structures of Jupiter and of Saturn (abstract), *Astron. J.*, 69, 565, 1964.
- Younkin, Robert L., *see also* Münch, Guido.
- Zirin, Harold, *see* Howard, Robert.
- Zwicky, Fritz, Compact galaxies, *Acta Astron.*, 14, 151-155, 1964.
- Zwicky, Fritz, Basic results of the international search for supernovae, *Ann. Astrophys.*, 27, 300-312, 1964.
- Zwicky, Fritz, Compact galaxies and compact parts of galaxies, I, *Astrophys. J.*, 140, 1467-1471, 1964.
- Zwicky, Fritz, The luminosity function of galaxies, *ibid.*, 1626-1628, 1964.
- Zwicky, Fritz, Durchmusterung der Himmelsobjekte, *Bild der Wissenschaften*, 1, 31-41, 1964.
- Zwicky, Fritz, Kompakte und sehr kompakte Sternsysteme, *Die Sterne*, 40, 129-130, 1964.
- Zwicky, Fritz, First list of compact galaxies, compact parts of galaxies, and eruptive and post-eruptive galaxies, California Institute of Technology, Pasadena, June 15, 1964.
- Zwicky, Fritz, Kompaktnie Galaktiki (in Russian), *Proc. Armenian Acad. Sci.*, 39, 167-170, 1964.
- Zwicky, Fritz, The 1963 Palomar supernovae search, *Publ. Astron. Soc. Pacific*, 76, 325-327, 1964.
- Zwicky, Fritz, Neutron stars, *Sky and Telescope*, 28, 79, 1964.
- Zwicky, Fritz, and Jeanne Berger, Area of the sky covered by clusters of galaxies, II, *Astrophys. J.*, 141, 34-42, 1965.
- Zwicky, Fritz, and Maria Karpowicz, Supernova 1956a of Type I in NGC 3992, *Astron. J.*, 69, 759-761, 1964.

## STAFF AND ORGANIZATION

Dr. Olin Eggen resigned on September 1, 1964, to accept an appointment at the Royal Greenwich Observatory.

Dr. Harold Zirin was appointed Staff Member of the Observatories as of September 16, 1964. With research interests mainly in the field of solar physics, Dr. Zirin comes from the High Altitude Observatory, Boulder, Colorado.

Mr. Bruce H. Rule was designated Chief Engineer of the Mount Wilson and Palomar Observatories.

Mr. Daniel L. Crotty took up a temporary appointment as Staff Associate, with responsibility for site testing in Australia, on August 1, 1964.

Mrs. Ester Bru Baum resigned as Librarian on June 30, 1965.

### *Research Division*

#### *Staff Members*

Halton C. Arp  
 Horace W. Babcock, Director  
 William A. Baum  
 Ira S. Bowen, Distinguished Service Staff Member  
 Edwin W. Dennison  
 Armin J. Deutsch  
 Olin J. Eggen<sup>1</sup>  
 Jesse L. Greenstein

<sup>1</sup> Resigned September 1, 1964.

Robert F. Howard  
 Robert P. Kraft  
 Robert B. Leighton  
 Guido Münch  
 J. Beverley Oke  
 Allan R. Sandage  
 Maarten Schmidt  
 Olin C. Wilson  
 Harold Zirin  
 Fritz Zwicky

*Staff Members Engaged in Post-Retirement Studies*

Harold D. Babcock  
 Alfred H. Joy

*Chief Engineer*

Bruce H. Rule

*Senior Research Fellows*

Stuart L. Ridgway  
 George Wallerstein

*Carnegie Fellows*

Leonard V. Kuhi  
 Hugo van Woerden<sup>2</sup>  
 Arthur H. Vaughan, Jr.  
 John B. Whiteoak<sup>3</sup>

*National Science Foundation Fellow*

Barry M. Lasker

*Research Fellows*

Peter S. Conti  
 Ivan J. Danziger  
 Rolf P. Fenkert<sup>4</sup>  
 John E. Gaustad<sup>5</sup>  
 Robert Kovar<sup>6</sup>  
 Antoni Stawikowski<sup>7</sup>  
 Robert Stoeckly  
 Henrietta H. Swope  
 Robert L. Wildey<sup>8</sup>

*Senior Research Assistant*

Dorothy D. Locanthi

<sup>2</sup> Resigned July 31, 1964.

<sup>3</sup> Resigned September 30, 1964.

<sup>4</sup> Resigned October 15, 1964.

<sup>5</sup> Resigned July 10, 1964.

<sup>6</sup> Resigned December 31, 1964.

<sup>7</sup> Resigned October 31, 1964.

<sup>8</sup> Resigned June 30, 1965.

*Research Assistants*

Frank J. Brueckel  
 Sylvia Burd  
 Thomas A. Cragg  
 Rowena Danziger  
 Howard Gates  
 Jack Harvey  
 Emil Herzog  
 Maria Karpowicz  
 Basil Katem  
 Margaret Katz  
 Charles T. Kowal<sup>9</sup>  
 A. Louise Lowen  
 George P. Mylonas<sup>10</sup>  
 Malcolm S. Riley  
 Gustav A. Tammann  
 Merwyn G. Utter  
 Philippe Veron

*Student Observers*

Christopher Anderson  
 Kurt Anderson  
 James Aries  
 Dennis Baker  
 James E. Gunn  
 Floyd Herbert  
 Douglas Keeley  
 Ernest Lorenz  
 Richard Nichol  
 Kenneth Nordsieck  
 Bruce Peterson  
 Philip Roberts  
 Jeffrey Scargle  
 Neil R. Sheeley  
 Alan M. Title  
 Laurence Trafton

*Photographer*

William C. Miller

*Librarian*

Ester Bru Baum<sup>11</sup>

*Instrument Design and Construction*

Lawrence E. Blakee, Senior Electronic Technician  
 Eileen I. Challacombe, Draftsman  
 Floyd E. Day, Optician

<sup>9</sup> Resigned January 9, 1965.

<sup>10</sup> Resigned August 30, 1964.

<sup>11</sup> Resigned June 30, 1965.



Kenneth E. DeHuff, Machinist<sup>12</sup>  
 Robert D. Georgen, Machinist  
 David C. Jermann, Machinist  
 Melvin W. Johnson, Optician  
 Rudolf E. Ribbens, Designer and Superintendent of Instrument Shop  
 Marlin N. Schuetz, Electronic Technician  
 John Shirley, Electronic Engineer  
 Benny W. Smith, Electronic Technician  
 Ralph W. Wilson, Machinist

### *Maintenance and Operation*

#### *Mount Wilson Observatory Offices*

Paul F. Barnhart, Chauffeur  
 Wilma J. Berkebile, Secretary  
 Hugh T. Couch, Superintendent of Buildings and Grounds  
 Helen S. Czaplicki, Typist Editor  
 Fanny G. Gabrielson, Stewardess  
 Eugene L. Hancock, Night Assistant  
 Mark D. Henderson, Gardener  
 Frank Hernandez, Laborer  
 Doris Jeffrey, Stewardess<sup>13</sup>  
 Fred Large, Laborer<sup>13</sup>  
 Anne McConnell, Administrative Assistant<sup>14</sup>  
 Leah M. Mutschler, Stenographer and Telephone Operator<sup>15</sup>  
 Bula H. Nation, Head Stewardess  
 Alfred H. Olmstead, Night Assistant  
 Ted C. Regulski, Accountant  
 Glen Sanger, Custodian  
 Henry F. Schaefer, Night Assistant  
 John E. Shirey, Laborer<sup>16</sup>  
 Elizabeth M. Shuey, Receptionist and Secretary

<sup>12</sup> Retired September 30, 1964.

<sup>13</sup> Temporary summer employee.

<sup>14</sup> Retired January 31, 1965.

<sup>15</sup> Retired May 31, 1965.

<sup>16</sup> Resigned April 30, 1965.

William D. St. John, Custodian and Relief Engineer  
 Benjamin B. Traxler, Superintendent

#### *Palomar Observatory and Robinson Laboratory*

Fred Anderson, Machinist  
 Jan A. Bruinsma, Custodian  
 Maria J. Bruinsma, Stewardess  
 Eleanor G. Ellison, Secretary and Librarian  
 Victor A. Hett, Night Assistant  
 Byron Hill, Superintendent  
 Helen D. Holloway, Secretary  
 Charles E. Kearns, Senior Night Assistant  
 J. Luz Lara, Ground Mechanic  
 Mildred Newton, Department Clerk  
 Robert D. Quinn, Maintenance Mechanic<sup>17</sup>  
 Gary M. Tuton, Night Assistant  
 Hendrika E. van Buuren, Stewardess  
 John E. van Buuren, Custodian  
 William C. Van Hook, Electrician and Assistant Superintendent  
 Betty A. Wallace, Secretary  
 Gus Weber, Assistant Mechanic<sup>18</sup>

### *Site-Testing Operations*

#### *Chile*

Manuel Casanova, Assistant Observer  
 Rolando H. Cortez, Assistant Observer  
 John B. Irwin, Staff Associate  
 Rolando Vega, Assistant Observer  
 Manfred Wagner, Observer

#### *Australia*

Daniel L. Crotty, Staff Associate

#### *Temporary Research Assistant*

Donald E. Johnson

<sup>17</sup> Resigned May 23, 1965.

<sup>18</sup> Retired June 30, 1965.

# *Geophysical Laboratory*

Philip H. Abelson  
*Director*

*Washington, District of Columbia*





Contents

Introduction . . . . .	63	melting composition in the system MgO-SiO <sub>2</sub> -TiO <sub>2</sub> . . . . .	135
Phase-Equilibrium Studies of Silicate and Oxide Systems . . . . .	69	Phase diagram for the system nepheline- quartz . . . . .	139
Melting relations of volcanic tholeiite and alkali rock series . . . . .	69	Shearing squeezer experiments with quartz and coesite . . . . .	141
Hawaiian alkali series . . . . .	72	Iron-titanium oxides . . . . .	144
Hebridean alkali series . . . . .	75	Pseudobrookite series . . . . .	146
Tristan da Cunha alkali series . . . . .	75	Ferrosilite . . . . .	148
Olivine nephelinites . . . . .	76	Ortho-clino inversion in ferrosilite . . . . .	148
Diopside-anorthite-water at five and ten kilobars and its bearing on explo- sive volcanism . . . . .	82	Intermediate iron-magnesium pyroxenes . . . . .	149
The reactions between forsterite and anorthite at high pressures . . . . .	89	Stability of (Fe <sub>0.95</sub> Mg <sub>0.05</sub> )SiO <sub>3</sub> . . . . .	150
Behavior of melilites in the join gehlenite-soda melilite-akermanite at one-atmosphere pressure . . . . .	95	Chemical analysis of synthetic ferrosilite . . . . .	150
Sides of the join gehlenite-soda melilite-akermanite . . . . .	95	Heat flow at Ajo, Arizona . . . . .	150
The join gehlenite-soda melilite-akermanite . . . . .	98	Statistical Petrography . . . . .	153
The join diopside-spinel at atmospheric pressure and the significance of the diopside-spinel assemblage . . . . .	100	I. The silica-alkali balance in Cenozoic basic volcanics . . . . .	154
The liquidus relations in the systems forsterite-CaAl <sub>2</sub> SiO <sub>6</sub> -silica and forsterite-nepheline-silica at high pressures . . . . .	103	II. The silica-alkali balance in basalts of the submarine ridges . . . . .	155
The system forsterite-CaAl <sub>2</sub> SiO <sub>6</sub> -silica . . . . .	104	III. On the level of silica saturation in andesite . . . . .	155
The system forsterite-nepheline-silica . . . . .	106	IV. On changes in composition effected by cyclic assimilation . . . . .	159
Coexistence of nepheline and enstatite at high pressures . . . . .	109	V. Some actual and potential petrographic applications of discriminant function analysis . . . . .	160
Clinopyroxene solid solutions at high pressures . . . . .	112	Geochronology and Isotope Geochemistry . . . . .	165
The join diopside-albite . . . . .	113	Lead isotopes and the age of the earth . . . . .	167
The join diopside-anorthite . . . . .	115	Isotopic composition of lead and strontium in crystalline rocks from the northern Cascade Range, United States . . . . .	171
The rhombic enstatite-clinoenstatite inversion . . . . .	117	The minimum age of the Glenarm series, Baltimore, Maryland . . . . .	174
Temperature-composition section for jadeite-diopside . . . . .	120	Radioactive heat production in peridotite . . . . .	176
Melting relations in the join diopside- forsterite-pyroxene at 40 kilobars and at one atmosphere . . . . .	123	Ore Minerals: Petrography and Experimental Studies . . . . .	177
Stability fields of spinel and garnet peridotites in the synthetic system MgO-CaO-Al <sub>2</sub> O <sub>3</sub> -SiO <sub>2</sub> . . . . .	126	Investigations of the nickel-copper ores and adjacent rocks of the Sudbury District, Ontario . . . . .	177
Aluminous diopsides in the three-phase assemblage diopside solid solution + forsterite + spinel . . . . .	134	The Strathcona ore body . . . . .	178
The effect of pressure on the minimum		Rock formations . . . . .	179
		Composition of olivine in xenoliths of hanging-wall breccia . . . . .	182
		Plagioclase composition in rocks near the mine . . . . .	183
		Structural state of the plagioclase . . . . .	185
		Biotite variation . . . . .	186



Geological history . . . . .	188	Tetraphenylporphyrin-silver (II) tetraphenylporphyrin solid solutions . . . . .	212
Sulfide-carbonate reactions . . . . .	188	Biogeochemistry . . . . .	215
Sulfide-silicate relations . . . . .	192	The extractable organic matter in Precambrian rocks and the problem of contamination . . . . .	215
The mercury-sulfur system . . . . .	193	Fatty acids from the oxidation of kerogen . . . . .	218
The lead-sulfur system . . . . .	195	Amino acid composition of some calcified proteins . . . . .	223
High-pressure differential thermal analysis . . . . .	197	Amino acid artifacts in organic geochemistry . . . . .	232
Crystallography . . . . .	200	Miscellaneous Administration . . . . .	235
Refinement of lattice parameters using systematic correction terms . . . . .	200	<i>Journal of Geophysical Research</i> . . . . .	235
Ferrosilite . . . . .	202	<i>Journal of Petrology</i> . . . . .	235
Clinoferrosilite and orthoferrosilite . . . . .	202	Lectures . . . . .	235
Ferrosilite III . . . . .	203	Petrologists' Club . . . . .	237
Thermal parameters and atomic coordinates of $\alpha$ quartz: a comparison of manual and automated diffractometer results . . . . .	204	References Cited . . . . .	237
Crystal morphology of rhombohedral species . . . . .	207	Summary of Published Work . . . . .	243
The structural relation of ardennite to epidote . . . . .	209	Bibliography . . . . .	248
Possible application of nuclear magnetic resonance to order-disorder study in the hydrogrossularite series . . . . .	210	Personnel . . . . .	250

## INTRODUCTION

A visitor to the Geophysical Laboratory sees what appears to be an establishment largely devoted to chemical research. In some rooms many silicate melts are in preparation or under study. In other rooms may be seen equipment and work in progress devoted to experiments at very high pressures. A comparatively large and busy machine shop lends an industrial aspect to part of the building, and there are laboratories with complex electronic equipment characteristic of modern chemical research facilities. It would require special knowledge to detect that the Laboratory is engaged in studies of the earth but overt evidence of these studies does exist—in the presence of petrological microscopes and occasional specimens of rocks and minerals.

Yet the visitor would be seeing only part of the picture. What is not so readily apparent is that our staff is at home in two laboratories. One is in Washington. The second encompasses the earth and part of the solar system. The Geophysical Laboratory staff has numerous close relations with the earth and has conducted studies on many meteorites. Almost all the experimental work has one of several direct connections with naturally occurring materials. For example, the investigations may be conducted with the rocks collected from localities that are scattered over almost all the earth's surface. Experiments with pure chemicals may be devised to explain what is seen in nature. For the most part our staff personally collects the rocks that we use. In the course of a few years this has involved travel throughout the United States and entailed field trips in many areas abroad. The close relation between our laboratory work and the earth's rocks is illustrated by some of our activities of the past few years.

To help them in their studies of organic matter in rocks, Hoering and Abelson have assembled and examined rocks from

Europe, Africa, Australia, and North America. They have also obtained core specimens from the continental shelves. The age group has dated specimens from all the continents except Antarctica and made isotope determinations on specimens from some of the oceanic islands. In his statistical analyses of Cenozoic basalts Chayes has drawn on most of the world's chemical analyses of such rocks. Tilley, Yoder, and Schairer have obtained and studied samples of analyzed basalts from all the continents and many of the oceanic islands.

Directly or indirectly, rocks from all over the world have been the source of most of the puzzles that are examined in the Laboratory. For their work investigators prefer to choose minerals that have wide occurrence or special significance as indicators of major geological events. Thus, one principal incentive in studies of basalts is their widespread occurrence. Investigations of sulfide minerals have relevance to ore deposits located everywhere. This broad connection with the whole earth is a source of satisfaction to our staff. There is a feeling of acquaintanceship with all the rocks of the earth, especially those from many famous localities, and of a common bond of friendship with scientists throughout the world who are interested in similar problems. Finally, there is the satisfaction of knowing that our work is of interest to an increasing number of scientists elsewhere. In 1957 reprints of material about our work were requested by 865 individuals or libraries in the United States and 576 in other countries. In 1965 the comparable figures were 1,142 here and 1,103 in foreign countries.

The broad pattern of investigation in significant geological problems was continued during the current report year. Naldrett and Kullerud have initiated a detailed study of processes of ore formation at the recently developed Strathcona



Mine at Sudbury, Ontario. Samples of the copper-iron-nickel sulfide ores and of the various types of associated rocks were obtained from numerous drill cores and locations in the mine. Intensive studies by a variety of techniques reveal that chemical and physical properties of certain minerals in the noritic hanging-wall rocks vary, depending on their distance from the ore bodies. Biotite at considerable distance from the ore is of the normal green variety, but as the ore is approached brown oxidized biotite is found to be increasingly common. Comparisons show that this oxidized biotite is identical with that previously obtained in sulfurization experiments. The composition of plagioclase also changes gradually and significantly and becomes increasingly more albitic as the ore is approached. Reaction zones extending to considerable distances from ores may be utilized in ore exploration.

Some of the world's largest ore deposits occur in sedimentary carbonate rocks. Although the ores generally are believed to be derived from hydrothermal solutions of igneous origin, igneous intrusions commonly do not occur within reasonable distances. By investigating reactions between carbonates and sulfur, Kullerud has shown that some sulfides are produced at 100°C in short periods of time. Carbonate rocks in which ores occur are usually interbedded with considerable amounts of sulfates as well as pyrite and organically derived sulfur. Sulfur and pyrite when mobilized react with the carbonates and produce sulfides, particularly of lead and zinc.

Using new and more versatile gas-chromatographic techniques, Hoering and Abelson have contributed further to the understanding of fatty acid residues in rocks. Such acids are major constituents of living organisms and could be expected to be abundant in both recently formed and old rocks. Palmitic and stearic acids with 16 and 18 carbon atoms per molecule, respectively, are the predominant saturated fatty

acids in cells. Both these compounds are found in rocks. The unsaturated fatty acids containing 18 carbon atoms are even more abundant in cells than is stearic acid, but no traces of unsaturated acids have been found in sediments more than a few years old. These same rocks contain relatively large amounts of acids with an odd number of carbons and with chain lengths greater than 20. It is apparent that profound changes occur rapidly in the concentration and molecular weight distribution of fatty acids in geological environments.

Hoering and Abelson have also observed that long, straight-chained aliphatic groups are present in the insoluble organic matter of rocks. These groups can be recovered as fatty acids after chemical oxidation. Just as in the case of the free fatty acids described above, the distribution of the acids produced on oxidation no longer resembles that in the organic detritus that was deposited in the sediments. Such aliphatic groups are characteristic products of the transformation of organic matter in post-Cambrian rocks and are very stable; it is significant that they have been identified in the kerogen of rocks as old as 1,600 million years (m.y.).

Hoering has observed that normal aliphatic hydrocarbons of long length can be isolated from some very old sedimentary rocks, including the 3,000-m.-y.-old Fig Tree shale of South Africa. This class of compounds is typical of sediments of all ages and arises from the transformation of organic matter that was once a part of living organisms. Hoering has examined the possibility that these hydrocarbons could have arisen from the migration of organic matter into the rock and that they may be younger than the rock. Since the insoluble portion probably could not have migrated far, it would seem to be indigenous to the rock. Hoering has examined the  $C^{13}/C^{12}$  ratio of this portion and compared it with the ratio in the extractable organic fluids that could have migrated in. The ratios agreed



in a number of young rocks, where there is every reason to believe that the soluble organic matter is in place. In several ancient rocks, with only a small amount of extractable organic matter, the ratios did not agree. The simplest interpretation is that the soluble organic matter migrated into the rocks under geological conditions and may not be the same age as the rock. Hoering concludes that the isotope method can give valuable clues about contamination and that one must be very cautious in interpreting the presence of aliphatic hydrocarbons in a rock.

The fossil record shows that whereas some animals have not evolved much, there have been dramatic changes in the hard parts of other forms. The evidence has led some paleontologists to suggest that the "sudden" appearance of multicellular life in the Cambrian was in reality a development from unpreservable organic hard parts to mineralized skeletons composed of calcium phosphate, calcium carbonate, or silica. By studying the hard parts of primitive and highly evolved animals obtained from many parts of the world, Hare and Abelson have found evidence for a related trend in the evolution of mollusks. A progressive sequence from organic-rich to organic-poor shells was seen; both the amount and the kind of organic matrix used in forming the shell varied. Hard parts from primitive forms contain 1-5 per cent organic matter, whereas those of highly evolved animals have a factor of 100 less. The proportions of the individual amino acids change.

Even more striking is a variation in content of glucosamine; shells of primitive forms contain  $10^4$  times more of this chemical than do highly evolved types. Glucosamine is related to chitin (a polymer of acetyl glucosamine) and a major constituent of hard parts of many phyla including some protista.

In analyzing low concentrations of organic components it is necessary to evaluate the problem of contamination,

and Hare has found that mere handling of samples can add recognizable amounts of amino acids that could easily obscure those present *in situ* in the sample. Fortunately, contamination from this source seems to be consistently characterized by relatively large amounts of serine and ornithine, components that are relatively low or absent in shell proteins.

The usual way of calculating the age of the earth is to assume that the earth originally contained lead having the same isotopic composition as that found in iron meteorites. The calculation involves finding the interval of time for radioactive decay required to produce "modern terrestrial lead," starting with the meteorite lead. Since there is a large variation in the isotopic composition of modern terrestrial lead, Tilton, Davis, and Steiger have been attempting to modify the method by working with lead from rocks that are 2.7 billion years (b.y.) old, expecting that the variation will be smaller. Last year preliminary data on old rocks from North America suggested an age of 4.7 b.y. for the earth instead of the commonly accepted value of 4.55 b.y. A coordinated study of granitic rocks and lead ores near Lake Superior in southern Ontario substantiates last year's result. Measurements from the middle portion of North America are now believed to indicate either that (1) the earth is 0.15 to 0.2 b.y. older than was previously thought, or (2) lead at the time of the earth's formation did not have exactly the same isotopic composition as that of iron meteorites.

Chayes has continued his study on the major-element geochemistry of Cenozoic volcanism. His work has centered on the silica saturation level of basic volcanics and andesites, a parameter conveniently characterized for any specimen by the amounts of normative quartz, olivine, and nepheline computed from its analysis. The first of these is always incompatible with the other two and in rocks of the kind under discussion the third usually occurs only if the second is also present.



In a collection of more than 2,000 analyses of basic volcanics it has been found that more than three quarters of the norms contain either  $Q$  or  $ne$ . The sample includes a very large proportion of the available data, and it is clear that the composition of each of the analyzed Cenozoic basic volcanics ordinarily lies outside the rather wide range that can be tolerated without the emergence of normative imbalance between alkalis and silica. Another broad data summary of this type has shown that the normative quartz content of analyzed specimens called andesite in the source references is such that in this respect barely a third of more than 1,500 such rocks satisfy the definitions proposed in the major chemical-petrographic systems. Quite apart from the substantive interest attaching to the results, what is particularly striking about these massive data reductions is the ease and speed with which they can now be obtained. The time consumed in the reading of this paragraph, for instance, insufficient for hand calculation of a single norm, is more than ample for the machine calculation of several hundred. Efficient exploitation of the vast accumulation of information concerning the chemical composition of rocks, not previously accomplished, though not in principle impossible, now requires little more than the preparation and maintenance of a suitable library of analyses.

During the report year much attention has been given to present and potential petrographic applications of discriminant function analysis, with particular stress on the interesting properties of linear and higher-order discriminants in the closed array. For the two-class partition of the members of any  $M$ -variable closed array, for instance, it has been found that there are  $M$  "most effective" polynomial discriminant functions of any given order and that all of them partition the data identically. There is thus no need to compute more than one, and any one will do. Moreover, whether or not the data

are closed, the objective of the discriminant function as a taxonomic device is very like that of the graphical procedure by which field boundaries are inserted in phase diagrams, and in trial calculations based on published data the results are gratifyingly similar. As long as the thermodynamic variance of a system is less than 4 a standardized nongraphical procedure for locating field boundaries, though perhaps often convenient, will hardly be essential. It becomes indispensable, however, in the systematic investigation of systems whose variance is such as to preclude graphical representation, for, if data points cannot be displayed on a graph or in a solid model, the location of field boundaries by inspection is *ipso facto* impossible. Their "location" by discriminant function or other multivariate computational technique would of course be subject to no such restriction.

Explosive volcanism ranks among the greatest of natural catastrophes. As much as 36 cubic miles of material was removed in a single explosion occurring in the East Indies in 1815. At Krakatoa in 1883 a famous and violent though somewhat smaller volcanic explosion occurred. Accompanying this event was a tremendous tidal wave. Ash from the explosion reached the stratosphere, where it remained for several years and affected world weather. The recurring violence of this type of volcanism and the widespread distribution of the ejected material are of special concern to many peoples of the world. At the Geophysical Laboratory there has been continuing awareness of this problem and consideration of potential mechanisms. An early idea of Morey's has been generally accepted. It was based on experiments conducted with potassium silicates and water at pressures up to 0.34 kb. He found that under special conditions gas pressure increased rapidly when the melt, saturated with crystals and gas, cooled. Although it was recognized that Morey's model was useful, it was considered by some not



generally applicable to natural systems. Yoder has now studied a silicate system more closely approximating natural basalts using pressures ( $\sim 10$  kb) more typical of those now believed to exist in the region in which magmas are generated. He has found that gas (mainly  $H_2O$ ) can be expelled from both saturated and undersaturated magmas when the containing pressure decreases. The water content of magma at depth (pressure) provides an adequate propellant for the natural phenomena that have been observed.

Tilley, Yoder, and Schairer, continuing their research on the experimental melting of basalts, extended their inquiry into the melting relations of the members of volcanic basalt-trachyte associations, exemplified in the oceanic alkali provinces of Hawaii and Tristan da Cunha and in the classic Hebridean region. Their study confirmed a direct relationship between liquid iron enrichment and liquidus temperature for the rocks of these provinces as in the work previously reported on the Hawaiian tholeiite series. Olivine, however, was early replaced by plagioclase as the liquidus phase in these successions, though phenocryst olivine persisted in the lavas themselves. The behavior of the investigated melts suggested that in the process of fractional crystallization the residual magma was enriched by inherited crystals of plagioclase acquired by flotation accumulation in this fractionating liquid.

When basalts are subjected to temperatures and pressures equivalent to those in the earth's upper mantle, eclogite rich in jadeitic pyroxene is formed. Delineation of the stability of pure jadeite was part of Bell and Roseboom's study of the nepheline-quartz system at high pressures and temperatures. Bell and Davis examined a system closer to the natural one by adding diopside to jadeite. At 30 kb and temperatures below  $1,425^\circ C$  they observed a two-pyroxene field in the temperature-composition plane.

In a continuing study of the basalt-eclogite transformation, reactions between forsterite and anorthite, reported last year, have been studied in detail by Kushiro and Yoder to determine the univariant curves of the reactions and to delineate the phase relations in the system  $CaO-MgO-Al_2O_3-SiO_2$  over a wide range of pressure-temperature ( $P-T$ ) conditions. The results yield information on the stability relations of basalts, basic granulites, pyroxenites, and eclogites. As part of the studies on the basalt-eclogite transformation the reactions between diopside and albite, and diopside and anorthite, have also been studied at high pressures. The results indicate the stability of diopside solid solutions containing considerable amounts of jadeite and Ca Tschermak's components at high pressures and give the amounts of both the components over a wide range of  $P-T$  conditions.

MacGregor has investigated melting relations in the system  $MgO-SiO_2-TiO_2$  in an effort to understand the bimodal distribution of  $TiO_2$  in basaltic rocks that was earlier discovered by Chayes. The composition of the minimum melting mixture in this ternary system was found to shift markedly with pressures up to 40 kb. If these melting relations are not substantially changed by the addition of other components it may be possible to interpret the variation of  $TiO_2$  in basalt as due to various depths of generation of basalt in the mantle. MacGregor has continued his study of the spinel peridotite  $\rightleftharpoons$  garnet peridotite reaction by evaluating the effect of  $CaO$  on this reaction. The addition of  $CaO$  leads to complex garnet and pyroxene solid solutions, but the basic relation in which low-pressure assemblages containing pyroxene with spinel react at high pressures to form garnetiferous assemblages is maintained.

Boyd and England have determined the curve for the reaction rhombic enstatite-clinoenstatite in the range up to 50 kb. Clinoenstatite has a stability field



that is little affected by pressure and is the equilibrium form of  $\text{MgSiO}_3$  below temperatures in the range  $600^\circ\text{C}$ – $700^\circ\text{C}$ . This rather wide field for clinoenstatite makes it puzzling that natural terrestrial enstatites are almost invariably rhombic. Although phase studies of synthetic silicates such as  $\text{MgSiO}_3$  have been predominantly applied to terrestrial rocks, they are equally applicable to extra-terrestrial occurrences. Both clinoenstatite and rhombic enstatite are found in chondritic meteorites. Inasmuch as glass is also found in these meteorites, it is probable that the clinoenstatite is not primary but that it has formed by rapid inversion from the high-temperature form, protoenstatite. If this inference is correct, the mineral assemblage in the meteorites formed in a restricted  $P$ – $T$  range at temperatures above  $1,000^\circ\text{C}$  and pressures below 8 kb.

Relations between monoclinic and orthorhombic ferrosilite are similar to those for  $\text{MgSiO}_3$ . Lindsley has found that in the range of 20–40 kb clinoferrosilite is stable below  $800^\circ\text{C}$  and orthoferrosilite above  $800^\circ\text{C}$ . The inversion curve is essentially independent of pressure in the range investigated. Preliminary data for the composition  $\text{Fe}_{0.4}\text{Mg}_{0.6}\text{SiO}_3$  indicate that clinopyroxene is stable below  $900^\circ\text{C}$  at 20 kb. Extrapolation of the high-pressure data to lower pressures indicates that clinohypersthene should be more common in many charnockites and metamorphosed pyroxenites and peridotites than has been reported.

Bell and Roy collected core samples and measured temperature gradients at Ajo, Arizona. After the field data were combined with laboratory measurements, a relatively high value of heat flow was calculated. A correlation between heat flow and subcrustal structure is suggested.

Bell, Simmons, and Hays utilized the shearing squeezer to extend previous studies of quartz-coesite to lower temperatures. Results at  $350^\circ\text{C}$ – $500^\circ\text{C}$  were consistent with values previously ob-

tained at higher temperatures. They have also been able to synthesize coesite at room temperature. Thus it is unnecessary to invoke high temperatures in explaining some occurrences of coesite in meteorite craters.

The capability of the Laboratory to carry out detailed crystal-chemical investigations of petrologically important systems has been significantly increased this year by the addition of an automated single-crystal diffractometer. This equipment has reduced the time needed to obtain precise X-ray diffraction data for crystal structure investigations by at least a factor of 3. Results already obtained with the instrument, reported by Burnham, indicate that increased measuring speed and flexibility have been achieved with a concomitant gain in precision. His studies of  $\alpha$  quartz, in conjunction with similar studies at the U.S. Geological Survey (USGS), show that atomic thermal models, which are strongly subject to systematic error, are reproducible on an interlaboratory basis with different measurement geometries.

Although no natural occurrences of ferrosilite ( $\text{FeSiO}_3$ ) have yet been reported, the crystal chemistry and phase relations of this end member and its polymorphs are critical to our understanding of the petrology of the common pyroxene constituents of basalts. Through single-crystal investigations of clinoferrosilite and orthoferrosilite, Burnham reports that the difference in molar volume between these two phases at room temperature is only  $0.06 \pm 0.02 \text{ cm}^3/\text{mole}$ , thus verifying the virtual independence of the experimentally determined phase boundary on pressure.

Studies of ferrosilite III, an  $\text{FeSiO}_3$  polymorph whose stability field is not yet known and that has no known enstatite ( $\text{MgSiO}_3$ ) analogue, have enabled Burnham to suggest that this phase is a pyroxenoid, closely related to such minerals as wollastonite ( $\text{CaSiO}_3$ ) and rhodonite ( $[\text{Mn}, \text{Ca}]\text{SiO}_3$ ), rather than a true pyroxene. Furthermore, he has demon-



strated that the structure of ferrosilite III will very likely contain a new pyroxenoid type of silicate chain with a repeat length along the chain of nine silicon tetrahedra—the longest repeat unit so far discovered among chain silicates. This proposed structure, once it is confirmed, will certainly have an important bearing on the crystal chemistry of both pyroxenes and pyroxenoids.

The phenomenon of solid solution, which gives rise to the so-called mixed crystals or isomorphous mixtures, is of fundamental importance in mineralogy—practically every mineral is a solid solution. For this reason the crystal structures studied so far, from the point of view of their ability to form solid solutions, are those having a predominantly ionic

character. In such mixed crystals ions nearly equal in size substitute for one another.

In molecular crystal structures, on the other hand, solid solutions may form if a whole molecule can replace another whole molecule. Although rarer than ionic ones, molecular solid solutions also exist in nature. Good examples are found among the biologically important porphyrins. In the case of tetraphenylporphyrins, Donnay has found that it is possible to establish that the free base and the silver salt form a complete series of solid solutions and that no significant change occurs in the volume of the cell of the crystal structure, as the composition varies from one end member to the other.

## PHASE-EQUILIBRIUM STUDIES OF SILICATE AND OXIDE SYSTEMS

### MELTING RELATIONS OF VOLCANIC THOLEIITE AND ALKALI ROCK SERIES

*C. E. Tilley, H. S. Yoder, Jr., and J. F. Schairer*

Melting relations in volcanic rocks, the determination of their liquidus temperatures, and the nature and sequence of phases crystallizing from the melts with falling temperature may reveal genetic relations between individual assemblages of a rock series. Studies of this character are exemplified in work previously reported from the Laboratory on basalts of tholeiitic type, and further inquiry may eventually be expected to test the nature of relationships, if any, existing between individual rock series. Such investigations should continue to aid materially in the ultimate interpretation of differentiation trends in igneous rocks.

Experimental studies on the melting relations of Hawaiian tholeiitic lavas under anhydrous conditions have been previously reported in *Year Books* 62 (pp. 77–84) and 63 (pp. 92–97). These studies have now been extended to cover

the behavior of additional tholeiitic lavas but principally lavas of the Hawaiian, Hebridean, and Tristan da Cunha alkali rock series.

Analytical data on some of these assemblages are reported in Tables 1 and 2; analyses of other lavas of these series experimentally treated are reported in the literature referred to in the legends of Figs. 1 and 2. The crystallization sequences of both tholeiitic and alkali rock series are summarized in Table 3.

In addition to the data on the Kilauean lavas of 1920 and 1921, the crystallization sequences in the picrite basalt ( $KI_{pb}$ ) of Kilauea Iki erupted in 1959 (Murata and Richter, 1965) and the glass ( $KI_g$ ) separated from this rock, but still containing a small percentage of olivine and showing quench pyroxene, have been determined.

The crystallization sequence of an oceanic high-alumina basalt tachylyte of the mid-Atlantic ridge is also recorded. The analysis of this rock reported by Nicholls, Nawalk, and Hays (1964) shows a close approach to that of the type of



high-alumina basalt of the Medicine Lake Highlands—the Warner basalt. The liquidus phase, however, is olivine (1,245°C), and plagioclase appears 30° lower. (For comparison the crystalliza- tion sequence of the Warner basalt is Pl, 1,240°; Ol, 1,230°; Cpx, 1,170°C; see Yoder and Tilley, 1962, p. 380, Table 15.) The more basic character of the oceanic assemblage is seen in its lower iron en-

TABLE 1. Chemical Analyses and Norms of Investigated Rocks (Chiefly Hawaiian Tholeiites)

	KI <sub>pb</sub>	KI <sub>g</sub>	1921 <sub>f</sub>	1920 <sub>ph</sub>	N	LB105	LB105a
Analyses							
SiO <sub>2</sub>	46.68	49.08	49.11	50.26	48.13	54.09	58.26
Al <sub>2</sub> O <sub>3</sub>	9.52	12.48	12.74	13.48	17.07	8.39	9.04
Fe <sub>2</sub> O <sub>3</sub>	1.57	1.59	3.23	1.55	1.17	3.65	3.93
FeO	10.30	10.05	8.40	9.57	8.65	6.54	7.04
MnO	0.17	0.18	0.17	0.17	0.13	0.15	0.16
MgO	19.52	10.20	10.31	7.04	10.29	13.03	14.04
CaO	8.26	11.05	10.73	11.45	11.26	5.46	5.88
Na <sub>2</sub> O	1.52	2.04	1.97	2.22	2.39	0.75	0.81
K <sub>2</sub> O	0.35	0.48	0.49	0.45	0.09	0.41	0.44
H <sub>2</sub> O <sup>+</sup>	0.00	0.09	0.07	0.27	0.27	4.66*	.....
H <sub>2</sub> O <sup>-</sup>	0.01	0.00	0.00	0.03	0.02	2.70	.....
TiO <sub>2</sub>	1.80	2.48	2.51	2.69	0.72	0.30	0.33
P <sub>2</sub> O <sub>5</sub>	0.18	0.24	0.27	0.26	0.10	0.07	0.07
Remaining	0.05†	0.06‡	.....	0.52§	.....	.....	.....
Total	99.93	100.02	100.00	99.96	100.29	100.20	100.00
Norms							
Qz	.....	.....	.....	2.64	.....	.....	15.96
Or	2.22	2.78	2.78	2.78	0.56	.....	2.78
Ab	13.10	17.29	16.77	18.86	20.44	.....	6.81
An	17.79	23.63	24.46	25.30	35.58	.....	19.74
Di	17.98	23.86	22.27	22.47	15.76	.....	7.19
Hy	11.54	18.10	22.84	18.62	4.25	.....	41.11
Ol	31.16	6.65	0.90	.....	20.18	.....	.....
Il	3.50	4.71	4.71	5.17	1.37	.....	0.61
Mt	2.32	2.32	4.64	2.32	1.62	.....	5.68
Ap	0.34	0.67	0.67	0.67	0.34	.....	0.17
Remaining	0.06	0.15	0.07	1.32	0.29	.....	.....
Total	100.01	100.16	100.11	100.15	100.39	.....	100.05

KI<sub>pb</sub>, picrite basalt, Kilauea Iki, Hawaii, pumice collected November 18, 1959. Analyst, D. F. Powers (Murata and Richter, 1965).  
KI<sub>g</sub>, glass separated from the picrite basalt (KI<sub>pb</sub>) of Kilauea Iki, Hawaii. Analyst, D. F. Powers (Murata and Richter, 1965).  
1921<sub>f</sub>, 1921 Kilauea lava, Hawaii. Analyst, C. O. Ingamells (Fudali, 1965, p. 1065, Table 1, No. 1.).  
1920<sub>ph</sub>, 1920 Kilauea, Pele's Hair, 2½ miles southwest of Halemaumau, Hawaii (Washington, 1923). Reanalyzed by C. O. Ingamells.  
N, tachylite margin of basalt, mid-Atlantic ridge (Nicholls, Nawalk, and Hays, 1964).  
LB105, "tholeiite," Cape Vogel area, Papua. Analyst, A. McClure (cf. Joplin, 1963, p. 199).  
LB105a, analysis of LB105 recalculated anhydrous.  
\* Loss on ignition.  
† Includes CO<sub>2</sub>, 0.02; Cl, 0.01; F, 0.02.  
‡ Includes CO<sub>2</sub>, 0.01; Cl, 0.02; F, 0.03.  
§ Includes CO<sub>2</sub>, 0.40 (as calcite); ZrO<sub>2</sub>, 0.02; Cr<sub>2</sub>O<sub>3</sub>, 0.02; V<sub>2</sub>O<sub>5</sub>, 0.04; SrO, 0.03; BaO, 0.01.  
|| Includes Ct, 0.90; H<sub>2</sub>O±, 0.42.

richment—defined by the ratio  $(\text{FeO} + \text{Fe}_2\text{O}_3)/(\text{MgO} + \text{FeO} + \text{Fe}_2\text{O}_3)$ —and the higher refraction of its glass (1.605, Warner basalt = 1.592).

In *Year Book 63* (p. 93) a tholeiite (LB) from the Cape Vogel peninsula, Papua, was discussed. Another rock (LB105) from this area carrying clinoenstatite phenocrysts, also recognized as inverted protoenstatite, yielded protoenstatite on the liquidus at 1,340°C, a result that may be compared with the liquidus (1,385°C) of the more magnesian tholeiite (LB). Though the anhydrous norm of this rock (LB105a) (*Year Book 63*, p. 93, Table 1) holds 16 per cent quartz, its plot in Fig. 1 of the present report is on the tholeiite liquidus in the region of the picrite basalts, indicating the important role of iron enrichment in the control of the liquidus of the tholeiite series.

TABLE 2. Chemical Analyses and Norms of Investigated Rocks (Alkali Types)

	Ha	X	6	U	O
Analyses					
SiO <sub>2</sub>	42.53	47.87	57.97	38.01	35.83
Al <sub>2</sub> O <sub>3</sub>	12.43	14.73	18.56	11.53	10.86
Fe <sub>2</sub> O <sub>3</sub>	2.68	3.84	1.82	3.57	6.43
FeO	11.23	8.38	4.81	8.25	10.17
MnO	0.16	0.19	0.24	0.19	0.23
MgO	12.17	6.02	1.95	12.40	11.09
CaO	11.80	10.42	3.32	15.49	12.21
Na <sub>2</sub> O	2.35	3.10	6.74	3.11	5.45
K <sub>2</sub> O	0.81	1.00	2.79	1.24	1.82
H <sub>2</sub> O <sup>+</sup>	0.03	0.37	0.18	1.16	0.72
H <sub>2</sub> O <sup>-</sup>	0.17	0.13	0.10	0.21	0.27
TiO <sub>2</sub>	2.92	3.88	1.06	3.10	2.64
P <sub>2</sub> O <sub>5</sub>	0.55	0.33	0.54	1.08	1.38
Remaining	.....	.....	.....	0.43*	0.68†
Total	99.83	100.26	100.08	99.77	99.78
Norms					
Or	5.00	6.12	16.68	Ks 4.11	Ks 6.00
Ab	5.24	26.20	56.59	.....	.....
Ne	7.95	.....	0.28	14.20	24.99
An	20.85	23.07	11.95	13.90	.....
Di	27.59	21.48	0.68	27.39	27.17
Hy	.....	5.05	.....	Cs 6.45	Cs 5.11
Ol	22.35	4.19	7.78	18.22	16.90
Il	5.47	7.45	2.13	5.93	5.01
Mt	3.94	5.57	2.55	5.10	9.28
Ap	1.34	0.67	1.34	2.48	3.23
Remaining	0.20	0.50	0.28	1.95	2.01
Total	99.93	100.30	100.26	99.73	99.70

Ha, Basanitoid, Haleakala lava flow of 1750 (1790?), E. Maui (Macdonald and Katsura, 1964, p. 122).  
X, (Feldspar-phyric) basalt, ½ mile north of Puu o Kawaiwai Kohala, Hawaii. Analyst, J. H. Scoon.  
6, Benmoreite, highway cut at McGregor Point, W. Maui (Macdonald and Katsura, 1964, p. 121).  
U, Melilite olivine nephelinite, Uvalde, Uvalde Co., Texas. Analyst, C. O. Ingamells.  
O, Melilite olivine nephelinite, Moiliili Quarry, Honolulu. Analyst, C. O. Ingamells.  
\* Includes ZrO<sub>2</sub>, 0.03; Cr<sub>2</sub>O<sub>3</sub>, 0.03; V<sub>2</sub>O<sub>5</sub>, 0.04; NiO, 0.04; SrO, 0.10; BaO, 0.07; CO<sub>2</sub>, 0.12.  
† Includes ZrO<sub>2</sub>, 0.04; Cr<sub>2</sub>O<sub>3</sub>, 0.025; V<sub>2</sub>O<sub>5</sub>, 0.045; NiO, 0.04; SrO, 0.17; BaO, 0.10; CO<sub>2</sub>, 0.26.



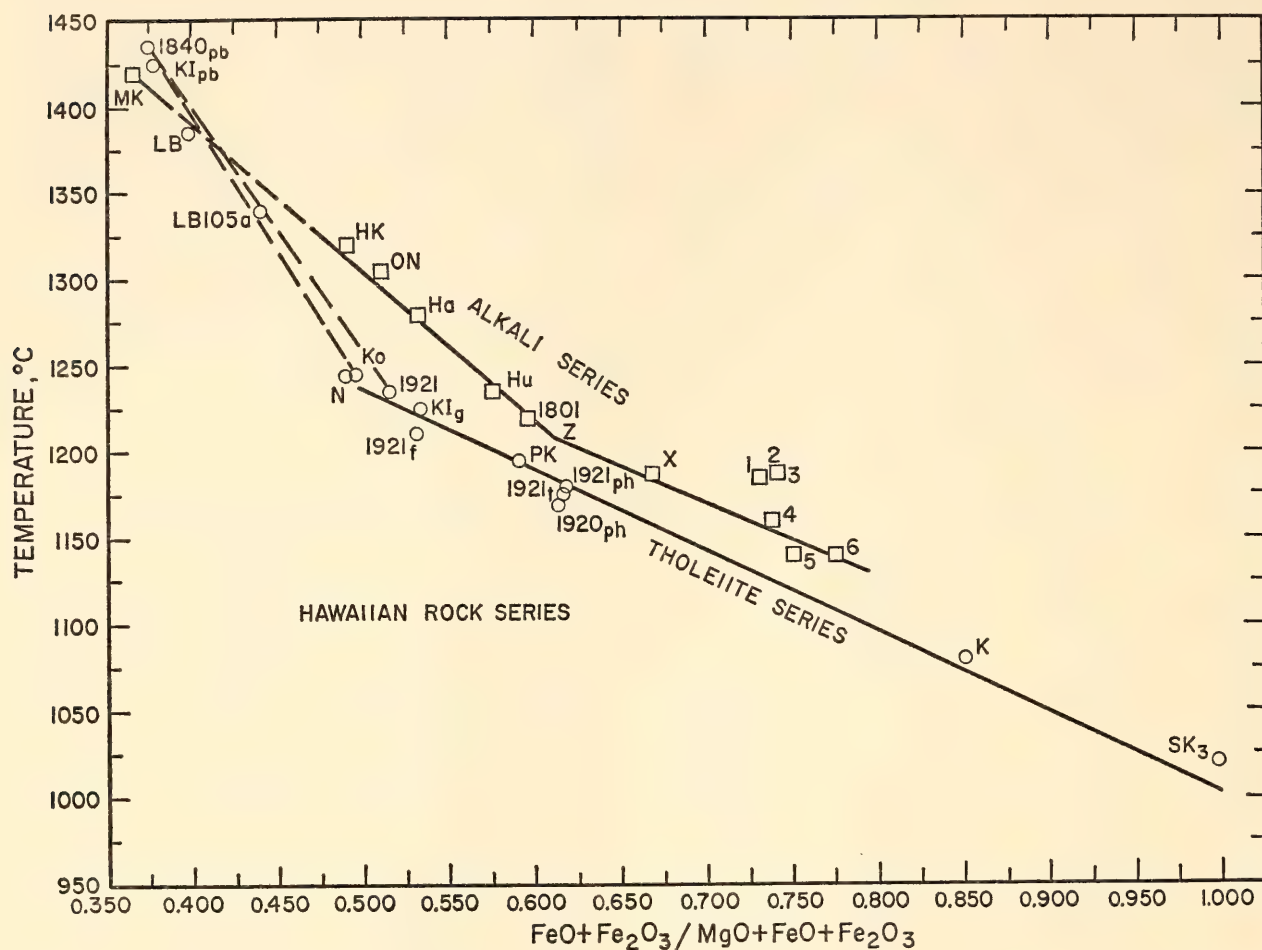


Fig. 1. Plot correlating liquidus temperature with iron enrichment. On tholeiite trend defined by points 1840<sub>pb</sub>-Ko-1921-PK-K-SK<sub>3</sub> (reproduced from Fig. 23, *Year Book 63*, p. 95), are plotted the data for the experimentally treated rocks KI<sub>pb</sub>, KI<sub>g</sub>, 1921<sub>f</sub>, and 1920<sub>ph</sub> (for analyses see Table 1), and of Kilauean lavas 1921<sub>ph</sub> and 1921<sub>t</sub> (Tilley, 1960a, Table 1, analyses 4 and 6, respectively). Points LB105a and N refer to a "tholeiite" holding clinopyroxene phenocrysts from Papua and a tachylyte of a high-alumina basalt from mid-Atlantic ridge (Table 1, analyses LB105a and N). Upper line MK-1801-6 defines trend of the temperature relations of rocks of Hawaiian alkali series. Points MK and HK refer to rocks previously investigated (*Year Book 63*, p. 93, Table 1, analyses MK and HK). Analyses corresponding to points Hu and ON are presented in Yoder and Tilley (1962, p. 362, Table 2, analyses 20 and 24). Additional points Ha, 1801, X, 1-6 represent newly investigated rocks of Hawaiian alkali series ranging from a Haleakala basanite (Ha) through basalts (1801, X), hawaiites (1-4), and mugearite (5) to a benmoreite (6); Z represents the point of change of liquidus phase. Analyses of Ha, X, and 6 are reported in Table 2 and analytical data for 1801, 1, 2, 3, 4, and 5 have been published in Yoder and Tilley, 1962 (1801 and 1: p. 362, Table 2, analyses 19 and 23; 2: p. 417, Table 23, analysis 4); and in Muir and Tilley, 1961 (4: p. 190, Table 4, analysis 3; 3 and 5: p. 192, Table 7, analyses 18 and 17).

### *Hawaiian Alkali Series*

The thermally treated rocks of this series include a range of compositions from picrite basalt (MK) through ankaramitic picrite basalts (HK, Ha), typical alkali olivine basalts (Hu, 1801), a group of hawaiites (1-4), a mugearite (5), and the intermediate rock benmoreite (6)

(Tilley and Muir, 1964) analyzed by Macdonald and Katsura (1964, p. 130, Table 6) and referred to by these authors as "trachyte trending towards mugearite."

In this series liquidus temperatures range from 1,420°C (MK) through to 1,140°C, benmoreite (6), with corresponding iron enrichment ranging from 0.36<sub>6</sub> to 0.77<sub>3</sub>. The trend of this alkali

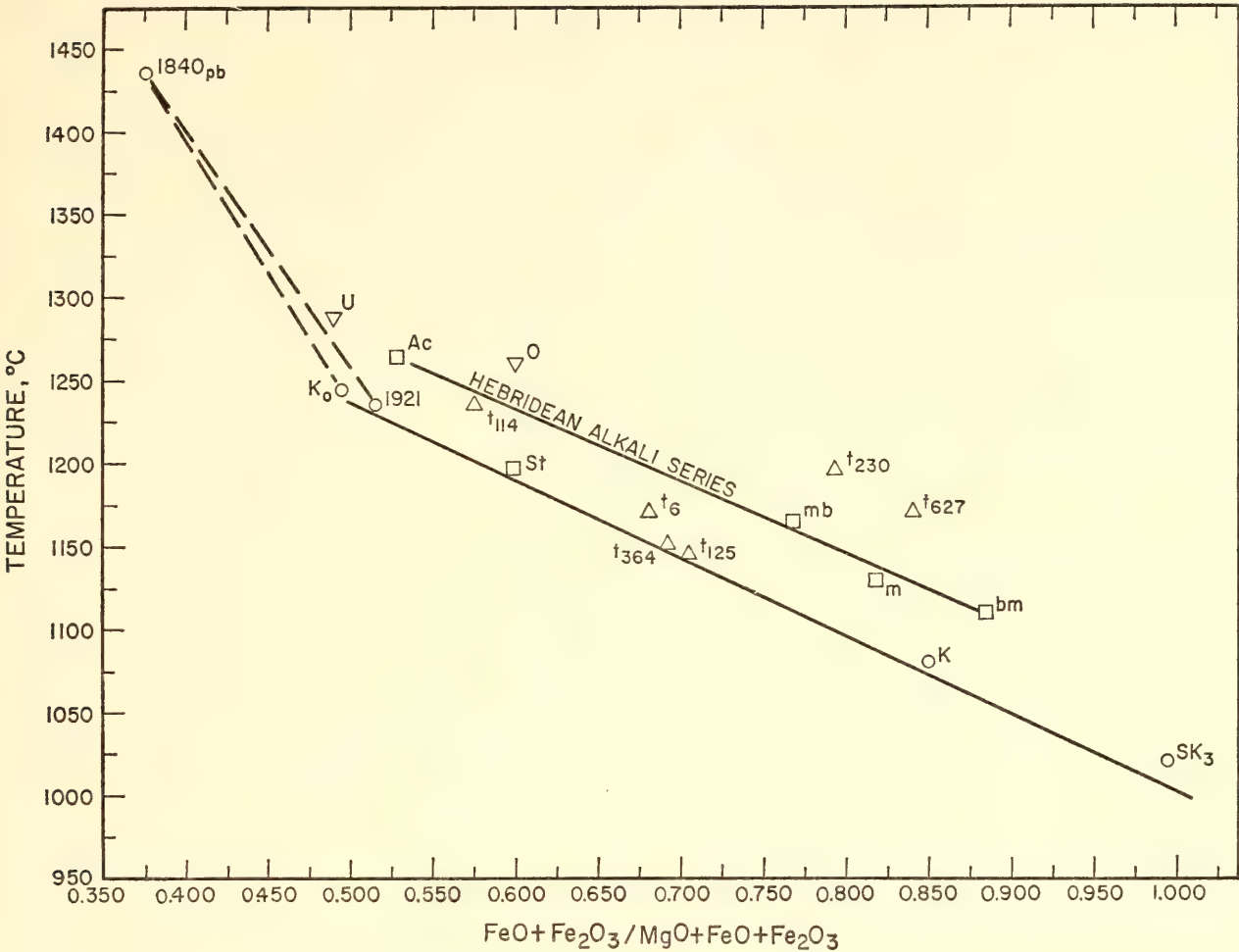


Fig. 2. Plot of positions of the rocks of Hebridean and Tristan da Cunha alkali rock series on a liquidus temperature-iron enrichment diagram. Hawaiian tholeiite trend of Fig. 1 is reproduced for comparison. Hebridean lavas Ac, St, mb, m, bm refer to series ranging from alkali olivine basalt (Ac, St) through hawaiiite (mb), mugearite (m), and benmoreite (bm), analyses of which are reported in Tilley and Muir, 1962 (Ac and St: p. 212, Table 3, analyses 1 and 2), and in Muir and Tilley, 1961 (mb, m, and bm: p. 190, Table 4, analyses 2, 1, and 10, respectively). Tristan da Cunha lavas  $t_{114}$ ,  $t_6$ ,  $t_{364}$ ,  $t_{125}$ ,  $t_{230}$ , and  $t_{627}$  thermally treated have analyses reported in Baker *et al.* (1964, p. 520, Table 6). In addition, liquidus temperatures of two melilite olivine nephelinites from Uvalde, Texas, and Honolulu, Oahu (analyses U and O of Table 2) are similarly plotted.

series is shown by the upper course in Fig. 1, separated there into two limbs (MK-Z and Z-6). The upper limb traces the trend with olivine on the liquidus; the rocks of the lower limb in contrast have plagioclase as the initial phase. Throughout, the liquidus temperatures of the members of the alkali series are higher than those of the rocks of the Kilauean tholeiite series of comparable iron enrichment except for the ultramafic picrite basalts (MK and 1,840<sub>pb</sub>, respectively); conversely the iron enrichment of the members of the alkali series is higher than that of the tholeiite series of

similar liquidus temperature. An alternative plotting of the relations of the tholeiite and alkali series is portrayed in Fig. 3, where total iron oxides are plotted against magnesia content, and in Fig. 5, where the plot is the variation of iron enrichment with total mafics ( $\text{FeO} + \text{Fe}_2\text{O}_3 + \text{MgO}$ ).

These plots reveal the contrasting trends of the two series. In the tholeiite series the two limbs signify the prime precipitation of olivine (upper limb) and of pyroxene (or pyroxene with plagioclase) dominant as the liquidus phases on the lower limb. The trend of the lower



TABLE 3. Results of Melting Experiments on the Tholeiite and Alkali Rocks of Tables 1 and 2 and Others\*

		<i>n</i> of Glass
<b>Hawaiian Lavas (Tholeiites) and Others</b>		
Picrite basalt, Kilauea Iki (KI <sub>pb</sub> )	Ol (1,425°), Cpx (1,165°), Pl (1,150°)	1.637
Glass of picrite basalt, Kilauea Iki (KI <sub>g</sub> )	Ol (1,225°), Cpx (1,165°), Pl (1,155°)	1.614
1921 Kilauea lava (1921 <sub>t</sub> )	Ol (1,210°), Cpx (1,165°), Pl (1,155°)	1.612
1921 Kilauea lava (Pele's Hair, 1921 <sub>ph</sub> )	Ol (1,180°), Cpx (1,160°), Pl (1,155°)	1.603
1921 Kilauea tachylyte (1921 <sub>t</sub> )	Ol (1,175°), Cpx (1,165°), Pl (1,155°)	1.605
1920 Kilauea (Pele's Hair, 1920 <sub>ph</sub> )	Ol (1,170°), Cpx (1,160°), Pl (1,155°)	1.603
High-alumina basalt (tachylyte), mid-Atlantic Ridge (N)	Ol (1,245°), Pl (1,215°), Cpx (1,165°)	1.605
"Tholeiite," Cape Vogel, Papua (LB105a)	Pl (1,340°)	1.576
<b>Hawaiian Lavas (Alkali Series)</b>		
Basanitoid, lava flow of Haleakala, Maui, erupted about 1750 (1790?) (Ha)	Ol (1,280°), Cpx (1,160°), Pl (1,150°)	1.634
1801 lava, Hualalai, Hawaii (1801)	Ol (1,220°), Pl (1,170°), Cpx (1,155°)	1.612
Feldspar-phyric basalt, Kohala, Hawaii (X)	Pl (1,187°), Cpx (1,170°), Ol (1,135°)	1.610
Hawaiiite, Mauna Kea, Hawaii (1)	Pl (1,185°), Cpx (1,160°)	1.597
Hawaiiite, Haleakala, Maui (2)	Pl (1,187°), Cpx (1,175°), Ol (1,130°)	1.597
Hawaiiite, Mauna Kea, Hawaii (3)	Pl (1,187°), Cpx (1,160°), Ol (1,110°)	1.580
Hawaiiite, Mauna Kea, Hawaii (4)	Pl (1,160°), Cpx (1,115°), Ol (1,115°)	1.580
Mugearite, Kohala, Hawaii (5)	Pl (1,140°), Cpx (1,115°), Ol (1,115°)	1.562
Benmoreite, West Maui (6)	Pl (1,140°), Cpx (1,110°), Ol (1,090°)	1.532
<b>Hebridean Lavas (Alkali Series)</b>		
Olivine basalt, Achdalean, Skye (Ac)	Ol (1,265°), Pl (1,180°), Cpx (1,175°)	1.612
Olivine basalt, Staffa, Mull (St)	Pl, Cpx (1,197°); Ol (1,170°)	1.607
Hawaiiite (7568), R. Rha, Skye (mb)	Pl (1,165°), Cpx (1,155°), Ol (1,130°)	1.590
Mugearite (9384), Druim na Criche, Skye (m)	Pl (1,130°); Cpx, Ol (1,090°)	1.564
Benmoreite (60444), Totardor, Skye (bm)	Pl (1,110°), Cpx (1,100°), Ol (1,090°)	1.524
<b>Tristan da Cunha Lavas (Alkali Series)</b>		
Ankaramite (t <sub>114</sub> )	Ol (1,235°), Cpx (1,190°), Pl (1,145°)	1.638
Olivine basalt (t <sub>6</sub> )	Cpx, Pl (1,170°); Ol (1,145°)	1.625
Trachybasalt (t <sub>364</sub> )	Pl (1,150°), Cpx (1,130°), Ol (1,065°)	1.600
Trachybasalt (t <sub>125</sub> )	Pl (1,145°), Cpx (1,100°)	1.568
Tristanite (t <sub>230</sub> )	Pl (1,195°), Cpx (1,115°)	1.547
Tristanite, 1961 lava (t <sub>627</sub> )	Pl (1,170°), Cpx (1,100°)	1.538
<b>Olivine Nephelinites</b>		
Olivine nephelinite, Pali, Oahu (ON)	Ol (1,305°), Cpx (1,280°), Ne (1,085°)	1.638
Melilite olivine nephelinite, Uvalde Co., Texas (U)	Ol (1,287°), Cpx (1,190°), Mel (1,130°), Ne (1,080°)	1.642
Melilite olivine nephelinite, Honolulu, Oahu (O)	Ol (1,260°), Cpx (1,160°), Mel (1,095°), Ne (1,085°)	1.640

\* See text and legends of Figs. 1 and 2.

limb of the tholeiite series (Figs. 3 and 5) shows continuous iron enrichment with approximately constant total iron oxides + magnesia, indicating that the phases

crystallizing from the liquid, dominantly pyroxene and plagioclase, are being withdrawn in the proportions necessary to preserve this relation. In contrast, the

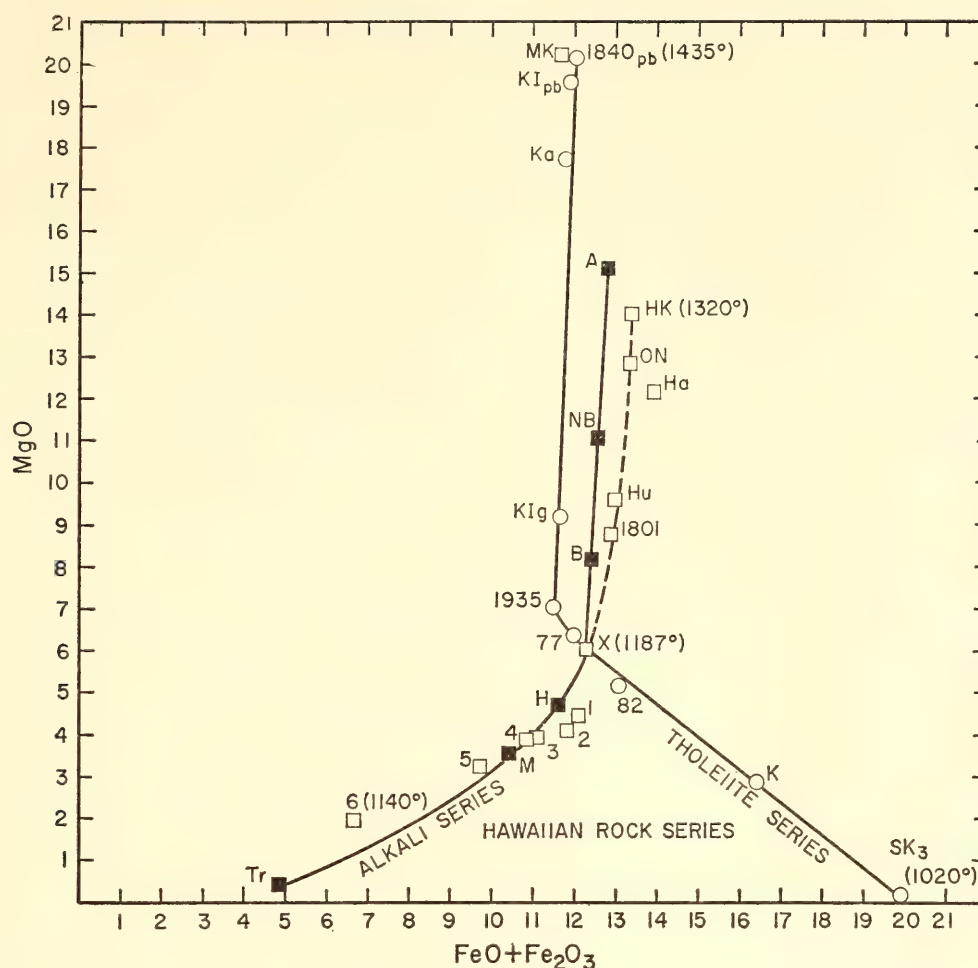


Fig. 3. Plot relating total iron oxides and magnesia of trends of Hawaiian tholeiite and alkali series. Numbered and lettered points correspond to those similarly plotted in Fig. 1. Circles, tholeiite series. SK<sub>3</sub>, fayalite ferrogabbro of the Skaergaard intrusion (*Year Book 63*, p. 93, Table 1). Squares, alkali series. Closed squares, plotted positions of averages of ankaramite (A), nepheline basanite (NB), alkali basalt (B), hawaiiite (H), mugearite (M), and trachyte (Tr) of the Hawaiian volcanic province (Macdonald and Katsura, 1964, Table 10, p. 124).

lower limb of the alkali series trend (Figs. 3 and 5) shows continuous iron enrichment with continuously falling total mafics (Fe and Mg oxides), indicating preferential subtraction of the mafic minerals.

#### *Hebridean Alkali Series*

The liquidus temperature versus iron enrichment trend of the Hebridean alkali series is shown in the plot of Fig. 2 (cf. Fig. 4). Like the alkali series of Hawaii, the trend lies above the tholeiite trend (Hawaiian). The rocks investigated range in composition from the alkali olivine basalt of Achtelean, Skye (Ac); through a hawaiiite (mb) of the River Rha, Skye; the type mugearite of

Druim na Criche, Skye (m); to the benmoreite (bm)—the “mugearite-trachyte” of Totardor, Skye, previously described (Muir and Tilley, 1961). The alkali basalt of Fingal’s Cave, Staffa (St), forms an exception in this series, but this rock is distinctive in being pyroxene rich and having pyroxene and plagioclase on the liquidus at 1,197°C followed by olivine at 1,170°C.

#### *Tristan da Cunha Alkali Series*

The rocks of the Tristan da Cunha alkali series that were investigated range from an ankaramite (t<sub>114</sub>) through an alkali olivine basalt (t<sub>6</sub>), trachybasalts (t<sub>364</sub>, t<sub>125</sub>), to intermediate members of the series (t<sub>230</sub>, t<sub>627</sub>) classified as tristanites



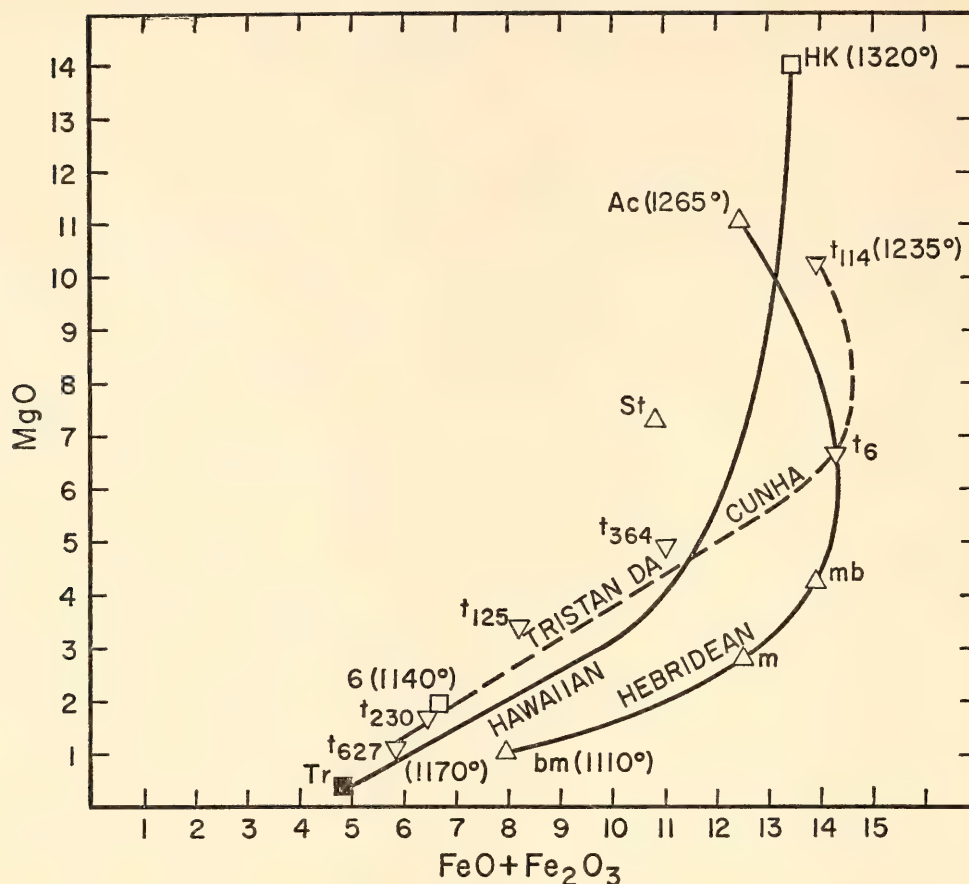


Fig. 4. Trend lines ( $\text{FeO} + \text{Fe}_2\text{O}_3$  versus  $\text{MgO}$ ) of the alkali series of Hawaii (reproduced from Fig. 3) and of the Hebridean and Tristan da Cunha provinces.

(Tilley and Muir, 1964). Leucite is recorded as a modal mineral in the trachybasalt ( $t_{125}$ ) and in the tristanite ( $t_{627}$ ) representing a lava of the 1961 eruption of the island. Leucite, however, is not a normative mineral (all the analyses hold nepheline in the norm).<sup>1</sup> As seen in the alkalis-silica plot of Fig. 6, the Tristan da Cunha series are markedly more alkalic compared with the Hawaiian and Hebridean series and are relatively enriched in potassium ( $\text{K}_2\text{O}$  content ranging from 1.47 ( $t_{114}$ ) to 5.03 ( $t_{627}$ ) (Baker *et al.*, 1964). The liquidus temperatures (Fig. 2) range from 1,235°C to 1,145°C and show a markedly less consistent relationship with iron enrichment than do the

Hawaiian and Hebridean alkali series. The relative trends of the Hawaiian, Hebridean, and Tristan da Cunha alkali series are plotted in Fig. 4, correlating total iron oxides and magnesia.

#### *Olivine Nephelinites*

Crystallization sequences have been determined for two melilite olivine nephelinites (ON), one from Uvalde, Uvalde Company, Texas, and the second from Moiliili Quarry, Honolulu, Oahu. The analyses and norms of these two rocks are recorded in Table 2 (analyses U and O, respectively). Assemblages of this type from Texas and Honolulu have been previously analyzed (Clarke, 1900; Cross, 1915), and the Honolulu type was described by Cross (1915) and later by Winchell (1947).

The crystallization sequence is olivine, clinopyroxene, melilite, and nepheline in both assemblages, but the Honolulu rock

<sup>1</sup> Baker *et al.* (1964, p. 528) have commented that a closer approach to the mode in rocks carrying modal leucite would result if in the norm calculation *or* was desilicated in preference to *ab*. Leucite would appear in the norm then but always with a calcium-bearing plagioclase.

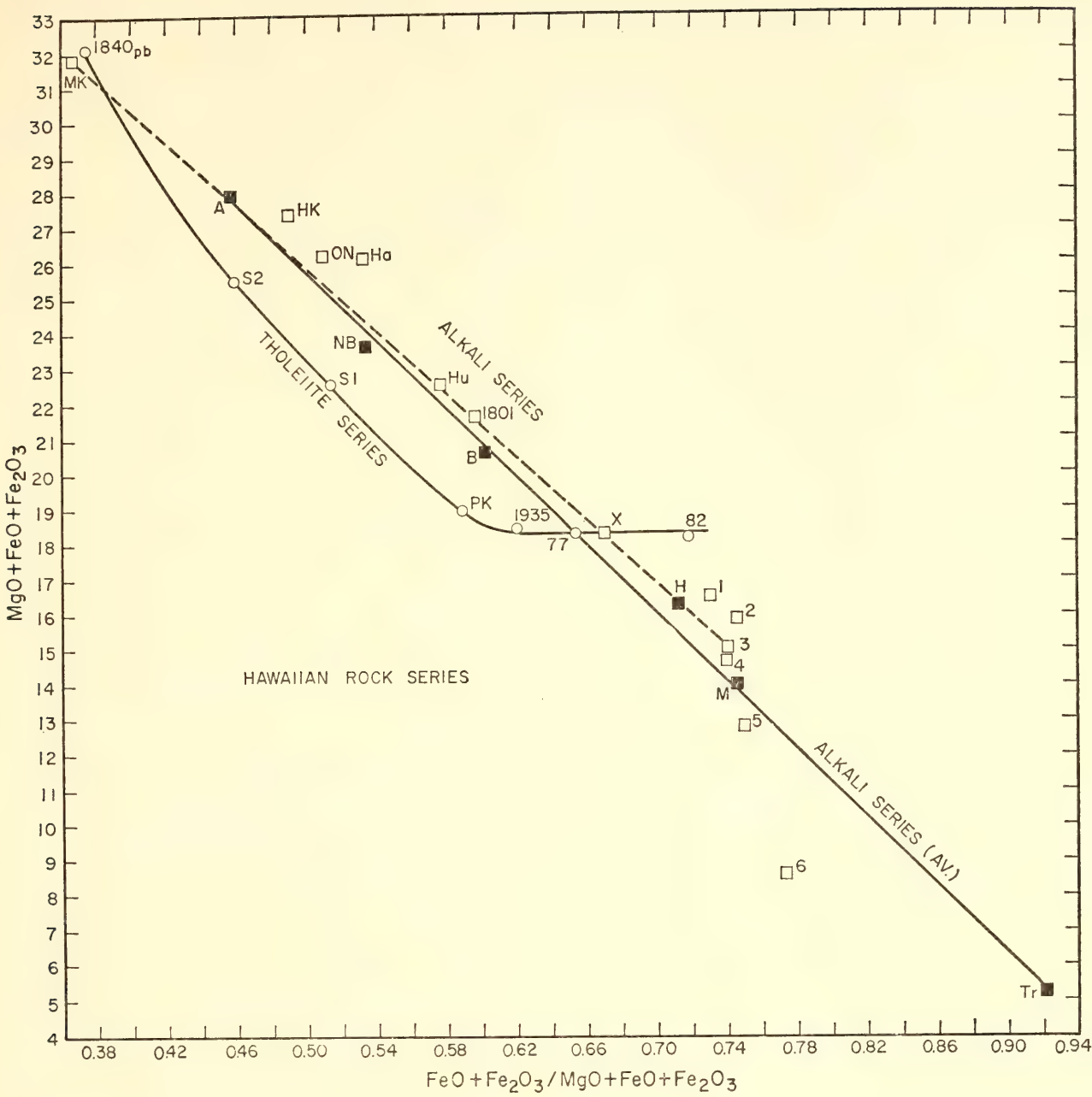


Fig. 5. Plot correlating total iron oxides + magnesia with iron enrichment for the Hawaiian volcanic series. Circles, trend of the tholeiite series; squares, the alkali series; closed squares, averages of the alkali series. Numbered and lettered points correspond to those indicated in Figs. 1 and 2. S1, S2, PK, and 1935 refer to analyses: S1 and S2 in Tilley (1960b, Table 1, Nos. 1 and 2); PK, Yoder and Tilley (1962, Table 2, analysis 7); 1935, a Mauna Loa lava (*Year Book 63*, p. 93, Table 1).

is much richer in nepheline. The textural relations of the melilite and nepheline phases differ in the two rocks. In the Uvalde rock nepheline crystallized late and is interstitial. In the Honolulu assemblage the periods of crystallization of the two phases were much closer together in time, the nepheline in part being idiomorphic. These contrasting features are brought out in the record of

the thermal treatment (Table 3); there it will be observed that the temperature interval between the initial precipitation of melilite and nepheline for the Uvalde rock is much longer than that recorded for the two phases in the Honolulu rock.

A modal analysis (volume per cent) of the Uvalde rock has been kindly carried out for us by F. Chayes. His results give the following figures: clinopyroxene, 43.1;



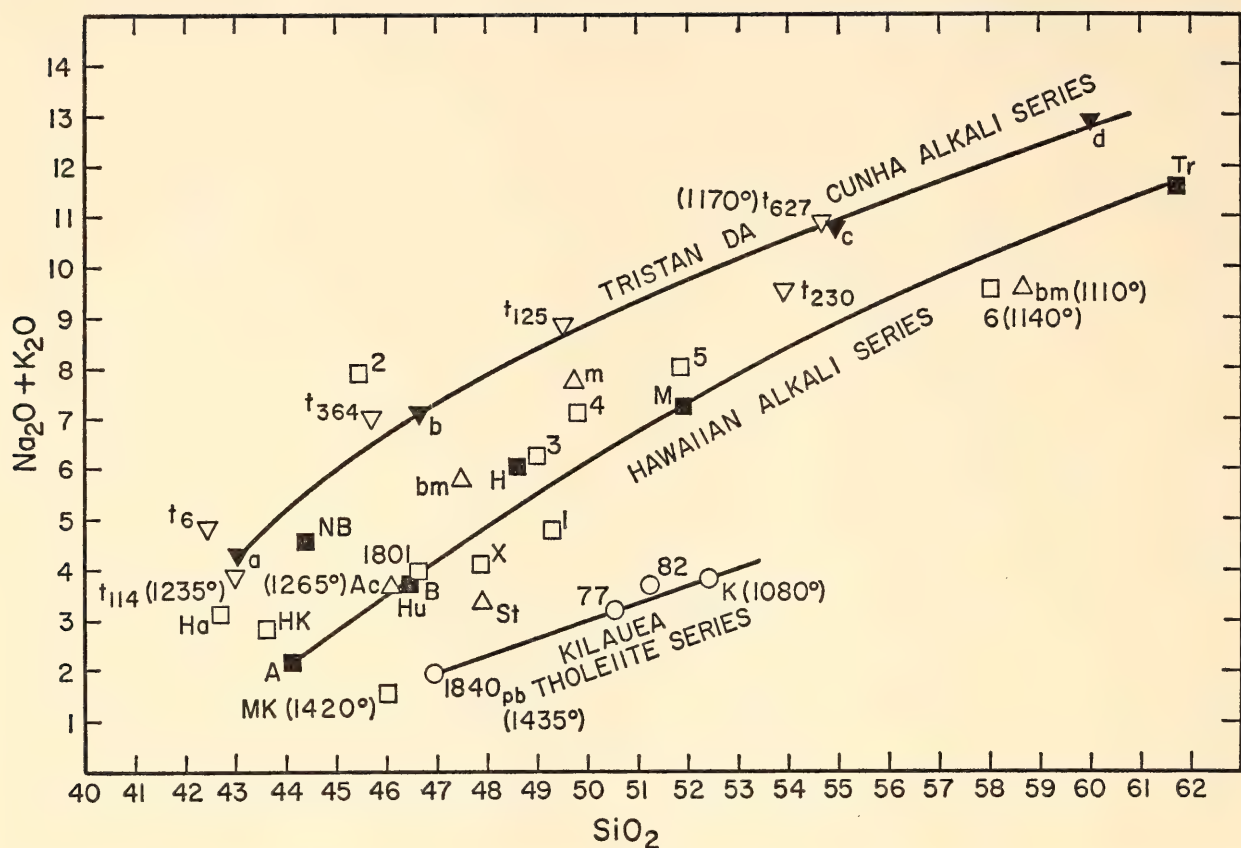


Fig. 6. Plot correlating silica and alkalis of the investigated rocks of the Hawaiian, Hebridean, and Tristan da Cunha series. Circles, Hawaiian tholeiite series; squares, Hawaiian alkali series; closed squares, averages of these; triangles, Hebridean alkali series; inverted triangles, Tristan da Cunha alkali series; closed inverted triangles, averages of this series (*a-d*) (Baker *et al.*, 1964, p. 531, Table 8, analyses 1-4).

olivine, 13.3; melilite, 13.1; nepheline, 18.9; opaques, 9.9; apatite, 1.2; biotite, 0.4. Natrolite is to be seen in the thin sections partly as an alteration of nepheline but also interstitially. Compared with the chemical data, apatite is deficient in this modal count, but Chayes has remarked that the rock examined in four thin sections was somewhat uneven in mineral distribution; the unevenness, combined with the thin-needle nature of the apatite, is probably responsible for this underestimate. The beginning of nepheline crystallization in the previously described ON from the Pali, Oahu, corresponds closely in temperature with that of the two melilite rocks at 1,085°C.

The consistently higher liquidus trend of the alkali series (Hawaiian and Hebridean) compared with the tholeiite trend of Kilauea may be considered in

terms of individual assemblages of (1) similar iron enrichment and (2) similar liquidus temperature in the contrasting series. Thus (1) the 1801 Hualalai lava may be contrasted with the prehistoric Kilauea lava (PK) of similar iron enrichment (0.59<sub>5</sub>, 0.58<sub>9</sub>, respectively; cf. Fig. 1). The corresponding liquidus temperatures are 1,220°C and 1,195°C. This difference of 25°C is explicable on the grounds of the more basic character of the 1801 lava as indicated by these data:

1801: SiO<sub>2</sub>, 46.59;

normative olivine, 18.51

PK: SiO<sub>2</sub>, 51.18;

normative quartz, 0.30

Alternatively, (2) the 1801 lava can be compared with a tholeiitic lava of similar liquidus temperature such as the glass of the 1959 Kilauea Iki picrite basalt.

1801: SiO<sub>2</sub>, 46.59; F/(F + M) = 0.59<sub>5</sub>; normative olivine, 18.51; liquidus, 1,220°C  
KI<sub>g</sub>: SiO<sub>2</sub>, 49.08; F/(F + M) = 0.53<sub>3</sub>; normative olivine, 6.65; liquidus, 1,225°C

The source of the 1801 lava could be traced to a less iron-enriched parent of the alkali series or alternatively to a tholeiitic parent clearly less iron enriched than the glass of Kilauea Iki. Such an origin from an olivine-enriched tholeiite under a high-pressure mechanism was discussed in *Year Book 63* (pp. 114–121). The relations between liquidus temperature and alkali content of the Hawaiian tholeiite and alkali series, and those of the Hebridean alkali series (see Fig. 7). Comparison with Figs. 1 and 2 demonstrates the fall of liquidus temperatures with both increasing alkali and iron enrichment; these indeed characterize the progressive felsic and mafic differentiation

of many rock series. Clearly, however, in the tholeiite series iron enrichment is the more effective factor in the lowering of the liquidus temperature, as seen in the plots of Figs. 1, 2, and 7; compare liquidus temperatures of 82 and K (tholeiite series) with 1801, Hu, and Ac of the alkali series of similar alkali content (Fig. 7). Discrepant relations (liquidus temperature vs. alkali and iron enrichment) exist among the Tristan da Cunha assemblages, commented on below.

In the alkali series, olivine is the liquidus phase for the more basic members (the Staffa basalt excepted). With increasing iron enrichment, assemblages of the composition of hawaiite and mugearite have, in the thermally treated rocks, plagioclase on the liquidus; and olivine appears later in the crystallization sequence. The change from olivine to pyroxene or plagioclase as the liquidus

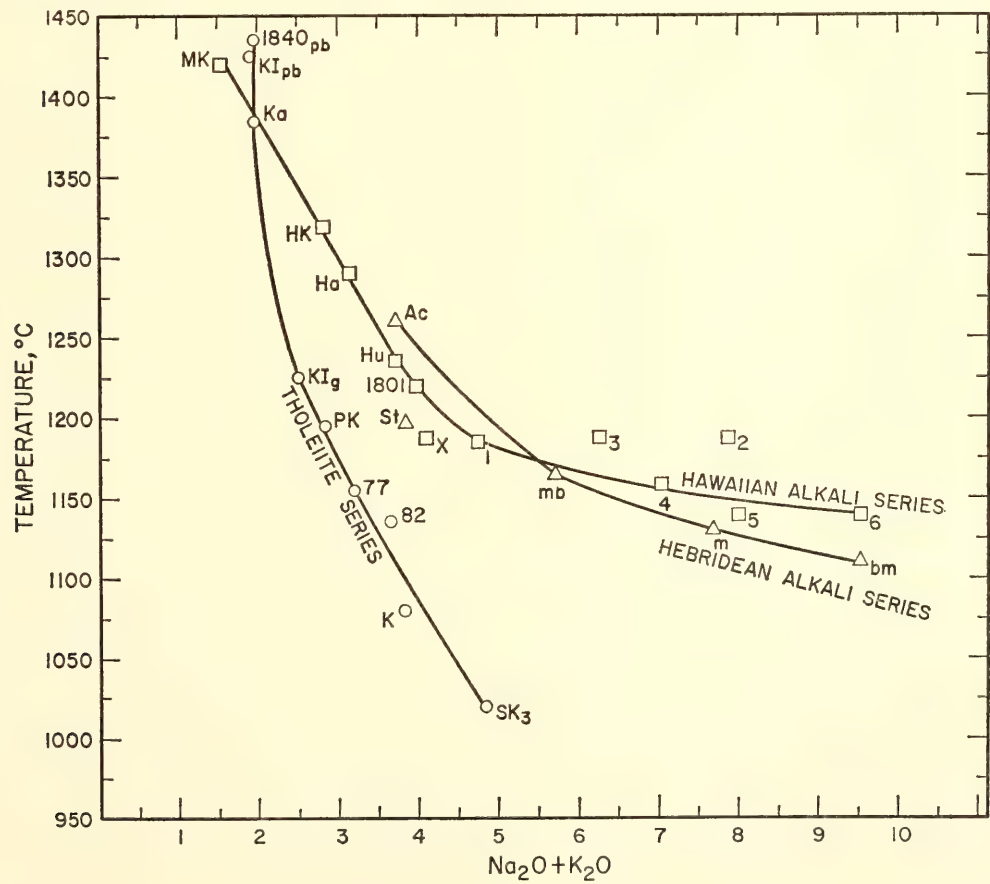


Fig. 7. Plot correlating liquidus temperatures with alkali content of the rocks of the Kilauea tholeiitic series and the alkali series of Hawaii and the Hebrides. Numbered and lettered points as in Figs. 1, 2, and 3.



phase in the tholeiite series may be explained on the basis of the reaction relation of olivine in tholeiitic liquids. Olivine disappears from the system and enters again only in strongly iron-enriched liquids.

The appearance of plagioclase on the liquidus of the thermally treated rocks of the alkali series is inconsistent with a simple crystallization differentiation sequence from a parental liquid of alkali olivine basalt composition. However, it would be consistent with a more complex differentiation process if selective segregation was operative. The continued precipitation of olivine, though at a later stage throughout the investigated series, denotes that a reaction relation, if existent, is ineffectual here.

The influence of oxidation, if any, on crystallization sequences may now be examined. The alkali series is consistently more heavily oxidized than the tholeiite series, as seen in the respective  $\text{Fe}_2\text{O}_3$ :FeO ratios of the two series and the prominence of magnetite in the groundmass of the alkali rocks. The average  $\text{Fe}_2\text{O}_3$ :FeO ratios of the investigated series of alkali rocks and the tholeiite series illustrate this feature: tholeiite series (0.19); Hawaiian alkali series (0.45); Hebridean alkali series (0.34); and Tristan da Cunha series, divisible into two groups—the four more basic assemblages (0.58), and the two tristanites ( $t_{230}$ ,  $t_{627}$ ) with the much higher figure of 1.11.

That oxidation has an effect of increasing the liquidus temperature but has been ineffective in changing the liquidus phase is seen in the case of the oxidized hawaiite of Mauna Kea (1 of Fig. 1). As previously recorded, this rock ( $\text{Fe}_2\text{O}_3$ , 4.11; FeO, 7.94) subjected to the normal thermal treatment gave these results (Yoder and Tilley, 1962, p. 380): plagioclase (Pl, 1,185°C; clinopyroxene (Cpx), 1,160°C. When the same rock was run experimentally under reducing conditions (sealed in a platinum tube, with iron filings in a separate open platinum foil in an evacuated silica tube) the results were:

Pl, 1,175°C; Cpx, 1,135°C; Ol, 1,110°C. Plagioclase remains as the liquidus phase, but the appearance of clinopyroxene is delayed, and olivine, absent in the normal run, appears now as a late phase. The normative olivine content of the rock is 1.8 per cent, but if all  $\text{Fe}_2\text{O}_3$  is reduced to FeO the normative olivine content rises to 13.7 per cent. Even if the reduction is only partial, to a level comparable to that holding in the tholeiite series, for example if  $\text{Fe}_2\text{O}_3$  is reduced to 1.50 per cent, the normative olivine is still considerable—10.5 per cent.

The appearance of olivine in the run under reducing conditions can be ascribed to this higher potential olivine content. The feldspar basalt (X, Table 2), occupying an intermediate position between the 1801 lava and the hawaiites of the Hawaiian alkali series, is characterized by the appearance of plagioclase on the liquidus.

Inspection of Table 3 shows that plagioclase in the alkali series (Hawaiian and Hebridean) is followed by clinopyroxene and olivine at considerably lower temperatures. The textural relations of the minerals as seen in the thin sections of the unheated rocks indicate that the sequence of minerals is not wholly consistent with the results obtained experimentally. All the rocks carry olivine, for the most part as a phenocryst or microphenocryst mineral, in some cases associated with plagioclase and less commonly with pyroxene, but olivine itself may be the only mineral detectable as phenocrysts, clinopyroxene and plagioclase then being confined to the groundmass. These textural relations are in harmony with the view that olivine may indeed be the liquidus mineral in the magma itself. The interpretation of the discrepant relations now revealed poses a problem needing further discussion.

In the succession of rock types in the Hawaiian alkali series the alkali olivine basalts may be associated with types poorer in olivine and markedly “porphy-



ritic" in feldspar. These types are further distinguished by exhibiting a significantly greater iron enrichment. Genetically they thus appear to be in the line of succession leading eventually through hawaiites to mugearites and trachytes. It may be recalled that in the Hebridean series the type mugearite is associated with a feldspar-phyric olivine dolerite as members of a composite lava flow (Kennedy, 1931).

In Hawaii a conspicuous example of such occurrences of feldspar-phyric basalts is found in the Hawi series of the Kohala Mountains, Hawaii. The basalt (X/66094, Table 2, X) is such an example that has been run experimentally (Table 3). This rock contains conspicuous plagioclase ( $\text{Ab}_{40}\text{An}_{60}$ ) seemingly as phenocrysts along with less abundant olivine phenocrysts. The norm carries 4.19 per cent olivine and 55.39 per cent feldspar. One possible explanation of the origin of this rock type is that it is derived from the alkali olivine basalts of the type of the Hualalai suite (Hu, 1801, Fig. 1), by removal of olivine by sinking, and the concentration of plagioclase by flotation accumulation.

That feldspars of the composition of the "phenocrysts" are lighter than the liquid of the rock in which they are found is suggested by the following data. The refraction of the glass X is 1.610, and the glass of the groundmass without the phenocrysts would be expected to exceed this value, for the refraction of the phenocryst feldspar glass ( $\text{Ab}_{40}\text{An}_{60}$ ) is only 1.54. For basalt glasses of this composition the density would approximate 2.85 as seen from the relations of refraction to density for natural glasses (Tilley, 1922). The density of a plagioclase of composition  $\text{Ab}_{40}\text{An}_{60}$  is  $\sim 2.70$  (Day and Allen, 1905, p. 71). Here is a sufficiently wide margin to indicate that such feldspars would float in a liquid of the composition of the whole rock or its groundmass.

The feldspar-phyric basalt as run has a liquidus of  $1,187^{\circ}\text{C}$  (Pl) followed by Cpx

at  $1,170^{\circ}\text{C}$  and Ol at  $1,135^{\circ}\text{C}$ . The difference between these results and those suggested by the textural relations of the rock might be explained if the plagioclase phenocrysts of the rock had accumulated by flotation. In the magma itself olivine might continue to be the liquidus phase, but in the thermally treated rock where the inherited feldspar phenocrysts (xenocrysts) become part of the liquid, the composition is such that plagioclase itself would be expected to be the liquidus phase.

The prominence of olivine as phenocrysts in the succession of rocks of the alkali series of Hawaii and the Hebrides and the appearance of plagioclase as the liquidus phase in the runs of these rocks may have their explanation along the lines suggested for the feldspar-phyric basalt (X), i.e., these rocks do not represent simple fractionated liquids but liquids with inherited crystals. The feldspar-phyric character of the later members of the series is unfortunately not so obvious, though in many of them "microphenocrysts" of plagioclase are found. However, there is no proof that such examples are strictly flotation accumulative as far as these microphenocrysts are concerned. Other factors as yet unrecognized may play a significant part—for example, the influence of water.

The problem raised by the melting phenomena of the alkali rocks of Tristan da Cunha is even more complex. Of the six rocks studied, olivine is found as phenocrysts only in three of the more basic rocks, and is confined to the groundmass in the trachybasalt ( $t_{125}$ ) and absent in the two tristanites ( $t_{230}$ ,  $t_{627}$ ). The normative olivine content of these three rocks is, respectively, 4.17, 0.45, and nil.

All the Tristan da Cunha rocks are porphyritic, and plagioclase is a "phenocryst" mineral in all except the alkali basalt ( $t_6$ ); all show a high  $\text{Fe}_2\text{O}_3 : \text{FeO}$  ratio. The more alkalic types are, moreover, rich in potash, and the tristanites carry phenocrysts of a brown amphibole. With the exception of the ankaramite



( $t_{114}$ ) plagioclase is the liquidus phase in the experiments, and olivine is a precipitating phase only in two of the remainder and then as the third phase after plagioclase and clinopyroxene. The relations suggest that accumulation phenomena have played a significant role in the consolidation of these rocks and may account for the anomalous liquidus temperature relations found among the series, despite the fact that there is a continuous progress in iron enrichment from the ankaramite through the trachybasalts to the tristanite phases (Fig. 2). Except for the nephelinites the investigated Hawaiian and Hebridean alkali basalts contain normative but not modal nepheline, the normative nepheline residing in the pyroxene or in an analcitic residuum. These basalts may be considered, therefore, to lie on or near the critically undersaturated plane in the simplified basalt tetrahedron (Yoder and Tilley, 1962, p. 350, Fig. 1, and p. 352, Fig. 2). The flow sheet for the simplified iron-free basalt system was presented by Schairer and Yoder in *Year Book 63* (p. 72, Fig. 8, and p. 73, Fig. 9), and on the basis of those data the alkali basalts free of modal nepheline appear to lie on or near a thermal maximum.

It is significant that these particular alkali basalts give rise most commonly to trachytes, which also appear to lie on or near a thermal maximum in the quartz-nepheline-kalsilite system. Such a differentiation trend, however, would be expected to be maintained by continued crystallization of feldspar, olivine, and pyroxene; nevertheless, the problem that emerges from the experimental work remains. The basalt-trachyte associations of the volcanic alkali series clearly offer a challenge in interpretation, which only continued investigation, including experimental study, can be expected to solve.

The writers are greatly indebted to the donors of the rocks under study in this account, particularly to the USGS for the rocks of Kilauea Iki (Table 1) and for

permission to record the two chemical analyses of these rocks, and to W. B. Dallwitz, J. E. Thompson, Dr. R. F. Fudali, Dr. R. W. LeMaitre, Professor G. A. Macdonald, Dr. G. D. Nicholls, and A. B. Spencer.

DIOPSIDE-ANORTHITE-WATER  
AT FIVE AND TEN KILOBARS  
AND ITS BEARING ON EXPLOSIVE  
VOLCANISM

*H. S. Yoder, Jr.*

Explosive volcanism is one of the most dangerous of natural hazards, with a total energy release estimated at  $10^{22}$ – $10^{25}$  ergs, equal to 1–100 megatons of TNT. The death toll at Mont Pelée, West Indies, was about 40,000, and some 36,000 lives were lost as a result of the Krakatoa eruption. The great need for devising methods to predict an explosion and alert a population requires an understanding of the mechanisms of the phenomenon. Knowledge of the physical chemistry of the explosion process could yield suitable geophysical techniques to provide some indication of potential hazards, for which purpose measurements of tumescence, heat flow, and seismic activity may prove helpful. It is hoped that the study here described of the influence of water on the melting process of simple silicate systems may contribute to an understanding of violent, gas-propelled volcanic eruptions.

Magmas of basaltic composition consisting of a pyroxene and a plagioclase are of greatest importance. A simple system representing the principal phases involves diopside and anorthite. A note on the relations of the diopside-anorthite-water system at 5 kb was given in *Year Book 53* (pp. 106–107); the results were not published in detail because the values obtained for the water content of the liquids were inconsistent. The system has now been studied at 10 kb, and a more reliable method employed for determining the water content of the liquids. Projections of the pseudo-

ternary joins through the diopside-Ca Tschermak's molecule-silica-water system at 5 and 10 kb are given in Figs. 8 and 9.

Optical and X-ray data indicate that the anorthite phase is close to  $\text{CaAl}_2\text{Si}_2\text{O}_8$  in composition; the pyroxenes, however, are believed to be members of the diopside-Ca Tschermak's molecule join. The excess silica expected in portions of the system as a result of the pyroxene solid solutions was not observed and is presumed to be wholly dissolved in the gas phase. The compositions close to and including anorthite usually yield some crystals of  $\beta$ -alumina as well as anorthite, and it is assumed in part that some compound of calcium as well as silicon is also dissolved in the gas phase. The anorthite appears to melt congruently if the appearance of the small amount of  $\beta$ -alumina

can be considered as residual from leaching by the gas phase.

In addition to the suspected leaching problem, the formation of metastable phases during quenching presents the most serious difficulty encountered in the system. Much of the diagram depends on the experimenter's judgment as to what are stable phases as opposed to quenching products. On examination of the cooled charge at room conditions the presence of a meniscus and balls of quenched gas phase together were regarded as evidence that liquid and gas coexisted under the conditions of the experiment. Where a gas phase was not present during the experiment, the ends of the charge were irregular and no meniscus was observed. Fortunately the crystalline quenching products are usually sufficiently distinctive in their morphology, commonly

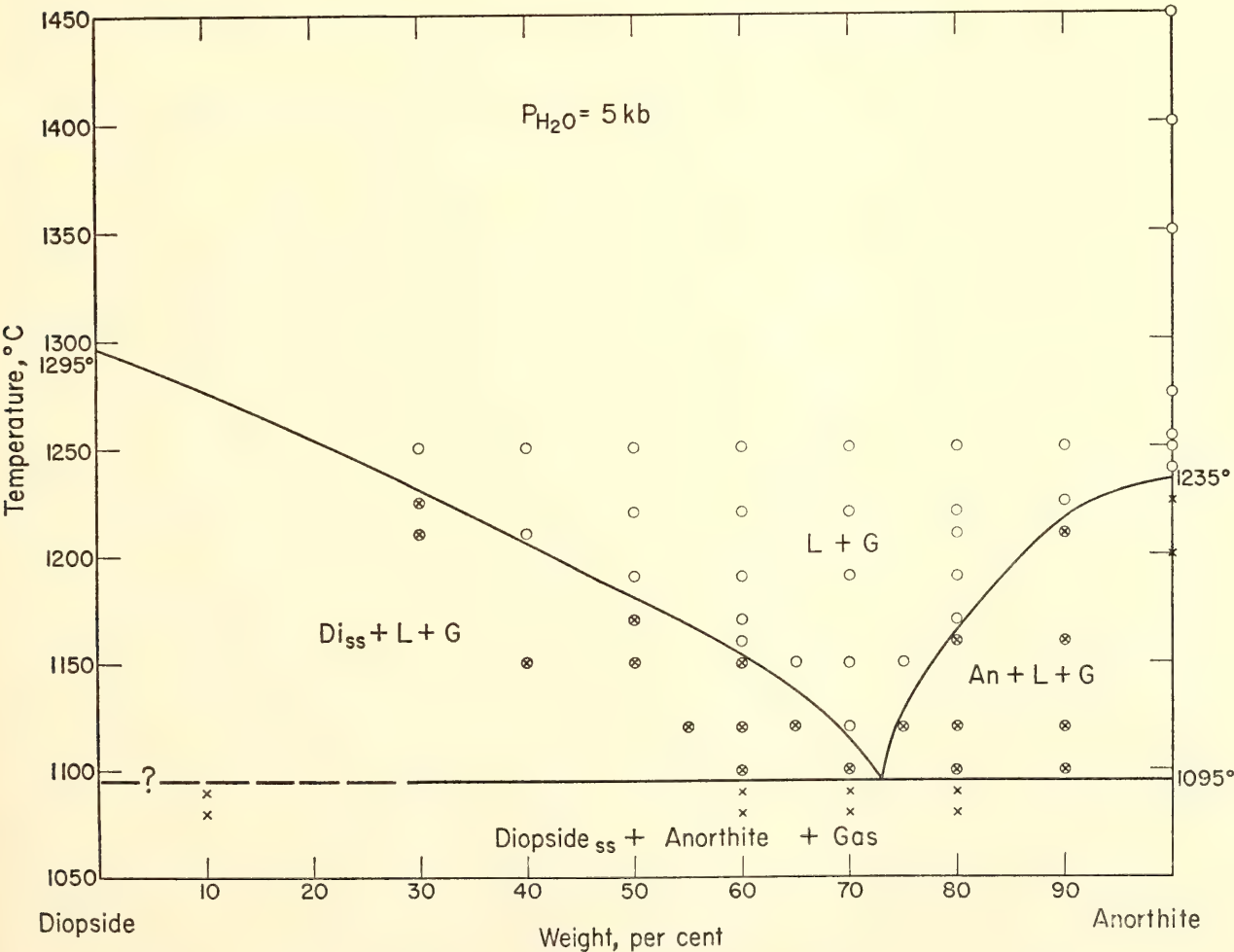


Fig. 8. Projection of the diopside-anorthite-water system at  $P_{\text{H}_2\text{O}} = 5 \text{ kb}$ .



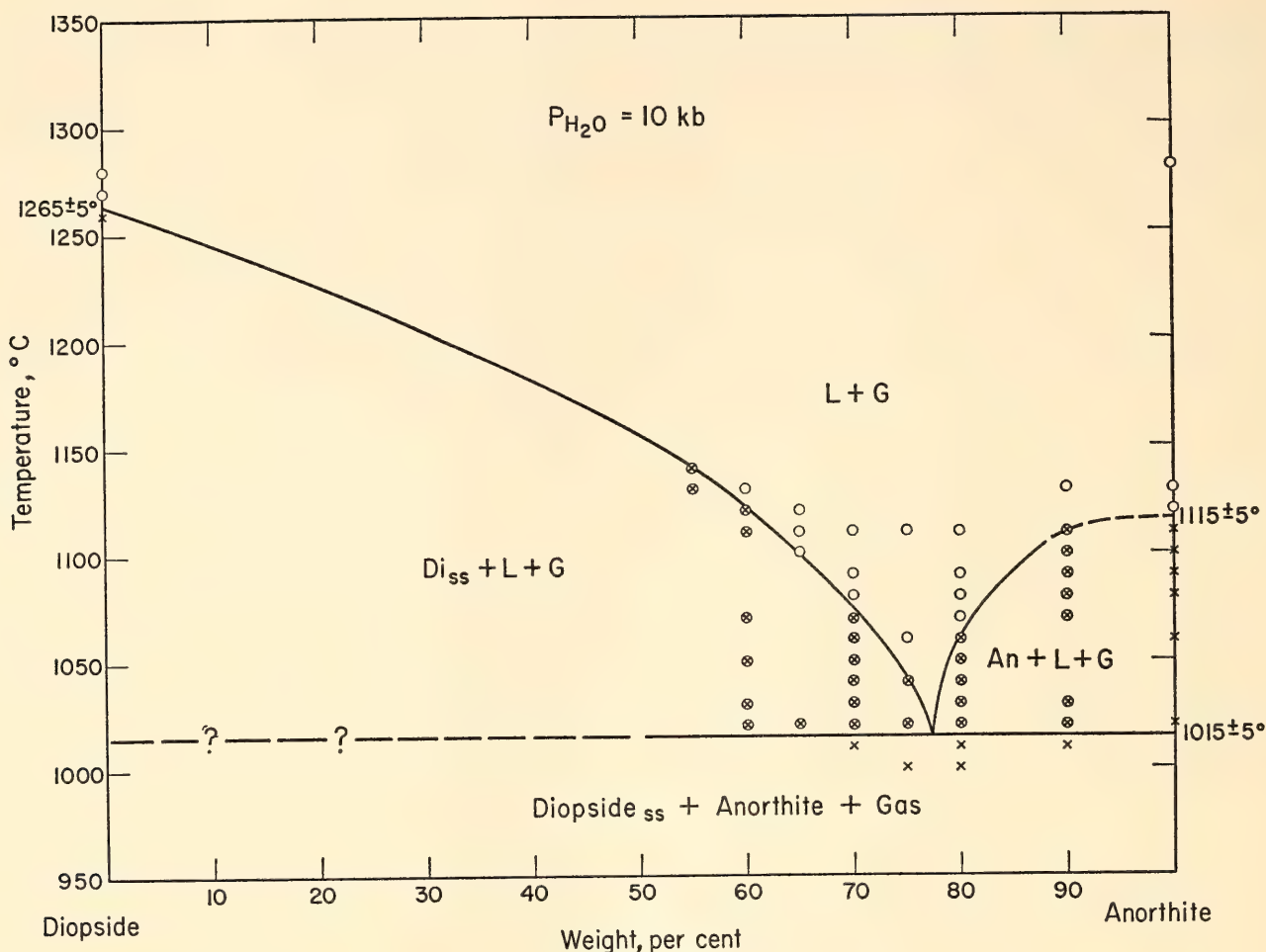


Fig. 9. Projection of the diopside-anorthite-water system at  $P_{H_2O} = 10$  kb.

by their larger size and fibrous nature, to be easily recognized in thin section and grain mounts. Persistence of residual (unchanged) phases also causes difficulty in interpretation, particularly in the gas-absent regions (in the so-called water-deficient compositions) where rates of reaction are slower.

On the basis of physical criteria, especially the morphology of the charge itself, a more precise estimate of the water content of the liquids may be made. With the technique outlined by Yoder, Stewart, and Smith in *Year Book 56* (pp. 206-209, especially Figs. 39 and 40), a section at 1,110°C and 10-kb total pressure was investigated; it is presented in Fig. 10. Some of the data points are not internally consistent, especially in the vicinity of field boundaries. It appears, however, that the maximum amount of water con-

tained in the liquids at this pressure and temperature is about  $9.5 \pm 0.5$  weight per cent ( $60.2 \pm 1.4$  mole per cent where the molar ratio of diopside to anorthite is 28/72). The fine, dashed tie lines in Fig. 10 are, of course, schematic; those shown extending to pure diopside probably project to a diopside solid solution involving alumina.

Data at liquidus temperatures now available on the diopside-anorthite system at various pressures with and without water are summarized in Fig. 11. The join at 20 kb is deduced from the preliminary work of Clark, Schairer, and de Neufville (*Year Book 61*, pp. 59-68), Boyd and England (*Year Book 60*, pp. 119-120), and E. C. Hansen (1965, personal communication). Although there are some discrepancies in the results, it is believed that diopside solid solutions

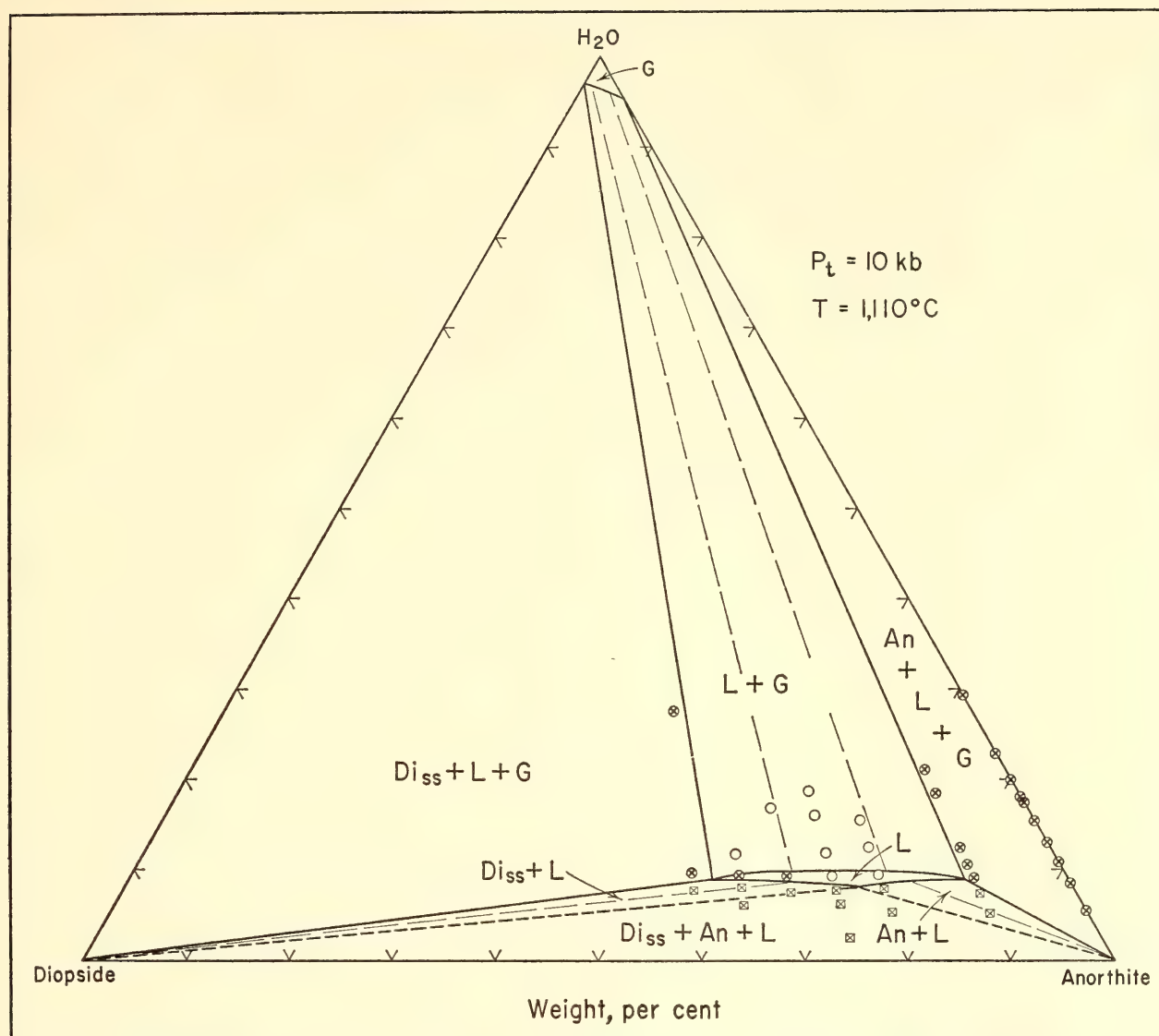
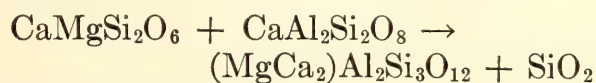


Fig. 10. Diopside-anorthite-water system at 1,110°C and  $P_{\text{total}} = 10$  kb. Note that tie lines to diopside are schematic since solid solution cannot be shown in this plane. Extent of gas field ( $G$ ) is assumed. The fields of  $\text{Di}_{\text{ss}} + G$  and  $\text{An} + G$  adjoining portions of the diopside- $\text{H}_2\text{O}$  and anorthite- $\text{H}_2\text{O}$  joins, respectively, are not illustrated because of their limited and undefined extent.

and anorthite have a common boundary at this pressure. The one-bar diagram is that of Osborn (1942) modified schematically to account for the ternary nature of the join shown by Clark, Schairer, and de Neufville. The diagrams for  $P_{\text{H}_2\text{O}} = 5$  and 10 kb are from Figs. 8 and 9. A reaction related to



which may take place at low temperatures in the solid state at these pressures is being investigated by Kushiro (described in a later section of this report).

The join itself is no longer stable above the breakdown of anorthite near 32 kb.

It is seen from Fig. 11 that pressure per se, as well as water under pressure, causes a significant shift in the initial coprecipitation point of a diopside solid solution and anorthite with lowering temperature. The importance of this behavior with regard to the formation of anorthositic magmas in nature has already been emphasized by Yoder (*Year Book 53*, pp. 106–107). The reversal in relative melting temperatures of diopside and anorthite in the presence of water (Fig. 12) has also been previously noted.



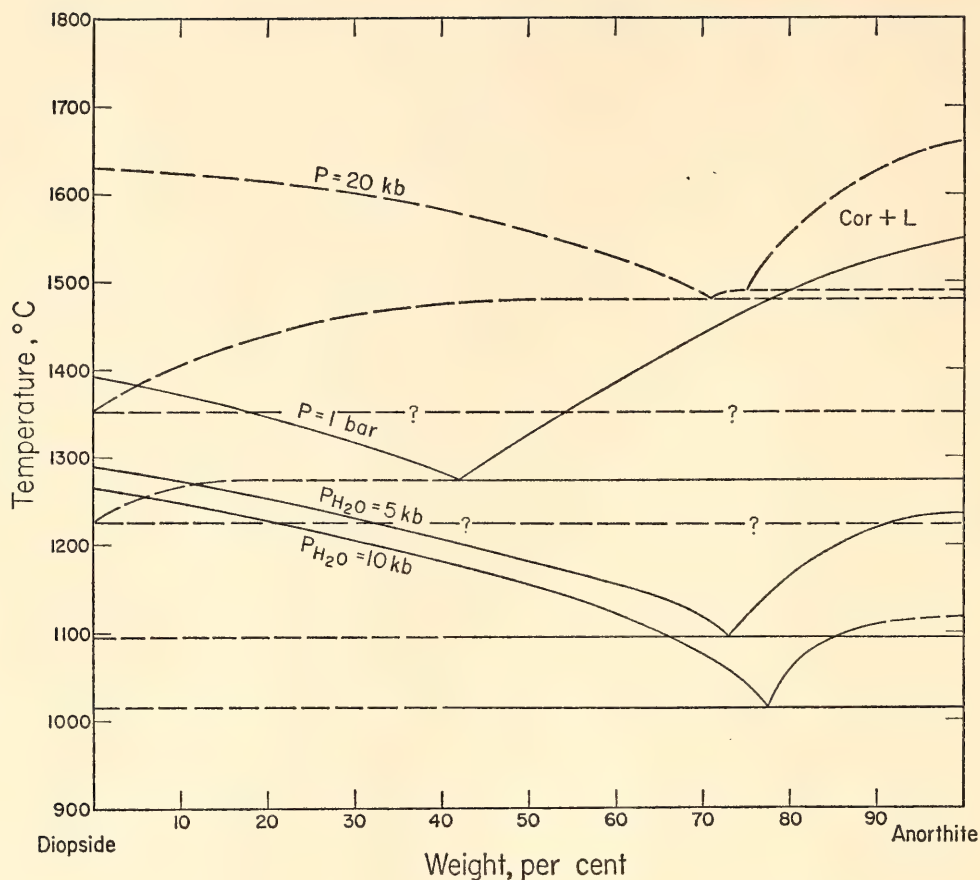


Fig. 11. Compilation of the projections of diopside-anorthite-water system at 20 kb, deduced mainly from Clark, Schairer, and de Neufville in *Year Book 61* (p. 67); at 1 bar, modified from Osborn (1942) in the light of Clark, Schairer, and de Neufville (*ibid.*, p. 66); at  $P_{H_2O} = 5$  kb and  $P_{H_2O} = 10$  kb from present studies. Completely crystalline assemblage probably includes a form of  $SiO_2$  as well as diopside solid solution and anorthite at all pressures illustrated. Cor, corundum.

Attention is now called to an application involving explosive volcanism.

First it is necessary to inquire into the potential water supply at depth. In most discussions of the rock types to be expected in the upper mantle (e.g., garnet peridotite) where magmas are believed to be generated, conditions are usually described as being nearly anhydrous yet sufficiently hydrous to provide a continuous supply of new volatiles to the oceans and atmosphere (Rubey, 1951). In addition, there is now coming to the fore a growing list of hydrous minerals more dense than their anhydrous equivalents (e.g., lawsonite,  $KAlSi_3O_8 \cdot H_2O$ ), and there are hydrous minerals that persist to very high pressures with or without polymorphic change (e.g., phlogopite, talc, glaucophane). It may be anticipated, therefore, that some hydrous minerals,

many as yet undiscovered, exist in the crystalline mantle, which can release water on decomposition or melting. The amount of water held by such minerals is perhaps small, not exceeding a low weight percentage. A mineral assemblage, consisting mostly of anhydrous but some hydrous phases and having negligible porosity, might contain an even smaller amount. As will be shown, it is not important that an accurate estimate of the water content of the crystalline mantle be made here. It is the great concentration of water that takes place on the initial formation of liquid that is critical.

Examination of the data indicates that the composition of the initial liquid formed on partial melting will always be just saturated with regard to water, no matter how small the water content of the

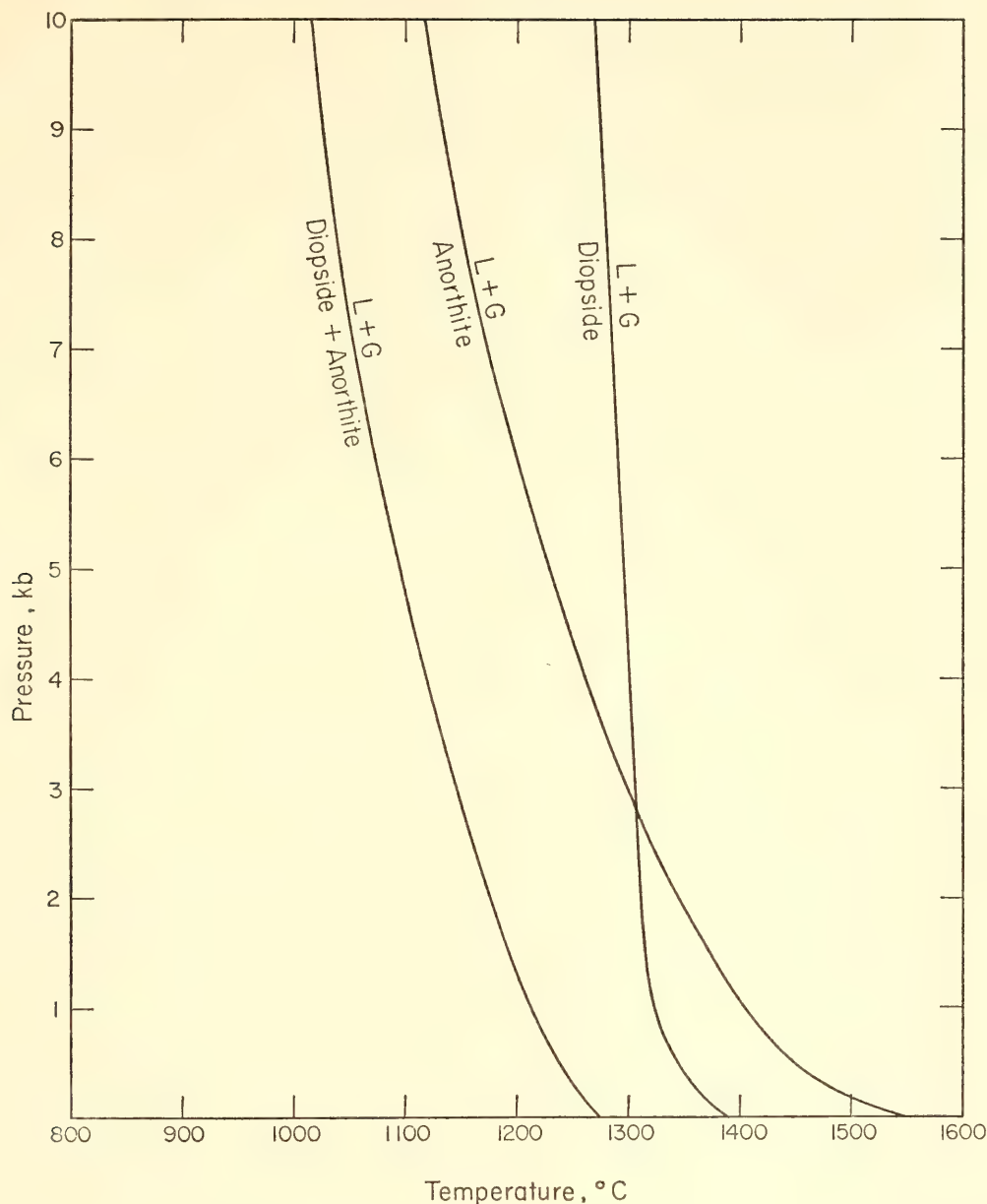


Fig. 12. Projection of the three-phase curves for the diopside-water and anorthite-water systems along with estimate of the four-phase curve for the diopside-anorthite-water system. *L*, liquid; *G*, garnet.

crystalline assemblage. This important observation can be appreciated by reference to the isothermal, isobaric section given in Fig. 10 for the diopside-anorthite-water system. The first liquid contains the components anorthite and diopside solid solution in the ratio of about 77/23. If the initial hydrous crystalline assemblage contains one per cent water, the first liquid will contain about nine per cent water. If the initial hydrous crystalline assemblage contains five per cent water, the first liquid will still contain about nine per cent water. As the tem-

perature is raised to about the initial melting temperature the relative water content of the liquid decreases. The basis of this conclusion can best be seen in the simple system  $\text{An-H}_2\text{O}$ , shown in Fig. 13. If the initial water content of the assemblage is one weight per cent under a total pressure of 10 kb, the water content of the liquid will progressively diminish with increasing temperature from point *A* through *B* and *C*, until complete melting is accomplished in *D*.

Consider now the resulting circumstances if the pressure on magma *A* (Fig.



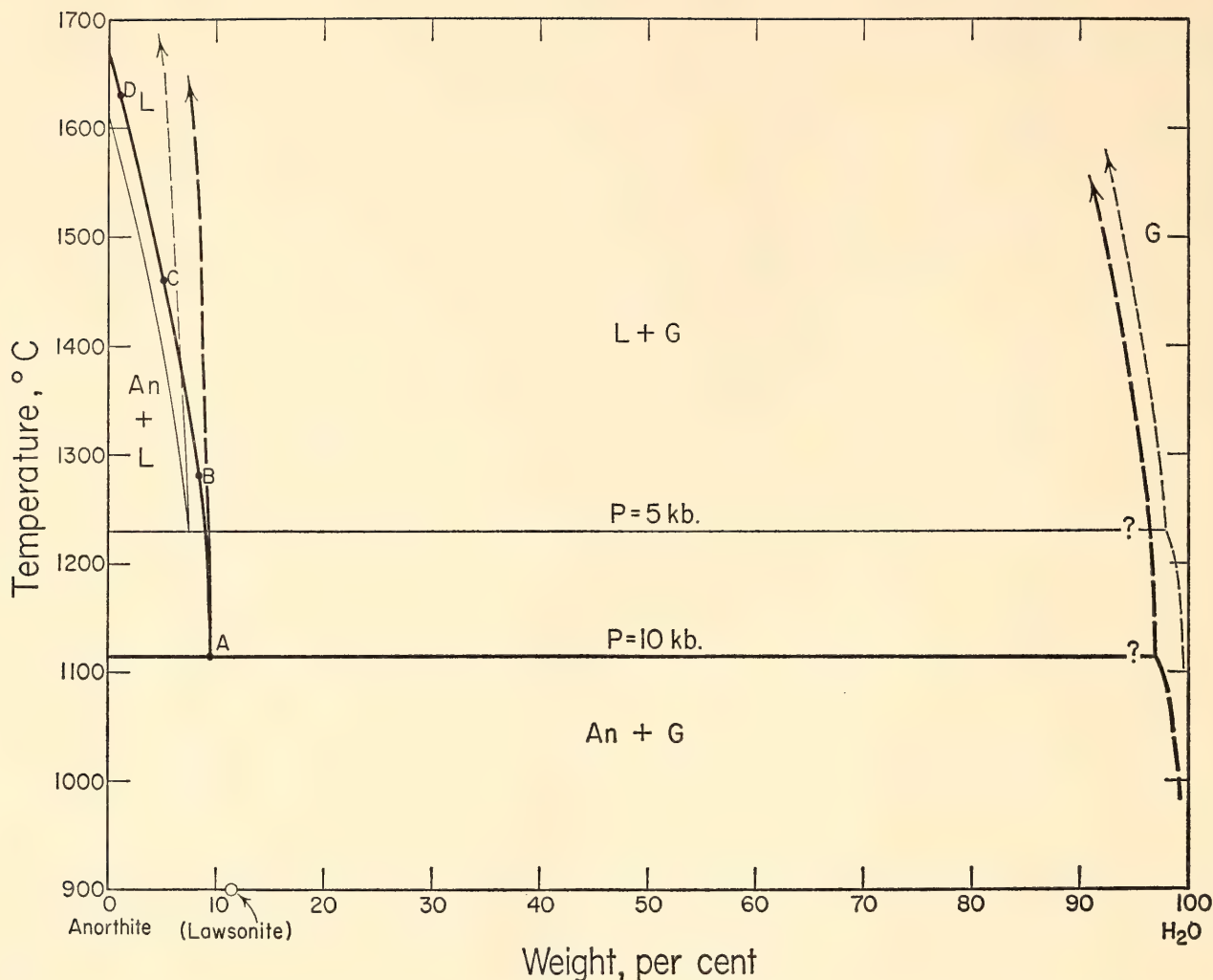


Fig. 13. Schematic illustration of the anorthite-water system at  $P = 5$  and  $10$  kb based in part on present work, assuming that  $dT/dP$  for anorthite is about  $12^\circ/\text{kb}$  and the composition of the gas phase. Points  $A$ ,  $B$ ,  $C$ , and  $D$  lie on the liquidus surface in the gas-absent region at a total pressure of  $10$  kb. Composition of lawsonite is shown although it is now believed to be unstable at these pressures and temperatures.

13) generated at  $10$  kb by the partial melting of a rock with one per cent water<sup>2</sup> (an anorthosite containing, for example, about  $10$  per cent of lawsonite, a phase believed to be metastable under these conditions), was suddenly reduced isothermally<sup>3</sup> to  $5$  kb. The magma would crystallize completely, become rigid, and

<sup>2</sup> Although no estimate of the water content of the mantle can be made with assurance, the writer favors the view that the water content is less than that of a gas-saturated basic magma in the region of generation.

<sup>3</sup> It is more likely that the pressure reduction will take place adiabatically; however, though the resulting drop in temperature of the whole magma is likely to be small, the parameters are not sufficiently well determined to estimate it.

release a gas phase filling the pores of the more dense crystalline mass, perhaps giving rise to miarolitic cavities. If the pressure on magma  $B$  generated in a similar way at a higher temperature were suddenly reduced isothermally to  $5$  kb, the fictive gas pressure would now greatly exceed that imposed by the new situation, and the magma would vesiculate as the gas phase was released. The mechanics of the vesiculation process have been outlined by Verhoogen (1951). If the pressure on magma  $C$ , also generated by partial melting at a still higher temperature, were suddenly reduced isothermally to  $5$  kb, the liquid phase would remain undersaturated with water, and

would be slightly superheated relative to the new liquidus surface. (It is conceivable, but not probable, that water could be added to the magma at this stage from an external source at a higher water pressure.) The quiescently erupting magma *C* is probably the common circumstance, vesiculating only after much of the expanding force of the gas has been dissipated. The behavior of magma *B* on pressure reduction could give rise to explosive volcanism. The pressure reduction can take place in several ways, for example, by deformation of the chamber or by emplacement of the magma into the upper crust. The effective gas pressure may then be sufficient to rupture the plug in the volcano or, more likely, the volcanic cone itself.

In circumstances in which the gas pressure is not in excess of that required for rupture, the rock, even slowly dissipating its volatiles, would be expected to crystallize with some evidence remaining of the vesiculation. In rocks of deep-seated origin, vesicles or cavities in general are conspicuous by their rarity or absence. It is known that a trapped gas phase would react with the crystallizing magma to form volatile-bearing minerals. For example, a gabbro may be converted into a hornblende gabbro as demonstrated by experiment (Yoder and Tilley, 1962, p. 449, Fig. 27). The vesicles are probably filled, therefore, during the recrystallization of the rock, the volatile phase consumed by reaction or expelled slowly by diffusion.

Explosive eruption resulting from sudden gas oversaturation of the magma may take place within a wide range of crystal content. The ashes so produced may be all glass or they may be highly charged with crystals as in the crystal tuffs. The presence of crystals may in fact accelerate the vesiculation process. A slow rate of diffusion of gas through liquid does seem to be necessary, and the new viscosity data of H. R. Shaw (personal communication, 1965) support this thesis. The mechanism is applicable to granitic as

well as basaltic magmas. The granitic magmas produce more ash deposits, presumably in part because of the greater water content ( $\sim 17$  weight per cent  $H_2O$  at 10 kb according to Luth, Jahns, and Tuttle, 1964) now believed to exist in the initial melts at the same pressure.

The concept briefly described differs considerably from the prevailing view first suggested by Morey (1922). He argued that very high pressures were developed during the cooling of a contained hydrous magma. It was necessary that the magma reach a condition of univariance before high pressure could develop. The large number of components in a magma makes the attainment of such a univariant condition unlikely (Yoder, *Year Book* 57, pp. 189–191).

It is perhaps not unwarranted to have some concern over the potentially explosive character of the stratovolcanos of the western United States. For example, there is a clear need to establish observatories near Mount Rainier and Lassen Peak. Remote monitoring of a network of tilt meters, seismometers, and shallow-well thermocouple strings would be a useful beginning on a systematic program of observation.

#### THE REACTIONS BETWEEN FORSTERITE AND ANORTHITE AT HIGH PRESSURES

*I. Kushiro and H. S. Yoder, Jr.*

In *Year Book* 63 (pp. 108–114) preliminary results on the reactions between forsterite and anorthite were reported by Kushiro and Yoder as a part of the studies on the basalt–eclogite transformation. Many additional experiments have been made on the compositions anorthite 1, forsterite 1 (in molecular ratio); and anorthite 1, forsterite 2, to determine more precisely the univariant curves for the solid reactions occurring in these two compositions. The revised  $P$ – $T$  diagram for the composition anorthite 1, forsterite 1, is shown in Fig. 14. The univariant



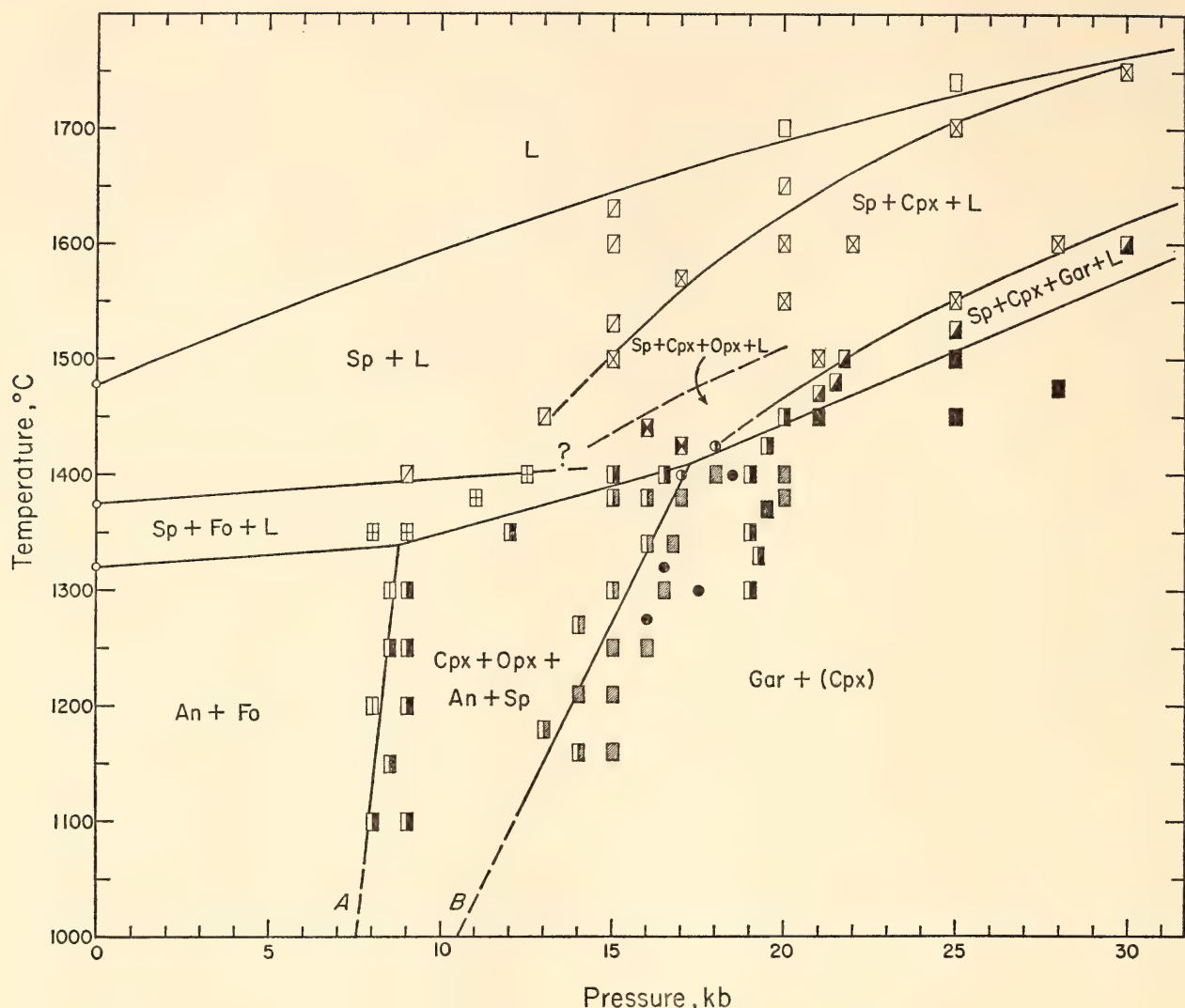


Fig. 14.  $P$ - $T$  plane for anorthite 1, forsterite 1 (molecular ratio) composition. An, anorthite; Cpx, clinopyroxene solid solution; Fo, forsterite; Gar, garnet;  $L$ , liquid; Opx, orthopyroxene solid solution; Sp, spinel. Symbols in the subsolidus region: closed rectangles, Gar + Cpx formed from An + Fo; half-closed rectangles, Cpx + Opx + An + Sp formed from An + Fo; shaded rectangles, Gar + Cpx formed from An + Fo when seeded with a small amount of Gar + Cpx; half-shaded rectangles, Cpx + Opx + An + Sp formed from An + Fo when seeded with a small amount of Gar + Cpx; open rectangles with vertical line, An + Fo unchanged; closed circles, garnet not broken down; half-closed circles, garnet broken down.

curve for the reaction anorthite + forsterite  $\rightleftharpoons$  clinopyroxene<sub>ss</sub> + orthopyroxene<sub>ss</sub> + spinel shown by curve A is nearly identical with that determined in the previous experiments. The univariant curve for the formation of garnet of the composition pyrope 2, grossularite 1, shown by curve B is located 2–3 kb lower than the previously published curve. The shift to lower pressures is based on experiments that use a different starting material.

The starting material used in the

previous experiments was a glass crystallized at 1 atmosphere (atm), consisting of very fine-grained forsterite and anorthite crystals. In the present experiments the crystallized glass is seeded with about 5 per cent of the high-pressure assemblage (garnet + clinopyroxene). Garnet grows rapidly from the seeded starting materials on the higher-pressure side of curve B, Fig. 14. On the lower-pressure side of curve B the garnet seeds disappear and the assemblage is clinopyroxene and orthopyroxene solid solutions + spinel +

anorthite. In a few experiments seeded starting material that was crystallized completely to garnet + clinopyroxene above curve *B* was used. Then garnet grows on the higher-pressure side of curve *B*, whereas it breaks down on the lower-pressure side of the curve. These experiments indicate that curve *B* is close to the univariant curve for the formation of a garnet equivalent in composition to anorthite 1, forsterite 1. Clinopyroxene also grows from seeded starting materials on the higher-pressure side of curve *B*, and it is still not certain whether the clinopyroxene is metastable.

As shown in Fig. 14, the slope ( $dT/dP$ ) of curve *A* is larger than that of curve *B*, and it seems possible that the curves

intersect at a low temperature. If this occurs an invariant point will be generated where six phases coexist—forsterite, anorthite, clinopyroxene<sub>ss</sub>, orthopyroxene<sub>ss</sub>, spinel, and garnet. At temperatures lower than that of the invariant point the garnet forms directly from anorthite + forsterite. The pyroxene-rich assemblage clinopyroxene and orthopyroxene solid solutions + spinel + anorthite would therefore be stable in a restricted triangular area between curves *A* and *B* and the melting region.

The reaction between anorthite and forsterite has also been studied on the composition anorthite 1, forsterite 2. The results are shown in Fig. 15. Curve *A*, along which the reaction anorthite +

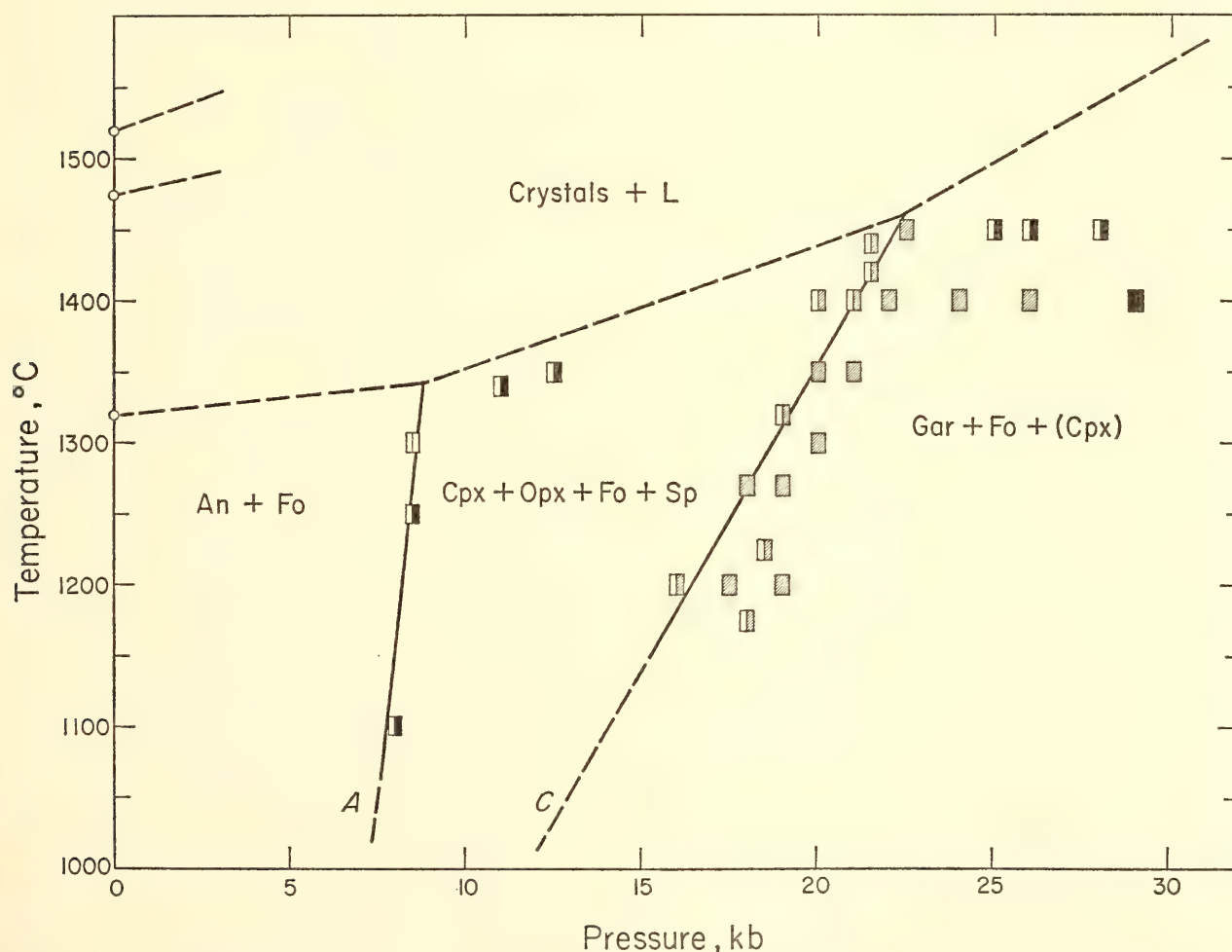


Fig. 15.  $P$ - $T$  plane for anorthite 1, forsterite 2 (molecular ratio) composition. Abbreviations as in Fig. 14. Solid rectangles, Gar + Fo + Cpx formed from An + Fo; half-closed rectangles, Cpx + Opx + Fo + Sp formed from An + Fo; shaded rectangles, Gar + Fo + Cpx formed from An + Fo when seeded with a small amount of Gar + Fo + Cpx; half-shaded rectangles, Cpx + Opx + Fo + Sp formed from An + Fo when seeded with a small amount of Gar + Fo + Cpx; open rectangles with vertical line, An + Fo unchanged.



forsterite  $\rightleftharpoons$  clinopyroxene<sub>ss</sub> + orthopyroxene<sub>ss</sub> + spinel takes place, is the same as that in Fig. 14. The position of curve *A* has been checked by three experiments, which are in agreement with those conducted on the composition anorthite 1, forsterite 1 (Fig. 14). On the higher-pressure side of curve *A* anorthite disappears and the assemblage is clinopyroxene and orthopyroxene solid solutions + spinel + forsterite, which is stable up to curve *C*. On the higher-pressure side of curve *C* garnet appears and the assemblage is garnet + forsterite with variable amounts of clinopyroxene. The amount of clinopyroxene relative to garnet and forsterite is small, however, and diminishes with longer experiments, suggesting that clinopyroxene is metastable on the higher-pressure side of curve *C*, so that above this curve garnet would have a composition pyrope 2, grossularite 1 (in molecular ratio). Curve *C*, therefore, is probably a univariant curve for the reaction clinopyroxene<sub>ss</sub> + orthopyroxene<sub>ss</sub> + spinel  $\rightleftharpoons$  garnet + forsterite. By using the glass crystallized at 1 atm into anorthite + forsterite and seeded with a small amount of the high-pressure assemblage (garnet + forsterite + clinopyroxene), curve *C* was found to lie on the higher-pressure side of curve *B* in Fig. 14. Between curves *B* and *C* a garnet of composition equal or close to pyrope 2, grossularite 1, is stable, but it cannot coexist with forsterite because the plane clinopyroxene<sub>ss</sub>-orthopyroxene<sub>ss</sub>-spinel is still stable, cutting, as will be shown later (Fig. 16), the garnet-forsterite join. The difference between the two curves is about 4 kb at 1,400°C and about 2.5 kb at 1,200°C. The  $dT/dP$  of curve *C* is smaller than that of curve *B* and in consequence they would intersect at a low temperature. Curve *C* would also intersect curve *A*, since its  $dT/dP$  is much smaller than that of curve *A*. If curves *A* and *C* intersect, an invariant point would be generated at which six phases (forsterite, anorthite, clinopyroxene<sub>ss</sub>, ortho-

pyroxene<sub>ss</sub>, spinel, and garnet) coexist, as in the composition anorthite 1, forsterite 1. The invariant point obtained by extrapolation of curves *A* and *B*, therefore, must be the same as that obtained by extrapolation of curves *A* and *C*, and further, there is no other possible intersection of *B* and *C*. The invariant point is in the vicinity of 700°C and 6 kb, but these estimates will of course be strongly influenced by small shifts of the univariant curves.

The phase relations in the four different areas of the  $P$ - $T$  conditions separated in part by curves *A*, *B*, and *C* are shown in the context of the system CaO-MgO-Al<sub>2</sub>O<sub>3</sub>-SiO<sub>2</sub> (Fig. 16). In  $P$ - $T$  condition I of the upper right  $P$ - $T$  diagram the An-Fo join is stable and consequently the Di<sub>ss</sub> + En<sub>ss</sub> + Fo + An assemblage is stable (stage I). This is the assemblage of olivine basalt or gabbro, although iron, sodium, and minor elements are neglected.

In  $P$ - $T$  condition II the An-Fo join is replaced by the plane Di<sub>ss</sub>-En<sub>ss</sub>-Sp and two different assemblages, Di<sub>ss</sub> + En<sub>ss</sub> + Fo + Sp and Di<sub>ss</sub> + En<sub>ss</sub> + Sp + An, are stable (stage II). The first-mentioned assemblage is that of the peridotite inclusions in basalts and some intrusive peridotites as described by many authors (e.g., Ross, Foster, and Myers, 1954). The second assemblage has been found in some metamorphosed olivine gabbro and norite in Canada, Norway, and other localities described by Barth (1927), Shand (1945), Osborne (1949), Oosterom (1963), and others. In these rocks the original olivine has reacted with plagioclase to form an intergrowth of pyroxenes and spinel that is known as pyroxene-spinel symplectite.

In  $P$ - $T$  condition III a garnet of the composition pyrope 2, grossularite 1, becomes stable, and garnet-bearing assemblages are stable, namely Di<sub>ss</sub> + Gar + Sp + An, Di<sub>ss</sub> + En<sub>ss</sub> + Gar + Sp, and Di<sub>ss</sub> + En<sub>ss</sub> + Gar + An (stage III). The second assemblage has been found as

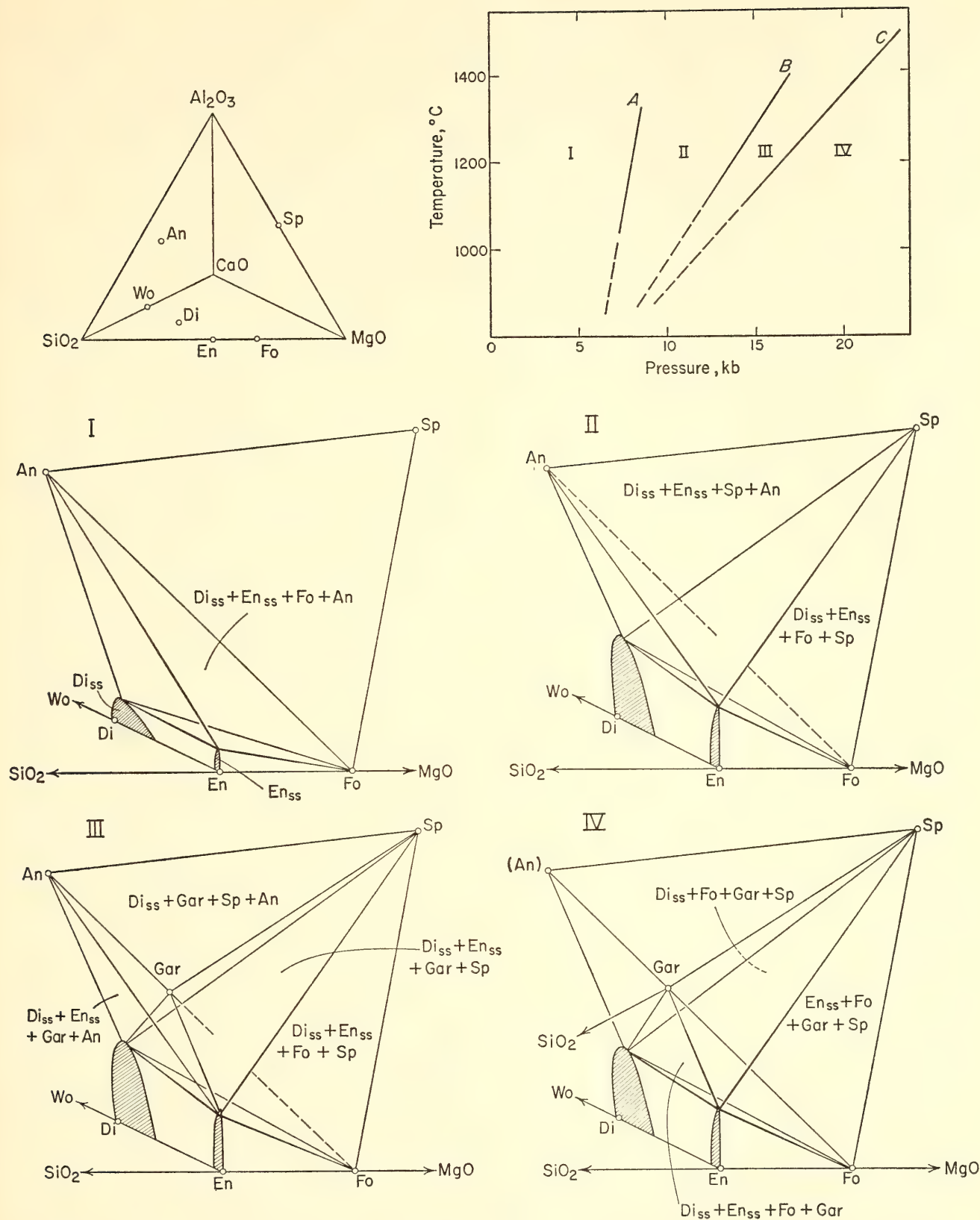


Fig. 16. Phase assemblages in a part of the system  $\text{CaO-MgO-Al}_2\text{O}_3\text{-SiO}_2$  in the four different  $P$ - $T$  conditions shown in the upper right  $P$ - $T$  diagram. Between stages III and IV there must be an intermediate stage in which the  $\text{Di}_{\text{ss}}\text{-En}_{\text{ss}}\text{-Sp}$  join is still stable but the  $\text{An-En}_{\text{ss}}$  join is replaced by the  $\text{Gar-Qz}$  join. Stages I, II, III, and IV may be called, respectively, the basalt, pyroxenite, granulite, and eclogite stages. Curves A, B, and C in the upper right  $P$ - $T$  diagram are those in Figs. 14 and 15. An, anorthite; Di, diopside;  $\text{Di}_{\text{ss}}$ , diopside solid solution (clinopyroxene solid solution); En, enstatite;  $\text{En}_{\text{ss}}$ , enstatite solid solution (orthopyroxene solid solution); Sp, spinel; Wo, wollastonite.



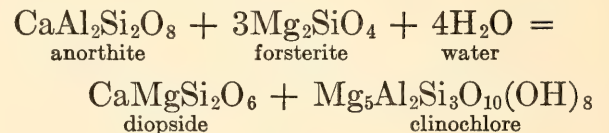
an ejected nodule in the tuff of Salt Lake Crater, Oahu Island, described by Yoder and Tilley (1962), and as ariegite in the Pyrenees, described by Lacroix (1900). The last assemblage is that of basic granulites and charnockites. The assemblage  $Di_{ss} + En_{ss} + Fo + Sp$ , characteristic of the peridotite inclusions in basalts, is still stable in this stage.

In  $P$ - $T$  condition IV the Gar-Fo join becomes stable and the assemblages of garnet peridotites are obtained (stage IV). The assemblage  $Di_{ss} + En_{ss} + Fo + Gar$  is well known from garnet peridotite inclusions in kimberlite. In this stage the An- $En_{ss}$  join is not stable, being replaced by the Gar-Qz join, as shown by Kushiro and Yoder (*Year Book 63*, pp. 108-114). Between stages III and IV there must be an intermediate stage in which the  $Di_{ss}$ - $En_{ss}$ -Sp join is still stable but the An- $En_{ss}$  join is replaced by the Gar-Qz join. With further increase of pressure the  $En_{ss}$ -Sp and  $Di_{ss}$ -Sp joins are replaced by the Gar-Fo joins, as shown by MacGregor (*Year Book 63*, p. 157, and this report), and anorthite breaks down into grossularite + kyanite + quartz (Boyd and England, *Year Book 60*).

The present experiments may throw light upon several petrological problems, such as the  $P$ - $T$  conditions of the basalt-eclogite transformation; the formation of pyroxene-spinel symplectite; the formation of pyroxenite; and the stability fields of granulites, charnockites, and the peridotite inclusions in basalts.

Because of the importance of the proposed invariant point forsterite + anorthite + clinopyroxene<sub>ss</sub> + orthopyroxene<sub>ss</sub> + spinel + garnet, it is now being studied in detail. The slow rate of reaction at low temperature requires hydrothermal technique, and we are now using the cold-seal type of hydrothermal quenching apparatus. In preliminary experiments at 4 and 5 kb  $P_{H_2O}$ , 500°C, 2 weeks, anorthite and forsterite (1:1 ratio) have reacted in the presence of

excess water to form the diopside<sub>ss</sub> + clinocllore assemblage. In these experiments forsterite was consumed, whereas a considerable amount of anorthite was left after the reaction. The reaction may be written schematically, without regard for solid solutions, as follows:



At 10-kb water pressure, however, anorthite reacts with forsterite to form the diopside<sub>ss</sub> + amphibole + spinel assemblage over 800°C, as shown by Yoder and Chinner (*Year Book 59*, p. 79). Therefore, a boundary curve between the chlorite-bearing and the amphibole-bearing assemblages is anticipated. The stability fields of these two assemblages would be bounded by those of the anhydrous assemblages clinopyroxene and orthopyroxene solid solutions + spinel + anorthite and garnet + (clinopyroxene). Experiments are in progress to determine the stability field of each assemblage and especially to estimate more closely the position of the invariant point, now believed to be in the water-deficient region. Preliminary results suggest that the mineral assemblage olivine + plagioclase, characteristic of olivine basalt or olivine gabbro, is unstable in the presence of excess water in the continental crust and probably even near the base of the oceanic crust. In the absence of water, as mentioned, garnet forms directly from the anorthite + forsterite assemblage at pressures and temperatures lower than those of the proposed invariant point. Although the univariant curve for the reaction has not been determined, it may pass near the  $P$ - $T$  condition corresponding to that of the oceanic Moho (M) discontinuity. It is suggested, therefore, that a phase change may take place in olivine basalts even near the oceanic M discontinuity and in the dry condition.



BEHAVIOR OF MELILITES IN THE  
JOIN GEHLENITE-SODA  
MELILITE-AKERMANNITE  
AT ONE-ATMOSPHERE PRESSURE

*J. F. Schairer, H. S. Yoder, Jr., and C. E. Tilley*

The studies of Schairer and Yoder (*Year Book 63*, pp. 65-74) showed the presence of melilites at all except two of the quaternary invariant points and of nepheline solid solutions at all of the invariant points in the complex system involved in the formation of simplified alkali basalts. Melilites are one of the most important key phases in the formation of basic alkaline rocks, and the melilite group is a major mineral group in such rocks.

During the past year some progress has been made in studies of the melting and crystallization behavior of ternary melilite compositions in the system gehlenite ( $\text{Ca}_2\text{Al}_2\text{SiO}_7$ )-soda melilite ( $\text{NaCaAlSi}_2\text{O}_7$ )-akermanite ( $\text{Ca}_2\text{MgSi}_2\text{O}_7$ ). So far 73 ternary melilite compositions have been prepared and studied. A knowledge of the melting and crystallization relations of ternary melilites is a prime requisite to an understanding of the change in melilite composition during the crystallization of these simplified rock magmas.

In the past progress has been possible in the study of five-component systems when they could be simplified and treated as four-component systems. The latter have been expressed geometrically as regular (equilateral) tetrahedra and studied by a series of slices and sections, usually lines or triangular joins, which link together the compositions of simple minerals involved in the equilibria. The relations between important quaternary invariant points have been presented by means of a simple "flow sheet" (see *Year Book 63*, p. 72, Fig. 8). This was done for the nepheline-normative and for the quartz-normative simplified basaltic compositions (*Year Book 63*, pp. 65-74). Somewhat detailed studies of the relations in the ternary melilite join

(gehlenite-soda melilite-akermanite) were undertaken during the past year, and are still in progress. The join cuts the tetrahedron nepheline-gehlenite-akermanite- $\text{CaSiO}_3$ , in which the relations are very complex owing to the appearance of diopsidic pyroxenes and possibly other solid phases in addition to nepheline solid solutions, wollastonite solid solutions, and pseudowollastonite. Because of the complexities of solid solutions, it has not been possible to determine the precise compositions of the coexisting mineral phases, even with a combination of the physical chemistry, the use of detailed examination with the petrographic microscope, and the X-ray powder pattern techniques. Clearly the original assumption that the melilite phase relations can be expressed by a simple tetrahedron is not valid; the loss of the simple geometry of a tetrahedron imposes serious theoretical and experimental difficulties.

*Sides of the Join Gehlenite-Soda  
Melilite-Akermanite*

*The sideline akermanite-soda melilite.* A preliminary diagram for the system akermanite-soda melilite appears in *Year Book 63* (p. 90, Fig. 20). On the basis of many additional data a more detailed data diagram for the system is given here as Fig. 17. The system lies within the join nepheline- $\text{CaSiO}_3$ -akermanite (*Year Book 63*, p. 67, Fig. 3), one of the limiting faces of the tetrahedron nepheline-gehlenite-akermanite- $\text{CaSiO}_3$ . In studies of the join akermanite-soda melilite difficulties were encountered in the identification of solid phases. Too little of some of the phases (principally pseudowollastonite, wollastonites, and diopsidic pyroxenes) was present for identification by X-ray powder pattern techniques. During the past year, however, more accurate identification of solid phases was accomplished by extensive and careful study with the petrographic microscope. There is no evidence of any change



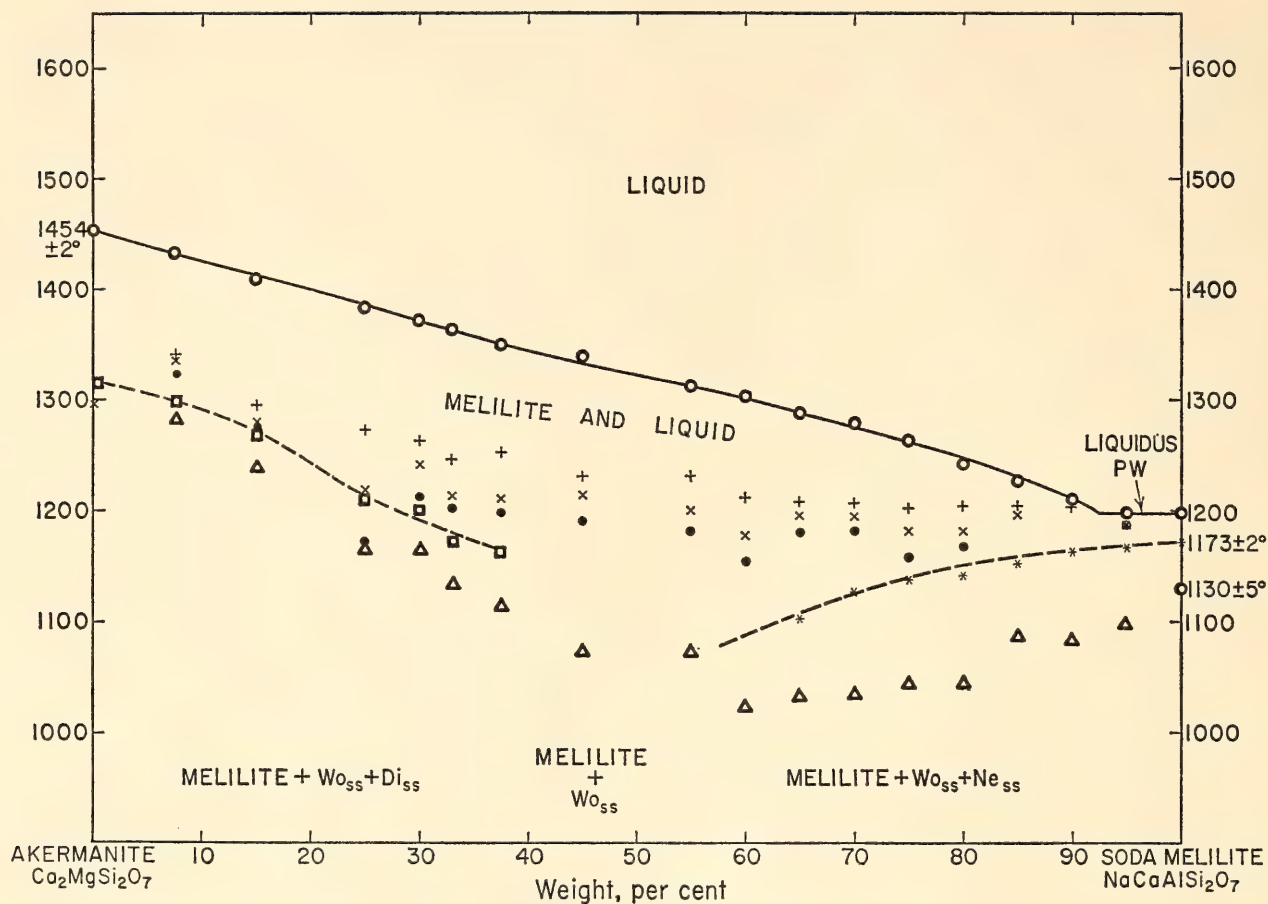


Fig. 17. Data diagram for mixtures between akermanite and soda melilite compositions. Circles, liquidus data; crosses, temperature of appearance of pseudowollastonite with decreasing temperature; Xs, temperature of appearance of wollastonites; closed circles, temperature of disappearance of pseudowollastonite; squares, temperature of appearance of diopsidic pyroxene; asterisks, temperature of appearance of nepheline solid solutions; circle with X inside, temperature of appearance of melilite; triangles, temperature of beginning of melting;  $Wo_{ss}$ , wollastonite solid solutions;  $Di_{ss}$ , diopsidic pyroxenes;  $Ne_{ss}$ , nepheline solid solutions.

in composition (possible soda volatilization) during the syntheses of these mixtures.

Pseudowollastonite appears as the primary phase or is the second solid phase to appear in all compositions. There is no optical evidence for any solid solution in this phase. It is joined by wollastonite solid solution, and there is a temperature interval in which both pseudowollastonite and wollastonite solid solution are present before the pseudowollastonite disappears by inversion as the temperature is lowered. In compositions between akermanite and  $Ak_{62.5}SM_{37.5}$ , diopsidic solid solutions appear at appropriate temperatures shown by a dashed curve in Fig. 17. In compositions between soda melilite

and approximately  $Ak_{42}SM_{58}$ , nepheline solid solutions appear at appropriate temperatures shown by a dashed curve. Temperatures at beginning of melting, which cannot be measured with precision, are shown by triangles. The behavior of mixtures of akermanite and soda melilite just described is complex and not even approximately binary. None of the melilite solid solutions present in these compositions can lie on the join, and they must contain other molecules.

*The sideline gehlenite-soda melilite.* Besides the data obtained by Goldsmith (1948) on three compositions, 10 additional compositions in the system gehlenite-soda melilite were prepared and studied. This system lies within the

triangular join nepheline-gehlenite- $\text{CaSiO}_3$ , another one of the faces of the tetrahedron nepheline-gehlenite-akermanite- $\text{CaSiO}_3$ . The results of quenching experiments for this join are given in Fig. 18; there is only one piercing point, *P*, at  $1,173^\circ\text{C} \pm 5^\circ\text{C}$ . The join is very similar to the join nepheline-akermanite- $\text{CaSiO}_3$  (*Year Book 63*, p. 67, Fig. 3), where the piercing point with the same solid phases lies at  $1,171^\circ\text{C} \pm 3^\circ\text{C}$ . Fig. 19 gives the phase equilibrium data for the system gehlenite-soda melilite.

Pseudowollastonite is the primary phase or the second phase to appear in compositions between approximately  $\text{Geh}_{32.5}\text{SM}_{67.5}$  and  $\text{Geh}_6\text{SM}_{94}$ , and there is then only a small temperature interval on cooling before wollastonite appears and pseudowollastonite disappears by inversion. In all compositions between approximately  $\text{Geh}_{47}\text{SM}_{53}$  and the soda melilite composition itself, crystals of a nepheline solid solution appear at the same temperature,  $1,173^\circ\text{C} \pm 5^\circ\text{C}$ . A solid line at  $1,130^\circ\text{C} \pm 5^\circ\text{C}$  shows the same beginning

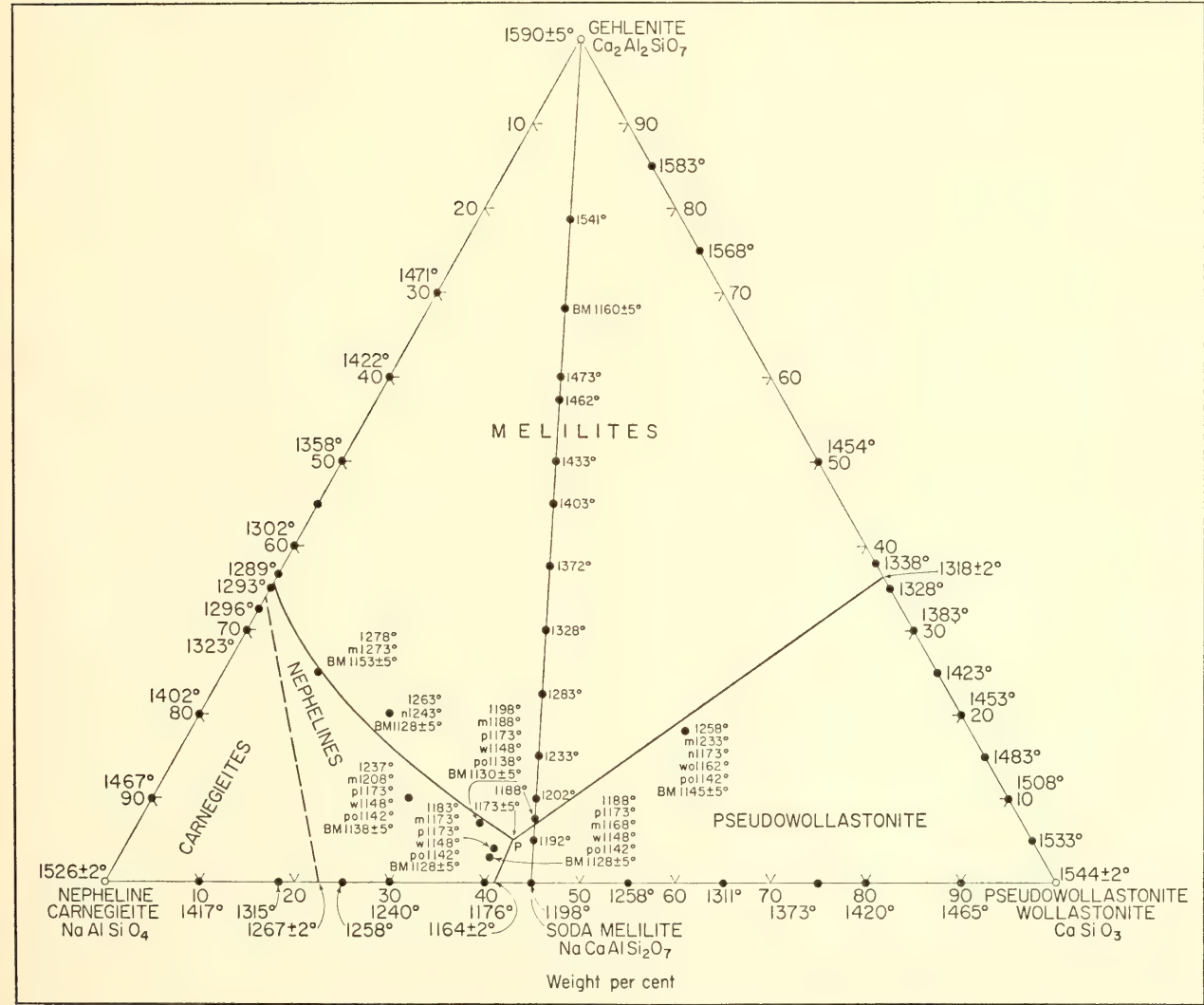


Fig. 18. Phase-equilibrium data for the join nepheline-gehlenite-wollastonite. Lower-case letters indicate the temperature of appearance of a phase with decreasing temperature for a specific bulk composition. First number is the liquidus temperature, and solid phase is indicated by field in which it lies: *m*, melilite; *p*, pseudowollastonite; *w*, wollastonites; *n*, nephelines; *cg*, carnegieites; *BM*, beginning of melting. Addition of letter *o* indicates that the phase has been consumed and is no longer present. Soda melilite composition is Ne 55.02, Wo 44.98 weight per cent. See Fig. 19 for details of gehlenite-soda melilite join. *P* at  $1,173^\circ \pm 5^\circ\text{C}$  is the piercing point of the line melilite + pseudowollastonite + nepheline solid solution + liquid.



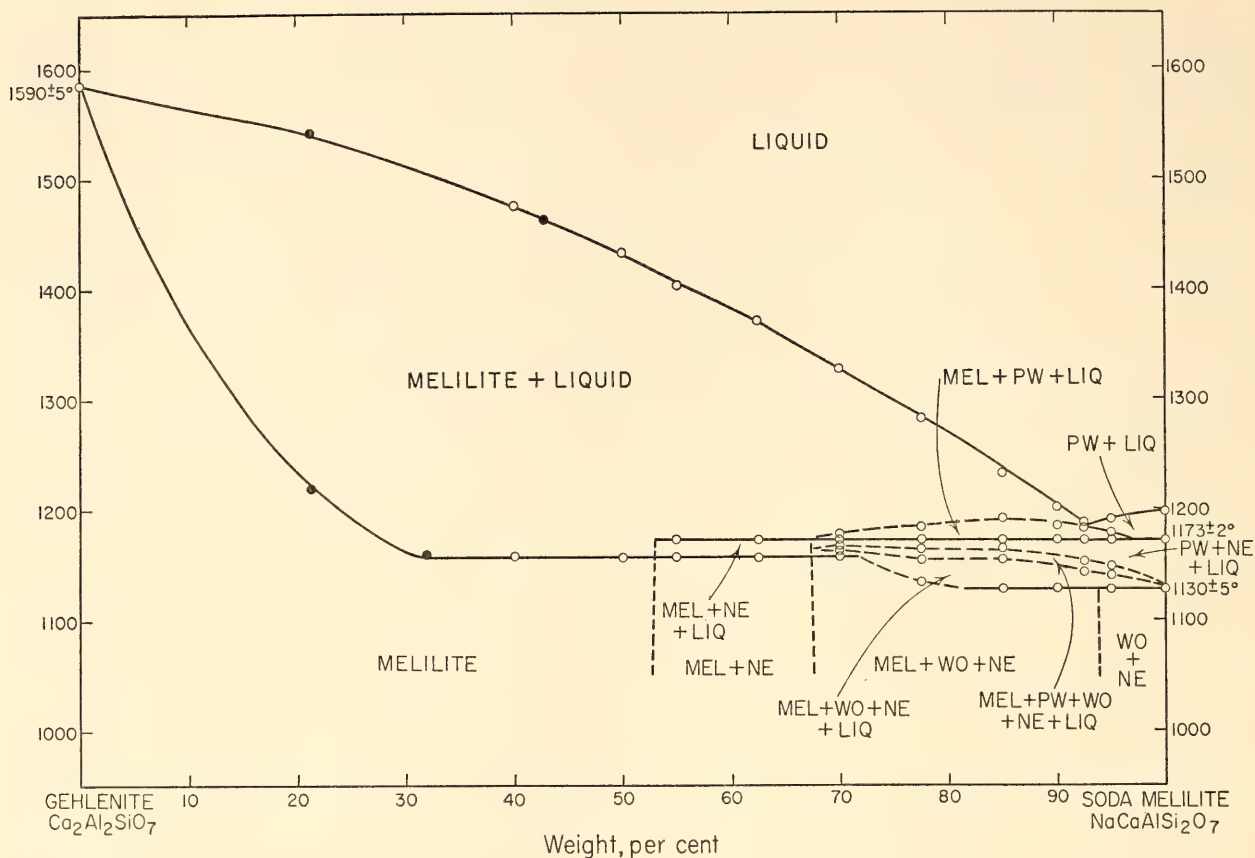


Fig. 19. Data diagram for mixtures between the gehlenite and soda melilite composition. Circles, data obtained in this study; closed circles, data of Goldsmith (1948); MEL, melilites; NE, nepheline solid solutions; WO, wollastonite solid solutions; PW, pseudowollastonite; LIQ, liquid. All lines outline observed phase assemblages and may not necessarily represent equilibrium boundary curves.

of melting temperature (within experimental error) for compositions between approximately  $\text{Geh}_{18}\text{SM}_{82}$  and the soda melilite composition itself. A solid line at  $1,155^\circ\text{C} \pm 5^\circ$  shows the beginning of melting for all compositions between approximately  $\text{Geh}_{69}\text{SM}_{31}$  and  $\text{Geh}_{28}\text{SM}_{72}$ . An examination of the join nepheline-gehlenite- $\text{CaSiO}_3$  (Fig. 18) shows that the three temperatures just noted— $1,173^\circ\text{C} \pm 5^\circ$ ,  $1,130^\circ\text{C} \pm 5^\circ$ , and  $1,155^\circ\text{C} \pm 5^\circ$ —correspond to the temperature of the piercing point *P* and to beginning of melting of some of the regions of bulk composition in this figure. The significance of these temperature correspondences is not yet apparent.

*The sideline gehlenite-akermanite.* This system was studied by Ferguson and Buddington (1920) and later by Osborn and Schairer (1941). It is binary at temperatures near and above the solidus.

Our studies now in progress indicate that many of these compositions, particularly those rich in akermanite, unmix at lower temperatures and show diopsidic pyroxenes, wollastonite solid solutions, and possibly other solid phases. These complexities will carry over into adjacent melilite compositions.

#### *The Join Gehlenite-Soda Melilite-Akermanite*

Liquidus data for the join are presented here as Fig. 20. The isotherms show that a temperature trough extends from the binary minimum in gehlenite-akermanite into the triangular diagram toward the soda melilite apex. It should be noted that there is a significant drop in liquidus temperature with increase in soda melilite components. The primary phase at the liquidus is a melilite solid solution, except for a small area near the

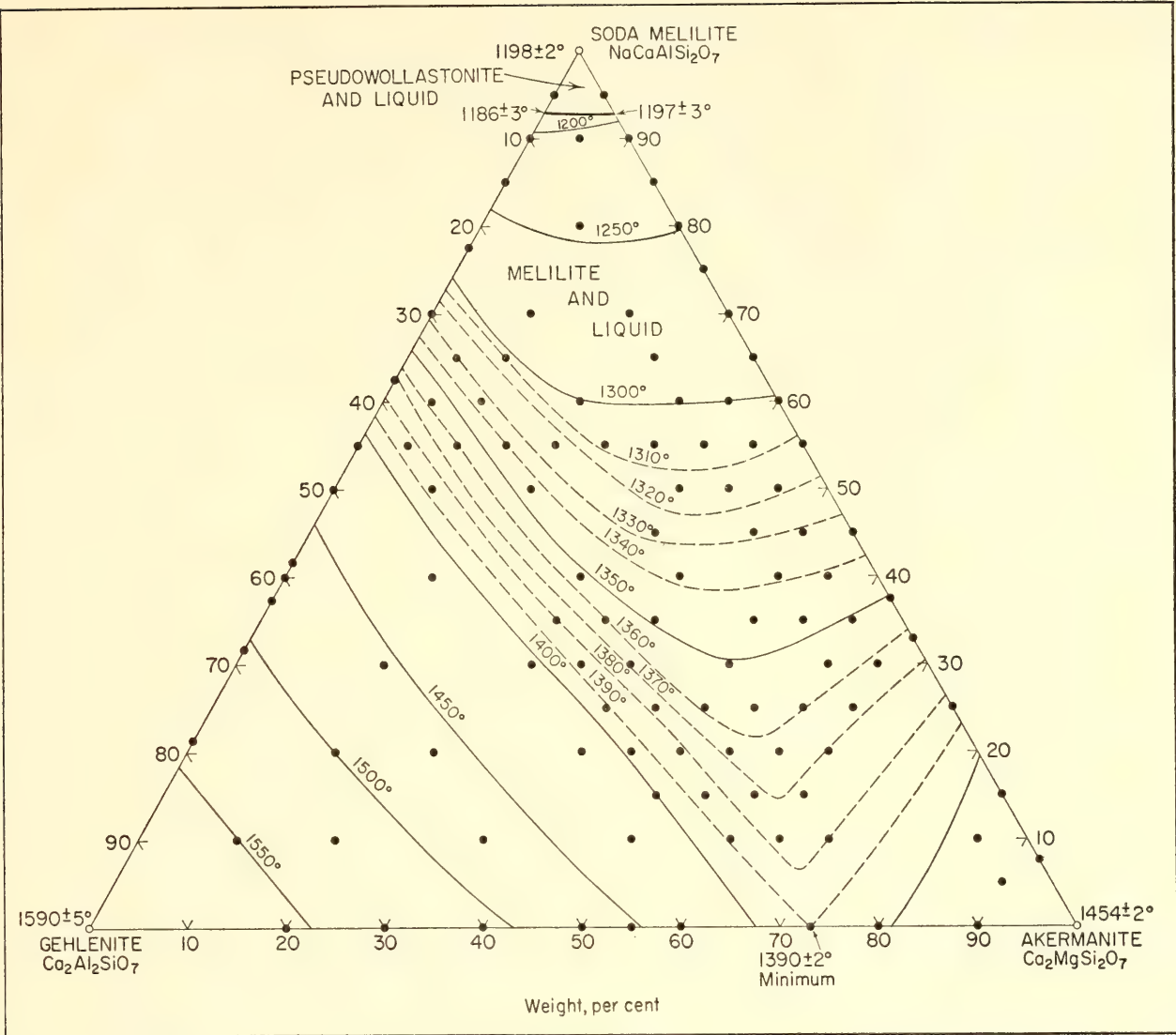


Fig. 20. Liquidus data for the join gehlenite-soda melilite-akermanite. Primary phase at the liquidus is a melilite solid solution except for very small area near the soda melilite apex. In temperature interval between 1,300°C and 1,400°C dashed isotherms at 10-degree intervals aid in defining temperature trough originating at temperature minimum in the sideline gehlenite-akermanite.

soda melilite apex (cf. Fig. 19). Many phase-equilibrium data are on hand at temperatures between the liquidus and solidus for the 73 ternary melilite compositions prepared so far. These data, which are not yet complete, indicate that there is a rapid change in composition of the melilite phase as soon as any liquid appears. The presentation of isothermal sections and their interpretation are reserved for the future.

The synthesis of a soda melilite at high pressures (4 to 10 kb) was described by Yoder in last year's report (*Year Book 63*, pp. 86-89). Examination of the product prepared at 10 kb and 1,100°C showed

crystals with characteristic melilite morphology—tetragonal prisms tabular on the base. The optical properties of homogeneous crystals free from any exsolved material gave values of  $\omega = 1.610$  and  $\epsilon = 1.593$ .

Glass of the composition  $\text{CaNaAlSi}_2\text{O}_7$  has a refractive index of 1.565. In the system gehlenite-soda melilite-akermanite under investigation, examination of the optical character of the melilite solid solutions showed that essentially isotropic compositions extend from the gehlenite-akermanite sideline at  $\text{Geh}_{45}\text{Ak}_{55}$ ,  $\omega$  and  $\epsilon = 1.651$  (Buddington, 1922, p. 42), in a linear course to approximately  $\text{Ak}_{68}\text{SM}_{32}$ ,

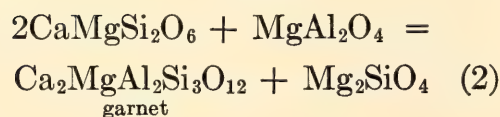
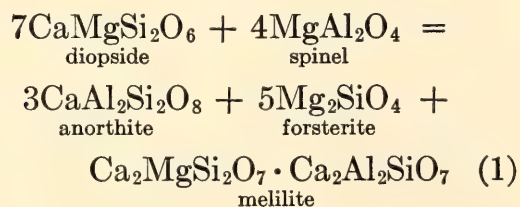


$\omega$  and  $\epsilon = 1.625$ ; therefore optically positive melilites are limited to the area enclosed by this line and the akermanite corner. Dispersion phenomena near the position of isotropism in the system are revealed in the abnormal interference tints, anomalous brown on the optically positive side and ultrablue on the optically negative side. On the Ak-SM sideline and in the region immediately adjacent in the system, melilites at the solidus contain a small amount of exsolved wollastonite or diopside so that the compositions of the studied melilites do not correspond exactly with the prepared glass compositions.

THE JOIN DIOPSIDE-SPINEL  
AT ATMOSPHERIC PRESSURE  
AND THE SIGNIFICANCE OF THE  
DIOPSIDE-SPINEL ASSEMBLAGE

*J. F. Schairer and I. Kushiro*

Diopside ( $\text{CaMgSi}_2\text{O}_6$ ) often coexists with spinel ( $\text{MgAl}_2\text{O}_4$ ) in metamorphic rocks and peridotites, although these two minerals commonly contain considerable amounts of iron, chromium, and other elements in solid solution. Diopside + spinel is isochemical with anorthite + forsterite + melilite and garnet + forsterite as shown by



The diopside + spinel assemblage therefore must have a stability field different from those of the other two assemblages. In the present experiments the join diopside-spinel has been studied at 1 atm, both at liquidus and subsolidus temperatures, by the quenching technique. In addition, several experiments have been performed at high pressures,

with both solid- and gas-media apparatus. The present experiments, particularly those at high pressures, have not been completed, but the results obtained so far would be useful in petrological problems.

Six mixtures were prepared along the join diopside-spinel in the composition range from  $\text{Di}_{95}\text{Sp}_5$  (weight per cent) to  $\text{Di}_{70}\text{Sp}_{30}$ . The preliminary diagram at 1 atm is shown in the diopside-rich portion of the join diopside-spinel (Fig. 21). Spinel appears on the liquidus for compositions more spinel rich than about  $\text{Di}_{76}\text{Sp}_{24}$ ; forsterite appears between the compositions  $\text{Di}_{76}\text{Sp}_{24}$  and  $\text{Di}_{92}\text{Sp}_8$ ; and diopside appears for compositions more diopside rich than  $\text{Di}_{92}\text{Sp}_8$ . X-ray powder patterns of spinel show no significant shift in lines from pure  $\text{MgAl}_2\text{O}_4$ . The liquids of compositions rich in diopside reach the divariant plane  $\text{Di}_{ss} + \text{Fo} + L$  and those of compositions near  $\text{Di}_{80}\text{Sp}_{20}$  reach another divariant plane,  $\text{Fo} + \text{An} + L$ . Except for liquids close to diopside, the liquids of compositions more diopside rich than  $\text{Di}_{80}\text{Sp}_{20}$  reach the univariant line  $\text{Fo} + \text{Di}_{ss} + \text{An} + L$  and finally crystallize into the  $\text{Di}_{ss} + \text{Fo} + \text{An}$  assemblage on the univariant line or the  $\text{Di}_{ss} + \text{Fo} + \text{An} + \text{Mel}$  assemblage at the invariant point. The temperature of the invariant point is  $1,220^\circ\text{C} \pm 5^\circ\text{C}$ , which is essentially the same as that obtained by de Neufville and Schairer (*Year Book 61*, pp. 56–59) and by O'Hara and Schairer (*Year Book 62*, pp. 107–115). The liquids of compositions rich in spinel follow the divariant plane  $\text{Sp} + \text{Fo} + L$  and the univariant line  $\text{Sp} + \text{Fo} + \text{Mel} + L$ , and attain the quarternary reaction point where spinel begins to react with liquid and anorthite begins to crystallize. The liquid is consumed at the invariant point, and the assemblage is  $\text{Sp} + \text{Fo} + \text{Mel} + \text{An}$ . For compositions near  $\text{Di}_{75}\text{Sp}_{25}$  liquid still remains after spinel disappears, and the liquids follow the univariant line  $\text{Fo} + \text{An} + \text{Mel} + L$  and finally crystallize into  $\text{Fo} + \text{An} + \text{Mel}$ .

From the crystalline mixture of the composition  $\text{Di}_{70}\text{Sp}_{30}$ , diopside solid solu-

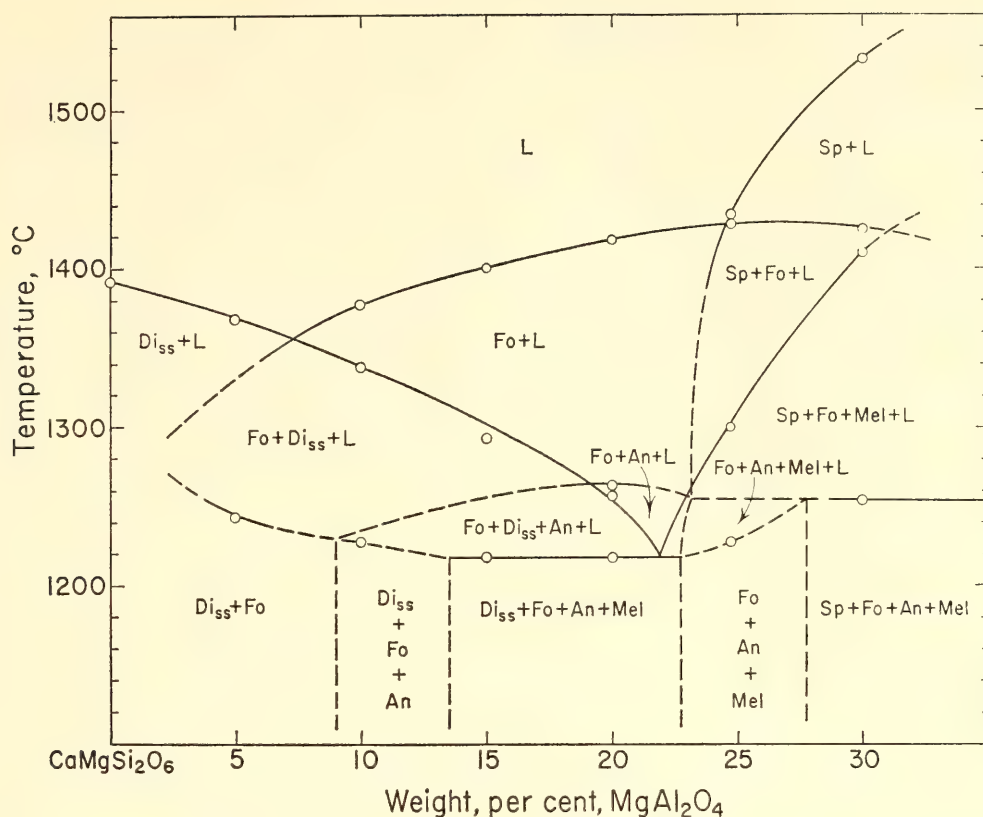
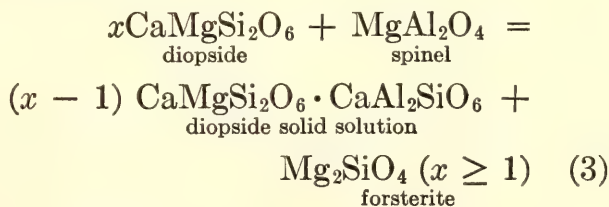


Fig. 21. Preliminary diagram of the diopside-rich portion of the join diopside ( $\text{CaMgSi}_2\text{O}_6$ )-spinel ( $\text{MgAl}_2\text{O}_4$ ) at 1 atm. An, anorthite;  $\text{Di}_{ss}$ , diopside solid solution; Fo, forsterite; L, liquid; Mel, melilite; Sp, spinel.

tion crystallizes at temperatures between  $1,215^\circ$  and  $1,235^\circ\text{C}$ , and five solid phases coexist in this temperature range: Sp, Fo, Mel, An, and  $\text{Di}_{ss}$ . Similar results have been obtained by Chinner and Schairer (1962) on the join grossularite-pyrope at 1 atm. The diopside solid solution, however, does not crystallize from glass of the same composition in the same temperature range; nor does it crystallize at any temperatures from either the crystalline mixture of glass of the composition  $\text{Di}_{75.27}\text{Sp}_{24.73}$ , more diopside rich than  $\text{Di}_{70}\text{Sp}_{30}$ . It is therefore most probable that the diopside solid solution is metastable and spinel and diopside solid solution do not coexist at solidus temperatures at 1 atm.

In the subsolidus region five different assemblages exist in the composition range of the present experiments:  $\text{Di}_{ss} + \text{Fo}$ ;  $\text{Di}_{ss} + \text{Fo} + \text{An}$ ;  $\text{Di}_{ss} + \text{Fo} + \text{An} + \text{Mel}$ ;  $\text{Fo} + \text{An} + \text{Mel}$ ; and  $\text{Fo} + \text{An} + \text{Mel} + \text{Sp}$ . A region where diopside solid

solution and spinel may coexist has not been found at subsolidus temperatures, at least above  $1,000^\circ\text{C}$ . At lower temperatures, however, it is possible for these minerals to coexist, as suggested by Osborn and Tait (1952). The range of the  $\text{Di}_{ss} + \text{Fo}$  assemblage extends from diopside to about  $\text{Di}_{90}\text{Sp}_{10}$  near solidus temperatures. The  $\text{Di}_{ss} + \text{Fo}$  assemblage on the diopside-spinel joint can be obtained by



Therefore, the diopside solid solution coexisting with forsterite must be aluminous. In the  $\text{Di}_{ss} + \text{Fo}$  region of Fig. 21 there may be a one-phase region of diopside solid solution. Glass of the composition  $\text{Di}_{90}\text{Sp}_{10}$  was crystallized to



diopside solid solution without any other phases at 800°C for 137 days and at 1,000°C for 28 days. At 1,050°C and 1,120°C, forsterite crystallizes out of diopside solid solution. Glass of the composition  $\text{Di}_{95}\text{Sp}_5$  was crystallized to diopside solid solution without any other phases at 1,000°C for 28 days and 1,050°C for 21 days. This evidence suggests that diopside may form a complex solid solution at temperatures at least between 800°C and 1,050°C. The range of diopside solid solution, if it exists, would be close to diopside with probably less than five per cent spinel in this temperature range. This diopside solid solution, although aluminous, may be similar to that obtained in the join diopside-forsterite (Kushiro and Schairer, *Year Book 62*, pp. 95–103). Forsterite coexisting with diopside contains a small amount of calcium as the monticellite ( $\text{CaMgSiO}_4$ ) molecule at high temperatures (Kushiro and Schairer, *Year Book 62*), and therefore it is expected that forsterite in this join also contains a small amount of monticellite at the liquidus and also near solidus temperatures. Reaction 3 would therefore be a simplified reaction.

The  $\text{Fo} + \text{An} + \text{Mel}$  assemblage is obtained by the simplified reaction 1. The composition of melilite coexisting with forsterite and anorthite changes with changes in the composition of the mixture. De Neufville and Schairer (*Year Book 61*, pp. 56–59) have shown that the composition of melilite coexisting with anorthite and forsterite changes from about  $\text{Ak}_{70}\text{Geh}_{30}$  to about  $\text{Ak}_{90}\text{Geh}_{10}$  on the join diopside- $\text{CaAl}_2\text{SiO}_6$ . The same composition range is expected in melilite in the three-phase region  $\text{Fo} + \text{An} + \text{Mel}$  of the join diopside-spinel, since the three-phase region is bounded by the two four-phase regions  $\text{Di}_{ss} + \text{Fo} + \text{An} + \text{Mel}$  and  $\text{Sp} + \text{Fo} + \text{An} + \text{Mel}$  as in the case of the join diopside- $\text{CaAl}_2\text{SiO}_6$ .

Previous experiments under high pressures indicated that diopside solid solution and spinel coexist both at liquidus

and subsolidus temperatures. In studies on the reaction between anorthite and forsterite (Kushiro and Yoder, *Year Book 63*, pp. 108–114, and this report) it was found that aluminous diopside coexists with spinel at pressures between 9 and 15 kb at 1,300°C and between 8 and 12 kb at 1,100°C. They also coexist in the presence of liquids at pressures higher than 15 kb. Yoder and Chinner (*Year Book 59*) have shown that diopside solid solution coexists with spinel at both liquidus and subsolidus temperatures at 10-kb water pressure. These experimental data indicate that diopside and spinel coexist at high pressures under either anhydrous or hydrous conditions. This coexistence should be expected from the volume relations. The diopside + spinel assemblage has a smaller volume than the forsterite + anorthite + melilite assemblage. Boyd (*Year Book 55*), however, reported the coexistence of aluminous diopside and spinel only at a 250-bar water pressure in the temperature range 860°C to 920°C and at 350 bars between 925°C and 1,060°C. This means that the diopside + spinel assemblage becomes stable instead of the forsterite + anorthite + melilite assemblage at a certain pressure between 1 atm and 350 bars at temperatures near 1,000°C. The univariant curve for reaction 1 would, therefore, lie in a very low-pressure region of the  $P$ - $T$  plane. The univariant curve for reaction 2 has been determined by MacGregor (this report). It is located at about 35 kb near 1,000°C and has a positive slope, indicating that reaction 2 takes place at much higher pressures than reaction 1. The stability field of the diopside + spinel assemblage has, therefore, a wide range of pressure and temperature conditions.

In the present study several experiments have been carried out on the composition  $\text{Di}_2\text{Sp}_1$  (molecular ratio) at pressures of 8–15 kb and temperatures of 1,100°C to 1,300°C, the conditions within the stability field of the diopside + spinel



assemblage. At 8 kb and 1,100°C, at 8.5 kb and 1,150°C and 1,250°C, and at 12 kb and 1,300°C, glass and crystallized glass of this composition were crystallized into  $\text{Di}_{ss} + \text{Fo}$  without spinel. This evidence indicates that the diopside solid solution is highly aluminous since the coefficient  $x$  in reaction 3 is equal to 2 for the composition  $\text{Di}_2\text{Sp}_1$ , and therefore the ratio of diopside to  $\text{CaAl}_2\text{SiO}_6$  is 1/1.

These experiments suggest that diopside coexisting with spinel is considerably aluminous at high pressures and high temperatures. Aluminous augites (fassaite) coexisting with spinel have been described in metamorphosed limestones in Ceylon and Tyrol (Tilley, 1938) and in Montana (Knopf and Lee, 1957). The fassaite in Helena, Montana, described by Knopf and Lee, containing 15.75 weight per cent  $\text{Al}_2\text{O}_3$  (the highest  $\text{Al}_2\text{O}_3$  ever recorded in clinopyroxene) and 6.10 per cent  $\text{Fe}_2\text{O}_3$ , with less than 0.1 per cent alkalis, coexists with spinel (60 molecular per cent  $\text{MgAl}_2\text{O}_4$ ), garnet, and a small amount of mica. The content of the Ca-Tschermak's components ( $\text{CaAl}_2\text{SiO}_6$  and  $\text{CaFe}^{3+}\text{AlSiO}_6$ ) is 42.7 weight per cent. The present experiments suggest that this pyroxene would have crystallized under a considerable pressure. However, the volume of the diopside + spinel assemblage is smaller than that of the aluminous diopside + forsterite assemblage; that is, the volume change in reaction 3 from left to right is positive and the content of alumina may decrease with increase of pressure at constant temperature or may increase with increase of temperature at constant pressure.

The preliminary experiments on the join diopside-spinel suggest that the diopside + spinel assemblage is not stable near atmospheric pressures and at high temperatures, whereas it becomes stable with increasing pressure and has a wide range of stability field, and that the diopside coexisting with spinel would contain a considerable amount of alumina.

# THE LIQUIDUS RELATIONS IN THE SYSTEMS FORSTERITE- $\text{CaAl}_2\text{SiO}_6$ -SILICA AND FORSTERITE-NEPHELINE-SILICA AT HIGH PRESSURES

*I. Kushiro*

Basalt magmas are believed to be generated in the upper mantle of the earth. The upper-mantle materials have been considered to be peridotite or eclogite on the basis of seismic data; and peridotite or garnet peridotite seems to be more acceptable than eclogite on the basis of petrological observations on the inclusions in kimberlite, in basaltic rocks, and in the peridotites of the mid-Atlantic ridge. Assuming the upper-mantle materials to be peridotite or garnet peridotite, the major constituent minerals in the upper mantle would be olivine, orthopyroxene, clinopyroxene, and garnet or spinel, all of which are solid solutions, and the process of producing basalt magmas would be partial melting. The compositions of the magmas produced by the partial melting of the upper mantle are closely related to the position of the invariant point in the systems including the constituents of the upper-mantle materials, since melting begins at or close to an invariant point. The position of the invariant point in the system including the constituents of the upper-mantle materials at high pressure is important, therefore, in considering the compositions of the magmas formed by the partial melting of the upper mantle.

Last year the liquidus relations of the ternary system diopside-forsterite-enstatite, one of the fundamental systems, were studied at 20 kb, and the invariant point and the olivine-pyroxene liquidus boundaries were determined (Kushiro, *Year Book 63*, pp. 105-108). In the present experiments the two ternary systems forsterite ( $\text{Mg}_2\text{SiO}_4$ )- $\text{CaAl}_2\text{SiO}_6$ - $\text{SiO}_2$  and forsterite-nepheline ( $\text{NaAlSi}_3\text{O}_8$ )- $\text{SiO}_2$  have been studied in the pressure range 10-35 kb, in relation to the posi-



tions of the invariant points and the olivine-pyroxene liquidus boundaries.

*The System Forsterite- $\text{CaAl}_2\text{SiO}_6$ -Silica*

The system forsterite ( $\text{Mg}_2\text{SiO}_4$ )- $\text{CaAl}_2\text{SiO}_6$ -silica (Fig. 22)—which contains enstatite ( $\text{MgSiO}_3$ ), anorthite ( $\text{CaAl}_2\text{Si}_2\text{O}_8$ ), and a garnet ( $\text{CaMg}_2\text{Al}_2\text{Si}_3\text{O}_{12}$ )—is one of the key systems in studies of basalt genesis. Andersen (1915) studied the liquidus relations of the system forsterite-anorthite-silica at 1 atm. The invariant point forsterite + clino-

enstatite (protoenstatite) + anorthite + liquid and the forsterite-clinoenstatite (protoenstatite) liquidus boundary determined by Andersen are shown by the solid curve in Fig. 22. Kushiro and Yoder (*Year Book 63*, pp. 108–114) carried out experiments on the composition pyrope 2, grossularite 1 ( $\text{CaMg}_2\text{Al}_2\text{Si}_3\text{O}_{12}$ ), up to 30 kb and found that the spinel liquidus covers this composition in the pressure range 1 atm to 30 kb. They also showed that the composition of point EAN-59 in Fig. 22 is covered by the spinel liquid-

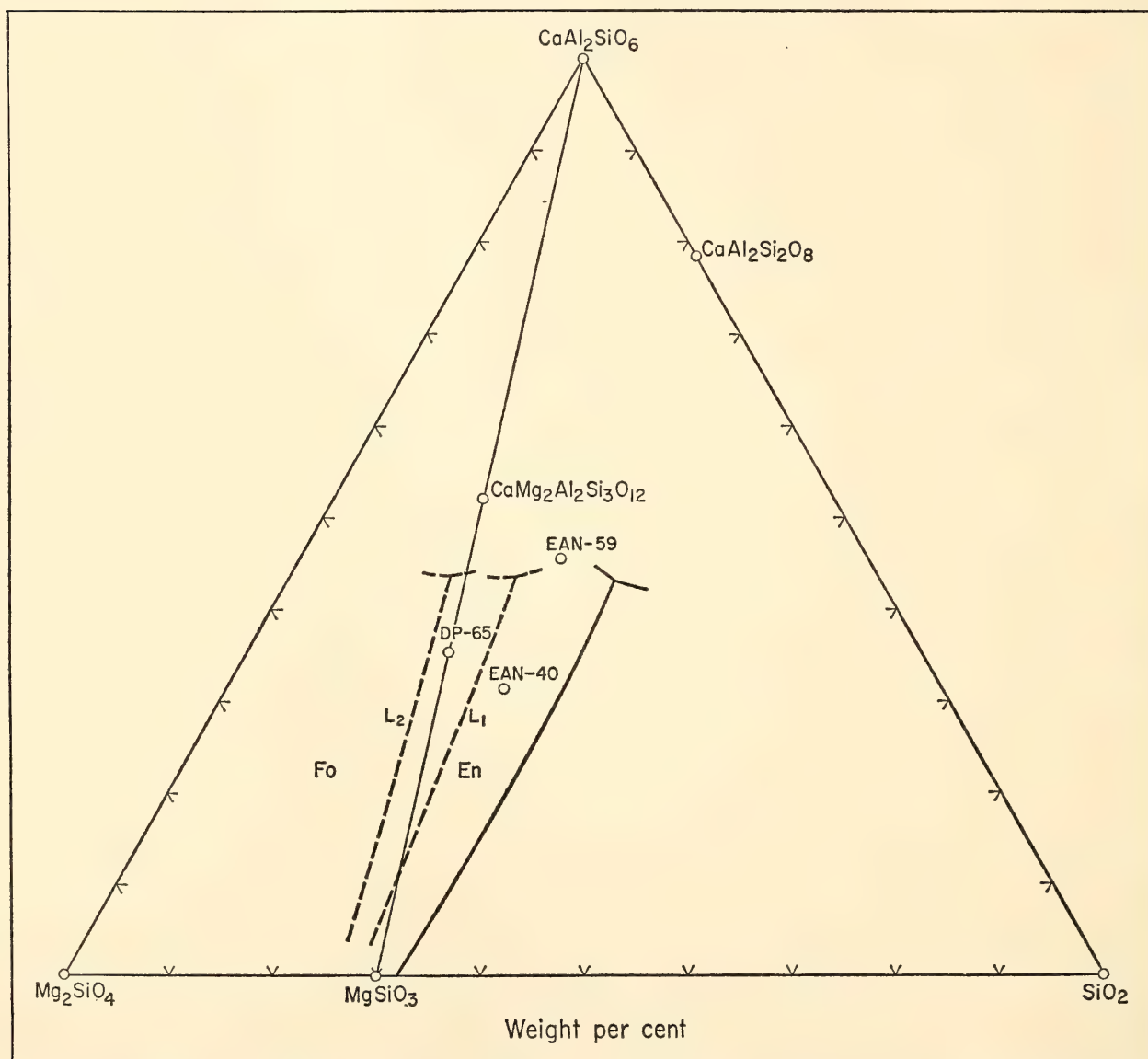


Fig. 22. The forsterite (Fo)-enstatite (En) liquidus boundary at different pressures in the system forsterite ( $\text{Mg}_2\text{SiO}_4$ )- $\text{CaAl}_2\text{SiO}_6$ -silica. Solid curve is a forsterite-clinoenstatite (protoenstatite) boundary at 1 atm determined by Andersen (1915). Dashed curves  $L_1$  and  $L_2$  indicate the forsterite-enstatite boundary curves at pressures near 20 and 30 kb, respectively.  $\text{MgSiO}_3$ ,  $\text{CaAl}_2\text{Si}_2\text{O}_8$ , and  $\text{CaMg}_2\text{Al}_2\text{Si}_3\text{O}_{12}$  show compositions of pure enstatite, anorthite, and a garnet (pyrope 2, grossularite 1, molecular ratio), respectively. EAN-59, EAN-40, and DP-65 are compositions studied.

us in the pressure range 10–22 kb.

In the present experiments the composition of point DP-65 in Fig. 22 has been studied in the pressure range 15–26 kb, using a solid-media, piston-cylinder type of apparatus similar to that designed by Boyd and England (*Year Books* 57, pp. 170–173, and 60, pp. 120, 121). The starting material is a crystallized glass of the composition diopside 35, pyrope 65 (weight per cent), prepared by O'Hara and Schairer (*Year Book* 62, pp. 107–115), which is very close to the composition enstatite 4,  $\text{CaAl}_2\text{SiO}_6$  1 (molecular ratio). The results of the experiments are shown in the pressure–temperature diagram for this composition (Fig. 23). As shown in the figure, forsterite is the primary phase to crystallize in the pressure range 1 atm to about 26 kb, indicating that this composition is covered by the forsterite liquidus up to about 26 kb. O'Hara (*Year Book* 62, pp. 116–119) found that orthopyroxene (aluminous enstatite) crystallizes as a primary phase for this composition at 30 kb. The Opx + L region determined by him is shown by circles in Fig. 23.

These experimental results indicate that a part of the forsterite-enstatite boundary is in the compositional field  $\text{MgSiO}_3\text{--CaAl}_2\text{SiO}_6\text{--SiO}_2$  in the pressure

range 1 atm to at least 26 kb as shown by the dashed curve  $L_1$  (Fig. 22); consequently the invariant point, which may be off the plane forsterite- $\text{CaAl}_2\text{SiO}_6$ -silica, is also in the same compositional field. Near 30 kb, however, they would be in the compositional field  $\text{Mg}_2\text{SiO}_4\text{--MgSiO}_3\text{--CaAl}_2\text{SiO}_6$  as shown by the dashed curve  $L_2$  (Fig. 22). B. T. C. Davis (*Year Book* 63, pp. 165–171) found that this composition is covered by the garnet liquidus at 40 kb, and the invariant or piercing point at 40 kb is most probably in the same compositional field as that at 30 kb. The enstatite in this system is aluminous at high pressures, and its composition would not be on the plane  $\text{Mg}_2\text{SiO}_4\text{--CaAl}_2\text{SiO}_6\text{--SiO}_2$ ; in consequence the compositions of the liquids coexisting with the enstatite would also be off this plane. For this reason forsterite and enstatite are joined by clinopyroxene at lower temperatures, as shown by Fig. 23, and at the invariant point, forsterite, enstatite, clinopyroxene, and spinel coexist with liquid.

EAN-40 has also been studied. The starting material is a crystallized glass of the composition enstatite 60, anorthite 40 (weight per cent), prepared by Hytönen and Schairer (*Year Book* 59, pp. 71, 72). It is found that this composi-

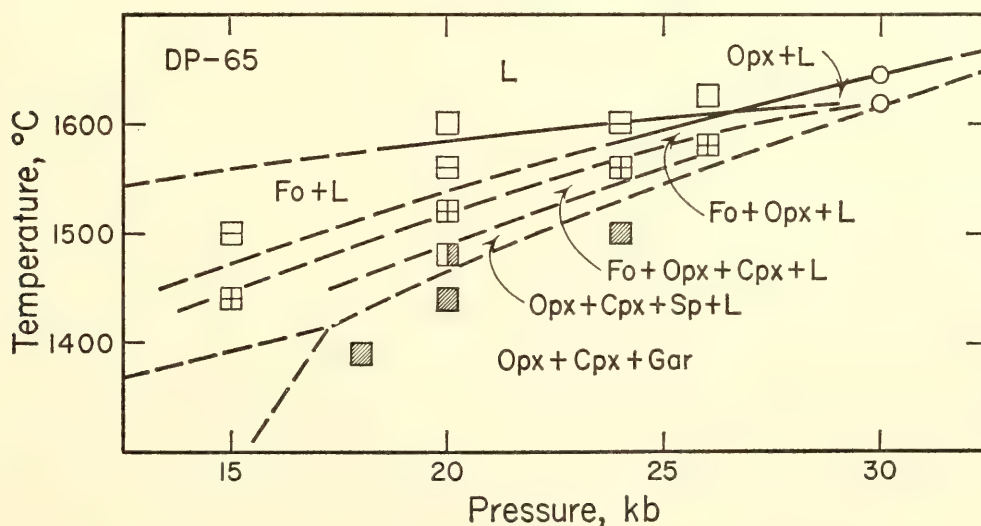


Fig. 23.  $P$ – $T$  diagram for the composition diopside 35, pyrope 65 (weight per cent). Circles at 30 kb are data from O'Hara (*Year Book* 62, pp. 76–77). Cpx, clinopyroxene; Fo, forsterite; Gar, garnet; L, liquid; Opx, orthopyroxene or enstatite; Sp, spinel.



tion is covered by the forsterite liquidus up to about 10 kb and covered by the enstatite liquidus above 10 kb. The dashed boundary curve  $L_1$  shown in Fig. 22, therefore, represents the forsterite-enstatite boundary curve in the pressure range 10 to 26 kb. It should be noted that the forsterite-enstatite liquidus boundary shifts from the silica-rich to the silica-poor side with increasing pressure and, in consequence, the invariant point would also shift toward the silica-poor side with increasing pressure.

### *The System Forsterite-Nepheline-Silica*

The system forsterite-nepheline ( $\text{NaAlSiO}_4$ )-silica (Fig. 24)—which contains enstatite, jadeite ( $\text{NaAlSi}_2\text{O}_6$ ), and albite ( $\text{NaAlSi}_3\text{O}_8$ ) as intermediate compounds—is another important ternary system used in the search for the genesis of basalt. Schairer and Yoder (*Year Book 60*, pp. 141–144) studied the liquidus relations of this system at 1 atm and showed that the invariant point forsterite + protoenstatite + albite +

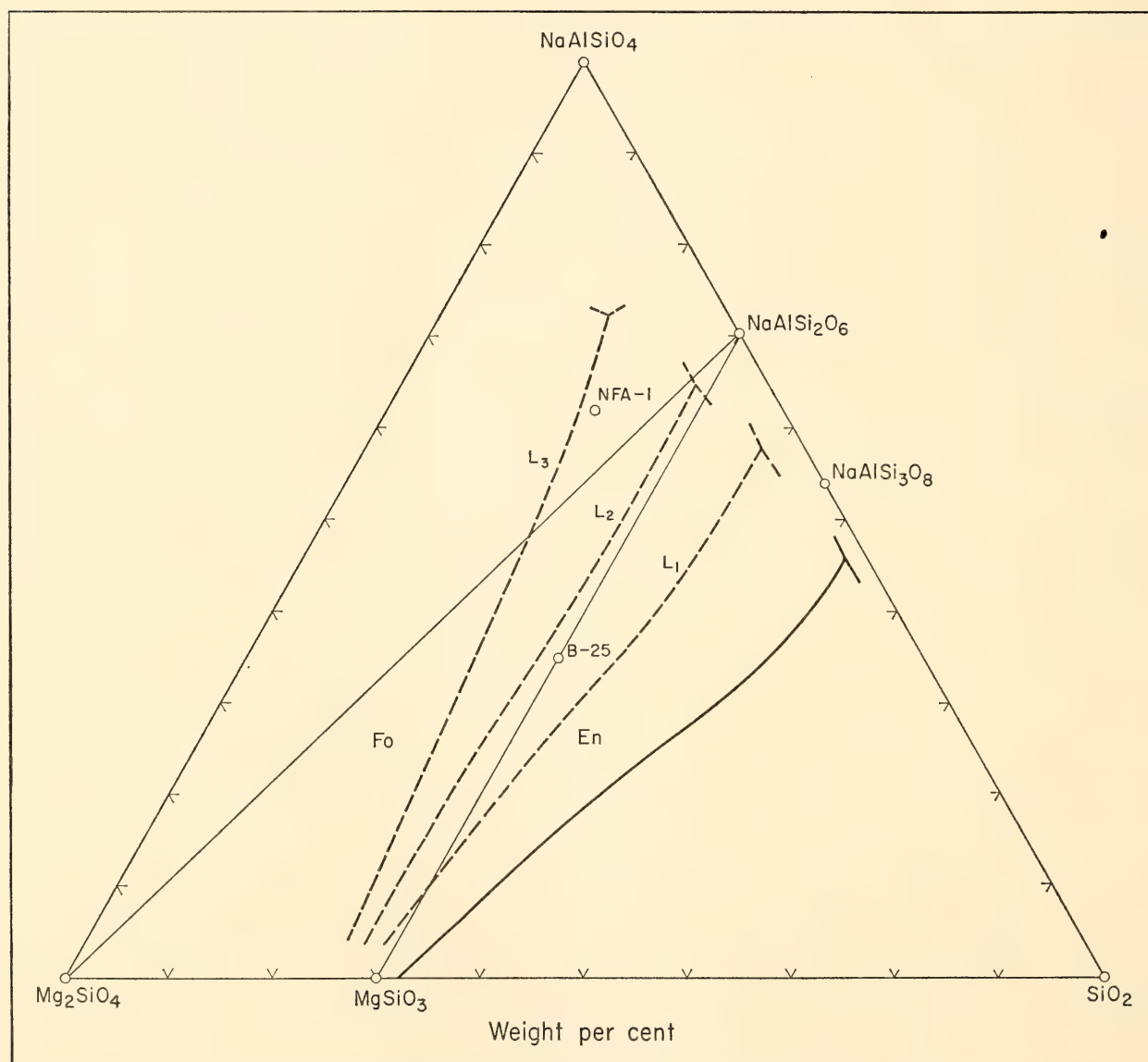


Fig. 24. The forsterite (Fo)-enstatite (En) liquidus boundary at different pressures in the system forsterite ( $\text{Mg}_2\text{SiO}_4$ )-nepheline ( $\text{NaAlSiO}_4$ )-silica. Solid curve is a forsterite-liquidus boundary at 1 atm determined by Schairer and Yoder (*Year Book 60*, p. 142). Dashed curves  $L_1$ ,  $L_2$ , and  $L_3$  indicate the forsterite-enstatite boundary curves at pressures near 10, 20, and 30 kb, respectively.  $\text{NaAlSi}_2\text{O}_6$  and  $\text{NaAlSi}_3\text{O}_8$  show compositions of jadeite and albite, respectively. B-25 and NFA-1 are compositions studied.

liquid and the forsterite-protosthenite boundary curve exist in the triangular field  $\text{MgSiO}_3\text{-NaAlSi}_3\text{O}_8\text{-SiO}_2$  as shown by the solid curve in Fig. 24. Yoder and Tilley (1962) conducted experiments on the composition forsterite 1, albite 1 (molecular ratio), shown by B-25 of Fig. 24 at 1,250°C and 33 kb, having suggested that the forsterite-albite join is replaced by the enstatite-jadeite join, which would be a new equilibrium thermal barrier at this pressure. It is expected, therefore, that the forsterite-enstatite (or pyroxene) liquidus boundary lies on the nepheline side of the enstatite-jadeite join at 33 kb. Yoder (*Year Book 63*, pp. 97–101) studied the forsterite-albite join at 9 kb and concluded that the join is binary at this pressure on the basis of the interpretation that enstatite crystallizing in the liquid is metastable. Based on his interpretation, the forsterite-enstatite liquidus boundary and the invariant point forsterite + enstatite + albite + liquid most probably lie on the silica-rich side of the join  $\text{MgSiO}_3\text{-NaAlSi}_3\text{O}_8$  at 9 kb.

In the present experiments the composition of B-25 has been investigated in the pressure range 13–25 kb. The preliminary  $P$ - $T$  diagram for this composition is shown in Fig. 25. As shown in the figure, forsterite crystallizes as a primary phase up to about 16 kb, and above this

pressure enstatite is the primary phase, indicating that this composition is covered by the forsterite liquidus up to about 16 kb and by the enstatite liquidus above about 16 kb. The compositions on the enstatite-jadeite join more jadeite-rich than composition B-25 would be covered by the forsterite liquidus up to pressures higher than 16 kb. It is suggested, therefore, that the invariant point, which may be off the plane forsterite-nepheline-silica, exists in the compositional field  $\text{MgSiO}_3\text{-NaAlSi}_2\text{O}_6\text{-SiO}_2$  at least up to 16 kb and possibly up to about 20 kb, as shown by the dashed boundary curve  $L_1$  (Fig. 24). At pressures higher than 20 kb, however, the forsterite-enstatite liquidus boundary and the invariant or piercing point exist in the compositional field  $\text{Mg}_2\text{SiO}_4\text{-MgSiO}_3\text{-NaAlSi}_2\text{O}_6$ , as shown by the dashed boundary curve  $L_2$  (Fig. 24). Enstatite crystallizing in the  $\text{Opx} + L$  region of Fig. 25 is sharply prismatic or rectangular, about 0.05 mm long, and appears to be a stable phase. There is still a possibility, however, that the enstatite in the liquid may be metastable, as mentioned by Yoder (*Year Book 63*, p. 98). If enstatite in the  $\text{Opx} + L$  region is metastable, the composition B-25 would be covered by the forsterite liquidus up to a pressure higher than 16 kb, and the forsterite-enstatite liquidus boundary and

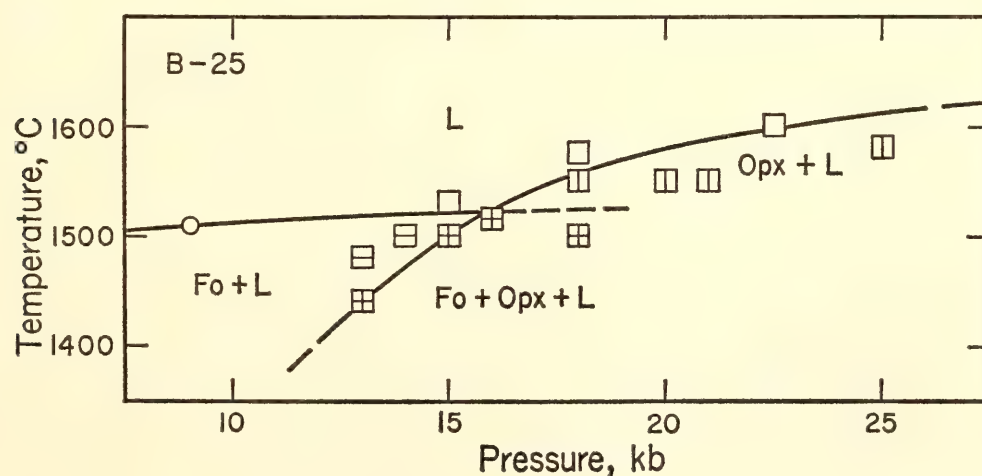


Fig. 25.  $P$ - $T$  diagram for composition forsterite 35, albite 65 (weight per cent). Abbreviations as in Fig. 23. Circle at 9 kb is from Yoder (*Year Book 63*, pp. 97–101).



the invariant point would lie on the silica-rich side of  $L_2$ .

The composition forsterite 18, nepheline 62, silica 20 (weight per cent), shown by point NFA-1 in Fig. 24 has been examined in the present experiments in the pressure range 10–35 kb. The results of the experiments in the liquidus region above 20 kb are shown in the  $P$ - $T$  plane for this composition (Fig. 26). As shown in the figure, the primary phase to crystallize is forsterite up to about 30 kb and enstatite at pressures higher than 30 kb. This evidence indicates that the invariant point and a part of the forsterite-enstatite boundary exist in the compositional field  $Mg_2SiO_4$ - $NaAlSiO_4$ - $NaAlSi_2O_6$  at pressures higher than about 30 kb, as shown by the dashed boundary curve  $L_3$  (Fig. 24). At pressures higher than 35 kb, clinopyroxene (jadeitic pyroxene) may be the primary phase for this composition. It should be noted that the forsterite-enstatite liquidus boundary and the invariant point shift drastically from the silica-rich to the silica-poor side with increasing pressure, as shown by Fig. 24, a fact of considerable interest in connection with the genesis of silica-deficient magmas.

Results obtained by present experiments on the systems forsterite- $CaAl_2SiO_6$ -silica and forsterite-nepheline-silica yield information on the compositions of

magmas formed by the partial melting of the mantle peridotites, for the compositions of mantle peridotites probably lie close to the forsterite-enstatite join in both of the present ternary systems (Figs. 22 and 24). The first liquid to form by the partial melting of such peridotites has a composition at or close to the invariant point where olivine and enstatite coexist. As already mentioned, the forsterite-enstatite liquidus boundary shifts from the silica-rich to the silica-poor side with increasing pressure, and consequently the invariant point where forsterite and enstatite coexist also shifts toward the silica-poor side with increasing pressure in both of the present systems. The forsterite-enstatite boundary and the invariant point in the system diopside-forsterite-enstatite also shift from the silica-rich to the silica-poor side with increasing pressure.

These facts indicate that the compositions of the magmas produced by the partial melting of the mantle peridotites become more silica poor with increase in the pressure at which melting occurs. It is suggested, therefore, that magmas of alkali basalt composition may be produced by partial melting at greater depths in the upper mantle than are magmas of tholeiite composition. This supports the hypotheses of Kuno *et al.* (1957), and Kushiro and Kuno (1963).

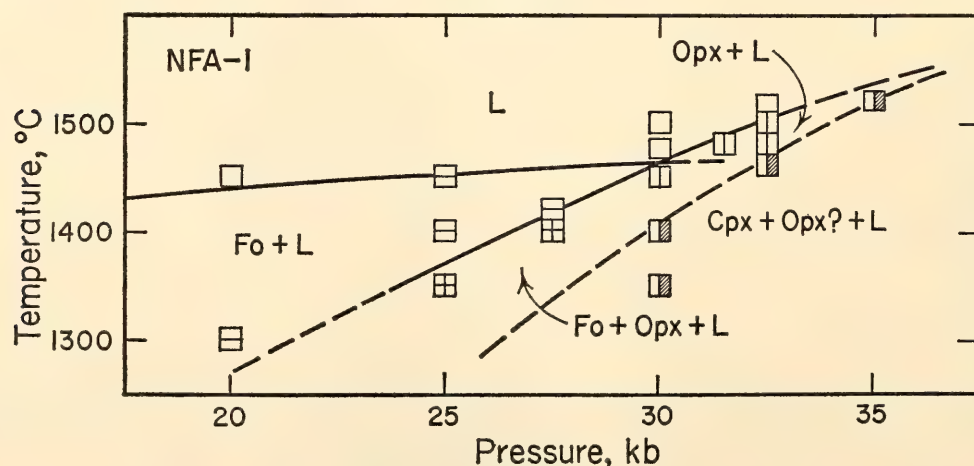


Fig. 26.  $P$ - $T$  diagram for composition forsterite 18, nepheline 2, silica 20 (weight per cent). Abbreviations as in Fig. 23.

As shown in Fig. 24, a part of the forsterite-enstatite boundary and the invariant point lie in the compositional field forsterite-nepheline-jadeite at pressures higher than about 30 kb. As the compositions in this triangular field are highly undersaturated with silica, including those of nepheline-basanite and nepheline-basalt, it is suggested that the magmas of such compositions can be produced by the partial melting of the mantle peridotite at depths greater than about 100 km.

The results of the present experiments also yield information on the crystallization course of basaltic magmas at high pressures. The fact that the forsterite-enstatite boundary shifts toward the silica-poor side with increasing pressure suggests that the fractional crystallization of olivine tholeiitic magmas produces more silica-poor magmas with increase in the depth of their crystallization, because the crystallization course of olivine tholeiitic magmas follows the olivine-enstatite boundary. This possibility has already been mentioned by Yoder and Tilley (1962) and Green and Ringwood (1964). In the depth range greater than 100 km it seems possible that olivine tholeiitic magmas yield even nepheline-basanite or nepheline-basalt magma by their fractional crystallization. It should be mentioned that enstatite can crystallize from such highly silica-undersaturated magmas at high pressures, which may suggest the possibility that some peridotite inclusions found in alkali basalts are the crystallization products of basalt magmas.

## COEXISTENCE OF NEPHELINE AND ENSTATITE AT HIGH PRESSURES

*I. Kushiro*

Nepheline ( $\text{NaAlSi}_3\text{O}_8$ ) and enstatite ( $\text{MgSiO}_3$ ) or hypersthene ( $[\text{Mg}, \text{Fe}]\text{SiO}_3$ ) have been considered incompatible minerals in rocks found in the surface (Shand, 1943) and in synthetic systems at 1 atm (Schairer and Yoder, *Year Book*

60). Nepheline + 4 enstatite is isochemical with albite ( $\text{NaAlSi}_3\text{O}_8$ ) + 2 forsterite ( $\text{Mg}_2\text{SiO}_4$ ). The latter assemblage is common in basic igneous rocks, but as albite exists as a component of plagioclase this assemblage is stable relative to the nepheline + enstatite assemblage in the  $P$ - $T$  conditions under which the basic igneous rocks crystallized. However, enstatite occurs as a main constituent of the peridotite nodules in the nepheline-bearing alkali basalts as described by several authors (e.g., Ross, Foster, and Myers, 1954) and as large phenocrysts in some alkali basalts (Kuno, 1965).

The occurrence of enstatite-bearing peridotite nodules in alkali basalts has been interpreted by nonequilibrium relations because of the accidental xenolith (e.g., Ross, Foster, and Myers, 1954; Kuno, 1959a; Wilshire and Binns, 1961) or equilibrium relations at high pressures (e.g., Frechen, 1948; Yoder and Tilley, 1962; O'Hara and Mercy, 1963). Miyashiro (1960) suggested on the basis of thermodynamic calculations that the nepheline + clinoenstatite assemblage is expected to be stable at high pressures instead of the albite + forsterite assemblage and that the extraction of clinoenstatitic pyroxene from olivine basaltic magma would produce magmas of the composition of feldspathoid-bearing rocks at high pressures. Yoder and Tilley (1962) have shown that the albite-forsterite join is not stable at 33 kb and is replaced by the enstatite-jadeite ( $\text{NaAlSi}_2\text{O}_6$ ) join, which is a new thermal barrier, indicating that the separation of enstatite<sup>4</sup> can produce alkali basalt magma having normative nepheline at high pressures, and that enstatite could occur in alkali basalts. Green and Ringwood (1964) suggested the same possibility on the basis of their high-pressure experiments on natural olivine

<sup>4</sup> Recently Tilley and Yoder (*Year Book* 63) reported that the separation of subcalcic augite would be a more likely process to produce alkali basalt magma.



basalts. However, the coexistence of nepheline and enstatite or hypersthene has not been reported. In the course of work on the system forsterite-nepheline-silica at high pressures it has been found that enstatite and nepheline may coexist stably.

A glass and a crystallized glass of the composition nepheline<sub>62</sub>forsterite<sub>18</sub>silica<sub>20</sub>, weight per cent (NFA-1 in Fig. 27) and a glass of the composition Ab<sub>65</sub>Fo<sub>35</sub> (B-25 in Fig. 27) both prepared by Schairer and Yoder (*Year Book 60*), were studied in the pressure range 10–35 kb at 1,050° to 1,400°C, with a solid-media piston-cylinder type of apparatus similar to that designed by Boyd and England (*Year Books 57 and 60*). The phases crystallized at subsolidus temperatures were fine grained and could be identified only by X-ray powder patterns, but those crystallized in the presence of liquid could be identified under the microscope.

Glass of composition NFA-1 was crystallized into forsterite + nepheline + albite at 10 kb and 1,100°C, whereas it was crystallized into enstatite + nepheline + albite at 15–20 kb and

1,100°C. At 12 kb and 1,100°C forsterite and albite coexist with nepheline and enstatite, indicating that the reaction begins to take place near this condition. Glass of composition B-25 was also crystallized into enstatite + nepheline + albite at 11, 14, and 17.5 kb at 1,100°C. At 9 kb this composition consists of forsterite and albite, as shown by Yoder (*Year Book 63*). These phase relations are shown in the system forsterite-nepheline-silica (Fig. 27). Figure 27A shows the tie lines below 11 kb at 1,100°C, and the solid lines in Fig. 27B show the tie lines at 11–20 kb and the same temperature. Enstatite would contain alumina under the conditions of the present experiments, however, and its composition may not be on this plane. The crystalline mixture of the forsterite + nepheline + albite assemblage was recrystallized into the enstatite + nepheline + albite assemblage at 22.5 kb and 1,200°C. At 1,125°C, however, the reaction rate is very slow, and forsterite and albite were not reacted in a two-hour experiment at 21 kb. At 22 kb and 1,100°C jadeitic pyroxene begins to crystallize from glass of composition

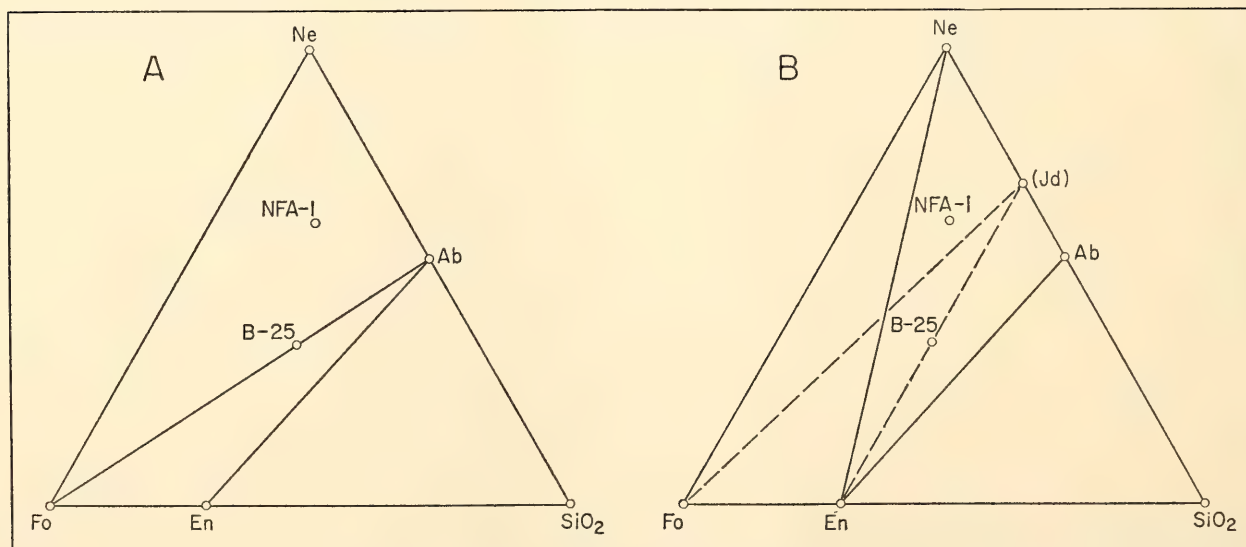


Fig. 27. Tie lines of coexisting phases in the system forsterite ( $\text{Mg}_2\text{SiO}_4$ )-nepheline ( $\text{NaAlSi}_3\text{O}_8$ )-silica. A. Solid lines indicate tie lines at pressures below 11 kb at 1,100°C. B. Solid lines are tie lines in pressure range 11 to 20 kb at 1,100°C; dashed lines indicate tie lines at 33 kb at 1,250°C given by Yoder and Tilley (1962). Ab, albite; En, enstatite; Fo, forsterite; Jd, jadeite; Ne, nepheline; NFA-1 and B-25 are compositions studied.

NFA-1, and above 25 kb glass of the same composition was crystallized into jadeitic pyroxene + nepheline. The jadeitic pyroxene may be a solid solution between jadeite and  $\text{MgSiO}_3$ . In the experiments at 20 and 24 kb at  $1,250^\circ\text{C}$ , nepheline and enstatite coexist in the presence of liquid. The enstatite in the liquid forms sharp prismatic or rectangular crystals 0.02 to 0.05 mm long.

It should be noted that the enstatite-nepheline join is not a thermal barrier on the liquidus surface at pressures where this join is stable. As shown in Fig. 24, the forsterite liquidus covers the composition NFA-1 up to about 30 kb, indicating that the forsterite liquidus covers a part of the enstatite-nepheline join up to about 30 kb. The liquidus relations in the system forsterite-nepheline-silica are discussed in another part of this report.

There is a possibility that enstatite coexisting with nepheline is metastable. The metastable formation of enstatite has been observed by Schairer and Yoder (*Year Book 60*) in the system forsterite-albite, and by Yoder (1952) and Chinner and Schairer (1962) in the pyrope composition. In these cases enstatite crystallizes in addition to the stable phases, that is, enstatite crystallizes with albite and forsterite from a glass on the join forsterite-albite and it crystallizes with spinel, cordierite, and forsterite from glass of pyrope composition. In the present experiments, however, forsterite is absent and enstatite is the only magnesian mineral of the new phase assemblage that satisfies the phase rule. In addition, the relative amount of enstatite did not decrease in a longer experiment at 20 kb and  $1,100^\circ\text{C}$ , and the nepheline + enstatite + albite assemblage was obtained from the forsterite + albite + nepheline assemblage immediately below the solidus temperature. These facts indicate that enstatite coexisting with nepheline is not metastable and that there is a  $P$ - $T$  region in which the nepheline + enstatite assemblage is stable, a conclusion supported by

thermodynamic calculations made by Miyashiro (1960) and by the following calculation.

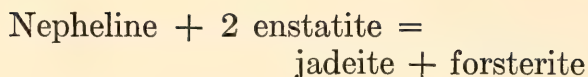
The univariant curve for the reaction albite + 2 forsterite = nepheline + 4 enstatite can be calculated from the thermochemical data of the four pure compounds given by Kracek *et al.* (*Year Book 52*) and Kubaschewski and Evans (1958). The volume change ( $\Delta V$ ), the standard heat ( $\Delta H^\circ_{298}$ ), and the standard entropy ( $\Delta S^\circ_{298}$ ) of the reaction are  $-9.4$  cc/mole,  $0.4$  kcal/mole, and  $-0.8$  cal/degree mole, respectively, using thermochemical data for clinoenstatite instead of enstatite. The free energy of the reaction at pressure  $P$  and temperature  $T$  is given by

$$\Delta G_{T,P} = \Delta H^\circ_{298} + \int_{298}^T \Delta C_p dT - T(\Delta S^\circ_{298} + \int_{298}^T \frac{\Delta C_p}{T} dT) + (P-1)\Delta V$$

As  $\Delta C_p$  (difference of the molar heat between the products and the reactants of the reaction) is close to zero in the solid reaction, the equation of the univariant curve for the reaction can be obtained from the condition  $\Delta G_{T,P} = 0$ . The equation thus obtained is  $P = 3.5T + 1,760$ , where  $P$  is in bars and  $T$  in degrees centigrade. The curve passes very near the point  $P \sim 6$  kb,  $T \sim 1,100^\circ\text{C}$ . Considering the nature of the assumptions and the uncertainty of the thermochemical data, the calculation is not inconsistent with the results of the present experiments. It is emphasized that the calculation based on the thermochemical data shows the existence of a stability field of the nepheline + enstatite assemblage at high pressures.

At 33 kb and  $1,250^\circ\text{C}$  the forsterite-jadeite join is stable, as shown in the experiments by Yoder and Tilley (1962). Therefore, the following reaction would take place at some pressure between 22 and 33 kb and a temperature between  $1,150^\circ\text{C}$  and  $1,250^\circ\text{C}$ :





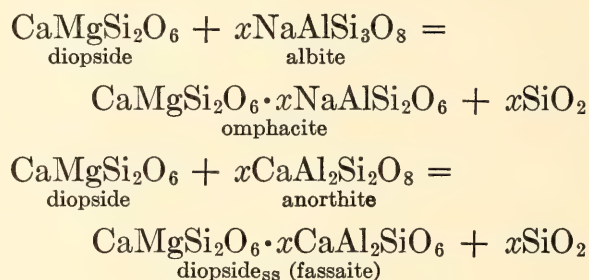
The tie lines between coexisting phases on the higher pressure side of the univariant curve for this reaction are shown by the dashed lines in Fig. 27B, which are the same as those given by Yoder and Tilley (1962).

The results of the present experiments are of significance for petrological problems. Forsterite and albite, which are essential constituents of olivine basalt or olivine gabbro, would react to form enstatite + nepheline. Although the univariant curve for the reaction has not been determined, the reaction probably occurs in the lower part of the continental crust. The reaction between forsterite and anorthite to form pyroxenes and spinel would also take place in the continental crust (Kushiro and Yoder, *Year Book 63* and this report). In addition, if diopside (or clinopyroxene) is present, both albite and anorthite react with diopside to form diopside solid solution at high pressures (Kushiro, this report). It is possible, therefore, that the mineral assemblages of olivine basalt or olivine gabbro may not be stable in the lower part of the continental crust and pyroxene-rich rocks may be formed. The coexistence of nepheline and enstatite at both liquidus and subsolidus temperatures suggests that enstatite in the peridotite inclusions in alkali basalts might be in equilibrium with host rocks or magmas at high pressures, although this does not mean that all the peridotite inclusions in alkali basalts are the crystallization products of basalt magmas. The large phenocrysts of aluminous orthopyroxene found in the alkali basalt at Takashima (Kuno, 1965) may be products of equilibrium crystallization at high pressures, as Kuno has suggested. The crystallization of enstatite in alkali basalt magma is discussed in the section on the system forsterite-nepheline-silica at high pressures (Kushiro, this report).

## CLINOPYROXENE SOLID SOLUTIONS AT HIGH PRESSURES

*I. Kushiro*

Clinopyroxene occurs in various kinds of igneous and metamorphic rocks, and it is expected that clinopyroxene will crystallize under a wide range of physicochemical conditions. The chemical analyses of the clinopyroxenes may be represented in terms of several pyroxene components in solid solution. Among the pyroxene components, jadeite ( $\text{NaAlSi}_2\text{O}_6$ ) and Ca-Tschermak's component ( $\text{CaAl}_2\text{SiO}_6$ ) seem to be important as indicators of the physical conditions. The diopside solid solutions containing the jadeite are obtained by the reactions between albite and diopside, and those containing Ca-Tschermak's components, by anorthite and diopside; the reactions are shown by



The diopside solid solution containing a considerable amount of Ca-Tschermak's component has been called fassaite. The molar volume of the assemblage on the right of each equality is smaller than that of the one on the left; accordingly, the contents of the Ca-Tschermak's and jadeite components would be expected to increase with increasing pressure at constant temperature.

The present experiments have been carried out to determine by synthesis the contents of the jadeite and Ca-Tschermak's components in diopside in a wide  $P$ - $T$  range. For this purpose the subsolidus phase relations have been studied on the joins diopside-albite and diopside-anorthite in the pressure range 8–37 kb and in the temperature range 1,050°C–1,350°C, with a solid-media piston-

cylinder type of apparatus similar to that designed by Boyd and England (*Year Books 57 and 60*). The starting materials are glass and crystallized glass of the compositions on these two joins prepared by Schairer. The phases after the experiments were identified by X-ray powder patterns in most cases.

*The Join Diopside-Albite*

The join diopside-albite at 1 atm has been studied in part by Bowen (1915) and more recently by Schairer and Yoder (1960), who found that this system is not binary, since sodic plagioclase appears at both liquidus and subsolidus temperatures. Figure 28 shows isothermal sections of the diopside-albite join at 1,350°C, 1,250°C, and 1,150°C in the pressure range 13–32 kb. Glass was used

as a starting material for all the experiments on this join. There are two different regions in phase assemblage in each isothermal section, namely, the region of the Omph + Qz assemblage and that of the Omph + Pl + Qz assemblage. The phase relations are shown in the ternary system  $\text{CaMgSi}_2\text{O}_6\text{-NaAlSi}_3\text{O}_8\text{-SiO}_2$ . The region of the Omph + Qz assemblage on the diopside-albite join corresponds to the two-phase region Omph + Qz in the ternary system, and that of the Omph + Pl + Qz assemblage corresponds to the three-phase region Pl + Qz + Omph of composition *S*. The boundary curve between the two assemblages Omph + Qz and Omph + Pl + Qz indicates the shift of the point *R* with changing pressure. At 1 atm sodic plagioclase appears in this system instead of pure albite as demon-

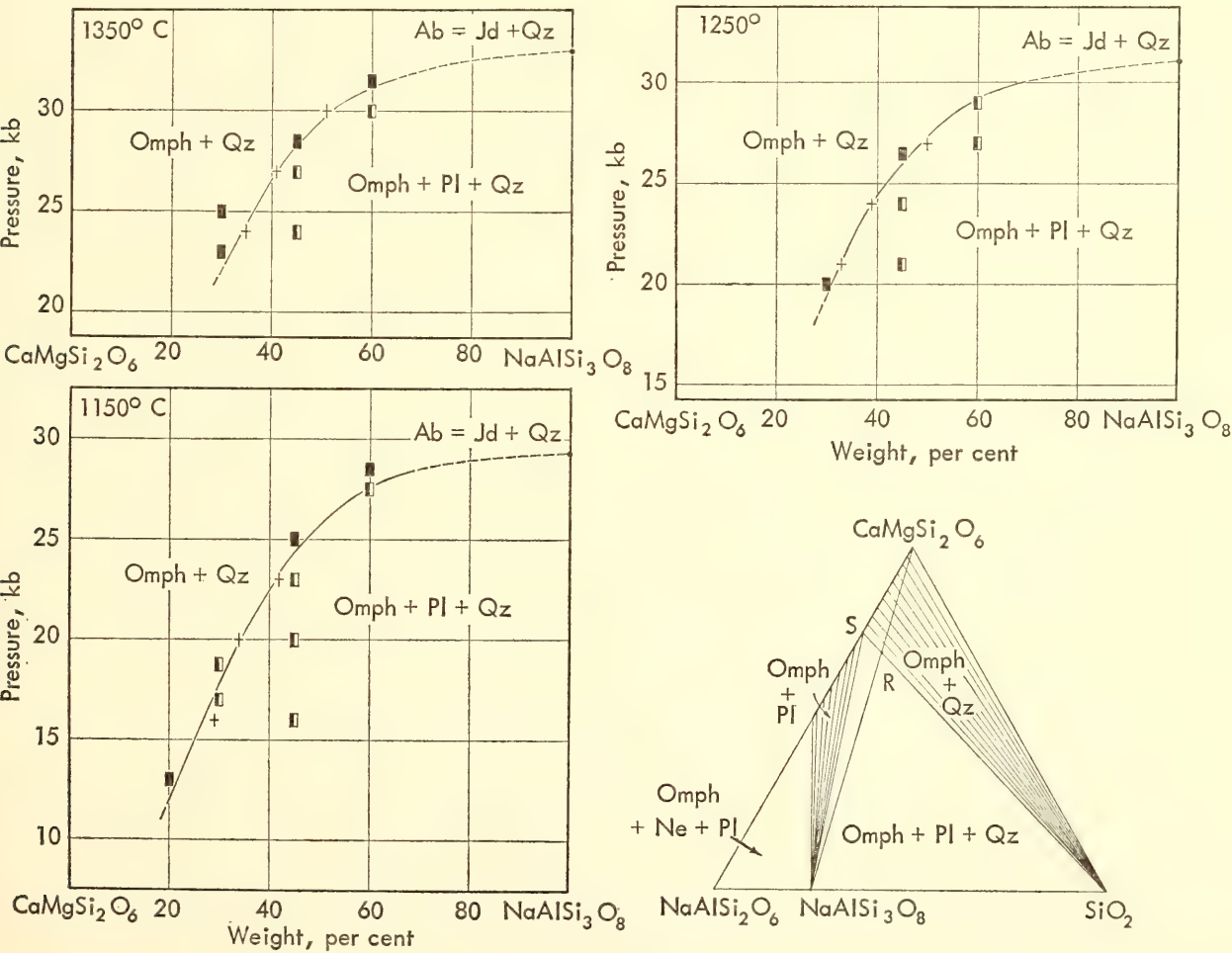


Fig. 28. Subsolidus phase relations on the join diopside ( $\text{CaMgSi}_2\text{O}_6$ )-albite ( $\text{NaAlSi}_3\text{O}_8$ ) at 1,350°C, 1,250°C, and 1,150°C. The lower right diagram is the ternary system diopside-jadeite ( $\text{NaAlSi}_2\text{O}_6$ )-silica showing the subsolidus phase relations. Omph, omphacite; Pl, sodic plagioclase; Qz, quartz.



strated by Schairer and Yoder (1960), and it is expected that sodic plagioclase will also appear in this system at high pressures. The composition of omphacite coexisting with sodic plagioclase, therefore, may not be on the diopside-jadeite join.

As shown in Fig. 28 the stable region of the Omph + Qz assemblage increases at the expense of that of the Omph + Pl + Qz assemblage with increasing pressure at constant temperature, indicating that the content of jadeite in omphacite increases with the increase of pressure. The curve finally terminates at the reaction point albite  $\rightleftharpoons$  jadeite + quartz, the  $P$ - $T$  conditions for which have been

determined by Birch and LeComte (1960). Crosses on the boundary curves are the points obtained from the compositions of omphacites coexisting with plagioclase and quartz, the composition of omphacite having been determined by the  $d$  value of the (311) reflection.

Figure 29 shows boundary curves at 1,050°C, 1,150°C, 1,250°C, and 1,350°C. The stable region of the Omph + Qz assemblage increases with decreasing temperature at constant pressure, so that the jadeite content in omphacite must increase with decreasing temperature at constant pressure. These boundary curves show the position of  $R$  in the system  $\text{CaMgSi}_2\text{O}_6$ - $\text{NaAlSi}_3\text{O}_8$ - $\text{SiO}_2$  (Fig.

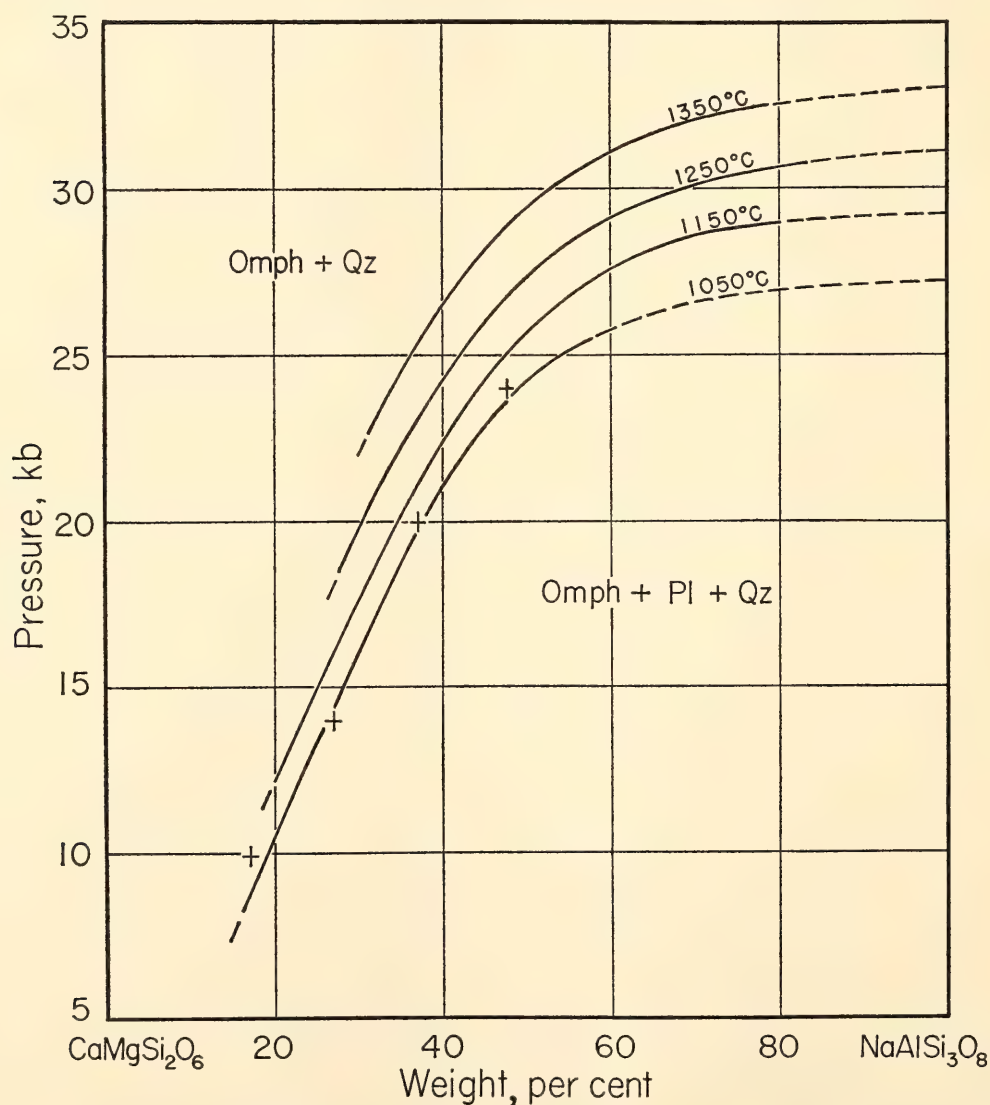


Fig. 29. Boundary curve between the two assemblages omphacite + quartz and omphacite + plagioclase + quartz at 1,050°C with those at 1,350°, 1,250°, and 1,150°C. The curve for 1,050°C was determined by omphacite composition; others are taken from Fig. 28.

28) in a wide  $P$ - $T$  range. The composition of omphacite coexisting with sodic plagioclase and quartz, shown by  $S$  in the ternary system of Fig. 28, can be obtained by projecting  $R$  onto the join diopside-jadeite from the  $\text{SiO}_2$  apex. In this fashion the composition of omphacite coexisting with sodic plagioclase and quartz, or the maximum content of jadeite in omphacite in the silica-saturated condition, may be obtained in a wide  $P$ - $T$  range. Figure 30 shows the equicomposition curves of omphacite on the basis of the boundary curves of Fig. 29. The equicomposition curves indicate the maximum solubility of jadeite in omphacite in the silica-saturated condition. That is, omphacite can contain  $X$  weight per cent jadeite along the equicomposition curve for  $X$  per cent jadeite in the silica-saturated condition. The curves also indicate the stability field of omphacite in the silica-saturated condition. That is, the omphacite with  $X$  weight per cent jadeite is stable on the higher-pressure side of the equicomposition curve for  $X$  per cent jadeite. The

curve for 100 per cent jadeite must be the same as the univariant curve for the breakdown of albite into jadeite + quartz, which has been determined by Birch and LeComte (1960). For omphacites containing more than 70 per cent jadeite the curves are close to the univariant curve for the breakdown of albite. The equicomposition curve for omphacite containing 40 per cent jadeite is close to the univariant curve for the formation of jadeite from nepheline + albite determined by Robertson *et al.* (1957), and by Bell (*Year Book 63*).

#### *The Join Diopside-Anorthite*

The join diopside-anorthite was studied at 1 atm by Osborn (1942) in his work on the system  $\text{CaSiO}_3$ -diopside-anorthite. He suggested that diopside in this system is aluminous and that, in consequence, the join is not binary. Hytönen and Schairer (*Year Book 60*) have shown that diopside in the system diopside-anorthite contains about three weight per cent Ca-Tschermak's component at  $1,135^\circ\text{C}$  at 1 atm. Clark, Schairer, and

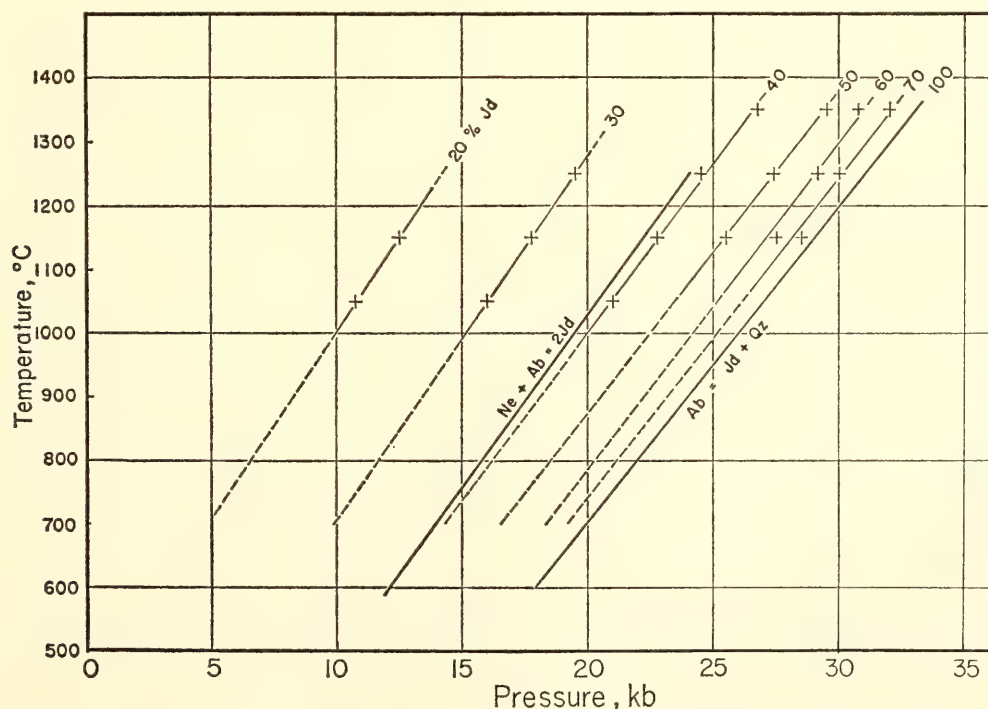


Fig. 30. Equicomposition curves of omphacite coexisting with quartz. Numbers indicate weight percentage of jadeite in omphacite. Univariant curves of the reactions  $\text{Ne} + \text{Ab} = 2\text{Jd}$  and  $\text{Ab} = \text{Jd} + \text{Qz}$  are from Robertson, Birch, and MacDonald (1957), and Birch and LeComte (1960), respectively.



de Neufville (*Year Book 61*), in their studies on the system diopside- $\text{CaAl}_2\text{SiO}_6$ -silica, found that anorthite melts incongruently at 20 kb and that diopside is highly aluminous near the liquidus temperatures at the same pressure.

Figure 31 shows the isothermal sections of the diopside-anorthite join at sub-solidus temperatures, 1,350°C and 1,150°C, in the pressure range of 8–37 kb. Glass was used as a starting material for all the experiments at 1,150°C, whereas crystallized glass was used for all the experiments at 1,350°C. As shown in the figure, there are three different regions in the phase assemblage: the  $\text{Di}_{\text{ss}} + \text{Qz}$  assemblage on the Di-rich side, the  $\text{Di}_{\text{ss}} + \text{An} + \text{Qz}$  assemblage on the An-rich side, and the garnet-bearing assemblage on the higher-pressure side for both the isothermal sections. At 1,150°C a small amount of anorthite coexists with garnet

and the assemblage is  $\text{Di}_{\text{ss}} + \text{Gar} + \text{An} + \text{Qz}$ , whereas at 1,350°C anorthite is absent and the assemblage is  $\text{Di}_{\text{ss}} + \text{Gar} + \text{Qz} + (\text{Ky})$ . Although kyanite was not detected in any runs at 1,350°C, it is probably present in the higher-pressure region of the isothermal section at 1,350°C, since anorthite breaks down into grossularite + kyanite + quartz above 30 kb near 1,350°C (Boyd and England, *Year Book 60*; E. C. Hansen, personal communication, 1965). The phase relations at lower pressures are shown in the ternary system  $\text{CaMgSi}_2\text{O}_6$ - $\text{CaAl}_2\text{Si}_2\text{O}_8$ - $\text{SiO}_2$  (Fig. 31). The region of the  $\text{Di}_{\text{ss}} + \text{Qz}$  assemblage on the diopside-anorthite join corresponds to the two-phase region  $\text{Di}_{\text{ss}} + \text{Qz}$  in the ternary system and that of the  $\text{Di}_{\text{ss}} + \text{An} + \text{Qz}$  assemblage corresponds to the three-phase region  $\text{Di}_{\text{ss}}(\text{Q}) + \text{An} + \text{Qz}$ . The boundary curves between the two

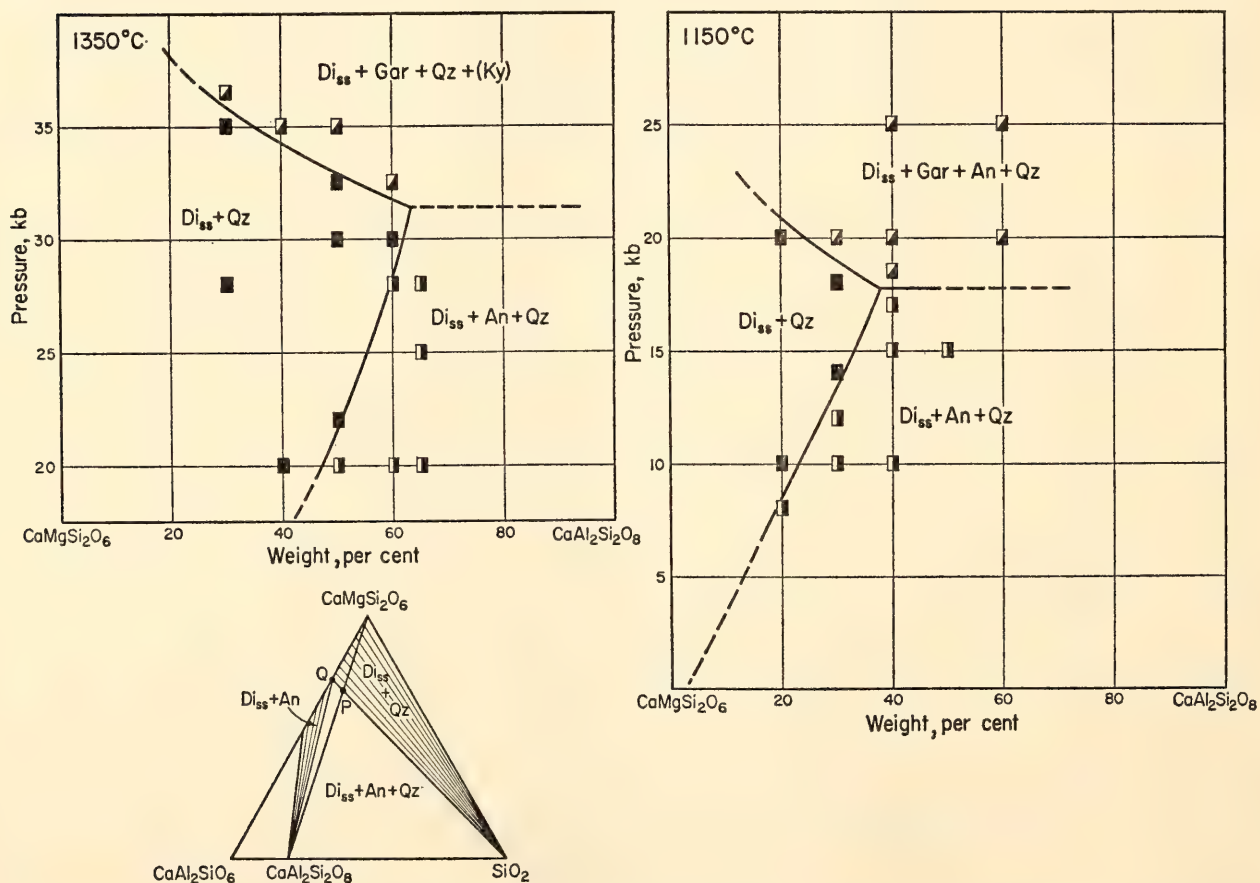


Fig. 31. Subsolidus phase relations on the join diopside-anorthite ( $\text{CaAl}_2\text{Si}_2\text{O}_8$ ) at 1,350° and 1,150°C. Lower left diagram is the ternary system diopside- $\text{CaAl}_2\text{Si}_2\text{O}_6$ -silica showing the subsolidus phase relations at lower pressures. An, anorthite;  $\text{Di}_{\text{ss}}$ , diopside solid solution; Gar, garnet; Ky, kyanite; Qz, quartz.

assemblages  $\text{Di}_{\text{ss}} + \text{Qz}$  and  $\text{Di}_{\text{ss}} + \text{An} + \text{Qz}$  indicate the shift of the point  $P$  with changing pressure.

As shown in Fig. 31, the range of the  $\text{Di}_{\text{ss}} + \text{Qz}$  assemblage increases, whereas that of the  $\text{Di}_{\text{ss}} + \text{An} + \text{Qz}$  assemblage decreases with the increase of pressure at constant temperature, indicating that the content of the Ca-Tschermak's component in diopside increases with the increase of pressure at constant temperature. On the other hand, if garnet is stable, the garnet field expands at the expense of the  $\text{Di}_{\text{ss}} + \text{Qz}$  field or the content of the Ca-Tschermak's component decreases as pressure is increased at constant temperature. Consequently, the area in which the  $\text{Di}_{\text{ss}} + \text{Qz}$  assemblage is stable and the content of Ca-Tschermak's component in diopside must have maximum values. The composition of the garnet formed at  $1,350^{\circ}\text{C}$  at 32.5 kb is about pyrope 1, grossularite 9 (molecular ratio), as measured by the (420) reflection, using the cell edge-composition relation proposed by Chinner, Boyd, and England (*Year Book* 59). The maximum content of the Ca-Tschermak's component is about 60 weight per cent, which is attained at about 30 kb at  $1,350^{\circ}\text{C}$ . At  $1,150^{\circ}\text{C}$ , however, the maximum content is about 40 weight per cent at about 18 kb. It is noted that there is no complete solid solution between diopside and the Ca-Tschermak's component under silica-saturated conditions. Under silica-undersaturated conditions complete solid solution would exist between diopside and the Ca-Tschermak's component, as shown by the experiments of Clark, Schairer, and de Neufville (*Year Book* 61).

Comparison of the isothermal sections of the join diopside-albite with those of the join diopside-anorthite at the same temperatures indicates that the content of the Ca-Tschermak's component in diopside coexisting with plagioclase is higher than that of jadeite under the  $P$ - $T$  conditions where garnet of the pyrope-grossularite series is not stable.

In the stability field of the garnet, however, the content of jadeite becomes higher than that of the Ca-Tschermak's component.

These possibilities are suggested by the results reviewed here: (1) At high pressures diopside coexisting with plagioclase may contain appreciable amounts of jadeite and Ca-Tschermak's components, and the contents of both may increase with increasing pressure below pressures at which garnet is stable. In the stability field of garnet of the pyrope-grossularite series, however, the content of the Ca-Tschermak's component decreases with increasing pressure. It is to be expected, therefore, that the content of Ca-Tschermak's component relative to the jadeite component will be small in the eclogite facies. (2) In the stability field of eclogite, outlined by Yoder and Tilley (1962), omphacite can contain at least 30 weight per cent jadeite in solid solution. (3) Assuming that the temperature of the M discontinuity under the continents is about  $500^{\circ}\text{C}$ , the maximum content of jadeite in omphacite would be about 40 weight per cent in silica-saturated environments of the continental crust.

#### THE RHOMBIC ENSTATITE-CLINOENSTATITE INVERSION

*F. R. Boyd and J. L. England*

The complex polymorphism exhibited by enstatite in laboratory experiments is curiously absent in terrestrial rocks. Magnesium-rich pyroxenes from a wide variety of ultramafic and mafic rocks are almost invariably rhombic enstatite. Only in meteorites do we commonly find the monoclinic form, clinoenstatite. Rhombic enstatite also appears in meteorites, and sometimes the two forms are intergrown in the same specimen. Natural occurrences of protoenstatite have not been discovered, and it is improbable that they will be because protoenstatite inverts so readily to clinoenstatite.

A phase diagram for  $\text{MgSiO}_3$  compiled from our present and previous results is



shown in Fig. 32. The high-temperature form, protoenstatite, is very difficult to quench; normally it inverts to clinoenstatite while a charge is being cooled to room temperature. High-temperature X-ray work (Foster, 1951), however, has demonstrated that protoenstatite has a true stability field. Until recently it was generally believed that clinoenstatite was a metastable form produced by inversion of protoenstatite on cooling. Rhombic enstatite was believed to be stable at all temperatures below the field of protoenstatite. Nevertheless, Sclar *et al.* (1964)

discovered clinoenstatite in the products of experiments made at high pressures and relatively low temperatures. They succeeded in reacting rhombic enstatite to clinoenstatite under these conditions and proved that clinoenstatite has a true stability field. Our determination of the rhombic enstatite-clinoenstatite inversion curve, shown in detail in Fig. 33, confirms the discovery of Sclar *et al.*, but it differs from the curve they obtained in that it lies at a temperature range about 75°C higher.

Quenching experiments that locate the

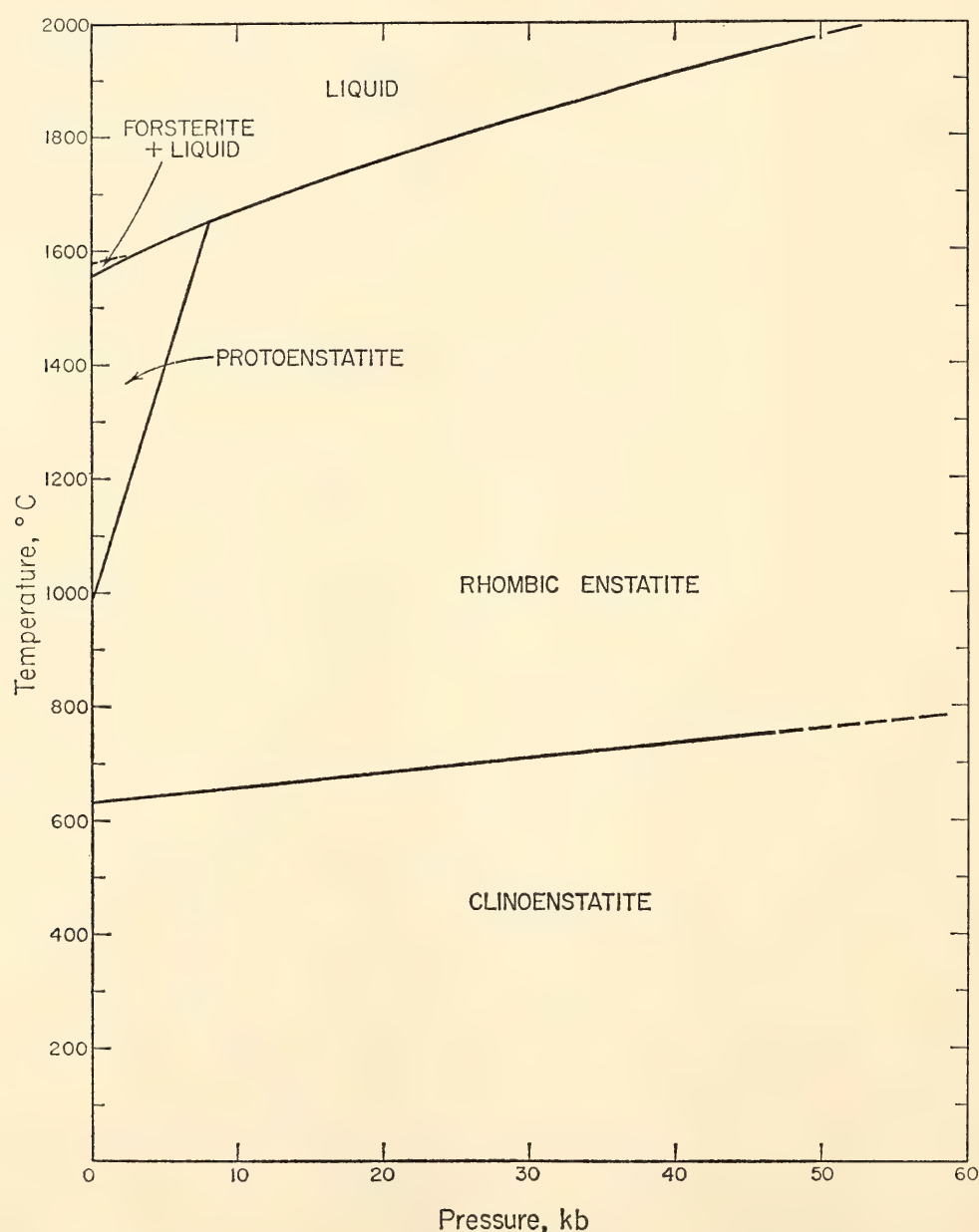


Fig. 32. Phase relations of enstatite,  $\text{MgSiO}_3$ . Liquidus data and the stability field of protoenstatite are from Boyd, England, and Davis (1964). The clinoenstatite  $\rightleftharpoons$  rhombic enstatite inversion curve is from this report.

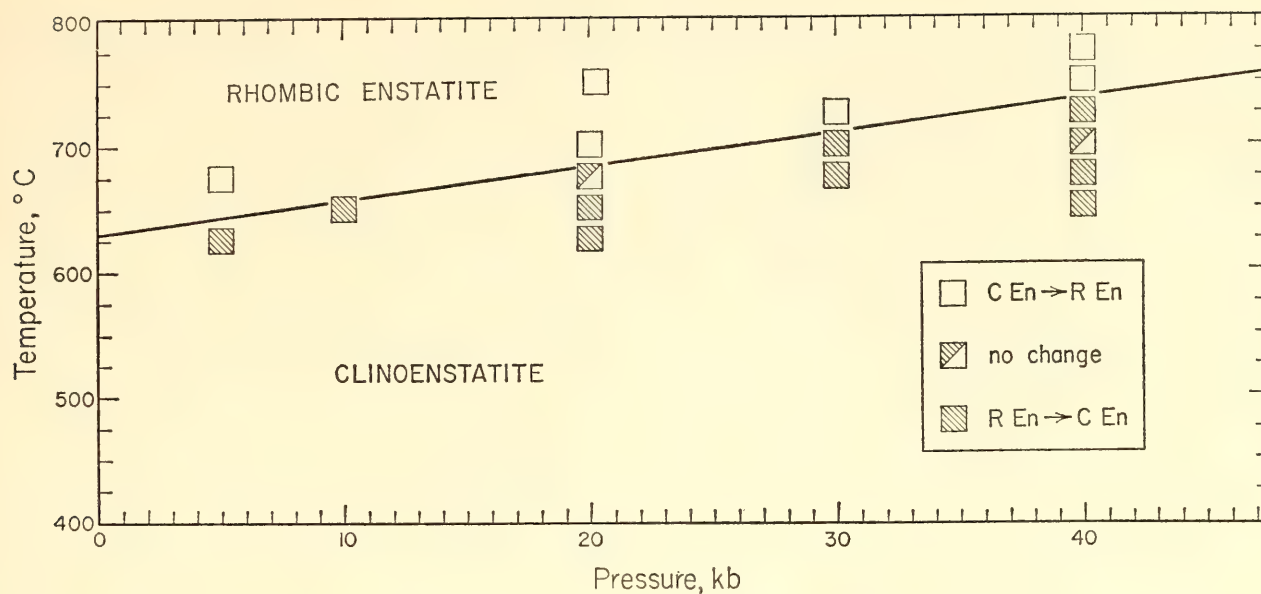


Fig. 33. Clinoenstatite-rhombic enstatite inversion. Equation for the curve is  $T = 630 + 2.6P$ , where  $T$  is in degrees centigrade and pressure ( $P$ ) is in kilobars.

curve were made with a starting mixture of about equal parts of rhombic enstatite and clinoenstatite. Close to the curve the reaction is sluggish and to obtain sufficient reaction it was necessary to make experiments up to six days in duration. Conversion of rhombic enstatite to clinoenstatite or vice versa was established by comparing the X-ray diffractometer pattern of a charge with that of the starting material. With this technique each bracket on the curve constitutes a reversal.

The  $dT/dP$  slope of the inversion is only  $2.6^\circ/\text{kb}$ . This is small in comparison with slopes of up to  $80^\circ/\text{kb}$  found for other solid transitions. However, the low slope is in harmony with the extremely small  $\Delta V$  found by J. V. Smith (personal communication, 1964) from determinations of cell dimensions of synthetic rhombic- and clinoenstatite. Smith's data show that clinoenstatite is denser than rhombic enstatite, but the  $\Delta V$  is so small as to be almost within the limits of error of the determinations. The inversion curve extrapolates to atmospheric pressure at about  $630^\circ\text{C}$ . We have not as yet attempted to bracket the transition with dry experiments at atmospheric pressure or at low  $\text{H}_2\text{O}$  pressures in hydrothermal

equipment. Nevertheless it is odd that the transition has not been found in studies of many systems containing enstatite in the dry and hydrothermal ranges.

Natural rhombic pyroxenes have compositions close to the join  $\text{MgSiO}_3\text{-FeSiO}_3$  with alumina, ferric iron, and lime as principal impurities. Lindsley's study of  $\text{FeSiO}_3$  (this report, section entitled "Ferrosilite") shows a pattern of polymorphism very similar to that which we have found for  $\text{MgSiO}_3$ . In particular the temperature range for the inversion of monoclinic  $\text{FeSiO}_3$  to rhombic  $\text{FeSiO}_3$  is close to that determined for  $\text{MgSiO}_3$ . Preliminary experiments by Lindsley on intermediate compositions, however, suggest the possibility of a maximum as high as  $900^\circ\text{C}$  on the inversion loop between  $\text{MgSiO}_3$  and  $\text{FeSiO}_3$ .

It is difficult to predict with much confidence the effects of lime and alumina on the inversion. Ca-rich pyroxenes are monoclinic, and one might expect that addition of  $\text{CaO}$  would expand the field of clinoenstatite. Natural enstatites contain an average of only about one per cent  $\text{CaO}$ , and it is unlikely that this would have a major effect. Alumina contents of rhombic pyroxenes, however,



range up to about nine weight per cent. The polymorphic relationship between the amphiboles anthophyllite (orthorhombic) and cummingtonite (monoclinic) is structurally similar to the rhombic enstatite-clinoenstatite inversion. Some natural anthophyllites contain large amounts of alumina, whereas cummingtonites contain very little. This relationship suggests that  $\text{Al}_2\text{O}_3$  might preferentially dissolve in rhombic enstatite and enlarge its stability field relative to clinoenstatite. However, we have as yet no experimental verification for this supposition.

It is nevertheless possible to apply with reasonable confidence the phase relations found for pure  $\text{MgSiO}_3$  to natural enstatites close to this composition. These include enstatites from ultramafic and some mafic rocks and enstatites from meteorites. Enstatites from igneous rocks have clearly crystallized at temperatures well above  $600^\circ\text{C}$ – $700^\circ\text{C}$  and hence well within the rhombic enstatite stability field. Absence of clinoenstatite formed from protoenstatite on cooling in such rocks can be attributed to their deep-seated origin and the fact that the field for protoenstatite is eliminated by relatively low pressures. Rhombic enstatites from plutonic rocks must, however, have been cooled rather slowly through the clinoenstatite stability field. Since the enstatite in such rocks is predominantly coarse grained, its tendency to invert to clinoenstatite would be inhibited. But still it is puzzling that there are not occasional instances where rhombic enstatite inverted to clinoenstatite during slow cooling.

The clinoenstatite found in some chondritic meteorites (Mason, 1962) might have inverted from protoenstatite or it might have formed over a wide pressure range at temperatures under the range of  $600^\circ\text{C}$ – $700^\circ\text{C}$ . The former alternative seems more probable because of the occurrence of glass in these meteorites (e.g., Dodd and Van Schmus, 1965). The glass implies high temperatures in the

magmatic range. Hence the process by which the mineral assemblage in these chondritic meteorites formed took place at high temperature but at rather low pressure, more specifically at temperatures over  $1,000^\circ\text{C}$  and pressures under 8 kb (Fig. 32).

#### TEMPERATURE-COMPOSITION SECTION FOR JADEITE-DIOPSIDE

*Peter M. Bell and B. T. C. Davis*

Omphacitic pyroxenes are among the most important constituents of eclogites. Experimental studies of jadeite, an important component of omphacite, have demonstrated that eclogites form under conditions of high pressures and temperatures. Knowledge of jadeite stability is not directly applicable, however, since the omphacites of most eclogites contain significant amounts of other components. Notably they include diopside, acmite, hedenbergite, and Tschermak's molecules. Of these, diopside is present in the greatest amounts and in most examples predominates over jadeite. One must therefore add the diopside component to jadeite in order to obtain a better approximation of natural omphacite. A solid solution of this composition might tend to increase the field of stability of jadeite in the subsolidus and melting regions. If so, such an increase could be used to explain the diversified natural associations of eclogite. The range of eclogite occurrences includes those found in inclusions with accessory diamond, which suggests deep subcrustal formation, and at the other extreme those continental eclogites that have evidently formed in various grades of crustal metamorphism. The formation processes thus range from melting to solid reactions.

In the present study, melting relations in the system jadeite-diopside were determined by quenching experiments at high pressure. The results of these experiments are presented in a temperature-composition section at 30 kb in Fig. 34. A melting phenomenon similar

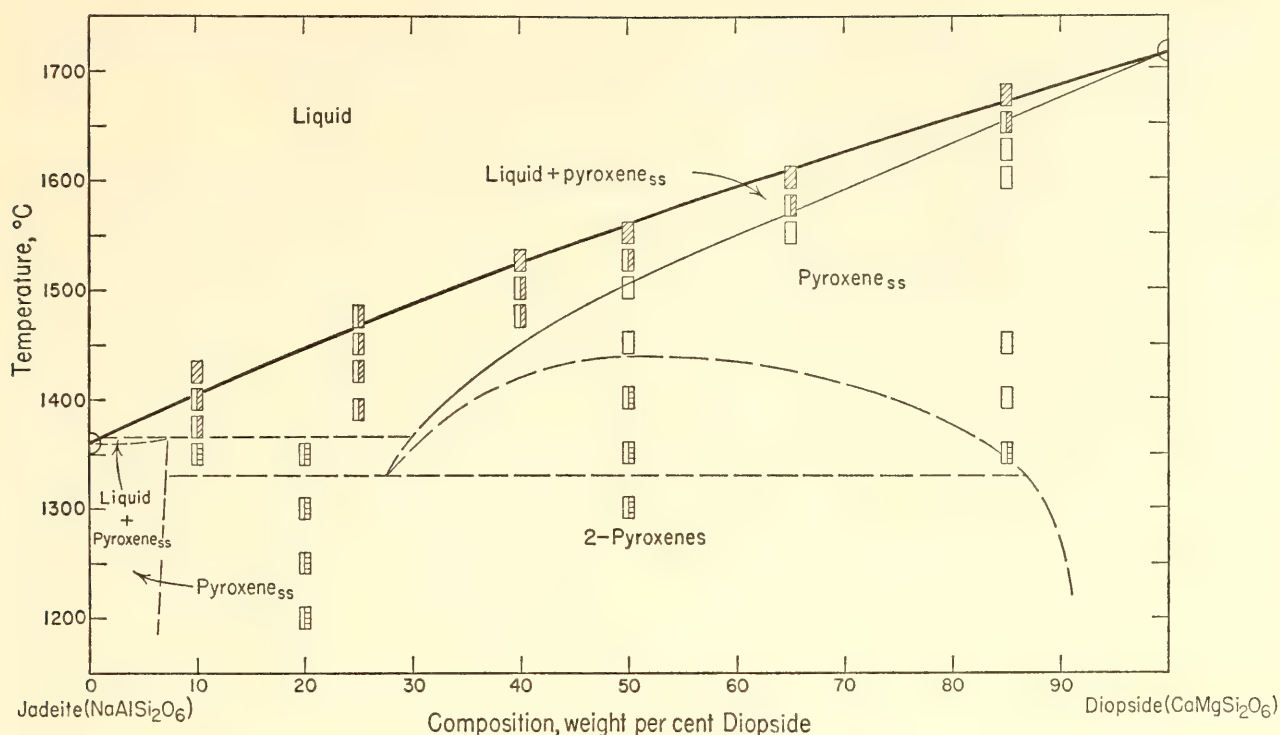


Fig. 34. Temperature-composition section at 30 kb for the system jadeite-diopside.

to that of the plagioclase system at 1 atm (Bowen, 1913) was expected, but little resemblance to the albite-anorthite melting interval was found. Instead, a narrow melting interval extends from diopside to about midway across the join and terminates in a three-phase equilibrium at the jadeite-rich end. One implication of the narrow melting loop is that in melts close in composition to diopside there is little concentration of sodium relative to calcium in the liquid. The steepness of the melting interval implies that fractionation would tend to concentrate jadeite in liquid and solid fractions under natural conditions. A pressure fall would probably accompany cooling, so that the trend of liquid toward liquid + diopside solid solution would change below about 25 kb to liquid + diopside solid solution + albite + nepheline.

Split peaks on X-ray diffractometer patterns of some of our experiments suggest the presence of a miscibility gap, indicated in Fig. 34 by dashed lines. The (220) reflection exhibits this feature clearly, but small spacing differences in other peaks of the two-pyroxene solid

solutions could not be resolved. Diopside and jadeite are quite similar in their optical, physical, and crystallographic properties, so it is not surprising that small spacing differences in solid solutions that are even closer in composition might not be apparent. Two (220) reflections were observed in the diffraction patterns of all samples quenched from the two-pyroxene fields in Fig. 34. The samples from the single-pyroxene field in every case show only one (220) peak, and the X-ray parameters give some indication of the composition shift along the binary join. It might be expected that natural omphacites would exhibit a more extensive miscibility owing to the presence of additional components. It seems probable, however, that unmixing would appear in eclogitic clinopyroxenes, even if only to a minor extent. In a recent study Coleman *et al.* (1965) point out that unmixing is a possible interpretation in some occurrences.

The effect of pressure on the solvus can be calculated. For this calculation only the shape of the solvus curve and the specific volume ( $\bar{V}$ ) as a function of composition are needed. A list of  $\bar{V}$  vs.



composition ( $x$ ) based on unit-cell volumes is given in Table 4. Values of a function for the excess volume of mixing ( $\bar{V}_m^e$ ) developed by curve fitting to the measured values are also listed in Table 4 for the calculations.

Starting from the measured temperature of critical unmixing ( $T_c$ ) at any pressure and the equations for critical unmixing in simple mixtures (Guggenheim, 1952), one can derive a value for the excess free energy of mixing ( $\bar{G}_m^e$ ). It is assumed that the entropy term ( $\bar{S}_m$ ) is of the form

$$-R[x_1 \ln x_1 + (1 - x_1) \ln (1 - x_1)]$$

and that  $\bar{G}_m^e$  is of the form

$$(x_1) (1 - x_1)w$$

Then

$$w = 2RT_c = 6,790 \text{ cal/mole} \\ (30 \text{ kb}, 1,708^\circ\text{K})$$

and

$$x_{1(T_c)} = 0.5$$

The fact that  $x_{1(T_c)}$  does in fact lie very close to 0.5 lends a certain degree of confidence to the simple-mixture approximation.

One may accordingly proceed a step farther and calculate  $dw/dP$  from the relation

$$\bar{V}_m^e = (x_1) (1 - x_1)(dw/dP) = \\ (x_1)(1 - x_1) 2.56$$

Accordingly

$$\Delta w_{(30 \text{ kb})} = \frac{2.56}{41.83} \int_{30 \times 10^3}^P dP$$

(where the factor 41.83 in the denominator arises from conversion from cc-bars to calories).

$$w_{(50 \text{ kb})} = 6,790 + \frac{(2.56)(20 \times 10^3)}{41.83} = \\ 8,015/\text{cal mole}$$

and

$$T_c(50 \text{ kb}) = w/2R = 2,015^\circ\text{K} = 1,742^\circ\text{C}$$

To derive this result it has been implicitly assumed that  $w$  is independent of  $T$ , by making the assumption for  $\bar{S}_m$ . With this proviso, it appears that pressure raises the critical solvus temperature about  $15^\circ/\text{kb}$ .

The reaction albite + nepheline  $\rightleftharpoons$  2 jadeite has attracted much attention as one of the principal reactions in the conversion of alkali basalt to eclogite. To improve our knowledge of the stability range of eclogite we would like to be able to predict the extent to which the solid solution of jadeite and diopside will expand the field of jadeitic clinopyroxene at the expense of albite + nepheline + diopside.

A preliminary evaluation of this effect can be obtained from a thermodynamic calculation of the reaction albite + nepheline +  $n$  diopside  $\rightleftharpoons$  omphacite ( $2/[2 + n]$  jadeite,  $n/[2 + n]$  diopside), assuming that the omphacite is a simple mixture (Guggenheim, 1952) and that diopside does not react with albite + nepheline at pressures less than those required to stabilize omphacite. Inasmuch as the solvus between jadeite and diopside permits only limited solution be-

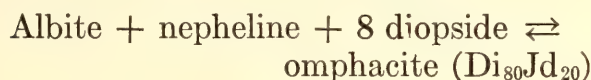
TABLE 4. Molar Volumes and Excess Volumes of Mixing

Jadeite, mole per cent	$\bar{V}$ cm <sup>3</sup> /mole, measured	$\bar{V}_m^e$ cm <sup>3</sup> /mole, measured	$\bar{V}_m^e$ cm <sup>3</sup> /mole = 2.56 ( $x_1$ ) (1 - $x_1$ )
15.0	.....	.....	0.325
15.8	65.61	0.355	.....
36.0	.....	.....	0.585
36.8	64.57	0.493	.....
50.0	.....	.....	0.640
51.8	63.88	0.632	.....
62.0	.....	.....	0.590
85.0	.....	.....	0.325

tween the pyroxenes, we limit the calculation to the composition  $\text{Di}_{80}\text{Jd}_{20}$ . Introduction of the simple-mixture assumption makes the effect of solution on free energy symmetrical about  $\text{Jd}_{50}\text{Di}_{50}$  so that the results obtained are valid also for the composition  $\text{Di}_{80}\text{Jd}_{20}$ , within the limits of this assumption.

The thermodynamics of the reaction albite + nepheline  $\rightleftharpoons$  2 jadeite have already been treated (Yoder and Weir, 1951). Addition of diopside to the reaction adds only an ideal entropy-of-mixing term to the free energy expression for the jadeite side of the reaction.

The first step is to calculate the pressure at which omphacite ( $\text{Di}_{80}\text{Jd}_{20}$ ) is stable at 298°K. For the reaction



we have

$$\Delta G^\circ_{298} = \Delta H^\circ - T\Delta S^\circ = RT(x_{\text{Di}} \ln x_{\text{Di}} + x_{\text{Jd}} \ln x_{\text{Jd}})$$

Substituting Yoder and Weir's (1951) values for  $\Delta H^\circ$  and  $\Delta S^\circ$  and recalling their demonstration (p. 693) that the rate of change of free energy with pressure of the reaction is negligible yields

$$\Delta G^\circ = -6,700 + 298(14.7) + (1.99)(298)(0.8 \ln 0.8 + 0.2 \ln 0.2) \approx \Delta V(P) = 33.8P/41.83 \text{ cal/mole}$$

For  $\Delta V$  we can substitute  $\Delta V$  of the reaction albite + nepheline  $\rightleftharpoons$  2 jadeite, for  $V_{\text{Di}}$  occurs on both sides of the equation and  $V_m^e$  at  $x_{\text{Di}} = 0.8$  is only about one per cent of  $V_{\text{ideal}}$ .

$P_{\text{equil}(298^\circ\text{K})} \approx -3.3 \text{ kb}$ ; i.e., omphacite is stable under standard conditions (STP). The contribution of the mixing term to the total free energy,  $-300 \text{ cal/mole}$ , is only 15 per cent of the free energy of reaction at STP. Next,  $dT/dP$  of the reaction is calculated with the Clapeyron equation and neglecting the dependence of both entropy change and volume change of the reaction on pressure and temperature.

$$\frac{dT}{dP} = \frac{\Delta V + 0.01\Delta V}{\Delta S + 0.8 \ln 0.8 + 0.2 \ln 0.2} =$$

$$\frac{31.03 \times 10^3}{(41.83)(14.7 + 0.5)} = 48^\circ/\text{kb}$$

where  $\Delta S$  and  $\Delta V$  are the entropy and volume changes of the reaction albite + nepheline  $\rightleftharpoons$  2 jadeite at STP, and the terms  $0.01\Delta V$  and  $0.8 \ln 0.8 + 0.2 \ln 0.2$  are the volume and entropy-of-mixing terms for an omphacite with the composition  $\text{Di}_{80}\text{Jd}_{20}$  at STP.

From  $dT/dP$  and  $P_{\text{equil}(298^\circ\text{K})}$  we may say that the omphacite with the composition  $\text{Di}_{80}\text{Jd}_{20}$  is stable below atmospheric pressure under about 175°C. This result agrees well with the calculated stability of pure jadeite under atmospheric pressure, so that one can conclude that the effect of solid solution of diopside has a negligible effect on the stability of jadeite.

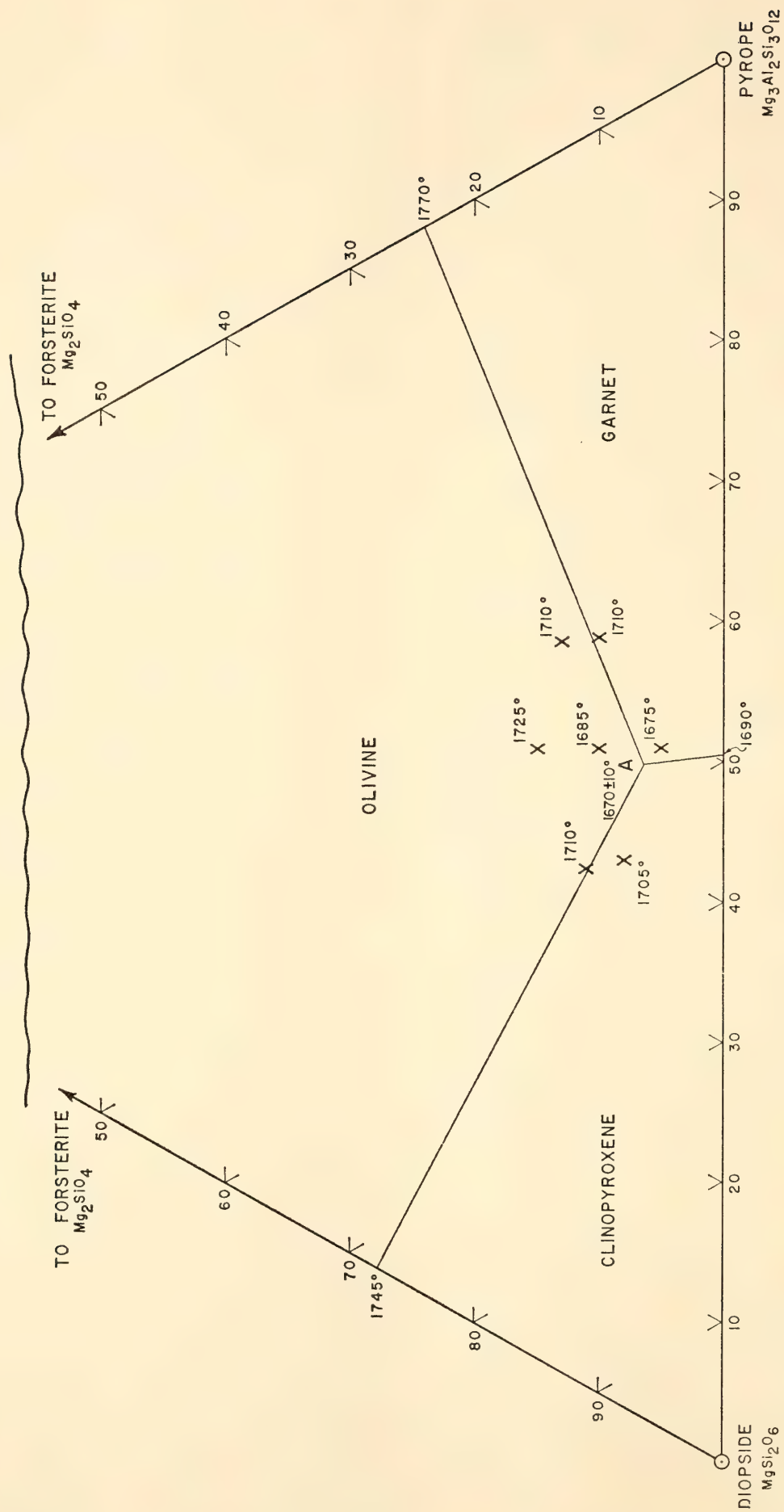
#### MELTING RELATIONS IN THE JOIN DIOPSIDE-FORSTERITE-PYROPE AT 40 KILOBARS AND AT ONE ATMOSPHERE

*B. T. C. Davis and J. F. Schairer*

The melting under high pressure of assemblages in the join diopside-forsterite-pyroxene may provide a satisfactory model for partial melting in the earth's mantle for two reasons. First, the components of this join—CaO, MgO,  $\text{Al}_2\text{O}_3$ , and  $\text{SiO}_2$ —include more than 90 weight per cent of the constituents of most garnet peridotites. Second, because of solid solution effects at more than 30-kb pressure, much of this join crystallizes to the assemblage clinopyroxene + orthopyroxene + garnet + olivine, the mineral assemblage of garnet peridotite. It is believed that this is the principal mineral assemblage of the upper mantle beneath continental areas (Boyd, MacGregor, and Ringwood, *Year Book 63*).

Last year the melting relations at 40 kb of the three joins that bound diopside-forsterite-pyroxene were presented (*Year Book 63*, pp. 165–171). Since then seven compositions in the triangular join were studied at 40 kb and also at 1 atm. Data on the primary phase fields, mineral





Weight, per cent

Fig. 35. Liquidus surface of diopside-forsterite-pyroxene at 40-kb pressure.

assemblages stable at the solidus, and the extent of the low-melting region are presented here. Data at 1 atm were obtained by the method of quenching, and the melting behavior at 40 kb was studied by means of the single-stage apparatus of Boyd and England (1960*b*). All products were examined both optically and by X-ray powder diffraction.

The liquidus surface of diopside-forsterite-pyrope at 40 kb is shown in Fig. 35. Only three phase fields—clinopyroxene, garnet, and olivine—are present, more details of which are shown in Table 5. The four-phase assemblage Cpx + Opx + Gar + Ol (compositions 4 and 5) begins to melt at the isobaric invariant point at 1,680°C ± 10°C. This temperature is higher than part of the liquidus of the clinopyroxene-garnet-olivine assemblage (Fig. 35), and the invariant point at 1,680°C ± 10°C is probably a reaction point at and above which orthopyroxene

disappears. Fractionation of the liquid at 40 kb must take place along the univariant curve clinopyroxene + garnet + olivine + liquid, passing through the join diopside-forsterite-pyrope at about Di<sub>47</sub>For<sub>6</sub>Py<sub>47</sub> at 1,670°C (point A of Fig. 35).

Although the exact composition of the reaction point Cpx + Opx + Gar + Ol + Liq has not yet been determined, its location can be greatly restricted from knowledge of the liquidus surfaces of the join diopside-forsterite-pyrope and previous data on the join diopside-pyrope-enstatite (Davis, *Year Book* 63, p. 169, Fig. 62). On both of these joins the four-phase point lies within 6 weight per cent of the midpoint of diopside-pyrope and within 10°C of the quaternary reaction point in question, which is, therefore, estimated to lie between the four-phase points at Di<sub>47</sub>For<sub>3</sub>Py<sub>47</sub>En<sub>3</sub> weight per cent at 1,680°C. The small uncertainty in the

TABLE 5. Results of Melting Experiments in the Join Diopside-Forsterite-Pyrope at 40 Kilobars

	Composition No.						
	1	2	3	4	5	6	7
Composition, Weight per cent							
Diopside	46.5	44	41.5	36	35	53	52
Forsterite	5.0	10	15.0	10	13	8	11
Pyrope	48.5	46	43.5	54	52	39	37
Phases Present							
Temp., °C							
1,740			L				
1,715			L, (Ol)	L		L	L
1,705		L	L, (Ol)	Gar, L	L, (Ol)		(Ol), L
1,690					Cpx, Gar, Ol, L	Cpx, L	
.....							
1,680	L	L, (Ol)	Ol, L	Cpx, Gar, Opx, Ol, (L)	Cpx, Gar, Ol, L, (Opx)		Cpx, Ol, L
.....							
1,670	Gar, L	Ol, Gar, L			Cpx, Opx, Gar, Ol		Cpx, Gar, Ol, L
.....							
1,660	Cpx, Gar, Ol, L	Cpx, Gar, Ol	Cpx, Gar, Ol	Cpx, Gar, Opx, Ol			
.....							
1,640	Cpx, Gar, Ol						
.....							

Cpx, clinopyroxene solid solution; Gar, garnet<sub>ss</sub>; L, liquid; Ol, olivine<sub>ss</sub>; Opx, orthopyroxene<sub>ss</sub>; parentheses indicate phases present in trace amounts.



location of this reaction point will have little effect on the qualitative conclusions that follow.

The primary liquid at 40 kb has a CIPW norm of An 32.4, Di 21.8, En 26.0, Fo 19.9 per cent. This composition is basaltic only in the broadest sense. It consists entirely of the essential and varietal normative constituents of basalt but the norm is that of an enstatite-rich picrite.

Inasmuch as the seven compositions studied under high pressure help to define the low-melting region for the garnet-two pyroxene-olivine assemblage in the system  $\text{CaO-MgO-Al}_2\text{O}_3\text{-SiO}_2$ , their crystallization histories under atmospheric pressure should have implications bearing upon the crystallization of natural primary magmas after eruption, and on the relations, if any, between primary magmas and basalt. The crystallization histories under atmospheric pressure are shown in Table 6.

In all seven compositions forsterite is the liquidus phase under atmospheric pressure, and in no case does a second phase begin to crystallize until the melt has cooled at least  $200^\circ$  from its liquidus. All compositions complete their crystallization at the quintuple point clinopyroxene-protoenstatite-forsterite-anorthite-liquid at  $1,248^\circ\text{C} \pm 5^\circ\text{C}$ . Clearly, low-temperature liquids from diopside-forsterite-pyroxene at 40 kb are not low-temperature liquids at atmospheric pressure.

The application of these results to the generation of natural magmas is an approximation in that at least three major components of basalt, the iron oxides, and  $\text{Na}_2\text{O}$  have not been included in this study. With this restriction it appears that the primary partial fusion extract of garnet peridotite is picritic rather than basaltic. Inasmuch as O'Hara (1965) has arrived at a similar conclusion for the primary fusion extract of hypersthene eclogite at 30 kb, one might expect picritic magmas to be a common feature of continental vulcanism when, in fact,

they are not. In general, picritic lavas and hypabyssal intrusives are few in number and restricted to the lower parts of both oceanic and continental volcanic columns (Muir and Tilley, 1957) and to sills (Walker, 1940) where crystal settling of olivine has played a dominant role. Even the picritic sills of the Hebrides, whose origin has been attributed to picritic magmas (Drever and Johnston, 1958), are a minor feature in a large basaltic magma province. However, the experimental evidence for the primary nature of picritic magma could be reconciled with the preponderance of basalt as opposed to picrite in extrusive situations if basalts were derived from a picritic parentage by a crystal-liquid fractionation at low pressure. The separation of olivine or olivine + orthopyroxene would be essential to the process, and such separation is consistent with the low-pressure courses of crystallization found in this study.

#### STABILITY FIELDS OF SPINEL AND GARNET PERIDOTITES IN THE SYNTHETIC SYSTEM $\text{MgO-CaO-Al}_2\text{O}_3\text{-SiO}_2$

*I. D. MacGregor*

Rocks of peridotite composition occur as four distinct mineral assemblages:

- a. Olivine + orthopyroxene  $\pm$  clinopyroxene + plagioclase
- b. Olivine + orthopyroxene  $\pm$  clinopyroxene + spinel
- c. Olivine + (clinopyroxene or orthopyroxene) + spinel + garnet
- d. Forsterite + orthopyroxene  $\pm$  clinopyroxene + garnet

Of these, assemblages *b* and *d* occur most commonly. Assemblage *a* may be seen occasionally as a minor phase of large spinel peridotite intrusions (Green, 1964), and assemblage *c* occurs occasionally as large separate masses (Lacroix, 1900).

Spinel peridotites are found as large intrusions in the axial regions of big fold belts (Hess, 1955) that have undergone low-grade to medium-grade regional

TABLE 6. Selected Results of Melting Experiments in the  
Join Diopside-Forsterite-Pyroxene at Atmospheric Pressure

	Composition No.						
	1	2	3	4	5	6	7
Composition, Weight per cent							
Diopside	46.5	44	41.5	36	35	53	52
Forsterite	5	10	15	10	13	8	11
Pyroxene	48.5	46	43.5	54	52	39	37
Phases Present							
Temp., °C							
1,520			L		L		
1,515			L, (Fo)		L, (Fo)		
1,505				L			
1,500		L	L, (Fo)	L, (Fo)			
1,495		L, (Fo)	L, (Fo)				L
1,490							L, (Fo)
1,485	L, (Fo)	L, (Fo)		L, (Fo)			L, (Fo)
1,480	L, (Fo)	L, (Fo)				L	L, (Fo)
1,475						L, (Fo)	
1,470						L, (Fo)	L, Fo
1,300					L, Fo		
1,295				L, Fo	L, Fo, (An)		
.....							
1,290	L, Fo			L, Fo, (An)	L, Fo, An		
.....							
1,285	L, Fo, (An)			L, Fo, An		L, Fo	L, Fo
.....							
1,280	L, Fo, (An)	L, Fo	L, Fo			L, Fo, (An)	L, Fo, (Cpx)
.....							
1,275	L, Fo, (An)	L, Fo, (An)	L, Fo			L, Fo, An, (Cpx)	L, Fo, Cpx, (An)
.....							
1,270		L, Fo, (An)	L, Fo, An		L, Fo, An		L, Fo, Cpx, (An)
.....							
1,265	L, Fo, An	L, Fo, (An)	L, Fo, An		L, Fo, An, (Pr)		
.....							
1,260	L, Fo, An, Cpx	L, Fo, An	L, Fo, An	L, Fo, An		L, Fo, An, Cpx	L, Fo, Cpx, An
.....							
1,255	L, Fo, An, Cpx	L, Fo, An, Cpx	L, Fo, An, Cpx	L, Fo, An, Pr	L, Fo, An, Pr		
.....							
1,250	L, Fo, An, Cpx	L, Fo, An, Cpx	L, Fo, An, Cpx	L, Fo, An, Pr	L, Fo, An, Pr	L, Fo, An, Cpx, (Pr)	L, Fo, Cpx, An
.....							
.....							
1,245	L, Fo, An, Cpx, (Pr)	L, Fo, An, Cpx, Pr	L, Fo, An, Cpx, Pr	L, Fo, An, Pr, Cpx	L, Fo, An, Pr, Cpx		
.....							

An, anorthite; Cpx, clinopyroxene; Fo, forsterite; L, liquid; Pr, protoenstatite; parentheses indicate phases present in trace amounts.

metamorphism, as nodules in alkali olivine basalt, and as intrusions along major fault zones. Garnet peridotites occur in fold belts that have been subjected to high-grade regional meta-

morphism and they occur as nodules in kimberlite pipes. Phase-equilibrium studies (MacGregor, *Year Book 63*) indicate that the garnet peridotites are the high-pressure equivalents of the



spinel peridotites. Further, the narrow range of peridotite bulk composition, in conjunction with its worldwide occurrence in the cores of old mountain belts and as nodules in anorogenic oceanic and continental regions, has led to the speculation that peridotites are the materials of the upper mantle. It is important, therefore, to understand the effect of pressure on the stability fields of the spinel and garnet peridotites.

The chemical composition of peridotites is closely approximated (88–92 weight per cent) by compositions in the four-component system  $\text{MgO-CaO-Al}_2\text{O}_3\text{-SiO}_2$ . The reaction enstatite + spinel  $\rightleftharpoons$  forsterite + pyrope has been studied in the three-component system  $\text{MgO-SiO}_2\text{-Al}_2\text{O}_3$  (MacGregor, *Year Book 63*), and the present study explores the effect of CaO on this reaction.

Three compositions were used in this study. They lie at the intersection of the joins garnet-forsterite and pyroxene-spinel with enstatite-diopside ratios of 25/75 (A), 75/25 (B), and 0/100 (C). In each case the boundary curve between the spinel- and garnet-bearing assemblages was determined with the use of crystalline starting materials composed of a 1/1 ratio of the high- and the low-

pressure assemblage. The boundary curves were determined by comparing the relative intensities of the Bragg reflections, on X-ray diffractograms, of the product with that of the starting material. On the low-pressure side of the reaction there was a significant decrease in the intensity of the garnet reflections and increase of the intensity of the pyroxene reflections. On the high-pressure side garnet peaks were significantly enhanced, whereas pyroxene peaks either diminished or disappeared. Since only minor amounts of spinel are present on both sides of the reaction, spinel reflections did not serve as a good indication of reaction. All these experiments were conducted with a piston-and-cylinder solid-media pressure apparatus (Boyd and England, 1960b).

For each of the compositions used, the assemblage clinopyroxene  $\pm$  orthopyroxene + spinel + forsterite is stable on the low-pressure side of the equilibrium, and the four-phase assemblage clinopyroxene + forsterite + garnet + spinel is stable on the high-pressure side. The reaction boundaries are shown on  $T$ - $P$  plots in Figs. 36 and 37. The equilibrium curves for compositions A and B are coincident, whereas the curve for pure diopside falls at considerably higher

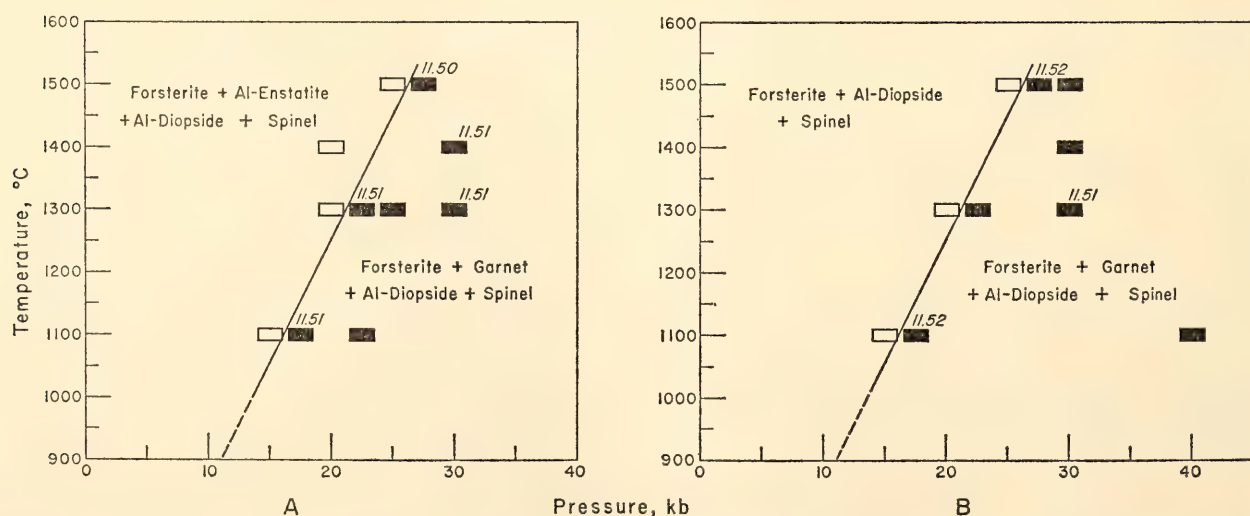


Fig. 36.  $T$ - $P$  plot of boundary between the two assemblages forsterite + aluminous enstatite + aluminous diopside + spinel (open rectangles) and forsterite + aluminous diopside + garnet + spinel (solid rectangles). Numbers on high-pressure side of equilibrium boundary represent garnet unit cell in Å. (A) Composition A (diopside/enstatite = 25/75); (B) composition B (diopside:enstatite = 75/25).

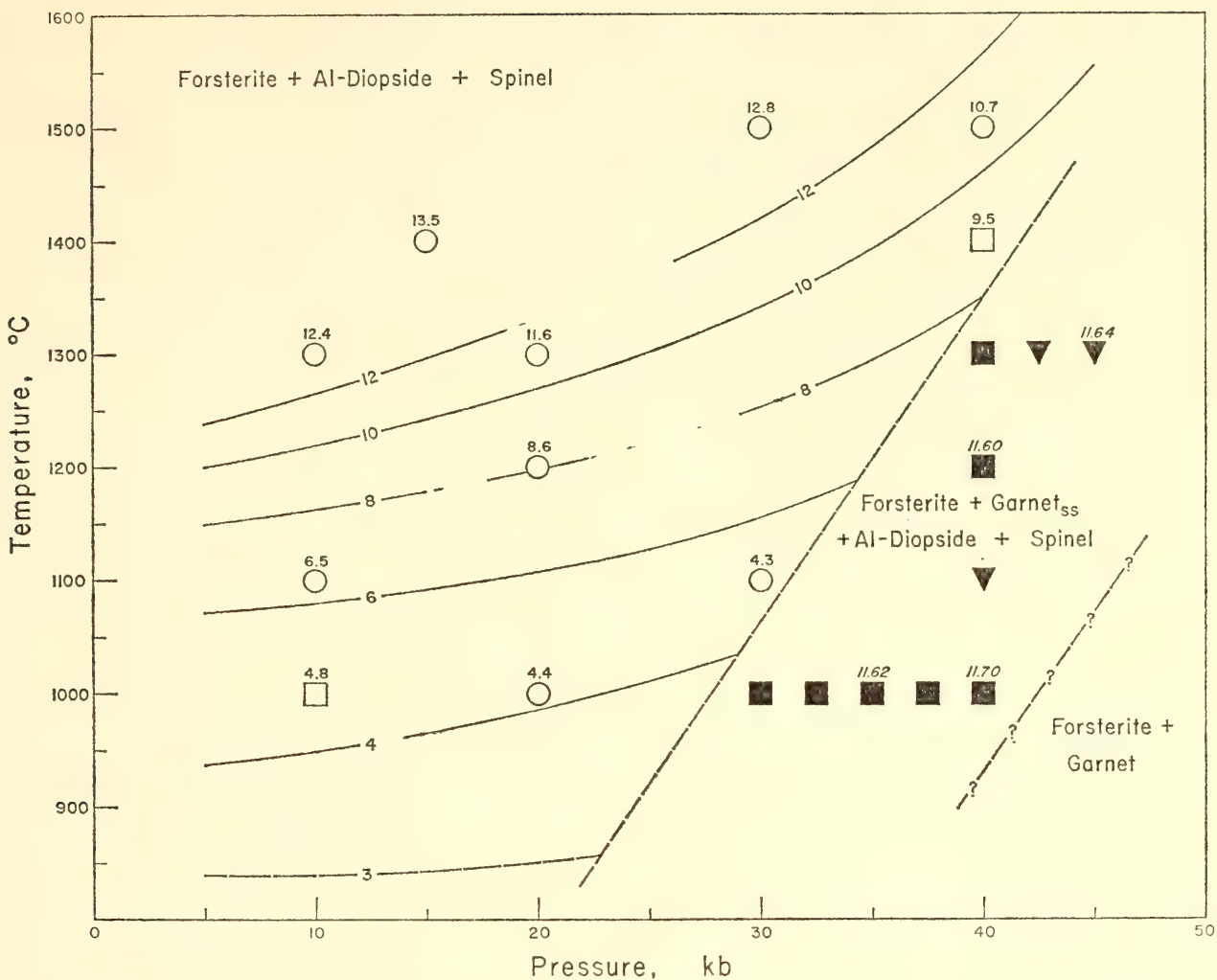


Fig. 37. *T*-*P* plot of boundary between the two assemblages forsterite + aluminous diopside + spinel (open points) and forsterite + aluminous diopside + garnet + spinel (solid points). Numbers on high-pressure side of equilibrium curve refer to garnet unit cells in Å; numbers on low-pressure side refer to weight per cent Al<sub>2</sub>O<sub>3</sub> in diopside; contours on low-pressure side are weight per cent Al<sub>2</sub>O<sub>3</sub> isopleths. Starting materials: circles, glass; squares (forsterite + aluminous diopside + garnet + spinel) + glass; inverted triangles (forsterite + aluminous diopside + garnet + spinel) + (forsterite + melilite + anorthite).

pressures (Fig. 38). It should be noted that the equilibrium curve (Fig. 38) for the composition with a diopside-enstatite ratio of 50/50 also falls close to the equilibrium boundaries for compositions *A* and *B* (Kushiro and Yoder, this report).

The unit-cell dimensions of garnets in the high-pressure field are shown in Figs. 36 and 37. Since in this system the garnet unit cell is a direct function of the Ca/Mg ratio of the garnet (Chinner, Boyd, and England, *Year Book* 59), it may be seen that for compositions *A* and *B* there is essentially no detectable com-

positional variation in the garnets as a function of temperature and pressure.

Moreover, for composition *A* the garnets in two experiments at 1,300°C and 30 kb for 4 hours and 17½ hours, and two additional experiments at 1,400°C and 30 kb for 35 minutes and 4 hours showed no compositional change with time (Fig. 36). It should also be noted that there is only a slight compositional variation between the garnets crystallized from compositions *A* (11.51 Å, Py<sub>87</sub>Gr<sub>13</sub>) and *B* (11.52 Å, Py<sub>86</sub>Gr<sub>14</sub>). The garnet has a lower Ca/Mg ratio than would be expected for a



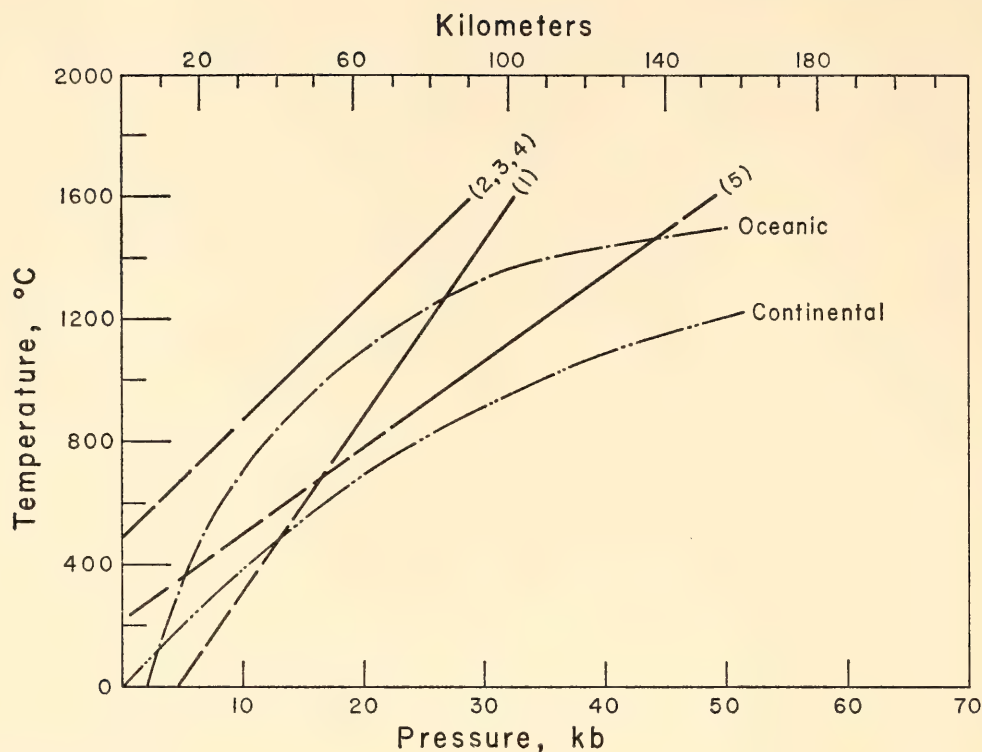


Fig. 38.  $T$ - $P$  plot combining equilibrium boundaries between model spinel and garnet peridotites for compositions  $A$  (2),  $B$  (3), and  $C$  (5). Also included is the reaction  $4\text{MgSiO}_3 + \text{MgAl}_2\text{O}_3 \rightleftharpoons \text{Mg}_3\text{Al}_2\text{Si}_3\text{O}_{12} + \text{Mg}_2\text{SiO}_4$  (1) (MacGregor, *Year Book 63*, p. 157) and the boundary curve for the reaction  $\text{CaMgSi}_2\text{O}_6 + 2\text{MgSiO}_3 + 2\text{MgAl}_2\text{O}_4 \rightleftharpoons \text{Mg}_2\text{CaAl}_3\text{Si}_3\text{O}_{12} + 2\text{Mg}_2\text{SiO}_4$  (4) (Kushiro and Yoder, p. 89). Geothermal gradients for continental and oceanic regions are shown.

garnet on the two-phase join garnet-forsterite. For composition  $C$  the limited number (four) of garnet unit-cell determinations indicates that the garnets become more calcic with increasing pressure (Fig. 37); their compositions are also significantly different from those for the compositions  $A$  and  $B$ , and, again, they have a lower  $\text{Ca}/\text{Mg}$  ratio than would be found for a garnet on the two-phase join garnet-forsterite. For each composition the garnet stable on the high-pressure side of the equilibrium boundary is more pyrope than would be expected for the two-phase assemblage forsterite-garnet.

No experiments have been carried out at sufficiently high pressures to give products that lie in the two-phase field forsterite-garnet. The increasing grossularite content, with increasing pressure, of the garnet for composition  $C$  (Fig. 37) indicates that the boundary between the four-phase and the two-phase assemblage should be at pressures well in excess of

those used in this experiment; an interpretive curve indicating this equilibrium is shown in Fig. 37. The latter equilibrium boundary should be present, but at various pressures, for the various compositions.

An interpretive diagram to indicate the different equilibria is shown in the isothermal section in Fig. 39. The figure indicates that for the range of enstatite-diopside ratios within the four-phase field forsterite + enstatite + diopside + spinel there will be five phases at equilibrium between the two four-phase assemblages forsterite + diopside solid solution + enstatite solid solution + spinel and forsterite  $\pm$  enstatite solid solution  $\pm$  diopside solid solution + garnet + spinel. In an isothermal section in a four-component system this represents an invariant situation and explains the coincidence of the equilibrium curves for compositions within the four-phase field. Figure 39 also shows a hypothetical curve for the boundary between

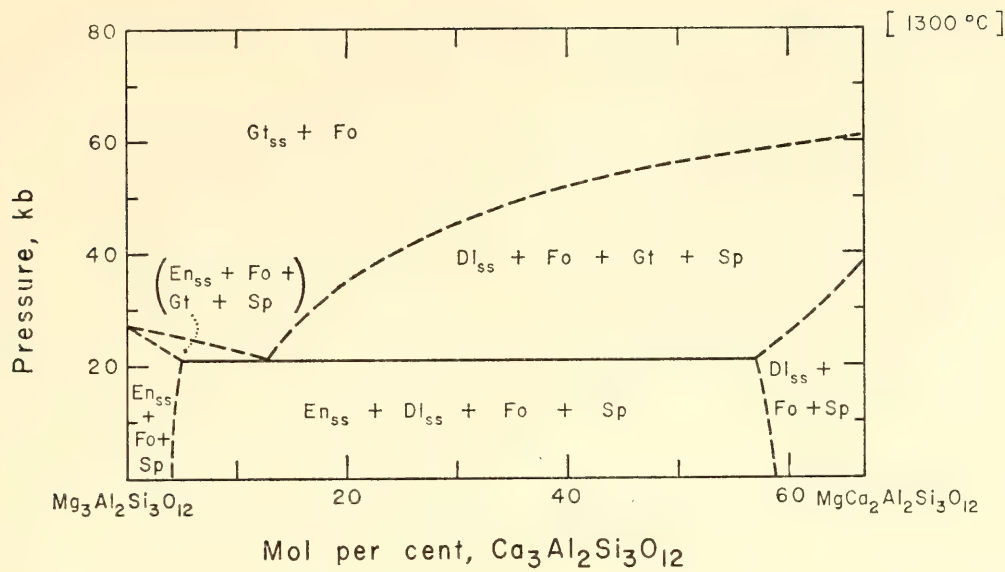
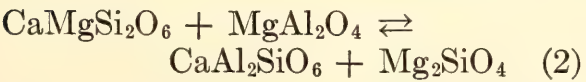
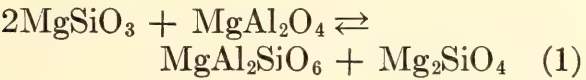


Fig. 39. Pressure-composition section at 1,300°C for a portion of the pyrope-grossularite join in the system MgO-CaO-Al<sub>2</sub>O<sub>3</sub>-SiO<sub>2</sub>.

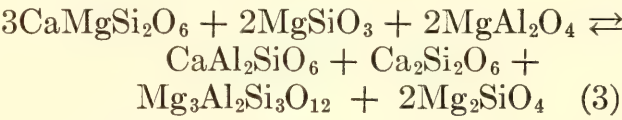
the four-phase assemblage pyroxene + forsterite + garnet + spinel and the two-phase assemblage garnet + forsterite. There will also be a composition at which the four-phase assemblage clinopyroxene + enstatite solid solution + forsterite + spinel converts directly to the two-phase assemblage garnet + forsterite. For other projections closer to the diopside-enstatite join, the range of compositions inverting directly from the four- to the two-phase assemblage will increase.

The small variation of the garnet unit cells for compositions within the four-phase assemblage forsterite + enstatite solid solution + diopside solid solution + garnet indicates that this garnet will have a composition close to  $\text{Py}_{87}\text{Gr}_{13}$  ( $A_0 = 1.51 \text{ \AA}$ ). Within the spinel peridotite stability field the solid solution of  $\text{Al}_2\text{O}_3$  in the pyroxene results in reactions of the following type:



giving rise to the three- or four-phase assemblage diopside solid solution ± enstatite solid solution + forsterite + spinel with solid solution of the Tschermak's molecule in the pyroxene.

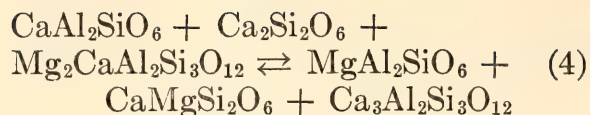
The first appearance of the garnet-forsterite join results in reactions of the type



The Ca/Mg ratio of the pyroxenes and garnets may vary depending on the original bulk chemistry. For compositions reacting to the enstatite solid solution + forsterite + garnet + spinel assemblage the Ca/Mg ratio of the garnet will be higher than that expected for the stoichiometric forsterite-garnet join, and the enstatite will lie along the join enstatite Mg-Tschermak's molecule because of  $\text{Al}_2\text{O}_3$  solid solution. For compositions reacting to the diopside solid solution + forsterite + garnet + spinel assemblage the Ca/Mg ratio of the garnet will be lower than that expected for the stoichiometric forsterite-garnet join, and there will be solid solution in the diopside toward Ca-Tschermak's molecule and wollastonite.

The increase of the Ca/Mg ratio of the garnets with pressure in the four-phase assemblage diopside solid solution + forsterite + garnet + spinel for composition C indicates that a continuous reaction of the type





occurs in this field. This type of reaction should occur for all compositions in the diopside solid solution + forsterite + garnet + spinel field as the two-phase field forsterite + garnet is approached.

From the above information it is possible to construct a series of isothermal projections of the four-component system from forsterite composition onto the plane  $\text{SiO}_2\text{-Al}_2\text{O}_3\text{-CaO}$  (Fig. 40). This plane will indicate the following sequence of assemblages.

1. At pressures of less than 20 kb (Fig. 40*B*) spinel peridotites are stable over a wide range of composition.

2. The first appearance of garnet is recorded at approximately 21 kb (Fig. 40*C*). The appearance of garnet results in the development of three four-phase fields:

- a. Forsterite + garnet + diopside solid solution + enstatite
- b. Forsterite + garnet + diopside solid solution + spinel
- c. Forsterite + garnet + enstatite solid solution + spinel

3. At pressures in excess of 27 kb (Fig. 40*D*) the join pyrope-forsterite is stable and the four-phase field forsterite + enstatite solid solution + garnet + spinel is replaced by the three-phase assemblage forsterite + garnet + enstatite solid solution and forsterite + garnet + spinel. No data are available to indicate the rate of increase of the three-phase assemblage with pressure, but the garnet in equilibrium with enstatite, forsterite, and spinel must become more pyropic with pressure.

4. There appears to be little change in the width of the four-phase field forsterite + diopside solid solution + garnet + spinel up to 38 kb. Above this pressure, however (Fig. 40*E*), the garnet in equilibrium with diopside solid solution, forsterite, and spinel becomes more

grossularite rich with pressure and the width of the three-phase field forsterite + diopside solid solution + garnet increases, probably as far as grossularite (Fig. 40*F*), to overlap the four-phase field forsterite + garnet + diopside solid solution + spinel.

5. The four-phase field forsterite + diopside solid solution + enstatite solid solution + garnet, or model garnet peridotite, is stable from 21 kb to at least 65 kb. Garnets within this field will show little compositional variation from 21 to 38 kb and will fall close to  $\text{Py}_{87}\text{Gr}_{13}$ . This narrow range of garnet chemistry is reflected in the small range of compositions found in natural garnet peridotites (O'Hara and Mercy, 1963). If the almandine content of these natural garnets is summed with pyrope the "pyrope"/grossularite ratio is essentially the same as that found for the synthetic assemblage. No data are available to indicate the garnet composition at pressures in excess of 38 kb.

To indicate the distribution of the different peridotite assemblages in the crust and upper mantle it is necessary to make some assumptions about the ambient geothermal gradient. The geothermal gradients for an oceanic and continental environment calculated by Clark and Ringwood (1964) have been superimposed on the different equilibrium curves (Fig. 38).

Since peridotites have a limited variation of chemical composition ( $\text{CaO}$ , 1–3.5 weight per cent;  $\text{Al}_2\text{O}_3$ , 0.5–5.0 weight per cent) the pertinent equilibrium boundaries between the spinel and garnet peridotites will lie between curves 1 and 2 of Fig. 38.

In continental areas at depths in excess of approximately 10 km most peridotite compositions fall wholly within the garnet peridotite stability field. This conclusion would have an important bearing on the origin of the large spinel peridotites found along the axes of old mountain belts and on the origin of spinel peridotite nodules in alkali olivine ba-

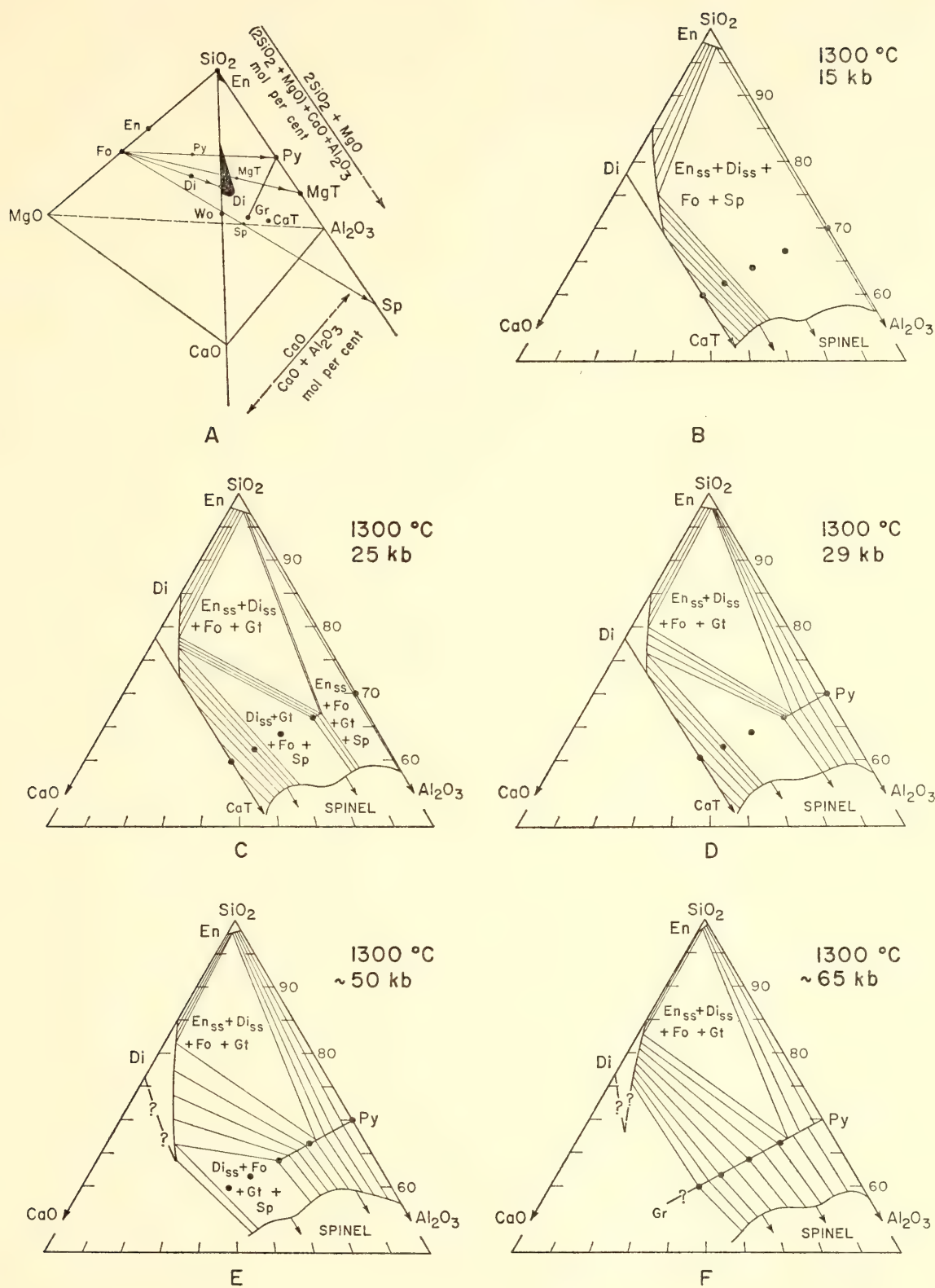


Fig. 40. A. Quaternary tetrahedron  $\text{CaO-MgO-Al}_2\text{O}_3\text{-SiO}_2$  showing method of projection of phases from forsterite onto the plane  $\text{SiO}_2\text{-CaO-Al}_2\text{O}_3$ . B-F. Successive isothermal ternary projections at increasing pressures to illustrate the phase assemblages stable with forsterite. Closed circles, compositions used for this projection; CaT, Ca-Tschermak's molecule; Di, diopside; En, enstatite; Fo, forsterite; Gr, grossularite; Gt, garnet solid solution; MgT, Mg-Tschermak's molecule; Py, pyrope; Sp, spinel; Wo, wollastonite; subscript ss, phases showing extensive solid solution.



salts. The spinel peridotites in continental regions, with normal geothermal gradients, have not formed by inversion from a high-pressure garnet-bearing assemblage but they must have formed directly at high temperatures and pressures on the low-pressure side of curve 2 (Fig. 38). This conclusion would indicate that these spinel peridotites have probably formed by fractional crystallization of basaltic magmas in or near the base of the crust. They do not therefore represent a primary upper-mantle composition. The pressures and temperatures attained in the high-grade regionally metamorphosed cores of ancient mountain belts lie well within the expected field of the garnet peridotites, and their occurrence under these conditions is consistent with the experimental data. Even with the abnormally high geothermal gradients expected during the metamorphism, peridotite compositions should be in the garnet peridotite field for approximately the first 10 km.

In oceanic areas there will be a delicate balance between the intersection of the geothermal gradient and the spinel-garnet peridotite equilibrium curve, depending on bulk composition and local variations in the geothermal gradient. At depths in excess of 20 km it would be possible to have these general conditions:

1. Spinel peridotites that are stable down to depths of approximately 70 km, beyond which garnet peridotite would be the stable assemblage.

2. A thin layer of garnet peridotite that passes downward into a zone (of varying thickness) of spinel peridotite and finally back at deeper levels to a garnet peridotite.

3. The oceanic mantle lying totally within the garnet peridotite stability field.

At approximately 20 km there is an intersection between the spinel-garnet peridotite and plagioclase-spinel peridotite equilibrium curves (Kushiro and Yoder, this report). Structural interpretation as to the distribution of peridotite types in the lower crust and upper mantle

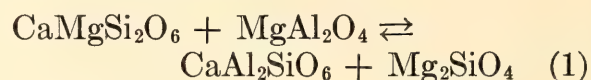
will thus depend on which of the two equilibrium boundaries mentioned is stable at shallower depths. No experimental evidence is now available to choose between these alternatives.

#### ALUMINOUS DIOPSIDES IN THE THREE-PHASE ASSEMBLAGE DIOPSIDE SOLID SOLUTION + FORSTERITE + SPINEL

*I. D. MacGregor*

The  $\text{Al}_2\text{O}_3$  content of diopsides in the three-phase assemblage diopside solid solution + forsterite + spinel was determined as part of a study of the spinel peridotite  $\rightleftharpoons$  garnet peridotite reaction. This information is useful in constructing phase diagrams of the sub-solidus relations in the  $\text{CaO-MgO-Al}_2\text{O}_3\text{-SiO}_2$  quaternary and could be used to indicate temperatures in rocks that contain these three minerals.

The composition 2 diopside + 1 spinel was used as a starting material. Both glasses and garnet-bearing crystalline assemblages were used as reactants. As a result of the reaction



any solid solution of  $\text{Al}_2\text{O}_3$  in diopside moves the diopside composition toward the Ca-Tschermak's molecule in composition and places the bulk composition in the three-phase field aluminous diopside + forsterite + spinel.

Experiments were conducted in the forsterite + diopside solid solution + spinel stability field in a piston-and-cylinder solid-media apparatus (Boyd and England, 1960b). The  $\text{Al}_2\text{O}_3$  content of the diopside in the products was determined by X-ray methods with the use of Sakata's data (1957). All suitable peaks were measured on a diffractogram against an internal standard (NaF, calibrated against gem diamond by B. Skinner) to an accuracy of  $\pm 0.02^\circ$ . For compositions in excess of 20 mole per cent  $\text{CaAl}_2\text{SiO}_6$  (9.40 weight per cent  $\text{Al}_2\text{O}_3$ ) a linear extension of the curve, from lower



$\text{CaAl}_2\text{SiO}_6$  contents, was used. It is estimated that the standard error of determination is  $\pm 0.75$  weight per cent  $\text{Al}_2\text{O}_3$ .

The results of this study are shown in Fig. 37. The contours ( $\text{Al}_2\text{O}_3$  weight per cent isopleths) were fitted visually from constructed temperature-composition and pressure-composition sections. As a result of the determination error, each curve will have a width of 0.75 weight per cent  $\text{Al}_2\text{O}_3$ .

As expected from the molar volume of the reactants and products of Equation 1, the  $\text{Al}_2\text{O}_3$  content of the diopsides decreases with increasing pressure at constant temperature. The increase in slope with increasing pressure of the isopleths seems to be required by the data, but the explanation is not evident. In the four-phase field forsterite + enstatite solid solution + diopside solid solution + spinel of the spinel peridotites the slope of the curves should be similar, but the  $\text{Al}_2\text{O}_3$  content will be less than that indicated for the three-phase assemblage (Fig. 37).

Caution should be exercised in the application of these curves to natural samples. The determined  $\text{Al}_2\text{O}_3$  isopleths refer only to subsolidus equilibria and not to crystal-liquid equilibria, and in addition most natural aluminous diopsides contain significant amounts of ferrous and ferric iron.

#### THE EFFECT OF PRESSURE ON THE MINIMUM MELTING COMPOSITION IN THE SYSTEM $\text{MgO-SiO}_2\text{-TiO}_2$

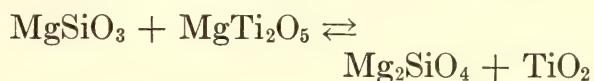
*I. D. MacGregor*

Chayes (1964), and Chayes and Velde (1965) have shown that  $\text{TiO}_2$  is by far the most useful single oxide in distinguishing between intraoceanic and circumoceanic Cenozoic basalts. Subsequent analyses of basalts from the mid-Atlantic ridge (Engel and Engel, 1964a) and the East Pacific Rise (Engel and Engel, 1964b) indicate that this classification is not entirely satisfactory for basalts dredged from the ocean floor. A bimodal  $\text{TiO}_2$

distribution is still noted, however, and Chayes's distinction holds firm if his intraoceanic group is reclassified to cover only the oceanic islands.

The  $\text{TiO}_2$  content of a basaltic magma could depend on a number of factors. Subsidiary reactions involving  $\text{TiO}_2$ -rich phases, solid solution of  $\text{TiO}_2$  in primary precipitating phases, and the effect of pressure on the movement of the liquid composition are factors that may have an important role in determining the final  $\text{TiO}_2$  content of a magma. Pressure is an important variable in determining the importance of each of these possibilities. This study reports the progress made on an investigation of the effect of pressure on the composition of the minimum melting compositions in the system  $\text{MgO-SiO}_2\text{-TiO}_2$ . At present sufficient data are available to indicate the nature of the 10- and 20-kb liquidus surfaces. For the future it is planned to study the 40-kb surface and investigate the effect of  $\text{CaO}$  on the present conclusions. The data supporting the current conclusions are to be published within the next year.

The stable subsolidus joins at 1 atm and at 10 and 20 kb are shown in Fig. 42A-C. Apart from the unchecked possibility that  $\text{MgTi}_2\text{O}_5$  decomposes to  $\text{MgSiO}_3 + \text{TiO}_2$  at higher pressures, the subsolidus equilibria at 20 kb remain unchanged to 40 kb. The only reaction that occurs from 1 atm to 20 kb is



The equilibrium curve for this reaction has not been accurately defined, but at solidus temperatures ( $1,440^\circ\text{C} - 1,540^\circ\text{C}$ ) the boundary is at  $15 \pm 1\frac{1}{2}$  kb. The magnesium titanates  $\text{MgTi}_2\text{O}_5$ ,  $\text{MgTiO}_3$ , and  $\text{Mg}_2\text{TiO}_4$  have not been found as separate mineral phases in nature, but they form important solid solutions with the minerals pseudobrookite, ilmenite, and magnetite, respectively.

Solidus and liquidus relations were investigated along the joins  $\text{MgSiO}_3\text{-TiO}_2$ ,  $\text{MgSiO}_3\text{-MgTi}_2\text{O}_5$ , and  $\text{Mg}_2\text{SiO}_4\text{-TiO}_2$ . Starting materials were composed of



oxide mixes, melted where convenient (i.e., for compositions whose liquidus, at 1 atm, are less than 1,550°C) and crystallized at 1 atm to the subsolidus assemblage. In each case the oxide mixes were thoroughly mixed before fusion or crystallization. The liquidus and solidus relations were determined by the quenching method with optical examination of the products. Except for  $\text{TiO}_2$ -rich compositions, little trouble was experienced in using the textural evidence to determine whether melting had occurred.

The experimentally determined liquidus and solidus curves for the 10- and 20-kb isobars are shown in Fig. 41. The comparable sections at 1 atm may be deduced from the data given by Massazza and Sirchia (1958). A check on the 1-atm join  $\text{MgSiO}_3$ - $\text{TiO}_2$  by J. F. Schairer shows that the eutectic temperature is probably some 10°C lower than indicated, but the eutectic composition is approximately correct.

The join  $\text{MgSiO}_3$ - $\text{TiO}_2$  (Fig. 41A and D) is a binary eutectic at all pressures from 1 atm to 40 kb. The eutectic compositions become more  $\text{TiO}_2$ -rich with increasing pressure; the greatest change in composition is from 1 atm to 10 kb (10 weight per cent  $\text{TiO}_2$ ), and at higher pressures the rate rapidly decreases to about 1 weight per cent  $\text{TiO}_2$  increase per 10 kb. Solid solution effects of  $\text{TiO}_2$  in enstatite have not yet been investigated. The solubility of  $\text{TiO}_2$  (less than 1 weight per cent) in enstatites in nature, however, suggests that it is minimal.

The join  $\text{Mg}_2\text{SiO}_4$ - $\text{TiO}_2$  (Fig. 41B and E) is pseudobinary at all pressures from 1 to 20 kb. At 1 atm two eutectics (one in the field  $\text{MgSiO}_3$ - $\text{Mg}_2\text{SiO}_4$ - $\text{MgTi}_2\text{O}_5$  at 1,440°C and the other in the field  $\text{MgSiO}_3$ - $\text{MgTi}_2\text{O}_5$ - $\text{TiO}_2$  at 1,390°C) are indicated for the field  $\text{MgSiO}_3$ - $\text{Mg}_2\text{SiO}_4$ - $\text{MgTi}_2\text{O}_5$ - $\text{TiO}_2$ . At 10 kb peritectic melting of compositions in the field  $\text{Mg}_2\text{SiO}_4$ - $\text{MgSiO}_3$ - $\text{MgTi}_2\text{O}_5$  results in the movement of minimum melting compositions

across the  $\text{MgSiO}_3$ - $\text{MgTi}_2\text{O}_5$  tie line into the  $\text{MgSiO}_3$ - $\text{MgTi}_2\text{O}_5$ - $\text{TiO}_2$  field, and there will only be one eutectic in the field  $\text{Mg}_2\text{SiO}_4$ - $\text{MgSiO}_3$ - $\text{MgTi}_2\text{O}_5$ - $\text{TiO}_2$ . At 20 kb the stable join  $\text{Mg}_2\text{SiO}_4$ - $\text{TiO}_2$  is pseudobinary because the primary phase field for  $\text{MgTi}_2\text{O}_5$  intersects this join.

The join  $\text{MgSiO}_3$ - $\text{MgTi}_2\text{O}_5$  is pseudobinary at 1, 10, and 20 kb. The incongruent melting of  $\text{MgSiO}_3$  at 1 atm and  $\text{MgSiO}_3 + \text{MgTi}_2\text{O}_5$  at 10 kb allows the appearance of  $\text{Mg}_2\text{SiO}_4$  at the liquidus for both these pressures. Because of the congruent melting of  $\text{MgSiO}_3$  at pressures in excess of 2.3 kb, however, it is possible that the primary phase field for  $\text{Mg}_2\text{SiO}_4$  disappears from the liquidus at pressures somewhere between 2.3 and 10.0 kb. At 20 kb the join  $\text{MgSiO}_3$ - $\text{MgTi}_2\text{O}_5$  is pseudobinary, and compositions in the field  $\text{Mg}_2\text{SiO}_4$ - $\text{TiO}_2$ - $\text{MgTi}_2\text{O}_5$  melt incongruently. This results in the movement of the minimum melting composition across the stable  $\text{Mg}_2\text{SiO}_4$ - $\text{TiO}_2$  join into the three-phase field  $\text{Mg}_2\text{SiO}_4$ - $\text{MgSiO}_3$ - $\text{TiO}_2$ . There will only be one eutectic composition in the field  $\text{Mg}_2\text{SiO}_4$ - $\text{MgSiO}_3$ - $\text{MgTi}_2\text{O}_5$ - $\text{TiO}_2$  at 20 kb.

Ternary liquidus surfaces for the field  $\text{Mg}_2\text{SiO}_4$ - $\text{MgSiO}_3$ - $\text{MgTi}_2\text{O}_5$ - $\text{TiO}_2$  have been constructed in Fig. 42A-C. At 1 atm (Massazza and Sirchia, 1958) two ternary eutectics are present, one at MgO 32.3,  $\text{SiO}_2$  33.0,  $\text{TiO}_2$  34.7 (weight per cent) and the other at MgO 33.6,  $\text{SiO}_2$  35.3,  $\text{TiO}_2$  31.1 (weight per cent). At 10 and at 20 kb there is only one eutectic composition, at MgO 27.0,  $\text{SiO}_2$  32.0,  $\text{TiO}_2$  42.0 (weight per cent) and at MgO 25.2,  $\text{SiO}_2$  24.8,  $\text{TiO}_2$  50.0 (weight per cent) respectively.

The composition of a basaltic melt at the earth's surface is dependent on two main processes—its origin as a complete or partial melt of some solid parental material at depth and its crystallization history during its ascent. Referring only to the simplified system  $\text{MgO}$ - $\text{SiO}_2$ - $\text{TiO}_2$ , primary liquids would lie in the field  $\text{Mg}_2\text{SiO}_4$ - $\text{MgSiO}_3$ - $\text{MgTi}_2\text{O}_5$  at pressures less than 15 kb and in the field  $\text{MgSiO}_3$ -

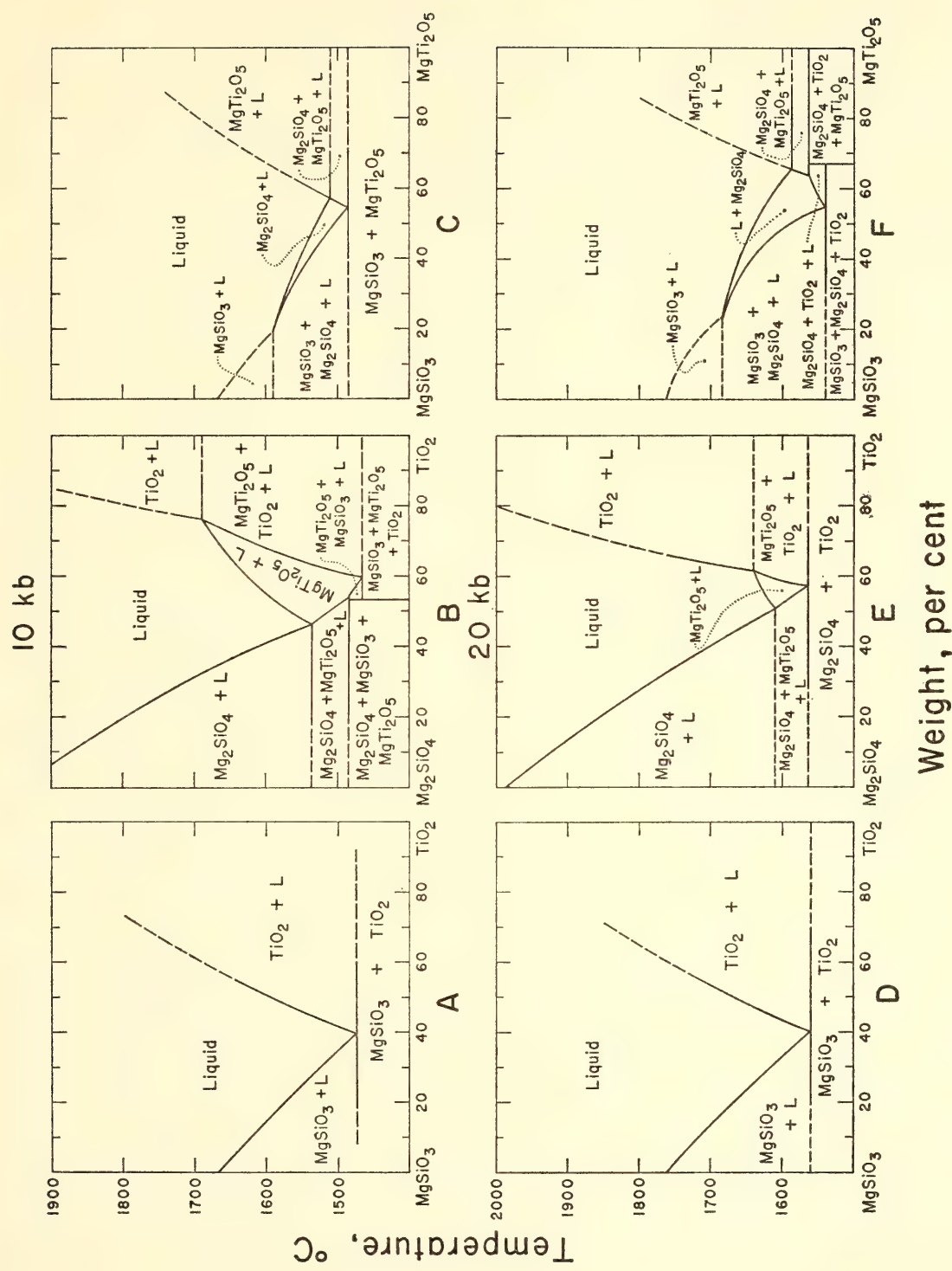


Fig. 41. Melting relations in binary and pseudobinary sections of the system  $\text{MgO-SiO}_2\text{-TiO}_2$  at 10 and 20 kb. All compositions given in weight per cent; continuous lines used where data available; dashed lines represent interpretation.



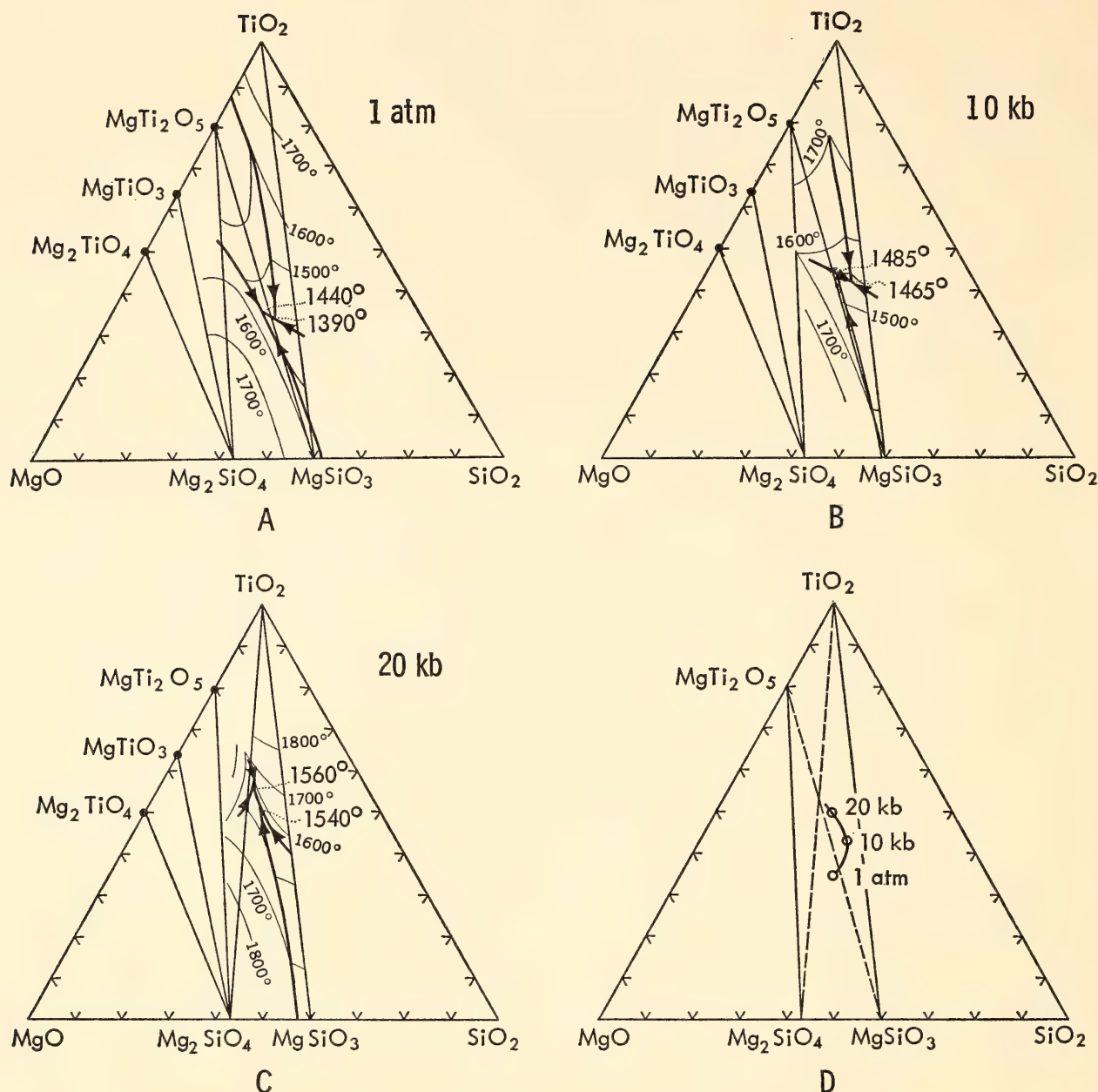


Fig. 42. Liquidus surfaces at 1 atm (A), 10 kb (B), and 20 kb (C) in the field  $\text{Mg}_2\text{SiO}_4\text{-MgSiO}_3\text{-MgTi}_2\text{O}_5\text{-TiO}_2$  in the system  $\text{MgO-SiO}_2\text{-TiO}_2$ . D. Ternary projection of minimum melting compositions for a model peridotite composition. Circles, minimum melting compositions at specific pressures; solid line, trend of minimum melting composition with pressure. Compositions in weight per cent.

$\text{Mg}_2\text{SiO}_4\text{-TiO}_2$  at pressures in excess of 15 kb; in both cases compositions would lie close to the join  $\text{Mg}_2\text{SiO}_4\text{-MgSiO}_3$ .

The change of the minimum melting composition or the composition of a primary magma with pressure is shown in Fig. 42D. With increasing pressure the  $\text{TiO}_2$  content increases, and the  $\text{MgO/SiO}_2$  ratio decreases from 1 atm to 10 kb but increases again from 10 to 20 kb. No data are available for pressures in excess of 20 kb, but presuming a linear

extrapolation, minimum melts at 30 kb and greater should be more titaniferous and lie in the three-phase field  $\text{Mg}_2\text{SiO}_4\text{-MgTi}_2\text{O}_5\text{-TiO}_2$ . Thus the composition of an initial primary liquid, derived by partial fusion of a solid parent, would become successively enriched in  $\text{TiO}_2$  with increasing pressure; it would also experience an initial minor  $\text{SiO}_2$  enrichment, but at pressures greater than 10 kb would become successively enriched in  $\text{MgO}$  and possibly at pressures in excess

of 30 kb would lie within the undersaturated field  $\text{Mg}_2\text{SiO}_4\text{-MgTi}_2\text{O}_5\text{-TiO}_2$ . During the ascent and cooling of this primary liquid the liquid would move into the primary phase field for  $\text{MgTi}_2\text{O}_5$  and become successively impoverished in  $\text{TiO}_2$ .

The extrapolation of this simple system to natural basalts is difficult. Three major components— $\text{CaO}$ ,  $\text{FeO}$ , and  $\text{Fe}_2\text{O}_3$ —form significant solid solutions with nearly all the phases in the ternary system. Thus major changes may be expected in both subsolidus and liquidus diagrams with the addition of these components. If the trends found in the ternary  $\text{MgO-SiO}_2\text{-TiO}_2$  may be projected into and are valid for the more complex system, however, it would indicate that the  $\text{TiO}_2$  content of a basalt may be significantly dependent on pressure. The bimodal distribution of  $\text{TiO}_2$  (Chayes, 1964) is possibly related to the depth from which the basalts have been tapped. Kuno (1959b) has noted a close spatial correlation between tholeiitic and alkali-rich basaltic provinces and belts of shallow and deep-seated earthquakes, respectively. Kuno's alkali-rich basalts fall in Chayes's (1964)  $\text{TiO}_2$ -rich group, whereas most tholeiitic basalts correspond to the  $\text{TiO}_2$ -poor group. The derivation of the more titaniferous basalts from greater depths would tend to agree with the experimental data in the ternary system  $\text{MgO-SiO}_2\text{-TiO}_2$ . Since the experimental data indicate a continuous variation of  $\text{TiO}_2$  content with pressure, the bimodal  $\text{TiO}_2$  distribution found by Chayes (1964) might indicate that most of the basalts are tapped from magma chambers at two widely separated levels in the mantle.

#### PHASE DIAGRAM FOR THE SYSTEM NEPHELINE-QUARTZ

*P. M. Bell and E. H. Roseboom, Jr.<sup>5</sup>*

Experiments were performed to determine melting relations for albite

composition at pressures in the range of 35–43 kb. A combination of the present data with those of earlier work, along with those for jadeite, quartz, and albite, permits delineation of most of the nepheline-quartz system. Even though more complex solid solutions are likely to be present in the natural analogues of the phases, the system as a whole is of value in considering field relations. It embraces the subsolidus and melting relations for the low-pressure phases albite, nepheline, and quartz, as well as those stable at high pressure, including jadeite and coesite.

The melting relations shown (Fig. 43) were determined with a starting material composed of jadeite, coesite, and quartz, prepared by holding glass of albite composition at 37 kb and 1,375°C for five hours. The results do not significantly alter location of the melting interval reported in a preliminary way last year. The liquidus was studied further by partially crystallizing glass of albite composition to jadeite + glass at 36 kb, 1,425°C; 39.5 kb, 1,460°C; and 43 kb, 1,475°C.

Data for albite and jadeite from this study have been used with all other available experimental data for the system to construct the nearly complete phase diagram (Fig. 44). All curves shown are univariant. The equilibrium curves for nepheline-albite-liquid, nepheline-albite-jadeite, albite-jadeite-liquid, jadeite-liquid, and jadeite-coesite-liquid are drawn from data obtained in this study in conjunction with the data of Robertson, Birch, and MacDonald (1957) and obtained at 1 atm by Schairer and Bowen (1947), Schairer and Yoder (1960), and Greig and Barth (1938). The curves for albite-liquid and quartz-coesite are after Boyd and England (1963) and Boyd (1964), respectively. The three dashed curves are based on extrapolated data as follows: (1) liquid-albite-quartz is based on a point at 1 atm (Schairer and Bowen, 1947; Schairer and Yoder, 1960) and the invariant point  $I_2$ ;

<sup>5</sup> U.S. Geological Survey, Washington, D.C.



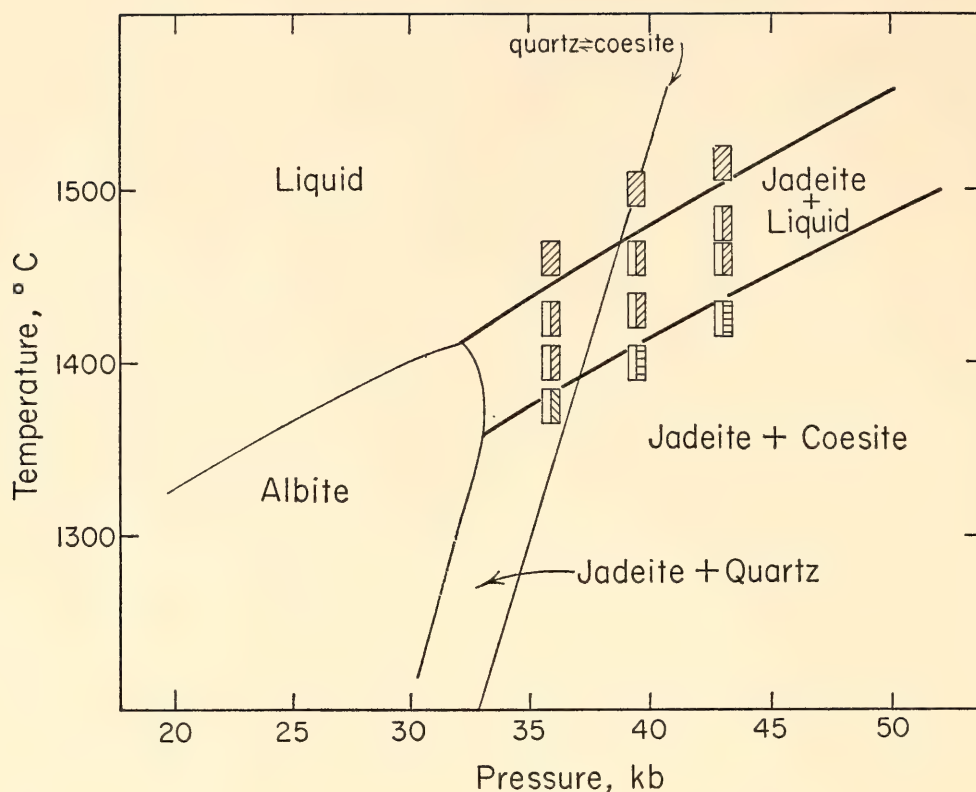


Fig. 43. Melting relations for albite composition in range 36–43 kb. Quartz-coesite equilibrium curve after Boyd (1964); albite melting curve after Boyd and England (1963); albite-jadeite + quartz equilibrium curve extrapolated after Robertson *et al.* (1957).

(2) liquid-jadeite-nepheline is based on invariant point  $I_1$  and is drawn with its slope roughly parallel to the other solidus curve; (3) albite-jadeite-quartz is based on a point at 1,000°C (Birch and LeComte, 1960) and the point  $I_2$ . The metastable extensions are dashed because they are inferred only on the basis of being thermodynamically correct. Details of the degenerate equilibrium that develops for jadeite-quartz-coesite-liquid probably include a change in slope of the solidus with metastable extensions in the jadeite-quartz and jadeite-coesite fields. They are not shown because the necessary information is unavailable and relatively unimportant for the diagram. Similarly, incomplete data on other phases of nepheline composition are not included.

The phase diagram as a whole shows some extraordinary features, one of which is the relation between the two singular points  $S_1$  and  $S_2$ , shown in expanded detail in the upper left-hand corner of Fig. 44. The incongruent melt-

ing curves of jadeite and albite start at  $I_1$  and  $I_2$ , and terminate at  $S_1$  and  $S_2$ . The points are connected by the eutectic curve for albite-jadeite along which the liquid changes composition from nepheline to quartz. One interesting consequence is that in crossing the curve  $S_2$ - $I_2$  by a rise in pressure at constant temperature albite melts to jadeite + liquid. The diagram also shows the phenomena that limit jadeite stability. Natural omphacite is seldom pure jadeite (Coleman *et al.*, 1965), and the resulting solid solutions can be expected to change the stability fields. It is significant that the field for jadeite + quartz, a common assemblage in nature, is narrow and the fields for less common jadeite and the assemblage jadeite + coesite, which has not been reported, are broad.

The main conclusion that can be drawn from these relations is that the melting of jadeite proceeds in a manner entirely analogous to that of albite. Both albite and jadeite have ranges of in-

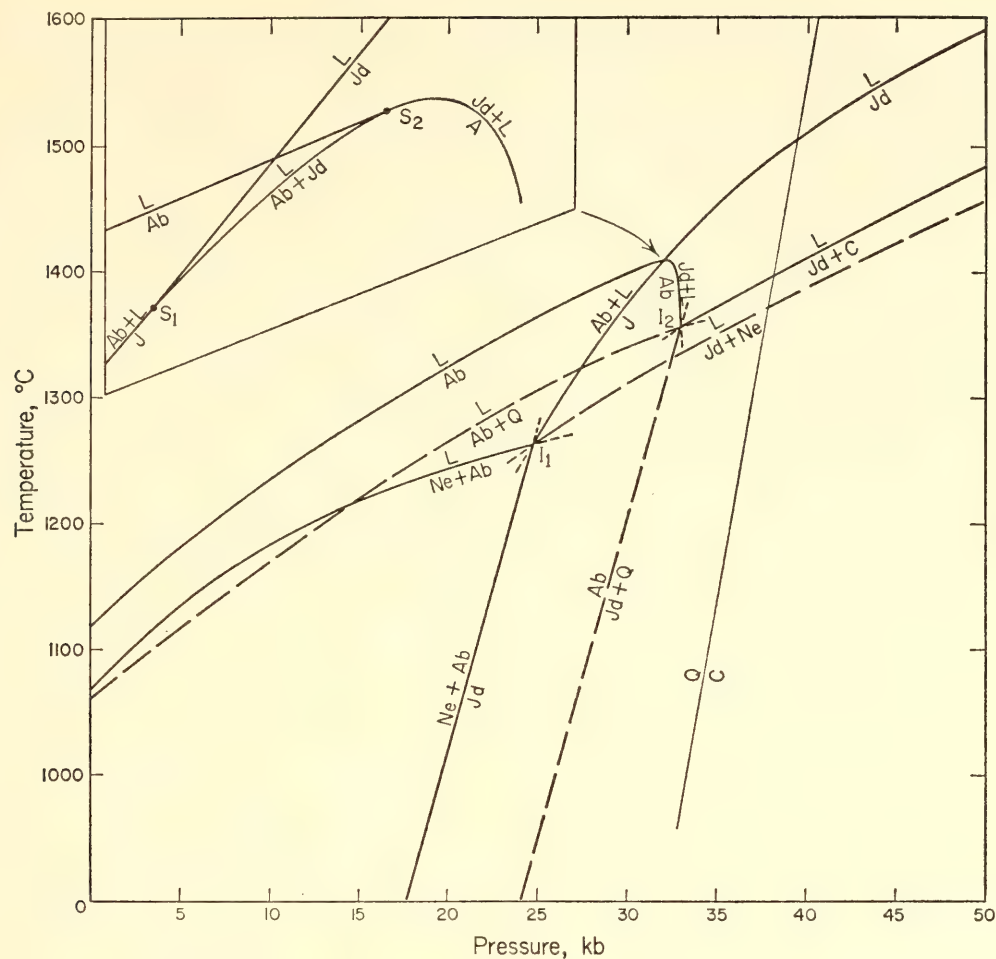


Fig. 44.  $T$ - $P$  plane for the system nepheline-quartz.  $I_1$  and  $I_2$  are binary invariant points. Inset (upper left) shows details concerning the two singular points,  $S_1$  and  $S_2$ . Ab, albite; C, coesite; Jd, jadeite; L, liquid; Ne, nepheline; Q, quartz.

congruent melting, although that of albite is favored by pressure increase and that of jadeite by pressure decrease. The congruent melting curves are similar; the liquid changes from albite composition to jadeite composition at about 32 kb. Subsolidus relations also show mirror symmetry on the phase diagram for the two compositions.

SHEARING SQUEEZER EXPERIMENTS  
WITH QUARTZ AND COESITE

Peter M. Bell, Gene Simmons,<sup>6</sup>  
and James F. Hays<sup>7</sup>

Equilibrium between quartz and coesite has been the subject of several experimental investigations. One motive was to provide a comparison calibration

for high-pressure apparatus. In addition, equilibrium relations of the quartz-coesite transition have become increasingly important owing to the reported occurrences of coesite at Meteor Crater, Arizona (Chao, Shoemaker, and Madsen, 1960), and the recent discovery of coesite in the Muong Nong tektites (Walter, 1965).

Previous studies in which equilibrium was demonstrated were limited by reaction rates to temperatures of 700°C or higher (Boyd and England, 1960a; Kitahara and Kennedy, 1964). Some reactions conducted under shearing conditions are greatly accelerated (Bell, 1963). Dachille and Roy (1962) have achieved synthesis of coesite at temperatures as low as 100°C by utilizing the shearing squeezer. Part of the present shearing squeezer experiments were designed to

<sup>6</sup> Southern Methodist University.  
<sup>7</sup> Harvard University.



determine equilibrium by reversing the quartz-coesite reaction in the temperature range below 700°C. The solid curve in Fig. 45 has been drawn by extrapolating  $P_{kb} = 19.5 + 0.0112 T(^{\circ}\text{C})$  from point A, the lowest point of reversed equilibrium determined by Boyd and England (1960a). Uncertainties in the present results are  $\pm 5^{\circ}\text{C}$  (measured) and  $\pm 1$  kb (estimated from hysteresis). Within these uncertainties, the present points of reversed equilibrium—at 350°C, 425°C, and 500°C—agree with the extrapolation of Boyd and England's (1960a) curve. More recently Boyd (1964) pub-

lished a revision for the curve in order to eliminate the -8 per cent correction included to account for the fraction of his single-stage apparatus (revised equation:  $P_{kb} = 21.2 + 0.0122 T(^{\circ}\text{C})$ ). The present points would not agree as well with the revised curve, but Boyd (personal communication, 1965) is currently making a study of the friction problem, so the matter is not yet settled.

In the present study these problems were investigated: (1) a comparison of equilibrium between the shearing squeezer and the static squeezer; (2) a comparison of equilibrium between experiments with

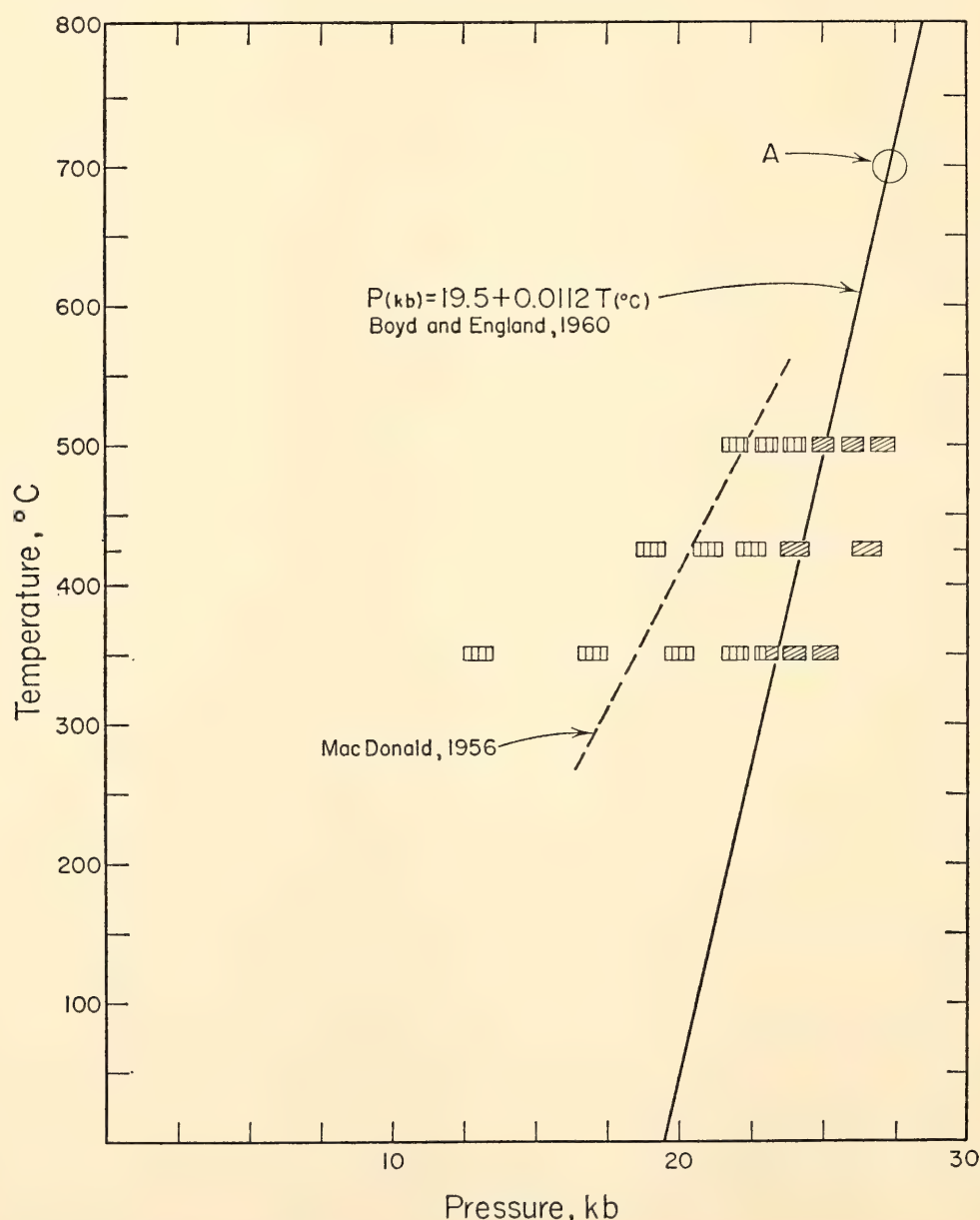


Fig. 45. Equilibrium curve for quartz-coesite. A is a point of reversed equilibrium determined by Boyd and England (1960a).

SiO<sub>2</sub> gel and crystalline SiO<sub>2</sub> as starting materials; and (3) the synthesis of coesite at room temperature.

Problem 1 was chosen because it was thought that addition of shearing to pressure might displace or otherwise upset equilibrium conditions. This proved not to be true. Results of the experiments (shown in Fig. 46) demonstrate that whereas the reaction boundary is smeared over a considerable pressure range (also observed by Boyd and England, 1960a) with the static squeezer, a rather low reaction hysteresis ( $\leq 1$  kb) exists with the shearing squeezer.

Problem 2 was important because MacDonald's (1956) early results with a static squeezer, which are based on SiO<sub>2</sub> gel as a starting material, do not agree with the present results or with the extrapolation of Boyd and England's (1960a) data (Fig. 45). After several experiments with shearing and without, it was soon obvious that the results obtained with the use of gel were not reproducible near the equilibrium curve.

Problem 3 was prompted by discovery of a growing number of natural occurrences of coesite that apparently have been due to "impact metamorphism" (Walter, 1965), a process that involves high pressures but not necessarily high temperatures. Therefore, it was interesting to supplement the low-temperature equilibrium results in Fig. 45 with efforts at synthesis at room temperature. It was found necessary to use SiO<sub>2</sub> gel with the shearing squeezer, at a pressure of 40 kb for 30 minutes. The temperature was actually 13°C owing to water cooling of the pistons. X-ray (film) and optical examination of the charge revealed the presence of coesite with quartz and unreacted gel. Only about five per cent reaction occurred, but this result demonstrates that high pressures alone are sufficient for coesite formation.

From the present experiments one can draw conclusions regarding quartz-coesite equilibrium and the shearing squeezer itself. Reversibility of the reaction demonstrated equilibrium, and the data points

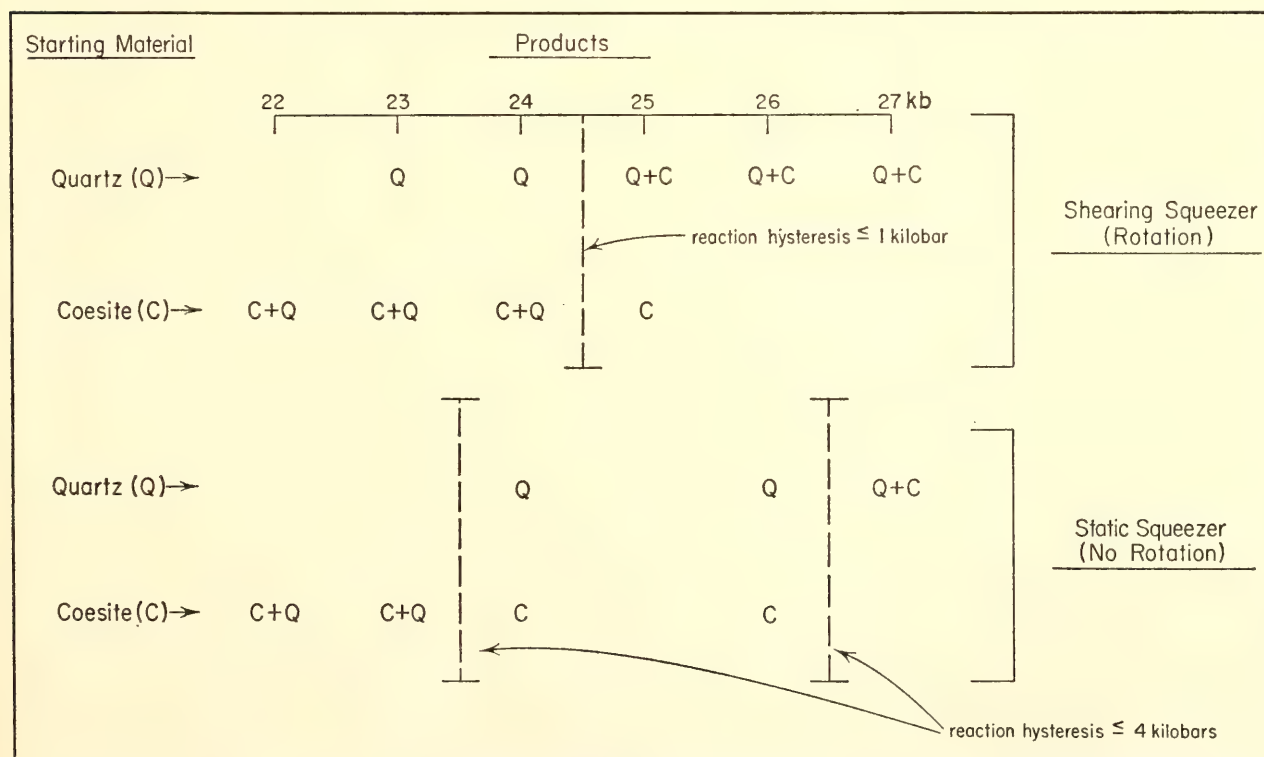


Fig. 46. Reaction hysteresis for quartz-coesite determined with the shearing and static squeezers at 500°C.



agree with an extrapolation of Boyd and England's (1960a) curve. The squeezer is unique in producing the observed reaction at low temperatures but it has limitations with respect to uniformity of pressure. It has been shown, however, that pressure uncertainty and reaction hysteresis are considerably reduced if a shearing squeezer is used rather than a static squeezer. A further advantage of the shearing squeezer is its great improvement in rates of reaction over the static squeezer, which permits synthesis of coesite at temperatures as low as 13°C. The temperature range of the present experiments, 13°C–500°C, may possibly be important in connection with explanations of the occurrence of coesite in tektites and impact products. For example, Walter's (1965) examination of Muong Nong tektites showed coesite, quartz, and

amorphous  $\text{SiO}_2$  (lechatelierite). These phases are essentially the same as those observed in the present 13°C results, and coincidentally, in about the same proportions. The implication is that in these specimens coesite must have formed at a pressure of at least 19.5 kb (although probably much higher), but a high-temperature rise was not necessary.

## IRON-TITANIUM OXIDES

*D. H. Lindsley*

Investigations are continuing in the system  $\text{FeO-Fe}_2\text{O}_3\text{-TiO}_2$  (Fig. 47). Previously the phase relations of the magnetite-ulvöspinel series (*Year Book 61*, pp. 100–106) and the hematite-ilmenite series (*Year Book 62*, pp. 60–63) were presented as functions of oxygen fugacity ( $f_{\text{O}_2}$ ) and temperature. This year attention has

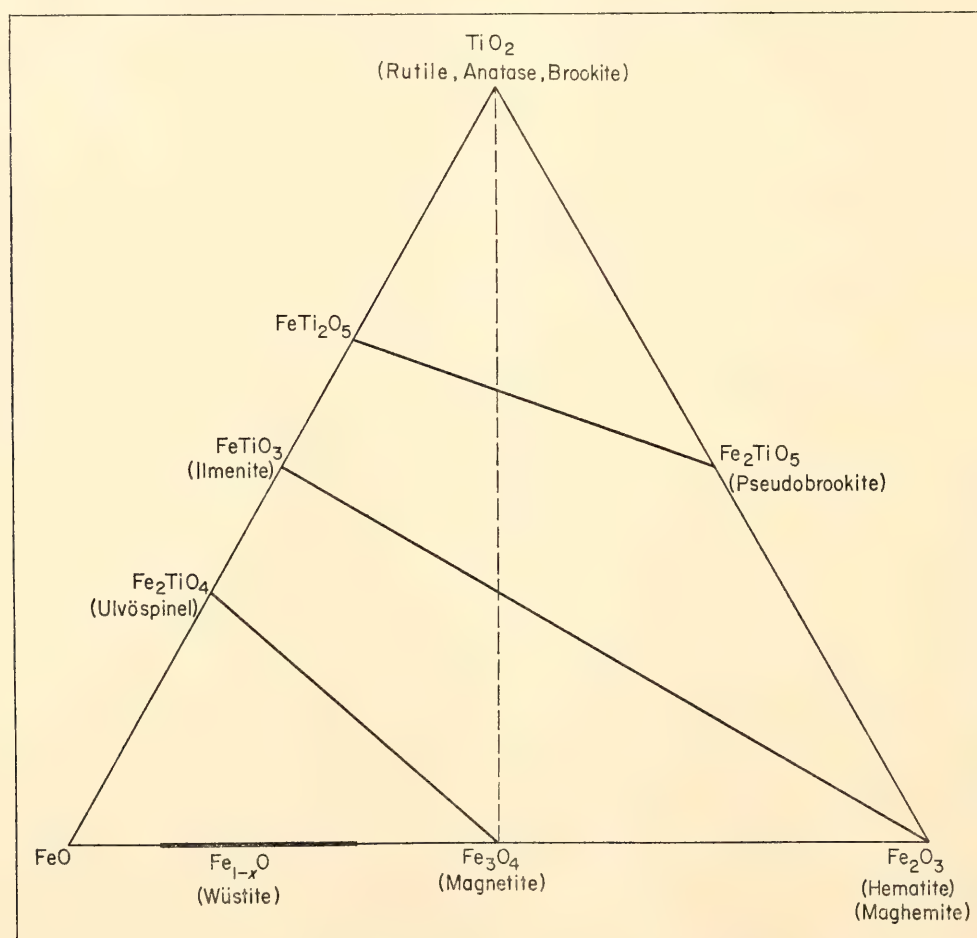


Fig. 47. Compositions of three solid-solution series in the system  $\text{FeO-Fe}_2\text{O}_3\text{-TiO}_2$ . At low temperatures the join magnetite-rutile (dashed line) becomes stable. Mole per cent.

focused on the variation of unit-cell parameters with composition in these two solid solution series and on the stability relations of the  $\text{FeTi}_2\text{O}_5$ - $\text{Fe}_2\text{TiO}_5$  (pseudobrookite) series (Fig. 47). The previous assumption that magnetite<sub>ss</sub>-ilmenite<sub>ss</sub> equilibria are essentially independent of total pressure is confirmed.

The effect of composition on unit-cell parameters in the magnetite-ulvöspinel and the hematite-ilmenite series is relevant to use of these minerals as oxygen barometers (*Year Book 62*, p. 64). Large molar volume differences between possible coexisting pairs would lead to a pressure effect on the free energy and hence the oxygen fugacity of a given equilibrium pair. Unit-cell parameters of standard samples previously synthesized in the magnetite-ulvöspinel and ilmenite-hematite series are presented in Figs. 48 and 49, respectively; molar volumes for

the two series are given in Fig. 50. The cell parameters were refined from X-ray diffractometer data with the use of the program of Burnham (*Year Book 61*, pp. 132-135).

Consider the effect of a pressure change at constant bulk composition and temperature on the compositions of coexisting ilmenite<sub>ss</sub> and magnetite<sub>ss</sub>. (Bulk composition remains constant and the coexisting phases remain binary if, for each mole of  $\text{Fe}_2\text{O}_3$  transferred from one phase to the other, 1 mole of FeO and of  $\text{TiO}_2$  is transferred in the opposite direction.) The assemblage  $\text{Usp}_{40}$  (40 mole per cent ulvöspinel, 60 per cent magnetite) +  $\text{Ilm}_{90}$  (90 mole per cent ilmenite, 10 per cent hematite) is stable at  $860^\circ\text{C}$  and  $10^{-12.7}$  atm  $f_{\text{O}}$  (*Year Book 62*, p. 64). The transfer of 1 mole each of FeO and  $\text{TiO}_2$  from the  $\text{Ilm}_{ss}$  to the  $\text{Usp}_{ss}$  and the back transfer of 1 mole of  $\text{Fe}_2\text{O}_3$  result in a

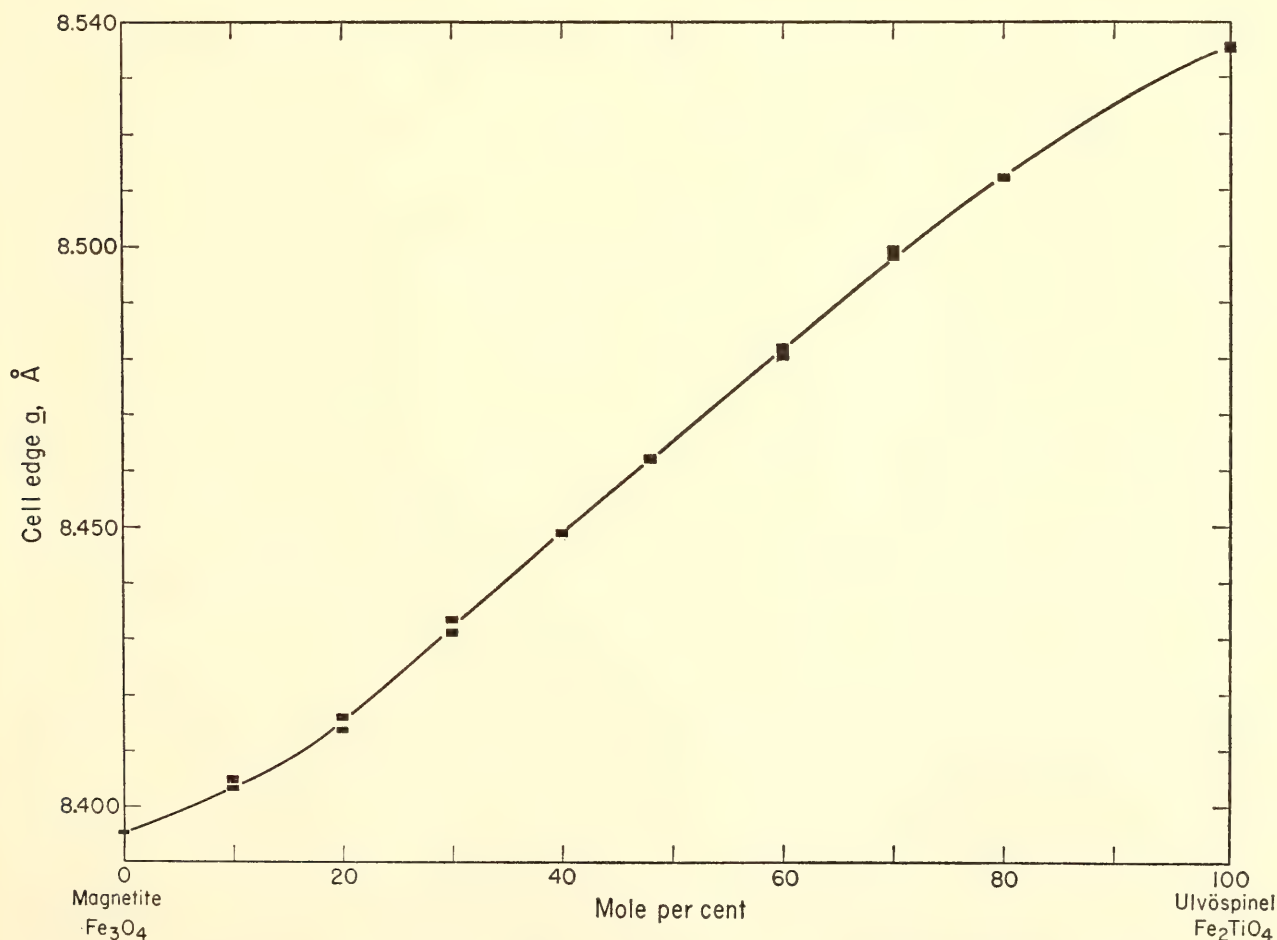


Fig. 48. Variation of cell edge  $a$  with composition in the magnetite-ulvöspinel solid solution series. Data for this and Fig. 49 were computed from X-ray diffractometer data using Burnham's program (*Year Book 61*, pp. 132-135).



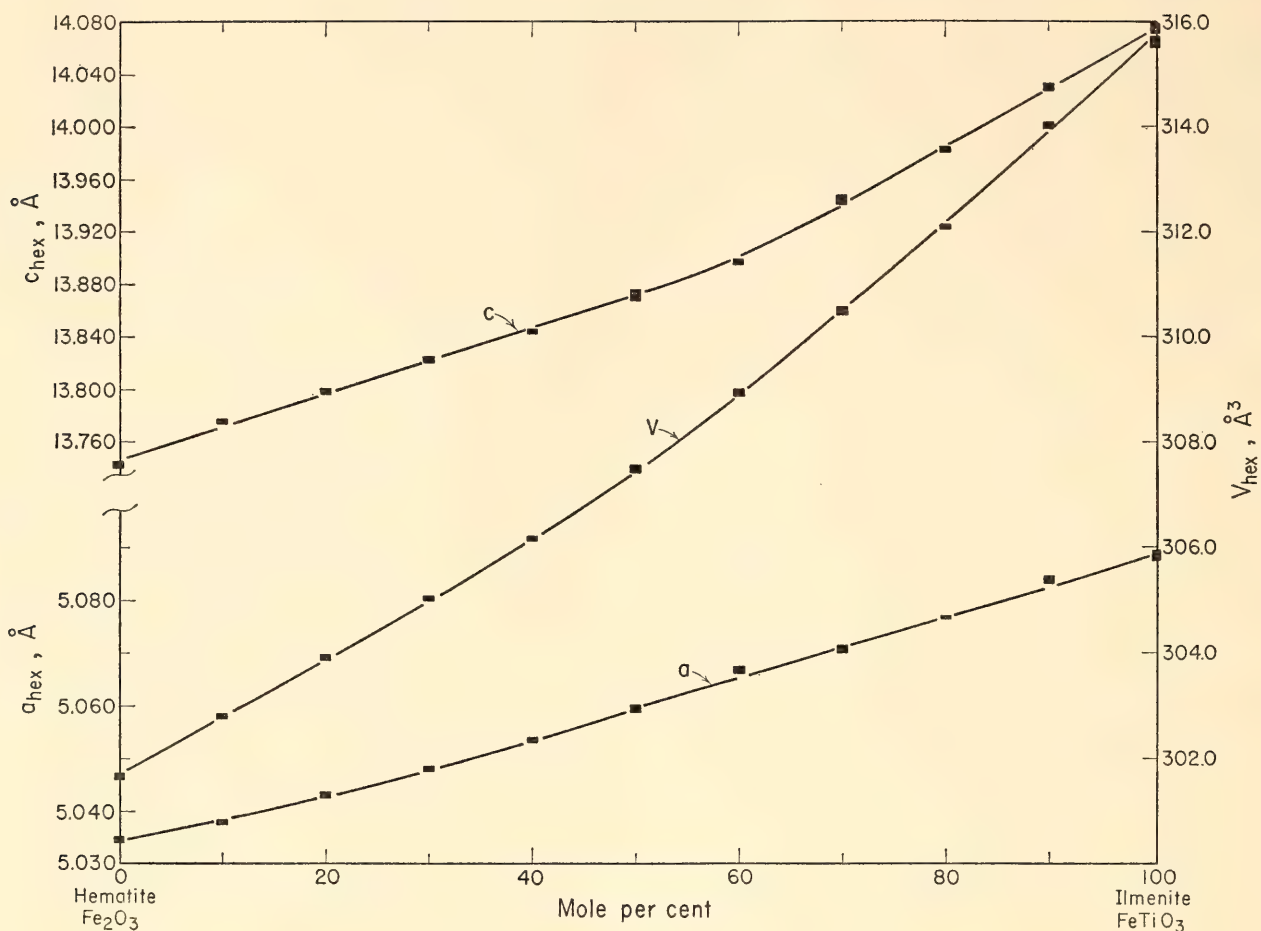


Fig. 49. Variation of lattice parameters with composition in the hematite-ilmenite solid solution series (*Year Book 61*, pp. 132–135).

molar volume increase of  $0.9 \text{ cm}^3$  or  $0.022 \text{ cal/bar}$ . Thus for a 1,000-bar pressure increase the contribution of this molar volume change to the free energy is only  $-22 \text{ cal/mole}$ , which is negligible compared with other free energies involved.

The total pressure effect on the  $f_{\text{O}_2}$  of the coexisting phases can be calculated following the method of Eugster and Wones (1962, pp. 91–92). Consider again the assemblage  $\text{Usp}_{40} + \text{Ilm}_{90}$ , stable at  $860^\circ\text{C}$  and  $10^{-12.7} \text{ atm } f_{\text{O}_2}$ , and allow the bulk composition as well as the composition of each phase to change. Isothermal oxidation accompanying a  $10^{0.5}\text{-atm}$  increase to  $10^{-12.2} \text{ atm } f_{\text{O}_2}$  yields the assemblage  $\text{Usp}_{32} + \text{Ilm}_{85}$  (*Year Book 62*, p. 64). The volume change per mole of  $\text{O}_2$  consumed in the reaction is  $3.6 \text{ cm}^3$  or  $0.086 \text{ cal/bar}$ . The free-energy change for a 1,000-bar pressure increase would therefore be  $-86 \text{ cal/mole}$ , corresponding to a

change in  $f_{\text{O}_2}$  of  $10^{-0.02} \text{ atm}$ . This effect is so small that it can be neglected in most applications of the magnetite-ilmenite oxygen barometer.

#### *Pseudobrookite Series*

Following common usage, the term “pseudobrookite series” is applied to the  $\text{FeTi}_2\text{O}_5\text{-Fe}_2\text{TiO}_5$  solid solution series (Fig. 47), although in the strict sense the term should be applied only to phases whose compositions approach  $\text{Fe}_2\text{TiO}_5$  composition. For convenience and at the expense of elegance the  $\text{FeTi}_2\text{O}_5$  end member (unknown as a mineral) is termed “ferropseudobrookite.” Akimoto, Nagata, and Katsura (1957) have shown complete solid solution in the series at  $1,150^\circ\text{C}$ . At lower temperatures, however, the pseudobrookite join must be broken to permit the assemblage magnetite + rutile found in low-grade metamorphic rocks. Experi-

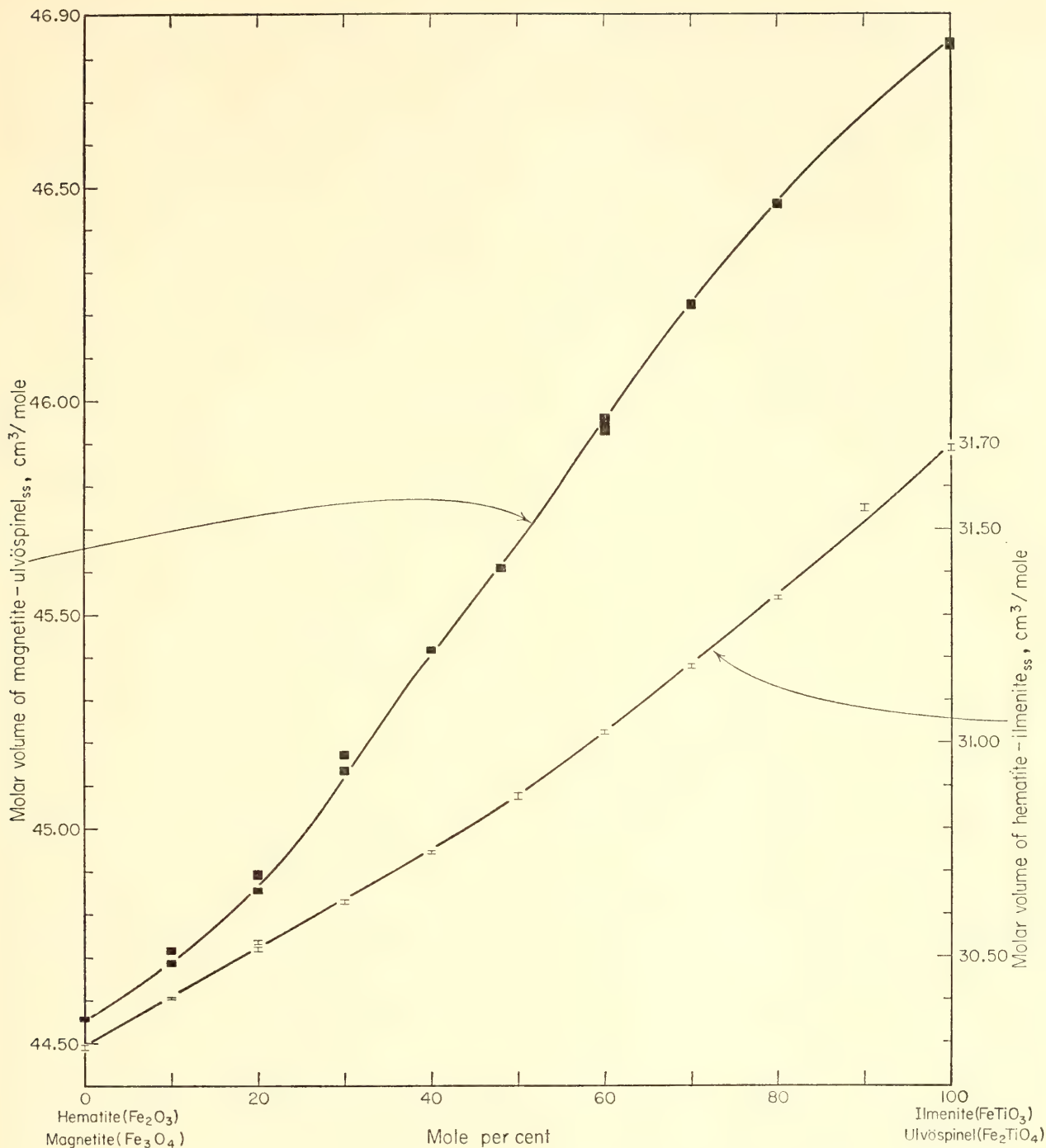


Fig. 50. Molar volumes of the magnetite-ulvöspinel and of the hematite-ilmenite solid solution series as functions of composition.

ments on the  $\text{FeTi}_2\text{O}_5$  end member have established the reversible reaction



at  $1,140^\circ\text{C} \pm 10^\circ\text{C}$ . This reaction explains the absence of natural occurrences of ferropseudobrookite. Hydrothermal experiments at 2 kb and the  $f_{\text{O}_2}$  of the magnetite-hematite buffer on inter-

mediate hematite-ilmenite solid solutions show that above  $700^\circ\text{C}$  the starting material is oxidized essentially to pseudobrookite ( $\text{Fe}_2\text{TiO}_5$ -rich solid solutions) whereas at  $600^\circ\text{C}$  the compositionally equivalent assemblage hematite<sub>ss</sub> + rutile occurs. Experiments 40 days in duration have been insufficient to demonstrate the breakdown reaction  $\text{Fe}_2\text{TiO}_5 = \text{Fe}_2\text{O}_3 + \text{TiO}_2$ ; however, experiments on inter-



mediate members of the pseudobrookite series suggest that the breakdown will take place at about 600°C. Solid solutions of the pseudobrookite series thus decompose to hematite-ilmenite<sub>ss</sub> + rutile, the decomposition temperature decreasing from 1,140°C at the FeTi<sub>2</sub>O<sub>5</sub> end to about 600°C at the Fe<sub>2</sub>TiO<sub>5</sub> end. The decomposition interval for intermediate compositions may intersect the hematite-ilmenite solvus, yielding the three-phase assemblage hematite<sub>ss</sub> + ilmenite<sub>ss</sub> + rutile; it has not yet been verified experimentally. It is clear that the entire pseudobrookite series becomes unstable at temperatures well above those at which the join magnetite-rutile is thought to exist (below ~400°C).

#### FERROSILITE

*D. H. Lindsley*

Work on the stability relations of FeSiO<sub>3</sub> (ferrosilite) has continued. As a result of further experiments in solid-media pressure apparatus, some revision has been made of subsolidus portions of the phase diagram presented last year (*Year Book 63*, p. 175); much of the diagram is now comparable in general to that for MgSiO<sub>3</sub>. Subsolidus relations for the intermediate Fe-Mg pyroxenes have been predicted from knowledge of the end members, and these predictions are now being tested.

#### *Ortho-Clino Inversion in Ferrosilite*

The phase diagram for ferrosilite has been extended down to 625°C (Fig. 51). Recent studies on stability relations of enstatite polymorphs (Sclar, Carrison, and Schwartz, 1964; see also Fig. 32) had led to the suggestion that the FeSiO<sub>3</sub> phase diagram should show at low temperatures a stability field of clinoferrosilite; at higher temperatures, a field of orthoferrosilite; and at still higher temperatures but below the solidus, a field of protoferrosilite, this last coinciding with the fields for ferrosilite III and clinoferrosilite reported last year (*Year*

*Book 63*, pp. 174–175). If the analogy with enstatite has validity, then the ferrosilite III and clinoferrosilite obtained from high-temperature experiments at 17–45 kb must have inverted from a non-quenchable phase—here called “proto?-ferrosilite.”

The postulated low-temperature stability field for clinoferrosilite has been confirmed experimentally. A reversible phase boundary between orthoferrosilite and clinoferrosilite lies at about 800°C between 20 and 40 kb (Fig. 51). The boundary has also been metastably reversed at 10 kb, in the stability field of fayalite + quartz; the metastable extension intersects zero pressure at about 800°C. A noteworthy feature of this curve is its virtual independence of pressure, suggesting that the molar volumes as well as compressibility dependence on pressure are identical for orthoferrosilite and clinoferrosilite. Molar volumes of the two polymorphs at room temperature and pressure are essentially identical (see p. 203).

Discovery of the low-temperature stability field of clinoferrosilite strengthens the hypothesis that the region of Fig. 51 between the orthoferrosilite field and the solidus is that of an unquenchable new polymorph, presumably proto?-ferrosilite. Direct evidence for its existence must probably await development of X-ray techniques for use at the requisite pressure and temperature. Some indirect evidence, however, does support this hypothesis. There is no detectable change in slope of either the solidus or the boundary with orthoferrosilite between ferrosilite III and clinoferrosilite (Fig. 51); this is consistent with the view that they are the boundaries of a single phase. Furthermore, runs on a pyroxene (Fe<sub>0.4</sub>Mg<sub>0.6</sub>) SiO<sub>3</sub> show a similar field from which the quench products are always polysynthetically twinned clinopyroxene, strongly indicative of an inversion from another polymorph. Synthetic protoenstatite commonly inverts to clinoenstatite upon quenching, so it seems reasonable to

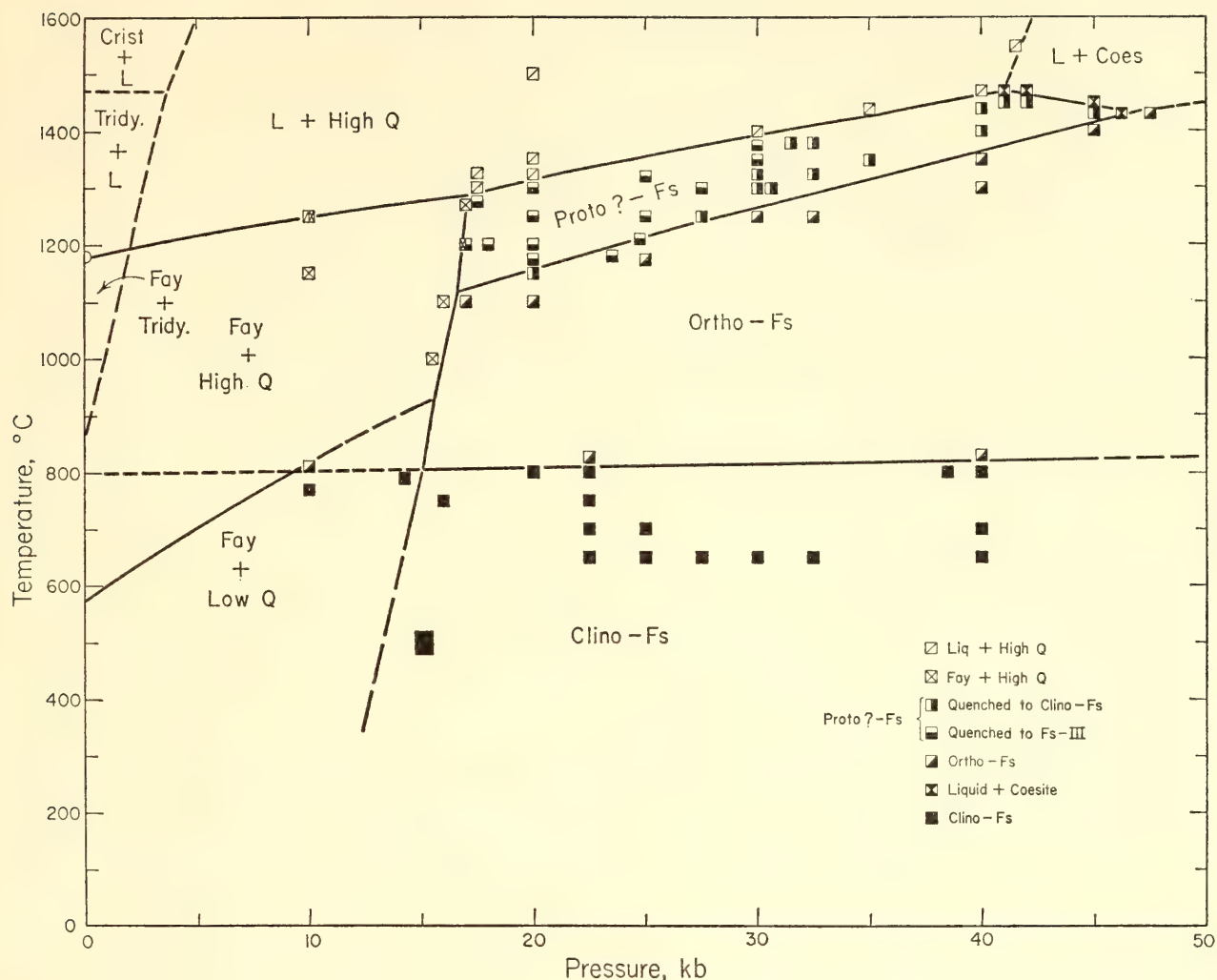


Fig. 51.  $P$ - $T$  diagram for the composition  $\text{FeSiO}_3$  in equilibrium with metallic iron. "Proto?-ferrosilite" is never found in the quench; quench products are ferrosilite III and clinoferrosilite. Experiments in the fayalite + quartz field bracketing the metastable extension of the ortho-clino curve show incipient breakdown to fayalite + quartz.

assume that clinoferrosilite and ferrosilite III might also form as quench products of proto?-ferrosilite. Inasmuch as the proto? to ortho inversion is sluggish (1–20 hours for partial reaction), it is suggested that the proto? polymorph persists metastably in the orthoferrosilite field during quenching. The proto? to clino inversion, however, takes place rapidly when the ortho-clino curve, or perhaps a metastable proto?-clino curve, is crossed. Experiments using differential thermal analysis at high pressure are planned to distinguish these possibilities.

No stability field has been found for ferrosilite III. Temperature quenches in the pressure apparatus employed in these experiments are necessarily accompanied

by a decrease in pressure, and it is suggested that ferrosilite III may form metastably upon quenching when the charge enters the field of fayalite + quartz before inversion to clinoferrosilite can take place.

#### *Intermediate Iron-Magnesium Pyroxenes*

A low-temperature stability field predicted for clinohypersthene (Fe-Mg pyroxene) has been confirmed. Orthopyroxene of the composition  $\text{Fe}_{0.4}\text{Mg}_{0.6}\text{SiO}_3$  inverts at least partially to clinopyroxene at 20 kb and at temperatures of 900°C and lower. Extrapolation of the data to lower pressures suggests the existence of an orthorhombic (hypersthene) field



above and a monoclinic (clinohypersthene) field below an inversion interval lying somewhere between 600°C and 900°C.

Thus natural calcium-poor pyroxenes that have crystallized below that temperature range—for example, pyroxenes in some charnockites and metamorphosed peridotites and pyroxenites—would be clinohypersthene on the basis of these experimental results. Authenticated reports of clinohypersthene in such rocks, however, are rare. Possible explanations of the apparent discrepancy between experimental results and reported field occurrences are that (1) extrapolation to lower pressures of data obtained at 20 kb may be invalid; (2) small amounts of Ca or other components may drastically affect stability relations of the polymorphs; or (3) occurrences of clinohypersthene may be more common than is generally supposed.

#### *Stability of $(\text{Fe}_{0.95}\text{Mn}_{0.05})\text{SiO}_3$*

Bowen (1935) suggested that the clinoferrosilites described by him from vugs in several obsidians might have been stabilized by the presence of components such as  $\text{MnSiO}_3$ . Recently Bown (1965) reported microprobe analyses of clinoferrosilite from Naivashan obsidian yielding a composition near  $(\text{Fe}_{0.95}\text{Mn}_{0.05})\text{SiO}_3$ . Pyroxene of this composition, readily synthesized at 25 kb, 1,300°, dissociates to olivine + tridymite *in vacuo* at 1,140° and to olivine + quartz at 600° and 800°C, 2 kb total pressure (mainly  $P_{\text{H}_2\text{O}}$ ), and the oxygen fugacity of the fayalite magnetite-quartz buffer. Thus manganiferous ferrosilites of this composition are stable, if at all, only at low temperatures at atmospheric pressure.

#### *Chemical Analysis of Synthetic Ferrosilite*

C. O. Ingamells' microchemical analysis of a portion of orthoferrosilite synthesized for use as a microprobe standard confirms the inference that ferrosilite synthesized in iron containers at high pressures and temperatures has the composition  $\text{FeSiO}_3$  (Year Book 63, p.

174). The sample was 98–99 per cent pure pyroxene by optical examination, the visible contaminants being metallic iron and quartz. The metallic iron is believed to account for the slightly high value reported for FeO (Table 7). Special thanks are owed to Ingamells for the extra care devoted to this analysis.

TABLE 7. Analysis of Ferrosilite Synthesized at 25 kb, 1,250°C for Several Hours in an Iron Capsule\*

	Synthetic Ferrosilite	Theoretical for $\text{FeSiO}_3$
$\text{SiO}_2$	45.10	45.54
$\text{TiO}_2$	0.00	.....
$\text{FeO}^\dagger$	54.72	54.46
$\text{MnO}$	0.00	.....
$\text{MgO}$	0.12	.....
$\text{CaO}$	0.02	.....
	99.96	

\* C. O. Ingamells, analyst.

† Total iron as FeO; includes some metallic Fe. Qualitative tests showed a small  $\text{CO}_2$  content.

#### HEAT FLOW AT AJO, ARIZONA

*Peter M. Bell and Robert F. Roy<sup>8</sup>*

Recently a rather striking relation between upper-mantle velocity ( $P_n$ ) and geography was demonstrated by Herrin and Taggart (1962). The western United States area is characterized by anomalously low velocities in the upper mantle. The low velocities may indicate that the upper boundary of the "low-velocity layer" of Gutenberg (1926, 1948) is coincident with the base of the crust. Inasmuch as the low-velocity layer may be caused by partial melting of the mantle (Press, 1959) as well as by a transition in chemical composition (Clark and Ringwood, 1964), it seems likely that anomalous temperatures are also involved (Birch, 1952; MacDonald and Ness, 1961). The present study is a measurement of heat flow at Ajo, Arizona (Fig. 52), which is located in an area of low  $P_n$  velocity.

<sup>8</sup> Harvard University.

In the Ajo area two prospecting wells with cored specimens were available. Temperatures were measured at 10-meter intervals in the wells (diamond drill holes Nos. HS-1 and HS-2) with a specially designed six-thermistor probe (accuracy  $\pm 0.02^{\circ}\text{C}$ , precision  $\pm 0.001^{\circ}\text{C}$ ). Thermal conductivities of the core specimens were measured with a divided-bar apparatus at  $20^{\circ}\text{C}$  and  $40^{\circ}\text{C}$ , and at 100 and 200 bars. Figure 53 shows a plot of the measured temperatures for HS-1. The vertical component of heat flow in each interval of a vertical drill hole can be calculated from the following equation (Roy, 1963):

$$fz = - \left( \frac{T_2 - T_1}{z_2 - z_1} \right) \left( \frac{z_2 - z_1}{\sum_i^n z_i / K_i} \right) \quad (1)$$

where  $fz$  = vertical component of heat flow;  $T_2 - T_1$  = temperature difference along depth interval,  $z_2 - z_1$ ;  $z_i$  = thick-

ness of the zone of influence of each  $K_i$ ;  $K_i$  = thermal conductivity average for each interval  $i$ ;  $n$  = number of  $K$ s that influence  $z_2 - z_1$ .

The mean temperature gradient and the average conductivity, which are the two terms on the right in Equation 1, are plotted for each interval in Fig. 53. Also plotted is the heat flow for the same intervals, which is the product of the two terms. The "best value" of heat flow for each conductivity unit was calculated by fitting a curve to a temperature vs. resistance-integral plot and measuring its slope. The temperatures were then recalculated from the fitted curve and its  $T$  intercept, and the residuals were examined. The residuals were  $\leq 0.01^{\circ}\text{C}$ .

A check on local geologic interpretations can be made by utilizing the intersection of the andesite dike (Fig. 53) with the porphyritic quartz monzonite. For situations of this kind Roy (1963) has taken into account refraction of the heat

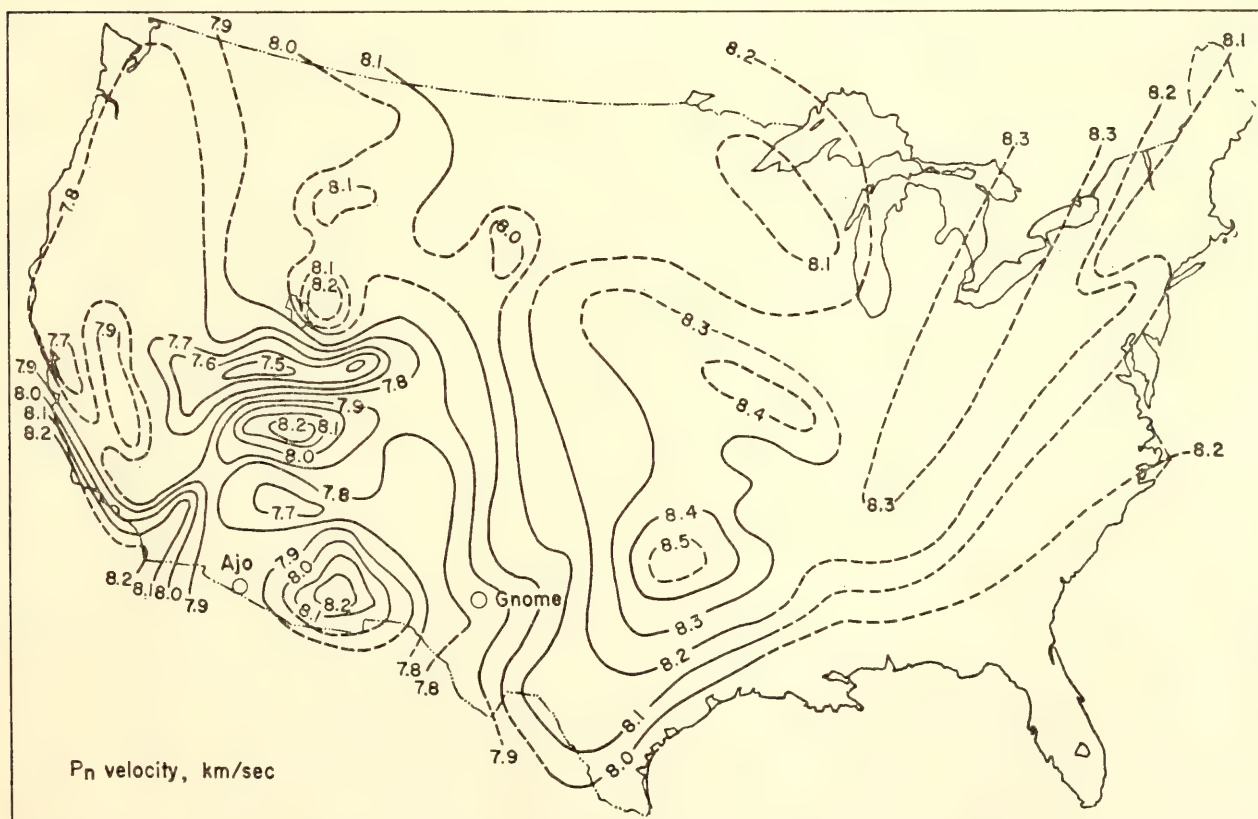


Fig. 52.  $P_n$  contours after Herrin and Taggart (1962). Diamond drill holes Nos. HS-1, HS-2, and K-1 are located at Knox claim approximately 15 miles south of Ajo, Arizona, in Organ Pipe Cactus National Monument.



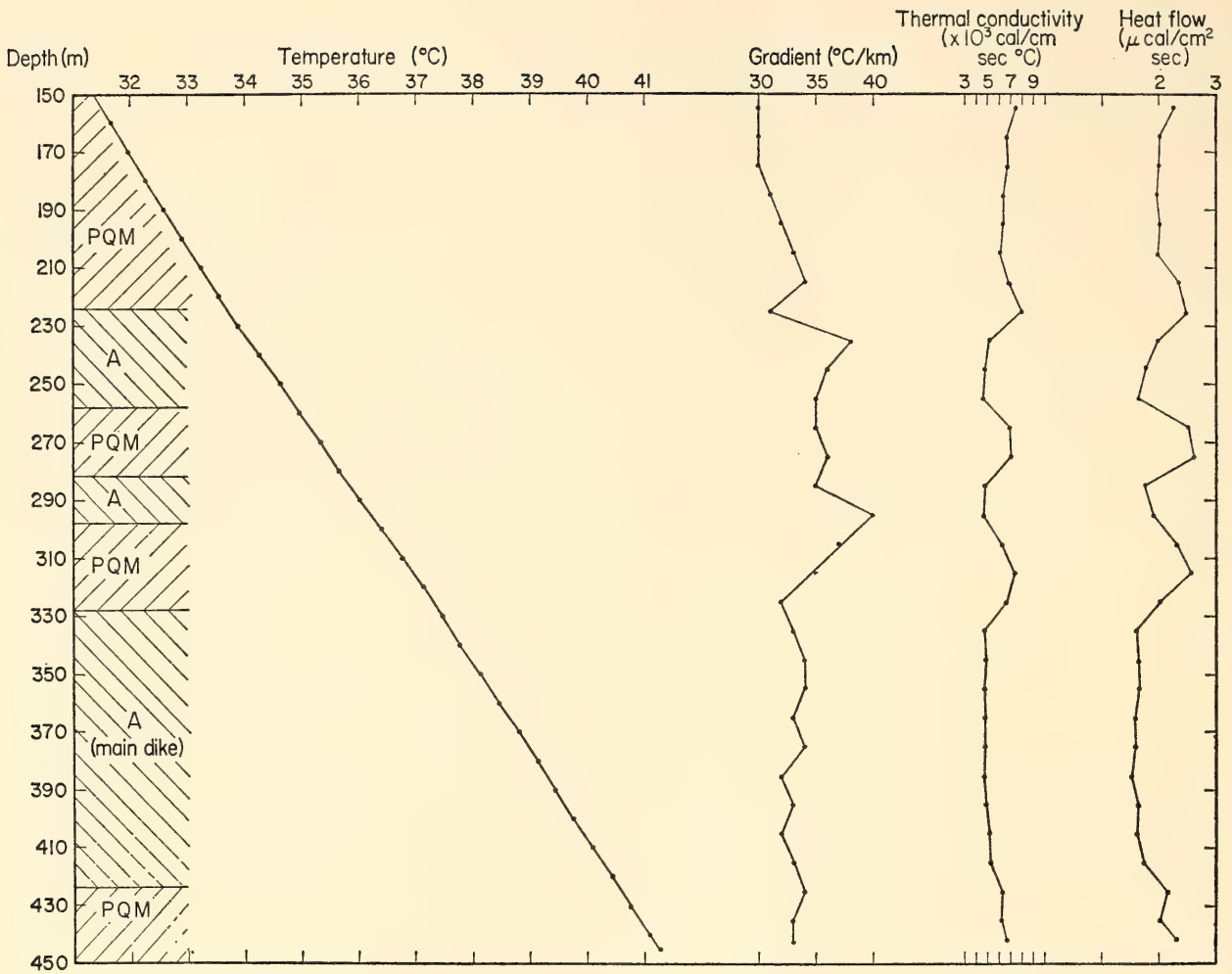


Fig. 53. Temperature, gradient, thermal conductivity, and heat flow as functions of depth. Data points plotted for HS-1. A, andesite; PQM, porphyritic quartz monzonite.

flow vector, and gives as the solution for a tabular dipping dike:

$$\sin \alpha_1 = \left[ \left( 1 - \frac{f2v}{f1} \right) \left( 1 - \frac{K_2}{K_1} \right)^{-1} \right]^{1/2} \quad (2)$$

where  $\alpha_1$  = angle of dip of the dike;  $f2v$  = vertical component of heat flow in the dike of conductivity  $K_2$ ; and  $f1$  = heat flow in the surrounding rock of conductivity  $K_1$ .

The values used (Table 8) were calculated by Equation 1 and substituted in Equation 2, giving  $\alpha_1 = 64^\circ$  for the base of the dike. This checks conveniently with the observed dip from the surface outcrop and well intersection of about  $65^\circ$ .

Corrections for the temperature and pressure coefficients of conductivity have been applied in the plots of Fig. 53. The steady-state terrain corrections (Birch,

1950) have been calculated to a horizontal distance equal to 10 times the

TABLE 8. Average Conductivities and Mean Heat Flows for Andesite Dike and Porphyritic Quartz Monzonite Intervals

Depth Interval, meters	Rock	Average Conductivity	Mean Heat Flow
155-220	Porphyritic quartz monzonite	6.79	2.14
220-260	Andesite	4.95	1.80
260-280	Porphyritic quartz monzonite	7.08	2.50
280-300	Andesite	4.88	1.83
300-320	Porphyritic quartz monzonite	6.70	2.33
320-420	Andesite (main dike)	4.36	1.62
420-445	Porphyritic quartz monzonite	6.33	2.17

depth of the holes. This introduces a further correction of no more than  $-2.5$  per cent. The resulting value of heat flow for HS-1 is  $2.1 \mu\text{cal}/\text{cm}^2 \text{ sec}$ . An additional correction might be necessary owing to the refraction effect of a nearby alluvium-filled valley. The estimated magnitude of this correction is less than 10 per cent of the heat flow.

A value of 2.1 is relatively high in comparison with most continental aver-

ages ( $1.2\text{--}1.5 \mu\text{cal}/\text{cm}^2 \text{ degree}$ , according to Clark and Ringwood, 1964), and by itself should not be considered representative for the region or for  $Pn$  lows in general. However, it is consistent with the possibility that high temperatures may be associated with the low  $Pn$  velocities in this region. Confirmation of this possibility will require further heat-flow observations in other areas of low  $Pn$  velocity.

## STATISTICAL PETROGRAPHY

*F. Chayes*

The account of an unusually large proportion of the work undertaken during the report year has either been submitted for publication or already appeared in print. It includes (1) a study of the silica-alkali balance in Cenozoic basic volcanics (part I), which, together with a proposed classification of basalt based on it, has been submitted for publication; (2) a detailed discussion of the use of discriminant functions in distinguishing oceanic-island and circumoceanic Cenozoic volcanics (part VA) published by Chayes and Velde; (3) a description of some of the geometrical properties of linear and higher-order discriminant functions in closed arrays (parts VB and VC), now in press. In addition, Zies has completed and submitted for publication his study of the rare titanium-rich mineral cossyrite, from the type locality in Pantelleria, and a discussion of the geometrical basis of modal analysis by Chayes has been published (see *Proceedings of the First Symposium on Quantitative Electron Microscopy* of the Armed Forces Institute of Pathology).

Since so much of the work of the year either already is or soon will be generally available, there is no need here for an extended review. The bulk of the year's work is essentially statistical, its immediate emphasis being in some instances substantive and in others procedural. Although there is nothing novel in the statistical basis of parts I, II, and III,

for instance, the results themselves are new and intrinsically interesting. On the other hand, the results obtained in parts VB, VC, and VD are provisional and inconclusive, but the methods by which they are reached are both promising and, in petrology at least, still rather uncommon.

Considering first the results of immediate substantive interest, there seem to be no earlier estimates of the relative abundance of analyses of Cenozoic basic volcanics of the three levels of silica saturation. That less than one quarter of the norms of such analyses lack both  $ne$  and  $Q$  may accordingly be expected by some readers and surprising to others. More than three quarters of the norms of the recently discovered submarine-ridge volcanics are of this type, however, and this curious distinguishing property of submarine volcanism seems to have escaped earlier notice. Indeed, whether it was curious or distinctive could hardly be surmised except in relation to the first estimate. And although the data upon which the first estimate is based have been public knowledge for years, data reduction techniques suitable for processing such masses of information are only now becoming generally available.

The discovery that most of the analyzed rocks called "andesite" would not be classified as andesite in the major petrographic systems (part III) reflects a similar inability to process the available



data by conventional methods. It is impossible to estimate with any precision the number of man-hours required to compute the requisite 1,500 norms, but despite the interest that would have attached to the result no such massive hand calculation has ever been attempted in connection with the delineation of a single rock type. Given the data on magnetic tape, however, passage from the raw analyses to the frequency distributions of Table 9 is a matter of something less than two minutes' work for a reasonably modern computer. Efficient exploitation of the vast accumulation of information about the chemical composition of rocks is now well within reach.

Except for the study of oceanic-island and circumoceanic basalts, however, the material on discriminant function analysis, reviewed in section V, is primarily of methodological interest. The effect of closure on the independence of discriminant functions based on different sets of variables is summarized, and some of the principal geometrical properties of such functions in ternary arrays are described. Higher-order terms can be introduced into any discriminant function, but the "cumulative polynomial" discriminant functions based on any  $(M - 1)$  variables of an  $M$ -variable closed array are analytically identical in the sense that each coefficient in one such function can be obtained as a linear combination of the coefficients of any one of the others. There is neither need for nor advantage in calculating more than one of these functions, for all will yield identical data partitions. If, furthermore,  $M = 3$ , as in the ternary closed array, they are all curves of identical locus in trilinear coordinates. The account concludes with an example suggesting that the discriminant function may provide a good numerical model of the graphical procedure by which field boundaries are located in phase-equilibrium diagrams.

### *I. The Silica-Alkali Balance in Cenozoic Basic Volcanics*

Conventions governing the allocation

of alkaline earths and ferrous oxides to *ol* and *px* provide a rather effective buffer against the appearance of *ne* or *Q* in the norms of basic volcanics, variation in the *ol/px* ratio being able to accommodate a considerable variation in silica and alkali content. Despite this buffering effect, however, the norms of most Cenozoic basic volcanics do in fact contain either *ne* or *Q*.

Excluding highly leucitic rocks, whose norms almost never lack *ne*, and the basalts of the submarine ridges, which have recently attracted much attention and are briefly discussed in part II, a literature survey conducted during the past three years has yielded a punch-card library containing 2,082 analyses of Cenozoic volcanic rocks called ankaramite, ankaratrite, basalt, basanite, diabase, dolerite, essexite, limburgite, nephelinite, oceanite, picrite, sakalavite, tephrite, tholeiite, trachybasalt, or trachydolerite in the source references. Of these analyses of basic volcanics, only 471, or 22.1 per cent, yield norms lacking both *ne* and *Q*. Although the collection is not exhaustive it now contains a large proportion of published analyses; of Cenozoic basic volcanics for which complete analyses have been published, almost certainly fewer than 24 per cent and probably fewer than 23 per cent yield norms lacking both *ne* and *Q*. The rather broad compositional range that can be tolerated without the emergence of normative imbalance between alkalis and silica is thus commonly exceeded by Cenozoic basic volcanics.

This interesting property forms the keystone of a proposed classification in which basic volcanics are divided into two major groups. More than three quarters of the available analyses of such rocks may be classified immediately as alkaline or subalkaline depending on whether they are *ne* or *Q* normative. Assignment of the remainder, whose norms lack both indicators, is accomplished by means of a discriminant based upon any pair of the normative parameters *ol*, *di*, *hy*, in a fashion reviewed in



part VC. A full description of the classification is awaiting publication.

## II. The Silica-Alkali Balance in Basalts of the Submarine Ridges

At the present writing there are 39 published analyses of basalts collected from submarine ridges at depths of more than 1,000 meters. It has already been pointed out (Engel and Engel, 1964a) that in most of these analyses  $\text{TiO}_2$  content is intermediate between the values recently proposed as characteristic of "circum-oceanic" and "oceanic" basalts (Chayes, 1964), the oceanic data upon which the proposal was based having been drawn exclusively from oceanic islands. This matter was discussed briefly in last year's report and at more length in a subsequent publication (Chayes and Velde, 1965), but neither discussion described the major normative distinction between previously known basalts and those of the submarine ridges.

In the preceding section it was suggested that probably more than 77 per cent of analyses of Cenozoic basic volcanics are either *ne* or *Q* normative. For "nominal basalts" (i.e., rocks in whose source-reference names the word basalt is the principal or only noun) the same data lead to a figure of 73 per cent. Of the 39 currently available analyses of submarine-ridge basalts, however, none is *ne* normative and only 7, or 18 per cent, are *Q* normative; in 4 of the 7 *Q* normative analyses, furthermore,  $\text{H}_2\text{O}$  content and  $\text{Fe}_3/\text{Fe}_2$  ratio suggest that extensive postconsolidation alteration may have seriously shifted normative parameters.

Although the submarine-ridge basalts are quite variable in composition, their variation, unlike that of most Cenozoic basic volcanics, nearly always lies within the range that yields no normative indication of silica-alkali imbalance. The principal normative parameters that compensate for this imbalance are *hy* and *ol*; other things being equal, the amount of compensation possible varies directly with the ratio  $(ol + hy)/di$ . In the sub-

marine-ridge basalts as a whole, however, as may be seen from Fig. 54, this ratio is not conspicuously high; in fact, except for materials from the Kilauean rift zone (Moore, 1965), it seems somewhat lower than in most Cenozoic basic volcanics. Since the submarine-ridge basalts tend to be intermediate in  $\text{TiO}_2$  content, it is worth noting that normative conventions concerning that oxide directly influence the alkali-silica balance, each mole of  $\text{TiO}_2$  freeing an equivalent amount of  $\text{SiO}_2$  that would otherwise be allotted to  $\text{FeO}$ .  $\text{Fe}_2\text{O}_3$  affects the alkali-silica balance in identical fashion, but both effects are ordinarily small.

There appears to be no simple—and probably there is no single—explanation for the remarkable scarcity of *ne* and *Q* in the norms of submarine-ridge basalts. In view of the present fever of speculation concerning these rocks it is perhaps as well to remind the unwary that little is known about them, despite the strenuous and highly productive effort recently expended in their study. Indeed, there are several small island groups for each of which there is more recorded information than is now available for all of the submarine ridges of all the oceans.

## III. On the Level of Silica Saturation in Andesite<sup>9</sup>

Of the common rock names that are thought to have reasonably clear connotations about chemical composition, few are as simply defined as andesite and perhaps none is so frequently misused. Systematists and textbook writers<sup>10</sup> are in almost complete agreement that modal and normative quartz are low or lacking in andesite. Harker's famous manual (1954, p. 163) says that quartz is "typically absent," though he recognizes a "quartz-bearing and more acid division, known as dacites or quartz-andesites." In Williams, Turner, and Gilbert (1954, p. 95) the only mention of primary quartz is as an intergrowth with alkali

<sup>9</sup> In collaboration with D. Velde.

<sup>10</sup> The latter with the clear but virtually sole exception of Moorhouse (1959).



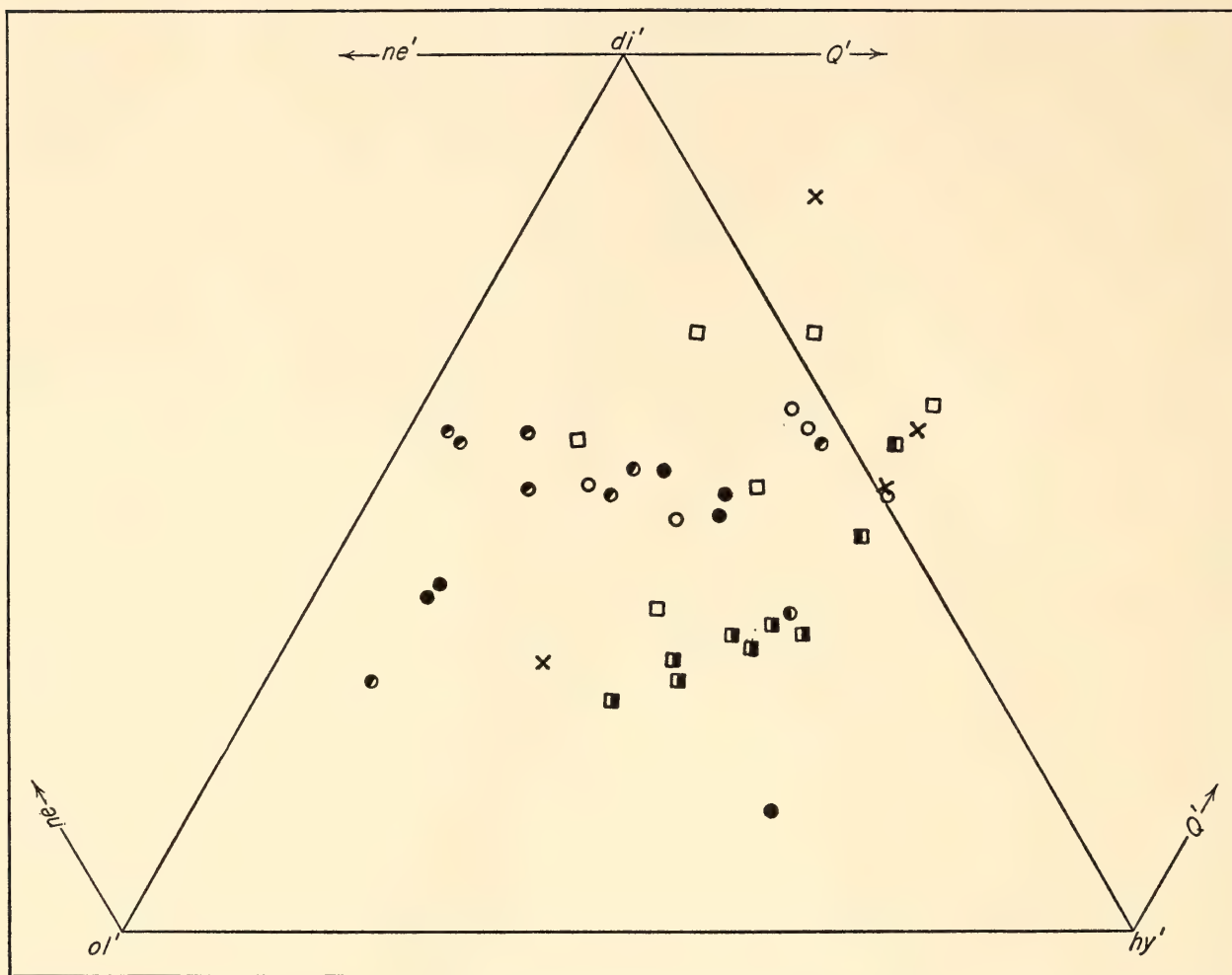


Fig. 54 Projection—in the normative ternaries *ne-ol-di*, *ol-di-hy*, and *hy-di-Q*—of all submarine basalts collected at depths greater than 1,000 m.

feldspar, “but any lava in which the total content of . . . potassic feldspars exceed 10 per cent should be called trachyandesite.” Heinrich (1956, p. 20) says simply that there is “no essential quartz” in the diorite-andesite family and adds (p. 72) that “quartz is rare in andesites, although it has been recorded as strongly resorbed phenocrysts (or xenocrysts?).”

In reference works and more advanced texts the situation is much the same, and has been for more than half a century. In the CIPW system the rang *andase*, taking its name “from andesite of the Andes” (Cross *et al.*, 1903, p. 262), is so defined that its normative *Q* content must be less, and will usually be very much less, than 12.5 per cent. In Vol. 2 of the great treatise of Iddings (1913), the

cornerstone of American petrography, the word “quartz” does not appear in the discussion of “andesites proper” and the presence of more than accessory amounts of either modal or normative quartz invariably leads to the use of varietal names that never found wide acceptance and have now been largely abandoned. Of the 21 andesite norms listed in Iddings’ tables, however, 9 contain more than five per cent of *Q* and only 4 lack it entirely; even this early there is some suggestion of conflict, though whether it is between rocks and systems or merely between norms and modes is not clear.<sup>11</sup>

<sup>11</sup> Volume 1 (Iddings, 1907, p. 372) contains one of the earliest suggestions that many dacites are mistakenly called andesites because their quartz escapes notice or is misidentified.

According to Rosenbusch and Osann (1923) the groundmass of andesites and porphyrites is rarely holocrystalline, and it is only in such instances that a little quartz may be found in it; their account makes no other mention of the mineral except as a foreign inclusion. Nor is it mentioned in the glossary definition of Holmes (1920). Johannsen (1937, p. 160) repeats Harker's dictum that andesites containing quartz are called quartz-andesites or dacites, and of the nine andesite modes he gives, one contains 0.5 per cent of quartz and the others none at all. Shand (1943) places andesite in the saturated class of his system, reserved for rocks "which contain neither free silica nor any unsaturated mineral," and similar or only slightly less restrictive definitions are given, for example, by Wahlstrom (1950), Barth (1962), and Niggli (1954).

Shand ultimately hedges his decision a little by describing the andesites in a chapter entitled "The saturated (and slightly oversaturated) rocks." Lacroix (1933) defines andesites as "rocks without or almost without quartz" and adds that in holocrystalline varieties the excess of silica usually finds expression as quartz; of the 12 andesites described in the body of his treatise, all are *Q* normative and in 8 *Q* exceeds seven per cent. Johannsen manfully remarks that despite the abundance of andesite he has been able to find record of only a few chemically analyzed specimens and "none of these is typical" (*op. cit.*, p. 168). In similar vein Rittmann (1962, p. 104) complains that Daly's average andesite "corresponds in chemical composition to a typical dacite" and his average dacite to rhyodacite.<sup>12</sup> After noting that the norm calculated from "average andesite" contains 15 per cent of *Q*, Tyrrell (1929, pp. 126-127) rejects this figure as too high, "for a critical revision of the analyses would certainly result in the rejection of some as not typical andesites." He nevertheless concludes that andesite lava "may contain excess silica

up to a maximum of about 10 per cent," and von Wolff (1951) puts the same upper limit on quartz content.

Judging from analyzed rocks described

TABLE 9. Distribution of *Q* in the Norms of 1,526 Analyses of Cenozoic Volcanics Called Andesite in the Source References

Per cent <i>Q</i> ≤	All Analyses		Analyses With H <sub>2</sub> O ≤ 2.0	
	Japan Only	All Localities	Japan Only	All Localities
0	10	56	7	44
2	24	46	23	42
4	30	61	30	56
6	49	101	47	89
8	61	134	60	123
10	52	125	44	103
12	59	163	57	138
14	88	167	82	143
16	82	153	78	124
18	65	127	57	95
20	64	124	58	91
22	53	92	42	73
24	42	69	34	50
26	28	47	21	28
28	15	24	10	14
30	12	18	4	6
32	4	7	2	4
34	3	5	3	3
>34	4	7	1	4
Σ	745	1,526	660	1,230

under the name "andesite," however, this is a considerable underestimate. Frequency distributions of normative quartz in Cenozoic volcanics called "andesite" in the source references are posted in Table 9, and Fig. 55 is a histogram of one of these; the interested reader may readily satisfy himself that deletion of all

<sup>12</sup> Rittmann's explanation of this curious confusion is that "many so-called andesites are in fact only hyaloandesites, containing occult quartz and sanidine in the glassy groundmass," but this can hardly account for such large average discrepancies if, as Johannsen (*op. cit.*, p. 160) maintains, andesites are "generally holocrystalline-porphyritic." *Caveat emptor.*



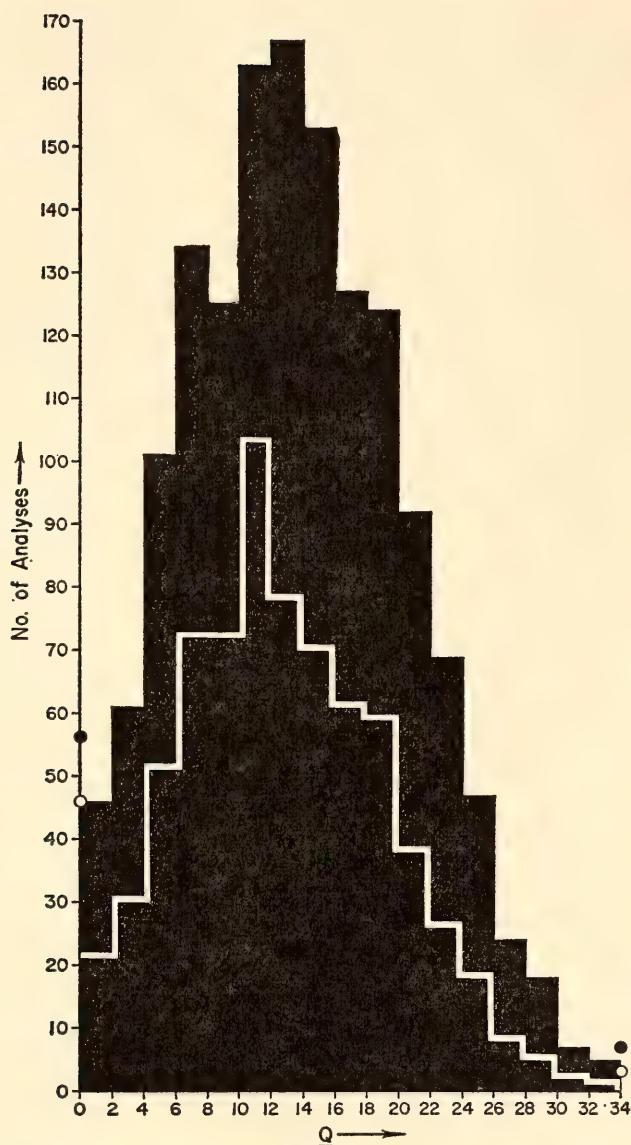


Fig. 55. Frequency distribution of  $Q$  in norms of 1,526 Cenozoic andesites. White line is trace of histogram of  $Q$  in norms of 781 non-Japanese Cenozoic andesites. Circles, frequencies of analyses whose norms contain either more than 34 per cent  $Q$  or none.

analyses containing more than two per cent  $H_2O$  does not materially change the character of the sample distribution. Of 1,526 Cenozoic rocks named "andesite," whose analyses are now included in our punch-card library, only 56, or less than four per cent, are devoid of normative quartz, and 1,003, or very nearly two thirds, carry more than Tyrrell's proposed maximum of ten per cent of excess silica. A considerable excess of molar silica over that required to express alkalis, available alkaline earths, and

$FeO$  as feldspars and pyroxenes is evidently highly characteristic of rocks referred to as andesites in detailed local descriptions.

What can have occasioned this marked incompatibility between systematists and descriptive petrographers, between, so to speak, the codifiers and users of rock names? The standard response, implicit in the way in which Johannsen and Tyrrell use the word "typical," would be simply that the descriptive petrographers either collect the wrong rocks or do not use the right names. We do not believe this is the correct explanation. Descriptive petrographers and petrographic systematists alike agree that andesite is an exceedingly common volcanic rock, second in abundance only to basalt, yet rocks which satisfy systematic definitions of andesite are evidently in short supply. Surely when the incidence of "erroneous" classification is as high as this it is appropriate to suggest that the classifications are hopelessly at variance with the facts, that the standard definitions of andesite are definitions not so much of rocks as of ideas about rocks.

Of course, as in every taxonomic argument, much more than taxonomy is involved. For one thing, in the basalt-andesite "sequence" there seems no longer room for doubt that saturated and slightly oversaturated materials are very much scarcer than those that are clearly over- or undersaturated. Further, silica saturation like that shown in the central region of Fig. 55, exceedingly common among volcanics, is not at all common among plutonic rocks of clearly igneous habit. Nockolds (1954), for instance, presents averages, and norms computed from them, of 36 common saturated or oversaturated plutonic rock types; in 10 of these  $Q$  is less than 6 per cent, in 21 it is more than 20 per cent, and in only 5 does it lie between 6 and 20 per cent; not one falls in the range 8–17 per cent, an interval that includes the mean, median, and mode of the andesite distributions shown in Table 9 and Fig. 55.



Clearly the genetic problems raised by the observed distribution of normative *Q* in rocks called andesite are as bothersome as the taxonomic ones. To most petrologists they will also seem more interesting and, alas, more important.

IV. On Changes in Composition Effected by Cyclic Assimilation

Since nearly all basalts are at least partly crystalline—true basalt glasses being both rare and of negligible volume—it is rather generally agreed that during its passage through the lithosphere basalt magma is little if at all above its liquidus temperature. Most assimilatory reactions are thought to be endothermic, and since the major if not the sole source of energy for them is the heat of crystallization of the invading magma it is usually considered that syntectic reaction between basalt magma and country rock must be of rather limited extent. Alleged extreme composition changes effected in this fashion are thus immediately suspect. In an example recently discussed (Chayes, 1965*b*; see Abstract 1435 in Summary of Published Work), for instance, one of the indirect consequences was reduction of the average amount of TiO<sub>2</sub> from 3.06 per cent in an initial alkali-basalt magma to 1.14 per cent in subalkaline-basalt magma formed, presumably, by remelting of the syntectic product. This would require the alkali-basalt magma to incorporate 1.68 times its own mass of a sial diluent free of TiO<sub>2</sub> and is patently absurd if the reaction is supposed to occur in the course of a single cooling cycle.

If the assimilation is to occur over several cycles of remelting, however, the situation is very different. Interest then centers not on the amount of assimilation possible in a single cycle but on the number of cycles required to effect some net change. Assuming that at each cycle the rejuvenated magma is able to assimilate the same proportion of its own volume before freezing, and that it assimilates material of the same composition, as in

the preceding stage, it may be shown that the number of cycles required to effect a net change of  $|\alpha - a_n|$  in constituent *X* is

$$n = [\log (\alpha - \beta) - \log (a_n - \beta)] / \log (1 + d)$$

where  $\alpha \equiv$  per cent of *X* in initial magma;  $\beta \equiv$  per cent of *X* in sial diluent; *d*  $\equiv$  amount of diluent added, as a proportion of the invading magma; *a<sub>n</sub>*  $\equiv$  per cent of *X* in syntectic rock at close of the *n*th cycle and in rejuvenated magma at the beginning of the (*n* + 1)th cycle. A number of cycles equal to the integral part of *n* will stop the process short of the desired point and a number equal to the first integer above *n* will carry it beyond.<sup>13</sup> The values of *n* as a function of different assigned values of *d* for the problem described are shown in Table 10.

TABLE 10. Number of Assimilatory Cycles (*n*) Required to Reduce an Initial Content of 3.06 Per Cent TiO<sub>2</sub> to a Final Value of 1.14 Per Cent for Various Amounts (*d*) of Diluent Containing No TiO<sub>2</sub>

(100 <i>d</i> )	<i>n</i>
1	99.3
5	20.2
10	10.4
15	7.1
20	5.4
25	4.4
35	3.4

The argument is, of course, a gross oversimplification, the assumption that the assimilatory capacity remains unchanged being particularly unrealistic if the only important source of thermal energy is indeed heat of crystallization. It probably materially underestimates *n*, and the assumption that constituent *X* is entirely lacking in the sial diluent would have a similar but less marked effect. Even ignoring this probable underestimate, however, the number of cycles

<sup>13</sup> Potential effects of cyclic fractional crystallization or remelting can of course be formulated in similar fashion.



required, for values of  $d$  that would be regarded as reasonable by most petrologists, seems considerably larger than would be expected in a single magmatic episode or even, for large masses of magma, in a series of such episodes. It seems much less of a strain on the imagination to suppose that the two types of basalt are tapped from different layers (or reservoirs) in the crust. Perhaps the assimilatory hypothesis could find application in speculations about the origin of these layers rather than of specific lavas, so that, in a time sense, its frame of reference would be geological rather than immediately petrological.

A further complication may be worth noting. The central problem of the circumoceanic environment is not the origin of subalkaline basalt but rather the origin of the far more abundant andesite, and, of course, syntectonic origin of andesite magma has been suggested many times. From the point of view of the  $\text{TiO}_2$  balance, however, this only makes matters more difficult, for the  $\text{TiO}_2$  content of andesite is considerably less than that of subalkaline basalt.

#### *V. Some Actual and Potential Petrographic Applications of Discriminant Function Analysis*

The extent to which a dichotomy based on one set of properties can be recaptured by means of information about a second set is often quite important to the naturalist. This is one of the principal questions the two-group discriminant function is designed to answer. It is supposed that each item in a sample may be unequivocally assigned to one of two mutually exclusive groups by means of some initial set of properties, and that for each of the items in the sample observed, values of each of a second set—the variables  $[X_{aj}]$ ,  $j = 1, 2, \dots, w$ —are available. From the latter a set of weighting coefficients,  $\lambda$ , is calculated in such fashion as to maximize the “distance” between the sample averages

$\bar{z}_1 = \bar{\mathbf{x}}'_1 \lambda$  and  $\bar{z}_2 = \bar{\mathbf{x}}'_2 \lambda$ , this distance being defined as the ratio

$$(\bar{z}_1 - \bar{z}_2)^2 / (n_1 \sigma_1^2 + n_2 \sigma_2^2) \quad (1)$$

where  $\sigma_i^2$  is the variance of  $z$ , and  $n_i$  the number of items, in group  $i$ . No other set of weighting coefficients for these particular variables can yield a larger distance, and if the number of variables is large enough it is most unlikely that a linear combination based on any other set of weighting coefficients will more nearly recapture the original partition.

The problem is a very general one, occurring at many levels in many branches of natural science, and the solution afforded by the discriminant function is intuitively appealing. Further, although the necessary calculations are so tedious that the method remained almost unused until the electronic computer became generally available, they are, in principle, simple and straightforward. If each item is characterized by a row vector

$$\mathbf{x}'_a = \{x_1, x_2, \dots, x_w\} \\ a = 1, 2, \dots, (n_1 + n_2)$$

in which each element is measured from its own group mean, and the matrix  $\mathbf{X}$  is the assemblage of such row vectors, the required weighting coefficients are the elements of the column vector

$$\lambda = (\mathbf{X}'\mathbf{X})^{-1}\mathbf{d}$$

where  $[d_j] = (\bar{x}_{1j} - \bar{x}_{2j})$ , the numerical subscripts here denoting groups and the barred values averages. Whenever a problem is overtly taxonomic or can be recast in taxonomic terms, discriminant function analysis offers a convenient and revealing procedure for sample description and data reduction.

*A. Distinguishing oceanic-island and circumoceanic basalts.*<sup>14</sup> Preliminary results, reported in *Year Book 63* (Chayes and Métais, p. 179), indicated that a binary discriminant based on  $\text{TiO}_2$  and  $\text{MgO}$  might be somewhat more efficient

<sup>14</sup> In collaboration with D. Velde.

than one based on  $\text{TiO}_2$  alone, but that more complex discriminants yielded no further increase in efficiency. These results have now been confirmed by a thorough study, a full account of which has already been published (Chayes and Velde, 1965); the abstract (No. 1441) is reproduced in the Summary of Published Work, below.

*B. Discriminant functions in closed arrays; the general case.* The fact that the sum of  $M$  variables in each item is a constant, the same for all items in the sample, exerts little direct influence on discriminant functions based upon  $N \ll M$  variables. As  $N \rightarrow M$ , however, this independence decreases, and when  $N = M - 1$  it vanishes entirely. It may be shown that (1) discriminants based upon all sets of  $(M - 1)$  variables partition the data identically, and (2) the discriminant and the coefficients of the discriminant function based upon any set of  $(M - 1)$  variables may be obtained as linear combinations of the coefficients and discriminant of any other set. If one is seeking the most efficient discriminant based upon  $N$  variables, it will usually be necessary to compute functions for most of the  $M!/N!(M - N)!$  possible sets if  $N < M - 1$ , but it will never be necessary to compute more than one function if  $N = M - 1$ .

This interdependence, which is both useful and intuitively reasonable, is either eliminated or greatly reduced if occasional higher-order terms are included in the calculation. If all terms of a cumulative polynomial expansion are used,<sup>15</sup> however, it may be shown that conditions 1 and 2 of the preceding paragraph again apply for all sets of  $(M - 1)$ -variable functions of the same order. This rather surprising result follows more from definition than from argument, but formulation of the defi-

nitions requires an extensive notation that would be out of place in a report of this kind. The matter is discussed in detail in a paper awaiting publication (Chayes, 1965a).

*C. Discriminant functions in ternary closed arrays.* One of the principal advantages of discriminant function analysis is that it permits simultaneous consideration of many variables, and there is of course no graphical analogue of a function based on more than three open or four closed variables. When the number of variables is small enough for graphical treatment, however, the geometrical properties of the discriminant function prove very striking. An example drawn from the paper mentioned above is shown in Fig. 56, in which  $X_1 \equiv di'$ ,  $X_2 \equiv hy'$ , and  $X_3 \equiv ol'$ . Since the members of the normative pairs  $(ne, hy)$  and  $(Q, ol)$  are incompatible, norms projecting in this ternary lack both  $ne$  and  $Q$ . In the diagram the open circles are projections of norms of rocks intimately associated with  $Q$ -normative Cenozoic volcanics, the solid circles of those associated with  $ne$ -normative Cenozoic volcanics. The taxonomic problem involved is the one already mentioned in part I, but the substantive context is of no immediate concern. The questions at issue may be very simply stated in terms of the symbols just defined: How, and how well, can one guess, from the position of a point in the diagram, whether it is the center of an open or solid circle? Both questions may be answered readily by means of discriminant function analysis.

The binary linear discriminant functions computed from the data are

$$X_1 + 0.866X_3 - 0.7297 = 0$$

$$X_2 + 0.134X_3 - 0.2694 = 0$$

$$X_2 - 0.155X_1 - 0.1566 = 0$$

and because of the closure restraint these are equations of identical locus in trilinear coordinates; their trace in the ternary is shown by the straight line in Fig. 55. The constant in each equation is

<sup>15</sup> That is, the discriminant is based upon all terms for each item in

$$\sum_{p=1}^q \left( \sum_{i=1}^{M-1} (X_i) \right)^p$$



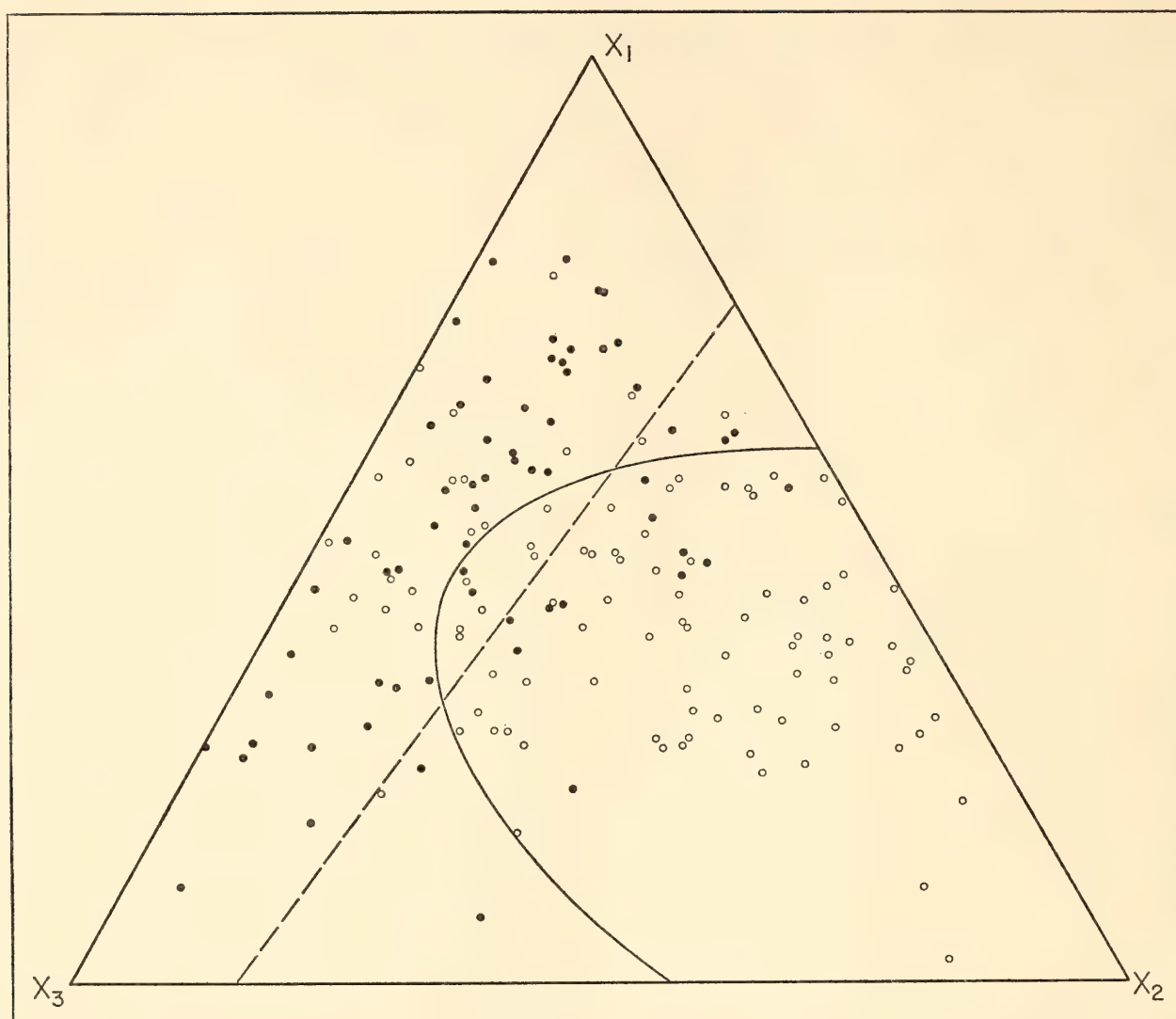


Fig. 56. Binary linear and quadratic discriminants in a ternary closed array. Projections of norms of rocks intimately associated with *Q*-normative Cenozoic volcanics (circles); *ne*-normative Cenozoic volcanics (closed circles).

the ternary equivalent of an intercept; when  $X_3 = 0$ , for instance,  $X_1 = 72.97$  per cent,  $X_2 = 26.94$  per cent. In similar fashion, the coefficient of the second term in each equation is a slope. Since the equations are of identical locus they partition the data identically, so that if one has been computed there is no need to compute either of the others.

From the first equation, to illustrate the use of the function, one would guess that a particular point was the center of an open or solid circle depending on whether its coordinates were such that the sum  $(X_1 + 0.866X_3)$  was greater or less than 0.73. The percentage of correct guesses tells how well the discrimination

is made in the sample; with adequate precautions about randomness in the sampling procedure it would also be legitimately interpreted as a prediction of how well the function may be expected to work in future samples. Similarly, the curve in Fig. 55 is the locus of the three possible discriminant functions of the form

$$\lambda_1 X_i + \lambda_2 X_j + \lambda_3 X_i^2 + \lambda_4 X_i X_j + \lambda_5 X_j^2 - \hat{z} = 0$$

$$0 < i \neq j \leq 3$$

For variables  $(X_2, X_3)$ , for instance, it is the trace of the equation

$$(X_2 + 1.119X_3) - (0.006X_2^2 + 0.014X_2X_3 + 0.011X_3^2) = 0.3226$$

Points lying above or to the left of this curve are classified by the discriminant function as centers of solid circles, those to the right of it as centers of open ones. Since 13 of the 63 solid circles actually fall to the right of the curve and 22 of the 97 open ones lie above or to the left of it, the efficiency of this discriminant is 125/160, or 78 per cent.

Whether a function whose efficiency is only 78 per cent will be of any practical use will depend entirely on the nature of the problem involved. In any event it should now be clear that the rationale of discriminant function analysis is remarkably similar to that of many taxonomic procedures common in chemical petrography, and that the diagram is a complete graphical analogue of the descriptive properties of the binary discriminant function in a ternary closed array.

*D. Locating field boundaries in phase diagrams.* Phase-equilibrium studies were among the first systematic experimental researches in petrology and are often cited as examples of "quantitative" investigation, as opposed to the "qualitative" or "descriptive" aspect of most other petrographic work. In fact, however, the student of phase equilibria is obliged to locate field boundaries by a dominantly qualitative appraisal of his quantitative data, the adjectives being used here without the customary and quite unrealistic pejorative connotation often attached to them in geological discourse. In principle his position is not very different from that of the naturalist who attempts to reclaim, from a study of variables, a classification based initially on attributes. The time sense is inverted, of course, but the field boundary is essentially a qualitative classification to be established by quantitative observations. It is true that most experimental petrologists do not use discriminant functions in their work, but neither do most naturalists. There is at present no systematic nongraphical procedure for locating field boundaries, but it is possible that discriminant function analysis might provide the basis for one.

A linear discriminant function based on temperature and pressure, for instance, is simply

$$\lambda_p P + \lambda_t T = \hat{z}$$

where, as before,  $\hat{z}$  and the  $\lambda$ 's are computed from the observed values of  $P$  and  $T$ . It may be written

$$P = (\hat{z}/\lambda_p) - (\lambda_t/\lambda_p)T$$

in which  $(\hat{z}/\lambda_p)$  is the intercept and  $(-\lambda_t/\lambda_p)$  the slope of a straight line in  $P$ - $T$  "space." The resemblance to an ordinary regression line is obvious but only skin deep. There is only one discriminant function for any set of data; its locus does not necessarily include the mean of either variable; there is no underlying assumption that either variable is dependent or independent in the regression sense; and the scatter of data points from the line has nothing to do with the goodness or badness of the "fit." The purpose of the line is to partition the data into two qualitatively distinct classes, and its success or failure is to be judged only by the number of correct classifications it makes.

Figure 57 is a display of data recently published by Akimoto, Fujisawa, and Katsura (1965) for the olivine-spinel transformation of  $\text{Fe}_2\text{SiO}_4$ . Solid circles denote  $P$ - $T$  coordinates at which spinel charges were unaffected or spinel grew in olivine charges; open circles denote  $P$ - $T$  coordinates at which olivine charges were unaffected or olivine grew in spinel charges. The solid line is the trace of the discriminant function computed from the data:  $P = 18.41 + 0.0375T$ . One of the solid circles falls below the line, and two of the open ones lie above it. The edges of the rectangles drawn around these points are proportional to the stated precision of the observations. Interpreting them as confidence intervals of unknown level, which is probably close to the sense in which they are intended, the true value for each point may lie anywhere in the rectangle that surrounds it. The trace of the discriminant function intersects each of the error rectangles. In this trial



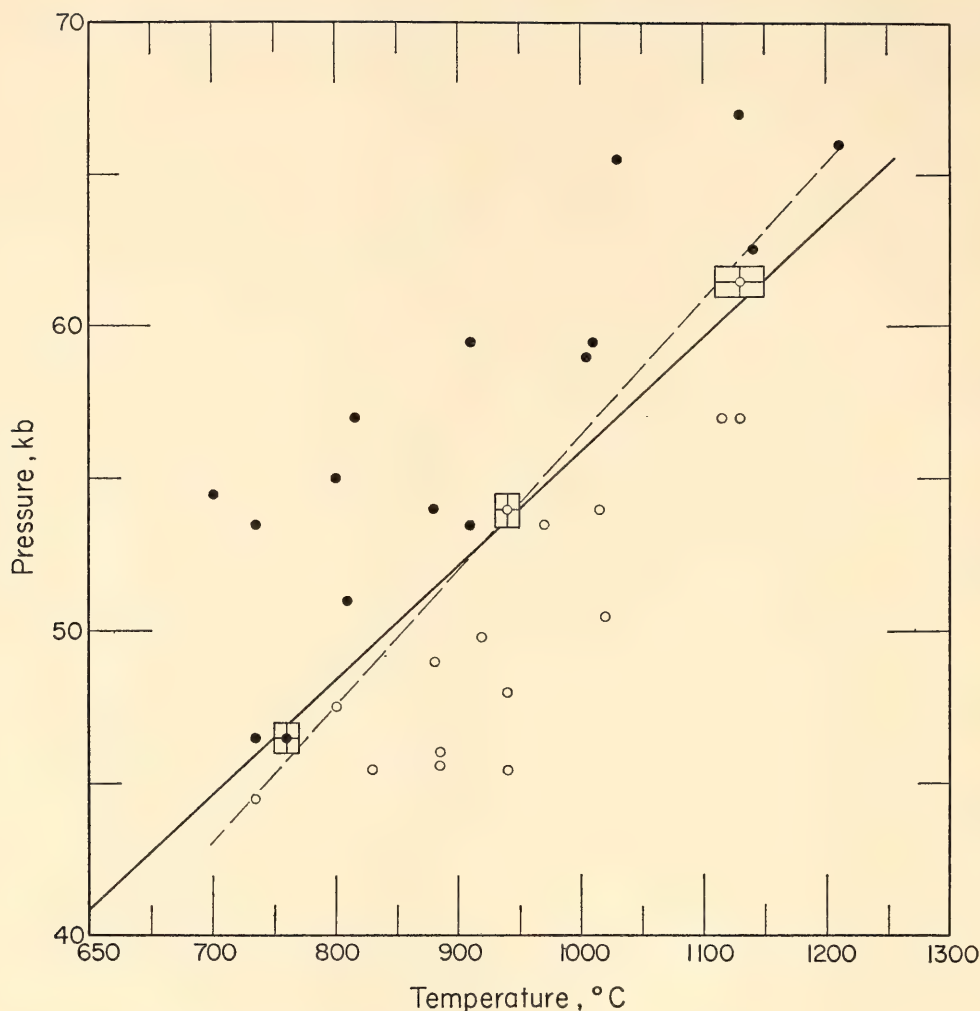


Fig. 57. Data of Akimoto, Fujisawa, and Katsura (1965) for olivine-spinel transition in  $\text{Fe}_2\text{SiO}_4$ . Dashed line, field boundary as published; solid line, field boundary as located by discriminant function; circle,  $P$ - $T$  coordinates at which olivine charges were unaffected or olivine grew in spinel charges; closed circle,  $P$ - $T$  coordinates at which spinel charges were unaffected or spinel grew in olivine charges.

calculation the discriminant function thus very nearly achieves an optimum partition.<sup>16</sup>

The purpose of this preliminary notice is largely to stimulate discussion for, despite its rather striking success with the data of Akimoto and co-workers, the method is open to serious criticism in several respects. Chief among these is the

<sup>16</sup> As the dashed line in Fig. 57 shows, Akimoto and co-workers have found, presumably by graphical means, an even more consistent one, but the line they draw is not the trace of the equation given in their text. The difference is slight but, for present purposes, rather critical. The two solid circles farthest to the right in Fig. 57, properly classified in their graph, lie below the plot of their text function.

fact that it gives equal weight to all data points regardless of their distance from the real or presumed field boundary; clearly the apparent efficiency of the partition may reflect nothing but the fact that points belonging to one class are all remote from those belonging to the other. In Fig. 56, for instance, had all runs at temperatures of less than  $900^\circ\text{C}$  been made at pressures greater than 60 kb, and all runs at temperatures over  $900^\circ\text{C}$  at pressures less than 50 kb, the passing of a line between fields occupied by open and solid circles would have been both simple and pointless. If the final curve fitting is to be by inspection, the investigator's desire to avoid wasting his time is usually

sufficient insurance against excesses of this kind, for in the end only solid and open circles that are close to each other will exert much influence on the path of the boundary. If all or a large percentage of the data points are to be used in some systematic computing procedure, however, a more formal basis for weighting the data or deciding which points are to be retained would be highly desirable.

On the whole, there is probably little advantage in locating the field boundary numerically rather than graphically if it is known in advance either that the boundary is linear in the region of interest or that only a linear approximation of it is required. Indeed, in either situation it is inefficient to spread the data points over the critical region; the best way to estimate the position of a line is to locate as well as possible two points on it that are as far as possible from each other. The results of this procedure neither require nor permit much statistical analysis. When the curvature of the field boundary is known or suspected to be appreciable, however, the situation is entirely different, for it will nearly always be preferable to estimate the shape and location of a curve by some form of calculation rather than inspection. Knowledge that such a procedure is available, furthermore, may suggest economies in the collection of data. Curve fitting by inspection, for instance, is extremely unsatisfactory unless there

are several points very close to the curve, and much of the experimenter's time may be devoted to obtaining them; for the method proposed here, however, such points are a rather desirable luxury but not in any sense a necessity. Although the example used here seems to warrant only the linear approximation, it is obvious from the discussion in part V, *B-C* that nonlinear terms of any desired form may be introduced whenever needed.

Finally, and perhaps most important, field boundaries cannot be located by inspection unless the number of variables is small enough to permit the data to be plotted on a graph or in a solid model. The location of field boundaries by means of discriminant functions is subject to no such restriction. Deprived of its customary geometric reference, the interpretation of field boundaries in multi-component "space" will no doubt be complicated and puzzling. If the discriminant function does in fact prove a satisfactory numerical analogue of the graphical procedures now in vogue, however, the mere "location" of such boundaries would pose no particular difficulty. The amount of computation required for calculation of the discriminant function increases rapidly with increase in the number of variables, but this is work for the computing machine, not for the experimenter, and in terms of machine time it is hardly likely to be of much consequence.

## GEOCHRONOLOGY AND ISOTOPE GEOCHEMISTRY

*G. L. Davis, G. R. Tilton, L. T. Aldrich,<sup>17</sup> S. R. Hart,<sup>17</sup> and R. H. Steiger*

Mineral age determination, based on the production of radiogenic lead and strontium in highly radioactive minerals, has helped to solve many geological problems over the past decade. In recent years investigators in isotopic geochemistry have begun careful studies aimed at using variations in the isotopic

composition of strontium and lead in rocks or minerals of very low radioactivity; these variations would act as natural tracers to delimit possible source materials for various rock types or to decipher genetic relationships among them. Whereas conventional age determination enables us to reach conclusions concerning the history of a rock since the time of its crystallization, the natural tracer work may give information about

<sup>17</sup> Department of Terrestrial Magnetism.



events that happened before the time of rock formation. Work in a number of laboratories has produced considerable data for strontium, but isotopic lead measurements are still relatively few.

In *Year Book 63* (pp. 241–247) we discussed some experiments involving variations in the isotopic composition of lead from potassium feldspars and basalts. A considerable part of our effort has again been directed toward lead tracer experiments. For example, we have continued to study the isotopic composition of lead in feldspars and galena from very old rocks in order to calculate the age of the earth. The usual method of calculation compares the isotopic composition of lead in a young rock or ore (modern terrestrial lead) with lead from the troilite phase of iron meteorites to obtain a  $Pb^{207}$ - $Pb^{206}$  age. The isotopic composition of modern terrestrial lead varies greatly; it may be desirable, therefore, to use lead from very old rocks because the processes responsible for the variations in isotopic composition would have operated over a shorter interval of time. The new studies at Manitouwadge, Ontario, which include age determinations and measurement of the isotopic composition of lead in feldspars and lead ore, strongly support the suggestion in *Year Book 63* that lead from the 2,700-m.y.-old rocks around Lake Superior can be used to obtain an age of 4,700 m.y. for the earth instead of the commonly mentioned value of 4,550 m.y. Results from a feldspar from a 2,700-m.y.-old pegmatite in South Africa when combined with available isotopic analyses of lead from galenas suggest that data from the African continent also give an age of 4,700 m.y. for the earth. We emphasize that much more sampling remains to be done to fully substantiate the new estimate. At present it appears that either the earth is about 200 m.y. older than was previously thought or, alternatively, the assumption that the earth initially contained lead of the same isotopic composition as that in meteoritic troilite is incorrect.

Another extension of the methods of geochronology is the beginning of an investigation using lead and strontium as natural tracers to study the genetic relationships between various igneous rocks in the Cascade Range of northwestern United States. The rocks investigated include tholeiite and high-alumina basalts, andesite, granodiorite, and basement gneiss. Preliminary measurements show important differences between the two basalt types, which indicate that it may be possible to distinguish between their derivative rocks. A major objective is to attempt to determine whether the andesites are related to one or both of the two basalt types, or whether they originate wholly or in part from crustal materials. Data obtained so far make the tholeiite basalts an unlikely source for the andesites at Mount Rainier and Mount Hood. The isotopic composition of lead and strontium in granodiorite from two plutons in the vicinity of Mount Rainier and in the andesite from the volcano are very similar. This finding, along with the chemical similarity of the rocks, implies a common source.

A major controversy in Appalachian geology has centered around the age of the sedimentary Glenarm series. The question is whether the series is contemporaneous with similar sequences of known Cambrian-Ordovician age occurring to the west of the Piedmont belt where the Glenarm is found, or whether the series predates the Paleozoic sediments and is of Precambrian age. Age measurements for the zircon from rocks intrusive into the youngest member of the Glenarm indicate ages of 550 to 600 m.y. These ages preclude deposition of any part of the series in Ordovician time, but indicate instead that deposition occurred in the Precambrian or early Cambrian era.

Another study has dealt with heat production by the radioactive elements uranium, thorium, and potassium in peridotite. In *Year Book 63* (p. 330)



we noted that a variation of more than a factor of 10 had been found in potassium contents for peridotites at St. Peter and St. Paul's Rocks on the mid-Atlantic ridge. We have now determined that the uranium content increases almost in proportion to the increase in potassium. The heat production in the sample containing the largest concentrations of potassium, uranium, and thorium is sufficient to account for the heat flow in oceanic regions should the outer 500 km of the earth's mantle consist of such material. The higher uranium and potassium concentrations correlate with an increase in the amount of hornblende in the rock, indicating that the radioactive elements are contained in that mineral. Since experimental data indicate that amphiboles are unstable at depths greater than approximately 50 km, it is necessary that the radioelement content not change greatly with the change in mineral composition if the heat production results are to be applicable at great depths in the mantle.

#### *Lead Isotopes and the Age of the Earth*

In *Year Book 63* (pp. 244–247) we discussed the calculation of the age of the earth from lead isotopes in igneous rocks and galena ores, and reviewed the assumptions underlying the calculation. Two important assumptions are that (1) the earth initially contained lead having the same isotopic composition as that observed today in the troilite phase of certain iron meteorites; and (2) leads of various isotopic compositions have evolved in systems chemically closed with respect to uranium and lead from the time of formation of the earth until the time of emplacement of the igneous rock or ore body. Subject to these assumptions the age of the earth can be determined by comparing terrestrial lead and the meteorite lead. The ratio of the increments of  $\text{Pb}^{207}/\text{Pb}^{206}$  yields a  $\text{Pb}^{207}\text{-Pb}^{206}$  age in much the same way that this age is determined for a mineral in more conventional geochronology. Most investiga-

tors have used data for lead from very young rocks and ores to calculate an age for the earth in this way. We showed in *Year Book 63* (pp. 243–244) that the isotopic composition of lead in young basalts (less than 10 m.y. old) is quite variable, proving that the closed-system assumption has been violated for these rocks. The spread in isotopic values for basalts leads to calculated age values from 4.42 to 4.63 aeons ( $\text{AE} = 10^9$  years). Data obtained in other laboratories in the past year extend these limits even further.

Because the closed-system assumption does not hold for young rocks the isotopic composition of lead in older rocks has been investigated. Failure of the closed-system assumption would introduce less error into the age calculation if lead from older rocks is used instead of lead from young rocks. In *Year Book 63* (pp. 246–247) we applied this method to feldspars from 2,700-m.y.-old granites and pegmatites from near Rainy Lake in northern Minnesota. A value of approximately 4.75 AE was found for the age of the earth by using the Minnesota feldspars, whereas commonly quoted values are about 4.55 AE. Since a rather restricted area was sampled in the Minnesota work and since the interpretation of the results depended rather critically on corrections for radiogenic lead produced by the small amount of uranium in the feldspars during the past 2,700 m.y., further measurements have been made on rocks collected at Manitouwadge, Ontario (location:  $49^{\circ}8'\text{N}$ ,  $85^{\circ}48'\text{W}$ ). This area was selected because of the presence of "conformable" galena deposits (Stanton and Russell, 1959) and of numerous pegmatites associated with so-called Algoman granites. The use of galena has the advantage that correction for radiogenic lead produced in the mineral by uranium is unnecessary and also that the large amount of lead present in the ore makes it less likely to be appreciably contaminated by lead from extraneous sources than the lead in



TABLE 11. Mineral Ages from Algonman Granites and Pegmatites at Manitouwadge, Ontario

Rock	Mineral	Age, million years				
		$\frac{\text{Pb}^{206}}{\text{U}^{238}}$	$\frac{\text{Pb}^{207}}{\text{U}^{235}}$	$\frac{\text{Pb}^{207}}{\text{Pb}^{206}}$	$\frac{\text{Pb}^{208}}{\text{Th}^{232}}$	$\frac{\text{Sr}^{87}}{\text{Rb}^{87}}$
MG-17-1	zircon*	2,500	2,610	2,700	2,710	.....
MG-17-d	zircon*	2,420	2,560	2,670	2,300	.....
MG-17	biotite	.....	.....	.....	.....	2,630
MG-20	microcline	.....	.....	.....	.....	2,590
MG-45	microcline	.....	.....	.....	.....	2,560

\* MG-17-1 and MG-17-d are light- and dark-colored fractions separated from a single sample of granite. The uranium content is 257 ppm in the light fraction, 701 ppm in the dark fraction.

feldspars, which is present only in trace amounts. On the other hand, ages of potassium feldspars can be determined by the conventional methods of geochronology, whereas the age of galena deposits must usually be inferred. Where possible it is best to work with lead from both sources.

Mineral age determinations were made

on zircon, potassium feldspar, and biotite from “Algonman” granites and pegmatites found at Manitouwadge. These results are summarized in Table 11. The zircon data are plotted in a concordia diagram in Fig. 58. The samples plot close to the line defined by the zircons from Rainy Lake and appear to have an age of about 2,750 m.y. The biotite age value shows that no

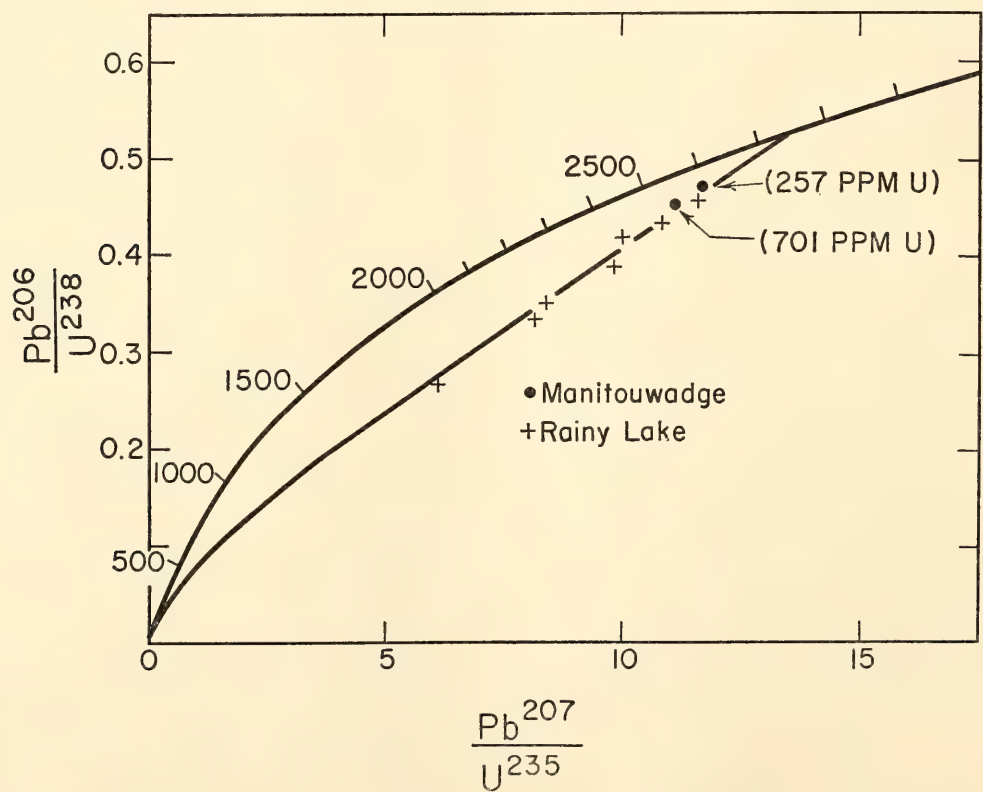


Fig. 58. Concordia diagram showing uranium/lead ratios in zircons from Manitouwadge and Rainy Lake, Ontario. Line through sample points represents pattern expected if the zircons are 2,700 m.y. old and have lost lead by continuous diffusion with a constant value of the parameter  $D/a^2$ , where  $D$  is diffusion coefficient and  $a$  is effective radius of the crystals.

severe metamorphism has affected the rocks in this area for the past 2,600 m.y. Whole-rock Rb-Sr age data, obtained on four granites, are consistent with an age of 2,600 m.y. From all the age data the Algonian rocks appear to have ages of 2,600–2,750 m.y.

The isotopic compositions of lead from four feldspar and two galena samples are given in Table 12. The isotopic compositions are for the samples as received without acid washing unless otherwise indicated. The isotopic ratios are shown graphically in Figs. 59 and 60. The line through the feldspar points in Fig. 59 is a “secondary isochron,” which gives the pattern expected should all feldspars initially have the same isotopic ratios as the galenas but contain additional radiogenic lead owing to the decay of the small amounts of uranium in the samples over the past 2,700 m.y. Within the limits of error the feldspar data conform to this hypothesis. It is also noteworthy that one sample, MG-45, contains less radiogenic lead than was found in any of the Minnesota feldspars. Without acid washing or any corrections for radiogenic lead produced by uranium in the sample, the isotopic composition of lead in MG-45 is nearly the same as that observed in the

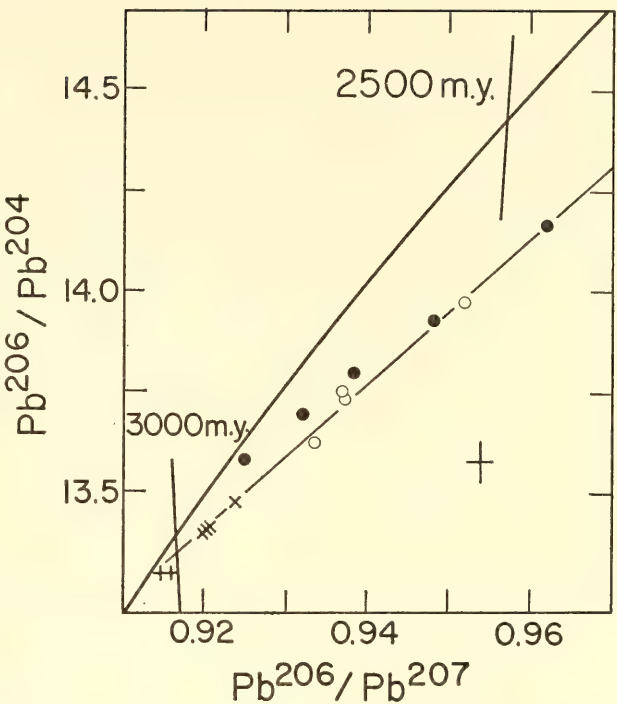


Fig. 59.  $Pb^{206}/Pb^{204}$  ratios plotted against  $Pb^{206}/Pb^{207}$  ratios for Superior province leads, North America. Circles, granites and pegmatites from Rainy Lake and northern Minnesota; solid circles, pegmatites near Manitouwadge, Ontario; Xs, Manitouwadge galena from Ostic (1963); crosses (+), Manitouwadge galena, this report. Cross at lower right represents approximate analytical uncertainty. Lines labeled in millions of years are isochrons based on an age of 4.55 AE for the earth and values of 9.54 and 10.27 for initial  $Pb^{206}/Pb^{204}$  and  $Pb^{207}/Pb^{204}$  ratios, respectively. See text for explanation of line through points.

TABLE 12. Isotopic Composition of Lead at Manitouwadge, Ontario

	$\frac{Pb^{206}}{Pb^{204}}$	$\frac{Pb^{206}}{Pb^{207}}$	$\frac{Pb^{206}}{Pb^{208}}$	$\frac{Pb^{207}}{Pb^{204}}$	$\frac{Pb^{208}}{Pb^{204}}$
Feldspar					
MG-19	13.69	0.9341	0.4076	14.66	33.59
MG-19 (acid washed)	13.57	0.9284	0.4057	14.62	33.45
MG-45	13.61	0.9245	0.4059	14.72	33.53
MG-20	13.92	0.9481	0.4148	14.68	33.56
MG-20 (acid washed)	13.71	0.9366	0.4089	14.64	33.53
MG-41	14.16	0.9616	0.4211	14.73	33.63
Galena					
Geco Mine	13.30	0.9166	0.3960	14.51	33.59
Willroy Mine	13.30	0.9149	0.3961	14.54	33.58
Average from three mines*	13.40	0.9202	0.3997	14.57	33.54
Standard					
Caltech lead standard, average of five determinations	16.63	1.0726	0.4574	15.51	36.35

\* Data from Ostic (1963).



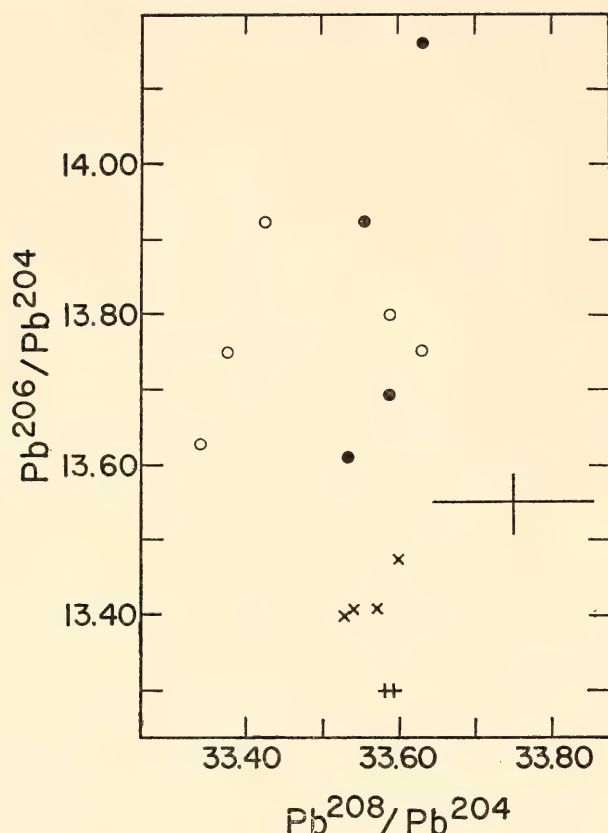


Fig. 60.  $Pb^{206}/Pb^{204}$  ratios plotted against  $Pb^{208}/Pb^{204}$  ratios for lead from Superior province samples. Code for identification of samples, same as used for Fig. 59. Cross gives analytical uncertainties of ratios.

galenas. The  $Pb^{208}/Pb^{204}$  ratios give further evidence of a close relationship between lead from potassium feldspar and galena. Figure 60 shows that the  $Pb^{208}/Pb^{204}$  ratios of all galena and feldspar samples at Manitouwadge agree within observational error limits. The newer studies at Manitouwadge considerably strengthen the suggestion made in *Year Book 63* (pp. 246–247) on the basis of the Minnesota work that the isotopic composition of lead in Manitouwadge galena represents lead associated with igneous activity 2,700 m.y. ago. As mentioned last year, if Manitouwadge galena lead is assigned an age of 2,700 m.y., a value of 4.72 AE is obtained for the age of the earth.

*Results from the African Continent.* To test whether the data for North America are typical of other continents as well we have determined the isotopic

composition of lead in potassium feldspar from the Bikita pegmatite in Southern Rhodesia. Ages of 2,700 m.y. have already been reported for lepidolite and monazite at this quarry. The isotopic composition of lead is  $Pb^{206}/Pb^{204} = 15.06$ ;  $Pb^{206}/Pb^{207} = 0.9794$ ;  $Pb^{206}/Pb^{208} = 0.4457$ . An interesting feature of the Bikita lead is that the  $Pb^{208}/Pb^{204}$  ratio agrees closely with the ratios found at Manitouwadge. The  $Pb^{206}/Pb^{204}$  and  $Pb^{207}/Pb^{204}$  ratios are unfortunately quite high owing to radiogenic lead. This condition is probably a result of the low concentration of lead in the sample—about 5 ppm. If the Bikita isotopic ratios are compared with the  $Pb^{206}/Pb^{204}$  and  $Pb^{206}/Pb^{207}$  ratios for Ontario and Minnesota plotted in Fig. 59, the point for Bikita does not lie on the secondary isochron through the North American feldspars, but rather it plots substantially *above* the isochron. This means that the isotopic composition of lead in the Bikita feldspar cannot be explained by assuming that 2,700 m.y. ago it was the same as that in Manitouwadge galena. Since the  $Pb^{208}/Pb^{204}$  ratios of the Bikita and North American feldspars are roughly the same it seems reasonable to compare galenas from the Superior Province of North America and from the Rhodesian Shield of southern Africa that have  $Pb^{208}/Pb^{204}$  ratios about equal to those in the feldspars.

Using data for galenas given by Russell and Farquhar (1960) we have found that galenas from Africa plot systematically *above* those from North America in a  $Pb^{206}/Pb^{204}$ – $Pb^{206}/Pb^{207}$  diagram like Fig. 59. The galenas from Africa, having the least radiogenic lead, give an age of approximately 4.7 AE for the earth if they are 2,700 m.y. old. These preliminary data suggest that isotopic measurements on lead from 2,700-m.y.-old rocks from North America and Africa yield the same age for the earth but that the uranium–lead ratios in the source for the lead from Africa were higher than those in the source for the leads from North America.

There are two simple ways of interpreting the results of these experiments. The earth may be approximately 200 m.y. older than was previously supposed, having an age of 4.7 to 4.75 AE. The age calculation contains the assumption, however, that the isotopic composition of lead in the earth was initially the same as that in the troilite phase of several iron meteorites, an assumption that may be incorrect. We emphasize that the calculation used to derive the value of 4.7 AE is as good as if not better than any of the previous calculations of the age of the earth. Since lead from young rocks or ores was used in all these calculations, errors owing to failure of the closed system assumption may be quite large. In any event, interesting effects have been found that indicate the desirability of obtaining new data for the isotopic composition of lead from very old rocks and ores on all continents.

We thank David Timms, Chief Geologist at the Willroy Mine, Manitouwadge, Ontario, for valuable assistance in the field, which facilitated the collection of samples at Manitouwadge. We also thank L. O. Nicolaysen, Bernard Price Institute for Geophysical Research, University of the Witwatersrand, Johannesburg, South Africa, for providing the sample of Bikita feldspar.

*Isotopic Composition of Lead and Strontium in Crystalline Rocks From the Northern Cascade Range, United States*<sup>18</sup>

The radioactive decay of the long-lived isotopes of uranium, thorium, rubidium, and potassium provides the basis for determining mineral ages, and is also used to determine the times of crystallization of metamorphism of rocks. The decay of these radioactive elements can provide other useful geological information. For example uranium, thorium, and rubidium

are continually producing natural tracers through characteristic labeling of their daughter products, lead and strontium. The isotopic composition of lead and strontium in surface rocks is highly variable, depending on the isotopic composition at the time the rocks were formed, their age, and the ratio of radioactive parent to stable daughter element. Thus, granitic rocks of Precambrian age are expected to contain lead and strontium that are enriched in radiogenic daughter isotopes in comparison with the lead and strontium without this enrichment in young volcanic rocks. Although the isotopic composition of lead and strontium in rocks of deep-seated origin, such as basalts, also varies, the isotopic compositions in specific locations may be quite uniform. (See *Year Book 63*, pp. 241-244, for a report on the isotopic composition of strontium and lead from basalts at Gough and Ascension Island along the mid-Atlantic ridge.) Under favorable circumstances the lead and strontium in rocks may serve as tracers for studying genetic relationships among different rock types. Magmas derived from fusion of crustal rocks or basic magmas heavily contaminated with crustal products might have lead and strontium isotopic ratios different from those in magmas derived from the mantle of the earth. We are attempting to apply these principles to problems concerning genesis of basalt, andesite, and granodiorite in the Northern Cascade Range.

Broadly speaking, two types of basalt are found in the area, tholeiite and high-alumina basalt. In Eocene time a large volume of tholeiitic basalt was extruded, principally to the west of the present range. Again in Miocene time voluminous tholeiite was extruded, mainly to the east of the range (Columbia River basalt). The olivine-bearing high-alumina basalt occurs in the Cascade Range and plateaus of southeastern Oregon, and is of Pliocene to Quaternary age. The andesites in the Cascades are chiefly of two types though

<sup>18</sup> In collaboration with C. A. Hopson and A. C. Waters, University of California, Santa Barbara.



there are gradations between them—olivine-hypersthene-augite andesite characterized by phenocrystic olivine and more silicic augite-hypersthene andesite. The olivine-bearing andesite occurs in localities where high-alumina basalt is found, and there are transitions between these. At Mount Rainier and Glacier Peak, where mainly augite-hypersthene andesite occurs, high-alumina basalt is absent. Both types of andesite may occur together, as at Mount Hood in Oregon. The age of the andesite varies from Pliocene for flows interbedded with high-alumina basalt along the Cascade Range to Quaternary for the large stratovolcanoes. It is interesting that many of the stratovolcanoes have plutons of granodiorite or quartz diorite cropping out beneath them or nearby. The plutons are older than the volcanoes, being of

Miocene age, but are similar in bulk chemical composition to the pyroxene andesite at Mount Rainier and Glacier Peak. North of Snoqualmie Pass the basement complex emerges from beneath the Tertiary cover, and forms much of the Northern Cascades. Schists, gneisses, migmatites derived from pre-Upper Jurassic sedimentary and volcanic rocks, and Cretaceous granitic batholiths comprise much of the basement.

Several relationships are being studied by isotopic tracer methods—the relationship between the tholeiitic and high-alumina basalts, that between the andesites from the stratovolcanoes and from the nearby Miocene granodiorite plutons, and that between the andesites and the basalts. Samples studied include three specimens of Columbia River basalt (tholeiite); two samples of high-alumina

TABLE 13. Isotopic Composition of Lead\* and Strontium† From Rocks of the Northern Cascade Range

Rock	Location	$\frac{\text{Pb}^{206}}{\text{Pb}^{204}}$	$\frac{\text{Pb}^{206}}{\text{Pb}^{207}}$	$\frac{\text{Pb}^{206}}{\text{Pb}^{208}}$	$\frac{\text{Sr}^{87}}{\text{Sr}^{86}}$	$\frac{\text{Rb}}{\text{Sr}}$
Tholeiitic basalt	{ Bridal Veil, Oregon	18.80	1.204	0.484	0.706	0.132
	{ Anatone, Washington	18.81	1.202	0.482	.....	.....
	{ Anatone, Washington	19.04	1.211	0.487	0.705	0.064
High-alumina basalt	{ Glenwood, Washington	19.29	1.232	0.497	0.705	.....
	{ Willard, Washington	18.95	1.216	0.492	.....	.....
Augite-hypersthene andesite	Mt. Rainier, Washington	19.01	1.215	0.490	0.706	0.093
Snoqualmie granodiorite	Snoqualmie Pass, Washington	18.89	1.215	0.489	.....	.....
Potassium feldspar from above‡	Snoqualmie Pass, Washington	18.92	1.216	0.491	.....	.....
Tatoosh granodiorite	Mt. Rainier National Park, Washington	18.95	1.217	0.489	0.709	0.076
Olivine-hypersthene andesite	Mt. Hood, Oregon	18.80	1.207	0.488	.....	.....
Hornblende-biotite quartz diorite gneiss	Chelan, Washington	{ 18.91	1.205	0.488	0.705	0.0037
		{ 18.83	1.205	0.489	.....	.....
Swakane biotite paragneiss	Chelan, Washington	19.48	1.246	0.497	0.712	0.065

\* Standard error of ratios: Pb<sup>206</sup>/Pb<sup>204</sup>, 0.3 per cent; Pb<sup>206</sup>/Pb<sup>207</sup>, 0.15 per cent; Pb<sup>206</sup>/Pb<sup>208</sup>, 0.2 per cent.  
† Estimated uncertainty in Sr<sup>87</sup>/Sr<sup>86</sup> ratios after normalizing all Sr<sup>86</sup>/Sr<sup>88</sup> ratios to 0.1194 is ±0.002.  
‡ Determination by B. R. Doe, U. S. Geological Survey.

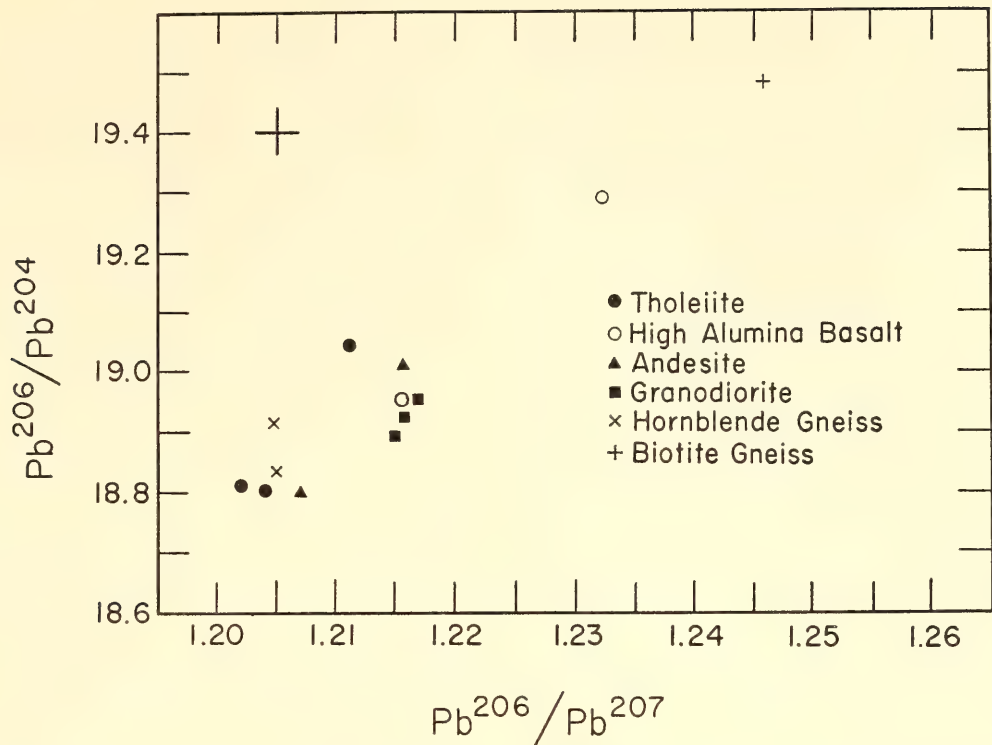


Fig. 61.  $Pb^{206}/Pb^{204}$  ratios plotted against  $Pb^{206}/Pb^{207}$  ratios for volcanic and crystalline rocks from Northern Cascade Range, Washington and Oregon. Cross at upper left gives approximate analytical uncertainties in the ratios.

olivine basalt; augite-hypersthene andesite from Mount Rainier; granodiorite from the neighboring Tatoosh and Snoqualmie plutons; olivine andesite from Mount Hood, and biotite paragneiss and two samples of migmatitic biotite-hornblende quartz diorite gneisses from the basement complex. The lead and strontium isotopic data are given in Table 13 and the lead data are displayed graphically in Figs. 61 and 62.

Several points are supported by these data. The high-alumina basalts appear on the average to have higher  $Pb^{206}/Pb^{204}$  and  $Pb^{206}/Pb^{207}$  ratios than do the tholeiite basalts, as can be seen in Fig. 61. Since the ratios  $Pb^{207}/Pb^{204}$  are nearly the same for all the basalts the distinction between the two basalt types in Fig. 61 depends primarily on difference in their content of radiogenic  $Pb^{206}$  (produced from  $U^{238}$ ). To make maximum use of the potential of the isotopic lead tracers, it is desirable to plot the data in a way that utilizes variations in  $Pb^{208}$  (produced by  $Th^{232}$ ) along with variations in  $Pb^{206}$ . Figure 62 is such a plot, showing that the

tholeiites form a group quite distinct from the high-alumina basalts. The

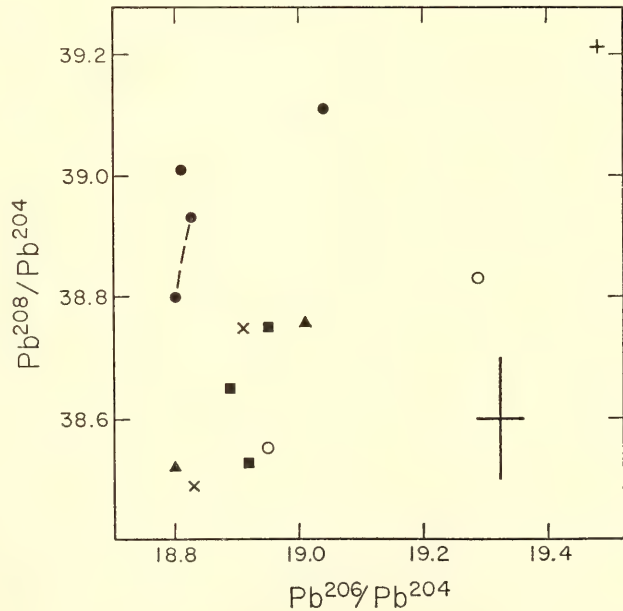


Fig. 62.  $Pb^{208}/Pb^{204}$  ratios plotted against  $Pb^{206}/Pb^{204}$  ratios for rocks from the Northern Cascade Range. Code for identification of samples, same as used in Fig. 61. The two tholeiite points connected by dashed line represent two separate determinations, including new chemical processing. Cross at lower right gives analytical uncertainty in ratios.



difference between the isotopic composition of lead in the two basalt types suggests that they are not simple differentiates from a common source material, but to reach firm conclusions more observations are necessary.

The isotopic compositions of lead in the andesite at Mount Rainier and in the Tatoosh and Snoqualmie plutons are identical within error limits, suggesting that these rocks have a common source. Fiske, Hopson, and Waters (1963) have postulated that the Tatoosh pluton did not cease its activity at depth in the late Miocene or early Pliocene but that pulses of quartz dioritic and granodioritic magma continued to rise during Pliocene and Pleistocene time, culminating in the building of Mount Rainier.

The isotopic evidence regarding the origin of the andesites is quite enigmatic. Perhaps of most significance is the fact that in Fig. 62 the andesites plot in the field of the high-alumina basalts and the hornblende-biotite quartz diorite gneisses from the basement complex, suggesting that the andesites are more likely to be related to the high-alumina basalts or to the hornblende-biotite gneiss than to the tholeiites. Two lines of field evidence support these hypotheses. Gradations in composition between high-alumina basalt and andesite are observed in the Cascades. Crowder (1959) describes the apparent development of quartz diorite magma in the vicinity of Glacier Peak by progressive migmatization, mobilization, and partial fusion of basement gneiss. Since the lead in andesite at Mount Rainier does not differ greatly from the lead in the hornblende-biotite gneiss, such a source for the granodiorite and andesite is not excluded by the data. The presence of hornblende in the hornblende-biotite gneiss indicates that the source materials probably include basic volcanic rocks, although metamorphism has obscured the nature of the original material (Crowder, 1959).

Besides additional isotopic work other measurements promise to help clarify

the andesite problem. Among these are determination of the thorium-uranium and potassium-rubidium ratios in the various rock types. Although the data given here are preliminary, they indicate that the Cascade tracer experiments have a reasonable sensitivity and that further work may lead to an improved understanding of the genetic relationships between the rocks in this area.

*The Minimum Age of the Glenarm Series, Baltimore, Maryland*<sup>19</sup>

The Glenarm series in the Washington-Baltimore area is a thick sequence of metamorphosed sedimentary rocks that lies unconformably on the 1,000-m.y.-old basement complex of Baltimore gneiss. During the early Paleozoic orogeny the Glenarm series was intruded first by gabbroic magma and its differentiation products under early kinematic to synkinematic conditions and later by a series of granitic rocks as synkinematic to late-kinematic events. The plutons of the gabbroic series and earlier granitic intrusions are cut by pegmatites dated at 440 m.y. by Rb-Sr (*Year Book* 58, p. 172).

Geologists originally assigned the Glenarm to the Precambrian era, but lately an early Paleozoic age has been favored. Those who prefer a Paleozoic age for this metasedimentary series think that the three major formations of the Glenarm—the Setters quartzite, the Cockeysville marble, and the Wissahickon schist—can be correlated with lower Cambrian quartzites, Cambro-Ordovician carbonates, and the Ordovician Martinsburg shales.

A minimum age of the Glenarm can be established by dating some of the plutons that intrude it. With this minimum age in mind one may attempt to correlate the Glenarm with rock formations of similar lithology and sequence of deposition.

Four new zircon ages of post-Glenarm

<sup>19</sup> In collaboration with C. A. Hopson, University of California, Santa Barbara.



intrusives are reported in Table 14 Included is an earlier analysis given in *Year Book 59* (p. 158). Petrographic, textural, and chemical data suggest that the Relay quartz diorite is a late differentiate of the earlier gabbroic magma series, whereas both the Norbeck quartz diorite and the Port Deposit granodiorite are early intrusions of the subsequent granitic series.

The zircon populations from these intrusives are of very uniform habit. Except for the quartz-diorite, in which clear, euhedral zircon crystals were found, the zircon crystals often have slightly rounded terminations and are turbid.

The Pb<sup>206</sup>-U<sup>238</sup> ages range from 320 m.y. for the Gunpowder granite to 495 m.y. for the Norbeck quartz diorite. The lead-lead ages spread from 470 m.y. for the Relay quartz diorite to 570 m.y. for the Norbeck quartz diorite. Some of these Pb<sup>207</sup>-Pb<sup>206</sup> ages have rather large errors, owing to the young ages and the relatively high content of common lead. The observed Pb<sup>207</sup>/Pb<sup>204</sup> ratios varied from 72 to 43. All ages are very discordant, suggesting some loss of lead.

The two analyses from the Gunpowder granite are of special interest. Field observations indicate that the Gunpowder granite is of migmatitic origin and represents a rheomorphic offshoot from the Baltimore gneiss that intruded the

mantling Glenarm metasediments. Near its type locality the Gunpowder granite is a distinctive fine- to medium-grained gneissic rock, with streaky biotite schlieren. Where the granite breaks through the Glenarm mantle it is relatively uniform. Traced back to its roots in the Baltimore gneiss, however, the granite is less uniform and begins to take on the characteristics of the gneiss.

The zircons separated from the Gunpowder granite consist of two populations that were separated by sieving. The coarse, -200-mesh fraction contains relatively short rounded zircons, which are often cloudy and pinkish, similar to zircons found in the Baltimore gneiss. The fine, -325-mesh fraction is composed of about 70 per cent clear needlelike, euhedral zircons; the remainder of rounded, cloudy, pink zircons. It appears that the fine fraction contains zircons that were predominantly freshly formed during the migmatization of the Baltimore gneiss, and that the coarse fraction contains zircons that may have been inherited from the original Baltimore gneiss. The two differently sized fractions were analyzed separately.

The age difference between the coarse and the fine fractions of the Gunpowder zircons is in the direction one would expect if the coarse material was inherited from the adjacent 1,000-m.y.-old Baltimore gneiss. If it was, the inherited zircons lost considerable lead as a result of the migmatization process. It appears that the age was lowered by a loss of lead and not an addition of uranium, since the coarse fraction has a uranium content of 600 ppm, which is lower than normal for zircons of the Baltimore gneiss, whereas the uranium content of the fine fraction is 900 ppm. Zircons separated from Baltimore gneiss interfingering with the Gunpowder granite at the type locality have a uranium content of 1,200 ppm as measured by alpha counting.

The lead-lead ages of most post-Glenarm zircons suggest an intrusion time at least 500 m.y. ago. The Pb<sup>206</sup>-U<sup>238</sup> age of

TABLE 14. Zircon Ages of Post-Glenarm Intrusives

	Age, million years		
	Pb <sup>206</sup>	Pb <sup>207</sup>	Pb <sup>207</sup>
	U <sup>238</sup>	U <sup>235</sup>	Pb <sup>206</sup>
Norbeck quartz diorite	495	510	570 ± 50
Port Deposit quartz diorite	325	350	525 ± 20
Relay quartz diorite	435	440	470 ± 50
Gunpowder granite			
Fine	320	355	500 ± 15
Coarse	485	510	615 ± 60



zircon from the Norbeck quartz diorite alone sets a probable lower limit of  $495 \pm 15$  m.y. for the intrusion of the Norbeck pluton.

On a concordia plot some of the post-Glenarm zircons (for additional data compare *Year Book 57*, p. 114) lie on a 550-m.-y. chord. None of them extrapolates to an age younger than 450 m.y. This is in agreement with the 450-m.-y. age of the pegmatites that cut some of the post-Glenarm plutons. The assumption of episodic loss of lead during the Paleozoic metamorphism or of continuous diffusion of lead would only increase the true age of the zircons measured. For these mechanisms ages of 600–700 m.y. are possible.

We conclude, therefore, that several of the post-Glenarm intrusives were emplaced at least 500 m.y. ago. Similar zircon ages of 520 to 550 m.y. have been determined from intrusives in the Wichita Mountains, Oklahoma, by Tilton, Wetherill, and Davis (1962). These rocks are overlain unconformably by the stratigraphically dated Upper-Cambrian Reagan sandstone. The similarity in ages of the zircons from Oklahoma and those from Maryland indicates that the Maryland rocks, particularly the Norbeck tonalite, must be of pre-Upper Cambrian age. This precludes a correlation of the upper Glenarm series, that is the Wissahickon schists, with the upper Ordovician Martinsburg shales. Since nothing in the Cambrian succession correlates well with the Wissahickon, one has to go further back in the time scale. In fact, Hopson (1964) has shown that the late Precambrian Ocoee–Lynchburg sequence, cropping out from Virginia southward, matches the Wissahickon almost perfectly. If the Wissahickon or upper Glenarm is Precambrian, then the whole Glenarm series must also be Precambrian.

#### *Radioactive Heat Production in Peridotite*

We presented measurements of the radioactive heat production in eclogite and in some ultramafic rocks in *Year Book 60* (pp. 195–197) and discussed the bear-

ing of these results on the problem of the composition of the outer mantle of the earth. A major conclusion of the investigation was that heat production in dunite and in olivine-pyroxene peridotite (lherzolite) is too low to account for heat flow in oceanic regions if such materials make up the outer mantle under the oceans. Heat production in eclogite more nearly meets the requirements.

In *Year Book 63* (p. 330) we reported data for the potassium content of six samples of mylonitized peridotite from St. Peter and St. Paul's Rocks on the mid-Atlantic ridge. The samples contain forsterite and enstatite; varying amounts of primary hornblende; and minor clinopyroxene, serpentine, and spinel. The potassium content varied from 100 to 1,400 ppm, the variations correlating primarily with the hornblende content of the samples, which was as high as 15 per cent. We pointed out that if the high-potassium samples had the potassium-uranium ratio of 10,000 generally found in igneous rocks their radioactive heat production would be high enough to explain the observed oceanic heat flow by conduction alone.

The concentrations of potassium, uranium, and thorium have been determined for three of the St. Peter and St. Paul's specimens covering a range of potassium concentrations. These data are given in Table 15. The uranium concentrations of the samples increase with increasing potassium content, and the potassium-uranium ratios are fairly constant. The radioactive heat production in WPIi, which contains about 15 per cent

TABLE 15. Concentration of Potassium, Uranium, and Thorium in Peridotite at St. Peter and St. Paul's Rocks

Sample No.	K, ppm	U, ppm	Th, ppm	K/U
WPIi	1,447	0.14	0.40	10,300
HI	502	0.015	.....	33,500
WC2	135	0.0045	0.013	30,000



hornblende, is sufficient to generate the observed oceanic heat flow if the outer 500 km of the earth's mantle consists of such material. The heat production is, in fact, more than twice that of eclogite as given in *Year Book 60*. Since amphiboles are unstable at high temperature and pressure, the mineral assemblage at depths greater than approximately 50 km would be different from the assemblage found in the peridotite now. It is not possible to say what would happen to the potassium, uranium, and thorium contents with the change in mineral composition, but the concentrations might not change drastically. Oxburgh (1964)

has pointed out that if basalts are assumed to be derived from the mantle the amount of potassium in basalts can be accounted for only if there are rocks in the outer mantle with more potassium than that in most dunites and peridotites. In any case, the new observations show that heat production in some kinds of peridotite is high enough to account for the heat flow in oceanic areas, and our previous objection to peridotite as a major constituent of the outer mantle must be qualified accordingly.

We are indebted to Dr. J. D. H. Wiseman of the British Museum for supplying samples WPII and WC2.

## ORE MINERALS: PETROGRAPHY AND EXPERIMENTAL STUDIES

### INVESTIGATIONS OF THE NICKEL-COPPER ORES AND ADJACENT ROCKS OF THE SUDBURY DISTRICT, ONTARIO

*A. J. Naldrett and G. Kullerud*

The Sudbury deposits of iron, nickel, and copper sulfides are associated with a body of rock known as the "nickel irruptive." This body outcrops as an elliptical ring with the long axis running 37 miles east-northeast and the short axis 17 miles long. It grades from an outer ring of augite norite or hypersthene gabbro, known locally as norite, through a transition to an inner ring of granophyric, alkali-feldspar-rich rock called the micropegmatite. Around much of its perimeter the outer contact of the body dips in toward the center between 30° and 50°. So far as is known, the inner contact always dips in toward the center.

The sulfide deposits that occur around the outer edge of the norite can be divided into two classes: offset deposits, associated with dike-like offshoots from the base of the norite; and marginal deposits, occurring at or close to the norite-footwall contact.

The origin of the deposits has been discussed for the last 80 years. Opinion is

divided into two main camps. One camp (Coleman, 1905; Coleman, Moore, and Walker, 1929; Collins, 1937) considers that the sulfides were introduced in solution in the irruptive magma, segregated from it as an immiscible sulfide liquid following intrusion, and then settled at its base. Evidence put forward in support of this view includes (1) the close spatial relationship between the norite and the ore bodies, (2) the presence of ore bodies at the base of the irruptive, (3) the zoning in the relative proportions of certain sulfide minerals and the downward transition from sulfide-poor norite through sulfide-rich norite to massive sulfides observed in certain deposits, (4) textural relations between sulfides and silicates present in certain deposits, and (5) the general absence of hydrothermal alteration.

Early proponents of this hypothesis considered that the sulfides had segregated and settled directly into the present sites of the ore deposits, but it is now clear that usually the marginal portions of the norite solidified before the sulfide ore was deposited. Howe (1914) and Bateman (1917) point this out and suggest subsequent intrusion of sulfide magma from a



deep-seated source. Hawley (1962) considers that the sulfides settled to the base of the irruptive and subsequently were injected in the liquid state along the frozen contact to present ore localities.

The second camp (Dickson, 1904; Knight, 1917; Wandke and Hoffman, 1924; Phemister, 1925) points to the epigenetic character of many of the deposits (since explained by Howe, Bateman, and Hawley's modifications of the original magmatic theory); the replacement of silicates by sulfides on both a macroscopic and a microscopic scale; the development of reaction rims between fragments and the surrounding sulfides; and the presence of hydrous minerals, silicification, and feldspathization in the wall rocks of certain deposits. They conclude that the sulfides were introduced by hydrothermal fluids.

Kullerud (*Year Book 62*, p. 187) suggested sulfurization as a mechanism through which the sulfides formed at Sudbury. Sulfurization is defined as the reaction between sulfur from an external source and cations such as iron, nickel, and copper in solid solution in common rock-forming minerals or in igneous magma. He bases his suggestion on experiments by Kullerud and Yoder (*Year Book 62*, pp. 215–218; *Year Book 63*, pp. 218–222), which show that reactions between iron-bearing silicates and sulfur result in the formation of pyrrhotite and pyrite or pyrite alone. In one experiment, where the silicate was a fayalite that contained some nickel, pentlandite also formed in the reaction.

The aim of the present investigation is to study the sulfide and silicate minerals in both ore and surrounding rocks of one of the marginal deposits in order to determine the sequence of geological events leading to the deposition of ore and the  $P$ - $T$  conditions at the time of mineralization. These results should point to the most likely mechanism of ore genesis.

The Strathcona ore body, owned and operated by Falconbridge Nickel Mines,

Ltd., has been chosen for detailed study because it is still being developed, and all parts of the mine are either accessible or well represented by core samples condensed from surface or underground drill holes. The structure, rock types, and mineralization at Strathcona have not been described previously. Accordingly the first step in the present project was an intensive study of the ore and surrounding rocks. Certain minerals have been examined in detail, and studies of other minerals are continuing. The data obtained so far permit the drawing of a provisional outline of the geological history of the deposit.

Falconbridge Nickel Mines has kindly permitted us to collect all the samples used in this study. We are indebted to the company's geologists who have supplied a great deal of information about the structure of the mine and the field relationships between the rock types.

#### *The Strathcona Ore Body*

The Strathcona deposit lies on the northern perimeter of the Sudbury basin, 20 miles northwest of Sudbury. It is one of a large number of deposits that occur close to the base of the nickel irruptive along a six-mile intensely mineralized stretch of the contact. This stretch contrasts strongly with the remainder of the northern perimeter, around which deposits of economic importance have not been reported.

The ore body runs roughly parallel to the base of the irruptive rock and extends approximately half a mile along strike. Ore accessible for sampling lies between the 1,600- and 3,150-foot levels in the mine. The overall dip of the base of the irruptive rock as examined from the mine workings varies between 30° and 45°S, though local irregularities are very common, and the dip is much steeper or much flatter, even horizontal in places.

A schematic plan of the 2,250-foot level of the mine is shown in Fig. 63. A "nose" of irruptive rock projects into the gneiss of the footwall. Granite breccia

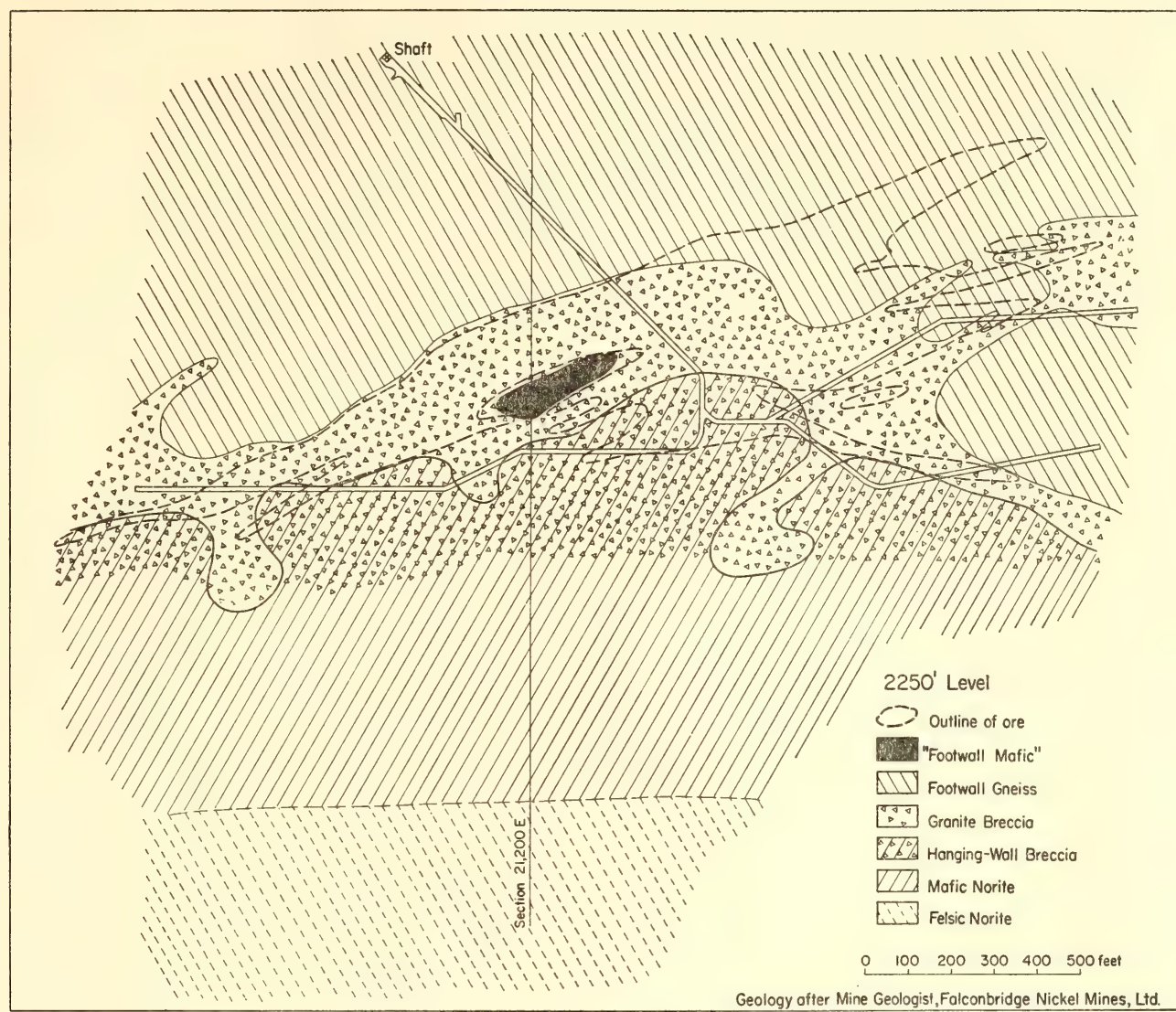


Fig. 63. Schematic plan of 2,250-foot level, Strathcona Mine, near Sudbury, Ontario.

occurs around this nose, extending as far as 600 feet away from the irruptive rock. The breccia also projects back into the irruptive rock.

Within the nose and along most of the remainder of the contact the irruptive rock itself consists of a breccia, the hanging-wall breccia. Farther back into the hanging wall the brecciated appearance is no longer so apparent; this phase is referred to as the mafic norite. Mafic norite extends up to 700 feet directly away from the contact, where another phase of the norite, felsic norite, appears. The hanging-wall breccia and mafic norite thin out at depth below the level where the ore starts to pinch out.

Most of the ore occurs in the granite

breccia formation, although ore stringers extend as far as 700 feet away from the contact out into the gneiss of the footwall in the eastern part of the mine. The matrix of the hanging-wall breccia is heavily mineralized in the vicinity of the nose, and zones of weaker mineralization occur in this breccia and the mafic norite elsewhere along the contact. Scattered sulfide specks are present in all the phases of the irruptive rock in the vicinity of the mine.

*Rock Formations*

Detailed descriptions of the five rock formations referred to above are given in Table 16. Three of these formations—the



TABLE 16. Petrographic Descriptions of Rock Formations in the Strathcona Mine

Rock Formation			Minerals Present in Rock Formation				Xenoliths in Rock Formation	
Name	Texture	Nature of Contact With Other Formations	Mineral	Per Cent	Form	Average Grain Size	Rock Type	Remarks
Felsic norite (known locally as "salc norite")	Coarse grained, holocrystalline, hypidiomorphic, granular	In most places, transitional contact over few tens of feet downward into mafic norite	Plagioclase	50-70	Subhedral tabular crystals with well-developed albite and carlsbad twinning	2.0 × 0.4 mm	None observed	
			Potash feldspar	5-10	1. Subhedral rectangular grains 2. Interstitial filling 3. Granophyric intergrowth with quartz	2.0 × 1.0 mm		
		In some places, sharp contact with mafic norite	Quartz	5-10	1. Interstitial masses 2. As in (3) above	0.6 mm diam.		
			Orthopyroxene Original content (Now 50-80% altered)	14-30	Subhedral tabular grains	2.0 × 0.8 mm		
Mafic norite (known locally as "lineated gray norite" or "quartz diorite")	Fine to medium grained, holocrystalline, hypidiomorphic, intergranular	Grades downward into hanging-wall breccia as xenoliths become more numerous	Augite Original content (Now 50-80% altered)	7-14	Anhedra masses molded about plagioclase Strong diallage parting		Poikilitic norite (known locally as "femic norite")	Zones of augite norite with large (5 mm diam.) plagioclase crystals enclosing mafic minerals poikilitically
			Biotite	2-6	Rectangular books	1.0 mm diam.		
			Anthophyllite Actinolite Chlorite Talc	10-30	Pseudomorphous after orthopyroxene and as irregular patches (?) after augite	0.7 × 0.4 mm		
			Apatite	<1	Small subhedral prisms	0.5 × 0.2 mm		
			Plagioclase	40-60	Fine grained subhedral tabular crystals with well-developed albite and carlsbad twinning Form matrix for mafic minerals	0.5 × 0.2 mm		
			Potash feldspar	1-2	Interstitial			
			Quartz	<1	Interstitial			
			Orthopyroxene	30-50	Subhedral to euhedral tabular grains	1.2 × 0.4 mm		
			Augite	15-25	Anhedra grains	1.0 mm diam.		
			Anthophyllite Actinolite Biotite	0-10	Developed around margins of pyroxene grains			
Hanging-wall breccia matrix (known locally as "quartz diorite breccia")	Similar to mafic norite	Contact with underlying granite breccia is sharp in some areas but difficult to	Apatite	1	Small subhedral prisms	0.5 × 0.2 mm	Poikilitic norite Olivine norite Pyroxenite Olivine pyroxenite	Xenoliths composed of varying proportions of orthopyroxene, augite, olivine, and
			Similar to mafic norite except that in sulfide-rich portions close to base of formation (1) proportion of plagioclase remains unchanged while proportion of pyroxene decreases as the sulfides increase, and (2) up to 5% quartz is present					

Granite breccia matrix (known locally as "granite breccia" or "late granite breccia")	Fine grained, holo- crystalline, xeno- blastic, granular	Adjacent to underlying gneiss, matrix is com- posed of gneiss frag- ments of all sizes down to limit of vision with a darker gray interstitial filling Stringers of this ma- terial encircle large (10 ft diam.) blocks of gneiss and tongues of the same material penetrate and finger out into the unbrec- ciated gneiss of the footwall	Plagioclase  Potash feldspar  Quartz  Orthopyroxene and augite Original content Now 80-100% altered  Anthophyllite Actinolite Biotite Chlorite Talc  Apatite	20-50  5-10  20-50  10-20  8-20  3-8	Mosaic of stubby to rounded grains with well-developed carls- bad and poorly de- veloped albite twin- ning  1. Anhedral grains 2. Interstitial  1. Anhedral interlock- ing grains 2. Interstitial  Mafic minerals occur as clusters of anhe- dral grains and ir- regular aggregates of hydrous alteration products after py- roxene	0.1 mm diam.  0.1 mm diam.  0.2 mm diam.	Footwall gneiss  Norite Pyroxenite Peridotite  Footwall gneiss	Rare corroded xenoliths  Most common close to hanging-wall but occur throughout  Most common close to footwall but occur throughout	cases plagioclase en- clozes mafic minerals poikilitically so that fabric of xenolith is in strong contrast to intergranular fabric of matrix
Footwall gneiss	Fine grained, holo- crystalline, xeno- blastic, granular	Mosaic of small anhe- dral equant grains with good carlsbad and poor albite twinning  As small anhedral masses enclosing pla- gioclase and quartz  1. Anhedral grains dotted among pla- gioclase 2. Lens-like segrega- tions of anhedral interlocking grains 3. Interstitial  Clusters of small anhe- dral grains  Irregular fringe around augite  Irregular masses around augite and also mantling actino- lite	Plagioclase  Potash feldspar  Quartz  Augite  Actinolite  Biotite  Apatite	40-50  2-3  15-40  12-16  5-10  1-5  <1	Small subhedral to euhedral prisms with hexagonal cross section  Mosaic of small anhe- dral equant grains with good carlsbad and poor albite twinning  As small anhedral masses enclosing pla- gioclase and quartz  1. Anhedral grains dotted among pla- gioclase 2. Lens-like segrega- tions of anhedral interlocking grains 3. Interstitial  Clusters of small anhe- dral grains  Irregular fringe around augite  Irregular masses around augite and also mantling actino- lite	0.06 mm diam.  0.25 mm diam.  0.12 mm diam.  0.3 mm diam.  0.3 mm diam.	"Footwall mafic"	Angular fragments, some drawn out and contorted, of a fine grained, very dark gray rock that has not been studied to date	



felsic norite, mafic norite, and hanging-wall breccia—are part of the nickel irruptive. The mafic norite is a later intrusion than the felsic norite. It is finer grained, and contains less quartz and potash feldspar and a much higher proportion of unaltered pyroxene than the felsic norite. The hanging-wall breccia is very similar to the mafic norite and is thought to be the same rock, rich in cognate xenoliths and modified in some areas near the footwall contact as a result of sulfide mineralization. Cognate xenoliths in the mafic norite and hanging-wall breccia range from norite to peridotite. Xenoliths derived from the footwall are also observed in the breccia in a few places. Plagioclase encloses the mafic minerals poikilitically in all the cognate xenoliths, in strong contrast to the intergranular texture of the surrounding matrix.

The texture and modal composition of the granite breccia matrix are very different from those of the hanging-wall breccia matrix. The texture is metamorphic rather than igneous and resembles that of the footwall gneiss. The modal composition of the granite breccia matrix is also similar to that of the gneiss except that (1) the breccia matrix is much richer in apatite and potash feldspar than the gneiss; (2) the pyroxene of the breccia matrix is much more altered than that of the gneiss; and (3) no orthopyroxene has been observed in the gneiss, whereas minor orthopyroxene (the exact amount is unknown because of the intense alteration) is present in the breccia matrix.

Both irruptive and footwall fragments occur in the granite breccia. Irruptive fragments are more numerous near the hanging wall, whereas footwall fragments occur almost to the exclusion of irruptive fragments near the footwall gneiss. The granite breccia-gneiss contact is explicable in terms of the hypothesis that the breccia matrix was derived as a result of fracturing and pulverizing of the gneiss and recrystallization of the pulverized material.

### *Composition of Olivine in Xenoliths of Hanging-Wall Breccia*

Olivine composition was determined in 22 xenoliths by the X-ray powder diffraction method described by Jambor and Smith (1964). Olivine was picked out of thin sections, pulverized, and mounted on silica glass spindles in a 114.6-mm-diameter Straumanis-type mounting camera. The films were exposed for about 20 hours with unfiltered Fe radiation. The position of the 174 reflection was measured on each film with the use of standard methods to compensate for film shrinkage and other systematic errors.

The precision of Jambor and Smith's method was tested by running the same powder mount 10 times, removing it from the camera, and recentering each time. The range in  $2\theta$  obtained was  $0.05^\circ$  and the standard deviation  $s$  for the 10 runs was  $0.015^\circ$ , which corresponds to a standard deviation of 0.2 mole per cent forsterite. Ten separate grains from a single thin section were then measured. The range in  $2\theta$  was found to be  $0.13^\circ$ , and the standard deviation  $0.04^\circ$  ( $= 0.46$  mole per cent forsterite).

Results of this study indicate a range in composition of 72.8–85.0 mole per cent forsterite. To determine whether there is a relation between the composition of the olivines and the nature of the individual xenoliths in which they occur, olivine composition is plotted against the modal per cent plagioclase in the appropriate fragment in Fig. 64. It is seen that there is a direct relation; the more ultramafic xenoliths contain the more magnesian olivine.

The presence of ultramafic cognate xenoliths in the hanging-wall breccia is evidence of an ultramafic portion of the "nickel irruptive" that does not appear at surface. The correlation between olivine composition and rock type indicates that the olivine-bearing rocks are zoned with respect to both relative proportions of their constituent minerals and composition of these minerals in a way similar to that observed in differentiated mafic

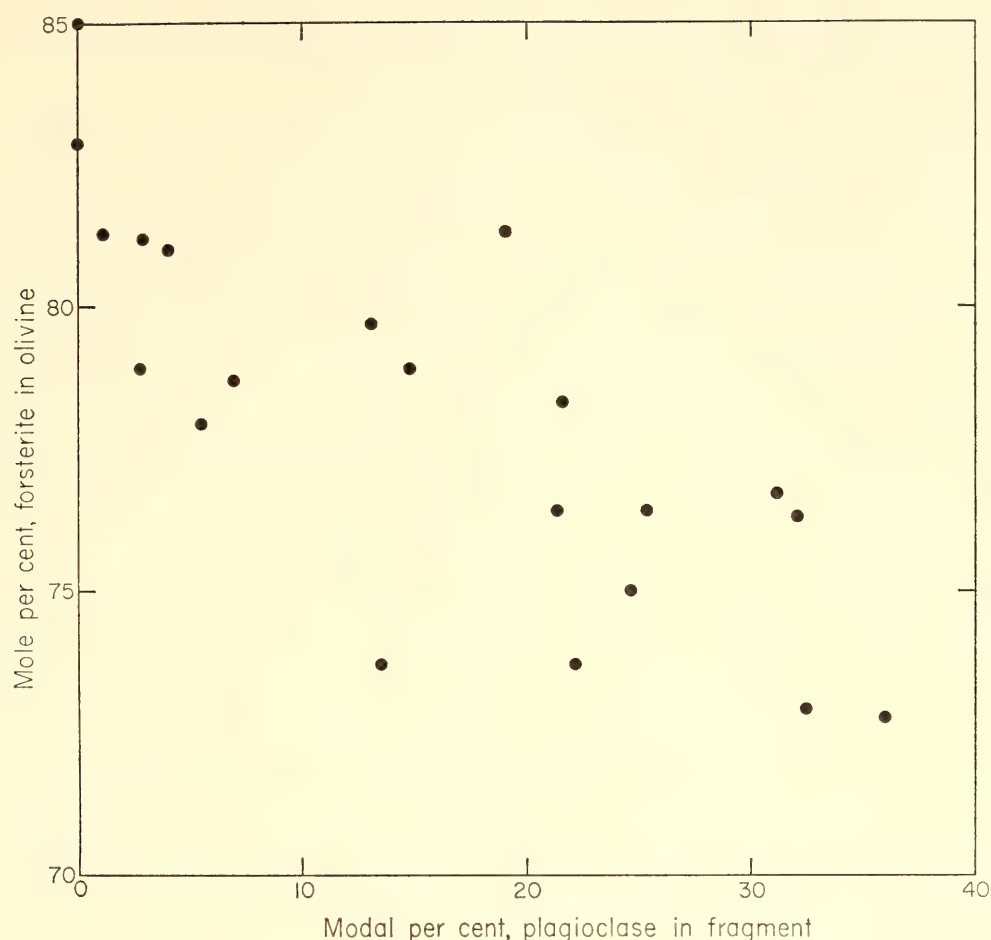


Fig. 64. Variation of olivine composition in fragments in hanging-wall breccia at Strathcona Mine with modal per cent plagioclase in appropriate fragment.

intrusions. Such similarity suggests that the fragments at Strathcona were derived from some hidden ultramafic accumulate within the irruptive.

This inference is in accord with Wilson (1956), who remarks on the points of similarity between the Sudbury nickel irruptive and large lopoliths such as the Bushveld Complex and the Great Dyke, and suggests that the irruptive is also a funnel-shaped lopolith with ultramafic layers hidden at depth. Hawley (1962) cites H. F. Zurbrigg's confirmation of crystal layering in the norite with a dip flatter than that of the footwall as important evidence in support of Wilson's suggestion.

#### *Plagioclase Composition in Rocks Near the Mine*

Plagioclase compositions were determined with the universal stage using the method described by Slemmons (1962).

Subsequently 26 plagioclases were re-determined by measuring the  $\beta$  refractive index with oils and comparing these readings with curves given by J. R. Smith in Hess (1960). Without exception the results of the two methods agree within 5 mole per cent anorthite.

Variation in plagioclase composition in rocks close to the mine is illustrated in Fig. 65. In the two breccia zones the plagioclase composition shown is that of the matrix and not the fragments. In general there is a progressive change in the anorthite content from a value of  $An_{65}$  in felsic and mafic norite well removed from the contact to a minimum of  $An_{30}$  in the granite breccia zone. The composition of plagioclase in the footwall gneiss is variable according to the part of the mine sampled, but all plagioclases fall between  $An_{30}$  and  $An_{42}$ . In most places the center of the granite breccia zone contains a more albitic plagioclase than



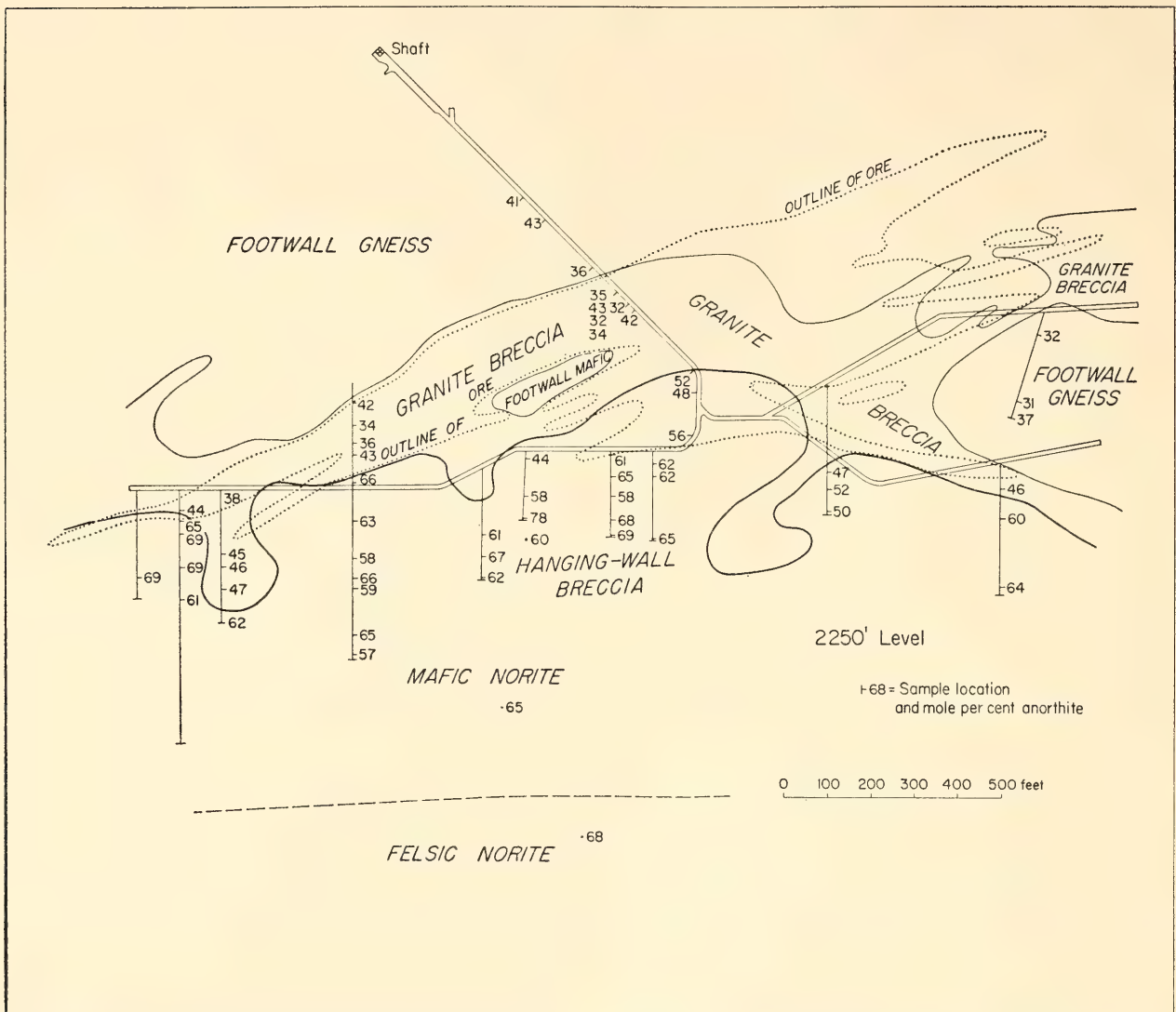


Fig. 65. Variation in plagioclase composition in rocks close to Strathcona Mine as illustrated by samples collected from the 2,250-foot level in mine.

either margin. Plagioclase in the matrix of the hanging-wall breccia ranges from  $An_{48}$  (close to the contact with the granite breccia) to  $An_{60}$  (well removed from the contact). Plagioclase in the gneiss, granite breccia, and hanging-wall breccia shows relatively little zoning.

Plagioclase composition in the pyroxenitic fragments of the footwall breccia ranges from  $An_{40}$  to  $An_{54}$ . In similar fragments in the hanging-wall breccia the range is from  $An_{52}$  to  $An_{72}$ ; in these the plagioclase is strongly zoned, not with concentric rings of differing composition, but very irregularly with areas and fingers of more sodic plagioclase occurring within and appearing to cut through material with a more calcic composition. Plagio-

clase in the mafic norite is only moderately zoned with selvages of more sodic composition, but plagioclase in the felsic norite is strongly zoned with cores containing up to  $An_{69}$  and margins as low as  $An_{40}$ .

The overall picture indicates that soda metasomatism has affected plagioclase in all rocks close to the contact between the irruptive body and the footwall rocks. The metasomatism is most intense within the granite breccia where even the composition of calcic plagioclase of ultramafic fragments is approaching that of the enclosing matrix. The effect on the hanging-wall rocks is most marked close to the contact; it gradually decreases in magnitude away from the contact and

disappears 200–300 feet into the hanging wall.

*Structural State of the Plagioclase*

Smith and Yoder (1956) have used the  $\Delta 2\theta$  separation of the 131 and  $\bar{1}\bar{3}1$  peaks in X-ray powder diffraction patterns to distinguish between series of plagioclases of different structural states. They point

out that when this separation is plotted against composition, most natural plagioclases in the range  $An_{30}$ – $An_{70}$  fall between the two curves (Fig. 66). The upper curve is defined by the plot of plagioclases synthesized from dry melts, and the lower one by plagioclases from thick stratiform mafic intrusions. Plagioclases in rocks that have been chilled

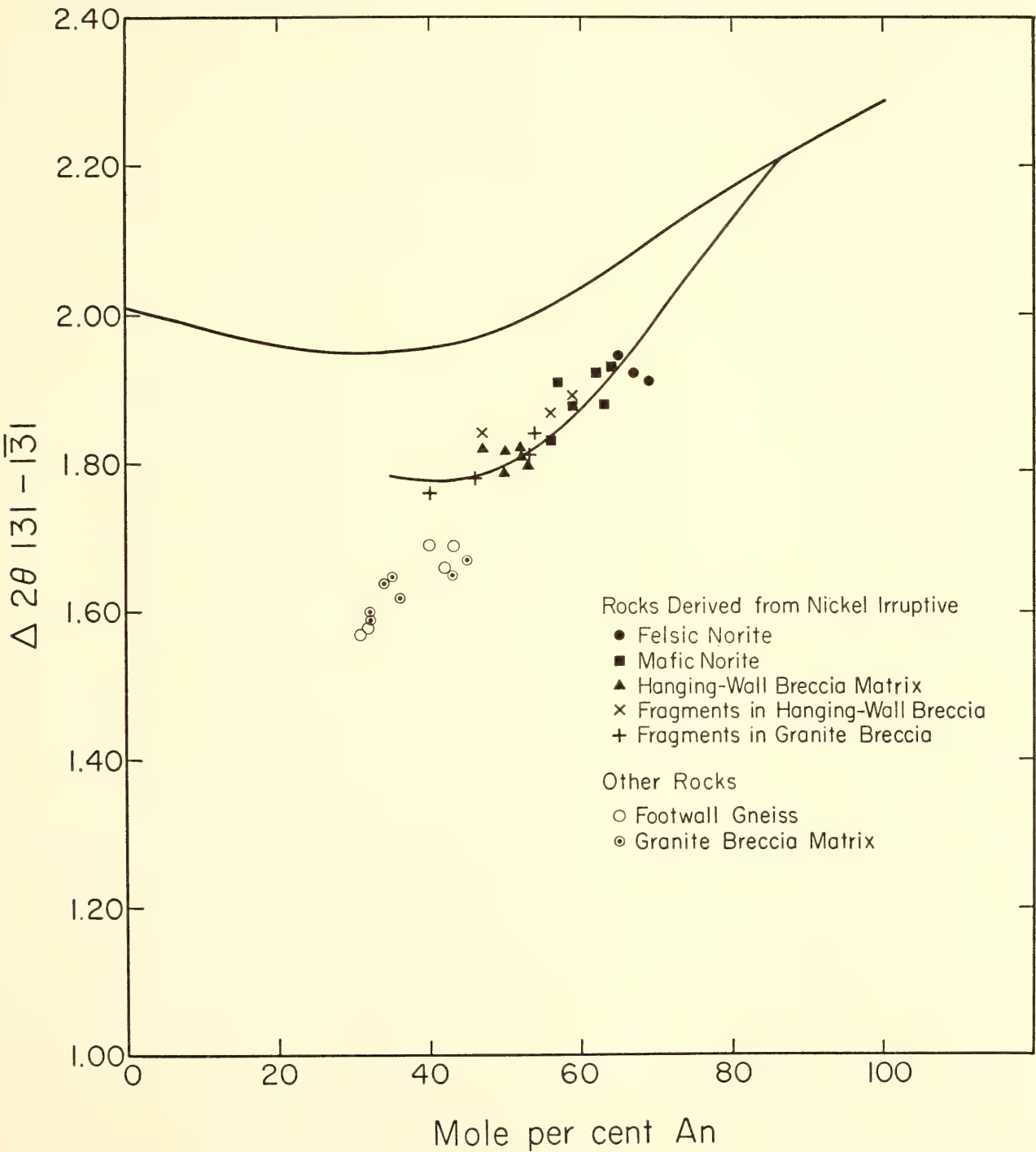


Fig. 66. Variation of  $\Delta 2\theta(131) - (\bar{1}\bar{3}1)$  with composition in plagioclases from rocks collected near Strathcona Mine.



rapidly from high temperatures fall closer to the upper curve and are interpreted as having a less ordered structural state than those in rocks that have been cooled more slowly, or have been annealed for a considerable time at lower temperatures and that fall closer to the lower curve.

In Fig. 66 the  $\Delta 2\theta$  131–131 separation has been plotted for 33 plagioclases from the Strathcona Mine against an estimate of their composition based on J. R. Smith's curve of the  $\beta$  refractive index (in Hess, 1960). Samples of irruptive rock (felsic norite, mafic norite, and matrix from the hanging-wall breccia) plot on or close to Smith and Yoder's lower curve. This is to be expected in view of the similarity between the nickel irruptive and other large mafic intrusions.

Samples from the footwall gneiss and the matrix of the granite breccia plot well below the lower curve. The explanation for this behavior is thought to be that the gneiss cooled sufficiently slowly or was annealed at a moderate temperature long enough for the plagioclase to reach an even more ordered structural state than that achieved by plagioclases from slow-cooling mafic intrusions. Although the metasomatism of plagioclase in the hanging-wall breccia matrix and ultramafic fragments in the granite breccia has involved the addition of much sodium and silicon and the removal of much calcium and aluminum, in each plagioclase studied the 131–131 separation remains close to the curve for large mafic intrusions. Smith and Yoder demonstrated that recrystallization does not necessarily result in change in this separation when they found no measurable change on recrystallizing a high-temperature synthetic plagioclase at 640°C and 10,000-bars water pressure. This experiment involved no change in chemical composition. It remains to be determined why recrystallization coupled with considerable chemical substitution such as that found at the Strathcona Mine has had little effect on the structural state as indicated by the 131–131 separation.

The similarity between the structural states of plagioclase in the gneiss and matrix of the granite breccia indicates that either plagioclase in the matrix of the breccia is derived from the gneiss and has subsequently recrystallized without changing its former low structural state, or that it crystallized from a magma of unusual composition at very low temperature.

Results of underground observations of the granite breccias at Strathcona, the granular mosaic texture of the matrix, and the evidence of the structural state of the plagioclase are compatible with Speers's (1956) conclusion that breccias of the Sudbury area akin to the granite breccia at Strathcona are essentially "crush breccias" formed by the comminution of the adjacent country rocks and modified to some extent by metasomatism. At the Strathcona Mine the high ratio of hydrous to anhydrous mafic minerals and the large amount of apatite in the breccia matrix, as well as the extensive sodium metasomatism both of fragments in the breccia and of the surrounding rocks, are evidence that the granite breccia here probably recrystallized under relatively high water pressure in an environment rich in phosphorus and sodium.

#### *Biotite Variation*

A schematic cross section through the ore deposit (section 21,200E) is shown in Fig. 67. Variations in the color and the  $\beta$  refractive index of biotites are shown on the section.

A deep brown, pleochroic biotite ( $n_\beta = 1.626\text{--}1.638$ ,  $2V = 5^\circ\text{--}10^\circ$ ) occurs throughout the ore deposit and the adjacent rocks in the footwall and hanging wall as far as 700 feet away from the ore. At distances greater than 700 feet from the ore the rocks in the hanging wall contain two biotites. One is again a deep brown variety ( $n_\beta = 1.628\text{--}1.638$ ,  $2V = 5^\circ\text{--}10^\circ$ ), which appears to be identical with that found in the ore zone and adjacent rocks; the other is a pleochroic green biotite ( $n_\beta = 1.616\text{--}1.621$ ,  $2V = 0$ ), which has no equivalent near the ore. The



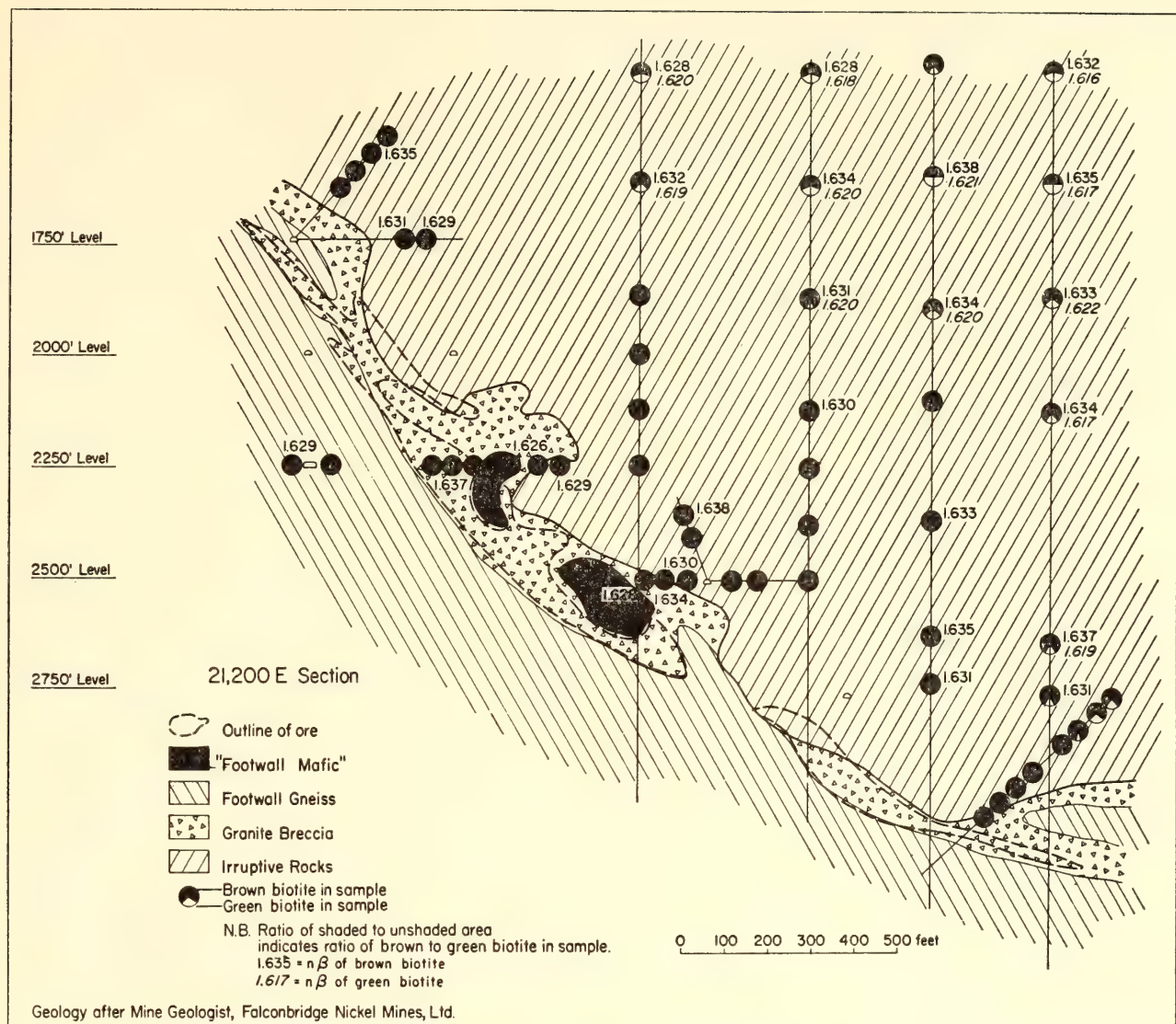


Fig. 67. Schematic vertical cross section (section 21,200E) through the Strathcona Mine showing the variation in color and  $n\beta$  of biotite about the ore body.

$c$ -lattice dimension of the unit cell for both green and brown biotites from a single sample was determined with a 114.6-mm-diameter X-ray powder camera using Fe radiation and silicon as internal standard. The  $c$  dimension of the brown biotite is  $10.17 \pm 0.04 \text{ \AA}$ , whereas that of the green is  $10.28 \pm 0.01 \text{ \AA}$ . The proportion of green to brown increases in samples collected farther away from the ore. The brown biotite appears to be secondary after the green and is particularly common around small specks of sulfide. Green biotite is never observed next to sulfide in a thin section.

Recent studies by Kullerud and Yoder (*Year Book 63*, p. 221) on the effect of

sulfur on hydrous iron-bearing silicates such as hornblende and biotite show that sulfur reacts with these minerals to form iron sulfides and possibly magnetite or hematite. The structure of the silicate remains unchanged except for a reduction in the unit-cell size. The brown color of the original silicate is intensified, and its refractive index increases. The reaction is interpreted as one in which some iron is removed from the structure while the remaining iron is oxidized up to the trivalent state to maintain charge balance.

The similarity between the changes observed in the laboratory and the variation present in the rocks from the



Strathcona Mine suggests that similar reactions occurred in both situations. Sulfur diffusing away from the ore deposit after its emplacement may have reacted with green biotite in the hanging wall to form sulfides and a partly oxidized brown biotite. If this is so, a reaction aureole of this type provides an important guide to ore. The validity of this hypothesis is being checked by chemical analyses of the biotites and examination of rocks along unmineralized portions of the contact.

### *Geological History*

A provisional outline of the geological history of the deposit follows:

1. Formation of the quartz-plagioclase-augite gneiss of the footwall.
2. Intrusion of the nickel irruptive rock followed by crystallization and formation of ultramafic zones at depth, possibly as stratiform layers that developed as a consequence of gravitational settling of olivine and pyroxene.
3. Fracturing of the chilled marginal portion of the norite followed by the intrusion of mafic norite, which brought with it fragments of olivine norite, ultramafic rock that had already consolidated at depth, and gneiss from the footwall. The existence of both gradational and sharp contacts between the mafic norite and the felsic norite is evidence that the felsic norite had only partly consolidated when the mafic norite was intruded.
4. Further fracturing, this time largely involving rocks of the footwall, which in part were ground to flour. A vapor phase consisting largely of water, but also rich in phosphorus and sodium, streamed into the new fracture zone and caused extensive recrystallization, deposition of apatite, and alteration of mafic minerals. The mixture of comminuted gneiss and vapor was injected back into fractures in the hanging wall and out into fractures in the footwall, gathering fragments of the irruptive rock and more gneissic fragments as it moved.

5. Introduction of ore. It is uncertain whether the ore was introduced into the granite breccia simultaneously with or after the other volatiles. It is clear that it was introduced and did not settle directly out of the overlying irruptive rock. Following mineralization, sulfur diffused away from the ore to attack biotite and other minerals in the surrounding rocks.

### SULFIDE-CARBONATE REACTIONS

*G. Kullerud*

Many of the world's important lead-zinc ore deposits occur in carbonate rocks of sedimentary origin. Such deposits are commonly not associated with observable igneous intrusives, and their origin has been debated heatedly for years. Some geologists regard the deposits as products of meteoric waters, and others maintain that the mineralogy indicates a hydrothermal origin from undisclosed igneous sources. To provide a possible basis for understanding the formation of sulfide ores in carbonate rocks a series of systematic studies of pertinent carbonate-sulfide systems has been conducted.

One of the important systems studied is Fe-S-O-CO<sub>2</sub>. In a series of experiments siderite (FeCO<sub>3</sub>) was reacted with sulfur in evacuated silica tubes at temperatures ranging from 100°C to 300°C. FeCO<sub>3</sub> decomposes, and FeS<sub>2</sub> forms together with a gas phase apparently containing CO<sub>2</sub> and SO<sub>2</sub> in a 2:1 ratio. In all experiments the FeS<sub>2</sub> phase occurs as euhedral crystals, and X-ray powder diffraction patterns and polished sections show that it is pyrite. Marcasite was not encountered even though all experiments were conducted in the *P-T* range in which this mineral appears to be stable. Similarly pyrrhotite does not form when sulfur reacts with FeCO<sub>3</sub>. Based on these new experiments and on already existing knowledge of the Fe-S-O system (Kullerud, *Year Book 56*, pp. 198-200) and the Fe-O-CO<sub>2</sub> system (French and Eugster, 1965), phase relations in much of the

quaternary system have been worked out.

These relations are shown in Fig. 68. They remain essentially unchanged over the temperature range in which  $\text{FeCO}_3$  is stable. For simplicity in presentation the solid solutions among some of the phases, such as  $\text{Fe}_{1-x}\text{S}$ , are not shown in the diagrams. Additional phases lying between  $\text{Fe}_{1-x}\text{S}$  and  $\text{FeS}_2$  in composition are not shown because they were not encountered in the present study. Such phases are monoclinic pyrrhotite, the  $\text{Fe}_3\text{S}_4$  phase, and marcasite, which appears to contain slightly less sulfur than is indicated by the  $\text{FeS}_2$  formula. In the simplified diagram of Fig. 68 the univariant mineral assemblages are iron + troilite + magnetite + siderite, pyrrhotite + pyrite + magnetite + siderite, and pyrite + magnetite + hematite + siderite.

In all experiments involving siderite and sulfur only pyrite and gas were produced. Thus these reactions involve only phases lying on the Fe- $\text{CO}_3$ -S plane in Fig. 68. The phase relations on this plane are shown in Fig. 69, with the same simplifications used in Fig. 68. Because of

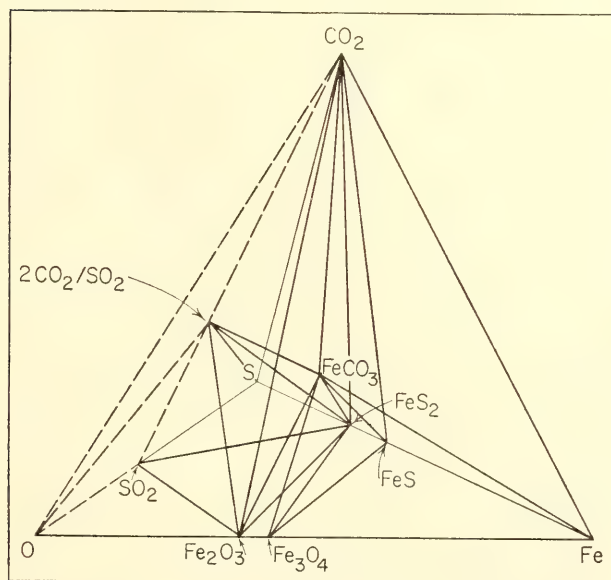


Fig. 68. Phase relations in the Fe-S-O- $\text{CO}_2$  system at temperatures where  $\text{FeCO}_3$  is stable. For simplicity, solid solutions among some of the phases are not shown, and some phases (marcasite, monoclinic pyrrhotite, etc.) not pertinent to the discussion are omitted.

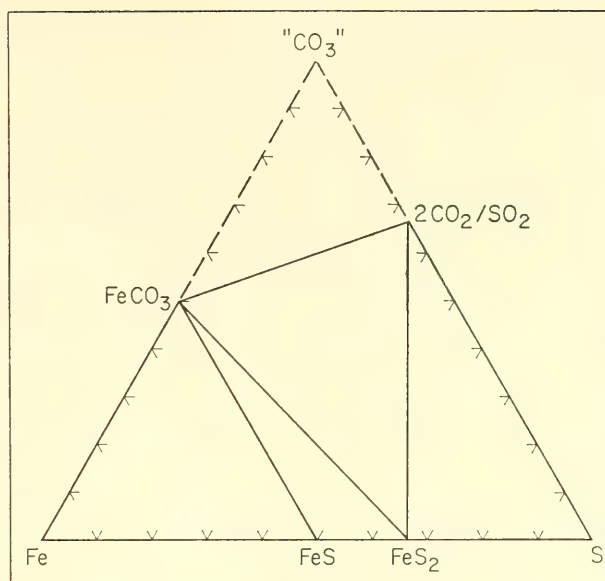
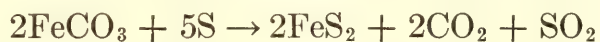


Fig. 69. Phase relations on the Fe-S- $\text{CO}_3$  plane in the temperature range of  $\text{FeCO}_3$  stability. Products of  $\text{FeCO}_3$ -S reactions lie on this plane.

the tie-line relations (shown by solid lines in the figures) addition of sulfur to react with  $\text{FeCO}_3$  can produce only the most sulfur-rich iron sulfide, which is pyrite.

The reaction between siderite and sulfur produces very high gas pressures, as may be inferred from the equation



The reaction rates are relatively rapid; clearly visible amounts of pyrite form at  $200^\circ\text{C}$  in 24 hours.

Experiments in the  $100^\circ\text{C}$ - $300^\circ\text{C}$  temperature range with cerussite ( $\text{PbCO}_3$ ) and sulfur produce galena ( $\text{PbS}$ ) and gas. Other phases were not encountered. Thus the reactions take place on the Pb- $\text{CO}_3$ -S plane and can be presented diagrammatically as shown in Fig. 70. The cerussite-sulfur reactions produce very high gas pressures similar to those resulting from the siderite-sulfur reactions. The cerussite-sulfur reaction can be expressed as



The  $\text{PbS}$  phase produced in these experiments gives X-ray diffraction patterns identical with those of natural galenas and occurs as well-developed



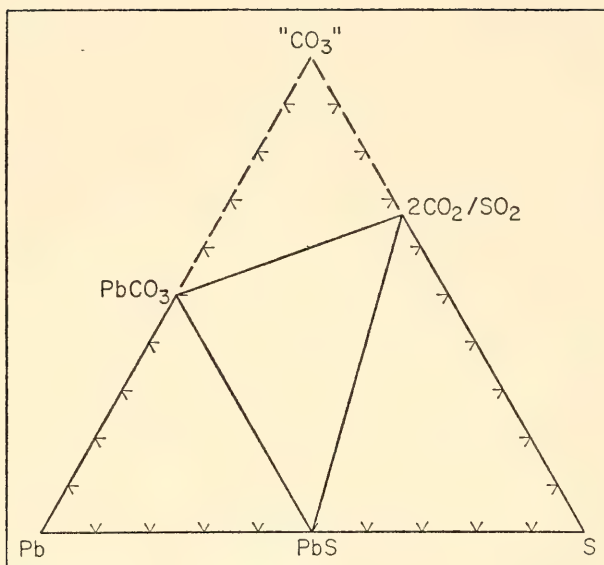


Fig. 70. Phase relations on the Pb-S-“CO<sub>3</sub>” plane in temperature range of PbCO<sub>3</sub> stability. Products of PbCO<sub>3</sub>-S reactions lie on this plane.

cubic crystals with cubes and octahedra as the most common forms. The reaction of PbCO<sub>3</sub> with S is more rapid than the reaction of FeCO<sub>3</sub> with S; at 200°C appreciable amounts form in one hour, and visible amounts form even at 100°C in 24 hours.

Because each of the carbonate-sulfur reactions described above is confined to a composition plane, phase relations involving two different carbonates and sulfur can be presented diagrammatically in a composition tetrahedron. Using the Fe-Pb-S ternary system (Brett and Kullerud, *Year Book* 63, pp. 202–204) as the base and “CO<sub>3</sub>” as the fourth corner of such a tetrahedron, the relations among all phases encountered in the present experiments can be expressed.

These relations are shown in Fig. 71. The stability of siderite has been studied by French and Eugster (1962) and by Weidner and Tuttle (1965), and that of cerussite by Grisafe and White (1964). Although the stability of the siderite-cerussite mineral pair has not been investigated, the phase relations as shown in Fig. 71 probably remain unchanged to at least 400°C.

From this figure it is seen that PbCO<sub>3</sub> and FeS<sub>2</sub> do not form a stable mineral

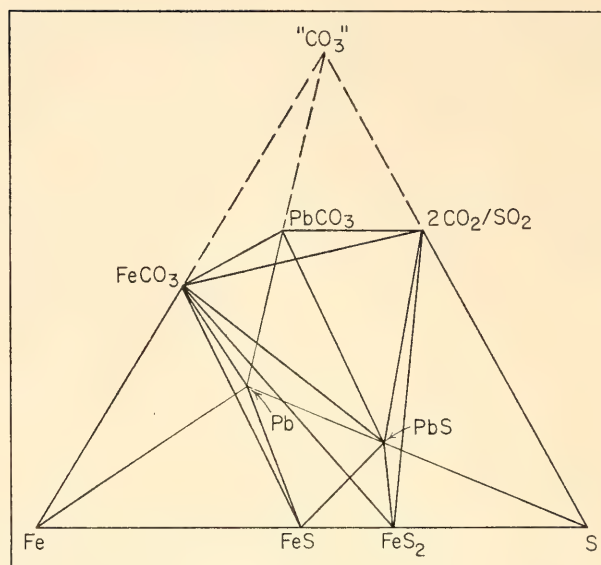
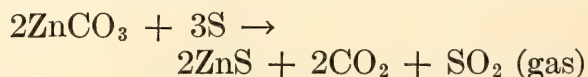


Fig. 71. Phase relations in the Fe-Pb-S-“CO<sub>3</sub>” system below about 400°C. For simplicity, some phases (between FeS and FeS<sub>2</sub>) and solid solutions among certain phases are not shown.

pair. Mixtures of the two will react, and the reaction products will be PbCO<sub>3</sub> + PbS + FeCO<sub>3</sub> + gas, or PbS + FeCO<sub>3</sub> + gas, or PbS + FeCO<sub>3</sub> + FeS<sub>2</sub> + gas, depending on the starting ratio of cerussite and pyrite. In this reaction PbCO<sub>3</sub> reacts first to produce PbS and gas. FeCO<sub>3</sub> is discolored by a thin, dark gray film that forms around grains, but it is only when the PbCO<sub>3</sub> supply is exhausted (the FeCO<sub>3</sub>-PbS-gas plane in Fig. 71) that FeCO<sub>3</sub> reacts beyond the stage of discoloration with the remaining sulfur to form pyrite and additional gas. If sufficient sulfur is present, all the FeCO<sub>3</sub> is consumed, and PbS and FeS<sub>2</sub> are the only remaining condensed phases.

Smithsonite (ZnCO<sub>3</sub>) and sulfur were reacted together in silica tubes at temperatures from 100°C to 300°C. Sphalerite (ZnS) and gas were the reaction products in all instances. The smithsonite-sulfur reaction, analogous to that involving PbCO<sub>3</sub> and sulfur, can be expressed as



The ZnS phase produced in these experiments is optically isotropic and gives an X-ray diffraction pattern identical to that of natural sphalerite. Wurtzite, the

hexagonal form of  $\text{ZnS}$ , was not produced. The reaction rates appear to be intermediate between those obtained when  $\text{PbCO}_3$  reacts with sulfur and those obtained when  $\text{FeCO}_3$  reacts with sulfur. Using  $\text{Zn}$ ,  $\text{S}$ , and " $\text{CO}_3$ " gas as end components the phases and phase assemblages partaking in the  $\text{ZnCO}_3$ - $\text{S}$  reactions can be represented in a composition triangle similar to the diagrams employed to demonstrate the  $\text{FeCO}_3$ - $\text{S}$  and  $\text{PbCO}_3$ - $\text{S}$  reactions. Because of the similarity, the  $\text{ZnCO}_3$ - $\text{S}$  reactions are not shown diagrammatically.

Reactions involving mixtures of  $\text{FeCO}_3$ ,  $\text{ZnCO}_3$ , and sulfur give further evidence of the similarity in behavior of  $\text{Pb}$  and  $\text{Zn}$  in carbonate systems. The phase relations in the quaternary system involving the carbonates and sulfides of  $\text{Fe}$  and  $\text{Zn}$  can readily be seen in Fig. 71 if  $\text{Zn}$  is substituted for  $\text{Pb}$  in the metal, sulfide, and carbonate phases. Thus it appears that cerussite and pyrite do not constitute a stable mineral pair. Mixtures of the two will react, and the reaction products will be  $\text{ZnCO}_3 + \text{ZnS} + \text{FeCO}_3 + \text{gas}$ , or  $\text{ZnS} + \text{FeCO}_3 + \text{gas}$ , or  $\text{ZnS} + \text{FeCO}_3 + \text{FeS}_2 + \text{gas}$ , depending on the starting ratio of smithsonite and pyrite.

Experiments using silica tubes in the  $100^\circ\text{C}$ - $300^\circ\text{C}$  temperature range were also performed on mixtures of rhodochrosite ( $\text{MnCO}_3$ ) and sulfur. The reaction rates are far slower than those observed in mixtures of  $\text{FeCO}_3$  and  $\text{S}$ ; less than one per cent sulfide was produced over a 30-day period in runs at  $250^\circ\text{C}$ . The sulfide phase occurred in amounts too small to be identified by X-ray power diffraction methods but was recognized as hauerite ( $\text{MnS}_2$ ) in polished sections. Neither the alabandite (green  $\text{MnS}$ ) phase nor any of the other reported  $\text{MnS}$  polymorphs were produced in these experiments. Carbonates in nature frequently contain appreciable amounts of lead, zinc, iron, and manganese. For instance, aragonite ( $\text{CaCO}_3$ ) from Friedensville, Pennsylvania, contains about 3.0 weight per cent  $\text{ZnO}$ , and aragonites

from Tarnowitz, Silesia (Traube, 1889), Tsumeb, Southwest Africa (O'Daniel, 1930), and Postenje, Serbia (Stephanović, 1922), contain 0.7, 5.2, and 15.10 weight per cent  $\text{PbO}$ , respectively. The  $\text{Zn}$  and  $\text{Pb}$  substitute for  $\text{Ca}$  in the aragonite structure. The dolomite group of carbonate minerals commonly contain considerable iron (ankerite) or manganese (kutnahorite) and in addition have been reported to contain cobalt and lead in appreciable quantities. The calcite group of the carbonate minerals includes calcite ( $\text{CaCO}_3$ ), siderite, and rhodochrosite. Calcite, which occurs in enormous quantities, has been reported to contain as much as 4.0 weight per cent  $\text{ZnO}$ , 2.0 weight per cent  $\text{CoO}$ , 1.5 weight per cent  $\text{PbO}$ , and several per cent of  $\text{Fe}$  and  $\text{Mn}$ . Siderite is commonly associated with hydrothermal replacement of metamorphic ore bodies and is the prominent gangue mineral in numerous large ore deposits as, for instance, in Erzberg, Austria; Freiburg, Germany; and Coeur d'Alene, Idaho. It often contains several per cent  $\text{MnO}$  and  $\text{CoO}$  and smaller quantities of  $\text{Pb}$  and  $\text{Zn}$ . Rhodochrosite is not so common but does occur as a gangue mineral in numerous metasomatic, metamorphic, and hydrothermal veins containing silver, lead, zinc, and copper sulfide ores. Although it generally contains several per cent iron substituting for manganese in its crystal structure, its zinc and lead contents are usually very low.

The experiments discussed show conclusively that carbonates containing metals such as lead, zinc, and iron will react with sulfur to form metal sulfides. Extensive carbonate deposits, as discussed, occur in nature, and large-scale reactions of the kind described may be expected to occur or to have occurred given some form of available sulfur. The carbonate rocks in which lead and zinc sulfide ores occur are frequently interbedded or closely associated with large amounts of pyrites and free sulfur of biologic origin.

Sulfur if mobilized would readily react



with the carbonates even at low temperatures, as indicated by the reaction rates observed in laboratory experiments. The metals, as demonstrated by experiments, would be extracted from the carbonates and converted to sulfides of lead, zinc, iron, and manganese in the order named. The gas phase produced by the carbonate-sulfur reactions would be augmented by  $H_2O$ , which invariably occurs in the rocks in question. In addition to the  $SO_2$  produced in carbonate-sulfur reactions this gas might contain significant amounts of sulfur acquired directly from an elemental source and thus serve as a carrier.

Judging from the pressures obtained in silica tubes considerable gas pressure may develop in carbonate rocks from carbonate-sulfur reactions even at  $100^\circ C$ . Provided sufficient sulfur is available and its solubility in the gas phase is significant, large-scale sulfide formation may take place when sulfur from the gas reacts with carbonates. Occasional release of pressure through fissures after a significant percentage of the carbonates locally have been transformed to dense sulfides and gas may result in the commonly observed slump structures.

The reactions taking place in experiments containing sulfur and carbonates of metals such as lead, zinc, iron, and manganese point out the role that sulfurization may have played in producing sulfide ores in carbonate rocks. The mechanisms and reactions of ore formation discussed above eliminate the need for igneous sources of the ore and may, when recognized in nature, provide new tools for ore exploration.

#### SULFIDE-SILICATE RELATIONS

*G. Kullerud and H. S. Yoder, Jr.*

Experiments have been performed on natural norites and ferrogabbros in the presence of excess sulfur in order to test the hypotheses of origin of associated ore bodies. Such ore bodies are thought either to have originated contemporane-

ously with the intrusives or to be dependent on later unrelated processes. If sulfur dissolves in the silicate magma, it will influence the crystallization behavior of the magma. The solution of sulfur in a silicate magma may be restricted in such a way as to yield two liquids, one silicate rich and the other sulfur rich, if appreciable sulfur is present. On the basis of this concept two schools of thought have emerged. One group believes that the ore is derived mainly through the expulsion of sulfides from the silicate-rich liquid, implying a relatively high solubility of sulfur in the silicate magma, about 0.1–0.2 weight per cent. The other group thinks that the ore body is produced by the sulfur-rich liquid, charged with metals, the immiscible silicate-rich liquid crystallizing separately yet contemporaneously with the ore-forming liquid.

The first test was to ascertain the influence of sulfur on the melting relations of two ferrogabbros having low liquidus temperatures from the Skaergaard intrusion (EG 4143 and EG 4330; see Tilley, Yoder, and Schairer, *Year Book 63*, pp. 92–97). In these experiments collapsible gold tubes could be used as sample containers to a temperature of  $1,000^\circ C$ . Gold melts at  $1,063^\circ C$  at 1 atm and probably melts below  $1,100^\circ C$  even at 10 kb. In the presence of ferrogabbro it may melt at an even lower temperature. For this reason attempts were made to use platinum sample containers at temperatures above  $1,000^\circ C$ . From previous experience (Kullerud and Yoder, 1959) it was known that sulfur reacts with platinum to produce  $PtS$  and  $PtS_2$ . It was thought possible that with an excess of sulfur present with ferrogabbro in platinum tubes some of the sulfur would react with platinum to form a relatively inert platinum-sulfide layer on the tube wall while the remaining sulfur would be available to react with the ferrogabbro. During such experiments the platinum-sulfide layer increases in thickness at a rapid rate as long as sulfur is available. It was therefore necessary to keep the tubes



at the desired pressures and temperatures only long enough to obtain equilibrium between ferrogabbro and sulfur.

Experiments lasting one hour at 1,150°C and 1,100°C at 10 kb produced partial melting of ferrogabbro. In addition, pyrrhotite and some magnetite occurred. The pyrrhotite in polished sections appeared to have crystallized from a liquid during the quenching period. Extensive reactions were observed to have occurred, however, between the pyrrhotite and the PtS and PtS<sub>2</sub> phases that formed in these experiments. The pyrrhotite, which is considerably grayer than pure Fe<sub>1-x</sub>S in reflected light, contains considerable Pt in solid solution.

In gold tubes sulfur reacted with the ferrogabbros at 1,000°C and 10 kb to produce pyrrhotite, magnetite, plagioclase, and pyroxene different from that of the ferrogabbro used as starting material. Much of the iron appears to have been removed as sulfide and oxide. No melting of the new assemblage was observed. It is concluded that a ferrogabbro cannot exist in the presence of an excess of sulfur. Therefore, either the sulfides coexisted with the ferrogabbro magma at the time of emplacement as miscible components or immiscible phases, or the sulfides were produced by reaction of sulfur with the crystallized ferrogabbro, presumably giving rise in a general way to the associated granophyric rocks as well as the ore body. These exciting observations clearly show that experiments with natural rocks in the presence of both sulfur and sulfides will contribute to our understanding of the relationship of ore bodies to silicate magmas.

#### THE MERCURY-SULFUR SYSTEM

*G. Kullerød*

Two sulfides of mercury, one red and one black, both having the composition HgS, are found in nature. The red sulfide, which has a hexagonal crystal structure, has the mineral name cinnabar; and the black sulfide, which has a cubic crystal structure, is called metacinnabar.

The cinnabar-metacinnabar relations were studied by Allen, Crenshaw, and Merwin (1912), who found three phases of HgS composition: cinnabar (specific gravity 8.176), which was prepared by digesting any other form of mercuric sulfide with a solution of ammonium sulfide or alkali sulfide; metacinnabar (specific gravity 7.60), which was precipitated from dilute acid solutions of mercuric salts by sodium thiosulfate; and hexagonal  $\beta'$ HgS (specific gravity 7.20), which was obtained by precipitation from concentrated neutral solutions of mercuric salts. Dickson and Tunell (1959) found that pure red HgS, cinnabar, inverts to black HgS, metacinnabar, at 344°C  $\pm$  2°C at 1 atm.

In the present study HgS was synthesized from the elements in silica tubes at 200°C, 300°C, 400°C, and 500°C. At 200°C and 300°C red cinnabar was produced, and at 400°C and 500°C black metacinnabar formed. This metacinnabar inverted to cinnabar in a few hours after quenching to room temperature. Differential thermal analyses (DTA) were performed on HgS enclosed in specially designed silica tubes with thermocouple wells. All experiments showed a sharply defined endothermic heat effect at 345°C on heating, an effect not observed on cooling. By means of a series of heating and cooling experiments in the 340°C–350°C range, however, it was shown that the cinnabar-metacinnabar inversion is reversible and that it takes place at 345°C  $\pm$  2°C, in agreement with the value of 344°C given by Dickson and Tunell (1959). In these experiments, after recording the effect at 345°C the heating process was stopped at 350°C. The temperature was then decreased to 340°C and after 30 minutes the sample was again heated to 350°C. In successive heating and cooling experiments the inversion was recorded without exception at 345°C on heating, whereas no sign of the inversion was recorded on cooling. DTA experiments on HgS at higher temperatures show that this compound melts con-



gruently at  $825^{\circ}\text{C} \pm 2^{\circ}\text{C}$ . Because of the high vapor pressure over  $\text{HgS}$ , a confining pressure of about 70 atm was applied on the DTA tubes in these experiments.

The  $\text{Hg-HgS}$  portion of the system was investigated by DTA experiments employing mixtures of liquid mercury and synthetic cinnabar. Confining pressures of about 150 atm were required at elevated temperatures because of the high vapor pressure over mercury. These experiments demonstrated the existence of a field of liquid immiscibility above  $792^{\circ}\text{C} \pm 2^{\circ}\text{C}$ . This field extends from  $0.7 \pm 0.2$  to  $8.5 \pm 0.3$  weight per cent S, as shown in Fig. 72. The cinnabar-metacinnabar inversion was recorded on heating at  $345^{\circ}\text{C}$  in all experiments containing 2.5 weight per cent S or more.

The  $\text{HgS-S}$  portion of the system was investigated by DTA experiments on

mixtures of synthetic  $\text{HgS}$  and S. Because of the high vapor pressure over sulfur at elevated temperatures, confining pressures of about 120 atm were required. As indicated in Fig. 72, liquid immiscibility exists in this portion of the system above  $795^{\circ}\text{C} \pm 2^{\circ}\text{C}$  and extends from  $24 \pm 0.5$  to  $76.5 \pm 0.5$  weight per cent S. The cinnabar-metacinnabar inversion at  $345^{\circ}\text{C}$  was again recorded only on heating. The occurrence of this inversion at  $345^{\circ}\text{C} \pm 2^{\circ}\text{C}$  in stoichiometric  $\text{HgS}$ , as well as when excess of Hg or S is used, indicates that little or no solid solution exists in  $\text{HgS}$  at this temperature. The lack of sharpness in curvature of the liquidus curve in the neighborhood of the melting point of  $\text{HgS}$  indicates that  $\text{HgS}$  is extensively dissociated in the liquid state.

Figure 72 also shows that  $\text{HgS}$  is readily soluble in liquid sulfur. The

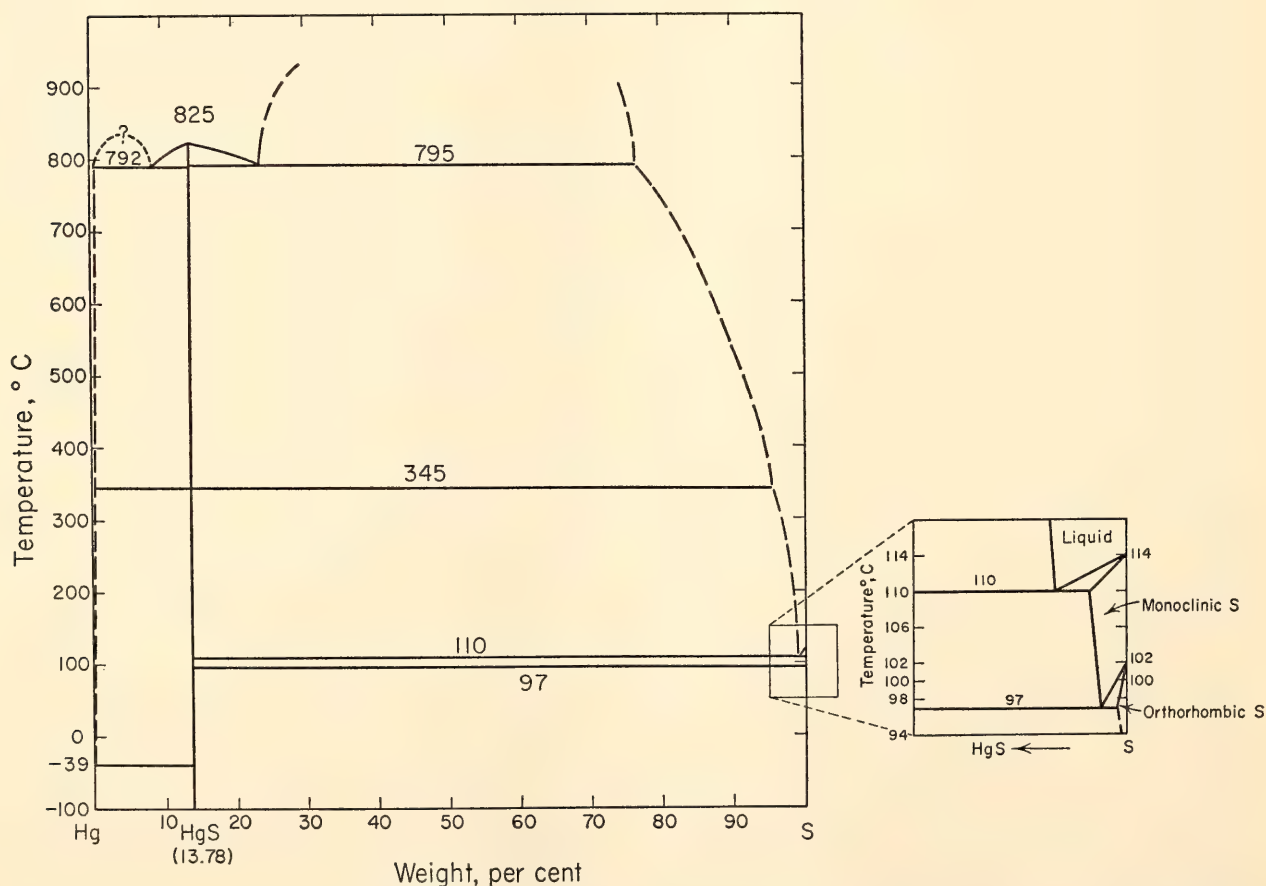


Fig. 72. Phase relations in the  $\text{Hg-S}$  system as determined in silica-tube experiments. Vapor occurs with all phases and phase assemblages.

amount dissolved reaches  $23.5 \pm 0.5$  weight per cent at  $795^\circ\text{C}$  and about 17.0 weight per cent at  $695^\circ\text{C}$ . On cooling, HgS crystallizes from the sulfur-rich liquid in dendritic or skeletal black metacinnabar crystals, which slowly invert to red cinnabar below  $345^\circ\text{C}$ . The solubility of HgS in S was not determined at low temperatures, but DTA experiments indicate that it is significant even at and below the melting point of sulfur. Details of the phase relations near the melting point of sulfur are given in the insert of Fig. 72. DTA experiments show that high-purity sulfur is orthorhombic below  $102^\circ\text{C} \pm 1^\circ\text{C}$ , where it inverts to a monoclinic polymorph. It melts at  $114^\circ\text{C} \pm 1^\circ\text{C}$ . These effects appear both on heating and on cooling. Experiments on mixtures of S and HgS, as indicated in Fig. 72, show that S saturated with HgS inverts to the monoclinic form at  $97^\circ\text{C} \pm 1^\circ\text{C}$  and melts at  $110^\circ\text{C} \pm 1^\circ\text{C}$ . Thus HgS decreases the inversion temperature by about  $5^\circ\text{C}$  and lowers the melting point by about  $4^\circ\text{C}$ .

In a number of experiments on compositions lying on the Hg as well as on the S side of HgS a very small exothermic effect was observed in the DTA heating curves at  $490^\circ\text{C}$ .

A high-temperature X-ray powder diffraction study is being conducted to determine whether observable structural changes occur at  $490^\circ\text{C}$ .

#### THE LEAD-SULFUR SYSTEM

*G. Kullerød*

In spite of the importance of galena (PbS) as a source of lead and the obvious desirability of developing low-cost commercial processes for metallurgical extraction of the metal from the ores, the lead-sulfur system has not been studied systematically before. In the present study PbS was synthesized from the elements in silica tubes with minimum vapor space at  $300^\circ\text{C}$ ,  $400^\circ\text{C}$ ,  $500^\circ\text{C}$ , and  $600^\circ\text{C}$ . The quenched products all gave X-ray powder diffraction patterns

identical with those of natural galenas. Differential thermal analyses performed on stoichiometric PbS enclosed in silica tubes with thermocouple wells showed that PbS melts congruently at  $1,115^\circ\text{C} \pm 2^\circ\text{C}$ . This melting temperature is in agreement with that given by Van Hook (1959) but is lower than the  $1,127^\circ\text{C}$  value given by Bloem and Kröger (1956).

The Pb-PbS portion of the system was investigated by DTA experiments on mixtures of Pb and synthetic galena. These experiments demonstrated the existence of a field of liquid immiscibility above  $1,043^\circ\text{C} \pm 2^\circ\text{C}$ , as shown in Fig. 73. This two-liquid field is rather narrow, extending from  $4.0 \pm 0.3$  to  $9.5 \pm 0.3$  weight per cent S.

The solubility of Pb in PbS is small. In experiments containing mixtures of Pb and PbS, strong heat effects were recorded at  $1,043^\circ\text{C} \pm 2^\circ\text{C}$  even when as much as 12.0 weight per cent S was present, corresponding to 90.0 weight per cent PbS and 10.0 weight per cent Pb. Since PbS contains 13.40 weight per cent S, these results indicate that the solubility of Pb in PbS is much less than 1.4 weight per cent. Furthermore, since the heat effect at  $1,043^\circ\text{C}$  is dependent on the presence of lead-rich liquid and since the effect would not be strong enough to be recorded unless an appreciable amount of this liquid were present, it can be concluded that the solubility of liquid Pb in PbS probably does not exceed 1.0 weight per cent even at  $1,043^\circ\text{C}$ . The solubility of PbS in liquid Pb is about 15.0 weight per cent (= 2.0 weight per cent S) at  $950^\circ\text{C}$  and about 26.0 weight per cent (= 3.5 weight per cent S) at  $1,013^\circ\text{C}$ . The melting point of pure lead was recorded at  $326.6^\circ\text{C} \pm 1^\circ\text{C}$ ; mixtures of Pb and PbS showed initial melting at  $326.5^\circ\text{C} \pm 1^\circ\text{C}$ . These experiments show that the temperature difference between the melting point of pure lead and the eutectic at which Pb, PbS, and liquid are in equilibrium is less than the experimental error.

In experiments on compositions con-



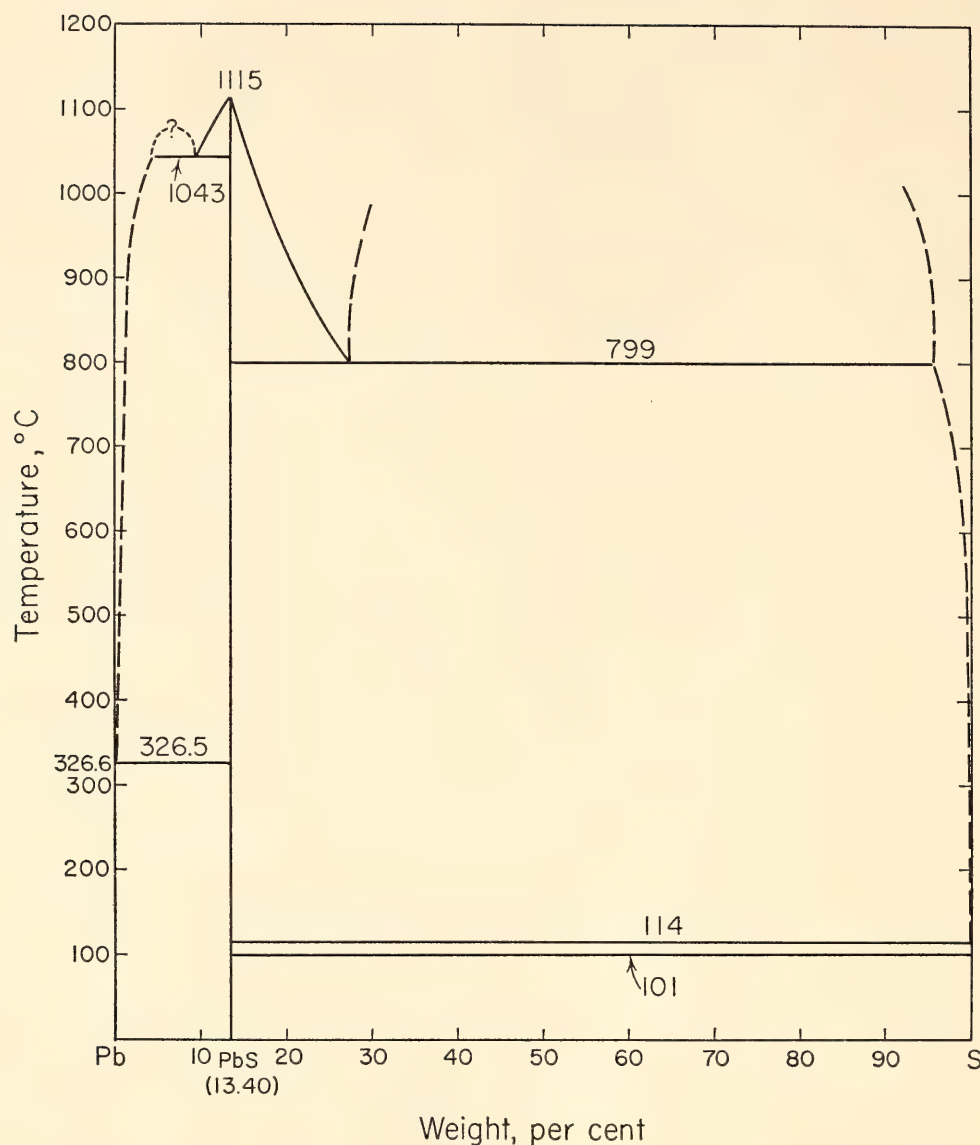


Fig. 73. Phase relations in the Pb-S system as determined in silica-tube experiments. Vapor occurs with all phases and phase assemblages.

taining more sulfur than is indicated by the PbS (13.40 weight per cent S) formula the liquidus curve was found to slope steeply to  $799^{\circ}\text{C} \pm 2^{\circ}\text{C}$ . Because of the high vapor pressure over PbS + S assemblages at elevated temperatures, the experiments in this portion of the Pb-S system were performed using confining pressures of about 50 atm on the DTA tubes. A second liquid immiscibility field exists in this system above  $799^{\circ}\text{C} \pm 2^{\circ}\text{C}$ , as noted in Fig. 73. This field is very wide, extending from  $27.0 \pm 0.5$  to more than 95.0 weight per cent S. The solubility

of PbS in liquid S is less than 6.0 weight per cent at  $799^{\circ}\text{C}$ . In comparison, the solubility of HgS in liquid S at about the same temperature is approximately 28.0 weight per cent, as discussed in another section.

In the presence of PbS, sulfur melts at  $114^{\circ}\text{C} \pm 1^{\circ}\text{C}$ , which is identical within experimental error with the melting point of pure sulfur. The orthorhombic-monoclinic inversion, which in pure sulfur appears at  $102^{\circ}\text{C} \pm 1^{\circ}\text{C}$ , was recorded at  $101^{\circ}\text{C} \pm 2^{\circ}\text{C}$  on mixtures of PbS and S.

Brett and Kullerud in *Year Book 63*

(p. 202) showed that a field of liquid immiscibility exists in the Fe-Pb-S system above  $717^{\circ}\text{C} \pm 3^{\circ}\text{C}$ . The new data on the Pb-S system show that this two-liquid field reaches the binary Pb-S boundary at  $799^{\circ}\text{C} \pm 2^{\circ}\text{C}$ .

#### HIGH-PRESSURE DIFFERENTIAL THERMAL ANALYSIS

*G. Kullerud, P. M. Bell, and J. L. England*

Numerous sulfide minerals at elevated temperatures undergo polymorphic inversions and chemical breakdowns that cannot be quenched; that is, as the temperature is lowered new crystalline forms or compounds may appear. Common ore minerals such as chalcocite, chalcopyrite, bornite, pyrrhotite, digenite, and cubanite are examples. They possess high-temperature crystal structures that on cooling invert to low-temperature polymorphs. Sometimes the inversion from the high- to the low-temperature crystal structure is accompanied by twinning. If twinning similar to that observed in the experimental sample is also observed in the corresponding samples from ore deposits it is likely that the mineral in question has experienced a temperature above that of the inversion point. The temperatures at which inversions occur have been determined for numerous sulfides by experiments employing DTA in silica tubes at the vapor pressures created by the minerals.

Another parameter that is important in geological processes of ore deposition is the influence of pressure on the temperatures of such inversions. During this last year the influence of pressure has been determined on the temperature of the inversion in chalcopyrite, troilite, pyrrhotite, and heazlewoodite.

In polished sections of ores chalcopyrite ( $\text{CuFeS}_{2-x}$ ) frequently displays twinning, probably because of an inversion that occurred at elevated temperatures. Experimentally Cheriton (1952) found that both natural and synthetic chalcopyrite invert from a low-temperature

tetragonal structure to a high-temperature cubic structure at  $580^{\circ}\text{C} \pm 20^{\circ}\text{C}$ . Yund and Kullerud (*Year Book 59*, pp. 111–114) determined the entire solid solution field of chalcopyrite and found, in agreement with Merwin and Lombard (1937), that this phase always contains less sulfur than is indicated by the  $\text{CuFeS}_2$  formula. Yund and Kullerud found the inversion to take place at  $547^{\circ}\text{C} \pm 5^{\circ}\text{C}$  in synthetic chalcopyrite containing the maximum amount of sulfur at this temperature. DTA experiments in silica tubes on natural chalcopyrites give results on the inversion in good agreement with this value. In the present study chalcopyrite of  $\text{CuFeS}_{1.92}$  composition was synthesized from the elements in silica tubes at  $600^{\circ}\text{C}$  as described by Yund and Kullerud. DTA experiments at high pressures were performed on this material in the range 2,500 to 40,500 bars (Fig. 74).

The inversion temperature decreases

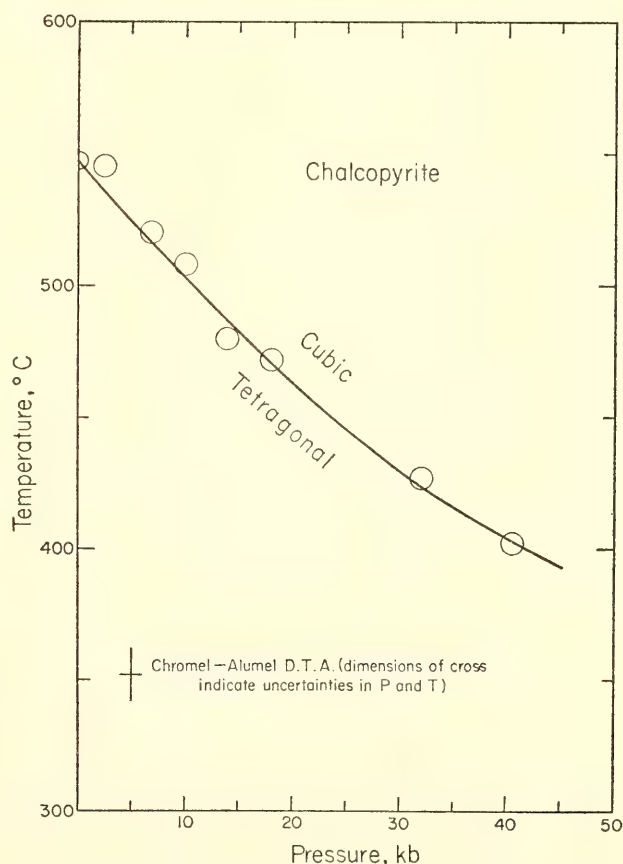


Fig. 74. Curve shows effect of pressure on tetragonal-cubic inversion in chalcopyrite of  $\text{CuFeS}_{1.92}$  composition.



markedly with increasing pressure and appears to be as low as  $400^{\circ}\text{C}$  at 40,000 bars. Thus the negative slope of the inversion is on the average almost  $4^{\circ}\text{C}$  per kb.

Kullerud (*Year Book 63*, p. 200) found by DTA that with a sample of  $\text{CuFeS}_2$  composition contained in silica tubes the solidus and liquidus were intersected at  $865^{\circ}\text{C} \pm 3^{\circ}\text{C}$  and  $895^{\circ}\text{C} \pm 3^{\circ}\text{C}$ , respectively. These curves nearly intersect

at  $898^{\circ}\text{C} \pm 3^{\circ}\text{C}$  for  $\text{CuFeS}_{1.92}$  composition.

The effect of pressure on the temperature of melting of  $\text{CuFeS}_{1.92}$  was investigated by DTA. At 14,000 bars melting was recorded at  $898^{\circ}\text{C}$ , and at 25,000 bars,  $920^{\circ}\text{C}$ . Apparently the melting temperature at first increases very little with pressure but increases more rapidly above 14,000 bars.

Unlikely chalcopyrite, the inversion in

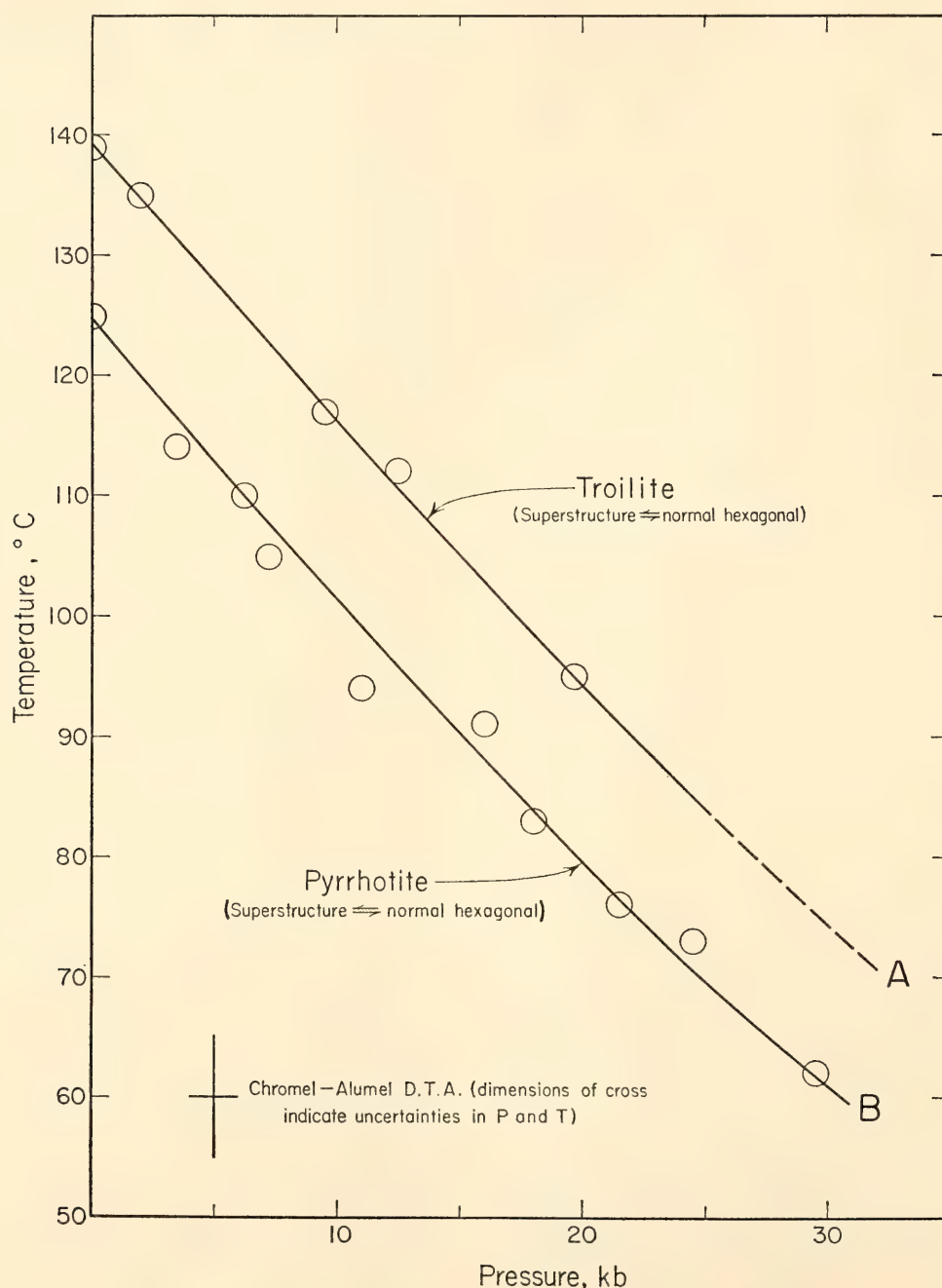


Fig. 75. Curve A, effect of pressure on superstructure-normal hexagonal inversion in troilite ( $\text{FeS}$ ); curve B, effect of pressure on superstructure-normal hexagonal inversion in pyrrhotite ( $\text{Fe}_{1-x}\text{S}$ ) containing 36.7 weight per cent S.

troilite (FeS) and in pyrrhotite ( $\text{Fe}_{1-x}\text{S}$ ) is a change from a normal *B8*-type hexagonal structure stable at elevated temperatures to a low-temperature hexagonal superstructure and is not accompanied by twinning. The temperature of this inversion at 1 atm was determined by Moh and Kullerud (*Year Book 63*, p. 207) as  $139^\circ\text{C} \pm 1^\circ\text{C}$  for stoichiometric FeS. DTA experiments at high pressures performed on troilite synthesized from the elements at  $550^\circ\text{C}$  demonstrate that the slope of the pressure-temperature curve for the inversion is negative (Fig. 75A). The inversion temperature was determined over the pressure range 2,000 to 19,700 bars. The effect of pressure is to lower the inversion temperature by about  $2.2^\circ\text{C}$  per kb. At 20,000 bars the inversion takes place at as low as  $95^\circ\text{C}$ .

Moh and Kullerud (*Year Book 63*, p. 207) determined the temperature of the inversion of pyrrhotite ( $\text{Fe}_{1-x}\text{S}$ ) from the normal hexagonal *B8*-type to the hexagonal superstructure as  $125^\circ\text{C} \pm 1^\circ\text{C}$  for  $\text{Fe}_{1-x}\text{S}$  containing 36.7 weight per cent S. The effect of pressure on this inversion has now been studied over the pressure range 3,500 to 29,500 bars (Fig. 75B). The slope of the lower curve is negative and, within the limits of error of the experimental methods, identical with that of the troilite equilibrium curve.

The mineral heazlewoodite ( $\text{Ni}_3\text{S}_3$ ) is hexagonal. On heating to  $556^\circ\text{C}$ , it inverts to a high-temperature tetragonal or pseudocubic polymorph (Kullerud and Yund, 1962). The high-low inversion is very rapid, and it can readily be detected in DTA experiments. The low-temperature form is not twinned. The inversion temperature has now been determined as a function of pressure to 14,400 bars. The material used in the experiments was stoichiometric  $\text{Ni}_3\text{S}_2$  synthesized from the elements at  $500^\circ\text{C}$  in silica tubes with minimum vapor space (Kullerud and Yoder, 1959). The results of the experiments are presented in Table 17. It is noted that the inversion temperature increases slightly with in-

TABLE 17. Inversion in Stoichiometric  $\text{Ni}_3\text{S}_2$

Temperature of Inversion, $^\circ\text{C}$	Pressure, bars
556	<1
$560 \pm 5$	1,700
$560 \pm 5$	3,300
$560 \pm 5$	4,000
$567 \pm 5$	6,000
$577 \pm 5$	10,700
$584 \pm 5$	14,400

creasing pressure. The slope of the *P-T* curve is about  $1.7^\circ\text{C}$  per 1,000 bars.

Heazlewoodite contains appreciable iron in solid solution when it coexists with pentlandite or when it is produced through breakdown of pentlandite. The influence of iron on the inversion of heazlewoodite was investigated. For this purpose mixtures of synthetic heazlewoodite and about 6.0 weight per cent pyrrhotite were heated together at  $550^\circ\text{C}$ . This amount of iron is sufficient to saturate the high-temperature heazlewoodite phase at this temperature and to produce a small amount ( $\sim 0.5$  per cent) of pentlandite. The results of DTA experiments at high pressures conducted on this material in the range 19,400–30,500 bars are given in Table 18. It is noted by comparison of the data in Tables 17 and 18 that the presence of Fe in solid solution decreases the inversion temperature below that of pure  $\text{Ni}_3\text{S}_2$  and decreases the slope of the inversion curve. This slope, as described above, is about  $1.7^\circ\text{C}$  per 1,000 bars for pure  $\text{Ni}_3\text{S}_2$  but is only of the order of  $0.3^\circ\text{C}$  per 1,000 bars for heazlewoodite saturated with iron.

TABLE 18. Inversion in Iron-Saturated Heazlewoodite

Temperature of Inversion, $^\circ\text{C}$	Pressure, bars
$534 \pm 5$	19,400
$535 \pm 5$	21,500
$535 \pm 5$	25,000
$537 \pm 5$	27,000
$537 \pm 5$	30,500



CRYSTALLOGRAPHY

REFINEMENT OF LATTICE PARAMETERS  
USING SYSTEMATIC CORRECTION TERMS

Charles W. Burnham

Lattice parameters of single crystals have been determined in this laboratory for the past two years by least-squares refinement of diffraction-angle ( $\theta$ ) measurements obtained with a precision back-reflection Weissenberg camera<sup>20</sup> (Buerger, 1937). Refinements have been carried out on the IBM 7094 computer using the method described in *Year Book 61* (pp. 132–135), which allows for inclusion of systematic error terms. For complete determination of all linear and angular parameters of a triclinic unit cell, photographs about all three crystallographic axes are required. The refinement operates on combined data from three films; hence three systematic film-shrinkage-error terms (one for each film) and three systematic absorption-error terms (one for each orientation of the crystal) are included in the refinement. In addition, an eccentricity-error term is included to account for instrumental error. The computation produces the best least-squares values for six lattice parameters and seven experimental systematic error parameters.

This year our first precision Weissenberg camera was replaced with a mechanically improved version. The geometry of both cameras is identical, and photo-

graphs of any crystal should therefore have been identical except for slightly different displacements owing to differing radius and film shrinkage errors, assuming both cameras to be perfectly aligned (zero eccentricity error). Such was not the case, however, and a marked lack of superposition of spots on films of the same crystal taken with the two cameras led to an investigation of the type of systematic error causing the disagreement and to a convincing demonstration of the power of this refinement technique.

Significant differences between the two supposedly identical cameras were first observed when *c*-axis photographs of R $\beta$ ec mullite (see *Year Book 62*, pp. 158–165) were compared. Some representative values of measured diffraction angles from the two films are listed in Table 19, illustrating the apparent lack of agreement between the two films.

A complete unit-cell refinement had already been carried out with the use of 56 measurements from *b*- and *c*-axis films obtained with the old camera. To check the least-squares procedure and make sure that the systematic error terms were actually compensating as they should, a set of 55 measurements from *b*- and *c*-axis films obtained with the new camera were subjected to least-squares refinement. Both refinements employed systematic error terms having the general form  $g(\theta)X$ , where  $g(\theta)$  is a trigonometric function of  $\theta$ , and  $X$  is an error parameter whose value is initially unknown and is

<sup>20</sup> Now available from the Charles Supper Company.

TABLE 19. Observed and Calculated Diffraction Angles  $\theta$  for Representative Reflections of R $\beta$ ec Mullite, CuK $\alpha_1$  Radiation

<i>hkl</i>	$\theta_{\text{obs}}$	$\theta_{\text{obs}}$	$\theta_{\text{obs}}$	$\theta_{\text{obs}}$	$\theta_{\text{calc}}$
	Uncorrected, Camera 1	Corrected, Camera 1	Uncorrected, Camera 2	Corrected, Camera 2	Combined Data
490	81.71	81.58	81.51	81.54	81.56
580	71.95	71.64	71.60	71.63	71.63
920	69.79	69.43	69.40	69.43	69.44
760	69.01	68.65	68.61	68.64	68.65
660	59.40	58.89	58.89	58.90	58.90

determined by the least-squares procedure (see *Year Book 61*, p. 133, Equations 5, 6, and 7). The coefficients  $g(\theta)$  follow.

Film shrinkage (separate terms,  $X_s$ , for each film):

$$g(\theta)_{\text{shr}} = \frac{4}{\lambda^2} \left( \frac{\pi}{2} - \theta \right) \sin 2\theta$$

Specimen absorption (separate terms,  $X_a$ , for each orientation of the crystal):

$$g(\theta)_{\text{abs}} = \frac{4}{\lambda^2} \cos^2 \theta \sin 2\theta$$

Eccentricity (one term,  $X_e$ , to allow for camera misalignment):

$$g(\theta)_{\text{ecc}} = \frac{4}{\lambda^2} \sin^2 2\theta$$

The results of the two independent refinements are listed in Table 20. The lattice parameters determined from the two sets of data are in very close agreement (the largest difference, in  $c$ , corresponds to about one part in 3,000). Comparison of the systematic error terms suggests two possibilities for differences between the cameras: (1) Film-cylinder radius errors are identical in form with shrinkage errors—hence the large values for  $X_s$  for camera 1 could arise from a radius error in that camera; (2) there is a definite possibility of a rather large eccentricity error in camera 1.

To gain further insight into the sources of systematic error, a least-squares refinement was performed using all measurements. Since the same crystal was used to obtain all films, there is only one set of true lattice parameters. Furthermore, the absorption error is a function of the sample only and does not depend on which camera was used. Hence the combined set of data was refined using eight systematic correction terms: four shrinkage terms,  $X_s$ , one for each film; two absorption terms,  $X_a$ , one for each orientation of the crystal; and two eccentricity terms,  $X_e$ , one for each camera. The resulting lattice parameters (Table 21) fall between those obtained from separate refinement (Table 20) and exhibit a minimum internal precision of one part in 7,000. The systematic correction terms show that there is little likelihood that the film cylinders of the two cameras have significantly different radii, assuming that the shrinkage of all films will be about the same. The two eccentricity error terms, however, are significantly different and strongly suggest that camera 1 is misaligned, i.e., that the crystal rotation axis is not coincident with the axis of the film cylinder, whereas the eccentricity error in camera 2 is small and may be zero.

After these refinements were completed, the alignment and film-cylinder radii of

TABLE 20. Results of Least-Squares Refinements of R $\beta$ ec Mullite (Orthorhombic) Lattice Parameters, Precision Weissenberg Cameras

	Camera 1 (old), 56 Observations	Camera 2 (new), 55 Observations
$a$ , Å	7.5791 ± 0.0008	7.5796 ± 0.0003
$b$ , Å	7.6870 ± 0.0006	7.6877 ± 0.0002
$c$ , Å	2.8883 ± 0.0007	2.8874 ± 0.0003
Volume, Å <sup>3</sup>	168.27 ± 0.06	168.25 ± 0.02
Shrinkage error, $X_s$ , $b$ -axis film	−0.026 ± 0.024	−0.008 ± 0.010
Shrinkage error, $X_s$ , $c$ -axis film	−0.022 ± 0.024	−0.007 ± 0.009
Absorption error, $X_a$ , $b$ -axis orientation	0.024 ± 0.018	0.013 ± 0.007
Absorption error, $X_a$ , $c$ -axis orientation	0.018 ± 0.017	0.009 ± 0.007
Eccentricity error, $X_e$	0.018 ± 0.010	0.001 ± 0.004



TABLE 21. Results of Least-Squares Refinement of R $\beta$ ec Mullite Lattice Parameters, Combined Data From Both Precision Weissenberg Cameras, 111 Observations

$a$ , Å	$7.5794 \pm 0.0005$
$b$ , Å	$7.6873 \pm 0.0003$
$c$ , Å	$2.8878 \pm 0.0004$
Volume, Å <sup>3</sup>	$168.26 \pm 0.03$
$X_s$ , $b$ -axis film, camera 1	$-0.019 \pm 0.014$
$X_s$ , $b$ -axis film, camera 2	$-0.015 \pm 0.014$
$X_s$ , $c$ -axis film, camera 1	$-0.015 \pm 0.014$
$X_s$ , $c$ -axis film, camera 2	$-0.013 \pm 0.013$
$X_a$ , $b$ -axis orientation	$0.018 \pm 0.010$
$X_a$ , $c$ -axis orientation	$0.013 \pm 0.009$
$X_e$ , camera 1	$0.016 \pm 0.005$
$X_e$ , camera 2	$0.004 \pm 0.005$

$X_s$ , shrinkage error;  $X_a$ , absorption error;  $X_e$ , eccentricity error.

the two cameras were carefully measured by the manufacturer (Charles Supper, personal communication, 1965). Within the limits of measurement, the film-cylinder radii were the same and equal to their designed value. Dial gauge measurements indicated that camera 1 was indeed misaligned as expected and that camera 2 was correctly aligned to within 1 mil (0.001 inch).

The lattice parameter of a sample of the pure silicon used as an internal standard in powder diffractometry at the laboratory has been determined by the methods just outlined. In this case a back-reflection powder photograph was made with camera 2, and least-squares refinement of the lattice parameter,  $a$ , and shrinkage and absorption correction terms was carried out with 18 measurements. The eccentricity error term was included, but its value was fixed at 0.004, as determined from the mullite refinements. The resulting value of  $a$  is  $5.43074\text{Å} \pm 0.00015\text{Å}$ . This should be compared with the value reported by Parrish (1960) of  $5.43054\text{Å} \pm 0.00017\text{Å}$ , which is an average of 25 determinations from 16 laboratories. The difference between our value and the average is 0.00020, which is slightly greater than  $1\sigma$  and corresponds to one part in 26,000.

From this investigation two important

conclusions can be drawn. First, the systematic errors inherent in any film technique cause significant errors in measured values of  $2\theta$  or  $d$  and must be taken into consideration when determining precise values of lattice parameters. Second, the least-squares technique discussed here is capable of determining the magnitude of systematic errors and automatically correcting for them to yield consistent results from data that are, before correction, inconsistent.

#### FERROSILITE

Charles W. Burnham

In *Year Book 63* (pp. 174–176) Lindsley, MacGregor, and Davis reported the synthesis of three polymorphs of ferrosilite,  $\text{FeSiO}_3$ , two of which are apparent structural analogues of the known polymorphs of enstatite,  $\text{MgSiO}_3$ . Results of a preliminary single-crystal investigation of the third polymorph, termed ferrosilite III, also reported in *Year Book 63* (p. 237), showed it to possess triclinic symmetry. This year single-crystal investigations of these materials have yielded precise unit-cell dimensions for clinoferrosilite and orthoferrosilite and have shown that ferrosilite III has a crystal structure similar to that of the pyroxenoids rhodonite and pyroxmangite, rather than to those of the clinopyroxenes.

#### *Clinoferrosilite and Orthoferrosilite*

Space groups of clinoferrosilite and orthoferrosilite have been determined by precession photographs as  $P2_1/c$  and  $Pbca$ , respectively. Unit-cell dimensions of both crystals have been determined by least-squares refinement of measurements from precision back-reflection Weissenberg photographs. Both refinements included systematic correction terms for specimen absorption, film shrinkage, and camera eccentricity. The results, based on 57 independent measurements for clinoferrosilite and 32 independent measurements for orthoferrosilite, are listed in Table 22. Since  $Z$ , the number of formula

TABLE 22. Unit-Cell Data for Clinoferrosilite and Orthoferrosilite

	Clinoferrosilite	Orthoferrosilite
<i>a</i> , Å	9.7085 ± 0.0008	18.431 ± 0.004
<i>b</i> , Å	9.0872 ± 0.0011	9.080 ± 0.002
<i>c</i> , Å	5.2284 ± 0.0006	5.238 ± 0.001
β	108.432 ± 0.004°	...
Volume, Å <sup>3</sup>	437.6 ± 0.1	876.7 ± 0.5
<i>Z</i>	8	16
Space group	<i>P</i> 2 <sub>1</sub> / <i>c</i>	<i>Pbca</i>

units per unit cell, is 8 in clinoferrosilite and 16 in orthoferrosilite, the unit-cell volume of the monoclinic form, 437.6 ± 0.1 Å<sup>3</sup>, should be compared with half the unit-cell volume of the orthorhombic form, or 438.4 ± 0.3 Å<sup>3</sup>. Conversion to molar volumes gives 32.952 ± 0.008 cm<sup>3</sup>/mole for clinoferrosilite and 33.008 ± 0.019 cm<sup>3</sup>/mole for orthoferrosilite. The increase in volume when transforming from “clino” to “ortho” is thus 0.056 ± 0.021 cm<sup>3</sup>/mole, and the basis for the small positive slope of the transformation curve determined by Lindsley this year (see Fig. 51, p. 149) is confirmed.

Intensity measurements from small single crystals of both clinoferrosilite and orthoferrosilite have now been obtained with the automated equi-inclination Weissenberg single-crystal diffractometer and the determination and refinement of both structures are being carried out.

Ferrosilite III

Preliminary precession photographs of ferrosilite III showed patterns similar to that of diopside obtained by precessing about the *b* axis. There were, however, several inconsistencies that indicated that this material is not monoclinic. Further study of several crystals revealed an unexpectedly short translation, which ultimately proved to be parallel to *c*\*. After photographing a crystal that exhibited one pronounced cleavage, a unit cell was selected on the basis of the cleav-

age being parallel to (010). It was immediately obvious that the cell bore an overall resemblance to those of the triclinic metasilicates or pyroxenoids. When the initial *a* and *b* axes are interchanged and the *c* axis is reversed to maintain a right-handed coordinate system, the cleavage becomes parallel to (100) and the analogy to the unit cell of pyroxmangite becomes obvious (see Table 23). The only major difference is that the *c* axis of ferrosilite III is longer than that of pyroxmangite by 5.23 Å. This difference is almost exactly equal to the length of the *c* axes of true pyroxenes, which corresponds to the repeat length of two SiO<sub>4</sub><sup>-4</sup> tetrahedrons along the pyroxene chain.

Liebau (1962), and Prewitt and Peacor (1964) have compared the known structures of the triclinic pyroxenoids and have shown that they may be described in terms of closest packing of oxygen atoms, with silicon cations filling tetrahedral interstices, and larger cations (Ca, Mn, Mg, Fe) occupying octahedral sites in such fashion that the structures consist of alternating layers of silicon cations and larger cations, separated by layers of oxygen anions. The silicon layers consist of tetrahedrons sharing vertexes to form continuous chains parallel to *c*. The essential difference between the structures is the length of the repeat unit along the chains; according to Liebau (1962) true pyroxenes contain *Zweierketten*, wollastonite and bustamite *Dreierketten*, rhodonite *Fünferketten*, and pyroxmangite *Siebenerketten*. The repeat units are illus-

TABLE 23. Comparison of the Unit Cells of Ferrosilite III and Pyroxmangite

	Ferrosilite III	Pyroxmangite (Liebau, 1959)
<i>a</i> , Å	6.57	6.67
<i>b</i> , Å	7.51	7.56
<i>c</i> , Å	22.68	17.45
α	115.3°	113.7°
β	80.5°	84.0°
γ	95.5°	94.3°



trated schematically in Fig. 76 (after Prewitt and Peacor, 1964).

Since the only significant difference between the unit cells of pyroxmangite and ferrosilite III is the increase, by approximately 5.2 Å, of the length of the  $c$  axis, which is a function of the length of the repeat unit in the chain, it is very likely that ferrosilite III is a pyroxenoid with a chain repeat of nine tetrahedrons or a *Neunerketten*. One possible chain configuration is shown in Fig. 76. Note that projections of ferrosilite III and diopside along a horizontal axis in the plane of the diagram are identical. Since that axis is parallel to the diopside  $b$  axis, the diopside-like precession patterns we obtained are not inconsistent with the suggested model.

Plate 1 contains two zero-level precession photographs of ferrosilite III. The  $a$ -axis photograph (Plate 1A) contains the  $c^*_m$  axis of the diopside-like pseudomonoclinic substructure. It should be noted that there is no apparent substructure

parallel to  $c^*$  in either photograph.

Single-crystal intensity data are now being obtained for ferrosilite III, and our structure determination will, it is hoped, confirm the first known example of *Neunerketten* in a pyroxenoid.

#### THERMAL PARAMETERS AND ATOMIC COORDINATES OF $\alpha$ QUARTZ: A COMPARISON OF MANUAL AND AUTOMATED DIFFRACTOMETER RESULTS

Charles W. Burnham

As our knowledge of silicate crystal chemistry broadens and becomes more detailed and complex, the demand for more precise structural information on the rock-forming silicates rapidly increases. To meet this increasing requirement for structural data and to afford us the practical ability to obtain such data under nonstandard temperature conditions, the manually operated single-crystal diffractometer has been replaced with an automated equi-inclination Weissenberg single-crystal diffractometer.

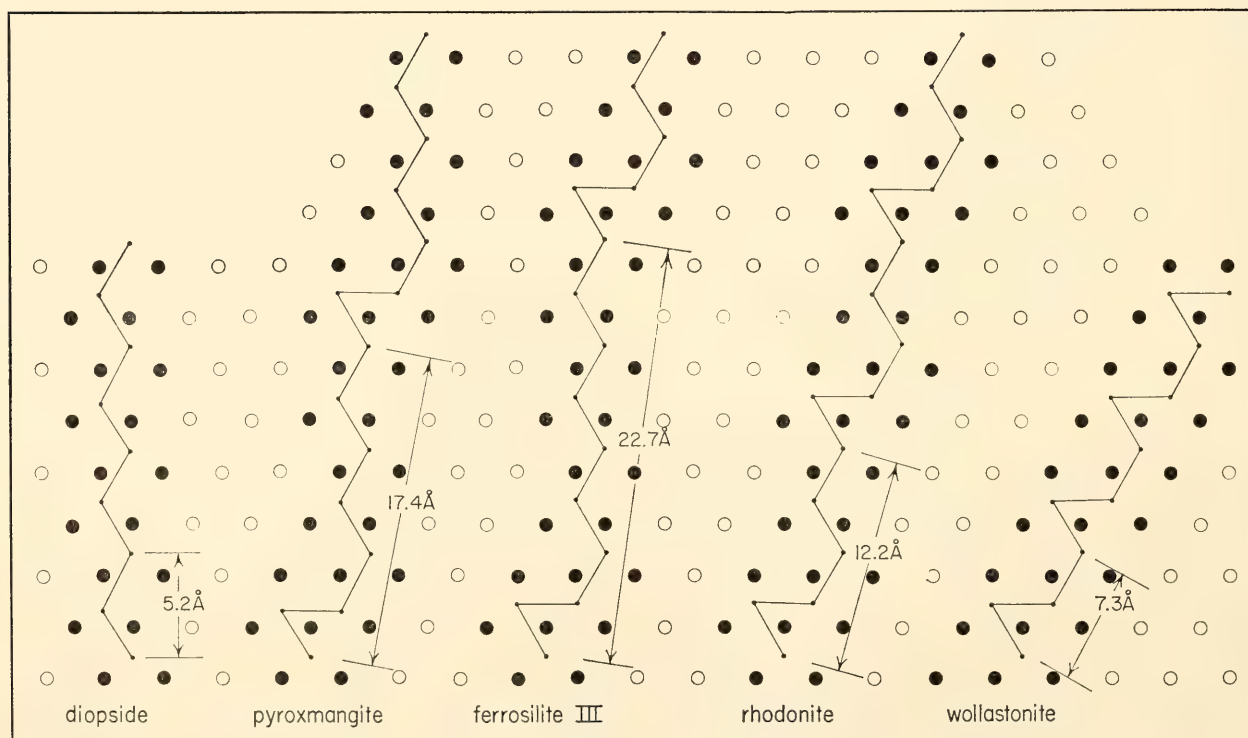


Fig. 76. Schematic representation of tetrahedral chains and octahedral cation distribution in pyroxenoids. Larger circles arranged in a hexagonal pattern represent octahedral sites; solid circles indicate occupied sites. The silicate chains are represented by lines connecting silicon atoms. The *Neunerketten* chain configuration for ferrosilite III represents one likely possibility and illustrates the similarity with pyroxmangite (diagram after Prewitt and Peacor, 1964).

This instrument, manufactured jointly by the Charles Supper Company and the Pace Controls Corporation, automatically drives the crystal-rotation angle,  $\phi$ , and the detector angle,  $\tau$ , by means of digital motors under direct control of punched paper tape. The resolution of both angles is  $0.01^\circ$ . Intensities are measured by either continuous or step scanning, and the scalar output is recorded on punched paper tape, which is easily converted to punched cards or directly to magnetic tape for data reduction on the IBM 7094 computer. Although the time required to measure one intensity is essentially the same as before, this instrument can consecutively record intensities for all Bragg reflections on one reciprocal-lattice level without any operator intervention, except for routine checks and for input and output paper tape changes.

To test and optimize the operating and measuring procedures the instrument was first used to collect intensity data on a sample of  $\alpha$  quartz. This crystal provided both internal and external precision checks because the structure has been refined twice using data from the same crystal—once by Dr. D. E. Appleman of the USGS on a G.E. XRD-5 goniostat using the  $\theta$ - $2\theta$  (moving crystal, moving detector) scan method, and again in this laboratory using the manual equi-inclination Weissenberg diffractometer with the  $\omega$  (moving crystal, fixed detector) scan method. In addition, three precise refinements of different  $\alpha$ -quartz crystals have been reported in the literature within the past three years, providing further external tests of agreement.

Both the automated and manual data were measured with Nb-filtered  $\text{MoK}\alpha$  radiation with the use of a Th-activated NaI scintillation detector and a Hamner N-302 pulse height analyzer set to pass 90 per cent of the characteristic wavelength. Only those independent reflections with  $\sin \theta/\lambda \leq 0.65$  were measured manually, whereas all independent reflections out to  $\sin \theta/\lambda = 1.0$  were measured automatically. With the manual instru-

ment each reflection was scanned continuously from low-angle background to high-angle background, and both backgrounds were measured using fixed-time counts. Positions of both background levels were set by visual inspection of a strip-chart record. Automatically measured intensities were obtained by step scanning in increments of  $0.05^\circ \phi$  through the reflection and by counting five seconds at each step. The total scan angle, a control parameter on the input tape, was computed according to an empirical relation developed by W. A. Dollase (personal communication, 1965):

$$sw = Kf[2.0 + 15L - (L - 1)^2]$$

where  $sw$  is the scan width in degrees,  $L$  is the Lorentz factor,  $K$  is an instrumental constant equal to 0.1 for the  $0.01^\circ$  resolution diffractometer, and  $f$  is an experimentally determined multiplier for each crystal to allow for variable factors affecting the intensity function, such as crystal size and perfection, and mosaic spread. For quartz a value for  $f$  of 1.0 was found to be suitable.

The raw step-scan data were converted to integrated intensities and estimates of their standard errors using formulas similar to those given by Cetlin and Abrahams (1963). Three steps on each side of the peaks were averaged to give background levels. The integrated intensity data were converted to a set of observed structure factors after being corrected for Lorentz, polarization, and absorption effects. No corrections were made for extinction.

The atomic coordinates and  $R$  values ( $= \Sigma ||F_o| - |F_c|| / \Sigma |F_o|$ ) resulting from least-squares refinement of both sets of data are listed in Table 24 along with the results obtained at the USGS (Appleman, personal communication, 1965) on the same crystal, and results obtained in three recent refinements by other workers. We have based our calculations on the orientation of the unit cell given in the *International Tables for X-Ray Crystallography* (Vol. 1, 1952, p. 257)



for space group  $P3_121$ . With this orientation the twofold axis passing through the origin is in the  $[110]$  direction, the oxygen atom is in the general position  $x,y,z$ , and the Si atom occupies position  $3a$  at  $u,u,0$ .

Comparison of the atomic coordinates in Table 24 shows that there is excellent agreement among the several workers and, in particular, that the results based on the same set of data from the same crystal with the use of different measurement geometries (manual data vs. USGS) are in close agreement. It is interesting to note that where results based on manual data and automated data differ the auto-

mated data give coordinates closer to those of previous workers. Of greatest significance is the fact that the automated data are as good as or perhaps slightly better than the manual data.

Tables 25 and 26 compare the atomic thermal models for oxygen and silicon obtained from this laboratory's two refinements with those obtained by Zachariasen and Plettinger (1965), and Smith and Alexander (1963). The reference axes are the same as those used by the previous workers (see Smith and Alexander, 1963, Figs. 3, 4, and 5), but note that their  $X$  axis is parallel to  $[110]$  with the *Inter-*

TABLE 24. Atomic Coordinates of  $\alpha$  Quartz

	$\lambda$	$n^*$	$u_{\text{Si}}^{**}$	$x_0$	$y_0$	$z_0$	$R$
Automated data	Mo	306	0.4699(2)	0.4154(4)	0.1470(4)	0.1186(2)	0.034
Manual data	Mo	106	0.4693(3)	0.4154(8)	0.1483(7)	0.1182(3)	0.033
Appleman (1965)	Mo	110	0.4693(4)	0.4144(9)	0.1475(8)	0.1184(4)	0.029
Z & P†	Cu	112	0.4697(2)	0.4125(4)	0.1463(4)	0.1188(2)	0.018
S & A‡	Cu	112	0.4698(3)	0.4145(8)	0.1483(7)	0.1189(3)	0.033
Y & P§	Mo	306	0.4705(3)	0.4152(7)	0.1474(6)	0.1184(3)	0.081

\* Number of observations. \*\* The transformation matrix for atomic coordinates from the standard setting used by us to that used by previous workers is  $(100/1\bar{1}0/001)$ .  
† Zachariasen and Plettinger (1965).  
‡ Smith and Alexander (1963).  
§ Young and Post (1962.)

TABLE 25. Thermal Ellipsoids of Oxygen

	Principal Axis	Rms Displacement, Å	Angle with respect to		
			$r$	$p$	$q$
Automated data	$r_1$	0.063(6)	20(5)	110(5)	85(3)
Manual data	$r_1$	0.060(12)	10(8)	93(13)	81(7)
Z & P*	$r_1$	0.086(5)	8	96	90
S & A*	$r_1$	0.084(8)	10(15)	83(18)	97(6)
Automated data	$r_2$	0.098(4)	70(5)	20(5)	91(7)
Manual data	$r_2$	0.093(8)	84(13)	15(19)	104(18)
Z & P*	$r_2$	0.111(4)	84	11	100
S & A*	$r_2$	0.102(7)	97(18)	8(17)	93(10)
Automated data	$r_3$	0.122(3)	94(3)	88(7)	5(3)
Manual data	$r_3$	0.111(8)	98(8)	76(19)	17(16)
Z & P*	$r_3$	0.138(3)	89	81	7
S & A*	$r_3$	0.132(6)	83(6)	86(10)	8(6)

\* See Table 24 for explanation of abbreviations; orthogonal axes  $r, p, q$  are the same as those defined by Smith and Alexander (1963).

TABLE 26. Thermal Ellipsoids of Silicon

	Principal Axis	Rms Displacement, Å	Angle		
			X[110]	Y	Z[001]
Automated data	$r_1$	0.055 (4)	90	23 (36)	67 (36)
Manual data	$r_1$	0.041 (10)	90	17 (18)	73 (18)
Z & P*	$r_1$	0.073 (3)	90	26 (23)	64 (23)
S & A*	$r_1$	0.051 (7)	90	6 (8)	96 (8)
Automated data	$r_2$	0.059 (3)	90	113 (36)	23 (36)
Manual data	$r_2$	0.059 (6)	90	107 (18)	17 (18)
Z & P*	$r_2$	0.078 (2)	90	116 (23)	26 (23)
S & A*	$r_2$	0.074 (5)	0	90	90
Automated data	$r_3$	0.064 (3)	0	90	90
Manual data	$r_3$	0.068 (6)	0	90	90
Z & P*	$r_3$	0.083 (3)	0	90	90
S & A*	$r_3$	0.080 (4)	90	84 (8)	6 (8)

\* See Table 24 for explanation of abbreviations.

*national Tables'* cell orientation. Comparison of rms displacements along the principal axes of the thermal ellipsoids shows that the current results are uniformly lower than the others. The ellipsoid orientations, however, are in remarkable agreement except for Smith and Alexander's interchange of  $r_2$  and  $r_3$  for Si, which is probably due to the fact that their restrictions on the temperature factor tensor  $\beta_{ij}$  for Si were incorrect. The automated data indicate the least relative anisotropy for Si (and consequently the largest orientation error), but one might reasonably expect that the true thermal vibrations of Si in quartz are indeed close to isotropic. At present the reason for the disagreement in rms displacements has not been determined. It is not due to instrumental differences, since the temperature factor tensors  $\beta_{ij}$  obtained by the USGS agree with those obtained in this laboratory. The automated data are now being corrected for extinction to test its effect on the thermal models, and in addition, intensities are being measured again with CuK $\alpha$  radiation to test the possibility of systematic differences due to wavelength changes.

The results of these tests have been gratifying for two reasons. (1) They

have shown that the procedures for measuring intensities automatically are valid and that the laboratory has the capability of getting precise data relatively quickly and easily for extensive refinement of complex structures. (2) They have demonstrated that reproducible results can be obtained from the same crystal using different measurement techniques and diffraction geometries not only for atomic coordinates, but for thermal models as well.

I should like to thank Dr. D. E. Appleman of the USGS for lending me the single crystal of quartz and for allowing me to quote the results of his refinement.

CRYSTAL MORPHOLOGY OF RHOMBOHEDRAL SPECIES

J. D. H. Donnay<sup>21</sup> and G. Donnay

It may be recalled that it was the morphology of tourmaline that gave the first indication that its lattice was rhombohedral (Buerger and Parrish, 1937). Early X-ray work had reported a hexagonal lattice (Kulaszewski, 1921).

The morphological prediction, based on

<sup>21</sup> The Johns Hopkins University.



the original law of Bravais (lattice  $R$ ) or its first generalization (space group  $R3m$ ), did not, however, account for the relative importances of the prisms. It made  $(11\bar{2}0)$  the most important prism, since  $(10\bar{1}0)$  must be written as  $(30\bar{3}0)$  to obey the rhombohedral criterion. The cross section should thus be essentially hexagonal, whereas a triangular cross section is one of the distinguishing features of tourmaline.

Buttgenbach and Mélon (1953, p. 660) summarize tourmaline morphology: "The crystals always show prisms, frequently elongated; the  $(10\bar{1}0)$  faces are reduced to three by hemihedry or, when all six faces appear, three of them are larger than the other three, thus resulting in a characteristic triangular cross section; the six  $(11\bar{2}0)$  faces are common." Rogers (1937, p. 485) refers to the cross section of tourmaline crystals as "being rounded triangular like a spherical triangle." Dana (1892, p. 552) gives this description: "...the triangular prism  $m(10\bar{1}0)$  [is] frequently predominating, the complementary form  $m_1(01\bar{1}0)$  then absent or subordinate; also ...  $a(11\bar{2}0)$  present alone; or, again,  $m$  with  $a$ ; ... ." The figures leave no doubt as to the predominance of  $m$  over  $a$ .

With the axial ratio  $c/a = 0.45$  established by X rays the list of net planes arranged in order of decreasing spacing in the  $R$  lattice is  $a(11\bar{2}0)$ ,  $r(10\bar{1}1)$ ,  $o(02\bar{2}1)$ ,  $m(30\bar{3}0)$ ,  $t(21\bar{3}1)$ , ... . In space group  $R3m$  the morphological effect of the mirrors (Year Book 63, p. 237) is to halve the spacing of the  $(11\bar{2}0)$  nets. The result of this effect is to make the hexagonal prism  $a$  recede in the list; now written as  $(22\bar{4}0)$ , it comes after  $t(21\bar{3}1)$ . The tourmaline cross section is thus satisfactorily accounted for. Conversely, starting with the X-ray cell we can determine the space group on morphological grounds.

Another example is provided by cesium and rubidium uranyl nitrates. These two compounds were first described by Sachs (1904), who gives for the  $(c/a)_{\text{gon}}$  axial ratio the values 1.0117 (for Cs) and

1.0074 (for Rb), and observes that both species have the same morphology:  $m(11\bar{2}0)$  and  $r(10\bar{1}1)$ , with habit "almost always columnar" parallel to  $c$ , so that  $m$  dominates over  $r$ . Sachs refers these species to the "hexagonal-rhombohedral system" but does not mention the point group, which can be either  $\bar{3}$  or  $\bar{3}2/m$ . The X-ray study of the rubidium salt by Hoard and Stroupe (1949) gave  $c/a = 2.0171$ , with aspect  $R^*c$ , for which  $R\bar{3}c$  and  $R3c$  are possible space groups; they propose a qualitative structure in  $R\bar{3}c$ . Malčić and Manojlović (1961) reach the same conclusions for the cesium salt. Like Hoard and Stroupe they find that the true cell is twice as high as the morphological cell:  $(c/a)_x = 2.0239$ . It follows that the X-ray setting and the morphological setting should be related by a  $180^\circ$ -rotation around the  $c$  axis and that the crystal forms must be reindexed:  $m(11\bar{2}0)$ ,  $r(01\bar{1}2)$ . We have correlated the two settings, by optical goniometry and precession diffractometry, with the help of John B. Newman, who kindly provided the  $\text{CsUO}_2(\text{NO}_3)_3$  crystals grown by him.

The classical law of Bravais, for  $c/a \sim 1$ , would predict the rhombohedron  $r(10\bar{1}1)$  to be dominant over the hexagonal prism  $m(11\bar{2}0)$ , contrary to observation. With the X-ray ratio  $c/a \sim 2$  and aspect  $R^*c$  the sequence is reversed:  $m(11\bar{2}0)$ ,  $r(01\bar{1}2)$ . If we now take into account the effect of the center and that of the glide plane (Donnay and Donnay, 1965), the sequence reverts to  $r(01\bar{1}2)$ ,  $m(22\bar{4}0)$  in  $R\bar{3}c$ , but it remains  $m(22\bar{4}0)$ ,  $r(02\bar{2}4)$  in  $R3c$ . The space group is thus twice confirmed by morphology, as the point group  $3m$  is ruled out by the rhombohedron  $r$  and the space group  $R\bar{3}c$  gives the wrong relative importance to  $m$  and  $r$ .

It is of interest to note that the morphological cell of Sachs, in the crystal structure, is a pseudo-cell that expresses the periodicity of the rubidium or cesium ions and the uranyl groups. The three nitrate groups that surround each uranium atom are oriented in two ways for successive uranium atoms along the  $c$  axis

(Hoard and Stroupe, 1949); this is the only structural feature that requires the doubling of  $c$ .

Space group  $R3c$  is represented by the ruby silvers: pyrrargyrite ( $c/a = 0.789$ ) and proustite ( $c/a = 0.804$ ). The list of net planes, read from the Mallard graph for the  $R$  lattice, is  $r(10\bar{1}1)$ ,  $a(11\bar{2}0)$ ,  $s(02\bar{2}1)$ ,  $e(01\bar{1}2)$ ,  $v(21\bar{3}1)$ ,  $m(30\bar{3}0)$ ,  $c(0003)$ ,  $d(12\bar{3}2)$ . For the aspect  $R^*c$  (Donnay and Harker, 1937) it becomes  $a(11\bar{2}0)$ ,  $e(01\bar{1}2)$ ,  $v(21\bar{3}1)$ ,  $r(20\bar{2}2)$ ,  $m(30\bar{3}0)$ ,  $d(12\bar{3}2)$ . Finally, if we let  $a(11\bar{2}0)$  be halved by the action of the planes of symmetry (Donnay and Donnay, 1965), we obtain  $e(01\bar{1}2)$ ,  $v(21\bar{3}1)$ ,  $r(20\bar{2}2)$ ,  $m(30\bar{3}0)$ ,  $d(12\bar{3}2)$ ,  $a(22\bar{4}0)$ . From available observations it is difficult to decide between the 1937 and 1964 sequences— $a(11\bar{2}0)$  is common; although placing it in first place is perhaps granting it too much importance, listing it in sixth rank seems like an overcorrection.

### THE STRUCTURAL RELATION OF ARDENNITE TO EPIDOTE

*G. Donnay*

Ardennite is a hydrated vanado-arseno-silicate of aluminum, manganese, and magnesium. It was found for the first time at Salm-Château in the Ardennes in Belgium. The mineral reported as ardennite from New Mexico (Sun and Weber, 1955) is not ardennite. Various analyses

in the literature show a widely varying atomic ratio of vanadium to arsenic and no constancy in the sum of arsenic plus vanadium, but a nearly constant ratio of the sum of vanadium, arsenic, and silicon to oxygen. The substitution of As and V for Si, which is therefore indicated, is of sufficient crystal-chemical interest to warrant an attempt at the structure determination.

Part of a hand specimen of ardennite collected by J. D. H. Donnay is now being chemically analyzed. An optimum-size crystal was used to obtain cell dimensions (Table 27) by means of precession photographs ( $\text{CuK}\alpha$  radiation,  $\lambda = 1.5418 \text{ \AA}$ ). The measured density,  $D_m \ 3.71 \pm 0.03 \text{ g/cm}^3$ , is somewhat higher than the value  $3.63 \pm 0.02$  in the literature (Gossner and Strunz, 1932). Eight Weissenberg layers around the  $c$  axis and four around the  $b$  axis have been taken with  $\text{MoK}\alpha$  radiation.

A possible relation of the ardennite crystal structure to that of zoisite was pointed out by Gossner and Strunz (1932). Inasmuch as zoisite has been shown to be structurally related to epidote (Fesenko, Rumanova, and Belov, 1955), we have looked for a relation between ardennite and epidote. Dr. A. Naldrett kindly provided a hand specimen (No. S-2183) from the Strathcona Mine, Sudbury area, Ontario, on which a suitable epidote crystal was found; its cell dimensions and space group were de-

TABLE 27. Cell Data on Epidote and Ardennite

	Epidote, Strathcona Mine	Epidote Cell Doubled by:		Ardennite
		Reflection in (100)	Reflection in (001)	
$a, \text{\AA}$	$8.88 \pm 2$	15.92*	18.32†	$18.50 \pm 5$
$b, \text{\AA}$	$5.63 \pm 2$	5.63	5.63	$5.81 \pm 2$
$c, \text{\AA}$	$10.22 \pm 3$	10.22	8.88‡	$8.72 \pm 2$
$\beta$	$116^\circ 20'$	...	...	...
Space group	$P2_1/m$	$Pm\bar{m}n$	$Pm\bar{m}n$	$Pm\bar{m}n$
Cell content	$\text{Ca}_4\text{Fe}_2^{3+}\text{Al}_4\text{Si}_6\text{O}_{24}(\text{OH})_2$	$2\{\text{Mn}_4(\text{MgAl})\text{Al}_4[\text{Si}, (\text{As}^{3+}, \text{V}^{3+})]_6\text{O}_{24} \cdot 3\text{H}_2\text{O}\}$		

\*  $2a \sin \beta$ .

†  $2c \sin \beta$ .

‡  $a$  of epidote.



terminated by the precession method (Table 27). Geometrically, two different cell-twinning operations can be applied to the epidote cell to obtain the approximate dimensions and the correct space group of the ardennite cell (Table 27). The cell derived from reflection in (001) is so close to the observed cell of ardennite that it was studied first. Eventually, however, it was ruled out on structural grounds as the following shows.

The epidote crystal structure is described in the literature as made up of chains of octahedra of O atoms and OH groups around Al atoms. The chains stretch along the  $b$  axis and make up the bulk of the structure (Ito, Morimoto, and Sadanaga, 1954; Belov and Rumanova, 1954). When we view the structure along the  $b$  axis (in the negative sense), we notice another kind of chains, the links of which are "mixed rings." Beginning with an oxygen octahedron around Al at (0,0,0) and turning clockwise, we first encounter an oxygen atom at height  $y = -1/4$ , which is shared by an  $\text{SiO}_4$  group with its Si atom at the same height. Another oxygen of the  $\text{SiO}_4$  group at  $y = -1/4$  is a corner of the octahedron around Al at (0,0,1/2). This octahedron and the one above it each share one oxygen (at  $y \sim 0$  and  $y \sim 1/2$ , respectively) with the  $\text{Si}_2\text{O}_7$  group that has both its Si atoms at  $y = 1/4$ . Two octahedra, one around the origin and one above, share two other corners of this  $\text{Si}_2\text{O}_7$  group, thus completing a five-membered ring of the "chair" form. Inversion through the centers of symmetry at the Al sites reproduces the ring and extends the chain along  $c$ . Thus the epidote crystal structure can be interpreted as consisting of thick sheets, parallel to (100), of composition  $\text{AlO} \cdot \text{SiO}_4 \cdot \text{AlOH} \cdot \text{Si}_2\text{O}_7$ . The calcium and ferric cations tie the sheets together.

A reflection of the epidote structure in (001) destroys the sheets; only a reflection in a mirror parallel to the sheet, namely (100), preserves them. Even so, the structure must be modified. By moving the chain at  $x = 1/2$  by 1.3 Å

along  $+c$  the ardennite space-group symmetry is obtained, but the unshared oxygens of the  $\text{Si}_2\text{O}_7$  group collide across the mirror (100) at  $x = 1/4$ . If these atoms are placed on the mirror, they have to be shared by adjacent sheets. As a result rings of four tetrahedrons,  $\text{Si}_4\text{O}_{12}$ , of symmetry  $mm2$  appear.

The following 98 reflections, not forbidden by the space group, are found to be structurally absent or so weak that they can be considered to be of zero intensity:  $hk0$  with  $h$  and  $k$  both odd,  $h01$ ,  $h41$ ,  $h81$ . Three cycles of least-squares refinement, with the Busing-Levy ORFLS program, used these reflections with zero  $F^2$ s as input data and the 33 atomic coordinates of the trial structure as the parameters to be adjusted. The idealized formula (Table 27) was used for the atomic scattering curves. The decrease in  $F^2_{\text{calc}}$  from cycle to cycle indicates that the trial structure is a promising one.

The reinterpretation just given of the epidote structure is novel in that it considers the sharing of oxygen corners between polyhedrons that are of different shapes (here tetrahedrons and octahedra) and that surround chemically distinct cations (here Si and Al). Its usefulness was demonstrated as it pointed out the dubiousness of the (001) cleavage of epidote reported as "perfect" throughout the literature. Such a cleavage would entail the breaking of several Al-O bonds and the destruction of the chains along  $c$ . Attempts to confirm this cleavage on epidote crystals from various localities have failed. If it exists at all, it must be extremely difficult to obtain.

#### POSSIBLE APPLICATION OF NUCLEAR MAGNETIC RESONANCE TO ORDER- DISORDER STUDY IN THE HYDROGROSSULARITE SERIES

*G. Donnay and A. Allerhand*<sup>22</sup>

As pointed out to us by Dr. H. S. Yoder, Jr., the solid solution grossularite-

<sup>22</sup> The Johns Hopkins University.



hydrogrossularite with formula  $\text{Ca}_3\text{Al}_2(\text{SiO}_4)_2(\text{SiO}_4)_{1-x}(\text{OH})_{4x}$  is now of special interest, since the crystal structure of  $\text{Ca}_3\text{Al}_2(\text{OH})_{12}$  has been refined (Cohen-Addad *et al.*, 1964). Unknown to the French authors, the structure had first been determined by Brandenberger (1933), but the oxygen atoms have now been shifted considerably and, moreover, the hydrogen atoms have been located with the help of neutron-diffraction data obtained from a powder sample. The hydrogen coordinates were used to calculate the second moment of the nuclear magnetic resonance (NMR) spectrum, which was compared with its observed value, obtained also from a powder sample.

As had been implied by Pabst (1937), the  $\text{SiO}_4$  tetrahedrons of the garnet structure are replaced by tetragonal disphenoids of four  $(\text{OH})^-$  ions. Rather than thinking of the replacement as a substitution of  $4\text{H}^+$  for  $\text{Si}^{4+}$  ions, one can, with Brandenberger, consider it an omission of  $\text{Si}^{4+}$  (the  $24d$  position in space group  $Ia3d$  is unoccupied in the hydroxygarnet), accompanied by the replacement of  $4\text{O}^{2-}$  by  $4(\text{OH})^-$  ions. All  $\text{H}_1\text{-H}_i$ ,  $\text{H}_1\text{-O}_i$ ,  $\text{O}_1\text{-O}_i$  and  $\text{H}_1\text{-Al}_i$  distances up to a maximum of 10 Å were calculated by us, and no unreasonably close approaches occur. The possibility of  $\text{OH} \dots \text{O}$  hydrogen bonding is thus ruled out. The closest O-O distances are 2.464 Å and 2.798 Å, which constitute the two edge lengths of the trigonal antiprism around Al. (These values were given as 2.29 Å and 3.72 Å by Cohen-Addad and co-workers, 1964.) The polyhedron around Al is considerably more distorted here than in any other garnet structure for which refined parameters are available but not more so than the one in andalusite, for example, in which the Al octahedral edges range from 2.469 Å to 2.794 Å (Burnham and Buerger, 1961).

To show that polyhedrons very different in size substitute for each other when an  $\text{SiO}_4$  group is replaced by four hydroxyl ions, we may compare the volumes of the tetragonal disphenoids that

have the centers of the oxygens as their corners. In grossularite (Abrahams and Geller, 1958) the O-O edges of the  $\text{SiO}_4$  group are two 2.56 Å long and four 2.73 Å long, giving a volume of 2.23 Å<sup>3</sup>. In hydrogarnet, two O-O distances are equal to 3.17 Å and four to 3.39 Å, corresponding to a volume of 4.26 Å<sup>3</sup>, that is, 91 per cent larger than that of the  $\text{SiO}_4$  group. This difference would be increased slightly if the additional volume occupied by the four H ions that fall outside the oxygen disphenoid (Pabst, personal communication) were taken into account. In ionic crystal structures Vegard's law predicts complete solid solution when the difference between the ionic radii does not exceed 15 per cent of the smaller radius, corresponding to a difference of 52 per cent between the volumes of substituting ions. Certainly an unusually deformable crystal structure is needed to accommodate the observed doubling of the volume of the disphenoid that is being replaced. The garnet structure is noted for its wide range of composition; the chances of finding four hydroxyl groups substituting for  $\text{SiO}_4$  elsewhere, even in other orthosilicates, where such a substitution should occur most readily, appear to be very slight on the basis of volume considerations.

We are exploring the possibility of obtaining information on the  $(\text{OH})_4$  environment in naturally occurring hydrogarnets of various  $\text{SiO}_4/\text{OH}$  ratios by comparing calculated and observed second moments of NMR spectra. The calculated second moment varies rapidly with the H parameter. A recalculation with the H coordinates given by Cohen-Addad and co-workers, corresponding to an O-H distance of 1.13 Å but with the range of H-H and H-Al distances extended to 10 Å, gives a  $\overline{\Delta H^2}$  value of 33.95 G<sup>2</sup>. (Cohen-Addad and co-workers had found 34 G<sup>2</sup>, with a 5-Å range.) When the H coordinates are changed from 0.142, 0.081, 0.806 to 0.150, 0.086, 0.806 and when H-H and H-Al distances up to 6.0 Å are included in the calculation, the value of  $\overline{\Delta H^2}$  drops to 23.81 G<sup>2</sup>. This second set of H



coordinates corresponds to an O-H distance of 1.0 Å (with the oxygen atom unmoved) which is the usual size of the hydroxyl group. The observed value of  $28 \pm 3 \text{ G}^2$  falls about halfway between the two calculated values, closer to 24 than to 34.

The contributions to the second moment made by the intradisphenoid H-H distances amount to 66.2 and 56.7 per cent of the total value of  $\overline{\Delta H^2}$  for O-H distances of 1.13 Å and 1.00 Å, respectively. But there is also a large contribution from a short H-H distance from a hydrogen in a neighboring disphenoid. It amounts to 23.4 per cent for O-H = 1.13 Å or 29.3 per cent for O-H = 1.00 Å. For crystals in which both  $\text{SiO}_4$  and  $(\text{OH})_4$  groups are present, this term, like all the other smaller contributions of interdisphenoid interactions, has to be weighted according to the short-range order, if any, that accompanies the substitution. It is hoped that, with hydrogen coordinates accurately determined by single-crystal neutron-diffraction studies, the observed second moment will permit an investigation of the short-range order of this very unusual substitution.

#### TETRAPHENYLPORPHYRIN-SILVER (II) TETRAPHENYLPORPHYRIN SOLID SOLUTIONS

*G. Donnay and C. B. Storm*<sup>23</sup>

Molecular solid solutions have received surprisingly little attention in the past, yet we must study them before we can hope to understand why their natural occurrence appears to be so much more limited than that of their inorganic counterparts. Examples might conceivably have escaped attention because single-crystal X-ray work has not been carried out on "impure" crystals. Porphyrins are well suited for solid-solution study. Because of their biological importance their molecular structure is known in detail from numerous refined

crystal structures that have appeared in recent years (references will be found, for example, in Hamor, Caughey, and Hoard, 1965). Methods of porphyrin synthesis have been perfected over many years in the laboratory of Professor A. H. Corwin at the Johns Hopkins University.

The triclinic modifications of tetraphenylporphyrin (TPP) and silver tetraphenylporphyrin (AgTPP) are isostructural, in space group  $P\bar{1}$ , and with one molecule per cell. Refined structure determinations (Silvers and Tulinsky, 1964; Tulinsky, personal communication, 1964) showed them to be similar enough for complete solid solution to be expected.

The end members as well as five intermediate compositions were synthesized as follows. The TPP was synthesized from pyrrole and benzaldehyde by a slight modification (Baker and Brookhart, personal communication, 1964) of the method of Ball, Dorough, and Calvin (1946). As to AgTPP, it was prepared by heating TPP with an excess of  $\text{AgNO}_3$  in pyridine on a steam bath for about 30 minutes (Dorough, Miller, and Hunnens, 1951). The pyridine is removed on a rotary evaporator; the AgTPP is dissolved in chloroform, passed over a short column of alumina, and crystallized from chloroform-methanol. The solubilities of the end members in ethylene dichloride were measured. AgTPP is about 1.5 times as soluble as TPP, 6.59 against 4.39 mM/l.

The solid solutions are obtained in this way: Portions of TPP and AgTPP are weighed on a micro balance and placed in a test tube. Ethylene dichloride (Fisher "Certified Reagent") is added in sufficient quantity to dissolve all the porphyrin mixture. This solution (~15 ml) is filtered through Whatman No. 1 filter paper into a  $28 \times 100$  mm test tube, which is then placed in a glass-stoppered jar with ~50 ml of methanol. The jar is put in a dark place at room temperature. The methanol slowly distills into the ethylene dichloride solution, and the porphyrin mixture crystallizes. No at-

<sup>23</sup> The Johns Hopkins University.

tempt was made to exclude air or moisture.

For any composition the crystals coming from a first batch are indistinguishable from those of later batches of crystallization as evidenced by the constancy of X-ray intensities on Weissenberg photographs (see below). This is, of course, to be expected for the pure end members. For intermediate compositions it is surprising.

Absorption spectra of samples of the solution were taken on a Beckman DK-2 recording spectrometer. The spectra of TPP and AgTPP differ sufficiently to be readily told apart; in the spectra of intermediate compositions the peaks of the two distinct molecular species are not resolved (for reasons not yet understood), and an intermediate type of pattern is obtained. In the course of crystallization the AgTPP/TPP ratio in the mother liquor increases. All crystals when redissolved in dichloroethylene give spectra similar to those of the original mother liquor.

The triclinic phase only is obtained for compositions of 0, 74.88, 85.85, and 100 mole per cent AgTPP. A few small tetragonal dipyrramids (101) appear, in addition to the triclinic crystals, when compositions of 8.84, 35.12, and 53.35 mole per cent AgTPP are crystallized. Since their cell dimensions change slightly with composition (Table 28), they must contain either the two kinds of molecules (TPP and AgTPP) or varying amounts of

solvent (chloroform, methanol, or water). Conceivably both effects may be present. Their Laue group is  $4/m$ ; the lattice is body centered, so  $I4/m$ ,  $I\bar{4}$ , and  $I4$  are possible space groups. A test for piezoelectricity kindly performed for us by Dr. D. Appleman of the USGS was negative. The morphology indicates  $I4/m$ , compatible with the test. The molecular volume, obtained from the triclinic crystals (Table 29), leads to two molecules in the tetragonal cell. The required molecular symmetry is therefore  $4/m$ . Fleischer, Miller, and Webb (1964) describe crystals of  $\text{ZnTPP}\cdot 2\text{H}_2\text{O}$ , which are almost identical with ours (Table 28). Their space group is  $I4/m$ ; their structure is known but has not yet been described in detail. We know, however, that the phenyl rings make an angle of  $90^\circ$  with the plane of the porphyrin ring, whereas in the triclinic phase the same angle is about  $62^\circ$ . Thus two very different looking molecules crystallize from one and the same solution.

The habit of the triclinic crystals varies from acicular to short prismatic along  $a$  but is not a function of the composition. The large faces, in order of decreasing importance, are designated (010),  $(0\bar{k}l)$ , (001), and the small terminal face (100). This indexing, which was used by Tulinsky (personal communication, 1964) for the silver end member, leads to cells (Table 29) in which  $(0\bar{k}l)$  becomes  $(0\bar{1}1)$ . (They can be transformed to the Bravais reduced cells by means of

TABLE 28. Tetragonal Crystal Data

Sample Description	D2	D1	D3	ZnTPP·2H <sub>2</sub> O*
Mole per cent				
AgTPP	8.84	35.12	53.35	....
$a$ , Å	13.37	13.37	13.42	13.44
$c$ , Å	9.73	9.70	9.72	9.715
$c/a$	0.727 <sub>7</sub>	0.725 <sub>5</sub>	0.724 <sub>3</sub>	0.722 <sub>8</sub>
Cell volume	1,739	1,734	1,751	1,755
Molecular volume	869.5	867.0	875.5	877.5

Lengths known to  $\pm 0.3$  per cent.  
\* Fleischer, Miller, and Webb (1964).



TABLE 29. Triclinic Crystal Data

Sample Description	TPP	D2	D1	D3	D4	D5	AgTPP
Mole per cent AgTPP	0	8.84	35.12	53.35	74.88	85.85	100
a, Å	6.45	6.45	6.45	6.45	6.40	6.39	6.37
b, Å	11.19	11.19	11.20	11.22	11.22	11.23	11.23
c, Å	12.43	12.43	12.43	12.43	12.45	12.47	12.47
α	100°50′	101°12′	101°15′	101° 0′	100°55′	100°55′	100°50′
β	80°48′	80°55′	81°10′	81°30′	81°50′	82° 0′	82°23′
γ	113°15′	113°15′	113°10′	113°10′	113° 0′	113° 1′	113° 1′
V, Å <sup>3</sup>	806 ± 6	805 ± 6	806 ± 6	809 ± 6	804 ± 6	807 ± 6	805 ± 6
ρ calc.	1.27 ± 1	1.29 ± 1	1.34 ± 1	1.38 ± 1	1.43 ± 1	1.45 ± 1	1.49 ± 1
I 004	7	7	6	6	2	0	3
I 005	4	3	6	7	6	7	8
I 006	6	5	0	1	0	5	6

Lengths known to ±0.3 per cent, angles to ±10′. Intensities are visual estimates on *a*-axis, zero-layer Weissenberg films taken with CuKα radiation. They are based on a scale of 10 (0 = unobserved).

the matrix  $\overline{110}/00\overline{1}/100$ .) Our choice of axes has the advantage that a single mounting of the crystal can be used to take the Weissenberg and precession photographs that are needed for the cell determination. For *a*-axis Weissenberg data (see intensities, Table 29), the main zone is adjusted in prism position on the two-circle goniometer. [The α\* angle can be measured between (010) and (001).] For precession work (100) is centered in polar position, involving a change of about 24° from the previous setting.

The changes in cell dimensions (Table 29) across the complete solid solution are insignificant except for a 1°35′ increment of the β angle. The cell volume remains constant at 806 ± 6 Å<sup>3</sup>, so that the calculated density is proportional to the molecular weight. All attempts to determine densities experimentally failed. Flotation in cyclohexane carbon-tetrachloride mixtures proved impractical because the porphyrin is sufficiently soluble to turn the liquid dark red, and the solution is too volatile. Fleischer (personal communication, 1964) reports that he determined the density to an accuracy of one per cent on a number of TPP derivatives by flotation in a pentane-carbon-tetrachloride mixture. We tried this mixture too but without

success. The wetting problem is severe even after the container is degassed. Centrifuging experiments are under way.

Even though there is complete solid solution between TPP and AgTPP, its existence would go undetected if only powder patterns were taken. The crystals are so soft that it is difficult to obtain a good powder, and the powder pattern shows broad diffuse halos. Even the patterns of the end members were indistinguishable. The intensities of reflections on single-crystal patterns, on the other hand, change so drastically with composition that it is possible to estimate the composition from selected intensities to about ±3 per cent. The silver atoms, which are located at cell origins, always add their maximum positive contribution to the structure factors.

The question now arises: Is there any ordering in the replacement of one type of molecule by the other? Determination of short-range order coefficients by diffuse X-ray studies would be very difficult, so another approach was tried. J. A. Leone of the Chemistry Department at the Johns Hopkins University studied the electron spin resonance spectra of our crystals. Even the one of lowest silver concentration, 8.84 mole per cent AgTPP,

showed such pronounced broadening of the hyperfine lines (owing to the silver-silver interactions in the crystal structure) that the data could not be used in quantitative calculations. Leone grew a crystal composed of 0.73 mole per cent AgTPP and 99.27 mole per cent TPP, which was  $0.1 \times 0.5 \times 2$  mm in size. Its

spectrum shows no line broadening. Crystals with compositions ranging between one and eight mole per cent AgTPP should give interpretable results, leading to information on the random nature of substitution of the paramagnetic AgTPP molecules.

## BIOGEOCHEMISTRY

### THE EXTRACTABLE ORGANIC MATTER IN PRECAMBRIAN ROCKS AND THE PROBLEM OF CONTAMINATION

*T. C. Hoering*

Sedimentary rocks of all ages contain reduced carbon. In severely metamorphosed formations the carbon is graphitic. Very old rocks can be found, however, that have experienced a mild thermal history, and any organic matter originally resident in them could be expected to have survived with only moderate degradation. We have assembled a good collection of old, carbonaceous, lightly metamorphosed rocks and have sought to identify some of the organic matter that can be extracted from them. We have found that sedimentary rocks even as old as 3,000 m.y. contain petroleumlike substances that can be extracted into organic solvents. The amounts of such material in Precambrian rocks are generally small, but there are several exceptions. We have found that a rock of the Nonesuch shale of upper Michigan with an age of 1,100 m.y. contains 3,100 ppm extractable organic matter. The McMinn shale of the Northern Territory of Australia, whose age is about 1,600 m.y., has 1,500 ppm of the weight of the rock as benzene-soluble material. Typically, however, the amounts are less than 80 ppm.

We have analyzed the extracts for straight-chained hydrocarbons in the range of  $C_{14}H_{30}$ – $C_{30}H_{62}$  and have found some of these compounds in all of them. Compounds of this type are known to

result from transformation of biologically produced organic matter. Before we can discuss the biogeochemical significance of finding this class of compounds in rocks of great age we must ask if they are indigenous.

Some of the ways that a rock may become contaminated can be evaluated. Inadvertent introduction of refined petroleum products is a potential hazard. The molecular weight distribution of the normal alkanes in them, however, is distinctly different from those in rock extracts. The problem of contamination during chemical processing can be assessed by running blanks and control experiments. A much more likely source of contamination of Precambrian rocks is the migration of petroleum fluids in the earth. Hedberg (1964) has reviewed the literature on the migration of oil. Although the mechanism and mode of such transport are not well understood, it is clear that petroleum can move for long distances and may appear in rocks of all kinds. Occurrences of petroleum in such unlikely places as igneous and metamorphic rocks are known.

The occurrence of biological-type alkanes in a rock older than 3,000 m.y. is described below, and a method of evaluating organic contamination is discussed. The Barberton area of eastern Transvaal in the Republic of South Africa contains some of the world's oldest rocks. Rocks of the Swaziland system have been dated by Nicolaysen as older than 3,000 m.y. This system contains the lower Onverwacht series of lava flows and the upper



Fig Tree series, consisting of pelitic rocks and great thicknesses of banded cherts, banded iron stones, and carbonaceous shales. The shales in some places have suffered surprisingly little metamorphism. Samples of them were collected in the Montrose Gold Mine.

An experiment was designed to determine the location of the extractable organic matter in the shale. The rocks were crushed into coarse pieces approximately  $\frac{1}{2}$  inch in size, and extracted in a Soxhlet extractor with 70 per cent benzene, 30 per cent methanol. The solvent was evaporated slowly under vacuum, and 13 ppm of extracted organic matter was obtained. The rock pieces were then crushed to  $-6, +30$  mesh size and extracted for 24 hours to give 30 ppm extractables. The crushed rock was then ball milled to 3–10 micron-sized particles and extracted to give 15 ppm. The ball-milled rock was demineralized with hydrofluoric and hydrochloric acid to give a kerogen concentrate. This was dried and extracted to give 6 ppm soluble matter based on the weight of the original rock. It appears that an appreciable amount of the extractable organic matter is on surfaces and grain boundaries that are easily accessible to the solvent.

The extracts were combined, and a nonpolar fraction was isolated by silica-gel chromatography using heptane as the eluant. The straight-chained hydro-

carbons were isolated by forming adducts with urea. They were recovered and analyzed by gas-liquid chromatography. The chromatogram is shown in Fig. 77. Although the individual compounds are easily detected, they each represent only about one part in  $10^7$  of the original rock. This assemblage of compounds is typical of hydrocarbons formed in association with biologically produced organic matter of all ages.

In most sedimentary rocks the bulk of the organic matter exists as an insoluble high polymer called kerogen. It is unusual to find a shale with more than a few per cent of its organic matter in a form that is soluble in benzene. Kerogen cannot migrate far, so it is of interest to compare the  $C^{13}/C^{12}$  ratio of the soluble and insoluble organic matter in a series of rocks. The rocks chosen had a wide range of ages and types. In some of them there is abundant extractable material, which is very likely related to the kerogen. Some of the Precambrian rocks contain only small amounts of extractable material and the relation of the extract to the kerogen is less certain.

Samples of finely ball-milled rocks were extracted in a Soxhlet extractor with benzene-methanol mixture, and the solvent was evaporated. The residual rock was dried and treated with hydrochloric acid to remove carbonates. The two fractions were quantitatively combusted

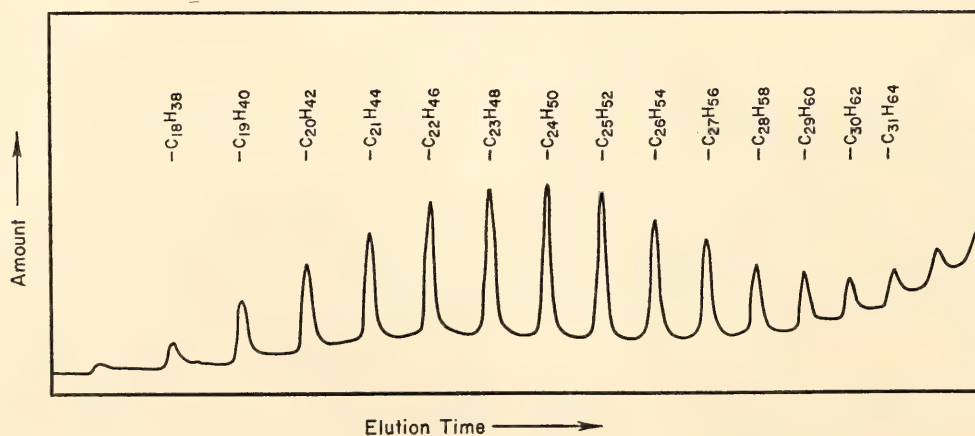


Fig. 77. Normal alkanes from Fig Tree shale of the Swaziland system. F and M Corporation Model 1609 hydrogen flame detector, 100-foot by 0.016-inch column coated with Apiezon L grease, 30 psi helium. Temperature programming from  $100^{\circ}\text{C}$ – $300^{\circ}\text{C}$ .

to carbon dioxide and analyzed in the mass spectrometer. The results, shown in Table 30, are expressed in parts-per-thousand difference in the  $C^{13}/C^{12}$  ratio compared with a standard (National Bureau of Standards isotope reference sample 20, limestone from Solenhofen).

$$\delta C^{13} = \frac{(C^{13}/C^{12})_x - (C^{13}/C^{12})_s}{(C^{13}/C^{12})_s} \times 1,000$$

where *x* refers to the sample and *s* to the standard.

In samples B through I, where there was an abundant amount of soluble material, the isotope ratios are within about two parts per thousand of each other. Sample A, the recent sediment, shows a relationship between the two fractions that is similar to that found between the "lipide" and "nonlipide" portions of living cells. In the Precambrian samples J, K, and L, where the extractable portion is less than 80 ppm, there is a considerable discrepancy. Sample M, the

shale from the Fig Tree series of the Swaziland system described earlier in this report, shows agreement.

To see how uniformly the carbon isotopes were distributed in a sample of rock extract, samples B, D, H, and I were fractionated by silica-gel chromatography. The sample was eluted successively with heptane, carbon tetrachloride, benzene, and methanol. Each fraction was combusted to carbon dioxide, and analyzed. There was little difference in the carbon isotope ratios between the four classes of compounds in every case. Thus a discrepancy cannot be explained by preferential loss of different portions of the organic matter in the rock.

The chemical pathways leading from biological organic matter to kerogen and extractable organic matter in rocks are not known. If the system has been closed since compaction of the rock, however, a consistent relationship would be expected between the carbon isotope ratios

TABLE 30. Carbon Isotope Ratios in the Extractable and Insoluble Organic Matter in Rocks

Rock		Location	Age	$\delta C^{13}$ Insoluble	$\delta C^{13}$ Soluble
A. Unconsolidated sediment		Aransas Bay, Tex.	Recent	-18.40	-22.01
B. Oil shale		Green River formation, de Beque, Colo.	Eocene	-28.80	-27.57
C. Shale		Chattanooga formation, Tenn.	Devonian	-27.46	-27.48
D. Shale		Woodford formation, Okla.	Mississippian	-27.82	-28.26
E. Shale		Alum formation, Sweden	Cambrian	-27.43	-26.19
F. Lignite coal		Fort Union formation, N. Dak.	Paleocene	-22.76	-23.60
G. Bituminous coal		Pittsburgh, Pa.	Pennsylvanian	-22.34	-22.84
H. Shale		Nonesuch formation, Mich.	Precambrian (1,100 m.y.)	-28.15	-28.14
I. Shale		McMinn formation, Northern Territory, Australia	Precambrian (1,600 m.y.)	-30.71	-30.59
J. Carbonaceous slate		Soudan formation, Minn.	Precambrian (2,500 m.y.)	-34.81	-25.00
K. Limestone		Transvaal system, South Africa	Precambrian (2,000 m.y.)	-38.21	-25.01
L. Shale		Ventersdorp system, South Africa	Precambrian (2,100 m.y.)	-36.86	-25.78
M. Shale		Swaziland system, South Africa	Precambrian (3,000 m.y.)	-26.94	-27.55



of the two, and this is what has been found empirically.

It is then necessary to understand the discrepancy in samples J, K, and L. The simplest explanation could be the migration of organic matter from an outside source. The values of  $\delta C^{13}$  found for the extractables in these rocks fall in the range of younger petroleums.

One possible explanation is that a process has removed or destroyed organic matter in a way that fractionated isotopic molecules. If this process preferentially removed  $C^{12}$ -containing compounds, the residue would be enriched in  $C^{13}$  compared with the insoluble organic matter. The agreement in the case of the Fig Tree shale could be fortuitous since the value of  $\delta C^{13}$  of  $-27.55$  found for the extractable organic matter falls in the range of most younger petroleums.

One must conclude that it is difficult to say whether the extractable organic matter in a very ancient rock is of the same age as the rock. Other criteria will have to be employed before it can be said that the  $n$  alkanes in the Fig Tree shale are diagnostic of biologically produced organic matter.

#### FATTY ACIDS FROM THE OXIDATION OF KEROGEN

*T. C. Hoering and P. H. Abelson*

The saturated fatty acids are prominent constituents of living organisms. They have an intrinsic chemical stability that would permit them to survive for long periods if protected in the proper environment. Previous work in this laboratory and by Cooper (1962, 1963) has shown that small amounts of fatty acids can be extracted from rocks by organic solvents. Several features of previous results are of interest. One is the relatively small amount of the organic matter in a rock that can be accounted for as a fatty acid. A second is the presence of acids with an odd number of carbon atoms in an amount comparable to that of the even-numbered acids in

some rocks; this is in contrast to living organisms, in which the acids have predominantly an even number of carbon atoms with  $C_{16}H_{32}O_2$  and  $C_{18}H_{36}O_2$  as the major components. A third feature is the greater relative abundance of high molecular weight acids than is found in living organisms.

In the light of the large possible number of isomers of the saturated hydrocarbons, the normal alkanes in petroleum are seen to be particularly abundant. This fact, along with others, has led many workers to speculate that the fatty acids are the biological precursors of such alkanes. Some of the intermediate steps in formation of the alkanes, however, are not at all clear. The amounts and molecular weight distributions of the naturally occurring  $n$  alkanes are greatly different from the corresponding distribution of biological fatty acids. Therefore, it is of some interest to determine whether long, straight-chained aliphatic structures are present in the insoluble organic matter (kerogen) of rocks.

The kerogen of rocks comprises the bulk of the organic matter on the face of the earth, but relatively little is known of its structure. It is evidently a high polymer formed from the condensation of organic debris and may contain fatty acid residues that can be cleaved off and identified.

The oxidative degradation of coal by chemical oxidizing agents has been used to yield a mixture of organic acids. This has given some insight into its chemical structure. Robinson *et al.* (1953, 1956) observed a wide range of organic acids of complex structures that were produced by the chemical oxidation of the Green River oil shale. The complexity of the mixture of the acids produced this way makes it difficult to separate and characterize the system. The advent of gas-liquid chromatography, especially in conjunction with high-resolution capillary columns, makes study of this problem more feasible.

In the following paragraphs an im-



proved procedure for the isolation of long-chained fatty acids from a mixture of organic acids is described. The technique was developed on the Green River oil shale, a rock conveniently rich in organic matter and complex enough to provide a good test. Preliminary results of the analysis of several rocks are presented.

In a typical experiment, the finely ball-milled rock was extracted with benzene-methanol mixture in an ultrasonic generator. The mixture was centrifuged, and the solvent was slowly evaporated under vacuum. The extract was partitioned between heptane and 90 per cent methanol, 10 per cent water. The heptane phase was retained for fatty acid analysis. The extracted rock residue was demineralized with hydrochloric acid and hydrofluoric acid. The resultant kerogen concentrate was oxidized with chromic acid in 3 molar sulfuric acid for six hours. The reaction mixture was covered with a layer of heptane and stirred vigorously while under reflux. The heptane layer contains some of the fatty acids produced by the reaction.

Some of the features of the production of fatty acids by oxidation were studied. Under conditions in which chromic acid or potassium permanganate reacted with kerogen each also reacted slowly with fatty acids. If the reaction was prolonged, the longer fatty acids degraded and eventually converted to acetic and carbonic acids. It was determined that the molecular weight distribution shifted to lower values with increasing time of oxidation, and an optimum yield of acids in the range of 14–30 carbon atoms was obtained at about five hours. Experiments with added  $C^{14}$ -tagged palmitic acid showed that an appreciable amount of the acids was tightly adsorbed on the unreacted residue after oxidation.

Since a very complex mixture of acid is produced by the oxidation of kerogen, it was necessary to devise a separation procedure that would enhance the concentration of straight-chained fatty acids

with respect to other components. To guide us in our procedure we added  $C^{14}$ -tagged palmitic acid to the reaction products. The crude mixture of acids was dissolved in a solvent containing 80 per cent methanol and 20 per cent water. This methanol phase was extracted with heptane, which contained the long-chained fatty acids. After removal of the solvent the acids were esterified with methanol- $BF_3$ , and the esters were extracted into heptane and exposed to a urea clathrate. The clathrate structure had been formed by treating urea with decane. Esters of the long-chained fatty acids entered the clathrate structure, but esters of branched chains tended not to be included even after an overnight exposure to the clathrate. These impurities can be removed by washing the solids with heptane. The esters were liberated from the urea adduct by addition of water, and the product was further purified by silica-gel chromatography. The esters were not eluted by heptane but were moved by benzene. As a result of these procedures the specific activity of the final product of fatty acid esters was increased 10–20 times over the initial crude oxidation mixture. An aliquot was analyzed by gas-liquid chromatography with a 100-foot capillary column coated with Apiezon L grease.

The chromatograms of the fatty acids from the extract of the Green River shale and those formed by chromic acid oxidation of the kerogen are shown in Figs. 78 and 79. Similar results were obtained when potassium permanganate in basic solution was used as the oxidizing agent, the solution being acidified after the reaction, excess oxidizing agent removed by sulfurous acid, and the solution and unoxidized residue extracted with benzene. Table 31 gives some quantitative results obtained from the chromatograms.

The results on the “free” acids, that is, those extractable from a rock by a solvent, are somewhat different and more comprehensive than those described previously. The new analytical procedure



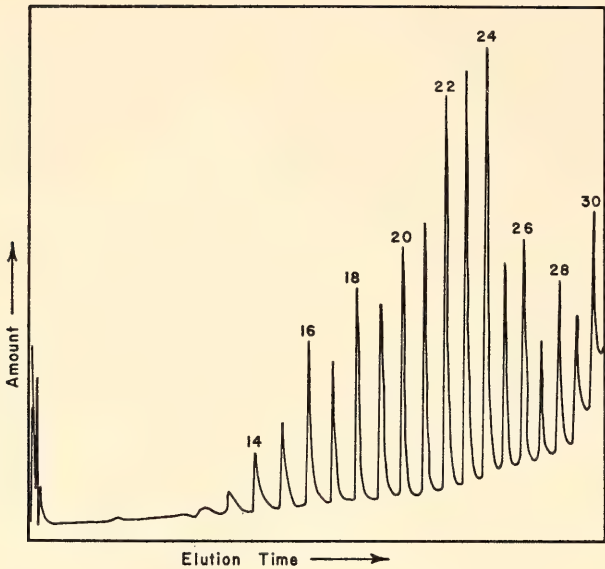


Fig. 78. Fatty acids extracted from Green River shale. Separation performed as described in Fig. 77.

permits detection of much higher molecular weight acids. We made special efforts to make certain of the identification of the purified fatty acids. The mixture of acids was chromatographed as their methyl esters on two completely different substrates: (1) a 100-foot  $\times$  0.016-inch capillary column coated with Apiezon L grease, and (2) a 10-foot  $\times$  0.125-inch outside diameter column packed with 5 per cent poly (ethylenglycol succinate) on Chromosorb W. Nearly identical chromatograms resulted. Individual methyl esters were separated by preparative gas-liquid chromatography by the use of a column packed with a nonpolar packing, silicone rubber SE-30 on Chromosorb P. The individual compounds were then re-chromatographed on the polyester-packed column, and each emerged as a single component at the expected retention time. The infrared spectra of the separated individual esters compared well with those of pure compounds and with those published in the literature. The mass spectra of several separated esters were compared with pure compounds and with values from the literature. The agreement was good. The analytical

TABLE 31. Saturated Fatty Acids in the Extract and Oxidation Products of Recent Sediment, San Nicolas Basin, California

Acid, carbon number	Micrograms Acid per Gram of Organic Carbon	
	Extractable	Chromic Acid Oxidation
14	2.8	34.0
15	0.2	27.0
16	6.0	126.0
17	0.1	47.0
18	1.1	166.0
19	0.07	26.0
20	0.77	33.0
21	0.06	8.3
22	1.1	14.0
23	0.2	5.9
24	2.1	8.4
25	0.22	5.2
26	2.1	5.9
27	0.14	3.1
28	1.7	4.0
29	0.19	2.3
30	0.66	3.7

separation appears to be specific and to yield fatty acids of sufficient purity.

The quantitative analysis of a mixture of compounds of such wide range in molecular weight is difficult. The methyl esters of acids with less than 14 carbon atoms are relatively volatile; they can be lost when the solvents are evaporated. The acids with 25–30 carbon atoms are not very soluble and could be partially lost through inefficient extraction. Although yields were monitored with C<sup>14</sup>-tagged palmitic acid, it is not entirely certain that this represents the actual yield of other components. Quantitative recovery of acids from the residue of the oxidation medium is difficult.

Figures 79 and 80 reveal several interesting points. The distribution of acids in the extract of the Green River shale is comparable to that produced by oxidation, especially if one considers the ratio of acids with an even number of carbon atoms to those with an odd number. A common source and chemical

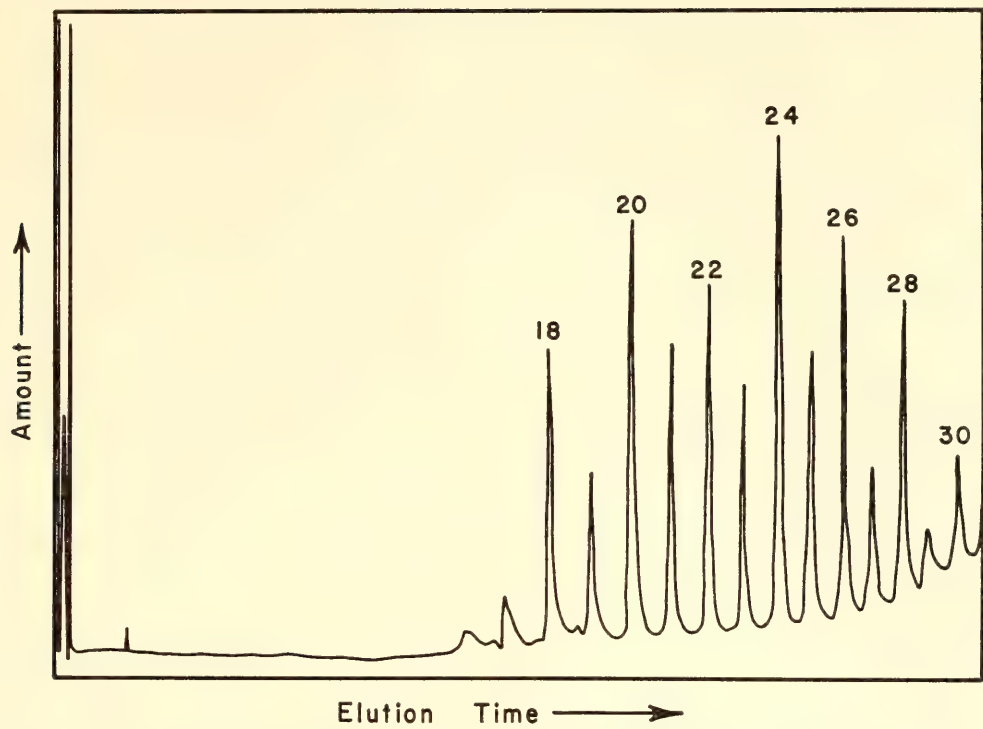


Fig. 79. Fatty acids from the chromic acid oxidation of Green River shale. Separation performed as described in Fig. 77.

pathways are suggested. Other workers have noted the abnormal abundance of *n* alkanes of very high molecular weight in this rock as compared with other rocks. It is tempting to speculate that the unusual environment of deposition for this rock favored the production and preservation of plant waxes, which have a higher range of molecular weights than the fatty acids. The highest acid of this

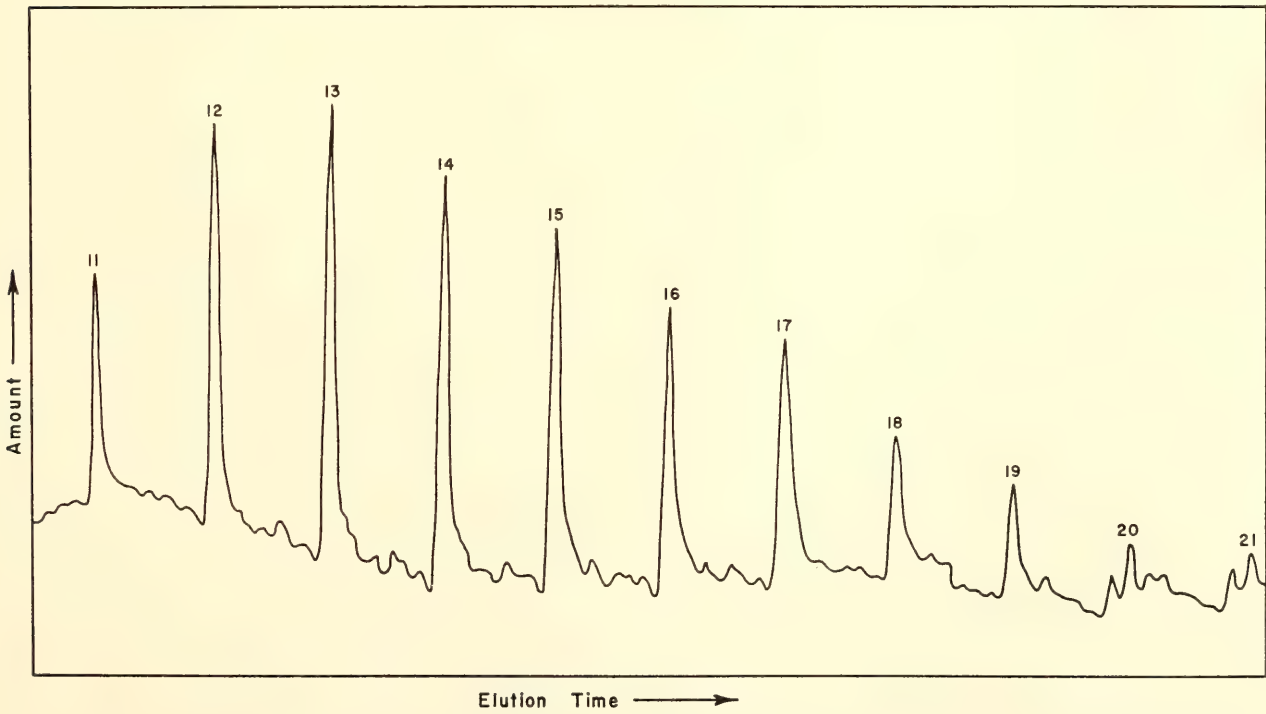


Fig. 80. Fatty acids from the chromic acid oxidation of McMinn shale (1,600 m.y. old). Separation performed as described in Fig. 77 except that a 0.010-inch-diameter column was used.



series that can conveniently be observed with our techniques is  $C_{30}H_{60}O_2$ , but on several occasions abundant amounts of higher acids were seen. It is not known how far they will go, and an experiment to determine those above  $C_{30}$  will be difficult.

The gas chromatograph was calibrated with a known amount of pure fatty acids. It was determined that 0.01 per cent of the organic carbon in the Green River shale could be extracted as fatty acids in the range of  $C_{14}$  to  $C_{30}$ , whereas 0.05 per cent could be isolated after chromic acid oxidation. Since about 10 per cent or more of the carbon in many types of living cells exists as lipides, which are mainly fatty acids, it is clear that great transformations have occurred in the original organic matter deposited in this sediment.

The fatty acids in the organic matter of a grab sample of recent sediment from the San Nicolas Basin off California were analyzed. Three hundred grams of wet mud was dried under vacuum and extracted, and the residue was demineralized and oxidized. The fatty acids were isolated as previously described. Approximately 0.012 per cent of the organic carbon in the sample could be accounted for as free fatty acids in the range of  $C_{14}$  to  $C_{30}$ , whereas 0.13 per cent of the carbon was released as fatty acids on chromic acid oxidation. Table 31 indicates the micrograms of the individual acids per gram of organic matter. It is apparent that substantial changes occur very rapidly to the fatty acids in sediments. The distribution of acids shown is greatly different from that found in marine organisms. Aliphatic residues are incorporated into the kerogen in a relatively short time. The relative amounts of odd-numbered acids are much greater in the fraction produced by oxidation than in the extractable acids, where the even-numbered acids comprise 94 per cent of the total. The amounts of acids relative to one another are probably correct to 30 per cent, but

the absolute amounts may have an error by a factor of 2 to 3.

Preliminary results on rocks of Paleozoic age or younger indicate that the amounts of acids decrease with age and metamorphism, with the relative amounts of odd-numbered fatty acids in carbon numbers increasing until there is an almost "smooth" distribution with little predominance of even-numbered acids.

The work has been extended to rocks of Precambrian age. The technique of observing straight-chained acids produced by the oxidation of the kerogen in these rocks holds great promise for tracing the record of life back in time. In another part of this report we have described the problems of contamination of ancient rocks by migrating organic fluids. Detection of molecular structures of probable biological origin in the kerogen fraction is somewhat safer, since it is less likely that this portion of a rock could become contaminated.

Figure 80 shows the chromatogram of the acids produced by the chromic acid oxidation of the McMinn shale from the Northern Territory of Australia. This extremely well-preserved rock has an age of approximately 1,600 m.y. The oxidation had been carried out for 20 hours and may account for the relatively low-molecular-weight range of the acids. Also, the acids were not separated by the urea adduction process, in spite of which the straight-chained acids predominate, showing that they are particularly stable in the kerogen matrix. Table 32 gives some quantitative results for the individual acids observed and shows that aliphatic structures are well preserved in the kerogen of rocks.

In this report we have shown that long, straight-chained aliphatic structures are incorporated rapidly into the insoluble organic matter of rocks. We have also shown that once they are in they can persist for great lengths of time and provide a suitable record of some facets of very ancient life on earth.

Several interesting questions are raised.

TABLE 32. Fatty Acids From the Chromic Acid Oxidation of the McMinn Shale

Acid, carbon number	Micrograms Acid per Gram of Organic Carbon
11	1.5
12	2.9
13	3.6
14	3.1
15	2.9
16	2.5
17	2.3
18	1.3
19	1.1
20	0.54
21	0.33

What is the mechanism of the reaction that binds fatty acids into the organic matter of recent sediments? What chemical reactions give rise to the acids with an odd number of carbon atoms? How are the acids of long-chain length synthesized in the sediments? What is the relation between the aliphatic chains in the kerogen and the *n* alkanes that can be extracted from rocks? The answers to these questions will give important clues to unraveling the complex chemistry of the organic matter in sedimentary rocks.

AMINO ACID COMPOSITION OF  
SOME CALCIFIED PROTEINS

*P. E. Hare and P. H. Abelson*

The geologic record provides impressive evidence of progressive changes in the nature of the skeletal hard parts of invertebrates. The relative scarcity of Precambrian fossils has been attributed by many (e.g., Glaessner, 1962) to a lack of preservable hard parts. Cambrian rocks contain remains of a variety of organisms that possessed hard parts of chitin, calcium phosphate, calcium carbonate, and silica.

The fossil record clearly shows that calcium-carbonate secreting organisms have increased in number and variety since early Cambrian time (Lowenstam, 1963). Many forms have appeared and

then later have become extinct. Some forms have appeared relatively recently, whereas a few have continued almost unchanged throughout a long geologic range.

The present study is concerned with the organic material associated with mineralized hard parts. The shells of living mollusks exhibit a variety of morphological forms. Calcium carbonate as aragonite, calcite, or a mixture of the two is intimately associated with an organic matrix which probably is involved in the shell-forming process. When cross sections of mollusk shells are viewed microscopically it is obvious that there are substantial variations in internal shell structure.

These structures can be broadly classified into a few basic types (Bøggild, 1930). Most shells exhibit more than one distinct structural layer. The nacreous aragonite structure is found in all three major molluscan classes. In an electron microscope this structure exhibits a "brick wall" pattern with aragonite layers about one micron thick, separated by still thinner layers of organic matrix. The structure is characterized by a relatively high proportion of organic material, usually between one and five per cent.

The prismatic structure, which may be aragonite or calcite, is often found as a distinct layer associated with the nacreous structure. It is also characterized by a high organic content and in the case of the bivalve *Mytilus* both the prismatic and nacreous structures have nearly identical amino acid compositions (Hare, 1963). The crossed lamellar shell structure is described by Bøggild (1930) as the most specialized and the most common structure and is found in all the classes of mollusks except the cephalopods. The mineral layers alternate at nearly right angles. Differences in the size of the lamellae vary widely. The chitons (Amphineura) have lamellar dimensions approaching one micron, whereas those of the shells of the Mesogastropoda and Neogastropoda have dimensions approaching one millimeter. Less common



shell structures restricted to particular taxonomic groups include a type of foliated structure present in some of the limpets (Archaeogastropoda) and some pectens (Anisomyaria) and an irregularly grained structure that is found in some cephalopods.

In the present study we have examined the protein content of about 200 shells. We find correlations between type of shell structure and the amount of organic material contained in them. The nacreous and prismatic structures are apparently restricted to shells of high organic content, whereas the crossed lamellar structure covers a wide range from about one per cent in the Amphineura to 0.01 per cent in some of the shells of Neogastropoda. Corresponding to this variation in organic content is a marked variation in the dimensions of the crossed lamellar structure, ranging from extremely fine lamellae in the Amphineura to very coarse lamellae in some shells of the Mesogastropoda and Neogastropoda. Summarized in Fig. 81 are the data on shell structure types and the amount of organic material found in mollusk shells.

Correlations also exist between the shell structure and the relative proportions of amino acids found in them. In this study quantitative comparisons of compositions are made to reveal to what extent similarities and differences exist between taxonomic groups. Because the amount of protein in shells of different taxonomic groups varies widely (0.01 per cent to 5 per cent) it is useful for comparative purposes to normalize the composition to 1,000 amino acid residues. Figure 82 compares data from three species of the genus *Mytilus* in the family Mytilidae. Compared with *M. edulis* the most significant difference in the closely related *M. californianus* is the glutamic acid. *M. veridus* (which some taxonomists consider a different genus) shows significant differences from *M. edulis* in aspartic acid, glutamic acid, serine, glycine, leucine, tyrosine, and phenylalanine. The morphology and shell structures of *M. edulis* and *M. californianus* are nearly identical, whereas *M. veridus* differs in having no outer prismatic layer.

We have found repeatedly that throughout the various taxonomic groups amino acid compositions are similar

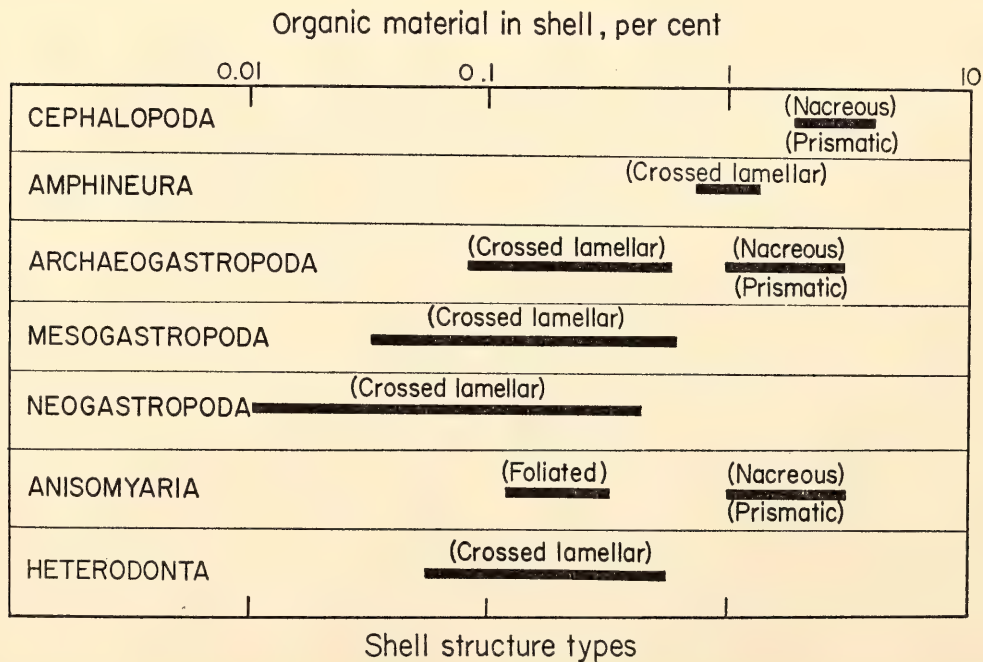


Fig. 81. Range of percentage of organic material found in mollusk shells with range of shell structure types described by Bøggild (1930).

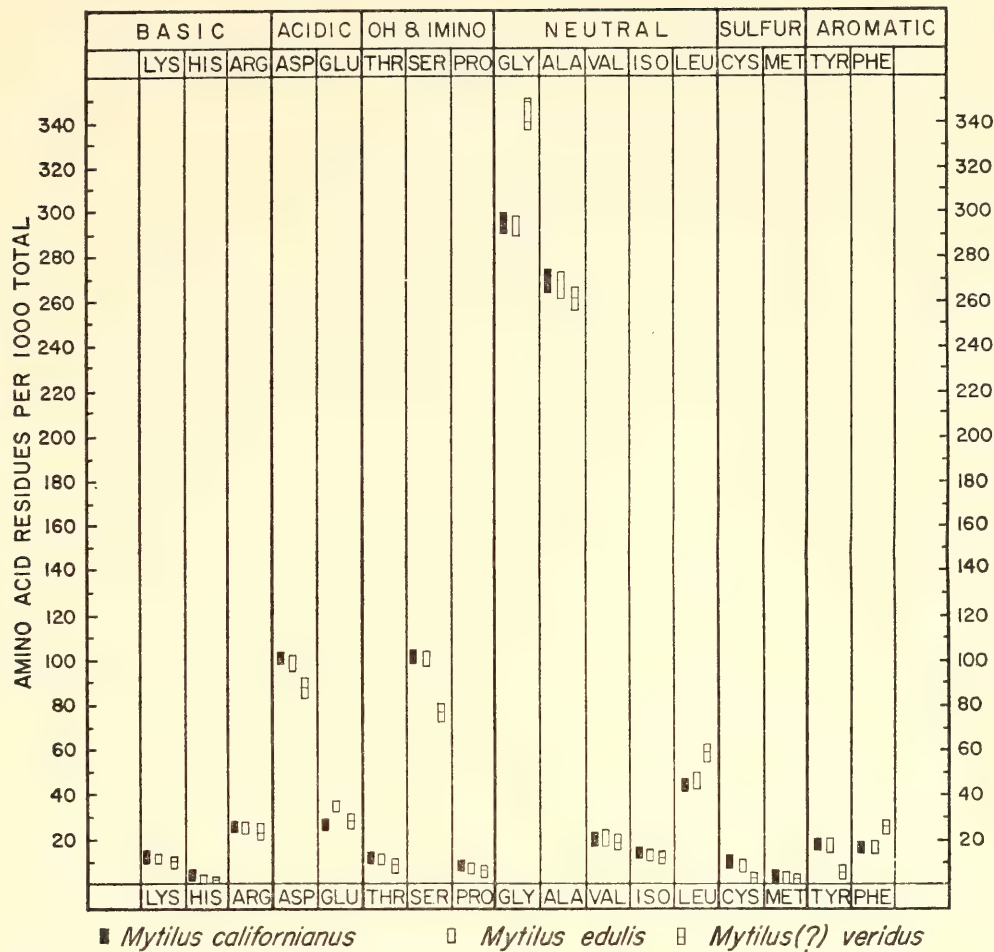


Fig. 82. Amino acid compositions of three species of *Mytilus*.

whenever morphology and shell structure are closely related. Figure 83 shows a similar comparison among three closely related genera of the family Veneridae. While differences in aspartic acid and glycine are apparent there are remarkable similarities in the three patterns.

In contrast, Fig. 84 compares the ranges of amino acid compositions found in the two families Veneridae and Mytilidae with widely different shell structures and morphology. Compositions for the two families show an overlap only in serine. The Veneridae (common clams, etc.) shells contain approximately one tenth the amount of protein found in the typical nacreous shells of the mussels in the family Mytilidae.

In some instances we found widely divergent amino acid compositions within a taxonomic family. Figure 85 shows the

results from two genera in the family Sanguinolaridae. *Tagelus* is morphologically distinct from *Sanguinolaria*. It seems significant that whenever gross differences in amino acid composition are found the shells exhibit either different morphology or greatly different shell structures.

The nacreous aragonite shell structure is found in all three major classes of mollusks and apparently is restricted to the more primitive representatives of these groups. Figure 86 shows the ranges in amino acid compositions found in the nacreous structures from the three major classes of mollusks. The Archaeogastropoda contain relatively more aspartic acid and less alanine and glycine. The pelecypod representatives are somewhat lower in arginine and glutamic acid and richer in glycine and alanine. The



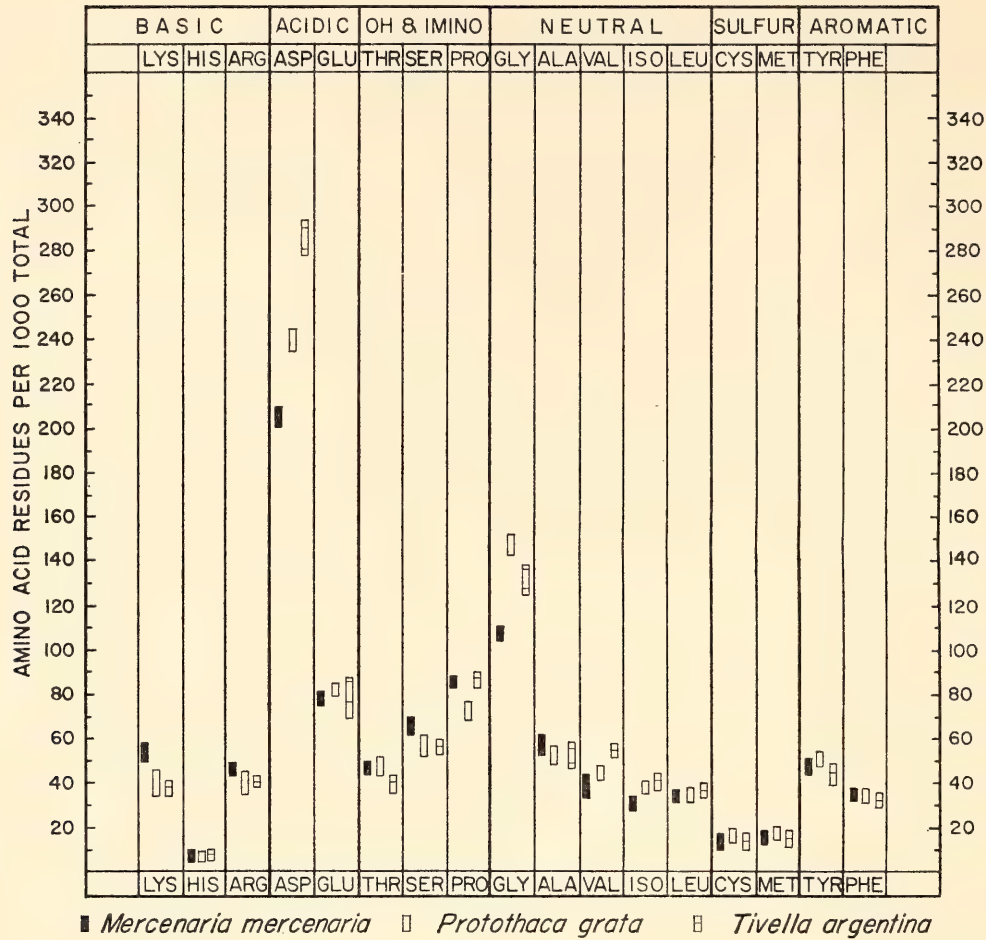


Fig. 83. Amino acid compositions of three related genera within the family Veneridae.

cephalopod *Nautilus*, often referred to as a living fossil, is relatively low in leucine and high in phenylalanine. Considering the major differences in taxonomic classification of these shells, the similarities in their amino acid compositions are remarkable and reflect the uniform nature of the nacreous structure.

Figure 87 compares the ranges in amino acid compositions for some non-nacreous shell structures of the gastropods. Although more than one type of shell structure is represented, the crossed lamellar structure is predominant. Again it may be seen that there exist broad similarities in composition.

The similarities in the amino acid contents of the nacreous structures of primitive mollusks suggested that a comparison with primitive forms of other phyla might be of interest. The brachiopod *Lingula* belongs to a superfamily

that has a fossil record from the lower-Cambrian to the present. Although the *Lingula* shell is phosphatic and chitinous, the phosphatic portions contain protein whose amino acid composition resembles that of the primitive mollusks. It differs from all carbonate shell proteins studied thus far in having appreciable amounts of hydroxyproline, an amino acid found in collagen and generally associated in phosphatic vertebrate structures. Comparative values of *Lingula* and nacreous gastropod structures are shown in Fig. 88.

Geologic evidence indicates that chitin may have preceded minerals as principal constituent of hard parts. It is interesting to note that chitin today is also found in the cell walls of green algae, fungi, and yeasts. Chitin rarely occurs alone even in the noncalcified exoskeletons of insects and other Arthropoda (Richard, 1951) but it is mixed with variable amounts of

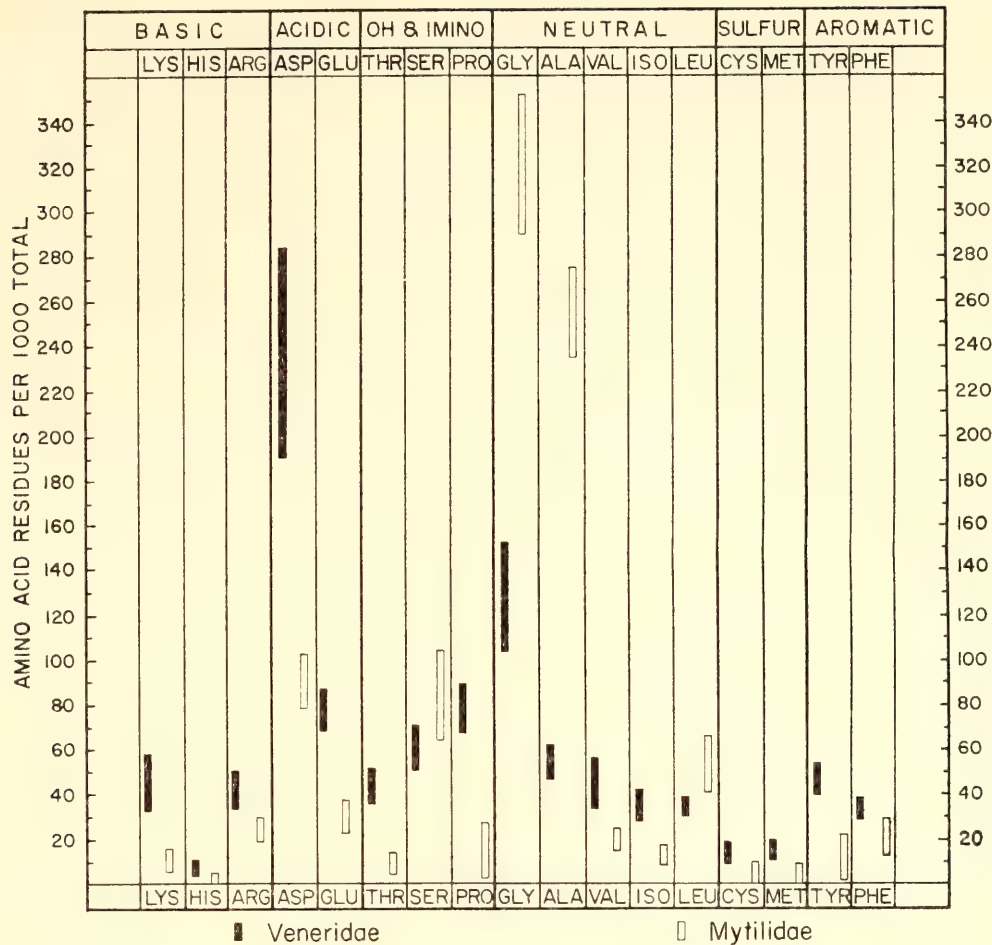


Fig. 84. Ranges of amino acid compositions found in two pelecypod families of widely differing shell structure and morphology, Veneridae (three genera) and Mytilidae (four genera).

protein. In view of the presumptive ancient origins of chitin, it seemed desirable to compare the glucosamine content of specimens representing a number of forms. Figure 89 is a plot of the glucosamine recovered on acid hydrolysis of the insoluble calcified organic matrices from various groups.

We have found large variations (over  $10^4$ ) in the amount of glucosamine in invertebrate hard parts. This was especially evident in a comparison among the mollusks. The primitive forms with nacreous or finely crossed lamellar shell structures were relatively rich in glucosamine, whereas some of the highly developed Neogastropoda contained less than 1/10,000 as much. Similarly the primitive pelecypods contained far more glucosamine than the more advanced Heterodonta.

The data shown in Fig. 89 are con-

sistent with the hypothesis that protein-chitin hard parts are more primitive than calcified structures. With the progressive development of calcification in the mollusks, chitin decreased not only in proportion to the total structures but also to the protein within the calcified structure.

Arthropod evolution, in contrast, has apparently followed a course where chitin remains dominant and calcification subordinate. *Lingula* may represent an early development of phosphatic calcification somewhat similar to the vertebrate structures of bone and teeth. The chitons (*Amphineura*) show a high glucosamine content and also show a primitive type of crossed lamellar shell structure, a rather interesting combination for what are generally considered the most primitive living mollusks (Shrock and Twenhofel, 1953, p. 358).



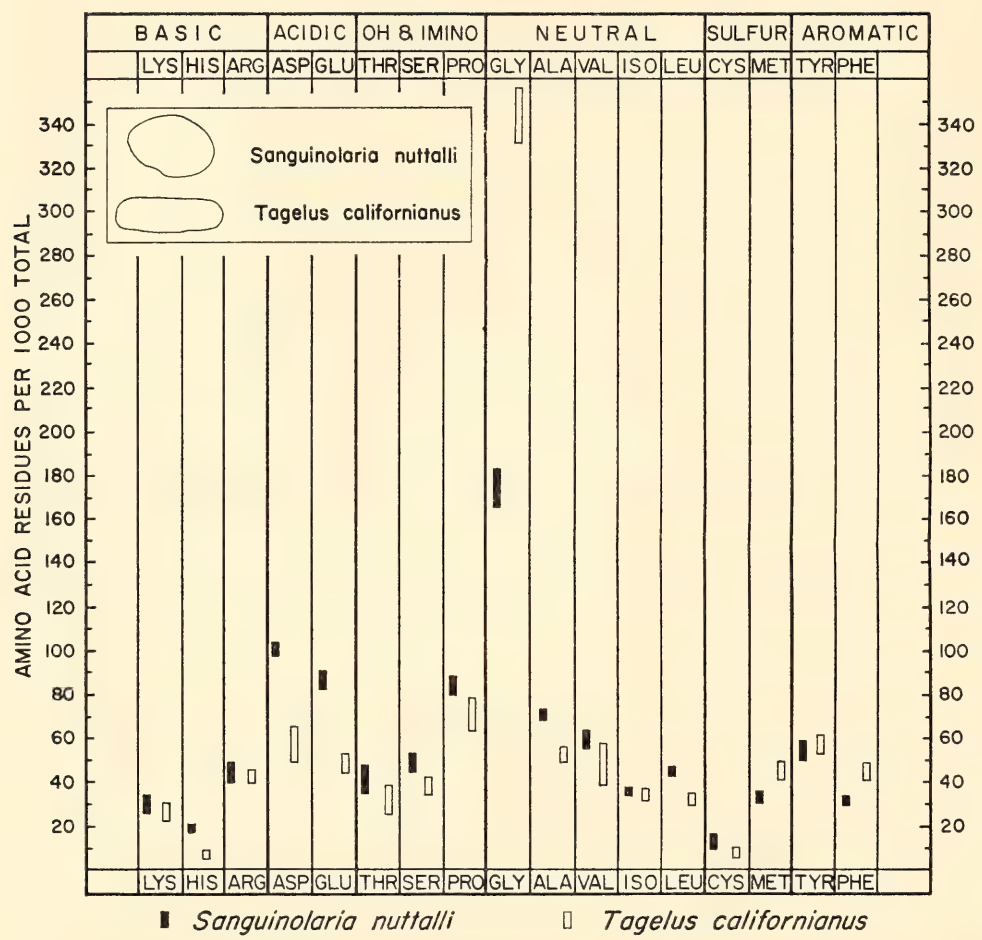


Fig. 85. Amino acid compositions from shells of two genera with widely differing morphology in the family Sanguinolaridae.

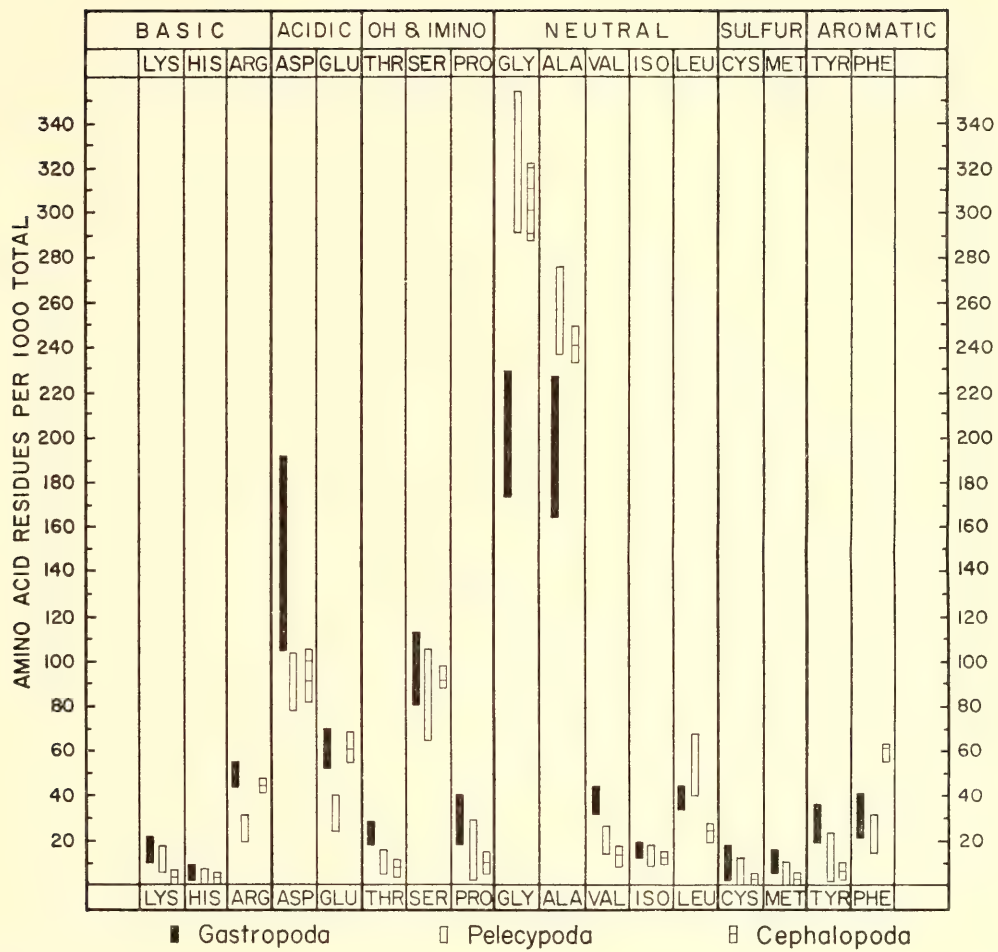


Fig. 86. Ranges of amino acid compositions for nacreous structures from three classes of mollusks.



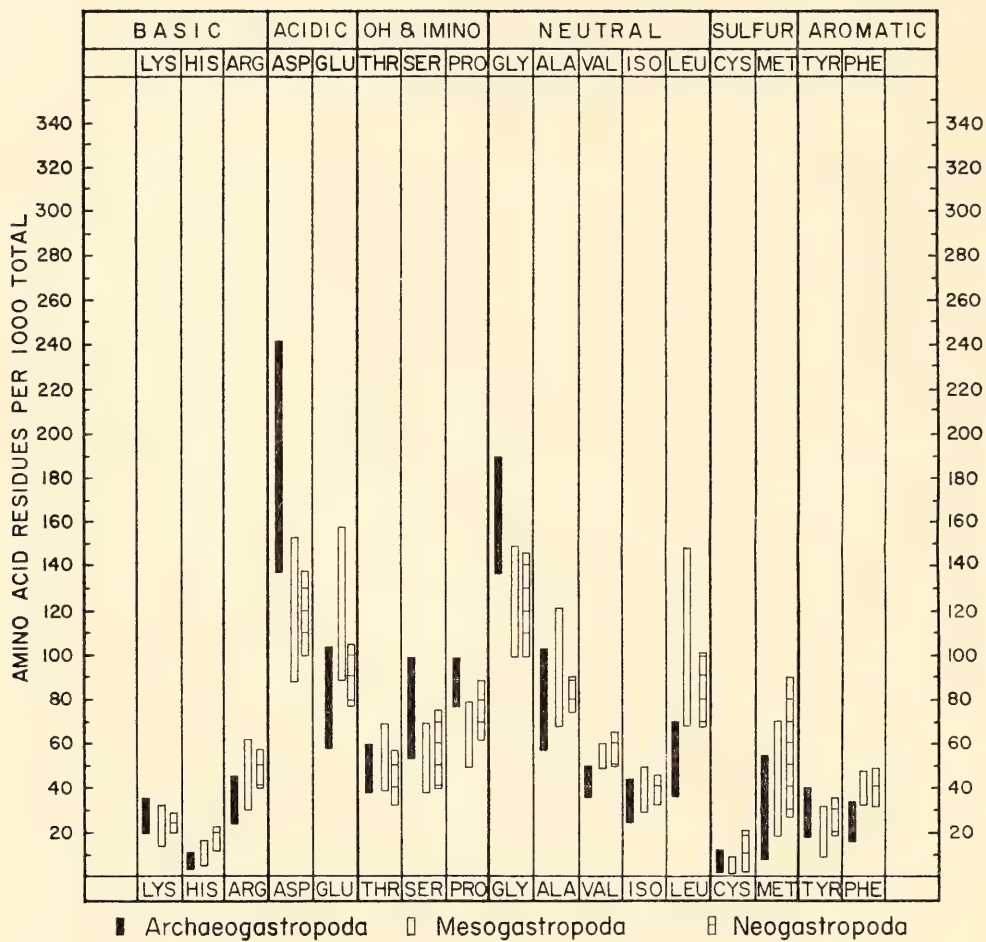


Fig. 87. Comparison of amino acid compositions for some nonnacreous shell structures of gastropods.

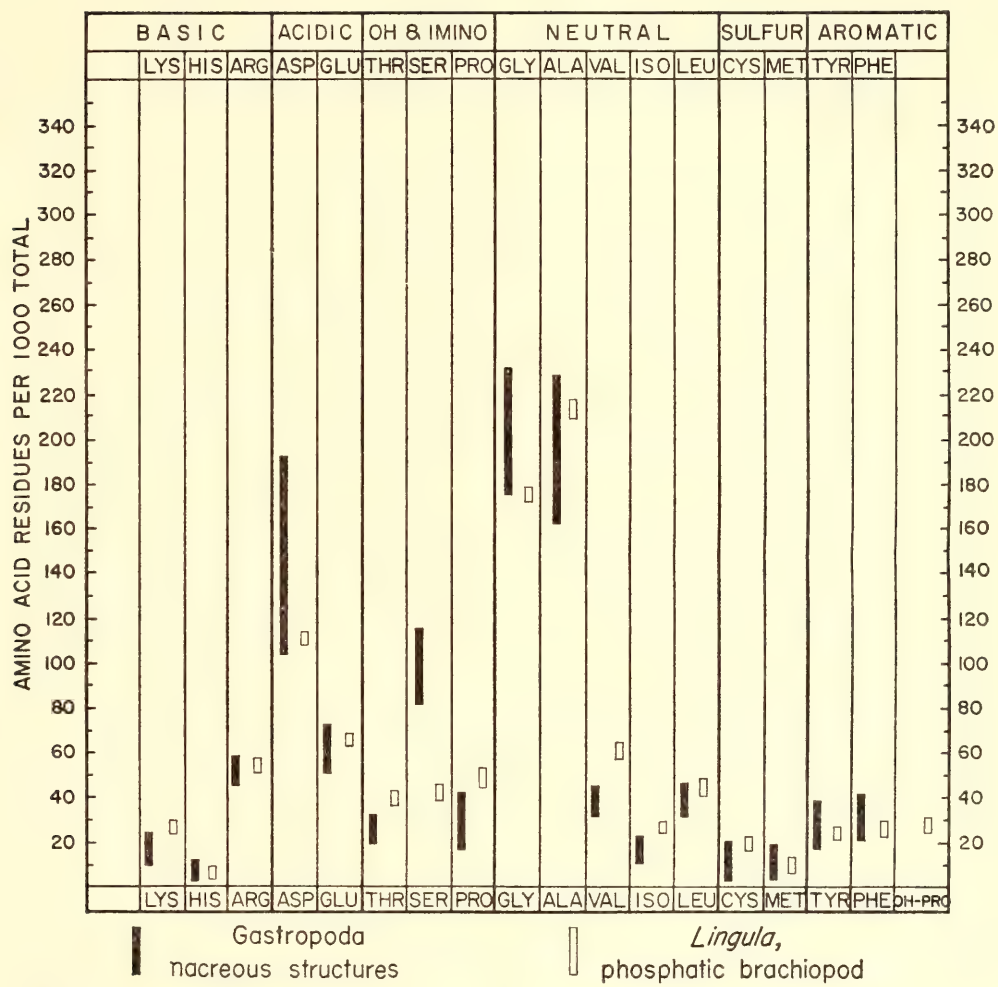


Fig. 88. Range of composition for nacreous shell structures of gastropods compared with *Lingula*, a phosphatic brachiopod.



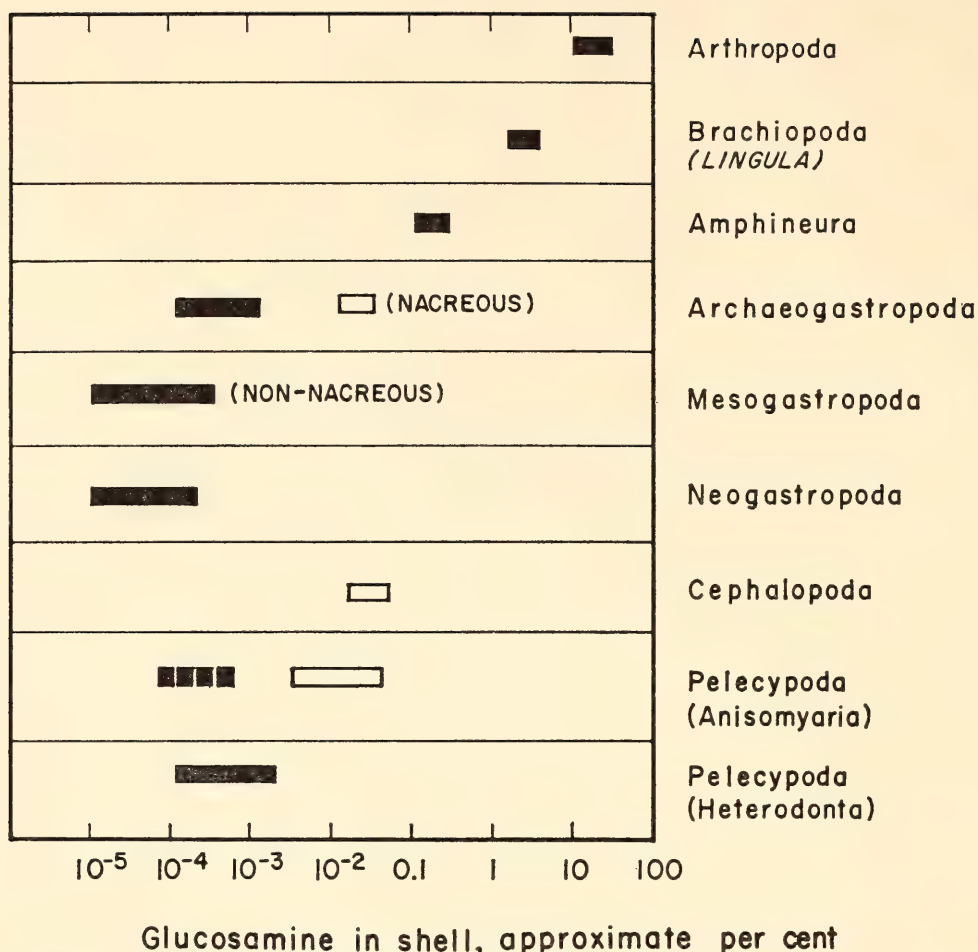


Fig. 89. Range of glucosamine contents in shell structures of various groups.

#### AMINO ACID ARTIFACTS IN ORGANIC GEOCHEMISTRY

*P. E. Hare*

The accurate measurement of small amounts of amino acids is made difficult by the ubiquitous occurrence of these compounds, which may contaminate chemicals and glassware. The present study is an attempt to evaluate some of the more obvious sources of contamination as well as the fate of certain amino acids during laboratory procedures for their separation and analysis. The equipment used was a sensitive ion-exchange amino acid analyzer described briefly in *Year Book 63* (p. 269).

A fingerprint on a piece of paper reacts with ninhydrin to form an easily measurable pattern. Oden and von Hofsten (1954) have detected 12-year-old fingerprints on paper documents by this

method. Substances from the hands, therefore, represent potentially significant sources of contamination in organic geochemistry since samples as well as glassware are usually handled at some stage in the process. Hamilton (1965) has evaluated the levels of amino acids in a single wet thumbprint and found approximately  $10^{-7}$  mole each of serine, glycine, and ornithine, and  $4 \times 10^{-7}$  mole urea. Most of the other amino acids were present in amounts somewhat greater than  $10^{-8}$  mole. Figure 90B shows the chromatogram produced when a single wet fingerprint was made inside a beaker and washed in a minimum amount of pH 2.0 citrate buffer, then added to the ion-exchange column. A standard amino acid pattern is shown for comparison in Fig. 90A. Serine (mixed with glutamine and asparagine) is the most abundant amino acid, followed by

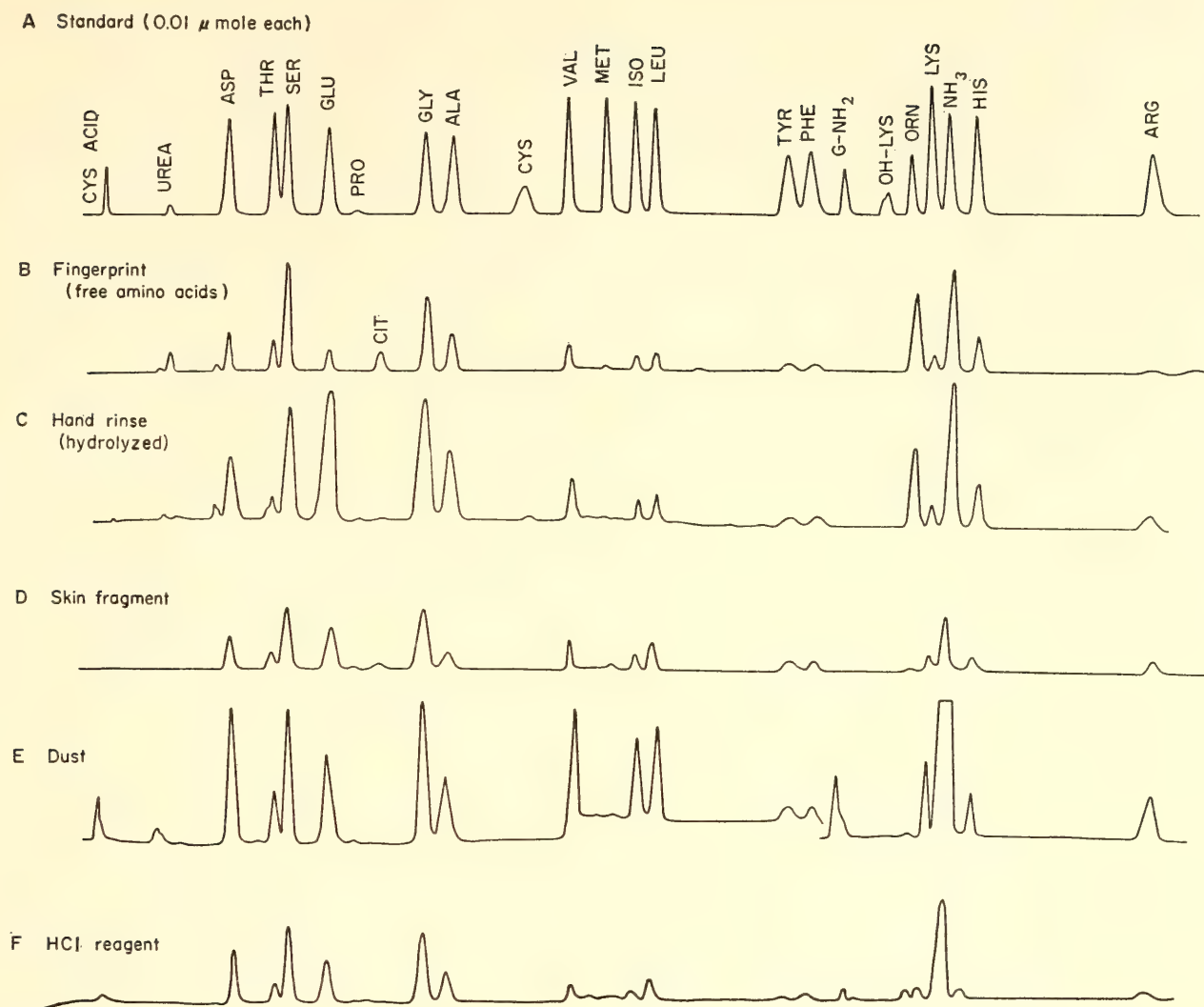


Fig. 90. Amino acid chromatograms from potential sources of contamination compared with standard amino acid pattern at top. ALA, alanine; ARG, arginine; ASP, aspartic acid; CIT, citrulline; CYS, cystine; CYS ACID, cysteic acid; GLU, glutamic acid; GLY, glycine; G-NH<sub>2</sub>, glucosamine; HIS, histidine; ISO, isoleucine; LEU, leucine; LYS, lysine; MET, methionine; NH<sub>3</sub>, ammonia; OH-LYS, hydroxylysine; ORN, ornithine; PHE, phenylalanine; PRO, proline; SER, serine; THR, threonine; TYR, tyrosine; VAL, valine.

glycine, ornithine, alanine, and aspartic acid. Notice the presence of citrulline, a nonprotein amino acid. Figure 90C shows a hydrolyzed sample of a hand rinse. Most of the amino acids show an increase, an indication of peptide-bound amino acids.

Hydrolyzed skin (Fig. 90D) has a somewhat similar amino acid chromatogram pattern, with high glycine and serine. Ornithine is much lower, whereas lysine is higher. The presence of citrulline, a nonprotein amino acid, suggests impregnation of the skin fragment with perspiration.

Dust was collected from a corner of the laboratory and hydrolyzed to give the pattern shown on the chromatogram in Fig. 90E. Glycine is present in greatest concentration, followed by valine, aspartic acid, serine, leucine, and glutamic acid. Also present are the amino sugars, glucosamine and galactosamine, possibly from the hydrolysis of chitinous material present in the dust.

Of the various reagents used in the separation and analysis of amino acids, only hydrochloric acid contained amino acids in the range of  $10^{-9}$  mole per liter or greater as shown in Fig. 90F. Five



hundred milliliters of acid was evaporated in a rotary evaporator, and the residue was analyzed. Hydrochloric acid furnished by two suppliers contained  $10^{-9}$  mole, whereas acid from another source was almost free of contamination. The amino acid pattern of high serine and glycine found in hydrochloric acid suggests hand contamination somewhere in its manufacturing or bottling procedure. Single distillation reduced the amino acid levels by a factor of 10 but did not eliminate them. A second distillation decreased the level to a point below detection.

Other reagents were tested, including glacial acetic acid (Fisher reagent grade), pyridine (Fisher certified reagent grade), ammonium hydroxide (B and A reagent grade), and hydrofluoric acid (B and A reagent, redistilled). No amino acids were

found. If present the amounts were less than  $10^{-10}$  mole per liter of reagent.

The fate of free amino acids during the separation and hydrolysis steps was determined for low-level amino acid concentrations. In Fig. 91B and C are shown the effects of hydrolysis in doubly distilled HCl of a mixture of free amino acids of  $0.025 \mu$  mole/ml of each. Again a standard amino acid pattern is presented for comparison (Fig. 91A). Figure 91B shows the effects of air in the sealed hydrolysis tube. Cystine has been quantitatively oxidized to cysteic acid, and nearly 60 per cent of the methionine has been destroyed. Flushing the tube with nitrogen (less than 5 ppm  $O_2$ ) before sealing and hydrolyzing improves the recovery as shown in Fig. 91C. Cystine and methionine are both recovered in better than 90 per cent yield.

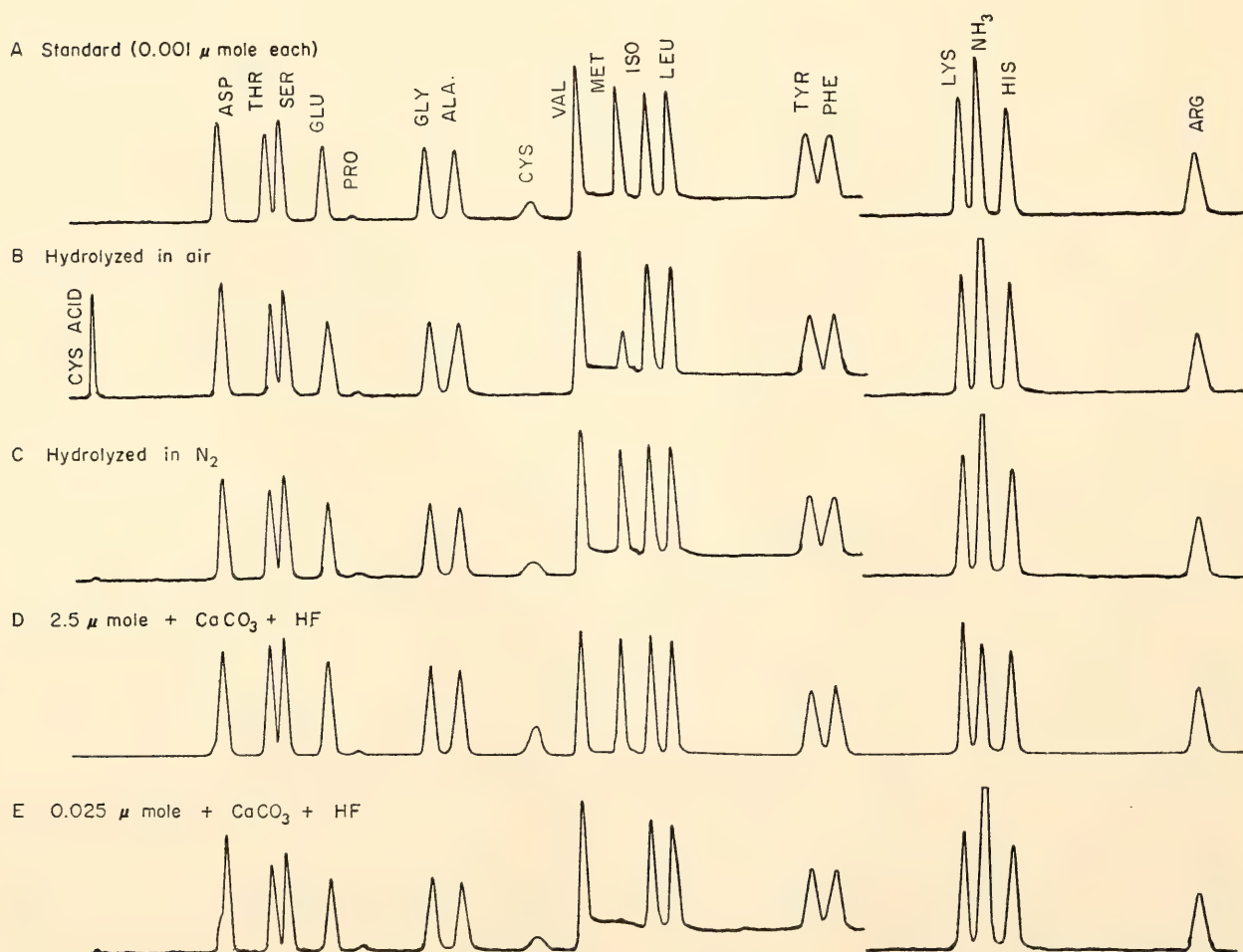


Fig. 91. Amino acid chromatograms showing results of laboratory treatments on standard amino acid mixtures. Recorder on expanded scale at  $10\times$  for all except D. Abbreviations as in Fig. 90.

A procedure for decalcifying solutions of  $\text{CaCO}_3$  shells has been developed that uses hydrofluoric acid to precipitate calcium.  $\text{CaF}_2$  is centrifuged off and washed with two separate volumes of water. The combined supernatant and washings are dried overnight in a vacuum desiccator over  $\text{NaOH}$  and  $\text{H}_2\text{SO}_4$ . The residue is then hydrolyzed if peptides are present or dissolved in pH 2 citrate buffer and analyzed directly. The results of an experiment in which a mixture of amino acids was added to 2 gm  $\text{CaCO}_3$  and decalcified by this procedure are shown in Fig. 91D and E for two different levels of amino acids. In the higher concentration of 2.5  $\mu$  moles/ml of each amino acid, recovery is excellent, with no tendency of

the  $\text{CaF}_2$  to selectively coprecipitate any of the amino acids. In the sample containing only 0.025  $\mu$  mole/ml of each amino acid, methionine is destroyed and its oxidation product appears as a leading shoulder on aspartic acid.

Only a few of the amino acids are subject to possible degradation during the sample preparation provided that reasonable care is maintained. Possible contamination by fingerprints should be indicated by abnormally large amounts of serine as well as by the presence of such "fingerprint" amino acids as citrulline and high amounts of ornithine. Evaluation of reported geologic occurrences of amino acids must include a critical appraisal of the contamination.

## MISCELLANEOUS ADMINISTRATION

### *Journal of Geophysical Research*

The *Journal of Geophysical Research* is published semimonthly by the American Geophysical Union, with P. H. Abelson (Geophysical Laboratory) and J. A. Peoples, Jr. (University of Kansas), as coeditors. About half the editorial work, consisting of manuscripts on the upper atmosphere and on space, as well as some of the papers involving geochemistry, are handled at this Laboratory. The *Journal* is regarded by many as the world's leading geophysical publication.

Though publishing about 6,000 pages a year, the *Journal* has one of the fastest publication records of any scientific journal. This accomplishment is due to the effective efforts of Dr. and Mrs. Peoples at Kansas, and the cooperation of Mrs. Lucile Stryker and Miss Mary Jane Miles of the Carnegie Institution, and Mr. A. D. Singer and Miss Marjorie E. Imlay of the Geophysical Laboratory.

### *Journal of Petrology*

During 1964 some 15 papers were published covering a broad spectrum of

petrology. The continued excellence of research work and concentration of new critical data have brought about a further increase in circulation. Four papers were authored wholly or in part by staff members of the Geophysical Laboratory, with Professor C. E. Tilley and Dr. H. S. Yoder, Jr., continuing to serve as editors. The *Journal* continues to operate successfully without a page charge or subsidy; however, in recent numbers of this publication some advertising has been included.

### *Lectures*

During the report year staff members and fellows were invited to present lectures as follows:

P. H. Abelson made a total of 17 invited public appearances: as lecturer ("Science in the service of society") at the dedication of a new science facility at State University College, Plattsburgh, N.Y.; as speaker ("The Midwest and the scientific revolution") at the Purdue University Symposium on Science and Public Policy: Evolving Institutions; as



lecturer ("Shaping our planetary environment") at Oberlin College; as speaker ("Needed changes in Federal support of research") at a government and science lecture series at Florida State University; as a participant ("Science and government") in the Galileo Quadricentennial Celebration at the University of Rochester; as lecturer ("Chemicals from ancient life") at Antioch College; and as the after-dinner speaker ("Relation of group activity to creativity in science") at the National Bureau of Standards Critical Points Conference.

P. M. Bell addressed the Geological Society of Washington.

F. R. Boyd lectured at the Geology Department of Northwestern University.

F. Chayes gave lectures at the Geology Departments of the University of Cincinnati and Northwestern University on the application of discriminant functions to petrographic classification and their properties in closed arrays.

G. L. Davis delivered two lectures at the Geological Society of Franklin and Marshall College.

During the first semester 1964-1965 G. Donnay taught a course on advanced inorganic chemistry in the Chemistry Department of the Johns Hopkins University. In February she lectured at the faculty seminar of the same department, "Crystallographic studies of solid solutions." In November she addressed the Officers' Club of Aberdeen Proving Ground. From October 13 to 16 she participated in a symposium, "Communication of two- and three-dimensional concepts," at the Ledgemont Laboratory of the Kennecott Copper Corporation in Lexington, Massachusetts.

P. E. Hare addressed the Geochemistry and Geophysics Colloquium at Yale University and the Paleoecology Seminar at California Institute of Technology.

T. C. Hoering gave a lecture, "Organic geochemistry and the record of Precambrian life," at the 10th International

Botanical Congress, Edinburgh, Scotland. He also addressed the Department of Botany at Cornell University and participated in a symposium, "The analysis of organic matter in carbonaceous chondrites," sponsored by the National Aeronautics and Space Administration.

As Visiting Professor in Geochemistry at Lehigh University, G. Kullerud gave a series of three monthly lectures on sulfide phase equilibria and supervised the research of four Ph.D. candidates. He was invited as a lecturer at a symposium at Heidelberg University honoring Professor Paul Ramdohr on his 75th birthday. While at Heidelberg University, Kullerud also gave a series of five talks at the Mineralogisch-Petrographisches Institut and a series of eight talks at the Physikalisch-Chemisches Institut. In addition, he gave lectures at the University of Georgia, University of Tübingen, Frankfurt University, University of Kiel, University of Liège, and the Falconbridge Mining Company at Sudbury.

D. H. Lindsley addressed the Department of Geology, Princeton University.

A. J. Naldrett lectured at the Department of Geology, Lehigh University, and addressed a group of geologists of Falconbridge Nickel Mines Ltd., at Falconbridge, Ontario.

As part of the Bicentennial Celebration Series at Brown University, J. F. Schairer lectured to the Department of Geology, "The nature of residual liquids in systems of rock-forming oxides and its bearing on the origin of igneous and metamorphic rocks." He also addressed the Geological Society of Franklin and Marshall College.

C. E. Tilley was another invited lecturer at the symposium at Heidelberg University honoring Professor Paul Ramdohr on his 75th birthday.

G. R. Tilton gave a series of lectures at the Sorbonne, University of Paris, the University of Kiel, Germany, the Swiss Federal Institute at Zürich, and the University of Bern, Switzerland. He also



addressed the International Conference on Absolute Geochronology at Nancy, France.

H. S. Yoder, Jr., participated in the first and second conference on Engineering for Executives sponsored by the University of Texas. Two days' seminars were conducted at each conference on the properties of rocks and minerals at high pressures and temperatures. A series of lectures was presented at the University of Alberta and the University of Oklahoma, the latter series being sponsored by the American Geophysical Union Visiting Scientist Program. The National Defense Education Act Fellowships Program supported a lecture series at Ohio State University. Yoder also was an invited speaker at the American Association of Petroleum Geologists Research Symposium: subject "Geophysical and geological properties of the crust and mantle." He gave a 20-lecture course, "Advanced problems in experimental petrology," during a two-week period at the University of Texas as Visiting Professor of Petrology.

### *Petrologists' Club*

Eight meetings of the Petrologists' Club were held during this, its 54th year. Topics spanned a broad range of experimental, theoretical, and field petrology:

"Petrology vs. thermodynamics," by James B. Thompson, Jr. (Harvard University).

"Aplites from quenched magmas," by R. H. Jahns (Pennsylvania State University).

"Synthesis and stability of siderite ( $\text{FeCO}_3$ )," by Bevan French (National Aeronautics and Space Administration).

"The Oka carbonatite complex," by D. P. Gold (Pennsylvania State University).

"Anisotropy in rock," by W. F. Brace (Massachusetts Institute of Technology).

"Isotopes and the bowels of the earth," by G. R. Tilton (Geophysical Laboratory).

"Partial melting of the upper mantle as a possible origin of basaltic magmas," by I. Kushiro (Geophysical Laboratory).

"Crystallization of tholeiitic basalt in Alea lava lake, Hawaii, by Dallas Peck and Thomas Wright (speaker) (Hawaiian Volcano Observatory).

Peter M. Bell was chosen as the new Secretary.

### REFERENCES CITED

- Abrahams, S. C., and S. Geller, Refinement of the structure of a grossularite garnet, *Acta Cryst.*, 11, 437-441, 1958.
- Akimoto, S., H. Fujisawa, and T. Katsura, The olivine-spinel transition in  $\text{Fe}_2\text{SiO}_4$  and  $\text{Ni}_2\text{SiO}_4$ , *J. Geophys. Res.*, 70, 1969-1978, 1965.
- Akimoto, S., T. Nagata, and T. Katsura, The  $\text{TiFe}_2\text{O}_5$ - $\text{Ti}_2\text{FeO}_5$  solid solution series, *Nature*, 179, 37-38, 1957.
- Allen, E. T., J. L. Crenshaw, and H. E. Merwin, The sulphides of zinc, cadmium, and mercury; their crystalline forms and genetic conditions, *Am. J. Sci.*, 34, 341-396, 1912.
- Andersen, O., The system anorthite-forsterite-silica, *Am. J. Sci.*, 39, 407-454, 1915.
- Baker, P. E., I. G. Gass, P. G. Harris, and R. W. LeMaitre, The volcanological report of the Royal Society Expedition to Tristan da Cunha, 1962, *Phil. Trans. Roy. Soc. London, Ser. A*, 256, 439-578, 1964.
- Ball, R. H., G. D. Dorough, and M. Calvin, A further study of the porphinelike products of the reaction benzaldehyde and pyrrole, *J. Am. Chem. Soc.*, 68, 2278-2281, 1946.
- Barth, T. F. W., Die Pegmatitgänge der Kaledonischen Intrusivgesteine im Seilandgebiete, *Skifter Norske Videnskaps-Akad. Oslo; I: Mat.-Naturv. Kl.*, 8, 123 pp., 1927.
- Barth, T. F. W., *Theoretical Petrology*, John Wiley & Sons, New York, 1962.
- Bateman, A. M., Magmatic ore deposits, Sudbury, Ont., *Econ. Geol.*, 12, 391-426, 1917.
- Bell, P. M., Aluminum silicate system: Experimental determination of the triple point, *Science*, 139, 1055-1056, 1963.
- Belov, N. V., and I. M. Rumanova, The crystalline structure of epidote, *Tr. Inst. Kristallogr. Akad. Nauk SSSR*, 9, 103-164, 1954.
- Birch, F., Flow of heat in the Front Range, Colorado, *Bull. Geol. Soc. Am.*, 61, 567-630, 1950.
- Birch, F., Elasticity and constitution of the earth's interior, *J. Geophys. Res.*, 57, 227-286, 1952.
- Birch, F., and P. LeComte, Temperature-pressure plane for albite composition, *Am. J. Sci.*, 258, 209-217, 1960.
- Bloem, J., and F. A. Kröger, The  $p$ - $T$ - $x$ -phase



- diagram of the lead-sulphur system, *Z. Physik. Chem. (Frankfurt)*, N. F., 7, 1-14, 1956.
- Bøggild, O. B., The shell structure of the mol-lusks, *Kgl. Danske Videnskab. Selskabs, Skrifter Naturvidenskab. Math. Afdel.*, 2, 232-325, 1930.
- Bowen, N. L., The melting phenomena of the plagioclase feldspars, *Am. J. Sci.*, 35, 577-599, 1913.
- Bowen, N. L., The crystallization of haplobasaltic, haplodioritic, and related magmas, *Am. J. Sci.*, 40, 161-185, 1915.
- Bowen, N. L., "Ferrosilite" as a natural mineral, *Am. J. Sci.*, 30, 481-494, 1935.
- Bown, M. G., Re-investigation of clinoferr-silite from Lake Naivasha, Kenya, *Mineral. Mag.*, 34, 66-70, 1965.
- Boyd, F. R., Geological aspects of high-pressure research, *Science*, 145, 13-20, 1964.
- Boyd, F. R., and J. L. England, The quartz-coesite transition, *J. Geophys. Res.*, 65, 749-756, 1960a.
- Boyd, F. R., and J. L. England, Apparatus for phase-equilibrium measurements at pressures up to 50 kilobars and temperatures up to 1750°C, *J. Geophys. Res.*, 65, 741-748, 1960b.
- Boyd, F. R., and J. L. England, Effect of pressure on the melting of diopside,  $\text{CaMgSi}_2\text{O}_6$ , and albite,  $\text{NaAlSi}_3\text{O}_8$ , in the range up to 50 kilobars, *J. Geophys. Res.*, 68, 311-323, 1963.
- Boyd, F. R., J. L. England, and B. T. C. Davis, Effects of pressure on the melting and polymorphism of enstatite,  $\text{MgSiO}_3$ , *J. Geophys. Res.*, 69, 2101-2109, 1964.
- Brandenberger, E., Kristallstrukturelle Untersuchungen an Calciumaluminathydraten, *Schweiz. Mineral. Petrog. Mitt.*, 13, 569-570, 1933.
- Buddington, A. F., On some natural and synthetic melilites, *Am. J. Sci.*, 3, 35-87, 1922.
- Buerger, M. J., The precision determination of the linear and angular lattice constants of single crystals, *Z. Krist.*, A, 97, 433-468, 1937.
- Buerger, M. J., and W. Parrish, The unit cell and space group of tourmaline, *Am. Mineralogist*, 22, 1139-1150, 1937.
- Burnham, C. W., and M. J. Buerger, Refinement of the crystal structure of andalusite, *Z. Krist.*, 115, 269-290, 1961.
- Buttgenbach, H., and J. Mélon, *Les minéraux et les roches*, Dunod & Liège, Vaillant-Carmanne, Paris, 8th ed., 1953.
- Carmichael, I. S. E., and W. S. MacKenzie, Feldspar-liquid equilibria in pantellerites: An experimental study, *Am. J. Sci.*, 261, 382-396, 1963.
- Cetlin, B. B., and S. C. Abrahams, Automatic diffractometer programs, *Acta Cryst.*, 16, 943-946, 1963.
- Chao, E. C. T., E. M. Shoemaker, and B. M. Madsen, First natural occurrence of coesite, *Science*, 132, 220-222, 1960.
- Chayes, F., A petrographic distinction between Cenozoic volcanics in and around the open oceans, *J. Geophys. Res.*, 69, 1573-1588, 1964.
- Chayes, F., Classification in a ternary diagram by means of discriminant functions, *Am. Mineralogist*, in press, 1965a.
- Chayes, F., Titania and alumina content of oceanic and circumoceanic basalt, *Mineral. Mag.*, 34, 126-131, 1965b.
- Chayes, F., and D. Velde, Distinguishing basaltic lavas of circumoceanic and oceanic-island type by means of discriminant functions, *Am. J. Sci.*, 263, 206-222, 1965.
- Cheriton, C. G., Disorder in chalcopyrite, Ph.D. thesis, Harvard University, 1952.
- Chinner, G. A., and J. F. Schairer, The join  $\text{Ca}_3\text{Al}_2\text{Si}_3\text{O}_{12}$ - $\text{Mg}_3\text{Al}_2\text{Si}_3\text{O}_{12}$  and its bearing on the system  $\text{CaO}$ - $\text{MgO}$ - $\text{Al}_2\text{O}_3$ - $\text{SiO}_2$  at atmospheric pressure, *Am. J. Sci.*, 260, 611-634, 1962.
- Clark, S. P., and A. E. Ringwood, Density distribution and constitution of the mantle, *Rev. Geophys.*, 2, 35-88, 1964.
- Clarke, F. W., Analyses of rocks from the laboratory of the U.S. Geological Survey, *U.S. Geol. Surv. Bull.* 168, 308 pp., 1900.
- Cohen-Addad, Cl., P. Ducros, A. Durif, E. F. Bertaut, and A. Delapalme, Détermination de la position des atomes d'hydrogène dans l'hydrogrenat  $\text{Al}_2\text{O}_3$ ,  $\text{CaO}$ ,  $6\text{H}_2\text{O}$  par résonance magnétique nucléaire et diffraction neutronique, *J. Phys. Radium*, 25, 478-483, 656, 1964.
- Coleman, A. P., The Sudbury nickel field, *Ann. Rept. Ontario Dept. Mines*, 14, Part 3, 1905.
- Coleman, A. P., E. S. Moore, and T. L. Walker, The Sudbury nickel intrusive, *Univ. Toronto Studies, Geol. Ser.*, 28, 1-54, 1929.
- Coleman, R. G., D. E. Lee, L. B. Beatty, and W. W. Brannoch, Eclogites and eclogites: Their differences and similarities, *Bull. Geol. Soc. Am.*, 76, 483-508, 1965.
- Collins, W. H., Life history of the Sudbury nickel irruptive (IV), *Trans. Roy. Soc. Canada, Sect. IV*, 31, 15-43, 1937.
- Cooper, J. E., Fatty acids in recent and ancient sediments and petroleum reservoir waters, *Nature*, 193, 744-746, 1962.
- Cooper, J. E., A postulated role of fatty acids in petroleum formation, *Geochim. Cosmochim. Acta*, 27, 1113-1127, 1963.
- Cross, W., Lavas of Hawaii and their relations, *U.S. Geol. Surv. Prof. Paper* 88, 97 pp., 1915.
- Cross, W., J. P. Iddings, L. V. Pirsson, and H. S. Washington, *Quantitative Classification of Igneous Rocks*, University of Chicago Press, 1903.
- Crowder, D. F., Granitization, migmatization, and fusion in the northern Entiat Mountains, Washington, *Bull. Geol. Soc. Am.*, 70, 827-828, 1959.
- Dachille, F., and R. Roy, Opposed-anvil pressure devices, in *Modern Very High Pressure*



- Techniques*, edited by R. H. Wentorf, Jr., Butterworths, Washington, D.C., pp. 163-180, 1962.
- Dana, E. S., *The System of Mineralogy*, John Wiley & Sons, New York, 6th ed., 1892.
- Day, A. L., and E. T. Allen, The isomorphism and thermal properties of the feldspars, *Carnegie Inst. Wash. Publ.* 31, 95 pp., 1905.
- Dickson, C. W., The ore deposits of Sudbury, *Trans. Am. Inst. Mining Engrs.*, 34, 1-67, 1904.
- Dickson, F. W., and G. Tunell, The stability relations of cinnabar and metacinnabar, *Am. Mineralogist*, 44, 471-487, 1959.
- Dodd, R. T., Jr., and W. R. Van Schmus, Significance of dispersed mineral compositions in chondrites (abstract), *Trans. Am. Geophys. Union*, 46, 122, 1965.
- Donnay, J. D. H., and G. Donnay, Four theorems in crystal morphology (abstract), *Geol. Soc. Am. Spec. Paper* 82, 48, 1965.
- Donnay, J. D. H., and D. Harker, Généralisation de la Loi de Bravais, *Compt. Rend.*, 204, 274-276, 1937.
- Dorough, G. D., J. R. Miller, and F. M. Hunnekens, Spectra of the metallo-derivatives of  $\alpha, \beta, \gamma, \delta$ -tetraphenylporphine, *J. Am. Chem. Soc.*, 73, 4315-4320, 1951.
- Drever, H. I., and R. Johnston, The petrology of picritic rocks in minor intrusions—A Hebridean group, *Trans. Roy. Soc. Edinburgh*, 63, 459-500, 1958.
- Engel, A. E. J., and C. G. Engel, Composition of basalts from the mid-Atlantic ridge, *Science*, 144, 1330-1333, 1964a.
- Engel, A. E. J., and C. G. Engel, Igneous rocks of the East Pacific Rise, *Science*, 146, 477-485, 1964b.
- Eugster, H. P., and D. R. Wones, Stability relations of the ferruginous biotite, annite, *J. Petrol.*, 3, 82-125, 1962.
- Ferguson, J. B., and A. F. Buddington, The binary system akermanite-gehlenite, *Am. J. Sci.*, 50, 131-140, 1920.
- Fesenko, E. G., I. M. Rumanova, and N. V. Belov, The crystalline structure of zoisite, *Dokl. Akad. Nauk SSSR*, 102, 275-278, 1955.
- Fiske, R. S., C. A. Hopson, and A. C. Waters, Geology of Mt. Rainier National Park, Washington, *U.S. Geol. Surv. Prof. Paper* 444, 93 pp., 1963.
- Fleischer, E. B., C. K. Miller, and L. E. Webb, Crystal and molecular structures of some metal tetraphenylporphines, *J. Am. Chem. Soc.*, 86, 2342-2347, 1964.
- Foster, W. R., High-temperature X-ray diffraction study of the polymorphism of  $\text{MgSiO}_3$ , *J. Am. Ceram. Soc.*, 34, 255-259, 1951.
- Frechen, J., Die Genese der Olivinausscheidungen von Dreisen Weicher (Eifel) und Finkenberg (Siebengebirge), *Neues Jahrb. Mineral. Geol. Palaeontol.*, 79, Abt. A, 317-406, 1948.
- French, B. M., and H. P. Eugster, Stability of siderite,  $\text{FeCO}_3$  (abstract), *Geol. Soc. Am. Spec. Paper* 73, 155-156, 1962.
- French, B. M., and H. P. Eugster, Experimental control of oxygen fugacities by graphite-gas equilibriums, *J. Geophys. Res.* 70, 1529-1539, 1965.
- Fudali, R. F., Oxygen fugacities of basaltic and andesitic magmas, *Geochim. Cosmochim. Acta*, 29, 1063-1075, 1965.
- Glaessner, M. F., Pre-Cambrian fossils, *Biol. Rev.*, 37, 467-494, 1962.
- Goldsmith, J. R., Some melilite solid solutions, *J. Geol.*, 56, 437-447, 1948.
- Gossner, B., and H. Strunz, Über strukturelle Beziehungen zwischen Phosphaten (Triphylin) und Silikaten (Olivin) und über die chemische Zusammensetzung von Ardenit, *Z. Krist.*, 83, 415-421, 1932.
- Green, D. H., The petrogenesis of the high-temperature intrusion in the Lizard area, Cornwall, *J. Petrol.*, 5, 134-188, 1964.
- Green, D. H., and A. E. Ringwood, Fractionation of basalt magmas at high pressures, *Nature*, 201, 1276-1279, 1964.
- Greig, J. W., and T. F. W. Barth, The system  $\text{Na}_2\text{O} \cdot \text{Al}_2\text{O}_3 \cdot 2\text{SiO}_2$  (nephelite, carnegieite)- $\text{Na}_2\text{O} \cdot \text{Al}_2\text{O}_3 \cdot 6\text{SiO}_2$  (albite), *Am. J. Sci.*, 35-A, 93-112, 1938.
- Grisafe, D. A., and W. B. White, Phase relations in the system  $\text{PbO}-\text{CO}_2$  and the decomposition of cerussite, *Am. Mineralogist*, 49, 1184-1198, 1964.
- Guggenheim, E. A., *Mixtures*, Clarendon Press, Oxford, 1952.
- Gutenberg, B., Untersuchungen zur Frage, bis zu welcher Tiefe die Erde kristallin ist, *Z. Geophysik*, 2, 24-29, 1926.
- Gutenberg, B., On the layer of relatively low wave velocity at a depth of about 80 kilometers, *Bull. Seis. Soc. Am.*, 38, 121-148, 1948.
- Hamilton, P. L., Amino acids on hands, *Nature*, 205, 284-285, 1965.
- Hamor, T. A., W. S. Caughey, and J. L. Hoard, The crystal and molecular structure of nickel (II) 2,4-diacetyldeuteroporphyrin-IX dimethyl ester, *J. Am. Chem. Soc.*, 87, 2305-2312, 1965.
- Hare, P. E., Amino acids in the proteins from aragonite and calcite in the shells of *Mytilus californianus*, *Science*, 139, 216-217, 1963.
- Harker, A., *Petrology for Students*, Cambridge University Press, 8th ed. rev., 1954.
- Hawley, J. E., The Sudbury ores: Their mineralogy and origin, *Can. Mineralogist*, 7, 1-207, 1962.
- Hedberg, H. D., Geological aspects of the origin of petroleum, *Bull. Am. Assoc. Petrol. Geologists*, 48, 1755-1803, 1964.
- Heinrich, E. W., *Microscopic Petrography*, McGraw-Hill Book Co., New York, 1956.
- Herrin, E., and J. Taggart, Regional variations



- in *Pn* velocity and their effect on the location of epicenters, *Bull. Seis. Soc. Am.*, 52, 1037-1046, 1962.
- Hess, H. H., Serpentine, orogeny, and epeirogeny, *Geol. Soc. Am. Spec. Paper* 62, 391-408, 1955.
- Hess, H. H., Stillwater igneous complex, Montana, *Geol. Soc. Am. Mem.* 80, 230 pp., 1960.
- Hoard, J. L., and J. D. Stroupe, Chapter 2, pp. 13-35, in *Spectroscopic Properties of Uranium Compounds*, by G. H. Dieke and A. B. S. Duncan, McGraw-Hill Book Co., New York, 1949.
- Holmes, A., *The Nomenclature of Petrology*, T. Murby and Co., London, 1920.
- Hopson, C. A., Geology of the crystalline rocks, in *The Geology of Howard and Montgomery Counties*, Maryland Geological Survey, 1964.
- Howe, E., Petrographical notes on the Sudbury nickel deposits, *Econ. Geol.*, 9, 505-522, 1914.
- Iddings, J. P., *Igneous Rocks*, Vol. 1, John Wiley & Sons, New York, 1907.
- Iddings, J. P., *Igneous Rocks*, Vol. 2, John Wiley & Sons, New York, 1913.
- Ito, J., N. Morimoto, and R. Sadanaga, On the structure of epidote, *Acta Cryst.*, 7, 53-59, 1954.
- Jäger, E., Rb-Sr age determinations on micas and total rocks from the Alps, *J. Geophys. Res.*, 67, 5293-5306, 1962.
- Jambor, J. L., and C. H. Smith, Olivine composition determination with small-diameter X-ray powder cameras, *Mineral. Mag.*, 33, 730-748, 1964.
- Johannsen, A., *A Descriptive Petrography of the Igneous Rocks*, Vol. 3, University of Chicago Press, 1937.
- Joplin, G. A., Chemical analyses of Australian rocks; I, Igneous and metamorphic, *Bull. Bur. Min. Resources (Canberra)*, 65, 446 pp., 1963.
- Kennedy, W. Q., On composite lava flows, *Geol. Mag.*, 68, 166-181, 1931.
- Kitahara, S., and G. C. Kennedy, The quartz-coesite transition, *J. Geophys. Res.*, 69, 5395-5400, 1964.
- Knight, C. W., *Report of the Royal Ontario Nickel Commission*, Toronto, 105-211, 1917.
- Knopf, A., and D. E. Lee, Fassaite from near Helena, Montana, *Am. Mineralogist*, 42, 73-77, 1957.
- Kubaschewski, O., and E. L. Evans, *Metallurgical Thermochemistry*, Pergamon Press, New York, 3rd ed., 1958.
- Kulaszewski, C., Über die Kristallstruktur des Turmalins, *Abhandl. Math.-Physik Kl. Säch. Akad. Wiss.*, 38, 81-117, 1921.
- Kullerud, G., and H. S. Yoder, Jr., Pyrite stability relations in the Fe-S system, *Econ. Geol.*, 54, 533-572, 1959.
- Kullerud, G., and R. A. Yund, The Ni-S system and related minerals, *J. Petrol.*, 3, 126-175, 1962.
- Kuno, H., Discussion of paper by J. F. Lovering, 'The nature of the Mohorovičić discontinuity,' *J. Geophys. Res.*, 64, 1071-1072, 1959a.
- Kuno, H., Origin of Cenozoic petrographic province of Japan and surrounding areas, *Bull. Volcanol.*, 2nd ser., 20, 37-76, 1959b.
- Kuno, H., Aluminian augite and bronzite in alkali olivine basalt from Taka-sima, North Kyusyu, Japan, *Advan. Frontiers Geol. Geophys.*, 1964, 205-220, 1965.
- Kuno, H., K. Yamasaki, C. Iida, and K. Nagashima, Differentiation of Hawaiian magmas, *Japan. J. Geol. Geography*, 28, 179-218, 1957.
- Kushiro, I., and H. Kuno, Origin of primary basaltic magmas and classification of basaltic rocks, *J. Petrol.*, 4, 75-89, 1963.
- Lacroix, A., Les roches basiques accompagnant les lherzolites et les ophites des Pyrénées, *8th Intern. Geol. Congr. Rept., Paris*, 806-836, 1900.
- Lacroix, A., Roches éruptives de l'Indochine, *Bull. Serv. Géol. Indochine*, 20, no. 3, 1933.
- Liebau, Friedrich, Über die Kristallstruktur des Pyroxmangits (Mn,Fe,Ca,Mg)SiO<sub>3</sub>, *Acta Cryst.*, 12, 177-181, 1959.
- Liebau, Friedrich, Die Systematik der Silikate, *Naturwissenschaften*, 49, 481-491, 1962.
- Lowenstam, H. A., Biologic problems relating to the composition and diagenesis of sediments, in *The Earth Sciences*, edited by Thomas W. Donnelly, pp. 137-195, University of Chicago Press, 1963.
- Luth, W. C., R. H. Jahns, and O. F. Tuttle, The granite system at pressures of 4 to 10 kilobars, *J. Geophys. Res.*, 69, 759-773, 1964.
- Macdonald, G. A., and T. Katsura, Chemical composition of Hawaiian lavas, *J. Petrol.*, 5, 82-133, 1964.
- MacDonald, G. J. F., Quartz-coesite stability relations at high temperatures and pressures, *Am. J. Sci.*, 254, 713-721, 1956.
- MacDonald, G. J. F., and N. F. Ness, A study of the free oscillations of the earth, *J. Geophys. Res.*, 66, 1865-1911, 1961.
- Malčić, S. S., and L. M. Manojlović, Crystal structure of cesium and uranyl nitrate, *Bull. Inst. Nucl. Sci. "Boris Kidrich" (Belgrade)*, 11, 135-139, 1961.
- Mason, B., *Meteorites*, John Wiley & Sons, New York, 1962.
- Massazza, F., and E. Sirchia, Il sistema MgO-SiO<sub>2</sub>-TiO<sub>2</sub>, *Chim. Ind. (Milan)*, 40, 460-467, 1958.
- Merwin, H. E., and R. H. Lombard, The system Cu-Fe-S, *Econ. Geol.*, 32, Supplement, 203-284, 1937.
- Miyashiro, A., Thermodynamics of reactions of rock-forming minerals with silica; Part I, Free energy of reactions and their petrogenetic significance, *Japan. J. Geol. Geography*, 31, 71-78, 1960.
- Moore, J. G., Petrology of deep-sea basalt near Hawaii, *Am. J. Sci.*, 263, 40-52, 1965.



- Moorhouse, W. W., *The Study of Rocks in Thin Section*, Harper and Brothers, New York, 1959.
- Morey, G. W., Relation of crystallization to the water content and vapor pressure of water in a cooling magma, *J. Geol.*, 32, 291-295, 1922.
- Muir, I. D., and C. E. Tilley, Contributions to the petrology of Hawaiian basalts; 1, The picrite-basalts of Kilauea, *Am. J. Sci.*, 255, 241-253, 1957.
- Muir, I. D., and C. E. Tilley, Mugearites and their place in alkali igneous rock series, *J. Geol.*, 69, 186-203, 1961.
- Murata, K. J., and D. H. Richter, 1959-60 eruption of Kilauea volcano, Hawaii, *U.S. Geol. Surv. Prof. Paper*, in press, 1965.
- Nicholls, G. D., A. J. Nawalk, and E. E. Hays, The nature and composition of rock samples dredged from the mid-Atlantic ridge between 22°N and 52°N, *Marine Geol.*, 1, 333-343, 1964.
- Niggli, P., *Rocks and Mineral Deposits*, W. H. Freeman and Co., San Francisco, English ed., 1954.
- Nockolds, S. R., Average composition of some igneous rocks, *Bull. Geol. Soc. Am.*, 65, 1007-1032, 1954.
- O'Daniel, H., Ein neues Tarnowitzitvorkommen von Tsumeb-Otavi und die Frage der wechselseitigen isomorphen Vertretung von Ca und Pb, *Z. Krist.*, 74, 333-362, 1930.
- Oden, S., and von Hofsten, B., Detection of fingerprints by the ninhydrin reaction, *Nature*, 173, 449-450, 1954.
- O'Hara, M. J., Primary magmas and the origin of basalts, *Scottish J. Geol.*, 1, 1-40, 1965.
- O'Hara, M. J., and E. L. P. Mercy, Petrology and petrogenesis of some garnetiferous peridotites, *Trans. Roy. Soc. Edinburgh*, 65[12], 251-314, 1963.
- Oosterom, M. G., The ultramafites and layered gabbro sequences in the granulite facies rocks on Stjernöy, *Leidse Geol. Mededel.*, 28, 177-296, 1963.
- Osborn, E. F., The system  $\text{CaSiO}_3$ -diopside-anorthite, *Am. J. Sci.*, 240, 751-788, 1942.
- Osborn, E. F., and J. F. Schairer, The ternary system pseudowollastonite-akermanite-gehlenite, *Am. J. Sci.*, 239, 715-763, 1941.
- Osborn, E. F., and D. B. Tait, The system diopside-forsterite-anorthite, *Am. J. Sci.*, Bowen Vol., 413-433, 1952.
- Osborne, F. F., Coronite, labradorite anorthosite, and dykes of andesine anorthosite, New Glasgow, P. Q., *Trans. Roy. Soc. Canada, Sect. IV*, 43, 85-112, 1949.
- Ostic, R. G., Isotopic investigation of conformable lead deposits, Ph.D. thesis, University of British Columbia, 1963.
- Oxburgh, E. R., Petrological evidence for the presence of amphibole in the upper mantle and its petrogenic and geophysical implications, *Geol. Mag.*, 101, 1-19, 1964.
- Pabst, A., The crystal structure of plazolite, *Am. Mineralogist*, 22, 861-868, 1937.
- Parrish, W., Results of the I.U.Cr. precision lattice-parameter project, *Acta Cryst.*, 13, 838-850, 1960.
- Phemister, T. C., Igneous rocks of Sudbury and their relation to the ore deposits, *Ann. Rept. Ontario Dept. Mines*, 34, Part 8, 1925.
- Press, F., Some implications on mantle and crustal structure from G waves and Love waves, *J. Geophys. Res.*, 64, 565-568, 1959.
- Prewitt, C. T., and D. R. Peacor, Crystal chemistry of the pyroxenes and pyroxenoids, *Am. Mineralogist*, 49, 1527-1542, 1964.
- Richards, A. G., *The Integument of Arthropods*, University of Minnesota Press, Minneapolis, 1951.
- Rittmann, A., *Volcanoes and their Activity* (translated by E. A. Vincent), John Wiley & Sons, New York, 1962.
- Robertson, E. C., F. Birch, and G. J. F. MacDonald, Experimental determination of jadeite stability relations to 25,000 bars, *Am. J. Sci.*, 255, 115-137, 1957.
- Robinson, W. E., J. J. Cummins, and K. E. Stanfield, Constitution of organic acids prepared from Colorado oil shale, *Ind. Eng. Chem.*, 48, 1134-1138, 1956.
- Robinson, W. E., H. H. Heady, and A. B. Hubbard, Alkaline permanganate oxidation of oil shale kerogen, *Ind. Eng. Chem.*, 45, 788-791, 1953.
- Rogers, A. F., *Introduction to the Study of Minerals*, McGraw-Hill Book Co., New York, 3rd ed., 1937.
- Rosenbusch, H., and A. Osann, *Elemente der Gesteinslehre*, Schweitzerbartsche Verlag, Stuttgart, 1923.
- Ross, C. S., M. D. Foster, and A. T. Myers, Origin of dunites and olivine-rich inclusions in basaltic rocks, *Am. Mineralogist*, 39, 693-737, 1954.
- Roy, R. F., Heat flow measurements in the United States, Ph.D. thesis, Harvard University, 1963.
- Rubey, W. W., Geologic history of sea water, *Bull. Geol. Soc. Am.*, 62, 1111-1147, 1951.
- Russell, R. D., and R. M. Farquhar, *Lead Isotopes in Geology*, Interscience, New York, 1960.
- Sachs, A., Über die Beziehungen des Rubidiums, etc., *Z. Krist.*, 38, 496-498, 1904.
- Sakata, Y., Unit-cell dimensions of synthetic aluminum diopsides, *Japan. J. Geol. Geography*, 28, 161-168, 1957.
- Schairer, J. F., and N. L. Bowen, Melting relations in the systems  $\text{Na}_2\text{O}-\text{Al}_2\text{O}_3-\text{SiO}_2$  and  $\text{K}_2\text{O}-\text{Al}_2\text{O}_3-\text{SiO}_2$ , *Am. J. Sci.*, 245, 193-204, 1947.
- Schairer, J. F., and H. S. Yoder, Jr., The nature of residual liquids from crystallization, with



- data on the system nepheline-diopside-silica, *Am. J. Sci.*, 258-A, 273-283, 1960.
- Sclar, C. B., L. C. Carrison, and C. M. Schwartz, High-pressure stability field of clinoenstatite and the orthoenstatite-clinoenstatite transition (abstract), *Trans. Am. Geophys. Union*, 45, 121, 1964.
- Shand, S. J., *Eruptive Rocks*, T. Murby and Co., London, 2nd ed. rev., 1943.
- Shand, S. J., Coronas and coronites, *Bull. Geol. Soc. Am.*, 56, 247-266, 1945.
- Shrock, R. R., and W. H. Twenhofel, *Principles of Invertebrate Paleontology*, McGraw-Hill Book Co., New York, 2nd ed., 1953.
- Silvers, S., and A. Tulinsky, The triclinic crystal form of  $\alpha, \beta, \gamma, \delta$ -tetraphenylporphine, *J. Am. Chem. Soc.*, 86, 927, 1964.
- Slemmons, D. B., Determination of volcanic and plutonic plagioclases using a three- or four-axis universal stage, *Geol. Soc. Am. Spec. Paper* 69, 64 pp., 1962.
- Smith, G. S., and L. E. Alexander, Refinement of the atomic parameters of  $\alpha$ -quartz, *Acta Cryst.*, 16, 462-471, 1963.
- Smith, J. R., and H. S. Yoder, Jr., Variations in X-ray powder diffraction patterns of plagioclase feldspars, *Am. Mineralogist*, 41, 632-647, 1956.
- Speers, E. C., The age relations and origin of the Sudbury breccia, Ph.D. thesis, Queen's University, 1956.
- Stanton, R. L., and R. D. Russell, Anomalous leads and the emplacement of lead sulfide ores, *Econ. Geol.*, 54, 588-607, 1959.
- Steiger, R. H., Petrographie und Geologie des südlichen Gotthardmassivs zwischen St. Gotthard- und Lukmanierpass, *Schweiz. Mineral. Petrol. Mitt.*, 42, 381-577, 1962.
- Stephanović, S. P., Sur quelques minéraux de la Serbie, *Ann. Géol. Pénins. Balkan. Beograd*, 7, 85-96, 1922; *Mineral. Abstracts*, 2, 116, 1923.
- Sun, Ming-Shan, and R. H. Weber, Ardenite from the Grants uranium district, New Mexico (abstract), *Am. Mineralogist*, 40, 338, 1955.
- Tilley, C. E., Density, refractivity, and composition relations of some natural glasses, *Mineral. Mag.*, 19, 275-294, 1922.
- Tilley, C. E., Aluminous pyroxenes in metamorphosed limestones, *Geol. Mag.*, 75, 81-86, 1938.
- Tilley, C. E., Differentiation of Hawaiian basalts: Some variants in lava suites of dated Kilauean eruptions, *J. Petrol.*, 1, 47-55, 1960a.
- Tilley, C. E., Kilauea magma 1959-60, *Geol. Mag.*, 97, 494-497, 1960b.
- Tilley, C. E., and I. D. Muir, The Hebridean Plateau magma type, *Trans. Edinburgh Geol. Soc.*, 19, 208-215, 1962.
- Tilley, C. E., and I. D. Muir, Intermediate members of the oceanic basalt-trachyte association, *Geol. Fören. Stockholm Förh.*, 85, 436-444, 1964.
- Tilton, G. R., G. W. Wetherill, and G. L. Davis, Mineral ages from the Wichita and Arbuckle Mountains, Oklahoma, and the St. Francis Mountains, Missouri, *J. Geophys. Res.*, 67, 4011-4019, 1962.
- Traube, H., Zinkhaltiger Aragonit von Tarnowitz in Oberschlesien, *Z. Krist.*, 15, 410-412, 1889.
- Tyrrell, G. W., *The Principles of Petrology*, E. P. Dutton, New York, 2nd ed., 1929.
- Van Hook, H. J., The ternary system  $\text{Ag}_2\text{S}-\text{Bi}_2\text{S}_3-\text{PbS}$ , Ph.D. thesis, Pennsylvania State University, 1959; see also *Econ. Geol.*, 55, 759-788, 1960.
- Verhoogen, J., Mechanics of ash formation, *Am. J. Sci.*, 249, 729-739, 1951.
- Wahlstrom, E. E., *Introduction to Theoretical Igneous Petrology*, John Wiley & Sons, New York, 1950.
- Walker, F., Differentiation of the Palisade diabase, New Jersey, *Bull. Geol. Soc. Am.*, 51, 1059-1106, 1940.
- Walter, L. S., Coesite discovered in tektites, *Science*, 147, 1029-1032, 1965.
- Wandke, A., and R. Hoffman, A study of the Sudbury ore deposits, *Econ. Geol.*, 19, 169-204, 1924.
- Washington, H. S., Petrology of the Hawaiian Islands, III, Kilauea and general petrology of Hawaii, *Am. J. Sci.*, 6, 338-367, 1923.
- Weidner, J. R., and O. F. Tuttle, Stability of siderite,  $\text{FeCO}_3$  (abstract), *Geol. Soc. Am. Spec. Paper* 82, 220, 1965.
- Williams, H., F. J. Turner, and C. M. Gilbert, *Petrography*, W. H. Freeman and Co., San Francisco, 1954.
- Wilshire, H. G., and R. A. Binns, Basic and ultrabasic xenoliths from volcanic rocks of New South Wales, *J. Petrol.*, 2, 185-208, 1961.
- Wilson, H. D. B., Structure of lopoliths, *Bull. Geol. Soc. Am.*, 67, 289-300, 1956.
- Winchell, H., Honolulu series, Oahu, Hawaii, *Bull. Geol. Soc. Am.*, 58, 1-48, 1947.
- Wolff, F. von, *Die Eruptivgesteine*, R. A. Lang Verlag, Pössneck, 1951.
- Yoder, H. S., Jr., The  $\text{MgO}-\text{Al}_2\text{O}_3-\text{SiO}_2-\text{H}_2\text{O}$  system and related metamorphic facies, *Am. J. Sci.*, Bowen Vol., 569-627, 1952.
- Yoder, H. S., Jr., and C. E. Tilley, Origin of basalt magmas: An experimental study of natural and synthetic rock systems, *J. Petrol.*, 3, 342-532, 1962.
- Yoder, H. S., Jr., and C. E. Weir, Change of free energy with pressure of the reaction nepheline + albite = 2 jadeite, *Am. J. Sci.*, 249, 683-694, 1951.
- Young, R. A., and B. Post, Electron density and thermal effects in alpha quartz, *Acta Cryst.*, 15, 337-346, 1962.
- Zachariasen, W. H., and H. A. Plettinger, Extinction in quartz, *Acta Cryst.*, 18, 710-714, 1965.



The summary of published work below briefly describes the papers published in scientific journals during the report year. In addition, the following papers have been prepared for publication: L. T. Aldrich, G. L. Davis, and H. L. James, "Ages of minerals from metamorphic and igneous rocks"; Charles W. Burnham, "Computation of absorption corrections, and the significance of end effect"; F. Chayes, "Classification in a ternary diagram by means of discriminant functions"; F. Chayes, "Alkaline and subalka-

line basalts"; J. J. Fawcett, "Alteration products of olivine and pyroxene in basalt lavas from the Isle of Mull"; G. Kullerud, "Covellite stability relations in the Cu-S system"; G. Kullerud, "Geologic thermometry"; N. Morimoto and G. Kullerud, "Polymorphism on the  $\text{Cu}_5\text{FeS}_4\text{-Cu}_9\text{S}_6$  join"; A. E. Ringwood, "Phases of the mantle"; B. Velde, "Phengite micas: Synthesis, stability, and natural occurrence"; E. G. Zies, "A new analysis of cossyrite from the island of Pantelleria."

## SUMMARY OF PUBLISHED WORK

- (1407) Fatty acids in sedimentary rocks. P. H. Abelson, T. C. Hoering, and P. L. Parker. In *Advances in Organic Geochemistry, Proceedings of the International Meeting in Milan, 1962*, pp. 169-174, Pergamon Press, New York, 1963.

Fatty acids have been extracted and identified from recent sediments and rocks as old as the Cambrian Alun shale of Sweden. The principal compounds found were C-14, C-16, and C-18 saturated acids. The amounts extractable from old rocks are in the range of  $2 \times 10^{-4}$  to  $10^{-5}$  g/g of organic matter.

- (1419) The system Mg-cordierite- $\text{H}_2\text{O}$  and related rocks. W. Schreyer and H. S. Yoder, Jr. *Neues Jahrb. Mineral., Abhandl.*, 101, 271-342, 1964.

The system  $2\text{MgO} \cdot 2\text{Al}_2\text{O}_3 \cdot 5\text{SiO}_2\text{-H}_2\text{O}$  was investigated at water pressures up to 10,000 bars and temperatures between 350°C and 1,300°C for the purpose of determining the stability limits, polymorphism, and water content of Mg-cordierite. At water pressures between 1,000 and 5,000 bars and temperatures of 475°C-550°C cordierite breaks down to chlorite + pyrophyllite + aluminosilicate; at water pressures about 5,000 bars and temperatures of 550°C-690°C, it breaks down to chlorite + quartz and metastable quartz + corundum (= aluminosilicate). At lower temperatures and all water pressures chlorite + pyrophyllite or montmorillonite-bearing assemblages are stable, respectively. At 5,000 bars, 350°C-450°C, the assemblage chlorite + montmorillonite + quartz was obtained. In the presence of water cordierite melts in-

congruently over a temperature range of as much as 50°C. Complete melting of cordierite in the presence of excess water vapor was obtained at 2,000 bars and 1,275°C, 5,000 bars and 1,110°C, and 10,000 bars and 970°C. Mullite, spinel, sapphirine, and corundum were among the incongruent melting products, the number and kinds of phases changing with pressure. At 5,000 and 10,000 bars the cordierite composition has a liquidus above 1,300°C and the first phase to crystallize is most likely corundum. Indirect evidence suggests that the cordierite field of stability is terminated at water pressures slightly higher than 10,000 bars through subsolidus breakdown into assemblages including talc, gedrite, aluminous enstatite, sillimanite, and quartz. Experimental determination of cordierite stability in the water-deficient region at low temperatures was found to be impracticable owing to the sluggishness of reactions.

At all water pressures investigated orthorhombic "low"-cordierite was found to be the stable polymorph up to the temperatures of incongruent melting. Hexagonal high-cordierite was obtained, however, as the first form to crystallize metastably. Its gradual transition to "low"-cordierite is accompanied by an increase of the optical axial angle  $2V_x$  and by development of the typical sector twinning of the cordierite crystals. The rate of this transition varies with temperature and water pressure.

Depending on the conditions of synthesis, the cordierites were found to contain variable amounts of water up to 2.75 weight per cent. In general the water content increases with



increasing water pressure and decreasing temperature; equilibrium water contents could not always be determined, however, because of insufficiently rapid quenching. There is a positive linear relation between water content and the mean refractive index of pure Mg-cordierites of identical structural states. Upon heating at atmospheric pressure, hydrous cordierites show a gradual water loss between 200°C and 700°C. Infrared absorption data, phase relations, and calculations of fictive densities, as well as of fictive mean indices of refraction, indicate that synthetic hydrous Mg-cordierites contain only absorbed molecular water, probably situated in the open channels of the cordierite structure, and that no substitutional water is present in the form of OH<sup>-</sup> groups.

Cordierite is a low-pressure mineral, unstable under the conditions below the continental Mohorovičić discontinuity. Within the earth's crust relatively high temperatures are required for the formation of cordierite in rocks of the requisite bulk composition; cordierite occurs in igneous rocks and is an important mineral of contact metamorphism. Whether or not cordierite may form in high-grade regional metamorphism under excess water conditions depends largely on the geothermal gradients prevailing within the particular orogenic belt. The influence of shearing stress on cordierite stability is considered equivalent to an increase of the mean pressure exerted on the crystal during deformation. Depending on the pressures and temperatures prevailing at a given depth under normal static conditions, therefore, cordierite may or may not become unstable when the enclosing rock is being deformed. The structural state of cordierite cannot be used in geothermometry but may act as a geologic timer for the crystallization history of the enclosing rock. Unless there is subsequent metastable hydration under low temperatures and pressures, the water content of natural cordierites may yield information about the minimum water pressures and maximum temperatures endured.

- (1426) The biogeochemistry of the stable isotopes of carbon in a marine bay. P. L. Parker. *Geochim. Cosmochim. Acta*, 28, 1155-1164, 1964.

The most abundant biological samples from Redfish Bay, a shallow marine estuary near Port Aransas, Texas, were collected, and  $\delta C^{13}$

for the total carbon, lipide carbon, and protein-carbohydrate carbon was measured. Some member of the community had an isotopic composition corresponding to every unit value of  $\delta C^{13}$  between -6 and -17;  $\delta C^{13}$  was found to be constant for different individuals of the same species to  $\pm 1$  per mil. The pure fatty acids or lipides, or both, were found to be from 0.5 to 15 per mil "lighter" than the total carbon of the organism that contained them. The organic matter of the sediment could have been supplied by the community according to the carbon isotope data. A 5-per-mil diurnal variation in  $\delta C^{13}$  of the inorganic carbon of the seawater of a simple marine community was observed.

- (1429) Studies of solubility in systems containing alkali and water; IV, The field of sodium hydroxide in the system sodium hydroxide-sodium carbonate-water. G. W. Morey and J. S. Burlew. *J. Phys. Chem.*, 68, 1706-1712, 1964.

The solubility of NaOH in H<sub>2</sub>O from 65°C to 300°C was determined by extrapolation along isotherms from the curve of mutual solubility of NaOH and Na<sub>2</sub>CO<sub>3</sub> to zero content of CO<sub>2</sub>. Along the curve for liquid saturated with both NaOH and Na<sub>2</sub>CO<sub>3</sub> the logarithm of the ratio of weight per cent CO<sub>2</sub>/Na<sub>2</sub>O increases linearly with the temperature, and the relation of temperature and H<sub>2</sub>O content is given by  $t = a - x/(b + cx)$ , in which  $x$  is mole fraction H<sub>2</sub>O,  $a = 287.9$ ,  $b = 5.25 \times 10^{-3}$ , and  $c = -7.24 \times 10^{-3}$ . A reversible polymorphic transition in NaOH was found in the neighborhood of 290°C; the melting point of NaOH is  $319^\circ \pm 2^\circ\text{C}$ , and the eutectic NaOH + Na<sub>2</sub>CO<sub>3</sub> is at  $287.9^\circ \pm 0.2^\circ\text{C}$  and 92.10 moles per cent NaOH.

- (1432) Trioctahedral one-layer micas; I, Crystal structure of a synthetic iron mica. G. Donnay, N. Morimoto, H. Takeda, and J. D. H. Donnay. *Acta Cryst.*, 17, 1369-1373, 1964.

The structure of a synthetic iron mica,  $K\text{Fe}_3^{2+}(\text{Fe}^{3+}\text{Si}_3)\text{O}_{10}(\text{OH})_2$ , determined from visually estimated intensities, shows very slight departure from Pabst's idealized biotite structure. The sextuple cell formerly used to describe micas accounts for the observed twinning.



- (1433) Sulfur-rich bornites. R. Brett and R. A. Yund. *Am. Mineralogist*, 49, 1084–1098, 1964.

Natural bornites in general remain homogeneous when heated and have cell edges close to that of stoichiometric  $\text{Cu}_5\text{FeS}_4$  (10.950 Å) before and after heating. Certain bornites exsolve chalcopyrite when heated at temperatures between 75°C and 400°C and have tetragonal cell edges less than 10.950 Å. Their cell edges after heating are close to 10.950 Å. The small initial cell edge and the induced exsolution can be correlated with a greater sulfur-to-metal ratio than is indicated by the stoichiometric formula  $\text{Cu}_5\text{FeS}_4$ . This conclusion is supported by studies on synthetic samples, and heating experiments on natural samples. Exsolution rate studies indicate that natural sulfur-rich bornites were deposited below about 75°C. Such bornites occurring in high-temperature type deposits, therefore, must have formed by later, possibly supergene processes.

- (1434) Isotopic composition of lead and strontium from Ascension and Gough Islands. P. W. Gast, G. R. Tilton, and C. Hedge. *Science*, 145, 1181–1185, 1964.

The isotopic composition of lead and strontium has been determined in a series of rock samples from two islands on the mid-Atlantic ridge. Both interisland and intra-island variations exist in the abundance of radiogenic isotopes of both elements. Lead from basalt of Ascension Island has a  $\text{Pb}^{206}/\text{Pb}^{204}$  ratio of 19.5, whereas the corresponding ratio at Gough Island is only 18.4. The  $\text{Pb}^{206}/\text{Pb}^{204}$  ratios from the two islands do not differ. Conversely, strontium from basalt of Ascension Island is less radiogenic than that from Gough Island basalts. The trachytes of both islands have lead and strontium that are more radiogenic than those found in the basalts. The interisland differences indicate the existence of regional variations in the uranium-lead and rubidium-strontium ratios of the upper-mantle source of these rocks and show that isotopic compositions are a means for investigating chemical heterogeneities in the mantle.

- (1435) Titania and alumina content of oceanic and circumoceanic basalt. F. Chayes. *Mineral. Mag.*, 34, 126–131, 1965.

Most circumoceanic basalts contain less than and most oceanic basalts considerably more than 1.75 per cent of  $\text{TiO}_2$ . The difference of  $\text{TiO}_2$  averages is large enough to require rejection of the hypothesis that circumoceanic basalt results from the assimilation of sial by oceanic basalt.

- (1436) Trioctahedral one-layer micas; II, Prediction of the structure from composition and cell dimensions. G. Donnay, J. D. H. Donnay, and H. Takeda. *Acta Cryst.*, 17, 1374–1381, 1964.

Atomic trimetric coordinates are predicted for 1 *M* trioctahedral micas of known compositions from the following data: tetrahedral and octahedral metal-oxygen distances, taken from the literature;  $b$  and  $d(001) = c \sin \beta$ , determined experimentally;  $a = b/\sqrt{3}$ , assumed. Predictions for ferri-annite and ferriphlogopite compare well with the known structures.

- (1437) Experimental data from the system Cu-Fe-S and their bearing on exsolution textures in ores. R. Brett. *Econ. Geol.*, 59, 1241–1269, 1964.

Controlled cooling experiments performed on solid solutions along the bornite-digenite, bornite-chalcocite, and bornite-chalcopyrite joins of the system Cu-Fe-S showed that exsolution lamellae persist in cooling experiments lasting for as long as seven months and are therefore not exclusively indicative of rapid cooling. Mutual boundary textures, lenses, wedges, and myrmekitic textures were also obtained as products of exsolution. No texture formed was diagnostic of any particular temperature or cooling rate. Quantitative data on the cooling rate or cooling conditions of natural sulfides in the system Cu-Fe-S, therefore, cannot be obtained through the study of exsolution textures.

Because exsolution produces mutual boundary, veining, and replacement textures, the textures observed in mineral pairs in which solid solution occurs are ambiguous as genetic criteria, at least in the system studied. A study of the literature on exsolution suggests that exsolution lamellae may develop and



persist even during slow cooling provided that the solid solution is not concentrated and that the degree of supersaturation is low. Lamellae are stable only as long as the lamellar phase is in crystallographic continuity with the host phase. When no continuity exists the most stable texture is a series of polyhedral grains or spheroids.

- (1438) Feldspar-liquid equilibria in peralkaline liquids—the orthoclase effect. D. K. Bailey and J. F. Schairer. *Am. J. Sci.*, 262, 1198–1206, 1964.

In at least three recently published discussions of pantellerites and related experimental liquids the compositions have been expressed in terms of normative *Q*, *or*, and *ab* and discussed by reference to their resulting positions in the composition plane  $\text{NaAlSi}_3\text{O}_8$ - $\text{KAlSi}_3\text{O}_8$ - $\text{SiO}_2$ . In presenting their experimental results, Carmichael and MacKenzie (1963) express the belief that this projection gives an undistorted view of the relationships. It has the usual drawback of all projections in that a dimension is lost, and this feature leads the proponents themselves to suggest that in each of their joins a “thermal valley” on the feldspar liquidus is a line of unique fractionation and crystallization, although the feldspar compositions lie outside the joins.

But there are at least three intrinsic deficiencies in this norm projection when used to depict peralkaline liquid compositions. First, it exaggerates the potential free silica in the liquid if *ns* forms part of the total composition because the compatibility expression of  $Q + ns$  should be quartz + sodium disilicate. Second, all the  $\text{K}_2\text{O}$  is arbitrarily allotted to *or*, peralkalinity being expressed only in terms of  $\text{Na}_2\text{O}$ , which is thereby lost in the projection; any liquid trends revealed by this mode of projection, therefore, may not be meaningful, inasmuch as the possibility is neglected that some of the  $\text{K}_2\text{O}$  may enter a phase other than feldspar. Such trends may even appear to be contrary to the actual changes taking place in the liquids. The third and most serious deficiency of the norm projection is that, by ignoring part of the  $\text{Na}_2\text{O}$  in peralkaline liquids, it conceals an important relation in the alkali balance between the liquids and their feldspar phenocrysts. When this is examined it is found that, in general, the feldspars separating from an oversaturated peralkaline liquid are

relatively more potassic than the parent liquid. This “orthoclase effect” means that separation of alkali feldspars from a slightly alumina-deficient liquid will fractionate alumina and eventually *potash*, leading to strongly peralkaline and sodic residual liquids.

- (1439) Dating of orogenic phases in the central Alps by K-Ar ages of hornblende. R. H. Steiger. *J. Geophys. Res.*, 69, 5407–5421, 1964.

The Gotthard massif in central Switzerland, part of the autochthonous basement of the Alps, has been metamorphosed during the Alpine orogeny. Structural studies of the metasedimentary hornblende rocks along the southern border reveal the existence of several mineral generations formed at various times and under differing conditions. The sequence of formation can be deduced from their mutual intergrowth and orientation relative to the fabric of the rock. Steiger (1962) concluded that the Alpine orogeny in this region consisted of two distinct tectonic phases separated by a thermal phase. The main tectonic phase was the dragging along of the Gotthard massif by the overlying northward-moving nappes. Most of the Pre-Alpine mineral assemblage was crushed and new minerals were formed that show preferential north-south orientation (direction of the nappe movements). The subsequent thermal metamorphism was linked with anatectic processes in the Lepontine region south of the Gotthard massif. At this time porphyroblastic minerals of random orientation were formed along the southern margin of the massif. A weaker tectonic phase consisting of an east-west contraction caused north-south oriented small folds and wrinklins in mica-rich schists, and produced cross biotites. Hornblende was formed in Pre-Alpine times as well as during both the main tectonic and the thermal phase of the Alpine orogeny. K-Ar ages were determined for 17 hornblendes. North-south oriented hornblendes show ages of 46 m.y. exclusively; random hornblendes yield ages of 23–30 m.y. Partially oriented hornblendes give apparent ages of 23–112 m.y. The hornblende ages are definitely higher than Rb-Sr ages of biotites (16 m.y.) from this region (Jäger, 1962). It is concluded that the north-south oriented hornblendes give a minimum age (46 m.y.) for major nappe movements in this region and that the random hornblendes approximately date the period



(23–30 m.y.) of the anatexis in the Lepontinic region. The Rb-Sr ages of the biotites (16 m.y.) appear to indicate the time of the east-west constriction of the massif and the Lepontinic region. Partially oriented horn-blendes cannot be related to any particular event. They may in part represent relics of Pre-Alpine origin which suffered differential loss of argon during the Alpine metamorphism.

(1440) Annual report of the Director for 1963–1964.

(1441) On distinguishing basaltic lavas of circumoceanic and oceanic-island type by means of discriminant functions. F. Chayes and D. Velde. *Am. J. Sci.*, 263, 206–222, 1965.

The basaltic lavas of the oceanic-island environment are much richer in titania than those found on the landward flanks of the great deeps margining the open oceans. Exceptions to this rule are rare; examination of a large body of data indicates that the efficiency of a classification based solely on  $\text{TiO}_2$  content would be nearly 93 per cent. Neither any other single oxide nor any unweighted combination of oxides other than  $\text{TiO}_2$  approaches the efficiency of  $\text{TiO}_2$ . Extensive discriminant function calculations indicate that (1) weighted linear combinations that include  $\text{TiO}_2$  may be a slight improvement over  $\text{TiO}_2$  alone; (2) any combination of oxides that does not include  $\text{TiO}_2$  is far less effective than  $\text{TiO}_2$  alone.

(1443) Determination of relative volume by sectional analysis. F. Chayes. *Lab. Invest.*, 14, 987–995, 1965.

Estimation of relative volumes of phases present in a solid is usually based on estimates of relative areas made on a plane surface. The measurement technique assures that the estimates of relative areas will be unbiased, but because of inadequate information about distribution of phases through the solid it usually cannot be established a priori that the relative areas are unbiased estimators of relative volumes. The question of bias can—and should—be examined experimentally.

Estimation of areas is usually based on points taken at the intersections of a rectangular grid. The actual “counting” or reproducibility error may be either greater or less

than the binomial variation corresponding to the same mean count, and must be determined experimentally when reliable estimates of reproducibility error are needed. Studies of the effect of grid constants on reproducibility error are essential if sampling schemes are to be chosen that will ensure that variations of substantive interest will not escape detection because of inadequate knowledge or control of error variance. An experimental evaluation of total analytical error is described.

(1444) Lead isotopes in feldspars from selected granitic rocks associated with regional metamorphism. B. R. Doe, G. R. Tilton, and C. A. Hopson. *J. Geophys. Res.*, 70, 1947–1968, 1965.

Paleozoic regional metamorphism of Precambrian gneiss near Baltimore, Maryland, altered the lead-isotope ratios in Precambrian feldspars but did not affect the Rb-Sr ages. This fact indicates that the alteration took place without solution and redeposition or melting of the feldspars. The metamorphism of amphibolite facies (kyanite zone) undoubtedly caused the observed differences in the lead-isotope ratios. The Paleozoic metamorphism was of lower grade to the west and had little effect on the isotopic composition of lead in feldspars of the pyroxene-bearing granitic rocks underlying Shenandoah National Park, Virginia. The feldspars of these rocks contain lead of uniform isotopic composition similar to those of younger granites of nearly equivalent age (about 1,000 m.y.) near Balmat, New York. The isotopic composition of lead in the Paleozoic granitic rocks and pegmatites near Baltimore, Maryland, is less uniform than in the 1,000-m.y.-old rocks at Shenandoah National Park. Age data and geologic relations suggest thermal effects sufficient to lower biotite ages by 50–150 m.y. This heating plus the fact that much older rocks (Precambrian) underlie the region, may account for the lack of a unique “Appalachian lead” through natural contamination. Isotopic uniformity of leads in the feldspars from the Vermilion granite, Minnesota, is comparable to that of the 1,000-m.y.-old granitic rocks at Balmat and Shenandoah National Park. Model lead ages are about 2,900 m.y., or approximately 350 m.y. greater than biotite K-Ar ages. This relation is in contrast to the Paleozoic and younger Precambrian granitic rocks of Maryland, Virginia, and New York,



for which the model lead ages are less than the biotite K-Ar ages.

- (1445) Experimental determination of muscovite polymorph stabilities. B. Velde. *Am. Mineralogist*, 50, 436-449, 1965.

Relative stabilities of the muscovite polymorphs have been determined by hydrothermal experiments with the result that  $2M_1$  was found to be the only stable form. The kaolinite + KOH  $\rightarrow$  muscovite reaction is used to demonstrate this conclusion by means of variations in the experimental parameters of time, temperature, and pressure. A discussion of the significance of this result in application to natural micas is given in the belief that polymorph relations of natural micas will be of significance in determining their genesis.

- (1447) Sulfide-silicate reactions and their bearing on ore formation under magmatic, postmagmatic, and metamorphic condi-

tions. G. Kullerud and H. S. Yoder, Jr. In *Symposium: Problems of Postmagmatic Ore Deposition*, Vol. 2, pp. 327-331, published by the Geological Survey of Czechoslovakia in the Publishing House of the Czechoslovak Academy of Sciences, Prague, 1965.

The reactions between sulfur and certain anhydrous silicates such as fayalite, olivine, hedenbergite, and Fe cordierite, were studied at 2,000 bars and 800°C using collapsible gold tubes as reaction vessels. Depending on the mole ratios of silicate and sulfur, these reactions produce pyrrhotite + magnetite and/or hematite, or pyrrhotite + SO<sub>2</sub> gas in addition to SiO<sub>2</sub> when fayalite is reacted; MgSiO<sub>3</sub> when olivine is used; CaSiO<sub>3</sub> + SiO<sub>2</sub> from hedenbergite; and Mg cordierite + Al<sub>2</sub>SiO<sub>5</sub> from Fe cordierite. These reactions indicate that sulfurization may be an important process in the formation of many magmatic, postmagmatic, and metamorphic ores.

## BIBLIOGRAPHY

- Abelson, P. H., T. C. Hoering, and P. L. Parker, Fatty acids in sedimentary rocks, in *Advances in Organic Geochemistry, Proceedings of the International Meeting in Milan, 1962*, pp. 169-174, Pergamon Press, New York, 1963.
- Bailey, D. K., and J. F. Schairer, Feldspar-liquid equilibria in peralkaline liquids—the orthoclase effect, *Am. J. Sci.*, 262, 1198-1206, 1964.
- Brett, R., Experimental data from the system Cu-Fe-S and their bearing on exsolution textures in ores, *Econ. Geol.*, 59, 1241-1269, 1964.
- Brett, R., and R. A. Yund, Sulfur-rich bornites, *Am. Mineralogist*, 49, 1084-1098, 1964.
- Burlew, J. S., see Morey, G. W.
- Chayes, F., Determination of relative volume by sectional analysis, *Lab. Invest.*, 14, 987-995, 1965.
- Chayes, F., Titania and alumina content of oceanic and circumoceanic basalt, *Mineral. Mag.*, 34, 126-131, 1965.
- Chayes, F., and D. Velde, On distinguishing basaltic lavas of circumoceanic and oceanic-island type by means of discriminant functions, *Am. J. Sci.*, 263, 206-222, 1965.
- Doe, B. R., G. R. Tilton, and C. A. Hopson, Lead isotopes in feldspars from selected granitic rocks associated with regional metamorphism, *J. Geophys. Res.*, 70, 1947-1968, 1965.
- Donnay, G., J. D. H. Donnay, and H. Takeda, Trioctahedral one-layer micas; II, Prediction of the structure from composition and cell dimensions, *Acta Cryst.*, 17, 1374-1381, 1964.
- Donnay, G., N. Morimoto, H. Takeda, and J. D. H. Donnay, Trioctahedral one-layer micas; I, Crystal structure of a synthetic iron mica, *Acta Cryst.*, 17, 1369-1373, 1964.
- Donnay, J. D. H., see Donnay, G.
- Gast, P. W., G. R. Tilton, and C. Hedge, Isotopic composition of lead and strontium from Ascension and Gough Islands, *Science*, 145, 1181-1185, 1964.
- Hedge, C., see Gast, P. W.
- Hoering, T. C., see Abelson, P. H.
- Hopson, C. A., see Doe, B. R.
- Kullerud, G., and H. S. Yoder, Jr., Sulfide-silicate reactions and their bearing on ore formation under magmatic, postmagmatic, and metamorphic conditions, in *Symposium: Problems of Postmagmatic Ore Deposition*, Vol. 2, pp. 327-331, published by the Geological Survey of Czechoslovakia in the Publishing House of the Czechoslovak Academy of Sciences, Prague, 1965.
- Morey, G. W., and J. S. Burlew, Studies of solubility in systems containing alkali and water; IV, The field of sodium hydroxide in the system sodium hydroxide-sodium carbonate-water, *J. Phys. Chem.*, 68, 1706-1712, 1964.
- Morimoto, N., see Donnay, G.
- Parker, P. L., The biogeochemistry of the stable

- isotopes of carbon in a marine bay, *Geochim. Cosmochim. Acta*, 28, 1155-1164, 1964.
- Parker, P. L., *see also* Abelson, P. H.
- Schairer, J. F., *see* Bailey, D. K.
- Schreyer, W., and H. S. Yoder, Jr., The system Mg-cordierite-H<sub>2</sub>O and related rocks, *Neues Jahrb. Mineral., Abhandl.*, 101, 271-342, 1964.
- Steiger, R. H., Dating of orogenic phases in the central Alps by K-Ar ages of hornblende, *J. Geophys. Res.*, 69, 5407-5421, 1964.
- Takeda, H., *see* Donnay, G.
- Tilton, G. R., *see* Doe, B. R.; Gast, P. W.
- Velde, B., Experimental determination of muscovite polymorph stabilities, *Am. Mineralogist*, 50, 436-449, 1965.
- Velde, D., *see* Chayes, F.
- Yoder, H. S., Jr., *see* Kullerud, G.; Schreyer, W.
- Yund, R. A., *see* Brett, R.



## PERSONNEL

*Scientific Staff*

*Director:* P. H. Abelson

*Emeritus Research Associate:* E. G. Zies,  
Chemist

*Physical Chemists:* F. R. Boyd, Jr., T. C.  
Hoering, J. F. Schairer, G. R. Tilton

*Petrologists:* C. W. Burnham, F. Chayes, D. H.  
Lindsley, H. S. Yoder, Jr.

*Geochemists:* G. L. Davis, G. Kullerud

*Organic Geochemist:* P. E. Hare

*Geophysicist:* P. M. Bell<sup>1</sup>

*Physicist:* J. L. England

*Crystallographer:* G. Donnay

*Fellows:* D. K. Bailey, Trinity College, Dublin;<sup>2</sup>  
P. M. Bell, Harvard University;<sup>3</sup> P. R.  
Brett, Harvard University;<sup>4</sup> B. T. C.  
Davis, Princeton University;<sup>5</sup> J. J. Fawcett,  
University of Manchester;<sup>6</sup> G. W. Fisher,  
Johns Hopkins University;<sup>7</sup> E. C. Hansen,  
Yale University; I. Kushiro, Tokyo Uni-  
versity; I. D. MacGregor, Princeton Uni-  
versity;<sup>8</sup> G. Moh, University of Heidel-  
berg;<sup>9</sup> A. J. Naldrett, Queen's University;<sup>1</sup>  
D. Presnall, Pennsylvania State University;  
A. E. Ringwood, Australian National  
University;<sup>10</sup> R. H. Steiger, Institut für  
Kristallographie und Petrographie, Zurich,  
Switzerland; B. Velde, Montana State  
University;<sup>11</sup> D. Velde, University of  
Paris.<sup>12</sup>

*Guest Investigators:* G. Allen, National In-  
stitutes of Health; A. Brown, Queen's  
University; J. R. Craig, Lehigh University;  
B. T. C. Davis, Southwest Center for  
Advanced Studies; J. D. H. Donnay, Johns  
Hopkins University; R. Hart, Yale Univer-  
sity; J. F. Hays, Harvard University;  
Odette James, Stanford University; J.  
Larimer, Lehigh University; I. D. Mac-  
Gregor, Southwest Center for Advanced  
Studies; R. M. Mitterer, Florida State  
University; R. Roy, Harvard University;  
C. E. Tilley, Cambridge University.

*Operating and Maintenance Staff*

*Executive Officer:* A. D. Singer

*Accountant:* E. T. Orozco

*Editor and Librarian:* Miss D. M. Thomas

*Stenographers:* Mrs. J. F. Etheart,<sup>13</sup> Miss A. L.  
Forsey,<sup>14</sup> Mrs. P. S. Garrett,<sup>15</sup> Miss M. E.  
Imlay

*Clerk:* H. J. Lutz

*Mechanic's Helper:* M. Ferguson

*Janitors:* C. Brooks,<sup>16</sup> R. L. Truesdale<sup>17</sup>

*Chief Mechanician:* F. A. Rowe

*Instrument Makers:* C. A. Batten, L. C.  
Garver, J. F. Kocmanek, W. H. Lyons,  
O. R. McClunin, G. E. Speicher

*Mechanic and Carpenter:* E. J. Shipley

*Electrician:* E. C. Huffaker

*Machinist:* J. R. Thomas

*Building Engineer:* R. L. Butler

<sup>1</sup> Appointment from August 1, 1964.

<sup>2</sup> Appointment terminated September 30,  
1964; to return to Trinity College.

<sup>3</sup> Appointment terminated July 31, 1964; to  
accept position on staff of Geophysical Labora-  
tory.

<sup>4</sup> Appointment terminated September 30,  
1964; to accept position with U.S. Geological  
Survey.

<sup>5</sup> Appointment terminated January 31, 1965;  
to accept staff position with Southwest Center for  
Advanced Studies, Dallas, Texas.

<sup>6</sup> Appointment terminated August 31, 1964;  
to accept position as Associate Professor in  
Department of Geological Sciences, University  
of Toronto.

<sup>7</sup> Appointment from December 1, 1964.

<sup>8</sup> Appointment terminated March 31, 1965;  
to accept staff position with Southwest Center for  
Advanced Studies, Dallas, Texas.

<sup>9</sup> Appointment terminated August 31, 1964;  
to return to University of Heidelberg.

<sup>10</sup> Appointment terminated September 30,  
1964; to return to Australian National Univer-  
sity.

<sup>11</sup> Appointment terminated December 31, 1964;  
to continue research at Laboratoire de Pétro-  
graphie at the Sorbonne, University of Paris.

<sup>12</sup> Appointment terminated December 31,  
1964; to return to University of Paris.

<sup>13</sup> Appointment terminated July 6, 1964.

<sup>14</sup> Appointment from July 10 to October 15,  
1964.

<sup>15</sup> Appointment from October 12, 1964.

<sup>16</sup> Appointment from January 6, 1965.

<sup>17</sup> Appointment terminated January 18, 1965.



Plate 1A.  $a$ -axis zero-level precession photograph of ferrosilite III,  $\text{MoK}\alpha$ ,  $\mu = 20^\circ$ , 40 hours;  $b^*$  and  $c^*$  axes are indicated, as is the pseudomonoclinic  $c_m^*$  axis of the diopside-like substructure.





Plate 1B. *b*-axis zero-level precession photograph of ferrosilite III,  $\text{MoK}\alpha$ ,  $\bar{\mu} = 20^\circ$ , 116 hours;  $a^*$  and  $c^*$  axes are indicated.

# *Department of Terrestrial Magnetism*

Merle A. Tuve  
*Director*

*Washington, District of Columbia*

Ellis T. Bolton  
*Associate  
Director*



# Contents

Introduction . . . . .	253
Experimental Geophysics . . . . .	256
The earth's crust . . . . .	256
Explosion studies . . . . .	257
Earthquake studies . . . . .	273
Isotope geology . . . . .	286
Heat flow . . . . .	296
Radio astronomy . . . . .	300
Continuum survey (234 mc/sec) . . . . .	300
Radio hydrogen . . . . .	301
Equipment development . . . . .	306
South American cooperation . . . . .	306
Theoretical and Statistical Geophysics . . . . .	307
Geomagnetic field of the equatorial ring current and its absolute value . . . . .	307
Cosmic-ray program . . . . .	309
Electrical conductivity anomalies in the earth's crust in Peru . . . . .	309
Laboratory Physics . . . . .	310
Nuclear physics . . . . .	310
Polarized protons . . . . .	311
Polarized deuterons . . . . .	313
Biophysics . . . . .	313
Interactions of nucleic acids . . . . .	314
Plant nucleic acids . . . . .	314
"Renaturation" of the DNA of higher organisms . . . . .	316
Lysogenic systems . . . . .	333
Substrains of <i>Escherichia coli</i> 15 bacteriophage . . . . .	334
Conditions influencing induction of lysis in lysogenic bacteria . . . . .	338
Ascites tumors in mice . . . . .	341
Cooperation . . . . .	345
Image Tubes for Telescopes . . . . .	345
References Cited . . . . .	347
Bibliography . . . . .	347
Major publication . . . . .	349
Personnel . . . . .	349







The radio sources in the southern sky are being studied by relatively few astronomers. The Department of Terrestrial Magnetism has evolved a cooperative program in Argentina, and has supplied a multichannel receiver for studies of the hydrogen clouds in our Galaxy and in the Magellanic Clouds, using a 100 foot parabolic antenna supplied by the Department and constructed near La Plata by the Department's staff, with the help of collaborators from the University of Buenos Aires, the University of La Plata, and the Consejo Nacional. The photograph shows the parabolic antenna in use for observations of the sky before being lifted up on its final equatorial mounting.

## INTRODUCTION

The activities of the Department of Terrestrial Magnetism (DTM) in recent years may be characterized as a set of very specific research studies carried out with the clear intention of testing whether a highly personal and individual approach to research is still valid and effective in various areas of modern physics, despite the vast expansion of research activities and support during the past two decades. For comparison one may examine the activities, fruits, and satisfactions of a similar small number of professionally trained men who have been spending their time and energies in a typical physics laboratory elsewhere, organized there on the more up-to-date basis of "team research" seeking new knowledge and developing procedures in some preselected and acknowledged research area. Our Departmental experiment in research administration based on the individual, and hence characterized by at least some degree of austerity, was deliberately undertaken just after World War II. It has been fully recognized as such an experiment by the participating staff members, who make their own evaluations of its risks and rewards.

One of the inevitable features of any departmental research program that grows out of a decision to emphasize personal research interests is a wide diversity of subject matter, simply because modern physics embraces the whole sweep of "natural philosophy." Recognition of the universal character of mathematics and the laws of physics and their bearing on a wide variety of problems in all sciences comes naturally to students of physics, and the applicability and usefulness of this physical approach even to biological studies have been a matter of great interest to several members of our staff for nearly two decades.

The reports following touch on current

activities in this Department relating to radio astronomy, photoelectric astronomy, isotope age measurements of ancient rocks, seismological studies of the earth's crust and mantle, heat flow outward from deep in the earth, magnetic induction in the earth due to changing electric currents in the ionosphere overhead, nuclear physics studies using polarized beams, and in biophysics a whole series of detailed studies of the mechanisms of inheritance and evolution in animals, plants, bacteria, and viruses, with their astonishing simplicities and their complex interrelationships.

Not the least valued feature of these highly personal activities is the sharing of our attitudes and experiences in personal research with selected individuals abroad, chiefly in Latin America, by direct colleague-to-colleague participation in half a dozen cooperative programs involving about as many professional colleagues in other countries as we have on our own staff. This kind of locally indigenous activity abroad can help leaders elsewhere evaluate the extent to which our type of dedication to the support of highly personal motivation and activity in research may be valid and useful in the rather different cultural patterns of their own countries. An endowment for an operating research establishment such as the Carnegie Institution is rare enough in the world to merit some active illustrations of its mode of operation actually functioning as examples in a few localities far removed from Washington, especially under the current circumstances of vast public support of research in the United States. This Department's activities in seismic and magnetic research in the Andes, and in radio astronomy near Buenos Aires, constitute a set of seven or eight such local examples of Carnegie Institution activity.

In these introductory remarks it is also



appropriate to describe briefly some of the specific stages of activity reached during the current year, and the results.

The long-term project seeking to utilize modern photoelectric surfaces for photography and spectroscopy with large telescopes, with an advantage of more than a factor of 10 over the best photographic emulsions for astronomy, came to fruition during this report year. These efforts have been carried forward by the Department over the past 11 years for the Carnegie Institution's Committee on Image Tubes for Telescopes, with substantial support in recent years from the National Science Foundation (NSF) for the industrial fabrication of tubes and for testing by actual use of these devices in astronomy. Distribution to half a dozen active astronomers of good image tubes fabricated by the Radio Corporation of America under the guidance of DTM and the Committee, along with the required auxiliary items provided by the Department for routine operation of these image tubes in observing programs, was carried out this year to round out the testing program. More tubes will be distributed later under the guidance of a Joint Allocations Committee.

Our radio astronomy program was largely occupied with technical preparations during the year, both at La Plata, Argentina, and at Derwood, Maryland. The new 100-foot parabolic antenna at La Plata was put to use for observations of hydrogen clouds beginning in April 1965 by our Argentine colleagues, who used it as a transit instrument pending the erection of the equatorial pedestal mounting. Similarly, after eight years of intermittent effort and disappointment, a satisfactory parametric amplifier for the multichannel H-line equipment at Derwood was evolved this year, yielding an effective input noise level of about  $220^{\circ}\text{K}$  (previously  $850^{\circ}\text{K}$ ). The chief trouble previously has been a shifting zero line, or base line. The Avery Road, Maryland, 100-foot parabolic antenna

was mounted and made ready for interferometer observations jointly with Derwood (two-mile spacing). A month-long series of observations at 230 Mc by our group using the 300-foot transit parabola at the National Radio Astronomy Observatory at Green Bank, West Virginia, sought to define and evaluate the so-called "galactic halo," a crudely spherical distribution of radio emission from all regions of our Galaxy. The intensity of this supposed "halo" should have exceeded  $200^{\circ}\text{K}$  if previous observations described in the literature were correct, but our observations show that, if the halo exists at all outside a narrow and well-known galactic "spur," the general emission does not exceed  $30^{\circ}\text{K}$  in intensity for the regions visible from our latitude.

Our program of magnetic observations in Peru and Bolivia, jointly with the Instituto Geofísico del Peru and the Instituto Geofísico Boliviano, seeks further to characterize the anomalously high electric conductivity at shallow depths (less than 100 km) that we discovered jointly two years ago in the Andes. This year our work was chiefly concerned with the "ocean-edge effect." In southern Peru the magnetic effects of electric currents known to be induced in the salty ocean are masked by the remarkably high conductivity under the land areas. This does not seem to be the case farther north in Peru, according to a preliminary examination of records from six instruments which were deployed along the coast and inland from January to June 1965. The instruments are being shifted to eastern Peru and later to Bolivia for further studies of deep conductivity.

The Lake Superior expedition of 1963 for explosion seismic studies of that region of the Canadian Shield, organized by our Department as a part of the United States contribution to the International Upper Mantle Project, gave a vast array of observations (3,500) of waves from the 77 shots in 1963, plus more data from about 40 shots in 1964,



but direct analysis of these records was difficult and led to contradictions. A long series of studies, finally using an "extended time-term analysis," led to the unequivocal finding that the structures under the lake are highly varied. The bottom of the crust slopes from a very shallow crust near Duluth to a very deep one north of the Keweenaw Peninsula, then up and down again going east. The velocity structure is also quite varied. This complexity under the Shield was not expected by most geologists.

The Andes seismic program of the Department, which has been given special impetus for two years as a part of the International Upper Mantle Project, has moved toward more analysis and somewhat reduced field troubles, although the determination of accurate times for specific shocks observed on the records, and confusion due to noisy observing sites are continuing obstacles. Marked differences in travel-time curves to the south and to the northwest are conspicuous for La Paz. Antofagasta has indications of similar azimuthal differences and additional local velocity structure, as Arequipa also has. Efforts to extend the scope of indigenous analysis procedures for the several local groups were made by establishing a temporary "Carnegie Analysis Center" in Antofagasta for two months; this effort *in situ* will be expanded. For comprehensive recording of earthquake wave amplitudes without distortion through a wide frequency range—30 c/s (cycles per second) to 50 sec—and a vast range of amplitudes (300,000/1) a complete system was designed and tested, comprising vertical and horizontal seismometers free from resonances and air disturbance and using linear amplifiers recording in multiple channels on slow magnetic tape. The first installation was made at Toconce, in northern Chile; a net of six or eight stations in the Andes and in the Far East are anticipated for observations specifically directed toward measurement of the  $Q$  (attenuation) of shear

waves in the upper mantle (300–600 km deep) beneath the Andes and beneath Japan.

The three wide-ranging geophysics programs mentioned—the Lake Superior project and the deep conductivity and seismic programs in the Andes—have been given special subsidies by the NSF to expedite the Department's efforts and extend their range in order to incorporate them as part of the United States program for the International Upper Mantle Project. This financial stimulus has greatly encouraged and enhanced our efforts.

Isotope studies of rocks in the Grenville province, a continuation of the age determination program using mass spectrographs, show that the 2,700-million-year (m.y.)-old rocks of the Superior province extend at least 100 miles into the Grenville province. These Superior province rocks were only partially metamorphosed by the metamorphism accompanying the extensive Grenville orogenic event 1,100 m.y. ago.

The nuclear physics program here continues to be directed toward the interactions of polarized nuclear particles (using polarized beams of protons and deuterons). Observations of 0.5–3.5 MeV have been completed on the scattering of polarized protons by helium ( $p, \alpha$ ) scattering and by hydrogen ( $p, p$ ) scattering and most of the data have been obtained for deuterium ( $p, d$ ) scattering. Current discussions of the next problems involve polarized reaction studies, and also include consideration of the emission spectra of ionized atoms (ion beams through thin foils) which are of considerable astrophysical interest.

The biophysics group has been concerned throughout the year with further probing of the processes of replication and preservation of the genetic information which is transmitted from cell to cell in the coded form of base sequences in the deoxyribonucleic acid (DNA) of the cell. The DNA provides the coded pattern for the various ribonucleic acid



(RNA) sequences which serve as the templates for the synthesis of proteins (enzymes).

Unequivocally homologous segments were found here several years ago for various bacteria, when fragmented DNA in suitable suspension was eluted from single-stranded DNA immobilized in agar. Closely related bacterial forms and their viruses showed very high degrees of homology. However, as reported last year, similar degrees of homology were readily observed, contrary to expectation, with mammalian tissue. Because of the very much larger number of gene sequences for a mouse it was expected that the rematching of like sequences with the use of fragmented mouse DNA on single-stranded mouse DNA in agar would be highly improbable. This conspicuous numerical discrepancy has required detailed study. Animal DNA is found to have numerous copies of identical or very nearly identical gene sequences. This finding stimulates various conjectures and estimates relating to species stability and variation in evolution.

The degree of homology indicated by the varying firmness of binding (temperature of redissociation of the fragments captured by the immobilized single DNA strand) is tied to the degree of sameness or identity of the gene fragments, both for the same species and for related animals. Furthermore, considerations related to the protection of essential genes (by many duplicates), and even the repair of gene damage (because the DNA helix is a double strand), offer much opportunity for

experimental study in relation to virus susceptibility, for example, and to differential dynamic processes such as those involved in tumor growth or inhibition and the predictably synergistic effects of different drugs or treatments when acting simultaneously.

A whole new phase of genetic and evolutionary studies of this general type was opened here a year ago when successful procedures were evolved for working with DNA from plants. The variety and complex relatedness of plant life and the varied responses of plant materials to the same (chemical) catalyst or stimulant provides a rich opportunity for studies of gene homologies. It is clear, of course, that DNA agar fragment-binding procedures provide only a rather crude physicochemical test of homology or sameness, but this coarse "filter" has remarkable usefulness when suitably combined with the more detailed and precise genetic data obtained by inbreeding and crossing. Indeed, one of its outstanding characteristics is that it provides quantitative data for situations in which genetics itself denies the possibility of crossbreeding.

It is clear from the wide range and the contemporary character of the research touched on in these brief remarks that the significance of this Department lies not merely in its professional posts and assignments but in the dedication of a small group of research men living and working together, sharing their interests, and their successes and failures, and enjoying the privilege, despite the inevitable stresses that accompany any intense work in research.

## EXPERIMENTAL GEOPHYSICS

### THE EARTH'S CRUST

The activities of the members of the Earth's Crust Section are a direct expression of the freedom granted the Carnegie Institution staff to pursue

with vigor the opportunities in personal and joint research. This is exemplified in two ways by the current activities of the Section. First, as this is written one staff member and two Fellows are in South America gathering special seismic



data as part of the DTM contribution to the International Upper Mantle Project. A second staff member is establishing personal contacts with geologists and geochronology laboratories, both active and potential, for future collaboration in studies of orogenic events that could be of great significance to continental drift hypotheses. The other members of the section are preparing for an ambitious effort to use the techniques devised for the Lake Superior data reported below to study the crustal structure of the Middle Atlantic states from the continental shelf to the Appalachian Mountains. This is a collaborative effort of the North American Explosion Seismology Group. The Carnegie measurements will be directed toward a broad areal understanding of the crust-mantle interface in the Middle Atlantic states. The effort, too, is a part of the United States program for the Upper Mantle Project and includes many individuals not listed on the rolls of the Earth's Crust Section.

A second example of Carnegie opportunity in geophysics is perhaps more intensive and is represented by the work of the Crust Section in heat flow. One of the participants is deeply involved in understanding the origin of the ultrabasic rocks from the data from isotopic abundance ratios. At the same time he is concerned with the problems of measuring heat flowing out of the crust. A novel adaptation of deep-sea techniques to measurements in deep fresh-water lakes has been completed, but there remains the problem of the corrections to the measured gradients by short-term temperature variations. Another participant has for several years been involved in the interpretation and understanding of seismic waves generated artificially by explosions. He, too, has joined in the concern for the interpretation of the heat flow measurements in lakes, and contributed the design of a simple, effective bottom-temperature recorder to provide accurate measures of the short-term variations

in the temperature of deep lakes. The effort to attack a new problem outside the main interest of either of the participants is but one example of the opportunities in the Crust Section, some of which are reported below.

### EXPLOSION STUDIES

*T. J. Smith, J. S. Steinhart, and L. T. Aldrich*

The ultimate goal of explosion studies of the crust and upper mantle of the earth is to learn about the distribution of rocks and their physical properties in many different types of geological provinces. With this knowledge we would hope to be able to infer how, in the sweep of geologic history, the continents and ocean basins were formed, the mountains raised, and the great oceanic trenches created. We have evinced, in previous *Year Books*, some dissatisfaction with the limited steps we have been able to take toward this goal. The models of crustal structure presented by us and by others are satisfactory as far as they go, but some doubt remains (since the data are analyzed in various ways) about which features of the structural interpretation of the data are persistent and unchangeable. We shall try in this summary of results from the 1963 Lake Superior experiment to treat an extensive body of data in several ways in the hope of exhibiting some of the features of crustal structure which are required by the data and are not merely possible or plausible results. The physical description of the experiment, and the difficulties of interpreting the data by classical techniques were discussed in *Year Book 63* (pp. 311-314).

Several analytical techniques have been employed to derive crustal structure from the data obtained in the 1963 Lake Superior seismic experiment conducted as a part of the United States and Canadian programs in the Upper Mantle Project. The Lake Superior region was found to have an unusual and rapidly varying crustal structure in comparison



with the Canadian Shield area surrounding it. In general, under the lake there is a high-velocity crust (6.67 km/sec) beneath 4–6 km of Keweenaw sediments and volcanics. The upper mantle velocity of 8.07 km/sec agrees closely with values found previously in adjacent areas. The depth to the M (the Mohorovičić discontinuity, which separates the crust from the upper mantle) varies from about 20 km in the area just west of the lake to 55 km or more in the eastern half of the lake—values that are among the most extreme yet observed in North America. A number of second-order structural features were also found in the M. The differences and the major structures persist for all reasonable assumptions about the velocity depth function.

Among the techniques used was the standard reversed-profile technique, which is poor for this complex structure, and the apparent velocity measurements provided limited information about the velocity depth function. The extended time-term technique developed and used here produced the most complete structural picture, and the general features of the structure are confirmed by a dip-projection method derived from apparent velocity data. Further studies in this area are required to determine the extent and detailed structure of this striking feature of the earth's crust.

*Time-term analysis.* The time-term method of seismic data analysis as formulated by Scheidegger and Willmore (1957)<sup>1</sup> deals with a set of observational equations in each of which the travel time  $t_{\mu\nu}$  from the  $\mu$ th shot to the  $\nu$ th receiver has been triply portioned to yield

$$a_{\mu} + b_{\nu} + \Delta_{\mu\nu}/V(\Delta) = t_{\mu\nu}$$

Here  $a_{\mu}$  and  $b_{\nu}$  are the time terms of the  $\mu$ th shot and the  $\nu$ th receiving station, respectively;  $\Delta_{\mu\nu}$  is the distance separating them; and  $V(\Delta)$  is some function of  $\Delta$ . The computational technique for  $V(\Delta) =$  constant as well as the assumptions

underlying its use have been thoroughly discussed from a number of points of view (Scheidegger and Willmore, 1957).<sup>1</sup> If there are  $m$  shots and  $n$  stations from which  $L$  ( $\leq m \times n$ ) observations are made we obtain  $L$  equations of the type of the equation to solve for  $m + n + 1$  variables ( $a_{\mu}$ ,  $b_{\nu}$ , and  $V$ ). These calculations and similar ones for the case when  $V = V_0 + V_1\Delta$  have been programmed for the CDC 3600 computer with maximum dimensions  $L = 350$  and  $m + n - 1 = 75$ . The routine, as now written, provides the option of obtaining one or two parameter velocity solutions and also permits the specification of a predetermined constant velocity. Statistical estimates of the uncertainties of the solutions have also been computed and, for the results that follow, the errors are given at the 95 per cent confidence level. Details of this analysis are given by Smith, Steinhart, and Aldrich (soon to be published).

*Stability, resolution, and reliability.* It will be seen from Fig. 1 that the Lake Superior experiment of 1963 was not designed to meet the suggested requirements of Willmore and Bancroft (1960).<sup>2</sup> Most of the observations are from three shot profiles in the lake, each of which was recorded at its extremities and, in the case of the Duluth–Otter Cove profile, at the center. The resulting data have several characteristics that militate against their being effectively analyzed by the time-term method. Despite the length of the profiles, areal coverage is comparatively small. Most shot and recording sites are tied to the network along no more than two azimuths, and for many of the recording stations observations are available in only one direction. There are few points at which similarly located shots and stations may be used for determination of the constant  $\alpha$ , which is introduced in eliminating the singularity of the observational system. Consequently, normalization of the solutions rests upon the continuity of the time-term structure at a few

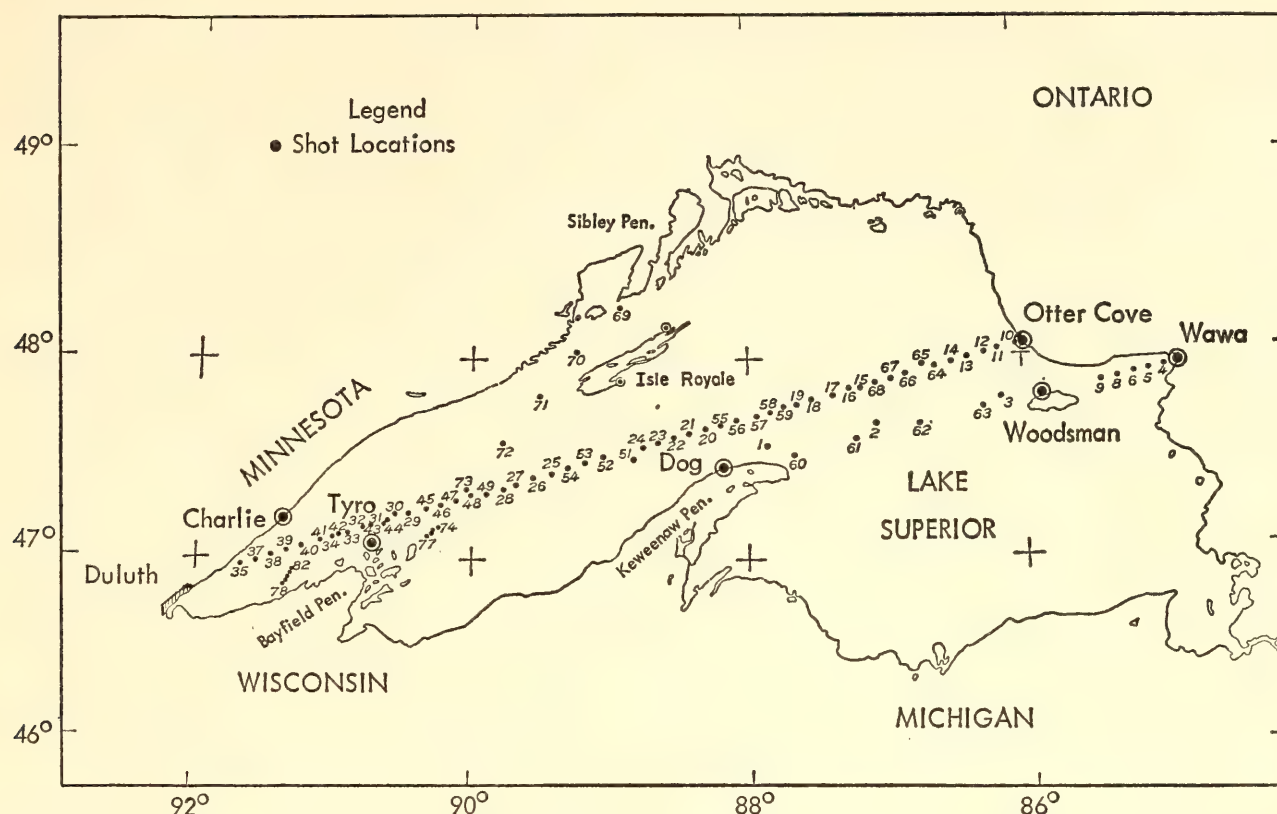


Fig. 1. Locations of shots in Lake Superior; principal attention is concentrated on line of shots from Duluth to Otter Cove, and on shorter line from Keweenaw Peninsula and Wawa.

isolated points where one is faced with the necessity of equating shot and station time terms whose principal recording azimuths differ by  $180^\circ$ . Finally, it should be noted that the density of stations on the western and southern sides of the lake greatly exceeds that on the eastern and northern shores, producing an imbalance in the data that might possibly be expected to bias the results in an unpredictable way.

Partially countering these disadvantages are the high level of redundancy in the experiment and the large amount of data available. These features make it possible to conduct meaningful and convincing tests of internal consistency without which many of the results would be open to criticism. More than 100 complete time-term calculations have been made on different selections of data from the Lake Superior experiment with techniques to be described later. Although the results from only one carefully controlled sequence will be presented, it can be said that the salient characteris-

tics of this final solution are exhibited by nearly all of its predecessors.

This study has largely been focused on the data taken along the two east-west profiles and their landward extensions. This simplification reduces the difficulty of interpreting the behavior of the time terms under changes in regional weighting, and facilitates the construction of realistic models to test conjectures. Thus, by sacrificing the comparatively small amount of areal information in these data, it is possible to obtain a more thorough evaluation of the reliability of the method as it applies to a profile experiment.

The treatment of the data has been predicated on the assumption, satisfactorily justified by the travel-time curves, that most of the Lake Superior first arrivals may be explained as refracted events from one or the other of two crustal interfaces. Observations lying on travel-time branches with gross apparent velocity between 6.0 and 7.0 km/sec have been called  $P_1$  arrivals,



while those on branches with velocity greater than 8.0 km/sec are referred to as  $P_n$  events. Transitional observations near the crossover have been excluded from the analysis.

Willmore and Bancroft have pointed out the difficulty in determining the velocities of crustal materials from time-term analysis. A crustal model depends critically on these velocities, a fact that prompted the following investigation of the repeatability of velocity determinations from the data.

The shot points were divided into two groups, here referred to as "circle" shots and "triangle" shots. Sorting the available data by group gave two data sets of very nearly identical size and quality from which independent solutions could be obtained and compared. Solutions were produced for each of the data sets for  $P_1$  arrivals from shots in the eastern end of the lake,  $P_1$  arrivals from shots in the western end of the lake, and  $P_n$  arrivals from all shots. Following each solution, observations with excessively high residuals were discarded and successive attempts were made. In no case, however, was an observation deleted from a data set unless its residual was at least five times as great as the standard deviation for that

station. Such a requirement for rejection of data may be more rigid than necessary. When further deletions were impossible under this criterion, the data sets were united and the same procedure followed to produce a maximally weighted solution based on the combined sets.

The velocities obtained from different sets, summarized in Table 1, show quite satisfactory agreement. In the course of refining the sets the velocities showed little tendency to fluctuate after the first rejection of unacceptable data, indicating that the determinations from different data sets are highly consistent if the recording geometries are essentially the same.

The same data sets as those just described were used to obtain the time terms plotted in Fig. 2. Time terms associated with the Duluth-Otter Cove profile have been distinguished from those for the Keweenaw-Michipicoten line to show the differences in structure. Data from these two profiles were, however, reconciled simultaneously. As with the velocities, the agreement between circle, triangle, and combined data is quite acceptable. In almost all cases the 95 per cent confidence intervals for the combined sets contain the circle

TABLE 1. Lake Superior Crustal Velocities From Final Time-Term Solutions

Profile	Velocity, km/sec	Observations	$\left(\frac{\sum \delta_t^2}{L-N}\right)^{1/2}$
<b><math>P_1</math> West</b>			
Circle	$6.63 \pm 0.02$	185	0.1064
Triangle	$6.64 \pm 0.02$	185	0.1095
Combined	$6.64 \pm 0.01$	322	0.0883
<b><math>P_1</math> East</b>			
Circle	$6.67 \pm 0.03$	153	0.1300
Triangle	$6.70 \pm 0.03$	167	0.1234
Combined	$6.69 \pm 0.02$	209	0.0957
<b><math>P_n</math></b>			
Circle	$8.07 \pm 0.04$	197	0.2252
Triangle	$8.08 \pm 0.05$	182	0.2750
Combined	$8.07 \pm 0.03$	332	0.1860

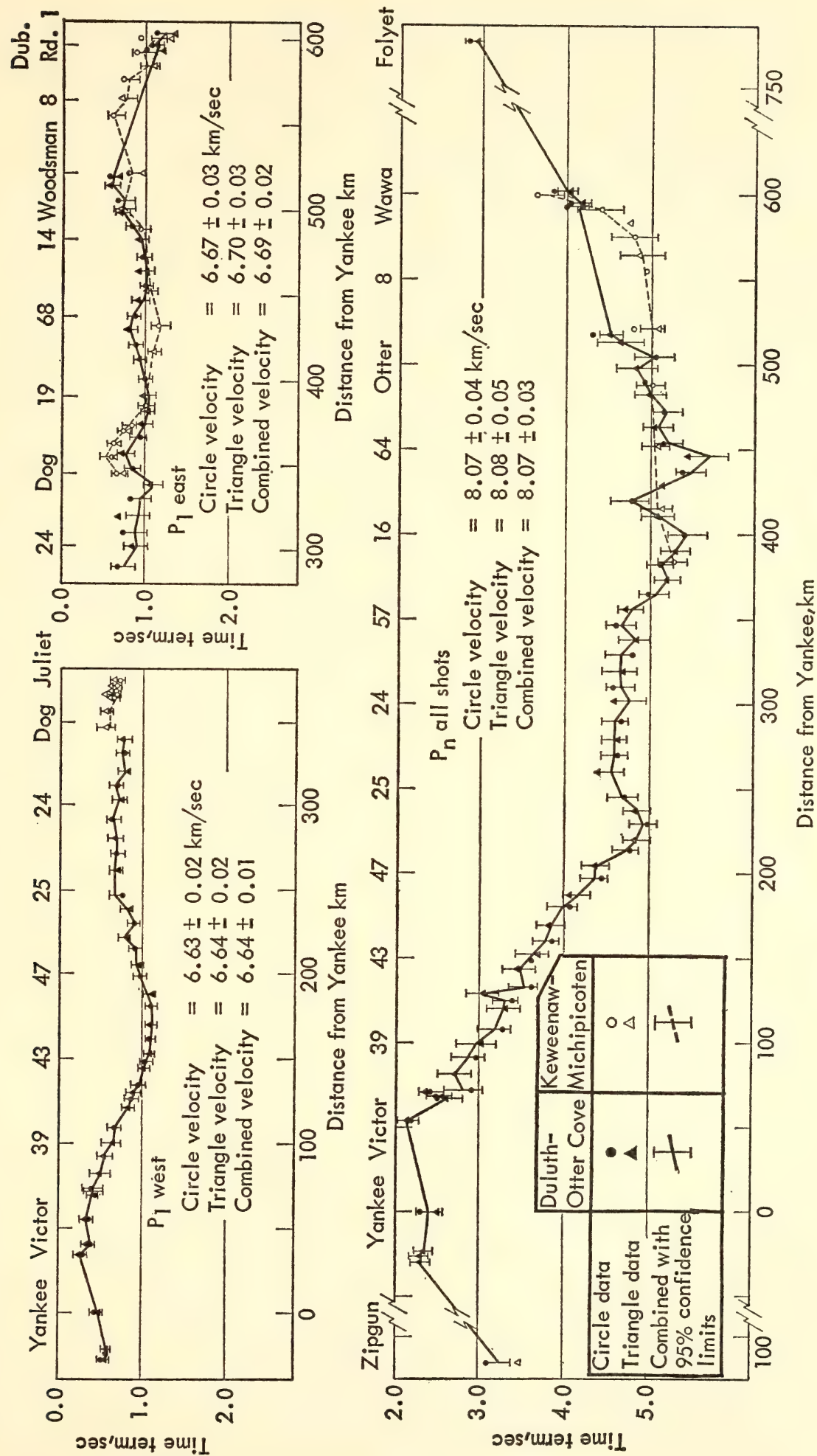


Fig. 2 Time-term results for the Lake Superior profiles.



and triangle determinations, again indicating good internal consistency in the data used. It should be mentioned that the obvious lack of continuity between the circle and triangle values for  $P_1$  east at the extremities of the profile can be completely accounted for by the discrepancy of 0.03 km/sec in the calculated velocities.

Since the structure indicated by these results fails so seriously to satisfy the requirements for exactness in the time terms, it was thought advisable to investigate the behavior of the time terms on some simple structures that were known to be at variance with the hypotheses of the method. Accordingly, a variety of models scaled to the Lake Superior  $P_1$  observations were constructed to test the resolution and validity of the analysis on profile data arising from domes, basins, faults, and undulating interfaces. Travel times for the models were generated by direct graphic measurement on the assumption that the minimal time path was in all cases appropriate. These travel times were then entered into the computer program, and a complete set of time terms was obtained for comparison with the known values. The only instances in

which the computed time term differed from the true value by more than its 95 per cent uncertainty occurred near sharp discontinuities in the model. The example of a step discontinuity, shown in Fig. 3, exhibits the compromise effected by the least-squares procedure when the time term has strong azimuthal dependence.

It remains to discuss the choice of the additive constant  $\alpha$  used to normalize the solutions. The rapidly changing structure under each of the shot-station interfaces made it inadvisable to require equality of time terms at these points. Instead, an  $\alpha$  was selected for each calculation which appeared to give simultaneously greatest continuity between all shot and station interfaces. This is admittedly a highly subjective procedure whose sole justification is that the difference between the extreme acceptable values of  $\alpha$  is less than the estimated uncertainty in the time terms.

*Apparent velocities.* Apparent phase velocities of seismic arrivals along the surface provide opportunities to obtain several kinds of information about the subsurface structure. If the velocity varies only with depth, then the velocity function may be determined by measurement of apparent velocities of the

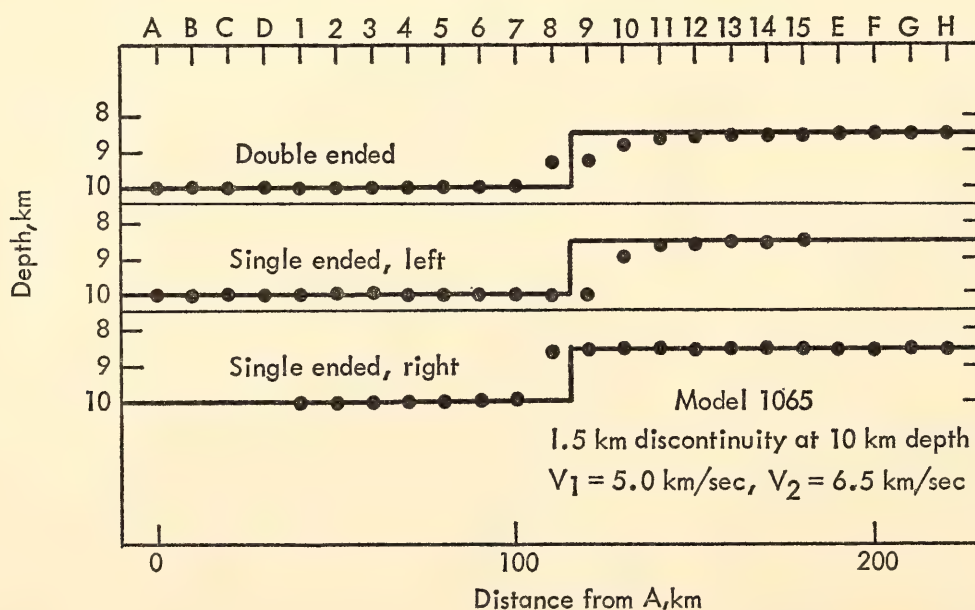


Fig. 3. Theoretical time-term results across a 1.5-km fault, showing single-ended results derived with use of constrained velocity, and double-ended results.

principal phases. In gradually dipping structures the velocity-depth function may also be determined provided apparent velocity measurements are available in two opposite directions. In principle these determinations of crustal structure may also be made from the travel times but the experimental problems are different. For example, to decide between a model with a layer of constant velocity and one with a region of slowly increasing velocity with depth requires measurement of curvature in the travel-time curve which may total only 0.1-sec difference from a straight-line fit over a range difference of 150 km. For the same model the change in apparent velocity is more than 10 per cent.

The results of apparent velocity measurements obtained with short (10-km) array are shown in Fig. 4.

In comparison with the velocities determined from the time terms it is remarkable how much higher the values were that were measured at Victor station than those obtained from the

time-term analysis. This difference in absolute value of the velocities correlates with the geology along the spread at Victor. The distance to bedrock was much greater on the east end than on the west end, and the whole array is underlain by the high-velocity Duluth Gabbro at the basement. Since  $V_{app} = V_1/\sin i$  the effect of both structure and basement velocity is to increase the measured values of apparent velocity.

There is no indication of apparent velocity increase with distance in the Victor data. Large errors attach to each of the measurements, especially as the distance increases, but it is still hard to find any encouragement for continuous velocity increase.

Yankee station was a 10-km linear array similar to Victor. The results for Yankee (Fig. 5) are much the same as for Victor, except that the absolute velocity values are all lower. Again there should be great uncertainties associated with the individual points, but the mean values show little indication of

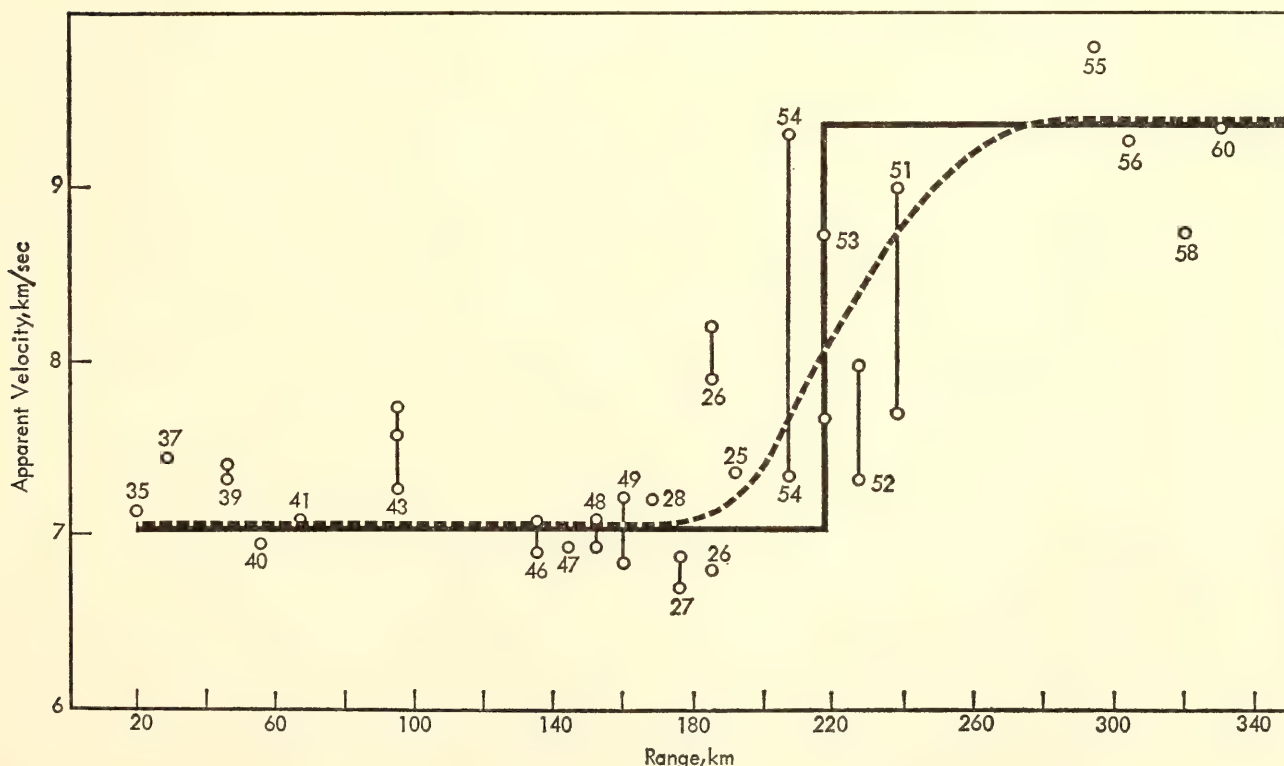


Fig. 4. First arrival apparent velocity measurements across 10-km Victor array.



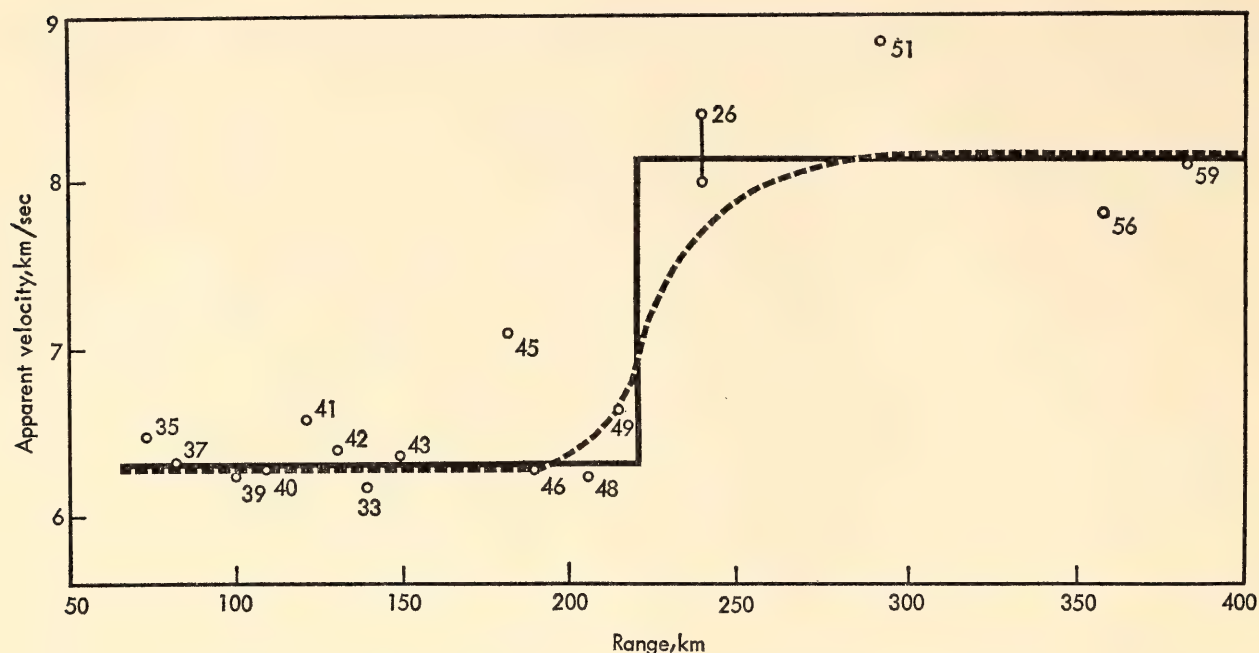


Fig. 5. Apparent velocity measurements for 10-km Yankee array.

velocity increase with distance. Other individual station results we have seen are somewhat similar. Tom station on the Keweenaw Peninsula and Otter Cove on the Canadian end show evidence that could be interpreted as velocity increase with distance, but there is much scatter, and the data could equally well be constant velocity in the  $P_1$  ranges with some dip to the structure.

*Apparent velocities from grouped stations.* One way to increase the resolution in the study of apparent velocities is to lengthen the array. Here this can be done by considering the stations in groups. The longest array of closely spaced stations is the group near the shore at the west end of Lake Superior. This group, here called the West Shore Group, produced the result shown in Fig. 6. Each shot was fitted by a least-squares technique, and where some stations were in gross disagreement they were left out in a recalculation. Thus, the 95 per cent confidence limits are on selected data and should be regarded as displaying only the degree of agreement in the data used. Efforts were made to avoid bias in removing bad data from the

analysis by discarding points only when they were in disagreement by more than 0.3 sec. Despite these qualifications the West Shore stations present the most impressive picture of continuous velocity increase with distance of any available. The slope of the dashed line is an increase in apparent velocity with distance of about 0.0027 km/sec/km. Slopes as low as 0.001 km/sec/km would also satisfy the data within the 95 per cent confidence limits. It would also be possible to fit one horizontal (constant velocity) line of 6.6 km/sec out to 120 km and another of about 7.0 km/sec beyond that distance to 250 km. It is difficult to choose between the possibilities from this data alone.

A second combined array 28 km long on the west end of the lake can be made up of stations Fox, Easy, Gamma, and Yankee, here called West FEGY Group. The results of this grouping are shown as Fig. 7. Either the 0.0027 km/sec/km or 0.001 km/sec/km gradients of apparent velocity with distance would be acceptable for these data. The third west end group, Tyro and the three Kudu stations, are technically

longer than the above arrays, but at a considerable angle with respect to the shot line, so that the effective length of the array is usually about 25 km, and the paths to each station differ. The results of this group (Fig. 8) show considerable scatter. That this scatter is the result of changing paths as the azimuth to

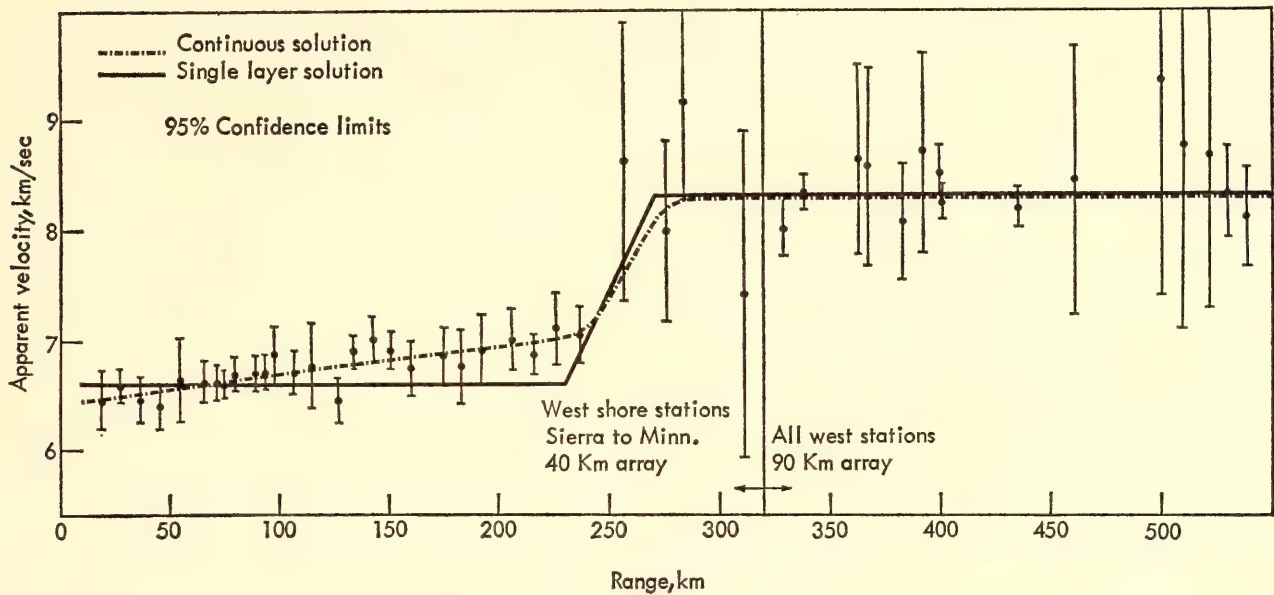


Fig. 6. Apparent velocity measurements for the West Shore Group. Solid-line slope at crossover for a layer model is due to length of the array.

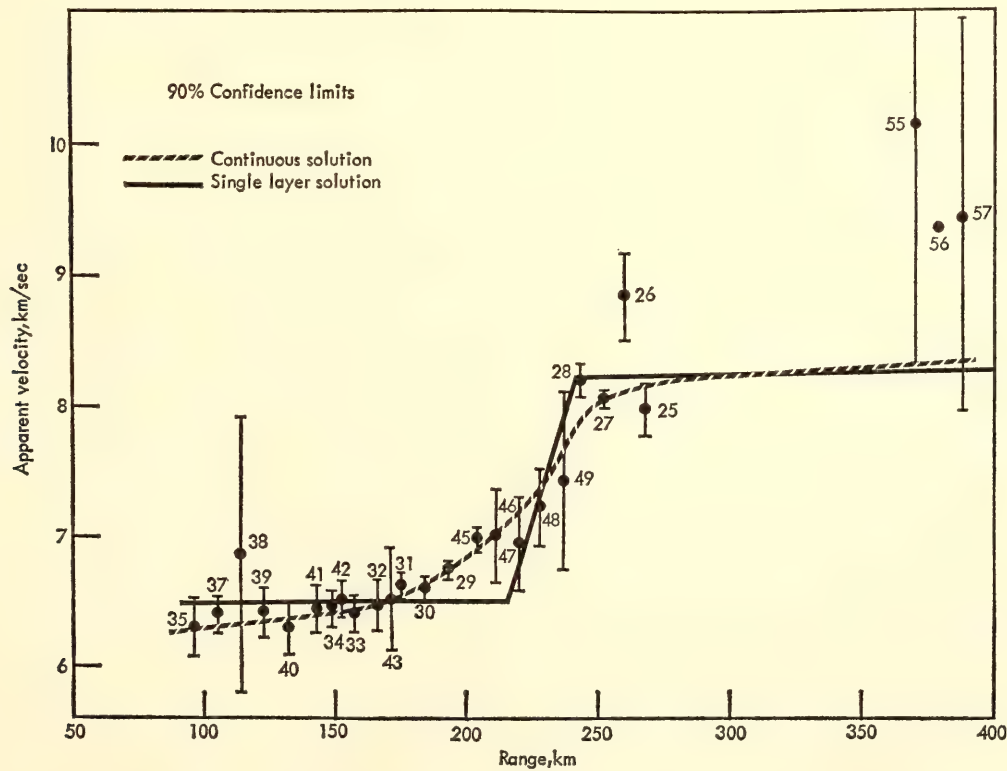


Fig. 7. Apparent velocity measurements for the West FEGY Group (plotted at Easy station ranges).



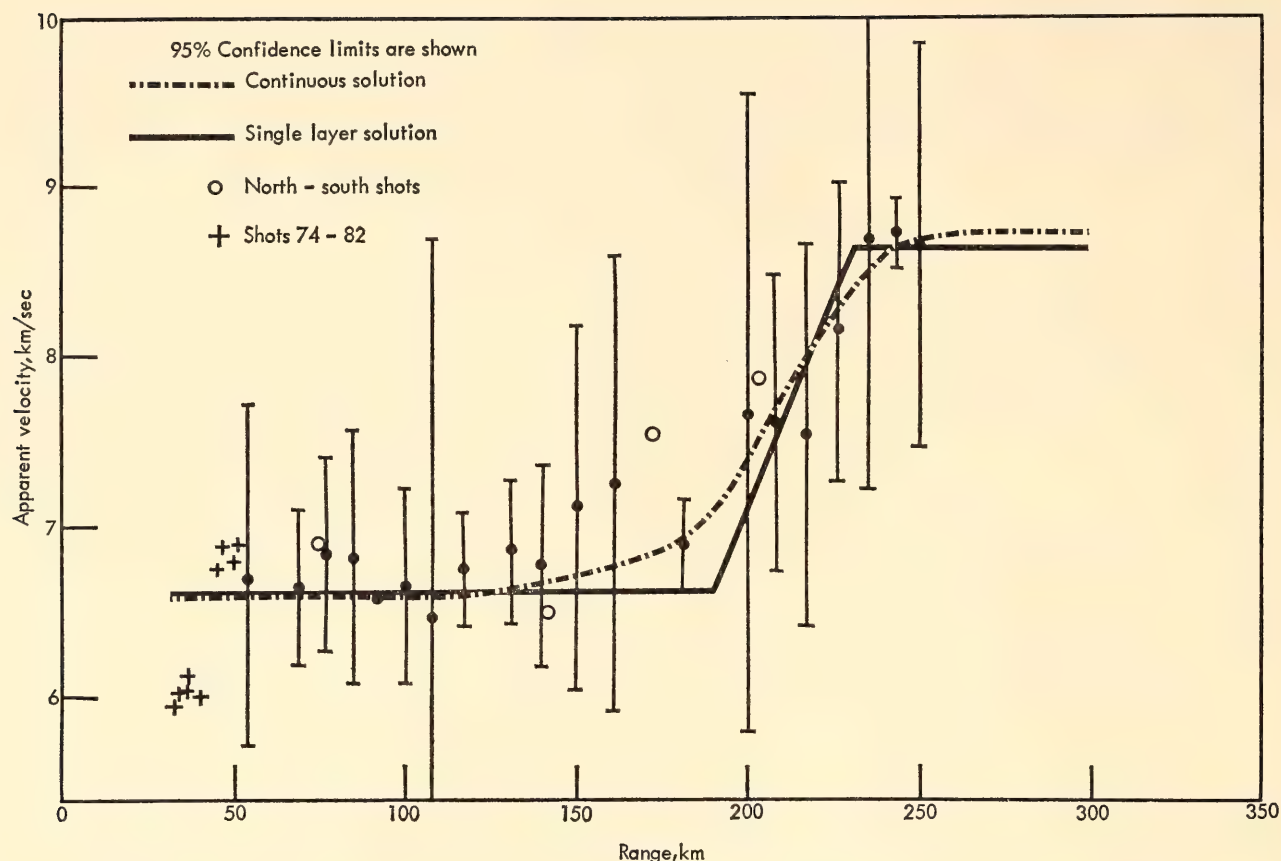


Fig. 8. Apparent velocity results for Tyro and Kudu stations 1, 2, and 3.

the shot changes is shown by the results (also in Fig. 8) for shots 74–82 which are along the line of the Tyro–Kudu array, and for which agreement from shot to shot is good. Although the mean values in Fig. 8 show some increase of velocity with distance, little significance can be attached to this result.

On the eastern end of the lake the stations were not spaced so densely and it is not possible to make up grouped arrays. Using the station pairs Wawa–Woodsman and Dubreuil Road–Otter Cove, it was possible to make some measurements of apparent velocity as a function of range. Because these are two-point measurements the accuracy may not be very good, and there is no way to estimate error. The results displayed in Fig. 9 do not support an apparent velocity increase with distance. There is a suggestion, especially on the Wawa–Woodsman pair (Fig. 9B), that the values depart from a single-layer solution.

Note that the very high  $P_n$  apparent velocities are obvious here, as they were on the travel times for the east end of the lake.

*Continuous velocity increase with depth.* There has never been any question but that the velocity changes continuously with depth. The question has been whether the change is large enough to be of concern in arriving at correct depths and whether the amount of change could be measured. Once again, from the results above, the answer is not entirely convincing. It was shown in the discussion of the two-parameter time-term results that different combinations of the data, which yielded the same stable time terms, gave different results for the existence and magnitude of the velocity increase with distance. The numbers for a linear increase of the  $P_1$  velocity with distance on the west end of the lake varied from 0.0005 km/sec/km to about 0.0015 km/sec/km, and were

at times barely significant statistically, and for other groupings slightly below significance. The velocity change of the eastern half of the lake was never consistent or statistically significant, and the data above yield the same result for the eastern end. The first conclusion is, then, that in the eastern part of the lake there is no measurable increase of velocity with distance (and hence with depth).

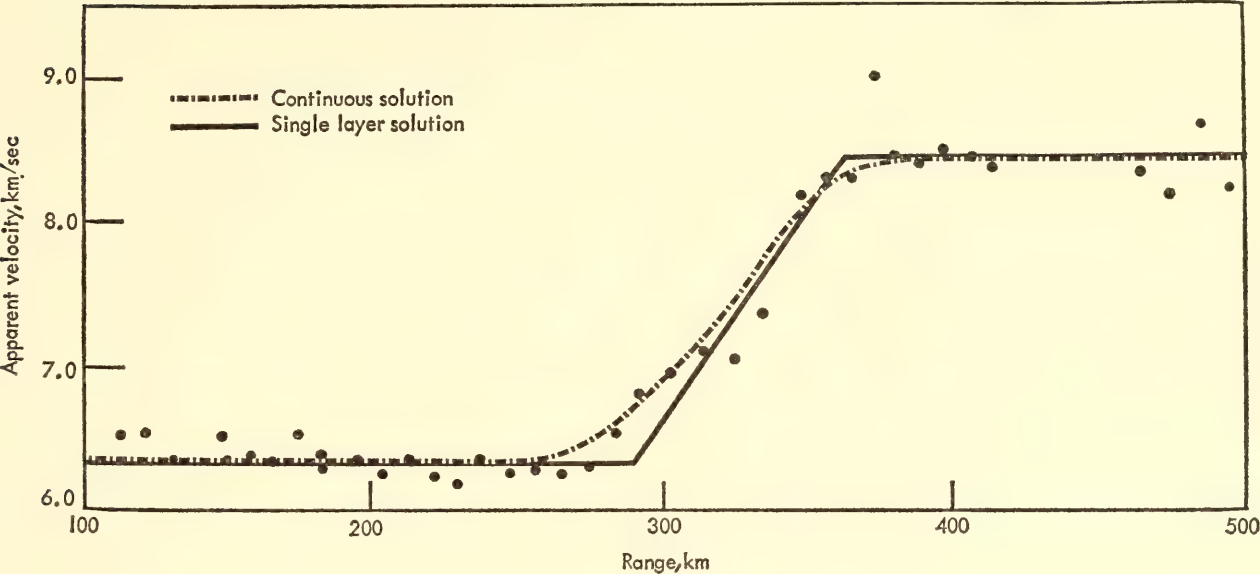


Fig. 9A. Apparent velocities measured on station pair Dominion Observatory (Dub 4)–Otter Cove.

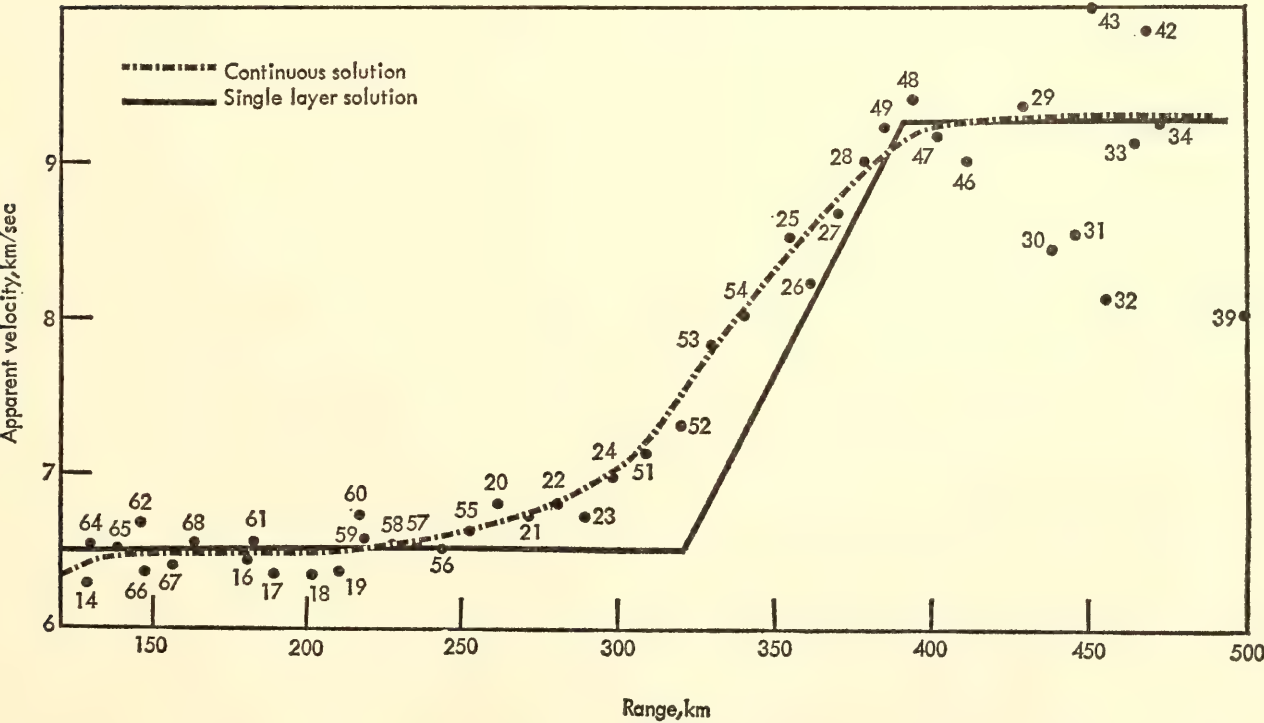


Fig. 9B. Apparent velocities measured on station pair Wawa–Woodsman.



For the western end there appear to be data that require such an increase, and the other western groups have nonsignificant indications of such an increase. The best numbers for these increases appear to be about 0.0027 km/sec/km, but somewhat smaller numbers would be acceptable. We feel that a continuous velocity increase with distance does exist for the western end of the lake and the linear approximation to the rate lies between 0.001 and 0.0027 km/sec/km. Choice of a linear fit to the apparent velocity distance data has certain detailed implications for the velocity depth function, as Bullen (1965)<sup>3</sup> has shown, which do not necessarily obtain in this case. Nevertheless, we may compute the velocity depth function for these two limiting cases; see Fig. 10. The graph shows the velocity depth functions for the two distance gradients 0.001 and 0.0027 km/sec/km. The termination of these models is at the maximum depth that would be sampled according to the data in Fig. 6. Both these models

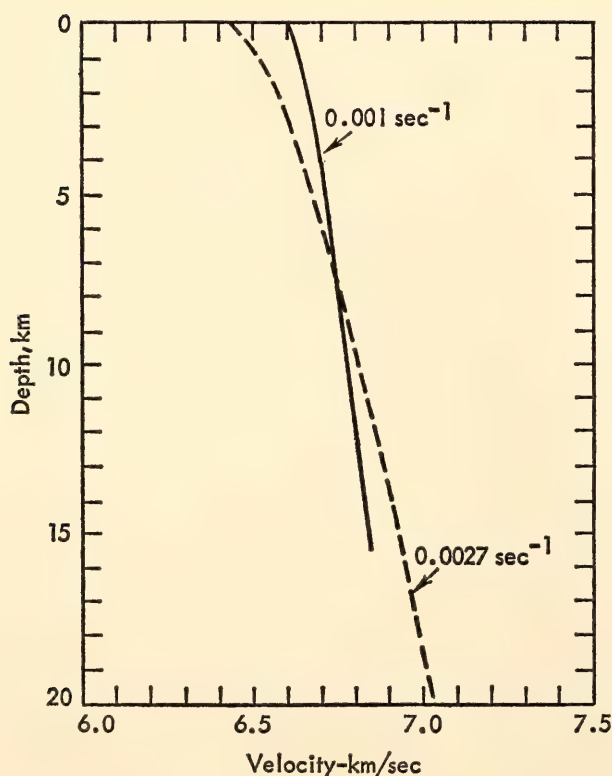


Fig. 10. Velocity depth function for west half of Lake Superior for the two extremes of the apparent velocity data.

would require some change in composition with depth, when they are compared with the laboratory results for the pressure-temperature effects on velocity. The smaller gradient is just at the limit of temperature-pressure effects alone (but with a rather small temperature gradient implied). Although the existence of such a gradient is of interest petrologically, it is clear that the single-parameter velocities derived from the time terms would be a good approximation for the purpose of calculating depths to deeper horizons.

*Dips from apparent velocities.* Another interesting use may be made of apparent velocity data when combined with time terms. We need only the assumption that the M is a sudden enough velocity change that we are justified in treating it as a refractor. Given the velocity below the M (which from above is 8.07 km/sec), we may convert any of the  $P_n$  apparent velocity observations to a value for the dip. If we consider points 3 and 4 in Fig. 11 as stations and look at the results from shots at, say, location 1, the measured apparent velocity  $V_{app}$  is related to the dip  $\phi$  by  $V_{app} = V_1/\sin(i \pm \phi)$ , the choice of sign depending on whether  $V_{app}$  is greater or smaller than  $V_2$ . Similarly, if locations 1 and 2 in Fig. 11 are shots we may plot the data for station 3 and calculate the dip under the shots. Since we know  $V_2$  from the time-term analysis above, we know  $i$  (the critical angle) from  $\sin i = V_1/V_2$ . There remains some question of exactly what value to use for  $V_1$ , but for this rough calculation the limits given above are precise enough. We used 6.7 km/sec for calculation of Fig. 12. The dips

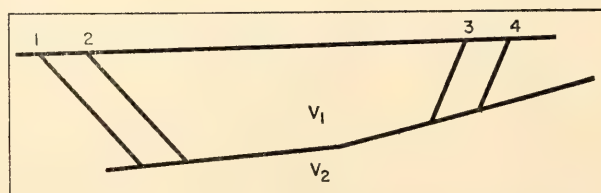


Fig. 11. Derivation of dips from apparent velocities.

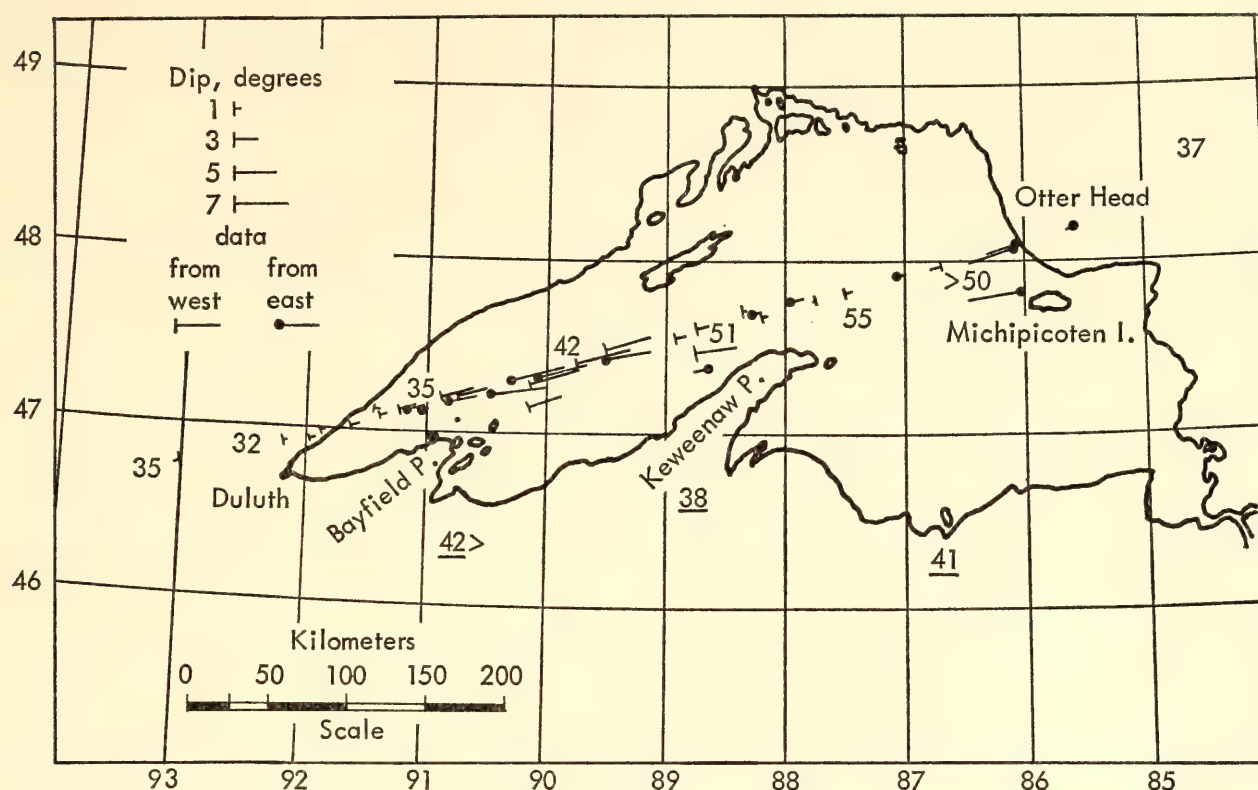


Fig. 12. Dips and depths in Lake Superior from apparent velocity data. Underlined depths are from previously published measurements.

calculated must, of course, be projected toward the shot (or station as the case may be) from the location where they apply. For these calculations this projection distance is 50–80 km depending upon the local thickness of the crust.

The data used are the apparent velocity data from individual and grouped arrays discussed above, and some individual array data obtained by other institutions in the Lake Superior experiment. In addition, the apparent velocities from the travel times from individual stations were used (the data were tabulated by Steinhart, 1964).<sup>4</sup> Frequently it was possible to obtain more than one dip from a travel-time graph. Because the structure is changing rapidly in the lake region, many of the travel times show two or more distinct slopes for various groups of the shots at  $P_n$  range. An example of such a travel-time plot may be seen in Fig. 13 from the Dubreuil Road station on the Canadian end.

The results of these rough dip calculations are shown in Fig. 12. It is reassuring

that these calculations, which are partly independent of the time-term results, show the same general picture of the structure along the profile. There are a few internal discrepancies in Fig. 12. They are probably due to the distortion of the apparent velocities by near surface dips (and thus should not be referred to the M), but the surprising fact is that there are not more. If the depth to the M at a single location is now assumed we may project the depths over the whole length of the profile from the calculated dips. This has been done by assuming 35 km to be the depth at the westernmost station (Zipgun), which is about in agreement with the time-term result. The underlined numbers in Fig. 12 are depths to the M from previous studies in this area and are shown for comparison. Even from these approximate calculations the remarkable depression in the upper mantle that underlies Lake Superior is obvious.

*Crustal structure in Lake Superior.* To convert the  $P_1$  time terms to a



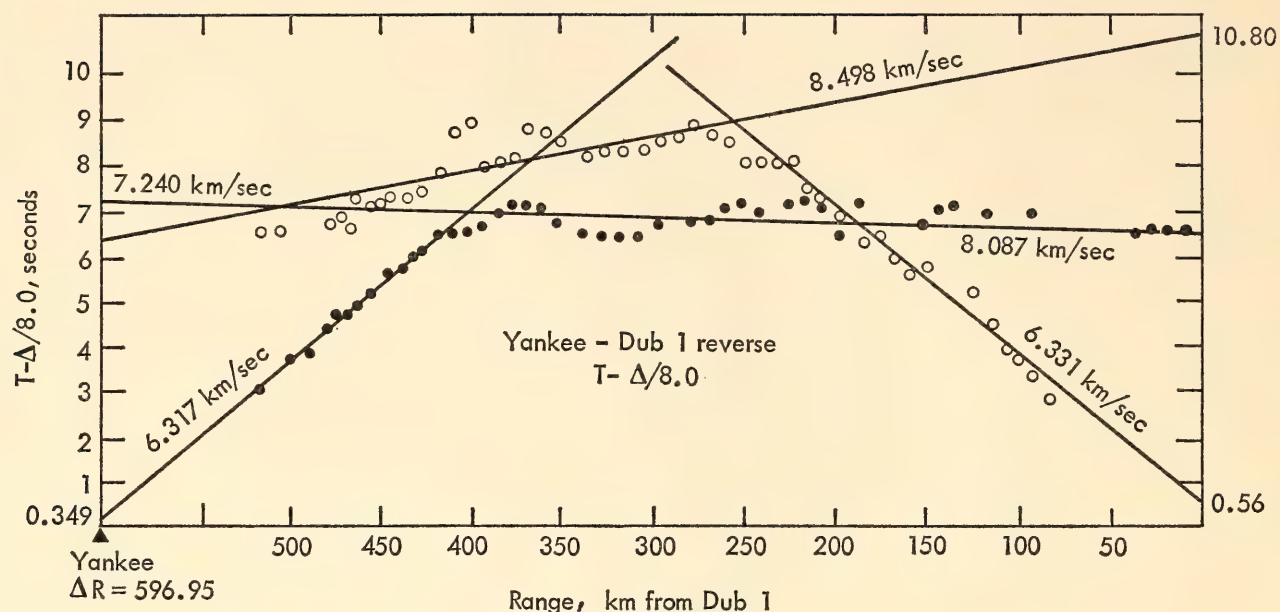


Fig. 13. Fitted reverse profile between Yankee and Dubreuil Road 1 stations.

structural picture we need mean velocities down to the depths at which the 6.6–6.7 km/sec velocities are measured. It must be stated at the outset that in deriving these mean velocities along the profile we are in some areas averaging several distinct near-surface layers and in others averaging a continuous increase of velocity with depth.

The derived velocity structure is shown in Fig. 14. We believe the choices to be well supported by evidence, except, perhaps, on the easternmost end of the lake.

For the region of the crust just below the  $P_1$  time-term depths we have the well-determined velocities of 6.64 km/sec in the western half of the lake and 6.69 km/sec in the eastern half. The average  $P_n$  velocity is precisely measured at 8.07 km/sec (Table 1). Unfortunately, the velocities in the lower portion of the

crust are uncertain, as they often are in crustal studies. We have examined later arrivals on three western stations and find no clear evidence for a layer of velocity intermediate between 6.7 and 8.0 km/sec. There are, however, some later phases on two of these travel-time graphs in the range of 100–200 km which might indicate an intermediate velocity cusp or, possibly, a poorly defined layer. A straight-line fit to these phases produces velocities between 6.95 and 7.2 km/sec. Their position with respect to the rest of the travel times indicates that the higher velocities could occupy, at most, the lowest 20 km of the crust. We have thus concluded that the mean velocity of the crust at depths greater than those appropriate to the  $P_1$  time terms must be between 6.67 km/sec and 6.9 km/sec (if the lower 20 km of the crust averages 7.2 km/sec).

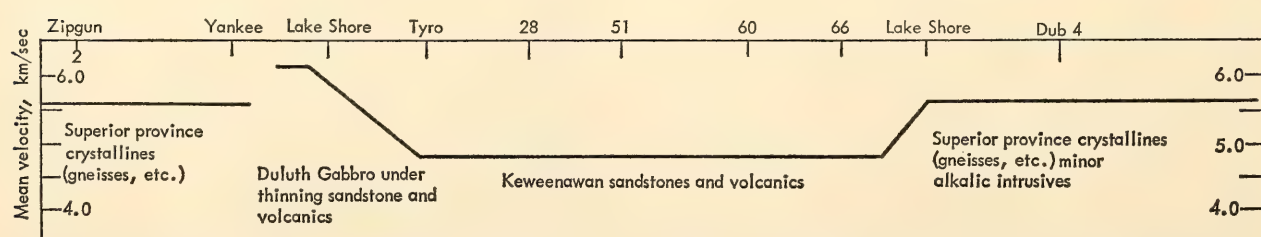


Fig. 14. Velocity values along Duluth–Otter Cove profile used to derive depths for  $P_1$  time terms.

*Discussion.* The velocities measured in this area are unusual in several respects. First, the measured crustal velocities in that portion of the crust below the basement complex are higher than those measured elsewhere in North America. Velocities of 6.6–6.7 km/sec are appropriate to a basic assemblage of minerals. Gabbro, for example, would be the likely candidate for a rock having these velocities (Birch, 1960).<sup>5</sup> The only other continental areas for which such high velocities have been reported so near the surface are in Arkansas where velocities of about 6.6 km/sec were observed at depths greater than 10 km and on the Keweenaw Peninsula (Steinhart and Meyer, 1961).<sup>6</sup> Of the rock exposed at the surface, only the Duluth Gabbro could be expected to have such a high velocity. Although it outcrops on the western end of the lake, no geological opinions known to the authors have been expressed that it occupies the whole of the Lake Superior basin. There can be no question, however, but that such high velocities exist at shallow depths beneath Lake Superior.

Horizontal changes in velocity are to be expected in an area of this size and were, in fact, observed even in the time-term analysis between the western and eastern half of the lake. The large-scale averaging of the time terms produces precise mean velocities. Most of the other techniques, although they are capable of more localized measurements, were not precise enough in this experiment to resolve the local variations. Somewhat larger lateral changes are required to connect these velocity measurements with the older measurements in central Minnesota, north central Wisconsin, and Ontario. Just how or where the transition occurs cannot be decided from the data at hand, although we feel that because of the localized nature of the unusual crustal structure, these horizontal transitions quite possibly occur near the edges of the deep depression in the crust found

in Lake Superior. To account for the mantle velocities no particular horizontal change is required from the seismic data, although a small lateral difference in the upper mantle is required to account for the gravity anomalies. The agreement between these and adjacent seismic measurements of  $P_n$  velocity is excellent. Our calculated  $P_n$  velocity is 8.07 km/sec and the measurements in Wisconsin and upper Michigan gave 8.04 and 8.08, respectively, while in central Minnesota Tuve and Tatel found 8.1 km/sec (*Year Book 52*, p. 104). These numbers differ by less than one per cent, but such close agreement may be fortuitous. The change required to account for the gravity anomalies is about one per cent. The variation of velocity of depth in the area is uncertain.

The apparent velocity analysis above indicates modest increase of velocity with depth in the uppermost 15–20 km, especially in the western portion of the lake. There is no compelling evidence for higher velocity intermediate layers, although some indication of higher velocities (6.95–7.2 km/sec) was found from the examination of later arrivals on the travel-time plots. The possibility of the existence of a low-velocity layer within the crust cannot be dismissed. If such a low-velocity layer exists it must occur at depths of more than 20 km, or we would expect to see a shadow zone for  $P_1$  arrivals. Further, if a low-velocity layer of any substantial thickness is introduced, difficulties in reconciling the observed gravity anomalies become still greater. The latitude given in the range of mean crustal velocities in Fig. 15 would permit a modest low-velocity layer within the crust, and the depths to the M would still be within the shaded band.

Comparison of the techniques of determining the crustal structure provides some ideas about which features of the structure are required by the data and which are produced by the analysis. It is clear, for example, that the standard



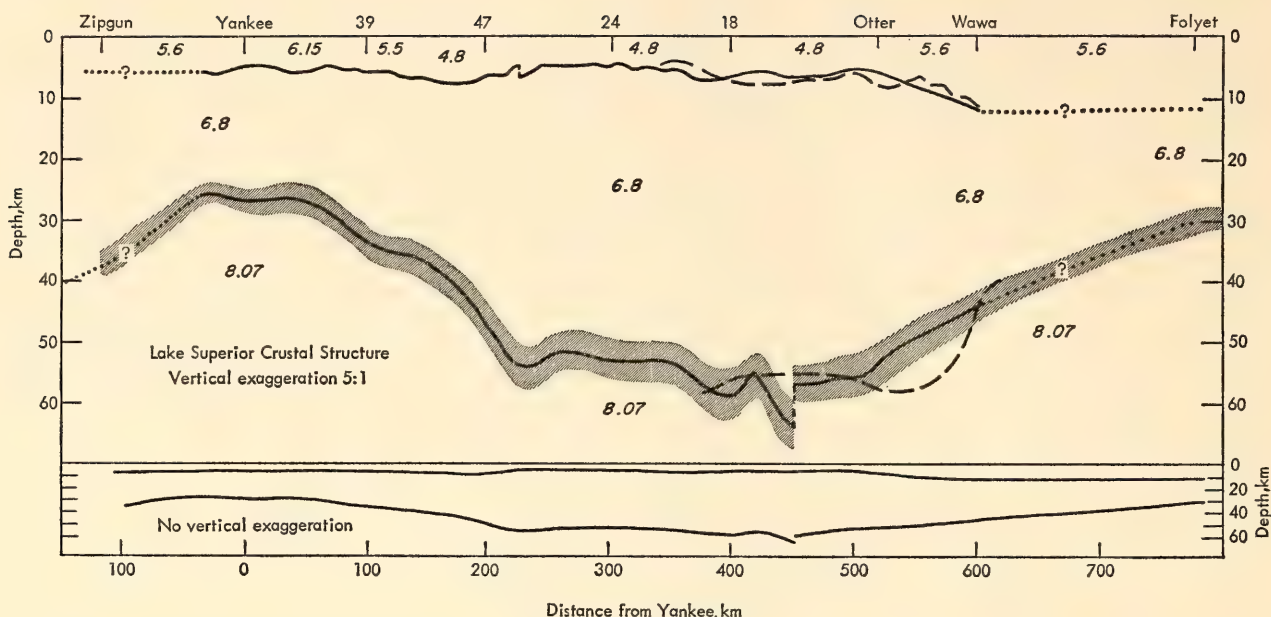


Fig. 15. Structure along Lake Superior profile. Locations at the top are keyed to Fig. 1. Dashed lines in the eastern lake are for the Keweenaw-Wawa profile.

reverse-profile method provides poor results in an area where structure is as complicated as at Lake Superior. The methods employing the apparent velocities were somewhat disappointing in yielding a velocity depth function, but the dips and depths obtained from apparent velocities shown in Fig. 12 correspond rather well to the time-term structure shown in Fig. 15. This technique seems to be a valuable adjunct to time-term analysis both because it employs some data independent of those used in time-term analysis and because the data used in both analyses are treated quite differently. To the extent that we must admit a certain amount of subjectivity to enter into our determination of the structure, it is advisable to try several methods in which the subjective contributions are different. On the whole, the time-term analysis produces the most interesting and detailed picture in the M discontinuity we have yet seen. As shown above, the structures are required by the data, even though some of them violate the formal assumptions of time-term analysis.

From our experiment we have the following facts: Crustal velocities are unusually high, especially in the upper portion of the crust; the crust is very

thick, and the structure exhibits considerable fluctuation from place to place; and the upper mantle velocities are normal. We must conclude further that this area at present is in isostatic balance or if not, that it will remain permanently out of balance. The evidence of other geophysical techniques contributes little to our understanding of the area. Heat-flow measurements by Birch (1954)<sup>7</sup> indicate normal heat flow for shield areas, and recent measurements by Hart and Steinhart (*Year Book 63*, pp. 326-328) in Lake Superior produce somewhat lower values that are accompanied by various uncertainties. Regional aeromagnetic coverage of part of the area has been completed (Wold, 1965),<sup>8</sup> which shows mostly that the geology of the rocks under the lakes is rather uniform horizontally and seems to indicate some basement fault structures. The fault structure shown in the basement from the time-term analysis is in an appropriate location to be considered an extension of the Douglas fault zone, as shown on the tectonic map of the United States. In the base of the crust we have drawn as a fault the abrupt change of the elevation of M discontinuity in the eastern part of the lake; it could possibly be a smooth but rapid

change. Its location can be correlated with the extension of the Keweenaw fault, but we know of no reason why the Keweenaw fault should find expression at the base of such a thick crust.

The structure of the crust under Lake Superior as revealed by this experiment is striking. In one region of relatively small dimensions we find both the thickest crust and nearly the thinnest crust observed on the North American continent, which, from classical geological hypotheses, is unexpected. Previous observations in the Canadian Shield areas have been almost monotonously similar. The Lake Superior basin itself is not a very impressive topographical feature: The maximum water depths are about 0.4 km, and the total relief from the deepest part of the lake basin to the surrounding higher lands is less than 1 km. Geological work in this area continuing for nearly 100 years has shown that the tectonic events are of Precambrian age, and isotopic age determinations indicate that no significant orogenic events have occurred in the last 1,000 m.y.

Van Hise and Leith (1911)<sup>9</sup> many years ago hypothesized that Lake Superior is a compressional feature of Precambrian tectonics. If this were so, one might expect to find normal or somewhat low-velocity crustal materials underlying the lake depression. We have shown that the reverse is true, and we suggest that Lake Superior may instead be a tensional feature in which the crust is made up of basic material somehow abstracted from adjacent areas or the mantle beneath. It does seem that the mantle has some special connection with the crust in Lake Superior. As shown in the data given by Steinhart (1964),<sup>4</sup> various stations of the Vela Seismological Center recorded these one-ton shots at distances ranging up to 2,500 km, and the amplitude obtained at these distances was far in excess of amplitude usually obtained under the circumstances; thus transmission of energy from Lake Superior into the mantle to distant stations is especially efficient. The reverse is

not true; that is, shots fired 2,500 km away from Lake Superior and recorded near, but not in Lake Superior, do not exhibit large amplitudes. The simplest explanation for the phenomena is that there is something anomalous about the structure beneath the lake.

We conclude that the crust is thick because the isostatic adjustment to the high-density crustal rocks would produce such depression and the initial sinking of the heavy crustal section. Just how an initial accumulation of basic rocks could have occurred we do not know, but the depression in the crust disappears to the southwest in the direction of the mid-continent gravity high, and to the east generally toward the northern part of Lake Huron. It would be interesting to conduct further experiments to see what connection this unusual crustal section may have to the mid-continent gravity high, to the Lake Huron basin, and to the Grenville province to the east. Conceivably, we could be confronted with a rift structure of Precambrian age, a sort of fossil rift.

#### EARTHQUAKE STUDIES

*I. S. Sacks, M. A. Tuve, R. Sumner,\* S. Suyehiro,† R. Cabre, S. J.,‡ and J. Careaga‡*

*Diffraction P-wave studies of the earth's core and lower mantle.* Observations of both spectral amplitude and velocity of *P* waves diffracted around the earth's core have indicated that the core must be larger than has been thought.

*Amplitude.* Further studies of the spectral behavior of *P* waves at distances between 70° and 165° have confirmed that the shadow boundary of the core is near 96°, rather than at 105° as has been assumed. A shadow boundary between 94° and 100° was suggested (*Year Book 63*, p. 300) from preliminary

\*Carnegie Institution Fellow; from University of Wisconsin.

†Carnegie Institution Senior Fellow; from Meteorological Research Institute, Tokyo, Japan.

‡Observatorio San Calixto, La Paz, Bolivia.



studies. Figure 16 shows the ray paths considered. Additional *P*-wave observations in the distance range of  $90^{\circ}$ – $100^{\circ}$  were obtained from records of the worldwide *Vela* network and from the three temporary tape-recording seismographs operated by R. Sumner in Peru for his study of absorption in the crust and upper mantle. Spectral analysis of the *Vela* records suggested a core boundary between  $96^{\circ}$  and  $98^{\circ}$ . The tape stations were fortunately situated with respect to the Alaskan earthquake of March 28, 1964, at distances of  $95.9^{\circ}$ ,  $96.5^{\circ}$ , and  $97^{\circ}$ . Some of the amplitude results are shown in Fig. 17. A shadow boundary between  $96^{\circ}$  and  $96.5^{\circ}$  is probable. Following the calculations of Jeffreys (1939),<sup>10</sup> this boundary location is compatible with a core radius of 3,550 km.

*Velocities.* An earlier determination

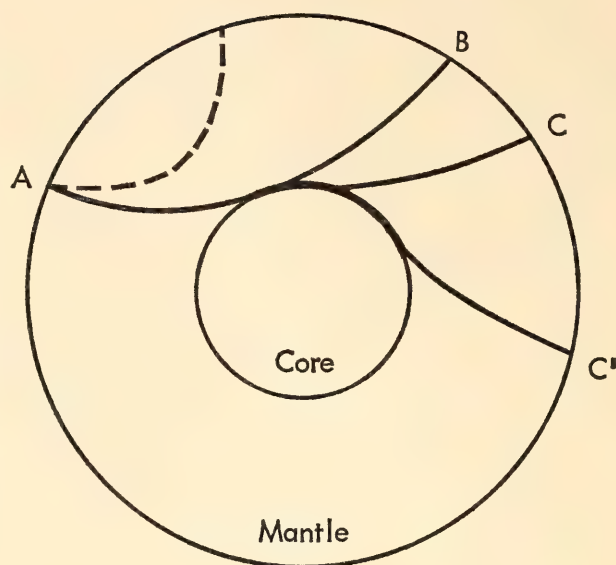


Fig. 16. The ray paths of direct and diffracted *P* waves. Distance at which the ray just grazes the core *AB* has been found to be  $96^{\circ}$ . Velocity at base of mantle can be determined from the difference in arrival time between stations *C* and *C'* since the mantle paths are identical.

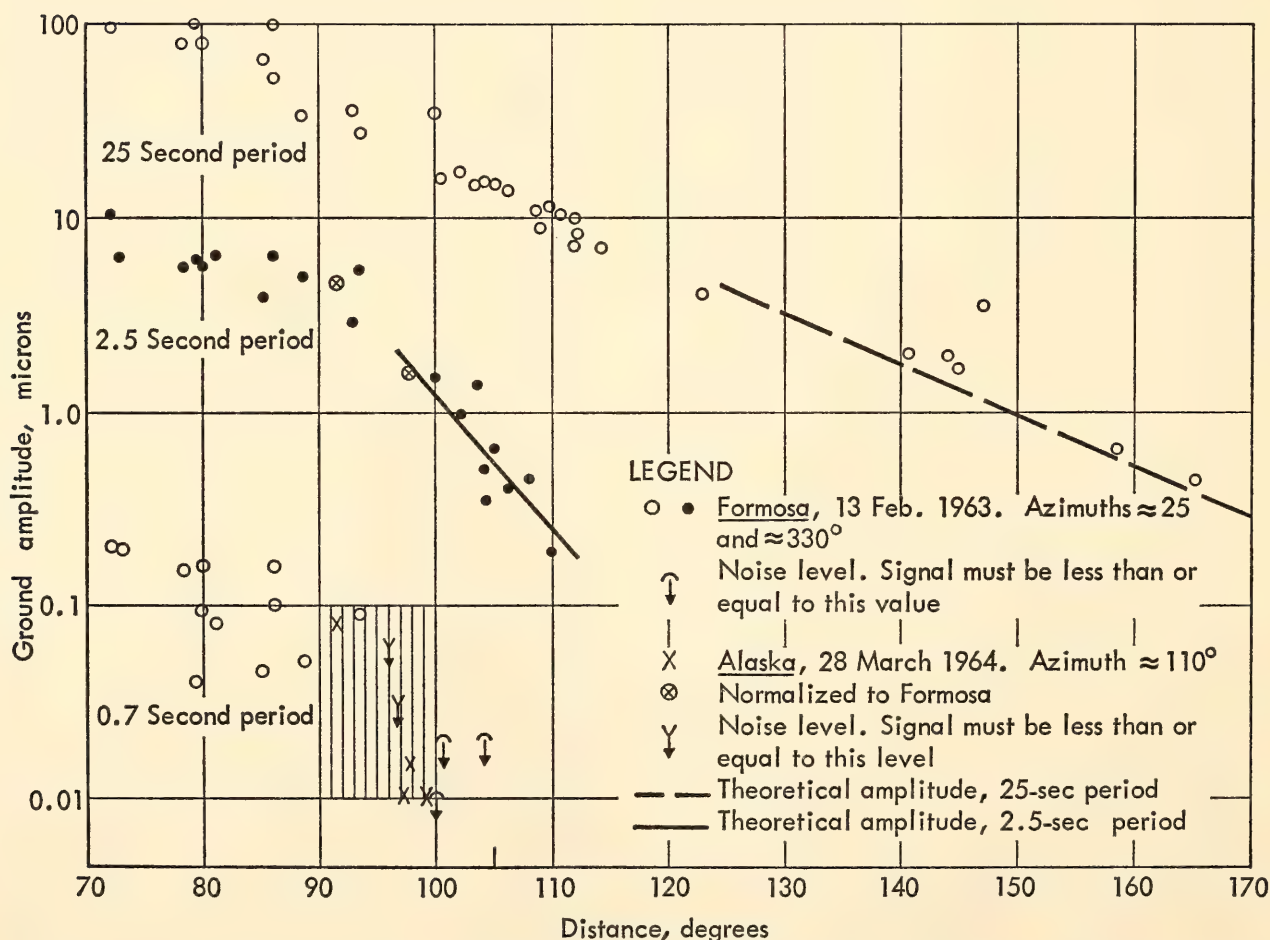


Fig. 17. Amplitudes of arrivals along same great circle paths at different periods, 25, 2.5, and 0.7 sec. Sharp decrease in amplitude of the 0.7-sec arrivals beyond  $96^{\circ}$  is due to shadow of earth's core. Agreement of amplitudes of 25- and 2.5-sec waves with theory suggests that diffraction adequately describes the behavior of these arrivals and therefore there are probably no strong velocity gradients or reversals near the mantle-core boundary.

of the velocity at the base of the mantle from diffracted *P* waves (*Year Book 63*, p. 300) had shown incompatibility with the accepted Jeffreys' core size of 3,473 km and lower mantle velocity of 13.62 km/sec. As shown in Fig. 18, the core size and lower mantle velocity may be determined from the phase velocity of diffracted waves measured at the earth's surface, and the Herglotz-Wiechert solution of the earth's structure derived from *P*-wave travel times. Onset times of diffracted *P* waves at great distances can be determined with limited accuracy because of the long-period nature of the arrivals, the shorter periods having been attenuated by the diffraction process (Fig. 19). However, since only relative arrival times are required for velocity determination they can be obtained with great accuracy by simple cross-correlation techniques, provided that only arrivals along great circle paths are compared. Figure 19 also shows the reduced travel times from two earthquakes which generated substantial long-period *P*-wave energy. The scatter is due to irregularities

in the transmission path, since the cross-correlation techniques give a relative timing accuracy of better than 0.5 second.

The velocity obtained from these results ( $24.55 \pm 0.08$  km/sec) combined with Jeffreys' determination of mantle structure gives a core size of  $3,537 \pm 9$  km (Fig. 18). This result is essentially the same as that obtained independently by means of the shadow-boundary determination. Both results, however, rely on the Herglotz-Wiechert solution of a *P*-wave travel-time curve. The calculated depth of penetration of any ray is sensitive to relatively small differences in  $dt/d\Delta$ , where  $t$  is the travel time of the ray at an epicentral distance  $\Delta$ . However, since the integrated value of  $dt/d\Delta$  is found to be essentially constant over the whole mantle (i.e., the travel time to  $96^\circ$ ), there is a functional relation between the lower mantle velocity and the depth of penetration for the slightly different integration paths used by various workers in this field. Figure 20 illustrates this relation. *P* travel-time curves giving deep ray penetrations will also give high

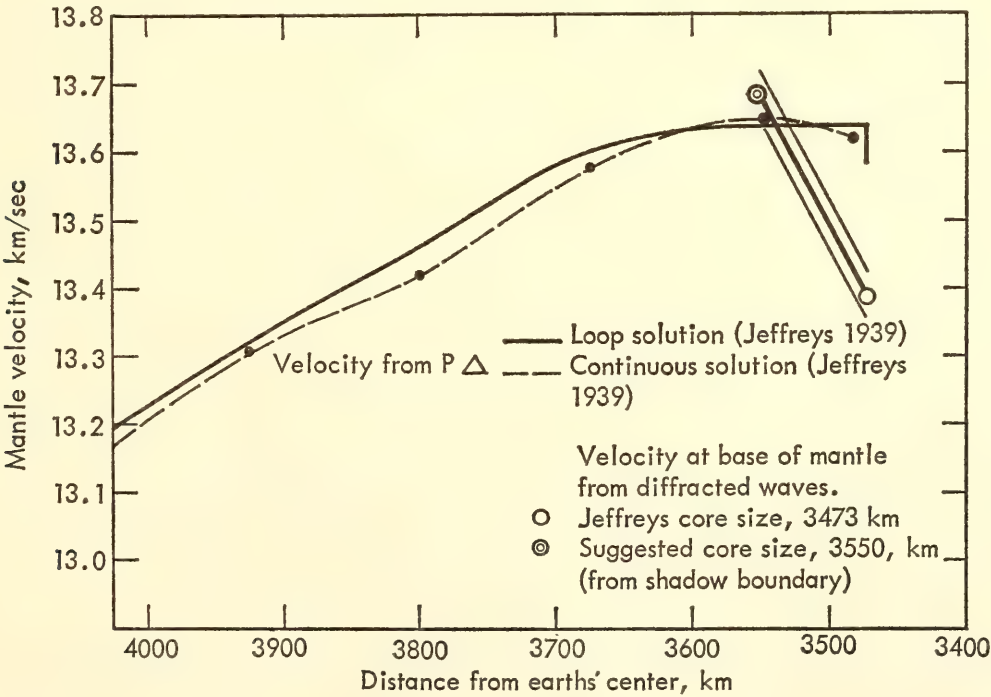


Fig. 18. Jeffreys' velocity-depth structure of lower mantle. Range of mantle velocities and core radii satisfying the diffracted waves and their probable errors is also shown. Intersection of this line and Jeffreys' Herglotz-Wiechert solution determine core radius as  $3,537 \pm 9$  km. Probable error indicated does not include uncertainties in Jeffreys' determination.



velocities in the region of deepest penetration, i.e., the base of the mantle in this study. The intersection of the best line through the various velocity-depth points

and the diffracted wave velocity gives both the velocity at the base of the mantle and the size of the core (Fig. 20). The resultant core radius is 3,553 km and the

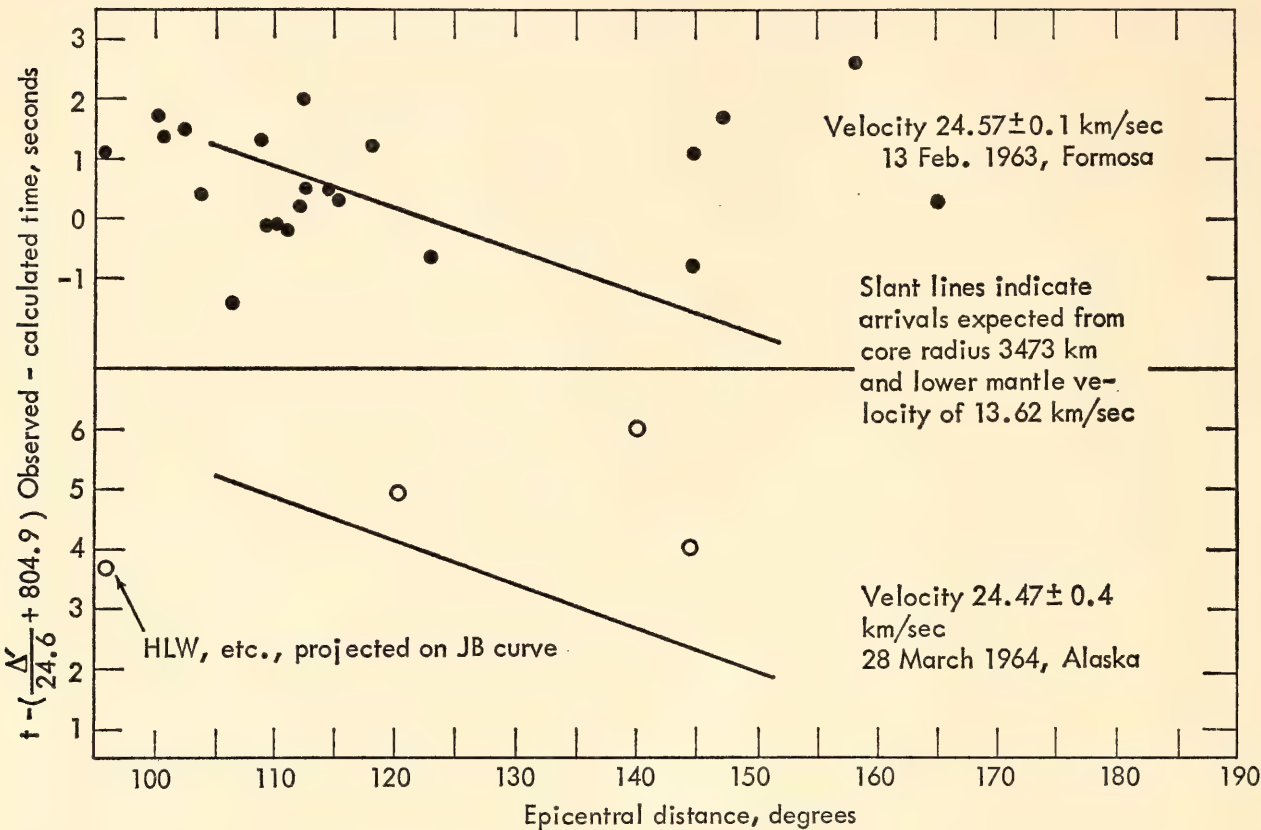


Fig. 19. Reduced travel times of diffracted *P* waves. Arrivals are clearly incompatible with Jeffreys' model core radius and lower mantle velocity.

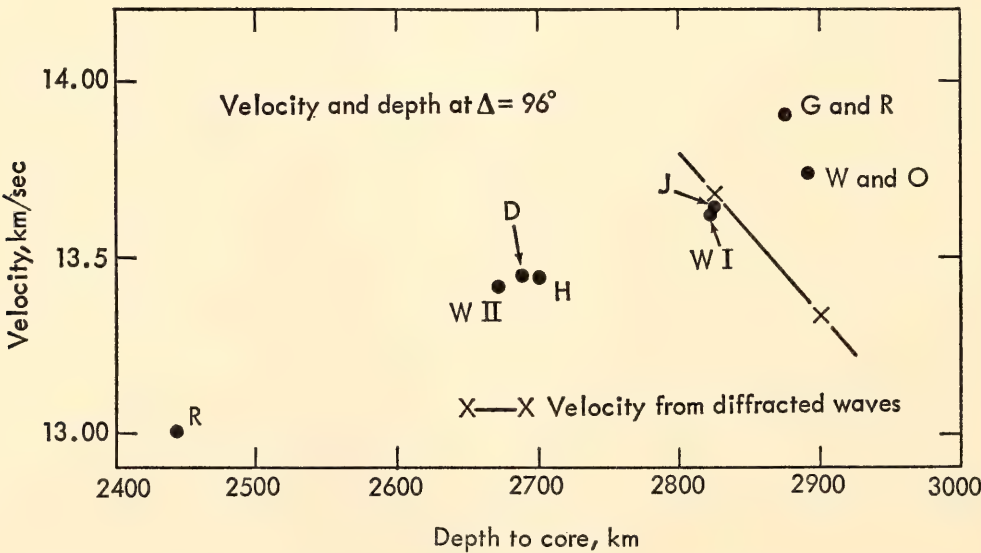


Fig. 20. Depth of penetration and lower-mantle velocity from waves at epicentral distances of 96°. Determinations shown are by Repetti, Witte I, Dahm, Hodgson, Witte II, Jeffreys, Gutenberg and Richter, and Wadati and Oki. Core radius and lower-mantle velocity are obtained from intersection of best line through the Herglotz-Wiechert solutions and range of velocities satisfying diffracted wave arrivals as measured at earth's surface. This velocity for any core radius is  $V_{\text{core}} = V_{\text{surface}} \times [(\text{radius core})/(\text{radius of earth})]$ .

velocity at the base of the mantle is 13.69 km/sec. It is suggested that this value ought to be adopted for the core radius in place of the earlier value of 3,473 km. It should be noted that the value of using both the shadow boundary and the phase velocity of diffracted waves to determine the core size and lower mantle velocity is that the result is not sensitive to small deviations or errors in the *P* travel-time distance curve.

*Rigidity.* The three-dimensional model

study results of Rykunov (1957)<sup>11</sup> showed that the amplitude decrease of diffracted waves was particularly sensitive to the rigidity of the core. Fig. 21 shows model study results (equivalent to the earth) compared with diffracted waves from a large earthquake. All the results lie within a region bounded by rigidity  $\mu = 0$  and  $\mu = 10^8$  dynes/cm<sup>2</sup>. The rigidity of the core must therefore be less than  $10^8$  dynes/cm<sup>2</sup>. The absence of any dispersion over the period range 2–60 sec indicates an uncomplicated lower mantle without

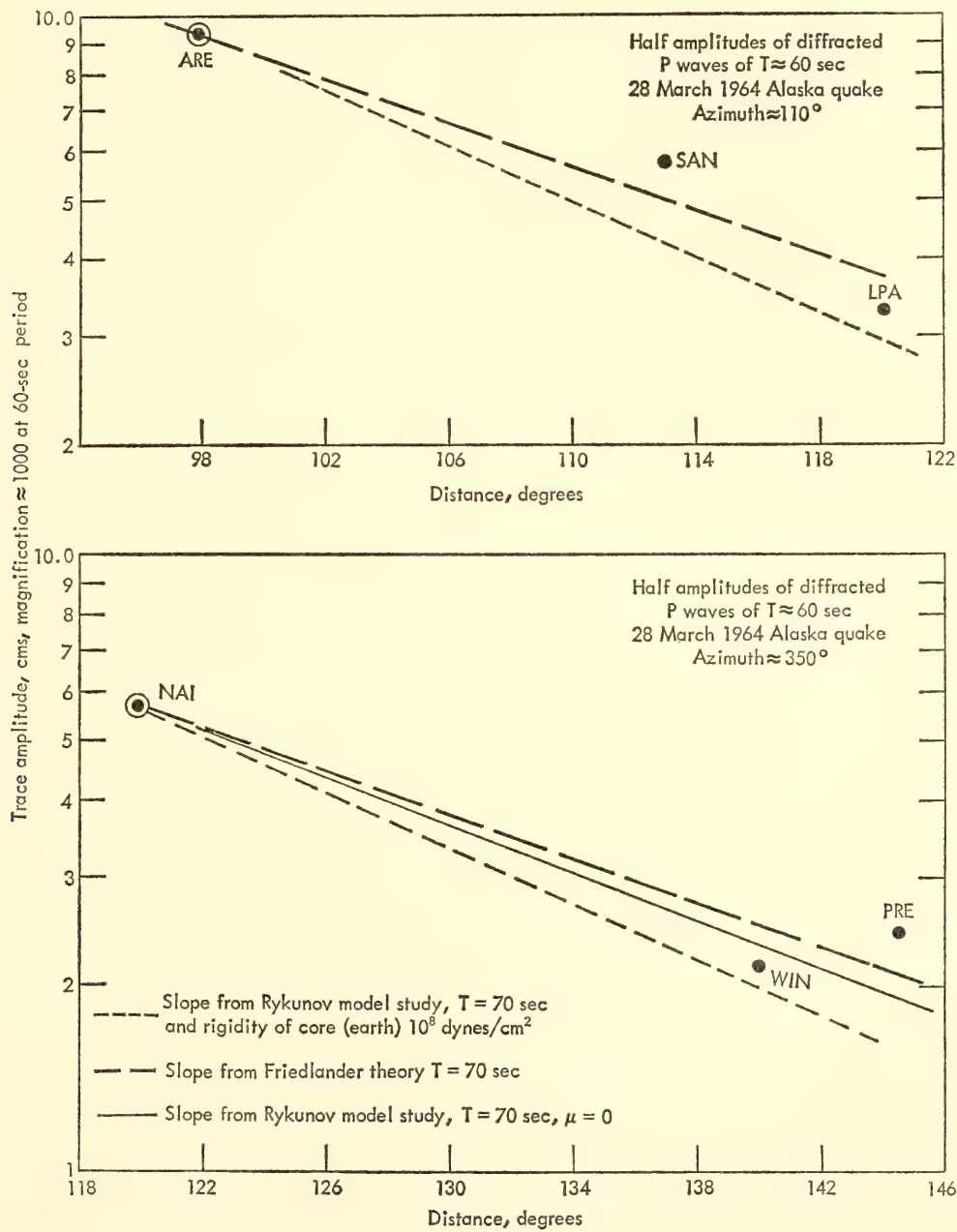


Fig. 21. Model results (Rykunov, 1957) and theoretical results compared with earthquake data. Results along two great circle paths are shown. Earthquake data suggest core rigidity less than  $10^8$  dynes/cm<sup>2</sup>.



any strong velocity gradient or low-velocity layers. Any diffusion of core material into the mantle must be rather limited, therefore, and may be less than 10 km in extent if it exists at all.

*Aftershocks and foreshocks in the relation of magnitude to frequency of occurrence for the 1960 Chilean earthquake.* The coefficient  $b$  in Gutenberg-Richter's equation  $\log N = a + bM$ , which represents the relation between frequency of earthquake occurrence and magnitude, is an important factor for the study of seismicity. Some difference in the value of  $b$  is seen among various seismic regions, and there have been many discussions of the significance of the difference. As far as the seismic activity in the same region is concerned, however, the coefficient seems unchanged in time including both ordinary and aftershock activities, according to sensitive observations made repeatedly in the same region.

When a small perceptible earthquake occurred only 18 km from a tripartite seismic net of high sensitivity in central Japan, a fairly large number of foreshocks were recorded as well as many aftershocks, and much difference was found (Suyehiro, Asada, and Ohtake, 1964)<sup>12</sup> between 25 foreshocks and 173 aftershocks in the relation of frequency of occurrence and magnitude. For that study the ratio of small foreshocks to large foreshocks was smaller than the same ratio in the aftershocks; i.e., the coefficient  $b$  is 0.35, which is abnormally small, for the foreshocks, and 0.76, which agrees well with that of the ordinary activity in the region, for the aftershocks (Fig. 22).

Many earthquakes in different parts of the world are reported to have been preceded by foreshocks but for lack of nearby sensitive stations little data have been available for study. The Chilean earthquake of 1960 was, however, exceptionally large, and many foreshocks and aftershocks were reported on the basis of teleseismic observations by the U.S. Coast and Geodetic Survey (USCGS) and the

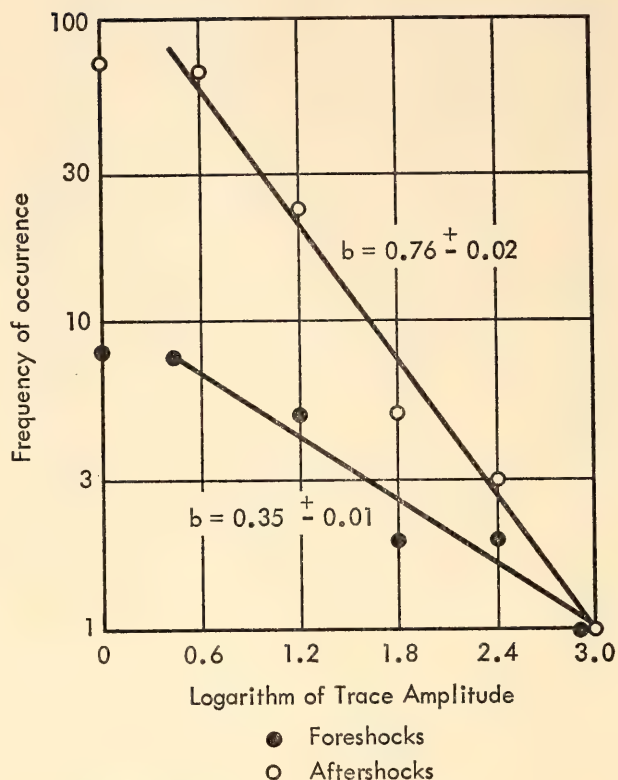


Fig. 22. Frequency of occurrence vs. logarithm of trace amplitude in foreshocks and aftershocks accompanying perceptible earthquake in Japan.

Bureau Central International Séismologique. From the published reports of these organizations, such difference in  $b$  was also found likely.

An investigation has been carried out to find the characteristics of the foreshocks for the Chilean earthquake of 1960, using the seismograms of four sensitive stations of the USCGS, namely, Eureka and Tucson to the north of the foreshock and aftershock region, and Byrd and South Pole to the south of the region.

*Location of foreshocks and aftershocks and estimation of magnitude.* According to the epicenters reported by the USCGS, the present foreshock and aftershock activity took place in a region from 71° to 77°W longitude and 37° to 48°S latitude. To locate as many foreshocks and aftershocks as possible in the region, in addition to those already reported, the difference of arrival times at the four stations was used.

As a measure of magnitude, the trace amplitude of *P* wave by vertical Benioff seismograph was used at the Tucson telemetering station where the record was available for all earthquakes except three large foreshocks, the trace amplitude of which was estimated from the record of a seismograph of lower sensitivity. The trace amplitude at other stations, as mentioned previously, was used for a further confirmation of the correspondence of earthquakes among the four stations. Assignment of magnitude itself was not made because only the relative comparison between the groups of foreshocks and aftershocks of one large earthquake was studied.

Most foreshocks were located near the northern edge of the quadrant region, whereas the aftershocks were more widely scattered, as shown in Fig. 23. The epicentral distance to Tucson, at which the standard trace amplitude was measured, ranges from  $76^{\circ}$  to  $85^{\circ}$ . No correction, however, was made on the trace amplitude according to the change in epicentral distance, for such a slight change at this distance would not appreciably affect the trace amplitude.

*Relation between frequency of occurrence and magnitude for the foreshocks and aftershocks.* The question arises as to whether it is adequate to consider the present earthquakes as a sequence of foreshocks, main shock, and aftershocks. The following facts are considered important: (1) The shock of 19h 11m 17s on May 22 was outstandingly larger by one or more in magnitude than the rest. (2) Although most shocks before the largest one occurred on the northern side, they shared the region with the shocks occurring after the largest one, as shown in Fig. 23. The present shocks can well be separated from the background activity, as will be shown. It will, therefore, be reasonable to assume that the initial breakage indicated by the foreshocks started near the northern end of the region, the main fracture developed

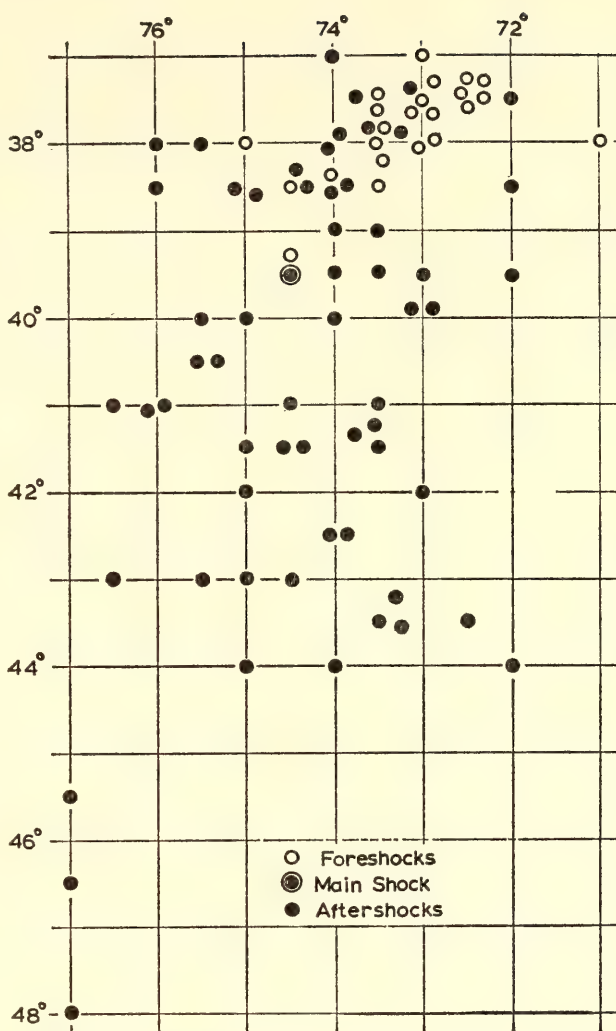


Fig. 23. Epicenters of foreshocks in period 33 hours before, and aftershocks after main shock of great Chilean earthquake of 1960 reported by USCGS.

to the south by the main shock, and the aftershocks took place all over the region.

The next question will be: When did the foreshock activity begin and when did the aftershock activity come to an end? The first question is easily answered; the beginning of the foreshock activity was undoubtedly sudden. As for the aftershock activity, only the period of the first 33 hours after the main shock, which is equal to the period of the foreshock activity, was taken into consideration.

Figure 24 shows the epicenters located in and near the southern part of South America reported by the USCGS in a period of six years from January 1954 to March 1960; the region indicated by the



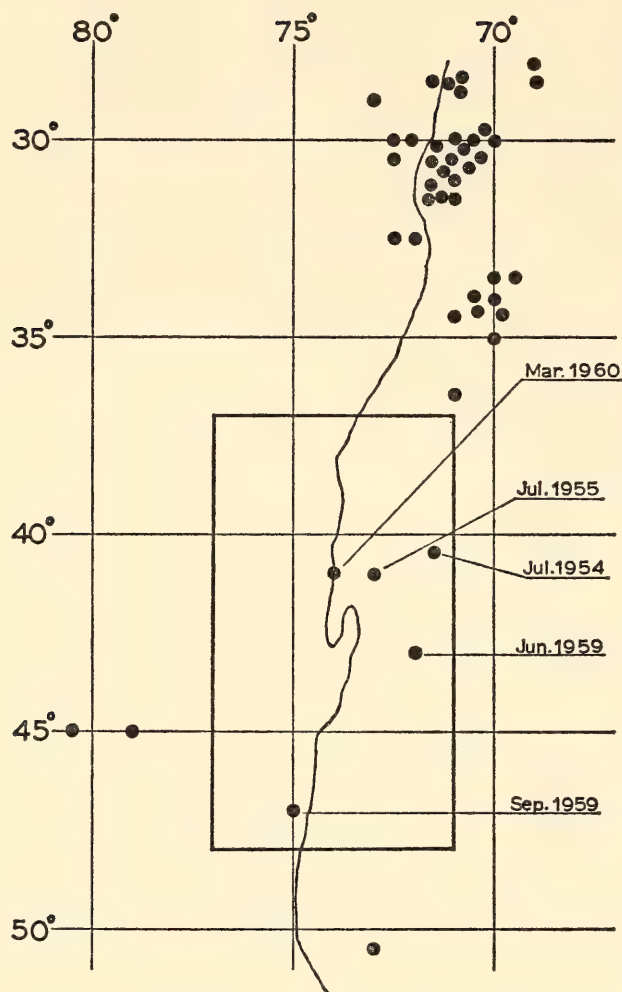


Fig. 24. Epicenters in southern part of South America reported by USCGS, Jan. 1954 to March 1960.

rectangle is of the present foreshocks and aftershocks. The ordinary seismicity in the region is much lower than in the other regions, the last shock reported in the region occurring about two months before the Chilean earthquake. In a period of 48 hours before the first reported foreshock no shocks could be

located in the region by the present method. The foreshock activity, therefore, probably started with the largest foreshock. Had it been preceded by small shocks, they would have been too small to contribute to the present statistics. For counting frequency of occurrence a logarithmic class interval of trace amplitude was employed which is more or less similar to the class interval by magnitude. The lowest level was set to 2 mm, above which no earthquakes could possibly be missed. The frequency of occurrence thus counted is given in Table 2.

The result is graphically presented in Figs. 25 and 26. The rates of increase in frequency of occurrence with decreasing magnitude in the foreshock and aftershock activities were calculated by the least squares with probable error as follows:  $b = 0.55 \pm 0.5$  for the foreshocks, and  $b = 1.13 \pm 0.04$  for the aftershocks.

Obviously a difference exists between the rates of frequency of occurrence with decreasing magnitude of the foreshocks and aftershocks. The cumulative frequency shows, furthermore, that the difference is not only in the rate of increase in the frequency of occurrence but in the frequency of occurrence itself; in other words, the frequency of occurrence is almost the same for larger shocks both in the foreshocks and aftershocks, but for smaller shocks a much higher frequency of occurrence is seen in the aftershocks in the same period of time, 33 hours.

*Discussion.* In the present case the

TABLE 2. Frequency of Occurrence with the Logarithmic Class Interval of Trace Amplitude

Class Interval, mm in trace amplitude	Foreshocks		Aftershocks	
	Frequency	Cumulative Frequency	Frequency	Cumulative Frequency
2-4	13	31	71	122
4-8	7	18	31	51
8-16	4	11	13	20
16-32	3	7	7	7
32-64	2	4	0	0
64-128	2	2	0	0

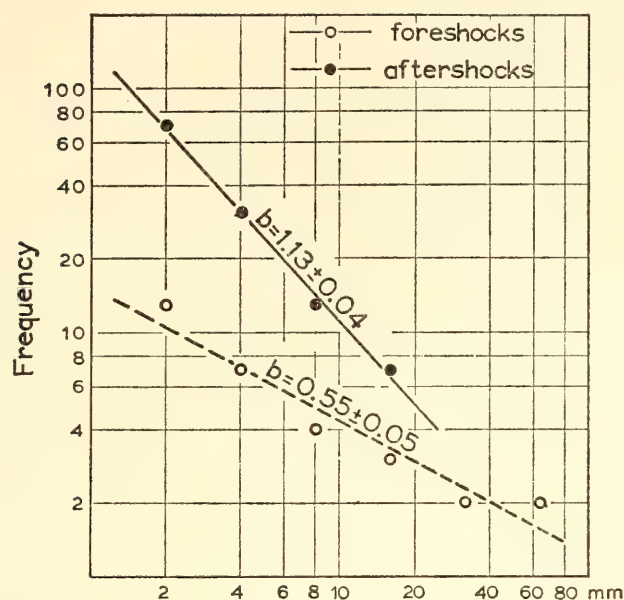


Fig. 25. Relation between frequency of occurrence and trace amplitude.

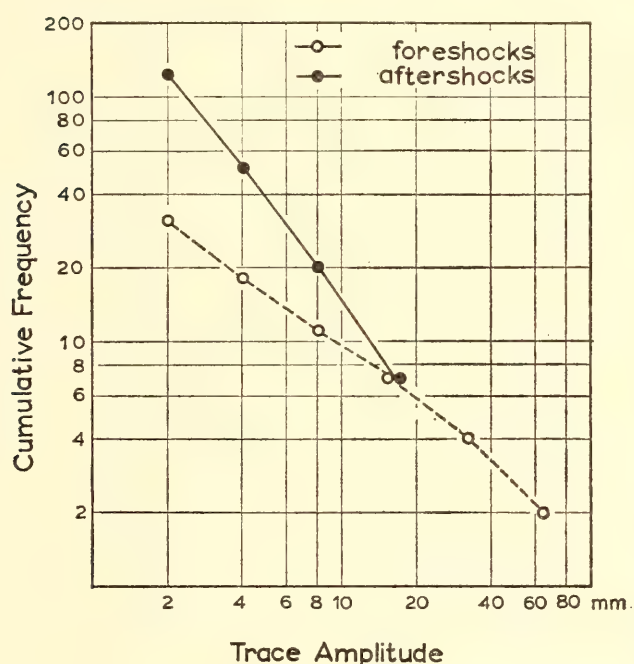


Fig. 26. Relation between cumulative frequency of occurrence and trace amplitude.

magnitude of the main shock and the region of the foreshocks and aftershocks are both of the largest scale, yet interesting comparisons may be made with the small shock that took place in Japan:

1. *Duration of foreshock activity and its beginning.* It is not certain whether the duration of foreshock activity depends on the magnitude of the main shock as it generally does in the after-

shock activity. Two examples are too scanty to be a basis for generalizations. An interesting point is that in both cases the foreshock activity started with one of the larger shocks.

2. *Difference of  $b$  between foreshocks and aftershocks.* It must be considered whether the difference is significant or not. According to Gutenberg and Richter (1954)<sup>13</sup> different values of  $b$  are assigned to comparatively large earthquakes in different seismic regions, ranging from 0.6 to 1.3. On the other hand, Suzuki (1959)<sup>14</sup> claimed virtually the same  $b$  value for both ordinary and aftershock activities in different seismic regions and, having studied small earthquakes, he showed how much the  $b$  value could fluctuate in the statistical process.

As to the Japanese foreshock activity, a number of sensitive observations had been repeatedly made in the region before the event, and the value of  $b$  had always fallen between 0.7 and 0.9 even where the total number of earthquakes was less than 50. The value of 0.35 obtained for the foreshocks deviates greatly from the established value of  $b$  in the region. Especially in comparing the foreshocks and aftershocks, the difference was found with the same mode of class interval and recording system; when the same period was considered before and after the main shock, large shocks occurred with almost the same frequency, whereas small earthquakes occurred more than six times more frequently in the aftershocks than in the foreshocks.

Similar comments can also be applied to the Chilean earthquake except for the regional seismicity of small earthquakes, data for which are not available. Therefore, the validity of the difference between the foreshock value of  $b$  and that of the aftershock sequence is better substantiated than in the mere comparison among  $b$  values obtained in different ways as to class interval, observation system, period, magnitude range, and so forth.

*Conclusions.* Some difference seems



probable in the manner of occurrence between foreshocks and aftershocks. No conclusion should be drawn at this moment, but in view of a possibility that the difference of *b* could serve for earthquake prediction much effort should be made to accumulate more information along this line. Two actions will be suggested: (1) Further laboratory experiments like the one made by Mogi (1963),<sup>15</sup> which demonstrated a possible difference in the value of *b* between foreshocks and aftershocks, should be pursued. (2) Observations should be made of high sensitivity in the regions where earthquakes are reported to have been preceded by foreshocks, preferably array observations, which are capable of locating epicenters and are easier to operate than multiple stations.

*Attenuation of P waves along the western*

*flank of the Andes.* The attenuation of longitudinal (*P*) waves generated by local shocks in southern Peru has been studied with three seismic stations equipped with identical vertical component seismometers (*T*<sub>0</sub> = 3.7 sec) and tape recorders located along the western flank of the Andes. The tape stations (SH, AT, and PV) and the epicenters of the 34 shocks used in the attenuation study are shown in Fig. 27. The shocks were recorded during March and April 1964 (*Year Book 63*, p. 304). Six tape-recorded earthquakes, located by the USCGS, were used to determine relative station effects.

Tapes were replayed through filters in several frequency bands to obtain maximum and average amplitude spectra (1½ to 27 c/s) for the first second of the *P* phase. The spectrum at each distant station (AT, PV) was normalized to the

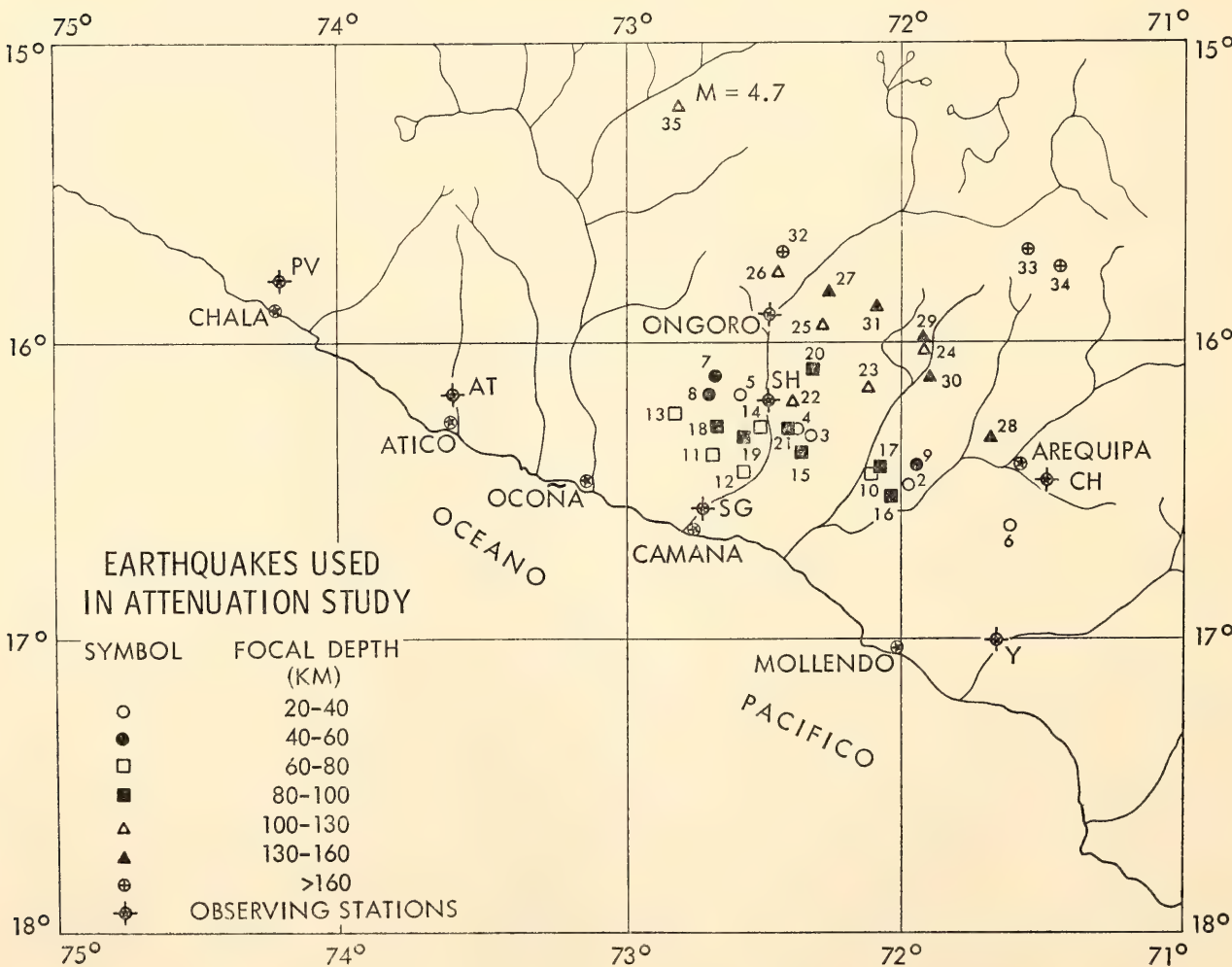


Fig. 27. Earthquakes used in attenuation study.

spectrum at the near source station (SH) and spectral amplitude ratios  $\exp [R(f)]$  were measured. In the analysis it was assumed that (1) each spectral amplitude contains the attenuation factor  $\exp (-\pi f D/QV)$ , where  $f$  = frequency,  $D$  = hypocentral distance,  $V$  = mean velocity of  $P$  waves, and  $Q$  = specific attenuation factor; and (2) other frequency-dependent factors cancel in the spectral amplitude ratios. The  $D/V$  difference in  $R(f)$  was replaced by the difference in  $P$  arrival times,  $\Delta t$ .  $Q$  was computed from the least-squares slope of the  $R$  versus  $f$  points. In combining maximum or average amplitude data from more than one shock or from the two station pairs (AT-SH and PV-SH) the  $\Delta t$  for each set of data was used as a weight function because the uncertainty in each computed  $Q$  is inversely proportional to  $\Delta t$ :  $dQ = Q^2 dR/\pi \Delta f \Delta t$ , where  $dR$  is the estimate of the mean uncertainty in the  $R$ s and  $\Delta f$  is the bandwidth.

Figure 28 shows the weighted means of maximum and average amplitude (squared) data points and the computed  $Q$  values for the focal depth range 20–183 km. From the computed  $Q$  values shown, uncorrected for relative station effects, and from the study of relative station effects, the conclusions about  $Q_p$  as a function of frequency are:

1. *For 1½–15 c/s.* The mean of the computed  $Q$  values, maximum and average amplitude data, is 580 in the frequency band 1½ to 10 c/s. However, results of the several methods used to determine relative station effects clearly indicate that the computed  $Q$ s are too small and that  $Q_p$  is greater than  $1 \times 10^3$ . The lower limit for  $Q_p$  of  $1 \times 10^3$  would require that the computed correction be in error by a factor of 4, which is considered unlikely. The computed values of  $Q$  in the frequency band 10–15 c/s are  $\gg 1 \times 10^3$ , with large uncertainties. Relative station effects account for the abnormally high values, but  $Q_p$  remains greater than  $1 \times 10^3$ . Therefore, the results of the study show that, for the

crust and uppermost mantle along the western flank of the Andes,  $Q_p$  is greater than  $1 \times 10^3$  in the frequency range 1½ to 15 c/s. The magnitude of  $Q_p$  indicates that the shape of the particle velocity spectrum for  $P$  waves in this band changes only very slightly with distance from the focus.

2. *For 15–17 c/s.* It was found that, for frequencies higher than 15 c/s, the frequency-dependent attenuation of  $P$  waves increases markedly. Relative station effects were found to be negligible in this frequency range.  $Q$  values computed separately for the two station pairs agree within limits of uncertainty. The increase in attenuation was observed for each focal depth range studied. The values computed from the combined data, for focal depths between 20 and 180 km, are given in Table 3.

TABLE 3. Values for 20–180 Km Focal Depths

Band, c/s	$Q_p$	90 % CL	Amplitude
16–27	720	240	maximum
15–27	560	140	average
21–27	590	330	maximum
19–27	400	110	average

The following evidence indicates that scattering, rather than anelasticity, is the principal loss mechanism more than 15 c/s:

1. Mean values of  $Q_p$  are smaller for the band 20–27 c/s than the band 15–27 c/s. Therefore,  $1/Q_p$  may be proportional to a higher power of frequency than the first.

2. The values of  $Q_p$  from average amplitude data are smaller than values of  $Q_p$  from maximum amplitude data.

3. Higher frequency energy appears to be progressively delayed with distance from the source in comparison with lower frequency energy (pseudo dispersion).

To study the possible variation of  $Q_p$  with depth, maximum and average



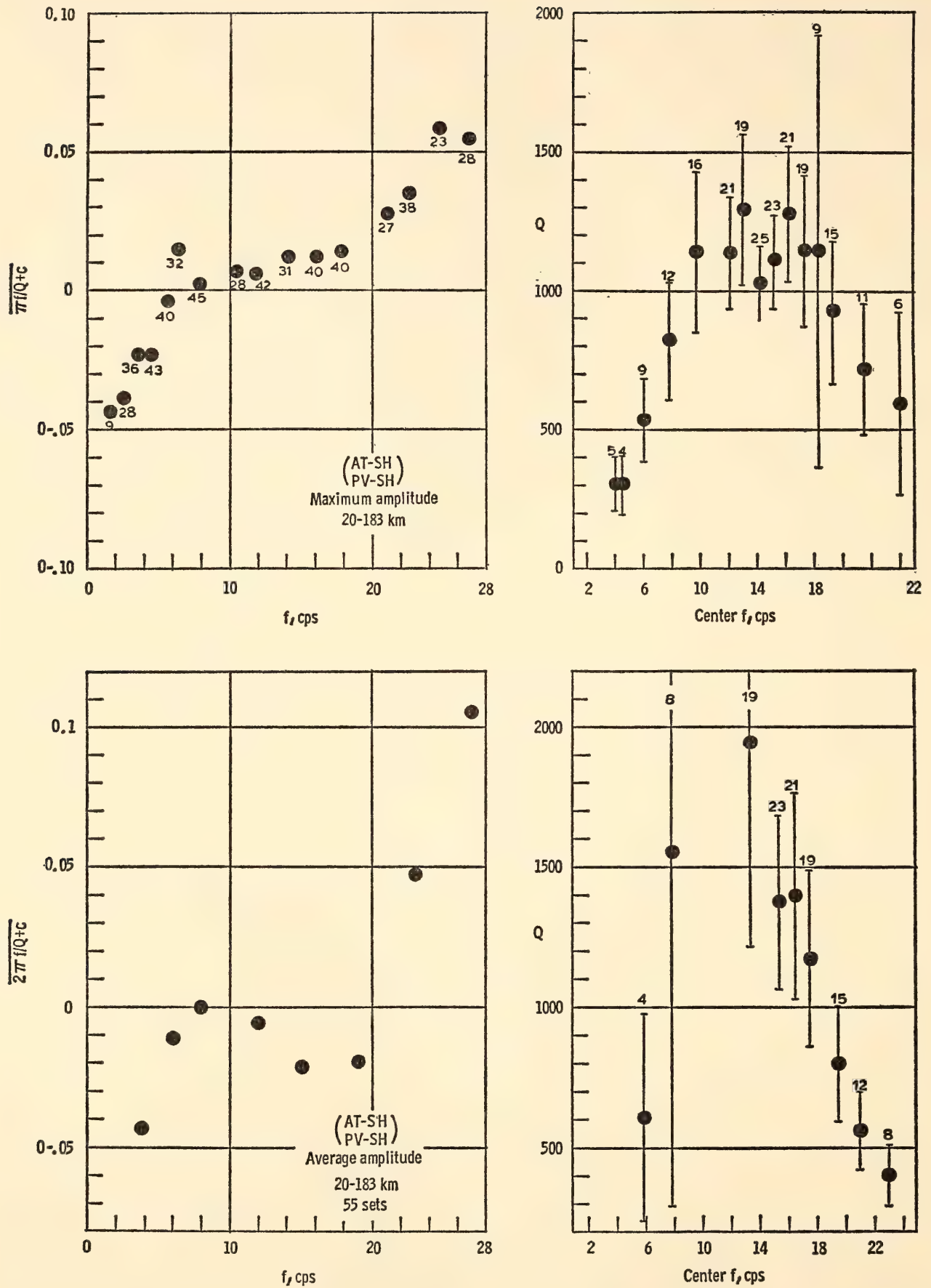


Fig. 28. Weighted mean data points and computed  $Q$  vs. center frequency results. Bandwidths (c/s) indicated over 90% confidence limit bars. Decrease in computed  $Q$  below 10 c/s is due to relative station effects. Decrease in  $Q$  over 15 c/s is attributed to scattering effects.

amplitude data for both station pairs were grouped into seven focal depth ranges and  $Q$ s were computed for a number of frequency bands. Thus, for each focal depth range and frequency band four values of  $Q$  were obtained. For the frequency band 15–27 c/s, where scattering effects prevail, the computed  $Q$ s show no significant variation with focal depth, suggesting that the effective inhomogeneity of the crust and uppermost mantle does not diminish significantly with depth down to 180 km.

For the frequency band  $11\frac{1}{2}$ –27 c/s the computed values of  $Q$  and their relative uncertainties show a minimum in the focal depth range 80–130 km. To test whether the apparent relative minimum in  $Q_p$  (80–130 km) is significant it is necessary to take into account the  $\Delta t$ s for the data used, since, if relative station effects are large compared to attenuation effects, the quantity  $\Delta t/Q$  will be approximately constant for all sets of data. For three focal depth ranges, 0–80, 80–130, and 130–180 km, the weighted mean logarithms of the spectral amplitude ratios at 27 c/s with respect to  $11\frac{1}{2}$  c/s ( $\bar{R}$ ) and standard deviations ( $\sigma_r$ ) were computed, where  $\bar{R}$  and  $\sigma_r$  are defined by

$$\bar{R}(1.5, 27) = \pi(27 - 1.5) / \left( \sum w_i Q_i / \Delta t_i / \sum w_i \right)$$

$$\sigma_r^2 = \sum w_i (R_i - \bar{R})^2 / \sum w_i$$

where  $R_i(1.5, 27) = \pi(27 - 1.5) \Delta t_i / Q_i$  and  $w_i = 1/90$  per cent confidence limit of  $Q_i$ .

In Fig. 29  $\bar{R}$  for the three focal depth ranges is plotted as a function of  $\bar{\Delta t}$ , the mean  $P$  arrival-time difference, and the corresponding value of  $\bar{Q}$ , where  $\bar{Q}$  is related to  $\bar{R}$  and  $\bar{\Delta t}$  by

$$\bar{R} = \pi(27 - 1.5) \bar{\Delta t} / \bar{Q}$$

Figure 29 shows that the zone 80–130 km is relatively more lossy for  $P$  waves than the zone from the surface to 80 km and that the attenuation may diminish again below 130 km.

*Seismic refraction south of La Paz, Bolivia.* We have done two parallel studies

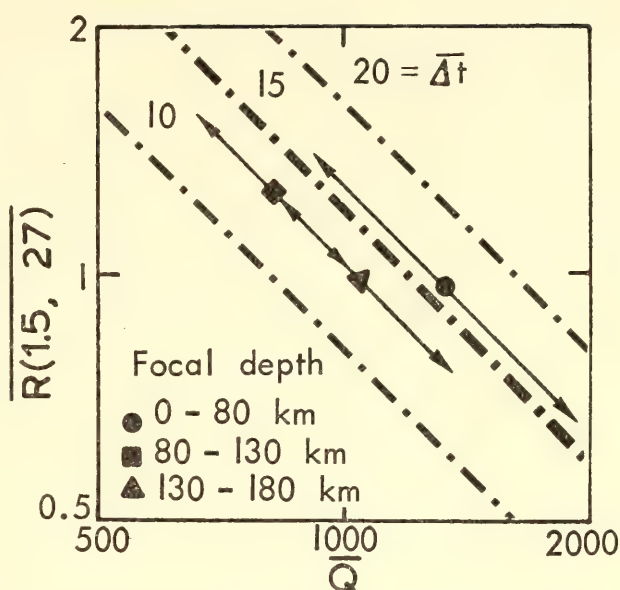


Fig. 29.  $\bar{R}(1.5, 27)$  as function of  $\bar{\Delta t}$  for three focal depth ranges. Error bars show relative uncertainty.  $\bar{Q}$  is related to  $Q_p$  by  $\bar{\Delta t}/\bar{Q} = \Delta t/Q_p + \beta$ , where  $\beta$  is correction for relative station effects.  $\beta$  is known to be positive for the data used. If  $\beta$  is identical for the three sets of data, the figure shows that  $Q_p$  has a relative minimum in the depth range 80–130 km.

of the velocity of seismic longitudinal waves in the upper mantle and the delay time of the  $P_n$  phase for two seismic stations near each other: La Paz (LPB of the USCGS standard network)  $16^\circ 31' 58''$ S,  $68^\circ 05' 54''$ W, 3.29 km above sea level (asl); and Desaguadero of the Andes network of the Carnegie Institution  $16^\circ 13' 54''$ S,  $68^\circ 30' 48''$ W, 3.805 km asl. Most of the foci used in this study lie between the meridians  $66^\circ$ W and  $71^\circ$ W and the parallels  $17^\circ$ S and  $25^\circ$ S. They were located by the USCGS and by the Antofagasta (Chile) networks. We have used 57 locations for the LPB records and 27 for Desaguadero.

We have plotted only the epicenters located at 320 km–1,120 km from the LPB and Desaguadero stations. The seismic under study occurred between February 1963 and June 1964. The method is similar to that used by J. Santa Cruz and R. Cabre, S.J., described in "Refraction profile in the central Andes northwest of La Paz" in *Year Book 63* (p. 309). For the calculations, data showing a discrepancy of more than eight



seconds with respect to the central line—obtained graphically—have been considered inconsistent. The results from both stations, compared with those previously obtained, are quite concordant. The comparison of  $P_n$  wave velocities may be summarized as follows:

1. R. Cabre, S.J., and J. Santa Cruz at La Paz, northwest  
 $V = 8.25 \pm 0.22$  km/sec  
 Delay time was  $8.65 \pm 2.39$  sec
2. R. Anzoleaga at La Paz, south  
 $V = 8.36 \pm 0.29$  km/sec  
 Delay time was  $9.9 \pm 2.7$  sec
3. R. Cabre, S.J., and J. Careaga at La Paz, south  
 $V = 8.03 \pm 0.33$  km/sec  
 Delay time was  $5.13 \pm 3.54$  sec
4. R. Cabre, S.J., and J. Careaga at Desaguadero, south  
 $V = 8.18 \pm 0.49$  km/sec  
 Delay time was  $6.55 \pm 5.06$  sec

Nine of the seisms studied in LPB records have been located at the same time by the USCGS and Antofagasta. For seven of them, the locations of the two centers correspond to points more than 100 km apart; but surprisingly the representative points on the travel-time curve were coherent in both locations; if we assume that nearby stations offer greater guarantee for an exact location, this would confirm the Antofagasta network suggestion that in the USCGS a systematic error might have been introduced because of the uneven distribution in azimuth of the teleseismic stations looking at this region.

Of the points plotted from USCGS locations, 28— or 90 per cent of those used—are in agreement; of those plotted from locations of the Antofagasta network 29— or 72 per cent—are in agreement.

In Desaguadero, because of interruptions with operation of the station or the slowly emergent beginning of the seism, we have operated with one half of the data available in Seguencoma (LPB). Four of these seisms were located jointly by the USCGS and Antofagasta.

## ISOTOPE GEOLOGY

*S. R. Hart, L. T. Aldrich, G. R. Tilton,\* G. L. Davis,\* T. E. Krogh,† and M. Yamaguchi.‡*

*Rb/Sr geochronology in the Grenville province of Ontario.* The Grenville province of the Canadian Shield is a region of high-grade metamorphic rocks extending from Georgian Bay on the east to the Labrador coast. It is bounded on the southeast by the St. Lawrence River and on the northwest by the Grenville front, a major fault commonly associated with a metamorphic transition. Both the more ancient basement (2,400–2,700 m.y.),<sup>16</sup> and the younger fold belts (with granites 1,500 and 1,750 m.y.)<sup>17, 18</sup> of the Superior province to the northwest have been truncated by this major structural feature, and although certain metamorphic equivalents of the older rocks are recognized south of the front, mica K-Ar ages in the Grenville province with few exceptions yield values of  $900 \pm 200$  m.y.

Before the present investigation whole rock isochron ages of about 2,700 and 2,400 m.y. have been determined in granite bodies lying 1 and 10 miles south of the front near North Bay, Ontario. Further, the earlier studies showed extensive granite emplacement into the typical Grenville sediments of southeastern Ontario at 1,000 to 1,100 m.y. ago.<sup>19</sup>

The investigation was initiated to evaluate the whole rock method for the detection of premetamorphic history. The region lying 0–100 miles south of the Grenville front, where typical Grenville sediments are rare or lacking, was studied. The rocks analyzed were collected from homogeneous granitic bodies which are foliated and hence are probably pre-tectonic or syntectonic (Fig. 30).

\*Geophysical Laboratory; Carnegie Institution.

†Carnegie Institution Fellow; from Massachusetts Institute of Technology, Cambridge.

‡Carnegie Institution Fellow; from Kyushu University, Fukuoka, Japan.

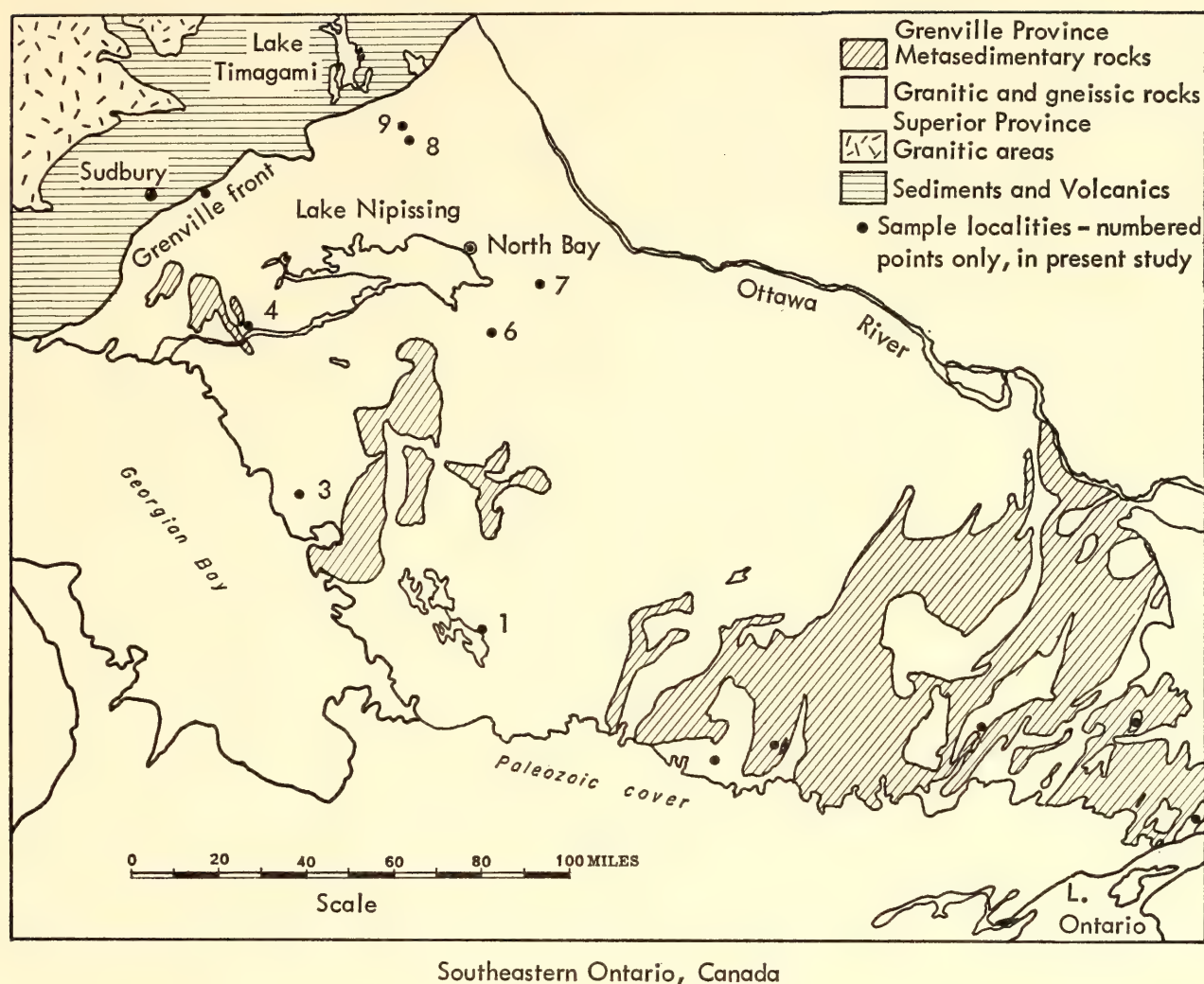


Fig. 30. Sample locations of rocks used in Grenville province study.

Figure 31 summarizes the results obtained including analytical data, the reference isochrons, and the distance of sample localities southeast of the Grenville front. An isochron for 1,100 m.y., the oldest granitic rock found in the southeastern Grenville area, is drawn to an initial ratio of 0.705 to allow a comparison of the two regions. In the southern region initial ratios for granitic rocks range from 0.704 to 0.7055, whereas marbles and gabbros have values of 0.705 and 0.703, respectively. Older rocks would probably have slightly lower initial ratios unless they were derived at least in part from preexisting sialic material. Granites sampled at localities 1, 3, 6, 7 (Fig. 30) were either emplaced about 1,400 m.y. ago with initial ratios close to 0.705, or about 1,100 m.y. ago

with initial ratios ranging from 0.708 to 0.713 (see Fig. 31). Allowing for a reasonable variation in initial ratio, the granites sampled at location 4 have an age of 1,600–1,800 m.y. and those at location 9, 2,200–2,500 m.y.

*Conclusions.* Granitic emplacement north of the Grenville front at 2,400, 1,750, and 1,500 m.y. have been determined by other workers in relatively unmetamorphosed regions. A comparison of these ages with those of the present determinations suggests that the whole rock system has remained essentially closed during the extensive regional metamorphism that reset some of the mineral ages in the area about 1,000 m.y. ago. Furthermore, the rocks studied lie in an area that extends for 120 miles into the Grenville metamorphic



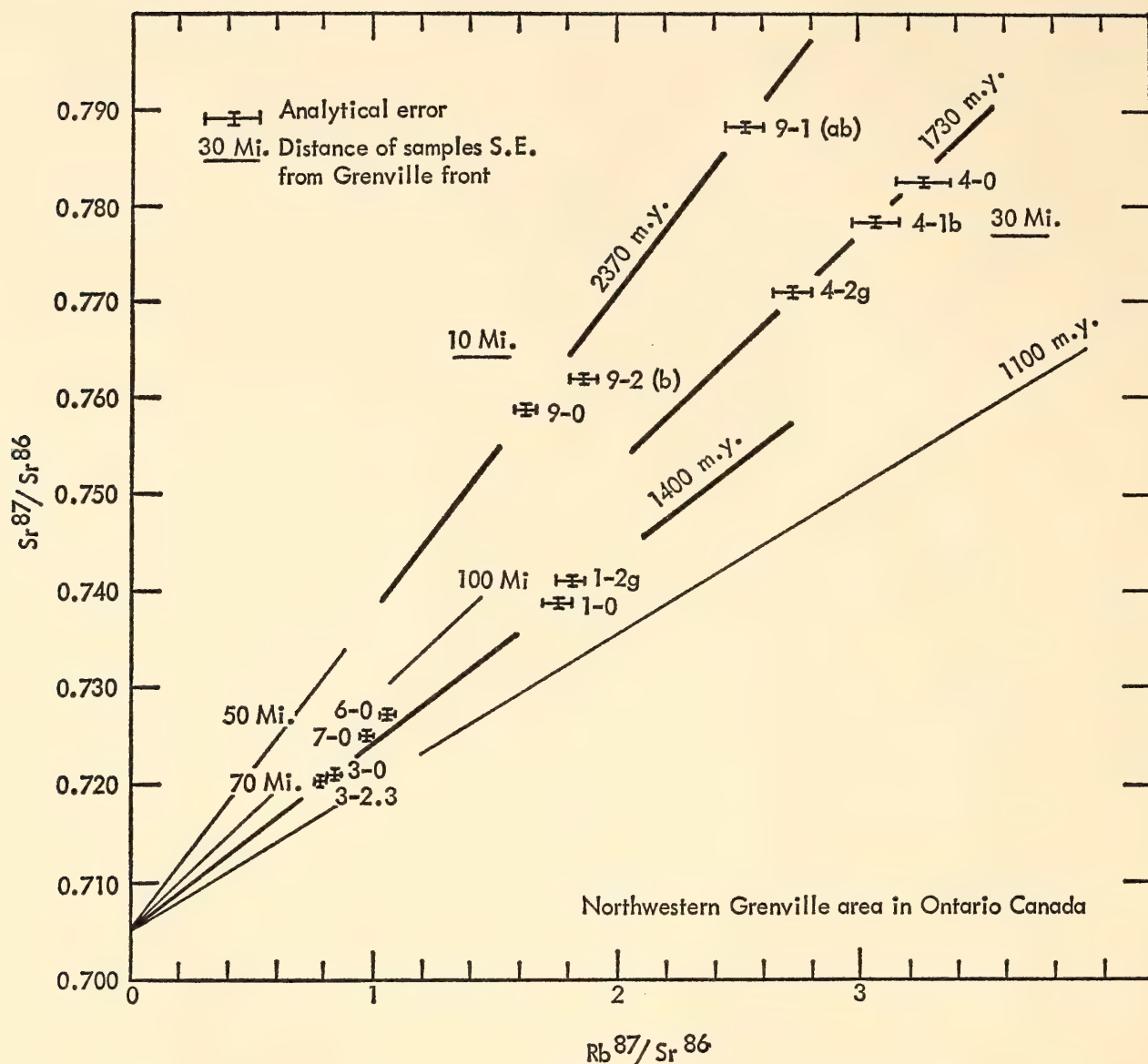


Fig. 31. Isochrons for rocks inside Grenville province. Note that all data points are above 1,100-m.-y. isochron. This is evidence of the history prior to 1,100 m.y.

region, to no more than 60 miles from the areas where granitic rocks were emplaced 1,000 to 1,100 m.y. ago. Further isochron studies and zircon investigations of selected granitic bodies are now under way to test this hypothesis.

*Excess radiogenic argon in rocks and minerals.* Radiogenic argon in excess of that produced by the *in situ* decay of potassium was first reported by Aldrich and Nier<sup>20</sup> for the mineral beryl. Damon and Kulp<sup>21</sup> reported a similar phenomenon in beryls, tourmaline and cordierite. Later work that we and others have done has shown that excess argon may also be present in pyroxene, quartz,

and fluorite. Because excess argon is a source of error in the K-Ar method of age determination, we have attempted to place limits on how much excess argon may be present in micas and other layered silicates. We have also tried to understand the way in which the excess argon is held in the various minerals. Finally, we have attempted to make use of this general phenomenon to learn more about the argon content of the mantle and the extent to which the mantle has been degassed.

Table 4 gives results of argon determination on a group of micas from Chester, Massachusetts. The muscovite

TABLE 4. Mica K-Ar Ages, Chester, Massachusetts

Rock	Mineral	K, %	Ar <sup>40</sup> *, cc/g	K-Ar Age, m.y.
Savoy schist	Muscovite	4.98	$7.18 \times 10^{-5}$	330
Rowe schist	Biotite	3.51	$4.80 \times 10^{-5}$	315
Emery deposit	Margarite	0.0515	$6.66 \times 10^{-7}$	300
Emery deposit	Chlorite	0.0021	$\leq 4.7 \times 10^{-8}$	...

and biotite ages place the time of the last metamorphism in the area at about 320 m.y. The margarite is a structural analogue of muscovite but depleted about a hundredfold in potassium, and for this reason any excess argon would show up readily in this mineral. In fact, the margarite age agrees within experimental error with the metamorphic age of the biotite and muscovite. From this we conclude that micas formed under metamorphic conditions similar to these will probably have less than  $6 \times 10^{-8}$  cc/g of excess argon. In a biotite this amount of excess argon would cause an error in the age of about 0.2 m.y.

A chlorite coexisting with the margarite was also analyzed. Since chlorite has a sheet structure similar to the micas, its ability to trap excess argon may also be similar. Because the potassium content of this chlorite was only 20 ppm, no radiogenic argon was detected. However, an upper limit on possible excess can be placed at  $3 \times 10^{-8}$  cc/g, a limit somewhat lower than that placed on margarite.

In earlier work, we found that the excess argon in quartz and fluorite was contained in fluid inclusions from which it could be completely released by heating briefly at 600°C–700°C. To find out if pyroxenes react similarly, a test (Table 5) was run on a pyroxene from Bear Moun-

tain, N.Y., previously shown to contain a large excess of argon. It has an apparent K-Ar age of 10,000 m.y. Heating at 910°C released only 14 per cent of the argon, which may be contained in very small fluid inclusions that do not decrepitate at 910°C. It is more likely, however, that the excess argon in pyroxenes is contained not in fluid inclusions but in much smaller structural defects. Similar evidence for the mineral olivine was obtained on material from a dunite nodule from recent Hawaiian lavas. The sample was supplied by E. Roedder of the USGS, who observed that about half the visible fluid inclusions were released by heating to 1,050°C. The sample clearly contains excess argon as shown by its 3,000-m.y. apparent age (Table 5). Heating at 1,080°C, however, released only three per cent of the argon from the sample, indicating that the argon in olivine is also more tightly held than the bulk of the fluid inclusions. The last sample in Table 5 is a granite xenolith from the young volcanics of Ascension Island, also supplied by Roedder. He noticed abundant fluid inclusions in both the quartz and feldspar and found that heating to 800°C was sufficient to release most of the visible inclusions. Our argon measurements give a K-Ar age of only 1.2 m.y., so there is no obvious content of excess argon indicated. Heating at 830°C released only

TABLE 5. Tests for Argon in Fluid Inclusions

Locality	Sample	K, %	Ar <sup>40</sup> *, cc/g	K-Ar Age, m.y.
Bear Mountain, N.Y.	Pyroxene	0.0086	$9.7 \times 10^{-6}$	10,000
Hualalai, Hawaii	Dunite nodule	0.0020	$5.5 \times 10^{-7}$	3,000
Ascension Island	Granite xenolith	5.73	$2.8 \times 10^{-7}$	1.2



10 per cent of the radiogenic argon, again showing that the argon is not contained in the visible fluid inclusions.

The data on the Hawaiian dunite nodule suggest that such nodules are not completely degassed while being brought to the surface in the molten lava. The nodules are believed to be either fragments of mantle or later crystal accumulates derived from settling in a magma chamber. In either event their depth of origin is probably subcrustal, and the gas they contain probably originates at similar depths. If ultramafic nodules originate in the mantle their argon content then should reflect the state of degassing of the mantle. To pursue this approach we analyzed other oceanic ultramafic samples—several additional nodules from Hawaii, two peridotites from St. Peter and St. Paul's Rocks on the mid-Atlantic ridge, and serpentinites dredged from the mid-Atlantic ridge and the Puerto Rico trench (Table 6).

The serpentinites contained no detectable argon, suggesting either that they represent a truly young material or that the process of serpentization is sufficient to expel any preexisting argon. The upper limit of radiogenic argon in the trench serpentinite was placed at  $4 \times 10^{-9}$  cc/g, which corresponds to a K-Ar age of less than 8 m.y. for this sample. This suggests that the Puerto Rico trench is a rather young feature, contrary to some of the present theories of ocean basin evolution.

The two pyroxenite nodules from

Hawaii contain rather high contents of radiogenic argon, and give apparent K-Ar ages of 1,900 and 1,500 m.y. The two peridotites from St. Peter and St. Paul's Rocks have argon contents essentially the same as the Hawaiian nodules. In addition, these two samples have potassium contents differing by a factor of 10, but with no corresponding variation in argon content. This shows that the argon is in some sense "excess," and that the apparent ages of 350 m.y. and 2,000 m.y. are not necessarily meaningful ages for the St. Paul's peridotite. It is the similarity in argon content of such widely separated occurrences as those of Hawaii and St. Paul's that is striking. Are we looking at a background level of argon that has been redistributed throughout the phases of the upper mantle? If so, we can estimate the degree to which the upper mantle has been outgassed. A 4,500-m.y. mantle with a potassium content of 500 ppm would contain about  $4 \times 10^{-5}$  cc/g of radiogenic argon. The ultramafics in Table 6 average about  $2 \times 10^{-6}$  cc/g, only five per cent of that for a hypothetical closed-system mantle. According to this argument, either the ultramafics themselves or their source regions have been rather well outgassed. In the coming year we intend to extend our coverage of argon in ultramafics to other oceanic localities, to see how general the phenomenon may be.

*Tracer studies of rocks from the Cascade Range, Washington (in collaboration with*

TABLE 6. Radiogenic Argon in Oceanic Ultramafics

Locality	Sample	K, %	Ar* <sup>40</sup> , cc/g	K-Ar Age, m.y.
Puerto Rico trench	Serpentinite	0.0125	$<3.9 \times 10^{-9}$	<8
Mid-Atlantic ridge	Serpentinite	...	$<1.2 \times 10^{-8}$	...
Salt Lake Crater, Hawaii	Pyroxenite	0.0190	$2.51 \times 10^{-6}$	1,900
	Hornblende- pyroxenite	0.0117	$2.03 \times 10^{-6}$	1,500
St. Peter and St. Paul's Rocks	Peridotite	0.0099	$1.37 \times 10^{-6}$	2,000
	Hornblende- peridotite	0.128	$1.95 \times 10^{-6}$	350

C. A. Hopson and A. C. Waters, *University of California, Santa Barbara*). The radioactive decay of the long-lived isotopes of uranium, thorium, rubidium, and potassium provides the basis for determining mineral ages and, from these, the times of crystallization or metamorphism of rocks. The decay of these radioactive elements can provide useful geological information in other ways. For example, uranium, thorium, and rubidium are continually producing natural tracers through characteristic labeling of their daughter isotopes of lead and strontium. The isotopic composition of lead and strontium in surface rocks is highly variable, depending on the isotopic composition at the time the rocks were formed, their age, and the ratio of radioactive parent to stable daughter element. Thus, granitic rocks of Precambrian age are expected to contain more radiogenic lead and strontium than young volcanic rocks do. Although the isotopic composition of lead and strontium in rocks of deep-seated origin, such as basalts, also varies, the isotopic compositions in specific locations may be quite uniform. (See *Year Book 63*, pp. 241-244, for a report on the isotopic composition of strontium and lead from basalts at Gough and Ascension Island along the mid-Atlantic ridge.) Under favorable circumstances lead and strontium in rocks may serve as tracers to study genetic relationships between different rock types. Magmas derived from fusion of crustal rocks or basic magmas heavily contaminated with crustal products might have lead and strontium isotopic ratios different from those of magmas derived from the mantle of the earth. We are attempting to apply these principles to problems concerning genesis of basalt, andesite, and granodiorite in the northern Cascade Range.

Broadly speaking, two types of basalt are found in the area—tholeiite and high alumina basalt. In Eocene time a large volume of tholeiitic basalt was extruded, principally to the west of the

present range. Again, in Miocene time voluminous tholeiite extruded, mainly to the east of the range (Columbia River basalt). The olivine-bearing high-alumina basalt occurs in the Cascade Range and plateaus of southeastern Oregon, and is of Pliocene to Quaternary ages. The andesites in the Cascades are chiefly of two types—olivine-hypersthene-augite andesite characterized by phenocrystic olivine, and more silicic augite-hypersthene andesite. Olivine-bearing andesite occurs in localities where high-alumina basalt is found, and there are transitions between them. At Mount Rainier and Glacier Peak, where mainly augite-hypersthene andesite occurs, high-alumina basalt is absent. Both types of andesite may occur together, as at Mount Hood in Oregon. The age of the andesite varies from Pliocene for flows interbedded with high-alumina basalt along the Cascade Range to Quaternary for the large stratovolcanoes. It is interesting that many of the stratovolcanoes have plutons of granodiorite or quartz diorite cropping out beneath them or nearby. The plutons are older than the volcanoes, being of Miocene age, but are similar in bulk chemical composition to the pyroxene andesite at Mount Rainier and Glacier Peak. North of Snoqualmie Pass the basement complex emerges from beneath the Tertiary cover, and forms much of the northern Cascades. Schists, gneisses, and magmatites derived from pre-Upper Jurassic sedimentary and volcanic rocks, and Cretaceous granitic batholiths comprise much of the basement.

Several relationships are being studied by isotopic tracer methods—the relationship between the tholeiitic and high-alumina basalts; that between the andesites from the stratovolcanoes and those from the nearby Miocene granodiorite plutons; and that between the andesites and the basalts. Samples studied include: three specimens of Columbia River basalt (tholeiite); two samples of high-alumina olivine basalt from Wash-



ington; augite-hypersthene andesite from Mount Rainier; granodiorite from the neighboring Tatoosh and Snoqualmie plutons; andesite from Mount Hood; and biotite paragneiss and two samples of magmatitic biotite-hornblende quartz-diorite gneisses from the basement complex. The lead and strontium isotopic data are given in Table 7. The  $\text{Sr}^{87}$  isotopic variation is too small to lend support to any relationship among the several rocks, doubtless due to the very low ratios, Rb/Sr.

Several hypotheses are supported by these data. (1) The high-alumina basalts appear on the average to have higher  $\text{Pb}^{206}/\text{Pb}^{204}$  and  $\text{Pb}^{206}/\text{Pb}^{207}$  ratios than do the tholeiite basalts. Since the ratios  $\text{Pb}^{207}/\text{Pb}^{204}$  are nearly the same for all the basalts, the distinction between the two basalt types depends primarily on differences in their content of radiogenic  $\text{Pb}^{206}$  (produced by the decay of  $\text{U}^{238}$ ). The distinction between the isotopic composition of lead in the two basalt types suggests that they are not simple

differentiates from a common source material. (2) The isotopic composition of lead in the andesite at Mount Rainier and in the Tatoosh and Snoqualmie plutons are identical within error limits, suggesting that these rocks have a common source. (3) The isotopic evidence regarding the origin of the andesites is quite equivocal.

Besides additional isotopic work, other measurements promise to help clarify the andesite problem. Among them are studies of the thorium-uranium and potassium-rubidium ratios in the various rock types. Although the data given here are of a preliminary nature, they indicate that the Cascade tracer experiments have a reasonable sensitivity and that further work can lead to an improved understanding of the possible genetic relationships between the rocks in this area.

The combined efforts of the Carnegie Institution's Geophysical Laboratory and this Department in the study of the problems of radioactive dating and the use of isotope tracers in the study of

TABLE 7. Isotopic Composition of Lead\* and Strontium† from Rocks of the Northern Cascade Range

Location	Rock	$\frac{\text{Pb}^{206}}{\text{Pb}^{204}}$	$\frac{\text{Pb}^{206}}{\text{Pb}^{207}}$	$\frac{\text{Pb}^{206}}{\text{Pb}^{208}}$	$\frac{\text{Sr}^{87}}{\text{Sr}^{86}}$	$\frac{\text{Rb}}{\text{Sr}}$
Bridal Veil, Ore.	Tholeiitic basalt	18.80	1.204	0.484	0.706	0.132
Anatone, Wash.	Tholeiitic basalt	{ 18.81	1.202	0.482	0.705	0.064
Glenwood, Wash.	High-alumina basalt	19.04	1.211	0.487		
Willard, Wash.	High-alumina basalt	19.29	1.232	0.497		
Mt. Rainier, Wash.	Augite-hypersthene andesite	18.95	1.216	0.492	0.705	
Snoqualmie Pass, Wash.	Snoqualmie granodiorite	19.01	1.215	0.490	0.706	0.093
	Potassium feldspar from above‡	18.89	1.215	0.489		
		18.92	1.216	0.491		
Mt. Rainier Nat'l Park, Wash.	Tatoosh granodiorite	18.95	1.217	0.489	0.709	0.076
Mt. Hood, Ore.	Olivine-hypersthene andesite	18.80	1.207	0.488	0.705	0.0037
Chelan, Wash.	Hornblende-biotite quartz diorite gneiss	{ 18.91	1.205	0.488		
		{ 18.83	1.205	0.489		
	Swakane biotite paragneiss	19.48	1.246	0.497	0.712	0.065

\*Standard error of ratios:  $\text{Pb}^{206}/\text{Pb}^{204}$ : 0.3%;  $\text{Pb}^{206}/\text{Pb}^{207}$ : 0.15%;  $\text{Pb}^{206}/\text{Pb}^{208}$ : 0.2%.

†Estimated uncertainty in  $\text{Sr}^{87}/\text{Sr}^{86}$  ratios after normalizing all  $\text{Sr}^{86}/\text{Sr}^{88}$  ratios to 0.1194 is  $\pm 0.002$ .

‡Determination by B. R. Doe, U.S. Geological Survey.

geological processes have been continuously fruitful. It is with no little regret that we must for the last time include Dr. George R. Tilton as a colleague in this report. Fourteen years of association have passed too quickly and we all join in wishing him continued productivity in his new post. The studies reported below are typical of the endeavors of the whole group.

*Potassium-rubidium studies of ultrabasic rocks in Japan.* Ultramafic intrusive rocks and the ultrabasic inclusions in basalts are the most probable sources of upper-mantle materials. Determining the concentration of radio elements in these rocks provides data for the estimation of heat production within the mantle and the behavior of the elements under high-temperature and high-pressure conditions. In this report, analyses of rubidium and potassium of ultramafic rocks and minerals are given, and the results are briefly discussed in terms of basalt petrogenesis.

The materials analyzed were collected from the fairly large ultramafic body

intruded into the core of strongly folded metamorphic rocks in Shikoku, and nodules in basaltic rocks from North Kyushu, Japan (Yamaguchi, 1961,<sup>22</sup> 1964<sup>23</sup>). The ultrabasic intrusive body of Shikoku is composed mainly of massive dunite, often schistose in places, and is serpentinized at the margins. Pyroxenite layers alternating with dunite are found occasionally, and eclogites, in lesser amounts, in the form of lenses and pools are enclosed in dunite or in pyroxenite.

Figure 32 gives the distribution of the ratio K/Rb to the concentration of potassium from these measurements and other published data on basalts and amphiboles. Analyses of potassium and rubidium are given in Table 8. The concentration of potassium and rubidium in dunite and peridotite (or diopside-bearing dunite) is extremely low, as expected, with a range of 10–20 ppm potassium and 0.03–0.1 ppm rubidium. The eclogites also show very low concentration of both elements.

The mineralogical composition of the

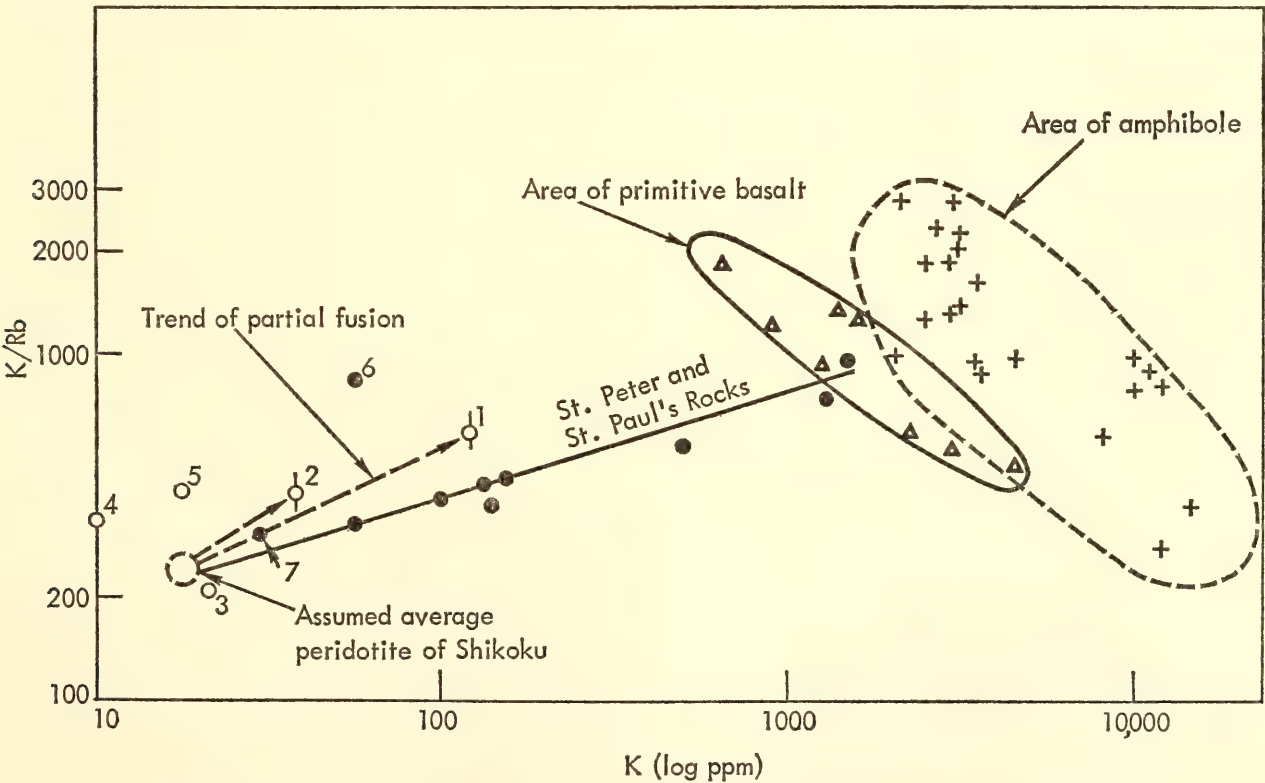


Fig. 32. Comparison of ultramafic rocks, basalts, and amphiboles with regard to potassium to potassium/rubidium ratios.



TABLE 8. Potassium and Rubidium in Ultramafic Rocks

Location	No.	Rock Type and Mineral	K, ppm	Rb, ppm	K Rb
Shikoku	1	Eclogite (A)	120	0.30	600
	2	Eclogite (B)	38	0.095	400
	3	Dunite	21	0.100	210
	4	Dunite (schistose, diopside-bearing)	10	0.03	330
	5	Pyroxenite	18	0.045	400
	6	Diopside in eclogite (B)	56	0.065	862
Karatsu	7	Augite of pyroxenite nodule in basalt	30	0.10	300

eclogite analyzed is very close to the eutectic of the garnet peridotite system reported by O'Hara (*Year Book 62*, pp. 71-76), and Davis (*Year Book 63*, pp. 165-171). It is as follows: garnet, 58.1; diopside, 41.6; chlorite, <0.1; olivine, <0.1; hornblende, <0.1; and rutile and chromite, <0.1. The analysis indicates that the eclogite may possibly be derived by partial fusion of garnet peridotite at high pressure and high temperature. If the deduction is valid, it follows that the dunite, pyroxenite, and peridotite (or diopside-bearing dunite) associated with eclogite may be explained as the remnant of the crystalline phases separate during this remelting process. Such a process should enrich the potassium and rubidium in the liquid phase. This is observed in the eclogite where the potassium and rubidium are enriched by a factor of 2 over the pyroxenite and dunite. It should be noted here that most potassium and rubidium of eclogite are incorporated in the diopside.

Potassium and rubidium concentrations in eclogite are far lower than those of primitive basalts, as shown in Fig. 33. Eclogite has essentially the same chemical composition as gabbroic or basaltic rocks except for the amounts of potassium and rubidium. This fact is subject to at least two interpretations: (1) The partial remelting of primary garnet peridotite does not always give the basaltic liquid; and (2) the eclogite treated here may be the crystal accumulated from the liquid of partial fusion of

primary garnet peridotite, as has already been suggested by O'Hara and Yoder (*Year Book 62*, pp. 66-71). The resolution of these two possibilities awaits adequate data on the other types of eclogites and associated rocks.

In many of the igneous rock series both potassium and rubidium are enriched in the later stage, rubidium at a faster rate than potassium; the ratio

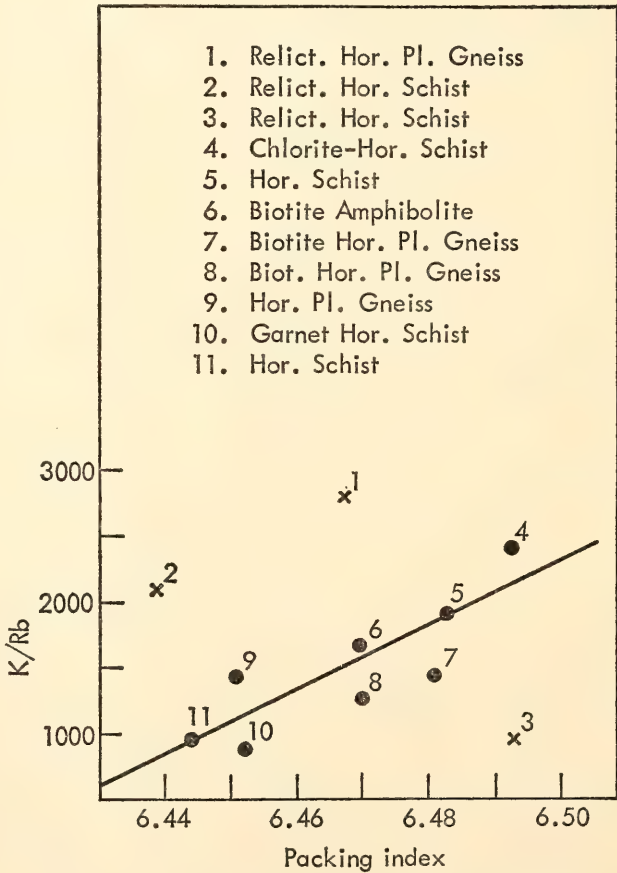


Fig. 33. Relation of potassium/rubidium ratio to packing index of hornblende from Tremola series.

K/Rb decreases in the later stage. Rocks from Skaergaard provide such an example. Thus, primitive basalt with low potassium content gives a very high K/Rb ratio—up to about 2,000 (Gast, 1965<sup>24</sup>). There has been discussion concerning the source material in the mantle from which the basalt is produced and whether the primitive mantle material would have a higher or lower K/Rb ratio than the primitive basalt (Gast, 1965,<sup>24</sup> Lessing *et al.*, 1963,<sup>25</sup> and Taubeneck, 1965<sup>26</sup>). As has been mentioned, dunite, pyroxenite, and eclogite have very low potassium content, while the K/Rb ratio is about 200/600. These natural relationships may be clarified by the following.

Potassium and rubidium have very similar chemical behavior, but the ionic radius of rubidium is larger than that of potassium. Rubidium minerals or the end member of rubidium minerals which make up the solid solution with potassium minerals are not known in nature. Thus, rubidium occurs in minerals entering into the vacant position of the crystal lattice or admitted in structure substituting for the position of potassium or both. The ratio of K/Rb fixed in the mineral would be controlled by the relative concentration of both elements in the initial system, the type of crystal structure, and the pressure and temperature of the system. Higher temperature would admit the rubidium in the lattice, while higher pressure would reverse the pattern.

If minerals crystallized from the same liquid are compared, the one at higher temperature but lower pressure and the other at higher pressure, the ratio K/Rb would be lower in the former and higher in the latter crystal, even though (K/Rb) liquid is always less than (K/Rb) crystal. To evaluate this concept the ratio K/Rb of hornblende has been compared with the packing index since the packing index is a function of  $P$ ,  $T$ , and the volume of ions. Because of the lack of sufficient data on potassium, rubidium, and crystal chemistry of hornblende, the samples

were arbitrarily selected from the metamorphic rocks of the Tremola series of the Gotthard massif in central Switzerland studied by Steiger (1961,<sup>27</sup> 1964<sup>28</sup>). The result is given in Fig. 33. The linear relation of the ratio K/Rb to the packing index is to be noted. The three points that fall outside the line are for mineral samples that have been shown by the petrological and age studies as relict minerals not in equilibrium with the main series (Steiger, 1964,<sup>28</sup> and oral communication). It is thus clear that the K/Rb ratio of the mineral varies during the metamorphism (diffusion in a closed system) as a function of  $P$  and  $T$ . The exact relation between these observations and the pattern of results in Fig. 32 is still not completely clear.

The scattered points of basalts (Gast, 1965<sup>24</sup>) plotted in Fig. 32, which apparently indicate a relation of increasing potassium concentration and decreasing K/Rb ratio, may not imply a series of fractional crystallization. They are collected arbitrarily from Pacific and Atlantic areas. There are no systematic variations between localities, the basalts being petrographically considered primitive. Rather, they may be independent primitive basalts produced from fusion, each of slightly different mantle material.

As already discussed, the eclogite of Shikoku, which was probably produced by partial fusion of a peridotitic rock, could not give rise to basalt magma. The difficulty encountered could be solved if we were to add some amount of hornblende in the primary mantle peridotite. Oxburgh (1964<sup>29</sup>) has suggested this possibility based on the ratio of sodium to potassium. Actually, the eclogite of Shikoku contains trace amounts (probably of the order of 0.1 volume per cent) of hornblende as an interstitial constituent, which is probably not of secondary origin. As we do not have enough knowledge of the chemical and physical properties of possible mantle hornblende, the potassium and rubidium content in some metamorphic rocks was tentatively plotted and compared with



basalt and ultramafic rocks (Fig. 32). It is clear that most amphibole has a potassium content and ratio K/Rb about the same as those of primitive basalts. Some mylonitized peridotite of St. Peter and St. Paul's Rocks (Hart, 1964, *Year Book 63*, p. 330), containing 20 per cent hornblende gave potassium content and K/Rb ratio very close to tholeiitic basalt dredged from the mid-Atlantic ridge (Gast, 1965<sup>24</sup>). Because of the very low content of potassium and K/Rb ratio of the peridotite, as estimated from this study (Fig. 32), the higher concentration of the St. Paul's peridotite could be reduced because of the presence of hornblende which contributed most of the potassium content of this rock. This also means that the hornblende in the peridotite has a close or higher potassium and K/Rb ratio than the average primitive basalts.

It has been previously noted (Yamaguchi, 1964)<sup>22</sup> that the dunite of Shikoku contains two types of olivine, one clear and the other turbid. Turbid olivine has been explained as the recrystallization product of serpentine. However, the turbid olivine might possibly be the remnant of hornblende that has undergone decomposition during the process of partial remelting.

It is now believed that the hornblende peridotite, such as is found at St. Peter and St. Paul's Rocks, is the mantle material that could most probably produce basalt magma by partial fusion. The variation of potassium concentration and K/Rb ratio of the primitive basalts is possibly due to the variation of the chemical composition and the amount of hornblende included in the peridotite, but the data are insufficient to lead to a conclusion. To confirm the hornblende peridotite as the basalt-yielding zone in the mantle, detailed studies of the physical and chemical properties of the hornblende, the mineralogical composition of the peridotite, and the seismic velocity of the rock remain for the future.

## HEAT FLOW

*J. S. Steinhart and S. R. Hart*

*Heat flow and thermal properties of Seneca Lake, N.Y.* The theories that attempt to provide an account of the large-scale processes by which mountain ranges are built and oceanic trenches created, and by which the face of the earth has been altered over the eons of geologic time, rely upon thermal energy as the energy source. Whether by expansion, contraction, or convection currents, it is the temperature differences and their history within the earth that could provide the basic understanding of the orogenic history of the earth. Radioactive decay of elements within the earth provides the main source of heat. Original heat, if any, and convection currents, if they exist, may provide small additional amounts of heat or change its distribution. Measurement of heat flow through the surface of the earth has shown an average value of about  $1.2 \times 10^{-6}$  calorie/cm<sup>2</sup>/sec. Regional variations from this mean value isolate areas where there are concentrations of radioactive elements in the upper portion of the earth or where, possibly, large-scale convection cells have transported additional heat into or out of the area. When these anomalous areas are well known we may be able to estimate the thermal imbalances that are now shaping the earth.

As observed in *Year Book 63* (p. 326) meaningful heat-flow values can be obtained only when steady-state conditions have been established. On land, because of atmospheric temperature variations, steady-state conditions are reached only at depths of several hundred meters and measurements must be made in mines and boreholes.

Using oceanic techniques for measurements at the bottom of deep lakes, where temperature variations are considerably reduced, one may greatly accelerate the heat-flow coverage of the lake areas, and preliminary studies in this direction were carried out in Lake



Superior in 1963. The results were very encouraging and led us this past year to carry out a more detailed program on Seneca Lake in New York.

The Naval Research Laboratory (NRL) maintains a large platform in 160 meters of water in the middle of Seneca Lake. Cooperation of the NRL and the Office of Naval Research made possible our work from this ideal facility. Studies completed to date at Seneca Lake include several temperature profiles to depths of seven meters in the bottom sediment, a series of detailed water-temperature profiles, conductivities, chemical analyses of near-bottom water samples, and a daily bottom-water temperature record for a period of nine months obtained with a self-contained *in situ* recorder.

The basic data required for a terrestrial heat-flow measurement in a lake are the temperature increase with depth in the bottom sediment and the thermal conductivity of the sediment. The temperature measurements are obtained from a series of thermistors attached to fins on a piston corer. For Seneca Lake, temperature gradients were measured in July and in October; the results are shown in Fig. 34. The agreement in the lower portions for the two measurements is quite good, the gradients there agreeing to within a few per cent. The

differences in the upper portions are caused by the seasonal variation in the temperature of the lake water. When this seasonal variation is known, its effect on the shallow parts of the gradient can be completely calculated. Since the sediment is a good insulator, the annual water variation is sharply attenuated with depth, below five meters producing only a 5–10 per cent effect on the gradient. The deeper gradients can therefore be used directly to calculate the heat flow. For this measurement of heat flow, thermal conductivities were determined from the water content of the sediment and found to vary from 0.0019 cal/cm sec°C at five meters to 0.0026 cal/cm sec°C at seven meters' depth. The thermal gradient in this interval was 0.075°C/meter. The product of gradient and thermal conductivity gives a heat-flow value of  $1.7 \times 10^{-6}$  cal/cm<sup>2</sup> sec. This value is distinctly higher than the continental average of  $1.2 \times 10^{-6}$  cal/cm<sup>2</sup> sec. There are no borehole measurements in the Seneca Lake region for comparison, so it is not yet certain whether this high value is real or represents some problem inherent in the method.

Aside from minor corrections for topography and sedimentation, the major uncertainty in the value obtained arises from the possible effects of long-term climatic variations. We have shown that short-period variations can be monitored and compensated. It is obviously impossible to monitor variations with periods longer than 10–50 years. Weather records from the Seneca Lake region, which are available back to about 1880, show evidence for long-term changes of as much as 1°C. This variation, if transmitted directly to the bottom water without attenuation, would penetrate the sediment to great depths and seriously alter the thermal gradient.

One way of assessing the effects of long-term air temperature fluctuations is to study the variation in mean annual deep-water temperatures for lakes that have widely differing mean annual air

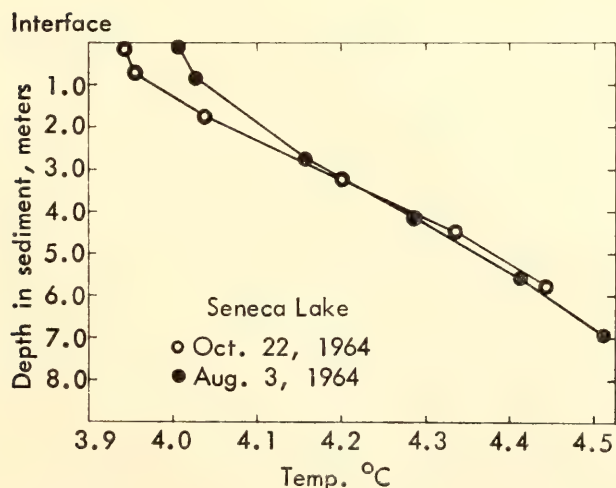


Fig. 34. Measured temperature gradients at bottom of Seneca Lake.



temperatures. Figure 35 is an assembly of such data from the literature. Most of the lakes represented are from the class of temperate lakes, that is, those that are cooled to the maximum density temperature (about  $4^{\circ}\text{C}$ ) at least once a year. The exceptions, Loch Ness, Loch Lomond, Lake Windermere, and Lake Ikedako, are from the class known as subtropical lakes. All the temperate lakes fluctuate only a few tenths of a degree from about  $4^{\circ}\text{C}$  although the mean annual air temperatures vary more than  $15^{\circ}\text{C}$ . Even these small fluctuations may be due to errors in the original measurements. With the exception of Seneca Lake, year-round water temperature values were compiled from diverse publications and may in some cases be unreliable. As stated above we measured daily temperatures in Seneca

Lake for nine months, and the mean bottom-temperature value for this lake is probably the most precise one ever determined. Similar measurements will be made in other lakes in the future.

For temperate lakes, the bottom water appears to undergo its yearly variation at about the temperature of maximum density of water. This means that the mean annual bottom temperature for most temperate lakes will be rather close to this maximum density temperature and will be independent of the long-term temperature variations as long as the lake remains in the temperate class. We believe this to be the correct explanation of the temperate lake data in Fig. 35, but for the present we cannot demonstrate that it is true. Until we can, the data in Fig. 35 suggest that a range of mean annual air temperature of  $15^{\circ}\text{C}$  will produce a

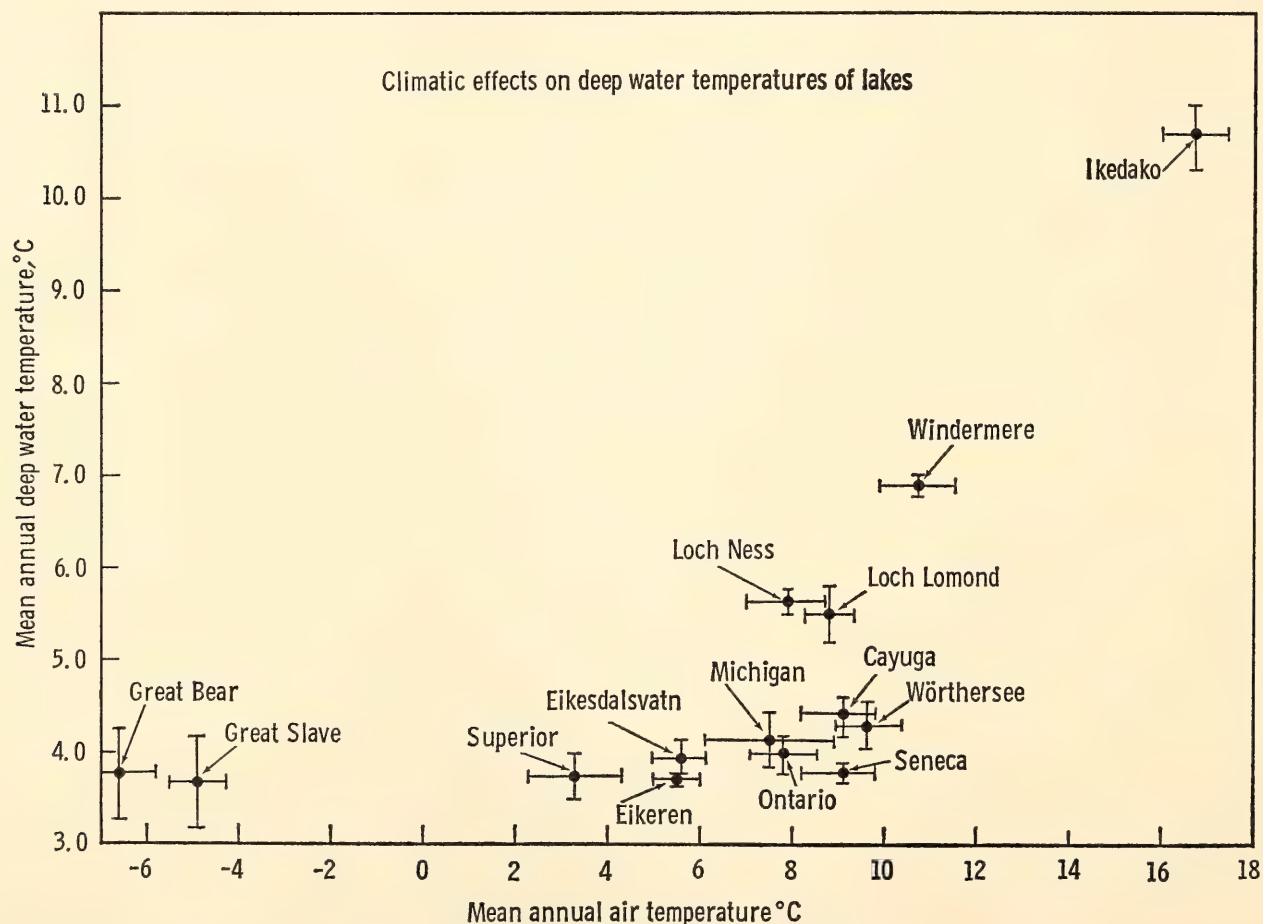


Fig. 35. Mean annual deep-water temperature plotted against mean annual air temperature, all corrected to 100-meter depth. Loch Ness, Loch Lomond, Lake Windermere, and Lake Ikedako are subtropical lakes. Note how the other (temperate) lakes are independent of mean annual air temperature.

few tenths of a degree change in mean bottom-water temperatures. This represents an attenuation factor of almost 2 orders of magnitude, and means that climatic changes of 10°C over the past 1,000 years would produce less than a 10 per cent error in a lake-bottom heat-flow measurement.

The bottom-water temperatures of deep temperate lakes have an annual temperature variation of about 1°C at about the maximum density temperature. To correct for this requires careful measurement of bottom-water temperatures throughout the year, and for this purpose we have designed and constructed a self-contained temperature recorder capable of unattended recording of daily temperatures for a year. Basically the device is a pinhole camera that takes pictures of an expanded scale thermometer. A battery-operated clock turns on the lights once a day for eight seconds and advances the film. One year's recording requires 60 inches of 35-mm film from which records can be read to 0.01°C, and the thermometers used can be calibrated to this accuracy. One of these recorders

has been operating in Seneca Lake since July 1964, from which date to April 1965 the observed temperatures are shown in Fig. 36. The results contain a few surprises. The long period of stable stratification in the warm months is shown in the slight increase from July to late November. Between November 28 and 29, however, the temperature changed abruptly by 0.4°C. This probably corresponds to the first top-to-bottom circulation of the whole lake. Throughout the winter months there are comparatively large day-to-day fluctuations in temperature, as shown in Fig. 36. These short-period variations have no perceptible effect on the annual correction we will apply to the measured thermal gradients. They do, however, resolve a difficulty that has persisted for many years in the limnological literature. Temperatures measured in lakes in winter seemed, at times, quite anomalous for the expected annual cycle. It is easy to see from Fig. 36 how the choice of a particular day might produce a single value difficult to reconcile with a smooth curve. For this reason we suspect that some of the values

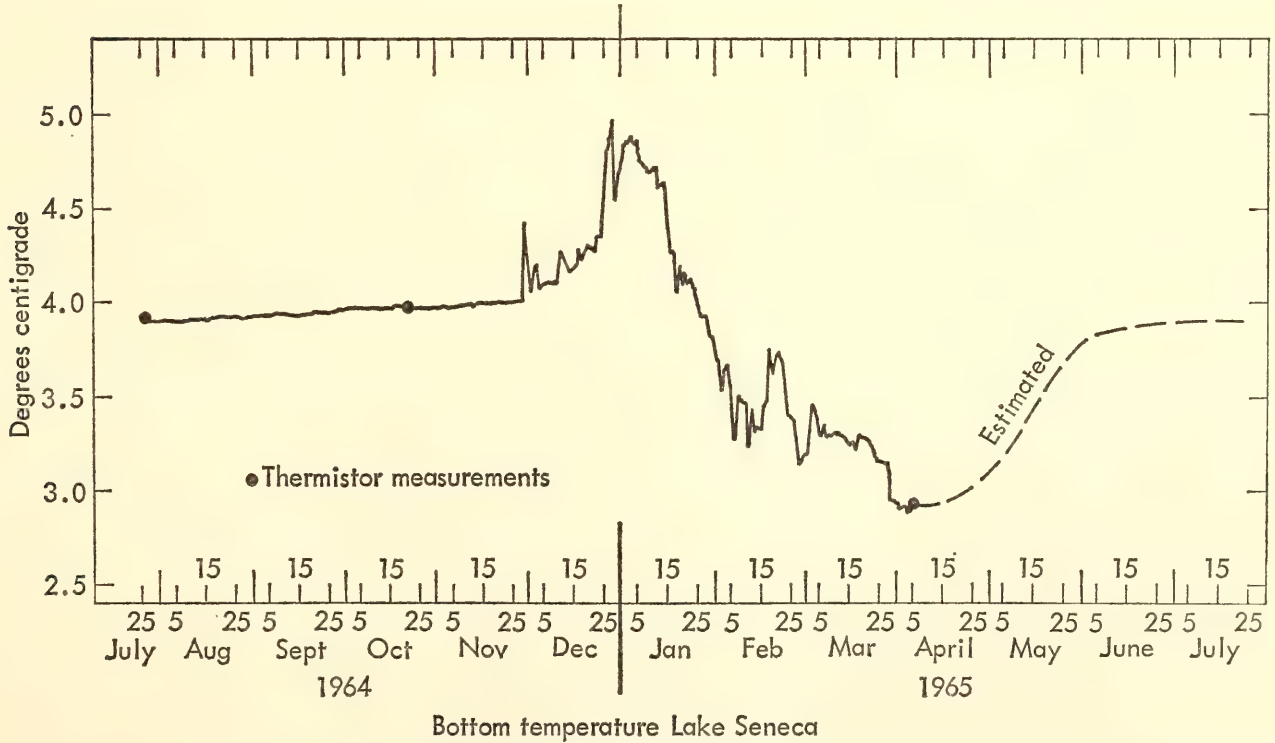


Fig. 36. Daily temperatures of bottom water in Seneca Lake.



from the literature used to construct Fig. 35 may be misleading.

### RADIO ASTRONOMY

*B. F. Burke, K. C. Turner, C. M. Varsavsky,\*  
and M. A. Tuve*

The radio astronomy program during the past year was concentrated in two principal areas—21-cm hydrogen-line spectroscopy and survey of the background continuum radiation at 234 mc/sec. The 21-cm studies have been closely linked with the development of a parametric-amplifier receiving system that increases sensitivity by a factor of nearly 4, enabling one to study much weaker interstellar cloud structures than before. Some of the clouds exhibit motions that were not expected from previous models of the interstellar medium, and neither their distance nor their origin is understood as yet.

Whereas the 21-cm observations involve the use of new electronics in an area in which we have long been active, the 234-mc/sec work, in contrast, has been pursued with conventional electronics, but in an area new to our group. The "galactic background," a distributed source of radio noise over the entire sky at all frequencies, is, in fact, the oldest known source of cosmic radio noise, for it was the variation of the sky background noise with sidereal time that led Karl Jansky to his discovery of cosmic radio emission. The explanation of the background radio noise has been a subject of dispute, with no general agreement on what fraction originated in our Galaxy. The distribution of the noise that does originate in our Galaxy has also been a subject of controversy, some surveys having been interpreted in terms of a galactic halo, a spheroidal distribution of radio emission surrounding the Galaxy, and possibly related to the origin of the cosmic rays,

while other surveys have shown only a galactic disk, a flattened system of radio emission concentrated in the plane of the Galaxy.

It is hoped that observations of the southern sky will shortly be under way with the 30-meter telescope we are now constructing in Argentina, with the cooperation of the Universities of Buenos Aires and La Plata. The dish is now completed on the ground and a hydrogen-line spectrometer is in operation, looking at parts of the Galaxy that pass close to the zenith. When the dish is mounted tracking operation will be possible, but in the meantime the electronic system can be checked out completely, and valuable experience will be gained by our colleagues in Argentina.

### CONTINUUM SURVEY (234 MC/SEC)

To help in reconciling the conflicting interpretations of the sky background a survey was undertaken of the entire sky available to the 300-foot telescope of the NRAO. A frequency of 234 mc/sec was selected as giving a combination of good resolution, relatively low frequency, and freedom from interference. At this frequency the 300-foot telescope has a beamwidth of  $1^\circ$  between half-power points. An antenna feed (a scaled-up version of the DTM 21-cm feed) and a transistor preamplifier for this frequency (giving a system noise temperature of about  $600^\circ\text{K}$ ) were constructed at the Department. The equipment was mounted on the 300-foot telescope during the last few days of October 1964, and observations were made throughout November. Use was made of a liquid nitrogen-cooled reference load, receiver, and digital and analogue data recording equipment kindly supplied by the NRAO.

Observation time was compressed by scanning the transit telescope north and south at  $10^\circ/\text{min}$  over a range of about  $50^\circ$ . Thus the sky was covered with zigzag tracks of observations which were interlaced on subsequent days. By the

\*Instituto Nacional de Radioastronomía and Universidad de Buenos Aires, Argentina.

end of November 1964 almost the whole sky visible with the 300-foot telescope had been observed twice every half-beamwidth.

It had been hoped that the major part of the data reduction could be done by computer. It has been found, however, that low-level, rather slowly varying interference is much too prevalent to allow this. The large amount of hand reduction now required has not yet been completed.

Two quiet days of interleaved observations in the region between 0° and 40° declination ( $\delta$ ) have been reduced, however, and this is sufficient to show the broad outlines of the distribution of galactic radio emission. An example is shown in Fig. 37. In particular, we may put an upper limit on the intensity of any halo-like distribution, i.e., any uniform spheroidal distribution of radio noise. Two model halos have been considered.

The first model is that of a spherical distribution, uniform inside the solar distance and zero outside. At any given galactic latitude this would give an observed intensity proportional to the cosine of galactic longitude for  $|\ell| < 90^\circ$  and constant outside that region. Figure

38 shows antenna temperature as a function of galactic longitude for several galactic latitudes, and Fig. 39 shows antenna temperature vs.  $\cos \ell$  for  $\ell < 90^\circ$ . It can be seen that any linear dependence gives less than a 30°K change as one looks toward the center. Most of this 30° is due to the two spurs seen in Fig. 37. It should be noted that the points shown in Fig. 38 for positive galactic latitudes are not used in Fig. 39. This is because almost half the northern hemisphere is filled with the great North Galactic Spur (see points labeled  $b = +20^\circ$  in Fig. 38).

The second model, that of a uniform spheroid of radiation, fits the data only with an axial ratio of 3.7:1, i.e., a very disklike halo indeed. The general conclusion is that a very weak halo may exist, but our observations neither require nor confirm it. More elaborate studies, together with discrete source investigations, are planned after a hand reduction of all the data has been completed.

RADIO HYDROGEN

*Hydrogen absorption.* The general problem of hydrogen-line radio astronomy is to determine, as a function of distance

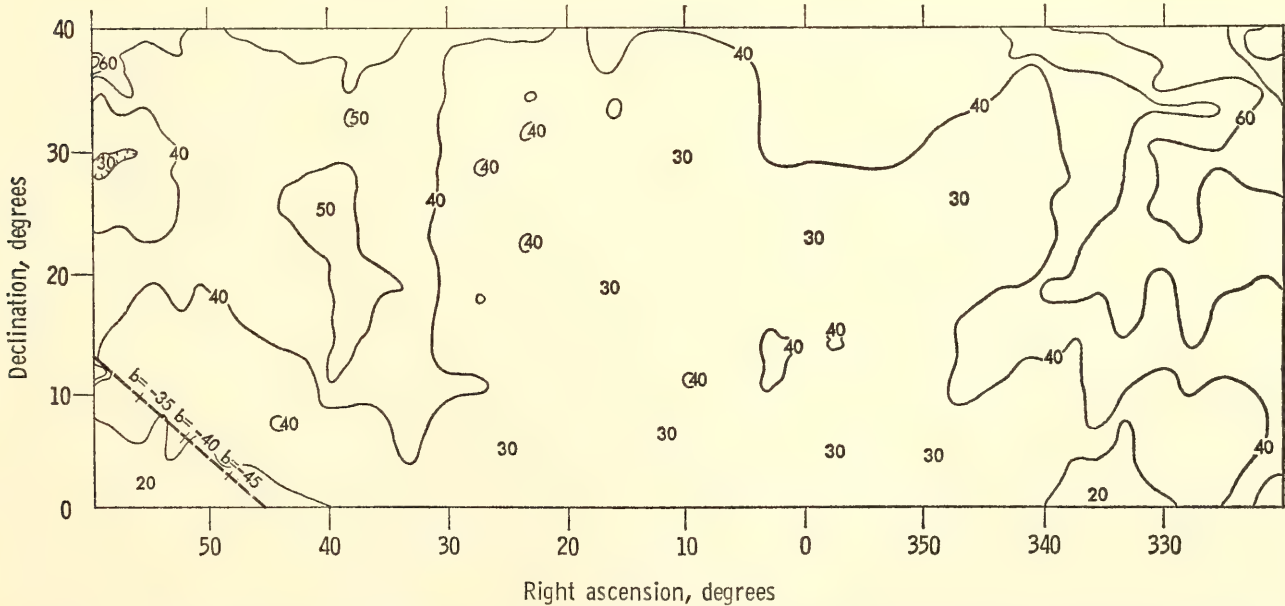


Fig. 37. Section of sky observed at 234 mc showing galactic background in region south of galactic plane.



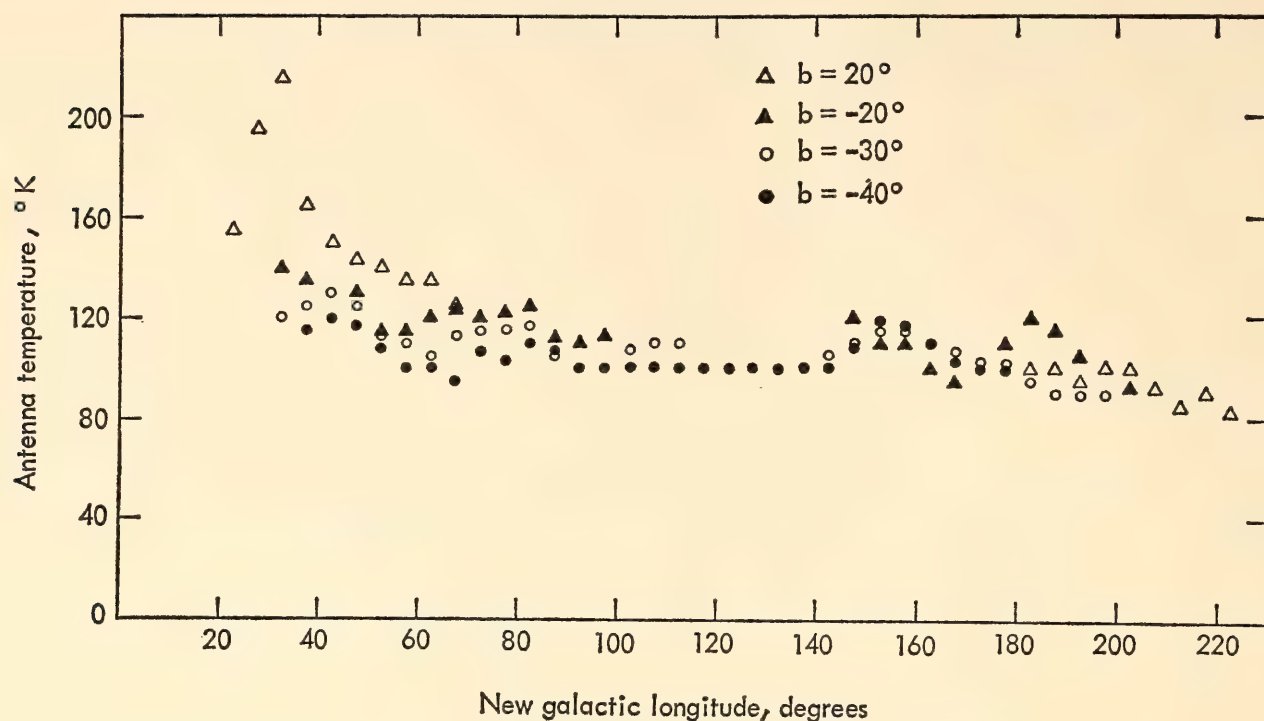


Fig. 38. Sky brightness at about 234 mc along circles of constant galactic latitude.

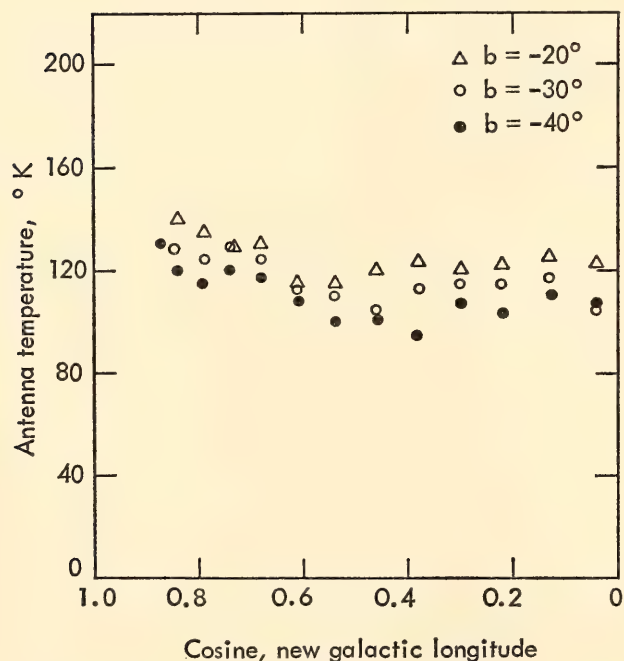


Fig. 39. Sky brightness at 234 mc along circles of constant galactic latitude plotted as function of  $\cos(\ell_{II})$  to show limits of spherical halo.

in a given direction, the velocity, temperature, and density of the interstellar atomic hydrogen. Since the number of variables is too large to permit a complete solution, dynamical models must be constructed to relate velocity and dis-

tance, but from emission-line profiles only, density and temperature cannot be separated. In those directions where one has a bright radio source, however, the optical depth can be measured, and a different functional relation of hydrogen temperature and density can be determined. If a reasonable "expected profile" (the emission-line profile that would be seen if the radio source were not present) can be constructed, limits can be placed on both hydrogen temperature and density. Previous studies by other workers have been made with frequency-switching receivers, which suffer from the disadvantage that a separate measurement of continuum temperature  $T_c$  must be made using a separately calibrated receiver. The brightness temperature in the direction of the radio source  $T_o$  is determined from the sum of the frequency-switched receiver output  $T_r$  and the continuum temperature  $T_c$ . If the source is small compared with the antenna beam, the optical depth is determined by solving

$$[(T_c + T_r - T_e)/(T_c)] = e^{-\tau}$$

where  $T_e$  is the expected temperature, the temperature that would be observed

in the absence of the source. It is clear that for large optical depth the numerator is a quantity that is small compared with  $T_c$ ,  $T_r$ , and  $T_e$ , and hence small errors in these quantities can have a large effect on  $\tau$ .

Because our parametric-amplifier receiver is a load-switching radiometer, it has the advantage that all quantities are observed with the same receiver, and  $T_o$  is determined from a single observation. The optical depth  $\tau$  is then determined from

$$[(T_o - T_e)/(T_c)] = e^{-\tau}$$

The absorption spectrum of the brightest radio source, Cassiopeia A, was chosen as a test case, because it exhibits three unusually sharp, deep absorption lines that have already been extensively studied. The expected profile was determined by observing the hydrogen emission in the vicinity of the radio source, and extrapolating to the position of Cas A. The results are shown in Table 9, which also shows the optical depth determined by other workers. In all cases the optical depth we deduce is less than previously measured. The reason for the discrepancy is not understood, although it is clear that the results are strongly influenced by the expected profile adopted. We also noted an interesting effect when the receiver was running close to saturation. Under these conditions the additional noise added by the radio source caused some overloading in the intermediate frequency (IF) system, and false results were obtained, with the apparent optical depths

much greater. We believe that sufficient precautions were taken to avoid such overload effects, and since our system is free of detector-law nonlinearity (because the detector of the channel at the line core is operating at nearly the same level both on and off the radio source) we suggest that the actual optical depths in the direction of Cas A, though large, may not be as large as previously believed.

The temperature of the absorbing hydrogen can be determined only if we can relate the expected profile taken with the resolution of our 60-foot telescope to the expected profile that would be obtained with a telescope whose beam is the same size as the radio source. Our experience in previous years with the 300-foot telescope, whose beam size of 10' is only slightly larger than Cas A (6'), indicates that differences can be expected, usually of the order of 30 per cent, and not a factor of 2 or 3. We can, therefore, relate the observed optical depth to the temperature of the expected profile and deduce the cloud temperatures, also given in Table 9. The temperatures are given for a scale in which the peak emission temperature at  $\ell^I = 50$ ,  $b^I = 0$  is adopted to be 100°. All three clouds have apparent temperatures that are significantly less than 100°. If this is generally true, the conventional calculations of optical depth are not correct, and the deduced hydrogen densities (for example in the Leiden models of BAN 475) are underestimates. The total amount of hydrogen in the Galaxy would be greater, by a factor of at least 2 or more, than the present estimate of five per cent. It should

TABLE 9. Optical Depths of Cassiopeia A Absorption Features

Cloud Velocity, km/sec	Optical Depth			Excitation Temperature, °K
	Jodrell Bank	Leiden	DTM	
-0.9	1.86	1.85	1.31 + 0.12 - 0.11	79
-37.8	3.32	2.6	1.71 + 0.41 - 0.29	74
-49.1	> 4.6	4.0	1.77 + 0.45 - 0.07	55



be emphasized, however, that the temperatures we have deduced depend upon the assumption that the expected profile is meaningful for an area comparable in size to the radio source, and is hence model dependent. Detailed studies with the 300-foot telescope of the emission in the vicinity of Cas A would clarify the validity of this assumption.

*High-velocity hydrogen clouds.* The increased sensitivity of the H-line receiver has enabled us to examine the weak, high-velocity clouds discovered by the Leiden workers. A detailed survey has been made of the strongest, highest velocity cloud, designated (I) in their initial list, and which we refer to as Leiden I. The peak temperature is  $4^\circ\text{K}$  and the radial velocity is  $-176\text{ km/sec}$ , with respect to the local standard of rest. Such a large radial velocity does not fit accepted notions of the hydrogen motions in the outer parts of the Galaxy. Oort has suggested that this cloud is intergalactic material swept up and decelerated by the gas in our Galaxy, and it was our hope that some clues might be gained from measuring internal motions of the cloud.

The hydrogen motion along an east-west line through the center of the cloud at  $\delta = +62.34^\circ$  is shown in Fig. 40. It is evident that systematic internal motions are not large, although the radial velocity of the eastern half may differ from the radial velocity of the western half by not more than  $4\text{ km/sec}$ . A more pronounced effect can be seen in Fig. 41, which represents the velocity profile for a north-south cross section  $2^\circ\text{W}$  of the adopted cloud center. Over a declination range of  $3^\circ$ , the velocity peak shifts by  $8\text{ km/sec}$ . This shift could be evidence for shear or rotational motion of the cloud, but an alternative explanation is possible. The profiles taken at the adopted center of the cloud  $\alpha = 135.00^\circ$ , and  $\delta = +62.34^\circ$  (1965) show an asymmetry that suggests that the profile is the superposition of two clouds, the weaker of the two having a radial velocity  $10$

$\text{km/sec}$  less negative than that of the main component. The change in velocity exhibited in Fig. 41 would then be attributed to the changing relative intensity of the two components. In any event,  $8\text{ km/sec}$  is an upper limit to the internal large-scale motions. The profile half-widths are remarkably constant over the

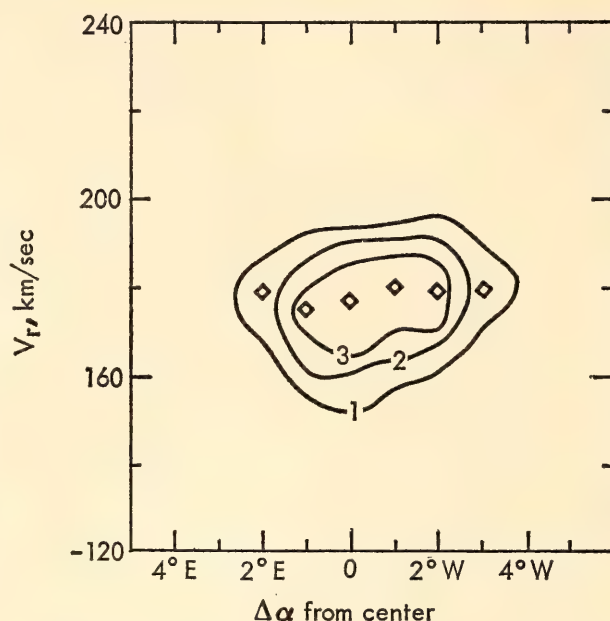


Fig. 40. Brightness contours as function of velocity and right ascension for cross section through high-velocity cloud, Leiden I.

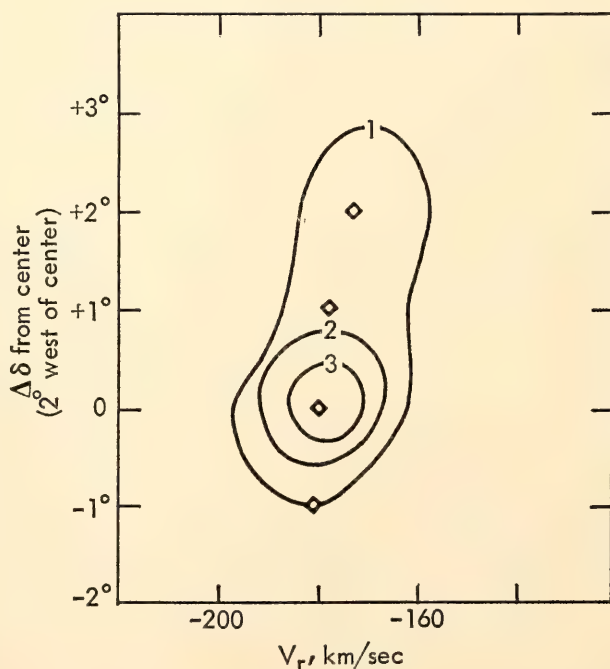


Fig. 41. Cross-section declination through high-velocity cloud, Leiden I.

areas studied. The largest half-width observed was 31 km/sec, and the smallest was 26 km/sec. If the cloud is, indeed, swept-up intergalactic material, the resulting body is remarkably homogeneous.

*The Andromeda Nebula.* In *Year Book 63* (p. 342) it was pointed out that some of the hydrogen clouds at the north-following end of the major axis of the Andromeda Nebula, M 31, could actually be foreground objects, belonging to our own Galaxy. The velocities were higher than those observed for the local gas,

but high-velocity clouds have now been observed so frequently that a survey of the surroundings of M 31 seemed advisable. Observations with our 60-foot telescope confirm this interpretation. Figure 42 shows an  $\ell, v$  diagram at  $b = -20^\circ$ , in which several such clouds can be seen at velocities ranging from  $-20$  to  $-60$  km/sec, and which in all probability are not associated with M 31. The consequences for the interpretation of M 31 are not serious, because the most intense ( $>5^\circ$  K) hydrogen is cer-

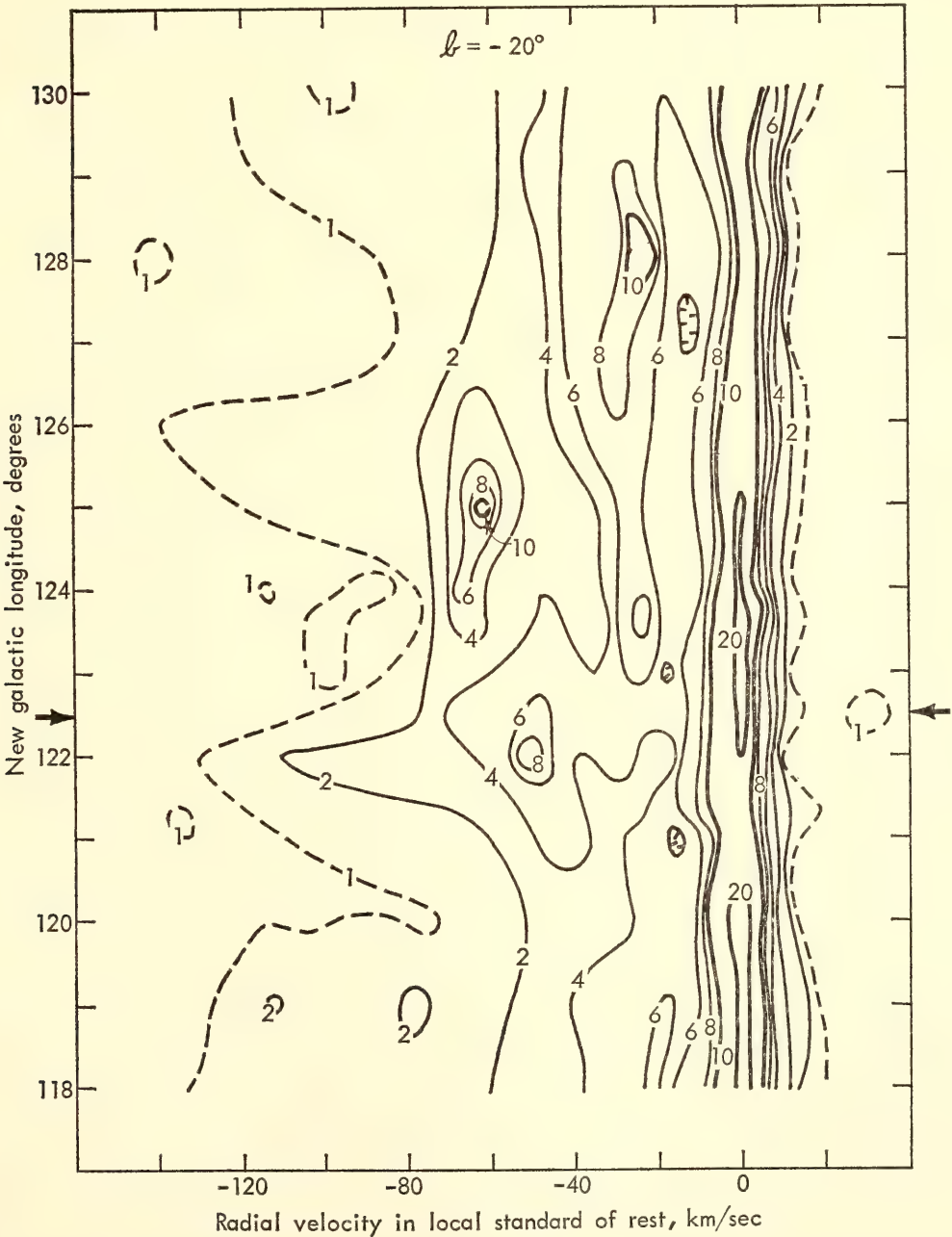


Fig. 42. Hydrogen brightness along cross section parallel to galactic plane passing through M 31.



tainly associated with M 31, but because of confusion from these high-velocity galactic clouds, the rotation curve along the north-following half of the major axis cannot be measured at distances greater than 100' from the center.

#### EQUIPMENT DEVELOPMENT

The parametric amplifier described in *Year Book 63* (pp. 348-349) occupied much of our attention during the year. A fundamental difficulty was uncovered when careful examination of the base-line stability was made. Over periods of about 15 minutes, the receiver base line could wander several degrees Kelvin, an effect that could completely mask the weak hydrogen features we wished to observe. Although the overall amplifier gain was stable, the drifts seemed to be associated with small changes in the shape of the amplifier pass band. Since the H-line spectrometer was a frequency comparison system in which the switching operation was performed after the parametric amplifier, such changes could not be canceled out, and a shift in base line occurred. The system was consequently changed to a comparison load receiver of the Dicke type, a system we have often used at lower frequencies. An L-band comparison switch using high-conductance diodes was constructed, and a cold load was developed that provides a stable comparison reference. The remainder of the H-line spectrometer needed no modification, and now the system can be used for observations of continuum sources as well as for radio hydrogen.

Some difficulties were encountered in developing the cold reference load. The load is immersed in liquid nitrogen, which provides a stable 77°K. Condensation of oxygen, CO<sub>2</sub>, or water vapor inside the load had a serious effect on the voltage standing-wave ratio of the load, and the receiver base line was no longer stable. Condensation was prevented by pressurizing the cold load

with helium, which prevents the entry of condensable vapors.

The new system has been operated for two months, during which time only minor adjustments were required by the parametric amplifier. The total system noise is approximately 250°K, and profiles can now be obtained in as short a time as 30 seconds, with a signal-to-noise ratio that is at least as good as we formerly obtained with an integration time of five minutes.

The construction of the 100-foot dish at our Avery Road field station, two miles east of the Derwood Laboratory, proceeded satisfactorily during the year. The dish was lifted from the ground and placed on the mount in May, and only a small amount of work remains to make it a working radio telescope. Construction of a microwave radio link to connect the two sites was under way at the close of the report year.

#### SOUTH AMERICAN COOPERATION

During the past year radio hydrogen from the southern sky was observed for the first time in South America as a result of our efforts to establish a center for radio astronomy in the southern hemisphere. E. T. Ecklund was in Argentina at the Villa Elisa field station from May to December, 1964. During this period the 30-meter dish was completed, the feed support towers erected, and the surface installed on the dish. The gear racks for the drive mechanism were constructed in Baltimore and shipped to Argentina, and partial assembly of the mount and drive system has been accomplished.

Before his return to Washington, Ecklund devised an interim tilting arrangement which allowed the dish to be tilted 5° from its present flat position. It was, therefore, possible to observe a strip of sky 10° wide centered at declination 34°S using the telescope as a transit instrument.

Under the direction of Dr. C. M. Var-

savsky, our South American colleagues completed assembly of the basic H-line receiver during the spring, including six channels of output (40–60 channels will eventually be installed), and successfully observed radio hydrogen from the southern sky.

During the fall of 1965 it is planned that Carnegie Institution personnel will return to Argentina to participate in the remaining construction and the erection of the dish on its mount.

Our southern colleagues, having gained experience from working with us on

the first telescope, have now begun construction of a second 30-meter dish which eventually will be used in conjunction with the first as an interferometer to measure radio source positions and brightness distributions. Materials for the second dish have so far been provided by the Carnegie Institution, but all of the layout and fabrication have been done by Dr. Varsavsky and his workers. At the close of the report year the central 40-foot-diameter hub was nearly finished and preparations were being made to start rib fabrication.

## THEORETICAL AND STATISTICAL GEOPHYSICS

### GEOMAGNETIC FIELD OF THE EQUATORIAL RING CURRENT AND ITS ABSOLUTE VALUE

*S. E. Forbush*

The procedure for determining the absolute value  $U_0$  of the southward horizontal geomagnetic field, which arises from the so-called equatorial ring current (ERC), was described in last year's report (*Year Book 63*, pp. 351–354), in which the variation of yearly means of  $U_0$  over a period of three solar cycles was shown. These results were based on data from the magnetic observatories at Tucson, Arizona, and at Huancayo, Peru. Similar but improved procedures have been used to derive  $U_0$  from data available in additional observatories at Abinger, England; Wingst, Germany; Honolulu, Hawaii; Apia, Samoa; Hermanus, South Africa; and Amberley, New Zealand. The results of this analysis provide a more reliable basis for determining  $U_0$  for periods of a day or less, which is essential for meaningful comparisons with results derived from data obtained in satellites. The same data required for deriving  $U_0$  at the several observatories provided material for investigating electromagnetic induction within the earth for the very low frequency of one cycle per six months.

The procedure for deriving  $U_0$  also provides reliable values of secular change at these observatories. The rates of secular change appear to be essentially constant over several years and then to change rather abruptly within an interval of a year or less. When secular change has been similarly derived from the several observatories in Europe it may be possible to determine whether the abrupt changes in the rate of secular change arise only from motions of sources in the earth's core or whether changes in the strength of these sources with time is also required.

The improved yearly mean values of  $U_0$ , derived from all the observatories mentioned, are well correlated with Bartels' magnetic activity measure  $u$ , based on the interdiurnal variability of monthly means of the geomagnetic horizontal component. Moreover, the linear relation between  $U_0$  and  $u$  indicates that  $U_0 = 0$  for  $u$  extrapolated to zero. The correlation between the amplitudes of the six-month waves in  $U_0$ , which have maxima near the equinoxes, are correlated with corresponding yearly means of  $U_0$ . Although the correlation is low, it suffices to indicate that on the average the amplitude of the six-month wave in  $U_0$  would become zero for zero annual mean of  $U_0$ . These two results check the



procedure used to derive  $U_0$  since for years with no magnetic activity and no six-month variation no ERC would be expected.

R. A. Hoffman and P. A. Bracken<sup>30</sup> analyzed data from a proton detector on the artificial satellite Explorer XII during a pass on August 27, 1961, through the Van Allen Belt that came closest to the equatorial plane. For this pass the investigators obtained the energy distribution of protons with energy above 100 keV, and their pitch-angle distributions in several energy bands. From a thorough analysis of these data they calculated the southward horizontal magnetic field at the earth's equator from the trapped particles to be  $9 \gamma$ , with an estimated uncertainty of  $\pm 5 \gamma$ . Using the data available from four magnetic observatories, we find  $U_0 = 18 \gamma$  for the corresponding time, which includes  $5 \gamma$  for the induced field within the earth. Thus our estimated external field for the ERC of  $13 \gamma$  is close to the value of  $9 \gamma$  calculated by Hoffman and Bracken.

Additional similar comparisons, and also comparisons of  $U_0$  with direct measurements from satellites of the ERC field, are of course required before the agreement indicated above can be established.

*Induction within the earth from variation of the six-month period in strength of the equatorial ring current.* Several investigators have separated the time-varying magnetic-field component at the earth's surface into parts of external and internal origin. This separation has been effected for frequencies in the external field variations from about one cycle per minute to about one cycle per day or two. Because the more slowly varying components of the external field induce currents at greater depth in the earth, such results have been used by investigators to estimate the variation of electrical conductivity with depth. Knowledge of the variation of electrical conductivity with depth would be improved if the induced field resulting from low-frequency

variations such as the six-month variation in the strength of the equatorial ring current could be reliably determined. Thus the amplitudes of the six-month waves in the horizontal  $H$  and in the vertical component  $Z$  were derived from the available published data for seven observatories, totaling about 200 observatory years. So large a number of years is desirable to reduce the statistical uncertainties in the small amplitude of the  $Z$  variation. The Fourier coefficients of the sine and cosine terms in the six-month waves in  $Z$  and in  $H$  were derived from monthly means of 24-hourly values for all days  $A$ , disturbed days  $D$ , and for quiet days  $Q$ . In addition the coefficients for the six-month waves in  $H$  and in  $Z$  were also derived from monthly means of bihourly averages centered at local midnight on quiet days  $QM$ . From these coefficients those for  $D - Q$  and  $A - Q + QM$  were derived.

The contribution to the coefficients, which may be due to variations in monthly means arising from variations with season, solar cycle, and latitude of the amplitude or phase of the diurnal variation, is eliminated in the coefficients for differences  $D - Q$  and  $A - Q$ . Thus these coefficients should arise from the six-month variation in the field of the ERC, which at the earth's surface is quite uniform. If there are no currents in the ionosphere near local midnight the coefficients for  $QM$  would also come only from ERC variations. Thus the coefficients for  $A - Q + QM$  would be those for all days with contributions from non-ERC variations eliminated.

For  $D - Q$  the maximum depth of currents induced in the earth is found to be about 0.10 earth's radius, and is in accord with that derived from annual means for disturbed- minus quiet-day means for 24 hours. For  $A - Q + QM$  the maximum depth of induced currents is tentatively found to be about 0.15 earth's radius. However, the variation with geomagnetic latitude of the coefficients for  $QM$  indicates that these coeffi-



cients, at least for stations near geomagnetic latitude  $54^\circ$  and near the geomagnetic equator, cannot arise entirely from ERC variations. The coefficients for stations between these latitude extremes may arise only from ERC variations; if so the value of 0.15 earth's radius for the maximum depth of induced currents would be correct. Further analysis of the data is in progress to determine if this uncertainty can be eliminated. In cooperation with Dr. Masahisa Sugiura of the Goddard Space Flight Center coefficients for the six-month waves were derived from selected data, continuous for 38 years, which had been effectively filtered (by digital computer) through a narrow band filter which passed only waves with a period near six months. These coefficients were for practical purposes equivalent to those that had been determined by the usual Fourier analysis. Thus the hoped for reduction due to random fluctuations was not realized.

#### COSMIC-RAY PROGRAM

*Observations and reduction of data.* Cosmic-ray ionization chambers were operated throughout the report year at Huancayo, Peru, and at Fredericksburg, Virginia. Scalings and reduction of records have been kept for both stations to date. While at the John A. Fleming Observatory at Huancayo to assist the program for electrical conductivity anomalies in Peru, advantage was taken of the opportunity to replace the original cosmic-ray control system with one of much improved design. The new system contains a well-regulated ac-dc voltage supply for the plates of the recording Lindemann electrometer. A similar installation at the Fredericksburg Magnetic Observatory has proved most reliable and results in essentially constant sensitivity which materially facilitates reduction of data.

*Cooperation in operation of cosmic-ray meters.* Grateful appreciation is expressed to the U.S. Coast and Geodetic

Survey and the staff of its magnetic observatory at Fredericksburg, Virginia, for efficient operation of the meters during the past report year, and to the Government of Peru, and the Director and staff of the Instituto Geofísico del Peru for making available cosmic-ray records from Huancayo.

#### ELECTRICAL CONDUCTIVITY ANOMALIES IN THE EARTH'S CRUST IN PERU

*U. Schmucker,\* O. Hartmann,\* A. A. Giesecke, Jr.,† M. Casaverde,† and S. E. Forbush*

The cooperative investigation, which was begun jointly in late 1962 with the Instituto Geofísico del Peru for the study of spatial distribution of geomagnetic variations, was continued in 1964 and 1965. The discovery of a marked conductivity anomaly in the region between Pucara and Cuzco in southern Peru was described in *Year Book 63* (pp. 354-362) together with the results of a preliminary examination of records indicating anomalous subsurface conductivity in much of southern Peru, including areas near the coast.

To investigate these anomalies further, adobe housings were constructed and Askania variographs installed in Peru at Casma, Huánuco, Cañete, Camaná, and Desaguadero. Variographs were also installed in the observatory at Arequipa and in the existing adobe housing at Abancay. These instruments have been in operation from about the beginning of November 1964.

Six of the Askantias comprise three sets of two, one of which is on the coast and the other inland on the same magnetic dip line. One set of instruments is on the dip equator, another north, and the third south of it. The instrument at Arequipa provides a third in the line south of the dip equator. Data from these will be used to investigate coast effects and anomalies.

\*Staff Associate.

†Instituto Geofísico del Peru.



Two of the Askantias were sent to the Instituto Geofísico Boliviano for use in a cooperative program with the Department for investigating conductivity anomalies and geomagnetic variations in Bolivia. Mr. Salvador del Pozo of the Instituto Geofísico Boliviano received training at Huancayo in the operation and maintenance of variographs. The two Askantias have been operating in adobe housings in Bolivia at Sicasica and Cochabamba since the end of January 1965. Data from these stations obtained simultaneously with those from stations in Peru should prove useful in investigation of anomalies and of electrojet effects.

For satisfactory analysis and interpretation of the conductivity structure it is essential to obtain reliable simultaneous registration at all variograph stations, especially of events such as magnetic storms, bays, and sudden commencements. Near the present phase of the solar cycle such events are not frequent, and not often extensive. Ten Askantia variographs were completely overhauled and adjusted at Huancayo before installation at the stations. The work included thorough adjustment of temperature compensation of the Z-variometers. Tests were made on the reliability of the temperature compensation of some of the Z-variometers by operating them, after compensation, in a building without much insulation. Comparison with results from other Askantias at constant temperature indicated differences such

that for reliable registration of the diurnal variation of the Z-component it would be necessary to provide adobe housing for the variographs at the field stations, where power for maintaining the instruments at constant temperature is not generally available.

Film copies of Askantia records have been received for the months of November 1964 through March 1965 from the stations in Peru. Records from all seven stations were obtained only from about mid-December 1964. A few small bays and other disturbances were simultaneously registered at all stations and these are now being examined to ascertain if they are adequate for analysis. Registration is continuing, and copies of more recent films are expected to indicate what further registration, if any, at the seven stations is necessary.

It is hoped to begin soon the construction of additional adobe shelters for the Askantias in the Cuzco-Lake Titicaca region to investigate more thoroughly the extent of the conductivity anomaly in that area and to provide further data that can be analyzed together with those already obtained there and with those which are being obtained in Bolivia.

We gratefully express appreciation to the U.S. Coast and Geodetic Survey for the loan of Askantia variographs and to the National Science Foundation for generous grants for the Department and to the Instituto Geofísico Boliviano in partial support of these programs.

## LABORATORY PHYSICS

### NUCLEAR PHYSICS

*L. Brown, H. A. Christ,\* and W. Träbslin\**

The most important development during the past year is the use of polarized protons as incident particles in elastic scattering. The transition from deuterons to protons was considerably easier than ex-

pected and has rewarded us with fundamental information about three simple nuclear interactions:  $\text{He}^4(p, p)\text{He}^4$ ,  $\text{C}(p, p)\text{C}$ , and  $\text{H}(p, p)\text{H}$ . Furthermore, a comparison of our measurements with beams of both kinds of particles leads to the solution of a problem in measuring deuteron polarization that has troubled all experimenters using similar sources of polarized deuterons. Analysis of the proton data is incomplete but shows a degree

\*Carnegie Institution Fellow and Fellow of Swiss National Foundation; from University of Basel, Switzerland.



of polarization nearer that of an ideal source than that determined for the deuteron beam with the  $\text{He}^3(d, p)\text{He}^4$  and  $\text{H}^3(d, n)\text{He}^4$  reactions. This adds evidence to a new theoretical explanation by L. C. McIntyre<sup>31</sup> of these two reactions. These reactions are used almost exclusively for determining deuteron tensor polarization, and theoretical predictions of their behavior were thought unassailable. The study of the  $\text{He}^3(d, p)\text{He}^4$  reaction as a function of energy, described in *Year Book 63* (p. 362), was completed, and the  $D(d, p)T$  reaction was investigated in search of the answer to a specific question about nuclear forces.

### POLARIZED PROTONS

The simplest interaction, scattering of protons by protons, shows very small polarization effects at energies of a few million volts and is of no use as an analyzer for a beam of polarized protons. The scattering of protons by  $\alpha$  particles has large effects at about 2 MeV and is also the easiest kind of reaction to consider, since the helium nucleus has neither spin nor structure in this energy range. The reason for the marked difference between proton-proton and proton-alpha scattering lies in the quantum nature of angular momentum. A proton experiences the nuclear force at greater distances when interacting with an  $\alpha$  particle than with a proton; furthermore, a proton has a higher center-of-mass velocity when incident on an  $\alpha$  particle than on a proton. These two facts lead to the onset of interactions with unit orbital angular momentum at lower energies in proton-alpha than in proton-proton interactions.

The scattering of polarized protons, or of any particle with a spin of one half, is considerably simpler than that of deuterons. Indeed, vectors suffice for the description. The incident beam is characterized by polarization vector  $\mathbf{P}_b$ . In our case the direction of this vector is determined by a magnetic field in the ion source, and the magnitude can be predicted for an ion source operating ideally.

All previous work with deuterons led us to believe that the direction of  $\mathbf{P}_b$  was well determined, but not its magnitude.

A polarized beam incident on some target nucleus is scattered according to the equation

$$\sigma_p(E, \theta, \phi) = \sigma_o(E, \theta) [1 + \mathbf{P}_b \cdot \mathbf{P}^a(E, \theta)]$$

where  $\sigma_o(E, \theta)$  is the distribution of an unpolarized proton beam of energy  $E$  scattered at an angle  $\theta$  and  $\sigma_p(E, \theta, \phi)$  is the distribution of a polarized beam scattered at reaction angle  $\theta$  and azimuthal angle  $\phi$ . The azimuthal dependence comes from the scalar product of  $\mathbf{P}_b$  and the nuclear function  $\mathbf{P}^a(E, \theta)$ . The latter is oriented perpendicular to the reaction plane and has a sign defined by the Basel convention as positive if it is in the direction  $\mathbf{k}_{in} \times \mathbf{k}_{out}$ , where  $\mathbf{k}_{in}$  and  $\mathbf{k}_{out}$  are the momentum vectors of the incident and outgoing particles, respectively.  $\mathbf{P}^a$  can have values only between  $-1$  and  $+1$ . Clearly  $\mathbf{P}^a$  is the object of our experiments, and from the equation it is seen that  $\mathbf{P}_b \cdot \mathbf{P}^a(E, \theta)$  is what we measure. Our first task is to determine  $\mathbf{P}_b$ , the polarization of our beam.

A prediction of  $\mathbf{P}^a$  can be made from the phase shifts imparted to the various partial waves by the interaction. Sets of phase shifts can be determined for target nuclei of spin zero from measurements of  $\sigma_o$  and the appropriate set selected by polarization measurement. In point of fact the phases are often more sensitive to  $\mathbf{P}^a$  than to  $\sigma_o$ ; consequently, in practice both quantities must be measured to determine the phases accurately. Knowledge of the phases is equivalent to knowledge of the scattering matrix; if all elements of the scattering matrix are known, then all the measurable information about the interaction is known.

Because of its fundamental nature we use the proton-alpha interaction to determine the polarization of our beam. The procedure, simple in concept, is tedious in practice. Using the quantum theory of scattering we seek the set of phase shifts for the  $S$ ,  $P_{1/2}$ , and  $P_{3/2}$  partial



waves plus a value of  $\mathbf{P}_b$  that best reproduces the measurements  $\sigma_o(E, \theta)$  and  $\mathbf{P}_b \cdot \mathbf{P}^a(E, \theta)$ . The phases are energy dependent, the beam polarization is not. We are measuring  $\mathbf{P}_b \cdot \mathbf{P}^a$  at 12 different scattering angles for each of 12 different energies. About 70 such polarization points have already been determined with accuracies ranging from 0.004 to 0.010 for  $\mathbf{P}_b \cdot \mathbf{P}^a$ . It is perhaps worth noting that during the 15 years since the first observations of nuclear polarization only six values of  $\mathbf{P}^a(E, \theta)$  have been reported in the energy range of our equipment, and these are less accurate. Examples of our measurements of the proton-alpha interaction are shown in Fig. 43.

The scattering of protons by carbon, which is 98.9 per cent pure  $\text{C}^{12}$ , illus-

trates the structure that can be observed with this instrument. Two levels, a  $P_{3/2}$  at 1,698 keV and a  $D_{5/2}$  at 1,748 keV, in the compound nucleus  $\text{N}^{13}$ , cause rapid fluctuations in  $\mathbf{P}^a$  with energy and angle, as illustrated in Figs. 44 and 45.

The target used for carbon is methane. At forward angles one can observe proton-proton scattering in addition to proton-carbon. These data show values of  $\mathbf{P}_b \cdot \mathbf{P}^a$  of about the same size as the experimental errors except for a few points where the polarization effects in carbon are large. We do not consider these proton effects meaningful, because they can result from counting protons scattered by carbon. The carbon data are not affected by the presence of hydrogen.

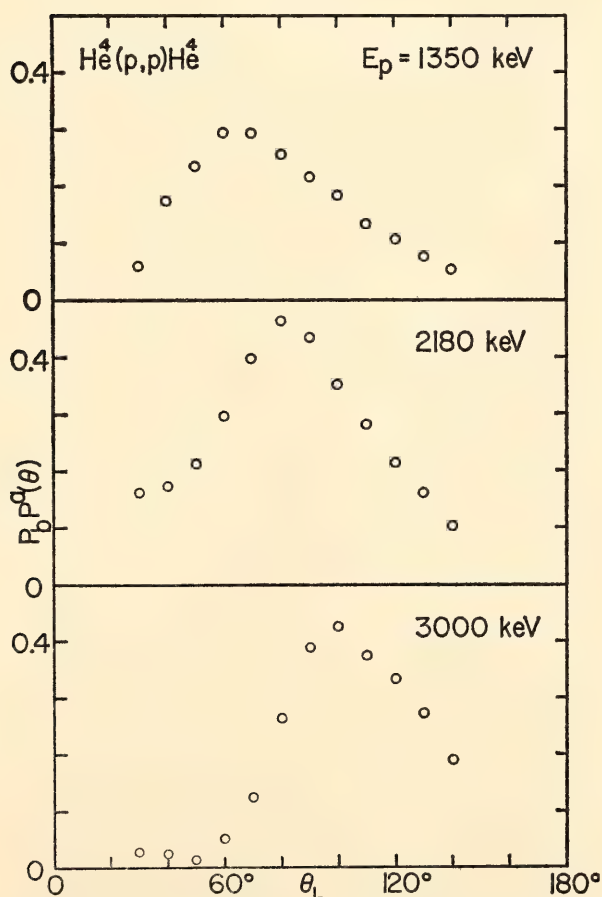


Fig. 43. Samples of function  $\mathbf{P}_b \cdot \mathbf{P}^a(\theta)$  in proton-alpha scattering for three energies. Errors due to counting statistics range from 0.004 to 0.009. Distribution at 2,180 keV indicates the high polarization of the beam, since  $|\mathbf{P}^a(\theta)| \leq 1$  and  $|\mathbf{P}_b| \geq 0.490$ .

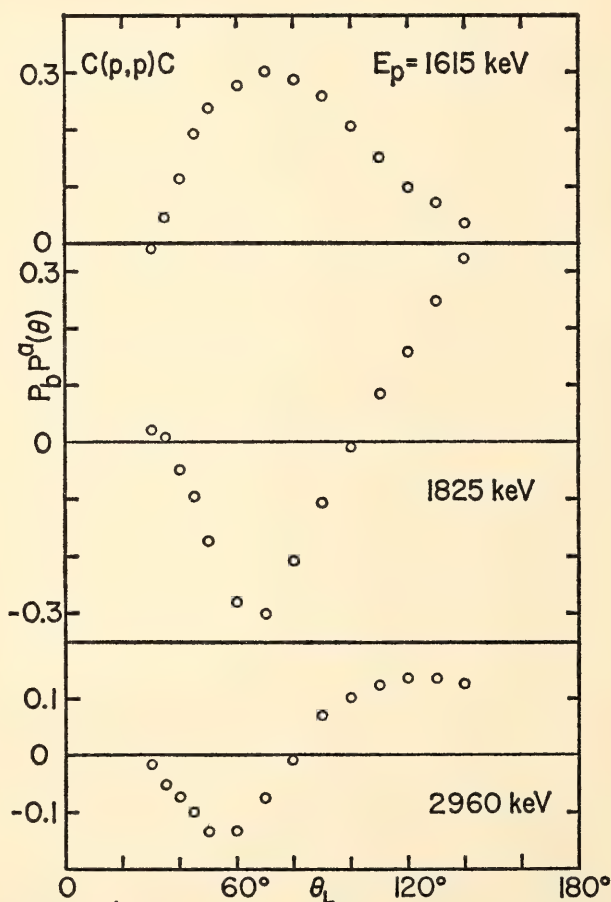


Fig. 44. Samples of function  $\mathbf{P}_b \cdot \mathbf{P}^a(\theta)$  in proton-carbon scattering for three energies. Errors due to counting statistics range from 0.002 to 0.007 for 1,615 and 1,825 keV and from 0.005 to 0.011 for 2,960 keV. Rapid change of polarization with energy of the first two distributions is due to a  $P_{3/2}$  level at 1,698 keV and a  $D_{5/2}$  at 1,748 keV.

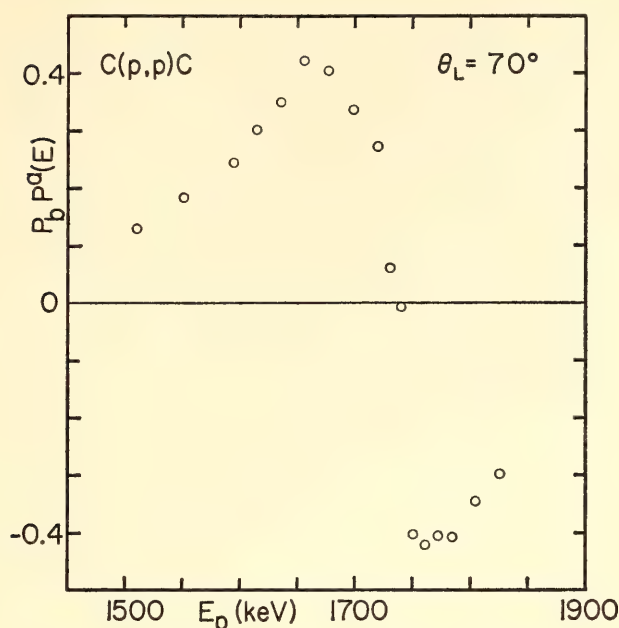


Fig. 45. Sample of function  $\mathbf{P}_b \cdot \mathbf{P}^a(E)$  in proton-carbon scattering for laboratory angle  $70^\circ$ . Errors due to counting statistics range from 0.004 to 0.008. Here the rapid change of polarization with energy, pointed out in Fig. 44, is again illustrated.

#### POLARIZED DEUTERONS

The study of the  $\text{He}^3(d, p)\text{He}^4$  reaction, as outlined in *Year Book 63* (pp. 362–365) is complete. L. C. McIntyre has explained the variation of the measurements with energy for bombarding energies below 1,000 keV satisfactorily. Furthermore, this theory can also explain why we obtained a value of deuteron polarization below that predicted for the ion source. Previously we ascribed this discrepancy

to experimental effects, but some values of  $\mathbf{P}_b \cdot \mathbf{P}^a$  obtained in proton-alpha scattering already exceed 0.47, indicating a beam polarization nearer the value for an ideal ion source (0.490) than was the case for deuterons.

The  $S$ -wave  $3/2^+$  resonances of the  $\text{He}^3(d, p)\text{He}^4$  and  $T(d, n)\text{He}^4$  reactions allow the distribution of the protons or neutrons to be calculated as a function of the tensor polarization of the deuteron beam, as discussed in previous reports. McIntyre notes that the selection rules allow the presence of an  $S$ -wave  $1/2^+$  state, even though it is not a resonance. For unpolarized deuterons such an interaction could scarcely be observed, but it appears as an interference term in the anisotropic distribution caused by tensor polarized deuterons.

The  $D(d, p)T$  reaction was investigated at deuteron energies below 1,280 keV to determine if transitions between the  $^3P_1$  deuteron-deuteron state and the  $^1P_1$  proton-triton state occur. According to a theoretical study by Rook and Goldfarb<sup>32</sup> this question may be answered by measurements of the kind used to study the  $\text{He}^3(d, p)\text{He}^4$  reaction. Our observations show that in the frame of Goldfarb's theory such transitions do take place. The occurrence of such transitions implies the presence of a spin-orbit force acting between proton and triton.

#### BIOPHYSICS

*E. T. Bolton, R. J. Britten, D. B. Cowie, R. B. Roberts, P. Szafranski,\* and M. J. Waring†*

Our studies this year have centered upon two major areas. In one area nucleic acid interactions have been exploited to reveal homologies among the DNAs of different species of higher plants and they

also have revealed homologies within the DNA of a given species of higher plant or animal. In the other area of study, the induction of lysis in lysogenic bacteria has been used as a guide for ascertaining events at the molecular level which are concerned with macromolecular organization in bacterial systems. The implications of the findings have provided a basis for a rational chemotherapy toward the control of the experimental ascites tumor in the mouse. Illustrative experimental results are presented in the

\*Carnegie Institution Fellow; from Institute of Biochemistry and Biophysics, Polish Academy of Sciences, Warsaw, Poland.

†Carnegie Institution Fellow; from Department of Biochemistry, University of Cambridge, England.



following paragraphs, and their significance for understanding evolutionary processes on the one hand, and the control of growth on the other, is discussed. These paragraphs reflect the continuing privilege of personal expression in the choice of our research and in the means by which it is conducted. They also reflect the results of interactions among colleagues who share in the intellectual excitement generated by new and basic findings and nurtured by new and basic ideas.

#### INTERACTIONS OF NUCLEIC ACIDS PLANT NUCLEIC ACIDS

Studies of homologies among the nucleic acids of higher plants have been initiated following the development of a general method for the preparation of high-molecular-weight plant DNA. The results are as yet tentative and relatively sparse. Nevertheless they demonstrate that the DNA-agar procedure described in earlier reports can contribute toward further understanding of genetic relationships and evolutionary connections among plants.

*Preparation of plant DNA.* The method outlined below for the isolation of DNA from seedlings of the common garden pea has been successfully applied to other legumes and to representative ferns, gymnosperms, and angiosperms. In general it is advantageous to use young and rapidly developing tissues such as seedlings, although well-expanded leaves of several dicotyledons and monocotyledons have also proved useful sources of DNA.

Ten grams of fresh weight of pea seedlings from which the cotyledons have been stripped are minced with scissors and ground by hand with a pestle and mortar. After one minute of vigorous grinding, 10 ml of a solution containing one per cent sodium dodecyl sulfate, 0.1 *M* sodium ethylene diamine tetraacetate, and 0.3 *M* sodium chloride are added, and grinding is continued for another minute. The resulting thick

paste is transferred to a stoppered bottle containing 20 ml of chloroform in which one per cent octanol is dissolved. The mixture is shaken rapidly by hand for 30 seconds and then centrifuged briefly to separate the phases. The upper aqueous layer, which contains the DNA, is poured into a bottle and heated to 70°C for five minutes. This extract is quickly cooled to room temperature and is adjusted to contain 1 *M* sodium perchlorate. It is again shaken with an equal volume of chloroform-octanol, and recentrifuged. The aqueous layer is then removed to a beaker, care being exercised to minimize shearing forces which damage DNA. Two volumes of 95 per cent ethanol are layered over the extract, and the DNA is wound on a glass rod. Should the DNA concentration be low, the nucleic acid will not wind efficiently. In this event the alcohol-precipitated nucleic acid can be collected by centrifugation and dissolved in a small volume of salt solution from which the DNA usually can be reclaimed by winding it on a glass rod after again adding two volumes of alcohol. The spool of DNA is transferred to a vessel containing 0.015 *M* sodium chloride, and the DNA is dissolved by gentle shaking. The procedure to this point usually requires about one half hour.

The DNA solution may be stored indefinitely at 4°C over a drop of chloroform, or the DNA may be further purified by treatment with ribonuclease and by shaking with phenol. This step is especially useful when the DNA is contaminated with plant pigments. The yield of DNA varies considerably depending upon the species of plant and particularly upon the stage of development of the tissue. Typically, 2–3 mg of highly polymerized DNA may be extracted from 10 grams of fresh young garden pea leaves, roots, or tendrils, while only about 0.1 mg of DNA has been prepared from 50 grams of well-developed fronds of a common fern (*Woodwardia Sp.*).

*Similarities among plant DNAs.* Some

results of experiments in which radioactive plant DNA fragments have been allowed to interact with single-stranded DNA immobilized in a matrix of agar are presented in Figs. 46 and 47. The radioactive DNA was prepared by the method just outlined from seedlings that had been allowed to develop while their roots were bathed in water containing  $P^{32}$ . The design of these experiments was to react radioactive DNA fragments of one species with homologous DNA in agar in the presence of increasing amounts of nonradioactive DNA fragments from the same or from a different species. Whenever there exist in the mixture radioactive and nonradioactive fragments that are similar in nucleotide sequence the nonradioactive fragments will compete with the radioactive ones for sites on the DNA immobilized in the agar. Hence, the amount of radioactivity bound to the

DNA-agar is decreased, and the decrement serves as a measure of the amount of similar DNA in the two forms.

Figure 46 shows the results of interactions of several plant DNAs with that of the common garden pea. Thus, about one half of the nucleotide sequences in the DNA of the hairy vetch (*Vicia villosa*) are similar to those in the pea, while only about one fifth are held in common between beans (*Phaseolus vulgaris*) and peas. A species of tobacco (*Nicotiana glauca*) DNA interacts to a much smaller extent and no interaction can be detected between rye (*Secale*) and pea DNA. The pea, vetch, and bean are members of the family *Leguminosae* and their DNAs interact to a greater degree than does the DNA from another dicotyledon of a different family (*N. glauca*) or that from a monocotyledon (rye). It would appear, therefore, that such interactions might usefully be applied to chart systematic

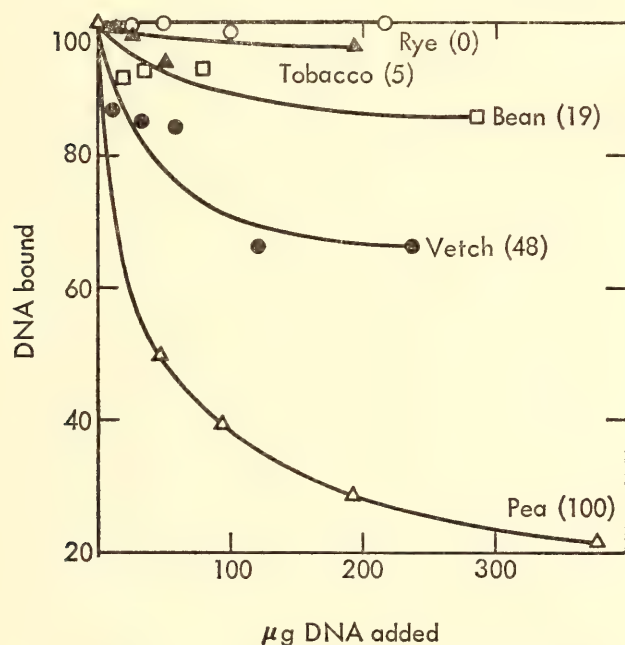


Fig. 46. Competition by unlabeled DNA fragments in reaction between labeled pea DNA fragments and agar containing high-molecular-weight single-stranded pea DNA. One microgram of  $P^{32}$ -labeled (Ca 1,000 count/min/ $\mu$ g) pea DNA fragments was incubated with 0.5 gram of agar containing Ca 160  $\mu$ g pea DNA in the presence of unlabeled DNA fragments from the species indicated. Percentage (relative to homologous test in absence of competitor) of labeled DNA fragments bound is plotted against amount of unlabeled DNA fragments added.

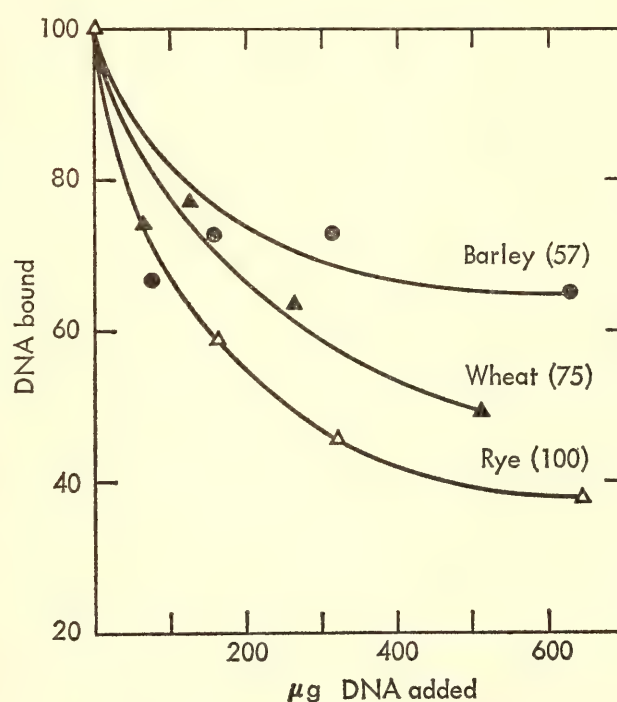


Fig. 47. Competition by unlabeled DNA fragments in reaction between labeled rye DNA fragments and agar containing high-molecular-weight single-stranded rye DNA. One-half microgram of  $P^{32}$ -labeled (Ca 1,000 count/min/ $\mu$ g) rye DNA fragments was incubated with 0.5 gram of agar containing 18  $\mu$ g rye DNA in the presence of unlabeled DNA fragments of the species indicated. Coordinates as for Fig. 46.



affinities and possible evolutionary relationships among the higher plants. It is of interest that within the family *Leguminosae* the relative genetic diversity as measured by these DNA interactions is at least as great as exists among orders of mammals as distantly related as men and mice. The basis for such diversity is not known. It may be that peas and beans, being cultivated forms and therefore strongly influenced in genetic composition by human intervention, have been submitted to a kind of "forced draft" evolution. In view of this consideration it will be of interest to compare DNA homologies among a series of cultivated forms and among a series of feral species of plants. Given an adequate archeological and paleontological record of the probable evolutionary progress of such forms it ought to be possible to assess how profoundly man has influenced the average rate of evolution within a group of plants.

The lack of interaction between the DNAs of monocots (rye) and dicots (pea) indicates a relatively rapid evolutionary change in nucleotide sequence homology. Among the vertebrates, similarities can be detected in the DNAs of primates and fishes whose common ancestors existed perhaps 450 million years ago, whereas the stock that gave rise to the monocots and dicots is thought to have existed as recently as 135 million years ago. Whether such relatively rapid change in the plant DNAs results from cultivation or from subtle causes deeply rooted in the mechanism of plant evolution poses a challenging problem.

Comparisons of similarities in the DNAs of rye, barley, and wheat have also been made and are illustrated in Fig. 47. It is evident that the wheat DNA contains more nucleotide sequences similar to those of rye than the barley DNA. These interactions of the DNAs of the cereal grains are especially intriguing because fertile hybrids of wheat and rye are a commonplace, while hybrids of barley and rye are not known. Approximately 60 per cent similarity exists in the DNAs of

rye and barley, while about 80 per cent obtains for those of rye and wheat. The possibility is thus offered that quantitative comparisons of DNA homologies may serve as indicators of genetic compatibility between plant species. It might be feasible, for example, to provide the plant breeder with a choice among possibilities for successful crosses which would have a high probability of giving rise to desirable offspring. Experiments along this line are being conducted in cooperation with Dr. G. R. Wiebe of the Bureau of Plant Industry at the U. S. Department of Agriculture, Beltsville, Maryland.

These experiments with DNAs extracted from plants are frankly probing, and the results so far achieved are tentative. Nevertheless, the application of the DNA-agar method to plant nucleic acids promises to yield new information concerning genetic relatedness and extent of taxonomic categories among plants, their evolutionary connections and possible mechanisms in plant evolution. In addition, a new criterion may be applied toward the evaluation of genetic compatibility among plant species.

#### "RENATURATION" OF THE DNA OF HIGHER ORGANISMS

The DNA-agar method has been successfully used to measure the evolutionary relationships among higher organisms. The method takes advantage of the fact that the fraction of nucleotide sequences held in common between various species can be measured quantitatively. Fundamental to this success was the separation of the two complementary strands of the DNA and the subsequent pairing of *matching* complementary strands. It has been shown for viral and bacterial DNA that this process of "renaturation" occurs readily under proper conditions and proceeds nearly to completion. Thus, most of the DNA can be re-formed into double strands with essentially the helical structure and stability of native DNA.

It was early realized, however, that the large amount and suspected diversity



of DNA in the cells of higher organisms presented a severe problem. The great dilution of individual nucleotide sequences, which results from the complexity of the genetic composition of higher organisms, was expected to prevent the rematching of complementary strands and thus the renaturation. The expectation was borne out when Marmur and Doty failed to detect evidence for renaturation through studies of the physical properties of calf thymus DNA. The success of the DNA-agar work has therefore remained an important and challenging puzzle. This section describes a number of findings leading to the resolution of the puzzle and indicates some far-reaching implications for the organization of the animal genome and, consequently, for understanding evolutionary processes.

New insight has come from work carried out during the report year at the DTM laboratory and by our close colleagues, Dr. Bill Hoyer, Dr. Malcolm Martin, and Dr. David Axelrod at the Laboratory of the Biology of Viruses, NIH. Complementary results have also been obtained independently by P. Walker and A. McLaren at the University of Edinburgh. The following summary of the important experimental results and conclusions has been drawn from the results of our colleagues' work as well as our own. "Renaturation" is used below in an inclusive sense and describes the process of strand pairing by nucleotide sequence matching even where the matching is imperfect and the renatured product differs from a native double-stranded helix.

1. Renaturation of animal DNA occurs between strands in solution as well as when one partner is partially immobilized by embedding in agar.

2. The resulting complementary strand pairs are only partly helical in structure, and the helical regions are disrupted at a lower temperature than that required to disrupt the helical structure of native DNA.

3. Temperature at which the renatured pairs can be disrupted depends on the

temperature at which they were formed.

4. Renaturation of animal DNA in solution leads to the formation of extended structures or three-dimensional networks in which any given strand forms helical base-paired regions with a number of other strands.

5. The formation of such networks involves species-dependent specific pairing of complementary base sequences.

6. The rate of renaturation of animal DNA is about the same as that of bacterial DNA. Based upon the quantity of DNA per cell, the animal genome is apparently a thousand times larger than that of the bacterium. Such a condition would be expected to lead to a thousandfold relative dilution of individual nucleotide sequences and thus a thousandfold increase in the time required for renaturation to occur.

7. Even when the DNA of an animal cell is sheared into millions of pieces and denatured, a majority of the single-stranded fragments find complementary strands with which to renature in a relatively short incubation period.

8. DNA from mouse tissues contains a fraction that has only a small number of distinct nucleotide sequences. These appear to be present in a very large number of copies (perhaps  $10^6$  per cell). This fraction constitutes between 10 and 20 per cent of the total DNA and can be separated from the remainder by virtue of the precision and rapidity with which it renatures.

It is concluded that many nucleotide sequences occur repeatedly in the DNA of higher organisms. The sets or families of repeated sequences may be characterized by the multiplicity of repetition (or number of members in the family) and the length and precision of repetition of the nucleotide sequences. These parameters can at present only be estimated. The rate of renaturation suggests that for mammals an average family has perhaps a thousand members. Since the majority of the millions of different sheared fragments do renature, there may be a few thousand such families. Figure





observed with the DNA-agar method might conceivably depend on some property of the milieu induced by immobilizing DNA in agar. Therefore, experiments were designed to look for such a property of the agar and to measure the extent of pairing in solution. No effect of agar was observed on the strand separation of native DNA embedded in agar. For this purpose melted agar was cooled to 50°C, mixed with a solution of native mouse DNA and poured in a thin sheet on a cold glass surface. The separation of the strands of DNA mounted in four per cent agar, as measured by the variation of its ultraviolet absorbancy with temperature, was identical with that in free solution. Thus, neither the gross physical immobilization nor the agar environment measurably influenced the denaturation process.

Several methods were used to show that *sheared* pieces of animal DNA in the single-stranded state do indeed pair in solution with single-stranded high-molecular-weight DNA. In these tests, denatured sheared labeled DNA was incubated at 60°C for 18 hours with denatured high-molecular-weight homologous DNA. In one experiment the high- and low-molecular-weight DNAs were separated by trapping the incubated mixture in agar at 50°C and then washing away untrapped DNA. Controls showed that sheared pieces incubated at low concentration were completely removed by the washing procedure. After incubation with high-molecular-weight DNA, the proportion of the sheared pieces retained by the agar corresponded to the amount of reaction observed in the usual DNA-agar method. Another experiment employed molecular sieves (columns of Sephadex-200 or one per cent agar operated at 60°C in 2 × SSC\*) to separate large and

small pieces of DNA after incubation. Again, the amount of radioactivity from small pieces that became associated with large fragments agreed with the values expected from experiments with the DNA-agar method.

Networks of high-molecular-weight DNA and any small associated pieces can be retained on filters of cellulose acetate allowing estimation of the extent of reaction (see Fig. 53). By this method species dependence of the attachment in solution was shown and the kinetics of the reaction were measured. By 18 hours approximately 60 per cent of the small pieces had paired with the high-molecular-weight DNA in solution. This extent of binding is higher than that ordinarily achieved in agar, presumably due to elimination of the competing reaction between sheared pieces and DNA which becomes detached from the agar.

A reaction in free solution is also demonstrated by the reduced capability for binding to agar-DNA of DNA that has previously been incubated under renaturation conditions. In a series of experiments carried out by M. Martin and B. Hoyer at the NIH, labeled, sheared, denatured mouse DNA was first incubated at various concentrations at 60°C in 2 × SSC and then diluted to a standard concentration (0.1 µg/ml) and incubated with homologous high-molecular-weight DNA embedded in agar. At low preincubation concentrations there was little loss of ability to bind to agar-DNA. At higher concentrations the capability to bind dropped rapidly to low values.

In a valuable additional series of experiments the preincubated ("inactivated") DNA was reactivated by heating at various temperatures before testing in the agar-DNA system. In this way the stability of the product of renaturation in solution was measured. The temperature for 50 per cent reactivation was found to be similar to the temperature required to elute 50 per cent of the sheared pieces bound to DNA-agar. Thus the type of

\*The buffers used in the course of this work had the following compositions. SSC: 0.15 M NaCl, 0.015 M trisodium citrate. 2 × SSC: 0.3 M NaCl, 0.03 M trisodium citrate. SET: 0.3 M NaCl, 0.001 M EDTA, 0.1 M tris-HCl buffer, pH 7.4. HMP: 0.001 M EDTA, 0.0075 M sodium phosphate buffer, pH 6.8, total Na<sup>+</sup> concentration, 0.013 M.



structure formed in solution is similar to that formed in agar, although neither is as stable as the native DNA.

Evidence for a reaction occurring in free solution has also been obtained from measurements of the optical hypochromicity of animal DNA. Figure 49 shows the relative optical density at 260  $m\mu$  as a function of temperature of sheared mouse DNA that had been denatured and incubated for 18 hours at 60°C in a high salt medium (SET).

The arrows (Fig. 49) indicate curves derived from data taken during the initial heating and cooling portions of a cycle lasting altogether about one hour. In subsequent cycles the optical density follows reversibly up and down the cooling curves shown. The DNA used in these experiments is not total mouse DNA but the principal fraction (85–90 per cent)

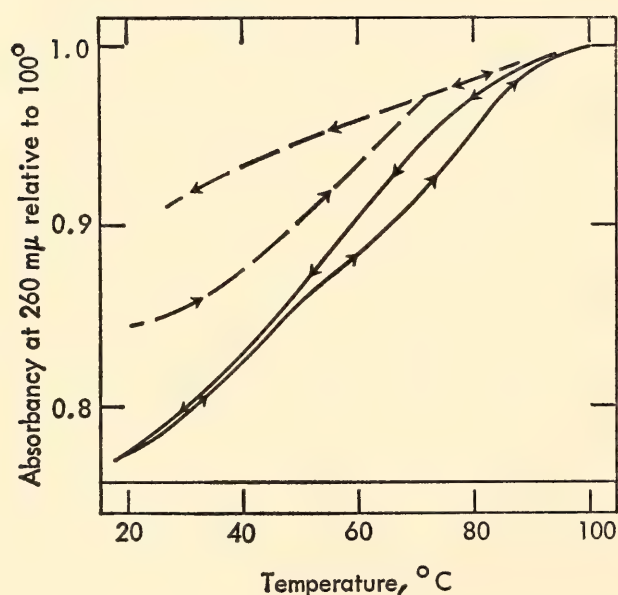


Fig. 49. Optical melting curves for renatured mouse embryo DNA. Preparatory to renaturation the DNA was sheared and denatured, yielding single-stranded pieces of about 400,000 mol wt. It was then incubated at 60°C for 18 hours in SET buffer. Solid curves were measured in buffer of high ionic strength (SET). Dashed curves were obtained after dialysis to low ionic strength (approximately HMP). Arrows indicate curves obtained during heating and cooling. As temperature is increased the complementary *inter*-molecular structures are gradually melted out; on subsequent cooling changes in absorbance reflect *intramolecular* associations and depend on the *pH* and the counterions present.

remaining after a very rapidly renaturing fraction had been removed by CsCl density gradient centrifugation.

It is clear that incubation under renaturation conditions affects the optical properties of the DNA. A reaction has occurred between molecules in solution, and it is not rapidly reversed by exposure of the product to low salt concentrations and modest temperatures. The dissociation of the reaction product occurs at a lower temperature and over a wider range of temperatures than the dissociation of the helical structure of native, double-stranded DNA (Fig. 50).

Marmur and Doty failed to observe a similar effect in their studies with calf thymus DNA. Their published measurements were carried out at 67°C at a high salt concentration equivalent to that of the solid curves in Fig. 49. Thus, the maximum hypochromicity expected would be about three per cent. This hypochromicity was further reduced since their measurements were carried out on high-molecular-weight DNA, which gives a lower hypochromic effect than sheared DNA. Further, at the concentration at

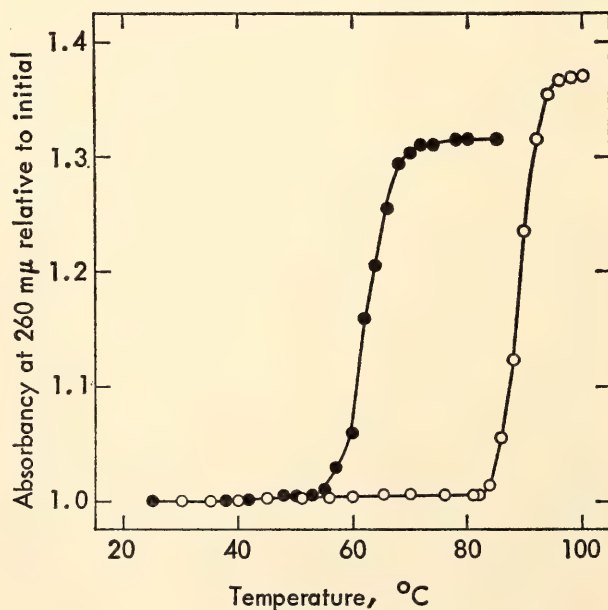


Fig. 50. Optical melting curves for native mouse embryo DNA, to be compared with those for renatured DNA shown in Fig. 49. Open circle, measured at high ionic strength (SET); dashed curve, at low ionic strength (HMP).

which the measurements were carried out the half-time for the reaction is about six hours. The combination of these features of the reaction reduces the expected hypochromic effect under their conditions to less than one half per cent in a two-hour observation period. Such a small change would be difficult to detect.

Measurements of strand association, inactivation, and optical properties of renaturation in free solution leave little doubt that renaturation also occurs in the liquid volume in DNA-agar preparations. This situation permits us to use the evidence from free solution reactions as an aid in interpreting the results from the DNA-agar method. Conversely, results obtained with the DNA-agar method may be used to assess the reaction in free solution. For example, "competition" experiments with the DNA-agar system (Fig. 46) show that renaturation *in solution* is species dependent and therefore rests on the matching of nucleotide sequences common to the species. In such experiments the addition of a great excess of sheared pieces of DNA from a distantly related plant or animal has little effect on the binding to the DNA in the agar of sheared pieces which are homologous to the agar-DNA. The homologous sheared pieces, therefore, do not pair to any great extent with the distantly related heterologous pieces in solution, although the heterologous pieces did pair with each other. Clearly, nonspecific aggregation does not occur to any great extent among sheared pieces of DNA of about  $5 \times 10^5$  molecular weight even at concentrations up to 1 mg/ml.

*The degree of order in renatured DNA.* Figure 49 shows hyperchromic (melting) curves for renatured mouse DNA and Fig. 50 presents a similar study of native mouse DNA for comparison. The optical properties of renatured mouse DNA differ very much from the native. From these data it appears that the renatured structure may be closer to that of denatured DNA than that of native DNA. Before attempting to analyze these and

other data in order to assess the precision of sequence matching, an important new phenomenon needs to be examined, namely, that the stability of renatured animal DNA depends on the conditions of renaturation.

P. Walker and A. McLaren have examined the thermal stability of the complexes between mouse DNA fragments and mouse DNA-agar formed at various temperatures. As mentioned, M. Martin and B. Hoyer have measured the temperatures required for the recovery of the capacity to bind to DNA-agar sheared pieces of DNA that were previously renatured in solution by incubation at a high concentration. Martin and Hoyer's experiments were carried out with the preincubation at several temperatures, and the final binding test was conducted at each of the temperatures. Thus, one set of experiments assesses the product formed in DNA-agar and the other the product formed in free solution. Nevertheless, the conclusions reached are identical and can be summarized as follows.

The renatured product formed at low incubation temperatures has a much lower dissociation temperature than that formed at high temperatures. Further, the percentage binding in the DNA-agar experiments is much greater at the lower temperatures. Both groups of workers have also carried out species cross reactions at different incubation temperatures and have found a higher degree of discrimination among species at the higher temperatures. Tests have not yet been carried out to show whether the discrimination disappears at low temperatures or is enormously broadened in its range.

These results lead directly to the conclusion that there must be a whole range of possible degrees of precision for nucleotide sequence matching within the DNA of a given animal, as well as between the DNAs of different species, and thus the selection of sequence matching to a given degree of precision is determined by the



incubation conditions. This conclusion stands in contrast to that from studies of viral and bacterial DNA renaturation, where the product is very similar to native DNA, and where, within reasonable bounds, only the rate of its formation depends on the conditions of incubation.

Thus, no simple answer can be given concerning the degree of precision of sequence matching in the renaturation of animal DNA. However, it is still of interest to set approximate bounds. The data in Figs. 49 and 50 supply two useful parameters, the distribution of melting temperatures and the total hyperchromicity. The deviation of these parameters from those of native DNA can be interpreted by comparison with the effects of known degrees of sequence mismatch. Figure 51 shows the results of a comparison experiment. Polyuridylic acid was irradiated with ultraviolet light while the low optical density solution was stirred to give homogeneous exposure. The number of residues damaged was estimated by the drop in absorbancy at 260  $m\mu$  since neither product of ultraviolet damage—hydrated uracil or the

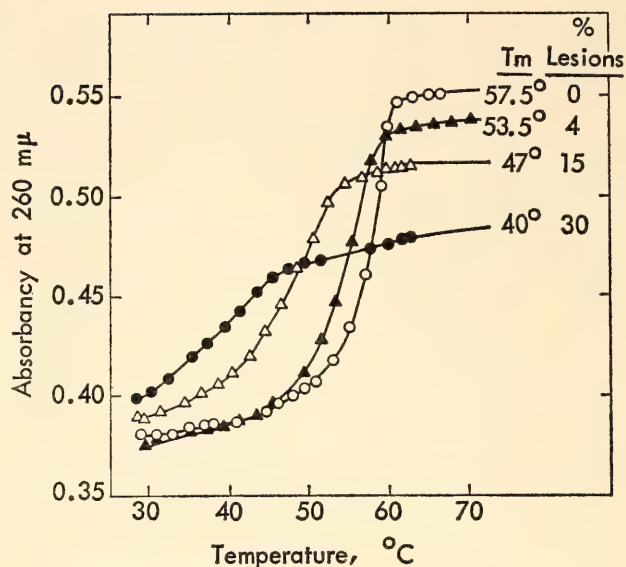


Fig. 51. Effect of ultraviolet irradiation of polyuridylic acid on stability of base-paired structures formed between it and polyadenylic acid. Solutions of poly U and poly A (prepared at an absorbancy of 0.500 in SSC containing 0.1% sodium dodecyl sulfate) were mixed after irradiation of the poly U solution. Column labeled "% lesions" records percentage reduction in absorbancy of poly U solutions due to irradiation (before addition of poly A solution). Since the lesions are most probably dimers, the average length of lesion-free helical regions formed with poly A will be about 200 divided by the percentage of lesions.

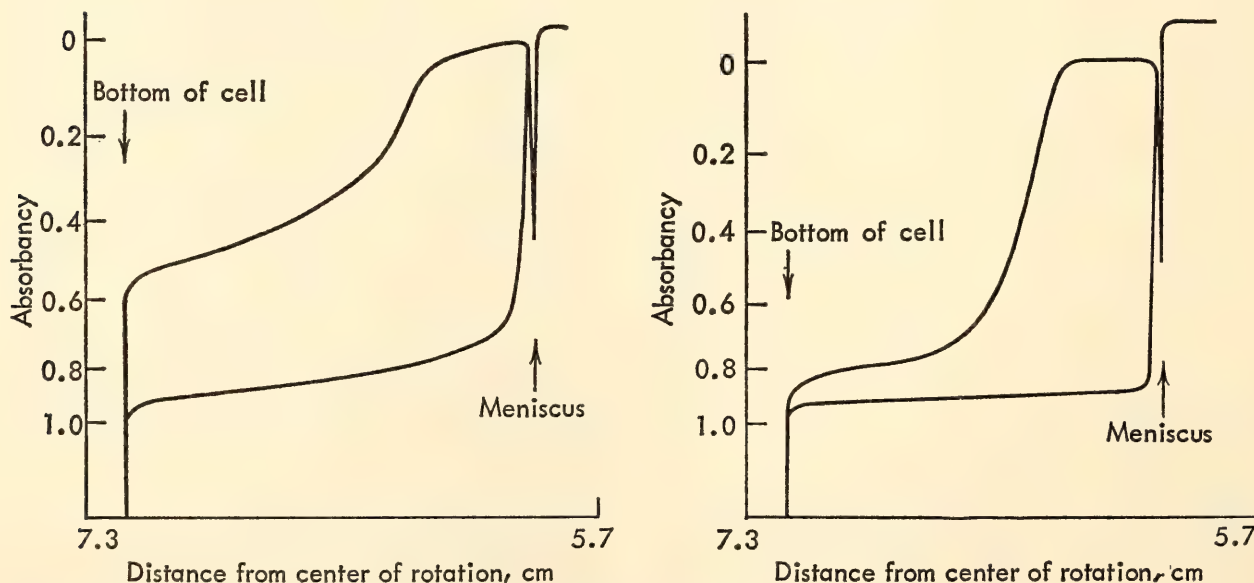


Fig. 52. Analytical ultracentrifugation of sheared denatured calf thymus DNA (right) and the same DNA after renaturation (left). Solution containing 500  $\mu\text{g}$  DNA per ml in SET was heated at 100° for 6 min, rapidly cooled, and separated into two portions. Preparation at left was then heated at 60°C for 3 hours while that at right was held at 0°C. Each solution was dialyzed to a low ionic strength (HMP) before centrifugation. Densitometer tracings are shown for exposures taken just after reaching 50 rpm, 740 rpm, and 80 minutes later.

uracil dimer—has a significant extinction coefficient. When the solution is boiled for five minutes, which reverses the hydration reaction, no recovery of the extinction coefficient is observed in the range of the irradiation dose that was used. It may be presumed, therefore, that the dominant part of the damage is due to dimerization of neighboring residues. The effect of these ultraviolet-induced lesions was assessed by adding polyadenylic acid and measuring the optical melting curves of the resulting imperfect helical structures.

When this calibration is applied to the data in Fig. 49, the reduction in the

melting temperature below that for native DNA suggests that the frequency of errors in the regions that are associated is fairly high, about one in seven residues. Further, the low hyperchromicity suggests that no more than a third of the nucleotides are paired. Thus, as the broad melting curve also indicates, there must be a wide range of degree of reactivation among various strands or regions of individual strands. The observation of low hyperchromicity, in spite of the fact that most strands participate in renaturation, implies that individual strands are paired for only part of their lengths (see Fig. 53 and next section).

The density of renatured DNA in CsCl equilibrium gradients provides another measure of the precision of sequence

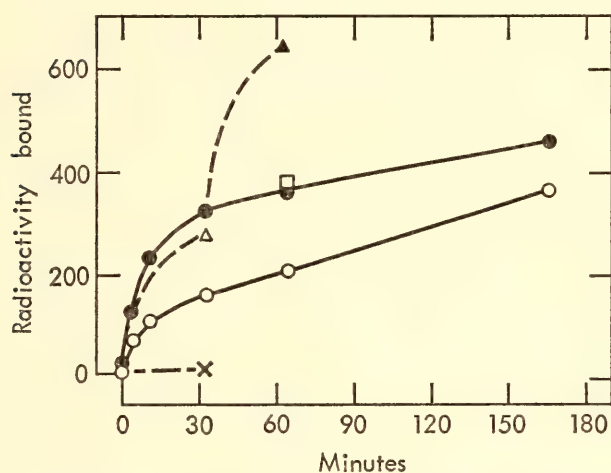


Fig. 53. Binding of  $C^{14}$ -labeled denatured sheared pieces of mouse DNA to networks previously formed from high-molecular-weight mouse DNA. Incubation was at  $60^\circ\text{C}$  in SET buffer. Closed circles: reaction mixtures contained  $1\text{ }\mu\text{g/ml}$  sheared pieces and  $500\text{ }\mu\text{g/ml}$  networks. Open circles: reaction mixtures contained  $0.2\text{ }\mu\text{g/ml}$  sheared pieces and  $100\text{ }\mu\text{g/ml}$  networks. Samples ( $0.1$  and  $0.5\text{ ml}$ , respectively) were diluted into  $3\text{ ml}$  of SET at room temperature and filtered through cellulose acetate filters (Gelman type GA-9; pore size  $0.1\mu$ ), and the filters dried and counted. In both cases, 500 on the ordinate scale represents binding of 50 per cent of sheared pieces present. Four control tests were carried out at the higher concentration. Closed triangle: another equal quantity of labeled sheared pieces added at 32 min and assayed at 64 min; square: another equal quantity of networks added at 32 min and assayed at 64 min; X: sheared pieces and networks preincubated separately for 32 min, mixed, and immediately assayed; triangle: sheared pieces and networks preincubated separately for 32 min, mixed, and incubated together for 32 min before assay.

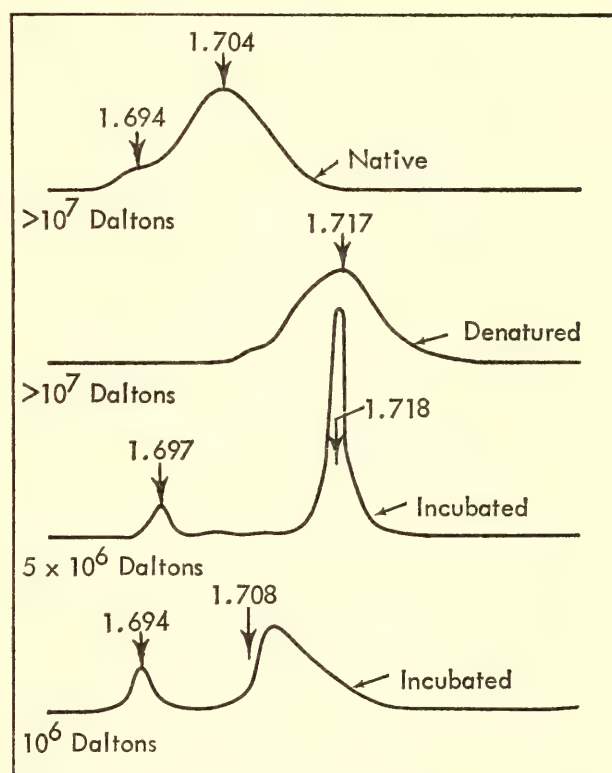


Fig. 54. Analytical CsCl density gradient centrifugation of the following mouse embryo DNA preparations. Top curve: native high-molecular-weight DNA; second curve: same DNA denatured for 10 min at  $100^\circ\text{C}$ ; third curve: DNA sheared lightly ( $500\text{ psi}$ ), denatured at  $100^\circ\text{C}$ , incubated for 18 hours at  $60^\circ\text{C}$  in SET buffer, diluted and dialyzed to low ionic strength (HMP) before adding to CsCl solution; bottom curve: DNA strongly sheared ( $12,000\text{ psi}$ ) and treated as for third curve.



matching. If the density of renatured DNA lies halfway between native and denatured, then the renatured material might contain about 50 per cent precisely matched regions and 50 per cent fully disordered regions. On this basis the lowest curve of Fig. 54 suggests that the product from sheared DNA which has been renatured is more than half precisely matched, although the better matched strands are probably overemphasized in this method.

Figures 54 and 55 show the effect of molecular weight on the matching nucleotide sequences in renaturation. High-molecular-weight DNA ( $\sim 10^7$  daltons) yields a product with little hyperchromicity and with the density of denatured DNA. This evidence shows that very little sequence matching occurs for long

strands of DNA and thus supports the indication mentioned above that sequence matching occurs over only short lengths.

*The formation of networks during renaturation.* Figure 48 has presented a model of the structure formed by renatured DNA. If, as shown on this diagram, only short separated regions are capable of renaturation, then nucleotide sequence pairing between two strands will terminate at the boundaries of such regions. Possibly the next capable regions along these two strands do not match each other; these regions might pair with other strands containing matching regions. In other words, a given strand may pair with several other strands, each along part of its length, and these in turn pair with several others. In this way

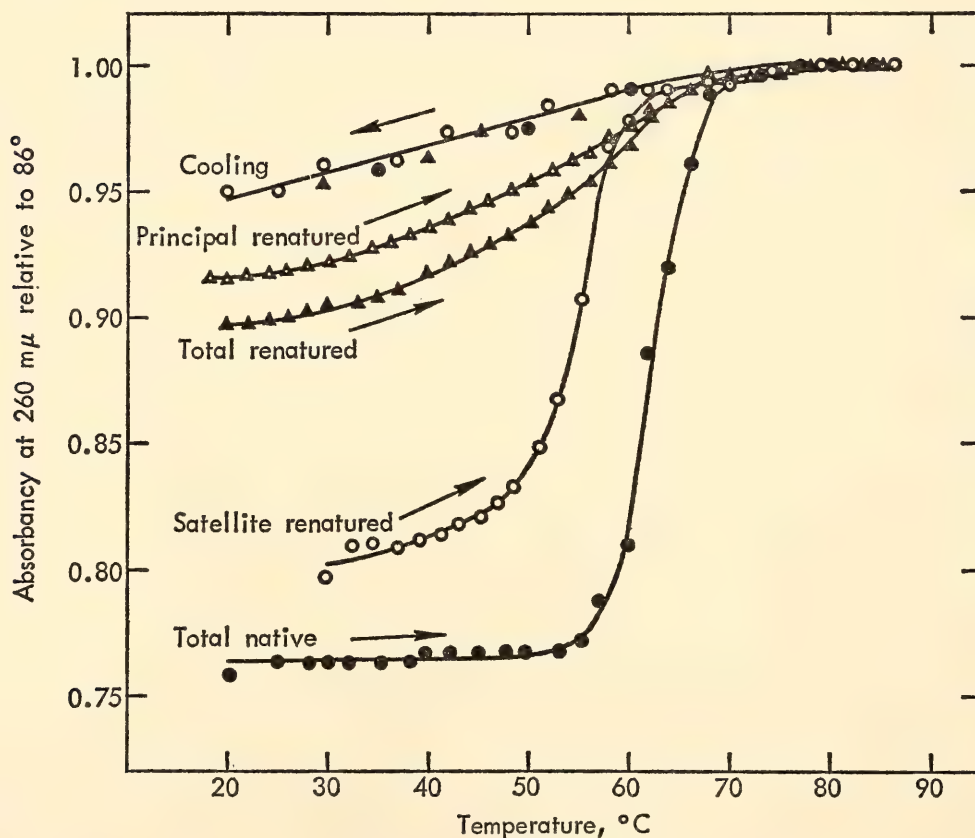


Fig. 55. Optical melting curves of satellite and principal fractions of high-molecular-weight mouse embryo DNA. The measurements were made in buffer of HMP. Closed circle: unfractionated native DNA; closed triangle: unfractionated networks prepared by denaturing DNA at 100°C for 5 minutes followed by incubation for 18 hours at 60°C in SET; circle: satellite fraction of networks; triangle: principal fraction of networks, isolated by preparative CsCl density gradient centrifugation. Absorbance changes for different materials during cooling were closely similar; only a few representative points have been plotted.

extended structures or networks could form that might be of indefinite extent. Probably the requirement for the formation of networks is that there be on the average more than two regions per strand capable of pairing with complementary regions on other strands. The following paragraphs discuss the evidence for the formation of networks and describe some of their properties.

When high-molecular-weight animal DNA is denatured and incubated under renaturation conditions the light scattering slowly increases and suspensions containing less than 100  $\mu\text{g}/\text{ml}$  become visibly cloudy. This observation has been made for calf thymus, mouse, rat, armadillo, rhesus monkey, pea, and euglena DNA. Centrifugation for 10 min at 100,000  $g$  will sediment more than 90 per cent of the gel formed with  $\sim 10^7$  daltons DNA incubated for 18 hours at 60°C in  $2 \times \text{SSC}$ . The gel particles may also be reasonably efficiently filtered out of solution with cellulose acetate membrane filters which were shown not to absorb single-stranded DNA.

Centrifugation yields a very transparent pellet containing from two to five per cent DNA. Such a pellet does not readily resuspend or dissolve and the gel is not dissociated by resuspension in or dialysis to low ionic strength ( $\text{Na}^+ = 0.01 M$ ) buffers. The gel may be decomposed by elevated temperatures, however.

The stability of the gel to thermal dissociation was determined by exposing samples to various temperatures and then measuring the fraction that was pelleted during 15 min at 40,000 rpm. By this criterion the gel is dissociated over a broad range of temperatures and the temperature for 50 per cent dissociation is about the same as the temperature for 50 per cent expression of the hyperchromicity (Fig. 49). For CsCl equilibrium density gradient centrifugation, DNA samples were denatured and incubated under renaturation conditions (60°C, SET, 18 hours), dialyzed overnight to low ionic strength (HMP), and

diluted and added to CsCl (final density of 1.61). The analytical ultracentrifuge cell was half filled with this solution, and then an equal volume of CsCl solution of density 1.79 was layered underneath. These densities were chosen to establish initially both the density and density gradient at the center of the cell near their equilibrium values.

This procedure has the advantage of preventing the pelleting of very rapidly sedimenting gel particles and of reducing the time required for the CsCl density gradient to reach equilibrium from 6 hours to about 1½ hours. Renatured high-molecular-weight calf thymus DNA gives an extremely sharp band at the density of denatured DNA with a width of about 0.1 mm at 27,960 rpm. This sharp band reflects the large size of gel particles and shows an extreme homogeneity (about 0.3 per cent spread in GC content) in average base composition. Since CsCl density gradient centrifugation shows that there is considerable spread (perhaps five per cent in GC) in the base composition among individual double-stranded molecules of  $10^7$  molecular weight, the gel particles must achieve their great homogeneity as the result of a very precise averaging. In other words, the particles are made up of many strands and, in general, individual particles are not formed from special groups of strands the composition of which differs from the average.

Specific network formation by DNA of moderate molecular weight is shown in Fig. 54 by the separation into two well-defined bands. A preparative CsCl density gradient equilibrium run on networks formed from mouse DNA of very high molecular weight also gave a good separation, but the presence of a slight amount of nonspecific aggregation could not be ruled out.

CsCl density gradient centrifugation resolves a mixture of separately renatured calf thymus and salmon DNA into two bands. The density difference is slight (about 0.004) but the resolution is com-



plete because of the extreme sharpness of the two bands. However, when *high-molecular-weight* calf thymus and salmon DNA are denatured and incubated *together*, only one band appears in the CsCl gradient. From the DNA-agar work reported last year it may be estimated that the two species would share five to ten per cent of their DNA nucleotide sequences in common. This small number of common sequences might well be enough to link together all the DNA from both species into network or gel particles. An opportunity is then presented to examine nucleotide sequence relationships among organisms so distantly related that the DNA-agar method fails to reveal them.

Sheared DNA of a molecular weight of only 400,000 (single stranded) also forms networks. The rate of formation is slower than for high-molecular-weight DNA, the gel particles are not as large and a fraction of the DNA does not appear to participate. Figure 52 shows some of the results of an experiment with calf thymus DNA which measures the approximate size distribution of such gel particles and shows among other features that incubation at 60°C is necessary for their formation. On the right is shown the sedimentation of sheared calf thymus DNA, which has been denatured, brought to high salt and dialyzed at 0°C overnight to low salt, then centrifuged in the latter solvent. No aggregation is observed, and 80 per cent of the DNA sediments between 3 and 6 S. On the left is shown the sedimentation of DNA, which has been denatured, brought to high salt and incubated for three hours at 60°C, and similarly dialyzed and centrifuged. Clearly, very rapidly sedimenting material is present, and perhaps only 20 per cent of the DNA retains its original sedimentation rate.

Analysis shows that a broad distribution of sizes is present, ranging from a sedimentation constant of 300 S down to the original 3 S. Although sedimentation characteristics of these networks are not known in detail, it seems likely that

particle molecular weights must range up to  $10^6$  times the sheared pieces and thus be greater than  $10^{11}$  daltons. It was also observed that incubating at 60°C for only one minute yielded little material sedimenting more rapidly than the single-stranded DNA. Studies with pea-root DNA provided similar results.

The species dependence and nucleotide sequence specificity of the network formation with *sheared* DNA follows from the earlier discussion of the specificity of renaturation. Although the best evidence remains the large number of successful DNA-agar competition experiments, some additional tests also show specificity. For example, sheared calf thymus and pea-root DNA were denatured and incubated *together* and the product analyzed by CsCl density gradient centrifugation following the procedure described above. Two well-resolved bands were observed.

The formation of networks with sheared pieces of DNA indicates the perhaps surprising result that pieces of DNA even as small as  $4 \times 10^5$  daltons have several independent regions capable of nucleotide sequence matching. Preliminary experiments suggest that there is a lower limit to the size of sheared pieces of DNA which will form networks. The measurement of such a limit is of considerable interest since it would determine the average spacing of regions in the DNA of the animal genome that are capable of nucleotide sequence matching. In two series of experiments calf thymus DNA solutions were forced through an orifice at pressures ranging from 15,000 psi to 125,000 psi using equipment at the Geophysical Laboratory of the Carnegie Institution through the kindness of England and Boyd.

Upon denaturation and incubation the 15,000 psi sheared DNA (pressure equal to standard shearing conditions) formed networks to the usual extent and about 70 per cent pelleted during centrifugation for 15 min at 40,000 rpm. After the same treatment only 10 per cent of the DNA sheared at 45,000 psi and higher was



pelleted. Sedimentation of the denatured DNA in HMP indicated that the molecular weight of the 45,000 psi sheared material was about 200,000, or about half the size of the usual sheared DNA. Treatment of 15,000 psi sheared DNA for two hours at 100°C suppresses network formation. Such a treatment should lead to about one strand scission per 500,000 daltons of single-stranded DNA and thus reduce the molecular weight to about the same as the 45,000 psi sheared DNA.

In another series of experiments networks were used to measure the kinetics of binding sheared pieces of DNA to high-molecular-weight DNA. For this purpose high-molecular-weight mouse DNA was denatured and incubated (60°C, SET buffer, 18 hours) and the resulting networks harvested by centrifugation and resuspended in buffer (SET). By filtration on cellulose acetate membrane filters about 80 per cent of the network particles could be harvested. On the other hand, sheared C<sup>14</sup>-labeled DNA passed through the filters without significant absorption. Figure 53 shows the results of the incubation of sheared C<sup>14</sup>-mouse DNA with high-molecular-weight network DNA. There is an initial rapid binding followed by a slower reaction. Sixty per cent of the available C<sup>14</sup> pieces were bound after an 18-hour incubation. After correction for the imperfect harvesting of the network particles it appears that at least 75 per cent of the sheared pieces actually paired with the high-molecular-weight DNA.

This result demonstrates that the great majority of DNA pieces 1,300 nucleotides long have at least one region capable of renaturation. The fact that more than two thirds of such pieces join in the formation of networks suggests that most of the pieces have more than one region capable of renaturation. These results and the tentative observation that pieces about 600 nucleotides long do not form networks suggest that regions capable of renaturation occur with an average

spacing of between 300 and 1,000 nucleotides. Interestingly, 300 nucleotides might also be taken to be the lower limit of the size of a gene since such a gene could code for a protein strand of only 10,000 mol wt.

*The rate of renaturation.* The renaturation of DNA is controlled by the collision of complementary nucleotide strands. Thus the rate of renaturation is determined by the concentration of each of the different nucleotide sequences present. Among different organisms the DNA of those with a larger and more complex genome will almost certainly contain a greater number of different nucleotide sequences. Accordingly, the rate of renaturation could be expected to be a measure of the "size" of the genome of an organism. This expectation is borne out for simpler organisms, such as bacteria, and also for the viruses. A number of renaturation rates are presented in Table 10. In spite of the enormous range of rates covered by the data shown, an inverse proportionality is maintained between the reaction rate constant and the amount of DNA in the genome. Some deviation is to be expected because of differences in experimental conditions and in molecular weights of the fragments.

The half-time for a particular initial DNA concentration is listed in Table 10 to permit ready visualization of the rates. In simple cases the renaturation of DNA in solution is a straightforward collision-controlled second-order rate process (see, for example, Fig. 56). In such a case the ratio of the concentration of unpaired strands  $C$  at any time  $t$  to that initially present  $C_0$  may be expressed by  $C/C_0 = 1/(1 + KC_0t)$ , where  $K$  is the second-order reaction rate constant. The half-time is therefore concentration dependent and has been listed for an initial concentration of 100  $\mu\text{g/ml}$ .

The time listed is also the time constant (decay to  $1/e$ ) for the first-order reaction between a small quantity of DNA binding to immobilized DNA (e.g., in agar or as networks). In this case, if the number



TABLE 10. Rate of Renaturation

Nucleic Acid	K liter	Half-Time, min	L Nucleotides	K $\times$ L $\times 10^6$
	mol sec			
Poly U + poly A	$1 \times 10^6$	$5 \times 10^{-5}$	(2)	2.0
SV-40 DNA	$3 \times 10^2$	1.5	$1.2 \times 10^4$	3.6
T-4 phage DNA	8.3	6.0	$4 \times 10^5$	3.3
<i>E. coli</i> DNA	0.37	170.0	$10^7$	3.7
Mouse DNA	...	120.0	$10^{10}$	...

The rates of renaturation of the DNAs listed in the first column were determined from measurements of the decrease in absorbancy at 260  $m\mu$  of sheared fragments (400,000 daltons) at 60° in high salt (SET). In addition, the mouse DNA renaturation was measured as described in Fig. 54. P. D. Ross and J. M. Sturtevant (1962)<sup>33</sup> measured the rate of renaturation of poly U and poly A using a stopped flow system to measure the rapid fall in absorbancy. The homopolymers had sedimentation constants similar to those of the DNA fragments. The rate was measured at optimum temperature (25°C) in 0.4 *M* NaCl. The second column lists the second-order reaction rate constant for the collision controlled part of the renaturation process. The third column lists the half period in minutes for a concentration of 100  $\mu\text{g/ml}$ . The fourth column lists the complement of DNA (expressed as number of nucleotides) present in each cell or virus particle. The fifth column lists the product of this number with the reaction rate constant.

of free sites in the immobilized DNA remains constant, the concentration of the minor component should decay exponentially as  $M/M_0 = e^{-K C_0 t}$  where  $C_0$  is the concentration of the immobilized DNA. Where a number of components with different rates of renaturation are present, as is surely true for the DNA of higher organisms, the rate constant is not listed and the half-time is listed as a qualitative index of the average rates. The half-times represent the collision-controlled (nucleation) part of the process of renaturation. In the very rapid cases the "zippering" phase might actually be rate limiting at this high concentration.

The conclusion may be drawn from Table 10 that animal DNA renatures much faster than would be predicted from consideration of the amount of DNA per cell nucleus. The average rate of renaturation for mouse DNA (Table 10; Fig. 53) is about 1,000 times faster than that predicted from the rates observed for DNA of bacteria. This result is consistent with measurements of the kinetics of DNA-agar binding, the rate of inactivation by incubation, the rate of network formation, and preliminary studies of the rate of development of hypochromicity. Similar studies have

been carried out with DNA from a number of different vertebrates. A detailed intercomparison is not at present justified. The renaturation of animal DNA does not follow the hyperbolic time

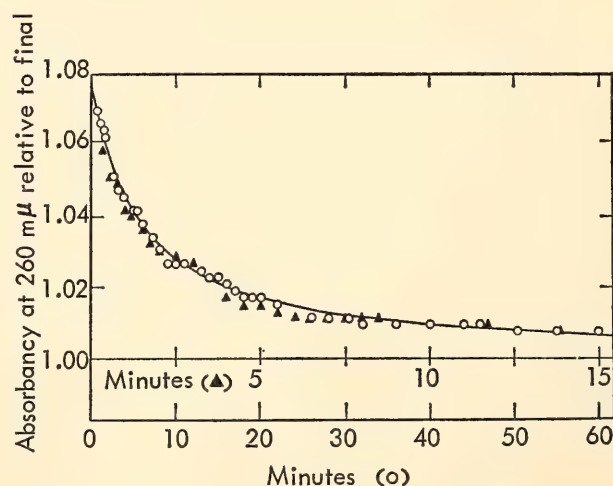


Fig. 56. Kinetics of renaturation of mouse satellite DNA. The DNA, dissolved in low ionic strength buffer (HMP), was denatured at 100°C for 4 min and returned to room temperature. At time zero salt concentration was brought to 0.09 *M* in  $\text{Na}^+$ , and the resulting hypochromic change was followed with time. Closed triangle: DNA concentration 24  $\mu\text{g/ml}$ ; absorbancy readings made using a 1-cm light path. Circle: DNA concentration 6  $\mu\text{g/ml}$ ; readings made using a 4-cm light path. Curve is theoretical, calculated for ideal second-order reaction.



course of a second-order reaction as does the renaturation of simpler DNA. Apparently a number of components are present with individual rates of renaturation distributed over a very wide range. The fastest component yet observed has a rate 100,000 times that expected in the absence of any repetition in the genome, and other components occur with rates between 10,000 and less than 1,000 times this expectation. Slower rates probably also occur but are as yet masked by the faster components.

There is little possibility that the very rapid renaturation could depend upon some as yet unknown chemical or physical difference between animal DNA and the simpler DNAs, because, as Table 10 indicates, even the relatively large differences between the ribonucleotide homopolymers and DNA have little effect. There appears to be no present alternative but to seek the explanation in the concentration of the sequences capable of renaturation. In this connection an extremely rapidly renaturing fraction of mouse DNA is described in the paragraphs below.

*Satellite DNA in the mouse.* Some years ago, S. Kit and W. Szybalski independently reported the presence of a satellite component in mouse DNA. It was revealed as a strong band in CsCl density gradients and appeared at a lower density than the principal fraction. The satellite was found in native DNA prepared from several strains of mouse and from all tissues examined, including mouse cell lines cultured in vitro. During the course of our work with mouse DNA the satellite was discovered to renature quite precisely at a very high rate.

Mouse embryo DNA extracted from a preparation of nuclei was gently sheared to a molecular weight of some  $5 \times 10^6$ , brought to 700  $\mu\text{g/ml}$  in SET, denatured by heating at 100°C for five minutes, and incubated at 60°C for four hours. A sample of the resulting suspension of networks was diluted with a neutralized CsCl solution and centrifuged to equi-

librium in a density gradient. Two extremely sharp and well-separated bands were observed (Fig. 54). The presence of two resolvable components in the original native DNA was then demonstrated by repeating the equilibrium centrifugation with an unsheared sample of the stock DNA. When the positions of the sharp network bands are compared with those of the native DNA it is clear that the satellite networks have a density close to that of the native form, but the density of the principal network band is higher than that of the principal component of native DNA by about 0.015 g/cm<sup>3</sup>. The density of the principal networks is almost equal to that of denatured mouse DNA, which gives a broad band under these conditions showing slight, if any, evidence of separation into two components (Fig. 54). These observations indicate (1) that the satellite DNA renatures almost completely when incubated at 60°C while the principal fraction hardly renatures at all, and (2) that the degree of base-sequence homology between the satellite and principal DNAs is too low to permit extensive cross reaction and formation of hybrid networks. Further experiments showed that networks prepared by incubating DNA sheared at 15,000 psi give rise to bands showing density decrease due to renaturation in both components (Fig. 54). The satellite band is broader but still lies at its "native" density, while the principal band is now much broader and skewed toward the lighter density side. Evidently breakage of the DNA into smaller pieces permits much more extensive base-sequence matching in the principal fraction.

Quantitative estimation of networks cannot be achieved in the analytical ultracentrifuge because of the errors introduced by the light-scattering properties of the particles. However, the difference in density between networks derived from the two components permits satisfactory separation in the preparative ultracentrifuge, which would be difficult



with native DNA because of the considerable overlapping between the satellite and principal bands. A suspension of networks was mixed with a CsCl solution of density 1.92 in proportions calculated to give 1 ml volume of solutions having densities 1.632, 1.648, 1.672, 1.696, and 1.724. The solutions were layered in order of density and the resulting step gradient centrifuged to equilibrium in an SW 39 rotor at 20,000 rpm for 72 hours. At the end of the run the two classes of networks were visible as sharp, light-scattering bands separated by about 8 mm. Fractions (four drops each) were collected and their absorbancy at 260  $m\mu$  measured. The separation achieved was not perfect but three fractions contained almost pure satellite DNA. The fraction of the total material constituted by the satellite was estimated to be 10–20 per cent.

The high degree of renaturation seen with satellite DNA was confirmed by dialyzing a suspension of satellite networks (purified as above) into HMP buffer and following the thermal denaturation profile (Fig. 55). The hyperchromic change given by this material was very high, almost as high as that of unfractionated native mouse DNA, and the  $T_m$  was 55°C compared with 62°C for the native DNA. The value of  $T_m$ , combined with the density observed in CsCl (Fig. 54), suggests that the base composition of the satellite is about 10 per cent lower in GC than that of the principal fraction. Compared with the melting properties of the satellite networks, the hyperchromic effect given by networks of the principal band is very much smaller and shows no distinct melting temperature. Figure 49 shows that principal band networks prepared from strongly sheared mouse DNA gave a hyperchromic effect about double that shown in Fig. 55, but the absorbancy still rose steadily between 40°C and 70°C. Thus, the extent of renaturation is less for the higher molecular-weight preparations of the DNA of higher organisms.

The most striking feature of the renaturation of mouse satellite DNA is

its rapidity. When denatured satellite DNA is incubated in the presence of moderate salt concentrations the hypochromic effect due to renaturation develops very rapidly, as shown in Fig. 56. Not only do the measured points fit closely to a theoretical curve for second-order kinetics, but a fourfold lowering in the concentration at which the DNA is incubated leads to a fourfold increase in the time scale of the reaction, as expected for a process requiring collision between reactive elements. The exact correspondence between the experimental points and the theoretical curve also shows that the reaction occurring over the period of the measurements is not significantly heterogeneous. Since the hyperchromicity of the product of renaturation of the satellite is not much less than that of native DNA, it appears that nearly perfect sequence matching occurs. The rate of satellite DNA renaturation is 14 times faster than that for simian virus-40 DNA. It must be concluded, therefore, that the concentration of reactive elements in satellite DNA per unit of ultraviolet absorbing material is much higher than that of viral DNA (mol wt  $3.5 \times 10^6$  daltons); in other words, its complexity is much lower. Thus, mouse satellite DNA represents a fraction of the mouse genome in which a relatively small piece of genetic information, possibly only a single gene, has been copied an enormous number of times. The best estimate at present (with considerable uncertainty) is two million copies of a 250,000-dalton stretch of nucleotide sequence.

The fact that a narrow satellite band is observed in native DNA in CsCl equilibrium centrifugation shows that the segment of DNA in which it occurs is at least several million in molecular weight. Further, the fact that networks of satellite DNA from high-molecular-weight DNA have native satellite density shows that such segments are almost entirely made up of satellite-type DNA. In other words, the 250,000-dalton repeating sequences are strung end to end



in sets of at least 10 and possibly very many more.

*Repetition of nucleotide sequences.* Since stretches of nucleotide sequence in animal DNA are capable of renaturation at more than 1,000 times the expected rate, it is evident that an excessive concentration of these nucleotide sequences exists. Moreover, many sequences must be sufficiently similar for complementary nucleotide sequence recognition and pairing to occur and yet not be identical over long stretches. Large numbers of long identical sequences would result in a large hypochromicity and a high melting temperature of the renatured DNA. However, only in the exceptional case of the mouse satellite DNA have such results been observed.

The average melting temperature of renatured mouse DNA (Figs. 49 and 55) is in fact about 10°C below that of native mouse DNA. This finding suggests that 10–20 per cent of the nucleotides in most of the regions that do pair must be mismatched as a result of the variations in actual nucleotide sequence of different segments in the DNA. Alternatively, the matching regions could be very short. Measurements of the melting temperatures of oligonucleotides in the poly U–poly A system suggest that if the stretches were perfectly matched they ought not to be longer than 20–50 nucleotides.

We may refer to the sets of sequences capable of pairing with each other as members of families. Such repetition could arise through occasional duplication of regions of the DNA and any given stretch of nucleotide sequence might very well have a complex parentage passing back through many steps of the duplication process. Membership in one family need not exclude membership in another. Our evidence concerning the existence of such sets of sequences at present derives entirely from families with very many members. The average families in mouse DNA have perhaps a thousand members and half their members renature in a few hours (at 100  $\gamma$ /ml total DNA concen-

tration). A family with only a tenth as many members would renature in about 10 times this period and thus not affect the results of experiments lasting over a relatively short period.

*Evolutionary implications.* The existence of a large amount of nucleotide sequence repetition in the DNA of higher organisms must deeply influence the processes of evolution. A detailed evaluation of the nature of the families of repeated sequences will surely yield new knowledge of the genetic mechanisms.

Some of the parameters that need to be determined and that may reflect the course of evolutionary change are: (1) The number of nucleotide sequences that are repeated. (2) The number of copies of each or, more realistically, the distribution of family membership count. (3) The average precision of repetition and the distribution of degrees of precision. (4) The average length of repeated segments. (5) The spacing along the DNA at which repeated segments occur. (6) The degree of interspersion of different family representatives in the DNA.

Since the various parameters are not completely independent of each other, and any single experimental observation will often be influenced by more than one parameter, a combination of different approaches will be necessary to characterize the material adequately. The following list indicates experimental observations that are dominantly influenced by one or another of the parameters: (1) The maximal hypochromicity achieved after incubation is chiefly a function of the number of repeated nucleotide sequences. (2) The rate of renaturation provides an estimate of the average multiplicity of repetition. (3) The thermal denaturation profile of renatured material gives information about the precision of matching of repeated sequences. (4) The renaturation properties of DNA after fragmentation into pieces of different lengths can be used to estimate the length and spacing of repeated segments. (5) The formation of networks



reflects the distribution or interspersion of repeated segments in the population of DNA molecules.

It will probably be years before the full implications of such studies and observations are realized because a large amount of experimental work will be required to assess the characteristics of the families of repeated sequences in a variety of organisms. Nevertheless, some evolutionary implications deserve comment. Since many DNA sequences exist in repetitive families composed of many members, new repetitions must be continually created during the evolution of a species. This becomes evident when it is realized that each of two species that have diverged significantly maintains large amounts of internal homology or repetition, but has lost some interspecies homology. Thus, in at least one of the species (and presumably both) new sets of multiple repeated sequences have arisen. A reasonable conjecture for the source of the repetitions is that they originate by multiple copying of preexisting genes. To account for the continual divergence of species the gene-

duplication process would have to occur frequently over a large fraction of geologic time. The genome of a present-day animal would, therefore, contain many nucleotide sequences that are the progeny of a gene that had been present in some earlier generation.

While the repeated sequences are able to pair with each other in tests for sequence complementarity, they need not be identical. Furthermore, the nucleotide sequence of a given gene may be made up of sections that exhibit complementarity with sequences in several other genes. Thus, the pattern of repetitions in the genome of a particular animal would result from a balance of processes such as duplication, translocation, point mutation, and deletion of nucleotide sequences, as suggested in Fig. 57.

From this view it is useful to regard the repetitive DNA sequences as relatives of each other—more or less distant, depending on their particular history and the selection pressure against or favoring change. Families of descendants could exist with any number of members from

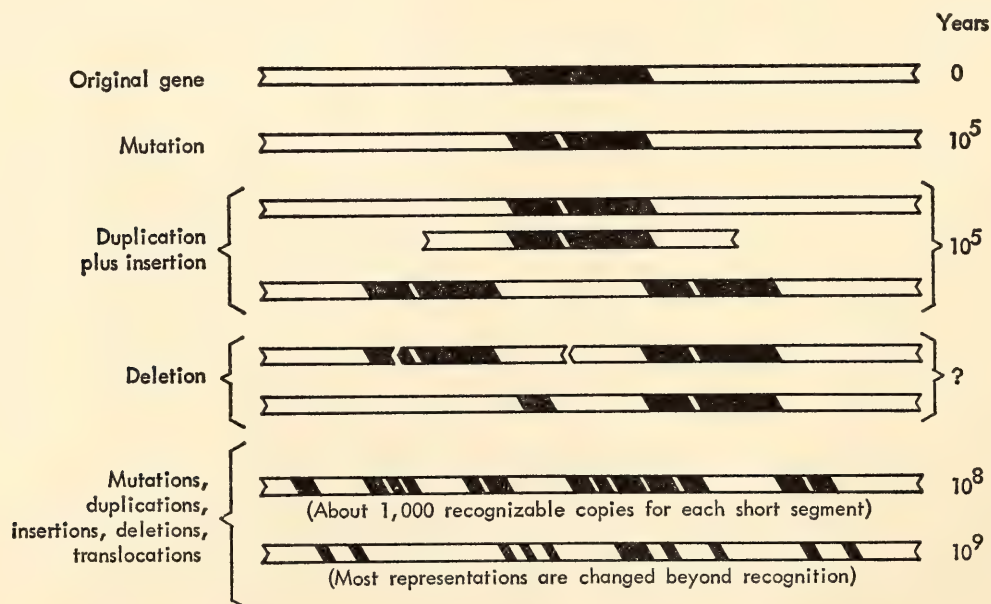


Fig. 57. Suggestive diagram of possible origin and history of a family of repeating sequences in DNA of a vertebrate. DNA of an arbitrarily chosen gene has been indicated in black, to show its contribution to nucleotide sequences in the descendants. Two regions of sufficient length which derive from same part of original gene can form complementary strand pairs that are stable in standard DNA-agar experiment. Times are indicated as general guides, not intended to represent rates of events themselves but approximate time of appearance of resulting DNA sequences in population of animals. Similar history is assumed for neighboring regions.



one or two to tens of thousands. Whether the relationships are created gradually by fairly common single duplications or catastrophically by rare events of extreme multiplication remains for the future to tell. The occurrence of the second possibility is suggested by the highly repetitive mouse satellite DNA.

The idea of gene duplication is not new; the striking evidence for earlier suggestions for at least limited occurrence has come from the degree of similarity of amino acid sequences among different, though related, proteins. However, the studies described above imply that gene duplication, or at least DNA nucleotide sequence duplication, is a very general phenomenon and leads to an enormous amount of internal relationship among nucleotide sequences in the genome of higher organisms.

The probable relation between gene duplication and the rate of evolution is also of interest. Once a gene has been duplicated, the risk of deleterious mutation is decreased. Further, if we may consider one copy (the effective gene) as being conserved relatively unchanged as a result of selection pressure, so that the function it specifies is neither lost nor adversely modified, other copies would be free to mutate as long as deleterious gene products did not result. These copies would initially have the capacity to specify a complete gene product—for example, an enzyme or part of a physiological system. As mutations occurred in the copies some elements might be lost or modified and other elements maintained. The capacity of some copies to specify the original function might well disappear entirely in the course of time in lines of animals that would not, on this ground, suffer a selective disadvantage.

The development of a gene specifying a new function from remaining elements of an older gene that had been protected from adverse selection pressure by copying seems to be far more probable than its development *de novo* from a random

nucleotide sequence, and would represent an evolutionary mechanism of consequence. A great source of variety in new structures might result from the combination (by translation of parts of duplicated genes) of elements from several pre-existing genes. If indeed duplication is responsible for the repetition of nucleotide sequences found in animal DNA it cannot occur uncommonly. The fact that most sheared pieces of DNA (1,300 nucleotides long, or a reasonable size for a structural gene) contain sequences shared by many other pieces implies that most sequences are derived from other sequences. In turn this suggests that most genes are derived at least in part from other genes.

Among the vertebrates the families of repeated sequences change at such a rate that the possibility of interspecies pairing is lost for half the members of the sequence families in 100 million years, as indicated by measurements under the conditions used in experiments with DNA-agar columns. At the same time new families are being created at about the same rate, each containing perhaps thousands of members. The production, on the average, of one new family member by duplication each 100,000 years could account for the observed rate of divergence. It is realized that the surprises already apparent in the characteristics of the extremely repetitive mouse satellite DNA and the somewhat similar feature in calf thymus DNA caution against premature conclusions, but it is also abundantly evident that a new area has been opened to exploration.

#### LYSOGENIC SYSTEMS

Studies of the induction of lysis can yield information in two different but possibly related areas. On the one hand they might provide some clues as to the association of viral DNA with that of the host. The viral DNA is said to be “integrated” into the bacterial genome, meaning that the viral DNA is replicated



once per bacterial generation and that the viral DNA is carried along with the host DNA during mating. Little is known about the nature of the association; the viral DNA could be inserted as a part of the host DNA strand or it could lie in some parallel association. Both views run into conceptual difficulties, and further information on the details of the release from this integration might favor one or the other of these views.

On the other hand, studies of the induction of lysis might have some implications for cancer chemotherapy. Some forms of cancer have been demonstrated to be caused by lysogenic virus. Furthermore, a high degree of correlation has been found between agents that induce lysis in  $K^{12}$  ( $\lambda$ ) bacteria and those having antitumor activity. During the course of the studies concurrent experiments with mice gave considerable encouragement to this hypothesis.

The experiments described below indicate that two stages are involved in the release of virus from lysogenic bacteria. Defects must be introduced into the DNA by one of a number of different agents. However, the defect alone is not sufficient to ensure subsequent lysis; repair mechanisms may come into play and remove the defect before the virus is released. Agents that presumably inhibit repair enhance the effectiveness of the original agent used to produce the defects. Thus a combination of agents, one to induce defects and another to prevent repair, is much more effective in altering a lysogenic state than either one used alone. This general principle seems to apply to the more complicated mammalian system as well as to the bacteria.

#### SUBSTRAINS OF *Escherichia coli* 15 BACTERIOPHAGE

*Escherichia coli* strain 15(TAU)<sup>-</sup>, when selected as a nonlysogenic strain for comparison with  $K^{12}$  ( $\lambda$ ) showed inductive characteristics similar to those of  $K^{12}$  ( $\lambda$ ).

Evidence supporting the conclusion that 15(TAU)<sup>-</sup> and several other substrains of *E. coli* 15 are in fact lysogenic is presented below. Because of the added versatility given by the three biochemical blocks, additional studies were carried out using 15(TAU)<sup>-</sup> as an example of a lysogenic bacterium.

*Induction of Escherichia coli* 15 (TAU)<sup>-</sup>. Treatment of lysogenic bacteria with mitomycin C results in cellular lysis and the release of mature bacteriophage. Our studies have shown that lysis of strain 15(TAU)<sup>-</sup> also occurs after exposure to various concentrations of mitomycin C, as shown in Fig. 58. These and similar results obtained with the lysogenic strain

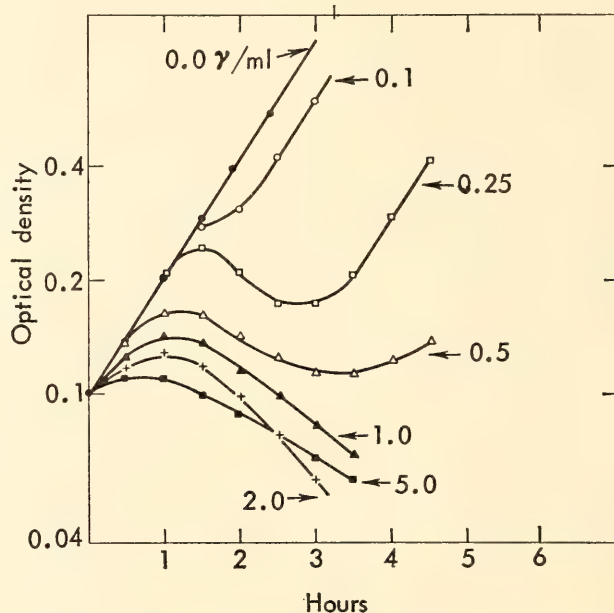


Fig. 58. Growth and lysis of *E. coli* strain 15 (TAU)<sup>-</sup> after exposure to mitomycin C. Culture of *E. coli* strain 15 (TAU)<sup>-</sup> growing exponentially in glucose-salts medium supplemented with thymine, arginine, and uridine was centrifuged and resuspended in 10 ml of same medium. Mitomycin C was added to give indicated concentrations and cells were treated for 15 min at 37°C without aeration. At end of period they were centrifuged and washed, then suspended in 100 ml of the growth medium with aeration at 37°C. Growth and lysis were observed by measuring optical density (at 650 m $\mu$ ) with Zeiss spectrophotometer. Mitomycin concentrations were as follows. Closed circle: 0.0  $\gamma$ /ml; circle: 0.1  $\gamma$ /ml; square: 0.25  $\gamma$ /ml; triangle: 0.5  $\gamma$ /ml; closed triangle: 1.0  $\gamma$ /ml; plus sign: 2.0  $\gamma$ /ml; closed square: 5.0  $\gamma$ /ml.

$K^{12}$  ( $\lambda$ ) differ significantly from results obtained with the nonlysogenic *E. coli* BB.

Bacteriophage induction also occurs when lysogenic bacteria are treated with ultraviolet. Figure 59 shows the growth and lysis of strain 15(TAU)<sup>-</sup> following various periods of exposure to ultraviolet light.

Transient thymine privation of thymineless *E. coli*, lysogenic for bacteriophages  $\lambda$  or  $P_{1b}$ , has been used to initiate the production of mature phage particles in lysogenic systems. Figure 60 shows the lysis induced by various periods of thymine privation of 15(TAU)<sup>-</sup> cells. Restoration of thymine to the cultures is required for completion of cellular lysis, a requirement also consistent with observations in other thymineless lysogenic systems.

Azaserine has been shown to be a bacteriophage-inducing agent. Figure 61 shows the growth and lysis observed

when 15(TAU)<sup>-</sup> are treated with various concentrations of azaserine.

In each of these examples, lysis of the 15(TAU)<sup>-</sup> cells occurs in a way characteristic of known lysogenic systems responding to the same inducing agents. These responses are not observed with nonlysogenic cells under identical environmental circumstances. An examination of (TAU)<sup>-</sup> cellular lysates was therefore undertaken to identify and describe the products of induction.

*Isolation of the virus.* Lysates of cultures of 15(TAU)<sup>-</sup> produced by each of these inducing procedures were found to contain bacteriophage. Residual cells and cellular debris were removed by centrifuging 10 minutes at 10,000 *g* in an SS-1

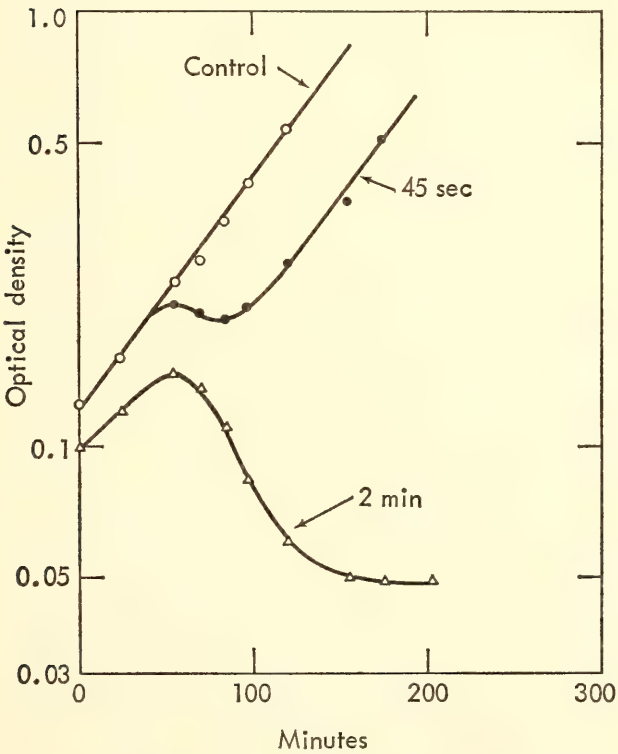


Fig. 59. Growth and lysis of *E. coli* strain 15 (TAU)<sup>-</sup> following exposure to ultraviolet light. Circle: control (no ultraviolet treatment); closed circle: 45-sec exposure; triangle; 2-min exposure.

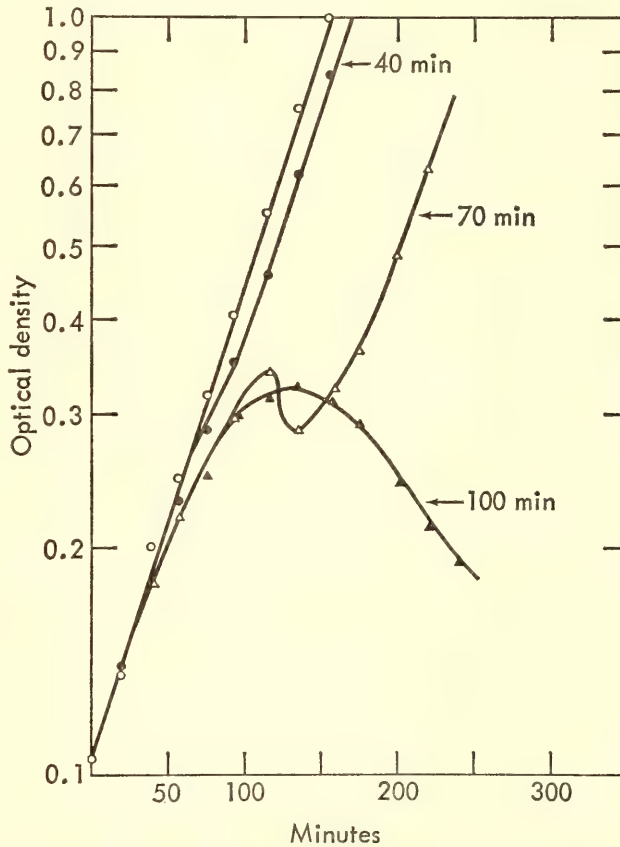


Fig. 60. Growth and lysis of *E. coli* strain 15 (TAU)<sup>-</sup> following transient thymine privation. A culture of cells growing exponentially in glucose-salts medium supplemented with thymine, arginine, and uracil was washed by centrifugation and resuspended in same medium without thymine supplement. Culture was divided and aerated at 37°C, and thymine restored at time 0 min (circle); 40 min (closed circle); 70 min (triangle); and 100 min (closed triangle).



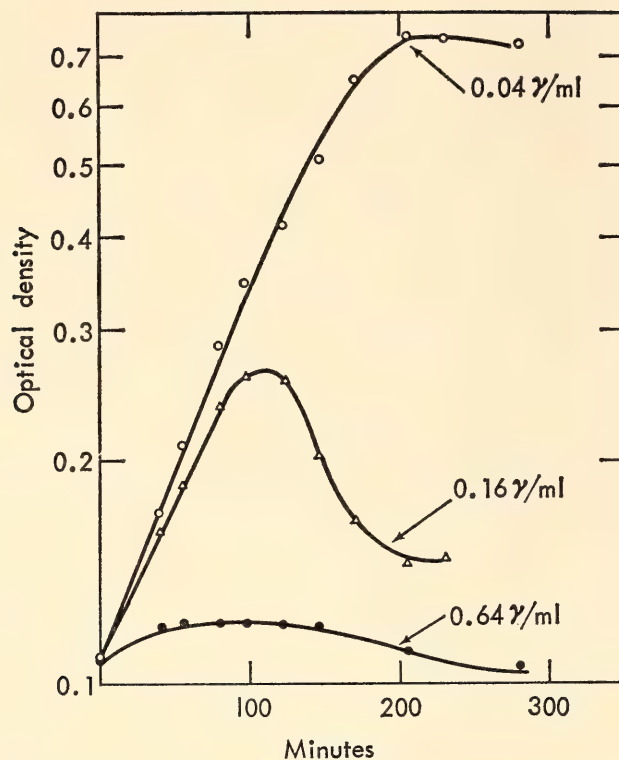


Fig. 61. Effect of azaserine on growth of *E. coli* strain 15 (TAU)<sup>-</sup>. Azaserine was added to aliquots of an exponentially growing culture at 0 time to concentration levels as indicated. Growth and lysis were observed by measuring optical density.

Servall centrifuge. Deoxyribonuclease was added to the supernatant fluid and re-centrifuged for 150 minutes at 50,000 *g* yielding a pellet that was resuspended in 2 × SSC and further purified by a second cycle of low-speed and high-speed centrifugation. The absorption spectrum of the purified material was typical of that for bacteriophage. The material is resistant to degradation by deoxyribonuclease and showed a sharp boundary sedimenting at roughly 300 S in the Spinco Model E analytical centrifuge.

Electron micrographs taken by Dr. Harold Morowitz of Yale University showed particles having hexagonal heads. Tail structures were unusual in that one eighth of the tail in the neck region was very narrow, the entire tail structure having a length of ~1,300–1,400 Å. The width of the tail, other than at the narrow neck region, was ~250 Å.

Attempts to infect other strains of *E. coli* with the viruses always gave negative

results. *E. coli* W3110, K<sup>12</sup> (λ), BB, and ML30 showed no plaque formation when fresh lysates or purified phage particles were used in attempts to infect these strains. The possibility exists that the particles are defective, but the range of bacteria tested is as yet inadequate to permit a firm conclusion.

*Homology of the viral DNA to bacterial DNA.* Virus-host genetic relatedness appears to be a feature common to lysogenic systems. A third of the λ genome has been shown to be homologous to *E. coli* DNA; P<sub>22</sub> appears to be even more related to its lysogenic host *Salmonella typhimurium*, and T3 shows a small genetic relatedness to *E. coli* in a semi-lysogenic system (*Year Book 63*, pp. 380–382). An extension of the DNA-agar technique has been employed to determine whether the 15(TAU)<sup>-</sup> lysogenic system shows this viral-host interrelationship.

In this method, binding of the labeled DNA fragments with the DNA trapped in agar has been investigated by obtaining thermal elution profiles of the reacting DNAs. Using this method, Cowie and Hershey showed that the sites of complementary base sequences between λ phage DNA and the DNA of its host were multiple and were distributed throughout the entire viral genome. Furthermore, the melting-out temperatures of the labeled λ fragments that had interacted with *E. coli* DNA-agar indicated that authentic matching of numerous base pairs accounted for the observed interaction of the two DNAs.

Figure 62 shows an elution profile obtained from the reaction between 15(TAU)<sup>-</sup> phage DNA fragments and the DNA of 15(TAU)<sup>-</sup> cells. Maximal elution of the bound fragments occurred when the temperature reached 70°C. As much as 25 per cent of the phage DNA fragments have been observed to bind to the *E. coli* DNA-agar when sufficient *E. coli* DNA is present in the agar.

Figure 63 shows corresponding elution profiles obtained from the reaction of:

(1) 15(TAU)<sup>-</sup> phage DNA fragments with 15(TAU)<sup>-</sup> phage DNA-agar (solid line), and (2) *E. coli* DNA fragments after incubation with *E. coli* agar (dotted line). Comparison of these thermal elution diagrams demonstrates that the average guanine-cytosine content of the phage DNA is slightly less than that of the *E. coli* DNA.

Segments of 15(TAU)<sup>-</sup> phage DNA

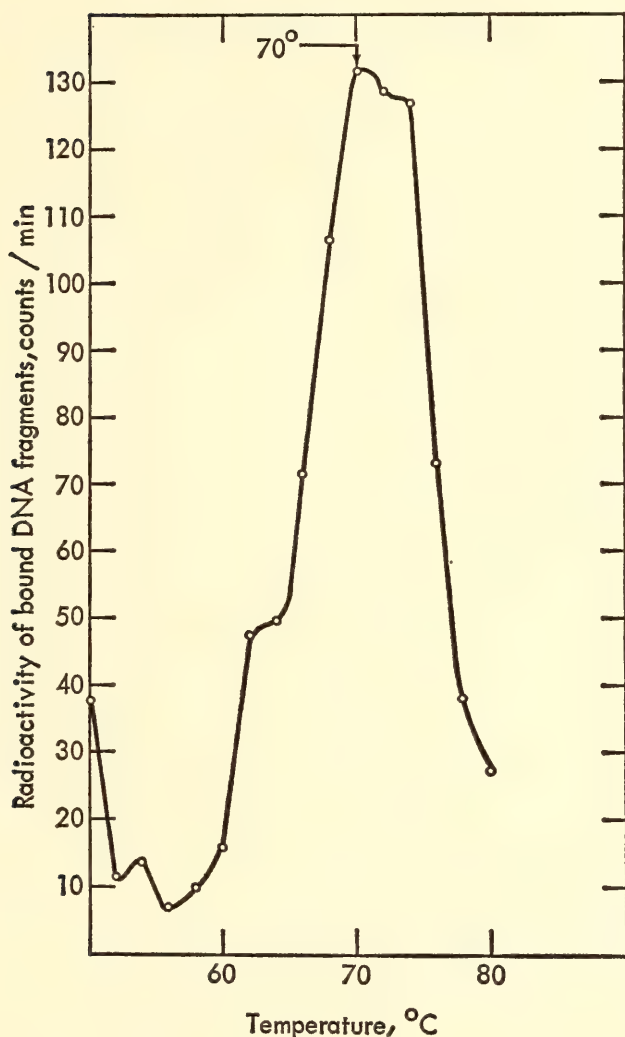


Fig. 62. Thermal chromatograms of complexes formed between *E. coli* strain 15 (TAU)<sup>-</sup> DNA and P<sup>32</sup>-labeled 15 (TAU)<sup>-</sup> phage DNA fragments. The mixed DNAs were annealed at 60°C in 2 × SSC overnight, transferred to a column, and washed with seven 15-ml portions of 2 × SSC at 50°C followed by two 15-ml portions of SSC/30 at 50°C. Thereafter the DNA, removed in a 10-ml single wash with SSC/30 at each of a series of temperatures, was measured. Results in this figure were obtained with 0.2 gram agar containing 256 γ *E. coli* DNA reacting with 2 γ of 15 (TAU)<sup>-</sup> phage DNA fragments.

that are homologous to *E. coli* (Fig. 62) are eluted from *E. coli* agar at a lower temperature than was observed for either of the homologous DNA reactions shown in Fig. 63.

*Lysogeny of other strains of E. coli 15.* Figure 64 shows the effects of mitomycin on substrains 15(TAU)<sup>-</sup> bar and 15 T<sup>-</sup>. Lysates from these cultures yielded bacteriophage similar to those obtained from 15(TAU)<sup>-</sup> described above.

When this report was being written a paper entitled "Inducible phage of *E. coli* 15" by Endo, Ayabe, Amako, and Takeya appeared in *Virology* (1965).<sup>34</sup> Our results, which have been described above, confirm their conclusion that this bac-

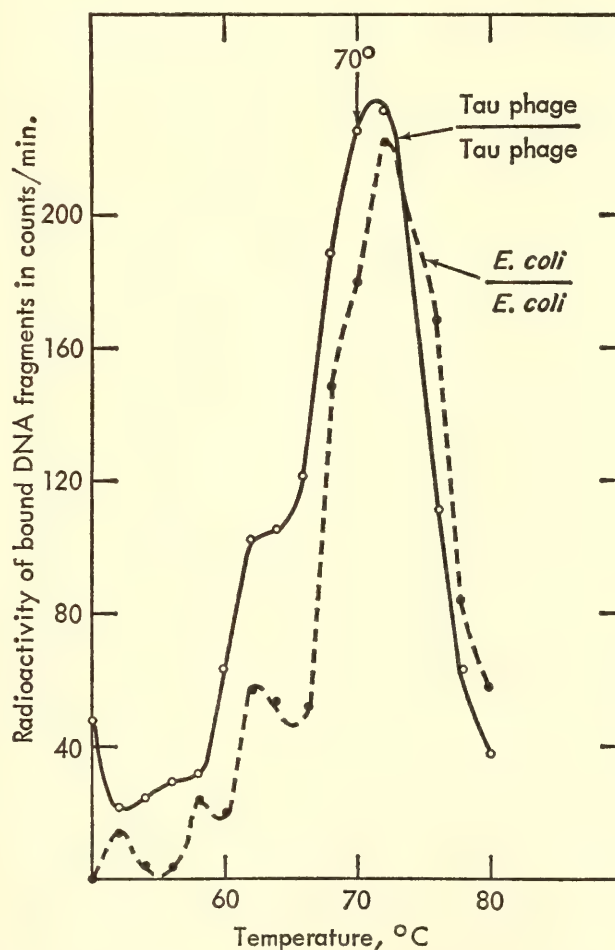


Fig. 63. Thermal chromatograms of complexes formed between 15 (TAU)<sup>-</sup> phage DNA-agar and 15 (TAU)<sup>-</sup> phage DNA P<sup>32</sup> labeled fragments (solid line), and *E. coli* strain 15 (TAU)<sup>-</sup> DNA-agar reacting with *E. coli* strain 15(TAU)<sup>-</sup> DNA fragments (dashed line). Method as described in Fig. 62.



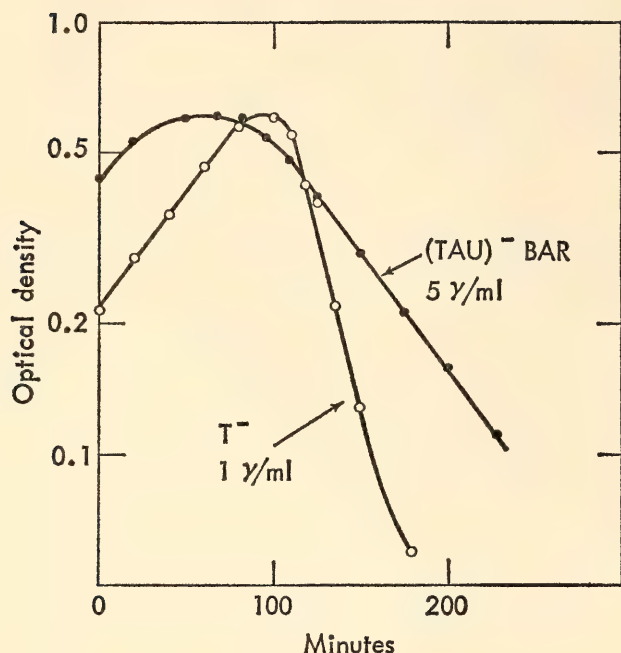


Fig. 64. Growth and lysis of *E. coli* sub-strains 15 (TAU)<sup>-</sup> bar (closed circle), and 15 T<sup>-</sup> (circle), following the addition of mitomycin (5 γ/ml and 1 γ/ml, respectively) to exponentially growing cultures of these cells.

terium is lysogenic, and demonstrate further that a portion of the phage genome is genetically related to the DNA of *E. coli* 15, another example of a viral-host DNA relationship in lysogenic systems.

The 15(TAU)<sup>-</sup> strain is ideal for the study of lysogeny and provides highly useful features for investigating the mode of attachment of prophage to host DNA. In addition, the induction of lysis by transient thymine privation raises some questions as to the nature of "thymineless death" frequently described as resulting from thymine starvation of *E. coli* 15 T<sup>-</sup> strains.

#### CONDITIONS INFLUENCING INDUCTION OF LYSIS IN LYSGENIC BACTERIA

*Potentiating effect of chelators.* Figure 58 shows the growth and lysis of 15(TAU)<sup>-</sup> after exposure to various concentrations of mitomycin C. The effect of the drug can be enhanced considerably by the addition of chelating agents during the period of growth after

treatment, as shown in Fig. 65. Initially we thought that the effect of ethylene diamine sodium tetraacetate was due to its binding of magnesium ions because similar results could be obtained by omitting magnesium from the growth medium. Magnesium, however, is not the ion of interest; calcium EDT is as effective as the sodium form, though it should have little influence on the concentration of free magnesium. Furthermore, cyclohexane 1,2 diamino sodium tetraacetate (CDT), a stronger chelator, is effective at  $10^{-4}$  M, which is only one fifth the molarity of the magnesium. CDT even at low concentrations causes a shift from exponential to linear growth but exponential growth can be restored by the addition of manganese or iron. Evidently a heavy ion is required both for exponential growth and for recovery from treatment with mitomycin.

The effect of the chelators is not limited to augmenting the lysis induced by mitomycin. Growth recovery remains slower in the presence of EDT after lysis

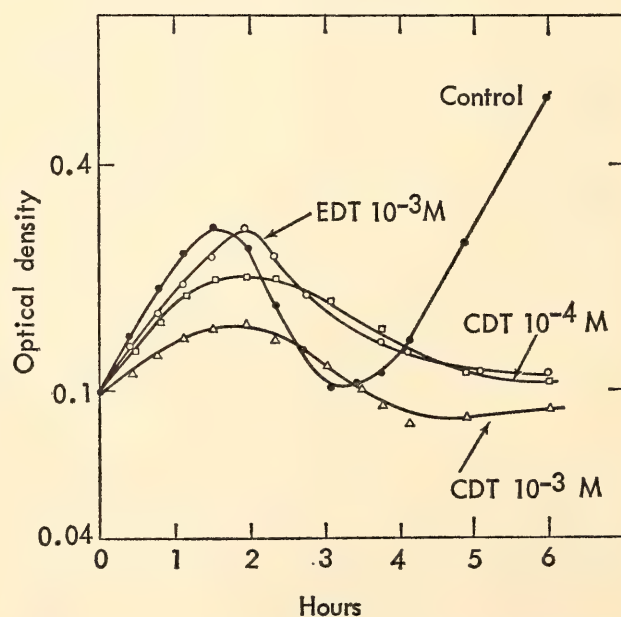


Fig. 65. Effect of chelators on lysis induced by mitomycin C. *E. coli* 15 (TAU)<sup>-</sup> cells were treated with mitomycin C at 0.25 μg/ml for 15 min as described in Fig. 58. They were then suspended in growth medium with chelators added at the indicated concentrations. Closed circle: control (no chelator); circle,  $10^{-3}$  M EDT; square:  $10^{-4}$  M CDT; triangle:  $10^{-3}$  M CDT.

induced by ultraviolet radiation, azaserine, or thymine deficiency.

*Effect of inhibitors of DNA synthesis.* Figure 66 shows how the extent of lysis and the rate of recovery can be markedly influenced by agents that affect the rate of DNA synthesis. Lysis is considerably reduced by the addition of nucleic acid precursors. In contrast, lysis is enhanced and recovery is delayed by agents that inhibit synthesis. Deprivation of thymine for 90 minutes has a drastic effect, but this prolonged deficiency of thymine is sufficient in itself to induce lysis, though it does enhance the effect of mitomycin. Hydroxyurea and phenethyl alcohol, when present in concentration sufficient to cause a partial inhibition of DNA synthesis, potentiate the mitomycin even though they cause only a slight inhibition of the growth rate of untreated cells. Other effective agents in-

clude: azaserine (0.04  $\mu\text{g}/\text{ml}$ ; 8 azaadenine (40  $\mu\text{g}/\text{ml}$ ); mercaptoethanol (20  $\mu\text{g}/\text{ml}$ ); and aminopterin (300  $\mu\text{g}/\text{ml}$ ).

These results can be interpreted in terms of the repair mechanism which comes into play after DNA is damaged by radiation or radiomimetic drugs. According to present evidence the defects caused by these agents are excised, leaving a gap in one of the strands of the DNA molecule. The gap is then enlarged (presumably by an exonuclease) and a considerable degradation of the DNA strand may ensue. Finally, the processes of degradation are reversed by a DNA polymerase which fills in the missing material by inserting bases complementary to the remaining intact strand. These mechanisms are sufficient to explain the effects observed in lysogenic cells if one additional assumption is made—that the initial defect is not sufficient to release a lysogenic virus but degradation is also required. In this situation, when conditions are favorable for DNA synthesis, the defects are filled in rapidly and the virus remains integrated with the genome of the host. When DNA synthesis is inhibited the degradation proceeds further and the virus is released to multiply independently.

*Effect of inhibitors of protein synthesis.* With *E. coli* 15 (TAU)<sup>-</sup> the synthesis of protein can be stopped by removing arginine from the medium. As shown in Fig. 67, growth resumes promptly when the arginine is restored. If, however, the cells have previously been treated with mitomycin a prolonged lag ensues. A period of inhibition as short as 30 minutes is sufficient to induce the prolonged lag; the inhibition need not be during the initial period after mitomycin treatment. Cells allowed to grow in the complete medium for 45 minutes and then subjected to 45 minutes' inhibition of protein synthesis show the same effect, which is quite general; the protein inhibition may be induced by 5-methyltryptophan, as well as by lack of arginine. Lack of uracil causes cessation of RNA synthesis and a

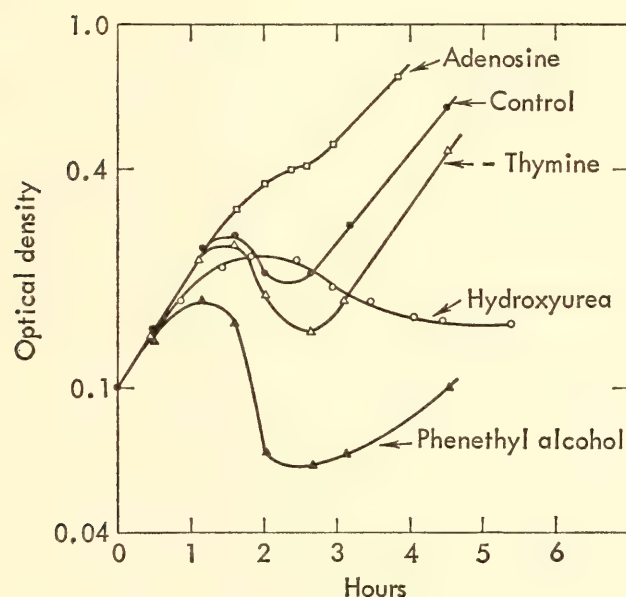


Fig. 66. Effect of inhibitors on lysis induced by mitomycin C. *E. coli* 15 (TAU)<sup>-</sup> cells were treated with mitomycin C at 0.25  $\mu\text{g}/\text{ml}$  for 15 min as described in Fig. 58. They were then suspended in media with the indicated additives. For inhibition by thymine privation the cells were washed and treated in media lacking thymine, and the thymine was restored after 40 minutes' incubation. Closed circle: control (complete growth medium); square: adenosine 0.15 mg/ml; circle: hydroxyurea 3.8 mg/ml; closed triangle: phenethyl alcohol 1 mg/ml; triangle: thymine privation.



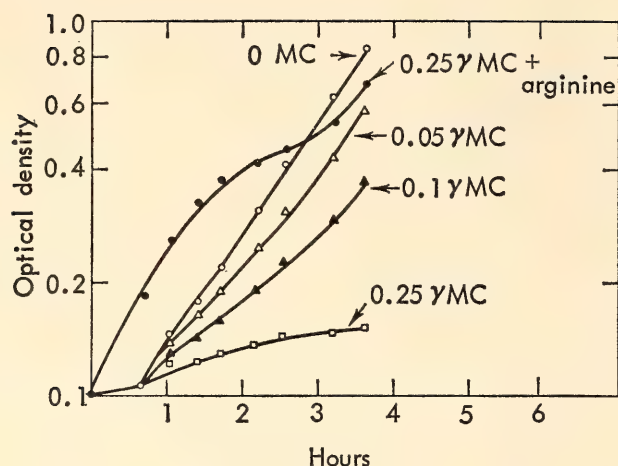


Fig. 67. Effect of inhibition of protein synthesis. *E. coli* 15 (TAU)<sup>-</sup> cells were treated for 15 min with various concentrations of mitomycin C and then subjected to a period of inhibition of protein synthesis resulting from arginine privation. For this experiment the cells were washed and treated in medium lacking arginine. Under conditions of various values of  $\mu\text{g/ml}$  of mitomycin C, with arginine restored at various lengths of time, the following symbols apply. Closed circle: 0.25  $\mu\text{g/ml}$  mitomycin C, arginine restored in 0 min; square: 0.25  $\mu\text{g/ml}$ , restoration at 45 min; closed triangle: 0.1  $\mu\text{g/ml}$ , 45 min; triangle: 0.05  $\mu\text{g/ml}$ , 45 min; circle: 0.0  $\mu\text{g/ml}$ , 45 min.

subsequent protein inhibition; *p*-fluorophenylalanine and 5-fluorouracil cause the synthesis of imperfect proteins; all these agents give long lags to mitomycin-treated cells (Fig. 68). In addition, similar lags are noted in cells exposed to ultraviolet radiation or to azaserine after a period of protein inhibition. In contrast, no such lag is observed when the non-lysogenic bacteria *E. coli* strain BB is treated with mitomycin followed by 5-methyltryptophan. Growth resumes as soon as the inhibition is reversed by the addition of tryptophan.

These results can again be interpreted, partly at least, in terms of inhibiting the repair mechanism. It was established several years ago that a period of protein synthesis was required before bacteria could resume DNA synthesis after exposure to ultraviolet or nitrogen mustard. This effect is undoubtedly present. There seem to be differences however, The prolonged lag after the removal of inhibi-

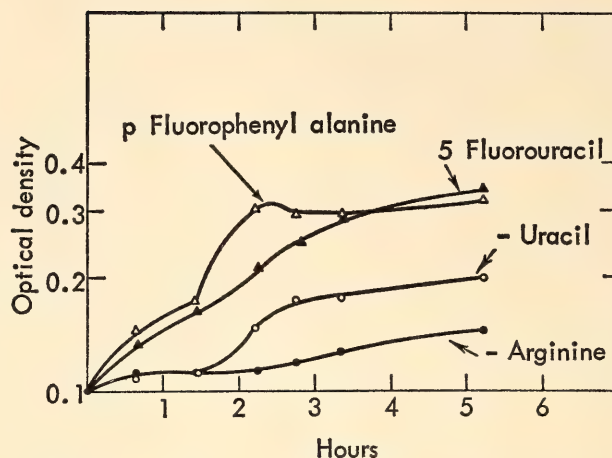


Fig. 68. Effect of protein synthesis inhibitors on mitomycin-treated cells. *E. coli* 15 (TAU)<sup>-</sup> cells washed and treated for 15 min with mitomycin C (0.25  $\mu\text{g/ml}$ ) in medium lacking arginine and uracil. Closed circle: uracil restored at 0 min, arginine at 90 min; circle: uracil restored at 90 min, arginine at 0 min; closed triangle: 5-fluorouracil present throughout, reversed by addition of uracil at 90 min, arginine restored at 0 min; triangle: arginine and uracil restored at 0 min, *p*-fluorophenylalanine (1 mg/ml) present throughout, reversed by addition of tyrosine and phenylalanine at 90 min.

tion is seen only in lysogenic cells, and an initial period of protein synthesis is not sufficient to ensure subsequent growth. We therefore believe that viral DNA may be synthesized during the period of protein inhibition and then may block the cell metabolism so that neither cell nor virus is synthesized. It seems possible that these cells are in an abortive state similar to that caused by the entry of ultraviolet inactivated virus.

Figure 69 shows a result of potential significance for chemotherapy. The addition of EDT makes the lag after protein inhibition more prolonged.

*Thymine-saturated cells.* When *E. coli* 15(TAU)<sup>-</sup> cells are grown for a period of 90 minutes with thymine, but without arginine or uracil, they continue to synthesize DNA at a decreasing rate until their DNA content has increased by 50 per cent. Experiments by Maaloe and Hanawalt indicate that these cells have finished off the DNA molecules already in replication, but no new round of replication can be started without a period of

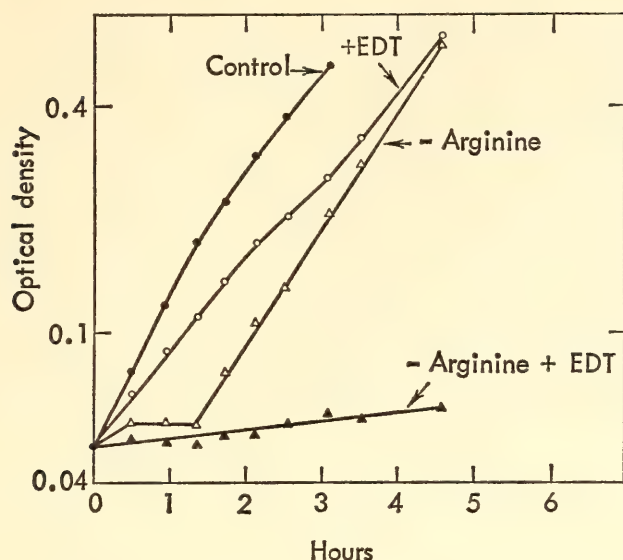


Fig. 69. Combined effect of EDT and inhibition of protein synthesis on mitomycin-treated cells. *E. coli* 15 (TAU)<sup>-</sup> cells were washed and treated in medium lacking arginine. Mitomycin concentration was 0.15  $\mu\text{g}/\text{ml}$  to give limited lysis. Arginine restored at 0 min (closed circle); at 0 min + EDT ( $10^{-3} M$ ) (circle); at 60 min (triangle); and at 60 min, + EDT ( $10^{-3} M$ ) (closed triangle).

RNA and protein synthesis. These cells are designated "thymine saturated." Maaloe and Hanawalt found that the cells in this condition were immune to thymineless death. Earlier work in this laboratory showed that they could not be induced to synthesize a new enzyme. In the course of the work we found that they were less sensitive to lysis whether induced by lack of thymine or by mitomycin. They were, however, subject to the prolonged lag caused by protein inhibition. The cells may be more similar to mammalian cells than are exponentially growing bacteria because few of the mammalian cells are in the phase of active DNA synthesis at any time.

*Selective repression of lysogenic cells.* Reich and Tatum have already shown lysogenic cells to be more sensitive to mitomycin than nonlysogenic ones. The experiments above suggest the following procedures to increase the differential: (1) Introduction of defects into the DNA by radiation or radiomimetic drugs, such as mitomycin. (2) Inhibition of the repair mechanism by use of agents to inhibit

DNA synthesis, such as hydroxyurea, phenethyl alcohol, or azaserine. (3) Inhibition of protein synthesis by drugs such as chloramphenicol, puromycin, or amino acid analogues; this treatment (reversed after an appropriate period) is particularly effective, as it results in a long lag in the lysogenic cells but not in the others. (4) The addition of a chelator such as EDT to amplify the effectiveness of the initial agent. In the next section it will be shown that these general principles carry over to the treatment of ascites tumors in mice.

### ASCITES TUMORS IN MICE

The experiments with bacteria were carried out at the Department, beginning in November 1964. Our interest was sustained and heightened by the progress of concurrent experiments with tumor-bearing mice which were carried out at the National Institutes of Health by Dr. Thomas L. Lincoln (Johns Hopkins University School of Medicine) and Dr. Albert Gelderman (National Institutes of Health). While we would not attempt to include a full account of their results in this report, we believe a partial summary is essential. Their experiments began in February when the potentiating effects of EDT had been established in bacteria. They have continued since then and information has been fully exchanged. It has been highly satisfying (although surprising) to find that the principles evolving from the bacterial experiments carried over to mammalian cells.

The ascites tumor was chosen because it grows rapidly and its progress can be estimated simply by daily weighing of the mice. In general, about  $2 \times 10^7$  tumor cells were injected and allowed to become established for three days before treatment was initiated. At that time a 20-gram mouse would contain roughly 2–3 grams of ascites cells and fluid. The object of the experiments was not to cure the mice but to establish whether or not the combinations of drugs found effective



in bacteria were equally effective against the tumor. For this purpose a single injection of one agent (usually mitomycin) was given either singly or in combination with other potentiating agents, and the subsequent growth of the tumor followed. As was done with the bacteria, a marginal dose was given, one that would have some effect but that allowed any enhancement to be observed.

To date, 11 experiments have been

carried out. In every case, the combinations suggested by the bacterial work have been more effective than the drugs used singly. Figure 70 presents the results of one of the later experiments, which tested the combination of mitomycin, puromycin, and EDT. The use of puromycin, an inhibitor of protein synthesis, was suggested by the effects of protein inhibition on the lysogenic bacteria, shown in Figs. 67 and 68. The ex-

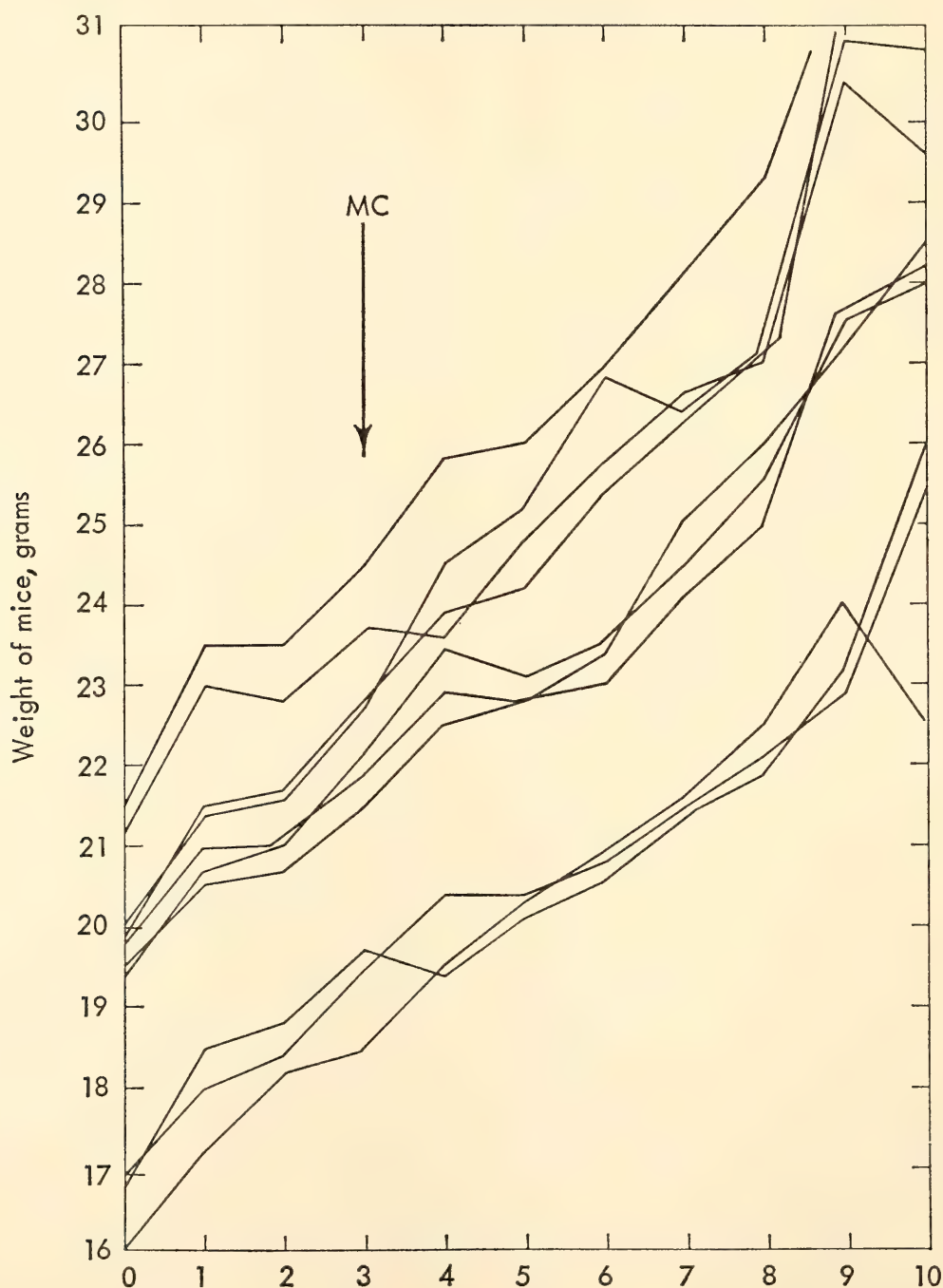


Fig. 70A. Days after transplantation.

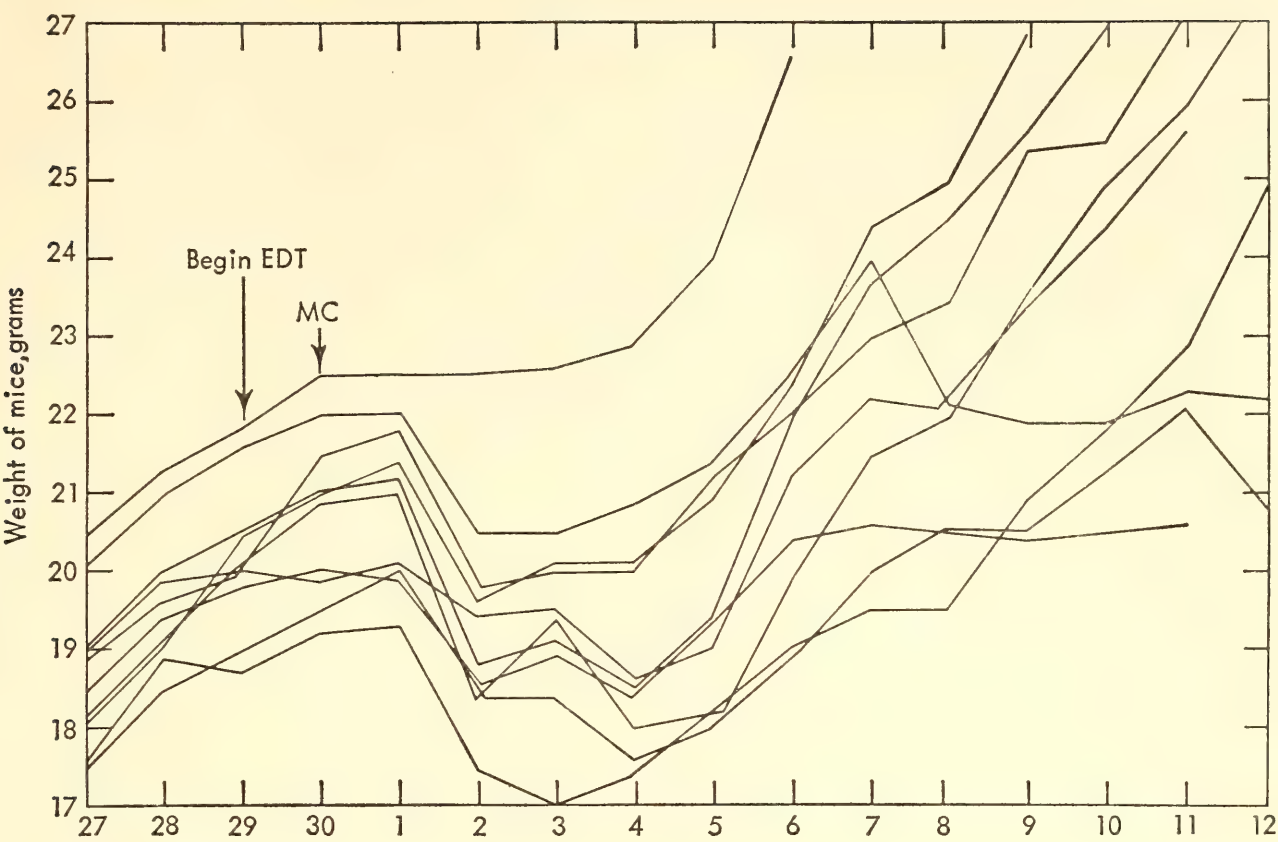


Fig. 70B. Days after transplantation.

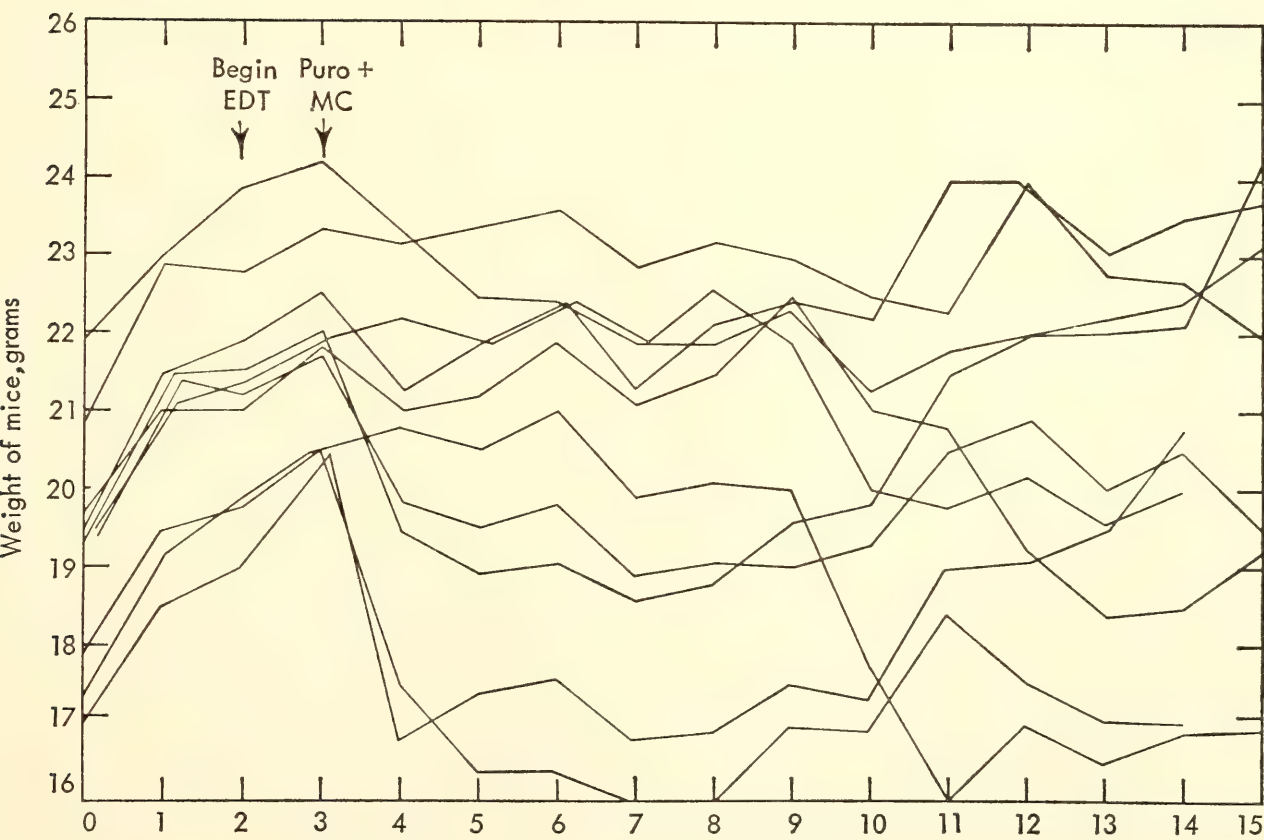


Fig. 70C. Days after transplantation.



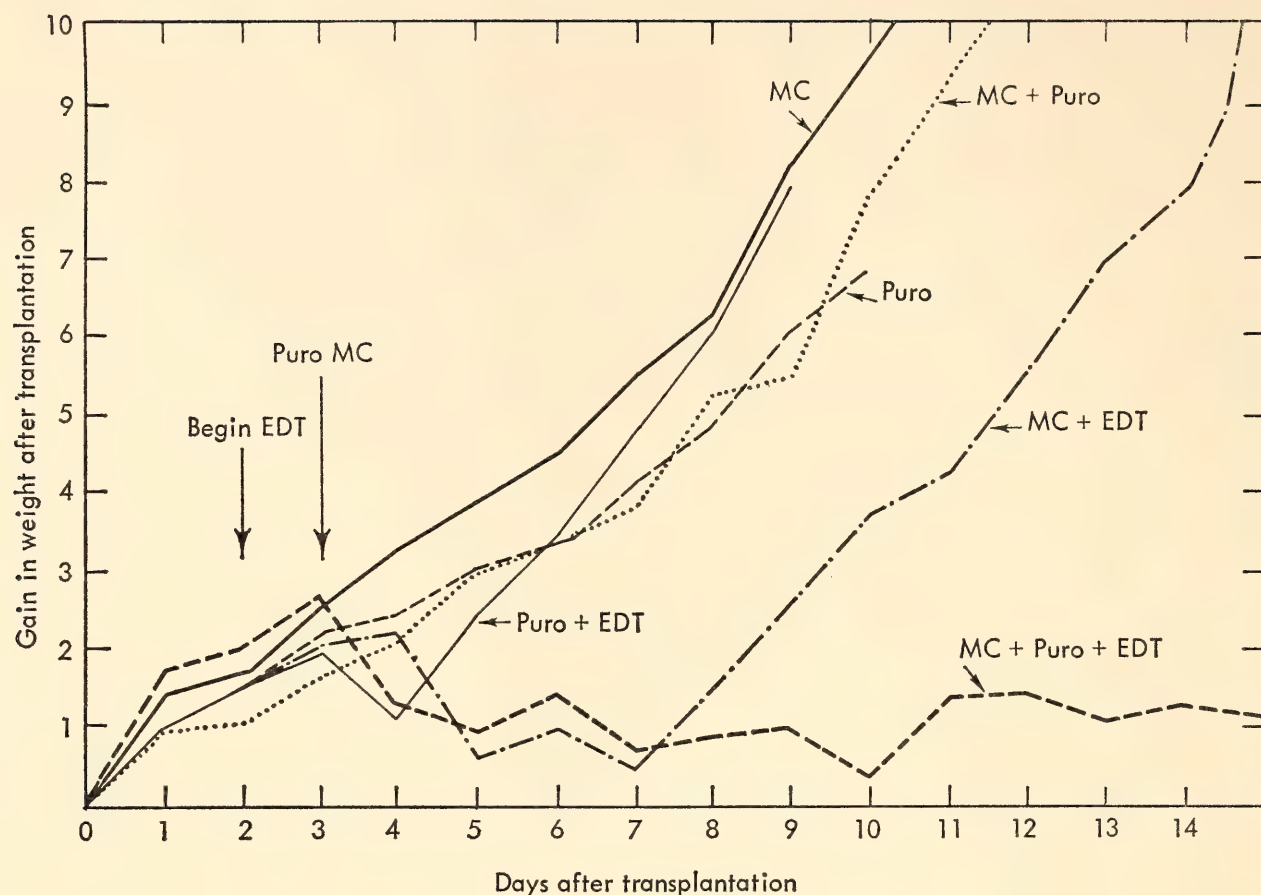


Fig. 70. Growth of ascites tumor in mice after various single treatments. C3H mice were injected with  $2 \times 10^7$  Ehrlich ascites cells on day 0. When EDT was used, 1 mg of  $\text{Na}_2\text{Ca EDT}$  was injected intraperitoneally and was added to the drinking water ( $10^{-3} M$ ) thereafter. Puromycin was injected intraperitoneally on day 3 at 0.2 mg per 20-gram mouse. Mitomycin C was injected intraperitoneally on day 3 one hour after the puromycin at  $50\mu\text{g}$  per 20-gram mouse. Curves A, B, and C (previous pages) show the weights of individual mice given mitomycin alone, mitomycin plus EDT, and mitomycin plus EDT plus puromycin, respectively. Curve D (above) shows the averages of the weights of these mice and of other groups of mice given other combinations.

periments illustrated in Fig. 69 were carried out to determine whether EDT should be added to the combination. The results seen in Fig. 70 show that these predictions were fully borne out. The combination of mitomycin C, puromycin, and EDT produced a prolonged inhibition of tumor growth even though the agents had no effect when used singly. Furthermore, the mitomycin was used at less than one fourth the level that mice can tolerate, and the puromycin was used at one fortieth the tolerance level. In more recent experiments chloramphenicol, another inhibitor of protein synthesis, which is much less toxic than puromycin, has been found equally effective.

It remains to be seen whether these

combinations will prove to be effective in solid tumors of animals and man. Since the additives markedly potentiate the agents that are at present marginal, it is difficult to believe that they could fail to do some good. In any event we believe that these experiments extend the correlation between agents that induce lysis and antitumor agents to a correlation between combinations of drugs that effect lysogenic bacteria and combinations that inhibit the ascites tumor. They also demonstrate the value of testing agents first in bacteria where the experiments can be completed in a day and secondly in ascites tumors where there is no problem of the drug reaching the tumor cells and where the experiments can be completed

in a week or two. The combinations that prove hopeful in these preliminary screening tests can then be used to treat a variety of tumors in experiments that need months for completion. We also hope that the rationale of using one drug to introduce defects in the DNA and other drugs to inhibit the repair of the defects may be a useful guide in cancer chemotherapy.

#### COOPERATION

Sharing with others the fruits of research experience continues to be a source of deepest satisfaction. We have been most fortunate in continuing old associations and also in making new ones. A number of gifted persons have contributed to our work at the laboratory bench and have aided importantly in the molding of new and constructive ideas. The work reported above on plant nucleic acids has benefited from

the advice and generous gifts of materials by Dr. G. R. Wiebe and Dr. Russell Steere of the Bureau of Plant Industry, U. S. Department of Agriculture. The studies of homologies among the nucleic acids of higher organisms have been furthered by the contributions of Dr. Bill Hoyer and Dr. Malcom Martin of the National Institutes of Health. Dr. Thomas L. Lincoln of the Johns Hopkins University School of Medicine and the University of Maryland and Dr. David Axelrod and Dr. Albert Gelderman of the National Institutes of Health have shared in the investigations of lysogenic systems and in the studies of mouse tumors. It is a pleasure also to acknowledge the contributions of Dr. A. D. Hershey of the Carnegie Institution's Genetics Research Unit and the long-standing association with Dr. L. B. Flexner and Dr. J. B. Flexner of the University of Pennsylvania.

#### IMAGE TUBES FOR TELESCOPES

Our Department has been the focus of activities for the Carnegie Committee on Image Tubes for Telescopes since it began its work in late 1953. After various discussions with the individuals involved, Dr. Vannevar Bush at that time asked the Trustees for a special initial grant of \$50,000 to start work on testing and developing image-intensifying devices for telescopes. The request was based on the fact that modern photoelectric surfaces are more efficient in cumulative response to faint light levels than even the best photographic emulsions, which respond well to short exposures but fail to accumulate fully the effect of exposure to very feeble light levels for periods of several hours, as is essential in astronomical work. The goal at the start was to seek a device that might be sufficiently effective to enable various medium-sized telescopes (70-120 inches) to study those very

remote objects that have been almost inaccessible to any telescopes but the 200-inch. Thus the initial stated aim was to minimize the highly privileged position occupied by the small group using the 200-inch telescope.

It appears that this goal has now been reached.

A two-stage cascaded image tube painstakingly developed at RCA during the past five years to meet the stringent requirements of astronomy, under the guidance of Dr. Ford of the DTM staff and the Carnegie Image Tube Committee (reported separately in each *Year Book*), was successfully put into production by RCA this year. Half a dozen active astronomers in major U.S. observatories have been supplied with tubes for actual use on their telescopes in research, as a final phase of the Committee's testing program. The Department has supplied all necessary auxiliaries with each of



these tubes, including magnets, high-voltage supply and controls, special lenses, focusing mount, and other items. Broadly speaking, these special RCA tubes operate with an overall gain or advantage of a factor of 10 or 12 above the best modern photographic emulsions used in astronomy. A total of 20 tubes with multialkali cathodes have been produced to tight specifications. The tubes show their highest sensitivity in the near ultraviolet and visible regions of the spectrum, yet with moderate response out to the near infrared beyond 8,000 Å.

Arrangements have been made for the distribution of a modest number of these very special tubes and their required auxiliary items to selected observatories and astronomers, under the direction of a Joint Allocations Committee of the Carnegie Institution and the National Science Foundation.

In addition to the multialkali tubes, RCA has made successful prototypes of similar tubes with infrared cathodes, sensitive out to 15,000 Å and beyond. These tubes are now in production for the Committee, to suitable specifications. Since no photographic emulsions have appreciable response in the range above about 10,000 Å the infrared tubes give an indefinitely large gain over photographic emulsions and open a new range of opportunity to the astronomer and the spectroscopist.

The efficiency of a modern photoelectric surface is such that on the average one photoelectron is emitted from the surface for every five or six "photons" (light-quanta) that strike it. A photographic emulsion, especially for long exposures, requires many more incident photons per developable silver halide grain. In 1953 the figure stood at about 1,000 photons per developable grain for emulsion 103aO, which is widely used in astronomy. This is still correct, but during the past two or three years it has

been found that the old standard emulsion, designated IIaO, when specially sensitized (by oven baking) prior to exposure, shows five or six times better effectiveness, yielding one developable grain for 160–200 incident photons. Hence, if we photograph the fine-grained output phosphor of the image tube using baked IIaO plates, a theoretical speed gain of 30–40 over the best emulsion for astronomy might be attainable. We actually measure speed increases of 30–45 (on stellar objects and spectra) in the "rate of blackening" of the emulsion, which photographs the image tube phosphor, in comparison with direct photographs without the image tube (a factor of about 80 over 103aO emulsion). Correspondingly fainter objects are thus measurable in a given available exposure time of, say, two hours.

For many kinds of astronomical studies this speed gain is a good measure of the advantage of using an image tube, but for many other types of observing, as in most spectroscopic studies, there is a diameter of the telescope by a factor of 0.6 or 0.7, due to the optical system and emulsion used to photograph the output phosphor of the image tube. The loss enters as the square, so the net overall advantage or "figure of merit" for such studies drops from a factor of 35 or more to about 12. However, this lower figure is not to be considered insignificant, as it corresponds to increasing the diameter of the telescope by a factor of roughly 3.5 for photographic procedures. It should be pointed out, of course, that image tubes offer no speed gain when compared with other photoelectric techniques (already in use on large telescopes) such as the measurement of individual stars or nebulae through a small pinhole aperture, with the use of filters (UBV) and a photomultiplier. Undeniably, astronomy still needs telescopes with the largest feasible apertures.

## REFERENCES CITED

1. Scheidegger, A. E., and P. L. Willmore, *Geophysics*, 22, 9-22, 1957.
2. Willmore, P. L., and A. M. Bancroft, *Geophys. J.*, 3, 419-432, 1960.
3. Bullen, K. E., *Geophys. J.*, 9, 265-274, 1965.
4. Steinhart, J. S., *J. Geophys. Res.*, 69, 5335-5352, 1964.
5. Birch, F., *J. Geophys. Res.*, 65, 1083-1102, 1960.
6. Steinhart, J. S., and R. P. Meyer, *Carnegie Inst. Wash. Publ.* 622, 409 pp., 1961.
7. Birch, F., *Am. J. Sci.*, 252, 1-25, 1954.
8. Wold, R. J., Ph.D. thesis, Univ. of Wisconsin, 1965.
9. Van Hise, C. R., and C. K. Leith, *U. S. Geol. Survey Monograph*, No. 52, 1911.
10. Jeffreys, H., *Monthly Notices Roy. Astron. Soc., Geophys. Suppl.*, 4, 520, 1939.
11. Rykunov, L. N., *Bull. Acad. Sci. U.S.S.R., Geophys.*, Ser. No. 10, 73-77, 1957.
12. Suyehiro, S., T. Asada, and M. Ohtake, *Papers Meteorol. Geophys. (Tokyo)*, 15, 71-88, 1964.
13. Gutenberg, B., and C. F. Richter, *Seismicity of the Earth*, p. 23, Table 9, Princeton Univ. Press, Princeton, N.J., 1954.
14. Suzuki, Z., *Science Reports Tohoku Univ., Fifth Ser.*, 11, 10-54, 1959.
15. Mogi, K., *Bull. Earthquake Res. Inst., Tokyo Univ.*, 41, 595-614, 1963.
16. Grant, J. A., *Science*, 146, 1049-1053, 1964.
17. Van Schmus, W. R., *J. Geophys. Res.*, in press.
18. Wetherill, G. W., G. L. Davis, and G. R. Tilton, *J. Geophys. Res.*, 65, 2461-2466, 1960.
19. Krogh, T. E., unpublished Ph.D. thesis, Mass. Inst. Technology, 1964.
20. Aldrich, L. T., and A. O. Nier, *Phys. Rev.*, 74, 1590-1594, 1948.
21. Damon, P. E., and J. L. Kulp, *Am Mineralogist*, 43, 433-459, 1958.
22. Yamaguchi, M., *Mem. Fac. Sci. Kyushu Univ., Geol. Ser.* 10, 233-245, 1961.
23. *Ibid.*, Ser. 15, 163-219, 1964.
24. Gast, P. W., *Science*, 149, 858-860, 1965.
25. Lessing, P., R. W. Decker, and R. C. Reynolds, Jr., *J. Geophys. Res.*, 68, 5851-5855, 1963.
26. Taubeneck, W. H., *J. Geophys. Res.*, 70, 475-478, 1965.
27. Steiger, R., *Schweiz. Mineral. Petrog. Mitt.*, 41, 127-156, 1961.
28. *Idem.*, *J. Geophys. Res.*, 69, 5407-5421, 1964.
29. Oxburgh, E. R., *Geol. Mag.*, 101, 1-19, 1964.
30. Hoffman, R. A., and P. A. Bracken, Magnetic effects of the quiet-time proton belt, Goddard Energetic Particles Preprint Series X-611-64-186, June 1964, *J. Geophys. Res.*, 70, 3541, Aug. 1, 1965.
31. McIntyre, L. C., thesis, University of Wisconsin, 1965.
32. Rook, J. R., and L. J. B. Goldfarb, *Nucl. Phys.*, 27, 79, 1961.
33. Ross, P. D., and J. M. Sturtevant, *J. Amer. Chem. Soc.*, 84, 4503, 1962.
34. Endo, H., K. Ayabe, K. Amako, and K. Takeya, *Virology*, 25, 469-471, 1965.

## BIBLIOGRAPHY

- Aldrich, L. T., *see* Smith, T. J.
- Axelrod, D., E. T. Bolton, and K. Habel, Homology of polyoma DNA to DNA of polyoma-free tumors (abstract), *Federation Proc.*, 23, pt. 1, 401, 1964.
- Axelrod, D., K. Habel, and E. T. Bolton, Polyoma virus genetic material in a virus-free polyoma-induced tumor, *Science*, 146, 1466-1469, 1964.
- Baum, W. A., J. S. Hall, L. L. Marton, and M. A. Tuve, Committee on Image Tubes for Telescopes, *Carnegie Inst. Wash. Year Book* 63, 405-410, 1963-1964.
- Bolton, E. T., Some observations on the work of the Biophysics Section, Department of Terrestrial Magnetism, Carnegie Institution of Washington, *Asahi Shimbun*, Sept. 3, 1964.
- Bolton, E. T., *see also* Axelrod, D.
- Britten, R. J., The concentration of small molecules within the microbial cell, 15th Symposium of the Society for General Microbiology, in *Function and Structure in Micro-Organisms*, pp. 57-88, Cambridge Univ. Press, England, 1965.
- Bullen, K. E., New evidence on rigidity of the earth's core, *Proc. Natl. Acad. Sci. U. S.*, 52, 38-42, 1964.
- Bullen, K. E., Models for the density and elasticity of the earth's lower core, *Geophys. J.*, 9, 233-252, 1965.
- Bullen, K. E., On compressibility and chemical inhomogeneity in the earth's core, *Geophys. J.*, 9, 195-202, 1965.
- Bullen, K. E., Seismic travel-time power-series expansions involving terms in  $\Delta^2$ , etc., *Geophys. J.*, 9, 265-274, 1965.



- Burke, B. F., *see* Turner, K. C.
- Cowie, D. B., and A. D. Hershey, Multiple sites of interaction with host-cell DNA in the DNA of phage  $\lambda$ , *Proc. Natl. Acad. Sci. U.S.*, 53, 57-62, 1965.
- Davis, G. L., *see* Wetherill, G. W.
- De La Haba, G., *see* Flexner, L. B.
- Flexner, J. B., *see* Flexner, L. B.
- Flexner, L. B., J. B. Flexner, R. B. Roberts, and G. De La Haba, Loss of recent memory in mice as related to regional inhibition of cerebral protein synthesis, *Proc. Natl. Acad. Sci. U.S.*, 52, 1165-1169, 1964.
- Forbush, S. E., Twenty-sixth award of the William Bowie Medal, April 21, 1964, citation, *Trans. Am. Geophys. Union*, 45, 281-283, 1964.
- Forbush, S. E., Absolute values for the terrestrial horizontal magnetic field due to the equatorial ring current (abstract), *Trans. Am. Geophys. Union*, 46, 115, 1965.
- Ford, W. K., Jr., Cascade image intensifiers for astronomical spectroscopy (abstract), *Astron. J.*, 69, 541-542, 1964.
- Habel, K., *see* Axelrod, D.
- Hammer, P. C., and T. J. Smith, Conditions equivalent to central symmetry of convex curves, *Proc. Cambridge Phil. Soc.*, 60, 779-785, 1964.
- Hart, S. R., Potassium, rubidium, and strontium in the ultramafic rocks of St. Paul's Islands (abstract), *Geol. Soc. Am. Program*, 77th Annual Meeting, Miami Beach, Fla., Nov. 19-21, 1964, pp. 86-87.
- Hart, S. R., The petrology and isotopic-mineral age relations of a contact zone in the Front Range, Colorado, *J. Geol.*, 72, 493-525, 1964.
- Hart, S. R., *see also* Rama, S. N. I.; Steinhart, J. S.; Wetherill, G. W.
- Hershey, A. D., *see* Cowie, D. B.
- Hopson, C. A., *see* Wetherill, G. W.
- Hoyer, B. H., *see* McCarthy, B. J.
- Hubbert, M. K., and M. A. Tuve, Foreword in *Solid-Earth Geophysics—Survey and Outlook*, vii-viii, National Academy of Sciences-National Research Council, Washington, D. C., Publ. 1231, 1964.
- McCarthy, B. J., and B. H. Hoyer, Identity of DNA and diversity of messenger RNA molecules in normal mouse tissues, *Proc. Natl. Acad. Sci. U.S.*, 52, 915-922, 1964.
- Pakiser, L. C., and J. S. Steinhart, Explosion seismology in the western hemisphere, in *Research in Geophysics*, 2, edited by H. D. Odishaw, pp. 123-147, M.I.T. Press, Cambridge, Mass., 1964.
- Rama, S. N. I., and S. R. Hart, Neon isotope fractionation during transient permeation, *Science*, 147, 737-738, 1965.
- Rama, S. N. I., S. R. Hart, and E. Roedder, Excess radiogenic argon in fluid inclusions, *J. Geophys. Res.*, 70, 509-511, 1965.
- Roberts, R. B., The synthesis of ribosomal protein, *J. Theoret. Biol.*, 8, 49-53, 1965.
- Roberts, R. B., *see also* Flexner, L. B.
- Roedder, E., *see* Rama, S. N. I.
- Sacks, I. S., Diffraction studies of the earth's core (abstract), *Trans. Am. Geophys. Union*, 46, 158, 1965.
- Sacks, I. S., *see* Smith, T. J.
- Smith, T. J., J. S. Steinhart, I. S. Sacks, and L. T. Aldrich, Explosion observations in the Lake Superior region (abstract), *Soc. Exploration Geophysicists Program*, 34th Annual International Meeting, Los Angeles, Calif., Nov. 15-19, 1964, pp. 60-61.
- Smith, T. J., J. S. Steinhart, I. S. Sacks, and L. T. Aldrich, Lake Superior crustal structure: comparison of several techniques (abstract), *Earthquake Notes, Eastern Section, Seis. Soc. Am.*, 35, 51, 1964.
- Smith, T. J., *see also* Hammer, P. C.
- Steinhart, J. S., Lake Superior seismic experiment: shots and travel times, *J. Geophys. Res.*, 69, 5335-5352, 1964.
- Steinhart, J. S., and S. R. Hart, A study of heat flow and thermal properties in Seneca Lake, New York (abstract), *Trans. Am. Geophys. Union*, 46, 176, 1965.
- Steinhart, J. S., *see also* Pakiser, L. C.; Smith, T. J.
- Suyehiro, S., Difference between aftershocks and foreshocks in the relationship of magnitude to frequency of occurrence for the great Chilean earthquake of 1960 (abstract), *Trans. Am. Geophys. Union*, 46, 152, 1965.
- Suzuki, Z., Maine seismic experiment: a study of shear waves, *Bull. Seis. Soc. Am.*, 55, 425-439, 1965.
- Tilton, G. R., *see* Wetherill, G. W.
- Turner, K. C., and B. F. Burke, A search for the galactic corona at 234 Mc/sec. (abstract), *Astron. J.*, 70, 332, 1965.
- Tuve, M. A., Solid-earth geophysics, *Trans. Am. Geophys. Union*, 46, 203-204, 1965.
- Tuve, M. A., *see also* Hubbert, M. K.
- Waring, M. J., The effects of antimicrobial agents on ribonucleic acid polymerase, *Molecular Pharmacology*, 1, 1-14, 1965.
- Wetherill, G. W., G. R. Tilton, G. L. Davis, S. R. Hart, and C. A. Hopson, Age measurements in the Washington-Baltimore area (abstract), *Trans. Am. Geophys. Union*, 46, 177, 1965.

## MAJOR PUBLICATION

*Studies in Macromolecular Biosynthesis*, edited by  
Richard B. Roberts. Octavo, xiii + 702 pp.,  
frontispiece, 1 pl., 360 figs. (1964).

## PERSONNEL

*Director*

M. A. TUVE

*Associate Director*

E. T. BOLTON

*Staff Members*

L. T. Aldrich  
E. T. Bolton  
R. J. Britten  
B. F. Burke  
D. B. Cowie  
S. E. Forbush

W. K. Ford, Jr.  
S. R. Hart  
R. B. Roberts  
I. S. Sacks  
T. J. Smith  
J. S. Steinhart

*Staff Associates*

L. Brown  
O. Hartmann  
Cinna Lomnitz<sup>1</sup>

A. Th. Purgathofer<sup>2</sup>  
Vera C. Rubin<sup>3</sup>  
Ulrich Schmucker<sup>4</sup>

K. C. Turner

*Section Chairmen*

Biophysics: R. B. Roberts  
E. T. Bolton, Deputy Chairman  
Earth's Crust: L. T. Aldrich

Radio Astronomy: B. F. Burke

Theoretical Geophysics: S. E. Forbush

*Fellows*

T. J. Byers, Fellow of U. S. Public Health  
Service.<sup>5</sup>  
H. A. Christ, University of Basel, Basel,  
Switzerland.<sup>6</sup>  
R. Green, University of Tasmania, Hobart,  
Tasmania.<sup>7</sup>  
D. E. James, Fellow of NSF.<sup>8</sup>  
A. Kamitsuki, Kansai University, Osaka,  
Japan.<sup>9</sup>

Y. Kato, Osaka Municipal Hygienic Labora-  
tory, Osaka, Japan.<sup>10</sup>  
T. E. Krogh, Massachusetts Institute of  
Technology.<sup>11</sup>  
M. Miranda, Universidade do Brasil, Rio de  
Janeiro, Brazil.<sup>12</sup>  
S. N. I. Rama, Tata Institute for Funda-  
mental Research, Bombay, India.<sup>13</sup>  
R. Sumner, University of Wisconsin.  
S. Suyehiro, Meteorological Research Insti-  
tute, Tokyo, Japan.<sup>14</sup>

<sup>1</sup> Through July 15, 1964.

<sup>2</sup> Through May 15, 1965.

<sup>3</sup> From April 1, 1965.

<sup>4</sup> On leave of absence from March 16, 1965.

<sup>5</sup> Through August 31, 1964.

<sup>6</sup> Through August 31, 1964.

<sup>7</sup> June 1965.

<sup>8</sup> From April 1, 1965.

<sup>9</sup> From November 1, 1964.

<sup>10</sup> Through November 15, 1964.

<sup>11</sup> From August 1, 1964.

<sup>12</sup> Through July 31, 1964.

<sup>13</sup> Through August 31, 1964.

<sup>14</sup> From December 1, 1964.



Z. Suzuki, Tohoku University, Sendai, Japan.<sup>15</sup>  
 P. Szafranski, Institute of Biochemistry and  
 Biophysics, Polish Academy of Science,  
 Warsaw, Poland.<sup>16</sup>  
 W. Trächslin, University of Basel, Basel,  
 Switzerland.<sup>17</sup>

C. Varsavsky, Universidad de Buenos Aires<sup>18</sup>  
 M. J. Waring, University of Cambridge,  
 England.<sup>19</sup>  
 M. Yamaguchi, Kyushu University, Fukuoka,  
 Japan.<sup>20</sup>

### *Junior Fellow*

R. Anzoleaga, Universidad Mayor de San  
 Andres, La Paz, Bolivia.

### *Collaborators and Visiting Investigators*

D. Axelrod, M. D., National Institutes of  
 Health.  
 K. E. Bullen, University of Sydney, Sydney,  
 Australia.<sup>21</sup>  
 R. Cabre, S. J., Observatorio San Calixto, La  
 Paz, Bolivia.  
 J. Careaga, Observatorio San Calixto, La  
 Paz, Bolivia.<sup>22</sup>  
 M. Casaverde, Instituto Geofísico del Peru,  
 Lima, Peru.  
 L. Fernandez, S. J., Observatorio San Calixto,  
 La Paz, Bolivia.<sup>23</sup>  
 E. Gajardo, University of Chile, Santiago,  
 Chile.  
 A. Gelderman, National Institutes of Health.  
 A. A. Giesecke, Jr., Instituto Geofísico del  
 Peru, Lima, Peru.  
 A. L. Hales, Graduate Research Center of the  
 Southwest, Dallas, Texas.

P. J. Hart, National Academy of Sciences.<sup>24</sup>  
 Bill Hoyer, National Institutes of Health.  
 K. E. Kissell, Ohio State University.  
 T. Lincoln, Johns Hopkins University and  
 University of Maryland.  
 M. Martin, National Institutes of Health.  
 H. Ohmoto, Princeton University.<sup>25</sup>  
 A. Rodriguez B., Universidad Nacional de  
 San Agustin, Arequipa, Peru.  
 G. Saa, S. J., University of Chile, Antofagasta,  
 Chile.  
 R. Salgueiro, Instituto Geofísico Boliviano, La  
 Paz, Bolivia.  
 F. Volponi, Universidad Nacional de Cuyo,  
 San Juan, Argentina.  
 J. P. Webb, University of Queensland,  
 Brisbane, Australia.<sup>26</sup>

### *Engineer and Research Assistant*

E. T. Ecklund

### *Research Assistants*

A. Bendich<sup>27</sup> (from September 8, 1964).      P. A. Johnson  
 J. B. Doak      C. A. Little  
                                  Mrs. A. Shirven

### *Laboratory Assistants*

Mrs. L. Beach      Miss M. Chamberlin  
 S. J. Buynitzky      G. R. Poe

<sup>15</sup> Through July 1964.

<sup>16</sup> April-June 1965.

<sup>17</sup> From December 1, 1964.

<sup>18</sup> From October 1, 1964.

<sup>19</sup> From October 1, 1964.

<sup>20</sup> From September 1, 1964.

<sup>21</sup> August 1964.

<sup>22</sup> September, October 1964.

<sup>23</sup> June 1965.

<sup>24</sup> June 1965.

<sup>25</sup> May, June 1965.

<sup>26</sup> June 1965.

<sup>27</sup> From September 8, 1964.

*Office*

Chief, Fiscal Section: Miss H. E. Russell  
 Office Manager: W. N. Dove  
 Librarian: Mrs. L. J. Prothro<sup>28</sup>  
 Secretary: Mrs. C. Ator

Stenographers: Mrs. D. Dillin  
 Mrs. E. K. Hill  
 Typist: Mrs. M. T. Sheahan<sup>29</sup>  
 Accounting Assistant: Miss G. J. Johnston

*Shop*

Chief Instrument Maker and Foreman of  
 Instrument Shop: J. G. Lorz  
 Instrument Makers: R. Hoffmaster, M.  
 Seemann

Machinist-Instrument Makers: D. E. Mossor<sup>30</sup>  
 C. Rinehart  
 Machinist: F. J. Caherty

*Buildings and Grounds*

Carpenter and Maintenance Foreman: L. J.  
 Haber  
 Caretaker: E. Quade

Assistant Caretakers: S. Gawrys, S. Swant-  
 kowski

*Part Time and Temporary Employees*

Pablo Aparicio  
 W. K. Burchard  
 Mrs. Dorothy Canter  
 M. F. Daly  
 Allen Forsbacka  
 Lin Ho  
 Alan Hoover  
 Raymond Mazza  
 Miss K. Mullin

J. Randall  
 J. Roddy  
 M. Roddy  
 Mrs. D. Titus  
 Miss J. Yates

<sup>28</sup> Part time.

<sup>29</sup> Part time.

<sup>30</sup> Through July 15, 1964.





# *Committee on Image Tubes for Telescopes*

Cooperative Project of Mount Wilson and Palomar Observatories  
Department of Terrestrial Magnetism, Lowell Observatory  
National Bureau of Standards, and United States Naval Observatory

W. A. Baum

*Mount Wilson and Palomar Observatories,  
and Lowell Observatory*

John S. Hall

*Director, Lowell Observatory  
Flagstaff, Arizona*

L. L. Marton

*National Bureau of Standards*

M. A. Tuve (*Chairman*)

*Department of Terrestrial Magnetism*



*Contents*

Review of Activities . . . . . 355

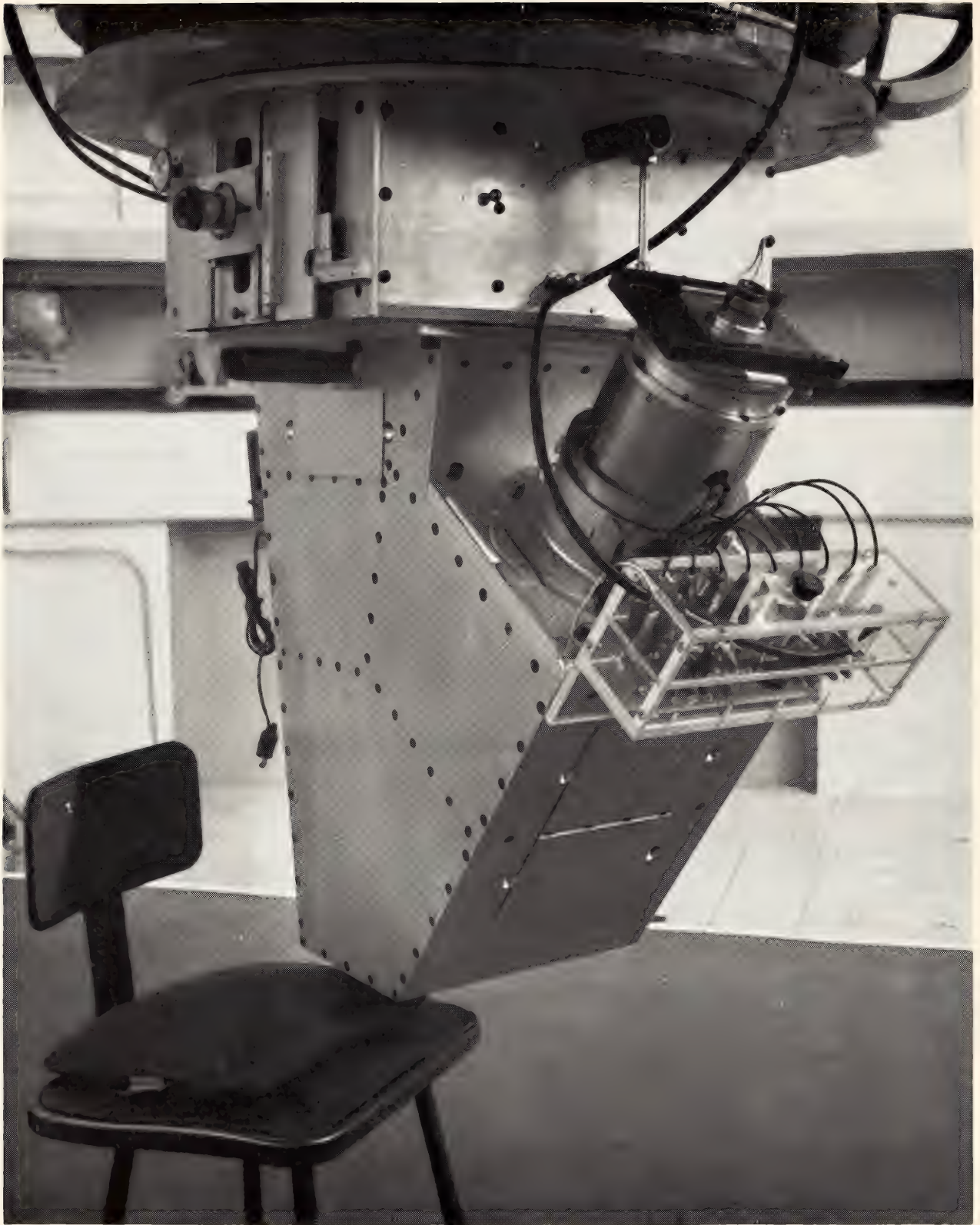
Test and Evaluation of Sample Tubes . . . . . 357

Collaboration with Other Astronomical  
Groups . . . . . 360

Acknowledgments . . . . . 361







The RCA Image Intensifier System on the DTM Spectrograph

Light from the telescope enters the spectrograph from above, is dispersed by a diffraction grating in the lower part of the spectrograph, and is focused by the spectrograph camera onto the photocathode of the image tube located in the protruding cylinder. The voltage divider (in plastic box) is just below the tube, and the focusing magnet is inside the cylinder. In this picture the plateholder has been replaced by an eyepiece, mounted in the plateholder slide, for checking the spectrograph camera focus.



## REVIEW OF ACTIVITIES

Image tubes are important in astronomical observations because for many problems they are more efficient than photographic emulsions. This higher efficiency can be used to obtain observations of fainter objects or, by reduced exposure time, to obtain a larger sample of objects, and it is correspondingly equivalent to increasing the aperture of the telescope with which the observations are made.

Image tubes developed during recent years by the Radio Corporation of America (RCA) for the Carnegie Image Tube Committee now give gains of 10–12 over the best photographic techniques when comparisons are made at the same resolution (line pairs per millimeter). Similarly, for the same final photographic density but with one half to two thirds of the resolution of direct photography, these tubes permit a decrease in exposure time by a factor of 40–50.

The Carnegie Institution's Department of Terrestrial Magnetism (DTM) has been the focus of activities for the Carnegie Committee on Image Tubes for Telescopes since the Committee began its work in late 1953. After various discussions with the individuals involved, Dr. Bush (then President of the Institution) asked the Trustees for a special initial grant of \$50,000 to start the work of testing and developing image-intensifying devices for telescopes. This action was based on the known fact that modern photoelectric surfaces are more efficient in cumulative response to faint light levels than even the best photographic emulsions. These emulsions respond well to short exposures but fail to integrate fully the effect of exposure to very feeble light levels for periods of several hours, an essential condition in astronomical work. Initially, the goal was to develop a device that would increase the effective range of

medium-sized telescopes (70–120 inches) so that other investigators could study those faraway objects that had been accessible only to astronomers using the 200-inch telescope.

It appears that this goal has now been reached.

The advantage offered by image tubes is derived from the fact that fewer photons are required to eject an electron from a good photoelectric surface than are required to produce a developable grain in a photographic emulsion. The task of the Carnegie Image Tube Committee has been to investigate various methods of image intensification that, in addition to making use of the increased sensitivity, will have the other prerequisites for an image-intensifying device for astronomy. These requirements are, briefly, that the resolution offered by the device must be at least comparable with that of the photographic plate which would otherwise be used, and that the intensifying device must not introduce any appreciable amount of spurious background. The granularity (or fluctuations) in the image produced by the device must be small, for fainter images can be detected on a smoother background, whether the images be faint threshold stars, galaxies, or weak absorption or emission lines in a spectrogram. Finally, the area of the intensifier must be of reasonable size. These needs have been fulfilled to a large measure by the cascade image tube developed by the Electron Tube Division of RCA in collaboration with the Carnegie Image Tube Committee.

The tube consists of a photocathode from which electrons are emitted, an intensifier membrane which multiplies the electrons, and a final phosphor screen which converts the intensified electronic image back into an optical image that can



be recorded with a camera and photographic emulsions. Because the electrons have been accelerated in the tube by an external power source, the amount of radiant energy emitted from the phosphor screen is large compared with the original faint optical input. The multiplication of the electrons in the "sandwich" is achieved by the combination of a phosphor screen and a second photocathode on a very thin and transparent supporting membrane. Scintillations in the phosphor from the primary photoelectrons are seen by the second cathode and "secondary" photoelectrons are emitted. Since this scheme is similar to two simple image tubes in series, the device is known as a cascaded image intensifier.

During the report year orders were placed with RCA for the production to high specifications of 20 of these image intensifiers. The 20 tubes have been fabricated by RCA and delivered to DTM. Our performance tests indicate that all these new tubes exceed in figure of merit the best of the prototype tubes we had measured previously and described in last year's report.

The astonishing rapidity with which the tubes have been produced has caused a major change of emphasis in the activities of the Carnegie Committee. The function of the Committee in the past has been to evaluate experimental tubes and to provide the manufacturers with a vigorous feedback of information and criticism based on the performance of the imaging device. Within recent months emphasis has shifted to the application of the cascaded intensifier to research problems by the Committee and its collaborators at other observatories.

Although this type of image tube does not represent the ultimate attainable in image intensification, it does represent a high level of performance that will be difficult to exceed with a commercially produced device for a number of years. One primary photoelectron for six incident photons represents a very high photoelectric efficiency. One developable

grain for 160 to 200 incident photons represents the best photographic efficiency measured to date (for baked IIa-O emulsions). The ratio is about 30. Our RCA tubes give an increase by this factor—or more (we measure 40 to 60)—in the "rate of blackening" of the IIa-O photographic emulsion which views the final phosphors with a small loss in resolution. It is reasonable, therefore, to proceed with the application of the tubes to research problems. Within the past few months complete cascaded intensifier systems have been provided for observational work at Yerkes Observatory, University of Chicago; Kitt Peak National Observatory; Lick Observatory, University of California; Lowell Observatory; and Mount Wilson Observatory. These tubes are being used and evaluated by our group and by other astronomers who have had experience with image tube techniques. The remaining tubes will soon be distributed to other observatories by a joint Carnegie-National Science Foundation Allocations Committee.

Professor J. D. McGee of the Imperial College, London, and W. A. Baum have continued experiments with a Lenard window tube which achieves "intensification" by recording photoelectrons directly in an electron-sensitive emulsion. The success of the device depends upon an exit window sufficiently strong to withstand atmospheric pressure, yet thin enough to permit penetration by electrons after acceleration to 40 kV. Successful work with the tube has been undertaken at Mount Wilson and is described in detail below.

An additional interest in image tube work lies in the possibility of extending the range of observations to new regions of the spectrum. It has been demonstrated by many workers that gains in the infrared, at one micron and beyond, are much larger than the gains that can be achieved with photographic emulsions. In the past, the Committee's activity in developing infrared-sensitive tubes has been, first, to support the development of



a magnetically focused, single-stage tube that can be used as a simple converter with modest gain, and second, to support the development of a mica-window tube with which exposures are made by pressing a photographic emulsion into contact with a thin window supporting a phosphor screen. In this tube the photoelectrons after acceleration impinge upon the screen and are converted to light which is then recorded by the photographic emulsion. During the report year, however, a third type of experimental intensifier was successfully built by the group at RCA. It is a cascaded tube with an infrared primary cathode,

but similar in other respects to the production type of cascaded tube described above. Many attempts have been made in the past to build such a tube, but the technological problems of processing have prevented the formation of stable photocathodes. With the support of the Carnegie group several tubes have been made with good infrared cathodes that appear to remain stable. The tubes have been used by Ford and Purgathofer at Lowell Observatory to obtain good spectra at  $1.0\text{--}1.1\ \mu$  of cool red stars. The success of these observations has led the Committee to place an order with RCA for a dozen tubes to our specifications.

## TEST AND EVALUATION OF SAMPLE TUBES

*Cascaded tubes.* The cascaded tubes made for us by RCA (their type C33011) have an S20 photocathode that is sensitive from 3,200 Å to 8,500 Å. The final screen is a fine-grain P11 (blue) phosphor. Typical photocathode sensitivities range from 120 to 150  $\mu\text{A}/\text{lumen}$  to 2,870°K tungsten radiation. The blue sensitivity as measured through a Corning 5113 filter (one-half stock thickness) is 9–10  $\mu\text{A}/\text{lumen}$ . The radiant energy gain of the tubes when operated at a total voltage of 20 kV is typically about 2,500. Relay lenses adequate to cover the 40-mm-diameter field are rarely faster than  $f/2$  when used at one to one.

A typical efficiency including transmission losses for such a relay lens, which might consist of a pair of  $f/2$  infinity conjugant lenses front to front, would be only about three per cent. The rate of blackening for the image tube system is the radiant energy gain of 2,500 times the three per cent lens efficiency, or a factor of 75. This rate-of-blackening gain is a sort of upper limit to the reduction in exposure time over Ila-O emulsion at the peak of the photocathode sensitivity. The quantum efficiency of the photocathode is about 15 per cent and the quantum efficiency of the photographic emulsion for long exposures is high—roughly 0.5

per cent. With a lens of this efficiency the gain of the intensifier system is adequate to give, on the average, 2.5 grains per photoelectron ( $75 \times 0.005$  divided by 0.15). For slower relay lenses having good definition and yielding statistically one developable grain per electron, typical gains in rate of blackening are 40 or 50 times that of the unaided photographic emulsion. These numbers are confirmed experimentally by comparing exposure time required to obtain a given density with blue light on Ila-O emulsions with that required to obtain the same density with the intensifier system using the same type of Ila-O emulsion to photograph the blue phosphor screen.

The resolution of the intensifier system measured on a Ila-O plate exposed to the system is approximately 25–30 lp/mm. It is roughly half that which can be adequately resolved with the unaided photographic emulsion. In general, the lower resolution can be compensated by enlarging the image going into the photocathode. The actual gain in exposure time for equal resolution and equal density then typically drops from 40 or 50 to 10 or 12. The gain in the rate of recording information, which is the appropriate criterion, may actually be higher than this because of the superior signal-to-



noise ratio that has been achieved by the magnification process. Since the grains of the photographic emulsion are large in comparison with those of the phosphor screen, the granularity (relative to a given image element) is deemphasized by the magnification process used to match the resolving power of the two systems.

The spurious background in these cascaded tubes consists of two components. One component is the thermally emitted electrons from the photocathode; the other is the result of cesium atoms being ionized and emitting bursts of electrons as they impinge upon the photocathode. These bunches of electrons are focused on the multiplying screen and appear as individual and infrequent bright scintillations at the output screen of the tube. In general, the thermal emission from the S20 photocathodes is sufficiently low under observing temperatures to permit exposures of many hours. The somewhat erratic ion emission is perhaps the most serious limitation of the present tubes. With some care in distributing the accelerating voltages along the electrodes of the intensifier the ion scintillation can be held to a sufficiently low value for one- or two-hour exposures. The duration of exposures when critical resolution is required is ordinarily limited not by the background but by the perturbing effects induced when the image tube moves through the earth's magnetic field while the telescope tracks on a celestial object.

Magnetic shields that operate efficiently around the focusing magnet required for the tube are usually large and bulky. Fortunately, it appears that the tube will give satisfactory images through exposures of several hours without shielding. Longer exposures will require either magnetic shields or simple servo systems to oppose and cancel the changing field.

In all the routine applications of these tubes we have used a permanent magnet array to simulate the focusing field of a solenoid. The array of permanent magnets is relatively light in weight and exhibits practically no drift with either

time or temperature. Our array of magnets has a 5-inch inside diameter, a  $6\frac{3}{8}$ -inch outside diameter, and a simple pole face to assist in the smoothing of the field. Fields of approximately 220 gauss are required to focus the tube at 10 kV per stage, or 20 kV total voltage. The magnet array is 25 cm in length and the photocathode is 6 cm inside the front pole piece. The inset of the tube inside the magnet array is a limitation as far as the placement of the tube on existing spectrographs is concerned. The overall length of the intensifying system depends in part on the relay camera. Our standard system is 18 inches from the front to the back and  $6\frac{1}{2}$  inches in outside diameter, including the shell supporting the tube. The magnet, tube assembly, and relay lens weigh 20 kg.

We have not found wholly satisfactory optics for the relay or transfer system. The most successful lenses are (1) a lens made by the Burke and James Co. of Chicago (their type 14011-A), a pair of  $f/2$  lenses front to front; (2) an Elgeet  $f/1.2$ , 86-mm focal length lens designed for one-to-one magnification; and (3) a Perkin-Elmer CRT-35 radar recording lens designed for operation at a magnification of 0.5. The Perkin-Elmer lens is best used for our purposes by turning it around to magnify by a factor of 2. The granularity of the photographic emulsion is deemphasized by the process, and the best resolution is obtained. With the Perkin-Elmer lens, however, the intensifier system is somewhat slower than needed. The Elgeet lens when stopped down to  $f/2$  for the infinity conjugate (i.e., when used at one to one at  $f/4$ ) is a well-corrected lens with uniform resolution and illumination across a 40-mm field. However, this lens too is slower than is desirable. The Burke and James lens gives good on-axis images and is fast enough, since it operates at  $f/2$  when used at one to one, but the uniformity of illumination and the resolution at the edge of the field are not satisfactory.

*Lenard window tubes.* Experimental



Lenard window tubes made by McGee and his collaborators at Imperial College were evaluated and tested at Mount Wilson in January 1965 by Baum and McGee. The tubes, 28 cm long, have a slotted window  $30 \times 5$ –10 mm and are  $3\frac{1}{2}$ – $4\frac{1}{2}$   $\mu$  thick. They are operated at 35–40 kV, and exposures are made by pressing an electron-sensitive emulsion into contact with the window. Photoelectrons penetrating the window form the latent image in the emulsion. Exposures were made on Ilford G5 and Ilford XM emulsions. With the XM emulsion the gain in exposure time is on the order of 40 times the gain that can be obtained directly with Ila-O. The resolution on XM is about 50 lp/mm, and on G5, 75–80 lp/mm. The Ilford G5 exposures are extremely fine grained. Those with the XM are considerably faster, but are quite grainy in comparison with direct exposures with Ila-O. The granularity of the electronographic exposures is voltage dependent. Actual electron tracks are being recorded, showing that at higher voltages the length of the track increases. The photocathodes of these tubes were made by EMI Electronics, Limited, in small capsules and introduced into the tube structure at Imperial College. The bialkali cathode sensitivities were approximately 35  $\mu$ A/lumen (2,870°K tungsten lamp). The tube background in the Mount Wilson exposures consisted mostly of light feedback from micro-discharges in front of the photocathode, which was operated at high voltage.

The gain of the Lenard window system with the XM emulsion is difficult to evaluate because of the increased granularity over photographic emulsion and because of the difficulty in assessing the storage capacity of the XM emulsions. It is estimated that the rms granularity may be  $1\frac{1}{2}$  times higher with this emulsion and that there may be a corresponding twofold reduction in storage capacity.

The principal advantage of the Lenard window scheme is that there is no photographic "inertia" in the log density-log exposure curve. Moreover, the system is nearly linear. The gain in rate of blackening, in the blue region of the spectrum, over a photographic system giving comparable resolution was 28 to 30. With improved photocathodes, perhaps with multialkali rather than bialkali photosurfaces, even larger rate-of-blackening gains can be expected.

*Infrared cascaded tubes.* Infrared cathodes (cesium oxide on silver, or S1) have a broad response from 0.9  $\mu$  to 1.0  $\mu$  and a tail that extends toward 1.3  $\mu$ . In March Purgathofer and Ford made exploratory exposures with a cascade tube having an S1 cathode. They used the Perkins 69-inch reflector of Ohio Wesleyan and Ohio State Universities at Lowell Observatory in Flagstaff, Arizona. The system was similar to that used previously for the S20 multialkali cascaded tubes except that cooling was required to suppress the thermal emission from the photocathode. The cooling was done with dry ice in a simple, circulating-fluid heat exchanger. Exposures of many hours could be made with no detectable background.

In April good quality spectra of several types of stars were obtained with this experimental equipment, and other observations were made by Ford with the collaboration of Dr. Peter B. Boyce of Lowell Observatory and Dr. Vera Rubin of DTM. In the second series of tests a systematic survey of spectra of M giants and supergiants between 0.96  $\mu$  and 1.1  $\mu$  was obtained. A few exposures were also made in the region between 1.15  $\mu$  and 1.35  $\mu$ .

Two other infrared cascaded tubes have recently been delivered. All three tubes have cathode sensitivities greater than 3.5  $\mu$ A/lumen measured with a 2,870°K tungsten lamp as seen through an infrared filter (Corning 2540).



## COLLABORATION WITH OTHER ASTRONOMICAL GROUPS

From the very beginning the purpose of the Carnegie Image Tube Committee's activity has been to develop an image-intensifying system that can be readily adapted to existing telescopes and spectrographs, and routinely applied to astronomical research problems. The tubes recently made by RCA for the Committee are specifically intended to provide a number of working intensifiers for various observatories. When the tubes from this production order first became available several colleagues in image tube work indicated that they were interested in making independent evaluations of them. Accordingly, image tube systems, based on a rather flexible design developed at DTM, have been made available to several groups outside the Carnegie Committee for practical testing in observing programs.

In February the first such system was put into operation at the Yerkes Observatory by Dr. W. A. Hiltner with the assistance of Ford and Purgathofer of DTM. Dr. Kron from Lick Observatory participated in the initial evaluation which was made on a laboratory spectrograph. The system will be used primarily for spectral classification, although the tube has already proved quite valuable in obtaining direct sky photographs with the Yerkes 40-inch refractor through narrow-band interference filters.

A second system was demonstrated in March by Ford, Purgathofer, and Tuve, and left at the Kitt Peak National Observatory, with Dr. Livingston and Dr. Lynds of the Observatory staff. The initial observations were made on the Kitt Peak National Observatory 60-inch solar telescope; the solar spectrograph was used to obtain high dispersion stellar spectra showing principally the resolution

of interstellar lines into components.

The third system has recently been sent to Lick Observatory where it is being evaluated by Dr. Kron. Preparations are being made for its installation at the coudé spectrograph of the 120-inch telescope during the summer of 1965. Another system is being set up at Lowell Observatory for the joint use of the Lowell Observatory and Ohio State University staffs and by Ford and Rubin. This system employs a small Cassegrain spectrograph weighing about 250 pounds, designed and built at DTM.

Another image tube system has been installed at the 100-inch telescope coudé spectrograph at Mount Wilson Observatory at the focus of the 73-inch schmidt camera. Ford and Baum with the collaboration of Wilson and Kraft had worked previously at the 114-inch camera. Depending on circumstances, the new installation will be a permanent one. The change from ordinary photographic spectroscopy to image tube spectroscopy at the focus of this camera can be made in a few minutes, representing a substantial improvement over the previous system.

To avoid any misunderstanding, it may be well to point out that image tubes offer no speed gain when comparison is made with the photomultiplier technique. This technique has been used for the measurement of individual stars and nebulae through a small pinhole aperture, characterizing their colors by using various filters (UBV in AR and others). The photomultiplier technique, applied to very remote single objects, of course utilizes the advantage of photoelectric sensitivity in comparison with photographic emulsions. There continues to be a requirement in astronomy for telescopes of the largest feasible apertures.

## ACKNOWLEDGMENTS

The primary acknowledgment of the Committee and its Chairman is to Dr. W. K. Ford, Jr., physicist-astronomer on the staff of the Department of Terrestrial Magnetism, for his sustained and intelligent efforts over more than a decade in direct technical activity for the Committee on many types of image intensifiers and with many laboratories, industrial firms, and observatories. Members of the Committee have helped identify and test the most important technical characteristics for the practical use of image tubes in astronomy, but without Dr. Ford's many contributions and his gently persuasive efforts the present happy result would have been long delayed or unattained.

Efforts by many industrial groups deserve thanks. In particular the Committee is under obligation to the tube development group at the RCA plant in Lancaster, Pa., under the general guidance of Dr. Ralph Engstrom, with the direct participation of E. G. Stoudenhimer, Allen Morehead, and Joseph C. Moore.

The encouragement and detailed participation of members of the Astronomy Section of the National Science Foundation have been major factors, quite apart from financial considerations, in pushing forward image tube efforts to the present level of practical usefulness in astronomy. Successive members of the Astronomy Section, including Dr. Helen Hogg, Dr. Frank Edmondson, Dr. Geoffrey Keller, and others in the early phases of the work, have been followed by the generous encouragement and interest of Dr. Gerald

Mulders and Dr. Harold Lane and their advisers in recent years, involving relatively large financial commitments. The Committee and the Institution have been pleased and impressed by the caliber of professional partnership exhibited in these relationships.

During the report year the Carnegie Committee has been fortunate in having the assistance of Dr. Alois Purgathofer who has been at DTM on leave from the Vienna University Observatory. Dr. Purgathofer's previous work has been in photoelectric photometry and instrumentation, and he contributed a great deal to the success of the image-intensifier camera systems while he was at DTM. The Committee will miss his capable support during the coming year.

We were fortunate in having Dr. Vera Rubin, formerly with the Georgetown College Observatory, join the staff at DTM in April. Her previous work in astronomical spectroscopy and radial velocity measurements in particular will be of great help in the application of tubes to observation problems.

The expense of bringing these image tubes into use, including the industrial costs for prototype tubes and for the production order of tubes for observatories, and the costs of additional spectrographs, lenses, and test equipment for the observatory testing, have been largely covered by grants from the National Science Foundation, supplementing the Carnegie outlay which covers salaries, shop time, and the cost of experimental or initial equipment items.





# *Department of Plant Biology*

C. Stacy French  
*Director*

*Stanford, California*



# Contents

Introduction . . . . .	365
Photosynthesis . . . . .	365
Experimental Taxonomy . . . . .	368
Staff Activities . . . . .	369
Biochemical Investigations . . . . .	370
Partial fractionation of natural chlorophylls <i>a</i> and <i>b</i> in aqueous extracts of certain algae by freeze-thawing . . . . .	370
Effects of detergents on the forms of chlorophyll <i>a</i> from different plants . . . . .	373
Fractionation of chlorophyll forms from <i>Euglena</i> and measurement of light-induced absorbance changes . . . . .	374
Separate action spectra for the photochemical systems of photosynthesis . . . . .	379
Localization of plastocyanin in the electron-transport chain of photosynthesis in relation to cytochrome <i>f</i> and components producing the 518-m $\mu$ absorbance change . . . . .	381
Partial inhibition of photosynthetic-electron transport by lack of oxygen . . . . .	390
An oxygen requirement for photosynthesis . . . . .	395
Kinetics of the two-light effect on the photosynthetic oxygen outburst . . . . .	397
Transients of oxygen exchange in <i>Chlorella</i> caused by short light exposures . . . . .	399
Studies on phytochrome transformation in vitro . . . . .	406
Electromotive-force measurements with a glass-membrane electrode . . . . .	412
Instrumentation . . . . .	414
Experimental Taxonomy Investigations . . . . .	415
Comparative physiological studies of ecological races of <i>Solidago</i> . . . . .	415
Measurements of the 591-m $\mu$ absorbance change . . . . .	416
Measurements of the Emerson enhancement effect . . . . .	418
Light utilization in ecological races of <i>Mimulus cardinalis</i> . . . . .	420
Photosynthetic rates of <i>Mimulus lewisii</i> . . . . .	425
Cytogenetic relationships within the Erythranthe section of <i>Mimulus</i> . . . . .	427
Cultures of <i>Mimulus</i> in vitro . . . . .	429
Vegetational and climatic contrasts within the Harvey Monroe Hall Natural Area . . . . .	431
References Cited . . . . .	435
Bibliography . . . . .	435
Speeches . . . . .	436
Personnel . . . . .	437

## INTRODUCTION

### PHOTOSYNTHESIS

The chemical composition and the function in photosynthesis of the pigment complexes in plants again have been the major concern of one group in the Department. This year efforts have been intensified to separate the two pigment systems without alteration of their characteristic absorption spectra or of their photochemical activity. Cornelis Bril, a research Fellow from Utrecht, has been collaborating with Jeanette S. Brown on the separation of the several forms of chlorophyll without removal of the pigments from their functional units.

The major problem in this work is to break apart the units of the chloroplasts that contain the individual pigment systems within the units. The separation methods used include the addition of detergents, which, within narrow ranges of concentration and under certain conditions, can liberate the distinct photosynthetic structures without loss of their function.

To determine if either separation or destruction of the pigment forms has been accomplished by the procedures used, the derivative absorption spectra of centrifugal fractions were measured. The test used for the retention of photochemical activity was a measurement of the light-induced changes of absorption by certain components with the apparatus constructed by David C. Fork. Wolfgang Urbach, a Kettering research Fellow from Würzburg, collaborated in the experiments on absorption changes.

Many exploratory experiments were made with various algae and with various detergents. The detergent deoxycholate yielded a supernatant fraction of the *Euglena* pigments that contains primarily a form of chlorophyll known as C<sub>a</sub>670 and a heavier fraction greatly enriched in C<sub>a</sub>695. Light-induced absorption changes indicate that these fractions retain differ-

ent portions of the photochemical transport chain. Dr. Bril was also able partially to fractionate pigment complexes from *Dunaliella* and *Ulva* by repeated freezing and thawing; a procedure that avoids the dangers of detergent treatment.

We were fortunate to have a week's visit from Dr. Keith Boardman, who, with his collaborator Dr. Joan Anderson, has previously achieved success in such separations. Next year Dr. Anderson will be with us as a research Fellow to correlate the findings of the Australian group and those of the workers in this Department on the separation and testing of the two pigment systems for their activity.

*Distinctive functions of the two pigment systems.* Studies of oxygen or carbon dioxide exchange and of the absorption change of various photosynthetic intermediates show that the two mutually dependent systems perform essential but very different functions. The main center of interest of many workers in photosynthesis now is the nature and sequence of the components of the electron pathway linking the two photochemical systems.

One of the simplest ways to study the two light reactions is to measure oxygen evolution from isolated chloroplasts without added substrates. Several years ago Dr. Fork found that, whereas excitation of system II in chloroplasts gives an oxygen outburst, excitation of system I regenerates their ability to give another oxygen outburst from a second illumination of system II (*Year Book 61*, pp. 334-343). William R. Griswold developed model schemes that were adequate to account for the time-course curves of a single oxygen outburst which qualitatively but not quantitatively describe the photochemical recovery process. Some further measurements were made for use in testing models. It was concluded that, to obtain adequate data, a different type



of electrode suitable for strictly comparable rate measurements on aliquots of a single sample should be built. We need but do not yet have a family of time-course curves for oxygen production by isolated chloroplasts adequate for a precise analysis of the kinetics of this reaction.

An effect in intact cells very similar to the oxygen outburst of isolated chloroplasts is the initial spike of the time course of oxygen evolution. This initial outburst of oxygen in *Chlorella* is also regenerated by illumination of system I, as found last year by Yaroslav de Kouchkovsky. This year Dr. de Kouchkovsky studied further the recovery of the outburst by system I and also its inhibition by illumination of system II (see p. 397). Strangely enough, he found that prolonged illumination at wavelengths mainly absorbed by system II caused not a further inhibition but rather an increase in the initial oxygen outburst. This complication arises from the fact that at the optimum wavelength (650 m $\mu$ ) for system II illumination, there is still an appreciable amount of absorption by system I. The relative reaction rates and pool sizes of the intermediates seemed to be of more significance than the wavelength of irradiation in determining the time course of the recovery.

Studies of the separate functions of the two pigment systems have been made in a different way by William E. Vidaver. In his experiments, intact algae were treated with a poison specific for the oxygen-evolving system. Algae so poisoned take up oxygen briefly when illuminated and in the dark soon recover the ability to do so again. The effectiveness of different colors of light in driving the oxygen uptake gave an action spectrum corresponding roughly to the absorption spectrum of the long-wavelength pigment complex, system I. Furthermore, Dr. Vidaver found that treatment of the algae overnight at a high oxygen concentration replaced the photochemical function of system I so that the influence of light on system II alone could be

determined. Its action spectrum is consistent with the absorption spectra of the system II fractions prepared from other algae.

*Kinetics of oxygen evolution and uptake.*

The uptake of oxygen, going on concurrently with oxygen evolution, is itself an essential part of the photosynthetic process. Attempts have been made this year to find out what step in the process is responsible for oxygen utilization. The results of Dr. Vidaver's experiments, and older work with *Porphyridium*, show that activation of the long-wavelength system I by light causes the oxygen uptake.

Results of experiments reported by Dr. Urbach and Dr. Fork show more directly how oxygen affects electron transport in photosynthesis. They found that lack of oxygen has a dramatic effect on absorbance changes of some photosynthetic intermediates. Apparently anaerobiosis produces a block of electron transport and thereby brings about changes in the redox state of these intermediates.

Immediately after algae have been illuminated there are complex changes in the rate of oxygen and of carbon dioxide exchange. As with the time course of photosynthesis at the start of a light period, these transient changes in rate after illumination have been used to draw conclusions about the mechanism of photosynthesis. The rate of oxygen exchange after a light exposure usually does not drop immediately to the preceding level of respiratory oxygen consumption but may decline slowly to that level. This effect has been interpreted in two ways: (1) Either oxygen evolution continues from a pool of material activated by light, or (2) respiratory oxygen uptake is inhibited by the light exposure. Both concepts, equally plausible without further evidence, lead to very different conclusions about the nature of the photosynthetic system. So far the experiments of other workers with isotope techniques have not established that either of the two concepts can be rejected. Further-



more, both a stimulation and an inhibition of oxygen uptake during the light period have been found in isotope studies.

The idea of postillumination survival of oxygen evolution has much support. But this year, experiments made by August Ried, a research Fellow from Professor Egle's laboratory in Frankfurt, seem to be more in line with the idea of the interaction of photosynthetic products with the plant's respiratory system than with the concept of continuing oxygen evolution.

Dr. Ried found that in *Chlorella*, large changes in rates of oxygen uptake that last for some minutes can be induced by illumination lasting only one second. These changes were absent in cells treated with glucose to make respiration go at its maximum value, or with antimycin A which poisons respiration but not oxygen evolution.

It thus appears that the transients in question show up only when the respiratory system is working at an intermediate rate so that it can be either speeded up or slowed down by the photochemical formation or removal of some intermediates. The observed transients, therefore, are ascribed to changes in the rate of oxygen consumption.

The effect of different wavelengths, light intensities, and exposure times on the subsequent oxygen exchange indicates strongly that the connection between the respiratory and photosynthetic systems (if indeed they are separate) is not a single link. Because clear transients in  $O_2$  exchange occur at specific times after various exposures, several such links must exist at different sites between the systems. The most extraordinary effect Dr. Ried found was the enormous stimulation of oxygen uptake produced by one second of blue light. The maximum rate of this light-induced stimulation came eight minutes after the exposure. Furthermore, the extra oxygen consumed was 500 times the amount of oxygen produced by the brief exposure to blue light. Such behavior may be connected with the effects of weak blue light on

photosynthesis driven by red light as found by Warburg, and with the carbon dioxide outburst found by Emerson.

The question of how plant respiration and photosynthesis interact is as old as the subject of plant physiology itself. Probably all conceivable types of interaction, as well as the lack of any coupling at all, have been proved convincingly for certain plants under certain conditions. Unfortunately, the interpretation of any measurements of photosynthetic rates necessarily implies some sort of an assumption about the nature of the interaction between the two processes.

*Absorption changes caused by light.* In last year's report the participation of the copper-containing protein plastocyanin in photosynthesis was described by Dr. de Kouchkovsky and Dr. Fork. Recently its location in the electron transport chain of photosynthesis has been more specifically established. Fork and Urbach found plastocyanin to act between the two light reactions before cytochrome *f*. They also found that the absorption change at 518  $m\mu$ , previously believed to be a characteristic of system II activity, is actually a complex effect. Part of the change at this wavelength must be attributed to system I. The chemical identity of the substance changing its absorption at this wavelength remains uncertain.

The apparatus for measuring absorption changes is also well adapted to studies concerning the kinetics of the reversible transformation of phytochrome between its active and inactive forms. Dr. Fork collaborated with Dr. Winslow Briggs of Stanford University on this problem. A second and previously unsuspected intermediate in the transformation of the inactive red-absorbing form to the active far-red-absorbing form was detected.

*Action spectra of photosynthetic pigments.* An adequate knowledge of the photosynthetic pigment system should make it possible to match an absorption spectrum of a live plant by adding together the spectra for the two functional systems after adjusting them by ap-



propriate factors. If this were done with reliable data for action spectra, any mismatch should show both the spectra of the photochemically inactive pigments and the possible participation of still other photochemical steps in photosynthesis. As far as we know, no sets of data adequate for this purpose exist.

Conceivably a third photochemical system may be present in the plants. Certainly effects of blue light on photosynthesis and on plant respiration are widely known, though poorly understood. To clarify the blue-light effect and its possible role as a third photochemical system of photosynthesis, much greater precision in action spectrophotometry of photosynthetic systems is required. The difficulties lie not in the physical measurements but in the varied responses of the cells following different light regimes preceding the measurements of action spectra. This year Dr. Vidaver found large differences in action spectra for *Ulva* caused by the long-lasting effects of previous light exposures. The effects are not at all clearly understood although a beginning has been made toward their clarification by Dr. Ried's experiments with the long-term effects of brief light exposures.

*Measurement of phosphate concentration.* The importance of phosphate metabolism in photosynthesis and in general biochemistry emphasizes the need for a way to determine inorganic phosphate by a rapid, continuously recording method that is not also sensitive to pH changes. James H. C. Smith has found that a calcium-sensitive glass membrane looks promising for this purpose. The principle is to determine phosphate ion indirectly in the solutions saturated with calcium phosphate through the solubility product relationship.

#### EXPERIMENTAL TAXONOMY

*Differences in the photosynthetic mechanism of contrasting climatic races.* For some years a significant part of the work of the Experimental Taxonomy group has

centered on quantitative measurements of the photosynthetic capacity of climatic races of plants native to contrasting environments. Appreciable differences have been reported by Harold W. Milner and William M. Hiesey between the photosynthetic responses of contrasting *Mimulus* races to light intensity, to temperature, and to long periods of illumination. The investigation continues to show differences in the photosynthetic ability of plants native to various climates. It was recently found that races of *Mimulus lewisii* from high altitudes require considerably higher light intensities to saturate photosynthesis than races of the closely related *Mimulus cardinalis*, which occurs at lower altitudes. In addition, the photosynthetic rates of *M. lewisii* show pronounced short-time variations not found in *M. cardinalis*.

The mechanism of photosynthesis consists of two separate light reactions driven by different pigments and of a number of enzymatically catalyzed steps independent of light. Olle Björkman has taken up the problem of finding out which particular steps in the process are responsible for the differing photosynthetic capacity of contrasting climatic races. His hypothesis is that in adapting to different environments, plants have evolved modifying devices for overcoming the major limiting external factors of their particular climatic niche. Genetic differences, therefore, are more likely to be revealed by investigating singly the capacity to carry on the individual steps of photosynthesis rather than by measuring overall rates. Variations in the capacity of each step of photosynthesis result from the interaction between the genetic makeup and the environment in which the plant is grown before measurement. It is essential to compare clones of diverse genetic constitution originating from contrasting natural environments grown under different sets of controlled conditions.

Dr. Björkman has in this connection studied the Emerson enhancement effect



in leaves grown at two light intensities. Leaves of a race of the goldenrod, *Solidago*, native to a shaded habitat, when grown at low intensity give a large enhancement effect with light beams of two appropriate colors. Leaves of the same clone grown at high intensity show only a small enhancement. In goldenrod plants native to shaded habitats the functioning of system II was found to be impaired in plants grown under high intensity. This was found both by measurements of enhancement and by the light-induced changes of absorbance in certain photosynthetic intermediates. In contrast, plants native to a high-light-intensity habitat have a more active system II when grown under high intensity than when grown under low intensity. The shade ecotypes are more efficient in the use of weak light, while those from bright-light habitats can use a high intensity more efficiently.

Further studies by Dr. Björkman and other staff members on the mechanics of light absorption and utilization in genetically distinct races of *Mimulus* reveal that the capacity to absorb light differs between races. The absorption also can be modified by growing the same clones under different light intensities. In either case the quantum yields are identical, and the differences in light utilization by photochemical processes are attributable to differences in capability of light absorption.

*Evolutionary relationships between species.* Continuous transplant studies on different combinations of first-generation hybrids of *Mimulus* at the three mountain stations support earlier findings that hybrids between contrasting climatic races display markedly greater vigor and tolerance to extreme environments than the parental races. Extending this study of the genetics of other distinct yet related species of *Mimulus*, Malcolm A. Nobs and Dr. Hiesey have made all possible crosses among five closely related members of one section of the genus. Comparative studies of the morphology,

growth, pollen fertility, and chromosome pairing were made on 200 cultures of 95 different first-generation hybrids. The work has revealed the existence of previously unknown genetic barriers between and within species, and, moreover, close relationship between components previously thought to be distinct. This clarification of evolutionary relationships in the *Erythranthe* section of *Mimulus* is of special significance in connection with the study of the genetics and the transplant responses of climatic races of *M. cardinalis* and *M. lewisii* being made concurrently in connection with physiological studies.

*Tissue cultures from contrasting climatic races.* A 2½-year exploratory study on the utilization of tissue cultures of *Mimulus* for comparing physiological and biochemical characteristics of ecological races is being successfully concluded. Various races are favored by various kinds of media, and the kind of growth among various types of tissues can be partly controlled by chemical additives. Use of uniformly established excised tissues of cloned plants in studies on comparative growth and respiration, and on biochemical and developmental projects is now a promising avenue for research.

Jens C. Clausen has continued his studies on the relation between microclimatic differences in the Harvey Monroe Hall Natural Area and their relation to the diversity of species and races found at high altitudes in the Sierra Nevada of California.

#### STAFF ACTIVITIES

Since many former members of the Department and their wives were to attend the 10th International Botanical Congress in Edinburgh, we were invited to Dunfermline by the Trustees of the Carnegie United Kingdom Trust, the Carnegie Dunfermline Trust, and the Carnegie Hero Fund on August 2, 1964. The arrangements were made by David Lowe, Secretary of the United Kingdom Trust, Mrs. Lowe, and their two



daughters. We were extraordinarily well entertained by Mr. and Mrs. Lowe. Mr. and Mrs. O. A. Cunningham, Mr. and Mrs. James Bonnar, Mr. and Mrs. J. W. Ormiston, and Mr. and Mrs. A. Reid also gave much thought and time to our pleasure and to our enlightenment about Andrew Carnegie's life as well as the present activities of his endowments. Those of our group who participated in this unusually delightful pilgrimage were Dr. Björkman, Dr. Clausen, Dr. Fork, Dr. and Mrs. C. Stacy French, Dr. and Mrs. Martin Gibbs, and Drs. Per Halldal, Arthur R. Kruckeberg, Jerome A. Schiff, Helen Sharsmith, and Hemming Virgin.

Papers were presented by Björkman, Clausen, and French at the Botanical Congress. Clausen was a vice-president of the Congress and the principal speaker at a dinner of the Botanical Society of Edinburgh honoring its foreign Fellows. He also participated in the six-day International Botanical Excursion to the central Scottish Highlands; on this expedition he compared the vegetation with the tree-line vegetations in other parts of the world.

During the year Dr. French was elected a member of the Deutsche Akademie der Naturforscher Leopoldina.

Harold W. Milner, who died on July 13, 1965, had joined the staff as a chemist in 1928. In collaboration with Dr. Spoehr he at first investigated the carotenoid

pigments of plants and later the plant carbohydrates. He was a gifted analyst who early mastered the technique of microanalytical chemistry, and was one of the pioneers in this field on the Pacific coast. Later he turned to problems in the large-scale culture of algae. Collaborating with Dr. Spoehr, he found that the chemical composition of algae could be controlled by the culture conditions chosen for their growth. He developed techniques for producing algae with a very high content of either protein or fat. In recent years he studied the differences in the photosynthetic response of various climatic races of plants to external conditions such as light intensity and temperature. Mr. Milner translated 300 Russian articles on aspects of photosynthesis closely related to the work of the Department. Microfilm copies of these translations have been widely distributed by the John Crerar Library in Chicago. In addition to engaging in scientific work Mr. Milner, the Department's most capable editor, willingly worked for long periods in editing the manuscripts of other members of the Department. Through his editorial work and his example, the entire laboratory benefited in standards of exactness and excellence of performance. Locally Mr. Milner was well known as an amateur astronomer and served effectively in both local and regional amateur astronomical organizations.

## BIOCHEMICAL INVESTIGATIONS

### PARTIAL FRACTIONATION OF NATURAL CHLOROPHYLLS *a* AND *b* IN AQUEOUS EXTRACTS OF CERTAIN ALGAE BY FREEZE-THAWING

*C. Brill*

Isolation of the various forms of chlorophylls to establish their nature and function requires as complete preservation as possible of their native states. As

will be described in a later section, disruption of chloroplast membranes by detergents is usually accompanied by spectral changes. This undesirable effect may lead to artifacts and to the measurement of photochemical activities that are not relevant to actual photosynthesis. An added disadvantage is that detergents cannot be removed completely after use, and they may inhibit enzymes and interfere with purification procedures. We



looked, therefore, for a method that avoids the application of these agents.

A well-known technique for disrupting biological structures and solubilizing some of their constituent proteins is repeated freezing and thawing, a procedure that has been successfully applied in a partial fractionation of chlorophyll complexes from the algae *Dunaliella* and *Ulva*.

*Methods.* *Dunaliella* cells, grown in an artificial seawater medium, were disrupted by forcing them through the needle-valve pressure cell, and the suspension was centrifuged at 10,000*g* for 20 minutes. To remove soluble cellular proteins the chloroplast fragments were subsequently spun down at high speed and rehomogenized in tris buffer, pH 8.5.

The marine alga *Ulva*, collected at Half Moon Bay, was washed with distilled water and its tough thallus macerated by passing it through an Acme Juicerator. After removing unbroken cells and debris by centrifugation at 1,000*g* for 10 minutes, the extract was forced through the needle valve. Chloroplast fragments were then purified as described for *Dunaliella*.

Samples of the chloroplast suspensions, brought to pH 10.5, were rapidly frozen in a dry-ice-acetone bath and slowly thawed at room temperature. The cycle was repeated 7 to 10 times. After this treatment the suspensions were dialyzed overnight against tris buffer and then subjected to two successive 20-minute runs at 10,000*g* and 50,000*g*, respectively, followed by a third run at 144,000*g* for one hour. The respective sediments were taken up in buffer. The final supernatant was free of chlorophyll.

*Results and discussion.* On spectral evidence, freeze-thawing causes no appreciable damage to the various chlorophyll *a* forms; sometimes a slight effect on C<sub>680</sub> is observed. Spectral differences exhibited by the centrifugal fractions demonstrate that fragmentation of the chloroplasts and a partial fractionation of complexes have occurred. Significant differences in chlorophyll *a*-to-*b* ratios are

evident from the derivative absorption spectra of the 10,000*g* and 144,000*g* fractions from both *Dunaliella* and *Ulva*. The difference was confirmed by the spectra of ether extracts from these fractions (Fig. 1). Compared with the original suspensions, the material sedimented at low speed is considerably enriched in chlorophyll *b*, whereas in the 144,000*g* fraction the chlorophyll *b*-to-*a* ratio is decreased. The difference of a few millimicrons in the main absorption maximum, together with the difference in inflection of the C<sub>680</sub> shoulder, indicates a partial fractionation of chlorophyll *a* forms also. The 50,000*g* fraction shows a spectrum very similar to that of the original suspension.

So far the best results were obtained when the materials were freeze-thawed at a strongly alkaline pH, followed by dialysis. When the procedure is carried out at a lower pH, irreversible aggregation takes place, increasing after each cycle, until part of the chloroplast material, enriched in chlorophyll *b*, flocculates. Separations under these conditions were poor.

Fractionation of the chlorophylls by the method described is reproducible for *Dunaliella*, but variable results were obtained with *Ulva*, collected at different times. Whether this reflects differences in the physiological state of the *Ulva*, or whether variables other than pH should be controlled during freezing is unknown.

Attempts to fractionate chlorophyll forms from two other algae, *Stichococcus* and *Euglena*, were unsuccessful under the same conditions. In addition, C<sub>695</sub> in *Euglena* chloroplasts is readily destroyed by freezing. Apparently chloroplasts from various algal species exhibit wide variations in resistance to freezing and thawing.

A similar fractionation of pigment complexes of both algae used in the present study can be achieved with digitonin. From an extract containing 0.5 per cent of this detergent, fractions are obtained by differential centrifugation



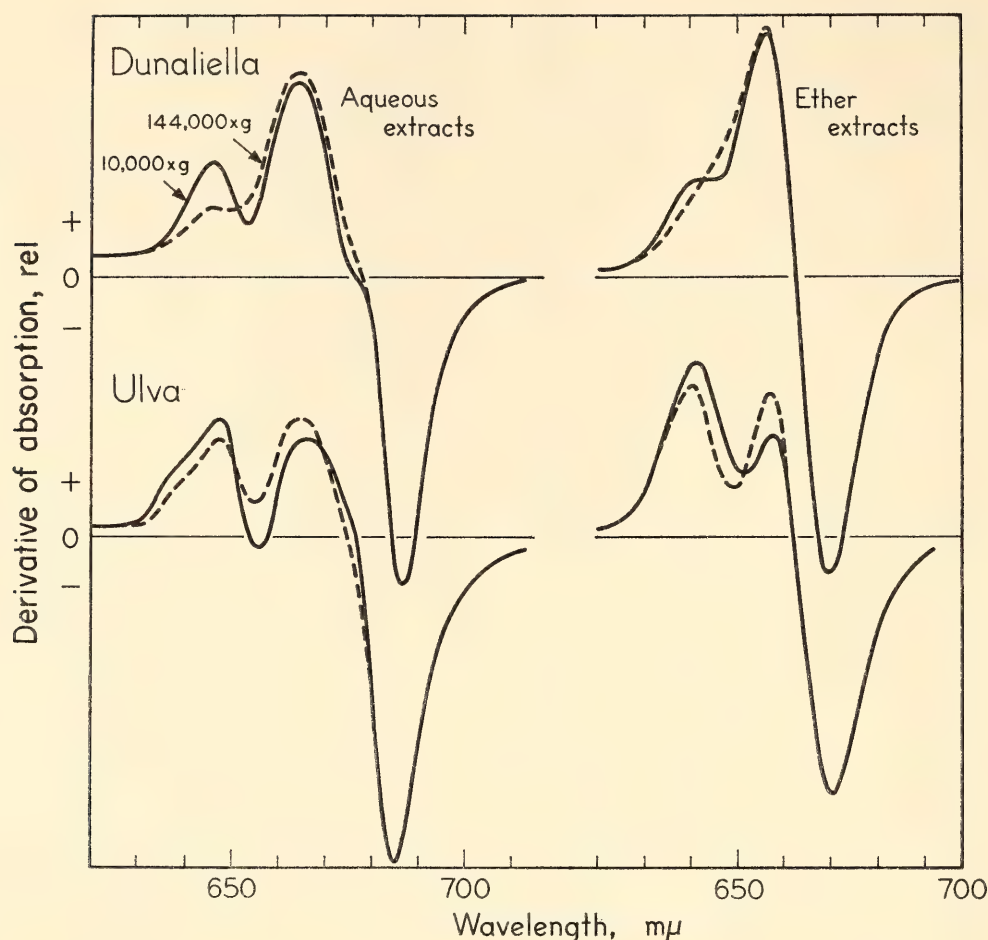


Fig. 1. Derivative absorption spectra of fractions obtained from *Dunaliella* and *Ulva* by differential centrifugation of extracts after freeze-thaw treatment.

that have spectral characteristics like those obtained after a freeze-thaw treatment—there is relatively more chlorophyll *b* in the low-speed fraction. In contrast to freeze-thawing, the detergent seriously affects  $C_{680}$ ; also a considerable amount of pigmented material with a changed absorption spectrum is rendered unsedimentable at a centrifugal force of 144,000*g*. Hence, the freeze-thawing technique is to be preferred.

The similarity between the results obtained with digitonin and freeze-thawing may not be coincidence. The observed fragmentation of the chloroplasts is certainly not a random process, and it seems likely that a basically similar mechanism operates during both treatments. There is reason to believe that the chloroplast membrane consists of a lipoprotein matrix covered with two types of functional units, commonly

referred to as systems I and II, each containing a set of similar pigment complexes, but in different proportions. Reports in the literature indicate that these units are separable. Digitonin blocks electron flow between the two photochemical systems in spinach chloroplasts (Wessels, 1962) and, as in our experiments, in its presence the same chloroplasts can be separated into fractions, which have tentatively been identified as systems I and II (Boardman and Anderson, 1964). Apparently the detergent breaks the bonds that hold one type of unit (system I) in the lipoprotein matrix, liberating these units as free particles. Being different in sedimentability, the particles can be separated from the membranous material, to which the system II units remain attached. Possibly freeze-thawing similarly strips the system I particles from the matrix by

rupturing the same binding forces as digitonin does. According to this picture the 50,000*g* fraction consists mainly of intact membranous material, unaffected by freeze-thawing.

EFFECTS OF DETERGENTS ON THE  
FORMS OF CHLOROPHYLL *a*  
FROM DIFFERENT PLANTS

*J. S. Brown and C. Bril*

Various forms of individual pigments, identified only by differences in their light-absorbing properties, occur in plants. One theory is that the spectral differences are caused by various modes of attachment of the pigment to its lipoprotein carrier. Last year (*Year Book 63*, pp. 480-482) a partial separation of chlorophyll *a* forms from each other and from chlorophyll *b* was accomplished by differential centrifugation of tobacco chloroplast material treated with sodium dodecyl sulfate. Allen, Boardman, Anderson, and Kahn have also made partial separations of different fractions of the photosynthetic pigment complexes.

Ideally such separations should be made without detergents, some of which may drastically alter the components

under study. In practice, attempts to fractionate the material without detergents are rarely successful. We have, therefore, made a study of the effects of a number of detergents at various concentrations on chloroplast material from nine kinds of plants. The objective is to define the usable type and amount of detergent that will allow separations to be made without changing the spectrum of the pigment complexes.

A suspension of chlorophyll-lipoprotein was prepared by a method suitable for the plant used. After adding a detergent, the mixture was subjected to differential centrifugation. Derivative absorption spectra of the fractions indicated whether pigment separation or destruction had or had not occurred.

Rather striking differences were observed in the effects of detergents on various chloroplast materials. The detergent concentration, time of action, temperature, ionic strength, and *pH* are critical factors in effecting a separation of chlorophylls. Each chloroplast material, even from such morphologically similar plants as spinach and Swiss chard, requires a different set of these factors. This indicates a difference in the struc-

TABLE 1. Effects of Low Detergent Concentration on Pigments in Suspended Chloroplast Material

Plant	Detergent			
	Sodium deoxycholate	Digitonin	Sodium dodecyl sulfate	Triton X-100
Pokeweed	....	....	—	....
Swiss chard	....	....	<i>D</i>	....
Spinach	....	....	<i>I</i>	....
<i>Porphyridium</i>	....	....	—	<i>D</i>
<i>Ulva</i>	....	+	—	....
<i>Dunaliella</i>	—	+	....	....
<i>Chlorella</i>	....	....	—	<i>D</i>
<i>Stichococcus</i>	<i>I</i>	—	—	<i>D</i>
<i>Euglena</i>	+	+	<i>D</i>	<i>D</i>

+ Separation of chlorophylls.  
— No separation or apparent change.  
*D* Chlorophyll complexes rapidly destroyed.  
*I* Inconclusive result.



tural matrix that bears the pigments in each plant.

By the use of roughly equal weights of detergent and chlorophyll in the suspensions, fractionation of the chlorophyll forms from different plants was attempted. The results are presented in Table 1. A good separation of pigment complexes was accomplished only with material from *Euglena*. The supernatant fraction contained mainly chlorophyll *a* 670, and the sediment was enriched in chlorophylls *a* 680, 695, and chlorophyll *b*, as described in a later section.

The absence of chlorophyll separation does not mean that the chloroplast material is unaffected by the low detergent concentration. With *Porphyridium* suspensions, sodium dodecyl sulfate solubilized all the phycocyanin, leaving in the sediment particles with an unchanged chlorophyll *a* spectrum.

An increased detergent concentration induces time-dependent spectral changes in the suspensions. The longest wavelength form of chlorophyll *a* is always destroyed first. Figure 2 shows an example

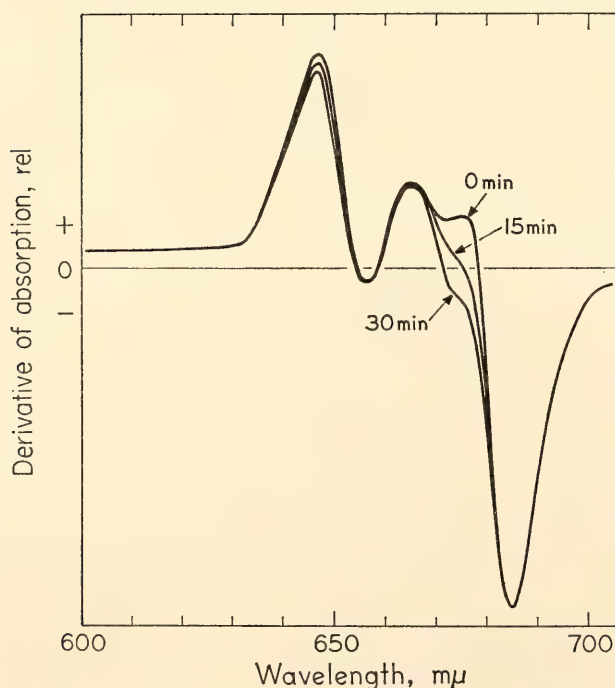


Fig. 2. Derivative absorption spectra of *Stichococcus* material at 0, 15, and 30 min after addition of 0.05% sodium dodecyl sulfate, at 20°C.

of this in material from *Stichococcus*. Still more detergent drastically alters the absorption spectrum of all chloroplast materials tested. The longer wavelength bands disappear and are replaced by a new band at about 667 mμ.

Separations attempted with too high detergent concentrations, therefore, may easily be misinterpreted. Nevertheless, under precisely controlled conditions a partial fractionation of the native forms of chlorophyll can be achieved.

#### FRACTIONATION OF CHLOROPHYLL FORMS FROM *Euglena* AND MEASUREMENT OF LIGHT-INDUCED ABSORBANCE CHANGES

*J. S. Brown, C. Bril, and W. Urbach*

*Euglena* has occupied a central position in the study of chlorophyll *a* forms because, in addition to the two absorbing forms, C<sub>a</sub>670 and C<sub>a</sub>680, that are present in most plants, this alga when grown with dim light contains a large proportion of a third form, C<sub>a</sub>695. In aqueous extracts of *Euglena*, C<sub>a</sub>695 is much more labile than the other two forms and always disappears first when the extract is heated, strongly irradiated, acidified, or differentially extracted with organic solvents. No separation of the different absorbing forms has been accomplished by differential centrifugation of the untreated aqueous extracts.

*Separation of chlorophyll forms.* During our general survey of the effects of detergents and of repeated freeze-thawing on plant extracts we observed that Triton X-100, sodium dodecyl sulfate, and freeze-thawing readily destroyed C<sub>a</sub>695. The contrasting effect of sodium deoxycholate and of digitonin is significant. When either of these detergents (about five parts by weight of detergent to one part of chlorophyll) is added to an extract of *Euglena* and the mixture is centrifuged differentially, the resulting fractions have different proportions of the forms of chlorophyll *a* and chlorophyll *b*. In one such experiment, digitonin was added to an extract and the mixture

centrifuged at 10,000*g* for 30 minutes. The supernatant layer was then subjected to two successive centrifugations, at 50,000*g* for 30 minutes and 144,000*g* for 60 minutes. The sediments were resuspended in buffer.

Figure 3 shows the derivative absorption spectra of the original untreated extract and of the sediments from 50,000*g* and 144,000*g*. The shoulder at about 650  $m\mu$  is caused by chlorophyll *b*. That the 50,000*g* sediment contained more chlorophyll *b* relative to *a* than the original extract, was confirmed from spectral measurements of acetone extracts of the fractions.

The derivative absorption curve crosses the zero line at the wavelength of the absorption maximum. The position of this maximum in our extracts depends on the relative amounts of  $C_a670$  and  $C_a680$ , which comprise the main chlorophyll *a* absorption band in vivo. The exact wavelength positions of the maxima of  $C_a670$  and  $C_a680$  forms are unknown and

may vary from one plant species to another. The 144,000*g* sediment contains primarily  $C_a670$ . The heavier, 50,000*g* sediment contains some  $C_a670$ , the same amount of or slightly more  $C_a680$  than the original, and it was considerably enriched in  $C_a695$ . A measure of  $C_a695$  is the relative size of the negative peak at 698  $m\mu$ . This is the first time we have observed a fraction with an increased amount of the very labile long-wavelength form of chlorophyll.

In another experiment, in which sodium deoxycholate was added to an aqueous extract of *Euglena*, a similar separation of the chlorophylls occurred. This time the mixture was centrifuged at 35,000*g* for 30 minutes. The resulting sediment corresponds to the 50,000*g* sediment of the first experiment, the supernatant layer to the 144,000*g* sediment. The spectral measurements were extended to the blue-wavelength region. In Fig. 4 these spectra show that the supernatant layer, containing about 10 per cent of the total chloro-

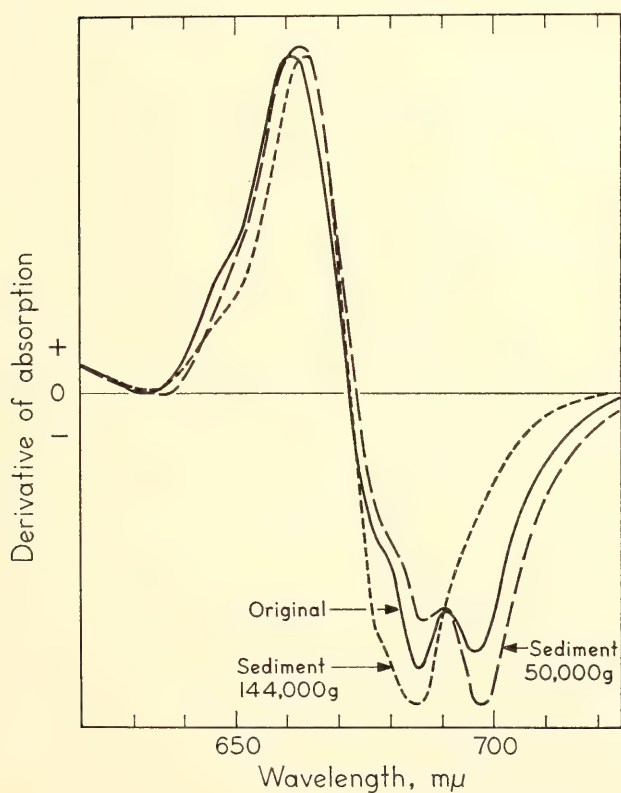


Fig. 3. Derivative absorption spectra of a digitonin-treated *Euglena* extract and of the 50,000*g* and 144,000*g* centrifugal fractions.

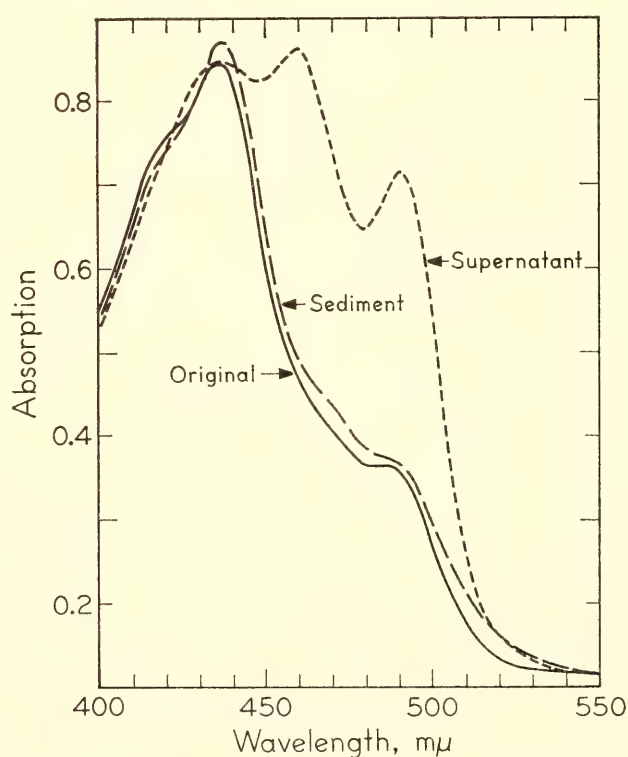


Fig. 4. Absorption spectra of deoxycholate-treated *Euglena* extract and of the sediment and supernatant layer after centrifugation at 35,000*g* for 30 min.



phyll, was considerably enriched in a carotenoid type of pigment having absorption maxima at 415  $m\mu$ , 433  $m\mu$ , and 485  $m\mu$  in acetone.

*Photo-induced absorbance changes in different pigmented fractions.* After obtaining cell fractions with different proportions of the pigments we looked for some type of photochemical activity that might be caused by a particular pigment form. Various types of activity, such as absorbance changes and fluorescence, have been extensively studied in intact cells, as well as in whole and broken chloroplasts. It is difficult to interpret results from these studies in terms of activity by a particular chlorophyll form because of the strong overlapping of the absorption bands.

We therefore looked for absorbance changes at 518  $m\mu$ , 591  $m\mu$  (plastocyanin), and also at 419  $m\mu$  (cytochrome *f*) induced by red plus far-red ( $> 630 m\mu$ ) or predominately far-red ( $> 670 m\mu$ )

actinic light. An instrument described by Fork was used (*Year Book 63*, pp. 435-436). Photo-induced changes were investigated in *Euglena* cells, in broken cell mixtures, in the insoluble fraction of broken cells (which includes all chlorophyll pigments), in the extract plus deoxycholate, and in centrifugal fractions of the detergent-treated extract. Absorbance changes of the supernatant and sediment fractions also were studied after the addition of a mixture of sodium ascorbate, 2,3,5,6-tetramethyl-*p*-phenylene-diamine (DAD), TPN, ferredoxin, and the colorless soluble cell extract. After the changes with these additions were observed, 3-(3,4-dichlorophenyl)-1,1-dimethylurea (DCMU) and salicylaldoxime were each added to aliquots and the measurements repeated.

Two types of absorbance changes were observed: (1) a large, slow change with a rate of rise  $10^{-3}$  OD  $\text{sec}^{-1}$  (seen especially in Fig. 5), and (2) a small, rapid change

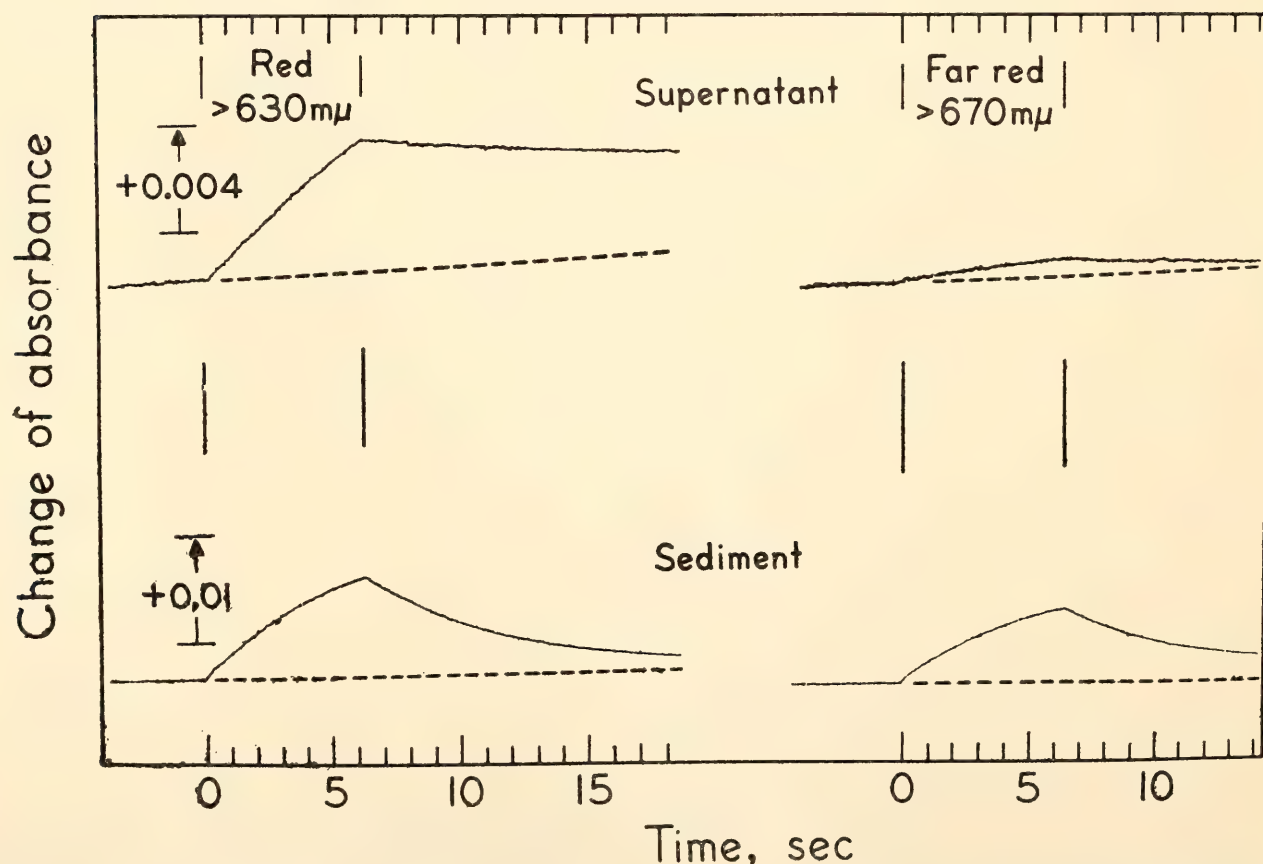


Fig. 5. Absorbance changes at 518  $m\mu$  in the supernatant layer and sediment without electron carriers induced by red plus far-red ( $> 630 m\mu$ ) and far-red ( $> 670 m\mu$ ) light.

with a rate of rise more than  $10^{-1}$  OD  $\text{sec}^{-1}$  (Fig. 6). Sometimes the two types of changes occurred simultaneously but they can be distinguished because of their different rates. Since these changes are probably caused by different substances or reactions, we will consider them separately.

Only slow increases in absorbance at  $518\text{ m}\mu$  in the fractions were observed before the addition of electron donors and acceptors (Fig. 5). The failure of the supernatant to respond to far-red actinic light correlates with its lack of absorption beyond  $700\text{ m}\mu$  (144,000g sediment, Fig.

3). That the sediment contained about twice as much chlorophyll per milliliter as the supernatant may account for the greater response of the sediment. Since similar slow absorbance increases were observed at  $518\text{ m}\mu$ ,  $591\text{ m}\mu$ , and  $419\text{ m}\mu$  in both fractions, this type of change is probably nonspecific with respect to wavelength.

After the mixture of ascorbate, DAD, TPN, ferredoxin, and the colorless soluble cell extract was added to each fraction, the slow absorbance increase shown by the supernatant layer practically disappeared (Fig. 6, upper traces) and that

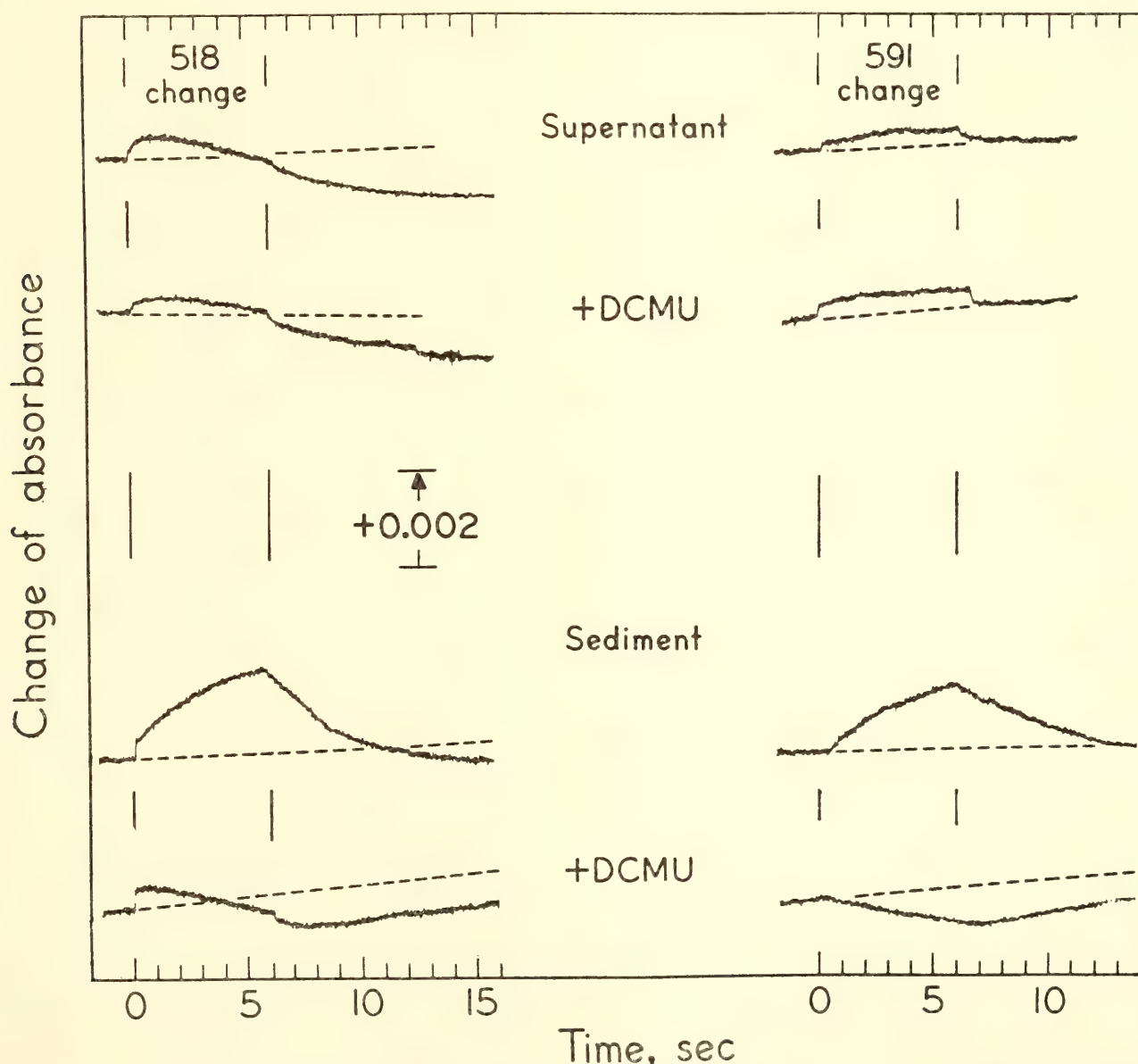


Fig. 6. Absorbance changes at  $518\text{ m}\mu$  and  $591\text{ m}\mu$  induced by red plus far-red light ( $> 630\text{ m}\mu$ ) in the supernatant and sediment fractions plus ascorbate, DAD, TPN, ferredoxin, and soluble cell extract before and after addition of DCMU.



of the sediment was much reduced (Fig. 6, lower traces). The further addition of DCMU to the sediment completely blocked the slow absorbance increase at 518  $m\mu$  as well as at 591  $m\mu$  (Fig. 6, lower traces). Packer (1963) has related photo-induced slow changes in the light-scattering of chloroplast fragments to phosphorylation coupled with electron transport. It seems highly probable that our light-induced, slow, and nonspecific absorbance changes are also caused by activity of the electron transport chain because they are inhibited by DCMU and also by salicylaldoxime.

The second type of more specific, rapid absorbance change occurred at 518  $m\mu$  and 591  $m\mu$  in our extracts only after the addition of electron donors and acceptors. Examples of this type can be seen in Fig. 6. The rapid increase in absorbance at 518  $m\mu$  was observed in both fractions but especially in the sediment. That it is small in our fractions as compared to known changes at 518  $m\mu$  in vivo probably results from nonoptimal concentrations and types of electron carriers.

DCMU did not inhibit the rapid 518- $m\mu$  change in either fraction because the DAD + ascorbate system, which was already present, supplied electrons after the DCMU block of the second light reaction, as described by Fork and Urbach in another section.

In contrast to these results at 518  $m\mu$ , the rapid change at 591  $m\mu$  was observed in the supernatant but not in the sediment after the addition of electron carriers. DCMU again did not inhibit the rapid 591- $m\mu$  change in the supernatant fraction but replaced the slow increase of absorbance in the sediment by a slow decrease. The fast 591- $m\mu$  change has been correlated by Fork, de Kouchkovsky, and Urbach, with the oxidation and reduction of plastocyanin. In algae this change can be inhibited by DCMU and restored by subsequent addition of DAD + ascorbate. Since DAD + ascorbate were already present in our extract mixtures, it was again expected that DCMU would

not inhibit the rapid changes. By contrast, the copper-chelating agent salicylaldoxime inhibited the 591- $m\mu$  plastocyanin change in the supernatant, and this type of inhibition cannot be overcome by DAD + ascorbate. The contrasting effect of DCMU on the rapid and on the slow absorbance changes demonstrates that they probably result from different chemical reactions. More specifically, the part of the electron transport chain that can receive electrons from DAD + ascorbate and not be inhibited by DCMU contributes to the rapid changes, and another part that is inhibited by DCMU causes the slow changes.

The fractional separation of chlorophyll-*a* forms from an aqueous *Euglena* extract treated with sodium deoxycholate also separated intermediates or different functioning parts, or both, of the electron transport chain. The particularly striking difference between the fractions was found in the 591- $m\mu$  absorbance change, where the fast change, attributed to plastocyanin, was only present in the supernatant and not in the sediment. With the donor system DAD + ascorbate present the change was not influenced by DCMU. The slow absorbance change was visible only in the sediment and was sensitive to DCMU. The rapid 518- $m\mu$  change, probably partially connected with system I, was observed in both fractions and was also insensitive to DCMU. The participation of two pigment systems in the 518- $m\mu$  change is discussed by Fork and Urbach in another section. The supernatant fraction did not respond to far-red light ( $> 670 m\mu$ ) because of the low absorption of  $C_{670}$ , predominant in this fraction.

These measurements of absorbance changes have contributed in several ways to our knowledge of the photochemical activity of the chlorophyll forms. We now know that it is possible, even in the presence of deoxycholate, to prepare very small chloroplast particles which still exhibit photo-induced absorbance changes. In addition, the particles will



perform other kinds of photochemical activity with electron donors and acceptors. Centrifugal fractions of the detergent-treated particles containing different proportions of the absorbing forms of chlorophyll *a* and chlorophyll *b* respond to actinic light in a manner correlated with their chlorophyll absorption. The responses of the two fractions are themselves different, indicating that a partial separation of portions of the electron-transport apparatus of photosynthesis has also taken place.

SEPARATE ACTION SPECTRA  
FOR THE PHOTOCHEMICAL SYSTEMS  
OF PHOTOSYNTHESIS

William Vidaver

*Contrasting effects of light on the photochemical systems.* Continuous far-red light produces different responses in algae that have been exposed to various treatments. In the green marine alga *Ulva* there is a constant O<sub>2</sub> evolution without pretreatment, a single O<sub>2</sub> uptake transient in tissue treated with DCMU, and a constant O<sub>2</sub> uptake after the alga has been exposed to high concentrations of O<sub>2</sub>. Shorter wavelength light superimposed on the far-red may increase O<sub>2</sub> production in the untreated tissue. It may have no effect on the alga treated with DCMU, and may induce in *Ulva*, after exposure to high O<sub>2</sub> tension, an O<sub>2</sub> evolution which competes with continuous O<sub>2</sub> uptake.

With the use of these effects, action spectra have been recorded that are believed to represent the two photochemical systems of photosynthesis in *Ulva*. Oxygen exchange was measured polarographically using a bare platinum electrode, a gassing system, and the recording action-spectrophotometer, all of which have been described previously.

A spectrum for system I was obtained by recording peak transient rates of O<sub>2</sub> uptake resulting from flashes of monochromatic light. Action spectra that may represent system I activity have been previously reported by this laboratory

(*Year Books* 60, p. 355; 62, p. 360; 63, p. 458). The spectrum for system II is from the measurement of continuous rates of O<sub>2</sub> evolution after a treatment that apparently replaced the functioning of system I.

*The spectrum for system I.* The transient O<sub>2</sub> uptake (*Year Book* 63, p. 453) saturates at lower light intensities than does O<sub>2</sub> evolution and is presumed to be mediated by system I. The spectrum for this uptake was obtained with *Ulva* treated with DCMU, which inhibits system II activity and suppresses O<sub>2</sub> production. Monochromatic light flashes of equal incident quanta per second were given at wavelength intervals of 5 mμ or 10 mμ. Flash intensity was about 500 ergs cm<sup>-2</sup> sec<sup>-1</sup> at 680 mμ. The duration of the light flashes was just long enough to allow the record of the uptake transient to reach completion. Completion time for the transient was least at the activity peak, about 678 mμ. The transient amplitude from which the action spectrum was plotted varied with wavelength and also reached its maximum near 678 mμ. Furthermore, the amount of the photoreductant formed, as measured by the total uptake following a flash, also appeared to vary with wavelength.

The action spectrum for system I of DCMU-treated *Ulva* (middle curve of Fig. 7) has a maximum at 678 mμ that corresponds to the maximum absorption by chlorophyll *a*. A small shoulder at 650 mμ suggests some participation of chlorophyll *b*. There is some variation in activity with decreasing wavelength but no prominent peaks appear at wavelengths between 650 mμ and 470 mμ, the shortest wavelength used. Considerable activity persists at wavelengths longer than 700 mμ. Some O<sub>2</sub> uptake is detectable at 750 mμ despite the low intensity of the light.

Reasons for presuming that this spectrum represents primarily the light activation of system I are: (1) The spectrum results from photochemical activity not culminating in O<sub>2</sub> evolution.



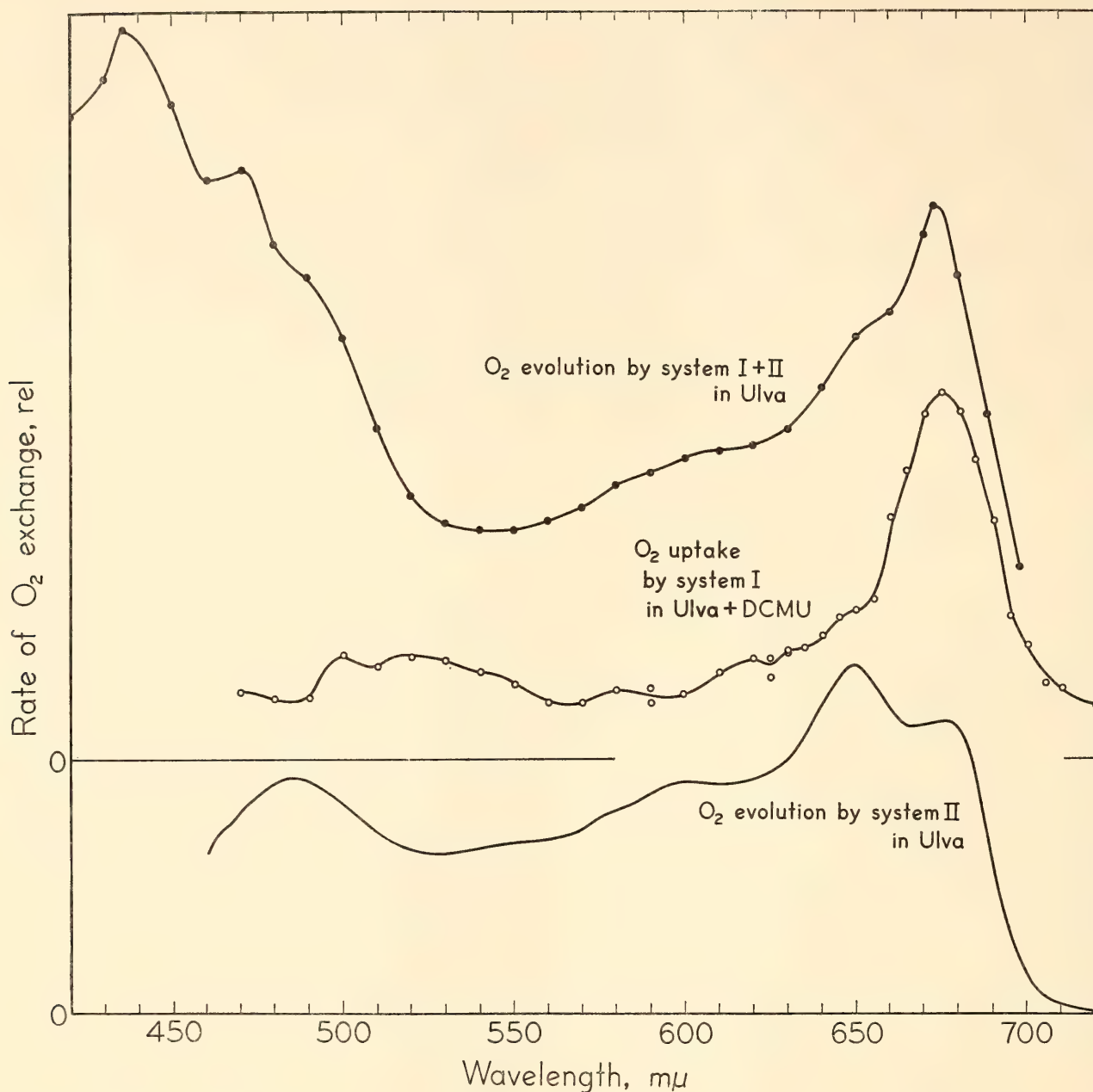


Fig. 7. Upper curve, action spectrum for O<sub>2</sub> evolution by *Ulva* (adapted from Haxo and Blinks, 1950). Middle curve, action spectrum for transient O<sub>2</sub> uptake obtained with 10<sup>-4</sup> M DCMU (system I). Lower curve, action spectrum for O<sub>2</sub> evolution after treatment with high O<sub>2</sub> tension (system II). Monochromatic light at different wavelengths was superimposed on constant 729-mμ illumination.

On the contrary, O<sub>2</sub> is consumed upon illumination. (2) Since DCMU suppresses O<sub>2</sub> production it is believed to inhibit system II activity. At concentrations that completely block O<sub>2</sub> evolution this inhibitor does not decrease the light-induced O<sub>2</sub> uptake. (3) Photoreductions and photophosphorylations presumed to be associated with system I have been reported to proceed at wavelengths longer than 700 mμ with light intensities that do

not induce O<sub>2</sub> production, or in partially isolated photosynthetic systems that do not evolve O<sub>2</sub>. The action spectrum shown here extends well into the far-red even though light intensity was very low. (4) A large portion of the action spectrum coincides well with the absorption spectrum of chloroplast preparations believed to be enriched for the system I fraction.

*The spectrum for system II.* After *Ulva* was treated for several hours in the dark

in an atmosphere of 50 per cent  $O_2$  and returned to air, it absorbed  $O_2$  continuously in light of any wavelength. The action spectrum (not shown in the figure) for this uptake had minima at  $650\text{ m}\mu$  and  $680\text{ m}\mu$ , probably because of competing  $O_2$  evolution.

The action spectrum for system II was obtained with *Ulva* treated in the same way using monochromatic light superimposed on a beam of far-red light having a peak wavelength of  $729\text{ m}\mu$  and an intensity of  $10^5\text{ ergs cm}^{-2}\text{ sec}^{-1}$ . The far-red beam, isolated with interference filters, induced the constant maximum rate of  $O_2$  uptake. The visible spectrum was swept with light from the monochromator using equal incident quanta per second and an intensity of about  $500\text{ ergs cm}^{-2}\text{ sec}^{-1}$  at  $680\text{ m}\mu$ . The action spectrum for  $O_2$  evolution by system II (Fig. 7, lower curve) results from a measured decrease in the rate of  $O_2$  uptake induced by light with wavelengths shorter than  $730\text{ m}\mu$ . It has a main activity peak at  $650\text{ m}\mu$ , a large shoulder corresponding to chlorophyll *a* absorption near  $680\text{ m}\mu$ , and another smaller peak near  $480\text{ m}\mu$ . The  $650\text{-m}\mu$  and  $480\text{-m}\mu$  peaks indicate the functioning of chlorophyll *b*. Accessory pigments, including chlorophyll *b*, are believed to function in system II and to be closely related to  $O_2$  production. In contrast to  $O_2$  uptake,  $O_2$  evolution under these conditions does not extend appreciably into the far-red. Beyond  $720\text{ m}\mu$  no  $O_2$  evolution was detected from *Ulva* that had been treated with high  $O_2$  tension and had its  $O_2$  uptake saturated with far-red light.

Decreased uptake in the combined beams can in principle result from one of two causes: either light induces inhibition of the uptake or stimulates competing  $O_2$  evolution. Acceptance of light-induced inhibition of the uptake as the explanation assumes that light can stimulate uptake in one instance (activity peak  $678\text{ m}\mu$  with DCMU-treated *Ulva*) and suppress the uptake at the same wave-

length in the tissue treated with high  $O_2$  tension. Competitive  $O_2$  uptake and evolution therefore appear to be a simpler and a preferable explanation.

The action spectra and kinetics for the two types of  $O_2$  exchange discussed here (uptake and evolution) are strikingly different and presumably result from the separate functions of the photochemical systems. If these responses do represent the individual systems, the action spectrum for sustained  $O_2$  evolution by untreated *Ulva* (upper curve, Fig. 7) should be a function of the sum of the separate spectra. This possibility is being explored.

#### LOCALIZATION OF PLASTOCYANIN IN THE ELECTRON-TRANSPORT CHAIN OF PHOTOSYNTHESIS IN RELATION TO CYTOCHROME *f* AND COMPONENTS PRODUCING THE $518\text{-m}\mu$ ABSORBANCE CHANGE

*David C. Fork and Wolfgang Urbach*

As a result of previous study (*Year Book 63*, p. 453), reversible light-induced absorbance changes at  $591\text{ m}\mu$  in green plants have been attributed to variations in the redox state of the copper-containing protein plastocyanin. An increase of absorbance at  $591\text{ m}\mu$  was linked to oxidation and a decrease to reduction of plastocyanin. In *Ulva* the excitation of system I with far-red light led to oxidation of plastocyanin. It was found that the dark decay that took place afterward (reduction) could be accelerated if red background light (absorbed by system II) was provided. This antagonistic effect of red and far-red light on the  $591\text{-m}\mu$  absorbance change led to the suggestion that plastocyanin probably functions as a component in the electron-transport chain between the two light reactions of photosynthesis, described later (Fig. 15).

In this study we attempted to localize the  $591\text{-m}\mu$  absorbance change more precisely. Because cytochrome *f* has been shown to operate between the two light



reactions, we studied the relation between the plastocyanin change and that of cytochrome *f* (419 m $\mu$ ). Results indicated that plastocyanin functions in the electron-transport chain after system II and before cytochrome *f*.

It is generally thought that the 518-m $\mu$  absorbance change is related to the functioning of system II. In many schemes of electron transport the 518-m $\mu$  absorbance change, like the plastocyanin change, is also put after system II and before cytochrome *f*. For this reason we investigated under identical experimental conditions the interrelation of the 518-m $\mu$  absorbance change and the 591-m $\mu$  (plastocyanin) absorbance change. The results showed that only part of the 518-m $\mu$  change is associated with system II; some of it must be associated with system I.

#### *Materials and Methods*

The *Chlorella pyrenoidosa* (Pringsheim 211/8b) used in these experiments was grown at 30°C in a completely synchronous culture in N5 medium according to Ried *et al.* (1963). A 16-hour light and 8-hour dark schedule was used. Young, recently divided cells were harvested about one hour after the start of the light period. They were kept in the dark, aerated with 5 per cent CO<sub>2</sub> in air, for at least three hours before the start of an experiment. Cells so treated did not grow, but remained "young," and exhibited reproducible absorbance changes for many hours, and in following experiments. A 5-ml aliquot of the algal suspension ( $7.5 \times 10^7$  cells/ml, 7.5  $\mu$ g chlorophyll/ml) was used in an open cuvette and inside a closed chamber, and it produced a path length of about 5 mm. A stream of 5 per cent CO<sub>2</sub> in air passed over the cells during the experiments, performed at about 20°C.

Light-induced changes of absorbance were measured as in previous work (Year Book 63, pp. 435-441). The changes were recorded on a Massa oscillographic recorder, model BSA-250A.

System I of photosynthesis was excited preferentially with monochromatic far-red light (716 m $\mu$ , half-bandwidth 12 m $\mu$ ); systems I and II with red light (668 m $\mu$ , half-bandwidth 10 m $\mu$ ). The intensities of the far-red and red beams were 4.10 and  $2.94 \times 10^{-8}$  einstein cm<sup>-2</sup> sec<sup>-1</sup>, respectively.

*The effect of salicylaldoxime on the 591-m $\mu$  and the 419-m $\mu$  absorbance changes.* The upper traces of Fig. 8 (A, A') show the 591-m $\mu$  (plastocyanin) absorbance changes observed in untreated *Chlorella* in far-red or in red actinic light. The changes (to be described) are different from and more complex than those described previously for *Ulua*. In far-red light a transient decrease of absorbance (reduction) is followed by an increase in absorbance (oxidation), which becomes constant in the light after six seconds. In red light the changes were similar but larger. The kinetics of the decay of the 591-m $\mu$  absorbance change after a red exposure is biphasic (seen more clearly in Fig. 12, A'). Analysis of this decay curve showed a fast ( $t_{1/2} \cong 0.05$  sec) and a slow component ( $t_{1/2} \cong 3.9$  sec), both decays following first-order (or pseudo first-order) kinetics. Although it does not appear so clearly here as it does with the 668-m $\mu$  exposure, the decay in the untreated material after 716-m $\mu$  actinic light is similarly biphasic and also consists of a fast ( $t_{1/2} \cong 0.23$  sec) and a slow ( $t_{1/2} \cong 1.75$  sec) component both following first-order kinetics.

Incubation of *Chlorella* in  $10^{-2}$  M salicylaldoxime for about 15 minutes inhibited plastocyanin oxidation but left a slow and smaller reduction at both wavelengths (Fig. 8, B, B').

The sample that produced the traces for Fig. 8 was also used for a comparison of the effect of salicylaldoxime on the 419-m $\mu$  (cytochrome *f*) absorbance change. The upper traces of Fig. 9 (A, A') show the changes produced before addition of the inhibitor. Far-red light (system I) produced predominantly oxidation (decrease of absorbance) of cytochrome *f*.

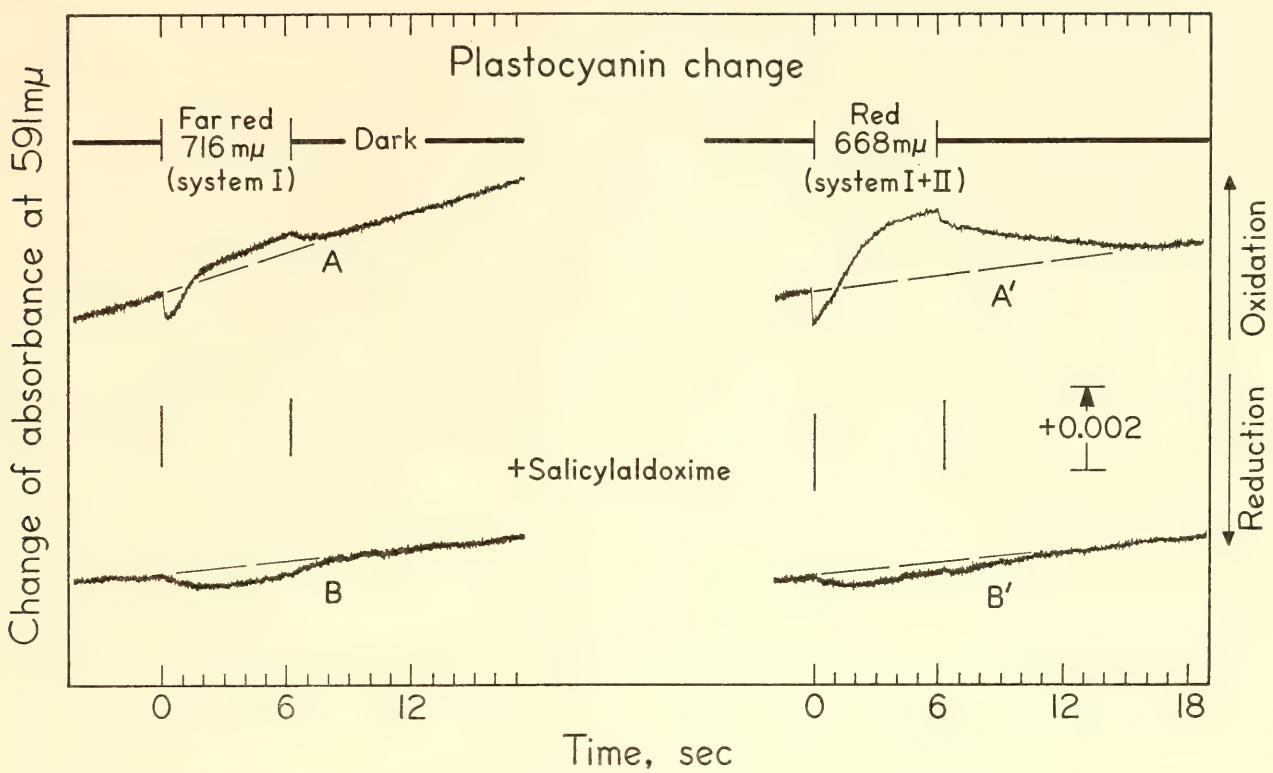


Fig. 8. Effect on 591-m $\mu$  absorbance change in *Chlorella* after a short incubation in 10<sup>-2</sup> M salicylaldoxime. The red exposure (B') was made 13.9 min after adding salicylaldoxime and the far-red (B) after 15.4 min.

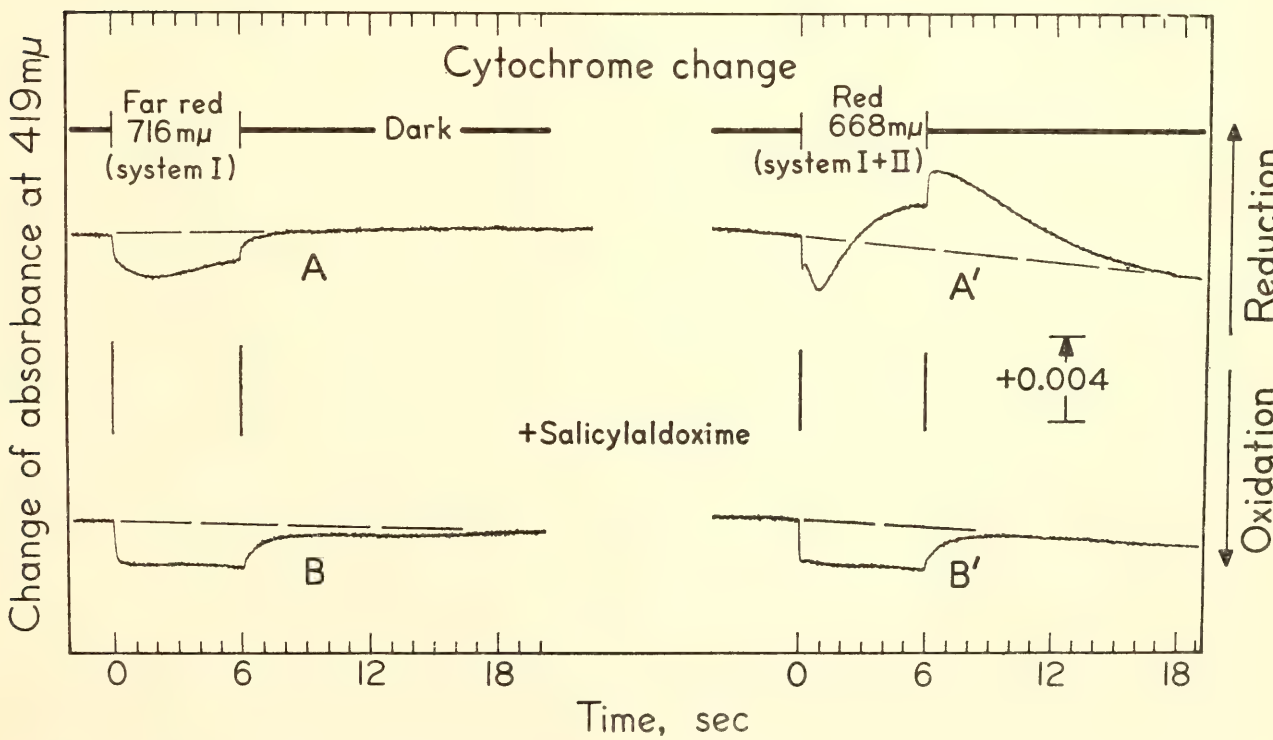


Fig. 9. Effect on 419-m $\mu$  absorbance change in *Chlorella* after short incubation in 10<sup>-2</sup> M salicylaldoxime. Exposure to red light (B') was made 28.6 min after adding salicylaldoxime and to far-red (B) after 30.4 min. Same sample of *Chlorella* produced traces in Figs. 8 and 9.



Red light (systems I and II), by contrast, produced initially an oxidation of cytochrome—with a transient—which was soon followed by reduction during the light. The red exposure produced a net reduction of cytochrome which became constant after six seconds. Dark reduction of cytochrome after red light was much faster than after far-red. This fast reduction in the dark after a red exposure was then followed by a slow oxidation of the cytochrome to its former dark level.

Short incubation in salicylaldehyde inhibited cytochrome reduction. After treatment the *Chlorella* produced only an oxidation of cytochrome in either wavelength (Fig. 9, B, B'). The dark reductions were slowed about equally after actinic light of either wavelength. The cyto-

chrome oxidation transient in red light was completely eliminated.

*The effect of salicylaldehyde on the 518-m $\mu$  absorbance change.* Figure 10 (A, A') shows the 518-m $\mu$  change produced in far-red and red light. Typical complex time courses for the 518-m $\mu$  change are shown. Far-red light induced a smaller 518-m $\mu$  change than did red light. The intensities of both wavelengths were near saturating for this change (Fig. 11, curves for untreated cells). Incubation in  $10^{-2}$  M salicylaldehyde for about one minute inhibited the 518-m $\mu$  change more in red than in far-red light (Fig. 10, B, B'). An unexpected result was that a longer incubation in salicylaldehyde increased the 518-m $\mu$  change (Fig. 10, C, C'). In this condition either red or far-

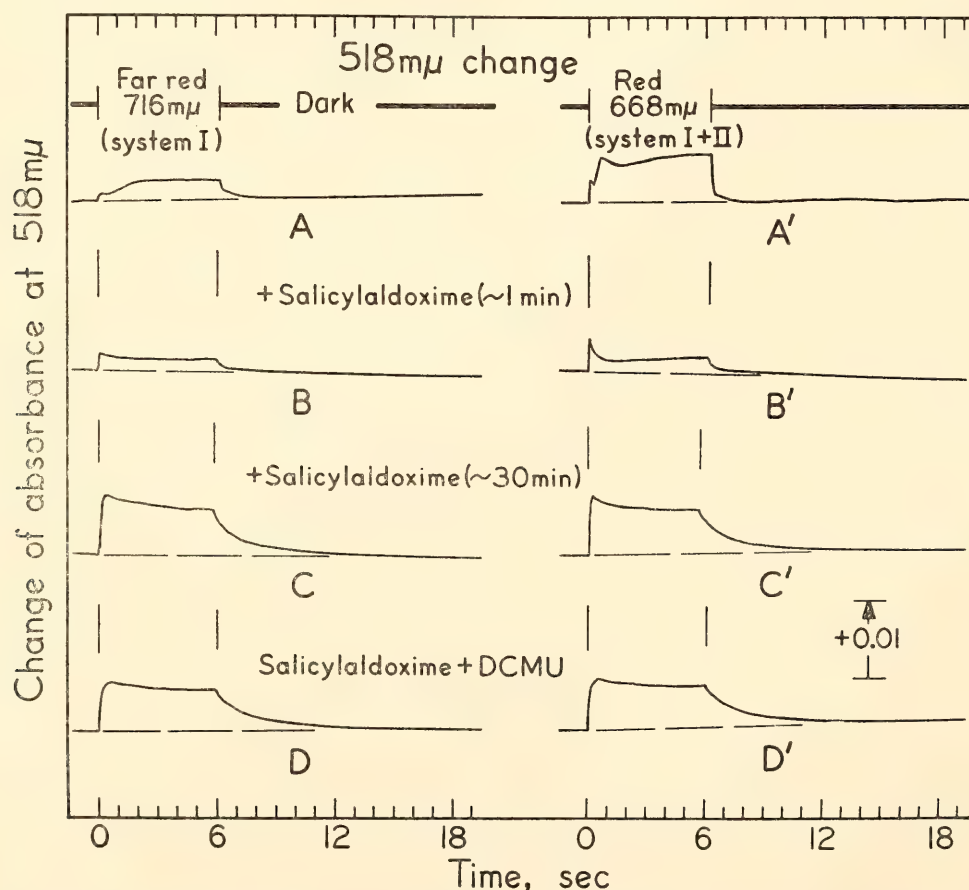


Fig. 10. Effect on 518-m $\mu$  absorbance change in *Chlorella* of a 1-min and of a 30-min incubation in salicylaldehyde and of salicylaldehyde plus DCMU. Exposures to far-red were made 1.7 min (B) and 26.0 min (C) after adding salicylaldehyde. Exposures to red were made 0.8 (B') and 27.3 (C') min after adding salicylaldehyde for the second and third traces, respectively. After the *Chlorella* had been in salicylaldehyde for 54 min, DCMU was added at  $5 \times 10^{-5}$  M. The 716-m $\mu$  exposure was then made 3.9 min after addition of DCMU (D) and the 668-m $\mu$  exposure after 6.8 min (D').

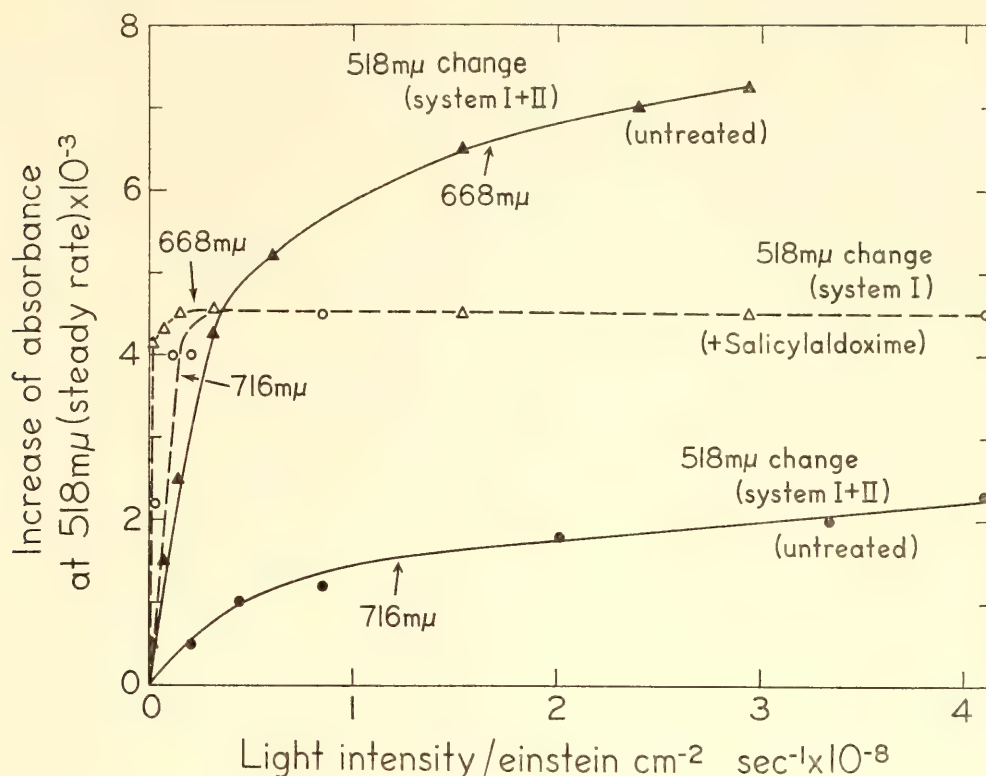


Fig. 11. Dependence of the steady-state 518-m $\mu$  absorbance change on intensity of red and of far-red light before and after treatment of *Chlorella* with  $10^{-2}$  M salicylaldoxime.

red light produced about the same amount of change, and the time courses were very different from those for the untreated cells. This 518-m $\mu$  change in salicylaldoxime-treated *Chlorella* saturated at much lower intensities of either wavelength than the untreated material (Fig. 11). DCMU now had no effect on the salicylaldoxime-stimulated 518-m $\mu$  absorbance change (Fig. 10, D, D') although it always partially inhibited the change in normal material (compare Fig. 14 B, B').

*Inhibition by DCMU of the 591-m $\mu$  absorbance change and its restoration by DAD and ascorbate.* Figure 12 (B, B') shows that DCMU at a concentration of  $5 \times 10^{-5}$  M completely inhibited the 591-m $\mu$  change in both red and far-red actinic light. Light-induced oxidation of plastocyanin was partly restored by the addition of a catalytic amount of 2,3,5,6-tetramethyl-*p*-phenylenediamine (DAD, kindly furnished by Professor A. Trebst) and a substrate amount of sodium ascorbate (Fig. 12, C, C'). The steady-

state change induced by both wavelengths was now the same ( $\Delta A = 5 \times 10^{-4}$ ) but showed large differences before treatment. The initial decrease of absorbance seen previously in 716- or 668-m $\mu$  light was absent. The dark decays after both wavelengths were now equal and followed first-order kinetics; both had a  $t_{1/2} = 0.2$  second.

*The effects of DCMU and DAD + ascorbate on the 419-m $\mu$  cytochrome change.* Figure 13 compares the effect of  $5 \times 10^{-5}$  M DCMU on the cytochrome change in the sample of *Chlorella* that was used for Fig. 12. After addition of the inhibitor, the fast oxidation produced immediately in far-red and red light was hardly influenced, but the subsequent transients were distinctly suppressed in both actinic lights (Fig. 13, B, B').

The light-driven reduction of cytochrome in red light was strongly inhibited by DCMU. The decay after red light (B') was much slower and resembled the decay after far-red (B). DAD and ascorbate regenerated the cytochrome reduction



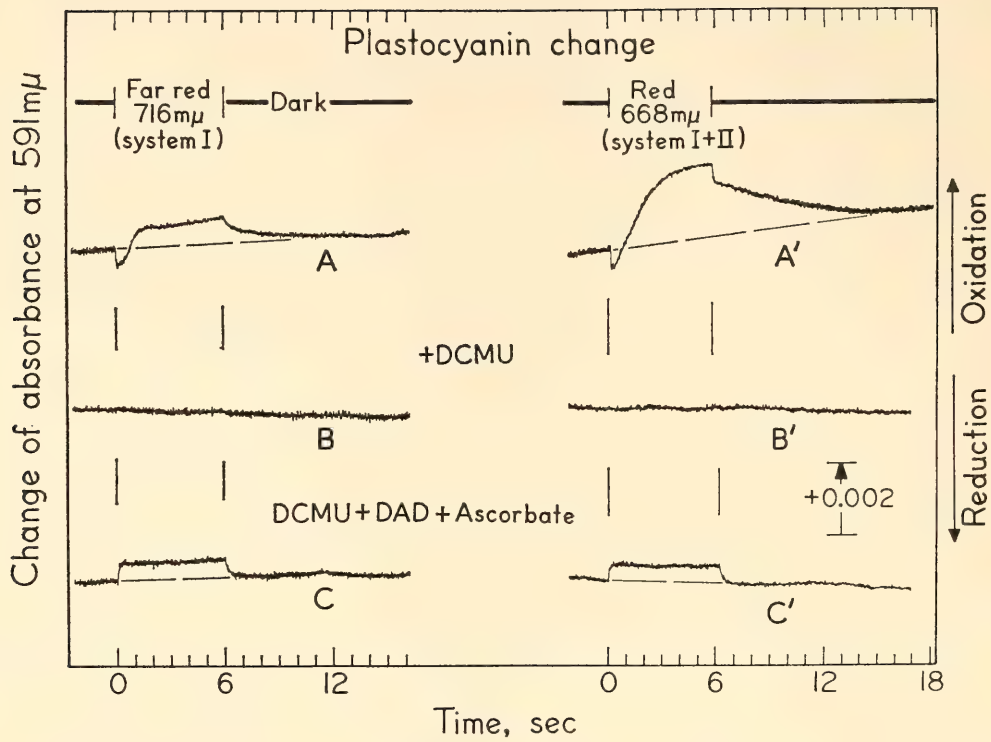


Fig. 12. Inhibition of the 591-mμ absorbance change in *Chlorella* by DCMU and its partial restoration by DAD + ascorbate. DCMU was added to a concentration of  $5 \times 10^{-5} M$ . Concentration of DAD was  $6.6 \times 10^{-5} M$  and of sodium ascorbate about  $5 \times 10^{-3} M$ . The *Chlorella* was in DAD + ascorbate about 10 min before turning on either actinic light.

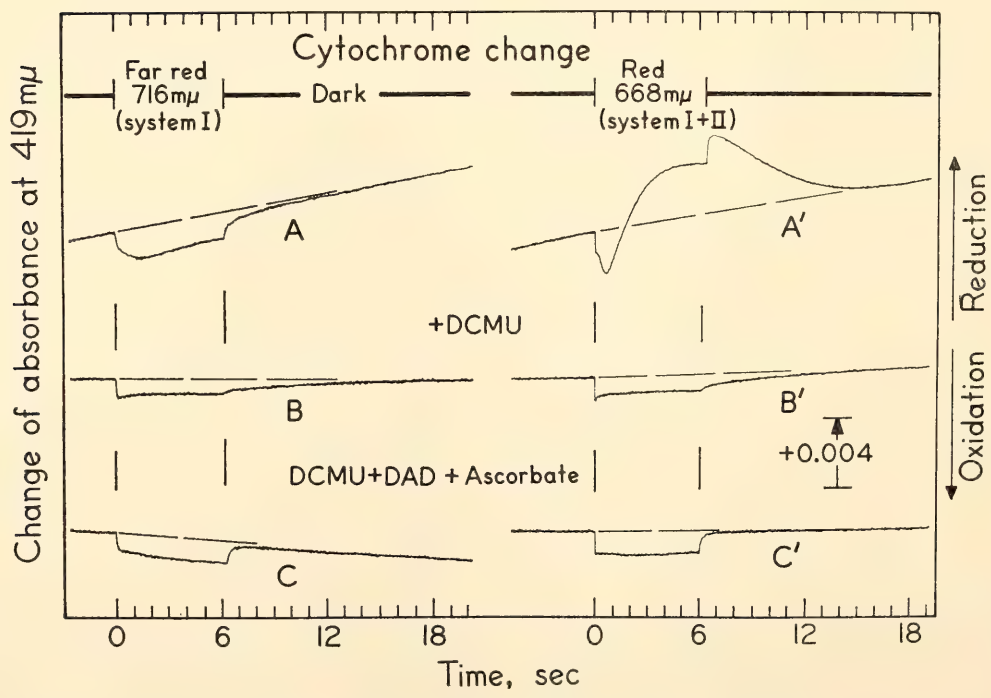


Fig. 13. Effect of DCMU and DAD + ascorbate on 419-mμ absorbance change in *Chlorella*. Same concentrations of DCMU, DAD, and ascorbate, and same sample as in Fig. 12.

(decay) after exposures but did not regenerate the light-driven reduction (Fig. 13, C, C'). The dark-decay times after exposure to both wavelengths were now about the same.

The effects of DCMU and DAD + ascorbate on the 518-m $\mu$  absorbance change. The sample used for Figs. 12 and 13 was also used to investigate the effects of DAD + ascorbate on the 518-m $\mu$  change in DCMU-treated *Chlorella*. The effects of  $5 \times 10^{-5}$  M DCMU on the 518-m $\mu$  change can be seen by comparing curves A and A' with B and B' of Fig. 14. The initial peak was higher at both wavelengths in the DCMU-treated *Chlorella*. The second, slower transient and the steady-state change were inhibited. The dark decay after either wavelength was greatly slowed by DCMU. Last year's report (Year Book 63, p. 446) gives a similar result for the 518-m $\mu$  change for the green alga *Ulva lobata*.

### Discussion

Many of the results observed in these experiments can be explained if we accept the Hill-Bendall type of scheme for photosynthesis with components arranged as shown in Fig. 15.

The observation that the 591-m $\mu$  change decays by first-order (or pseudo first-order) reactions suggests that plastocyanin is reduced in the dark via a large pool of a reduced substance. This pool may be provided by a plastoquinone (PQ in Fig. 15) which may also be responsible for the oxygen burst seen in chloroplasts lacking an added Hill oxidant (Year Book 61, p. 334). The decay of the 591-m $\mu$  change after two different first-order reactions suggests that either another substance or a different species of plastocyanin is producing the slower, larger 591-m $\mu$  change seen clearly in red light. In any case, salicylaldehyde sup-

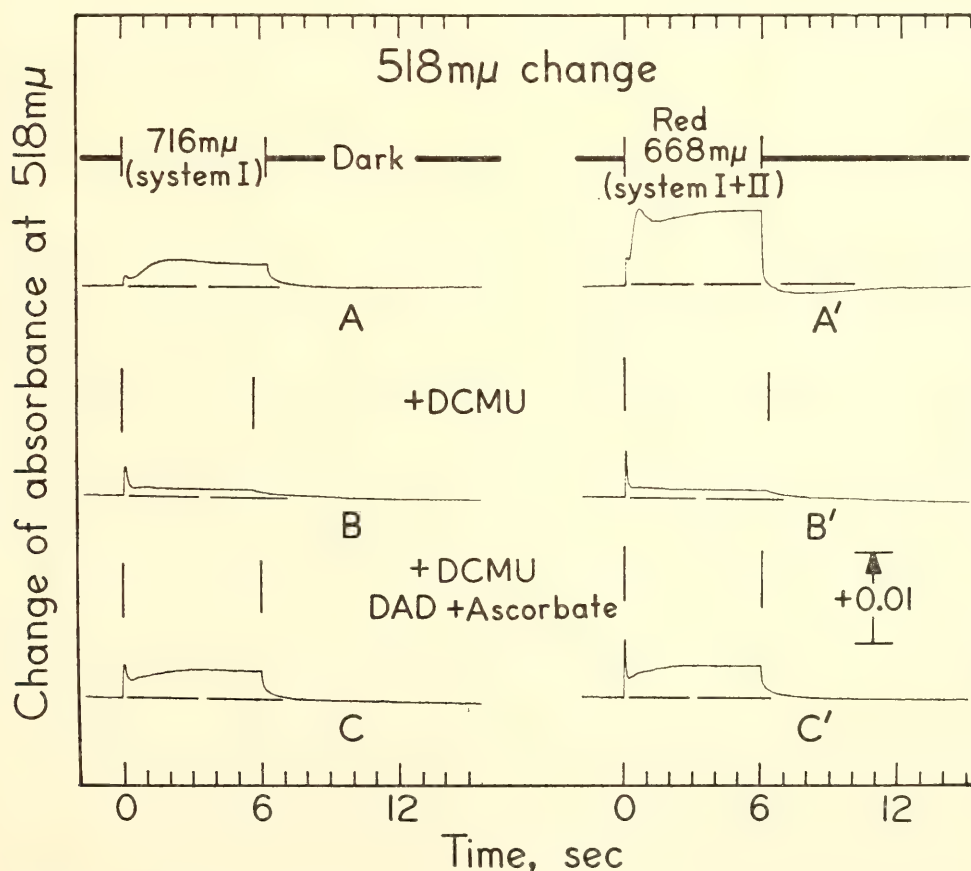


Fig. 14. Effect of DCMU and DAD + ascorbate on the 518-m $\mu$  absorbance change in *Chlorella*. Same concentrations of DCMU, DAD, and ascorbate, and same sample as in Fig. 12.



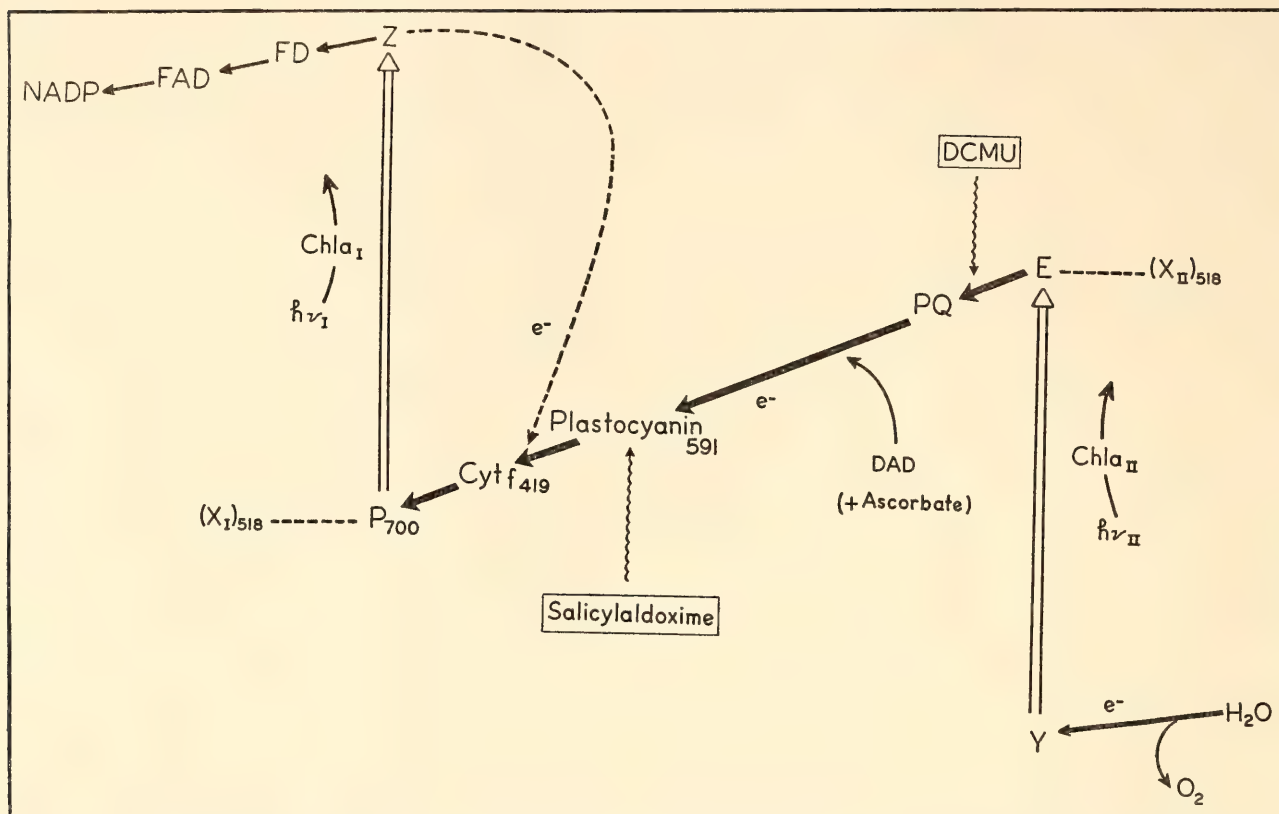


Fig. 15. Hill-Bendall type of diagram for photosynthesis to show presumed site of plastocyanin function in the electron-transport chain in relation to the cytochrome-*f* (419-m $\mu$ ) change and the compounds ( $X_I$  and  $X_{II}$ ) responsible for the 518-m $\mu$  changes. *PQ*, plastoquinone; *E*, (Duysens' "Quencher"), electron acceptor for the second light reaction; *Z*, acceptor for the first light reaction; *Y*, oxidized photo-product of system II. Unshaded arrows indicate light reactions; other arrows, dark reactions.

pressed both the fast and the slow components.

This inhibition by the copper-complexing reagent, salicylaldoxime, seems to be specific for the plastocyanin change. It did not inhibit cytochrome oxidation. Inhibition of plastocyanin oxidation by salicylaldoxime gave a parallel inhibition of light-dependent cytochrome reduction mediated by system II. This observation makes it reasonable to place plastocyanin before cytochrome *f* in the flow of electrons coming from the second light reaction (Fig. 15) rather than in a side position.

Since plastocyanin oxidation appears to follow from excitation of system I, it was not expected that DCMU would have any effect because it is a specific inhibitor of  $O_2$  evolution mediated by system II. The inhibition of the plastocyanin change by

DCMU may have occurred because plastocyanin oxidation can only be observed if the substance is first reduced. The reduction normally becomes possible by the presence of electrons made available by the action of system II. DCMU interrupts the reduction and in turn abolishes the plastocyanin change. The inhibiting effect of DCMU on plastocyanin oxidation appears to be an indirect one. Thus the DCMU-inhibited plastocyanin oxidation was partly regenerated after addition of the electron-donor system, DAD + ascorbate, because DAD catalyzed the reduction of plastocyanin by ascorbate.

The partial regeneration of plastocyanin oxidation by the donor system was paralleled by a regeneration of the fast dark reduction of cytochrome. This partial regeneration of the plastocyanin

and cytochrome absorbance changes by the donor system after DCMU had prevented electron flow from light reaction II suggests that electrons were feeding into the chain from ascorbate via DAD at some site after the second light reaction but before plastocyanin as shown in Fig. 15. The suggestion is supported by these observations: a disappearance of the initial transient reduction of plastocyanin; the red-light-driven reduction of cytochrome; and the regeneration of only light-dependent plastocyanin oxidation.

In untreated material the rapid component of plastocyanin reduction in the dark was faster after red (more system II excitation) than after far-red. But when DAD + ascorbate served as a substitute electron source for system II, the dark decays were the same in both cases. This chemical reduction of plastocyanin proceeded by first-order kinetics because ascorbate was present in great excess.

It is interesting to note that only the rapid component of the 591-m $\mu$  change was regenerated by DAD + ascorbate. The large, slow change seen especially clearly in red light was absent in the regenerated condition. The nature of this slow component is not yet clear.

The observation of a 518-m $\mu$  spike, which is higher with DCMU in either red or far-red actinic light, can be accounted for if DCMU does not interfere with the photochemical functioning of system II, but rather prevents electron transfer from the primary acceptor (*E*) of the second light reaction to a substance such as plastoquinone (Fig. 15). Joliot and de Kouchkovsky recently found that *E* is present in an amount 10 to 20 times less than the compound causing the O<sub>2</sub> burst of chloroplasts without added Hill oxidants. Duysens has already postulated this site of DCMU inhibition on the basis of fluorescence and other studies. A block at this site would account for slowing of the decay of the 518-m $\mu$  absorbance change by DCMU (Fig. 14, *B*, *B'* and *Year Book 63*, p. 446).

Partial regeneration of both the plasto-

cyanin and cytochrome changes by DAD + ascorbate was also paralleled by partial regeneration of the 518-m $\mu$  absorbance change. The above observations suggest that only system I is functioning after DCMU-treated *Chlorella* is regenerated by DAD + ascorbate. If we apply this idea to the results obtained with the 518-m $\mu$  absorbance change we must conclude that the regenerated portion of the change is associated with system I. (The association of the 518-m $\mu$  change with system II was discussed in *Year Book 62*, p. 357.) Assignment of part of the 518-m $\mu$  change to system I appears justified because either red or far-red actinic illumination produced equal steady-state 518-m $\mu$  changes in *Chlorella* regenerated with DAD + ascorbate (Fig. 14, *C*, *C'*). In addition, the prolonged treatment of *Chlorella* with salicylaldoxime produced a stimulation of the 518-m $\mu$  absorbance change that was the same in either red or far-red actinic light. Moreover, the kinetics of the change at either wavelength were identical and were very different from those seen before treatment. It appears that the steady-state 518-m $\mu$  absorbance change is a reflection of the activity of system I alone, because salicylaldoxime inhibits plastocyanin function and blocks electrons coming from system II. In addition, the salicylaldoxime-stimulated 518-m $\mu$  change was unaffected by DCMU.

A further indication that this 518-m $\mu$  change is associated with system I is the early saturation of the change in salicylaldoxime-treated material (Fig. 11). Evidence reported in previous *Year Books* shows that system I saturates at lower light intensities than does system II. The steady-state 518-m $\mu$  absorbance change seen in salicylaldoxime-treated *Chlorella* suggests that a cyclic flow of electrons enters the transport chain after plastocyanin, which is blocked by this inhibitor and can no longer transfer electrons originating in water.

The acceleration of the decay of the 518-m $\mu$  absorbance change in the presence



of DCMU and DAD + ascorbate is difficult to understand. Evidence has accumulated to show that this decay is related to an oxidation; therefore DAD + ascorbate should slow the decay, not accelerate it. We can understand the accelerated decay of the 518-m $\mu$  change by the DAD system if we assume that the change appears simultaneously with oxidation of a pigment in system I ( $P_{700}$ ?).

### Summary

The reversible light-induced absorbance change at 591 m $\mu$ , which reflects changes in the redox state of the copper-containing protein, plastocyanin, has been studied in conjunction with the cytochrome-*f* change at 419 m $\mu$ . The results suggest that plastocyanin functions in the electron-transport chain of photosynthesis and before cytochrome *f*.

The 518-m $\mu$  absorbance change was also studied in relation to the cytochrome-*f* and plastocyanin changes. Only part of the 518-m $\mu$  change is associated with system II activity; another part appears to be related to functioning of system I.

### PARTIAL INHIBITION OF PHOTOSYNTHETIC-ELECTRON TRANSPORT BY LACK OF OXYGEN

Wolfgang Urbach and David C. Fork

Little is known about the involvement of oxygen ( $O_2$ ) in the electron-transport chain of photosynthesis. An examination of the interaction of  $O_2$  with components of the transport chain during photosynthesis has therefore been undertaken. The results lead to the conclusion that lack of  $O_2$  interrupts electron transport in photosynthesis, possibly by altering relative rates of noncyclic and cyclic electron flow.

### Materials and Methods

For these investigations *Chlorella pyrenoidosa* (Pringsheim 211/8b) was grown synchronously in N5 medium, and changes of absorbance were measured as described in the preceding report.

Far-red actinic light (716 m $\mu$ ) was used

to excite system I preferentially, and red light (668 m $\mu$ ) was used to excite both systems simultaneously. The intensities and spectral properties of these actinic wavelengths are described in the preceding section.

The intensity of the 419-m $\mu$  measuring beam was 200 ergs cm $^{-2}$  sec $^{-1}$  and of the 518-m $\mu$  beam, 169 ergs cm $^{-2}$  sec $^{-1}$ . The filter set for the 591-m $\mu$  measuring beam, consisting of Balzer Filtraflex DT (green) and Corning 3482, passed a wide spectral band of 42-m $\mu$  half-width with an intensity of 828 ergs cm $^{-2}$  sec $^{-1}$  at the *Chlorella* sample. To avoid interference by red excitation light, a Bausch & Lomb 591-m $\mu$  interference filter of about 10-m $\mu$  half-width and glass cutoff filters were placed between sample and photomultiplier.

A 5-ml aliquot of the *Chlorella* suspension (7.5  $\mu$ g chlorophyll/ml) was used in an open cuvette and placed in a closed chamber through which air or nitrogen ( $N_2$ ) + 5 per cent carbon dioxide ( $CO_2$ ) was passed.

Anaerobic studies on photosynthesis are difficult because  $O_2$  is evolved by the process. Measurements of absorbance changes require a weak measuring beam which itself causes some  $O_2$  evolution. It was found to be generally impossible to obtain sufficiently anaerobic conditions even with a strong flow of  $N_2$  + 5 per cent  $CO_2$  when the measuring beam illuminated the sample. To ensure anaerobiosis, complete darkness together with a strong stream of  $N_2$  + 5 per cent  $CO_2$  was necessary until just before measuring.

*Inhibition of light-induced cytochrome reduction by lack of  $O_2$  and its partial regeneration by DAD + ascorbate.* Figure 16 shows the effects of lack of  $O_2$  on the 419-m $\mu$  cytochrome-*f* change. Under aerobic conditions typical cytochrome changes (*A*, *A'*) were seen which were the same as those described in Fig. 9 (*A*, *A'*).

After the algal suspension had been gassed for 5–10 minutes with  $N_2$  + 5 per cent  $CO_2$  in the dark with the measuring beam off, there was a strong inhibition of light-driven reduction of

cytochrome mediated by system II, but only a small inhibitory effect on cytochrome oxidation. Anaerobically, the absorbance changes in either far-red or red actinic light showed almost the same time course (Fig. 16, *B*, *B'*). Anaerobic conditions also suppressed the oxidation transient in the light and slowed the dark decay after either wavelength.

The inhibiting effect of  $O_2$  deficiency could be observed only for the first light exposure after complete darkness in  $N_2 + 5$  per cent  $CO_2$ . Even the second exposure showed a different time course because of  $O_2$  produced during the first exposure. After 5 to 10 light exposures (still in  $N_2 + 5$  per cent  $CO_2$ ) the absorbance changes were similar to those observed in air. Anaerobic conditions

were maintained when DCMU, which prevents evolution of  $O_2$ , was added to the suspension gassed with  $N_2 + 5$  per cent  $CO_2$ . Subsequent addition of the electron-donor system DAD + ascorbate, which feeds electrons into the transport chain after system II and before plastocyanin (described in the preceding section) produced an acceleration of the dark reduction of cytochrome following a light exposure (Fig. 16, *C*, *C'*).

*Inhibition of plastocyanin oxidation in the light by lack of  $O_2$  and its partial regeneration by DAD + ascorbate.* Since it was concluded from the preceding section that plastocyanin functions after system II and before cytochrome *f*, the effect of  $O_2$  deficiency on the plastocyanin change was studied. In Fig. 17 (*A*, *A'* and

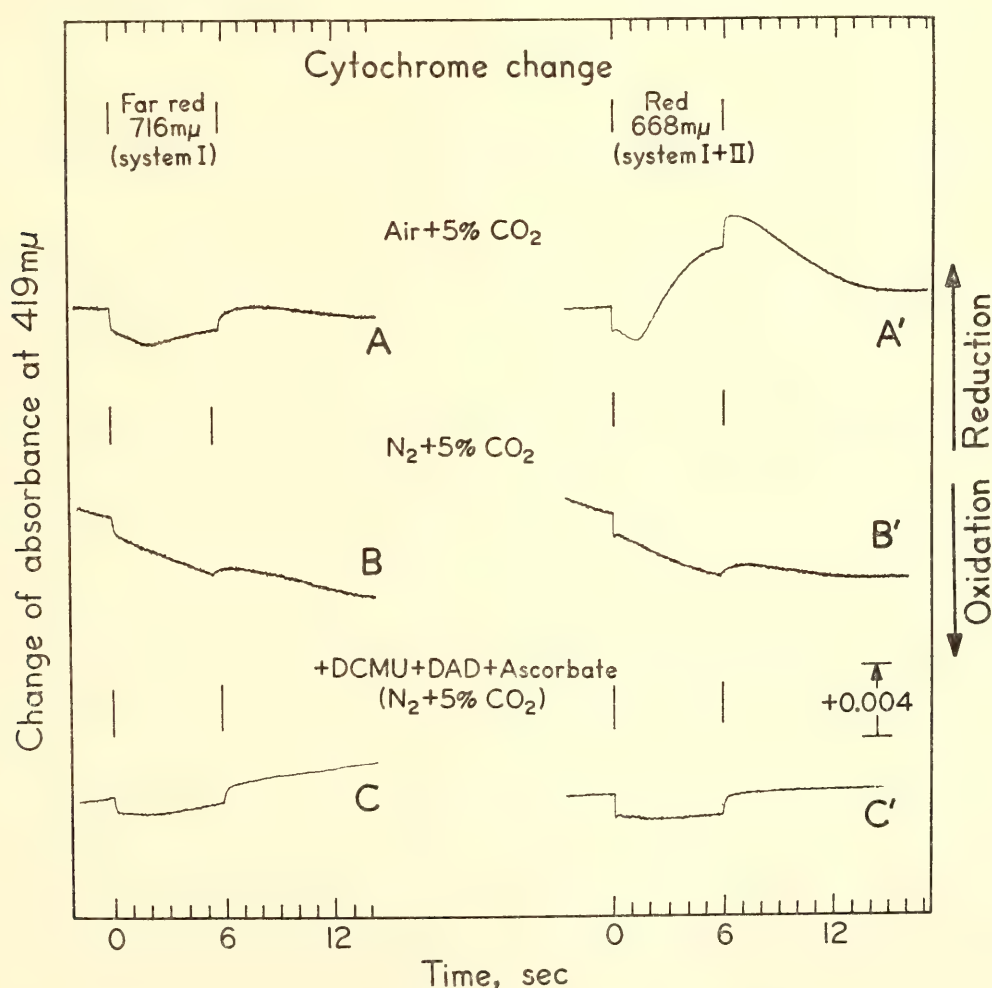


Fig. 16. Effect of lack of  $O_2$  and DCMU, DAD + ascorbate on the 419 mμ cytochrome absorbance change in *Chlorella*.  $N_2 + 5$  per cent  $CO_2$  was passed over the algal suspension (5 ml, 12 cm<sup>2</sup> surface, 5 mm pathway in cuvette, 37.5 μg chlorophyll) in the dark for 3–5 min. Additions used in these final concentrations: DCMU,  $5 \times 10^{-5}$  M; DAD,  $6.6 \times 10^{-5}$  M, ascorbate about  $5 \times 10^{-3}$  M. Changes were measured 5–10 min after adding the substance. The first absorbance changes after dark treatment were used. After darkening of the cell suspension the base line drifted down occasionally, because the photomultiplier sensitivity varied following a dark period.



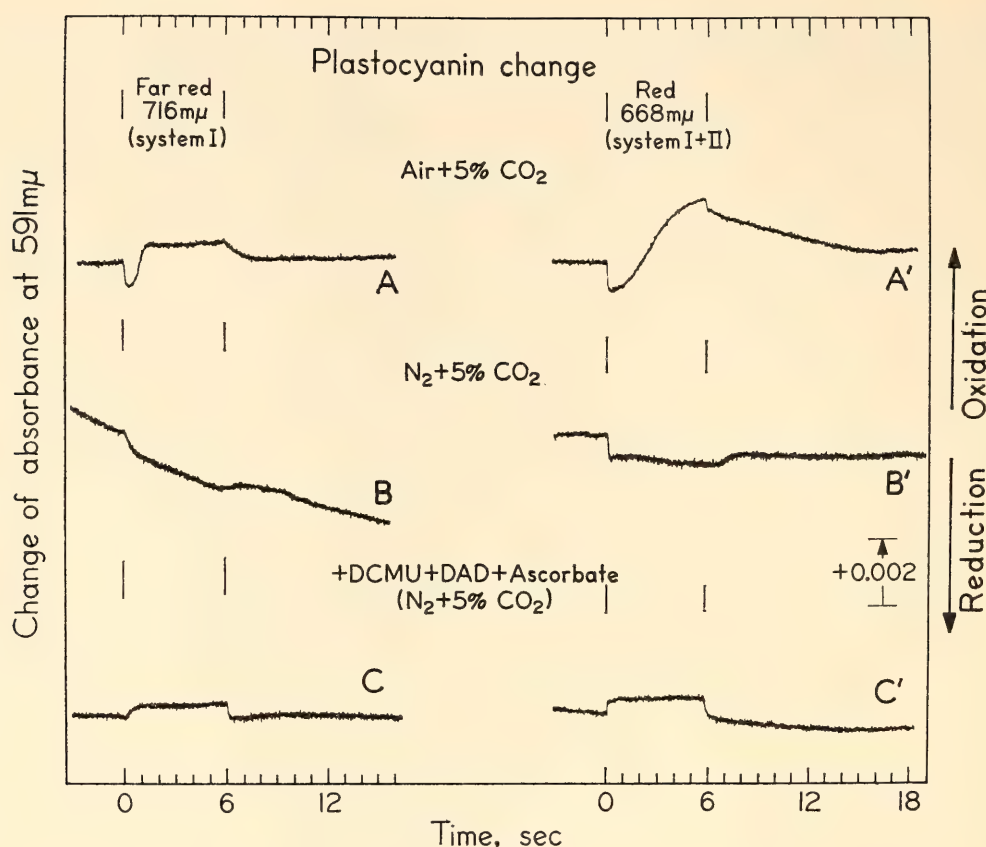


Fig. 17. Effect of lack of  $O_2$  and added DCMU, DAD + ascorbate on 591-m $\mu$  plastocyanin absorbance change in *Chlorella*; same concentrations of additions and sample as in Fig. 16.

*B, B'*) compare the 591-m $\mu$  plastocyanin change with and without  $O_2$ . Under anaerobic conditions only reduction of plastocyanin (decrease of absorbance at 591 m $\mu$ ) in either red or far-red actinic light could be seen. Moreover, when the light was turned off, a slow oxidation of plastocyanin to its former level took place. Addition of DCMU and the donor system, DAD + ascorbate, made it possible to oxidize plastocyanin again with far-red or red actinic light (Fig. 17, *C, C'*).

*Partial inhibition of the 518-m $\mu$  absorbance change from lack of  $O_2$  and the effect of DAD + ascorbate on this change.* Figure 18 (*A, A'* and *B, B'*) compares the 518-m $\mu$  absorbance change under aerobic and anaerobic conditions. An inhibitory effect of  $O_2$  deficiency on the 518-m $\mu$  absorbance change has been noted previously by other workers. Under anaerobic conditions the first rapid transient of the 518-m $\mu$  absorbance

change was unaffected; however, the other components of the change were almost completely suppressed either in red or far-red actinic light. The effect of DCMU was parallel to that of anaerobiosis on the 518-m $\mu$  absorbance change as shown in Fig. 14 (*B, B'*) of the preceding section and Fig. 18 (*B, B'*) here. Anaerobiosis does not prevent the regeneration by DAD + ascorbate of the 518-m $\mu$  change inhibited by DCMU. The preceding section shows the regeneration in air of the DCMU-inhibited 518-m $\mu$  absorbance change by DAD + ascorbate (Fig. 14, *C, C'*).

*Effect of a dark treatment prior to the measurement of the 419- and 591-m $\mu$  absorbance changes in air.* Darkening the cells in air + 5 per cent  $CO_2$  until just before the light exposure had some effects on the plastocyanin and cytochrome absorbance changes as is shown in Fig. 19. The first absorbance change obtained after a dark time of 2–30 minutes without

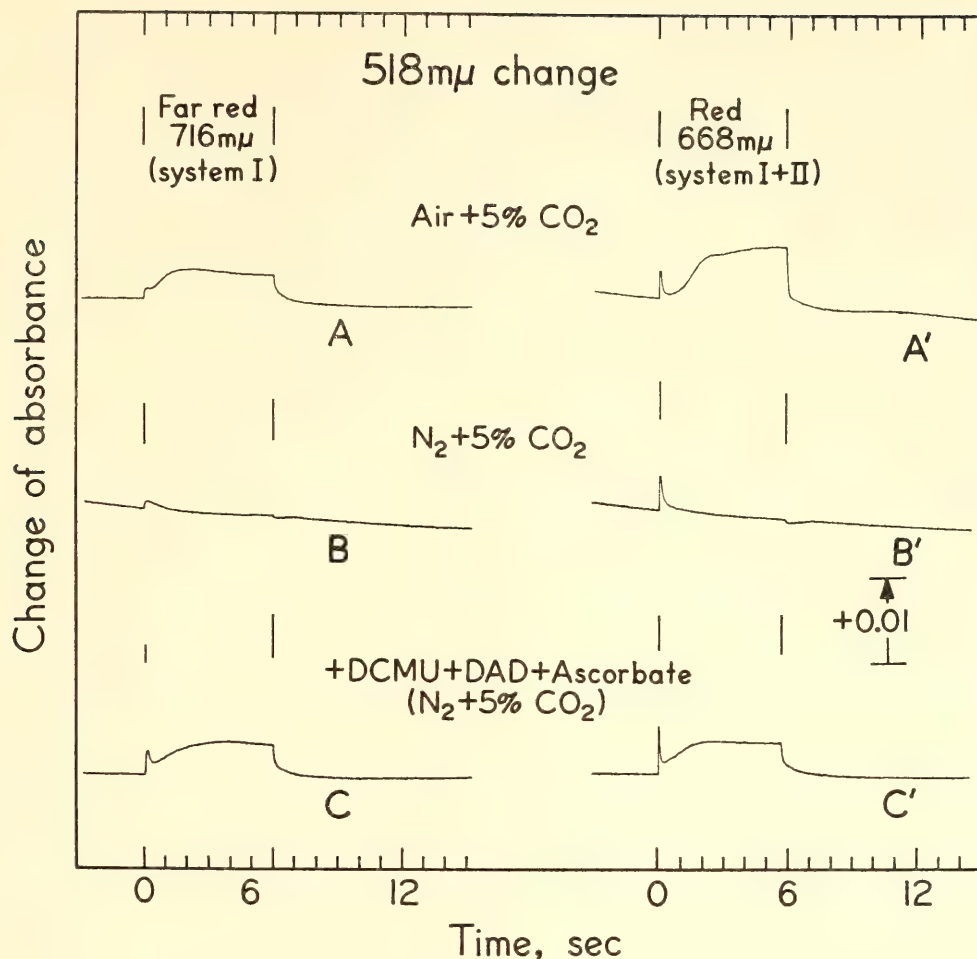


Fig. 18. Effect of lack of  $O_2$  and added DCMU, DAD + ascorbate on 518- $m\mu$  absorbance change in *Chlorella*. For details see Fig. 16.

the measuring beam showed a retarded light-driven reduction of cytochrome compared with the second or following changes measured at 18-second intervals with only the measuring beam on. The effect of a previous dark period on the plastocyanin absorbance change (at 591  $m\mu$ ) was opposite that on the cytochrome change (at 419  $m\mu$ ). After the dark pretreatment the reduction of plastocyanin (decrease of absorbance) caused by system II was longer lasting, and oxidation was retarded. As shown previously (*Year Book 63*, p. 445) the time course of the 518- $m\mu$  absorbance change was also influenced by a previous dark treatment.

#### Discussion

The results obtained demonstrate that a short period of anaerobiosis had a dramatic effect on certain intermediates of the electron-transport chain of photo-

synthesis. These effects could not be produced only by a period of darkness. Dark pretreatment, however, did give small effects parallel to those of anaerobiosis. The parallelism may have been caused by partially anaerobic conditions resulting from cellular respiration.

The three absorbance changes investigated were influenced differently by anaerobiosis. The results can be explained by an  $O_2$  requirement for the activity of system II because lack of  $O_2$  inhibited the light-driven cytochrome reduction mediated by system II. It also partially inhibited the 518- $m\mu$  absorbance change as did DCMU, an effect described in the preceding section and in *Year Book 63* (p. 446). The idea that system II requires  $O_2$  is not supported by the results obtained with the 591- $m\mu$  absorbance change because lack of  $O_2$  permitted only reduction of plastocyanin.



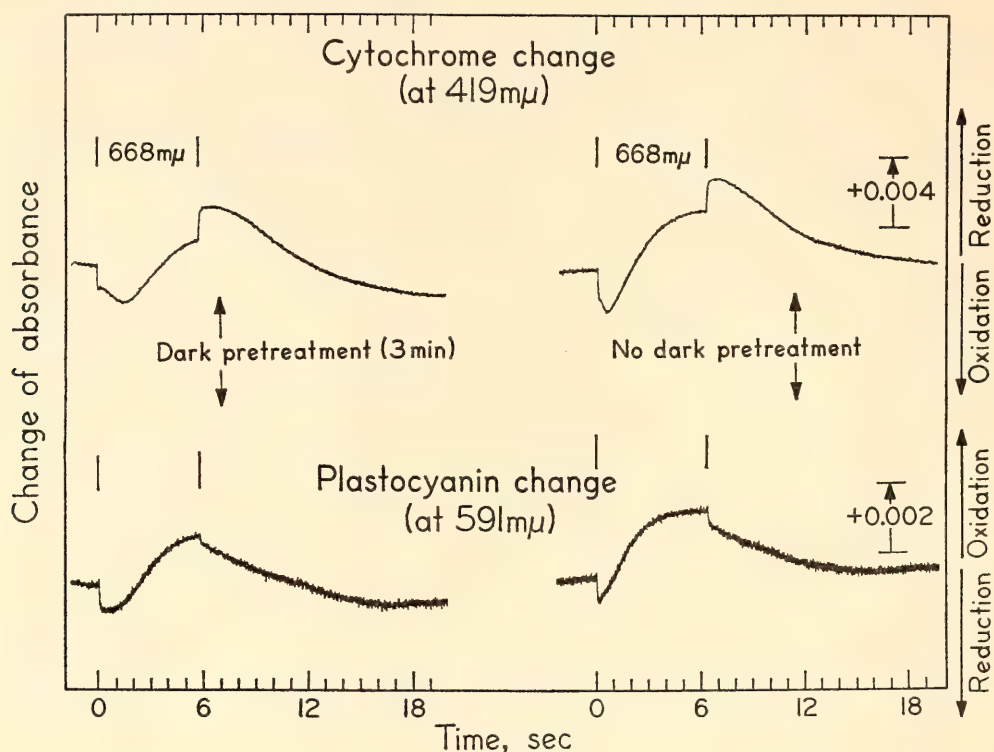


Fig. 19. Effect of dark pretreatment on the 419  $m\mu$  and the 591  $m\mu$  absorbance changes in *Chlorella* in air + 5 per cent  $CO_2$ . First light exposure (left) was made after 3 min dark and about 10-sec illumination by measuring light. Second light exposure (right) followed 18 sec after first exposure (measuring beam still on) without dark pretreatment.

Another explanation for the results observed is that lack of  $O_2$  prevented normal electron transport between plastocyanin and cytochrome. Such an interruption at this site would give rise to the effects observed, since only oxidation of cytochrome, by system I, and reduction of plastocyanin, by system II, could take place. This block could be caused by a link between a cyclic electron pathway and the main electron chain at the site (Fig. 15, previous section). Under anaerobic conditions accumulation of reduced products such as  $NADPH_2$  and ferredoxin may accumulate and force a cyclic flow of electrons upon the system. An increase in electron flow in the cyclic pathway would compete with electrons coming from system II. If the common link between the cyclic flow and the electron flow originating in water is located between plastocyanin and cytochrome, a competition at this point would act as a block to electron flow from system II to system I. The block could lead to the

observed plastocyanin reduction and cytochrome oxidation. It would also retard steady-state  $O_2$  evolution (*Year Book 63*, p. 462).

Lack of  $O_2$  had no effect on the plastocyanin or cytochrome changes seen when the electron-donor system DAD + ascorbate served as a substitute electron source for system II as in Figs. 16 (C, C') and 17 (C, C') as compared with Figs. 13 (C, C') and 12 (C, C') of the previous section. The reducing potential of the donor system may be such that a competition between cyclic and noncyclic electron flow strongly favors the noncyclic flow; anaerobiosis would have no effect on the regenerated changes.

#### Summary

Anaerobiosis had a dramatic effect on certain light-induced absorbance changes. Lack of  $O_2$  caused plastocyanin to accumulate in its reduced form while cytochrome *f* accumulated in its oxidized form. An accumulation of reduced end

products of photosynthesis (NADPH<sub>2</sub>, ferredoxin, etc.) under anaerobic conditions may accentuate a cyclic electron flow. An effective competition between a cyclic electron flow linked to the main pathway between plastocyanin and cytochrome would act as a block of electron flow from system II to system I, and lead to the effects observed.

#### AN OXYGEN REQUIREMENT FOR PHOTOSYNTHESIS

*William Vidaver*

In green-plant photosynthesis, oxygen (O<sub>2</sub>) is usually considered a waste product. Although it can be produced at once in the light, it is also believed to participate as a reactant in photosynthesis. So-called "pseudocyclic photophosphorylation" as described by Arnon evolves and consumes equal amounts of O<sub>2</sub> in the light. Warburg found that two molecules of O<sub>2</sub> were consumed for every three evolved photosynthetically. Our workers and others have described light-induced O<sub>2</sub> uptake during photosynthesis by pigment system I. Presumably this uptake results from either the back oxidation of a photoreductant or oxidations that are part of the photosynthetic process rather than light-induced stimulation of respiration. The relation between respiratory O<sub>2</sub> consumption and photosynthesis is poorly understood.

Experiments were made to determine whether the lack of endogenous O<sub>2</sub> has any effect on photosynthetic rates under various light conditions. Determinations of O<sub>2</sub> evolution by *Ulva lobata* were made polarographically. The electrodes and gassing system were similar to those described in *Year Book 63* (p. 467). Monochromatic light of up to  $1.5 \times 10^6$  ergs cm<sup>-2</sup> sec<sup>-1</sup> intensity was isolated from incandescent lamps by interference and glass filters. Steady-state-rate determinations were made in decrements of light intensity at constant wavelength.

A single tissue sample was used for all measurements at each wavelength.

*Rates of O<sub>2</sub> evolution in air and N<sub>2</sub> at various intensities and wavelengths.* The rate of O<sub>2</sub> evolution as a function of light intensity at four wavelengths was measured in air + 5 per cent CO<sub>2</sub> and in N<sub>2</sub> + 5 per cent CO<sub>2</sub>. At low light intensities, O<sub>2</sub> evolution is less anaerobically than in air at all wavelengths. The inhibition of O<sub>2</sub> evolution produced by lack of O<sub>2</sub> varies with wavelength and is generally more pronounced as wavelength increases. Figure 20 illustrates these relations.

*Relative inhibitions of O<sub>2</sub> evolution under N<sub>2</sub>.* Figure 21 is derived from data shown in Fig. 20. The ratio of the rates of O<sub>2</sub> evolution under N<sub>2</sub> to the rate under air is plotted as a function of intensity. This ratio is strongly dependent on wavelength.

*Wavelength dependency of anaerobic inhibition.* Figure 22 shows a partial action spectrum for the effect of low O<sub>2</sub> tension on O<sub>2</sub> evolution. It was prepared from data similar to and including that used in Figs. 20 and 21. The points represent the ratios of the rates of O<sub>2</sub> evolution in air to those obtained under N<sub>2</sub> when the light intensities were adjusted to give 25 per cent of the light-saturated rate in air.

*Discussion.* The wavelength dependence of anaerobic inhibition of O<sub>2</sub> evolution in *Ulva* suggests that the amount of inhibition depends on the proportion of the light that is absorbed preferentially by one of the two photochemical systems of photosynthesis. Photochemical system I (the long wavelength system) mediates transient O<sub>2</sub> uptake (*Year Book 63*, p. 453). An explanation for anaerobic inhibition of photosynthesis could be the inability of system I to function in the absence of O<sub>2</sub>. Short-wavelength system II carries out O<sub>2</sub> evolution. If O<sub>2</sub> is required by system I it must be supplied by system II activity.

The action spectra for the two systems



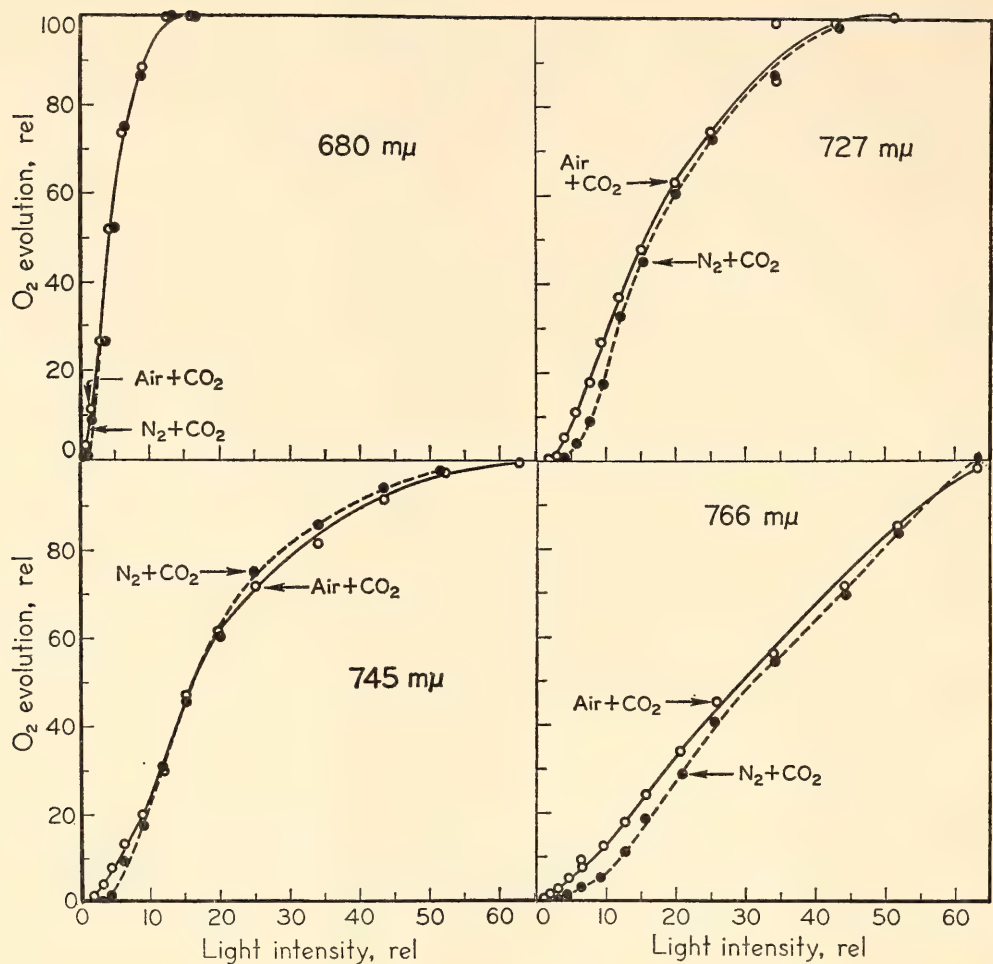


Fig. 20. Light intensity curves for  $O_2$  evolution in air and in  $N_2$  at  $20^\circ \pm 2^\circ$ . Gas mixtures contained 5 per cent  $CO_2$ . Scales for  $O_2$  evolution are identical for all wavelengths but the relative intensity scales for the various wavelengths are not comparable.

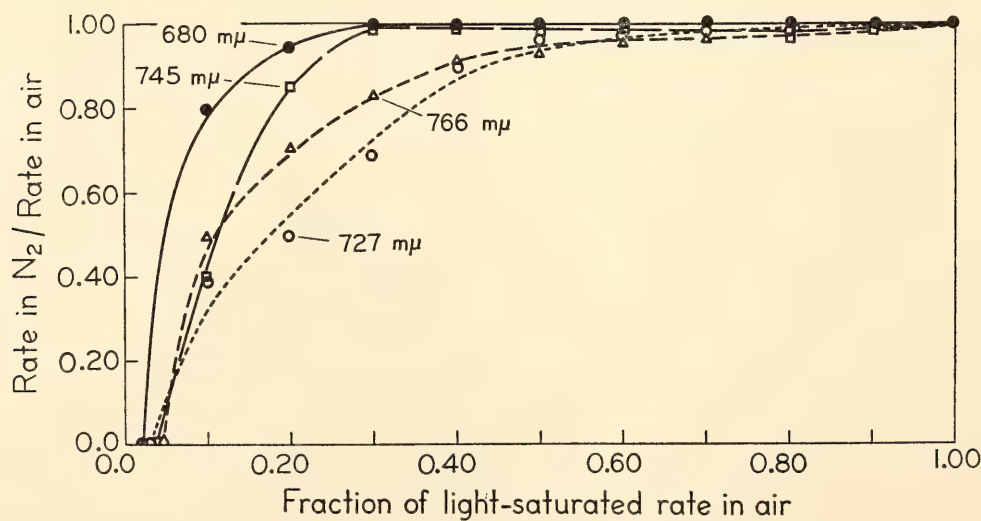


Fig. 21. Fraction of the photosynthetic rate in air achieved under  $N_2$  at light intensities giving different rates in air. The abscissa is the fraction of the maximum rate of  $O_2$  evolution in saturating light. This relation permits the rate of  $O_2$  evolution to be calculated independently of light intensity. The ordinate indicates the ratios of the rates in  $N_2$  and air. Had there been no inhibition in  $N_2$  all curves would be horizontal lines with a value of 1.

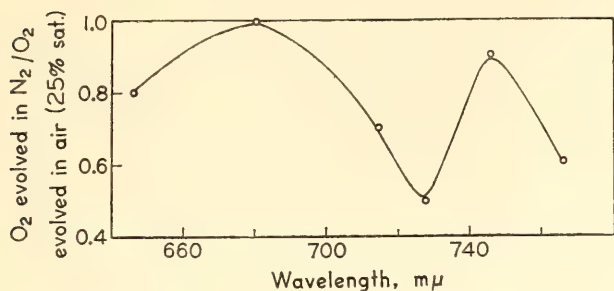


Fig. 22. Partial action spectrum indicating inhibitory effect of lack of O<sub>2</sub> at different wavelengths. Ratio of O<sub>2</sub> evolution ratios in N<sub>2</sub> and in air compared at light intensities that induced 25 per cent (25 ordinate units in Fig. 20) of maximum rate in air for each wavelength.

overlap but do not coincide. System II activity is highest at 650 mμ, where chlorophyll *b* absorbs most strongly, and is only slightly lower at 675 mμ. The activity of system I corresponds to the absorption peak of the long-wavelength form of chlorophyll *a* near 675 mμ and extends further into the far-red than does system II. If there is an O<sub>2</sub> requirement for system I, anaerobic inhibition should be least at the region where the activities of the two systems have the greatest overlap. Inhibition is least near 680 mμ. The anaerobic inhibition of O<sub>2</sub> evolution is greatest at 727 mμ and decreases again in longer wavelengths.

The reason for the rise at longer wavelengths is not clear. Perhaps some respiratory stimulation occurs around 730 mμ. Alternatively there could be a secondary activity peak for system II near 745 mμ.

#### KINETICS OF THE TWO-LIGHT EFFECT ON THE PHOTOSYNTHETIC OXYGEN OUTBURST

Yaroslav de Kouchkovsky

It was reported that preillumination with far-red light, which acts on system I, will increase the transient outburst of O<sub>2</sub> by chloroplasts or algae when given bright

light of shorter wavelength (*Year Books 61*, pp. 339–343, and *63*, pp. 447–453). Short enough flashes of far-red light inhibited rather than enhanced the burst in an alga (*Year Book 63*, pp. 447–453). It was thought that preillumination by red light (absorbed predominately by pigment system II) would inhibit the burst. This report compares the effects of weak red and far-red preillumination on the O<sub>2</sub> burst induced by red light of higher intensity.

*Methods and results.* The rates of O<sub>2</sub> exchange by *Chlorella vulgaris* were recorded with a stationary bare platinum-electrode assembly (*Year Book 60*, pp. 362–363). Monochromatic light was isolated with interference and cutoff filters (half-bandwidth about 9 mμ). Preilluminations were made with low intensities at 713 mμ or 646 mμ. The electrode assembly was filled with the culture medium containing 0.1 *M* KCl. A mixture of air + 5 per cent CO<sub>2</sub> was bubbled through this medium and the temperature was kept at 22°C.

The experimental procedure (*Year Book 63*, p. 449) utilized one-minute cycles. Each cycle consisted of a 3-second exposure to bright 651-mμ light (about  $4 \times 10^4$  ergs cm<sup>-2</sup> sec<sup>-1</sup>), followed by a 57-second interval which was either all dark, part dark and part 713-mμ (or 646-mμ) light, or all 713-mμ (or 646-mμ) light.

First, cycles with 57-second dark intervals were repeated until a constant value of the O<sub>2</sub> burst, as measured by the height of the initial spike, was reached. Then, the dark interval was progressively replaced by preillumination periods of various durations up to the 57-second maximum immediately before the next 3-second 651-mμ exposure. The enhancement or inhibition of the O<sub>2</sub> burst by preillumination is expressed as  $(P - D)/D$  where *P* is the height after preillumination and *D* is the height after a dark period.

Figure 23 shows these results as a function of the preillumination time in a



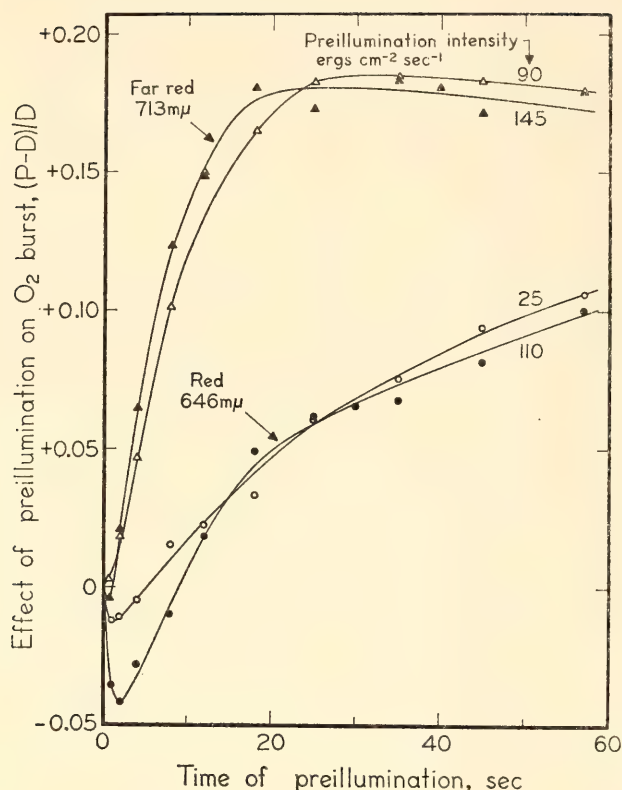


Fig. 23. Effect of red or far-red preillumination for various times on the  $O_2$  burst of *Chlorella*. Negative ordinate, inhibition; positive ordinate, stimulation.

typical experiment. Similar curves for the far-red preillumination effect were published last year (*Year Book 63*, p. 451). As expected, there was inhibition by preillumination with red light. Surprisingly, the present results show that longer preillumination with red light stimulates rather than inhibits the outburst. Furthermore, in this experiment the stimulatory effect is nearly as great as that obtained with far-red preillumination, although more time is required.

**Discussion.** At any wavelength the absorbed light is divided between the two photochemical systems. In the far-red at 713  $m\mu$  the absorption of system I predominates. At 646  $m\mu$ , near the peak of chlorophyll-*b* absorption, the situation is reversed, so more of the light is absorbed by system II than by system I.

The  $O_2$  outburst produced by bright 651- $m\mu$  light presumably depends on the

rapid photochemical utilization by system II of an oxidized intermediate X. In the dark, nonphotosynthetic metabolism gives a certain ratio of X to the reduced form  $X^-$  according to Goedheer and also *Year Book 63*, p. 452. The inhibition of the outburst by a short preillumination is thought to be due to the reduction of X from its metabolically produced level to a lower concentration level. This is done by that fraction of the light that is absorbed by system II.

Because the photoreduction of X is faster than the photooxidation of  $X^-$ , the inhibition of the  $O_2$  outburst is seen before its stimulation.

Why does prolonged preillumination with weak 646- $m\mu$  light stimulate, whereas strong red or far-red light, as is well known, inhibits the  $O_2$  outburst? The following hypotheses may explain these phenomena.

(1) On the one hand, at any wavelength light is distributed between the two pigment systems and the resulting photochemical reactions proceed at a rate that is a function of the number of the quanta absorbed and of the concentration of the photochemical reactants. On the other hand, the dark metabolism may be more or less reductive, thus varying the concentration of the substrates for these reactions between wide limits.

(2) For low light intensity, the reoxidation (by NADP?) of the reduced product formed by system I does not limit the rate of light reaction I. An equal amount of an oxidized product, which oxidizes  $X^-$ , corresponds to this reduced product. With a strongly reductive dark metabolism (high initial concentration of  $X^-$ ), the balance will then be in favor of the accumulation of X, and a stimulation of the burst will result; see Fig. 23.

(3) For any wavelength there will be a value of light intensity above which the reoxidation of the system-I reduced product will limit the light reaction I and, therefore, the formation of the corresponding oxidized product: hence the inhibition of the  $O_2$  burst.

# TRANSIENTS OF OXYGEN EXCHANGE IN *Chlorella* CAUSED BY SHORT LIGHT EXPOSURES

August Ried

A single light exposure of a few seconds or less may induce in *Chlorella* a long sequence of oxygen ( $O_2$ ) exchange transients. An effort was made to characterize the time courses of individual transients and to obtain information about their causes.

*Chlorella pyrenoidosa* (Pringsheim 211/8b) was grown synchronously as described by Soeder (*Year Book 63*, pp. 477–480). Unless otherwise noted, experiments were made with young cells harvested one to three hours after the start of the light period. Relative rates of  $O_2$  exchange were measured polarographically with the

Teflon-covered electrode described by Fork (*Year Book 61*, p. 343). The desired wavelengths were isolated from the light of an incandescent lamp by Balzer interference filters having a half-bandwidth of about  $10\text{ m}\mu$ .

*Experimental results.* The upper curve in Fig. 24 shows the whole series of transients called  $T_1, T_2, \dots, T_8$ , that may result from a short light exposure. Even numbers symbolize minima (negative peaks, enhanced  $O_2$  uptake or reduced  $O_2$  evolution), and odd numbers symbolize maxima (positive peaks,  $O_2$  evolution or reduced  $O_2$  uptake). Each transient can be identified by the time ( $tm$ ) between the end of the light period and the appearance of its maximum or minimum. The  $tm$  values have a limited and regular variation, depending on experimental

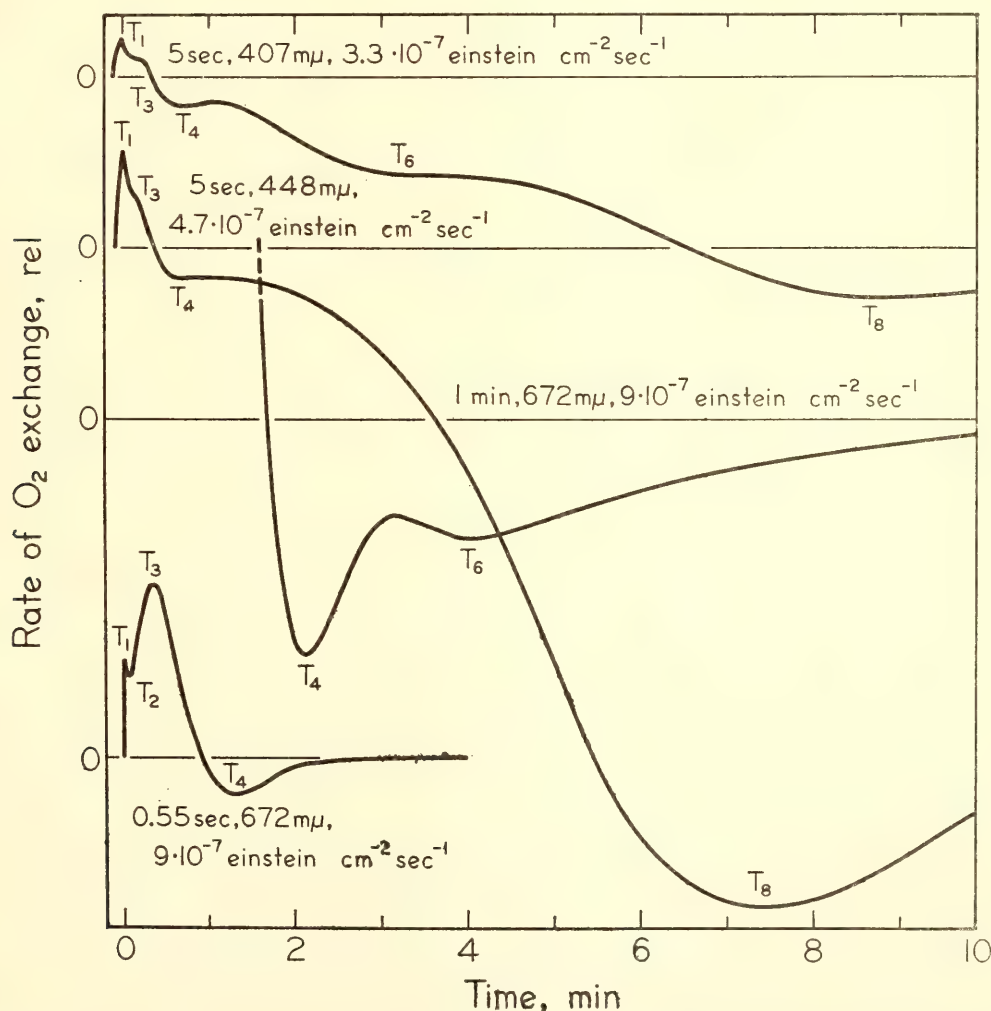


Fig. 24. Transients in rate of  $O_2$  exchange after a short light period. Exposures were chosen to show all the transients (upper curve), or to emphasize separate transients (lower curves).



TABLE 2 Characterization of Individual Transients

Transient	Time, seconds			Exciting Wavelength, mμ	Duration of Flash	DCMU, $5 \times 10^{-6} M$	DNP, $1 \times 10^{-4} M$	CCCP, $1 \times 10^{-5} M$	Antimycin A $1 \times 10^{-5} M$
	Least	Mean	Longest						
$T_1$	...	...	...	as for photosynthesis	steady state in 1-2 min	†	†	§	§
$T_2$	3	13	26	>700 *	...			...	†
$T_3$	10	25	53	>700 *	maximum after 10 sec	§		†	†
$T_4$	54	98	166	>700 *	rising to >15 min			†	†
$T_6$	155	207	285	as for photosynthesis	rising to 15 min	†	§	...	†
$T_8$	360	485	600	<540	...	§	...	...	...
Steady state $O_2$ evolution	...	...	...	...	...	†	§	†	§

\* Strongly effective. Effects observed: † nearly complete inhibition (80% to 100%); ‡ partial inhibition (50% or less); § almost no inhibition; || stimulation.

conditions. Table 2 shows mean and extreme values from 200 exposures, where the light time varied from 0.025 second to 15 minutes and light intensity of different wavelengths varied from  $9 \times 10^{-8}$  to  $6 \times 10^{-6}$  einstein  $\text{cm}^{-2} \text{sec}^{-1}$ . There is only a small overlap between the  $tm$  values of successive positive or negative transients. Therefore, the  $tm$  value may be used in a manner similar to  $rf$  values in chromatography.

The individual transients differ strongly in their dependence on experimental conditions as shown in Table 2. By the choice of appropriate conditions, some transients may be made larger, others smaller. Thus, single transients may be separated to some extent, as shown in Fig. 24. The individual transients are characterized as follows:

$T_1$ , the first positive peak, is caused by photosynthetic  $\text{O}_2$  evolution and has some characteristics similar to those of steady-state photosynthesis. Some obvious differences, such as the much greater sensitivity of  $T_1$  to DCMU and DNP, are understandable if partial steps

that are rate-limiting during the induction period are other than those limiting in the steady state.

$T_2$  ( $tm = 13 \text{ sec}$ ), the dip between  $T_1$  and  $T_3$ , may result, at least in part, from the time lag between photosynthetic  $\text{O}_2$  evolution accompanying the light flash ( $T_1$ ) and the appearance of  $T_3$ . Under some conditions the curve drops below the base line between  $T_1$  and  $T_3$  (Fig. 25). This actual stimulated net  $\text{O}_2$  uptake has characteristics similar to the "negative spike" reported by French and Fork (*Year Book 60*, pp. 351–357) in *Porphyridium* and by Vidaver and French (*Year Book 63*, p. 453) in *Ulva*. It has not yet been possible to determine whether or not such a light-stimulated  $\text{O}_2$  uptake is always involved in  $T_2$ .

$T_3$  ( $tm = 25 \text{ sec}$ ), the second positive peak, is certainly of a very different nature from  $T_1$ . Appropriate inhibitors can suppress either  $T_1$  or  $T_3$  completely without affecting the other.  $T_3$  can be isolated by adding  $2 \times 10^{-6}$  to  $5 \times 10^{-6} M$  DCMU or  $5 \times 10^{-5}$  to  $1 \times 10^{-4} M$  DNP (Fig. 25), whereas only  $T_1$  remains after adding  $1 \times 10^{-5} M$  antimycin A (Fig. 28) or  $1 \times 10^{-5} M$  CCCP.  $T_3$  is further characterized by its saturation at a light intensity about 0.1 the intensity required to saturate photosynthesis. Half-saturation occurs at about  $1.5 \times 10^{-7}$  einstein  $\text{cm}^{-2} \text{sec}^{-1}$  (Fig. 26). The maximal value is reached after 5–10 seconds' exposure, half-saturation after about one second (Fig. 27), whereas photosynthetic  $\text{O}_2$  evolution  $T_1$  is still increasing with exposure times greater than one minute.  $T_3$  never exceeds or even reaches the compensation point. It also differs from  $T_1$  in its wavelength dependence (Fig. 25). At intensities giving the same steady-state rate, light at 727  $m\mu$  is much more effective in producing  $T_3$  (and  $T_4$ ) than 672- $m\mu$  light.

$T_4$  ( $tm = 98 \text{ sec}$ ), the transitory stimulation of dark  $\text{O}_2$  uptake, appears immediately after  $T_3$  and lasts one to two minutes. It shows a dependence similar to  $T_3$  on light intensity and wavelength

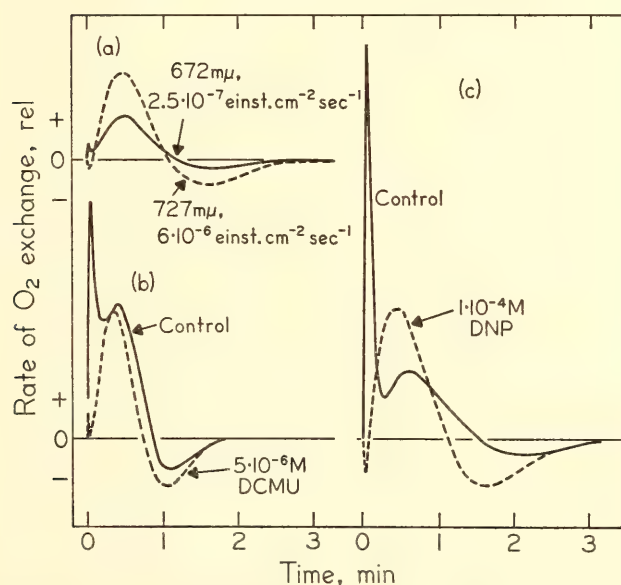


Fig. 25. Comparison of the second maximum,  $T_3$ , and photosynthetic  $\text{O}_2$  evolution,  $T_1$ , from 0.55 flashes. (a) Wavelength dependence. Light intensities at 672  $m\mu$  and 727  $m\mu$  gave about the same steady-state  $\text{O}_2$  evolution. (b, c) Effect of DCMU and DNP on  $T_1$  and  $T_2$ . Light intensity,  $3 \times 10^{-6}$  einstein  $\text{cm}^{-2} \text{sec}^{-1}$ ; wavelength, 672  $m\mu$ .



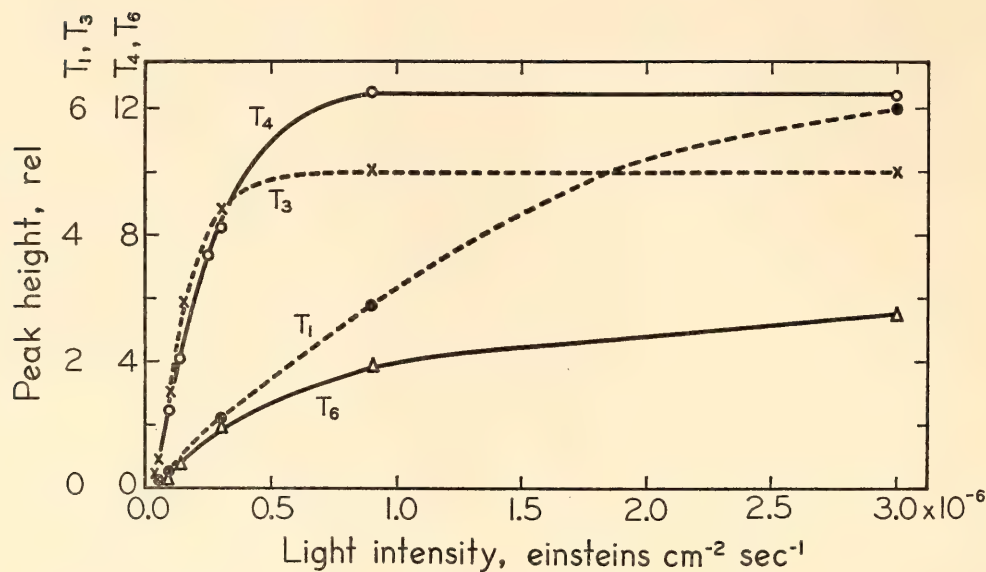


Fig. 26. Magnitudes of the transients as functions of light intensity.  $T_1$  and  $T_3$  were measured after 0.55-sec exposures,  $T_4$  and  $T_6$  after 2-min exposures to monochromatic 672-m $\mu$  light.

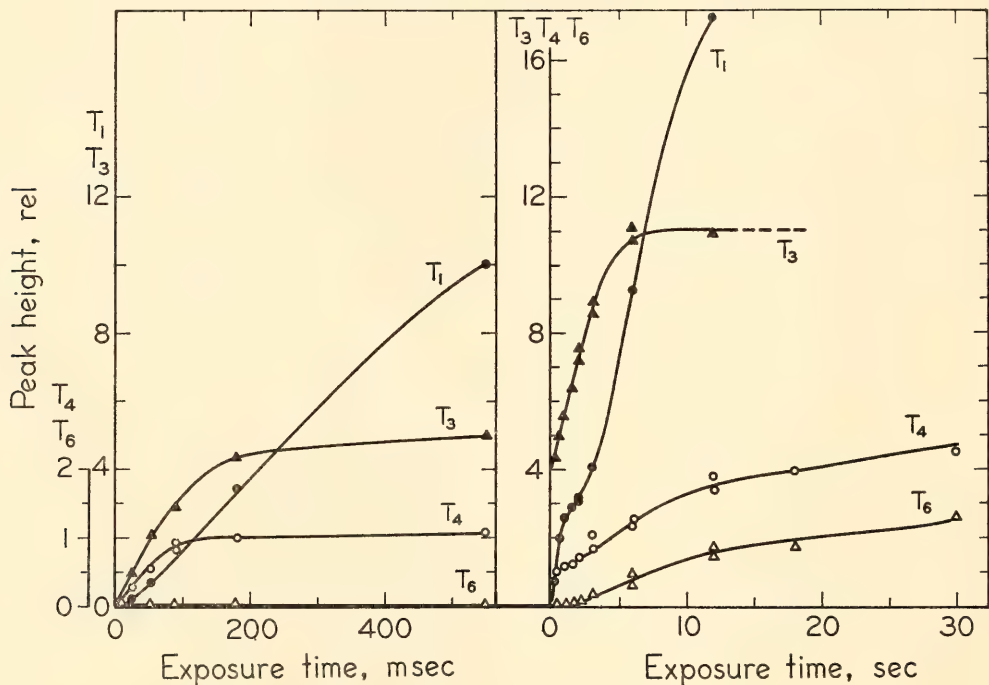


Fig. 27. Magnitudes of the transients as functions of flash duration. Wavelength, 672 m $\mu$ ; intensity,  $3 \times 10^{-6}$  einstein cm<sup>-2</sup> sec<sup>-1</sup>.

as well as in sensitivity to diverse inhibitors, at least when the light exposure does not exceed one second. But the magnitude of  $T_4$  continues to increase with exposure time up to several minutes. Possibly this long-continued increase of  $T_4$  is related to overlapping by  $T_6$ .  
 $T_6$  ( $t_m = 207$  sec), the next peak of enhanced O<sub>2</sub> uptake, culminates three to

four minutes after darkening. It occurs only after light periods greater than one to two seconds (Fig. 27), and reaches appreciable size only after more than one minute of illumination. This seems to be a frequently observed type of enhanced O<sub>2</sub> uptake after exposure to red light. Because of its wavelength dependence, it appears to be linked with photosynthesis.

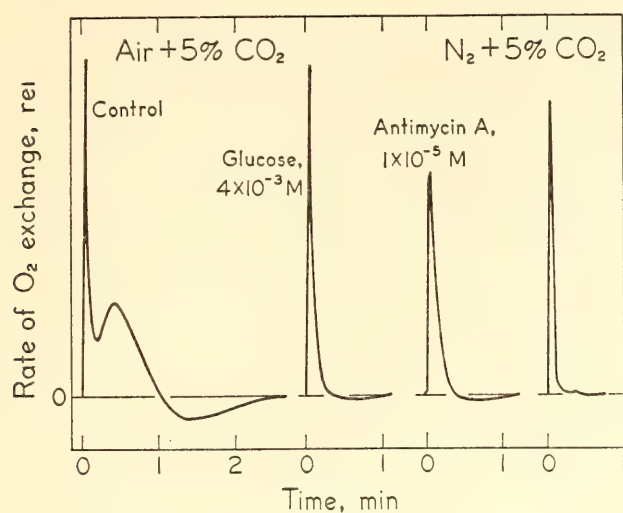


Fig. 28. All transients except  $T_1$  are suppressed when  $O_2$  uptake is maximal with glucose, or is reduced with antimycin A or by removal of  $O_2$ . Flashes were 0.55 sec, 672  $m\mu$ , intensity  $3 \times 10^{-6}$  einstein  $cm^{-2} sec^{-1}$ . Apparently faster decay of  $O_2$  evolution under  $N_2$  may be caused partly by the high concentration difference for  $O_2$  inside and outside the cells.

$T_8$ , the largest and longest-lasting transient, appears only after short-wavelength ( $< 540 m\mu$ ) illumination following a dark period of several hours. Under optimal conditions the amount of  $O_2$  taken up after a short-wavelength flash may be more than 500 times as great as the amount evolved photosynthetically during the flash (Fig. 24). The maximum effect can be obtained only once after a long dark-interval. This appears to be the effect described by Emerson and Lewis (1943) for several wavelengths near 470  $m\mu$ . It does not seem to depend on photosynthesis, but on a separate photo-reaction.

**Discussion.** All these transients except  $T_1$  almost disappear under three extreme conditions: (1) when the respiratory  $O_2$  uptake is completely suppressed by removing  $O_2$  or by adding antimycin A; (2) when the respiratory  $O_2$  is stimulated to a maximum rate by adding glucose (Figs. 28 and 29); or (3) when endogenous  $O_2$  uptake is maximal during cytoplasmic cleavage (Fig. 29).

We therefore assume that all transients except  $T_1$  consist of changes in the respiratory  $O_2$  uptake. This assumption

is further supported by the relation between the rates of respiratory  $O_2$  uptake and the manifestation of the transients, their magnitudes, and especially their  $tm$  values, observed best during cell development. Dark  $O_2$  uptake drops from a maximum during cytokinesis in autospore mother cells to a minimum in darkened young cells (Ried, Soeder, and Müller, 1963). Parallel with this drop,  $T_3$  and  $T_4$ , absent in curves from mother cells, appear in young cells, with continuously increasing  $tm$  values (Fig. 29). In young cells with minimal dark  $O_2$  uptake, the magnitude of the transients is strongly reduced. A series of similar curves, beginning with those showing only a  $T_3$  shoulder, can be obtained from young cells when the rate of dark  $O_2$  uptake drops to a minimum during a long dark-time following several hours in the light. The reverse effect is obtained when glucose is added in rising concentrations to such dark-adapted young cells (Fig. 29). The ways in which the transients disappear and reappear seem not to be the same. DNP at  $1 \times 10^{-4} M$  stimulates  $O_2$  uptake to a submaximal rate and, parallel with this, increases  $T_3$  and  $T_4$ , and shortens the  $tm$  values in a manner similar to  $5 \times 10^{-4} M$  glucose (Figs. 25 and 29).

The strong differences in the dependence of individual transients on experimental conditions show that each successive change in the respiratory activity is caused by a different process, induced more or less directly by the light-flash. The special effectiveness of long-wavelength light in producing  $T_2$ ,  $T_3$ , and  $T_4$ , and their at least partial insensitivity to DCMU (Fig. 25), may be taken as an indication that these transients are caused, although in different ways, by some interaction of system I with the respiratory system. One connection between the photosynthetic and respiratory systems may be through the adenylate system. The long lag phase between the light-flash and the single transients seems to exclude



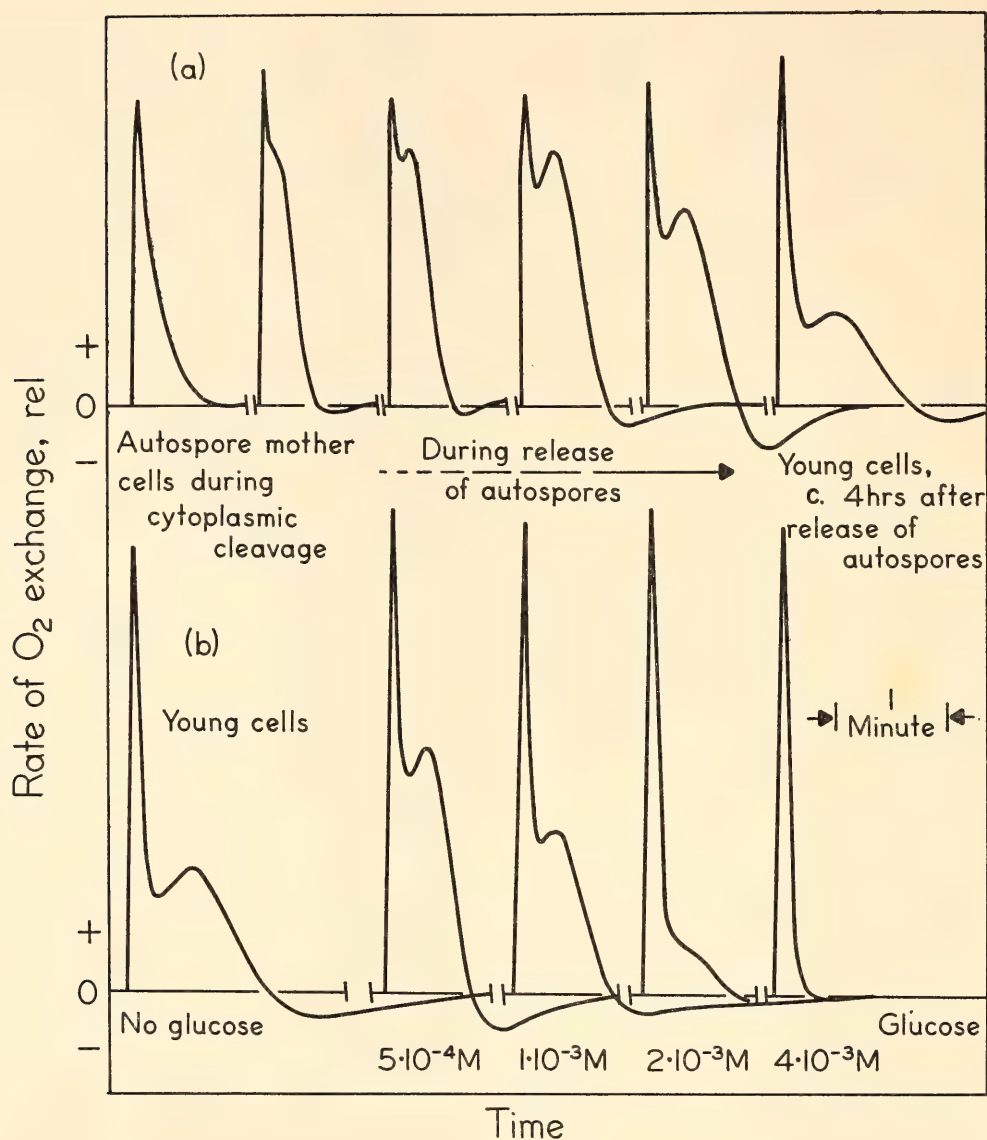


Fig. 29. (a) Reappearance of transients with decreasing respiration during cell development. (b) Their disappearance in young cells when respiration is increased by adding glucose in ascending concentration. Flashes, 0.55 sec at 672 m $\mu$ , intensity,  $3 \times 10^{-6}$  einstein cm<sup>-2</sup> sec<sup>-1</sup>.

a more direct interaction between electron carriers of both systems and supports strongly such a loose connection. In this sense,  $T_3$  is assumed to reflect a lowering of ADP concentration by photophosphorylation (Heber and Santarius, 1964), and the minima  $T_4$ ,  $T_6$ , and  $T_8$  a rise in ADP concentration resulting from different energy (ATP)—requiring processes connected with photosynthesis or, in the case of  $T_8$ , a separate photoreaction.

In agreement with this concept,  $1 \times 10^{-5}$  M CCCP, an uncoupler of both photosynthetic and oxidative phosphorylation, suppresses  $T_3$  and  $T_4$  nearly

completely, but stimulates or does not affect  $T_1$ . In contrast, the uncoupling of only oxidative phosphorylation by  $1 \times 10^{-4}$  M DNP stimulates  $T_3$  and  $T_4$ . This is to be expected if the DNP uncouples only two of the three phosphorylating sites in the electron chain (Ernster and Lee, 1964). The strict dependence of the transients on respiratory activity is further proof of the validity of the interpretation given. Best expression of the transients can be expected when respiratory activity is most effectively controlled by the ADP-ATP level. As shown by the effectiveness of DNP in

stimulating  $O_2$  uptake, such conditions are found at medium and moderately low rates of  $O_2$  uptake. Although other explanations are possible, there is no evidence against the working hypothesis proposed, and it is preferred for its simplicity.

Kinetic studies on the effects of different light intensities and durations make it fairly sure that the transitory suppression of respiratory  $O_2$  uptake *after* short flashes ( $T_3$ ) is identical with the inhibition of respiration *during* longer exposures (also depending on system I), as observed by Hoch, Owens, and Kok (1963). The intensity curves for  $T_3$  and for the steady state give further evidence

for the identity of  $T_3$  with the Kok effect. The Kok effect is the steeper initial rise of photosynthetic rate with intensity at very low intensities. Saturation of  $T_3$  and the Kok-effect bend in the steady-state curve occur at the same light intensity (Fig. 30). Also, the quantitative relation between the two effects is satisfactory. When the values for  $T_3$  in Fig. 30 are multiplied by 2.2 to give the maximum magnitude for  $T_3$  found after longer illuminations (Fig. 27), and the products are subtracted from the steady-state values, the Kok effect vanishes and a nearly linear theoretical photosynthesis curve results (Fig. 30). The Kok effect and the transients disappear together after the addition of

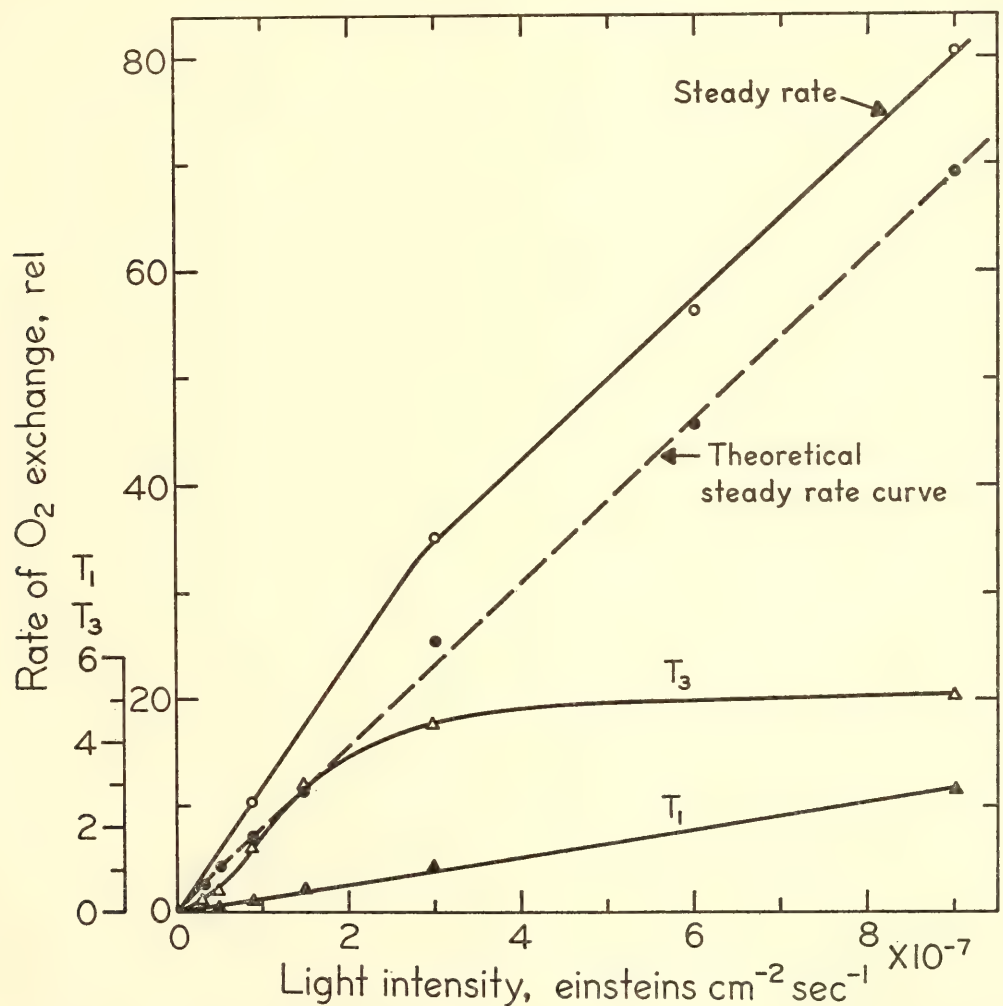


Fig. 30. Relation of  $T_3$  and Kok effect. Curves for  $T_3$  and  $T_1$  from 0.55-sec exposures, and of steady rate as function of light intensity, at 672  $m\mu$ . Dashed line, theoretical curve for the steady rate, drawn through zero point and parallel to second branch of the measured curve; closed circles, measured values of steady rate minus maximum values for  $T_3$  (2.2 times the measured values). All data were from one experiment. Some points on the theoretical curve were derived by interpolation on the curve for  $T_3$ .



antimycin A or glucose at  $2 \times 10^{-3} M$ .

The possible use of short light-flashes to isolate in time the inhibition of  $O_2$  uptake (responsible for the Kok effect) from photosynthetic  $O_2$  evolution offers a simple way to study the effect kinetically. It is remarkable that this suppression of  $O_2$  uptake by system I, saturated at much lower light intensities, reaches appreciable values after much shorter flashes than  $O_2$  evolution does. It may be the only observable effect of a short flash (25 to 200 msec) at medium or low intensity. This seems to mean that a special activity of system I, possibly cyclic photophosphorylation, precedes the non-cyclic electron flow connected with  $O_2$  evolution.

*Summary.* Light exposures of about one second produced transient increases or decreases in the succeeding rate of respiration. Different transients appeared at various times after the exposure, and some lasted for several minutes, showing that there must be more than one type of linkage between the photosynthetic and the respiratory mechanisms of plant cells.

Exposures to certain wavelengths of blue light caused a very large increase in the succeeding rate of respiration, the peak of which came eight minutes after the one-second light exposure. The extra amount of oxygen taken up as a result of this exposure to blue light amounted to more than 500 times the amount of oxygen evolved by the cells during the light exposure. The implication is that this blue-light effect is not an inherent part of the photosynthetic system but may in some way activate an enzyme of the cellular respiratory mechanism.

#### STUDIES ON PHYTOCHROME TRANSFORMATION IN VITRO

*Winslow R. Briggs and David C. Fork*

The pigment phytochrome mediates a broad range of red to far-red reversible responses in plants ranging from mosses

to angiosperms. Techniques for its purification from dark-grown oat seedlings were published recently by Siegelman and Firer. The pigment is a chromoprotein, and evidence from Siegelman indicates that its prosthetic group is a linear tetrapyrrole, perhaps similar to that of phycocyanin. The pigment exists in either of two relatively stable spectral forms:  $P_r$  with absorption maxima at about 380 m $\mu$  and 665 m $\mu$ ; and  $P_{fr}$ , with absorption maxima at about 410 m $\mu$  and 725 m $\mu$ . Red light (665 m $\mu$ ) transforms  $P_r$  to  $P_{fr}$ , and far-red light (725 m $\mu$ ) transforms  $P_{fr}$  to  $P_r$ . The absorbance changes induced by sequential alternation of red and far-red irradiation are easily measured by difference spectrophotometry. Such measurements constitute the sole available assay for the pigment. Extensive studies at the Laboratory of Plant Physiology, Pioneering Research Group, U.S. Department of Agriculture, Beltsville, Maryland, and elsewhere, have suggested that  $P_{fr}$  is the biologically active form in those cases examined.

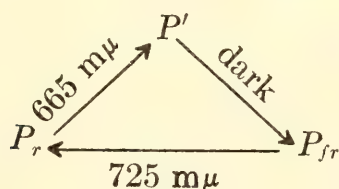
Butler, Lane, and Siegelman recently found that the pigment appearing in dark-grown grass seedlings is in the  $P_r$  form which is normally stable, and transformation to the  $P_{fr}$  form results in rapid enzymatic degradation, detected as loss of absorbance and spectral reversibility. The degradation requires oxygen. Butler, Siegelman, and Miller showed that partially purified extracts of phytochrome were normally stable in the presence of protein-denaturing agents such as 5  $M$  urea or *p*-chloromercuribenzoate (PCMB) as long as the pigment was kept in the  $P_r$  form. The slight spectral changes induced in the pigment by these agents could be reversed by removal of the agents through Sephadex column chromatography. Under similar conditions,  $P_{fr}$  was irreversibly denatured. Again, the criteria for denaturation were loss of absorbance and spectral reversibility. These experiments all suggest that phytochrome transfor-

mation may involve a protein conformational change.

Butler, Siegelman, and Miller showed also that while neither  $P_r$  nor  $P_{fr}$  were particularly affected by proteolytic enzymes such as trypsin or pronase, spectral reversibility and absorbance were lost if the enzymes were present during the  $P_r$  to  $P_{fr}$  transformation. But no such denaturation occurred when the enzymes were present during the  $P_{fr}$  to  $P_r$  transformation only. These experiments suggest that the pathway from  $P_r$  to  $P_{fr}$  is not a simple reversal of the  $P_{fr}$  to  $P_r$  pathway. During transformation of  $P_r$  to  $P_{fr}$  an intermediate susceptible to proteolytic enzymes must exist.

Flash photolysis experiments by Linschitz, Butler, and Siegelman revealed such an intermediate,  $P'$ . The intermediate had greater absorbance than  $P_r$  on the short-wavelength side of the 665-m $\mu$  absorption maximum of  $P_r$ , although its own absorption maximum was apparently at longer wavelengths than that of  $P_r$ . The intermediate could not be detected spectrally during  $P_{fr}$  to  $P_r$  transformations, but time-course studies suggested that other colorless intermediates might exist during this latter reaction. The spectrally detectable intermediate,  $P'$ , decayed in the dark to  $P_{fr}$  with no detectable reversion to  $P_r$ . The decay characteristics of the intermediate in the dark suggested something more complex than simple first-order kinetics.

*Detection of the intermediate ( $P'$ ) under steady-state conditions.* The denaturation and flash photolysis experiments described above suggest the following scheme for phytochrome transformation:



Thus, simultaneous irradiation of phytochrome with high-intensity red and far-red light should cause the above system to

cycle. At steady state, one should detect an accumulation of  $P'$ , the amount of which should depend upon total pigment concentration, relative intensities of red and far-red light, and the rate constants for the three reactions. Instrumentation for this type of experiment has been described previously (*Year Book* 63, pp. 435–436).

Partially purified phytochrome was prepared from dark-grown oat seedlings using Siegelman and Firer's method with minor modifications. Extraction with buffer was followed by Sephadex and calcium phosphate chromatography, then by ammonium sulfate fractionation. Following precipitation by ammonium sulfate, the phytochrome was taken up in dilute phosphate buffer, yielding approximately 10-fold purification and about 20-fold concentration. Further purification (about 200-fold) did not appear to alter the spectral properties of the pigment. Thus, all the experiments were done with 10-fold purified material. Some of the later experiments should be verified with more highly purified material.

One technical note should be mentioned: maintaining the pigment entirely as  $P_r$  during ammonium sulfate precipitation, and subsequently redissolving in buffer increases the final yield by about 20 per cent. This result is consistent with the relative stability of the  $P_r$  form of phytochrome to denaturation and enzymatic degradation (see above). Since both incandescent and fluorescent illumination establish a steady-state equilibrium of the pigment with a substantial portion as  $P_{fr}$ , the ammonium sulfate step was carried out under very dim green light.

Seedlings were grown in total darkness for five days at 25°C, and then chilled to 4°C in the dark before harvest in the light. All purification steps were carried out at 4°C. Unless otherwise noted, all spectral measurements were made on samples kept below 5°C. A thermistor was used to monitor continuously the sample tem-



perature in the ice-jacketed cell, which was 2 cm thick and 3 cm in diameter.

The actinic light from a Sun Gun lamp, after passing through 5 cm of water and a Corning 2030 filter to remove wavelengths  $< 620\text{ m}\mu$ , had an intensity of  $1.33 \times 10^6\text{ ergs cm}^{-2}\text{ sec}^{-1}$  between  $620\text{ m}\mu$  and  $850\text{ m}\mu$  at the sample level. An incandescent lamp and interference filter provided the low-intensity,  $543\text{-m}\mu$  measuring beam. This wavelength was selected for two reasons. First,  $P'$  has substantially greater absorbance here than either  $P_r$  or  $P_{fr}$ . Thus, chances of detecting low levels of  $P'$  at steady state seemed reasonably good. Second, in view of the relatively low absorbance of both  $P_r$  and  $P_{fr}$  at this wavelength, the measuring beam itself should drive the cycling reaction only extremely slowly. Consequently, it should not interfere with measurements of absorbance changes induced by the actinic beam.

A typical oscillographic recorder tracing of the absorbance changes at  $543\text{ m}\mu$  produced by the actinic beam is shown in Fig. 31. The sample was illuminated before the measurement to bring the pigment to an approximate photostationary equilibrium between  $P_r$  and  $P_{fr}$ . A lower base line would indicate a greater proportion of  $P_{fr}$ , a higher base line, a greater proportion of  $P_r$ . The anticipated

absorbance increase appears with illumination, then decays without any measurable lag after the end of the light period.

The half-time for decay (0.5 sec) is considerably slower than the Beltsville workers found ( $< 0.1\text{ sec}$ ) with flash photolysis. Thus, the possibility arises that the signal seen here is not caused by phytochrome at all, but by some other pigment. Three lines of evidence suggest that the light-induced absorbance changes shown in Fig. 31 belong to phytochrome:

The first line of evidence is that samples that are purified an additional 20-fold give results qualitatively and quantitatively similar to those in Fig. 31.

The second line of evidence is illustrated by Fig. 32. Here, the pigment was first driven entirely into the  $P_r$  form with far-red light before making the upper tracing. Then, red light was flashed (flash length, 0.13 sec; intensity,  $7.7 \times 10^5\text{ ergs cm}^{-2}\text{ sec}^{-1}$ ). Each flash caused a rapid decrease in  $543\text{-m}\mu$  absorbance because of the disappearance of  $P_r$ . The characteristic dark decay, presumably representing the disappearance of a small amount of  $P'$  formed during illumination could be seen after the end of each flash. Many of the flashes progressively reduced the amount of  $P_r$  present at the start of illumination, and the magnitude of the observed dark decay became progres-

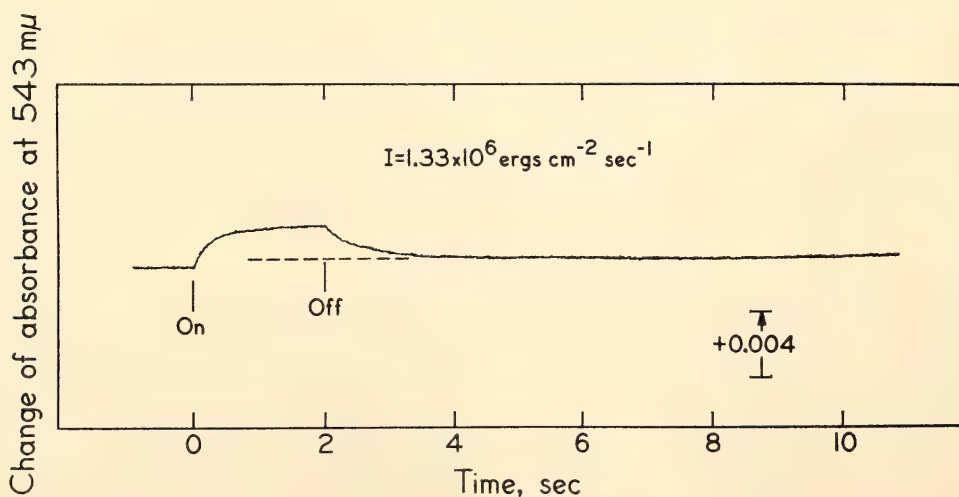


Fig. 31. Absorbance change at  $543\text{ m}\mu$  induced in a phytochrome preparation by high-intensity actinic light (mixed red and far-red,  $1.33 \times 10^6\text{ ergs cm}^{-2}\text{ sec}^{-1}$ ).

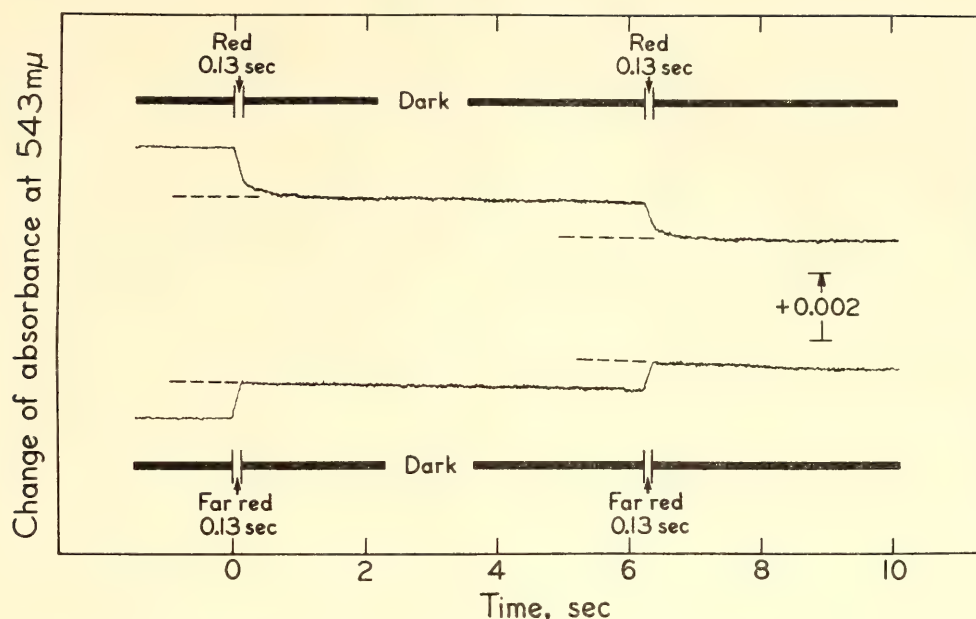


Fig. 32. Behavior of phytochrome preparation when red light ( $7.7 \times 10^5$  ergs  $\text{cm}^{-2} \text{sec}^{-1}$ ) is flashed on  $P_r$  (upper tracing) and when far-red light ( $1.0 \times 10^6$  ergs  $\text{cm}^{-2} \text{sec}^{-1}$ ) is flashed on  $P_{fr}$  (lower tracing).

sively smaller. Thus, the amount of decay was directly proportional to the amount of  $P_r$  present at the start of each flash. No such dark decay was observed when the pigment was present mostly as  $P_{fr}$  at the beginning of the experiment, and far-red light ( $1.0 \times 10^6$  ergs  $\text{cm}^{-2} \text{sec}^{-1}$ ) was flashed (Fig. 32, lower tracing). Only an absorbance increase, reflecting the appearance of  $P_r$  during illumination, was detected.

The third line of evidence is based on two observations: first, lower intensities of actinic light produce smaller signals; and second (observed by the Beltsville workers),  $P'$  decays stoichiometrically to  $P_{fr}$ . The  $P_r/P_{fr}$  ratio should therefore be higher after low-intensity actinic illumination (less  $P'$  to decay to  $P_{fr}$  after the light period) than after high-intensity actinic illumination. It should be possible to detect this altered ratio as a base-line shift—the less  $P_{fr}$  in the mixture, the higher the base line. Such base-line shifts were consistently found when low- and high-intensity 12-second exposures were alternated.

Knowing the total possible base-line shift, obtained by driving the  $P_r$  as far as possible to  $P_{fr}$  (see below), the approxi-

mate amount of the total phytochrome present as  $P'$  after any given light exposure can be calculated from the small base-line shifts described. With the full intensity of the actinic beam used for 12 seconds, about 6 per cent of the pigment is present as  $P'$ . With the actinic beam reduced to 30 per cent of full intensity, the amount falls to about 2 per cent.

*Decay characteristics of  $P'$ .* Another series of experiments was carried out using a wide range of light intensities and exposure times to determine the decay characteristics of  $P'$ . With a fixed intensity (100 per cent) the amount of  $P'$  present at the end of the light exposure could be varied by varying exposure time. Under these conditions the half-time for decay of  $P'$  increased linearly with increase in the amount of  $P'$  present. Thus, one was not observing simple first- or second-order decay reactions, but rather something more complex. But if the amount of  $P'$  present at the end of the light exposure was varied by keeping the exposure time constant and varying intensity, a similar analysis showed the decay half-time to be independent of  $P'$  concentration, characteristic of a first-order reaction.



The apparent paradox was resolved by doing detailed kinetic analyses of the decay curves obtained under the various conditions. If  $\log$  of  $P'$  is plotted against the time after the end of the light exposure (or what is equivalent, if the amount of  $P'$  is plotted as the ordinate on semilog graph paper as was done in Fig. 33) a curve is obtained that can be shown to be the sum of two straight lines. Thus, the observed decay of  $P'$  is the result of simultaneous first-order decay of two components,  $P_1'$  and  $P_2'$ . In Fig. 33 the top solid curves represent the total amount of  $P'$ , or  $P_t'$ . The linear portions of the upper curves extrapolated to zero time (dashed lines) represent decay of  $P_2'$ , and the lower solid straight lines obtained by plotting the actual numerical difference between the upper solid and dashed lines represent decay of  $P_1'$ . For each of the two decay reactions, the amount of a given  $P'$  at any given time can be expressed as  $A = Ke^{-t/\tau}$  where  $K$  is equal to  $P'$  at time zero,  $t$  is the observed time, and  $\tau$  is the time necessary for the given  $P'$  to decay to  $1/e$  times its original value. This provides a measure of the rate of a given decay reaction. For

decay of  $P_1'$  and  $P_2'$  at  $5^\circ\text{C}$ , the temperature at which the curves shown in Fig. 33 were obtained, the values of  $t$  are 0.22 and 1.17 sec, respectively. Since the extinction coefficients for  $P_1'$  and  $P_2'$  at  $543\text{ m}\mu$  are not known, it is not possible to determine precise concentrations at any time. What is actually measured is the product of extinction coefficient times concentration. Values for the products for  $P_1'$  and  $P_2'$  at the end of the light period may be determined from the intercepts of the straight lines with the ordinate.

Inspection of Fig. 33 reveals that at a fixed intensity (100 per cent of actinic light), short light-flashes (left) yield a higher  $P_1'/P_2'$  ratio than longer exposures (right). Analysis of a series of tracings from experiments with constant (100 per cent) intensity and exposure time ranging from 0.13 to 24 seconds showed that in every case both  $P_1'$  and  $P_2'$  were formed. The relative amounts of each form present at the end of the various light exposures were determined from the intercepts of the appropriate straight lines with the ordinates on graphs similar to those shown in Fig. 33. The relative

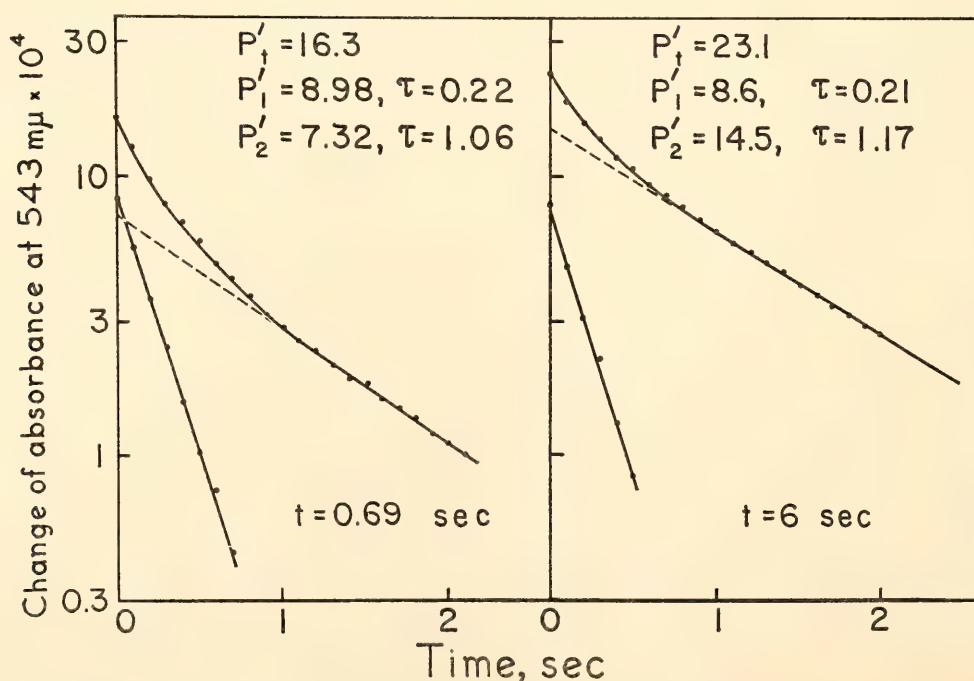


Fig. 33. Kinetic analyses of  $P'$  decay following end of light exposures of same intensity ( $1.33 \times 10^6$  ergs  $\text{cm}^{-2} \text{sec}^{-1}$ ) but different durations (see text).

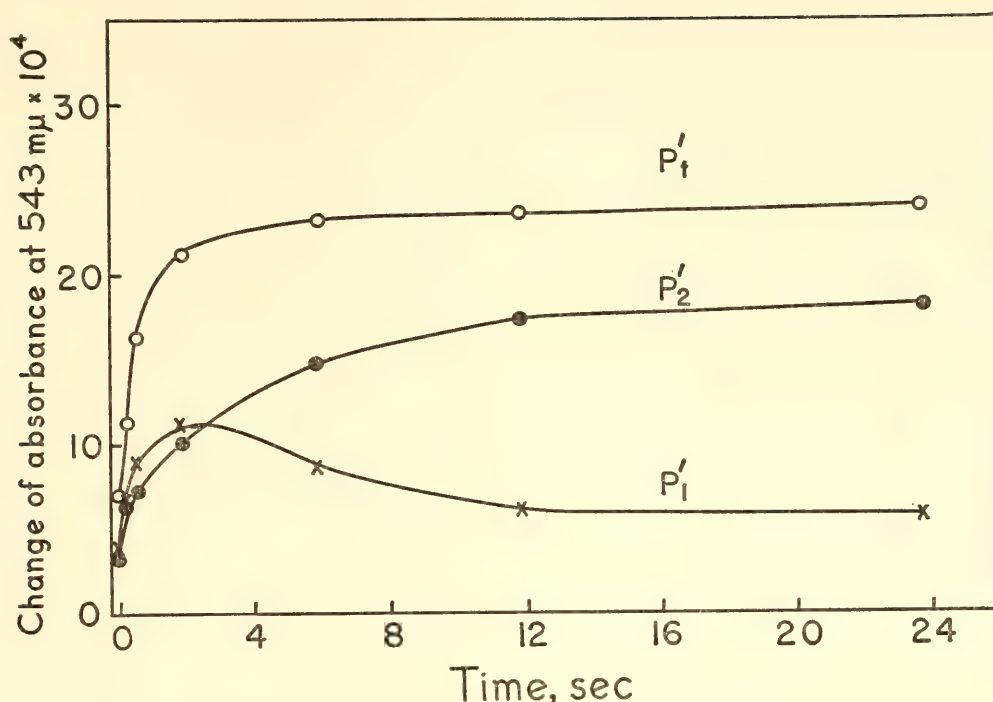
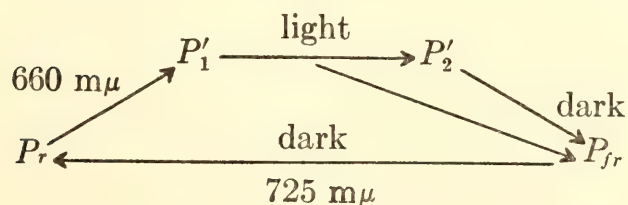


Fig. 34. Relative amounts of total intermediate ( $P'_t$ ),  $P_1'$ , and  $P_2'$  vs. exposure time. Intensity constant,  $1.33 \times 10^6$  ergs  $\text{cm}^{-2} \text{sec}^{-1}$ .

amounts of each form present at the end of the light period as a function of exposure time are plotted in Fig. 34. The upper curve shows total  $P'$  ( $P'_t$ ), while the lower curves show  $P_1'$  and  $P_2'$ .  $P_1'$  appears rapidly, reaches its maximum concentration after about two seconds, and then declines.  $P_2'$  appears more slowly, and continues to increase while  $P_1'$  declines. The most logical explanation for these changes is that  $P_1'$  is being transformed to  $P_2'$  by light. Thus the steady-state level of  $P_1'$  is substantially lower than the level reached within the first two seconds of illumination. According to Linschitz *et al.*,  $P'_t$  decays only to  $P_{fr}$ .

The following kinetic scheme accounts for the observations made to date:



The rapid rise in concentration of  $P_1'$ , and the subsequent decrease that accompanies the increase in  $P_2'$  concentration suggests

that  $P_2'$  is formed from  $P_1'$  by a light reaction. Nothing is known about the action spectrum for this proposed light reaction. The kinetics require that decay of both components must proceed independently by first-order reactions.

Analyses similar to those shown in Fig. 33 were made of experiments in which the light-exposure time was kept constant, at six seconds, and the amount of  $P'_t$  was varied by varying intensity. Over a three-fold intensity range, the  $P_1'/P_2'$  ratio remained constant at the end of the six-second exposure. The results are consistent with the kinetic scheme proposed above. Thus, when one varies  $P'_t$  by keeping intensity constant and increasing exposure time, the increased decay half-time measured for  $P'_t$  represents a decrease in the ratio of  $P_1'$  to  $P_2'$ . When one varies  $P'_t$  by keeping exposure time constant and varying intensity, the half-time appears independent of  $P'_t$  concentration, since the ratio of  $P_1'$  to  $P_2'$  is independent of intensity, at least over the range of intensities used, and the decay of both components is first order.

Not shown in either Fig. 33 or Fig. 34 is the appearance of a very small amount of



a third and still more stable form of  $P'$  with 24-second exposures. The amount found was far too small for detailed kinetic analysis. Nevertheless, longer exposure time may produce more quantitative information about it.

*Effect of temperature on phytochrome transformation.* On two occasions phytochrome samples were intentionally allowed to warm from the normal experimental temperature of 4°C–5°C to room temperature (24°C). Temperature was continuously monitored by means of a thermistor probe inserted into the sample. On both occasions half-times were determined for three reactions: (1) decay of  $P'_t$  following 12 seconds, 100 per cent actinic light, (2) transformation of  $P_r$  to  $P_{fr}$ , and (3) transformation of  $P_{fr}$  to  $P_r$ . The  $Q_{10}$  for complete pigment transformation in either direction was almost exactly 1 (1.0 in one experiment, 1.06 in the other). The  $Q_{10}$  for  $P'_t$  decay—probably primarily  $P'_2$  following 12-second illumination (see Fig. 34)—was between 1.9 (4°–14°C) and 2.3 (14°–24°C). The amount of  $P'_t$  present at the end of the 12-second exposure decreased considerably with increasing temperatures because of the increased decay rates. Thus it was not possible to separate the temperature dependence of  $P'_1$  and  $P'_2$  decay by kinetic analysis, since the absorption changes were too small for accurate measurement at the higher temperatures. Activation energies, therefore, could not be calculated for the two reactions, but it is possible to state that under the conditions used in these experiments for complete transformation of  $P_r$  to  $P_{fr}$  and back, dark decay of the intermediates was not a rate-limiting step.

*Failure to obtain complete transformation of  $P_r$  to  $P_{fr}$ .* When phytochrome was driven by far-red light as far as possible into the red-absorbing form (as determined by the absence of any further absorbance increase at 543 m $\mu$ ) and the far-red light was turned off, there was no further change in absorbance. But when

$P_r$  was driven as far as possible toward  $P_{fr}$  by red light, and the red light was then turned off, characteristic decay of the intermediate could be seen. Thus the suggestion of the Beltsville group, based on physiological evidence and absorption spectra, that overlapping absorption of both  $P_r$  and  $P_{fr}$  at 655 m $\mu$  should prevent complete transformation to  $P_{fr}$ , is verified by direct measurement of intermediate red-light treatment at the end of extended red-light treatment. Even with red light alone some cycling of the pigment system is revealed. No such cycling could be detected with far-red actinic light.

#### ELECTROMOTIVE-FORCE MEASUREMENTS WITH A GLASS-MEMBRANE ELECTRODE

*James H. C. Smith*

Experiments carried out during the past year were aimed at the determination of phosphate ion by means of a glass electrode. At present there seems little likelihood of obtaining a glass electrode specific for estimating phosphate ion directly, but the possibility exists for determining it indirectly. If an electrode is found that responds quantitatively to an ion whose concentration is controlled by phosphate ion, the goal of determining phosphate ion electrochemically may be achieved.

Calcium-ion concentration is controlled by phosphate-ion concentration in a solution saturated with calcium phosphate through operation of the solubility-product relation. The basis of this relation is that the calcium-ion concentration is inversely proportional to the phosphate-ion concentration. Under some conditions where phosphate ion is being consumed, as in certain biological processes, the calcium-ion concentration will increase, and this increase will be registered through electromotive-force (EMF) changes.

In recent years glass electrodes have been developed that are relatively specific for sodium, potassium, and silver ions.



A calcium-ion glass electrode now seems within reach. (Truesdell and Pommer, 1963; and Garrels *et al.*, 1962). Thanks to Professor R. M. Garrels, Harvard University, and to N. C. Herbert, Corning Glass Works, a sample of Corning Glass No. 916-P responsive to calcium ion was obtained. The glass is being tested for its suitability to estimate calcium ion directly and phosphate ion indirectly. It was ground to membranes from 0.05 mm to 0.07 mm thick by Ruperto Laniz of the Petrography Laboratory, Stanford University. Each membrane was sealed with Lakeside 70 cement to the plane-ground end of a glass tube, 10 mm in diameter and 100 mm long. The tube was filled with either sodium or potassium chloride (KCl), 1.0 *M*, into which a Beckman calomel electrode was dipped. This assembly served as cathode. Another Beckman calomel electrode served as anode. The voltages that developed between these electrodes when immersed in various ionic solutions were measured and correlated with the concentrations. A model G Beckman *pH* meter was used for measuring the EMF.

Fortunately this electromotive-force cell was relatively insensitive to change in hydrogen-ion concentration. As expected from the work of others, it was sensitive to sodium, potassium, and calcium ions. The work this year has centered on evaluating the electrode's electrochemical response to individual ions and mixed ions in various concentrations.

Unfortunately several difficulties developed in the use of the electrode: (1) The seal between membrane and tube was easily ruptured. (2) The reproducibility of response was poor; measurements of the same solution at various times gave different EMF values. (3) At times the change of voltage with concentration was consistent, but at other times this also varied. (4) The sensitivity of the electrode deteriorated with time. (5) The response time varied.

These obstacles to reliable measurements have not been overcome but some

progress has been made in removing them: (1) Paraffining the seal strengthens it greatly. (2) Properly cleaning the containers for the solutions with organic solvents, acids, etc., rather than with detergents, decreases variability. (3) Wiping the exposed surface of the membrane with organic solvents—dioxane, methanol, petroleum ether—often restores sensitivity of response. Such small details are evidently important for successful operation of the electrode.

Although definitive measurements cannot be reported, the general behavior of the electrode corresponds to the results reported in the articles cited. The simplest mathematical expression for EMF vs. concentration for a single univalent salt is (Rechnitz, 1965)

$$E = E^{\circ} + (RT/nF) \ln ([A^{+}] + K [B^{+}])$$

which reduces to

$$E = E^{\circ} + k \log ([A^{+}] + C)$$

(see also Fig. 35)

where  $E$  is the measured EMF;  $E^{\circ}$ ,  $k$ , and  $C$  are constants; and  $[A^{+}]$  is the concentration of the univalent cation. Results obtained with KCl at various concentrations from  $10^{-1}$  to  $10^{-4}$  molar are compared with a calculated curve in Fig. 35, curve 1. From the reasonably good agreement of the experimental points with the curve, it is clear that this type of equation is applicable.

Figure 35 shows the effects of mixed salts on the EMF of the glass-membrane electrode. Curves 1 and 2 were obtained with solutions containing the individual salts KCl and calcium chloride ( $\text{CaCl}_2$ ); curves 4 and 5 were obtained with various KCl concentrations in solutions containing different fixed concentrations of  $\text{CaCl}_2$ . Curve 3 shows the effect of various KCl concentrations in solutions saturated with calcium phosphate  $[\text{Ca}_3(\text{PO}_4)_2]$ .

It is evident that the  $\text{CaCl}_2$  concentrations control the voltage obtained until the KCl concentration exceeds the  $\text{CaCl}_2$  concentration. Furthermore, the difference in EMF between the two curves at



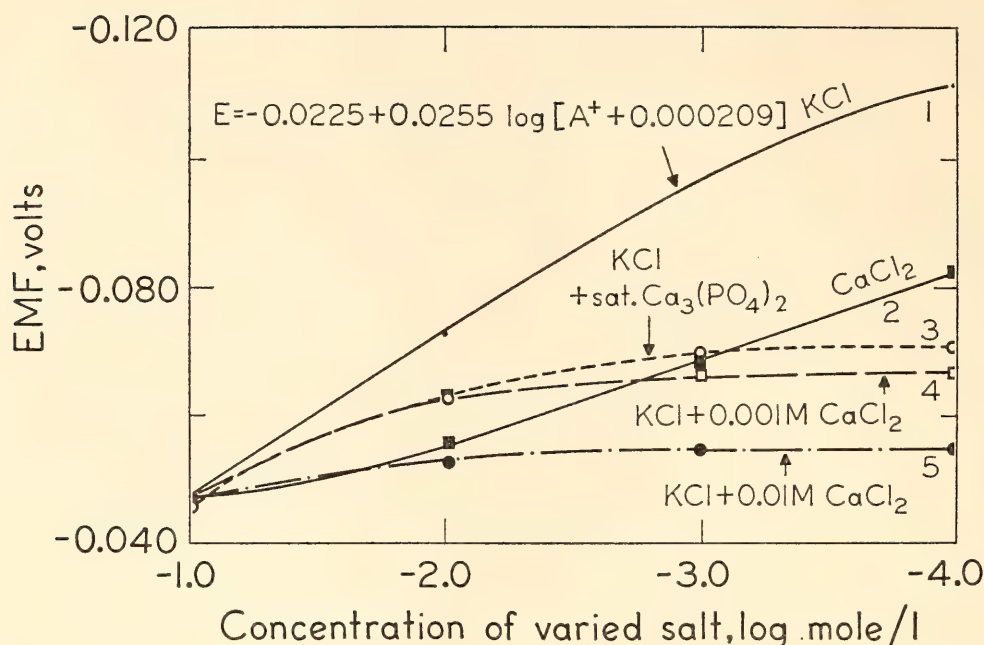


Fig. 35. A plot of the EMF measurements with Corning Glass electrodes (196-P) against logarithms of the concentrations of various electrolyte solutions (see text).

low or zero concentrations of KCl is the same as the difference in EMF between the two concentrations of  $\text{CaCl}_2$  alone. The behavior is what would be expected with mixed salts.

From the curves it is evident that the calcium ion from  $\text{Ca}_3(\text{PO}_4)_2$  is less than  $10^{-3}$  but greater than  $10^{-4}$  molar. Calculation puts the value at  $4.9 \times 10^{-4}$ , which is in reasonable agreement with the calcium-ion concentration,  $5.43 \times 10^{-4}$  molar, calculated from the data of Holt, LaMer, and Chown (1925) for solutions saturated with  $\text{Ca}_3(\text{PO}_4)_2$  at pH 6.15, the experimentally determined pH for our solutions.

The conclusion is that the Corning Glass membrane, 916-P, may prove satisfactory for the electrochemical estimation of phosphate indirectly.

#### INSTRUMENTATION

C. S. French

Some years ago the equipment used for measuring fluorescence spectra was taken apart and its components built into an apparatus for measuring action spectra of photosynthesis. We are now setting up an

improved apparatus for measuring fluorescence spectra.

We wish to investigate the fluorescence spectra and the relative efficiency of energy transfer between pigments in the fractionated preparations of photosynthetic pigments obtained by Brown and Bril.

During the year Adolph Fejfar, a Stanford University student in electrical engineering, helped to improve the performance of the curve analyzer. The major improvement is in the wave form of the signal voltage. It was previously taken directly from the power line but now is passed through a tuned power amplifier. The instrument operated well in the analysis of derivative spectra of fractionated pigment-protein complexes.

Several years ago we had developed a simple model scheme to describe the interaction of the two pigment systems of photosynthesis in *Porphyridium*. With a borrowed analogue computer we explored the response of the model to changes in the values of the assumed constants. That model gave hypothetical time-course curves for  $\text{O}_2$  evolution very similar to those measured in *Porphyridium* (Year

*Book 60*, pp. 357–362). Last summer, William Griswold, a recent Stanford University graduate in biology, similarly investigated other models. A small Donner analogue computer was purchased and we plan to expand its capacity for multiplication.

No further work has been done on the surveying instrument described in *Year Book 62* (pp. 382–386) and again mentioned in *Year Book 63* (pp. 488–489) during the year.

The Research Corporation has taken over the responsibility for attempting to find a commercial developer of the device. The eventual profits, if any, are to be divided equally between the Research Corporation and Carnegie

Institution. We are most fortunate that the Research Corporation was willing to undertake this venture, since our own attempts to find a competent organization interested in pursuing the matter were not successful.

An instrumentation problem of great concern to us which has not yet been solved is to design a rate-measuring electrode of the Blinks type into which reproducible amounts of an algal or chloroplast suspension may be serially introduced. Such an electrode could make rapid comparable rate measurements of oxygen evolution, from aliquots of a single suspension, with the speed of response only achievable by electrical methods.

## EXPERIMENTAL TAXONOMY INVESTIGATIONS

Substantial advances in three principal areas of our multiple approach to the study of plant relationships were made during the current year. Comparative physiological studies of ecological races were strongly accelerated when Olle Björkman joined our group, introducing the techniques and plant materials that he and his collaborators had used previously at Uppsala, Sweden.

Physiological studies on the mechanics of light utilization by races of *Solidago* were continued, and related measurements were made on races of *Mimulus cardinalis*. Races of *Mimulus lewisii* from high altitudes show photosynthetic characteristics that distinguish them from races of *M. cardinalis* that grow at lower elevations.

Continued cytogenetic studies on intraspecific and interspecific hybrids in the Erythranthe section of *Mimulus* reveal important new details that greatly clarify basic biosystematic relationships in this evolutionally close-knit but ecologically diverse section of the genus.

The aseptic culture in vitro of excised portions of *Mimulus* plants has advanced sufficiently to show clearly the value of

this technique for comparative physiological and biochemical study of ecologically diverse races and species. A composite picture resulting from such diverse experimental approaches centering on the *M. cardinalis-lewisii* species-complex will be the subject of a new monograph in the series "Experimental Studies on the Nature of Species."

Clausen has studied further the ecological aspects of the Harvey Monroe Hall Natural Area. Attention was given to the diversity of races within the native species and to microclimatic differences existing in the area.

### COMPARATIVE PHYSIOLOGICAL STUDIES OF ECOLOGICAL RACES OF *Solidago*

*Olle Björkman*

Ecological races of *Solidago virgaurea* from shaded and exposed habitats differ strikingly in their response to light intensity during leaf development (Björkman and Holmgren, 1963).

Plate 1 illustrates the response of two clones brought from dormancy to active growth in controlled environments in growth chambers. Each clone was grown



under both low and high light intensity. The clone native to shaded environments grows rapidly under low light intensity but under high intensity growth is markedly retarded. In contrast, the clone native to exposed environments grows rapidly under high intensity. Under low intensity the leaves of this clone at first develop at a moderate rate, but the longer the plants are kept under low light intensity the slower the rate of leaf development becomes. After a period of several weeks no further growth can be observed, presumably because of the depletion of stored food.

In clones native to shaded environments, leaves grown under high light intensity show a greatly reduced slope of the linear part of the curve for photosynthesis as a function of light intensity, compared with leaves of the same clone grown under low intensity. This and other evidence indicate that the light-absorbing part of the photosynthetic machinery is severely impaired by high intensity during leaf development. The detrimental effect becomes greater with longer exposure of the leaves to high light intensity.

In clones native to exposed environments the slope of the linear part of the curve for photosynthesis as a function of light intensity is about the same regardless of whether the light intensity under which the leaves were grown is high or low. There is no evidence of a detrimental effect of high light intensity on the clones native to an exposed environment. The photosynthetic rate at saturating light intensities is considerably higher when the leaves of clones from exposed habitats have developed under high light intensity. This has tentatively been ascribed to a higher capacity of enzymatic processes.

The current investigations are designed to isolate in greater detail the parts of the photosynthetic machinery that are damaged by high light intensity in clones from shaded environments, in comparison with the contrasting response to light

intensity of clones from exposed environments.

The action spectrum for  $\text{CO}_2$  uptake and the spectrum for light absorption measured on the same leaf show that not only a lowered capacity for capturing light incident upon the leaf, but also a reduced yield per absorbed light quantum, is responsible for the low photosynthetic efficiency of clones native to shaded environments when grown under a high light intensity. In leaves developed under low intensity the action spectrum is at a maximum close to  $650\text{ m}\mu$ , whereas the absorption spectrum is at a maximum at about  $675\text{ m}\mu$ . In leaves developed under high light intensity the action spectrum closely follows the absorption spectrum (at  $\lambda > 580\text{ m}\mu$ ) and the maximum for both is at  $675\text{ m}\mu$ . The shift in the decline of quantum yield toward longer wavelengths when the leaves are grown under high intensity suggests a less efficient functioning of the short-wavelength system (system II).

One method for distinguishing between the functioning of the two photochemical systems is by measurement of changes in absorbance at  $591\text{ m}\mu$  that take place when the leaf is illuminated with light, preferentially exciting one or the other of the two systems. An independent and perhaps more direct method is the measurement of the Emerson enhancement effect on  $\text{CO}_2$  uptake. Both methods yield closely agreeing results. All measurements of action spectra, absorbance changes, and Emerson enhancement were made on individual leaves attached to intact plants.

#### *Measurements of the 591-m $\mu$ Absorbance Change*

*Olle Björkman, with  
David Fork and Wolfgang Urbach*

The light-induced absorbance change at  $591\text{ m}\mu$  was described by Fork and collaborators in previous *Year Books*. It is probably caused by changes in the redox level of plastocyanin, a copper pro-

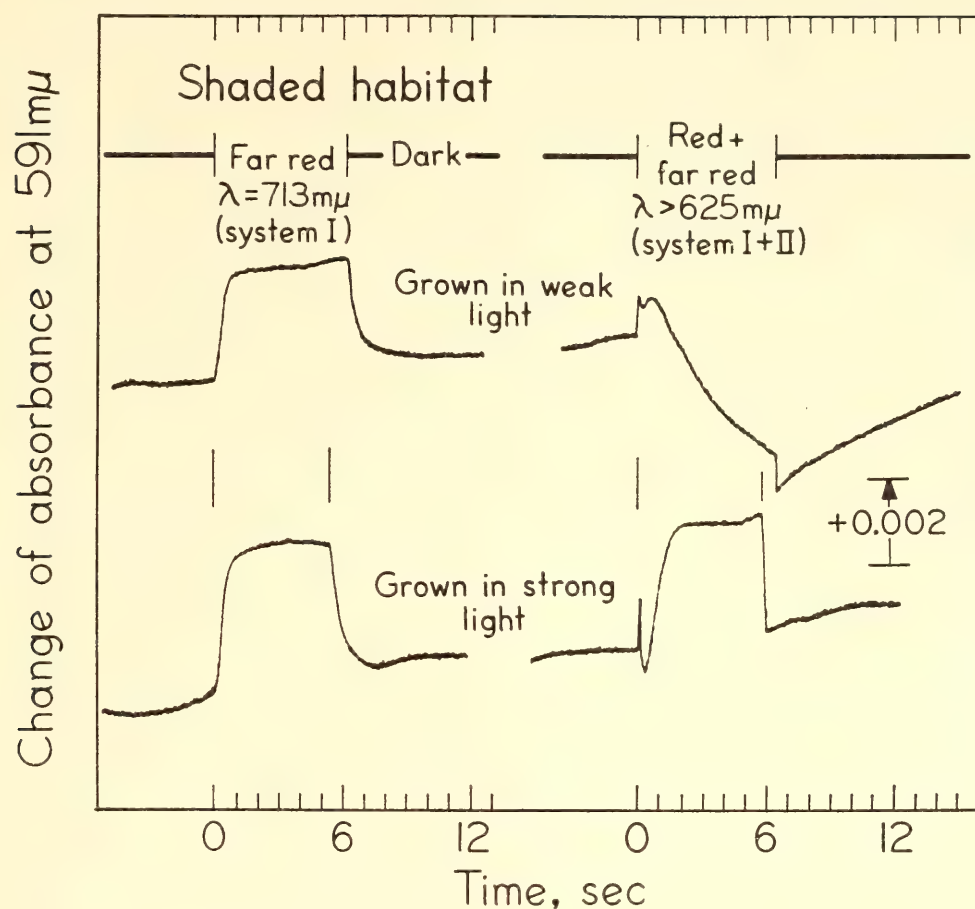


Fig. 36. Effect on the 591-m $\mu$  absorbance change of growing same clone native to a shaded habitat of *Solidago virgaurea* in weak and strong light. All measurements shown in figures were made on mature leaves attached to the plant.

tein believed to function between the two systems in the electron carrier chain. Excitation of system I causes an oxidation of plastocyanin resulting in an increased absorbance. Excitation of system II reduces plastocyanin, thus giving a decrease in absorbance.

Figure 36 shows the response of clone HV 124 native to a shaded habitat on Hallands Väderö, in southern Sweden. The effect produced by far-red light alone (which excites primarily system I), is about the same, regardless of the light intensity under which the leaves are grown. In contrast, the effect produced by far-red + red light (which would excite both systems I and II) differs strikingly between leaves that are grown under low and high light intensities. In leaves developed at low intensity, a net reduction takes place during the light

exposure, which indicates a strong functioning of system II; in those developed under high intensity, the result is net oxidation, indicating that the activity of system II is very weak in comparison with system I. Apparently the functioning of system II is impaired when leaves of this clone, native to a shaded environment, are grown at a high light intensity.

Figure 37 shows the response of clone B 039 native to an exposed habitat at Beskades, in northern Norway. Again the effect produced by far-red light alone (excitation mainly of system I) is about the same, regardless of the light intensity at which the leaves were grown. In this clone a strong reducing effect produced by system II when the leaf is illuminated with far-red + red light is seen in leaves grown under high intensity. However, leaves grown under low intensity show only a



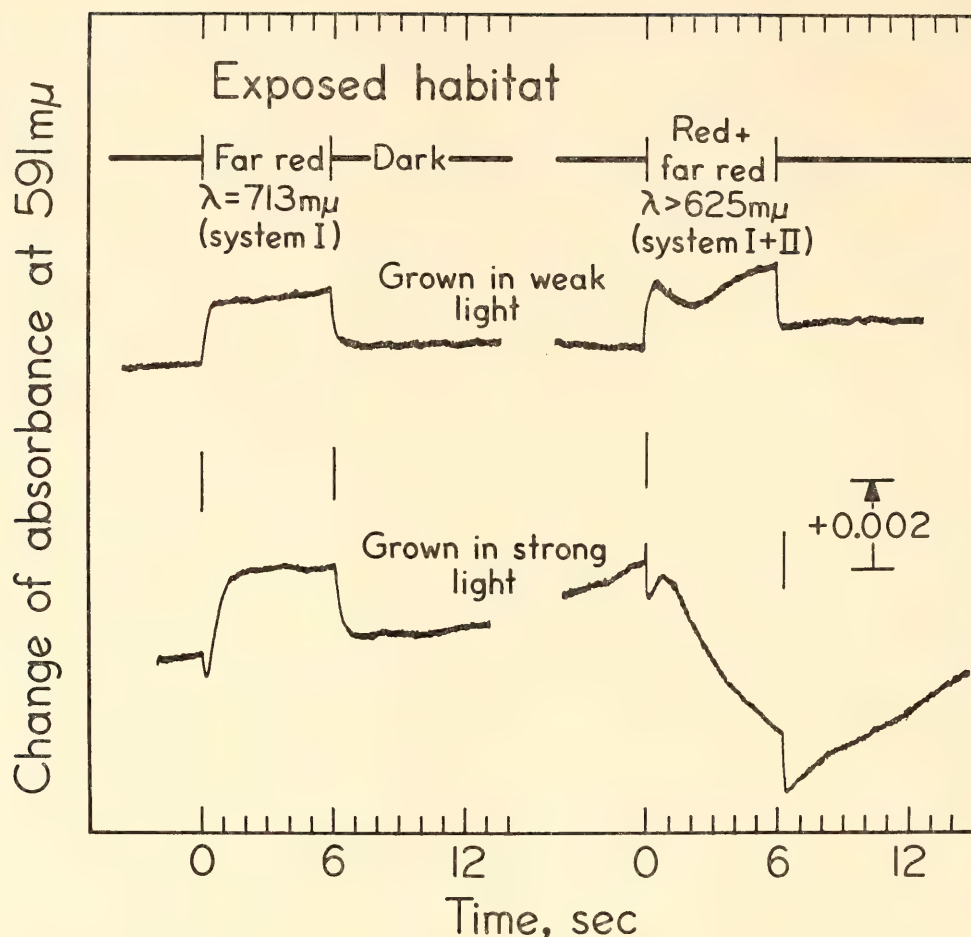


Fig. 37. Effect on the 591-m $\mu$  absorbance change of growing same clone native to an exposed habitat of *Solidago virgaurea* in weak and strong light.

slight reducing effect of system II, a reversal of the responses found on the clone from Hallands Väderö.

#### *Measurements of the Emerson Enhancement Effect*

The Emerson enhancement effect has been demonstrated on photosynthetic oxygen evolution in various algae, and also on TPN-reduction in isolated spinach chloroplasts. Although to our knowledge the Emerson enhancement of photosynthetic CO<sub>2</sub> uptake by intact leaves in higher plants has not been reported previously, it has generally been assumed a universal phenomenon common to all green plants. The measurement of action spectra of Emerson enhancement was therefore attempted in leaves of clone HV 124 originally from the shaded habitat, grown under both low and high light intensity. This was accom-

plished by using two light beams, one of a constant wavelength of 700 m $\mu$ , and one of a shorter wavelength. The two beams were superimposed on the same leaf by a beam splitter. The intensities of the two beams were adjusted so that the CO<sub>2</sub> uptake produced by the shorter wavelength beam alone was many times that produced by the 700-m $\mu$  beam alone. Enhancement is expressed as the rate of CO<sub>2</sub> uptake produced by the 700-m $\mu$  beam on a background of shorter selected wavelengths of light relative to the CO<sub>2</sub> uptake produced by the 700-m $\mu$  beam alone. Presumably this provides an expression for the action spectrum of system II. The greatest enhancement would therefore be expected to take place at about 650 m $\mu$ .

As shown in Fig. 38, leaves of clone HV 124 developed under low light intensity exhibit marked enhancement

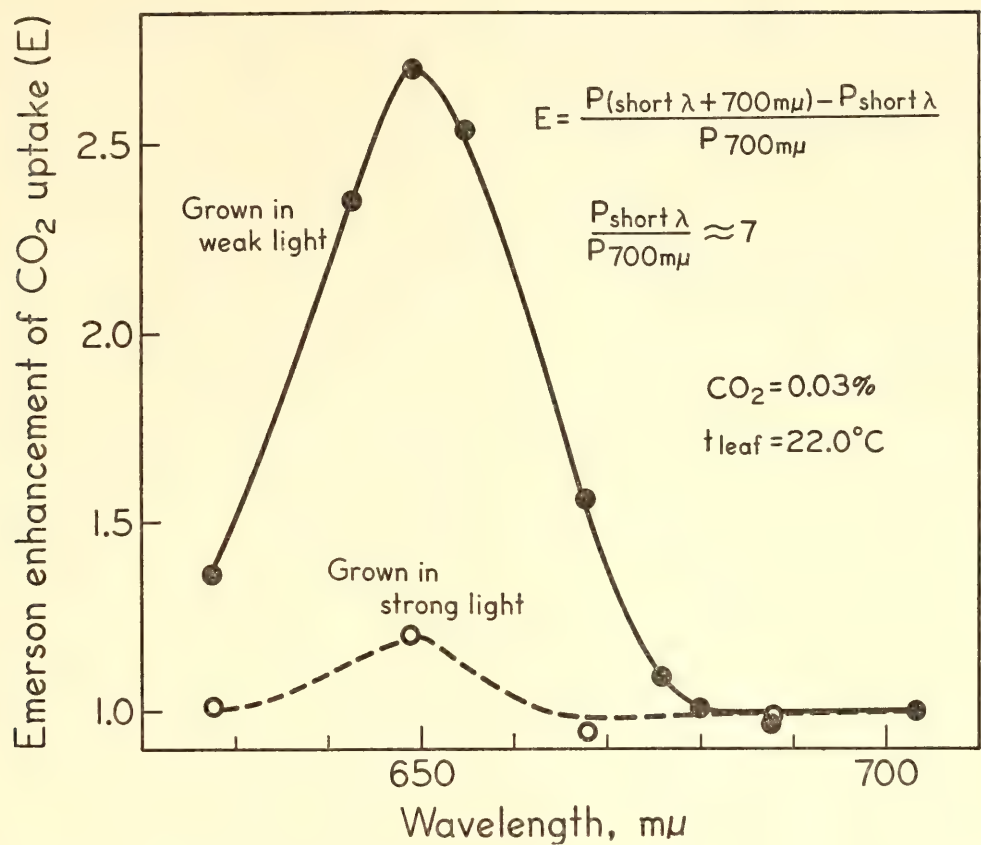


Fig. 38. Action spectrum for Emerson enhancement of CO<sub>2</sub> uptake of same clone from shaded habitat of *Solidago virgaurea*, grown in weak and strong light.

with a peak activity at about 650 mμ, thus indicating a strong functioning of system II. In contrast, leaves of the same clone developed under a high intensity show only a very weak enhancement. This evidence, together with the reduced yield per absorbed light quantum, indicates that system II operates with low efficiency.

**Conclusions.** When ecological races of plants native to shaded environments are grown at high light intensity, their photosynthetic efficiency is impaired. Results of several kinds of independent measurements consistently indicate that this impairment is attributable to an inactivation of system II. In contrast, genetically distinct ecological races of the same species native to exposed environments show a strong functioning of system II in leaves grown under a high light intensity.

The measurements of light-induced changes in absorbance indicate a weak activity of the reaction caused by system

II in the exposed habitat clone when grown under low intensity. A tempting hypothesis is that this phenomenon is a direct effect of a poorly developed system II in leaves that have been grown under a low light intensity. Nevertheless, the data on photosynthetic measurements indicate that the main difference between leaves developed under high and low intensities is a higher capacity of the former to utilize light of saturating intensities, whereas the efficiency in utilizing light of low intensities does not appear to vary markedly. It is difficult to understand why the capacity of a light reaction would influence strongly the photosynthetic rate at nonlimiting light intensities and not at the same time drastically affect the initial slope of the rate as a function of light intensity. One likely theory is that enzyme-controlled reactions are involved. Measurements are planned of the activity of photosynthetic enzymes, particularly ribulose diphosphate carboxylase, further



investigating the differences in photosynthetic performance between leaves of clones from exposed habitats, grown under high and low light intensities.

#### LIGHT UTILIZATION IN ECOLOGICAL RACES OF *Mimulus cardinalis*

Olle Björkman, William M. Hiesey,  
and Malcolm A. Nobs

Previous studies (*Year Book 61*, pp. 313–317) show that differences in photosynthetic rate among climatic races of *Mimulus cardinalis* can be demonstrated when light intensity, temperature, or carbon dioxide (CO<sub>2</sub>) is varied.

Such results raise questions regarding the basic mechanics of light absorption and utilization in photosynthesis by leaves of higher plants, a subject still inadequately understood. Answers to these questions are essential for a critical interpretation of any kind of observed photosynthetic response of a given ecological race to a particular environment. The current studies are directed toward clarifying the problem.

The mechanics of light utilization in photosynthesis may be resolved into three major steps: (1) the capacity of leaves to capture light energy, (2) the efficiency of the photochemical processes in light utilization, and (3) the capacity of enzyme-controlled dark processes and of CO<sub>2</sub>-diffusion processes that limit the rate of CO<sub>2</sub> uptake at saturating light intensities. The present report is concerned only with the first two steps; the third will be the subject of a later discussion.

There is now abundant evidence that the photosynthetic performance of an individual plant may be considerably modified by the light intensity during the development of the leaf. In *Solidago virgaurea* the modifications are profound and they differ greatly among ecological races from contrasting environments, as described in the preceding section. Preconditioning to light intensity is therefore given special emphasis in the present study on two clones of *M. cardinalis*.

One clone was of the Jacksonville race from the warm region of the Sierra Nevada foothills, the other of the San Antonio Peak race from a 2,600-meter altitude in southern California. These races represent extremes within *M. cardinalis* in regard to original habitat, response to transplanting at the altitudinal stations, and leaf morphology. The two clones were grown in controlled cabinets at a high and a low light intensity,  $1.5 \times 10^5$  and  $3 \times 10^4$  ergs cm<sup>-2</sup> sec<sup>-1</sup> (about 5,000 and 1,000 foot-candles), respectively. The light was from Sylvania VHO cool white fluorescent tubes supplemented with incandescent lamps. Illumination for 16 hours at 22°C was followed by 8 hours' dark at 15°C each day. The plants were grown in perlite, a chemically inert medium, with nutrient solution added. Air humidity was uncontrolled.

The growth response of the two clones to different light intensities is shown in Plate 2. While both clones grow well under both low and high light intensity, the growth rate is greater under the high light intensity, especially in the high-altitude San Antonio Peak race. Under the high intensity the leaves of both clones are thicker than under the low, as shown in Fig. 39. Fewer intercellular spaces occur in leaves grown under high intensity in both clones, and in the San Antonio Peak clone an extra layer of palisade parenchyma is developed.

*Light absorption.* The light-intercepting capacity (absorptance) of the leaves was measured in an Ulbricht integrating sphere at a number of photosynthetically active wavelengths. A quartz-iodine lamp (Sylvania DWY), appropriate lenses, heat filters, and interference filters (Balzer Filtraflex, half-bandwidth 10 mμ) provided the monochromatic light beams. The absorptance  $A_\lambda$  at each wavelength  $\lambda$  was computed by the expression  $A_\lambda = 1 - (T_\lambda + R_\lambda)$  where  $T_\lambda$  is the spectral transmittance and  $R_\lambda$  is the spectral reflectance of the leaf.

Although the spectral properties of a

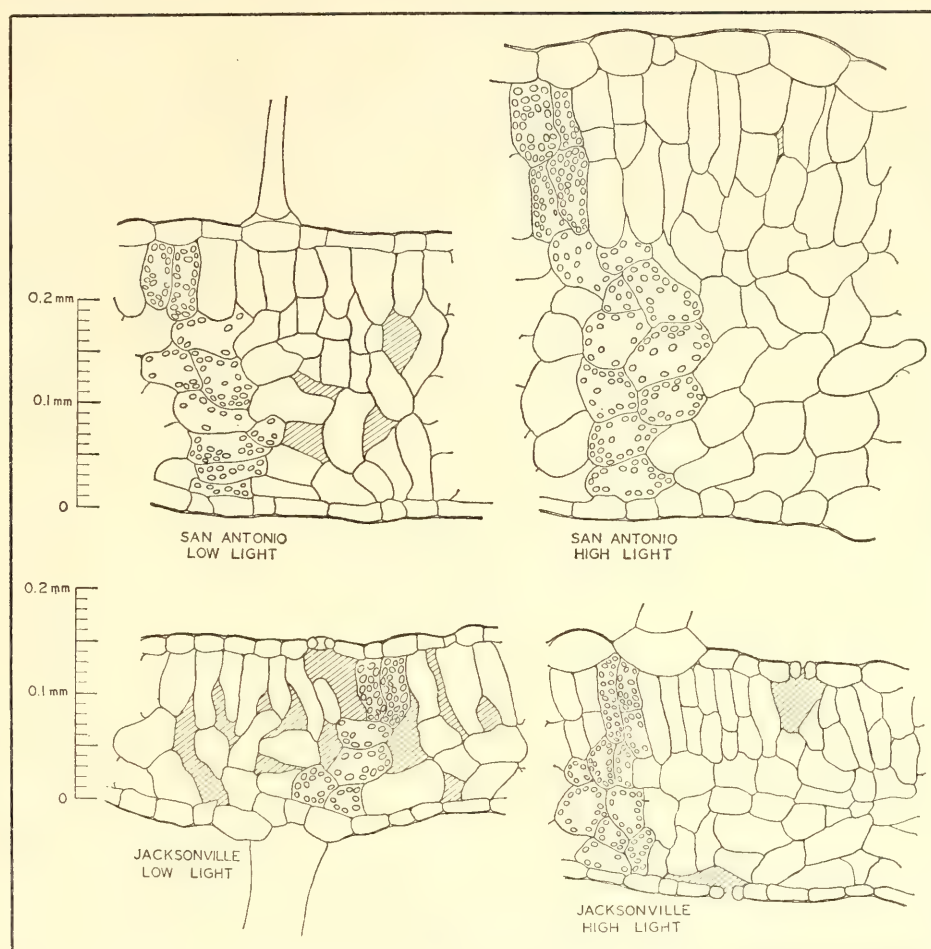


Fig. 39. Sections of fully expanded leaves of Jacksonville and San Antonio Peak clones of *Mimulus cardinalis* grown under low and high light intensity. Cross-hatched areas indicate intercellular spaces.

leaf are influenced by its structure, the approximate relation between its absorptance and its pigment content can be expressed as  $A_\lambda = 1 - e^{-k_\lambda c}$ , where  $e$  is the base of the natural system of logarithms,  $k_\lambda$  is a constant at wavelength  $\lambda$ , and  $c$  the amount of pigment per leaf area. An increase either in the concentration of pigment-per-leaf volume or in the thickness of the leaf will thus increase the absorptance. At normal chlorophyll concentrations the effect of an increase in pigment on the absorptance is smaller at wavelengths where the absorptance is high than at those where it is low. The increase in total absorptance that results from an increased chlorophyll content will therefore be due mainly to a broadening of the absorption bands.

The absorption characteristics of the two races grown at low and high light

intensities are shown in Figs. 40 and 41. The greater thickness of the leaves in each clone when grown at high light intensity is correlated with a higher absorptance. Similarly, when compared at the same light intensity, the thicker leaf of the San Antonio Peak race has a higher absorptance than one of the Jacksonville clone. As expected from the equation given above, the differences in absorption between the leaves lie mainly in the wavelength region between the major absorption peaks of the chlorophylls, and in the far-red region.

*Action spectra and quantum yields.* At low light intensities  $\text{CO}_2$  uptake is linearly related to light intensity (the Kok effect excepted) and the efficiency of light conversion is at a maximum. The capacity of the photochemical part of the photosynthetic processes is limiting the



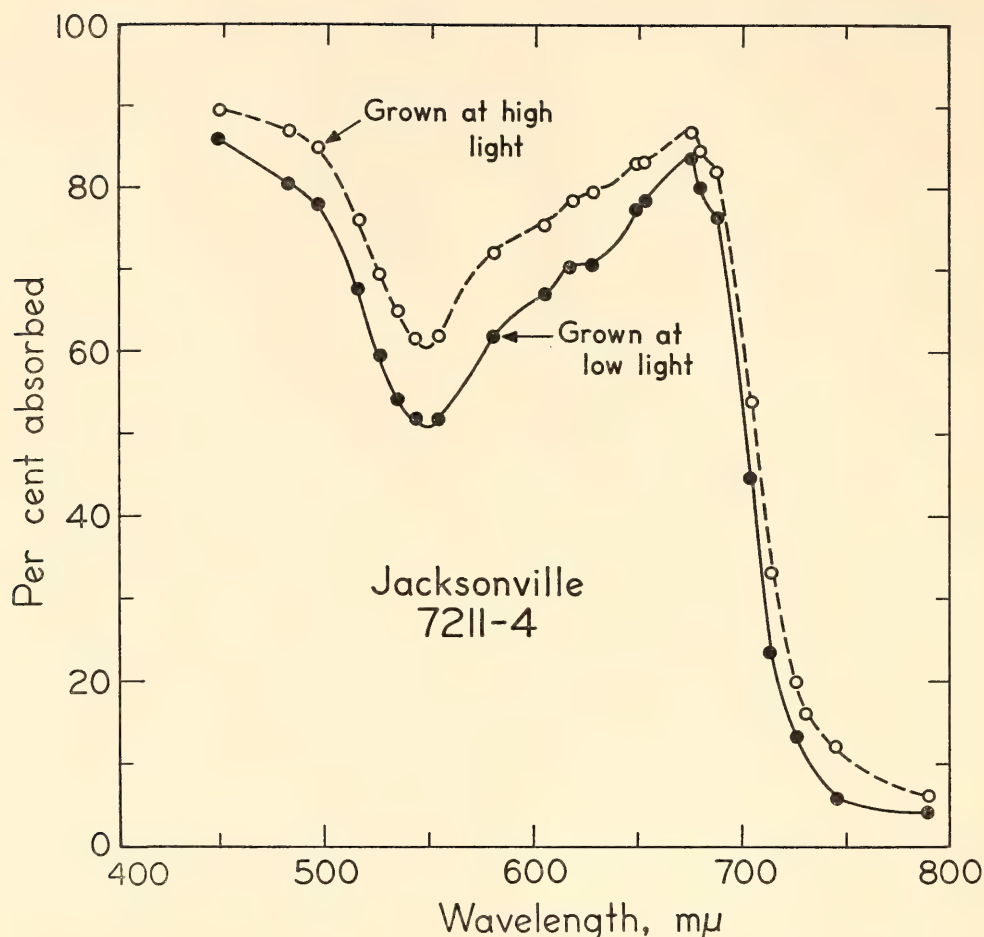


Fig. 40. Spectral absorbance of leaves of Jacksonville clone of *Mimulus cardinalis*, grown at low and high light intensity.

photosynthetic rate. It can be measured as the number of moles of  $\text{CO}_2$  absorbed per mol quantum of light incident upon the leaf.

The rate of  $\text{CO}_2$  uptake as a function of wavelength was measured with the apparatus previously described (*Year Book 63*, pp. 430–431). Monochromatic light was obtained as in the leaf absorbance measurements described above. The light intensity was adjusted so that at each wavelength  $2 \times 10^{15}$  quanta  $\text{cm}^{-2} \text{sec}^{-1}$  were incident on the leaf. In this intensity region the steady-state uptake of  $\text{CO}_2$  was a linear function of light intensity at all wavelengths; action spectra that were measured by adjusting the number of incident quanta, so that the same rate was obtained at all wave-

lengths, were the same as those obtained when the number of quanta was kept constant and the rate measured. All measurements were made at  $22^\circ\text{C}$  and with 280 ppm–320 ppm  $\text{CO}_2$ . Under the experimental conditions the rate of  $\text{CO}_2$  uptake was independent of its concentration. Young but fully expanded leaves attached to the intact plant were used in all determinations of action spectra.

Action spectra of  $\text{CO}_2$  uptake for the same leaves, used in the absorbance measurements, are shown in Figs. 42 and 43. All the curves have a maximum close to  $650 \text{ m}\mu$ ; the position of the minimum varies from about  $520 \text{ m}\mu$  to  $550 \text{ m}\mu$ . Within each clone the efficiency in utilizing incident light energy is higher

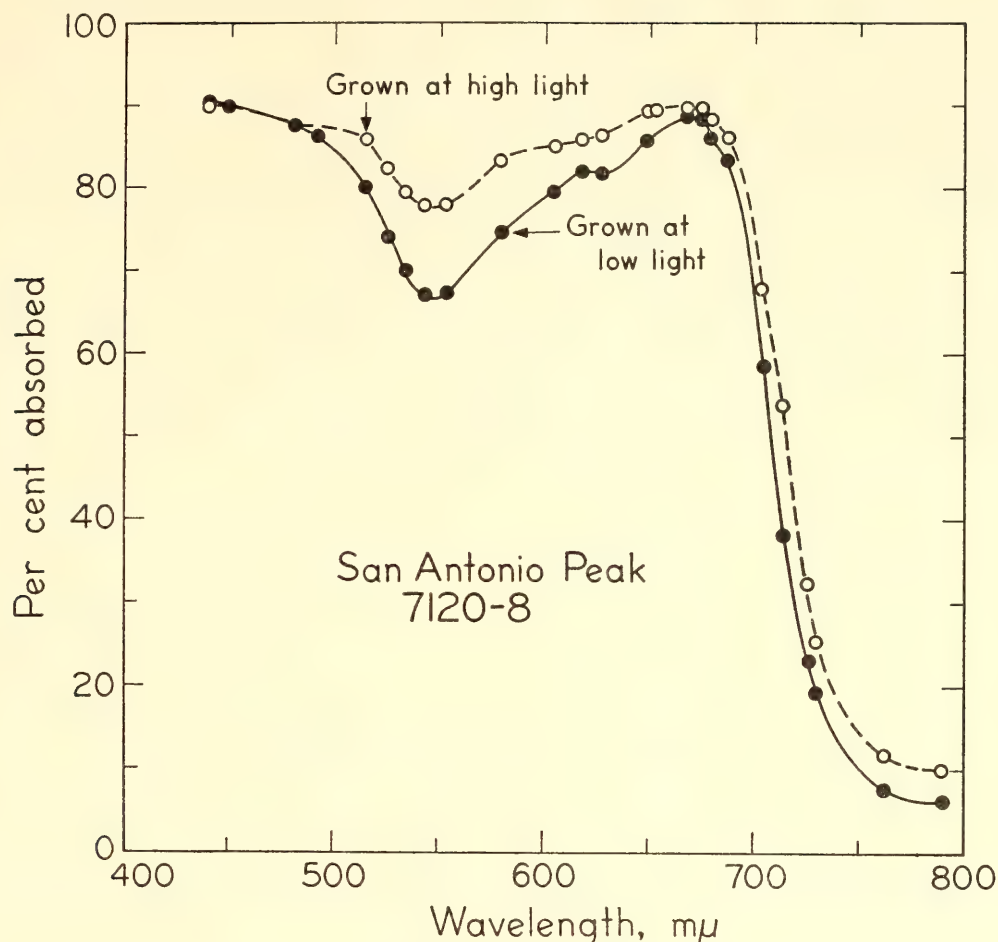


Fig. 41. Spectral absorbance of leaves of San Antonio Peak clone of *Mimulus cardinalis*, grown at low and high light intensity.

when the leaves are developed under high light intensity. At a given light intensity the San Antonio Peak clone has a higher efficiency than the Jacksonville clone. The curves for the efficiency of  $\text{CO}_2$  uptake per absorbed light quantum (quantum yield), also seen in Figs. 42 and 43, show that the differences in efficiency of utilizing incident light are entirely due to the differences in absorbance. The quantum yield is remarkably constant; both the wavelength dependence and the absolute value are essentially the same in both races and are not significantly influenced by the light intensity under which the leaves have grown.

The lower quantum yields at wavelengths  $< 550 \text{ m}\mu$  are in agreement with those found by other workers in green

algae, and have commonly been attributed to the absorption by carotenoids. Of particular interest is the drop in quantum yield at wavelengths  $> 655 \text{ m}\mu$ . Results on *S. virgaurea* described in the previous section support the supposition that this drop in quantum yield beyond  $655 \text{ m}\mu$  is due to a progressively decreasing absorption by system II in relation to that by system I beyond  $650 \text{ m}\mu$ .

**Conclusions.** The results clearly indicate that (1) the clones of the two races of *Mimulus* differ in their capacity to absorb light of photosynthetically active wavelengths; (2) the efficiency of utilizing incident light is directly proportional to the light-intercepting capacity of the leaf; and (3) the utilization of the light absorbed by the leaf, or quantum



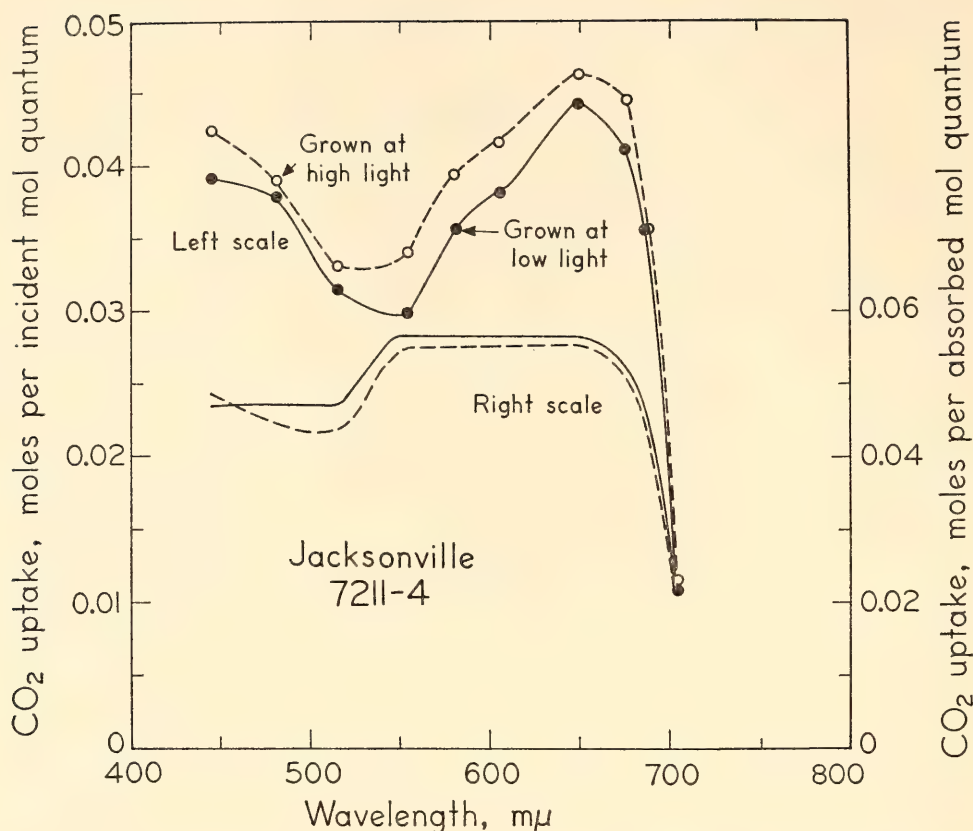


Fig. 42. Action spectra and quantum yields for photosynthesis of leaves of Jacksonville clone of *Mimulus cardinalis*, grown at low and high light intensity.

efficiency, is the same in both races and is independent of the light intensity under which the leaves have grown.

High light intensity during growth in both races increases the light-intercepting capacity of the leaves; this is attributable to an increased leaf thickness and thus longer path for the light, and not to an increased concentration of chlorophyll per leaf volume.

The difference in absorption between leaves grown under high and low light intensity corresponds exactly to the difference in light utilization of the photochemical processes of photosynthesis. The fact that the quantum yield is the same in leaves grown under high and low intensity shows that the photochemical part of the photosynthetic machinery in neither race of *M. cardinalis* is impaired by exposure to strong light during growth. Measurements of light-induced changes in absorb-

ance at 591  $m\mu$  and of the Emerson enhancement effect provide additional evidence of active functioning of both systems I and II in leaves grown at high light intensity (see the preceding section).

Both *Mimulus* races used in this study are found in open rather than shaded habitats, and both differ profoundly in their responses as compared with *S. virgaurea* from the shaded habitat of Hallands Väderö described in the preceding section.

Although the *Mimulus* races share more of the characteristics of the Beskades race of *Solidago* native to an exposed habitat, they differ in having a greater tolerance for low light intensity. Comparison between races of *Mimulus* and *Solidago* and of the two genera with regard to the capacity of processes that limit the photosynthetic rate at saturating light intensities is still to be made.

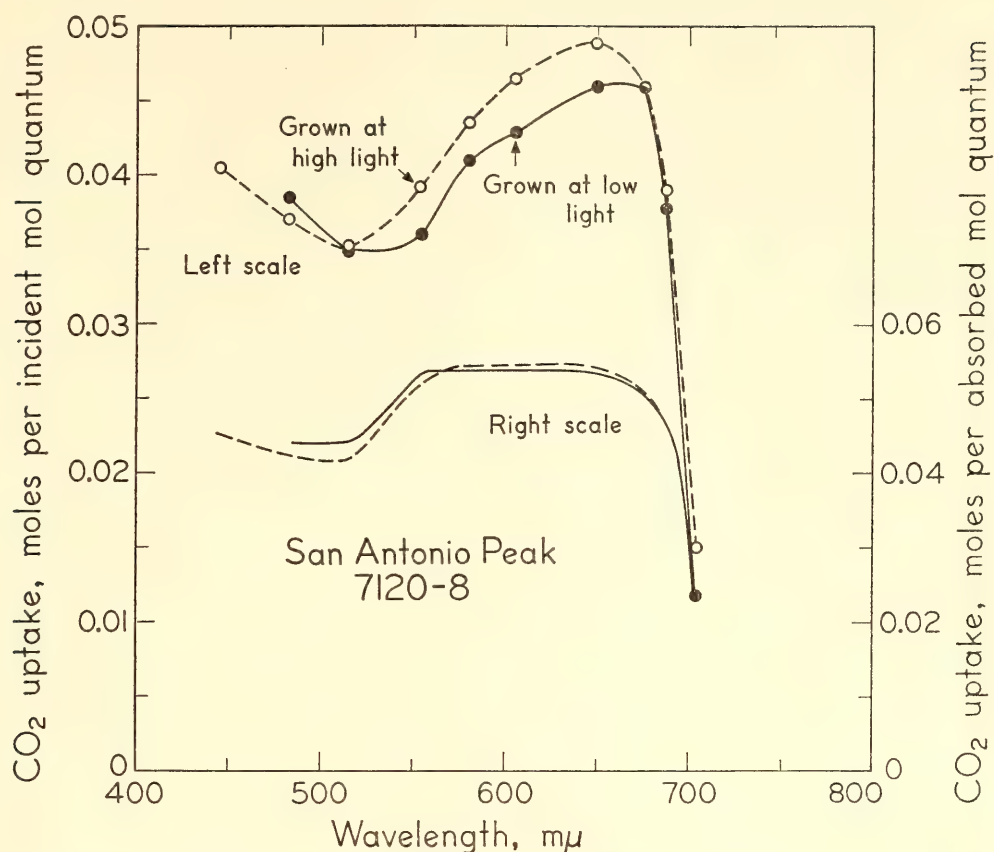


Fig. 43. Action spectra and quantum yields for photosynthesis of leaves of San Antonio Peak clone of *Mimulus cardinalis*, grown at low light intensity.

#### PHOTOSYNTHETIC RATES OF *Mimulus lewisii*

Harold W. Milner and William M. Hiesey

Preliminary measurements comparing the photosynthetic responses of *Mimulus lewisii* and *Mimulus cardinalis* were reported last year. Further work confirmed that the most striking difference between the components of the *M. cardinalis*-*lewisii* complex is in the reproducibility of photosynthetic rate measurements. Consecutively determined rates of *M. cardinalis* are nearly always the same, rarely differing as much as one per cent, whereas successive rate measurements on *M. lewisii* seldom agree within one per cent, usually showing random variations of several per cent.

Unidentified factors cause a difference in response of the photosynthetic mechanisms of *M. lewisii* and *M. cardinalis* to changing carbon dioxide ( $\text{CO}_2$ ) concentration. In our method of measuring

photosynthesis, the plant diminishes the available  $\text{CO}_2$  in a closed system for three minutes, and from the resulting change in  $\text{CO}_2$  concentration the rate of apparent photosynthesis is calculated. *M. cardinalis* accomplishes the same degree of  $\text{CO}_2$  depletion in successive trials; *M. lewisii* does not. We reach this conclusion because in Björkman's apparatus (Year Book 63, p. 430), in which measurements are made at constant  $\text{CO}_2$  concentration, both *M. lewisii* and *M. cardinalis* show steady photosynthetic rates. Furthermore, the photosynthetic rate of *M. lewisii* adapts more slowly to a change in light intensity or temperature than the rate of *M. cardinalis* does.

These circumstances dictate a different experimental regime to obtain rate measurements of *M. lewisii* that have the same precision as those readily obtained for *M. cardinalis*. The *M. lewisii* plant is maintained at the same temperature and light intensity for one hour after the



initial drift in photosynthetic rate has ceased. During this hour 15 to 20 rate measurements are made. The standard deviations of these rates from the mean and the probable error of the mean are computed. When the probable error of the mean is less than  $\pm 0.5$  per cent of the mean value, the mean is accepted as the rate under the stated conditions. Then, following a change in light intensity or temperature, the series of operations is repeated. In this way, rate vs. temperature and rate vs. light intensity curves are obtained for *M. lewisii*.

At first, rate measurements of *M. lewisii* were made with about 400 ppm CO<sub>2</sub>, the same as for *M. cardinalis*. To test whether the unsteadiness of *M. lewisii* rates might be caused by too much CO<sub>2</sub>, an effect found with *M. cardinalis* above 500 ppm CO<sub>2</sub>, the measurements were repeated with 250–300 ppm CO<sub>2</sub>. The random variation between consecutive rates was only a little less at the lower CO<sub>2</sub> level. Nevertheless, 250–300 ppm CO<sub>2</sub> was adopted for rate measurements of *M. lewisii*, in keeping with the lower available grams per liter of CO<sub>2</sub> at the high elevations where *M. lewisii* occurs as compared with the lower elevations of *M. cardinalis* habitats.

The long time required to observe the effect of changes in light intensity or temperature on the rate of *M. lewisii* demands consideration of possible changes in rate with time during the measurements. To this end, rate vs. time curves were measured for 12 hours' continuous photosynthesis with saturating light intensity and at different temperatures. Such curves are evaluated (*Plant Physiol.*, 39, 746, 1964) by a performance index (*PI*): the observed total CO<sub>2</sub> uptake in 12 hours expressed as the percentage of the calculated uptake in 12 hours at the maximum observed rate. The *PI* for 20 clones of *M. cardinalis* ranged from 82 to 95. For any one clone of *M. cardinalis*, the *PI* shows little change with temperature between 20° and 35°C. Here again *M.*

*lewisii* differs from *M. cardinalis*. The *PI* for one clone of *M. lewisii* at 20° and 2,560 footcandles was 77, whereas at 35° and 6,250 footcandles the *PI* was 95. The single *M. lewisii* clone at two temperatures shows a greater difference in *PI* than was observed among 20 clones representing six races of *M. cardinalis*.

The light intensity required to saturate photosynthesis of *M. lewisii* varies with temperature in a manner similar to that found for *M. cardinalis*. For example, a clone of the Tamarack Flat race, native at 1,830-meter altitude, shows light saturation at 1,640 footcandles at 10° and 7,800 footcandles at 35°. The highest saturation values found for *M. cardinalis* at these temperatures were 1,500 and 5,200 footcandles, respectively. Other data for *M. lewisii* also show a higher saturation intensity than for *M. cardinalis*.

Incomplete data for *M. lewisii* indicate that it and *M. cardinalis* reach their maximum photosynthetic rates at or near 30°C. The loss in rate below 10° and above 40° appears to be greater in *M. lewisii* than in *M. cardinalis*.

The rate measurements were made on *M. lewisii* plants raised in controlled growth chambers. One chamber is placed outdoors and receives natural illumination. The other is inside and is lighted for 12 hours per day at 1,200 footcandles by fluorescent lamps. The day temperature is 22°–25° and the night temperature 15°–17° in both cabinets. Clone members from the indoor and outdoor cabinets showed no significant difference in light saturation requirement or in the effect of temperature change on rate. This observation on *M. lewisii* is in agreement with the former finding that *M. cardinalis* grown in the greenhouse and in the controlled cabinets shows no real difference in photosynthetic behavior. It also confirms that races of *Mimulus* differ in this respect from the races of *Solidago* already discussed.

The data obtained so far point out



some similarities and some striking differences in photosynthetic responses of *M. lewisii* and *M. cardinalis*. When further data are obtained on clones and races of *M. lewisii*, a more quantitative expression will be given to the similarities and differences between the two.

CYTOGENETIC RELATIONSHIPS WITHIN  
THE ERYTHRANTHE SECTION  
OF *Mimulus*

Malcolm A. Nobs and William M. Hiesey

Earlier reports (*Year Books* 59, pp. 319–322; 60, pp. 381–386; 62, pp. 387–391; 63, pp. 432–435) emphasize the genetic segregation, the recombination and coherence, and the transplant responses in hybrid derivatives among highly interfertile altitudinal races of the *Mimulus cardinalis-lewisii* complex, members of the Erythranthe section of the genus *Mimulus*. This section is a closely related group of six species among the some 140 species in the genus. New cultures of interspecific and intraspecific hybrids provide critical data that clarify the broader relationships between species of the Erythranthe section.

Relationships among five of the species, *M. cardinalis*, *M. lewisii*, *M. eastwoodiae*, *M. verbenaceous*, and *M. nelsonii*, were explored. Experimental material was not obtained for the sixth member of the group, *M. rupestris*, which is known only from a single collection made by Pringle in 1900 in the state of Morelos, Mexico. Data were obtained from about 200 cultures of 95 different  $F_1$  combinations. Comparative studies were made on the morphology and growth of parental races and their  $F_1$  hybrids, on chromosome pairing during meiosis, and on pollen fertilities.

*M. cardinalis* and *M. lewisii* have the widest geographic distribution, occurring over a wide range of altitudes and latitudes in western North America. *M. verbenaceous* extends from southern Utah through Arizona into northern Mexico.

*M. eastwoodiae* is limited to a small area in southeastern Utah and northeastern Arizona. *M. nelsonii* has been found only in central Mexico.

Each of the morphologically and ecologically distinct species has  $n=8$  chromosomes. All possible interspecific hybrid combinations among them, and also numerous interracial crosses within *M. lewisii* and *M. cardinalis*, were obtained. A high degree of chromosome homology among all five species is evidenced by the extent of pairing during meiosis in  $F_1$  hybrids. Even in the genetically most diverse combinations at least a small percentage of the pollen mother cells show normal pairing.

*Genetic differentiation within species.* Differences in chromosome structure sufficient to cause some irregularity during meiosis have evolved within *M. cardinalis* and *M. lewisii*. A race of *M. cardinalis* from the Santa Catalina Mountains of Arizona when crossed with any of several *M. cardinalis* races from the Pacific coast or the central Sierra Nevada in California produces  $F_1$  hybrids that have one tetravalent or trivalent plus a single chromosome in about 50 per cent of the pollen mother cells. Others show regular pairing of all eight chromosomes, but often one or two pairs are loosely attached. At least one reciprocal translocation in the Arizona race distinguishes it from the coastal and Sierran populations of *M. cardinalis*. Pollen infertility increases to 20–35 per cent in  $F_1$  hybrids with the Arizona race, compared with 3–7 per cent in various hybrids between five coastal and Sierran races. Pairing at meiosis is highly regular in the Sierran group, with no evidence of any structural differences among any of the pairs of chromosomes.

In *M. lewisii*, also, two groups of races are similarly differentiated. One group occurs northward from the Warner Mountains in California to British Columbia and eastward to the Rocky Mountains, the other in the Sierra



Nevada or California. When any of four northern races (Warner Mountains, California; Stevens Pass, Washington; Mount Rainier, Washington; and Logan Pass, Montana) are crossed among themselves in any combination, all the  $F_1$  hybrids show regular pairing at meiosis and high pollen fertility. The same is true when six races of *M. lewisii* from the central Sierra Nevada are intercrossed. Pollen infertility in each of these two groups of  $F_1$  hybrids ranges from 6 to 18 per cent. In contrast,  $F_1$  hybrids between any of the northern and any of the Sierran group consistently show irregularities in chromosome pairing, with two sets of quadrivalents either in chains or rings at first metaphase, and a pollen infertility of 44–67 per cent. This confirms the earlier report (*Year Book 59*, pp. 320–322) of meiotic irregularity in an  $F_1$  hybrid between a Stevens Pass race and one from our Timberline station.

*Differentiation between species.* Although they differ distinctly in vegetative character and in natural distribution, *M. verbenaceous*, *M. eastwoodiae*, and *M. nelsonii* form a genetically inter-compatible unit. Hybrids are obtained easily in any combination of the three species, and regular chromosome pairing during meiosis is the rule. A low pollen infertility, 7–20 per cent, is consistent with the cytological finding. The exact degree of genetic intercompatibility among the three species can be evaluated properly only after studies of seed fertility of the  $F_1$  hybrids have been made, and the viability of the  $F_2$  progenies has been determined.

The most highly developed genetic barrier in the *Erythranthe* section appears between the inter-compatible three species just mentioned and *M. cardinalis*. The Arizona and California forms of *M. cardinalis* are about equally incompatible with the *M. verbenaceous-eastwoodiae-nelsonii* complex. In the initial cross, less than one per cent of the seed harvested on the female parent of these combinations survives to yield mature  $F_1$  plants. Moreover, viable seed can usually be obtained

only when *M. cardinalis* is the mother plant. Once obtained, the  $F_1$  hybrids are highly vigorous, but reduction divisions in the pollen mother cells are irregular. Reduced pairing and multivalent chains are evident, and pollen infertility reaches between 79 and 90 per cent.

Second-generation progenies of hybrids between *M. cardinalis* and members of the *M. verbenaceous-eastwoodiae-nelsonii* complex are yet to be grown. They are needed to supply details of the extent of the genetic incompatibilities between the two subgroups of *M. cardinalis* and members of the other complex. In flower structure and color, *M. verbenaceous*, *M. eastwoodiae*, and *M. nelsonii* resemble *M. cardinalis* so closely that taxonomists often regarded the first three species as varieties or subspecies of *M. cardinalis*. But the genetic evidence makes their biological distinctness unmistakable.

It is now clear that a genetic barrier exists between the components of the *M. verbenaceous-eastwoodiae-nelsonii* complex and both subgroups of *M. lewisii*, and that the barrier is somewhat similar to the one between the first group and *M. cardinalis*. But neither the Sierran nor the northern races of *M. lewisii* exhibit any initial incompatibility when crossed with any member of the *M. verbenaceous-eastwoodiae-nelsonii* group. The  $F_1$  hybrids are easily obtained and vigorous, but their meiosis is irregular, with loose chromosome association, lack of pairing, and frequent multivalent associations. The pollen in all combinations is poor, with 78–88 per cent of the grains aborted.

The two subgroups of *M. lewisii* have different degrees of genetic compatibility with *M. cardinalis*. The Sierran member of *M. lewisii* and the coastal and Sierran members of *M. cardinalis* are completely interfertile genetically. The genetics of hybrids between contrasting altitudinal races of these species was studied in some detail through the  $F_3$  generation, and was described in *Year Book 63*. In contrast, members of the northern group of *M. lewisii* when crossed with the same races



of *M. cardinalis* consistently show meiotic irregularities. Two sets of quadrivalents are evident at first metaphase in the majority of the pollen mother cells, and pollen infertility is high, 60–78 per cent.

The Arizona races of *M. cardinalis* show a high degree of genetic incompatibility with either the northern or Sierran races of *M. lewisii*. The  $F_1$  hybrids in both instances are about 87 per cent sterile, and in some cultures they are sublethal. When  $F_2$  progenies become available the relative degrees of genetic relationship can be clarified further.

*Species relationships.* The genetic evidence now available gives the broad outline of relationships within the Erythranthe section of *Mimulus*. A major evolutionary divergence appears to have occurred between the three southern and inland species, *M. verbenaceous*, *M. eastwoodiae*, and *M. nelsonii*, as one group. Although any race of one complex is capable of a limited gene exchange with a race in the other complex, the sterility barriers are probably great enough to maintain the biological distinctness of each complex as a natural taxonomic entity.

Differentiation has taken place within both components of the *M. cardinalis-lewisii* complex. A series of ecological races has evolved in the northern group of *M. lewisii*. These races are partially incompatible with the Sierran group of races farther south. The Arizona race of *M. cardinalis* has become differentiated from the California coastal and Sierran races.

In the light of these findings, the interfertility between the Sierran forms of *M. lewisii* and coastal and Sierran forms of *M. cardinalis* can be viewed in new perspective. In this instance, a striking and unusual differentiation of both morphological and physiological characters has taken place on a genic level without any change in the basic chromosome structure that might affect the mechanism of normal inheritance patterns governing specific character differences.

## CULTURES OF *Mimulus* IN VITRO

Kathe A. Picken, William M. Hiesey, and  
Frank Nicholson

The cultivation of excised parts of *Mimulus* under aseptic conditions has shown the practicality of this approach for comparative studies on ecological races and species. Examples of the interaction between some of the major variables encountered in this type of study and the consequent opportunities for future studies using these techniques are presented.

*Culture media.* Earlier reports (*Year Book* 63, pp. 431–432; 62, pp. 392–394) described studies using media containing high (*H*) and low (*L*) salt concentrations. This year a third intermediate (*M*) salt concentration was also tested. Both liquid and agar forms of these media were used, often with added hormones, indole acetic acid (IAA), naphthalene-acetic acid (NAA), 2,4-dichlorophenoxy-acetic acid (2,4-D), and 6-furfurylaminopurine (kinetin). The compositions of the three basic media are shown in Table 3.

*Establishment of cultures.* Two methods for establishing cultures appear to be about equally useful in the study of the various races of *Mimulus*. One is to start with peeled internodes of healthy, actively growing young stems of cloned plants grown under favorable conditions either in the greenhouse or in controlled cabinets. Callus, root, and leafy tissues were established in this manner. The kind and rate of growth are strongly influenced by the composition of the medium, and also by the genetic constitution of the races. For example, callus cultures of two Sierran foothill races of *M. cardinalis* (Jacksonville and Priest's) established in this manner in *L* medium were maintained through 21 transfers for over two years, and still continue. Corresponding cultures of a mid-Sierran race (Yosemite) died after eight transfers within about a year, and another race from a higher altitude (San Antonio Peak) grew slowly and survived only through



TABLE 3. Compositions of Basic Media

Elements and Supplements	<i>L</i> , Low Salt,* mg/l	<i>M</i> , Intermediate Salt,† mg/l	<i>H</i> , High Salt,‡ mg/l
Nitrogen	12.4	46.7	840.8
Potassium	16.9	65.0	783.5
Calcium	12.7	50.9	119.9
Magnesium	2.5	74.0	36.5
Sulfur	3.3	142.6	48.1
Phosphorus	5.7	4.2	38.7
Glycine	....	3.0	2.0
Nicotinic acid	....	0.5	0.5
Thiamine	....	0.1	0.1
Pyridoxine	....	0.1	0.5
Myo-Inositol	....	.....	100.0
Coconut milk	15% by volume	.....	.....

\* Laetsch and Briggs, modified medium (*Year Book* 61, p. 323).

† P. R. White (1963).

‡ T. Murashige and F. O. Skoog (1962).

six transfers, and for less than a year. Attempts to use the same technique to establish callus cultures from races of *M. lewisii* have failed.

The other method is to germinate seeds on nutrient agar and then to establish clones by transferring selected seedlings to liquid media from which subcultures are made. When the subcultures are started from apexes of branched stems, complete plants may be regenerated. Other excised parts can be used to establish various kinds of cultures. For example, leaves of a subalpine race of *M. lewisii* transferred to agar slants with *M* medium containing 1 mg/l kinetin plus 0.1 mg/l NAA produced uniformly reproducible callus cultures. They are the first successful callus cultures of *M. lewisii* that have been obtained and are in active growth after three transfers and 14 weeks. The growth is rapid and the callus formed is extremely friable and easily separable into chains of cells or single cells. The earliest growth is translucent and slightly yellowish, but later the callus becomes reddish tan. Excised leaves of a foothill race of *M. cardinalis* treated in the same way developed very differently: they remained green, and instead of developing callus, produced roots at the base of the cut

leaves. The stock plants of *M. lewisii* were grown in *H* medium and those of *M. cardinalis* in *L* medium. The possibility of carry-over effects from these media influencing the development of the leaf cultures in *M* medium cannot therefore be excluded.

*Interaction between various media and races.* In either *L* or *H* liquid media, stem apexes of *M. cardinalis* and *M. lewisii* show marked differences in growth. *M. lewisii* grows much better in *H* than in *L* medium. In both media, *M. cardinalis* usually grows better than *M. lewisii*, but in *M* medium the growth differential between the two nearly vanishes. *M. cardinalis* grows less actively in *M* medium than in *L* or *H*, and *M. lewisii* grows more slowly in *M* than in *H*.

The use of *L* medium reduces the frequency of transfer needed to maintain rapidly growing *M. cardinalis* clones in liquid culture. In contrast, *H* medium is required to provide reasonably rapid growth for *M. lewisii*. Cultures of stem apexes of the two species grown at room temperature in these media require transfer every four to six weeks. Clones of *M. cardinalis* are still growing after 6 transfers, and of *M. lewisii* after 13.

Additions of hormones to agar *M*

medium were tested for stimulation of callus growth on peeled internode cultures of *M. cardinalis*. Medium *M* containing 10 mg/l IAA plus 1 mg/l kinetin stimulated abundant growth of bright green chlorophyllous roots but very little callus. Under the same conditions, except with 1 mg/l kinetin plus 0.1 mg/l 2,4-D, abundant, soft, friable callus tissue developed, the best of the media tested for obtaining abundant reproducible callus tissues of *M. cardinalis*. If 1 mg/l NAA is used in place of the 2,4-D, thick stunted roots develop in addition to vigorous callus growth. In general, when agar media are used for studies of comparative growth rates, better replication of results in similarly treated cultures is obtained with *M* medium than with *L* or *H* medium.

*Temperature effects.* Liquid cultures of peeled internodes of a race of *M. cardinalis* from a high altitude in the Santa Catalina Mountains of Arizona developed an abundance of roots and callus at 15°C, whereas at 25°C the growth rate was markedly reduced. A reverse response was observed in corresponding cultures of another high-altitude race of *M. cardinalis* from San Antonio Peak in California in which growth of roots and callus was appreciably faster at 25°C.

As mentioned in last year's report, differential growth response between alpine *M. lewisii* and foothill *M. cardinalis* at the same two temperatures was found in aseptic seedling cultures. The growth differentials observed at the two temperatures were not so striking as those found between the two contrasting races of *M. cardinalis* from higher altitudes, mentioned above. More data are needed on the growth of excised parts of clones of contrasting races at different temperatures.

In the comparisons described in this section, 5 to 15 replications were routinely made in each experiment. The cultures were grown under weak diffuse light. Studies using light intensity or

light period as controlled variables have not been made, although these variables may be important factors influencing growth in such cultures.

*Conclusions.* Available data show that the interaction between the major sets of variables in the cultivation of excised parts of *Mimulus* clones provides an opportunity to analyze in detail many aspects of developmental, metabolic, and biochemical problems relating to clones, races, and species of *Mimulus*. The use of cultures in vitro thus provides a potentially useful supplement to other methods in the comparative study of ecological races and species.

#### VEGETATIONAL AND CLIMATIC CONTRASTS WITHIN THE HARVEY MONROE HALL NATURAL AREA

*Jens Clausen*

Intermittent field studies have been made within the Harvey Monroe Hall Natural Area during the last 30 years, especially within the five square kilometers that include the Slate Creek Valley where the Timberline transplant station is located. The Hall Area was established in 1932 by the U.S. National Forest Service in cooperation with the Institution (*Year Book* 32, pp. 20-21, 180, 194-196).

Slate Creek Valley is on the east side of the Sierra Nevada at altitudes between 3,000 and nearly 4,000 meters. It runs from west to east and has climatically contrasting steep slopes facing north and south. The western third of the valley is granite; the eastern two thirds is in heavily metamorphosed sedimentary rock. No limestone has been observed. Vegetation is denser in the metamorphic than in the granitic sector, but no species occurs exclusively on either of the two soil types.

The Harvey Monroe Hall Natural Area is typical of the recently glaciated high-altitude valleys on the east side of the Sierra Nevada. These valleys are topo-



graphically young. Great uplifts occurred along the eastern escarpment between the glacial periods. The uplifts changed the local climate, and glaciers and rejuvenated streams sculptured the landscape, providing many new niches for specialized plants.

It is reasonable to assume that before the uplifts some of the present plant species of the region or their relatives existed here and that the mountains rose with the plants in position. The uplifts changed the selective pressures, permitted immigration of related forms from other regions, followed by crossings, recombinations, and subsequent release of latent, hitherto unexpressed variability. The uplifts and changes in vegetation would be relatively gradual, from montane to subalpine to alpine. East of the mountains the climate of the Great Basin region became gradually drier as the heightened mountains shielded the basin against the humidity from the Pacific Ocean.

A list of the species of pteridophytes and flowering plants that now grow within the Harvey Monroe Hall Natural Area has been assembled. The list now stands at 353 species, all but two being represented within the Slate Creek Valley, the botanically richest of the three valleys in the area. Compared with other parts of the world the number of species is unusually high for this altitude. A preliminary report on the tree species was presented in *Year Book 62*, pp. 394-398, and the completed analysis has now been published.

*Species grouped according to their distribution outside the Hall Area.* The species of the Hall Area can be roughly divided into four groups, some of which have subgroups. A small group of 28 species are local alpine endemics limited to the high Sierra Nevada between Tehachapi Pass and Lake Tahoe. They could have survived the periods of heaviest glaciation on ice-free peaks. Presumably they are the most specialized of the four.

A group of 74 are widely distributed circumpolar to circumboreal species that are found at high latitudes in all the northern hemisphere continents. They include such species as the high-latitude *Sibbaldia procumbens* and mid-latitude *Potentilla fruticosa*, both of the rose family. Their distribution patterns suggest that they invaded the area via the mountain chains of western North America.

Another category of 69 species complexes extends to the mild Pacific coastal region. They have evolved series of ecological races that have enabled them to ascend the Sierra and to cross passes to the east-side subalpine valleys. Examples of such species complexes are the colorful thistle *Cirsium andersonii* and the crucifer *Streptanthus tortuosus*.

The fourth group is more heterogeneous, containing the 182 species that do not belong to the other three groups. All of them are found in the continental region between the Sierra Nevada and the Rocky Mountains, although some may also extend to wider ranges. Ecological extremes within this continental group include the typical Great Basin plants of arid areas, such as the sagebrushes of the *Artemisia tridentata* complex and the rabbit-brushes related to *Chrysothamnus nauseosus*, both of which have high-altitude forms in the Slate Creek Valley and spill over the summits to mid-altitudes on the west side of the mountains.

Others of the continental group are high-altitude but nonendemic species with disjunct distribution from the high Sierra Nevada to the high peaks in the intermountain region and the Rocky Mountains. They are generally rare plants exemplified by a species such as *Potentilla diversifolia*.

Slate Creek Valley species that have been classified with the continental group include also a subgroup of about 30 wide-ranging species complexes that go far north but are not circumboreal. In North America they extend almost from



the Pacific to the Atlantic, with continental forms in between. Some of them are species associated with forests, such as the honeysuckle, *Lonicera involucrata*; an orchid, *Habenaria dilatata-leu-chostachys*; the five-finger fern, *Adiantum pedatum*; and elephant's head, *Pedicularis groenlandica*. Having such a distribution, they could have existed in the region from the time when the mountains were still low.

Species now in the Hall Area therefore appear to have arrived during various geologic epochs from regions with highly diverse climates. Within the area they occupy distinct habitats—solid rock cliffs, alpine pavements, moraines, talus slopes, gravel beds, stream banks, lake shores, bogs, and alluvial meadows. These habitats are replicated at different altitudes and different slope exposures. During periods of geologic change the varying topography provided local refugia for displaced species and new invasions. Meanwhile ecological races suited to new situations have evolved through crossing and natural selection.

*Recent geologic activities.* The presence of the still active Mount Conness glacier is evidence of recent glaciation. As it retreated, the former Slate Creek glacier left striations on the steep slopes high above the valley bottom, huge erratic boulders, and about 11 terminal moraines inside the valley. The latest raw moraines are now populated by forest strips, but permanent although inactive snow patches within the Slate Creek and other cirques indicate the recency of the glacial activity.

Although the area is on the edge of the Mono basin and outside the major volcanic activities of the basin, a geologically recent volcanic eruption occurred on a steep south-facing slope in the western part of the metamorphic sector. From what appears to be a fissure in the rock, a lava core, 7 to 8 meters high, projects, ending in a downhill lava flow about 50 meters long, which contains many small lava blocks. Lava blocks

extend some 200 meters eastward beneath the rock talus.

The lava core is between the fourth and fifth terminal moraines from the Slate Creek cirque and is unglaciated. Only three species of higher plants have arrived on the lava core: *Sitanion hystrix*, one of the commonest grasses in the Hall Area; the prickly phlox *Leptodactylon pungens*, and a single shrub of the alpine currant, *Ribes cereum*, perhaps 50 years old. Several colorful lichens are present.

*Climatic contrasts within the valley.* Plant species of climatically contrasting regions exist together within the Slate Creek Valley, and there are obvious differences among the vegetations of the north- and south-facing slopes. Temperature measurements were sporadically recorded in recent years by Nobs and Clausen at various sites within the valley. These observations confirmed the supposition that striking microclimatic differences can exist within such a valley.

During 1962 a seven-week residence within the valley to study tree distribution made it possible to obtain readings at three contrasting sites. The period, August 5 to September 17, covered the major growth period of the brief summer and fall seasons.

Table 4 lists the minimum and maximum readings within alternating three- and four-day intervals for the sites. One site was on a steep north-facing slope, about 70 meters above the valley bottom; another on a south-facing slope nearly as steep, 200 meters above the valley; and the third in a direct line between the other two, in the bottom of the valley at a 3,000-meter altitude. The distance between the slope sites was about 800 meters.

The north-slope temperatures are similar to summer temperatures in coastal regions near the Arctic Circle: low day temperatures and frostless nights, the daily amplitudes averaging only 12°C. As at high latitudes, the sun's rays reach the north slope only at small angles.

In contrast, on the south-facing slope



TABLE 4. Summer and Fall Temperatures in Slate Creek Valley

Dates, 1962	Degrees Centigrade					
	North-facing slope, 3,070 meters		Valley bottom, 3,000 meters		South-facing slope, 3,200 meters	
	min.	max.	min.	max.	min.	max.
August						
5-6	4.5	14.0	-1.0	27.0	2.5	27.0
7-10	2.5	15.0	-4.5	21.0	1.0	21.0
11-12	4.5	19.0	-0.5	22.5	0.0	26.5
13-16	8.0	19.5	0.0	25.5	0.0	29.0
17-19	3.5	17.0	-0.5	21.5	3.0	29.0
20-23	6.5	16.5	-1.5	25.0	2.5	27.0
24-26	5.0	16.0	-0.5	22.0	6.0	28.0
27-29	1.0	16.5	-2.5	19.5	0.0	26.5
30-						
September						
2	2.0	15.5	-6.5	22.0	0.0	28.0
3-5	3.0	15.5	-4.5	24.0	6.0	27.5
6-9	3.0	14.5	-3.0	20.5	1.5	29.0
10-12	3.0	13.5	-3.0	18.0	1.5	27.5
13-15	2.5	13.0	-4.0	20.5	2.0	29.5
16-17	5.0	13.0	-2.0	21.5	2.0	29.5
Mean	4.0	16.3	-2.4	22.2	2.0	27.5

the solar radiation arrives at nearly right angles during the summer midday, as in lower latitudes, and the maximum day temperatures may rise to nearly 30°C. Even at the higher altitude of this site the nights were free of frost, but the average daily amplitudes were 25°C, being typically continental and more than twice the amplitude of the north slope.

In the valley bottom, strong temperature inversions occur during quiet nights. Only one three-day period was free of frost during the seven weeks. Both day and night temperatures were about 5°C lower than at the south slope, although the daily amplitudes were comparable and of the continental type. Temperature differences of the order of those between the south slope and the valley bottom during the growing season are of high importance for vegetation and they are accentuated by the occurrence of night frosts near the valley bottom.

The temperature inversions are comparable with those found by Billings

(1954) at about a 1,900-meter altitude in the Virginia Mountains of Nevada. Billings, however, did not find appreciable temperature contrasts between north and south slopes, probably because of gentler slopes than the approximately 45° slopes at the Slate Creek Valley sites.

Many species in the Slate Creek Valley occupy distinct kinds of slope. Species almost entirely limited to the north slopes include the arctic rush, *Luzula spicata*; arctic sorrel, *Oxyria digyna*; and roseroot, *Sedum rhodiola*. Species predominantly on the south slopes include *Potentilla glandulosa nevadensis* and *Achillea lanulosa alpicola* as well as the sagebrushes and rabbit-brushes. Some plants can occupy both kinds of slope, including the prominent trees, *Pinus albicaulis* and *P. murrayana*, although the former is best developed on northern slopes and the latter on southern and eastern slopes.

*Conclusions.* Groups of species from at least four major climatically contrasting regions appear to have converged in the

Harvey Monroe Hall Natural Area, a region representative of the eastern side of the high Sierra Nevada. Subalpine and alpine races of the species of these groups evolved and were able to find suitable habitats among the topographically, edaphically, and climatically diverse sites in this area. Microclimatic niches exist within the area that in some respects, during the growth period of the plants,

are comparable to coastal and continental areas, and to low- and high-latitude environments.

The dynamic changes during active mountain building in a geologically young area appear to have made it possible for previously separated species to come together, thereby providing a means for further evolution through hybridization and natural selection.

## REFERENCES CITED

- Billings, W. D., *Butler Univ. Bot. Studies*, 11, 112-114, 1954.
- Björkman, O. E., and K. P. Holmgren, *Physiol. Plantarum*, 16, 889, 1963.
- Boardman, N. K., and J. M. Anderson, *Nature*, 203, 166, 1964.
- Emerson, R., and C. M. Lewis, *Am. J. Botany*, 30, 165, 1943.
- Ernster, L., and C. Lee, *Ann. Rev. Biochem.*, 33, 729, 1964.
- Garrels, R. M., M. Sato, M. E. Thompson, and A. H. Truesdell, *Science*, 135, 1045, 1962.
- Haxo, F. T., and L. R. Blinks, *J. Gen. Physiol.*, 33, 389, 1950.
- Heber, U., and K. A. Santarius, *Ber. Deut. Botan. Ges.*, 77, 1, 1964.
- Hoch, G., O. Owens, and B. Kok, *Arch. Biochem. Biophys.*, 101, 171, 1963.
- Holt, L. E., Jr., V. K. La Mer, and H. B. Chown, *J. Biol. Chem.*, 64, 509, 1925.
- Murashige, T., and F. O. Skoog, *Physiol. Plantarum*, 15, 473-497, 1962.
- Packer, L., *Biochim. Biophys. Acta*, 75, 12, 1963.
- Rechnitz, G. A., *Anal. Chem.*, 37, No. 1, 29A, 1965.
- Ried, A., C. J. Soeder, and I. Müller, *Arch. Mikrobiol.*, 45, 343, 1963.
- Truesdell, A. H., and A. M. Pommer, *Science*, 142, 1292, 1963.
- Wessels, J. S. C., *Biochim. Biophys. Acta*, 65, 561, 1962.
- White, P. R., *Cultivation of Animal and Plant Cells*, Second Ed., Ronald Press, New York, 1963.

## BIBLIOGRAPHY

- Butler, Warren L., *see* Menke, Wilhelm.
- Clausen, Jens, New combinations in Western North American violets, *Madroño*, 17, 173-197, 1964.
- Clausen, Jens, Synthesis (Experimental taxonomy), *Genetics Today, Proc. 11th Intern. Congr. Genet.*, 2, 447-449, 1964.
- Clausen, Jens, and Øjvind Winge, *Naturhistorisk Tidende*, 28-29, 60-66, 1964-1965.
- Clausen, Jens, Population studies of alpine and subalpine races of conifers and willows in the California High Sierra Nevada, *Evolution*, 19, 56-58, 1965.
- Clausen, Jens, Microclimatic and vegetational contrasts within a subalpine valley, *Proc. Natl. Acad. Sci. U. S.*, 53, 1315-1319, 1965.
- de Kouchkovsky, Yaroslav, and David C. Fork, A possible functioning *in vivo* of plastocyanin in photosynthesis as revealed by a light-induced absorbance change, *Proc. Natl. Acad. Sci. U. S.*, 52, 232-239, 1964.
- Fork, David C., and Wolfgang Urbach, Evidence for the localization of plastocyanin in the electron-transport chain of photosynthesis, *Proc. Natl. Acad. Sci. U. S.*, 53, 1307-1315, 1965.
- Fork, David C., *see* de Kouchkovsky, Yaroslav.
- French, C. Stacy, Fluorescence spectra of sharp cut-off filters, *Appl. Opt.*, 4, 514, 1965.
- French, C. Stacy, Review of *Photosynthetic Mechanisms of Green Plants*, National Academy of Sciences-National Research Council Publ. 1145, *Radiation Botany*, 5, 71-72, 1965.
- French, C. Stacy, Review of *Primary Processes in Photosynthesis*, by Martin Kamen, *Photochem. Photobiol.*, 4, 638-639, 1965.



- French, C. Stacy, *see also* Vidaver, William; Menke, Wilhelm.
- Hiesey, William M., The genetic-physiologic structure of species complexes in relation to environment, *Genetics Today, Proc. 11th Intern. Congr. Genetics*, 2, 437-445, 1964.
- Hiesey, William M., and Harold W. Milner, Physiology of ecological races and species, *Ann. Rev. Plant Physiol.*, 16, 203-216, 1965.
- Hiesey, William M., *see also* Milner, Harold W.
- Menke, Wilhelm, C. Stacy French, and Warren L. Butler, Über die durch Trocknen bewirkten Absorptions-Änderungen von Chloroplasten und Algen, *Z. Naturforsch.*, 20b, 482-487, 1965.
- Milner, Harold W., and William M. Hiesey, Photosynthesis in climatic races of *Mimulus*. II. Effect of time and CO<sub>2</sub> concentration on rate, *Plant Physiol.*, 39, 746-750, 1964.
- Milner, Harold W., *see also* Hiesey, William M.
- Urbach, Wolfgang, *see* Fork, David C.
- Vidaver, William, and C. Stacy French, Oxygen uptake and evolution following monochromatic flashes in *Ulva* and an action spectrum for system I, *Plant Physiol.*, 40, 7-12, 1965.

## SPEECHES

- Björkman, Olle, Metabolic differences within species and their adaptive relation to climate, Symposium, 10th International Botanical Congress, Edinburgh, Scotland, August 1964. Abstract: *Abstracts, Proc. 10th Intern. Botan. Congr.*, p. 144, 1964.
- Björkman, Olle, Intraspecific differences in photosynthetic properties, Seminar, Botany Department, University of California, Berkeley, April 1965; Department of Life Sciences, University of California, Riverside, May 1965.
- Bril, Cornelis, Detergent-induced changes in fluorescence spectra of bacterial chromatophores, Biophysical Society, San Francisco, California, February 1965. Abstract: *Abstracts, Biophys. J.*, 5, 80, 1965.
- Bril, Cornelis, and Jeanette S. Brown, Partial separation of chlorophylls *a* and *b* in aqueous extracts of certain algae by digitonin and by freeze-thawing, American Society of Plant Physiologists, Western Section, Riverside, Calif., June 1965.
- Bril, Cornelis, *see also* Brown, Jeanette S., *et al.*
- Brown, Jeanette S., Cornelis Bril, and Wolfgang Urbach, Partial fractionation of the absorbing forms of chlorophyll *a* in *Euglena* by deoxycholate, American Society of Plant Physiologists, Western Section, Riverside, Calif., June 1965.
- Brown, Jeanette S., *see* Bril, Cornelis.
- Clausen, Jens, What the wild plants tell us about evolution, Symposium on Man in the Evolving Universe, College of Notre Dame, Belmont, Calif., July 1964.
- Clausen, Jens, Population studies among conifers around tree line in the Sierra Nevada, Symposium on Plant Sociology and Phytogeography, 10th International Botanical Congress, Edinburgh, Scotland, August 1964. Abstract: *Abstracts, Proc. 10th Intern. Botan. Congr.*, p. 291, 1964.
- Clausen, Jens, A causerie on historical and recent political and botanical connections between Scotland, Denmark and California, Botanical Society of Edinburgh, Edinburgh, Scotland, August 1964.
- Clausen, Jens, Botanical explorations within the Harvey Monroe Hall Natural Area, California Botanical Society, Berkeley, February 1965.
- Clausen, Jens, Microclimatic and vegetational contrasts within a subalpine valley, Annual Meeting, National Academy of Sciences-National Research Council, Washington, D.C., April 1965. Abstract: *Science*, 148, 664, 1965.
- Clausen, Jens, The forest at tree line, Public lecture, Biology Department, San Diego State College, San Diego, Calif., June 1965.
- de Kouchkovsky, Yaroslav, Mechanisms of photosynthesis, Seminar, Laval University, Quebec, Canada, July 1964.
- de Kouchkovsky, Yaroslav, Function of plastocyanin in photosynthesis, 6th International Congress of Biochemistry, New York, N.Y., July 1964.
- de Kouchkovsky, Yaroslav, The role of plastocyanin in photosynthesis, Department of Biochemistry and Biophysics, Faculty of Science, University of Tokyo, Tokyo, Japan, September 1964.
- Fork, David C., Two light reactions in photosynthesis in relation to the evolution of O<sub>2</sub> and the 515-m $\mu$  absorption change, 4th International Congress on Photobiology, Oxford, England, July 1964. Abstract: *4th Intern. Congr. Photobiol.*, p. 120, 1964.
- Fork, David C., Kinetic studies of the 515-m $\mu$  absorption change, Photosynthesis Conference, Queen Mary College, London, England, July 1964.
- Fork, David C., Studies on the localization of plastocyanin *in vivo* in the electron-transport chain of photosynthesis, Seminar, Department of Physiology, University of California, Berkeley, February 1965.

- Fork, David C., and Wolfgang Urbach, Evidence for the localization of plastocyanin in the electron-transport chain of photosynthesis, American Society of Plant Physiologists, Western Section, Riverside, Calif., June 1965.
- French, C. Stacy, The interaction of two pigment systems as seen in the time-course of O<sub>2</sub> exchange, Photosynthesis Conference, Queen Mary College, London, England, July–August 1964.
- French, C. Stacy, Pigment function in photosynthesis, Symposium on Energy Conversion in Photosynthesis, 10th International Botanical Congress, Edinburgh, Scotland, August 1964. Abstract: *Abstracts, Proc. 10th Intern. Botan. Congr.*, p. 151, 1964.
- French, C. Stacy, Effect of intensity on the time course of O<sub>2</sub> evolution from chloroplasts without added substrates, Biophysical Society, San Francisco, Calif., February 1965. Abstract: *Abstracts, Biophys. J.*, 5, 54, 1965.
- French, C. Stacy, Some contrasting ideas about the mechanism of photosynthesis, Seminar, Department of Life Sciences, University of California, Riverside, May 1965.
- French, C. Stacy, and William E. Vidaver, Energy conversion and the photosynthetic unit, Contribution to Rapporteur Session, 4th International Congress on Photobiology, Oxford, England, July 1964. Abstract: *4th Intern. Congr. Photobiol.*, p. 120, 1964.
- Hiesey, William M., see Milner, Harold W.; Picken, Kathe A.
- Milner, Harold W., and William M. Hiesey, Differences in photosynthetic rates of *Mimulus* races, American Society of Plant Physiologists, Boulder, Colo., AIBS Meeting, August 1964. Abstract: *Plant Physiol.*, 39 (supplement), xlvi, 1964.
- Picken, Kathe A., and William M. Hiesey, Studies on cultures of *Mimulus in vitro*, Botanical Society of America, Boulder, Colo., AIBS Meeting, August 1964. Abstract: *Am. J. Botany*, 51, 676–677, 1964.
- Urbach, Wolfgang, Intracellular translocation of P<sub>i</sub>, ATP, ADP, and PGA between chloroplasts and cytoplasm during photosynthesis, Seminar, Department of Physiology, University of California, Berkeley, April 1965.
- Urbach, Wolfgang, see also Fork, David C.; Brown, Jeanette S.
- Vidaver, William, Photosynthetic mechanisms, Seminar, University of South Carolina, Columbia, December 1964; State University of New York, Stonybrook, December 1964.
- Vidaver, William, Science and Education, Seminar, Newark State College, Union, N. J., December 1964.
- Vidaver, William, An O<sub>2</sub> requirement for sustained photosynthesis in far-red light, Biophysical Society, San Francisco, Calif., February 1965. Abstract: *Abstracts, Biophys. J.*, 5, 54, 1965.
- Vidaver, William, see also French, C. Stacy.

## PERSONNEL

*Biochemical Investigations*

*Staff:* C. Stacy French, *Director*; Jeanette S. Brown, David C. Fork; James H. C. Smith, *Emeritus*

*Carnegie Corporation Fellows:* Yaroslav de Kouchkovsky, Alexander Müller

*Institution Research Fellows:* William E. Vidaver, Cornelis Bril

*Charles F. Kettering Research Fellows:* Wolfgang Urbach, August Ried

*Technical Assistants:* Shirley G. Landsman, Mark Lawrence, Adolph Fejfar, William R. Griswold

*Experimental Taxonomy*

*Staff:* Jens C. Clausen, *Emeritus*; William M. Hiesey, Harold W. Milner,<sup>1</sup> Malcolm A. Nobs

*Institution Research Fellow:* Olle Björkman

*Summer Research Assistant:* Allan Oakley Shields

*Technical Assistants:* Frank Nicholson, Kathe A. Picken

*Clerical Assistant:* Marylee H. Eldredge

*Gardeners:* Joseph S. Chang, John F. Emmel

*Administrative Assistant:* Wiley Knight, Jr.<sup>2</sup>

*General Department Secretary:* Gloria Thomas

*Mechanic:* Richard W. Hart

*Custodian:* Jan Kowalik

<sup>1</sup> Died July 13, 1965.

<sup>2</sup> Resigned April 7, 1965.





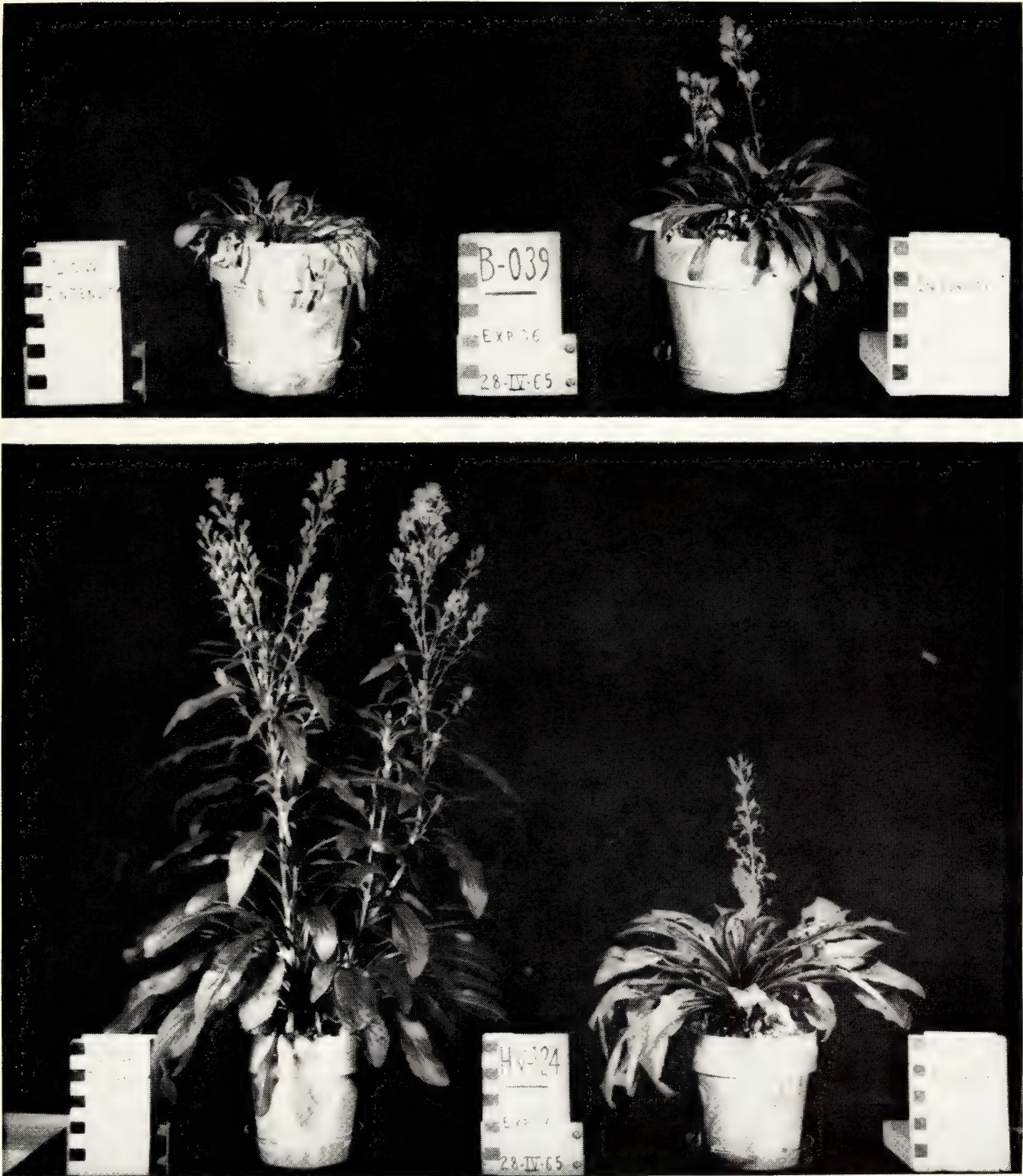


Plate 1. Plants of a clone of *Solidago virgaurea* originally from an exposed habitat in northern Norway (top) and from a shaded habitat in southern Sweden (bottom) grown at low light intensities (left) and high light intensities (right).



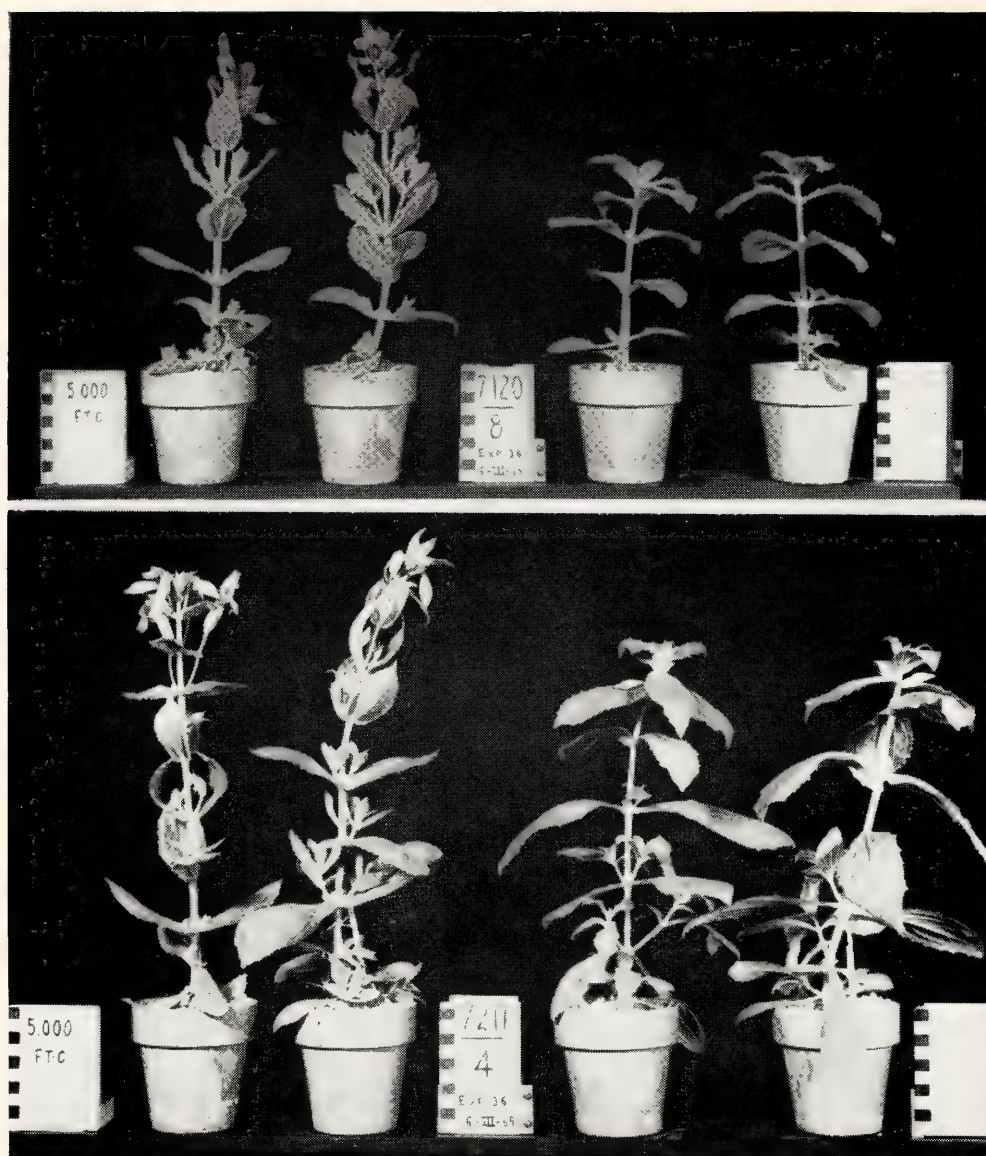


Plate 2. Plants of a Jacksonville race clone (bottom) and of San Antonio Peak race clone (top) of *Mimulus cardinalis*, grown at high light intensity (left) and low light intensity (right).

# *Department of Embryology*

James D. Ebert  
*Director*

*Baltimore, Maryland*





# Contents

Introduction. . . . .	443
Cellular Regulatory Mechanisms . . . . .	446
Development of machinery for protein synthesis . . . . .	446
The RNA of the unfertilized egg . . . . .	448
Quantitative analysis of the three classes of RNA newly synthesized during development	448
Aggregation of ribosomes during development . . . . .	450
Synthesis of messenger RNA studied by the agar-DNA technique . . . . .	452
DNA in amphibian eggs . . . . .	465
Clonal and Biochemical Studies of Myogenesis . . . . .	469
Clonal analysis . . . . .	469
Biosynthesis in cultured muscle cells . . . . .	470
Chemistry and Physiology of the Developing Heart . . . . .	471
A mitochondrial factor that prevents the effects of antimycin A on myogenesis . . . . .	471
Pacemaker cells in the embryonic heart . . . . .	471
Cultivation of embryonic heart cells . . . . .	472
Electrophysiological properties of cultured heart cells . . . . .	474
Formative movements in the early chick embryo . . . . .	477
Inductive Tissue Interactions . . . . .	481
Origin of feather specificity . . . . .	481
Ribosomes and polysomes in epidermis and dermis during feather induction . . . . .	482
“Heterogeneous inductors” . . . . .	482
Effect of thioglycolic acid . . . . .	482
Animal Viruses and Embryos . . . . .	483
Infection of embryonic muscle cells by Rous sarcoma virus . . . . .	483
Production of infectious centers in muscle cell cultures . . . . .	483
Transformation of muscle clones by Rous sarcoma virus . . . . .	484
Susceptibility of kidney and cartilage cells to Rous sarcoma virus . . . . .	486
The Graft-Versus-Host Reaction . . . . .	486
The granulocytic response . . . . .	486
Immunologically Induced Aspermatogenesis . . . . .	495
Testicular sorbitol dehydrogenase . . . . .	496
The Embryo in Relation to its Environment. . . . .	504
Mechanisms of implantation of the ovum . . . . .	504
Anatomy and physiology of the placenta . . . . .	506
Radioangiography of the placental circulation . . . . .	506
Uterine activity . . . . .	507
The fetal circulation . . . . .	508
Vasculature of the pregnant human uterus and placenta . . . . .	509



The Collection of Human Embryos . . . . . 510  
    Complete dysraphism in a 14-somite human embryo: a contribution to normal and  
        abnormal morphogenesis . . . . . 510  
    The initial appearance of ossification in staged human embryos . . . . . 510  
    Publication of *Contributions to Embryology* . . . . . 511  
  
Apparatus and Techniques . . . . . 511  
    Culturing tissues of invertebrates . . . . . 511  
  
Staff Activities . . . . . 512  
  
Bibliography . . . . . 514  
  
Personnel . . . . . 515

## INTRODUCTION

In *Heredity and the Nature of Man*, Theodosius Dobzhansky enters an eloquent plea that biological research be pursued on a broad front, and not allowed to become funneled in a single direction, no matter how promising it may seem at present to be. "Modern man is, however, so accustomed to expect science to produce miracles," he wrote, "that some scientists and popular writers talk and write about them as though they were accomplished facts. A little overdose of optimism is perhaps not undesirable here and there in our Age of Anxiety; barring unforeseen calamities, new and important discoveries in biological science may confidently be anticipated. *What cannot be anticipated is just what these discoveries will be and in just what fields they will be made.*" (Italics added.)

The first clear evidence of extranuclear deoxyribonucleic acid (DNA) was presented in 1924, yet nearly forty years passed before proof of the localization of DNA in chloroplasts and mitochondria was forthcoming and was generally accepted, and before the role of extranuclear DNA became a central topic of discussion among biologists. Admittedly the evidence for DNA in mitochondria in the intervening years was less than crucial but, curiously, it did not stimulate very much critical inquiry, especially in view of the increasing information on cytoplasmic inheritance, some of which pointed to the involvement of mitochondria. Although the issue of protein synthesis in mitochondria is no longer a matter of contention, and the presence of DNA in cytoplasmic particulates in a variety of organisms is entirely clear, our satisfaction must be tempered by the admission that we do not know the role of extranuclear DNA. It cannot yet be stated with certainty that the DNA found in mitochondria is responsible for any of the information required for the

synthesis and development of mitochondrial structure.

The role of the "cytoplasmic" or "egg" DNA in the eggs and early embryos of several animals, including the anurans, is especially puzzling. However, the confusions and difficulties still so daunting in this field throw into sharper relief the critical information now available.

It was reported in *Year Book 63* (p. 515) that the eggs of *Xenopus laevis* and *Rana pipiens* contain 100–300 times the amount of DNA present in diploid somatic cells of the same species. Igor Dawid had isolated this DNA and found it to be double stranded; the evidence available suggested that the earlier hypothesis of others that preformed DNA is used directly during cleavage in the formation of chromosomal DNA might be incorrect. During the current year Dawid has continued to explore the relation of the egg DNAs to the somatic DNAs of these species. Earlier, Brian J. McCarthy and Bill Hoyer had shown that DNA samples from different somatic tissues of animals of the same species are indistinguishable in competition experiments using the agar-DNA technique, a finding extended by Herman Denis to embryos and adults of *Xenopus laevis*. Dawid has applied the same technique and, in addition, in an elegant application of an even more sensitive test, he has studied the direct hybridization of complementary ribonucleic acid (RNA), prepared with egg DNA as a template, and liver DNA. The findings in both kinds of experiments show that the fraction of liver DNA homologous to egg DNA lies between 0.1 and 5.0 per cent. Egg DNA is thus shown to be a specialized DNA, further suggesting that it may have a specific function, and that it does not serve simply as a depot, providing materials for cleavage.

Even though Dawid's evidence points to a cytoplasmic, and in fact mitochon-



drial localization of egg DNA, the evidence presented so far falls short of being crucial. However, although the techniques are now available to provide a satisfactory answer to the question of localization, the role of egg DNA continues to puzzle us.

It has long been known that agents interfering with the pathways of aerobic phosphorylation embodied in the mitochondria in developing embryos disrupt the normal course of differentiation. In earlier reports we have discussed the inhibition of the developing heart and somites in chick embryos cultivated in media containing low concentrations of the antibiotic antimycin A. Neither ectodermal nor endodermal tissues are affected significantly when the inhibitor is added via the hypoblast. The heart, however, is absent or rudimentary, and the number of somites is drastically reduced. Irwin R. Konigsberg has shown that the treatment of colonies of muscle cells for 24 hours with antimycin A results in the selective destruction of multinuclear cells. Neither myoblasts nor fibroblasts are destroyed at concentrations that eliminate all the multinucleated fibers in a culture.

Minocher C. Reporter and James D. Ebert have continued to explore the mechanism and site of action of this inhibitor of electron transport in myogenesis. They have described the isolation of a mitochondrial factor that affords protection against antimycin A. Embryos recover that are cultivated in a medium containing as much as 0.035  $\mu\text{g}/\text{ml}$  of the inhibitor for six hours, and are transferred to normal medium containing the factor. The factor also prevents the action of antimycin A in monolayer cultures of embryonic skeletal muscle. The properties of the factor, which are discussed in the body of this report and in an article to appear in *Developmental Biology*, suggest that it is a protein containing nonheme iron. The authors advance the hypothesis that the factor, which they have shown to be

present in early embryos, represents the extracted mitochondrial site of action of antimycin A. If this hypothesis proves to be correct, the protein may prove to be a useful "marker" in studying the development of mitochondrial structure, and in relating one site in the now familiar fine structure of the mitochondrion with its enzymatic role.

The importance of such markers or other objective criteria cannot be overlooked. Progress reported by David W. Bishop suggests that he has been able to develop an objective criterion for evaluating the onset and extent of immunologically induced aspermatogenesis. His continuing study of the mechanism of this reaction has long been hampered by lack of such an assay. Now he has been able to show that the activity of the enzyme sorbitol dehydrogenase provides a reliable quantitative measure of functional germinal epithelium.

Progress is reported in another of the Department's continuing programs. M. E. Kaighn, Pauline Stott, and Ebert have provided evidence that myoblasts can be infected by Rous sarcoma virus (RSV). Of 23 isolated muscle colonies (ringed clones), 19 produced infectious virus, providing the first convincing evidence of the infection by RSV of a cell capable of differentiation. It is clear that, since partially and totally transformed muscle colonies have been obtained from single myoblasts infected at the time of plating, the infectious process does not necessarily prevent fusion of myoblasts. It is not yet clear whether multinucleate myotubes are sensitive to infection.

But why this emphasis on what we might call "viral susceptibility and embryonic differentiation"? Ample attention is being paid to the effects of viruses, including the tumor viruses, on replicative mechanisms in animal cells, but little effort is being directed toward understanding what types of cells a tumor virus will infect and transform. We could say with assurance until now that RSV could transform "fibroblasts" in vitro, that it



would transform at least some of the mesenchymal cells of the chorioallantois, and that it would produce tumors when injected into the breast or wing of the susceptible fowl. It had not been established that prospective muscle cells or other differentiating cells could be transformed. Ephrussi and Temin had provided evidence that RSV-infected cells derived from the chicken iris epithelium undergo morphological changes similar to those exhibited by infected fibroblasts, but the iris epithelial cells were not clonally derived. Saxen, Vainio, and their colleagues in Helsinki have shown that polyoma virus infects only relatively undifferentiated cells in developing kidney rudiments in vitro. However, the techniques employed are not crucial, for it is impossible to say just which cell types in the culture have been infected. It now appears possible to determine how such viruses interact with cells at precise times in their life histories, to determine how the "state of differentiation" of a cell influences its susceptibility to viruses, thanks to the techniques for cloning differentiating cells, in which Konigsberg pioneered and which are now being exploited in several laboratories.

Experiments are now in progress to determine the amount and rate of viral synthesis in muscle at each major point in its development, and to compare the infectivity of muscle clones with clones of cartilage cells and with clones of fibroblastic cells. A comparison of muscle, cartilage, and fibroblastic clones may be especially meaningful when one considers their origin in the early embryo.

The cloning techniques should permit advances not only in studies of the behavior of viruses toward cells, but in studies of the behavior of cells toward one another. In the somite, for example, do developing cartilage and muscle cells influence each other? Tokindo Okada has emphasized that a comparison of the cloning techniques for chondroblasts and myoblasts, developed, respectively, by Coon at Brandeis University and by

Konigsberg, and the relative ease with which cartilage cells can be subcloned (as contrasted with muscle cells) suggests that cartilage cells—either those overtly synthesizing collagen and matrix or cells with fibroblastic morphology, which may be covert cartilage cells (Grobstein's terminology)—may be more independent than developing muscle cells.

But the most difficult questions involving the behavior of cells toward one another lie in the field of morphogenetic movements. During the year, working in consultation with Robert L. DeHaan, Glenn C. Rosenquist provided evidence that appears to answer an old question. By following the fate of small fragments of radioactively labeled chick embryos transplanted orthotopically in unlabeled hosts, he has shown that cells of the epiblast may be observed in autoradiographic preparations in sites approaching the primitive streak and leaving it, and in the streak itself. These findings, which will be presented in detail in volume 38 of *Contributions to Embryology*, confirm Spratt's earlier observations (recently questioned by Spratt himself) that the primitive streak is in fact an elongated blastopore.

Faithful readers of these reports must have been impressed over the years by the extent of the contributions made by the Department's Fellows and graduate students. The year under review has been no exception. In addition to the findings already mentioned, by Dawid, Reporter, Kaighn and Rosenquist, the reader will find in the sections that follow studies to which nearly three dozen visiting investigators have contributed, for varying periods. It may be helpful to those reading the body of the report to glance at the following "cast of characters," which identifies most of those who have been in residence a major part of the year.

It should be noted first that Dawid, a Fellow of Carnegie Institution, spent the second half of the year at the Max-Planck-Institut in Tübingen, Germany,



where, in consultation with W. Beermann, he is beginning to look into possibilities of isolating and characterizing DNA of *Chironomus*. He is expected to return to the Department as a member of the staff.

Reporter has assumed a new position in the Charles F. Kettering Research Laboratory, Yellow Springs, Ohio.

DeHaan enjoyed the cooperation of two Fellows in addition to Rosenquist: Iva A. Ajdukovic of Zagreb, Yugoslavia, a Carnegie predoctoral Fellow, and Melvyn Lieberman, a Fellow of the U.S. Public Health Service, who has begun to examine the electrophysiological properties of cultured heart cells.

In his second year Herman Denis, Carnegie Fellow from Belgium, continued his study of the synthesis of "messenger" RNA (mRNA) in *Xenopus laevis*, using the agar-DNA technique.

Heinz Tiedemann completed his stay as a Fellow of the Institution and has organized a group in developmental biology at the Max-Planck-Institut für Meeresbiologie in Wilhelmshaven.

During the year, four additional investigators joined the Department as Fellows of Carnegie Institution. Okada of Kyoto, Japan, spent about six months working with Kaighn and Ebert on the susceptibility of cartilage and kidney cells to Rous sarcoma virus. Yoheved Berwald of Israel's Weizmann Institute joined Konigsberg's group to help initiate clonal studies of mammalian muscle cells. John

B. Gurdon of Oxford University, whose long-range collaborative efforts with Donald D. Brown have previously been recorded in these reports, arrived for a six-month stay in the spring of 1965. And in June 1965 Carl Weber, a recent graduate in biochemistry at the University of Illinois, joined the Department to work in cooperation with Brown.

The team of Elizabeth M. Ramsey, C. B. Martin, Jr., and Martin W. Donner of Johns Hopkins Department of Radiology, again enjoyed the collaboration of Harry S. McGaughey of the University of Virginia. During the year, two new co-workers, Peter Eckstein of the University of Birmingham, England, and Edward J. Quilligan of Western Reserve University, joined the team for brief periods and also took part in interactions "at a distance."

Oleg E. Viazov of Moscow spent about two months in the Department in the fall of 1964, largely in Bishop's laboratory. As might be expected, his stay was too short to permit a fruitful collaboration, but his visit was instructive. The visit permitted a comparison of the problems considered important and the ways they are being approached in the two countries; and techniques were exchanged.

Other visitors to the Department, some of whose studies are reported, included J. W. S. Harris, R. E. Marshall, Catherine A. Neill, Ronan O'Rahilly, Dorcas H. Padget, John Papaconstantinou, Edward C. Roosen-Runge, and E. C. Sensenig.

## CELLULAR REGULATORY MECHANISMS

### DEVELOPMENT OF MACHINERY FOR PROTEIN SYNTHESIS

In amphibian embryos, three classes of RNA are synthesized at rates that differ from each other and that vary with the stage of oogenesis or embryogenesis. During the past year D. D. Brown has developed techniques for measuring the amount (in micrograms) of all three classes of RNA which are synthesized at

each stage of development. These measurements shed additional light on the pattern of RNA synthesis during development and provide information on the factors regulating the synthesis of each class of RNA. The specific activity of the nucleotide pool is measured, permitting the calculation of a direct conversion from radioactive counts per minute to micrograms for each class of RNA.

Embryos of *Xenopus laevis* have again

been labeled with inorganic phosphate ( $P^{32}$ ) according to a method devised by Kutsky. The isotope is introduced into the eggs and embryos by intraperitoneal injection into the gravid female. During ovulation the eggs become radioactive by coming directly into contact with the isotope in the body cavity. This technique has the advantage of eliminating problems of permeability. And, more important, the isotope enters such a large pool of inorganic phosphate that nucleotide precursors remain radioactive over the first four days of development.

The nucleotide pool at all times consists largely (90 per cent or more) of triphosphates; the two terminal phosphates have much higher specific activities than the alpha phosphate. It is the alpha phosphate which is incorporated into nucleic acids; it was therefore necessary to develop a technique to hydrolyze the two terminal phosphates yielding all four 5' mononucleotides. The acid-soluble extracts are adsorbed on acid-washed activated charcoal and hydrolyzed in

NHCl at 100°C for 30 min. The charcoal is washed and eluted with an ethanol-ammonia solution. This eluate is then concentrated and chromatographed on Dowex-1-formate (Fig. 1) according to Hurlbert's method. Adsorption on charcoal preserves the normally labile purine-riboside linkages. In the unfertilized egg, the relative specific activities of the four nucleotide alpha phosphates are

$$\text{AMP:GMP:UMP:CMP} = 1.0:1.6:0.52:0.34$$

These differences gradually decrease during development and by the swimming stage are insignificant.

During development the total acid-soluble radioactivity drops gradually as the  $P^{32}$  is converted into acid-insoluble macromolecules; at the same time, the specific activity of the nucleotides rises (Fig. 2), the amount of nucleotides in the pool being maintained at a constant level by new synthesis of nucleotides from the radioactive inorganic phosphate pool. A decrease in the specific activity of the pool

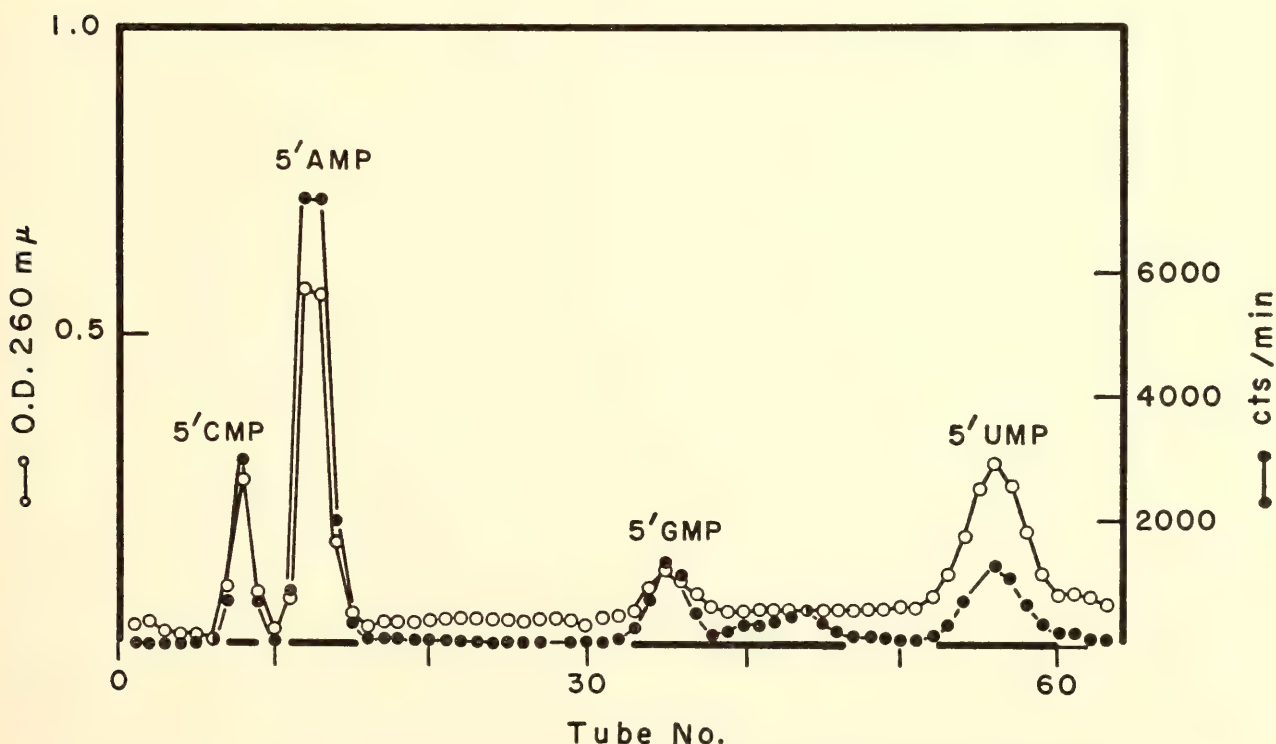


Fig. 1. Separation of  $P^{32}$ -labeled 5' ribonucleotides prepared from acid-soluble fraction of unfertilized eggs by hydrolysis of triphosphates. Nonlinear gradient of formic acid was used to elute nucleotides from a Dowex-1-formate column.



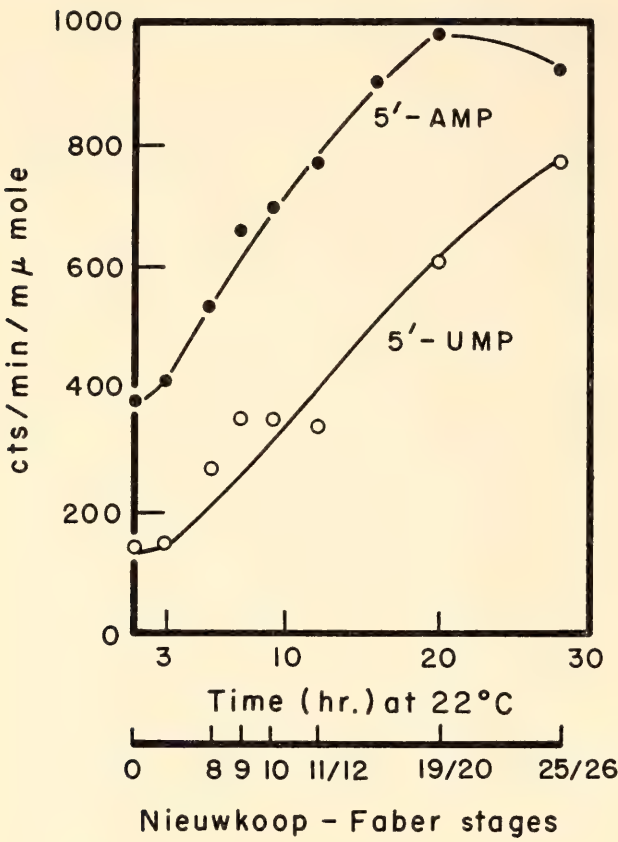


Fig. 2. Specific activity of P<sup>32</sup> nucleotides during development.

begins at the early swimming stage as the result of the more rapid release of non-radioactive yolk phosphate.

The change in specific activity of the nucleotides in the pool is so gradual during early development that only a minor correction need be made when the amounts of radioactive RNA synthesized during a given period of differentiation are compared.

Finally, a convenient measurement validates this technique. During development, deoxyribonucleic acid (DNA) is synthesized, presumably from the same pool of precursors as RNA. Therefore, DNA has been analyzed at different stages, first by the specific activity technique, i.e., calculation of micrograms of DNA from counts per minute in purified DNA, and the known specific activity of the pool. The calculated values have been compared with assays of the same sample by direct measurement. The two values are in good agreement.

*The RNA of the Unfertilized Egg*

The unfertilized egg contains predominantly ribosomal RNA. During ovulation, however, heterogeneous DNA-like RNA (dRNA) is synthesized (*Year Book* 63, pp. 498-499). By specific activity measurements of the pool, a *minimal* value of 1 mμg can be assigned to this dRNA. The small content of 4S RNA has been measured by fractionation on Sephadex and methylated albumin (MAK); (see Fig. 3). Most of the 4S RNA in the unfertilized egg is associated with ribosomes. It is not yet known whether this 4S RNA can accept amino acids. Table 1 summarizes Brown's best estimates for the RNA and DNA content of the unfertilized egg and compares the values with those of the nucleic acids of adult liver.

TABLE 1. RNA and DNA of the Unfertilized Egg of *Xenopus Laevis*

	mμg/mg Wet Weight	
	Egg	Liver
rRNA	4,000	8,000
4S RNA	70	1,200
dRNA	> 1*	80†
DNA	3‡	2,000

\* Value estimated from pool measurements; it is a minimal value.

† Value obtained by assuming that about 1% of the total RNA is dRNA.

‡ Value taken from the work of Dawid.

*Quantitative Analysis of the Three Classes of RNA Newly Synthesized During Development*

Total RNA was isolated from sibling *Xenopus* embryos at different stages and then passed through a column of Sephadex G-100. Both ribosomal RNA (rRNA) and dRNA pass through the column in the void volume while 4S RNA is retarded and therefore separated from the other two types. In Fig. 4 the optical density and radioactivity profiles of purified RNA are shown for each developmental stage. The first class of RNA to be syn-

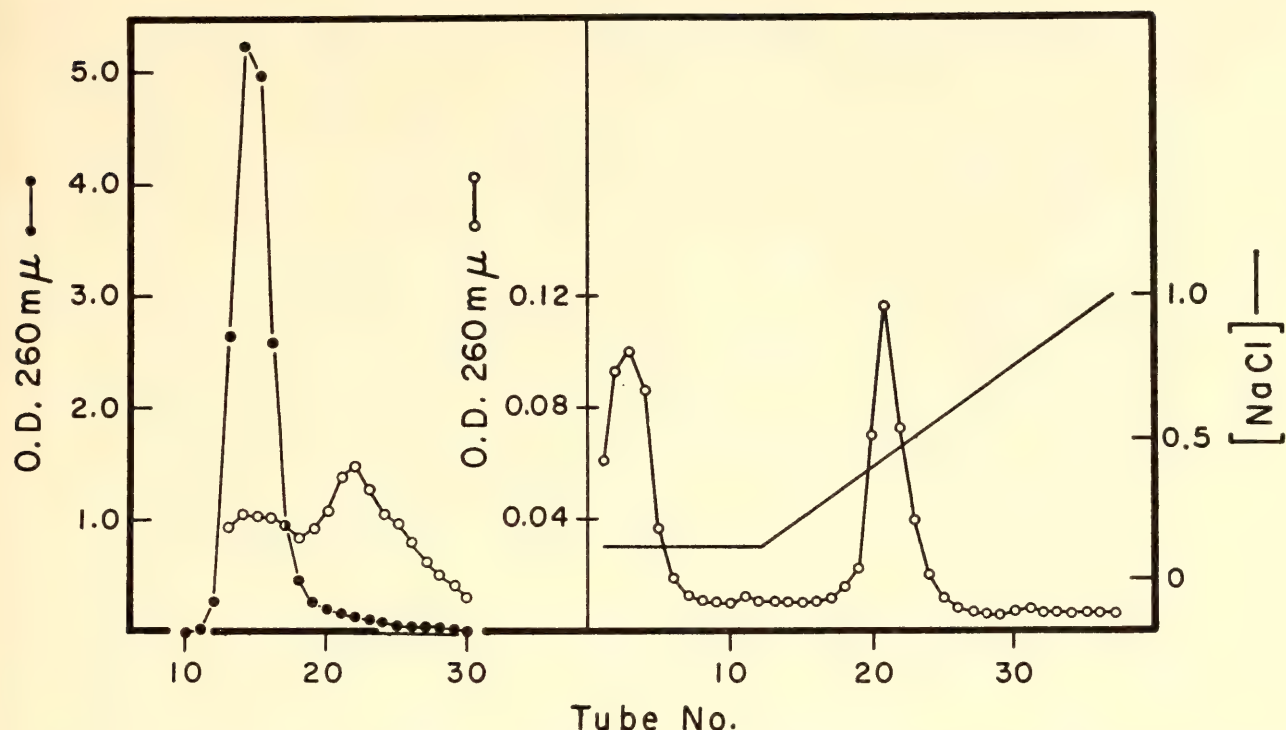


Fig. 3. Isolation of 4S RNA from unfertilized eggs. Postmitochondrial supernatant fluid was extracted with phenol and the aqueous phase passed through a Sephadex G-100 column (left). After the first passage (closed circles) the region following the large peak was concentrated and passed through another column. The procedure was repeated a third time, resulting in the optical density profile represented by the open circles (left). The peak of RNA which had been retarded on the Sephadex column was then fractionated on a methylated albumin column (MAK), and a peak of 4S RNA was eluted at about 0.5 M NaCl (right).

thesized is dRNA. About two hours later, 4S RNA synthesis begins. Base composition of the RNA in the void volume from the column has a progressively higher percentage of G-C content, documenting again the fact that the early embryo is greatly enriched in newly synthesized dRNA in comparison with rRNA. The relative contribution of each class of RNA in the void volume is calculated by assuming that the base composition reflects the arithmetic sum of the two classes, pure dRNA and pure rRNA having overall base compositions of 42 and 60 per cent G-C, respectively (Fig. 5). The total counts per minute, therefore, for each of the three classes has been calculated. At each stage the specific activity of the alpha phosphates of the four nucleotides in the acid-soluble pool was measured. From this value, the actual millimicrograms of all three classes of RNA have been calculated. In Fig. 6

these values are presented on a semilog plot along with the values for DNA content of *Xenopus laevis* embryos as measured by Dawid. The remarkable similarity in the shapes of the 4S RNA, dRNA, and DNA curves is confirmed by plotting the values in Fig. 6 as amount of newly synthesized RNA/DNA at each stage (Fig. 7).

The results demonstrate the striking fact that the embryo accumulates newly synthesized dRNA and 4S RNA in amounts that are a constant when expressed per amount of DNA. Newly synthesized ribosomal RNA, on the other hand, follows an entirely different pattern per cell. To interpret these findings, it will be necessary to know whether dRNA and 4S RNA are labile or stable during this developmental period. For example, if they are completely stable (as ribosomal RNA has been shown to be), then the constant value per DNA reflects a cumu-



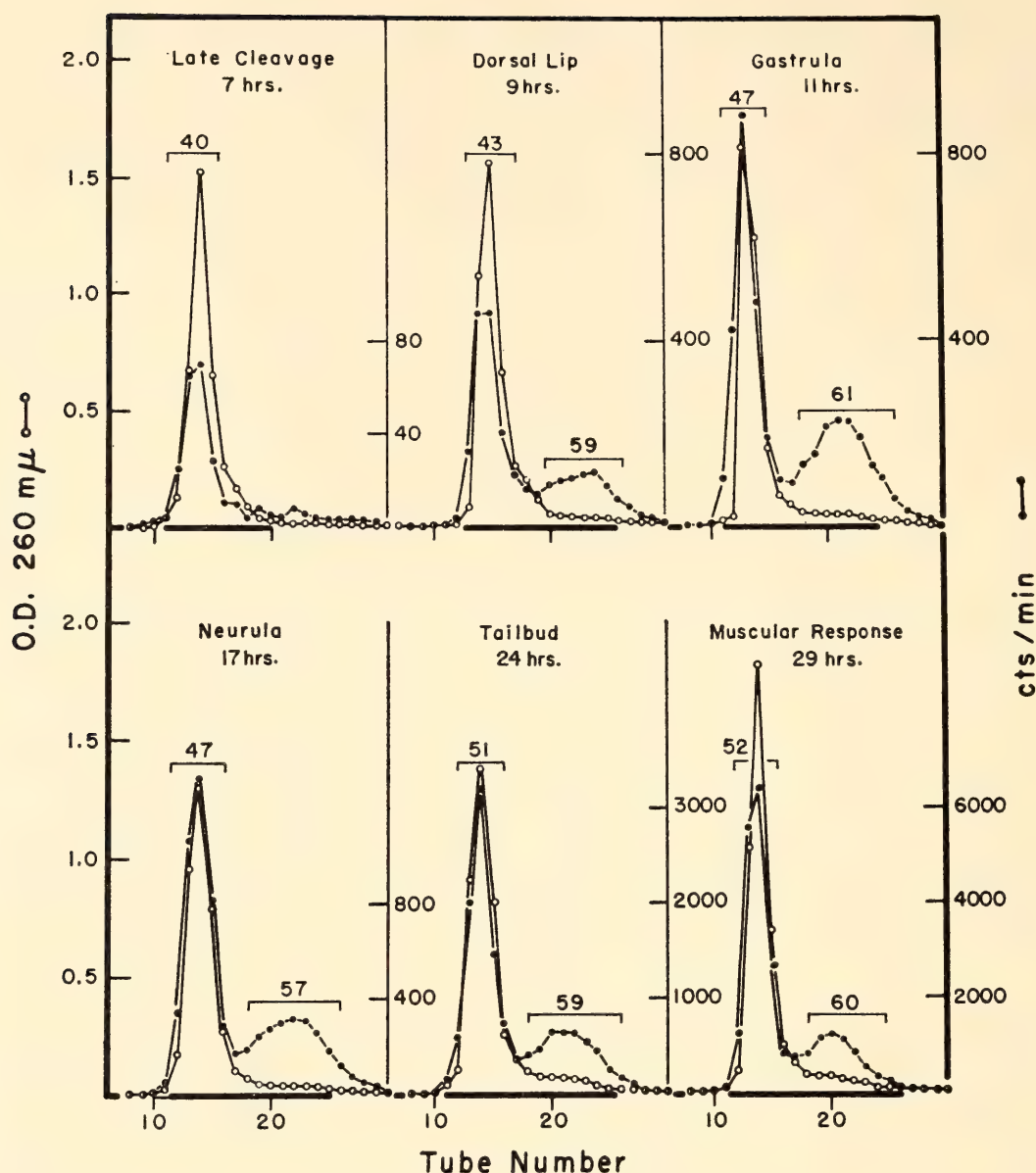


Fig. 4. Sephadex G-100 fractionation of RNA isolated from whole  $P^{32}$ -labeled embryos at varying stages of development. Numbers over brackets refer to guanylic-cytidylic acid (per cent G-C) content of labeled RNA.

lative curve, and the finding means that each time the embryo doubles in cell number it also doubles its amount of the particular class of RNA. On the other hand, if the RNA should turn over rapidly with a short half-life, the interpretation would be different. Brown is now trying to assess the stability of these two classes of RNA during development (see pp. 457-465). An understanding of these events may be useful in postulating mechanisms of regulation involved in the synthesis of the three classes of RNA.

#### *Aggregation of Ribosomes During Development*

Several years ago, when these studies had just begun, Brown and his colleagues observed that the content of "free" ribosomes decreased strikingly as development proceeded. By the tail-bud stage, the embryos seemed to be practically devoid of free ribosomes. At the same time, the fraction of homogenates that could be pelleted at low speed became rich in RNA.

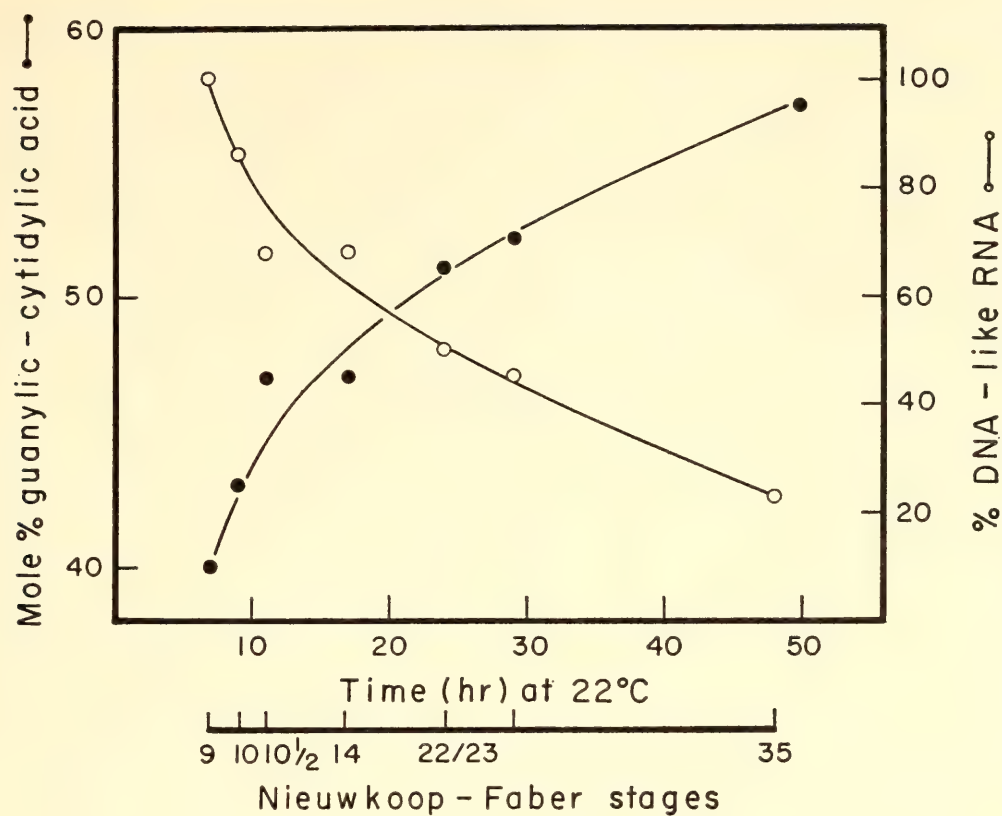


Fig. 5. Summary of base composition of  $P^{32}$ -RNA which passes through the Sephadex column in the void volume. Results obtained from experiment shown in Fig. 4.

As there was no gain or loss of these original egg or “maternal” ribosomes (a term Brown uses to distinguish them from new ribosomes synthesized later) during this period, it was apparent that some structural modification must be taking place. By the tail-bud stage most of the ribosomes have become associated with a cell fraction sedimenting at low speeds. The addition of deoxycholate to homogenates of embryos releases the majority of these “bound” ribosomes.

Brown has begun to analyze this phenomenon in view of the recent demonstrations in other species that ribosomes appear to be active in protein synthesis only when they are aggregated in functional units termed “polyribosomes,” or “polysomes.” The polysomes have been shown to contain all three classes of RNA. Following the addition of deoxycholate, an analysis for ribosomal aggregates has

been performed in embryos of different stages (see Fig. 8 for results). It is clear that at early stages the bulk of the ribosomes are present as monosomes. As development proceeds, an increasingly larger fraction of these original ribosomes becomes aggregated until finally, when the population of monosomes has almost disappeared, the *net* amount of ribosomes (both monosomes and aggregates) begins to increase, marking the time when new synthesis of ribosomes has become very active. The nature of these aggregates has not been completely investigated, and for this reason Brown hesitates to use the term “polysome.” These experiments have not been designed to show the actual *in vivo* size of the aggregates, nor have all appropriate ribonuclease controls and RNA analyses been completed on the different-sized classes of aggregates. Nevertheless, it is clear that the same



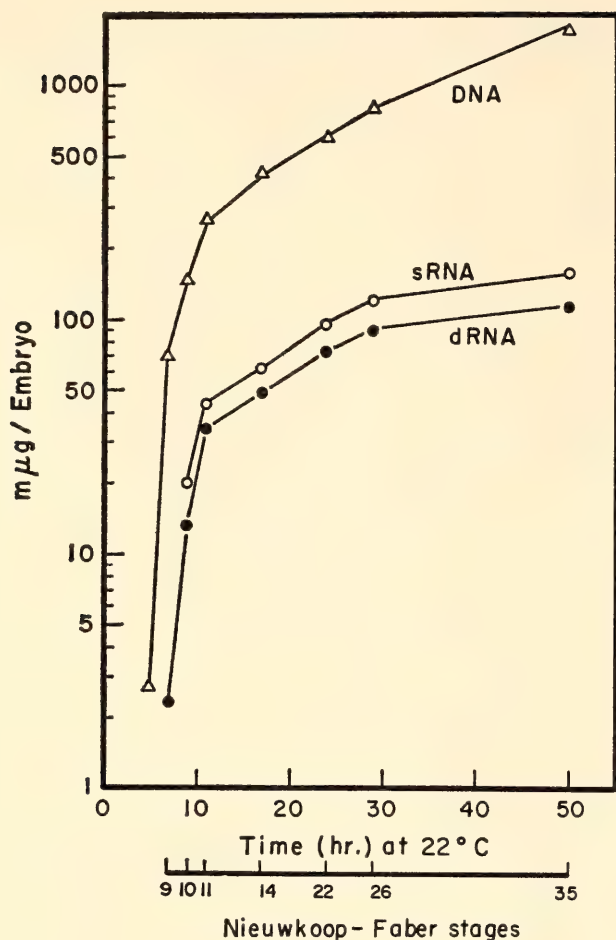


Fig. 6. Actual content of  $P^{32}$ -4S RNA and dRNA at each stage of development. Values from Fig. 4 experiment converted to  $m\mu g$  by means of specific activity method. Curve for DNA content taken from experiments of Dawid.

ribosomes that were initially present predominantly as individual monosomes become aggregated during the course of development.

*Résumé.* These experiments, coupled with the analysis of RNA in the unfertilized egg, have led to the following generalized explanation of the sequence of events that occurs during amphibian embryogenesis. The unfertilized egg is an immature system for protein synthesis since it has a preponderance of only one of the three classes of RNA—ribosomal RNA. During development, RNA synthesis acts to correct this imbalance by greatly increasing the content of 4S RNA and dRNA per embryo. These newly synthesized molecules can be found in

association with the maternal ribosomes (those synthesized during oogenesis). During this period the maternal ribosomes aggregate to an increasing extent, presumably into polysomal complexes now active in support of protein synthesis.

At the tail-bud stage, only a small percentage of the maternal ribosomes are still in the free state (monosomes) and concomitantly, the synthesis of new ribosomes becomes very active.

#### *Synthesis of Messenger RNA Studied by the Agar-DNA Technique*

H. Denis has continued his description of the pattern of synthesis of dRNA during the development of *Xenopus laevis*. DNA-like RNA (dRNA)—presumably mRNA, the direct product of gene action—can be isolated and studied by virtue of its property of forming a molecular hybrid with DNA; mRNA is hybridized with DNA extracted from adult tissues, e.g., blood or liver. The use of adult DNA for studying embryonic RNA is valid only if embryonic DNA can be shown to contain the same nucleotide sequences as adult DNA. The validity of Denis's approach is established by two experiments: (1) A small amount of erythrocyte DNA entrapped in agar is incubated with increasing amounts of radioactive DNA from embryos. The DNA is sheared by sonication and denatured. Under these conditions, 70 to 75 per cent of the nucleotide sequences of adult DNA can be saturated by embryonic DNA (Fig. 9), a level of saturation close to the maximum obtained when adult DNA is incubated with a large excess of DNA of the same origin. (2) Fragments of radioactive DNA from embryos are incubated with erythrocyte DNA immobilized in agar in the presence of increasing amounts of non-radioactive ("cold") sheared DNA either from embryos or from various adult tissues (Fig. 10). If the nonradioactive DNA is complementary to the labeled DNA, it competes for the same sites on the trapped DNA, and the fraction of

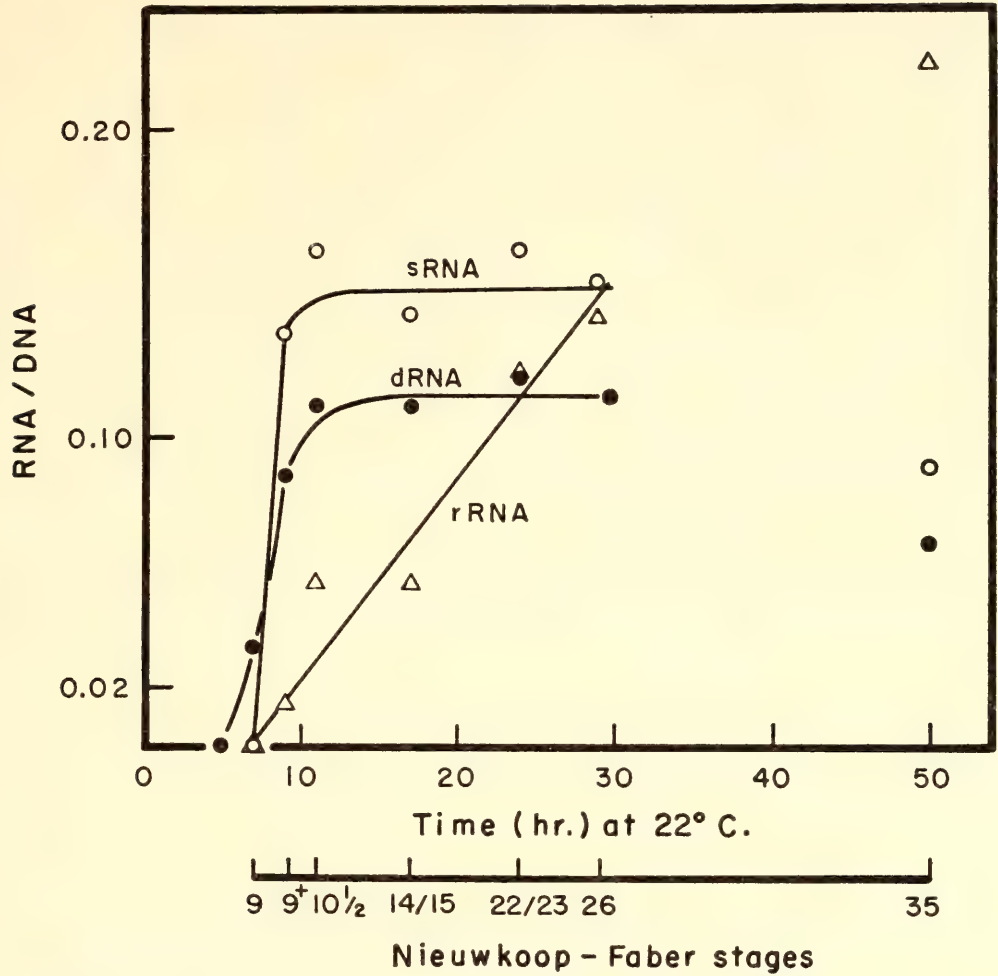


Fig. 7. All three classes of RNA plotted per DNA. Same experimental values from the experiments in Figs. 4-6 expressed in relation to DNA.

radioactive DNA that is hybridized decreases. All the DNA preparations tested were equally competitive versus embryonic DNA, so no detectable difference has been demonstrated between embryonic and adult DNA except for the "cytoplasmic" DNA of the egg and early cleavage stages (see pp. 465-469).

*Hybridizable RNA.* Among the characteristics by which Denis has defined mRNA are the following:

1. Hybridizable RNA from various developmental stages is DNA-like in base composition, containing about 40 per cent G-C, whereas nonhybridizable RNA has the high G-C content (60 per cent) characteristic of ribosomal RNA.

2. Hybridizable RNA is unstable. We have already referred to Kutsky's technique of injecting labeled inorganic

phosphate ( $P^{32}$ ) into the female anuran before ovulation is induced, so that a large quantity of radioactive phosphate enters eggs and remains available throughout embryonic development. When the percentage of radioactive RNA that can be hybridized at various stages of development with a given amount of DNA is examined, it is found to decrease steadily during embryogenesis (Fig. 11). Denis interprets this observation to mean that the hybridizable RNA is continuously being degraded and resynthesized, whereas the nonhybridizable RNA (sRNA and rRNA), when synthesized, remains stable and accumulates.

3. Hybridizable RNA "melts" at a definite temperature which does not vary by more than 2°C during development (Fig. 12). The melting temperature of



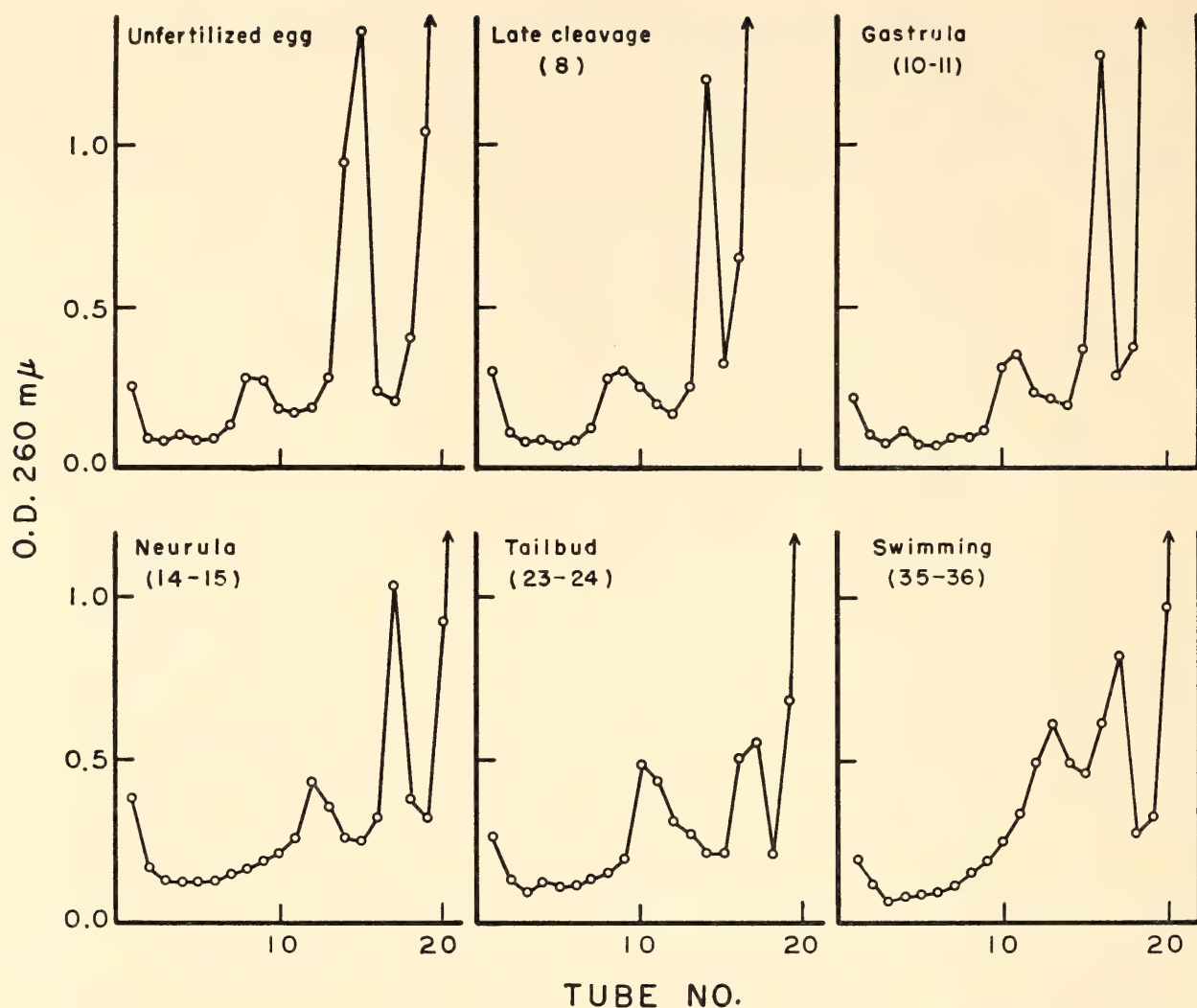


Fig. 8. Sucrose gradient sedimentation of postmitochondrial supernatant fractions from embryos at different stages of development. Linear gradient from 15% to 30% sucrose containing tris-magnesium buffer; centrifugation: 2 hours at 25,000 rpm.

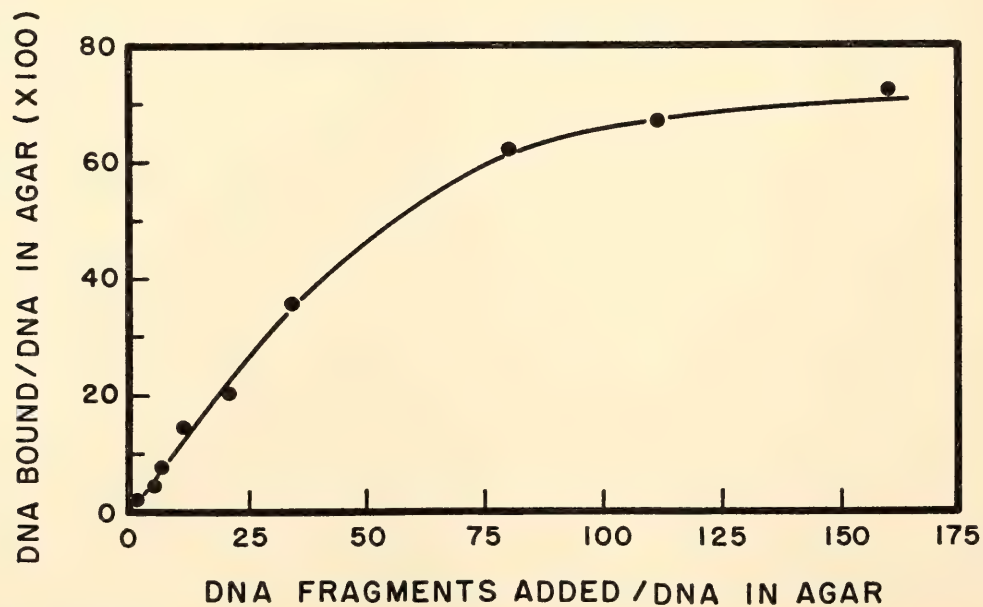


Fig. 9. Saturation of adult DNA with embryonic DNA; 5  $\mu$ g of erythrocyte DNA entrapped in agar incubated at 60°C with increasing amounts of single-stranded DNA fragments extracted from swimming tadpoles.

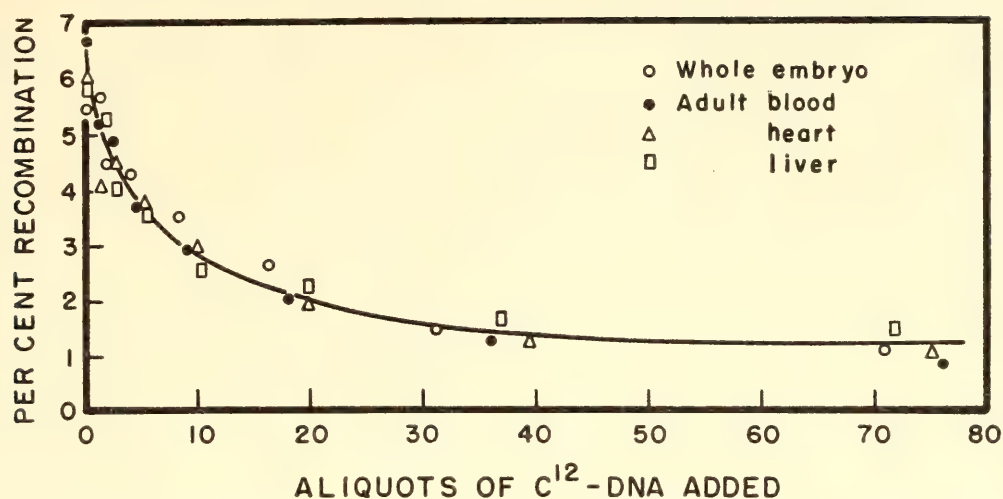


Fig. 10. Competition experiment between DNA fragments from whole embryos and various adult tissues; 5  $\mu$ g of labeled DNA fragments from whole embryos incubated with 50  $\mu$ g of erythrocyte DNA immobilized in agar together with increasing amounts of nonradioactive DNA fragments from various origins.

embryonic mRNA is determined in the following way. P<sup>32</sup>-RNA from one stage is mixed with C<sup>14</sup>-RNA from the same or another stage and hybridized with DNA in agar. After extensive washing in concentrated saline to remove unbound RNA, the hybrid is transferred to a water-jacketed column. The salt concentration is lowered and the temperature is progressively raised. The amount of radioactivity released as P<sup>32</sup> and C<sup>14</sup> at each temperature is measured. The melting point curves for C<sup>14</sup>-RNA and P<sup>32</sup>-RNA from the same stage (e.g., gastrula)

were found to be exactly the same. By this method, RNA is fractionated according to its base composition (the molecules with the lowest G-C content melting first); the results show that hybridizable RNA from every stage contains a wide variety of molecules melting over a range of more than 20°C.

4. Hybridizable RNA represents a fixed proportion of the rapidly labeled RNA (10 to 15 per cent after a 1-hour pulse). If RNA first hybridized with DNA is melted, recovered, and reincubated with the same amount of fresh DNA, about 80 per cent of this RNA hybridizes again during the "rerun" (Fig. 13). Thus, the efficiency of the hybridization technique is about 80 per cent.

5. The hybrid between DNA and embryonic RNA is entirely resistant to RNase but sensitive to DNase, suggesting that the molecular hybrid between DNA and RNA is perfectly helical in structure.

*Species specificity of DNA-RNA and DNA-DNA hybridizations.* The recombination between DNA and embryonic RNA shows a characteristic species specificity. Some recombination takes place between embryonic RNA from *Xenopus laevis* and DNA from genetically related species. The amount of recombination is roughly proportional to the number of nucleotide sequences shared in common

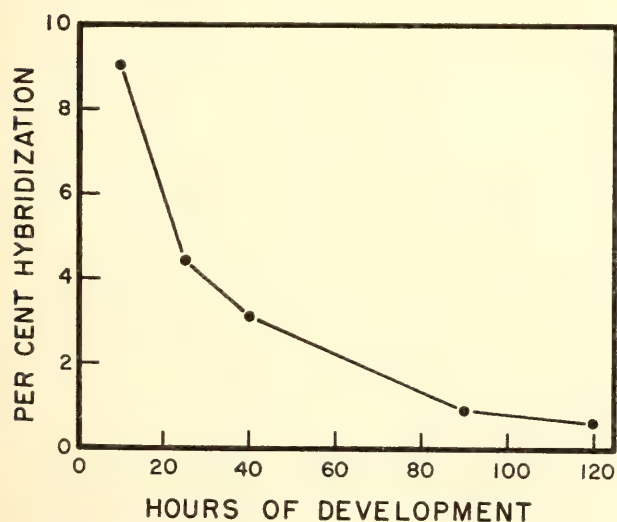


Fig. 11. Change in percentage of hybridizable P<sup>32</sup>-RNA during development; 30  $\mu$ g of RNA labeled by injection of P<sup>32</sup> into the female hybridized with 150  $\mu$ g of DNA trapped in agar.



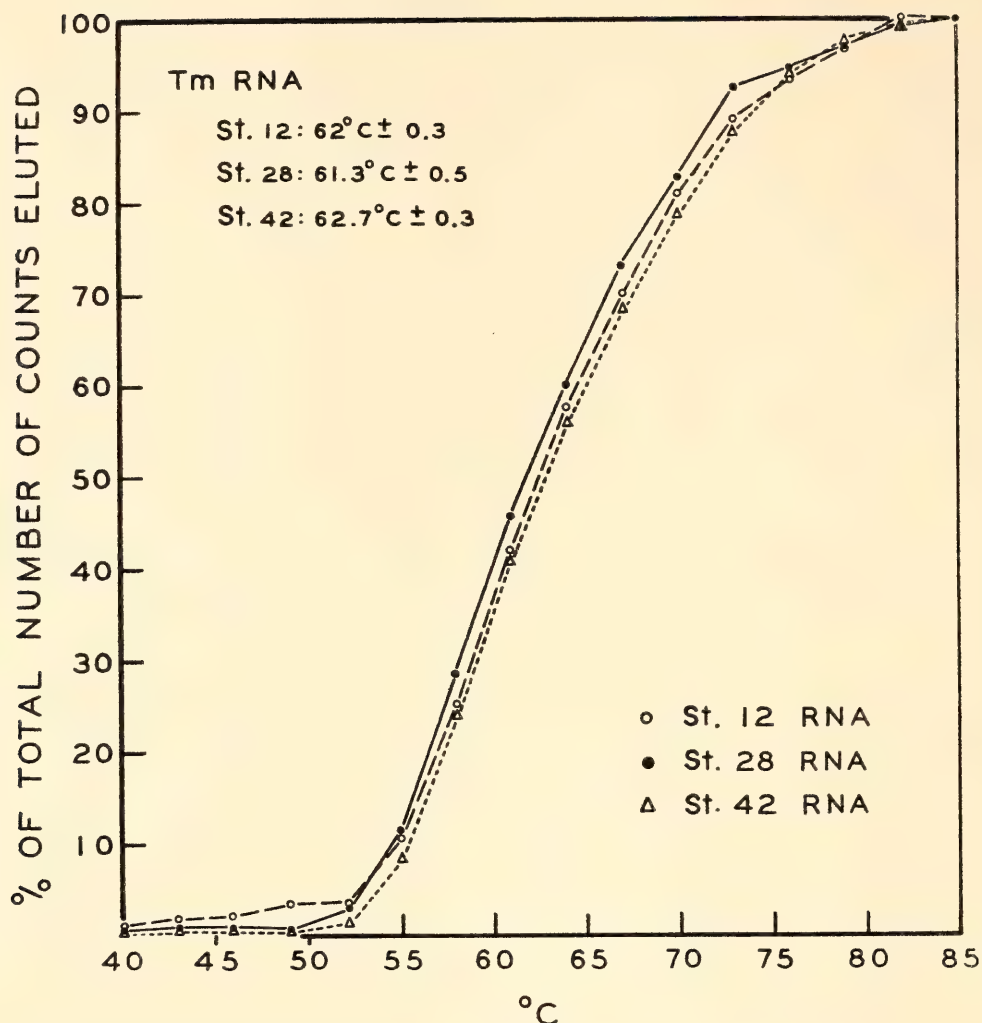


Fig. 12. Melting curves of embryonic RNA of different stages. For experimental details, see text.

between the DNA of the two species. No hybridization occurs between *Xenopus* RNA and bacterial DNA.

The specificity of the recombinations taking place between the DNAs of *Xenopus* and those of related species has been examined in a series of competition experiments. Radioactive DNA from *Xenopus* is sheared by sonication, denatured, and incubated with a fixed amount of *Xenopus* DNA entrapped in agar. An increasing amount of nonradioactive DNA from the same species or from another species is added to the incubation mixture. "Cold" DNA from *Xenopus* is, of course, very competitive versus "hot" DNA of the same origin (Fig. 14). In this type of competition experiment, the radioactive DNA is progressively replaced in the duplex with DNA in agar by nonradio-

active DNA so that the apparent percentage of recombination falls as more and more cold DNA is added. The curve obtained is the reference curve for all the comparisons with other species. Non-radioactive DNA from *Rana pipiens* or *Rana sylvatica* is able to reduce by a definite percentage the recombination that takes place between DNA fragments of *Xenopus* and single-stranded DNA of the same species trapped in agar. The amount of competition obtainable between heterologous DNA and *Xenopus* DNA is thought to be a measurement of the number of nucleotide sequences common to the DNA of the species studied.

Figure 14 shows several of the competition experiments. Many others have been carried out; see Table 2. Some of the experiments were performed in the re-

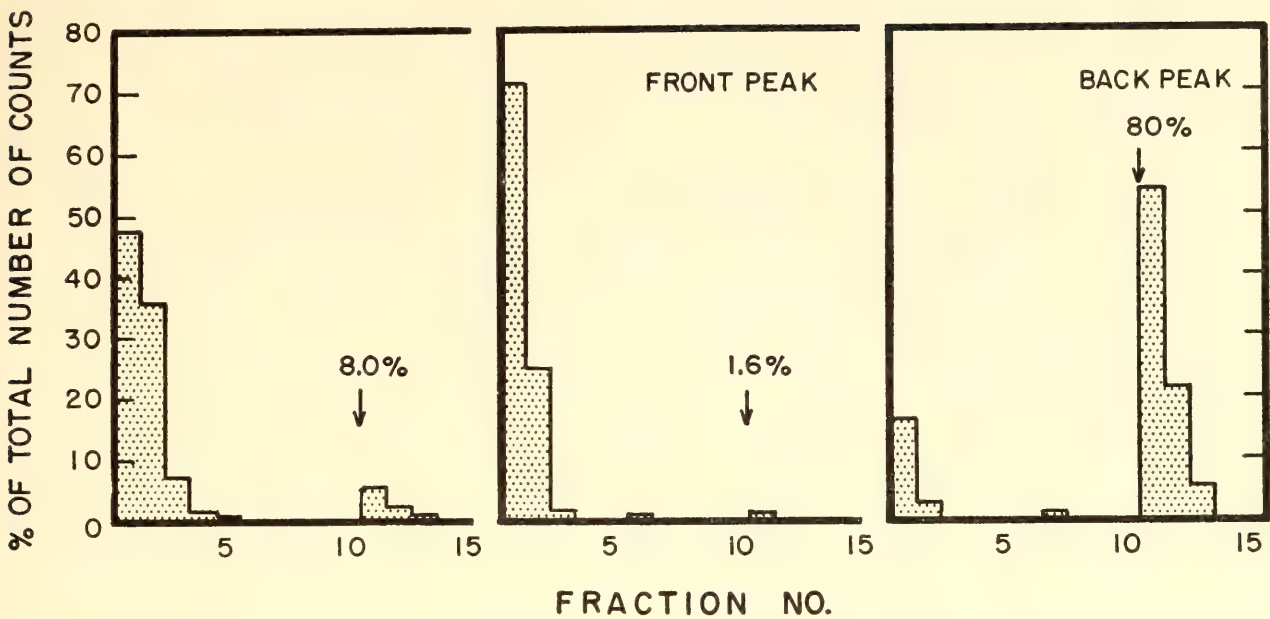


Fig. 13. Experiment to test the efficiency of hybridization techniques; 1.3 mg of pulse-labeled RNA from stage-42 embryos incubated with 420  $\mu$ g of DNA trapped in agar. After 10 washes in concentrated saline ( $2 \times$  SSC at 60°C), the hybrid was “melted” by raising temperature to 75°C and lowering salt concentration to  $0.01 \times$  SSC. The front peak (nonhybridized material) and the back peak (hybridized material) were recovered, concentrated, and incubated again with the same amount of DNA in agar.

TABLE 2. Comparisons of Nucleotide-Sequence Occurrence, Per Cent

	Competition	
	Direct	Reverse
<i>Xenopus laevis</i>		
Occurrence in common with:		
<i>Rana pipiens</i>	28.0	27.0
<i>Rana sylvatica</i>	22.0	—
<i>Amblystoma tigrinum</i>	19.0	9.0
<i>Triturus viridescens</i>	14.0	—
Ox	6.0	4.0
Chicken	2.0	5.5
Salmon	11.0	11.0
<i>Escherichia coli</i>	—	—
<i>Rana pipiens</i>		
Occurrence in common with:		
<i>Xenopus laevis</i>	41.0	—
<i>Rana sylvatica</i>	53.0	—
<i>Triturus viridescens</i>	34.0	—
<i>Escherichia coli</i>	—	0.1

verse direction, meaning that the portion of the DNA of different species that can form a duplex with *Xenopus* DNA has been determined.

The data presented in Table 2 are in good agreement with the existing classification. The number of nucleotide se-

quences shared in common between two given species decreases when one compares species at the level of genus, order, class, and phylum; see Table 3.

*Stability of mRNA in developing Xenopus laevis.* Coming back to the characteristics of mRNA during development, the stability of this fraction has been examined in a series of pulse-chase experiments. In a first experiment, 1,500

TABLE 3. Comparisons of Nucleotide-Sequence Occurrence Showing Order of Decrease in Percentages

Specimens	Classification in Common	Sequences in Common, %
<i>Pipiens</i> }	genus <i>Rana</i>	53
<i>Sylvatica</i> }		
<i>Rana</i> }	order Anura	22-41
<i>Xenopus</i> }		
<i>Xenopus</i> or <i>Rana</i> }	class Amphibia	14-34
<i>Amblystoma</i> or }		
<i>Triturus</i> }		
<i>Xenopus</i> }	phylum Vertebrata	2-11
Ox, salmon, or chicken }		



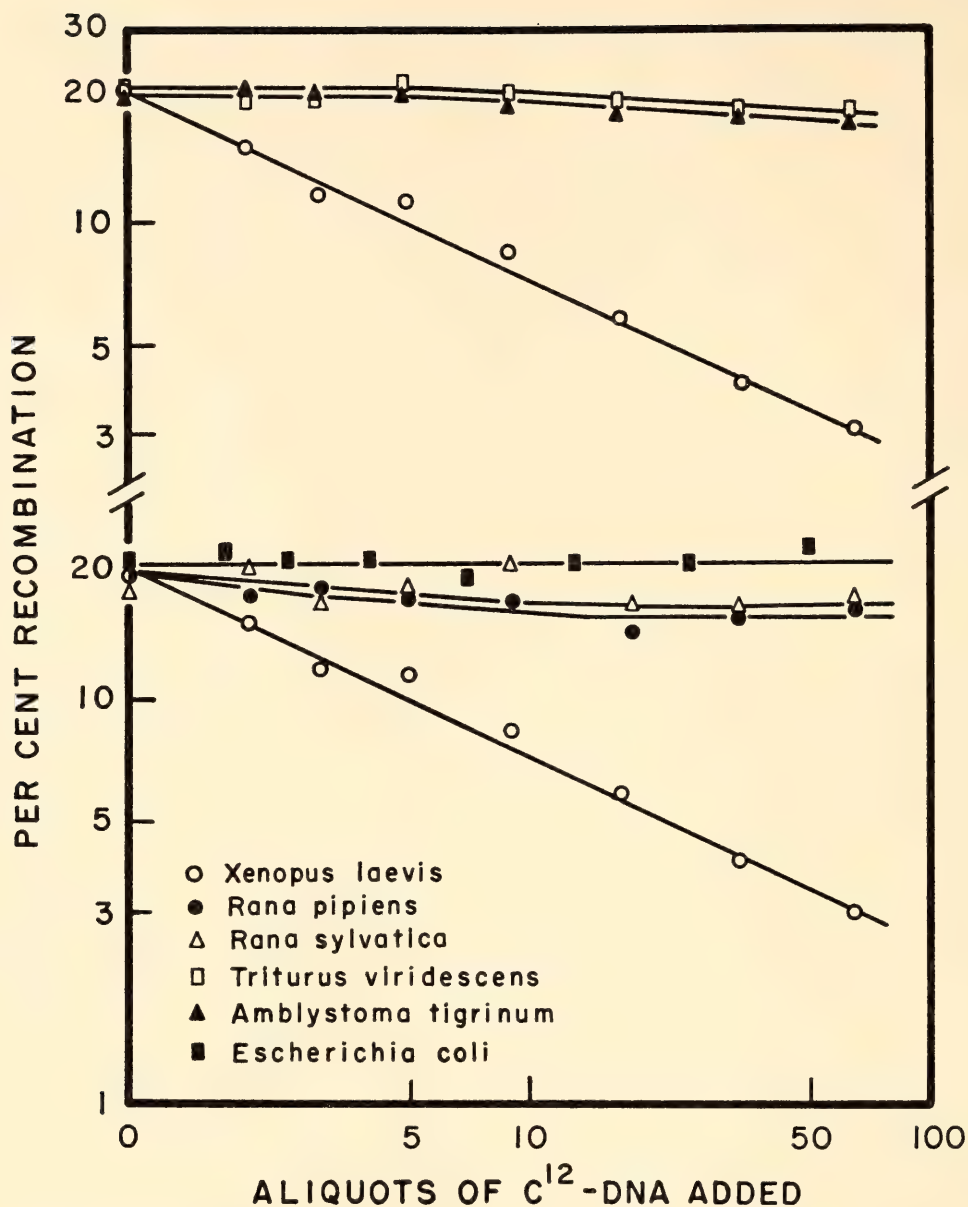


Fig. 14. Competition between DNAs of different species; 5  $\mu$ g of labeled DNA fragments of *Xenopus laevis* incubated with 100  $\mu$ g of *Xenopus* DNA in agar in the presence of larger and larger amounts of nonradioactive DNA fragments of *Xenopus* or other species.

gastrulae were given a 1-hour pulse in  $C^{14}O_2$  and then allowed to grow in non-radioactive medium for two days. At various intervals 100 embryos were removed, RNA was extracted and its radioactivity determined. The amount of radioactivity present in RNA increases during the first 35 hours of chase (Fig. 15), showing that the precursor pool is large into which  $C^{14}O_2$  is incorporated. The RNA isolated after each chase was hybridized with a given amount of DNA. The number of counts in RNA hybridizable with DNA increases during the

first 6 hours after the pulse, reaches a maximum, and then drops sharply (Fig. 15).

The ratio of hybridizable counts to total counts present in RNA, i.e., the percentage of hybridization, decreases steadily during the first 30 hours of chase (Fig. 16). The data shown in Figs. 15 and 16 can be used to calculate the rate at which the percentage of counts hybridized after each chase should decrease, assuming a definite half-life for the mRNA. When a half-life of two hours is adopted for the hybridizable fraction of RNA, a

good fit is obtained between the calculated and experimental decay curves (Fig. 16), indicating that the half-life of mRNA in early embryos (gastrula, neurula, and early tail-bud stages) is about two hours at 22°C.

Two other pulse-chase experiments

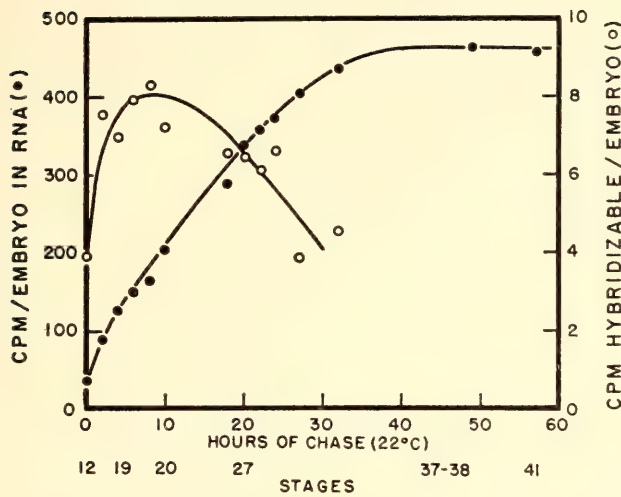


Fig. 15. Pulse-chase experiment at gastrula stage. After 1-hour pulse in  $C^{14}O_2$ , gastrulae were allowed to grow in normal medium. At recovery after different periods of chase total number of counts in RNA and the number of hybridizable counts per embryo were measured.

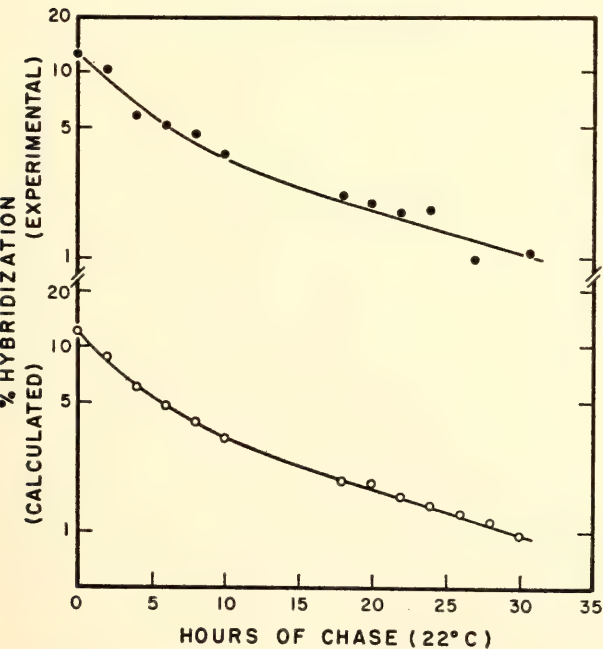


Fig. 16. Change in hybridization rate of RNA extracted after various periods of chase; data from Fig. 15. Open circles show decay curve to be expected if a half-life of 2 hours is adopted for hybridizable RNA.

were performed with older embryos (swimming tadpoles, stage 42). The results obtained in these experiments were similar, but differ strikingly from those obtained with gastrulae. The percentage of hybridization decreases sharply during the first 3 hours of chase (Fig. 17) and much more slowly from the fifth hour on.

Assuming half-lives of varying lengths of mRNA, agreement cannot be obtained between the calculated and the experimental decay curves. Fig. 17 shows how the percentage of hybridization should drop during the chase when a half-life of one hour is assumed for mRNA. It is necessary to postulate the existence of at least two different mRNAs having different half-lives. The data can be interpreted by assuming two classes of mRNA molecules: one with a half-life of 1 hour and another with a half-life of about 45 hours. This line of thought suggests that the older embryo contains some mRNA molecules of considerable stability, whereas all the mRNA of the early embryo seems to turn over at a rapid rate.

*Patterns of mRNA synthesis.* The mRNAs made by embryos at different stages of development have been examined in a series of competition experiments. In the first experiment, RNA from embryos at stage 39 labeled by injection of  $P^{32}$  into the female was used. If cold RNA from embryos at the same stage is added to the incubation mixture containing  $P^{32}$ -RNA and DNA, a competition is observed: the percentage of hybridization falls from 2.3 to 1.4 when 10 aliquots of cold RNA are added (Fig. 18). Nonradioactive RNA from cleaving eggs does not compete with  $P^{32}$ -RNA from embryos at stage 39. RNA extracted from neurulae (stages 22–26) shows some competitiveness, and RNA from tail-bud embryos (stages 28–32) is about half as competitive versus stage 39 RNA as stage 39 RNA itself. This experiment shows that the mRNA present in the swimming tadpole has nothing in common with that in the cleaving egg. This finding might have been expected because it has been repeat-



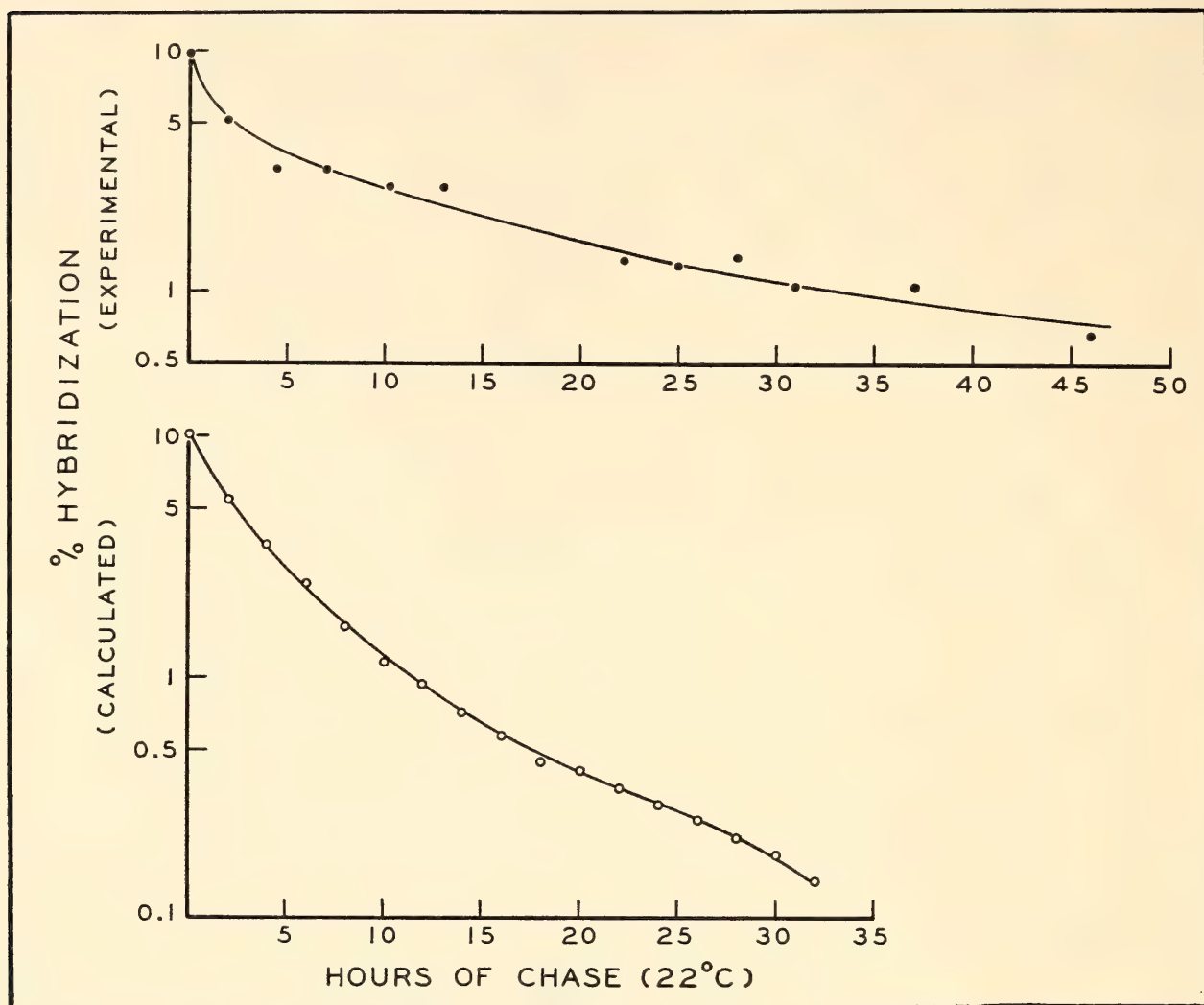


Fig. 17. Change in the hybridization rate of RNA extracted from stage-42 embryos after various periods of chase. Lower curve shows decay rate expected assuming a half-life of 1 hour for hybridizable RNA.

edly shown that cleaving eggs synthesize little mRNA. The neurula contains a small portion of the mRNA of the swimming tadpole; the tail-bud larvae have more of it.

In another experiment, pulse-labeled RNA from tail-bud embryos was challenged against cold RNA from other stages (Fig. 19). RNA from embryos in late cleavage does not compete with RNA from embryos at stages 26–28. RNAs from gastrulae and neurulae do compete with tail-bud RNA; however, the shape of the competition curves suggests to Denis that the difference between gastrula and tail-bud RNAs is mainly qualitative, whereas the difference between neurula

and tail-bud RNA is mainly quantitative, in that the tail-bud embryo contains all the specific mRNAs present in the neurula, but in a larger number of copies. RNA from swimming tadpoles (stages 35–38 and stage 42) seems to be more competitive versus tail-bud RNA than tail-bud RNA versus itself, again suggesting that all the mRNAs present in the tail-bud embryo are also present in older embryos, but in a larger number of copies.

A competition experiment between neurula mRNA and mRNA from other stages gave results similar to those described, the only difference being that mRNA extracted from older embryos is

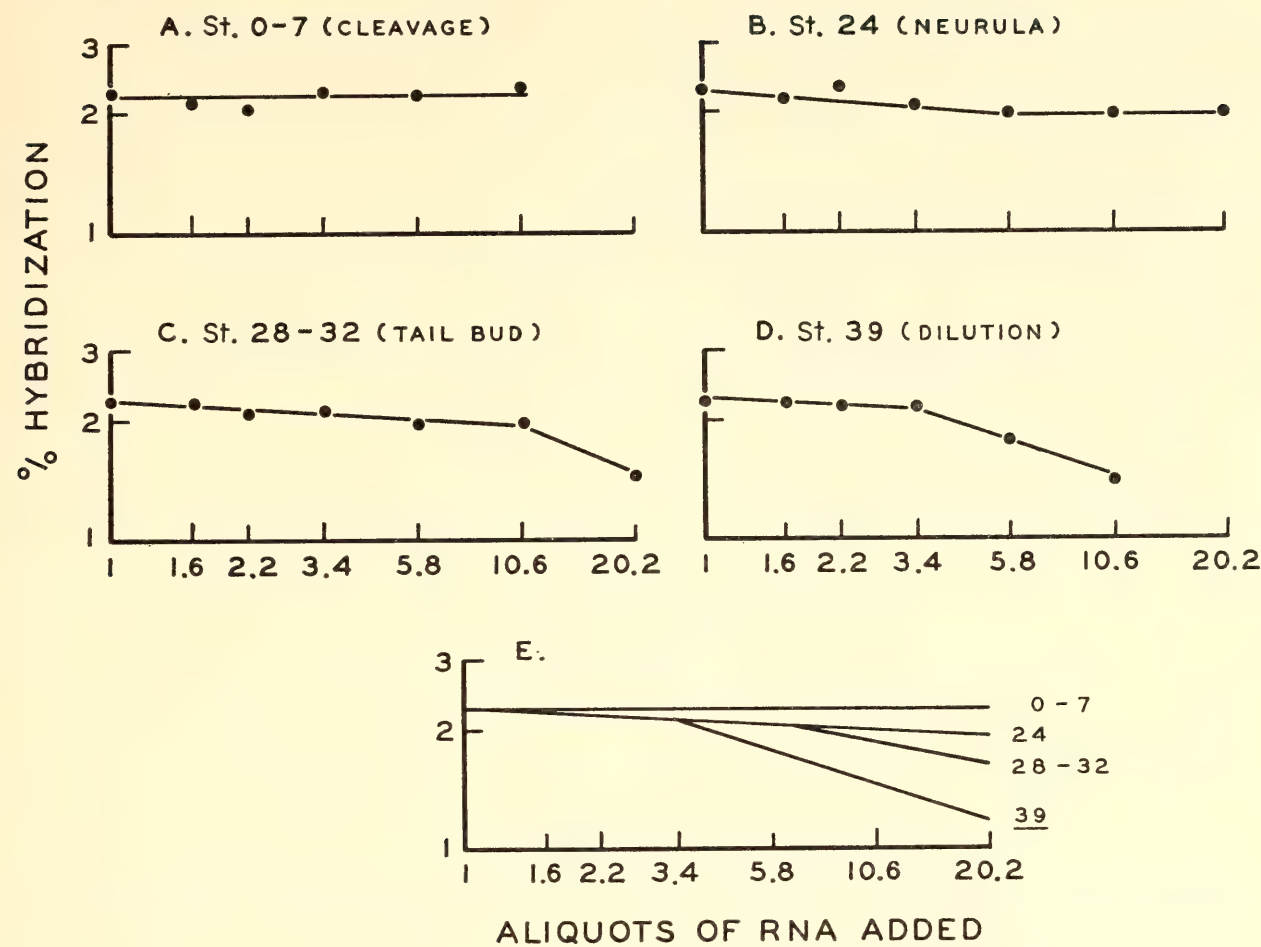


Fig. 18. Competition between  $P^{32}$ -RNA from stage 39 and "cold" RNA from other stages; 64  $\mu$ g (= 1 aliquot) of labeled RNA incubated with 110  $\mu$ g of erythrocyte DNA in agar together with 0, 0.6, 1.2, 2.4, 4.8, 9.6, and 19.2 aliquots, respectively, of nonradioactive RNA. In E, data are summarized on per embryo basis.

slightly less competitive versus neurula RNA than neurula RNA versus itself.

A similar observation was made when gastrula mRNA (Fig. 20) was coupled with mRNA from older embryos. About 25 to 30 per cent of the hybridization that takes place between gastrula mRNA and DNA cannot be blocked by mRNA from swimming tadpoles, suggesting that the early embryo contains nucleotide sequences not found in the older embryo.

Denis has summarized and interpreted the data obtained in numerous competition experiments as follows:

1. Much of the mRNA in the early embryo (gastrula through neurula) is identical with that in the swimming tadpole. Furthermore, the early embryonic stages contain a small number of mRNAs

that are specific for those stages and that would result from the activity of transient genes. When RNA from a whole adult is tested versus pulse-labeled RNA from gastrulae (Fig. 21), adult RNA is about as efficient a competitor versus gastrula RNA as gastrula RNA itself. Heart and liver RNA tested separately are slightly less competitive than RNA from the whole adult, showing that a large part of the RNA made by the gastrula belongs to a generalized type that is widely distributed in the adult organism. Other experiments with RNA present in older embryos gave similar results. The organ specificity of the RNA present in swimming tadpoles is, however, much more pronounced than that of the gastrula RNA. Compared with RNA extracted



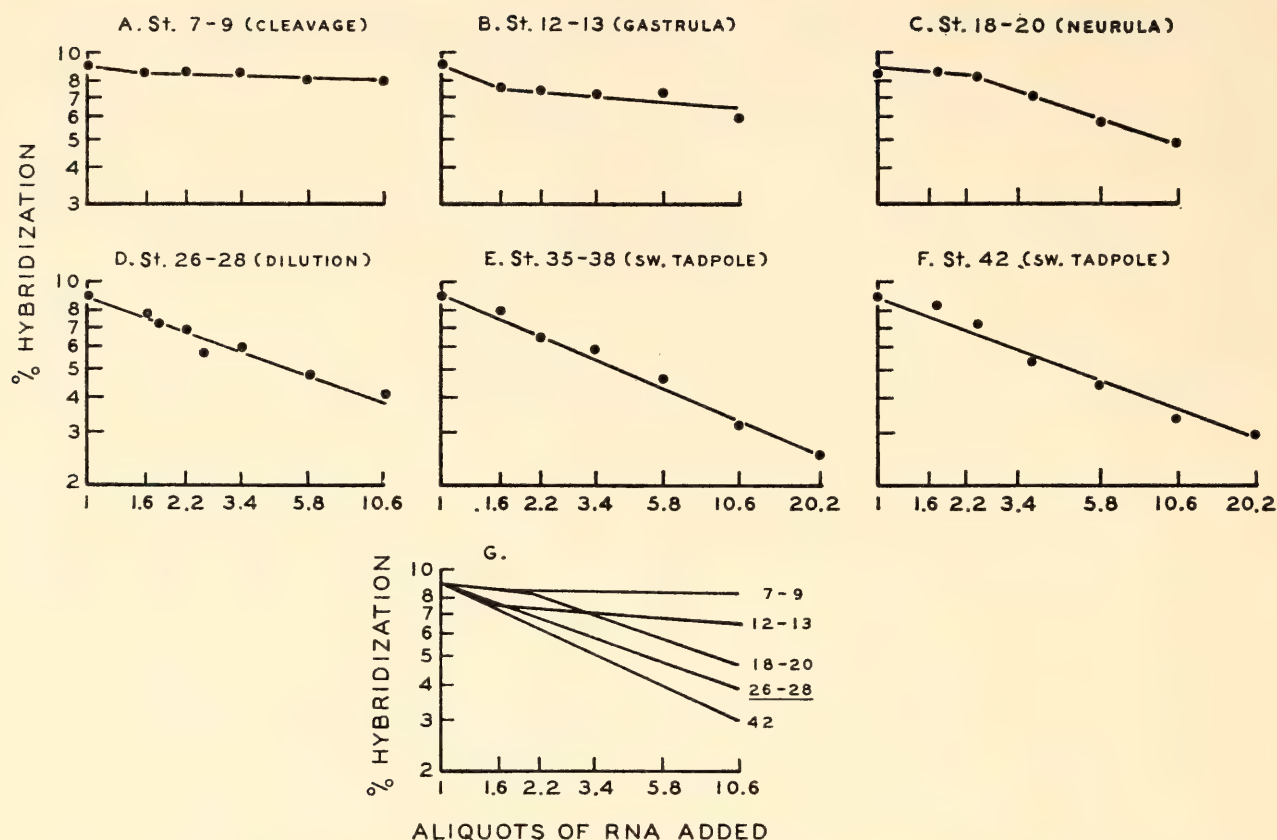


Fig. 19. Competition between pulse-labeled RNA (1 hour) from stages 26 to 28 and RNA from other stages. One aliquot (38  $\mu$ g) of labeled RNA incubated with 46  $\mu$ g of DNA in agar together with increasing amounts of "cold" RNA. In G, data plotted on per embryo basis.

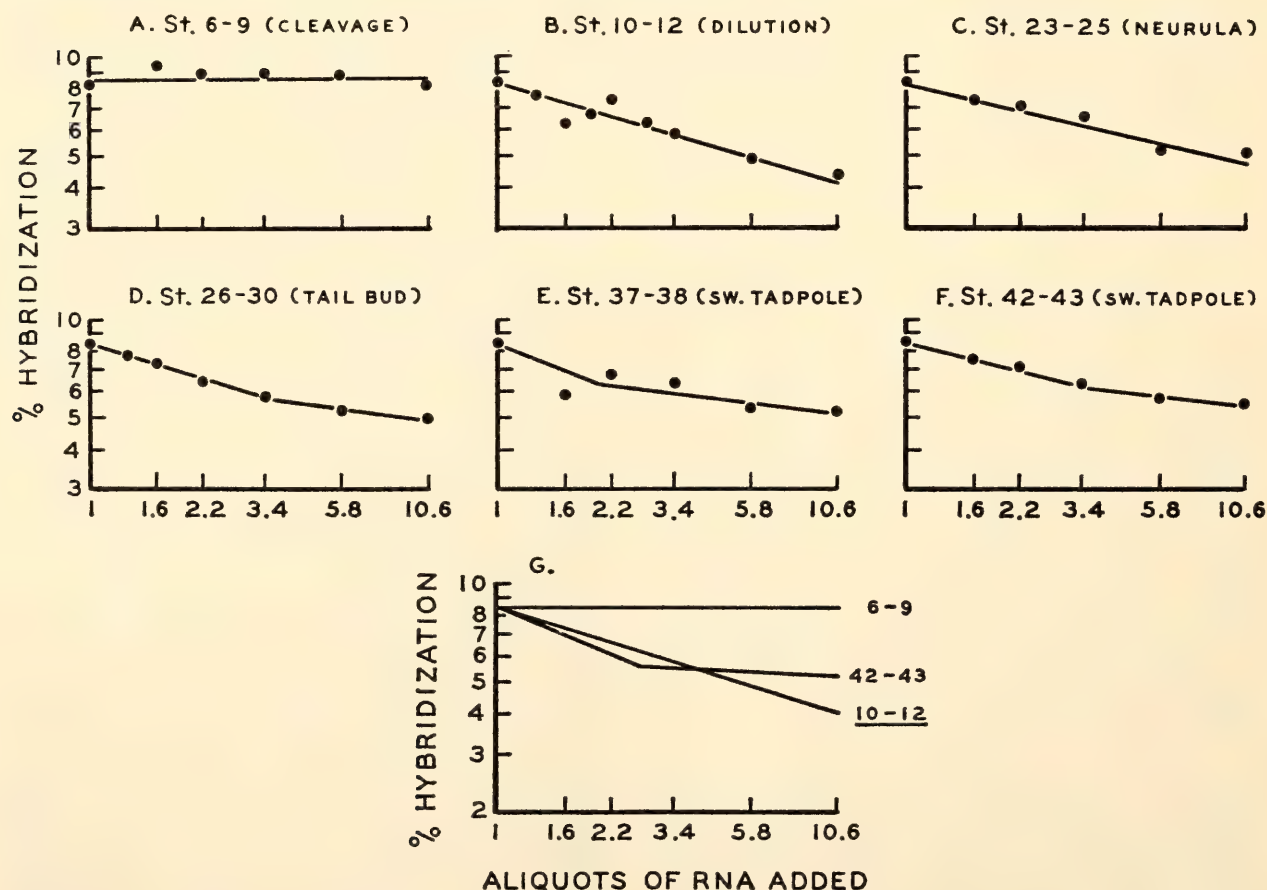


Fig. 20. Competition between pulse-labeled RNA (1 hour) from stages 10 to 12 and RNA from other stages. One aliquot (88  $\mu$ g) of gastrula RNA incubated with 104  $\mu$ g of DNA in agar.

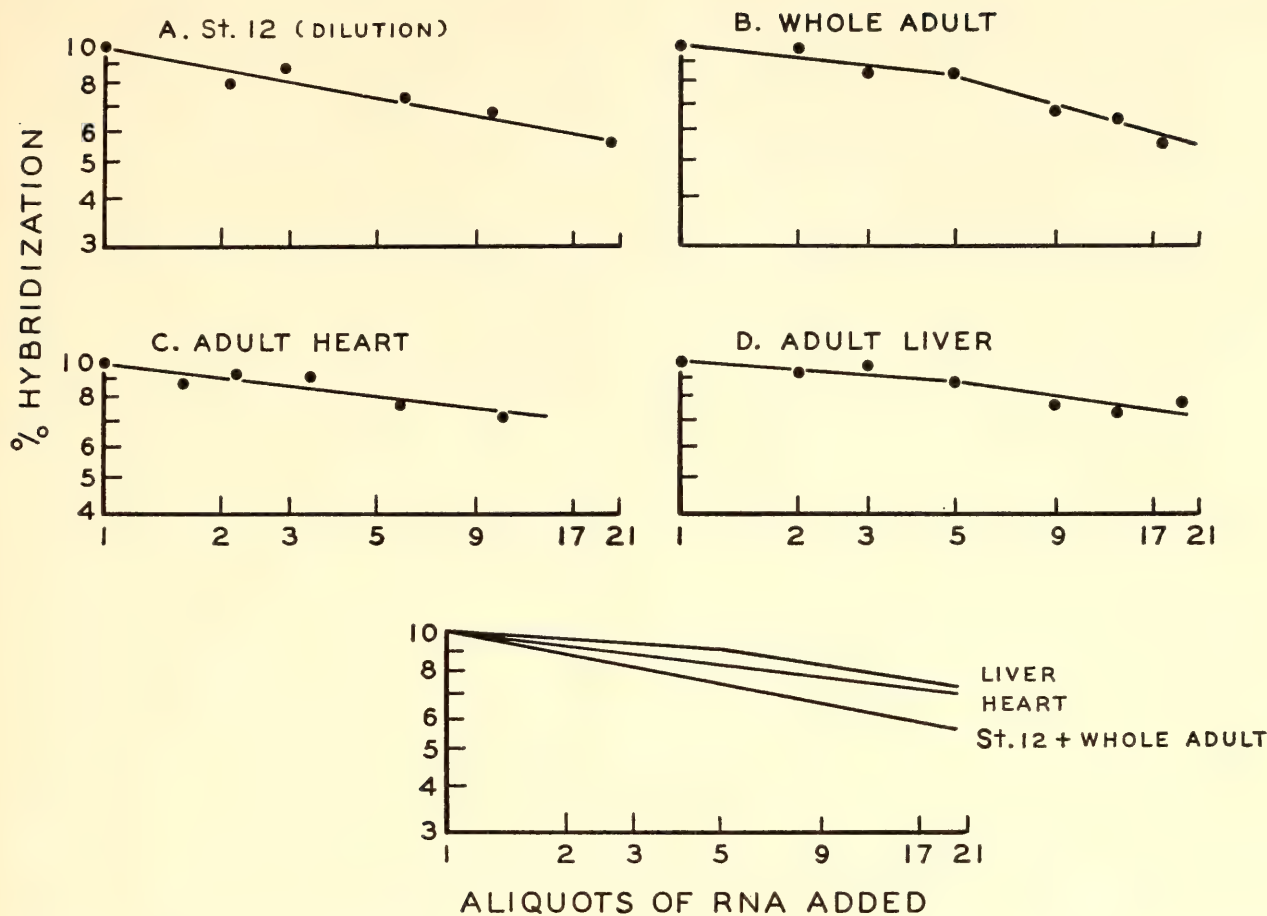


Fig. 21. Competition between pulse-labeled RNA (1 hour) from stage 12 and RNA extracted from either whole adult or different adult tissues; 1 aliquot (57  $\mu$ g) of gastrula RNA incubated with 208  $\mu$ g of DNA in agar. Data summarized on RNA basis in final graph.

from the whole adult, liver RNA is only slightly competitive versus RNA from stage 42 embryos.

2. The developing embryo contains a wider and wider variety of messenger molecules. Attempting to prove this point Denis undertook a series of saturation experiments. What portion of the DNA can be saturated by RNA from different stages of development? To convert to micrograms the number of counts per minute bound to DNA, the specific activity of mRNA must be obtained; as already shown, this is done by measuring the activity of the free nucleotides from which mRNA is synthesized. The pool of mono-, di-, and trinucleotides was extracted from embryos at the same time as mRNA. The di- and trinucleotides were then hydrolyzed to mononucleotides and chromatographed on Dowex. Each fraction (5'-AMP, 5'-CMP, 5'-GMP, and

5'-UMP) was further purified by paper chromatography. Knowing the base composition of hybridizable RNA (about 40 per cent G-C) and the specific activity of each nucleotide, we have seen how it is possible to calculate the specific activity of the messenger fraction. A number of saturation experiments were carried out and the results are summarized in Fig. 22.

If  $P^{32}$  injected into the female is used as a precursor of RNA, all the molecules made since the beginning of development are radioactive.  $P^{32}$ -labeled RNA from gastrula saturates 2.4 per cent of the genome; RNA from tail-bud embryos labeled in the same way saturates 5 per cent of the genome, and RNA from swimming tadpoles (stage 39) is complementary to 7.5 per cent of the DNA, showing that, as development progresses, the variety of molecules present in the embryo increases.



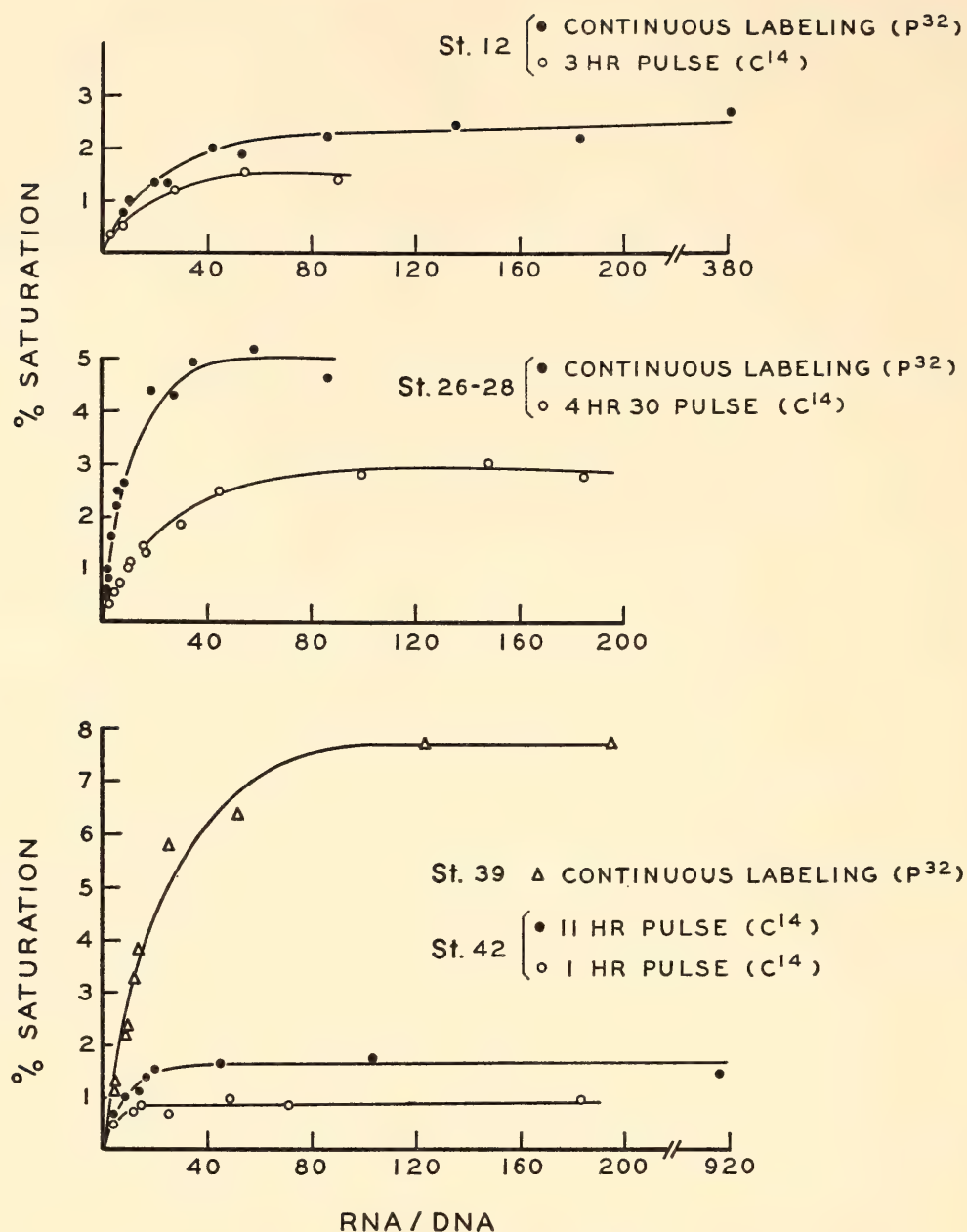


Fig. 22. Saturation of DNA with RNA from different stages; 15  $\mu$ g of erythrocyte DNA in agar saturated with RNA labeled by  $P^{32}$  injected into the female or with RNA labeled with  $C^{14}O_2$  for a shorter time. Specific activity of hybridizable fraction measured in precursor pool.

The actual number of genes active at any one given moment, however, is not necessarily larger in differentiated embryos than in early embryos. The point is suggested by a few saturation experiments performed with pulse-labeled RNA. At stages 12 and 26-28, RNA labeled for a short time with  $C^{14}O_2$  saturates more than half the DNA sequences complementary to  $P^{32}$ -RNA. This observation is taken to mean that the mRNA of embryos up to tail-bud stage is in rapid

equilibrium with the precursor pool. After 3 to 4 hours more than half the messenger molecules bear the label. At stage 42, however, RNA labeled for 1 hour and for 11 hours in  $C^{14}O_2$  saturates only 0.8 per cent and 1.6 per cent, respectively, of the DNA, whereas  $P^{32}$ -RNA saturates 7.5 per cent of it. Thus, in these embryos, there is a large population of molecules that do not equilibrate with the precursor pool and that must have a considerable stability. The finding con-

firms the results obtained by pulse-chase experiments. The mRNAs of older, differentiated embryos probably cannot be labeled by a short pulse because they are complementary to regions of the genome which are no longer being transcribed. In other words the older embryo has more messengers produced by genes that have been active in earlier stages but are now "switched off." Differentiation seems to be accompanied by a stabilization of gene products.

3. Early embryos have a certain number of transient genes. This argument can be amplified by a two-step saturation experiment (Fig. 23). A small amount of

DNA in agar is saturated with  $P^{32}$ -RNA from embryos at stage 39. When the saturation plateau is reached, an increasing amount of  $C^{14}$ -RNA from gastrulae is added to the incubation mixture. The results show that there is a small region of the DNA that is complementary to gastrula RNA and that cannot be covered by swimming tadpole RNA. The length of the genome corresponding to gastrula "genes" ranges between 0.5 to 0.75 per cent of the total nucleotide sequences. The complementary experiment (Fig. 23, upper part) shows that the gastrula RNA covers only a small part of the DNA on which swimming tadpole RNA is transcribed, once again showing that differentiation is accompanied by a progressive release of the information contained in DNA.

#### DNA IN AMPHIBIAN EGGS

It was reported in *Year Book 63* (pp. 510-516) that the eggs of two amphibian species, *Rana pipiens* and *Xenopus laevis*, contain DNA in excess of the amount expected for single cells. I. Dawid isolated this DNA and found it to be double-stranded material of high molecular weight. Further characterization of egg DNA will be reported below.

The isolation method described last year was improved by initial proteolytic digestion of the egg proteins by the enzyme pronase. Further purification was achieved by phenol-detergent treatment and centrifugation in cesium chloride gradients. The recovery of DNA by this method was measured by the addition of small quantities of radioactive DNA and was found to be 80 per cent with *R. pipiens* eggs and 30 per cent with eggs of *X. laevis*. By correcting the amounts of DNA obtained for quantitative recovery, it was found that eggs contain 300 to 500 times the quantity of DNA present in diploid somatic cells (Table 4).

It was reported in *Year Book 63* that the "cytoplasmic" DNA of *R. pipiens* eggs has the same density as liver DNA of that species. The egg DNA in *X. laevis*

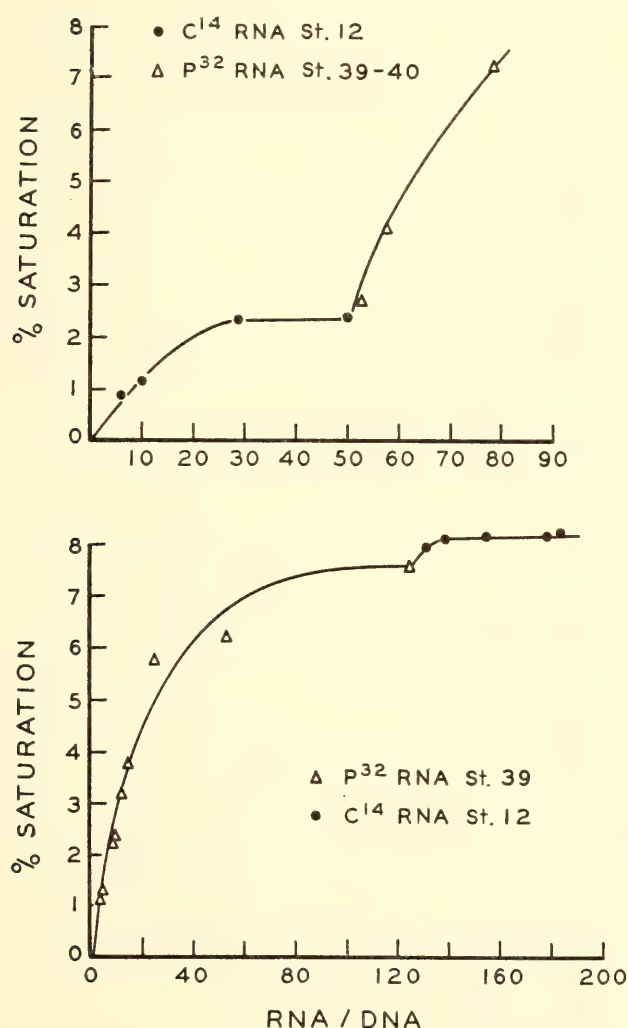


Fig. 23. Double saturation experiment with RNA from 2 different stages; 15  $\mu$ g of DNA in agar (upper part of figure) saturated with  $C^{14}$ -RNA from gastrulae and then offered increasing amount of  $P^{32}$ -RNA from stage 39. Lower part of figure shows the reverse experiment.



TABLE 4. DNA Content of Amphibian Eggs

	mμg Per Cell	
	Egg	Erythrocyte
<i>Rana pipiens</i>	4.5	0.015
<i>Xenopus laevis</i>	3.1	0.006

Note: DNA content of erythrocytes was determined using the diphenylamine reaction. The value for eggs was obtained by correcting the amounts found in the band in CsCl for 100% recovery with the aid of an isotope dilution method (see text).

is more dense than the somatic DNA (Fig. 24). This observation was the first indication of a qualitative difference between egg and somatic DNAs. To explore further the relation of these DNAs, hybridization experiments were performed using the agar-DNA technique. Since attempts to label egg DNA in vivo were not successful, direct hybridization of egg DNA to somatic DNA could not be tested. This difficulty was circumvented by (1) competition experiments, and (2) using highly labeled complementary-RNA synthesized with egg DNA as template.

DNA samples from different somatic tissues of animals of the same species are indistinguishable in the competition ex-

periments, as shown by McCarthy and Hoyer for the mouse and by Denis for *X. laevis*. The results of a competition experiment are presented in Fig. 25. The agar contained erythrocyte DNA, the labeled DNA fragments being obtained from whole tadpoles and the nonradioactive fragments being derived from liver DNA. In contrast to liver DNA, egg DNA fragments do not compete with the labeled DNA, and the degree of hybridization remains unchanged (Fig. 25). Small amounts of labeled fragments were incubated with relatively large agar samples, resulting in scattering of the points. Small experimental variations in the amount of fragments added produce large differences in the fraction hybridized, a fact illustrated by the steepness of the curve in its initial phase. Competition experiments with eight independent preparations of egg DNA from *X. laevis* gave results similar to those shown in Fig. 25. *It can be concluded that egg DNA cannot be complementary to more than 5 per cent of the somatic DNA*, since this is the limit of sensitivity of the competition experiments.

Direct hybridization is a more sensitive test for complementarity than competition. This approach became possible by



Fig. 24. Density comparison of *X. laevis* DNA. Egg DNA, 8 μg, and labeled somatic DNA, 0.7 μg containing 840 count/min, centrifuged in CsCl in a volume of 5 ml. A total of 230 fractions collected; only those containing the band are shown. Open circles, absorbancy at 260 mμ; closed circles, radioactivity.

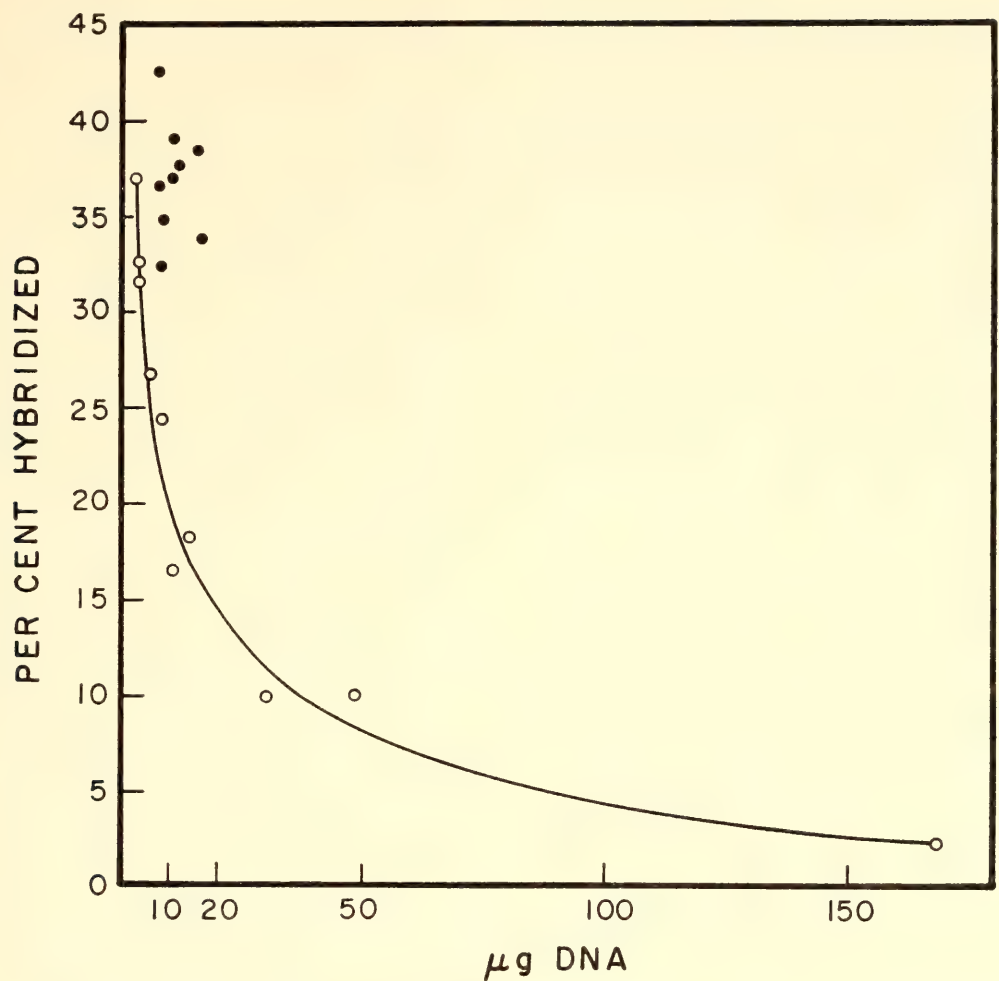


Fig. 25. Samples of agar (80 mg) containing 50  $\mu\text{g}$  *R. pipiens* erythrocyte DNA incubated with denatured DNA fragments prepared from mixtures of 3  $\mu\text{g}$   $\text{C}^{14}$ -labeled DNA from tadpoles and carrying amounts of liver DNA (open circles) or egg DNA (closed circles).

the preparation of complementary RNA (c-RNA) of high specific activity, which was prepared with RNA-polymerase from *E. coli* and egg DNA as a template. It is well established that RNA synthesized with RNA polymerase is complementary to the DNA template used. Therefore, c-RNA was regarded as a copy of the DNA, and transcription made it possible to obtain the sequence of egg DNA in a highly radioactive form. Table 5 shows the results of hybridization experiments with c-RNA. Liver c-RNA (meaning, as it does in analogous cases, c-RNA synthesized with liver DNA as template) hybridizes 40 to 50 per cent with all agar-DNA samples. Egg c-RNA formed duplexes with liver DNA in agar, but the fraction hybridized was lower (Table 4). Hybridization between egg c-RNA and

erythrocyte agar was still lower, although the agar preparation was very efficient in binding liver c-RNA. To interpret these findings, it must first be pointed out that the amount of DNA in the agar was 3,000–100,000 times the quantity of c-RNA added. Despite the excess of DNA, only 48 per cent of the liver c-RNA is bound, although all of its sequences are complementary to the DNA. The hybridization of liver c-RNA observed is thus a maximum value and in the range studied, independent of the amount of DNA-agar used (Table 5). In contrast, the hybridization of egg c-RNA is not at a plateau level. Hybridization increases with increasing amounts of DNA, but not in a linear fashion. The fact that liver c-RNA hybridizes at a maximal proportion at all DNA-RNA ratios used,



TABLE 5. Hybrid Formation Between c-RNA and Agar-Trapped DNA

Agar, mg	DNA in Agar Source	c-RNA		c-RNA Source
		$\mu\text{g}$	%	
47	whole liver	32	41.0	liver ( <i>R. pipiens</i> )
47	liver nuclei	19	42.0	
40	erythrocyte	25	48.0	
44	whole liver	30	7.0	egg ( <i>R. pipiens</i> )
215	whole liver	148	15.0	
43	liver nuclei	17	2.0	
226	liver nuclei	91	7.0	
42	erythrocyte	26	0.7	
193	erythrocyte	122	2.0	egg ( <i>X. laevis</i> )
45	whole liver	19	9.0	
201	whole liver	84	17.0	
46	liver nuclei	14	14.0	
223	liver nuclei	67	22.0	
47	erythrocyte	42	1.0	
216	erythrocyte	192	6.0	

Two  $\mu\text{g}$  (1,000 cts/min) c-RNA were used in each reaction. In 9 control experiments with empty agar and agar containing *E. coli* DNA, an average of  $0.8\% \pm 0.2\%$  of the c-RNA was found to be retained. The values presented are corrected for this background.

whereas egg c-RNA hybridizes at a lower, still increasing proportion, means that egg c-RNA is complementary to only a small part of the liver DNA. This conclusion is in agreement with the competition experiments which demonstrated that at least 95 per cent of the sequences of somatic DNA are not present in egg DNA. The relation is similar to that of ribosomal RNA and DNA. Ribosomal RNA does not compete with messenger RNA, which, in bacteria, represents a copy of most sequences of the DNA; ribosomal RNA itself, however, hybridizes with DNA, and the hybrid can be detected if the specific activity of the RNA is sufficiently high.

From considerations of the extent of hybridization observed at different DNA to RNA ratios and the limit of sensitivity of the competition experiments, *it can be concluded that the fraction of liver DNA homologous to egg DNA lies between 0.1 and 5.0 per cent.*

The opposite question concerns the portion of the egg DNA that is comple-

mentary to sequences in liver DNA. If 48 per cent hybridization is regarded as maximal (Table 5, representing experiments with liver c-RNA), the highest egg-liver combination of 22 per cent proves that 45 per cent of the egg DNA is complementary to liver DNA. This is a minimal value, since there is no indication that the plateau has been reached.

Since egg DNA is probably cytoplasmic, agar preparations containing DNA from whole livers and liver nuclei were compared. It was considered possible that egg DNA might be complementary to a fraction of DNA present in the cytoplasm of liver cells. The expectation was not borne out by the experiments (Table 5), since agar preparations containing DNA from whole liver and liver nuclei were about equally efficient in binding egg c-RNA. Because the preparation of liver nuclei used was a crude one and certainly contaminated with cytoplasmic material, the experiment cannot be interpreted unequivocally. A striking difference was observed with agar containing erythrocyte DNA: the hybridization is low but clearly above background. Whether this small homology is present in the DNA of the erythrocytes or is due to white-cell contamination is not known. As already mentioned, no difference can be detected between erythrocyte and liver DNA in binding liver c-RNA or fragments of tadpole or kidney DNA or in competing with these fragments for sites on identical agar samples. The difference between liver and erythrocyte DNA is therefore small but apparently it affects the same part of the total DNA that contains the egg-liver homologies.

In an article accepted for publication in the *Journal of Molecular Biology*, Dawid suggests that it might be more fruitful to try to understand the phenomenon of excess DNA in eggs by considering oogenesis rather than embryogenesis. In the oocyte the cytoplasmic constituents are greatly enriched in relation to the nuclear ones. Also, in eggs, storage materials are present which have no

counterpart in somatic tissues. It has been reported that different cell organelles contain DNA, and it is not surprising to find that cytoplasmic DNA is enriched in eggs, surpassing the chromosomal contribution. The association of egg DNA with particles sedimenting at 20,000 *g* supports the idea that it may be part of certain organelles. The low recombination of egg c-RNA with erythrocyte DNA also supports the view that egg DNA is cytoplasmic, because erythrocytes have lost many organelles, in particular most of their mitochondria. Doubt is cast on this interpretation because egg c-RNA hybridized well with DNA from liver nuclei. However, the preparation of nuclei was a crude one, and it is likely that it was contaminated with cytoplasmic material. It is therefore still possible to regard the liver DNA that is homologous to egg DNA as cytoplasmic. It may then be

suggested that the bulk of egg DNA is mitochondrial DNA. This view is based on the presence of DNA in mitochondria of other organisms; the abundance of mitochondria in eggs and their virtual absence from erythrocytes; and the association of egg DNA with particles that have sedimentation characteristics similar to those of mitochondria. Alternatively, it might be assumed that the sequences homologous to egg DNA are present in liver nuclei. With this assumption it must be postulated that the nuclear DNA of erythrocytes undergoes some changes during maturation, which could possibly be connected with the inactive state of the DNA in these cells. It is apparent, though, that egg DNA is a specialized type of DNA, a fact that argues against its being a storage material and suggests that it has a specific function.

CLONAL AND BIOCHEMICAL STUDIES OF MYOGENESIS

CLONAL ANALYSIS

With the assistance of F. J. Kupres, I. R. Konigsberg has continued experiments on the subcloning of primary muscle colonies. The cumulative data of a large series of individual transfers are presented in Table 6. In the vast majority of subcloning experiments, the daughter colonies breed true to the parental type. The relatively few transfers in which both muscle and fibroblastic daughter colonies developed most likely represent

instances in which the colony to be transferred was not cleanly isolated from an adjacent colony of the contaminating type. In transfers yielding both colonial types, for example, the contaminating type is represented by only a few colonies.

The original question posed, however, was whether or not the mononucleated cells that are still present in the vast majority of colonies after two weeks of culture are still competent to initiate the entire process of growth and differentiation involved in the formation of a macroscopic muscle colony. Subcloning by trypsinization yields cell suspensions which contain, in addition to these mononucleated cells, fragments of myotubes of various lengths. It is conceivable, although unlikely, that only these fragments are viable, and that these alone give rise to the secondary daughter muscle colonies. To settle the question, it would be necessary to eliminate the fragmented myotubes from the secondary suspensions.

TABLE 6. Distribution of Morphological Type in Second-Generation Cloning Cultures Derived from Individual Primary Colonies

Type of Parent Colony	Total	Type with Respect to Parent Colony		Abortive Transfer
		True	Mixed	
Muscle	126	99	16	11
"Fibroblastic"	39	23	5	11



It was reported in *Year Book 63* (pp. 516–517) that in muscle colonies exposed to antimycin A, only the differentiated myotubes are destroyed. By pretreating cultures with antimycin A, Konigsberg is able to remove myotubes selectively and prepare cell suspensions of muscle colonies which contain mononucleated cells exclusively. By subculturing these cells, secondary cultures of well-differentiated macroscopic muscle colonies are obtained. Konigsberg concludes, therefore, that the mononucleated cells in the older (two-week) colonies are competent progenitors and can reestablish muscle clones capable of differentiating further. In the cloning analysis, two additional lines of investigation have been initiated, but because the studies have just begun, only a brief description is warranted.

In cooperation with Konigsberg, Stephen D. Hauschka is studying the cytological fine structure of muscle clones. Since the material offers several difficult technical problems, he has had to explore a variety of fixing and embedding schedules and to devise procedures for orienting the small amounts of tissue with which he is working. He is now able to obtain good-quality electron photomicrographs of cells in monolayer culture and is turning his attention to studying the various stages in the development of muscle clones.

Both the genetics and cytogenetics of the chicken present so many difficulties that it would be advantageous to establish conditions for cloning muscle cells from mammalian embryos. Yoheved Berwald has been working with Konigsberg with this objective in mind. Preliminary studies of various media and culture conditions have been completed. Monolayer cultures of rat muscle grown to confluency contain large numbers of myotubes. In similar cultures of mouse muscle cells, however, myotubes are relatively scarce. Single-cell plating on either irradiated feeder layers or in conditioned medium confirm the differences. However, as the mouse represents a better

organism from the standpoint of available genetic stocks, comparative studies of mouse and rat tissues will be continued in an effort to determine the basis of the difference between them.

One curious finding has emerged from the studies. Conditioned medium prepared with mouse cells supports higher plating of rat cells than of the homologous cell type.

#### BIOSYNTHESIS IN CULTURED MUSCLE CELLS

Konigsberg, with the assistance of Henry Burr, has continued his studies of the biosynthetic activities of primary mass cultures of muscle cells. Uridine incorporation into the trichloroacetic acid-insoluble fraction of homogenates of confluent cell monolayers was studied as a measure of RNA synthesis in the presence and absence of actinomycin D. The studies were initiated as a first step toward measuring the rates of decay of the unstable RNA fraction in log and stationary phase cultures. Concentration curves were established for the effect of actinomycin D on incorporation during the first hour after a 20-minute preincubation with the analogue. Incorporation falls precipitously at concentrations ranging from 0.02  $\mu\text{g/ml}$  to 0.2  $\mu\text{g}$ , reaching values on the order of 5 per cent of the control level at a concentration of 1  $\mu\text{g/ml}$ . At concentrations between 5  $\mu\text{g/ml}$  and 15  $\mu\text{g/ml}$ , the level of actinomycin-resistant RNA synthesis remains at the low level. To determine the extent to which protein synthesis can occur in stationary cultures in the presence of actinomycin D, the uptake of radioactive valine into the cell protein fraction was measured. Measurements of valine incorporation were made in the presence of concentrations of actinomycin D ranging from 0.5  $\mu\text{g/ml}$  to 15  $\mu\text{g/ml}$ . At all concentration levels the rate of valine incorporation was depressed to the same extent (40 to 60 per cent below the control level) but continued at the same level for a five-hour period.



## CHEMISTRY AND PHYSIOLOGY OF THE DEVELOPING HEART

A MITOCHONDRIAL FACTOR THAT  
PREVENTS THE EFFECTS OF  
ANTIMYCIN A ON MYOGENESIS

Antimycin A, together with a number of other agents that interfere with or inhibit oxidative phosphorylation in isolated mitochondrial systems, also interferes with normal development of myogenic elements in explanted chick embryos and monolayer cultures of muscle. The effects of these agents are quantitative, with both morphological and biochemical indexes, at millimolar to micromolar concentrations. It is concluded that normal growth and maintenance of myogenic elements initially require structural integrity as well as a balanced oxidative state of membrane elements involved in aerobic phosphorylation.

In *Year Book 63* (pp. 523–525) and in an article to appear in *Developmental Biology*, M. C. Reporter and J. D. Ebert have described a factor isolated from aqueous extracts of chicken liver mitochondria that affords protection against antimycin A. Embryos recover that are cultivated in a medium containing as much as 0.035  $\mu\text{g}/\text{ml}$  of the inhibitor for 6 hours, and transferred to normal medium containing the factor. The factor also prevents the action of antimycin A in monolayer cultures of embryonic skeletal muscle. It does not protect embryos against effects of oligomycin. The factor is isolated and purified by passage through a Sephadex G-200 column, followed by adsorption on hydroxyapatite columns and stepwise elution with phosphate buffer. The protein coming off at a concentration of 0.06 *M* phosphate, pH 7.3, is active and can be treated with light petroleum ether followed by dialysis against 0.002 *M* phosphate without loss of activity. Activity is lost in 30 minutes at pH 4 (25°C), but at pH 5.5 no reduction in activity is observed. Activity is destroyed by heating at 60°C for 15 minutes.

Neither DNase nor RNase affect the activity of the factor; it is not destroyed completely by mild trypsin treatment.

The factor is antigenic in rabbits. Two groups of rabbits were injected with 0.2 to 0.4 mg of protein from crude liver extracts and the purified factor, respectively, after they had been mixed with an equal volume (1–2 ml) of Freund's complete adjuvant. The injections were repeated thrice at intervals of 15 days. Antigen-antibody reactions were studied; the technique of agar gel diffusion and that of agar immunoelectrophoresis were used, as described by Ouchterlony, and Grabar and Williams, respectively.

Freshly isolated samples of the factor gave single bands when tested against antiserum to crude liver extracts as well as to antiserum to the factor itself. Aged samples of the factor or samples that had been repeatedly frozen and thawed showed at least two bands with the technique of immunoelectrophoresis or a broad, hazy precipitation pattern in Ouchterlony plates. Antiserum to the factor gave positive reactions with whole homogenates of explanted chick embryos and anomalous precipitation bands with cultured leg muscle homogenates.

Antisera to the factor were not toxic to explanted embryos when included in albumen medium in concentrations as high as 660  $\mu\text{g}$  protein per ml. The antisera did not prevent the action of antimycin A (0.025–0.03  $\mu\text{g}/\text{ml}$  medium) on explanted embryos. No positive precipitation bands of the antisera have been obtained in preparations from mitochondria of porcine or bovine hearts, such as NADH-cytochrome *c* reductase or NADH-CoQ reductase.

PACEMAKER CELLS IN THE  
EMBRYONIC HEART

As in previous years, R. L. DeHaan's attention has been centered on problems of the early development of the heart,



specifically on the movements of the precardiac mesoderm cells and the development of pacemaker function.

By labeling small regions of mesoderm and endoderm in early chick embryos with tritiated thymidine, and using autoradiographic techniques to trace the movements of the labeled cells, G. C. Rosenquist, working in consultation with DeHaan, has confirmed and greatly extended DeHaan's observation that the paired lateral regions of precardiac mesoderm move over the endoderm in an anteromedial direction, rather than being carried passively by the endoderm into the midline. With these techniques, he has also been able to map the heart-forming regions and other areas of the embryo, at several stages, with a degree of precision not heretofore available (see below, pp. 477-481).

Since 1957 three groups of investigators (Fange, Personn, and Thesleff; Crill, Rumery, and Woodbury; and Lehmkuhl and Sperelakis) have demonstrated electrophysiologically that transmembrane potentials recorded from embryonic chick heart cells, in densely populated cultures, have properties in common with the myocardial cell *in situ*. Thus, the cultured heart cell appears to offer a system in which some of the basic questions concerning the development of electrical activity in the heart may profitably be investigated.

During the year DeHaan has directed most of his effort to studies designed to find the optimal conditions for spontaneous activity of pacemaker cells *in vitro*. At the same time, working in cooperation with him, M. Lieberman has been trying to develop a technique by which intracellular recordings may be obtained from isolated cultured heart cells.

#### *Cultivation of Embryonic Heart Cells*

In *Year Book 63* (pp. 531-535), it was reported that the percentage of embryonic heart cells exhibiting spontaneous activity *in vitro* is dependent on the culture con-

ditions. Mode of tissue dissociation, initial cell density of cultures, and amount of embryo extract in the culture medium were all shown to affect both the quality of the culture and the percentage of spontaneously active cells.

In establishing optimal conditions, the following factors have now been assessed: (1) age and condition of horse serum used in the medium, (2) use of nutritional supplements such as Puck's medium N-16, (3) cell density during the dissociation procedure, (4) duration of trypsinization, and (5) pH of the trypsin disaggregation medium. Each of these factors has been found to influence the percentage of beating cells in a culture, and an optimal condition with regard to each has been determined.

DeHaan's observation that the use of chick embryo extract in the medium diminishes spontaneous activity has also been examined more fully. Chick embryo extract (CEE) contains a wide variety of biological substances of all classes and molecular dimensions. One of its obvious characteristics, however, is that it is a mixture of both intracellular and extracellular components. It has long been recognized that a major difference between the extracellular milieu (i.e., serum) and cytoplasm is that serum is high in sodium ions and low in potassium, whereas the reverse is true of cell sap. DeHaan reasoned that embryo extract should have a significantly higher concentration of potassium ions than serum. It is also known that high external potassium levels tend to depress spontaneous activity of heart tissue. These considerations led to the working hypothesis that the smaller number of beating cells observed in media containing embryo extract might be related, at least in part, to their potassium ion concentration.

To test this hypothesis, flame photometric analyses were made on several preparations of embryo extract. The concentration of potassium in different samples was found to range between 24-

31 mEq/l. In contrast, normal serum potassium is 4–5 mEq/l. Although a medium may be made up in a balanced salt solution (BSS) designed to have 5 mEq/l of potassium, that medium may have twice that concentration of potassium after it has been supplemented with 25 per cent embryo extract. Cultures of 7-day embryonic chick heart, dissociated and cultured for 24 hours, were assayed for the number of spontaneously active cells in medium supplemented with CEE at from 0 to 25 volumes per cent. Aliquots of the media were also analyzed for potassium content. Results of the tests are shown in Table 7. As predicted, a medium containing 25 per cent CEE (4513A), which permits only 10 per cent of the heart cells to beat spontaneously, contains 10 mEq/l of potassium. As the amount of CEE is reduced to zero (4511B; 4513B), and the amount of potassium decreases to normal serum levels, the number of beating cells increases to about 22 per cent. When the growth medium components (serum, CEE, and N-16) were combined with a potassium-free BSS, reducing the potassium level still further, the number of spontaneously active cells again increases significantly (media 463D, 468A).

A definitive test of the hypothesis was performed by reproducing the depressive effects of CEE with potassium chloride alone. A potassium-free culture medium was made up by combining potas-

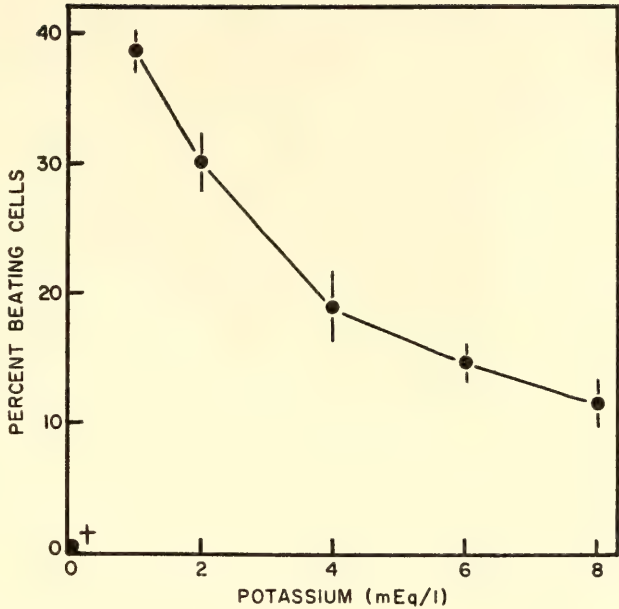


Fig. 26. Effect of external potassium-ion concentration on spontaneous activity of 7-day embryonic heart cells in potassium-free tissue culture medium.

sium-free BSS, horse serum dialyzed for 24 hours against potassium-free BSS, and medium 199 made up without potassium. Aliquots of a cell suspension of 7-day heart were then plated in the medium, to which potassium chloride had been added back to yield a final concentration of 0, 1, 2, 4, 6, and 8 mEq/l. After 24 hours, the number of spontaneously active cells in culture was counted (see Fig. 26).

In a completely potassium-free medium, all cells die. However, at normal serum levels of potassium, about 20 per

TABLE 7. Effect of Varying Composition of Medium on Percentage of Beating Cells

Medium	Composition of Medium, %				Total K <sup>+</sup> mEq/l	Beating Cells, %
	Serum	CEE	BSS	N-16		
4513A	5	25	50	20	10.0	10.3 ± 1.7
456B	15	15	50	20	8.0	11.2 ± 0.9
456A	20	10	50	20	6.9	13.1 ± 0.5
448	25	5	50	20	6.1	15.1 ± 1.5
4511A	28	2	50	20	5.4	19.1 ± 1.6
4511B	30	0	50	20	4.8	23.1 ± 0.7
4513B	50	0	30	20	4.5	22.3 ± 1.7
463D	30	0	50*	20	2.1	31.6 ± 0.9
468A	30	0	65*	5	1.2	33.9 ± 1.3

\* BSS made without potassium.



cent of the cells beat. As the external potassium concentration is increased, spontaneous activity is depressed in about half those cells. As the potassium is decreased down to mEq/1, progressively more cells are active to a maximum of about 40 per cent. Thus, potassium alone mimics the effect of CEE.

CEE has another well-known effect on cell cultures—it promotes growth. Studies by Eagle, Harris, Kutsky, and others have demonstrated that primary cultures of most embryonic tissues (including heart) proliferate rapidly only if embryo juice or other tissue extracts are present in the medium. In DeHaan's cultures, this effect was obvious as soon as he began comparing cultures in media with and without CEE (see Plate 5, Fig. 2, in *Year Book* 63). It became necessary to test whether the depression of physiological activity of heart cells by CEE might be secondary to its stimulation of mitosis, an example of the classic embryological concept of the antagonism between growth and function.

Such a test was easily devised as soon as it became apparent that the repression of spontaneity by CEE could be reproduced by potassium chloride. If the depressive effect of CEE is not a direct action but is dependent on mitotic stimulation, then (1) it should take some time to act on beating cells, and (2) the repression of spontaneity and the stimulation of growth should not be separable.

Accordingly, cultures were prepared in media containing no CEE and 1 mEq/1 of potassium ions. After 24 hours, approximately 40 per cent of the cells were beating spontaneously. Addition of potassium chloride to the cultures, to a final concentration of 10 mEq/1, or of CEE at 25 volumes per cent, immediately (within 30 seconds) caused 90 per cent of the beating cells to become quiescent. With either CEE or potassium chloride, the quiescence was completely reversible by washing the plates and replacing the original low-potassium medium. Thus, the depressive effect of CEE is immediate.

The second point was tested by dialyzing CEE against potassium-free BSS. Such a preparation retains its growth-promoting activity, but no longer decreases the number of beating cells; in this system, no real antagonism between growth and function exists. Cultures plated in low-potassium media containing dialyzed CEE exhibit both rapid proliferation and levels of spontaneous activity similar to, or slightly greater than static cultures lacking CEE.

These studies have now provided the background information necessary to begin studying the population dynamics of pacemaker cells in the developing heart. How many cells in the early heart are capable of spontaneous activity? Does this population increase or decrease with development? Is there a limited "seed" population of prepacemaker cells present in the cardiogenic mesoderm of the early embryo? Do some precardiac cells differentiate into quiescent myocardial cells, while others form spontaneously active components of the conduction system, and if so, why?

Experiments now in progress are beginning to provide answers to some of these questions, but many problems still require clarification. For example, Holtzman and Agin have recently shown that treatment of skeletal muscle fibers with trypsin elicits spontaneous contractions. On the one hand, some of the spontaneous activity of heart cells in culture could result from trypsin-induced alterations of their plasma membranes. On the other hand, it has recently been reported that trypsinization of embryonic chick heart may disrupt myofibrillar structure within cells. Thus, some cells in culture with spontaneously active pacemaker membranes may not be beating visibly as a result of a nonfunctional intracellular contractile mechanism.

#### *Electrophysiological Properties of Cultured Heart Cells*

We have seen that under favorable conditions two functionally distinct cell



populations—beating and quiescent—emerge when embryonic heart cells are cultivated in vitro. However, M. Lieberman has emphasized that definitive statements regarding the percentage of pacemaker cells in any given culture must be based primarily on electrophysiological findings for these reasons: (1) Transmembrane potentials provide an accurate index of the electrical changes associated with cardiac cell excitability; (2) cardiac cells have been shown to be electrically excitable in the absence of a contractile response; (3) cells of the specialized conducting system of the heart are capable of developing spontaneous activity at levels of extracellular calcium and potassium, which do not normally support contraction.

To study the electrical activity of embryonic chick heart cells in cultures it was necessary to arrive at a medium that would maintain its pH upon exposure to atmospheric conditions for a prolonged period of time and would duplicate the observed findings obtained in the bicarbonate CO<sub>2</sub> buffered medium.

Lieberman first confirmed that the cultured heart cell apparently responds to changes in [K<sup>+</sup>]<sub>0</sub> and [Ca<sup>++</sup>]<sub>0</sub> in a manner similar to the intact adult heart cell (see Table 8), after which a bicarbonate-free medium (L5114) containing 50 per cent phosphate-buffered salt solution—(NaCl 130 mM; MgSO<sub>4</sub> · 7 H<sub>2</sub>O 0.8 mM; NaH<sub>2</sub>PO<sub>4</sub> · H<sub>2</sub>O 2.6 mM; Na<sub>2</sub>HPO<sub>4</sub> 10.4

mM; dextrose 5.5 mM; CaCl<sub>2</sub> · 2 H<sub>2</sub>O 1.4 mM), 20 per cent medium 199, 30 per cent horse serum (potassium-bicarbonate-free)—was found to be satisfactory. However, attempts to record from cells attached to the bottom surface of the plastic petri dish (Falcon 35 × 10 mm) of a sparsely populated cell culture (5 × 10<sup>4</sup> cells/ml) in this medium were unsuccessful. The cell membranes were extremely difficult to penetrate with microelectrodes. In addition, limitations imposed by the Prior micromanipulators made it impossible to eliminate high-frequency electrical signals which appeared every time the electrode was advanced in the direction of the cell.

Numerous experiments were then performed in which cells were grown on agar (1 per cent in L5114), in an agar suspension (0.8 per cent in L5114), on a plasma clot, in grooves scribed on the surface of the culture dish, and on reconstituted rattail collagen. Unfortunately, it was still not possible to successfully impale the cells until additional procedural changes were incorporated into the protocol. The procedures included (1) alteration in the trypsinization procedure so that disaggregated cells were exposed to 0.05 per cent trypsin (NBC 1-300) for no longer than eight minutes, (2) omission of phenol red from the culture medium, (3) use of bicarbonate-free medium 199, (4) increase in the density of the cultures to approximately 1.5 × 10<sup>5</sup> cells/ml, (5) use of a bicarbonate-buffered medium which was gassed with a 5 per cent carbon dioxide mixture during cell incubation in a humidified closed chamber, and then gassed with 10 per cent CO<sub>2</sub> for electrophysiological study in room conditions.

*Apparatus.* Intracellular glass capillary microelectrodes filled with 3 M KCl (DC resistance 20–50 megohms) were used to record transmembrane potentials. The microelectrode was rigidly mounted on a Leitz micromanipulator. The reference electrode was an agar-3 M KCl bridge immersed in the culture medium. Both electrodes were connected to the

TABLE 8. Beating Cells as a Function of the External Potassium and Calcium Concentrations, Per Cent

Medium	K <sup>+</sup> , mM/L	Ca <sup>++</sup> , mM/L	BC, %
4105B	1.1	2.5	48.8
41120C*	1.1	2.5	45.6
463B	4.9	2.5	31.2
4930F†	5.9	2.1	22.6
4930E†	6.9	2.0	13.8
4930D†	8.9	1.8	6.1

\* Chick embryo extract dialyzed against potassium-free salt solution was added.

† Chick embryo extract was added to increase potassium.



recording system by means of Ag/AgCl wires. A high-impedance preamplifier with an input capacity neutralization system (Bioelectric Instruments), a dual-beam oscilloscope (Tektronix 502A), and an oscillographic camera (Grass C4) were used for recording the action potentials.

The culture dish was placed in an aluminum chamber which was maintained at a constant temperature by continually pumping water at 50°C through the channels in the chamber from a thermostatically controlled water container. The temperature in the culture dish was maintained between 35°C and 37°C. A layer of nontoxic mineral oil (Klearol 7617) was poured over the surface of the culture medium to prevent its evaporation during the course of an experiment. A humidified mixture of 90 per cent oxygen and 10 per cent carbon dioxide constantly streamed over the surface of the culture dish from a circular brass ring with 12° openings positioned above the dish. The cells were observed with the aid of a Bausch & Lomb light microscope (150X). With the exception of the oscilloscope and camera, all the equipment was housed in a grounded aluminum screen cage.

*Preliminary electrophysiological results.* Transmembrane potentials have been recorded from cells in culture for 24–75

hours in media containing 1.1 mM  $K^+$ , 2.5 mM  $Ca^{++}$  (Figs. 27, 28, 30), 4.1 mM  $K^+$ , 2.5 mM  $Ca^{++}$  (Fig. 29, A and B), and 4.85 mM  $K^+$ , 2.5 mM  $Ca^{++}$  (Fig. 29 C). In future experiments it will be necessary to record from cells bathed by media containing varying amounts of  $K^+$  and  $Ca^{++}$  to determine whether the electrical activity of the cultured heart cell will respond to these cations in a manner similar to the intact heart cell.

It is of interest to note that transmembrane potentials have been recorded from cells that were in contact with other cells—either in clumps, monolayers, or areas of reassembled cells (Figs. 27–30)—but not from isolated single cells. Furthermore, the potentials recorded from cells in culture less than 48 hours were more difficult to obtain than the potentials recorded from cells in culture more than 48 hours. Apparently the physical characteristics of the younger differ from those of the older cell membrane. The cells in culture for 24 hours have a “stickier” membrane than those in culture for 48 and 75 hours. Upon impalement, cellular material from 24-hour cultured cells adheres more readily to the tip of the electrode than cellular material from the 48-hour cells. In a number of experiments, insertion of the microelectrode into a

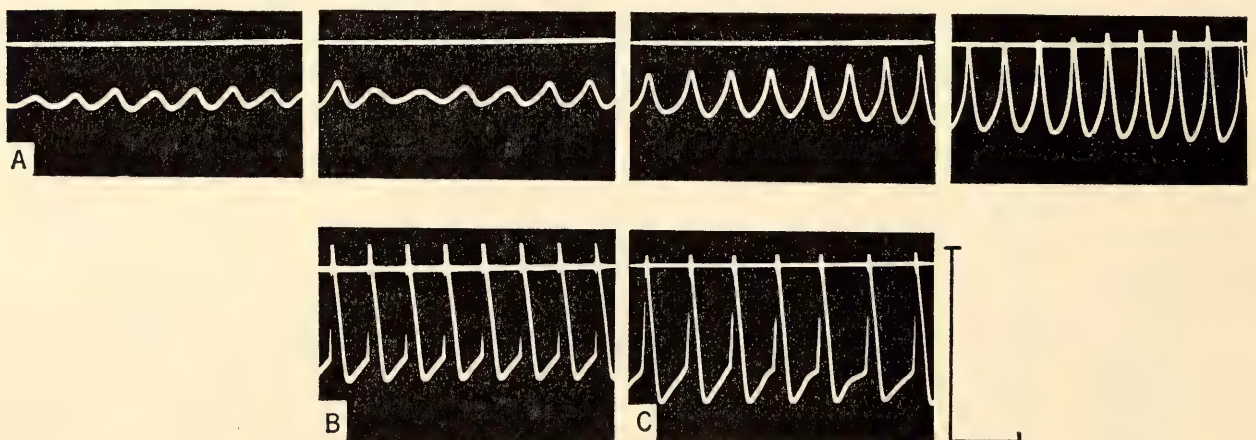


Fig. 27. Transmembrane potentials recorded from spontaneously active trypsin-dispersed embryonic chick heart cells. A. Recorded from a 24-hour cultured cell. Consecutive sweeps show development of pacemaker activity as noted by gradual transition from phase 4 (diastolic period) to phase 0 (rapid upstroke). B. Recorded from 48-hour cultured cell. C. Recorded from 75-hour cultured cell. Note the more abrupt transition from phase 4 to phase 0 in B and C, typical of a latent pacemaker cell. Vertical bar, 100 mv; horizontal bar, 1 second.



beating 24-hour cultured heart cell resulted in the cessation of rhythmic contractions. When it occurred the membrane potential remained constant for a short period, after which subthreshold, rhythmic oscillations appeared. The oscil-

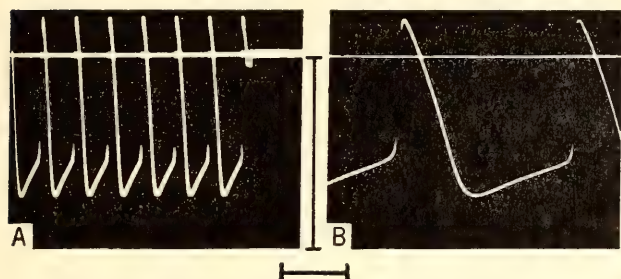


Fig. 28. Pacemaker potentials recorded from cardiac cells cultured for 48 hours. *A* and *B* are responses obtained from the same cell at increasing sweep speeds. Note withdrawal of the electrode at end of *A*. Vertical bar, 100 mv; horizontal bar, 1 sec (*A*), and 200 msec (*B*).

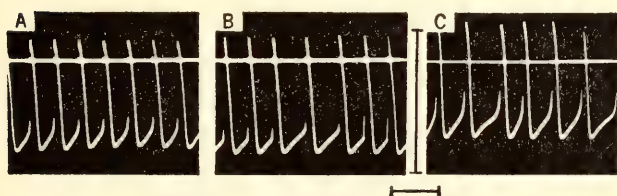


Fig. 29. Transmembrane potentials recorded from cardiac cells in culture for 48 hours. *A*. Recording from pacemaker cell. *B*. Recording from latent pacemaker that escaped driving pacemaker domination for two beats. Note decrease in frequency caused by change in level of threshold potential. *C*. Recording from a pacemaker cell. Note change in frequency caused by decrease in slope of phase 4. Vertical bar, 100 mv; horizontal bar, 1 sec.

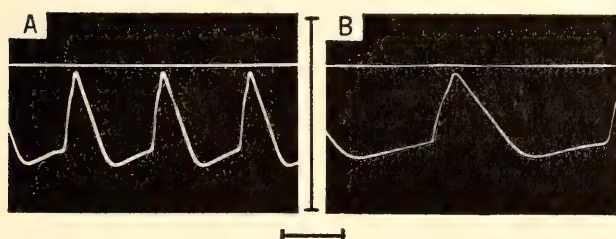


Fig. 30. Transmembrane potentials recorded from a "bridge" of cardiac cells connecting two actively contracting areas in culture for 48 hours. *A* and *B* are responses obtained from the same cell at increasing sweep speeds. Note slowly rising, notched upstroke, a characteristic response of slowly conducting cells. Vertical bar, 100 mv. Horizontal bar, 400 msec (*A*) and 200 msec (*B*).

lations gradually increased in amplitude and eventually gave rise to a pacemaking type of action potential (Fig. 27*A*); at the same time cellular contractions reappeared. This response was never observed in the older cells.

One of the questions asked at the outset of this study was whether it would be possible to distinguish between the transmembrane potentials of sinoatrial (pacemaker), atrial, ventricular, and His-Purkinje cells in culture. Thus far it is apparent that nearly all the 113 impaled cells are capable of behaving as pacemakers; that is, almost every action potential is characterized by an unsteady resting potential (phase 4, diastolic depolarization). It is also important to note that the phase of prolonged repolarization (plateau) characteristic of the intact embryonic and adult heart cell is observed infrequently. It now remains to be determined whether or not these observations are a result of the procedures employed to produce the cell cultures from the intact heart. With phase optics it will be possible to relate accurately the state of mechanical activity of the cell type in question to its electrical profile, determining whether or not pacemaker activity may be recorded from a quiescent cell. Furthermore, if the physical characteristics of the cell membrane are a function of cell population and age, it may be possible to eliminate the problems heretofore encountered while attempting to record from isolated heart cells by culturing cells in a conditioned medium. The procedure for preparing the medium will be based on a modification of the techniques at present employed by Konigsberg.

#### FORMATIVE MOVEMENTS IN THE EARLY CHICK EMBRYO

In experiments carried out in consultation with DeHaan, Rosenquist has been attempting to resolve some of the thorny questions raised in studies of formative movements in the early chick blastoderm. Initially Rosenquist centered his attention on the relations of mesoderm and



endoderm in cardiogenesis, a natural outgrowth of DeHaan's interest. However, the method proved sufficiently precise and reliable to warrant extension of the program to a more comprehensive examination of the functions of the primitive streak.

Our knowledge of formative movements in the early chick embryo has been based primarily on marking experiments in which either particulate matter (carmine or carbon particles) or vital dyes are placed on various parts of the embryo, and their movements recorded, a technique useful for following surface movements only. Our knowledge of the differentiative fate of various parts of the early blastoderm has been based on experiments in which it is divided into pieces, which are then allowed to differentiate in a suitable, isolated environment. As a result of such experiments, numerous, often conflicting hypotheses have been advanced for the role of the primitive streak.

As recorded in *Year Book 63*, pp. 530-531, Rosenquist has used a technique of transplanting grafts labeled with tritiated thymidine to unlabeled recipient embryos which are then reincubated to later stages. Embryos at primitive-streak and head-process stages have served as donors and recipients. The grafted cells participate normally in the subsequent growth and differentiation of the host, as shown by the distribution of cells in radioautographic reconstructions. Series of labeled grafts from representative areas of the blastoderm provide information about movements and differentiation of all three germ layers.

In the first series of grafting experiments, the mesoderm-endoderm layer of the right side of the head-process embryo was divided into 25 pieces, Plate 1A, and transplanted to the homologous area of a recipient unlabeled embryo, Plate 1B. After one to two hours, the wound had healed, Plate 1C. Sections through such an embryo at the 1-somite stage (two additional hours of incubation) show that

(1) the labeled mesoderm cells have preceded the corresponding endoderm cells of the graft to a more cephalic area of the embryo, Plate 1D, (2) this mesoderm appears on the same section with endoderm at a more caudal area, Plate 1E, but (3) is not present further caudally, where labeled endoderm appears alone, Plate 1F.

By studying such migration patterns Rosenquist has been able to show that the endoderm at these stages radiates from ventral parts of the streak, where a pool of such cells is apparently maintained, into the area pellucida. However, it does not appear to cross into the area opaca as recently suggested by Spratt. The endoderm squares elongate as they migrate toward the upper end of the blastoderm. Gut formation begins by invagination of a midline area approximately halfway above Hensen's node, followed by a subsequent infolding of concentric areas of surrounding endoderm. By stage 12, approximately one third of the endoderm has been invaginated into the gut.

Mesoderm, on the other hand, has its own path of cephalic and peripheral migration between endoderm and ectoderm, but radiating in all directions from the streak. The more medial and cephalic migrating areas are folded between the endoderm of the gut and the ectoderm of the neural tube and head. More lateral areas continue into the yolk sac, where their route takes them into the area vasculosa. Areas adjacent to those migrating into the head swing around to form the alae of the area vasculosa (Fig. 31).

Mesoderm moving into the head may contribute to the paraxial mass, the nephrotome, or the lateral plate. After the lateral plate separates into somatic and splanchnic layers, the splanchnic limb folds over to the midline ventrally, meeting the opposite fold so that the heart is formed. Through continued folding and cephalic migration the heart continues to be augmented by more caudal zones as demonstrated in Fig. 32.

The primitive streak appears to per-

form three functions. First, at least at stages 3 through 5, it is a source of cells for the endoderm layer; second, its cephalic tip contains a source of notochordal cells; and third, it is the route of invagination of mesoderm.

The additional information concerning the streak comes from Rosenquist's study of the fate of labeled homologous grafts of the epiblast layer, where a zone of premesoderm can be demonstrated in an oval area extending from the tip of the

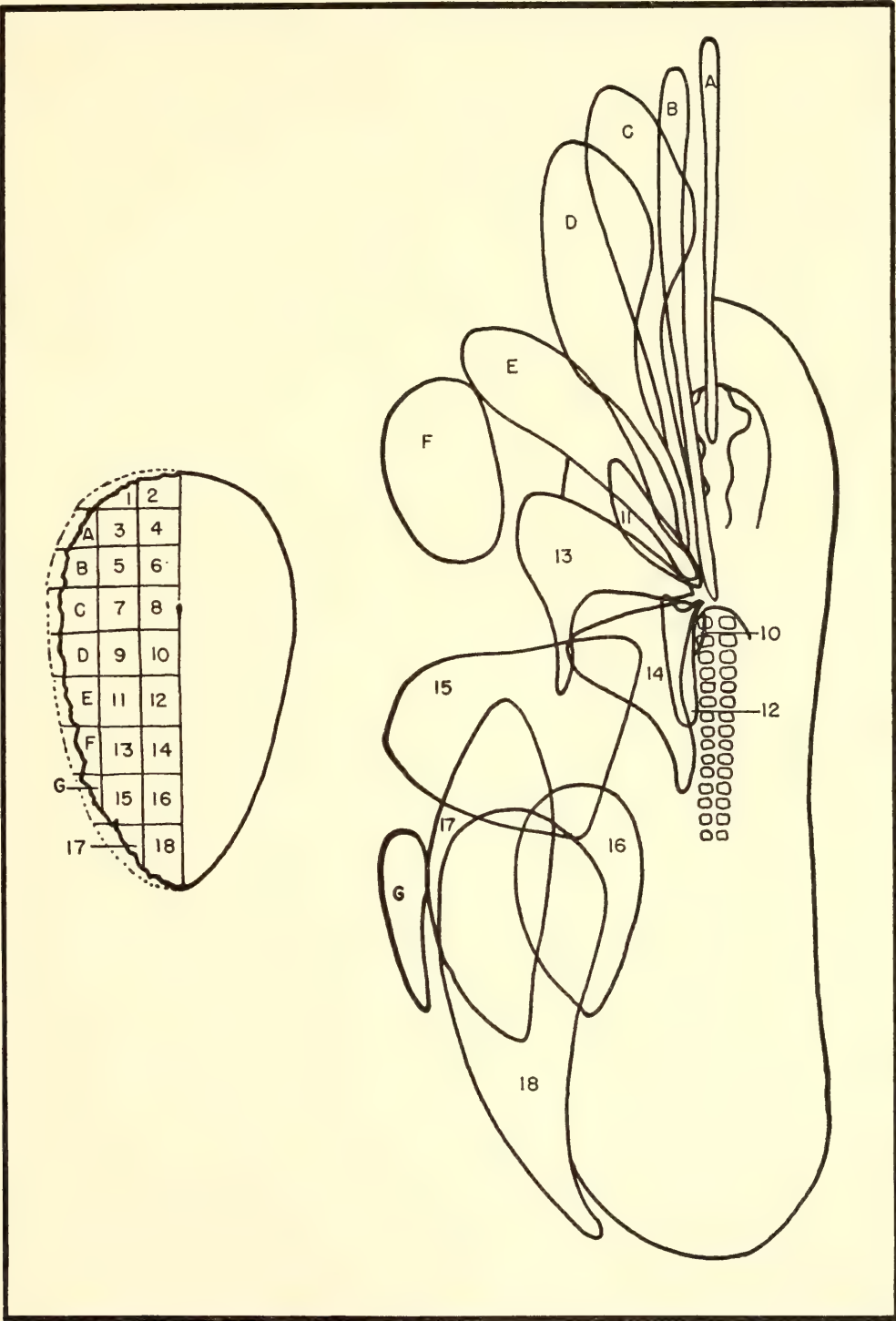


Fig. 31. Left: Endoderm-mesoderm layer of one half of a stage-5 chick embryo divided into 25 squares. Right: distribution of the grafted labeled squares in nonlabeled recipient embryos incubated to stage 12. Drawings, to scale, illustrate general movements of the mesoderm squares away from the streak in a cephalic and peripheral direction and formation of the alae of the area vasculosa. Head mesoderm not included.



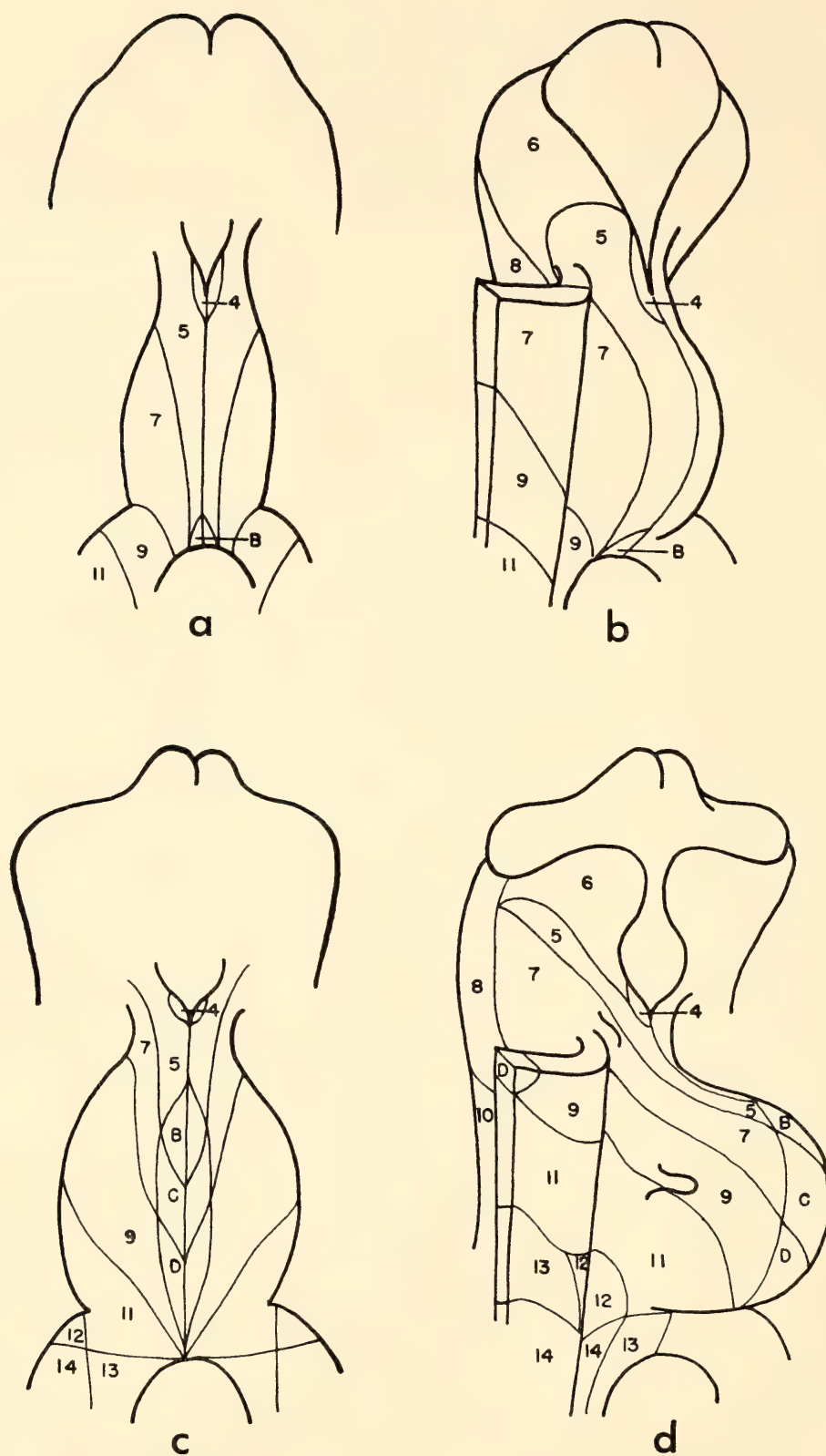


Fig. 32. Cephalic end of chick embryos with endoderm removed to show distribution of labeled mesoderm squares in heart and great vessels (*a, b* at stage 10; *c, d* at stage 12). Drawings at right (similar to those at left but seen from a 45° angle) also show head mesoderm as it surrounds the neural tube and a cutaway flap of somatic mesoderm extending from nephrotome to left into yolk sac. Anatomic ventral border of heart (line separating right from left sides of heart in left drawings) corresponds to the most peripheral border of the myocardial zone prior to formation of the splanchnic fold. In righthand figure, this line has moved away from the midline as myocardium falls away from ventral mesocardium. Stage 12 heart also differs from that in stage 10 by augmentation with more caudal mesodermal squares. Numbers refer to Fig. 31.

streak laterally, nearly to the area pellucida margin, but tapering toward the midline in more caudal regions. The pre-mesodermal cells are progressively invaginated into the streak, where considerable mixing occurs. The invaginated cells, now mesodermal, stream from the streak to their positions in the mesoderm layer already described. This premesoderm is preparaxial in an area adjoining the upper streak, prelateral plate material toward the center of the streak, and preextra-embryonic mesoderm at the lower part of the streak.

Beyond the outer limits of the pre-mesodermal zone is a zone of preectodermal cells. The most medial areas of these are destined to be the floor of the neural tube. More lateral areas become,

respectively, walls of neural tube, embryonic surface epithelium, and extraembryonic epithelium. The route of movement of ectodermal cells from this zone is similar to that described for endoderm and mesoderm in the lower layers, i.e., in a cephalic and peripheral direction. In fact, ectodermal cells often precede the mesoderm and endoderm in their migration to the cephalic areas of the blastoderm. These movements also result in the same elongation of grafts as was described for endoderm and mesoderm. The ectodermal areas of the blastoderm thus come to lie in arcs around the node, with a central core of neural tissue surrounded by an arc of embryonic surface epithelium and the more peripheral arc of extra-embryonic areas.

## INDUCTIVE TISSUE INTERACTIONS

### ORIGIN OF FEATHER SPECIFICITY

During the past year Mary E. Rawles has made a number of attempts to devise a method that would permit the normal succession of plumage types (down, juvenile, and adult) in grafts, after reciprocal exchange of epidermis and dermis from prospective feathered and nonfeathered regions of the chick embryo. Heretofore, in exchange experiments of this sort, feather development has not been followed beyond the down-feather stage; consequently no information has been obtained concerning the origin of the marked regional specificity displayed by the later plumages.

The down feathers are the first to arise from the papillae of the various tracts (pterylae) established during embryogenesis. Structurally they are the simplest and most uniform of all feather types, consisting of a circlet of delicate filamentous barbs attached to a short calamus, without a shaft. The first set of contour feathers of the juvenile plumage begins to form from the papillae before

the down is shed, but thereafter a feather does not begin to regenerate until its predecessor is molted or plucked. Thus, whereas the down feathers occupy the same position within a particular feather tract as the definitive or contour feathers which replace them, they show neither the structural complexity nor the marked regional specificity of the definitive feathers appearing later.

That structurally normal down feathers can be readily produced in grafts, from a variety of unique epidermal-dermal recombinations, has been demonstrated in Rawles's earlier experiments (*J. Embryol. Exp. Morphol.*, 11: 765-789). For instance, dermis from the middorsum, prospective dorsal feather tract, induces normal down feathers in overlying "foreign" epidermis from the foot (tarso-metatarsus), beak, and lateral apterium—regions that normally do not participate in feather formation. If the successive juvenile and adult feathers could be followed in such cases, one might expect to obtain interesting and pertinent information concerning the origin of feather



specificity. Attempts in this direction are continuing.

#### RIBOSOMES AND POLYSOMES IN EPIDERMIS AND DERMIS DURING FEATHER INDUCTION

As we have seen, differentiation of avian skin involves an interaction of dermal and epidermal cells resulting in the formation of feather keratin by the epidermal cells. Although feather formation requires an interaction of these cell layers, keratin is synthesized specifically by cells of the epidermis. John Papaconstantinou of the University of Connecticut visited Rawles's laboratory briefly during the winter of 1965, where he began an investigation designed to determine whether differences can be observed in the state of aggregation of ribosomes of the epidermis and dermis before, during, and after feather induction. In addition, because the dermis and epidermis can be separated by trypsinization, it was the purpose of these experiments to initiate a series of studies on the biochemical mechanisms of feather induction.

We have already remarked that protein synthesis appears to be correlated with the aggregation of ribosomes into polysomes. Initial experiments by Papaconstantinou and Rawles have shown that there is a specific polysomal population in the epidermis and dermis associated with the formation of feather papillae. The polysomes in the two layers are approximately the same size as determined by their sedimentation in a 15-30 per cent gradient. The absence of these polysomes in 6-day skin is a further indication that they are associated with feather formation. In the 8-day skin, the development of feather papillae is well advanced, and these polysomes are still found in the epidermis. In the dermis, however, the polysomes are no longer detectable. Thus, the retention of the polysomes that appear during formation of papillae in the epidermis is related to the continued synthesis of feather keratin.

Their disappearance in the dermis may be related to the end of the active inductive role of these cells in feather formation. At this stage, possibly, the polysomes become sensitive to the extraction procedure and may be easily broken down into ribosomes. Since these are only preliminary observations, further interpretation is not warranted.

#### "HETEROGENEOUS INDUCTORS"

##### *Effect of Thioglycolic Acid*

Heinz Tiedemann continued his exploration of the chemical nature of the mesodermal and neural inductors prepared from chick embryos. He found that the implantation of a highly purified mesodermal-inducing factor in the blastocoel of early gastrulae results in the spreading of endoderm over the ectoderm. During the year his finding was published in *Science*, 147, 167-168. In this article he and his colleagues Ursula Kocher-Becker and Hildegard Tiedemann argued that the spreading can be explained by a change in cell affinities in the ectoderm, induced by the factor.

In further experiments, crude fractions prepared from chick embryos were implanted as pellets into the blastocoel of early gastrula stages of *Amblystoma punctatum* (see *Year Book* 63, p. 537). These pellets induce mainly hindbrain structures in the ventral ectoderm. After treatment with thioglycolic acid or thioglycolic acid and catalase (to destroy  $H_2O_2$  formed by autoxidation of thioglycolic acid), the fractions preferentially induce archencephalic structures. Histological examinations of the induced tissues have confirmed the observations. The untreated fraction induces ear vesicles, rhombencephalon, muscle, and in a few cases mesenchymic tails, whereas the thioglycolic-acid-treated fraction preferentially induces eyes, noses, prosencephalon and diencephalon. In a further experiment highly purified mesodermal-inducing factor was treated with thio-

glycolic acid. The factor is completely inactivated by the treatment. Thus, the mesodermal factor is inactivated by treatment with thioglycolic acid whereas

the neural factor remains active. A conversion of the mesodermal into the neural factor by thioglycolic acid can be excluded.

ANIMAL VIRUSES AND EMBRYOS

INFECTION OF EMBRYONIC MUSCLE CELLS BY ROUS SARCOMA VIRUS

During the year, J. D. Ebert, M. E. Kaighn, and P. M. Stott have continued their investigation of the effects of Rous sarcoma virus (RSV) on differentiating skeletal muscle of the chick embryo. The problem of the susceptibility of single myoblasts to RSV has been attacked directly, using the method of clonal culture of myoblasts developed by Konigsberg. The effect of the virus on the cell types found in cell suspensions prepared from skeletal muscle (myoblasts and fibroblasts) can be examined separately. Several of the questions posed in *Year Book 63* (pp. 539-540) can now be answered or phrased more precisely.

Many of the technical problems that arose at the outset of this study have now been resolved. In August 1964 Kaighn had the opportunity of consulting with Harry Rubin at the University of California, Berkeley, and since then, no difficulty has been encountered with the focus assay or other routine procedures involved in the virus work.

Production of Infectious Centers in Muscle Cell Cultures

Cultured muscle cells are assayed by the infectious center technique in order to determine the fraction of cells infected by virus. The effects of virus concentration and incubation of the cells in conditioned medium either before or after infection have also been studied. Some preliminary results are shown in Table 9.

Several facts emerge from a consideration of these data. First, regardless of the prior history of the cell (in a primary or secondary culture) a maximum of 3 per

TABLE 9. Muscle Cells Registering as Infectious Centers, Per Cent

Cells	Virus Added, ffu/cell†	Interval in Culture After Infection, hour*		
		0	18-22‡	46§
Primary	0.20	2.7	2.9	14
Secondary	0.25¶	2.5	—	—
	0.34**	—	2.9	96
	1.0**	—	3.5	100
	1.7**	—	2.6	33

\* Primary muscle suspensions were prepared from 12-day chick leg muscle by the method of Konigsberg (*Science*, 140, 1273-1284, 1963). Aliquots of 1 ml ( $2 \times 10^6$  cells) were added to 60 mm Falcon petri dishes containing 4 ml conditioned medium.

† Calculated from a parallel titration of the virus used to infect the cells (focus forming units/cell). The Bryan high-titer strain (7B) used in these studies was obtained from Harry Rubin and passed twice in chickens in this laboratory.

‡ Corrected for cell-associated virus by subtracting the total number of foci obtained with frozen and thawed cells.

§ Counts of foci were probably low because of excessive number of foci per plate.

|| Cultures were washed with Saline G, incubated for 30-60 minutes with medium containing RSV antiserum, rinsed with Saline G, and treated with 0.0025% trypsin in Saline G for 8 minutes at room temperature. These cells were assayed as infectious centers (H. Rubin, *Proc. Natl. Acad. Sci.*, 46, 1105-1119 (1960).

¶ Cultured 13½ hr before infection.

\*\* Cultured 22 hr before infection.

cent of cells *appear* to be infected when assayed up to one day after infection. This fraction rises sharply by the second day after infection. The results are similar to those of Rubin for chick embryo fibroblasts except that a sharp increase in the fraction of overtly infected cells occurs only one day after infection in Rubin's experiments. There



is an increased probability that an infected cell will produce a focus if plated after advanced infection.

Since the media used for cell attachment and growth in this assay system are inimical to the growth of myoblasts, it follows that a low efficiency of plating of freshly infected cells will be observed. Alternatively the increased plating efficiency could be due to a sharp increase in the proportion of fibroblasts in the culture. After two days in conditioned medium considerable fusion of myoblasts to form myotubes has occurred. In fact, when primary or secondary muscle cells grown in conditioned medium for up to 24 hours are cloned, at least 50 per cent of the total colonies are muscle colonies, whereas after 46 hours in culture, more than 95 per cent of secondary cells give rise to fibroblast clones. It is clear that the infectious center method cannot give decisive information about the sensitivity of myoblasts to RSV infection.

*Transformation of Muscle Clones by Rous Sarcoma Virus*

The effect of RSV infection of single myoblasts on their subsequent growth and differentiation has been examined. In the experiment summarized in Table 10, cells were infected either at the time of cloning or 3 days later. Uninfected controls, and cultures infected with various virus concentrations plus anti-RSV serum were included. It is evident that a substantial fraction of both muscle and fibroblast clones have been transformed. Why is the fraction of transformed muscle clones apparently larger than that of transformed fibroblast clones? Possibly fibroblast clones transform more uniformly and hence become detached more readily from the surface of the dish. There is no doubt that this transformation is due to the virus since no transformation occurs in the presence of antiserum. Unfortunately the anti-

TABLE 10. Effect of RSV Infection at the Myoblast Stage on Growth and Morphology of Muscle Clones\*

Time of Infection	Virus Concentration†	Anti-RSV Serum‡	P.E., %§	M <sub>f</sub> , %	TM, %¶	TF, %¶
Control	—	—	26.9	81.0	0	0
Antiserum control	—	+	14.8	59.0	0	0
0	1 × 10 <sup>6</sup>	+	13.5	86.5	0	0
0	1 × 10 <sup>6</sup>	—	18.0	75.7	7.4	9.4
0	5 × 10 <sup>5</sup>	+	15.6	94.7	0	0
0	5 × 10 <sup>5</sup>	—	17.7	74.5	17.9	5.8
0	1 × 10 <sup>5</sup>	+	13.1	82.3	0	0
0	1 × 10 <sup>5</sup>	—	22.0	77.2	17.7	2.3
3 days**	1 × 10 <sup>5</sup>	+	26.7	73.7	0	0
3 days**	1 × 10 <sup>5</sup>	—	26.3	45.6	39.5	11.4

\* Primary muscle cultures were plated at 2 × 10<sup>6</sup> cells in conditioned medium. After 22 hr, the plates were washed and the fractions of cells that were suspended by treatment with 0.0025% trypsin for 8 min at room temperature were used for cloning (300 cells/plate in 2 ml conditioned medium). Medium was changed every 3 days. Clones were fixed and stained on the 8th day of culture.

† Focus-forming units (ffu/ml).  
‡ Anti-RSV serum was added at time of plating.  
§ Per cent of cells forming clones.  
|| Per cent of total clones forming normal muscle.  
¶ Per cent of total clones forming transformed fibroblasts.

\*\* Two clone plates were washed and infected with 1 × 10<sup>5</sup> ffu in 1 ml conditioned medium each. After 3 hours, the plates were rinsed and 2 ml conditioned medium was added. The control plates received 0.1 ml anti-RSV serum. Nineteen clones, consisting of 6 to 30 cells each, were marked.

serum used in this experiment appears to be toxic, especially to freshly trypsinized myoblasts, as its presence reduces both plating efficiency and percentage of muscle. It is interesting that the concomitant presence of virus seems to ameliorate this toxicity to some extent.

The effect of the virus on fibroblast and muscle colonies is illustrated in Plate 2. Insets *A* and *B* are a control culture and a culture infected at 3 days from the experiment recorded in Table 10. With the plating efficiency in control, and virus plus antiserum and virus-treated plates the same (about 26 per cent), 51 per cent of all clones were transformed in the infected plates. The nature of this transformation is seen in Plate 2, insets *E* and *F*. As in the transformation of fibroblasts, grapelike clusters of cells appear in the muscle colonies. In addition muscle syncytia are sometimes distended by large numbers of refractile vacuoles. Whether this is an additional manifestation of the infectious process or merely moribund tissue remains to be investigated.

The most convincing evidence that muscle cells have indeed been infected

by RSV would be a demonstration of the production of infectious virus by physically isolated muscle colonies. Table 11 gives the results of such an experiment. Six days after infection 23 clones were ringed, and the medium changed. The next day virus assays were carried out on the medium above these colonies. The assay plates in 19 of the isolated colonies produced large amounts of virus. In the four negative plates, 3 of the colonies were very small, and only one was a normal muscle colony.

These experiments clearly demonstrate that both cell types present in embryonic chick skeletal muscle are sensitive to RSV infection, exhibit the characteristic transformation, and produce infectious virus. However, the transformation of a muscle colony differs from that of a fibroblast colony because of the formation of myotubes. It is not yet certain whether these multinucleate myotubes are sensitive to infection. It is clear, however, that, inasmuch as partially and totally transformed muscle colonies have been obtained from single myoblasts infected at the time of plating, the infectious process does not necessarily

TABLE 11. Production of RSV by Isolated Muscle Clones\*

Plate No.	Clone No.	Clonal Morphology When Isolated	RSV Foci, Transformation
CS-I	1	small, diffuse muscle	0
	3	small muscle	0
	4	ca. 100 cells, type?	0
	5	normal muscle	0
	6	muscle, grapelike clusters	nearly confluent
CS-II	1-4	average to large myotubes, transformed	}
	5-9	sparse muscle, transformed	
CA-I	1	normal muscle (bulging myotubes)	}
	2	muscle with clusters of round cells	
	3	like 1	
	4	like 2	
CA-II	6	completely transformed muscle, "ring form"	}
	1-4	transformed muscle, "ring form"	

\* Four 10 cm Falcon plastic plates were seeded with 300 secondary muscle cells in 5 ml conditioned medium (see asterisk, Table 9). After 2 days in culture, the plates were infected. The medium was removed and 1 ml of conditioned medium containing  $1 \times 10^6$  ffu RSV added. After 1 hour at 37°C, 4 ml of conditioned medium was added. The medium was replaced every 2 days. On the 6th day after infection, individual muscle colonies were isolated in porcelain cylinders. Next day, entire contents of each cylinder were assayed for RSV.



prevent fusion of myoblasts. The point is of some interest since RSV matures at the cell membrane. Experiments are either in progress or are planned, to determine the amount and rate of viral synthesis in muscle compared with fibroblast clones, and whether the more highly organized muscle syncytia are sensitive to RSV.

#### SUSCEPTIBILITY OF KIDNEY AND CARTILAGE CELLS TO ROUS SARCOMA VIRUS

From September 1964 to February 1965, T. S. Okada of Kyoto University joined Ebert and his colleagues to collaborate in their study on the susceptibility of embryonic cells to RSV. Working closely with Kaighn and Stott, Okada explored the possibility of examining the susceptibility of a cell system other than muscle. The two systems chosen for study were 12- to 14-day chick metanephros, because of Okada's familiarity with this tissue, and 12-day femoral cartilage, which might be expected to provide a relatively homogeneous suspension of chondrocytes. Initially it was found that clones could be obtained from primary cultures of both these tissues using a muscle-conditioned medium similar to that of Konigsberg. Plating efficiencies observed were 23 per cent for kidney and 27 per cent for cartilage. For the most part the clones consisted of cells of fibroblastic morphology with a few small epithelioid colonies from kidney. When the clones were challenged with RSV after 6 days in culture and examined 6 days later, 58 per cent of the clones derived from cartilage contained characteristic altered foci, while 7 per cent of

153 kidney colonies showed only doubtful alteration. Since the changes were not seen in control cultures, or when anti-RSV serum was present, the alteration must have been due to the virus. Furthermore, the altered colonies produced virus by direct assay, and the cells produced infectious centers. These experiments suggest that cells derived from kidney are less sensitive than those from cartilage.

When freshly dissociated cartilage cells were treated with virus at the time of plating rather than at 6 days, no altered colonies formed. However, the plating efficiency and colony size were reduced in infected cultures, so the failure to observe transformation could be due to a toxic effect of the virus preparation rather than resistance to infection.

An experiment was carried out to determine whether clones derived from precartilage (5½- to 6-day chick limb) differed from cultures prepared from differentiated cartilage in viral susceptibility. If clones from precartilage were infected 6 days after plating, a plating efficiency was observed of 15 per cent with 17 per cent transformation compared with plating efficiency of 26 per cent and 58 per cent transformation in the case of clones from 13-day femoral cartilage.

These studies, though highly suggestive, must be regarded as only preliminary because no specific criteria were used to identify "cartilage" cells. Where a plating efficiency of about 27 per cent was obtained, however, at least in the case of femoral cartilage, it seems likely that many of the transformed cells were derived from cartilage cells. Further studies should clarify the problem.

### THE GRAFT-VERSUS-HOST REACTION

#### THE GRANULOCYTIC RESPONSE

Previous work in this and other laboratories has shown that grafting fragments of adult chicken spleen onto the chorio-

allantois or injecting suspensions of cells from the lymphoid tissues or blood of the adult chicken leads within a few days to a number of pathologic changes in the embryo, usually culminating in



death. Perhaps the most conspicuous element of this syndrome is the striking enlargement of the host's spleen. The initial stage, the "graft-versus-host reaction," is immunologic in nature. However, the nature of the subsequent stages in the reaction are not clearly defined. The increase in size of the host's spleen, which may be as much as ten- to twenty-fold, is granulocytic, most of the proliferating elements being derived from the host.

Little is known of the role of granulocytes in this reaction or of the factors regulating their proliferation. During the year, in consultation with J. D. Ebert, C. B. Kimmel continued his study of the granulocytic response.

Recent evidence from several laboratories is beginning to shed light on the function of granular leucocytes in immunologic reactions. In immune responses, granulocytes are known to be active in the phagocytosis of antigen and antibody-antigen complexes. This process is accompanied by a striking change in the morphology of the cell; the granules disappear under phase contrast observation and at the same time lose their staining properties. This process of "degranulation" is now well substantiated. Hirsch and Cohn have demonstrated that leucocyte granules contain a full complement of lysosomal digestive enzymes, and that, accompanying degranulation, the enzymes are released from the granules in a fully active state. Ingested material is found in the cell enclosed in vesicles. The membranes of the granules fuse with those of the vesicle in such a way that hydrolytic enzymes are liberated into it. Thus, disappearance of the granules from the cytoplasm can be correlated with the beginning of intracellular digestion of the phagocytosed material.

Granulocytes have also been shown to play a central role in hypersensitivity reactions. Skin inflammatory responses, such as the Arthus and Schwartzman reactions, do not occur unless granulo-

cytes are present in large numbers at the site, where they appear to be active in endocytosis and degranulation. Thomas has demonstrated that a suspension of granules injected into such a site can partially replace the requirement for the cells themselves. He has argued that the release of relatively high concentrations of hydrolytic enzymes results in tissue breakdown leading to inflammation.

Parallels may be drawn between these systems and the graft-versus-host reaction. Both show the conditions of an immune reaction accompanied by reactions of the granular leucocyte. The first objective of Kimmel's study is to follow the granulocytic response in the graft-versus-host reaction more closely, with emphasis on the role of lysosomes and lysosomal enzymes. He has asked what changes occur in the properties of lysosomes in the spleen as a consequence of the reaction. In *Year Book 63* (pp. 541-547), evidence was presented that the embryonic spleen is rich in lysosomal enzymes and that the major part of the activity is associated with the granulocytes. After implantation of adult spleen on day 9, the activities were found to be increased in the enlarged host spleens.

Most of the enzyme assays were outlined last year. Aryl sulfatase is measured by the method of Dodgson and Spencer in which the release of nitrocatechol is followed spectrophotometrically after incubation of nitrocatechol sulfate with the enzyme solution at pH 5.7, and alkalization. Cytochrome oxidase, which is assayed as a mitochondrial marker, is measured by the method of Straus. Acid phosphatase activity is assayed by (1) the method reported last year with carboxy-phenyl phosphate as the substrate, and (2) the method used by de Duve, following inorganic phosphate release with  $\beta$ -glycerophosphate as the substrate.

To avoid confusion, the activities obtained by method 1 are denoted as acid *phenyl* phosphatase, and by method 2 as acid phosphatase, although no attempt has been made to show that these are



indeed two different enzymes. Enzyme units are expressed as  $\mu$ moles of product released per minute in the reaction mixture for all of the lysosomal enzymes, and as change in optical density  $\times 1,000/\text{minute}$  for cytochrome oxidase and lactic dehydrogenase (LDH). Splenomegaly has been elicited by inoculating blood leucocyte suspensions into vessels in the chorioallantois on the 11th or 12th day of incubation. This method produces splenomegaly more rapidly and more uniformly than chorioallantoic grafting. Cobb White Rock roosters served as donors and could be used several times. White Leghorn embryos served as hosts.

Table 12 summarizes the results of an experiment in which enzyme contents of day-17 normal embryonic spleens are compared with five-fold enlarged spleens from embryos injected on day 12 and recovered on day 17. Sucrose homog-

enates were frozen and thawed, and sonicated prior to assay, to release lysosomal enzyme activities in a fully active form. The activities of three lysosomal enzymes (cathepsin, RNase, and aryl sulfatase) increase proportionally to spleen weight, and the increase of the others ( $\beta$ -glucuronidase, acid phosphatase, and DNase) is significantly greater than the increase in weight. The increases in a mitochondrial enzyme, cytochrome oxidase, and the soluble enzyme LDH, are not so dramatic. The results are in agreement with those reported last year from pH 5.0 extracts.

Table 13 presents a similar experiment in which assays from 10- to 18-fold enlarged spleens are compared with controls. The results from the group enlarged 10-fold (E2) are in agreement with those in Table 12; in the group of greatly enlarged spleens (E3), only the specific

TABLE 12. Comparison of Enzyme Activities in 17-Day Chick Spleens from Control and Injected Embryos

Group	No.	No. Cells Injected (day 12)	Mean Wet Wt. Spleen, mg (day 17)	
C1	5	...	10.2	
C2	5	...	11.0	
E1	5	$5 \times 10^5$	54.4	

Enzyme	Group	Specific Activity $\pm$ S. E., units/mg wet wt.	Ratio (E/C)	Probability, <i>t</i> test
Cytochrome Oxidase	C1	$10.2 \pm 0.6$	0.8	$0.05 > P > 0.025^*$
	E1	$7.8 \pm 0.7$		
LDH	C1	$46.4 \pm 2.8$	0.8	$0.025 > P > 0.01^*$
	E1	$37.1 \pm 1.3$		
$\beta$ -Glucuronidase	C1	$0.268 \pm 0.007$	1.5	$P < 0.001^*$
	E1	$0.400 \pm 0.011$		
Acid phosphatase	C2	$1.33 \pm 0.08$	1.4	$0.005 > P > 0.001^*$
	E1	$1.91 \pm 0.08$		
Acid DNase	C2	$0.81 \pm 0.04$	1.5	$0.010 > P > 0.005^*$
	E1	$1.23 \pm 0.11$		
Cathepsin	C2	$0.082 \pm 0.006$	0.8	$0.2 > P > 0.1$
	E1	$0.065 \pm 0.004$		
Acid RNase	C1	$13.8 \pm 1.2$	1.0	$P > 0.5$
	E1	$13.3 \pm 0.6$		
Aryl sulfatase	C1	$1.44 \pm 0.18$	0.7	$0.1 > P > 0.05$
	E1	$1.01 \pm 0.06$		

\* Difference significant at 5% level.

TABLE 13. Comparison of Enzyme Activities in 17-Day Chick Spleens From Control and Injected Embryos

Group	No.	No. Cells Injected (day 12)	Mean Wet Wt. Spleen, mg (day 17)
C3	5	...	10.8
C4	5	...	9.8
E2	5	3 × 10 <sup>6</sup>	105.9
E3	3	3 × 10 <sup>6</sup>	182.0

Enzyme	Group	Specific Activity ± S.E., units/mg wet wt.	Ratio (E/C)	Probability, <i>t</i> test
β-Glucuronidase	C4	0.303 ± 0.021		
	E2	0.478 ± 0.022	1.6	<i>P</i> < 0.001*
	E3	0.419 ± 0.015	1.4	0.025 > <i>P</i> > 0.01*
Acid Phosphatase	C4	1.95 ± 0.10		
	E2	2.91 ± 0.11	1.5	<i>P</i> < 0.001*
	E3	2.25 ± 0.12	1.2	0.2 > <i>P</i> > 0.1
Acid DNase	C3	1.67 ± 0.05		
	E2	3.82 ± 0.26	2.3	<i>P</i> < 0.001*
	E3	1.68 ± 0.58	1.0	<i>P</i> > 0.5
Cathepsin	C3	0.077 ± 0.013		
	E2	0.082 ± 0.004	1.2	<i>P</i> > 0.5
	E3	0.074 ± 0.012	1.0	<i>P</i> > 0.5
Acid RNase	C4	22.6 ± 1.4		
	E2	23.2 ± 1.0	1.0	<i>P</i> > 0.5
	E3	16.0 ± 1.0	0.7	0.025 > <i>P</i> > 0.01*
Aryl Sulfatase	C4	1.04 ± 0.04		
	E2	0.96 ± 0.12	0.9	0.5 > <i>P</i> > 0.4
	E3	0.60 ± 0.04	0.6	<i>P</i> < 0.001*

\* Difference significant at 5% level.

activity of β-glucuronidase is significantly increased, whereas that of RNase and aryl sulfatase is significantly decreased. Perhaps this finding, a general lowering of specific activities in very large spleens, is due to degenerative changes that become histologically more evident as the spleen size increases.

In the experiment presented in Fig. 33A, embryos were inoculated on day 12 with 5 × 10<sup>5</sup> cells. On day 13 and daily thereafter to day 17, randomly chosen groups of 5 embryos were killed along with 5 unoperated controls of the same age. Spleens were weighed and stored frozen until the series was complete. Assays were carried out as above on sucrose homogenates that had been frozen and thawed, and sonicated.

As seen in Fig. 33, spleen weights in the experimental group are not signifi-

cantly increased until day 15—three days after inoculation—a finding in agreement with the results of other laboratories and earlier results of this laboratory. In Fig. 33, *B*, *C*, and *D* show the results of assays of these spleens for acid phenyl phosphatase, β-glucuronidase, and aryl sulfatase. In each case there is a progressive increase in the specific activity in the control spleens with time. In the experimental group the specific activities of acid phenyl phosphatase and β-glucuronidase also show the progressive increase. Acid phenyl phosphatase increases significantly over controls by the first day after injection, and β-glucuronidase by the second day. Thus, the changes that lead to detectable increases in enzyme content of the spleens occur at least as quickly and probably more quickly than those that lead to an in-



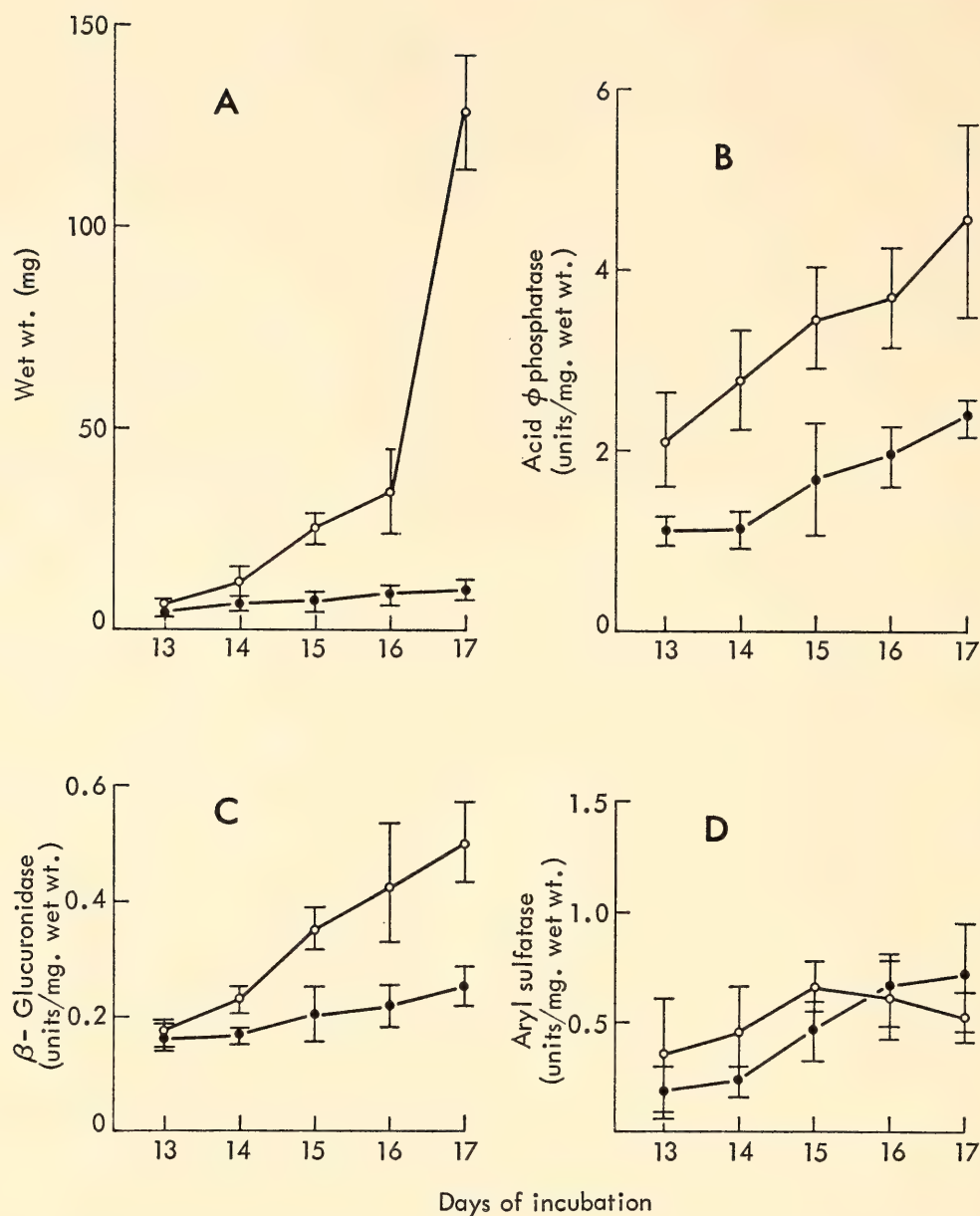


Fig. 33. Lysosomal enzyme activities in developing chick spleen: changes induced by inoculation of adult blood leucocytes on day 12. *A*: changes in wet weight with development. *B*, *C*, and *D*: changes in enzyme specific activity with development. Each point is the mean of five determinations, and length of vertical line through the mean corresponds to a 95% confidence interval (*t* test). Closed circles, uninjected control spleens; open circles, spleens from embryos inoculated on day 12 with  $5 \times 10^5$  cells.

crease in spleen size. Aryl sulfatase, on the other hand, does not show a progressive increase in the experimental group. On no day during the experiment does it show a significant difference from the respective control activities, the means falling above those of the rising control group in the first few days and below them in the last. Other experiments show that this trend is repeatable.

We may conclude from this experiment

and the others described in this section that, although generally the increase in size of the spleen following inoculation is accompanied by similar increases in all of the lysosomal enzymes studied, significant differences among the enzymes are found when the increase is compared in relation to wet weight. These differences are dependent not only on the enzyme being studied, but also on the time after injection and the relative degree of enlarge-

ment of the spleen. Cytochemical methods are available for the study of two of the enzymes that have been found to differ (acid phosphatase and aryl sulfatase) and may be of some help in the resolution of the differences.

Kimmel's second approach to this problem was a study of the distribution of the lysosomal enzymes among subcellular fractions and characterization of the spleen lysosomes. Three methods were used—differential centrifugation of spleen homogenates, study of enzyme latency, and isopycnic centrifugation of lysosomes through sucrose gradients. A major problem encountered early in the studies was how to find a way to disrupt the spleen cells without damaging the hydrolase-containing particles. After trying various procedures, a controlled manual homogenization with a Dounce tissue grinder using ion-free 0.25 *M* sucrose as the suspending medium was found to yield intact lysosomes, the majority of the cells being disrupted. Differential centrifugation of the homogenate was then carried out. The material obtained in the pellets was checked microscopically and assayed after disruption of the particles for enzyme activities. The most satisfactory technique is:

1. Centrifugation of the homogenate at 500 *g* for 5 minutes. Free nuclei, erythrocytes and unbroken leucocytes, and a number of granules are sedimented in a fraction designated the "nuclear fraction."

2. Centrifugation of the supernatant from step 1 at 1,000 *g* for 10 minutes. Remaining nuclei and intact cells and the largest of the free granules are sedimented. The characteristic spindle-shaped granules of the mature heterophil and larger spherical granules are found in this fraction, designated the "large granule fraction."

3. Centrifugation of the supernatant from step 2 at 4,000 *g* for 10 minutes. Mitochondria and specific granules of a wide range of sizes are sedimented, the

product being designated the "mitochondrial fraction."

4. Centrifugation of the supernatant from step 3 at 30,000 *g* for 20 minutes. Small granules and a number of particles barely discernible with the light microscope are sedimented, the fraction being designated the "light mitochondrial fraction."

5. The supernatant from step 4 is assayed intact.

Further centrifugation (for example, to obtain a microsomal fraction) does not lead to appreciable sedimentation of lysosomal enzymes.

Results of fractionations carried out as above with day-17 normal and experimental spleens are presented in Figs. 34 and 35, respectively. The specific activity obtained in a fraction in relation to total recovery from the homogenate is plotted on the ordinate. The amount of protein obtained in a fraction as a percentage of the total recovery of the homogenate is plotted on the abscissa. The height of a column, then, gives the extent of purification of a fraction, while the total area of a column shows the total amount of recovery of the enzyme in that fraction. For example, in the first plot in Fig. 34, the mitochondrial fraction (third column) contains about 60 per cent of the cytochrome oxidase obtained in all the fractions. The purification is about fivefold. The lysosomal enzymes do not show the homogeneous distribution of cytochrome oxidase; rather, the data of Fig. 34 suggest that particles of a wide variety of sizes have acid hydrolase activities. These data also show that, although the heterogeneity is characteristic of the lysosomal enzymes as a group, all the enzymes follow a similar pattern. Nonsedimentable activities (supernatant fraction) amount to 5–20 per cent of the total, depending on the enzyme being assayed.

Comparison of Figs. 34 and 35 shows that several changes have occurred in the enlarged spleens. In replicate experiments three major changes are found: (1) an



increase in the heterogeneity among the group of lysosomal enzymes; (2) an increase in the relative amount of protein recovered in the supernatant fraction at the expense of the other fractions; and (3) an increase in the supernatant activi-

either hypothesis might be regarded as plausible.

The well-known phenomenon of latency of lysosomal enzymes has been studied using whole homogenates as well as granule-rich fractions. Treatments

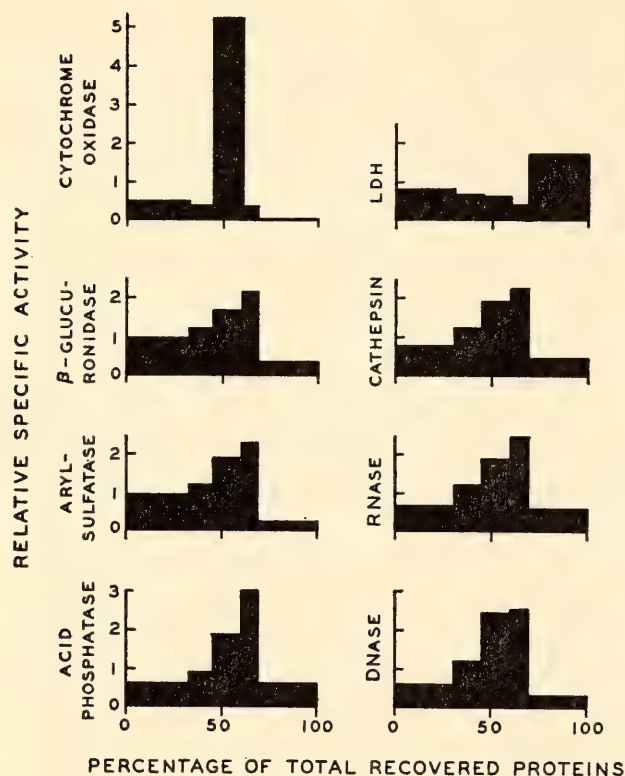


Fig. 34. Intracellular distribution of enzymes in homogenates of day-17 control spleens. Pooled spleens were homogenized and fractionated as described in text. Fractions, from left to right, are nuclear, large granule, mitochondrial, light mitochondrial, and supernatant. Assays were carried out on frozen-thawed and sonicated sucrose resuspensions. Proteins were measured by the biuret procedure using BSA as the standard.

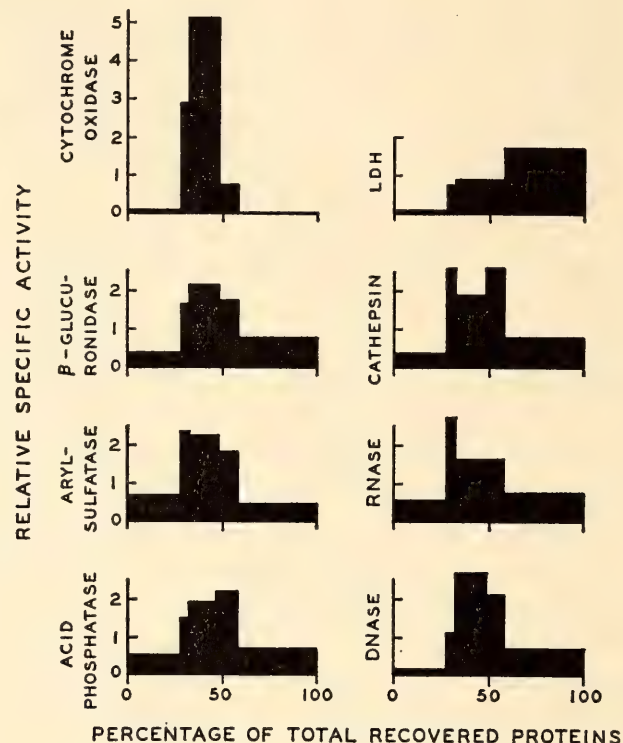


Fig. 35. Intracellular distribution of enzymes in homogenates of day-17 tenfold enlarged spleens (see Fig. 34 and text).

ties of the lysosomal enzymes, above that of LDH. Two possible explanations may be offered; either more of the enzymes are found in the free state in intact enlarged spleens, or the particles become more fragile and sensitive to mechanical disruption. The data at present do not permit distinguishing between the two, and

thought to disrupt membranes are effective in increasing the free activities of the enzymes. They include freeze-thaw cycles, sonication, incubation at low pH, and treatment with detergent (Triton X-100). In Dounce homogenates of day-17 control spleens, free activities of lysosomal enzymes amount to 5-25 per

cent of that found after the homogenate has been treated to disrupt the lysosomes, figures that agree well with those found for nonsedimentable activities. Furthermore, free activities of homogenates of the experimental enlarged spleens are consistently higher than those of the controls (Table 14).

Analysis of spleen lysosomes by means of isopycnic centrifugation indicates that there is no significant change detectable in the buoyant densities of the particles as a result of inoculation. Figs. 36 and 37 on the following pages show the distribution of lysosomal enzymes, protein, and cytochrome oxidase on gradients. In these experiments, 0.5 ml of a homogenate from which the nuclear and large granule fractions had been removed served as the load volume. It was layered on a 4.5 ml linear gradient from 0.5 *M* to 2.25 sucrose and centrifuged at 4°C for 2 hours at 35,000 rpm in the SW-39 rotor of the Spinco model L-2 ultracentrifuge. Fractions were collected as drops from a needle hole in the bottom of the tube. Material found in the top of the gradient (Fractions 15–17) corresponds to soluble proteins and free enzymes which do not move from the original load volume during centrifugation.

It may be seen from Fig. 36 that the general distribution of lysosomal en-

zymes is similar from one to another, yet clearly different from that of the mitochondrial enzyme, cytochrome oxidase. The major part of the lysosomal enzyme activity is found in a rather wide distribution around a peak at density 1.20, whereas cytochrome oxidase has a much sharper peak at a density of 1.18. The significance of this heterogeneity is not clear, nor is that of the lighter peak or shoulder (Fraction 12), which is characteristic of some of the enzymes. Comparison of Figs. 36 and 37 shows that there are no significant differences in the distribution of these enzymes after injections of adult cells.

These data suggest that, as a consequence of the reaction, there is an increase in the heterogeneity of the size but not of the density of granules containing hydrolases. There is also an increase in the proportion of lysosomal enzymes not associated with the granules in the homogenates of enlarged spleens. Both changes have been noted in other studies where cells are undergoing active endocytosis or other granulocytic processes, and the events may indeed be a major part of the splenomegaly reaction. Correlation of these results and those of cytological studies now in progress may serve to put this interpretation on a firmer basis.

TABLE 14. Free Activities of  $\beta$ -Glucuronidase and Aryl Sulfatase in 17-Day Control and Experimental Chick Spleens

Enzyme	Mean Activity $\pm$ S.E.				Probability, <i>t</i> test
	Control*		Experimental†		
	Total,‡ units/mg	Free,§ % of total	Total,‡ units/mg	Free,§ % of total	
$\beta$ -Glucuronidase	0.21 $\pm$ 0.01	20.5 $\pm$ 2.0	0.24 $\pm$ 0.02	28.3 $\pm$ 2.1	0.05 > <i>P</i> > 0.025
Aryl sulfatase	0.84 $\pm$ 0.02	5.1 $\pm$ 0.5	0.51 $\pm$ 0.11	10.0 $\pm$ 0.6	<i>P</i> < 0.001

\* Five determinations on groups of 6 pooled spleens.  
† Five determinations on single spleens enlarged about sixfold.  
‡ Homogenates assayed in the presence of Triton X-100 (0.05%).  
§ Homogenates assayed in the presence of 0.25 *M* sucrose to prevent osmotic lysis of the lysosomes.



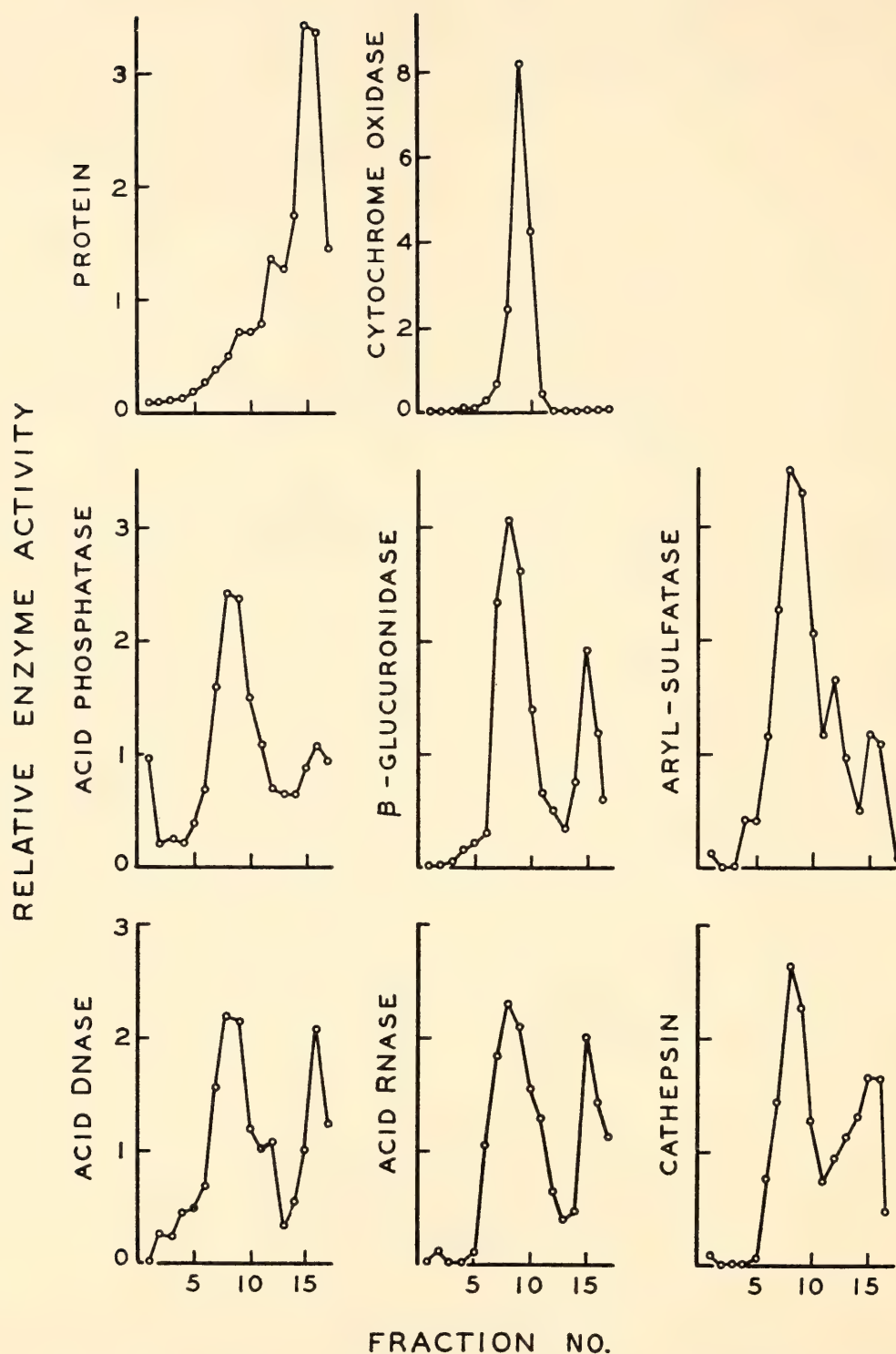


Fig. 36. Distribution of enzymes from day-17 control spleens after centrifugation through a linear sucrose gradient (0.5 *M* to 2.25 *M*) in water. The relative activity (ordinate) is the ratio of the observed activity to that which would have been found if the enzyme had been homogeneously distributed throughout the whole gradient. Proteins were measured by the Lowry procedure (see text).

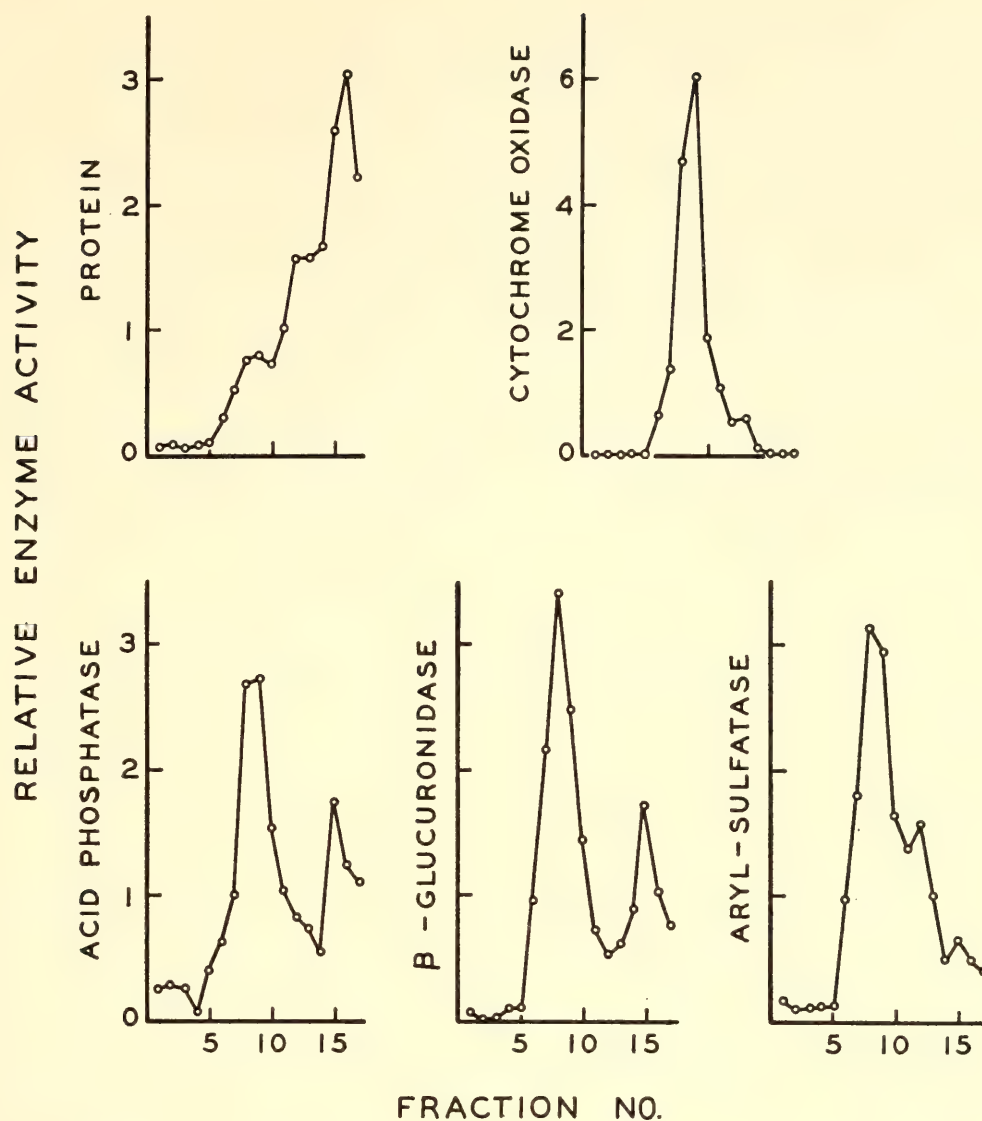


Fig. 37. Distribution of enzymes from eightfold day-17 enlarged spleens after centrifugation through a linear sucrose gradient (0.5 *M*–2.25 *M*) in water (see Fig. 36 and text).

## IMMUNOLOGICALLY INDUCED ASPERMATOGENESIS

Recent studies of immunologically induced aspermatogenesis have been impeded by the lack of an objective criterion for evaluating the onset and extent of damage to the germinal epithelium. With the assistance of Arlyne Musselman, D. W. Bishop has now developed a reliable assay which avoids the subjective analysis based on histological examination alone; permits the sampling of more tissues and the averaging of results within an experimental series; and gives an accurate, quantitative value for the amount of germinal tissue present, a more precise

estimate than that afforded merely by testicular weight determinations.

The activity of the enzyme, sorbitol dehydrogenase (SDH), provides the quantitative measure of functional germinal epithelium.

The assay has permitted a more precise evaluation of change in the germinal epithelium, including (1) brain-induced aspermatogenesis, and (2) intramuscularly induced aspermatogenesis. These studies, reported earlier, are now being prepared for publication.

During the year two extensive experi-



ments were conducted attempting to transfer aspermatogenesis from actively sensitized donor guinea pigs to inbred (strain 13) secondary recipients by intravenous administration of heavy suspensions of lymph-node cells. Despite the ready transfer of a state of delayed hypersensitivity, based on skin tests, and of humoral antibodies, no germinal epithelial impairment has been induced. Thus far no explanation, other than the possible failure of transplanted lymphoid cells to survive and proliferate, is suggested for the negative results.

#### TESTICULAR SORBITOL DEHYDROGENASE

Previous studies by Mann, Williams-Ashman, and their colleagues have demonstrated that sorbitol dehydrogenase (SDH) is present in mammalian reproductive tissues; responds to androgen stimulation of male accessory glands; reflects more accurately atrophy of the germinal epithelium than do other dehydrogenases (e.g., malic, succinic); and that it is DPN-dependent and can therefore be assayed simply by spectrophotometric methods.

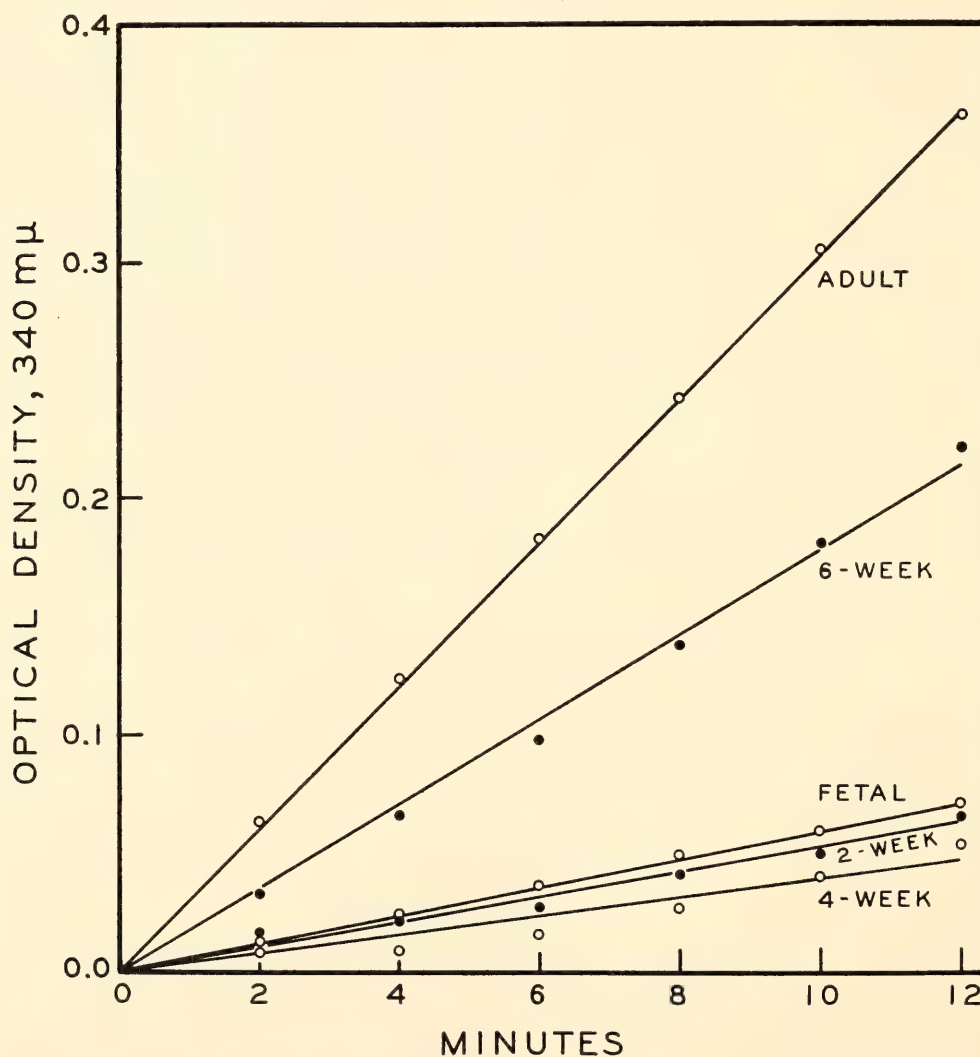


Fig. 38. Sorbitol dehydrogenase assays of guinea pig testes of various ages. Spectrophotometric plots show linear relation of DPNH-formation with time. Unless otherwise noted, all data throughout obtained on 0.2 ml sample (in 3.0 ml total tris-buffered incubation medium, pH 8.2) of 15,000*g* supernate of tissue homogenized (1-3 w/v) in saline-bicarbonate, read at 340 mμ at room temperature (23°-25°C).

Although the literature concerning this enzyme, or family of enzymes, is increasing, only one study—an as yet unpublished recent dissertation of Paul R. Libby at the University of Chicago—has delved in much detail into the enzyme's characteristics, extraction procedures, and correlation with related enzymes. Libby investigated xylitol dehydrogenase of the rat liver, responsible for the oxidation of xylitol to D-xylulose with the reduction of the cofactor DPN to DPNH. His extracted preparations also reversibly catalyzed the conversion of sorbitol to fructose

and were reactive with other polyol substrates such as ribitol and D-arabitol. Presumably Bishop is dealing with the same, or a closely related enzyme system in the guinea-pig testis.

Activity of the enzyme has been shown to increase with the age of the animal, a pronounced change occurring four weeks after birth, at a time when spermatocytes first appear in the gonad (Fig. 38). Fractionation and sedimentation in 0.34 *M* sucrose indicate that, of the several fractions, most of the activity is in the supernatant following centrifugation at

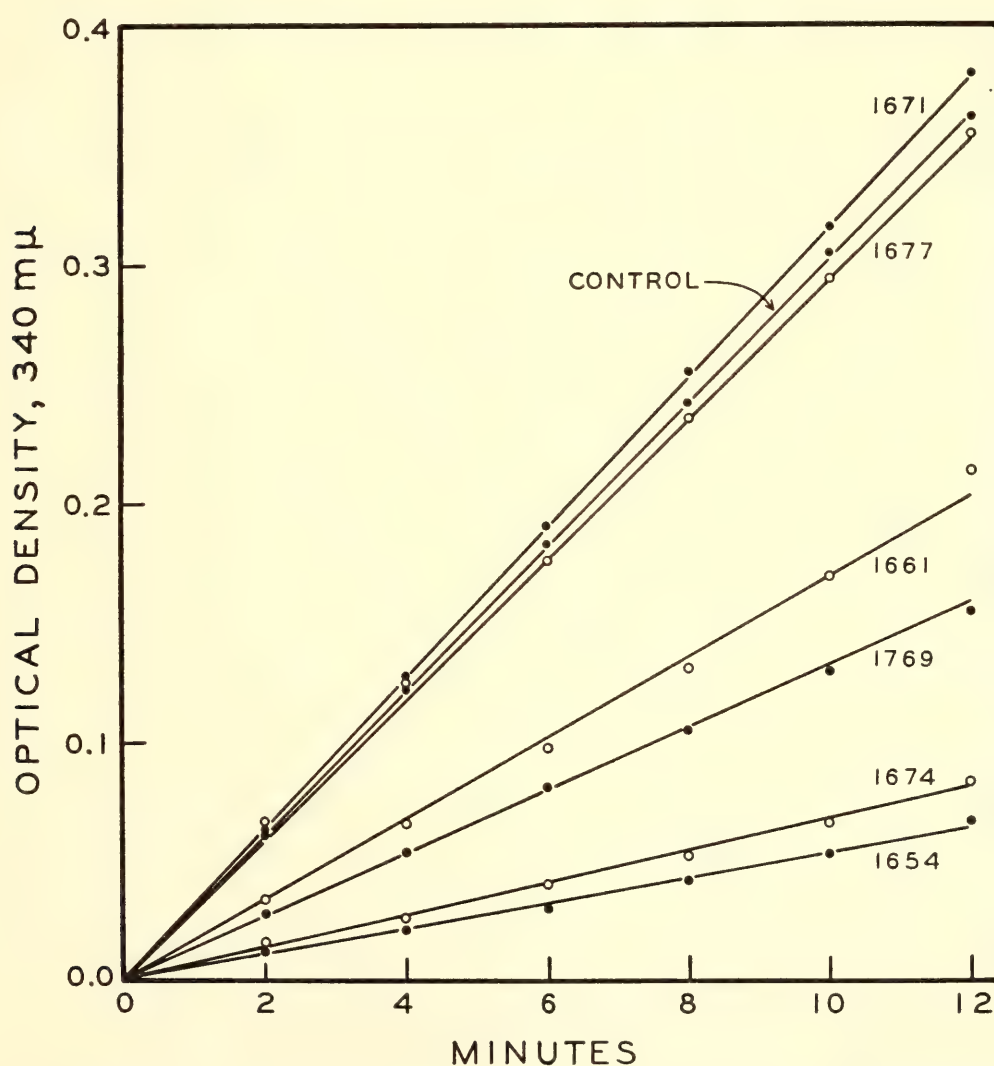
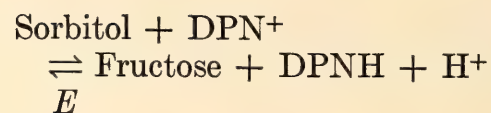


Fig. 39. SDH assays of normal, control, and impaired testes showing different degrees of germinal epithelial damage. Untreated control 1671 (sensitization with aspermatogenic factor in incomplete adjuvant), and 1677 (injected with complete adjuvant only) all have high levels of enzyme activity. 1654 and 1674 (sensitized with aspermatogenic factor in complete adjuvant) both show severe histological damage; 1769 and 1661 (similarly sensitized) are only moderately damaged.



105,000 *g*. The enzyme, in whole testicular tissue and in supernatants following low-speed (15,000 *g*) centrifugation, withstands freezing and thawing. Absolute values of enzyme activity may be calculated from the curves as plotted in Fig. 38 and expressed as micromoles of DPNH formed per minute per sample, e.g., 1.9, 8.7, and 14.8  $\times 10^{-3}$   $\mu$ mole DPNH/minute for 4-week, 6-week, and adult testes, respectively. The overall enzyme reaction system may be written as



The test for SDH in testes of animals sensitized against testicular aspermato-genic factor correlates excellently with histological anomalies present in the tissue. With increasing extent of damage a decreasing level of SDH occurs (Fig. 39). In testes in which the germinal epithelium has been totally destroyed vir-

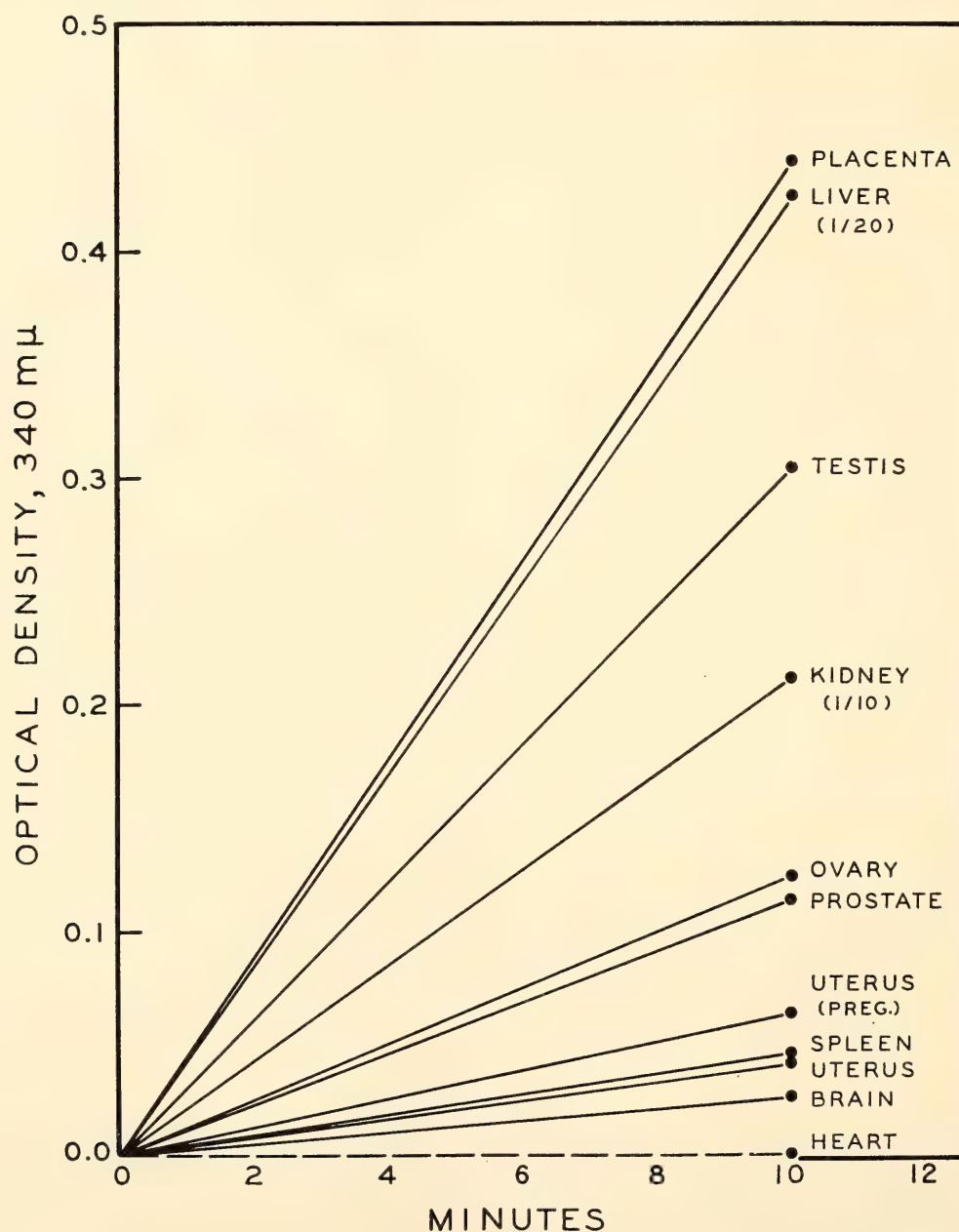


Fig. 40. Sorbitol dehydrogenase activity in various tissues of the guinea pig. Liver diluted 1/20 and kidney 1/10 compared with standard procedure; 10-minute enzyme assay.

tually no enzyme activity can be detected. In such immunologically damaged testes both interstitium and lymphatic infiltration may be observed, indicating that SDH activity in the testis is a function of the germinal epithelium. The enzyme assay is being used in connection with studies to determine onset of the testicular response, minimal effective doses of antigen, role of adjuvant components, and reversibility of the testicular reaction.

The increase in SDH activity in the developing testis, its relation to SDH activity in other tissues, and the possible occurrence of isozymes have stimulated interest in the enzyme itself. The distribution of SDH in other tissues of the

adult guinea pig is shown in Fig. 40. Placenta, liver, and kidney, expressed in wet weight of tissue, exceed testis; all other tissues assayed in the adult show less activity. Of the testes of the chicken and the several mammals that have been tested, the guinea-pig testis has the greatest SDH activity (Fig. 41). Possibly correlated with this fact is the occasional but unexplained high serum level of SDH in the guinea pig, contrary to that of the rat and of man except in cases of severe liver damage.

Substrate specificity of the testicular enzyme of the guinea pig roughly parallels that found by Libby for rat-liver SDH (Fig. 42). Sorbitol, ribitol, D-xylitol, and mannitol are oxidized, in decreasing order

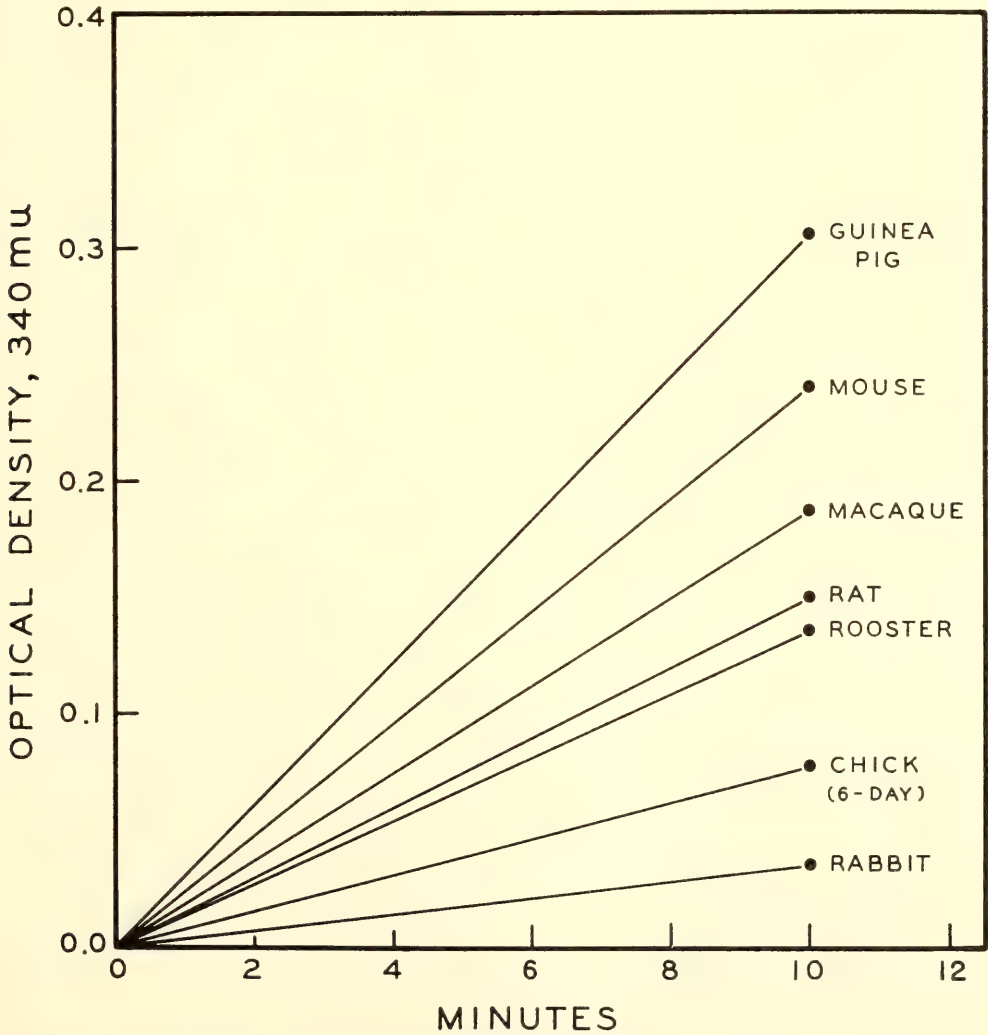


Fig. 41. Species variation in testicular sorbitol dehydrogenase activity in preparations run under identical conditions; 10-minute assay.



of preference, by Bishop's crude enzyme preparations; D-arabitol, dulcitol, and inositol are not.

Whereas DPN is the physiological co-factor of SDH, in vivo, the use of the analogue 3-acetylpyridine-DPN (3-AP-DPN) in vitro, increases sensitivity of the reaction eight- to tenfold (Fig. 43). The use of 3-AP-DPN, read at 360  $m\mu$ , is advantageous in assays involving small amounts of fetal tissue and consequent greater dilution with incubation medium.

Guinea-pig testes, impaired in a variety of ways other than by immunological means, have been employed in SDH assays. At 8 days after experimental cryptorchidism, cadmium chloride injection, or X irradiation (800 r), enzyme activity is less than normal (Fig. 44). In one series of unilateral cryptorchid animals, assays of the abdominal testes at 3-day intervals showed decreasing enzyme activity, first evident at 3 days, before histological changes became very ob-

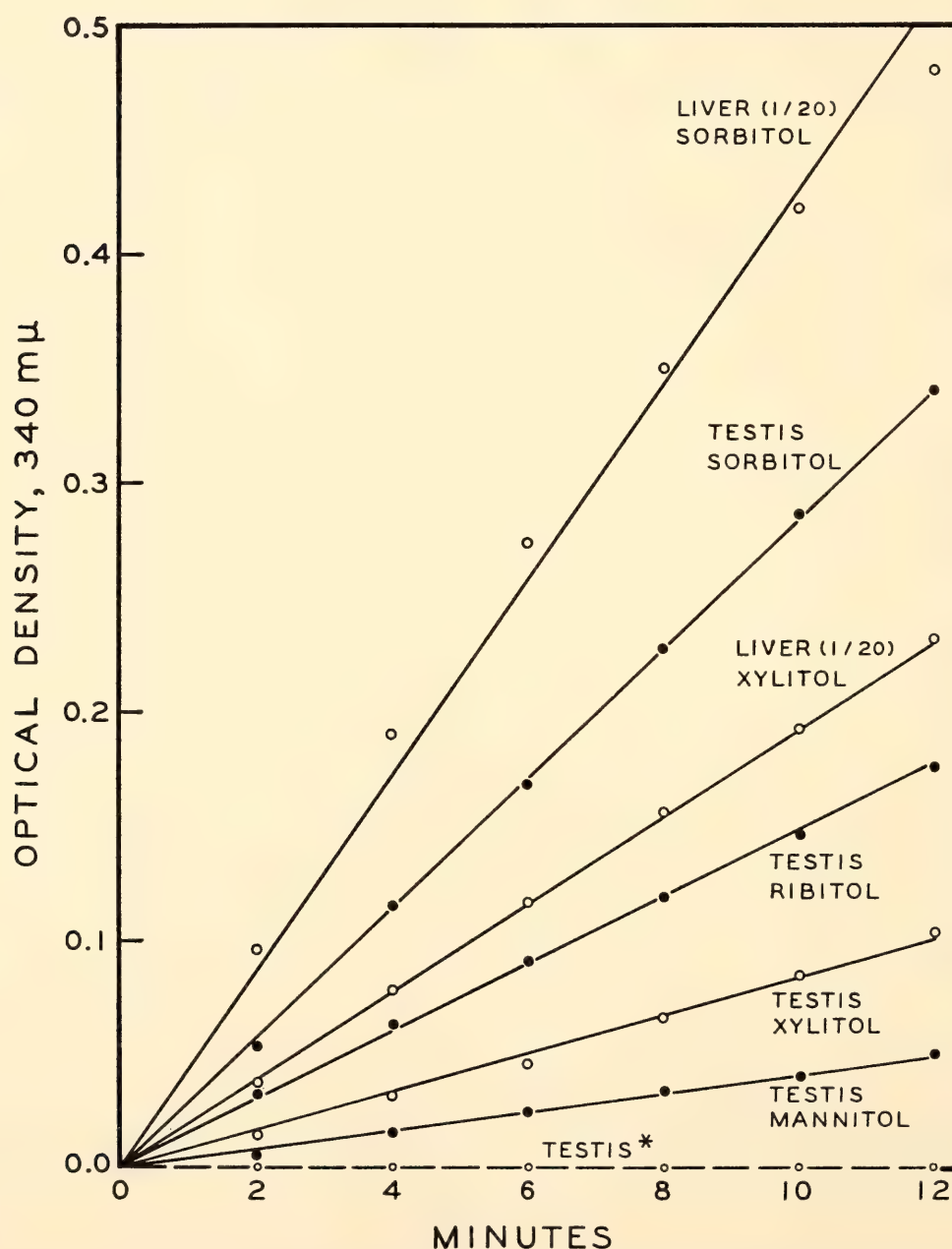


Fig. 42. Substrate preference of guinea pig liver and testis SDH. "Testis\*" indicates lack of activity with D-arabitol, dulcitol, or inositol.

vious (Fig. 45). The differences in enzyme levels of the cryptorchid testes and their paired normal scrotal controls are indicated in Fig. 46.

The apparent distribution and characteristics of testicular sorbitol dehydro-

genase have thus suggested several possibly rewarding lines of investigation—cellular localization in the developing testis, relation to spermatogenesis, and possible isozyme patterns, to mention only a few.

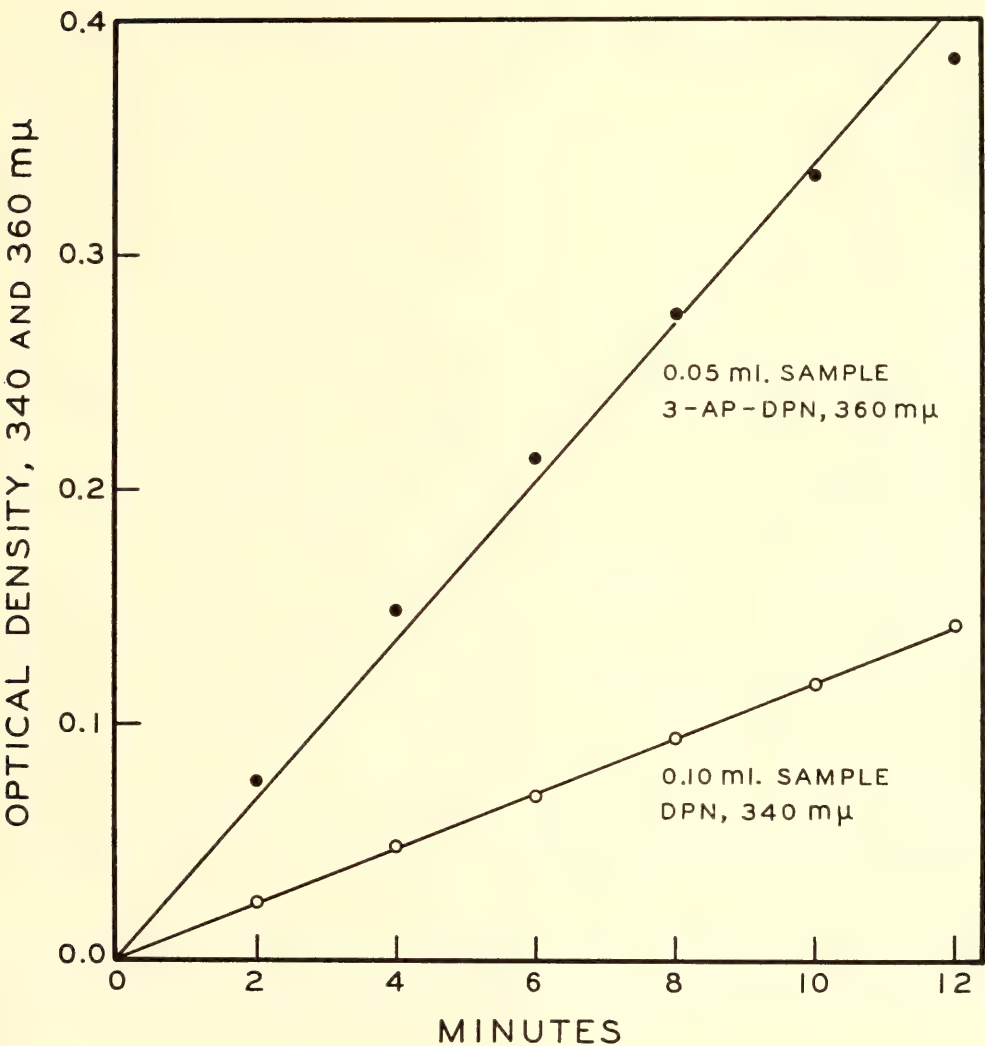


Fig. 43. SDH reaction rates with DPN (340 mμ) and the analogue 3-acetylpyridine-DPN (360 mμ). Note sizes of samples, both diluted 1-9 from standard.



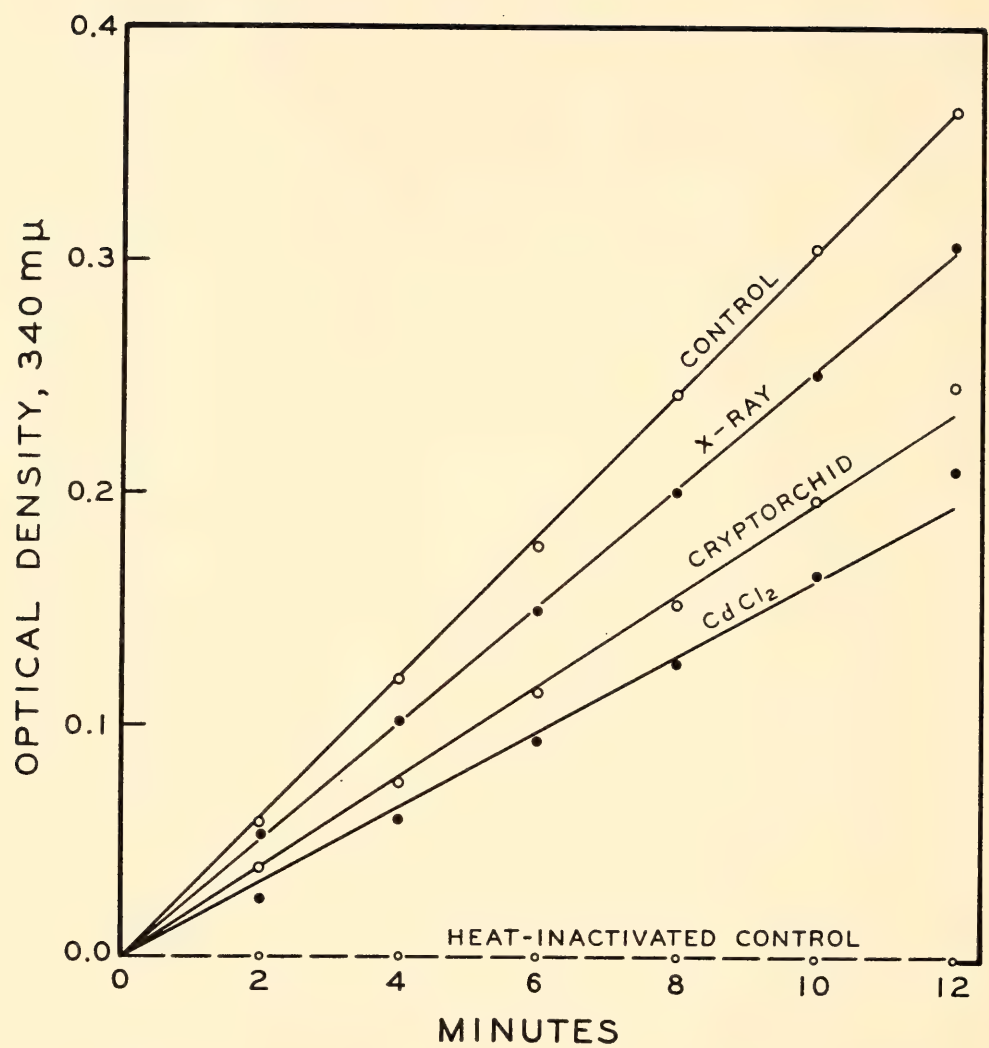


Fig. 44. Testicular SDH response to 800 r X irradiation, experimental cryptorchidism, and injection of cadmium chloride (0.24 mg/100g body wt, subcutaneously); assayed at 8 days.

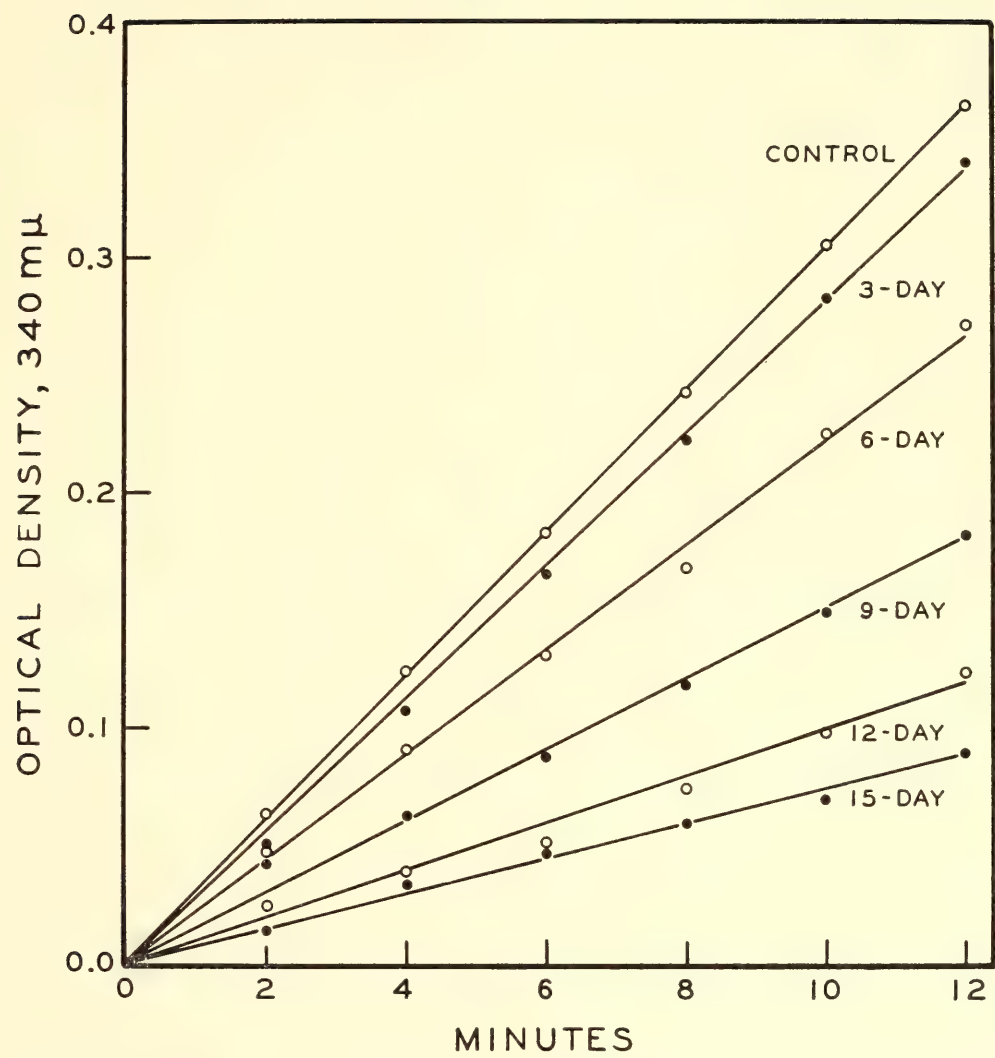


Fig. 45. SDH activity in abdominal testes of unilateral experimental cryptorchids at 3-15 days. Control from a selected normal animal.



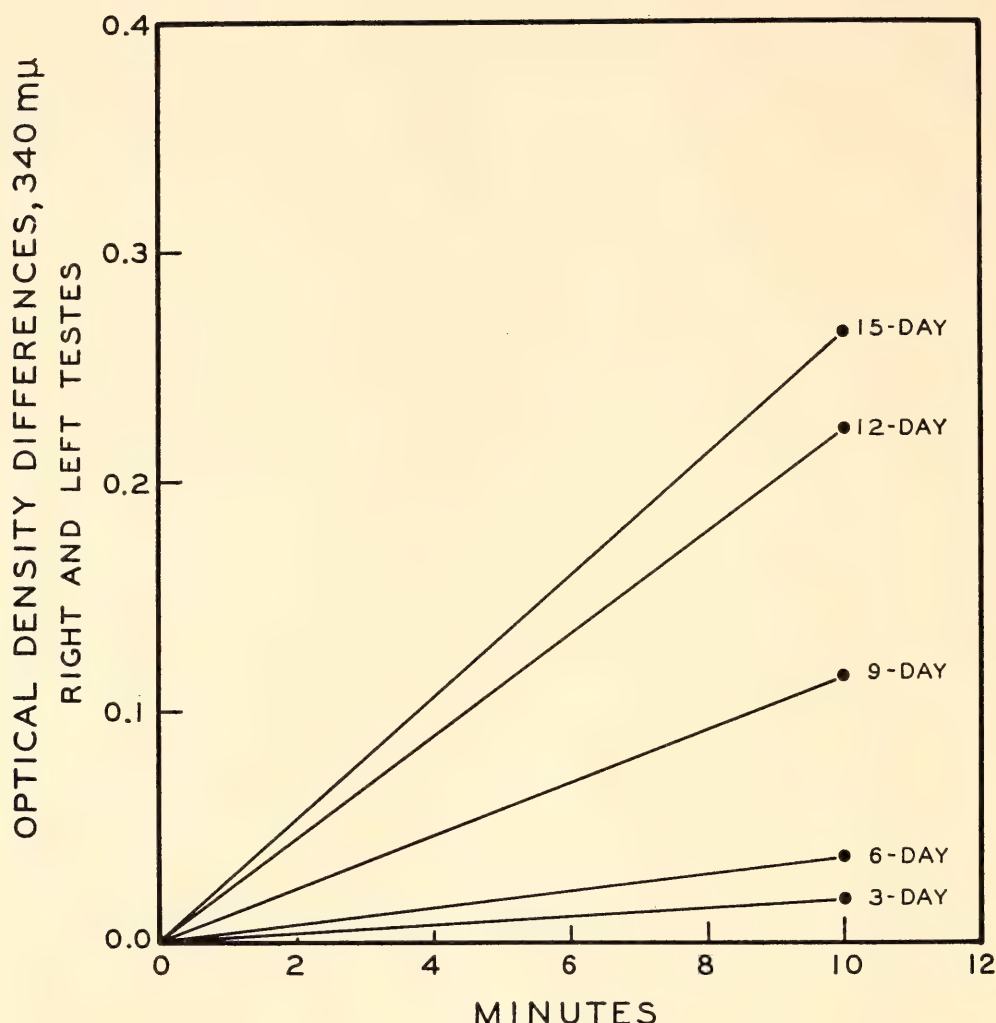


Fig. 46. Differences in optical density readings in enzyme preparations from abdominal cryptorchid testes and paired scrotal control testes at 3–15 days; SDH assay at 10 minutes.

## THE EMBRYO IN RELATION TO ITS ENVIRONMENT

### MECHANISMS OF IMPLANTATION OF THE OVUM

Having completed, for publication in the fall of 1965, a major contribution ("Anatomy of Reproduction") to the 13th edition of *Obstetrics*, edited by J. P. Greenhill, B. Böving returned to the laboratory late in the year covered by this report.

Fig. 47 brings up to date a summary of mechanisms of implantation in the rabbit, similar to the summary presented in *Year Book 57* (p. 314).

In renewing his investigations, Böving first sought experimental verification of the role of trophoblast "knobs" (aggre-

gates of syncytium) in penetration of the uterine epithelium.

Histological evidence that penetration is effected by extrusion of the contents of a trophoblast knob through an epivascular gap common to cytotrophoblast and epithelium was presented in *Year Book 63* (pp. 554–556). Experimental evidence may now be added in support of the hypothesis that the extrusion is induced by alkalinity—which normally is generated epivascularly. Blastocysts ready to implant were removed from a rabbit uterus and placed under the microscope in a plastic dish specially shaped to immobilize them for micromanipulation. They were viewed tangentially, and knobs on the visual

DAYS AFTER MATING		MECHANICAL		CHEMICAL		STIMULUS ( P = progesterone dependent )	EFFECTOR	ACTION	RESULT
3						"spontaneous"	uterine muscle	well-propagated contraction	blastocyst transport rapid with random arrangement
4							progesterone	uterine muscle	decreasingly propagated contraction
5						P 2-5mm blastocyst distention	uterine muscle	dome & grasp	transport stopped, endometrium flattened, blastocyst held antimesometrially
6						progesterone	uterine muscle		
7						P over 5mm blastocyst distention	maternal circulation	$2\text{HCO}_3^- \rightleftharpoons \text{H}_2\text{CO}_3 + \text{CO}_3^{=}$ (alkaline) carbonic anhydrase $\updownarrow$ (residue) $\text{H}_2\text{O} + \text{CO}_2 \rightarrow$ (to maternal circulation)	epivascular alkalinity
						P carbonic anhydrase increase	uterine epithelium		
						epivascular alkalinity	lemmas	adhesion	first attachment (fixes blastocyst orientation, always abembryonic & antimesometrial)
							?	lysis	lemmas disintegrated abembryonically (aids chemical exchange, uncovers trophoblast)
							trophoblast knobs	adhesion	epivascularly localized attachments (aim subsequent penetrations at vessels)
							trophoblast knob	cell dissociation	gap in cytotrophoblast
							uterine epithelium	cell dissociation	gap in epithelium
						?	trophoblast knob	extrusion of syncytiotrophoblast	penetration to vessel
8						penetration to vessel	early yolk-sac placenta	anchor	holds blastocyst while lemma remnants are shed
						maternal circulation	uterine epithelium	chemical exchange	alkaline reaction becomes diffuse
						progesterone		becomes syncytial	undissociable
						presence of trophoblast			basis for pH rise eliminated
9						continued & improved chemical exchange	late yolk-sac placenta	$\text{HCO}_3^-$ gradient eliminated	penetration stops

Fig. 47. Mechanisms of rabbit blastocyst transport, orientation, and yolk-sac placentation tabulated in terms of the stimulus, effector, action, and result. Each mechanism is both mechanical and chemical in nature, but the predominance differs from one mechanism to another, and there appears to be a degree of orderliness to the fluctuation. It is suggested that the oscillation may help one mechanism to be succeeded by the next, whereas in the absence of mechanical-chemical fluctuation the mechanism in operation tends to reach a steady state.



horizon were squirted with a stream of alkaline solution (sodium carbonate, 0.15 *N*). Aside from random and probably degenerative bleb formation, the usual specific reaction was a diffuse disruption of all trophoblast reached by the alkali. The hypothesis was confirmed, however, by a few instances limited to highly localized "popping" of a knob by the alkaline stream. An experiment recorded by time-lapse cinematography is illustrated in Plate 3, insets *A-F*. Observations are preliminary. As mentioned in last year's report, it was considered possible that most knobs ready to rupture might do so as a result of carbon dioxide loss to the atmosphere, and consequent spontaneous rise in *pH* while the blastocyst was being taken from the uterus to the microscope stage. Attempts to work under carbon dioxide were not obviously helpful, nor did variously buffered solutions give adequate control. Further efforts will be required to determine to what extent Böving's difficulties with the system lie in inadequate technique or inadequate understanding of biological factors.

#### ANATOMY AND PHYSIOLOGY OF THE PLACENTA

##### *Radioangiography of the Placental Circulation*

E. M. Ramsey, C. B. Martin, Jr., and M. W. Donner were again joined by H. S. McGaughey of the University of Virginia who paid a brief but productive visit to the laboratory at the height of the monkey pregnancy season during May.

In the active experimental season in the spring of 1965 several new avenues of experimentation were opened and new concepts evolved. It was deemed advisable this year to accumulate additional data to test the validity of the tentative conclusions in *Year Book 63* (pp. 556-558). "Verifying experiments," necessary as they are, have less appeal than pioneering work, but they are gratifying when, as in the present instance, they provide both

confirmation and amplification of previous observations.

*Arterial inflow to the intervillous space of the placenta.* In one group of monkeys, radiopaque dye was introduced through the femoral artery according to the techniques previously employed. In a second group, the following modifications were introduced: The catheter for injection of the dye was inserted extraperitoneally into the left external iliac artery and threaded as far as the origin of the hypogastric artery. The free end of this catheter was buried in a superficial subcutaneous site where it was readily accessible through a small incision carried out with minimal anesthesia. In one or two instances a corsetlike binder was closed posteriorly, out of reach of the monkey, with concealed safety pins. Intra-arterial injections of dye were made in the animals on alternate days for periods up to two weeks. The intra-amniotic catheter for monitoring myometrial activity was introduced percutaneously.

The results in both types of experiment were similar to those of previous years: the dye entered the intervillous space in characteristic spurts; the spurts slowly spread peripherally and coalesced; the dye cleared from the center of the spurts before disappearing at the periphery. Again it was found that different spurts appeared in successive injections carried out in tonus. The previous interpretation of the central clearing in the spurts as the result of negative washout by aftercoming blood was substantiated by the injection of a second bolus of dye while the peripheral ring persisted. The new spurts so occasioned appeared within the area of negative washout.

A start was made toward studying the possible relations between the intermittent opening and closing of spiral arterioles and the regulation of uteroplacental blood flow. Epinephrine has been shown to increase uterine vascular resistance and decrease uterine blood flow in sheep and dogs. The drug was therefore given intravenously to two pregnant monkeys after



control placental arteriograms had been obtained. The epinephrine dosage was 0.25  $\mu\text{g/kg/minute}$  in one animal, and 0.50  $\mu\text{g/kg/minute}$  in the other. After several minutes of the infusion another arteriogram was carried out. The effects of the drug were equivocal with the lower dosage; they were dramatic in the second animal. There was a marked decrease in number of entries (spurts) visualized after infusion, and most of those that did appear were smaller and fainter than in the control films. Even here, though, a few spurts were large and distinct. This spectrum, from complete disappearance of some entries to rather complete development of others, suggests differing sensitivities of individual spiral arterioles to the sympathetic neurohormone epinephrine.

These results are taken as confirmation of the existence of independent vasomotion in the spiral arterioles.

*Venous drainage of the intervillous space.* A series of injections of radiopaque dye directly into the intervillous space was carried out without change in technique over previous years. Cineradiograms showed findings identical with those already reported. Again, as in the past, it has been exceedingly difficult to get a catheter into the intervillous space even when the placenta is sharply localized at laparotomy by transillumination of the uterus. Clinicians can tap the intervillous space of the human placenta more easily. The cause of this discrepancy is unknown, but it is hoped that anatomical studies now in progress may cast some light upon the underlying factors.

It will be recalled that drainage from the intervillous space was only vaguely discernible following intra-arterial injection of the dye. With the modified technique of arterial injection noted above, venous channels in the uterine wall and pelvis have been visualized. They are far less distinct than those seen when the dye is introduced directly into the intervillous space, and it might not have been possible to recognize them at all had not

the intervillous space injections been carried out in advance. It is gratifying, however, that it is now possible to trace dye into, through, and out of the intervillous space after a single injection. Possibilities for study of time of transit and allied phenomena may be envisioned.

It is to be noted that in both the arterial and venous studies the effect of myometrial contractions, spontaneous or drug induced, has been similar in all respects to that previously observed.

### *Uterine Activity*

Preliminary observations of the uterine contraction patterns of nonpregnant rhesus monkeys were reported in *Year Book 63* (pp. 558–561), and the studies were continued during the experimental season just past. Two very significant advances occurred. The first was the development, with the collaboration of P. Eckstein of the Anatomy Department, University of Birmingham, England, of a technique for inserting the recording catheter into the uterine cavity through the tortuous monkey cervix. Recordings could then be obtained at more frequent intervals and with much less trauma to the monkeys. The second step came when Eckstein provided monkey-sized models of one of the intrauterine contraceptive devices and the equipment for inserting the coils.

Intrauterine pressure tracings thought to be typical of the contraction patterns during various phases of the menstrual cycle were presented in *Year Book 63*. As the number of observations has increased, it has become apparent that the earlier patterns were not entirely representative. In particular, the activity during the follicular phase of the cycle appears to be usually much greater than was indicated by the early experiments. In the follicular phase the contractions become increasingly rapid and irregular. One contraction follows another with only a few seconds or even incomplete relaxation intervening. Major peaks may occur as frequently as three a minute. This degree of uterine



activity continues for about a week past the time of ovulation at midcycle. In the final, premenstrual week contractions become less frequent and longer in duration, and a resting interval appears between contraction waves on the recording. The intensity of contraction varies considerably from animal to animal and even from hour to hour in the same animal; but in general contraction pressures of from 50 to over 100 mm Hg are recorded throughout the intermenstrual interval.

At the onset of menstruation, the contractions come to resemble in their smooth and rapid buildup and subsidence the expulsive contractions of advanced labor. The greatest contraction pressures, as high as 300 mm Hg, are recorded at this time. Later in the menstrual period, the contractions diminish in intensity and break up into the more rapid and irregular waves of the follicular phase.

When the ovary is inactive, as it is during the summer amenorrhea, the uterus is also quiescent, although not absolutely so; even then occasional weak contractions may be recorded.

Confidence in the monkey as a subject for reproductive studies applicable to humans is heightened by the similarity of these records of uterine activity to those obtained in women by C. H. Hendricks of Western Reserve University. Except for the greater contraction pressures observed in monkeys—perhaps the result of the smaller size of the uterine cavity—the resemblance is quite remarkable.

*The intrauterine contraceptive device (IUCD).* Studies with the IUCD have been directed toward the question, "What is the effect (if any) of these devices on uterine activity?" This query is of dual interest, as it is believed that accelerated uterotubal transport of ova may be important in the pregnancy-preventing effectiveness of the devices, and as a large proportion of clinical failures of the device result from its expulsion by the uterus.

It has been suspected that the uterus responds to the presence of the device by increased activity. Such an increase in

both frequency and intensity of contraction after insertion of the device was indeed recorded in some monkeys, but only when the preexisting activity was low, as in animals with irregular cycles. In most instances the effects of the device are not so simple to assess. When the uterus is contracting with the frequency and intensity usually found during the follicular and early postovulatory portions of the cycle, quite a different change is observed. As soon as the IUCD is inserted the contractions become less frequent and of longer duration. Their intensity does not seem to be consistently altered under these circumstances. Moreover, this effect appears to be a chronic one, for the slow pattern has been recorded through the cycle in one animal with the device in place during the whole cycle. The contraction pattern during menstruation seems unchanged by the presence of the device either immediately after insertion or in place for some weeks.

That the IUCD does affect uterine activity is apparent from these observations. It is equally apparent that the observed effect of the device on the contraction pattern is not, on the surface, a uniform one. One interpretation that lends consistency to the observations is that the preexisting activity is changed toward the pattern of labor or menstruation. The direction of the observed change varies according to the base-line pattern. Thus, when activity is low, increase in intensity and frequency of contraction is produced; but when contractions are rapid, a slowing results. During menstruation, no change occurs. It is generally held that the contractions of normal labor or menstruation represent coordinated, expulsive activity. According to this tentative interpretation, then, the IUCD produces a qualitative improvement in the uterine contraction pattern, though not always a quantitative increase.

#### *The Fetal Circulation*

During the 1965 monkey pregnancy season the placental physiology team



turned their attention across that barrier to the fetal circulation. In this venture the group was joined by E. J. Quilligan of the Department of Obstetrics at Western Reserve University. Quilligan's visit brought the additional benefit of his considerable experience with studies of fetal lamb and human circulations.

Studies of the fetal circulation were aimed at a dual target. The first was the development of means of continuously and simultaneously monitoring such fetal parameters as blood pressure, heart rate, and oxygen tension. The second was the investigation of the effects of uterine contractions upon these parameters. In each area there was partial success.

The plan of the experiments was to insert a shunt into the intraplacental vessels, those fetal arteries and veins that course in the chorion between the primary and secondary of the monkey's two placental discs. Blood pressure and heart rate would be recorded from one side arm of the shunt. Into the other side arm, a polarographic electrode would be inserted so that the tip lay just within the stream of fetal blood. Technical problems were encountered in maintaining blood flow through the shunt, so that the desired continuous recording of  $pO_2$  was achieved only twice, and then only for short periods. In each instance, however, the oxygen tension of the fetal blood showed the expected decrease with uterine contractions. This decrease reflects the diminished maternal perfusion of the placenta so well shown in the radioangiographic experiments of former years.

Although the shunt experiments proved a temporary disappointment, alternative techniques yielded very interesting insights into fetal physiology. Fetal blood pressure and heart rate could be monitored over long periods from small catheters threaded into intraplacental or femoral arteries. Samples of fetal blood drawn at intervals from the catheters

provided glimpses of the status of fetal oxygenation, if not the panorama hoped for at the outset.

Fetal blood pressure remained constant in relation to intrauterine pressure throughout uterine contractions. The fetal heart rate remained normal and steady between and during contractions, even though the fetal arterial oxygen tension had been reduced to very low levels (5 mm Hg or less) by excessive uterine activity. Only when the anoxic stress had been prolonged did bradycardia, accompanied by widening of the pulse pressure, appear late in the course of a uterine contraction. If the interference with oxygenation continued still longer, the periods of bradycardia became more prolonged, and eventually the slow rate persisted between, as well as during, contractions. Recovery was possible if the excessive uterine activity interfering with maternal placental perfusion was terminated.

These results indicate that the monkey fetus possesses considerable resistance to acute anoxemia. Further, they show that disturbance of the fetal heart rate, generally considered to be the best clinical indicator of fetal asphyxia, may indeed be a very late reflection of fetal distress.

Of three fetuses left *in utero* at the conclusion of the experiment, one continued to thrive for six weeks, indicating that long-term observations of this sort on the monkey fetus may be possible.

#### *Vasculature of the Pregnant Human Uterus and Placenta*

E. M. Ramsey's collaborative study with J. W. S. Harris, of London, dealing with the vasculature of the pregnant human uterus and placenta, has moved ahead. It was completed and a manuscript prepared for publication during the summer of 1965, when Harris spent several weeks in the Department.



## THE COLLECTION OF HUMAN EMBRYOS

In the year covered by this report, E. M. Ramsey and C. B. Martin, Jr. examined 61 specimens sent by 12 physicians and laboratories from four states and the United States Army, Berlin. Of these specimens, 43 were discarded as of no research value at the end of 3 months after reporting to the donor and in the absence of instructions to the contrary, and 18 had sufficient research value to justify preservation.

From cases of maternal rubella 7 specimens were received, bringing to 24 the total of such cases that have been sent to us; 22 of them were loaned to G. C. Rosenquist for histological study.

COMPLETE DYSRAPHISM IN A  
14-SOMITE HUMAN EMBRYO:  
A CONTRIBUTION TO NORMAL AND  
ABNORMAL MORPHOGENESIS

Studies of congenital malformation in young human embryos are essential for the understanding of definitive teratological anomalies present in a proportion of newborn infants and in later life. Such studies may also provide important clues for elucidation of normal morphogenesis during embryonic stages. Thus, there exists a clear need for accumulation of well-documented material concerning aberrations of development. So far only a few human embryos with total dysraphism have been reported in the literature. A. S. Dekaban and G. W. Bartelmez have now studied embryo 779 of the Carnegie Collection, the youngest known totally dysraphic embryo (14 somites). Their observations are recorded in a paper published recently in the *American Journal of Anatomy*. This embryo has been reconstructed from the microscopic sections and studied in detail. Although the neural folds failed to close throughout the dorsal extent of this 14-somite embryo, the beginning of independent closure took place rostrally at the torus opticus. The last feature has been shown to be the usual event in normal embryos of this stage.

Careful examination of structures other than the nervous system reveals only minor abnormalities. Thus, the dispersion of cells of somites I and II as well as loosening of other sclerotomes in this region has begun prematurely. On the other hand, some retardation in the development of the pharynx, heart, and nephros has been noted. Specifically, the chorda, the mesenchyme, blood vessels, and gut have been found to be normal.

The literature pertaining to the closure of the neural folds has been discussed, as well as the reports on experimental inhibition of the formation of the neural tube, which are accorded special emphasis. The available evidence refutes the contention that the closure of neural folds is induced by adjacent structures of whatever derivation. It appears plausible, as Davis demonstrated, that biochemical reactions within the neural epithelium may be involved in the process of normal closure of the neural folds.

Morphological findings in the present embryo do not support most of the previously advanced theories relating to the pathogenesis of dysraphic states.

THE INITIAL APPEARANCE OF OSSIFICATION IN STAGED HUMAN EMBRYOS

R. O'Rahilly and Ernst Gardner have presented the following preliminary account of the most recent chapter in their continuing study of ossification.

Serial sections of 36 embryos aged from 6 to 8 postovulatory weeks (12–31 mm C.R.) were examined. The clavicle and the mandible began to ossify during stages 18, 19, or 20, the clavicle, frequently at least, by means of two centers. The maxilla followed rapidly (stages 19–20). The premaxilla was found in continuity with the maxilla proper, either as a mesenchymal condensation or as an ossific area (stages 20–21). The next elements to commence ossification were the humerus (stages 21–22), the radius (21–23), and the femur, tibia, and ulna (22–



23). By stage 23, the following were also undergoing ossification in at least some cases: intraparietal, supraoccipital, anterior process of malleus, squamous temporal, palatine, medial pterygoid plate, zygomatic, frontal, vomer, scapula, and distal phalanges of hand. Cellular invasion was found in the clavicle and in the bone collars of the radius, ulna, and femur at two prenatal months. The cartilages (Meckel's) approached the median plane (stage 20) but did not fuse in the embryonic period proper; their cartilage underwent a localized hyper-

trophy by stage 23, but endochondral ossification did not occur until the fetal period.

#### PUBLICATION OF "CONTRIBUTIONS TO EMBRYOLOGY"

It is expected that volume 38 of *Contributions to Embryology* will appear in the spring of 1966. The following *Contribution* numbers have been assigned: 259, J. W. S. Harris and E. M. Ramsey; 260, R. O'Rahilly; 261, A. S. Dekaban and G. W. Bartelmez; 262, G. C. Rosenquist and R. L. DeHaan; 263, G. C. Rosenquist.

### APPARATUS AND TECHNIQUES

#### CULTURING TISSUES OF INVERTEBRATES

Over the past several years, one of DeHaan's continuing interests has been the spatial organization occurring in those embryos that exhibit mosaic development. In certain invertebrate forms such as dipteran insect larvae and the embryos of annelids and molluscs, the organization of the various body parts is more or less rigidly predetermined at an early stage. The embryological mechanisms involved in this type of development are little known. What are the roles of intercellular adhesion and cell migration in the processes of morphogenesis in these forms? It was in an attempt to begin attacking these questions that DeHaan spent the year 1962-1963 in the laboratory of Ernest Hadorn in Zürich, trying to work out methods of maintaining and handling *Drosophila* imaginal disc tissues in vitro (see *Year Book* 62, pp. 444-447). During the past year, in collaboration with Ajdukovic, he has continued this program. Ajdukovic has been able to improve upon the culture medium by supplementing it with Puck's medium N-16, and by the use of Mycostatin in low doses as a fungistatic agent. The most important innovation, however, has been in the biological assay.

Imaginal disc tissues do not differen-

tiate in tissue culture. To determine the condition of a tissue fragment, it must be forced to undergo metamorphosis. The method for its accomplishment was devised by Ephrussi and Beadle three decades ago when they injected freshly dissected fragments of imaginal discs into the body cavity of host *Drosophila* larvae. After pupation and metamorphosis of the host into an adult fly, the injected fragments could be found in the host abdomen, also having differentiated into adult structures. The major difficulty with this technique is that *Drosophila* larvae are small (1-2 mm in diameter) and therefore difficult to use as hosts. The injection technique is laborious, and the number and size of fragments that can be injected are severely restricted. For these reasons, Ajdukovic and DeHaan are injecting *Drosophila* discs into host larvae of another, larger dipteran species. Thus far they have enjoyed some success using prepupae of the calliphorid fly, *Phormia*. With this relatively large form (3 mm diam  $\times$  8-10 mm long), several entire wing discs can be injected into a single host. Tests of the survival of whole discs after long periods of culture, and of fragments compounded of multiple discs should now be possible.

The marine snail *Ilyanassa obsoleta* is another classic example of an embryo that



exhibits mosaic development. During the summer of 1964, while serving as an instructor at the Marine Biological Laboratory, Woods Hole, Massachusetts, DeHaan attempted to work out media for the culture of cells of this molluscan species. In collaboration with two students, Bonnie Sue Ebstein of Yale University and Miriam D. Rosenthal of Brandeis University, these preliminary

attempts proved successful. In a medium composed of 5 per cent horse serum, 1–5 per cent Eagle's basal medium, and 94 per cent pasteurized seawater, fibroblast-like cells have been maintained for 8 days after isolation from the embryo, during which time at least some cells developed the capacity for spontaneous contractions. This project was continued in the summer of 1965.

### STAFF ACTIVITIES

Members of the staff were privileged to serve, along with their colleagues in Johns Hopkins Department of Biology, as hosts for the International Conference on Organogenesis held in Baltimore, September 6–12, 1964.

Those charged with arranging the program believed that the time had come for reemphasizing the study of development "beyond the ribosome." Acting on the conviction that ample attention was being given to problems of coding and protein biosynthesis, Professor Etienne Wolff, President of the International Institute of Embryology, under whose auspices the Conference was held, invited the Organizing Committee to develop a program that would center attention on supermolecular aggregates, cells, and cell associations. Thus, at the Conference the primary focus was on the behavior and interactions of cells and cell groups in the fashioning of complex ordered tissues.

Within the International Union of Biological Sciences, the International Institute of Embryology represents developmental biology. In addition to its publishing and research programs, centered in the Hubrecht Laboratory, the Institute has convened a series of successful international conferences. Happily, the International Conference on Organogenesis was no exception. Its success was attested by the genuine enthusiasm of the 400 participants and the prompt, willing cooperation of speakers, discussants, and other contributors to the book *Organo-*

*genesis*, being edited by DeHaan and Heinrich Ursprung. It is scheduled for publication in October 1965.

Other international conferences in which members of the group participated included the Fourth World Congress of Gynecology and Obstetrics, held at Mar del Plata, Argentina; the Symposium on Biology of Skin and Hair Growth, in Canberra, Australia; a Workshop on the Molecular Basis of Differentiation, at Naples, Italy; the Japanese-American Cooperative Science Program, in Tokyo, Japan; and a Symposium on Effects of Labor on the Fetus, at Montevideo, Uruguay.

The staff took part in a number of national conferences: a conference on developmental and metabolic control mechanisms and neoplasia at the M. D. Anderson Hospital, Houston; a symposium on the molecular basis of differentiation at the annual meeting of the American Association for the Advancement of Science, Montreal; a workshop on developmental immunology at Sanibel Island, Florida; another on fetal homeostasis at Princeton; two workshops on the embryological background of congenital heart disease, at Purchase, New York, and Washington, D. C., respectively; and two on the uterus and placenta, at the University of Washington, Seattle, and Woman's Medical College of Pennsylvania, in Philadelphia.

During the year staff members, Fellows, and visiting investigators presented lec-



tures at a number of campuses, including Albert Einstein College of Medicine, California Institute of Technology, Columbia University, Goucher College, Jefferson Medical College, Marquette University, Medical College of Georgia, Michigan State University, Syracuse University, Tulane University, and the Universities of California (San Francisco and Santa Barbara), Florida, Illinois (Chicago), Kyoto, Michigan, Nagoya, Pennsylvania, Tokyo, Virginia, and Washington (Seattle); Washington University (St. Louis), and Wayne State University.

Other research centers at which lectures were given included Baltimore City Hospitals, Francis Delafield Hospital, Marine Biological Laboratory, and National Institutes of Health.

Members of the group took part in meetings of a number of learned societies, including, in addition to those already mentioned, the American Association of Anatomists, American College of Obstetricians and Gynecologists, American Institute of Biological Sciences, American Physiological Society, American Society of Biological Chemists, American Society for Cell Biology, American Society of Zoologists, Federation of American Societies for Experimental Biology, National Foundation, National Institute of Science, Society for Experimental Biology and Medicine, Society for the Study of Development and Growth, Society of General Physiologists, and Society for Gynecologic Investigation.

Advisory and consultative services included membership on the editorial boards of *International Journal of Cancer*, *Journal of Embryology and Experimental Morphology*, *Journal of Experimental Zoology*, and *Excerpta Medica* (section on Human Developmental Biology); and on the board of consulting editors of *Current Topics in Developmental Biology* and *Developmental Biology*. Members of the staff continued to serve on the Divisional Committee for Biology and Medicine and the Science Development Advisory Panel, National Science Foundation; the Sub-

committee on Congenital Malformations, U. S. National Committee on Vital and Health Statistics; and the Visiting Committees of the Departments of Biology, Massachusetts Institute of Technology and Western Reserve University. Others rendered service on the National Science Foundation's Panel on Regulatory Biology and the Training Committee of the National Institute of Child Health and Human Development.

Members of the staff acted in these capacities: president, Society of General Physiologists and vice-president of the 24th International Congress of Physiology; secretary, Section F, American Association for the Advancement of Science (AAAS); member, Newcomb Cleveland Prize Award Committee, and Committee on Nominations and Elections, AAAS; vice-president and chairman, and committeeman-at-large, Section N, AAAS; chairman of the National Science Foundation's Committee for Postdoctoral Fellowships (through the National Research Council); member of the Executive Committee and representative to the national Research Council of the American Association of Anatomists; member, AIBS Governing Board; member of Advisory Committee for *American Men of Science*, and trustee, Marine Biological Laboratory.

One member of the group continued to serve as chairman of the Maryland Academy of Sciences' Scientific Council.

Other activities directed largely toward teaching included the participation of several members of the Department in the Embryology Training Program, Marine Biological Laboratory, Woods Hole, Massachusetts; and service on the Commission on Undergraduate Education in the Biological Sciences. As in the past, members of the group took part in teaching programs in Johns Hopkins University School of Medicine, in the Departments of Anatomy, Biology, Obstetrics and Gynecology, and Pediatrics. One staff member offered a series of holiday science lectures, sponsored jointly



by the AAAS, Case Institute of Technology, and Western Reserve University.

*Seminars.* The roster of speakers at the seminars organized by the Department to serve all those working in developmental biology in the area included Everett Anderson, University of Massachusetts; David Epel, University of Pennsylvania; Colin A. Finn, Wye College, University of London; Gary Free-

man, University of Pennsylvania, Alberto Monroy, University of Palermo, Italy; Robert T. Schimke, National Institutes of Health; Robert L. Searls, University of Virginia; Sheldon J. Segal, The Population Council; Louis Sokoloff and Gordon Tomkins, National Institutes of Health; Robin Wallace, Biology Division, Oak Ridge National Laboratory.

## BIBLIOGRAPHY

- Bartelmez, G. W., *see* Dekaban, A. S.
- Beck, F., The utilisation of yolk by the chick blastoderm—a histochemical and biochemical study, *Am. Zoologist*, **4**, 288, 1964.
- Beck, F., The distribution of acid phosphatase in the chick blastoderm, *Exptl. Cell Res.*, **37**, 504–508, 1965.
- Brown, D. D., RNA synthesis during amphibian development, *J. Exptl. Zool.*, **157**, 101–114, 1964.
- Brown, D. D., *see also* Gurdon, J. B.
- DeHaan, R. L., Cell interactions and oriented movements during development, *J. Exptl. Zool.*, **157**, 127–138, 1964.
- Dekaban, A. S., and G. W. Bartelmez, Complete dysraphism in 14 somite human embryo. A contribution to normal and abnormal morphogenesis. *Am. J. Anat.*, **115**, 27–41, 1964.
- Donner, M. W., *see* Martin, C. B., Jr.
- Donner, M. W., *see* Ramsey, E. M.
- Ebert, J. D., Review of *Biological Science: Molecules to Man*, by Biological Sciences Curriculum Study, *Quart. Rev. Biol.*, **39**, 189–191, 1964.
- Ebert, J. D., *Interacting Systems in Development*, Holt, Rinehart and Winston, New York, 227 pp., 1965.
- Ebert, J. D., *see also* Reporter, M. C.
- Fuerst, C. R., *see* Kaighn, M. E.
- Gardner, E., *see* O'Rahilly, R.
- Gurdon, J. B., and D. D. Brown, Cytoplasmic regulation of RNA synthesis and nucleolus formation in developing embryos of *Xenopus laevis*, *J. Mol. Biol.*, **12**, 27–35, 1965.
- Kaighn, M. E., M. A. Moscarello, and C. R. Fuerst, Purification of murine encephalomyocarditis virus, *Virology*, **23**, 183–194, 1964.
- Kaighn, M. E., *see also* Moscarello, M. A.
- Kaiser, I. H., *see* Martin, C. B., Jr.
- Kocher-Becker, U., Heinz Tiedemann, and H. Tiedemann, Evagination of newt endoderm: Cell affinities altered by the mesodermal inducing factor, *Science*, **147**, 167–169, 1965.
- Konigsberg, I. R., The embryological origin of muscle, *Sci. Am.*, **211**, 61–66, 1964.
- Konigsberg, I. R., Muscle, differentiation in, in *Year Book of Science and Technology*, McGraw-Hill Book Company, New York, pp. 274–276, 1965.
- Lieberman, M., and A. Paes de Carvalho, An electrophysiological study of functional differentiation in embryonic chick hearts, *Federation Proc.*, **23**, 249, 1964.
- Lieberman, M., and A. Paes de Carvalho, An electrophysiological study of AV conduction in embryonic chick hearts, *The Physiologist*, **7**, 192, 1964.
- Martin, C. B., Jr., H. S. McGaughey, Jr., I. H. Kaiser, M. W. Donner, and E. M. Ramsey, Intermittent functioning of the uteroplacental arteries, *Am. J. Obstet. Gynecol.*, **90**, 819–823, 1964.
- Martin, C. B., Jr., *see also* Ramsey, E. M.
- McGaughey, H. S., Jr., *see* Martin, C. B., Jr.
- Moscarello, M. A., and M. E. Kaighn, The amino acid composition of three plaque-type mutants of encephalomyocarditis virus, *Biochim. Biophys. Acta*, **90**, 161–163, 1964.
- Moscarello, M. A., *see also* Kaighn, M. E.
- Muecke, E. C., The role of the cloacal membrane in exstrophy: The first successful experimental study, *J. Urol.*, **92**, 659–667, 1964.
- O'Rahilly, R., and E. Gardner, The initial appearance of ossification in staged human embryos, *Anat. Record*, **151**, 394, 1965.
- Paes de Carvalho, A., *see* Lieberman, M.
- Ramsey, E. M., Placenta, in *Laboratory Technique in Biology and Medicine*, edited by V. M. Emmel and E. V. Cowdry, Williams & Wilkins, Baltimore, 345–348, 1964.
- Ramsey, E. M., Placental hemodynamics, Apartado del tomo de Relatos del 4° Congreso

- Mundial de Ginecología y Obstetricia, Mar del Plata, Argentina, September 1964.
- Ramsey, E. M., C. B. Martin, Jr., and M. W. Donner, Radiographic studies of the venous drainage of the placenta in rhesus monkeys, *Obstet. Gynecol.*, *25*, 417-418, 1965.
- Ramsey, E. M., C. B. Martin, Jr., and M. W. Donner, Radioangiographic demonstration of the circulation in the maternal placenta of rhesus monkeys, *Anat. Record*, *151*, 492, 1965.
- Ramsey, E. M., *see also* Martin, C. B., Jr.
- Reporter, M. C., Amino acid incorporation by isolated mitochondrial fractions of unfertilized *Arbacia* eggs and late gastrula embryos, *Biol. Bull.*, *127*, 386-387, 1964.
- Reporter, M. C., and J. D. Ebert, A mitochondrial factor which prevents the effects of antimycin A on myogenesis, *J. Cell Biol.*, *23*, 77A, 1964.
- Rosenquist, G. C., Radioautographic mapping of endoderm-mesoderm movements in head process chick embryos, *Am. Zoologist*, *5*, 215, 1965.
- Tiedemann, Heinz, *see* Kocher-Becker, U.
- Tiedemann, H., *see* Kocher-Becker, U.

## PERSONNEL

*Year Ended June 30, 1965*

(including those whose services began or ended during the year)

*Research Staff*

David W. Bishop, General Physiology  
 Bent G. Böving, Physiology  
 Donald D. Brown, Biochemistry  
 Robert L. DeHaan, Experimental Embryology  
 James D. Ebert, Director  
 Irwin R. Konigsberg, Experimental Embryology  
 Elizabeth M. Ramsey, Placentology; Pathology  
 Mary E. Rawles, Experimental Embryology

Melvyn Lieberman, Fellow of the U. S. Public Health Service  
 C. B. Martin, Jr., Fellow of Carnegie Institution  
 Tokindo Okada, Fellow of Carnegie Institution  
 Oscar Ramirez-Toledano, Fellow of Carnegie Institution  
 Glenn C. Rosenquist, Fellow of the U. S. Public Health Service  
 Heinz Tiedemann, Fellow of Carnegie Institution  
 Carl Weber, Fellow of Carnegie Institution

*Assistant Investigators*

M. Edward Kaighn  
 Minocher C. Reporter

*Research Associates (Extramural)*

Louis B. Flexner, Philadelphia  
 Arthur T. Hertig, Boston  
 Chester H. Heuser, Augusta, Georgia  
 Samuel R. M. Reynolds, Chicago

*Fellows*

I. A. Ajdukovic, Predoctoral Fellow of Carnegie Institution  
 Felix Beck, Fulbright Visiting Scholar  
 Yoheved Berwald, Fellow of Carnegie Institution  
 Igor Dawid, Fellow of Carnegie Institution  
 Herman Denis, Fellow of Carnegie Institution  
 John B. Gurdon, Fellow of Carnegie Institution

*Students*

G. R. Djavadi, Undergraduate, Biology, Johns Hopkins University  
 R. L. Hallberg, Graduate, Biology, Johns Hopkins University  
 S. D. Hauschka, Graduate, Biology, Johns Hopkins University  
 C. B. Kimmel, Graduate, Biology, Johns Hopkins University  
 Sharon Nelson, Graduate, Art as Applied to Medicine, Johns Hopkins University School of Medicine  
 F. Shafa, Undergraduate, Biology, Johns Hopkins University

*Visiting Investigators*

Frank D. Allan, Washington, D.C.  
 J. George Coslet, Philadelphia  
 Louis E. DeLanney, Crawfordsville, Ind.  
 Martin W. Donner, Baltimore  
 Peter Eckstein, Birmingham, England



J. W. S. Harris, London, England  
 M. Kostowiecki, Philadelphia  
 A. C. Kulangara, Madras, India  
 R. E. Marshall, Bethesda, Md.  
 Harry S. McGaughey, Jr., Charlottesville,  
 Va.

Benjamin C. Moffett, Jr., Detroit  
 Catherine A. Neill, Baltimore  
 Ronan O'Rahilly, St. Louis  
 Dorcas H. Padget, Baltimore  
 John Papaconstantinou, Storrs, Conn.  
 Edward J. Quilligan, Cleveland  
 Edward C. Roosen-Runge, Seattle  
 E. C. Sensenig, Birmingham, Ala.  
 C. B. Severn, Ann Arbor, Mich.  
 W. L. Straus, Jr., Baltimore  
 Oleg E. Viazov, Moscow, U.S.S.R.  
 Bernice G. Wedum, Washington, D.C.  
 J. Zwaan, Amsterdam

#### *Clerical and Technical Staff*

James E. Abbott, Recorder  
 Mary N. Barton, Librarian (part time)  
 James Blackwell, Custodian  
 Paul Blackwell, Custodian  
 George Boettinger, Porter  
 Henry Burr, Technician  
 William I. Cleary, Recorder  
 Nina Douglas, Laboratory Helper  
 William H. Duncan, Senior Technician  
 Ernest W. Edwards, Custodian  
 Raymond Fado, Assistant Recorder  
 Wilbur F. Garde, Assistant Recorder  
 Norman R. Gortt, Assistant Recorder  
 Richard D. Grill, Photographer

Charles E. Hargett, Assistant to the  
 Director

Ernest Harper, Chief Custodian  
 Shirley Hicks, Laboratory Helper (part  
 time)

Virginia Hicks, Laboratory Helper

Jeannie Hubbard, Technician

Eddie Jordan, Laboratory Helper

Elaine C. Kerby, Stenographer

Leo Kormann, Technician

Francis J. Kupres, Technician

Elizabeth Legum, Technician

Edna G. Lichtenstein, Secretary

Elizabeth Littna, Technician

Arlyne Musselman, Technician

John Pazdernik, Building Engineer

Margaret J. Proctor, Secretary

Arthur G. Rever, Fiscal Officer

Bessie Smith, Laboratory Helper

Pauline M. Stott, Technician

Isabel P. Williams, Technician

John L. Wiser, Machinist

Ann Wisotzki, Technician<sup>1</sup>

#### *Student Assistants*

John Chase, Drew University

Kurt Johnson, Johns Hopkins University

John A. Kloetzel, Johns Hopkins University

Frederick Rosen, Sandy Spring Friends  
 School

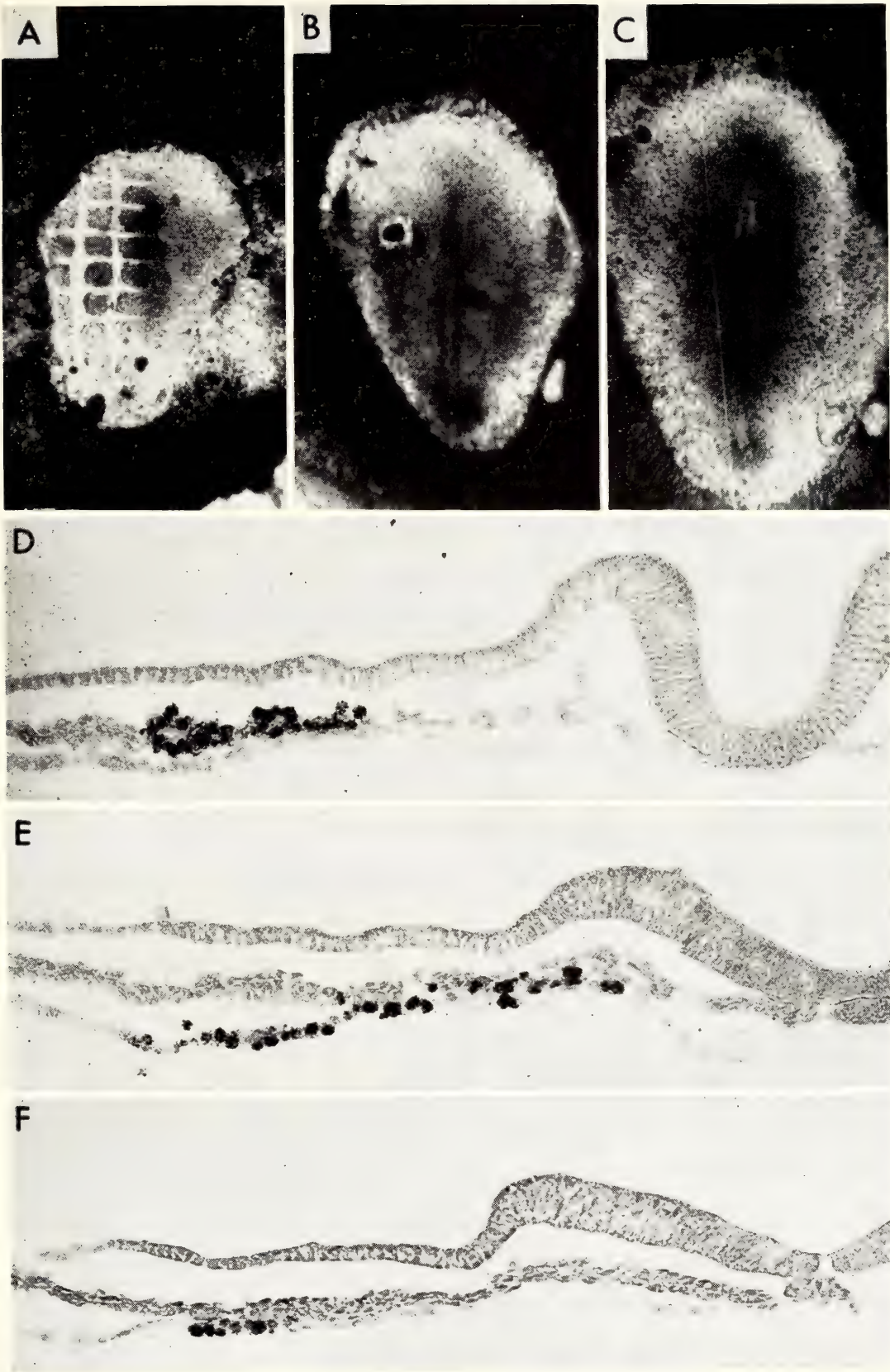
Robert Sachs, Johns Hopkins University

Winslow Schrank, Haverford College

Merry Youle, Brown University

<sup>1</sup> Resigned September 15, 1964.

Plate 1. (A-C) Explanted chick blastoderms. (A) Donor embryo (stage 5) in which endoderm-mesoderm of left half is divided into 25 squares. (B) Recipient embryo, also at stage 5. Square 7 has been removed from the donor and put into the homologous site in the recipient. (C) Same recipient embryo 1½ hours later (stage 6). The edges of the graft have expanded to meet the endoderm-mesoderm of the recipient. Graft site no longer visible. (D-F) Photomicrographs of sections through 3 levels of chick embryo fixed at stage 7. Labeled endoderm-mesoderm graft was inserted 5 hours previously (stage 5). Independent movements of endoderm-mesoderm portions of the square illustrated in (D). A 10μ section just below anterior intestinal portal. Labeled mesoderm only in cells with concentration of silver granules over nuclei. (E) Level in which mesoderm and endoderm appear together, and (F) more caudal level in which labeled endoderm alone is seen.





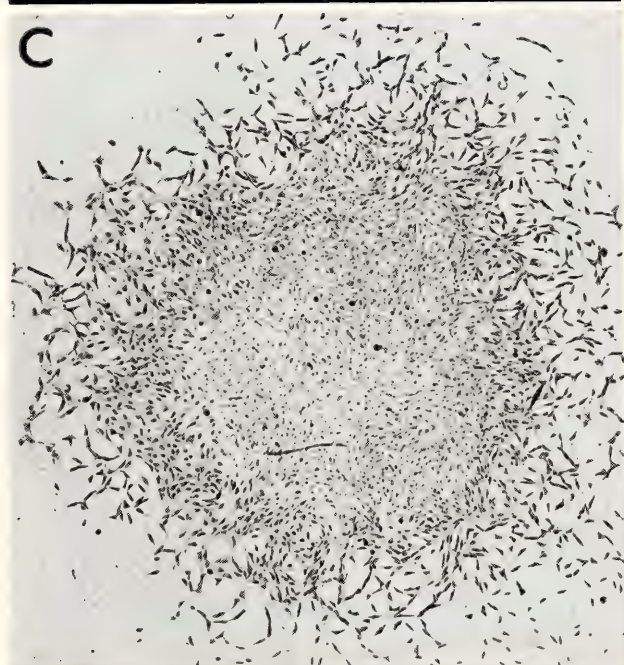
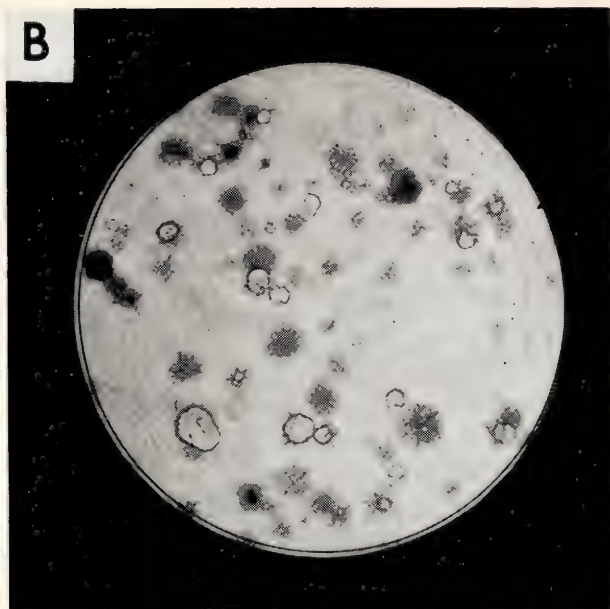
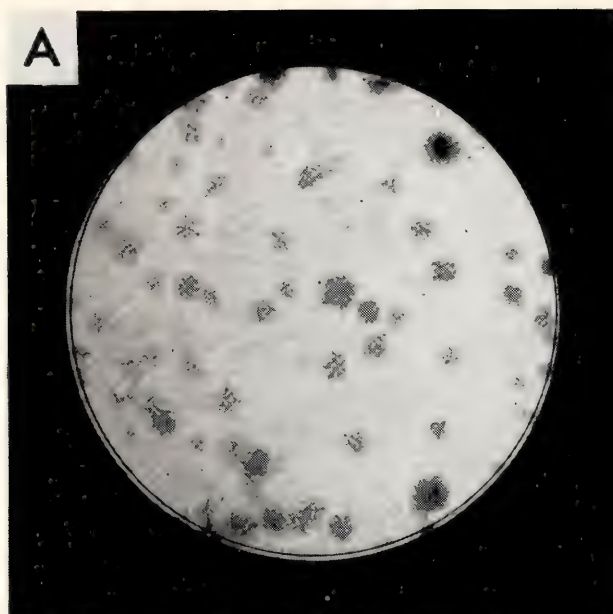


Plate 2. Clonal cultures of secondary cells derived from 12-day chick leg muscle. Inocula consisted of 300 cells per plate fixed and stained on 8th day of incubation. (A) Control plate. (B) Infected with RSV on third day of culture. Transformed muscle and fibroblast colonies are present. (C) Normal fibroblast colony. (D) Normal muscle colony. (E) Virus-transformed fibroblast colony. (F) Virus-transformed muscle colony.



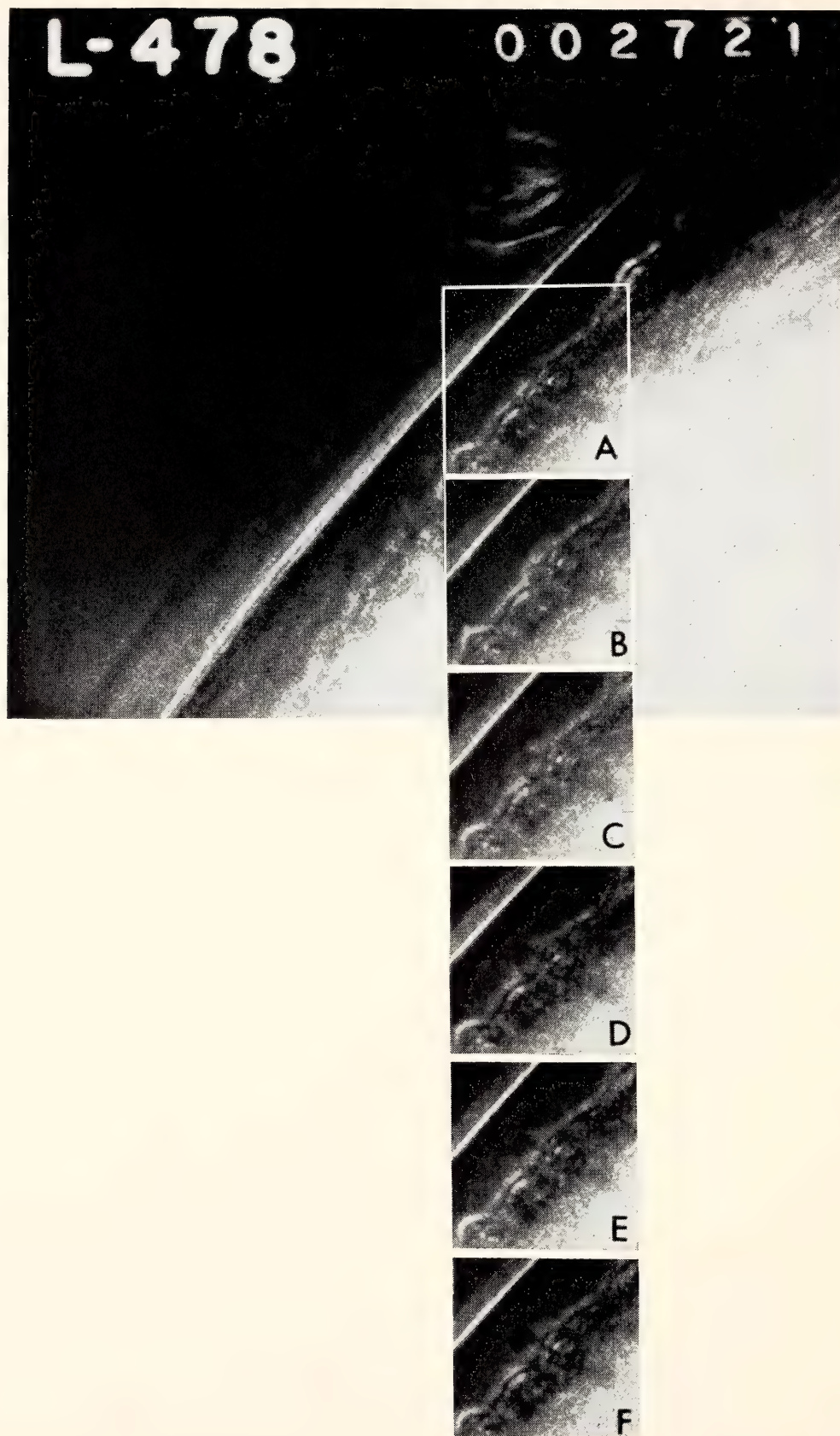


Plate 3. Complete frame of a 16-mm time-lapse movie. From top down the (broken) tip of a pipet from which alkaline solution is streaming, a diagonal bright line of lemmas or egg envelopes, and (from corner to corner of the square) the periphery of the rabbit blastocyst. (B) Region enclosed by the square in (A) shown 2 seconds later with a bulge at center from the beginning extrusion of a knob's contents. (C) At 4 seconds after (A); most of the knob contents have been extruded. (D-F) At 6, 8, and 10 seconds after (A) there is a little outward movement of the knob contents, but extrusion is essentially complete.

# *Genetics Research Unit*

Alfred D. Hershey  
*Director*

*Cold Spring Harbor, New York*



# Contents

Introduction . . . . .	519
Structure and Function of Phage DNAs . . . . .	519
Lambda DNA . . . . .	520
Weak spots in T5 DNA . . . . .	520
T4 phage particles with incomplete genomes . . . . .	521
Genetic recombination with exceptional particles of phage T4 . . . . .	523
Genetic linkage in T4 DNA molecules . . . . .	524
Replicating DNA . . . . .	524
Genetic transcription in bacteria infected with phage lambda . . . . .	526
Components of Action of the Regulators <i>Spm</i> and <i>Ac</i> . . . . .	527
The component of <i>Spm</i> responsible for preset patterns of gene expression . . . . .	530
Transmission of the preset pattern . . . . .	531
Components of action of <i>Ac</i> . . . . .	532
Bibliography . . . . .	534
Personnel . . . . .	535

## INTRODUCTION

Work in the laboratory at Cold Spring Harbor can be described at various levels. First, it demonstrates a philosophy: not, to be sure, a moral principle consciously chosen, but a pattern that an observer might discern in our activities. We have the freedom and the obligation to look at natural things. We look at them with vision that is both sharpened and restricted by the tools at our disposal and the direction our curiosity has taken. What we first see is an element of novelty, without which nature and art cannot charm. Perceiving that element, we have already in a measure succeeded. But we should like to prolong our surprise, to savor it fully, to communicate it. So we formulate a question, and find ourselves trying to solve a problem. It is always the same sort of question: Why is this object constructed as it is? And always the same kind of problem: How can our question be framed and answered in conveyable terms? In its particular example, the problem may be solved or not, with varying degrees of success or failure. In any event, excepting the worst failures, we have prolonged and illuminated our surprise and can hope to share our experience with others.

Research, including ours, exemplifies other philosophies as well. For instance, it can start with a problem that appeals to us mainly because we have an idea how to

solve it, or mainly because a solution is urgently needed. Our research, if different from anybody's, differs in exhibiting as a major ingredient the philosophy first stated.

To place the element of novelty at the center of endeavor may strike some readers as frivolous. Though at a tangent to the purpose of these paragraphs, I would go further. I would argue that the sophistication and costliness of contemporary research are necessary because the threshold of human surprise is rising. We don't exhaust our natural surroundings; we exhaust our ability to respond to them. This may be the secret and real price of the scientific vitality of our time. Except for the element of novelty, ritual could take the place of research.

At a second level of description, work in our laboratory can be identified by subject matter. The writer and his colleagues are studying the structure and function of the nucleic acids of phage particles. Barbara McClintock is exploring mechanisms of control of gene action in maize. These two areas of research have some aims in common, notably to understand cooperation among biological elements, but they differ greatly in materials and methods.

At a third level of description, we present in the following pages edited versions of nine laboratory notebooks.

## STRUCTURE AND FUNCTION OF PHAGE DNAs

*A. D. Hershey*

The DNAs isolated from phage particles of different species, though possessing a basic structure in common, show a surprising number of individual differences. A few years ago my colleagues and I began studying some of them, pursuing the thought that elucidation of the differences in structure should contribute

to an understanding of the common features.

Different phage DNAs must also perform common as well as individually distinct functions and, indeed, the structural features are mainly interesting as clues to function. DNA molecules in phage particles are inert products of



replication, and can furnish only indirect clues. For this reason several people in our laboratory and elsewhere have inquired into the structure of phage DNAs in the replicating state by extracting them from infected bacteria. Here too it appears that the different phages show both common features and individual differences, though further work will be needed before these can be understood or even adequately described.

A rather different approach to DNA function has been initiated by Anna Marie Skalka, who is taking advantage of the internal differentiation in lambda DNA to look for signs of order in the functioning of genes. She finds that after infection of bacteria with phage lambda, transcription of genetic information begins somewhere in the right half of the DNA molecule, and only later on extends to both halves.

The group studying DNA molecules this year includes Ruth Ehring and Edward Goldberg (Carnegie Institution Fellows), Mervyn G. Smith (Damon Runyon Fellow), Anna Marie Skalka (American Cancer Society Fellow), Elizabeth Burgi, Laura Ingraham, Gisela Mosig, and A. D. Hershey. The work is partly supported by grant HD 01228 from the National Institute of Child Health and Human Development, U.S. Public Health Service.

### *Lambda DNA*

*Burgi and Hershey*

Burgi is continuing her analysis of the structure of the ends of lambda DNA molecules, and has arrived at a specific but still hypothetical model that should be testable in due course.

One of the requirements in this and other work is a practical method for the separation of right and left halves of lambda DNA molecules. In collaboration with C. I. Davern, we found that equilibrium density-gradient centrifugation in an angle rotor is a serviceable method. It is based on the principle that bands

formed at an oblique angle to the tube axis in the spinning rotor spread apart when the rotor is stopped and the tube is brought to a vertical position. Although there is no theoretical gain in resolution under these circumstances, resolution is in fact improved because the expanded bands are less subject to mechanical mixing when the fractions are collected. Details of the method have been published by Hershey *et al.* in *Biochemical and Biophysical Research Communications*.

Another promising method, which is likely to facilitate our work, has been introduced by Nandi, Wang, and Davidson. In this method the density difference between molecular halves is increased by addition of mercury ions, which combine preferentially with parts of the molecule rich in adenine and thymine.

### *Weak Spots in T5 DNA*

*Ingraham and Hershey*

When a solution of T5 DNA is stirred to generate the minimum rate of shear that will break the molecules, fragments 0.4 and 0.6 of the original molecular length are produced. These can be separated by chromatographic or centrifugal fractionation. When the fragments of 0.6-unit length are broken in turn, fragments 0.4 and 0.2 unit long appear. This behavior must be contrasted with that of some other phage DNAs, which do not show preferred breakage points but pull apart near their centers for purely mechanical reasons.

The breakage pattern of T5 DNA can be explained by several models, at least three of which are potentially distinguishable.

1. Two weak spots may lie at positions 0.4 and 0.6 of the molecular length from either end. According to this model, the 0.4-unit fragments resulting from the first and second breaks would be identical mixtures of pieces from both ends of the molecule.

2. Two weak spots may lie at positions



0.4 and 0.8 of the molecular length from a specified end. In this model, the 0.4-unit fragments resulting from the first and second breaks would represent different and nonoverlapping segments of the molecule.

3. The molecule may contain four weak spots dividing it into five segments of equal length. In this model, the 0.4-unit fragments resulting from the first break would be an equal mixture of the two ends, and those resulting from the second break would consist partly of ends and partly of subterminal sections. Thus the second breakage product would contain parts absent from the first, but not vice versa.

We explored these possibilities by application of the DNA homology test of Bolton and McCarthy. The experiments showed that the 0.4-unit fragments resulting from the first and second breaks each contain sequences absent from or less frequent in the other, but also contain many common sequences. These results exclude models 1 and 2 but not 3, and suggest additional possibilities.

Besides model 3, two principal alternatives remain. The structure may resemble that of model 1 if the two weak spots are of unequal strength or are situated at slightly unequal distances from the molecular center. Or model 2 may be correct if different parts of the molecule contain both unique and common base sequences. The interesting possibility that different molecular parts contain similar sequences has already arisen in our work with lambda DNA and will have to be pursued with that DNA, whose parts can be isolated without ambiguity.

The structure of the weak spots is unknown. One obvious possibility is that they are points at which one of the two polynucleotide chains of the molecule is already broken. The hypothesis is plausible inasmuch as several people have found evidence of single-strand breaks in T5 DNA but not in some other phage DNAs. Such breaks are detected by

measuring molecular weights in terms of sedimentation rates of the DNA in single-stranded form. In our experience the results do not support the hypothesis, because the sedimentation rates do not indicate sufficient uniformity of size of the polynucleotide chains to explain the rather precise locations of the weak spots. Both the method and its application to T5 DNA require further study.

The foregoing description refers to the DNA of a heat-stable mutant of T5. Irwin Rubenstein at Yale University has found that DNA of the wild-type phage differs from that of the mutant both in length and in location of weak spots. His results make the structure of T5 DNA more interesting but even more puzzling than it was before.

*T4 Phage Particles  
With Incomplete Genomes  
Mosig*

Exceptional particles of phage T4 can be isolated that prove to contain a single DNA fragment two thirds of the standard length (*Year Book 63*, pp. 588–589). The particles are individually noninfective, but have the interesting property that two or more of them can cooperate, in a single bacterium, to regenerate complete chromosomes. Apparently the particles have incomplete genomes, and the missing parts are different in different particles, so that one particle can supply what is absent in another. That idea underlies the following experiments.

When a single bacterium is simultaneously infected with a normal phage particle and with a defective particle that is genetically marked, the marker from the defective particle may appear in the phage progeny. In this type of experiment different markers are “rescued” from the defective particles with identical frequencies, independently of their map position. The actual frequency of rescue of a single marker is about two thirds, as expected from the length of DNA in the particles. These



results show that the rescue is highly efficient, that the DNA molecule and the genome are colinear, and that the two-thirds length is cut at random from an effectively circular genome. The results are consistent with other evidence that the genetic map of phage T4 is circular, and that the DNA molecules are "circularly permuted."

If, in the experiments just described, the defective phage particles are doubly marked, both markers can be rescued from the same defective particle even when they are widely separated in the genetic map. The frequency of joint rescue depends on the marker pair, providing a test of linkage. The linkage measures obtained in this way agree roughly but not precisely with distances on the genetic map. The discrepancies are unexplained but the following considerations apply. The rescue of a single marker from a DNA fragment appears to depend only on the presence or absence of the marker in the fragment. If so, the frequency of joint rescue of two markers from a continuous fragment of fixed length is a direct measure of the physical distance between them. The genetic map, on the other hand, is based on recombination frequencies that may be influenced by factors other than distances between markers.

In another type of experiment, bacteria are infected with defective phage particles only, to measure the efficiency of cooperation among them. This kind of cooperation may be called mutual complementation, to distinguish it from marker rescue by viable phage particles. If a bacterium is infected with one defective particle, phage growth fails, by hypothesis because phage genes are missing. If it is infected with two or more defective particles, phage growth may succeed or fail, by hypothesis depending on whether or not at least one copy of each gene is supplied by one or another of the particles. Theoretically, two phage particles, each containing a random segment representing two thirds of a circular

genome, furnish a complete set of genes with a probability of one third. For three particles, the probability is two thirds. These probabilities define a theoretical upper limit to the efficiency with which defective phage particles of the specified number and kind can complement one another to produce phage progeny. In strain B of *Escherichia coli* the measured efficiency is equal within limits of error to the theoretical maximum. This result shows that cooperation among two or three chromosome fragments is highly efficient, that the DNA molecule and the genome are colinear, and that the two-thirds length is cut at random from an effectively circular genome, confirming and extending the conclusions from marker rescue experiments.

In several other bacterial strains, the efficiency of mutual complementation is lower; in some, practically zero. The efficiency measured by this test in different bacterial strains is correlated with the efficiency with which two or more phage particles damaged by ultraviolet light can cooperate to produce phage progeny. Neither efficiency is correlated with the sensitivity of the bacteria themselves to ultraviolet light, or with other known properties of the strains. The frequency of marker rescue also depends, though less strongly, on the bacterial strain. Linkage measured from the frequency of joint rescue of two markers does not.

The bacterial properties affecting cooperation among phage particles are unknown, but suggest a possible means of analyzing the mechanism of cooperation. *Marker rescue* (cooperation between intact and defective chromosomes to produce chromosomes of double parentage) and *mutual complementation* (cooperation between two defective chromosomes to produce intact biparental chromosomes) both call for DNA replication and genetic recombination. In mutual complementation, but not in marker rescue, recombination must precede replication, unless chromosome



fragments themselves can replicate. The results show that both rescue and complementation occur with perfect or nearly perfect efficiency in some bacterial strains but not in others. The bacterial defect therefore interferes with some event common to the two phenomena, an event that is especially critical in mutual complementation. The event recognized in this way may be an early genetic recombination, prerequisite for replication of fragmented chromosomes. Comparative experiments with different bacterial strains may serve, with Mosig's material, to determine whether or not chromosome fragments can replicate, and otherwise to analyze the functional competence of the fragments.

The same bacterial defects that interfere with mutual complementation among chromosome fragments also interfere with cooperation among radiation-damaged chromosomes, and the same considerations apply to both phenomena. Radiation damage is more complicated than a missing chromosome segment, because the number and kinds of radiation damages cannot be adequately specified, and because radiation damages are subject to repair as well as complementation. Incidentally, mutual complementation among chromosome fragments confirms the principle by which Luria proposed, in 1947, to explain cooperation among radiation-damaged phage particles: that a complete set of intact genes in two or more phage particles suffices to initiate phage growth. The quantitative failure of his theory for irradiated phage particles should probably be attributed to the complications mentioned.

Another phenomenon from the classical radiobiology of phage should be recalled in this connection. Krieg found that the radiosensitivity of the function of a specific gene, measured from the frequency with which that gene in an irradiated phage particle can complement its mutant allele present in an unirradiated phage particle, is improbably high in view of the small target size of the

gene. No doubt the explanation must be sought in the complicated nature of radiation damages. The present experiments show that one must also take into account the efficiency with which two defective chromosomes can cooperate, which depends on properties of the bacterium as well as on the nature of the defects.

During the summer of 1964 Frances Womack of Vanderbilt University joined our group with the intention of studying crosses between defective phage particles carrying multiple genetic markers. The experiments failed because the numerous amber mutations in the phages interfered with mutual reactivation, presumably because the mutant genes function too poorly in the permissive bacterial host. A second try will be made if the difficulty can be circumvented.

The work with phage T4 was critically aided by A. H. Doermann, Robert Edgar, Ruth Hill, Frances Womack, and Michael Yarus, who provided phage and bacterial strains and information about them.

*Genetic Recombination With  
Exceptional Particles of Phage T4*

*Ehring*

Mosig's present work began with her observation that genetic recombination frequencies in phage T4 were correlated with the buoyant densities of the phage particles entering into the crosses. In particular, particles of low density showed high recombination frequencies. The particles of low density were subsequently resolved into two classes (*Year Book* 63, pp. 587, 588): viable particles with slightly curtailed DNA molecules (class 3) and inviable particles with DNA molecules only two thirds the normal length (class 5). Particles of class 5 yield many recombinants for understandable reasons: the phage progeny are necessarily multiparental in origin. Ehring has now made crosses with purified particles of class 3. Yields of recombinants do not differ from those in comparable crosses with particles



of average DNA content. Therefore recombination frequencies in crosses with phage particles of the majority class do not depend on the lengths of chromosomal redundancies, or at any rate this test failed to reveal such dependence.

### *Genetic Linkage in T4 DNA Molecules*

*Goldberg*

Modified bacteria (spheroplasts) can be infected with modified T4 phage particles (particles treated with urea to alter the specificity of attachment). If T4 DNA is present at the time of infection, a few per million of the phage progeny will show genetic markers derived from the DNA. The complicated system (first developed by van de Pol, Veldhuisen, and Cohen) is probably needed to get DNA into the cells, or to get it in without excessive enzymic degradation. The efficiency is inconveniently low with present techniques, but that does not seriously interfere with the experiments. The unusual feature of the system is that fragmented and denatured DNA can still contribute genetic markers. Since DNA fragments are not infective by themselves, even in principle, the genetic contribution by the DNA may be thought of as a rescue of markers by incorporation of specific nucleotide sequences into multiplying chromosomes.

If the DNA is doubly marked, the frequency of joint rescue of both markers provides a measure of genetic linkage. The actual measurement takes the form of a ratio between the number of phage particles showing both markers and the total number showing a specified one of them. This measure is influenced both by the initial rescue and by subsequent genetic recombinations, and is therefore inferior in principle to Mosig's test, which apparently depends only on the presence or absence of markers in the DNA fragments. The advantage of the system introduced by the Dutch workers is that the DNA fragments can be experimentally modified.

Figure 1 shows the effect of varying the size of the fragments on the frequency of marker rescue. It will be seen that rescue of a single marker is little affected by limited enzymic hydrolysis of the DNA. The frequency of joint rescue of two markers, however, decreases progressively with the amount of enzymic degradation. Since, after enzymic treatment, the DNA is denatured, the chief variable is the length of the single polynucleotide chains entering the bacterial cells. This method too, then, must measure the physical distance between markers.

The actual sizes of the fragments are not known and, indeed, precise methods of physical measurement are only now being worked out. The genetic data suggest that fragments of the order of size of single genes can be rescued. It should be possible now to construct a detailed physical map of the chromosome.

### *Replicating DNA*

*Smith*

Frankel began several years ago to study DNA isolated from bacteria infected with phage T2 (*Year Book 61*, p. 448). He found a component of very high molecular weight but his work was hampered for a long time by the difficulty of extracting DNA from the cells without degradation.

Smith, in Burton's laboratory at Oxford, explained part of the difficulty in work with bacteria infected with phage T5. He found that bacteria treated with detergent and phenol in the usual way yielded two fractions of DNA, one going into solution in the aqueous phase, the other remaining in insoluble form at the interface between phenol and water. Appropriate isotopic labeling showed that the insoluble DNA was precursor to the soluble, and that the soluble fraction contained DNA derived from finished or nearly finished phage particles. The insoluble fraction thus became the center of interest. It turned out that the insoluble DNA was still trapped inside

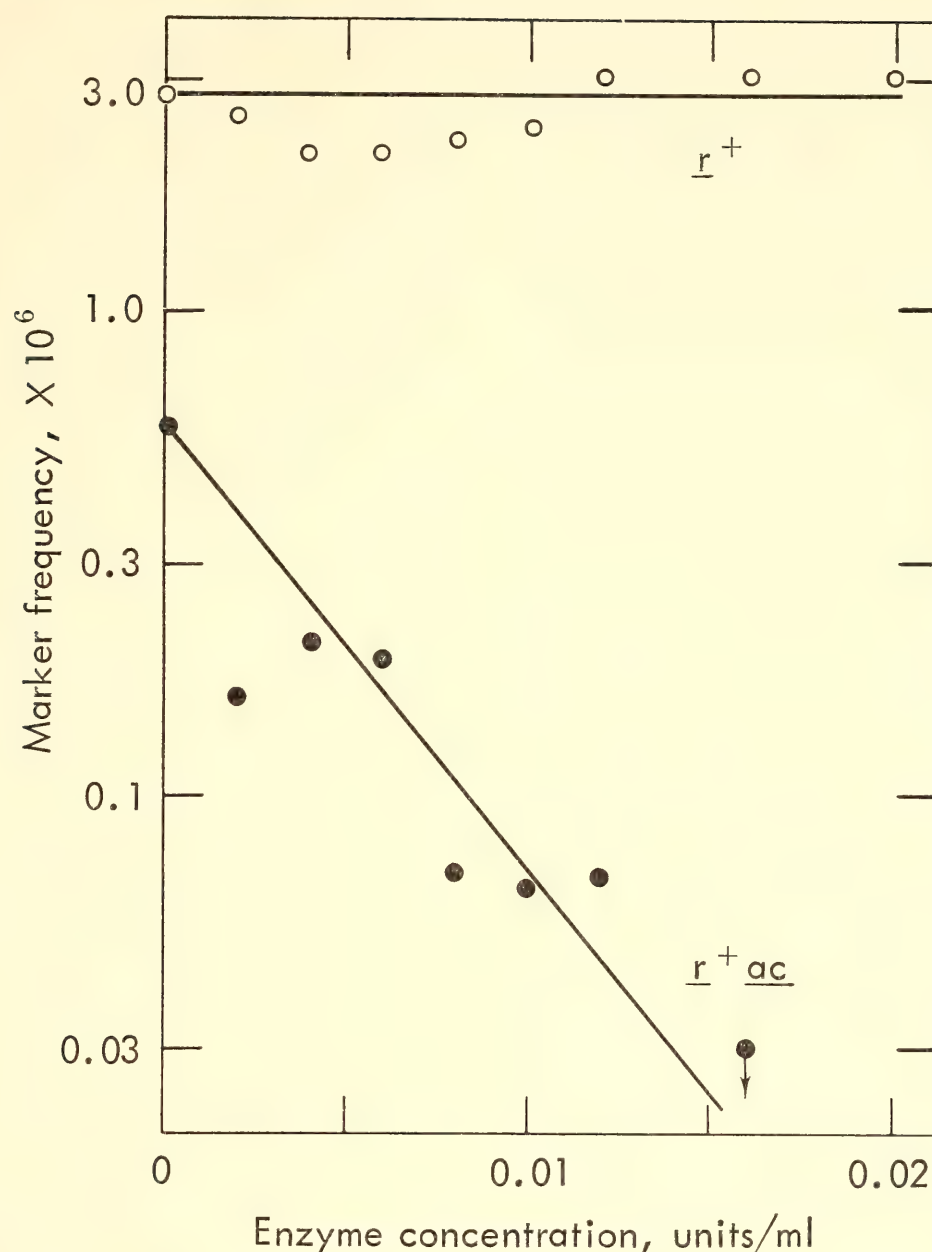


Fig. 1. Frequency of marker rescue from polynucleotides of varying length. Digestion mixtures contained 1  $\mu$ g T4 DNA, carrying the marker pair  $r\gamma 3^+ ac41$ , and the indicated amount of pancreatic deoxyribonuclease (Worthington Biochemical Corp.) expressed in units measured by the manufacturer. The enzyme was allowed to act for 5 minutes at room temperature before the mixtures were boiled. Open circles indicate recovery of  $r^+$  phage, irrespective of the  $ac$  allele; filled circles, recovery of  $r^+ ac$  phage; both expressed as fractions of the total yield of phage in the test system.

partly dissolved bacteria, from which it could be released, somewhat erratically, by treatment of the cells with lysozyme, an enzyme that hydrolyzes mucopolysaccharides in the bacterial cell wall.

Since joining our group, Smith has studied the properties of the phage-precursor DNA. Its density is the same as that of DNA extracted from phage T5, which shows that it has the expected base

composition and is not attached to appreciable amounts of non-DNA material. It sediments as a single, very broad band, most of which moves faster than DNA extracted from phage particles. The fast-sedimenting DNA is sufficiently fragile under shear to suggest a long, threadlike structure. An examination in the electron microscope by MacHattie at The Johns Hopkins University showed,



in fact, long threadlike structures without noticeable branching. Fragmentation of the DNA has not yet revealed any preferred subunit length. On denaturation in alkali the DNA sediments more or less like denatured DNA from phage particles, at a rate suggesting that both are composed of relatively short polynucleotide chains.

Frankel (now at the University of Pennsylvania), Smith, Skalka, Mosig, and others are extending work along these lines with several phages. It appears that the formation of very long structures is a common feature of the replication of phage DNAs. The results depend somewhat on the time during the growth cycle at which the DNA is labeled, on the time at which it is extracted, and on the phage species. Under certain circumstances a putative ring form of lambda DNA can be seen, as first found by Young and Sinsheimer. Detailed kinetic studies with several phage species may reveal an intelligible sequence of events.

*Genetic Transcription in Bacteria  
Infected With Phage Lambda*

*Skalka*

It is known from the classical observations of genetics that not all genes function at the same time. According to the operator theory of regulation of gene action, control is exerted at the primary step by which information coded in DNA is transcribed into complementary base sequences in messenger RNA. At any rate it has been shown recently that the specific messenger accumulates only when a given protein is being synthesized.

Transcription of specific genes can be studied only in a few favorable instances. In phage lambda, gross differences in base composition of the two halves of the DNA molecule (*Year Book 63*, pp. 581-583), permit analysis along somewhat different lines. One can ask, for instance: Where in the molecule does transcription start?

An appropriate experiment is performed as follows. Bacteria are infected

with phage lambda. At any desired time thereafter, radiophosphate is fed to the culture for a period of two minutes, the culture is promptly chilled to stop synthetic activities, and RNA is extracted from the cells. The significant experimental variable is the time after infection at which the examination is made.

The labeled RNA extracted from the cells consists of several types, among which only that matching lambda DNA in base sequence is of interest in the present context. It is isolated, and its amount judged, by annealing to lambda DNA according to the technique of Bolton and McCarthy.

The labeled RNA isolated by annealing to lambda DNA is analyzed in the following ways. Its base composition is determined by alkaline hydrolysis and electrophoretic separation of the resulting nucleotides. Its purity is verified by annealing to lambda DNA a second time. This time the annealing is 60 to 80 per cent efficient (close to the maximum attainable by the method), and the base composition is not altered by the second annealing. Finally, the RNA is tested for its ability to anneal to the separated right or left halves of lambda DNA.

The yield and composition of lambda-specific RNA at different times after infection are illustrated in Table 1, which shows that lambda messenger RNA comprises only about 5 per cent of the total RNA labeled at early times after infection, but amounts to 30 per cent of the RNA labeled at 30 minutes. The same trend has been reported by Sly and Adler. The guanine-plus-cytosine content of the

TABLE 1. Lambda-Specific RNA  
From Infected Bacteria

Interval of Synthesis, minutes	Yield, % of total	Guanine + Cytosine, mole %	Purines, mole %
5-7	6	45.4	52.6
15-17	5	48.5	54.6
30-32	32	53.9	52.6



RNA, not previously measured, is low at early times and high at late times. This trend is reproducible, as are the individual analyses, but the absolute values vary somewhat in different experiments. Finally, the purine content of the labeled RNA is high at all times (in double-stranded DNA it is necessarily 50 per cent), probably because only the pyrimidine-rich strand of the DNA is read, as has been shown directly for phages SP8 and alpha.

One interesting feature of these data is the difference in guanine-plus-cytosine content of the RNA labeled at different times. In principle it could arise from trivial changes in RNA precursor pools in the cells, but that is unlikely because precursor nucleotides have their phosphorus at the 5' end whereas the nucleotides analyzed have their phosphorus at the 3' end, a shuffling that should tend to cancel out a bias of the sort mentioned. Otherwise the data show that different parts of the DNA are transcribed at different times, and suggest that transcription starts in the right half of the molecule, which is low in guanine plus cytosine.

That transcription does start mainly in the right half of the DNA molecule is confirmed by annealing tests. Messenger RNA synthesized at early times anneals almost exclusively to right halves of lambda DNA, whereas messenger synthesized between 30 and 32 minutes after infection anneals with equal efficiency to both halves.

These results can, of course, be interpreted in any of the ways previously considered in connection with problems of gene regulation. The unique feature is

that lambda DNA represents a "hybrid" chromosome consisting of two parts differing from each other in base composition just as much as chromosomes of different species usually differ. In general, perhaps, one must postulate mechanisms of control operating at some step in the functioning of individual genes or small groups of related genes. Instead of or in addition to this, there may be in lambda a broader category of control regulating simultaneously all or most genes lying in the same half of the DNA molecule. At any rate, if the composition of DNA reflects the composition of genes, different genes in lambda must use somewhat different coding vocabularies, and perhaps different punctuation marks, depending on their positions in the molecule. These differences may or may not be pertinent to mechanisms controlling transcription. Seemingly we have the opportunity, if we can muster the skill, to explore such possibilities.

A second interesting feature of the data in Table 1 is the increased rate of transcription from both halves of the molecule seen at late times. The rate change implies a second mechanism of control that is neither gene specific nor dependent on base composition. It could reflect simply the increased amount of DNA in the cells at late times, but other explanations are equally plausible.

Nada Ledinko, now at the Salk Institute, started the work described above in our laboratory. We were also assisted by generous advice from Sly and Adler, who independently began work along related lines at the University of Wisconsin.

## COMPONENTS OF ACTION OF THE REGULATORS *Spm* AND *Ac*

*Barbara McClintock*

Gene control systems other than those associated with the regulators *Spm* (Suppressor-mutator), *Ac* (Activator), and *Dt* (Dotted) are known to be present

in maize. Just as proved true of the *Ac* and *Spm* systems, aspects of which still need to be elucidated, many types of test extending over a number of years will be



required to identify these additional systems, their components, and their modes of operation. Because time will not be available for such extended studies, it was decided to concentrate attention during the past year on some of the unresolved aspects of the *Ac* and *Spm* systems.

The Suppressor-mutator control system is so called because its regulator element, also designated *Spm*, has two components of action. The suppressor (or inhibitor) component, component-1, directly regulates the expression of a gene that has come under the control of the *Spm* system. Such control, it will be remembered, arises through insertion of the operator element of the system at the locus of a gene. When component-1 of *Spm* is in an active phase, the expression of the gene is suppressed; when it is inactive, gene action is expressed. One exception to this general rule concerns the modified gene locus  $a_1^{m-2}$ . This gene is active when component-1 is active, and suppressed when it is inactive. Component-2 of *Spm* is the mutator or transposition-inducing component. The response of the operator element to component-2 often gives rise to a mutant expression of the gene that releases it from control by the *Spm* system. Some responses, on the other hand, effect other modifications that are not associated with release but instead alter the subsequent types of response of the operator element to the components of *Spm*. These modifications have been called "changes in state" of the gene locus. With some altered states, the operator element loses its capacity to respond to component-2, although it retains its ability to respond to component-1. No further mutations occur, nor is the gene released from control by the system. Its action remains permanently under the control of component-1 of the *Spm* regulator element.

Both components of *Spm* may undergo change. Component-1 exhibits alternating cycles of activity and inactivity,

whose regulation has been outlined in previous reports. Changes of component-2 resemble mutations in that they arise from single events, each of which alters the effectiveness of this component, both for inducing responses of the operator element that lead to changes in gene expression, and for inducing transpositions of *Spm*. Such alterations in action of component-2 have been detected only in those cells of the plant in which component-1 is active. Some alterations eliminate all activity of component-2 whereas others effect altered times and frequencies of occurrence of mutation-inducing responses of the operator element. Each mutant of component-2 may undergo still further mutation, the frequency of occurrence differing with different mutants.

The components of *Spm* and their characteristic modes of action were detected originally in observations of the activity of one gene that is under the control of the *Spm* system. Although it is possible to distinguish a change in action of either component through such observations, distinctions are greatly facilitated when two or more genes, each under the control of the system, are present in a plant or kernel. The operator elements at the different gene loci respond in like manner to modifications affecting either of the components. Through such combinations it has been possible to determine with a considerable degree of accuracy the types of modification undergone by each of the components of *Spm*.

Although direct evidence is lacking, the mechanism that releases a gene from the control of the *Spm* system is believed to be transposition of the operator element away from the gene locus. This assumption is based on studies of the *Ac* system, which have provided direct evidence of release of a gene from its control through transposition of the operator element away from the gene locus. Transpositions of the regulator element *Spm*, on the other hand, may be readily detected, and indirect evidence



had suggested that component-2 regulates them. Tests designed to obtain direct evidence were completed during the year, and are described below.

The original state of  $a_1^{m-2}$  has at the  $a_1^{m-2}$  locus an *Spm* element with a highly active component-2. This *Spm* is designated *Spm<sup>s</sup>*. It induces many germinal mutations at the  $a_1^{m-2}$  locus, and the events responsible for them are usually associated with transposition of the *Spm* away from the gene locus. Often the event is accompanied by release of the gene from control by the *Spm* system. The germinal mutants that have been released from *Spm* control may be placed in two categories: those that resemble the wild-type gene in their action, and those that give rise to the diffuse-mottled phenotype, described in *Year Book 61* (pp. 448-460). In plants carrying the original state of  $a_1^{m-2}$ , component-2 of *Spm* may undergo a mutation that alters its capacity to induce mutations at  $a_1^{m-2}$  and to induce similar responses of the operator element at other gene loci. One of these mutations alters component-2 in such a manner that it induces change in gene action only very late in the development of a tissue, and in only a few cells. This mutant is designated *Spm<sup>w</sup>*. In plants carrying *Spm<sup>w</sup>* at the  $a_1^{m-2}$  locus, no germinal mutants are produced. Also, this *Spm* is not removed from the  $a_1^{m-2}$  locus in those cells of the plant that contribute to formation of the gametes. If component-2 back-mutates to a high level of activity, germinal mutants appear and *Spm* in many instances is transposed away from the gene locus. One *Spm<sup>w</sup>* isolate, however, proved to be very stable; back-mutation of component-2 was rare. This isolate was selected for the tests to be described.

It was suspected that this *Spm<sup>w</sup>* would undergo early transpositions if an *Spm* with a highly active component-2 was also present in the nucleus. To obtain direct evidence and to determine whether or not the components of *Spm<sup>w</sup>* would be maintained unaltered after such a trans-

position, testcrosses were conducted with plants that commenced development with the selected *Spm<sup>w</sup>* at the locus of  $a_1^{m-2}$  in chromosome 3 and an *Spm<sup>s</sup>* located close to the *pr* marker in chromosome 5. The constitution of the plants was *Spm<sup>w</sup>*  $a_1^{m-2}$  *Sh*<sub>2</sub>/ $a_1$  *sh*<sub>2</sub>; *Pr/pr* *Spm<sup>s</sup>*; *wx/wx*. The presence of *Spm<sup>s</sup>* induced some germinal mutations at the  $a_1^{m-2}$  locus, most of them giving rise to the diffuse-mottled phenotype in the kernel. Kernels with this phenotype were detected on ears produced on the plants by a cross with plants that were homozygous for  $a_1$ , *sh*<sub>2</sub>, and *pr* and had no active *Spm*. (In general the kernels on these ears were similar to those illustrated in *Year Book 63*, plate 1B, following page 601.)

Plants were grown from 30 of the kernels exhibiting a diffuse-mottled phenotype; 27 of the selected kernels had purple pigment and thus had received the *Pr* marker from the heterozygous parent, and three were red, having received the *pr* marker from this parent. Five of the plants derived from the *Pr* kernels contained *Spm<sup>w</sup>* but no *Spm<sup>s</sup>*, as shown by the response given to *Spm<sup>w</sup>* by the gene *wx<sup>m-8</sup>*, which had been introduced by the pollen parent in some of the crosses. All 30 plants were tested for the presence of *Spm*, its type, and its location with reference to the genetic markers carried in the plants.

In all, 78 fertile ears were produced by the 30 plants. The pollen parents in the crosses were of several types: homozygous for  $a_1^{m-1}$ , *sh*<sub>2</sub>, *pr*, and *wx<sup>m-8</sup>* and having no active *Spm*; homozygous for  $a_1$ , *sh*<sub>2</sub>, *pr*, and *wx<sup>m-8</sup>* and having no active *Spm*; or homozygous for  $a_1^{m-1}$ , *sh*<sub>2</sub>, and *wx*, having no *Spm*, and either homozygous or heterozygous for the *Pr* marker. One particular state of  $a_1^{m-1}$  was utilized in these crosses because it responds in a very clear way to activity of the components of *Spm* and also allows the type of *Spm* in a plant to be registered in both the *Sh*<sub>2</sub> and the *sh*<sub>2</sub> class of kernels on the ears of the plant. The presence of *wx<sup>m-8</sup>* in a kernel serves as an additional means of



scoring the *Spm* elements it may contain.

The tests revealed the following. Among the five plants derived from *Pr* kernels that were known to contain *Spm<sup>w</sup>*, two had one *Spm<sup>w</sup>* element, carried in chromosome 3 and linked with the diffuse-mottled locus but removed from it. Two others had one *Spm<sup>w</sup>*, not linked with the diffuse-mottled locus. The fifth plant had two *Spm<sup>w</sup>* elements, neither of which was linked with that locus. Of the remaining 22 plants derived from *Pr* kernels, 12 had no *Spm*, 4 had one *Spm<sup>w</sup>* linked to the diffuse-mottled locus but removed from it, 3 had one *Spm<sup>w</sup>* not linked with that locus, and 2 had one *Spm<sup>s</sup>* closely linked with the *Pr* marker. One of these two plants had in addition an *Spm<sup>w</sup>*, not linked with the diffuse-mottled locus. The remaining plant of the 22 had one *Spm<sup>s</sup>* not linked with *Pr* or with the diffuse-mottled locus. Of the three plants derived from the *pr* kernels, one had one *Spm<sup>s</sup>*, one had two *Spm<sup>s</sup>*, and one had one *Spm<sup>s</sup>* and also one *Spm<sup>w</sup>*, not linked with the diffuse-mottled locus.

The evidence obtained from the tests indicates that an *Spm<sup>w</sup>* element that is unable to induce its own transpositions early in development will undergo such transpositions if a potent component-2 is supplied by an *Spm* located elsewhere in the chromosome complement. It also indicates that the transposition event does not modify the components of the *Spm<sup>w</sup>*; they remain unaltered after the event.

#### *The Component of Spm Responsible for Preset Patterns of Gene Expression*

To identify the component of *Spm* that is responsible for inducing the preset patterns of gene expression discussed in *Year Book 63* (pp. 594–599), plants carrying state 7977B of *a<sub>1</sub><sup>m-2</sup>* and no active *Spm* were crossed with plants that had *Spm<sup>w</sup>* at the locus of *a<sub>1</sub><sup>m-2</sup>*, or *Spm<sup>w</sup>* at the locus of *a<sub>1</sub><sup>m-5</sup>*, or *Spm<sup>w</sup>* linked with *Pr* in chromosome 5. Other crosses were made that introduced into some of the kernels

an *Spm* with a highly active component-2. From the ears produced by these crosses, kernels were selected that had and that had not received the *Spm*. Plants were grown from both types of kernels, and testcrosses were conducted with their ears to determine whether or not they would bear kernels exhibiting types of anthocyanin distribution similar to those illustrated in *Year Book 63*, Plate 2B.

Sixty-one plants derived from kernels that had received the introduced *Spm* were tested. Since most of them produced two to four fertile ears, different types of tests could be conducted with many of them. At least one ear, and usually more than one, took part in a cross with a plant that was homozygous for *a<sub>1</sub>*, *sh<sub>2</sub>*, and *wx<sup>m-8</sup>* and had no active *Spm*. On all the ears there were kernels that exhibited preset patterns of anthocyanin distribution and showed no indication of the presence of an active *Spm*. There was no evidence that would relate the type of preset pattern to the particular *Spm* present in the ear-bearing parent: *Spm<sup>s</sup>* and *Spm<sup>w</sup>* were equally effective in this regard. This observation suggested that component-1 of *Spm* is responsible for induction of preset patterns. Confirmation was provided by the kernel types on ears of four additional plants, which carried an *Spm* whose component-1 remained in an inactive phase throughout plant development but returned to an active phase in many cells during development of the kernels. No kernels with preset patterns appeared on any of the ears produced by these four plants.

Sixty-one plants derived from kernels that had not received *Spm* from the pollen parent were also examined. On 68 of the ears on these plants, produced either by self-pollination or by crosses with plants that were homozygous for *a<sub>1</sub>* and had no active *Spm*, kernels exhibiting preset patterns did not appear. The kernels were colorless or nearly so. In addition, 49 ears produced by 36 of the plants were utilized in a cross that introduced an active *Spm<sup>s</sup>*. No kernels



with preset patterns appeared on these ears. The phenotype expressed by  $a_1^{m-2}$  (state 7977B) in those kernels that received *Spm* was typical: deep-pigmented spots in a lighter-pigmented background. Kernels that did not receive *Spm* from the pollen parent were colorless or nearly so.

#### *Transmission of the Preset Pattern*

In the study of preset patterns described in *Year Book 63*, pp. 594–599, it was found that the patterns usually did not reappear in the following generation. Most of the ears of plants derived from kernels exhibiting preset patterns showed no evidence of retention of the patterns: their kernels were colorless or nearly colorless. On a few ears, however, produced by plants carrying state 7995 of  $a_1^{m-2}$ , several kernels exhibited a pattern of anthocyanin distribution resembling that in the kernel from which the plant was derived. Five such exceptional kernels were present on one ear, four on another, and two on a third. This year, plants were grown from the exceptional kernels to determine whether or not the pattern would again reappear.

The constitution of the plants derived from these kernels was  $a_1^{m-2}$  (state 7995)  $Sh_2/a_1 sh_2$ ,  $wx/wx$ , and no active *Spm* was present in any of them. Nineteen of the fertile ears on these plants were utilized in a cross with a plant that was homozygous for  $a_1$ ,  $sh_2$ , and  $wx$  or  $wx^{m-8}$  and had no active *Spm*. If more than two ears were produced by a plant, one of them was used in a cross with a plant that was homozygous for  $a_1$  and  $sh_2$  and had one or more *Spm* elements. This cross, conducted with one ear on each of five of the eleven plants, was made to test whether some modification had occurred at the  $a_1^{m-2}$  locus that would be revealed by the locus's response to an active *Spm* element. On all five ears the response to *Spm* was normal: deep-pigmented spots appeared in a lighter-pigmented background.

The 19 ears produced by the first-mentioned cross were examined for kernels with patterns of anthocyanin distribution and intensity resembling those in the parent and grandparent kernels. On the ears produced by plants derived from the parent ear that had four such kernels, no kernels of this type appeared. All were colorless or nearly so. On one or more of the ears produced by the remaining seven plants, some parent-type kernels did appear, in numbers ranging from one to five per ear. Their distribution on an ear was not random: most were located in the upper third, several at the base of the ear. When more than one was present on an ear, they were not clustered, exhibiting in that respect the same distribution as on the parent ears. There is no evidence that contamination contributed to their presence on the progeny ears, as all the remaining kernels were colorless or nearly so.

The exceptional kernels had pigment intensities resembling those of the kernels from which their respective plants arose. They did not show the wide range of intensities represented among kernels with preset patterns appearing on ears of plants that have an active *Spm*. It seems probable, therefore, that the condition responsible for a particular expression of a preset pattern was retained for two plant generations in the ancestor cells that produced the exceptional kernels, but was lost from those ancestor cells that produced the remaining kernels on the same ears. At present there is no adequate explanation for this phenomenon. Some of its aspects recall a type of gene expression that is produced by one of the operator elements of the *Ac* system. This operator functions at the loci of  $c_1^{m-2}$ ,  $wx^{m-1}$ , and  $wx^{m-5}$ . It was noted that some responses of the operator to *Ac* did not immediately result in a stable expression of the gene; instead, the level of expression appeared to oscillate. This behavior was observed in the descendent cells of a cell in which such a response had occurred. The results were apparent in kernels that



had received one such "excited" gene locus from the pollen parent. Plants were grown from some kernels that exhibited this type of metastability at the  $wx^{m-5}$  locus. In kernels on the ears of the plants the level of action of the  $Wx$  gene was now uniformly expressed throughout the cells of the endosperm. The "oscillation" had ceased. Furthermore, no responses of the mutant locus to  $Ac$  occurred thereafter. The locus had acquired stability.

#### *Components of Action of Ac*

Study of  $wx^{m-7}$ , first reported in *Year Book 63* (pp. 599-601), was extended in order to examine the activity cycles of  $Ac$  in greater detail. The  $wx^{m-7}$  modification arose by insertion of  $Ac$  at the  $Wx$  locus in chromosome 9. The initial effect was a marked reduction in activity of the gene. Transposition of  $Ac$  away from the locus restores a high level of gene action and releases the gene from control by the  $Ac$  system.  $Ac$  is known to regulate the time and frequency of occurrence of self-transposition and of responses of the operator element at other gene loci. Initially this  $Ac$  at the  $wx^{m-7}$  locus exhibited the type of dose expression that characterizes  $Ac$ : the higher the dose, the later the time of occurrence of such responses. It was observed that this  $Ac$  undergoes cycles of activity that alter the component responsible for the responses and for induction of transpositions. When that component is inactive, no such responses occur nor does the  $Ac$  contribute to dose expressions should an active  $Ac$  also be present elsewhere in the chromosome complement. It responds, however, to such an active  $Ac$  by undergoing transposition that releases the  $Wx$  gene from further control by the  $Ac$  system, and the time and frequency of occurrence of transposition reside in the active  $Ac$ . When the  $Ac$  at the  $Wx$  locus returns to an active phase, its capacity to induce responses of the operator element located elsewhere, to induce its own transpositions, and to contribute to

dose expressions is restored. Thus, the activity cycles affect a component of  $Ac$  that is comparable to component-2 of  $Spm$ , but different in that it is also responsible for dose expressions, which are not exhibited by component-2 of  $Spm$ . No component of  $Ac$  comparable to component-1 of  $Spm$  has yet been identified.

A fascinating aspect of inactive  $Ac$  at  $wx^{m-7}$  relates to its control of the level of action of the  $Wx$  gene in the starch-bearing cells of the endosperm. Different levels of action are induced during kernel development. To examine this aspect it was necessary to utilize a technique that could reveal these levels in individual cells. The  $Wx$  gene is responsible for the production of amylose starch in the pollen grain, the embryo sac, and the starch-bearing cells of the endosperm of the kernel. The associated enzyme, which has been identified by O. E. Nelson, is affixed to the starch-forming granules within the cells. When the  $Wx$  gene is acting normally, approximately 25 per cent of the starch in the endosperm is amylose, the remainder being amylopectin. If the activity of the gene is reduced, the amount of amylose formed is also reduced. If the gene is totally inactive, all the starch is amylopectin. The two types of starch stain differentially with a solution of potassium iodide and iodine: the amylose stains blue and the amylopectin red-brown. The red-brown stain may be removed, either by hot water or by exposure of the cells to the rays of a lamp. To examine the level of  $Wx$  gene action in different cells of the endosperm of a kernel, a cut is made to expose a surface of endosperm cells, which are then stained with an I-KI solution. The intensity of blue coloring in the starch granules of different cells may be compared. It was learned many years ago that the intensity of this staining in the granules of a cell reveals the level of  $Wx$  gene action in that cell. It is believed, therefore, that the observed differences in intensity of blue coloring among the



endosperm cells of an individual kernel reflect differences in level of *Wx* activity in the cells. Such differences are illustrated in Plates 1 and 2.

To aid in interpreting the illustrations, a brief review should be made of endosperm development, some aspects of which were first revealed during the course of this study. The primary endosperm nucleus, produced by fusion of a sperm nucleus with two haploid nuclei contributed by the female gametophyte, divides in two, and then each nucleus divides again. Each of the resulting four nuclei gives rise by subsequent divisions to a column of nuclei, before cell walls are formed. The columns are arranged around a central, nonnucleated core. Cell-wall formation occurs later, but does not eliminate the central core, often visible in the mature kernel. The cells in the columns divide tangentially, and the outermost cells continue to divide, leaving behind cells in which endoreduplication of the chromosomes occurs. In the mature kernel the innermost cells of the endosperm are highly polyploid and very large, containing many starch granules. The degree of polyploidy becomes lower in cells farther removed from the middle of the kernel, and the cell size is correspondingly reduced. The chromosomes in the nuclei of cells toward the periphery do not undergo endoreduplication, and these cells are small. The aleurone layer is the outermost layer of cells of the endosperm; only in these cells is anthocyanin pigment produced. Although a change in control of action of a gene contributing to anthocyanin pigment formation may occur within a cell during endosperm development, it can be expressed only in cells of the aleurone layer that are descended from that cell.

To examine the effects produced by *Ac* in its active and inactive phases, it is necessary to know when it is in one or the other. This is made possible by the presence of a gene that is associated with anthocyanin pigment formation and is under the control of the *Ac* system.

The modified *A<sub>1</sub>* locus *a<sub>1</sub><sup>m-3</sup>* was chosen for the purpose. The state of *a<sub>1</sub><sup>m-3</sup>* selected for the experiments produces a lightly pigmented aleurone layer when *Ac* is absent or inactive. When *Ac* is active, the responses it induces in the operator element at the *a<sub>1</sub><sup>m-3</sup>* locus give rise to altered *A<sub>1</sub>* gene expressions, often restoring full or nearly full activity to the gene. The time of occurrence of these responses is controlled by the *Ac* element that is present in the kernel. An illustration is given in Plate 1A. The responses to the active *Ac* in this kernel were registered in like manner by *a<sub>1</sub><sup>m-3</sup>* and *wx<sup>m-7</sup>*; they occurred late in development of the kernel.

Kernels that commence development with *a<sub>1</sub><sup>m-3</sup>* and an inactive *Ac* at the locus of *wx<sup>m-7</sup>* will show no deeply pigmented areas in the aleurone layer at maturity if the *Ac* remains inactive throughout endosperm development. If *Ac* returns to the active phase in an individual cell during development, it will induce responses of the operator element leading to change in gene action at *a<sub>1</sub><sup>m-3</sup>* in some of the progeny of that cell. The event will be evidenced by an area in the aleurone layer that exhibits pigmented spots. *Ac*'s return to activity will also induce many reversions of the *Wx* gene to full expression. The size of an area having pigmented spots indicates the time during development when the change of phase occurred.

Progeny were obtained from a number of plants that developed from kernels having *a<sub>1</sub><sup>m-3</sup>* and an inactive *Ac*, for examination of the cycles of activity that *Ac* would subsequently undergo. Only that aspect of the study relating to control of expression of the *Wx* gene will be reported here. In a number of progeny kernels, the action of *a<sub>1</sub><sup>m-3</sup>* gave no indication of a change of phase of *Ac* from inactivity to activity. The level of *Wx* gene expression in the starch-bearing cells of these kernels was not uniform, as shown in Plate 1(C, D, and E). Although most such kernels exhibit a basic pattern of *Wx* gene action, produced by



a low level of this action in the cells of the upper mid-region and at the base of the endosperm, many changes in level may occur during endosperm development. It was noted that the initial level of *Wx* gene expression imposed by the inactive *Ac* at the time of fertilization, regardless of whether it was contributed by the male or by the female gametophyte, had a marked effect on the levels of *Wx* gene expression appearing in the kernel. Some kernels commenced development with a low level of *Wx* gene action (Plate 1C), others with a much higher level (Plate 1D and E). If such kernels had started development with one active *Ac*, located elsewhere than at  $wx^{m-7}$ , both  $a_1^{m-3}$  and  $wx^{m-7}$  would have responded to it. Early and late changes in  $A_1$  gene expression and changes to full *Wx* gene expression would have occurred, in the manner exhibited by the kernel in Plate 1F. In that kernel the pattern of *Wx* gene expression produced by the presence of active *Ac* is superimposed on the pattern produced by inactive *Ac*.

The kernel shown in Plate 1B and all three kernels shown in Plate 2 illustrate the responses of  $a_1^{m-3}$  and  $wx^{m-7}$  to a change in phase of *Ac* from inactive to active during endosperm development. The legends give the constitutions of the kernels and describe the effects produced by the changes in phase. It can be noted particularly in Plate 1B and Plate 2B and C that the progeny cells of a cell in which *Ac* underwent activation are

readily distinguished because they express either a low or a high level of *Wx* gene action. In cells where *Ac* remained in an inactive phase throughout endosperm development, on the other hand, a wide range of levels may be expressed, resembling the range exhibited by kernels in which *Ac* remains inactive throughout development.

In conclusion, it may again be stated that the resemblance between the regulators *Ac* and *Spm* resides in a component of each that initiates responses of the respective operator element and of the regulator itself which effect transpositions. If the component is inactive, such responses do not occur. It is this component of *Ac* that is comparable to component-2 of *Spm*. In *Ac*, but not in *Spm*, the component is also responsible for dose effects. The operator element of the *Ac* system has not yet given evidence of differential control of action of the gene in response to activity cycles of *Ac*, in the manner exhibited by the operator element of the *Spm* system. Thus, *Ac* has no recognizable component that corresponds to component-1 of *Spm*.

It is possible that the different levels of *Wx* expression produced by inactive *Ac* at  $wx^{m-7}$ , the "preset" patterns within the *Spm* system, and the "oscillations" in gene expression produced by responses to active *Ac* of one *Ac* operator may all reflect a common type of event occurring at the locus of a gene to initiate temporary metastability of its action.

## BIBLIOGRAPHY

- Burgi, E., *see* Hershey, A. D.  
 Cowie, D. B., and A. D. Hershey, Multiple sites of interaction with host-cell DNA in the DNA of phage  $\lambda$ , *Proc. Natl. Acad. Sci. U.S.*, 53, 58-62, 1965.  
 Davern, C. I., *see* Hershey, A. D.  
 Hershey, A. D., and E. Burgi, Complementary structure of interacting sites at the ends of lambda DNA molecules, *Proc. Natl. Acad. Sci. U.S.*, 53, 325-328, 1965.  
 Hershey, A. D., E. Burgi, and C. I. Davern, Preparative density-gradient centrifugation of the molecular halves of lambda DNA, *Biochem. Biophys. Res. Commun.*, 18, 675-678, 1965.  
 Hershey, A. D., *see also* Cowie, D. B.  
 Ledinko, N., Occurrence of 5-methyldeoxycytidylate in the DNA of phage lambda, *J. Mol. Biol.*, 9, 834-835, 1964.

PERSONNEL

*Year Ended June 30, 1965*

Boeskay, Elizabeth M. (Mrs.), Chief Clerk  
Buchanan, Jennie S. (Mrs.), Curator of  
Drosophila Stocks  
Burgi, Elizabeth, Associate in Microbiology  
Ehring, Ruth, Carnegie Institution Fellow  
Fisher, Agnes C., Secretary to Director;  
Editor  
Goldberg, Edward, Carnegie Institution  
Fellow  
Hershey, Alfred D., Director  
Ingraham, Laura J. (Mrs.), Research  
Assistant  
McClintock, Barbara, Cytogeneticist  
Mosig, Gisela, Associate in Research  
Skalka, Anna Marie, Postdoctoral Fellow,  
American Cancer Society

Smith, Mervyn G., Fellow, Damon Runyon  
Memorial Fund  
Wilson, Carole E. (Mrs.), Technical Assist-  
ant

*Temporary and Part-Time*

Taylor, Albert E., Technical Assistant  
Treible, Kathryn E.,<sup>1</sup> Research Assistant  
Womack, Frances C., Guest Investigator  
Wolfowitz, Paul D.,<sup>1</sup> Research Assistant

<sup>1</sup> NSF Undergraduate Research Participation  
Program, Cold Spring Harbor Laboratory of  
Quantitative Biology, summer 1964.



Plate 1. Exposed starch-bearing cells of the endosperm of the kernels have been stained with a solution of potassium iodide and iodine.

A. Top view of a kernel with crown cut off to expose a surface of starch-bearing cells. The constitution of this kernel was  $a_1^{m-3}/a_1/a_1$ , active  $Ac\ wx^{m-7}/active\ Ac\ wx^{m-7}/wx$ . The two doses of active  $Ac$  produced late-occurring mutations at  $a_1^{m-3}$ , revealed by dots of pigment in the aleurone layer, and late mutations to full  $Wx$  gene expression, as shown by the cells with intensely staining starch granules.

B. Top view of a kernel with crown cut off to expose a surface of starch-bearing cells. This kernel commenced development with the constitution  $a_1^{m-3}/a_1/a_1$ , inactive  $Ac\ wx^{m-7}/wx/wx$ . Early in development, the inactive  $Ac$  mutated to an active phase. The cell in which the activation occurred produced the large sector (lower right) exhibiting many cells with full  $Wx$  gene expression. The gene  $a_1^{m-3}$  also responded to the activation, as seen by the pigmented spots in the aleurone layer of this sector.

C-E. Longitudinal sections of three kernels having the constitution  $a_1^{m-3}/a_1/a_1$ , inactive  $Ac\ wx^{m-7}/wx/wx$ . In each of these kernels,  $Ac$  remained in its inactive phase throughout endosperm development. Note, however, the differences in level of  $Wx$  gene expression induced in different cells by the inactive  $Ac$ .

F. Two views of the same half of a longitudinally sectioned kernel. The constitution of this kernel was  $a_1^{m-3}/a_1/a_1$ , inactive  $Ac\ wx^{m-7}/wx/wx$ . It had, in addition, one active  $Ac$  element not linked with these markers. Note effect of the active  $Ac$  in one dose on mutation at  $a_1^{m-3}$  and at  $wx^{m-7}$ .

G. Longitudinal section of a kernel that had the same constitution as those in C-E and commenced development with an inactive  $Ac$  at  $wx^{m-7}$ .  $Ac$ , however, was activated in some cells during kernel development. It was active in cells in the upper right-hand quarter and inactive in cells in the upper left-hand quarter.

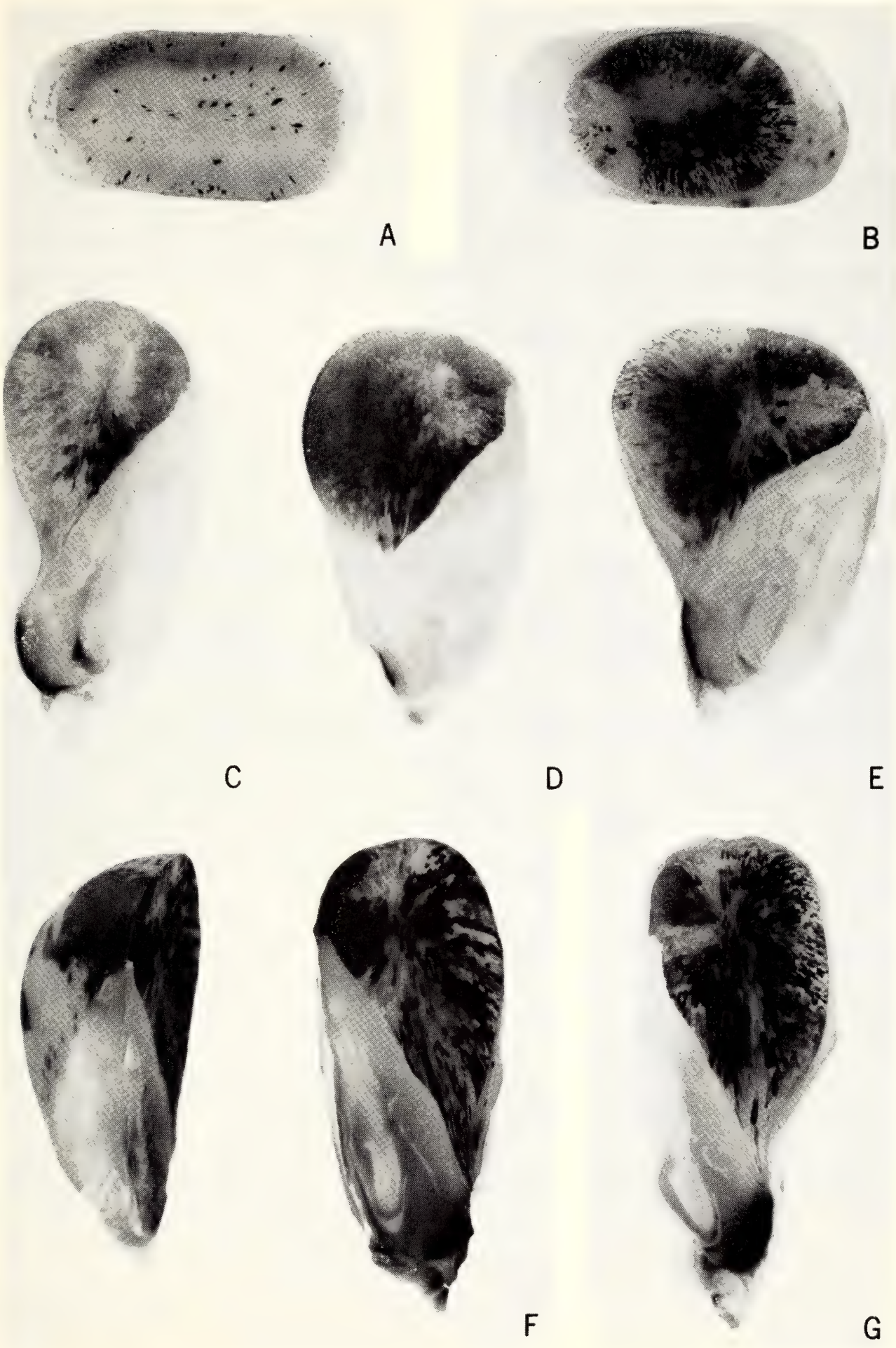
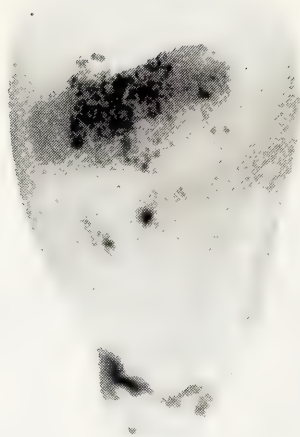
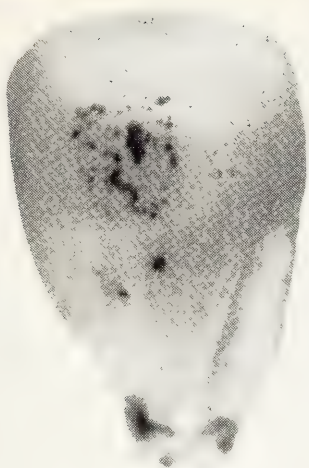




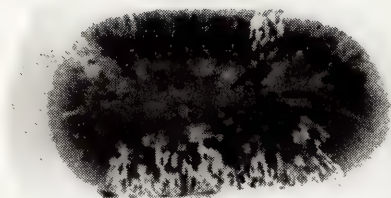
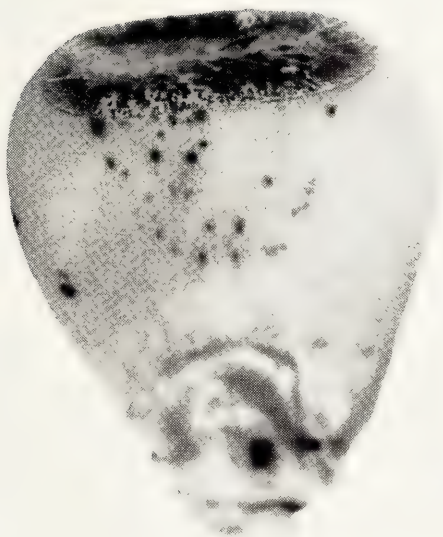
Plate 2. A. Side view of a kernel that commenced development with the constitution  $a_1^{m-3}/a_1^{m-3}/a_1$ , inactive  $Ac\ wx^{m-7}/inactive\ Ac\ wx^{m-7}/wx$ .  $Ac$  returned to an active phase in some cells during development. One of the activations occurred early; the descendent cells produced a large area in the aleurone layer containing many pigmented spots, as shown in the left-hand photograph. Three small areas with  $A_1$  dots are also visible, indicating activation of  $Ac$  in other cells but later in kernel development. To show that these activations also resulted in many mutations of  $wx^{m-7}$  to full  $Wx$  expression, a strip of the aleurone layer, running across the large area and into a nearby smaller area, was scraped off to expose a surface of underlying starch-bearing cells. These cells were stained with an I-KI solution, as shown at right. Note the many cells underlying the spotted sectors that exhibit full  $Wx$  gene expression, and the absence of such cells under the unspotted areas. Number of  $A_1$  spots per area is smaller than number of  $Wx$  spots because some responses of  $a_1^{m-3}$  to active  $Ac$  do not lead to pigment formation, whereas nearly all such responses at  $wx^{m-7}$  give rise to full  $Wx$  gene expression.

B. In this kernel, which commenced development with the constitution  $a_1^{m-3}/a_1/a_1$ , inactive  $Ac\ wx^{m-7}/wx/wx$ , a large area and several smaller areas of the aleurone layer had pigmented spots. To show that the large area was derived from a cell in which  $Ac$  had become active early in development, the crown of the kernel was cut off to bisect that area, and the exposed cells were stained as usual. Cut kernel is seen side view at left, top view at right. Large sector containing active  $Ac$  is clearly delimited by the expression of both gene loci. A small sector of cells having active  $Ac$  is also visible in the cut surface, above and slightly to right of center. All other cells in this cut surface had an inactive  $Ac$ .

C. Three views of same half-kernel. The kernel commenced development with the constitution  $a_1^{m-3}/a_1/a_1$ , inactive  $Ac\ wx^{m-7}/wx/wx$ . When mature, it showed a very large area of pigmented spots in the aleurone layer. The kernel was cut longitudinally to bisect that area as well as the area lacking such spots. The center photograph is a front view of the cut surface. The cells in the right half of this surface, and some in the middle of the endosperm, had an active  $Ac$  element, as shown by the intensely staining starch granules. In the cells of the large area to the left,  $Ac$  was inactive. Effects of active and inactive  $Ac$  on responses of  $a_1^{m-3}$  are revealed by the side views.



A



B



C





# *Cytogenetics Laboratory of the Carnegie Institution*

Helen Gay

*University of Michigan, Ann Arbor*



Contents

Organization of Chromosomes in Higher Forms . . . . . 539

    Introduction . . . . . 539

    Fine structure of chromosomes . . . . . 540

        Development of salivary-gland chromosomes . . . . . 540

        Perichromatin vesicles of *Tradescantia* mitotic chromosomes . . . . . 542

    Mitotic cycle and DNA replication in *Haplopappus gracilis* . . . . . 544

    DNA of mitotic chromosomes of *Drosophila* . . . . . 546

    Base composition of heterochromatic DNA in *Drosophila melanogaster* . . . . . 548

Bibliography . . . . . 552

# ORGANIZATION OF CHROMOSOMES IN HIGHER FORMS

## INTRODUCTION

During the report year our investigations have again been centered on problems of fine structure and molecular organization of chromosomes in higher plants and animals. That an understanding of the structure and function of the more complex carriers of fundamental genetic information is important need not be repeated here. Cytologists and cytogeneticists have continued in their attempts to bridge the gap between the highly variable mitotic chromosomes or the differentiated chromosomes of such specialized units as gametes or actively secreting cells, and the essentially "naked" genetic material of microorganisms. The work appears on the surface to proceed at a frustratingly slow pace. But it is only by successive probings in analysis of the structure and behavior of these different types of chromosomes with the numerous experimental methods at our disposal that a common underlying pattern of organization may be revealed and its evolutionarily derived variants determined.

With this as our basic premise, we have continued to investigate the intricacies of the structure of the giant salivary-gland chromosome of *Drosophila* by electron-microscope analysis of the development of the polytene chromosome from the earliest stages procurable. Presumably the giant chromosomes arise by synapsis of mitotic-type progenitor homologues, each containing two chromonemata. Our aim was to determine the nature of the basic chromonematic unit and to trace it through known developmental stages up to the time of formation of the fully developed polytene chromosome.

At the molecular level our concern has been primarily with deoxyribonucleic acid (DNA)—the analysis of its replication in the mitotic type and in the giant chromosomes, and determination of its

base composition in heterochromatic and euchromatic regions of the chromosomes. Although the basic pattern of DNA replication in mitosis has been defined, the many examples of unorthodox segregation of chromosomal DNA we observed led us to believe that study of these exceptions with refined radioautographic analysis should provide evidence of the number of strands within the chromosome. Use of an organism with two pairs of chromosomes, each with readily distinguishable morphological features, has permitted analysis of individual chromosomes through three successive replication cycles of DNA.

Our chemical analyses of DNA have been centered on determination of the base composition in heterochromatin as compared with that in euchromatin. In *Drosophila melanogaster* heterochromatin has been demonstrated as relatively "inert" genetic material and its quantity within the genome is sufficient to render it amenable to chemical analysis. Unfortunately the DNA of *Drosophila* is refractory to isolation and the material obtained is of a low molecular weight, making highly refined analyses of specific nucleotide sequences of DNA impossible at the moment. By determination of base composition, however, it is possible to compare *Drosophila* heterochromatin with euchromatin. By these methods we have found that the two types—"inert" and "active" chromatin—are essentially similar in DNA composition.

These investigations have been pursued with the able collaboration of several associates. Dr. Elisabeth Peveling terminated her Carnegie Institution Fellowship in February 1965 and completed her electron-microscope analysis of the development of the polytene chromosome. The electron microscope used in these studies was provided by National Science Foundation grant GB-290 to Dr. Berwind P. Kaufmann. The other studies described



have been carried out in collaboration with Dr. Kaufmann and his associates, Dr. Elio Sparvoli, William J. Perreault, and Mrs. Kay Forward, under the sponsorship of U.S. Public Health Service research grant GM-10499 to the University of Michigan. The advantages to the author and other members of the Cytogenetics Laboratory of working in close association with this group are gratefully acknowledged. Miss Mary Lee, who served as interim Research Assistant, resigned in July 1965, and was replaced in September 1965 by Mrs. Betty J. Moberly.

#### FINE STRUCTURE OF CHROMOSOMES

##### *Development of Salivary-Gland Chromosomes*

Over the years, a number of observations by experimental methods, such as radiation or radioautographic techniques, and direct examination at both the light- and electron-microscope levels of resolution have substantiated the fact that the fully developed salivary-gland chromosomes of *D. melanogaster* are polytenic; that is, they are made up of many longitudinal elements whose number has not been determined precisely. These studies have also revealed that the lengthening that takes place as the salivary-gland chromosome develops is not uniform in all parts of the chromosome. For example, the proximal heterochromatic regions adjacent to the centromeres represent 1/20th to 1/30th of the total length of the giant chromosome, whereas they may constitute (as in the X) at least one third of the length in the mitotic-type chromosome. How these giant chromosomes arise from the mitotic-type precursors is one of the problems of chromosomal differentiation to which we have directed attention in the past year.

At the time of compiling the annual report for *Year Book 63*, Dr. Elisabeth Peveling's electron-microscope studies of the salivary-gland chromosomes of *D. melanogaster* had just been initiated.

Those preliminary studies provided a basis for determining the course of investigations during the remainder of her stay in our laboratory. The research was directed toward the preparation and selection of true transverse sections of chromosomes in cells of third-instar larvae (so that the degree of polyteny could be ascertained) and the analysis of early developmental stages in first- and second-instar larvae before the chromosomes become highly polytenic. The latter approach, which represented the first ever made at the electron-microscope level of resolution, proved most fruitful in our efforts to obtain information about the polytenic aspects of chromosome structure and the changes occurring in euchromatin and heterochromatin during chromosomal differentiation.

To place in proper perspective the electron-microscope observations on salivary-gland chromosomes during early larval development, the current picture of the fully developed late third-instar giant chromosomes will be described. As noted in *Year Book 63* (p. 607), Dr. Peveling's techniques showed that in longitudinal section the chromosome appears to be composed of many chromonemata, 75–125 m $\mu$  in diameter.

Although we have not been able to trace the individual chromonemata through the 25 longitudinal sections needed to cut through a chromosome about 3  $\mu$  in width, we have obtained a cross section (Plate 1) indicating that the chromosomes are cylindrical in shape. Using the measured chromosomal width of 3  $\mu$  and the chromonemal width of 0.1  $\mu$  as a basis for calculating both chromosomal and chromonemal cross-sectional areas, we can determine that about 900 chromonemata, 100 m $\mu$  in diameter, would fit into a chromosome 3  $\mu$  wide (and about 2,500 into a 5- $\mu$  chromosome, which is the largest observed in late third instar). This calculation implies that either 1,024 or 2,048 chromonemata (multiples of two would reflect the degree of chromonemal dupli-



cation) are present in the fully developed third-instar salivary-gland chromosome. Dr. Peveling consistently found that the  $0.1\text{-}\mu$  chromonemata are made up of subchromonemata,  $100\text{--}200\text{ \AA}$  in diameter, but had not determined how many constitute the chromonema. It would seem, however, that each  $0.1\text{-}\mu$  chromonema must contain at least two of the  $100\text{--}200\text{ \AA}$  subchromonemata. If so, Dr. Peveling's derived value for chromonemata multiplied by two would correspond reasonably well with previous estimates by various workers, including the author, of the number of fine strands in the giant chromosome.

At the light-microscope level of resolution, Hertwig's earlier determinations of the degree of polyteny by measurements of nuclear volume, and Swift and Rasch's determinations of amounts of DNA by microspectrophotometry suggested that 9 or 10 chromosomal replications take place in the formation of the third-instar salivary-gland chromosome. These results imply that the DNA of chromosomes and the nuclear volumes have increased 1,024 times—a conclusion supported by our electron-microscope studies of the increase in number of chromonemata.

Dr. Peveling has previously indicated how the characteristic bands of the giant chromosome are formed by the coiling of the chromonemata (*Year Book 63*, Fig. 10, following p. 614). She has now demonstrated a point suggested in earlier studies with ultraviolet and electron microscopy: that many of the bands, which appear single with the ordinary light microscope, are resolvable into several small bands. Her evidence is as follows: The largest bands in the light-microscope image of the chromosome are about  $1.0\text{--}1.5\text{ }\mu$  in thickness. In electron micrographs, similar dense regions of equivalent length along the chromosome reveal several dark bands with interband distances of less than  $0.18\text{ }\mu$ . It is apparent that the small bands would not be resolvable with the light microscope and that the complex of small

bands would appear as a single structure. These observations have a direct bearing on the question whether a band represents a complex of structural and operator genes—in essence an operon.

In her study of the development of the giant salivary-gland chromosomes Dr. Peveling was concerned mainly with the multiplication of the longitudinal strands—the chromonemata. Could the basic chromonema be found in the earlier stages and would its dimensions be the same as those of the third-instar chromosome? On the basis of about 1,000 measurements made on 10–20 electron micrographs of both acid- (Ernst's fluid) and osmium-fixed tissues from each of the three larval instars, the  $75\text{--}125\text{ m}\mu$  chromonema was the most common fibrous strand in all stages of development, but subchromonemata,  $100\text{--}200\text{ \AA}$  in diameter, were always present. In the first-instar salivary-gland nucleus, which is only about  $4\text{ }\mu$  in diameter, the chromosomal material exists as fine strands, most of which are  $75\text{--}125\text{ m}\mu$  in diameter. These units are the same size as those found in chromosomes of the neuroblast interphase nucleus, which is also  $4\text{ }\mu$  in diameter.

Because in mitotically active neuroblast cells Dr. Peveling has been able to determine that the  $75\text{--}125\text{ m}\mu$  fibers make up the chromatids, we conclude that our use of the term chromonemata for these strands in both neuroblast and salivary-gland nuclei is valid. Although chromonemata are almost exclusively composed of subchromonemata  $100\text{--}200\text{ \AA}$  in diameter, strands  $300\text{ \AA}$ ,  $500\text{ \AA}$ , and  $700\text{ \AA}$  in diameter do occur with a relatively low frequency. They are assumed to be aggregates of subchromonemata, similar to those detected in our earlier studies.

During larval development, although the chromosomal diameter increases from  $0.15\text{ }\mu$  in the first instar, to  $0.7\text{ }\mu$  in the second, and  $3\text{ }\mu$  in the third instar, the chromonemal diameter remains constant at  $75\text{--}125\text{ m}\mu$ . The first appearance of banding of the whole chromosome is



detectable in the second instar, although the chromonemata themselves show faint banding in all three instars (Plate 2). At the chromosomal level the banding is apparently caused by coils of the component chromonemata; it may be postulated that at the chromonemal level, coils of the subchromonema form a pattern of banding, although this conclusion must be held in abeyance until the number of subchromonemata and their arrangement within the chromonema are ascertained. Dr. Peveling has determined that the chromonemata occur in relationally coiled pairs in the early stages of development and occasionally form chromomere-like coils. Future studies should tell whether these phenomena are related to formation of the bands.

The outlines of the chromocenter—the fused heterochromatic regions lying adjacent to the centromeres in all the chromosomes—are readily seen in the first-instar nucleus. As development proceeds through the second and third instars, the chromocentral region does not enlarge proportionately. Dr. Peveling's studies have shown that the chromonematic strands within the chromocenter are about  $0.2\ \mu$  in width during both second and third instar. At first instar, the chromocentral region is so tightly packed that it is impossible to measure included strands, but emerging from the chromocenter are chromonemata  $0.12\ \mu$  in diameter. Using radioautography, we are endeavoring to determine whether DNA synthesis occurs in this region during very early larval development. An examination of some slides obtained in previous experiments had suggested that  $H^3$ -thymidine might be incorporated in the chromocenter during early hours of first-instar development; however, a specially designed experiment will be needed to determine the point.

Rudkin has raised the question whether differential DNA synthesis in heterochromatic and euchromatic regions of the salivary-gland chromosomes could be the

factor determining the proportionate reduction of heterochromatin in the fully developed salivary-gland chromosomes. If the morphological differences in heterochromatin observed between first instar and second or third instars are significant, they may reflect heterochromatin in a synthetic or nonsynthetic phase. We are now developing methods of electron-microscope radioautography that should enable us to determine with more precision than is possible at the light-microscope level any differential DNA synthesis during development of the salivary-gland chromosome.

By using the classical chromosomal technique of acid fixation, Dr. Peveling has disclosed strands that she believes are the basic chromonemata within the polytene chromosomes. These strands are below the limits of resolution of the light microscope and appear to be present in the *Drosophila* salivary-gland chromosome from the first instar on throughout larval development. The fully developed salivary-gland chromosome is cylindrical and appears in cross section to contain 1,024 or 2,048 component chromonemata, which are made up of subchromonemata, 100–200 Å in diameter. The similarity at the electron-microscope level of the salivary-gland and neuroblast nuclei has raised a question about the time at which polytenic replication in the first-instar salivary-gland chromosomes is initiated. A full-scale microspectrophotometric study, now in progress, of the amount of DNA in salivary-gland nuclei from all stages of development, for comparison with mitotically active neuroblast cells from several stages of development and with spermatozoa, should give a basis for determining the degree of polyteny.

#### *Perichromatin Vesicles of Tradescantia Mitotic Chromosomes*

In the course of our electron-microscope investigations of chromosomal changes during mitosis in the apical cells



of staminate hairs of *Tradescantia*, reported briefly in *Year Book 63* (p. 606), Dr. Elio Sparvoli repeatedly observed small ringlike structures, not previously described, in close association with the chromatin. Because they are preferentially located at the periphery of chromatin masses or chromosomes, they have been designated "perichromatin vesicles" (pv).

The electron micrographs reveal the pv as an easily identifiable ellipsoidal ring, generally darker than the surrounding chromatin, with major and minor axes, about 600 Å × 400 Å, and a limiting membrane about 100 Å thick (Plate 3). The interior of the vesicle appears homogeneous, and the exterior is often surrounded by a clear zone, 150 Å wide, which delimits the vesicle from the chromatin in which it is embedded. The pv are always associated with chromatin, except possibly during late anaphase stages. Since they are almost invariably located at the periphery of the chromatin or chromosomal mass and are never found in the nucleolus, we believe they are not related to the particles and granules of nucleolar origin that have been previously described by several investigators.

Analysis of the frequency of the pv in the longitudinal sections of dividing cells (whose mitotic phases could be accurately identified and selected by using the open-face embedding technique perfected by Dr. Sparvoli) denoted a change in number during the mitotic cycle. Because the vesicles are small enough to be included within a single ultrathin section, they are infrequently cut, and it is therefore possible to evaluate the number per nucleus by counting the number of vesicles in successive serial sections, finding the average number per section, and calculating the total in the whole nucleus. An estimated section thickness of 700 Å and actual measurements of nuclear diameter are used.

As Table 1 shows, the number of pv

TABLE 1. Number of Perichromatin Vesicles During Mitosis in *Tradescantia* Staminate-Hair Cells

Duration, hours*	Mitotic Stage	Vesicles Per Cell, number
14.8	Interphase (S + G <sub>1</sub> )	60
2.7	Preprophase (G <sub>2</sub> )	150
1.6	Prophase	60
0.3	Metaphase	100
0.6	Early anaphase	340
	Late anaphase	500(800)†
	Early telophase	700
	Mid-telophase	200
	Late telophase	100

\* According to D. E. Wimber, *Am. J. Botany*, 47, 828, 1960.

† Includes vesicles inside the chromosomes and those very close to the chromosomes.

is about 60 during interphase and prophase. But from metaphase on, the number increases rapidly and in early telophase there are about 10 to 12 times the number in interphase. In late telophase the number is reduced quickly to approximately the interphase value. Two values for the number of vesicles at late anaphase are recorded. The lower figure indicates the number strictly associated with chromatin, and the higher one includes the first value plus vesicles of the same size and appearance that lie in the dense zone around the chromosome and might also be classified as small cytoplasmic vesicles (Plate 4). Differences in density of the enveloping membrane usually distinguish pv from cytoplasmic vesicles, but we have not relied on this subjective appraisal in making our estimates.

The significance of the change in number of the pv during mitosis can only be surmised. Michael Watson earlier described perichromatin granules, about



350 Å in diameter, which contained nucleic acid. The pv we have seen have a distribution similar to that of these granules, and are similarly surrounded by a clear zone, but they differ in their internal morphology (being vesicular), and in size and shape. Without further study, we must of course entertain the possibility that differences in fixation and preparation, as well as source of material, might be responsible for the observed differences.

Nonetheless the changes in number detected in the analysis suggest the intriguing possibility that structures concerned in nucleocytoplasmic relations might be involved. It is true that the pv are quite similar to the smaller cytoplasmic vesicles and in late anaphase it seems arbitrary to make a distinction between them. However, because the pv have a constant size and shape and are so closely associated with the chromosomal material, we are inclined to think of them as specialized structures connected with the nucleus, rather than as the usual cytoplasmic vesicles occasionally trapped in the nucleus after nuclear membrane formation at telophase.

Whether the pv are vesicles which migrate from the cytoplasm and accumulate on the chromosomes during mitosis or whether they are special vesicles which originate in the chromosome and produce new cytoplasmic vesicles for special functions in the cytoplasm cannot be determined from our observations. A working hypothesis might be that both cytoplasmic vesicles and pv form the nuclear membrane, but that the less numerous pv have a special function caused by their chromosomal association and thus could impart special properties to a localized region of the nuclear membrane.

Whether the pv contain nucleic acid remains to be determined. Further observations bearing on their origin, behavior, and function are needed to confirm our assumption that they may be significant in nucleocytoplasmic reactions.

#### MITOTIC CYCLE AND DNA REPLICATION IN *Haplopappus gracilis*

In our former radioautographic investigations of replication of DNA during the mitotic cycle of *Vicia faba* and *Allium cepa* we became aware that precise chromosomal analysis was greatly hampered by inability to adequately flatten and separate the large and numerous chromosomes of these species. We have frequently observed in second-division metaphases of *Vicia*, *Allium*, or *Crepis* that the chromosomes reveal a similar pattern of distribution of silver grains over corresponding segments of both chromatids of a chromosome (called "isolabeling" by Peacock), a pattern that is most readily explainable if a chromosome is multistranded. Although the frequency of isolabeling sometimes appeared high, precise evaluation of the data was difficult because good analyzable preparations were few in number.

During the past year, Dr. Sparvoli developed a technique for obtaining a good qualitative and quantitative evaluation of distribution of  $H^3$ -thymidine label in constituent chromatids of a chromosome. He used the composite *Haplopappus gracilis*, which has the lowest chromosome number reported for a flowering plant ( $n = 2$ ). First, he developed methods to induce good germination and growth of the *Haplopappus* seedlings so that the root-tip meristems were highly active mitotically. The process involved soaking the seeds in 10 per cent Chlorox for 10–15 minutes and then thoroughly rinsing in running water for three to four hours in an effort to remove a substance in the seed coat that inhibits root growth.

Next, Dr. Sparvoli worked out improved squashing techniques, so that the four Feulgen-stained chromosomes of the diploid complement of a root-tip cell were well separated from each other and easily distinguishable. Chromosome A is a long submetacentric, and chromosome



B is a shorter subtelocentric with a secondary constriction and small satellite. It was found that at late prophase there was greater radioautographic resolution along the longitudinal axis of the chromosome than at metaphase, when normal and colchicine-induced contraction combined to produce markedly shortened chromosomes. (Short development of the Kodak AR-10 stripping film which covered the squashes for radioautography produced very fine silver grains giving better resolution than had been obtained in previous studies.)

Finally it was necessary to determine accurately the length of the mitotic cycle in *H. gracilis* under prescribed growing conditions, so that the extent of the *S* (synthetic) period—during which  $H^3$ -thymidine is incorporated into DNA—could be specified with accuracy in order to gauge the optimum time of treatment and the times for sampling the metaphase stages of the first and second divisions thereafter in our experimental design. Summarized below are the results of these investigations and some preliminary observations on label distribution at the third prophase after labeling the chromosomes of *H. gracilis* with tritiated thymidine.

In its essentials, the method for determining the length of the mitotic cycle involves analysis of a block of cells, tagged with  $H^3$ -thymidine during the synthetic period, as they progress through the mitotic cycle. The experiment is continued long enough to include at least two divisions after the label is administered.

In our experiment,  $H^3$ -thymidine at a concentration of  $1 \mu\text{C}/\text{ml}$  (specific activity  $6.7 \text{ c}/\text{mM}$ ) was administered to the seedling for one half hour at  $24^\circ\text{C}$ . After repeated rinsing the seedlings were returned to tap water and samples were collected every half hour for the first three hours and every hour thereafter. The sampled seedlings were fixed in acetic alcohol (1/3); fixation was followed by a standard Feulgen reaction,

after which the root tips were squashed and then coated with AR-10 stripping film. In our experiment, 10 to 15 root tips were scored in each sample.

In Fig. 1, the analysis of the percentage of labeled metaphases among all the metaphases is graphically recorded. From this curve we can obtain some basic values concerning the duration of certain phases of the mitotic cycle. The distance between the mid-points of the two peaks gives 10.5 hours, the length of one generation. The flatness of the first peak reflects the length of the synthetic period. The skewness of the ascending curve reflects the variability of the  $G_2$  + prophase + labeling time and the skewness of the descending curve, the variability of the  $G_2$  + prophase + synthesis + labeling time. Consequently, the average length of the *S* period can be calculated as the distance between the 50 per cent points of the ascending and descending curves minus the labeling time, or  $4.5 - 0.5 = 4$  hours. Similarly  $G_2$  + prophase can be estimated as the distance between the origin and the 50 per cent intercept of the abscissa with the ascending curve, or 2.5 hours.

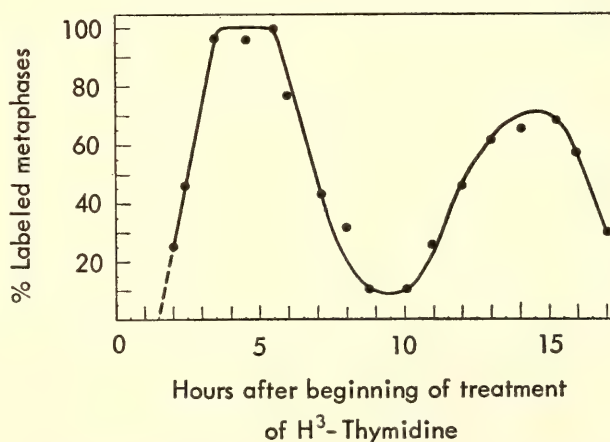


Fig. 1. Percentage of labeled metaphases plotted against time after beginning of a pulse label of 30 min. Distance between the two peaks is 10.5 hours and is the measure of average length of generation time. Distance between the 50% points of ascending and descending portion of curve is 4.5 hours and corresponds to average length of the period of DNA synthesis (*S* period) plus labeling time.



To obtain further information about the length of the other phases, it is necessary to use additional microscopic analysis. Since, in a population of asynchronously dividing cells, the number of mitotic figures in each stage of the cycle is proportional to the time spent in each stage, it is possible, if the duration of one stage and the numerical proportion of cells in each stage are known, to derive the length of the other stages.

A proportion can be set up:

$$nS:nP:nM:nAT = tS:tP:tM:tAT$$

where  $n$  = number,  $S$  = synthesis,  $P$  = prophase,  $M$  = metaphase,  $AT$  = anaphase + telophase, and  $t$  = time.

From our pulse-labeling experiment, the synthetic period + labeling time was found to be 4.5 hours. By scoring 50 root tips the frequency per thousand was obtained:  $nS = 735$ ;  $nP = 174$ ;  $nM = 48$ ;  $nAT = 43$ . By substituting in this proportion we find prophase time = 1.05 hours, metaphase time = 0.29 hour, and anaphase + telophase time = 0.26 hour.

We can conclude that in *Haplopappus* the generation time of 10.5 hours is composed of the following stages:  $G_1 = 3.45$  hours; synthesis = 4.0 hours;  $G_2 = 1.45$  hours; prophase = 1.05 hours; metaphase = 0.29 hour; anaphase + telophase = 0.26 hour.

With this information in hand Sparvoli initiated a series of experiments with *H. gracilis* to analyze the frequency of isolabeling in the second and third divisions after  $H^3$ -thymidine labeling. As noted, Peacock had found a high frequency of isolabeling in *Vicia faba* and had interpreted this as evidence that the chromosomes were multistranded. But the question remained whether the isolabeling could be the result of multiple exchanges between single-stranded chromosomes. To discriminate between isolabeling caused by multistranded chromosomes and that caused by multiple exchanges, a quantitative analysis of the frequency of the two patterns of isolabeling is necessary. Theoretically,

two types of isolabeling can be expected: single isolabeling, which is the presence of label over the same segment of two chromatids of the same chromosome; and twin isolabeling, which is the presence of label over the same segment of four chromatids of two sister chromosomes. Verification of the occurrence of both these forms of isolabeling in *H. gracilis* is a preliminary step to evaluation of the measure of isolabeling. Once this measure is established, a quantitative analysis of the occurrence of all forms of exchange (single and twin sister chromatid exchange and single and twin isolabeling) can give us more detailed information about the origin of isolabeling. Moreover, grain counts over the isolated regions, with the improved resolution afforded by the study of prophase, may give us the quantitative information needed to determine whether isolabeling is due to multistrandedness.

Preliminary results indicate that, as predicted, all chromosomes at the first division are labeled in both chromatids (Plate 5), while at second division there is segregation of label between the sister chromatids (Plate 6). Examples of single and twin isolabeling found in the second division are shown in Plate 6. Our results at the moment confirm that both single and twin isolabeling occur in the second division of *Haplopappus*, but there is not yet sufficient quantitative data available to explain the frequency or origin of isolabeling.

#### DNA OF MITOTIC CHROMOSOMES OF DROSOPHILA

In last year's report we presented preliminary findings by Dr. C. C. Das, based on microspectrophotometric determinations of DNA, showing that among neuroblast cells of *Drosophila melanogaster* larvae with the diploid chromosome number there were two populations of metaphases with respect to DNA content. In them the DNA values differed by a factor of 2. This finding suggested that metaphases with the higher DNA



values had arisen because DNA replication was not followed by separation of chromatids in a normal anaphase or by establishment of a tetraploid nucleus. The observed condition thus appears to reflect a state of polynemy attained by formation of multistranded chromosomes. The chromosomes would not be regarded as polytenic since their DNA content was determined in mitotically active diploid cells ( $2n = 8$ ).

To further substantiate these results, Mrs. Kay Forward has repeated during the current year DNA measurements on metaphase plates from ganglia of first-instar larvae (16 hours old), second-instar larvae (5 hours after the molt), and third-instar larvae (3–4 hours before the time of eversion of the anterior spiracles). In our previous experiments colchicine had been used to increase the number of metaphase plates, but in the present series this alkaloid was omitted to eliminate the possibility that it might be a factor in producing the observed doubling in the amount of DNA. In our former experiments we assumed that the lower of the two DNA values recorded was the true diploid DNA amount. To determine the validity of this assumption, squashes of the posterior region of the testes from mature male flies were prepared, and the total amount of DNA for a small number of identifiable spermatozoa was determined. All squash preparations of neuroblasts and spermatozoa were treated simultaneously by the standard Feulgen reactions, i.e., 14 minutes of hydrolysis in 1 N HCl at 60°C and staining for two hours in Schiff's reagent. All measurements were made with the optical system used previously.

These more carefully controlled experiments have given results that are essentially the same as those reported in *Year Book 63*. Two classes of diploid metaphases have been found in the ganglia of *Drosophila* larvae: One has a mean value in arbitrary units of 0.02185, the other a value of 0.0110. The haploid or C value for a *Drosophila* sperm

(obtained by readings made on five groups, containing, respectively, 25, 20, 18, 15, and 9 spermatozoa) was 0.0027 arbitrary unit. When the values for the two classes of metaphases were subjected to statistical comparison they were found to be significantly different at the 99 per cent confidence level. On this basis we conclude that metaphases with the lower DNA value, 0.0110, contain the normal diploid amount of DNA (4C in metaphase) for *D. melanogaster* and those with the higher value, 0.02185, are 8C cells containing mitotically functional polynemic chromosomes which have arisen by replication and nonseparation of chromonemata.

One might assume that these 8C metaphase chromosomes were diplochromosomes, composed of four chromatids loosely held together by a single centromere; but they would then be expected to fall apart at anaphase to form a polyploid cell. We have not observed any mitotic figures with more than the normal diploid chromosome number. Our efforts are now being directed to microspectrophotometric measurements of anaphase chromosome groups to determine whether some contain the diploid chromosome number but the 4C amount of DNA.

How could polynemic chromosomes arise? We might postulate that the greater amount of DNA in metaphase chromosomes has arisen by two rounds of replication during a single interphase. Or, alternatively, a normal mitotic cycle might be interrupted at metaphase, whereupon a telophaselike despiralization of chromosomes ensued, followed by a second synthetic interphase. McGrath has reported that under the influence of X rays, early prophase nuclei in grasshopper neuroblasts may be "returned" to an interphaselike condition, and DNA synthesis reinitiated. Radioautographic analysis now in progress of  $H^3$ -thymidine incorporation into mitotic chromosomes of neuroblast cells of *D. melanogaster* may give us a clue to the origin of their polynemic nature.



BASE COMPOSITION OF HETERO-  
CHROMATIC DNA  
IN *Drosophila melanogaster*

Although there has been much discussion about the differences between heterochromatin and euchromatin, these two types of chromosomal materials have not been precisely characterized either cytologically, cytochemically, genetically, or biochemically. Several years ago Sueoko and Cheng described a bimodal distribution of DNA extracted from testes of two species of crab. The two DNAs differed markedly from each other in their base composition, one being essentially an A-T copolymer. This observation might be construed to indicate the existence in a given individual of two kinds of chromosomal DNA. Then T. C. Hsu found that the heterochromatic regions of chromosomes were highly susceptible to breakage by 5-bromodeoxyuridine (BUDR), and has postulated that since the analogue is incorporated into DNA in place of thymine, the heterochromatic regions could be rich in the A-T bases.

With current methods of extraction and characterization of DNA perfected so that analyses of *Drosophila* adults are feasible, provided that sufficient numbers of flies are used, it seemed appropriate to test the hypothesis that heterochromatin differs from euchromatin in base composition. In collaboration with Dr. Kaufmann and W. J. Perreault, we undertook this problem (outlined in *Year Book 63*, pp. 613-614) using *D. melanogaster* in which the proximal heterochromatin (the heteropycnotic regions adjacent to the centromeres) has been carefully identified as a specific fraction of the total mass in each chromosome. For our experimental analysis it was necessary that the flies differed from one another by measurable amounts of heterochromatin. The Y chromosome in *Drosophila* is completely heterochromatic and adult male flies can be obtained that are either XY or XO (the latter without

any Y chromosome). Using a *D. melanogaster* stock in which the X and Y chromosomes had been combined to form a single monocentric structural entity (XY), we could obtain XO and XY males, and XXY females. From other stocks, XY and XX flies were obtainable. These four types (XO, XY, XX, XXY) were used to study the base composition of the DNA in flies that were relatively "heterochromatin rich" and "heterochromatin poor." Approximately 10 grams of flies of each of the four karyotypes were required in each experiment to get a good analyzable yield of DNA.

Table 2 indicates the relative heterochromatic and euchromatic mass of each *D. melanogaster* chromosome and shows how this determines the percentage of heterochromatin within the different types of flies analyzed. As can readily be seen, the maximum difference in amount of heterochromatin between the two extreme classes, namely, XO males and XXY females, is 9.8 per cent (i.e., 31.0 - 21.2). It was believed that if heterochromatic DNA were highly rich in the A-T bases or grossly different in some other respect from euchromatic DNA, it should be detectable by a comparison of these two karyotypes, differing by about 10 per cent in the amount of heterochromatin. Some idea of the limits of the amount of change that could be detected by the methods used among the various karyotypes can be demonstrated in the following way.

If it is assumed that DNA is distributed uniformly throughout the chromosomes, in both heterochromatic and euchromatic segments, then the total guanine + cytosine content ( $\Sigma$ GC), expressed as per cent molar composition, is equal to the sum of the total heterochromatic plus the total euchromatic GC. The total is found by multiplying the per cent molar GC composition of heterochromatin (*het* GC) by the heterochromatic mass as proportion of total chromatin (per cent *het*), shown in Table 2, plus the total euchromatic GC, (*eu* GC)

TABLE 2. Heterochromatin and Euchromatin in *Drosophila melanogaster* and Their Contribution to Classes of Karyotypes, Per Cent

Chromosome	Dimensions, $\mu$	Volume $\times 10^2$	Ratio, $Het/Eu$	Relative Mass Per Chromosome		Heterochromatic and Euchromatic Mass in Karyotype					
				Per Chromosome		XO		XY		XX	
				Het	Eu	Het	Eu	Het	Eu	Het	Eu
X	$1.8 \times 0.3$	12.7	1/2	4.24	8.46	4.24	8.46	4.24	8.46	8.48	16.92
Y	$1.9 \times 0.3$	13.4	1/0	13.40	...	...	...	13.40	...	...	...
II	$2.6 \times 0.3$	18.4	1/4	3.68	14.7	3.68	14.7	...	...	...	...
III	$3.2 \times 0.3$	22.6	1/4	4.50	18.1	16.36	68.40	16.36	68.40	16.36	68.40
IV	$0.2 \times 0.2$	1.4	0/1	...	1.4	...	...	...	...	...	...
Total	...	...	...	...	...	20.60	76.86	34.00	76.86	24.84	85.32
Per Cent	...	...	...	...	...	21.20	78.80	30.80	69.20	22.40	77.60
										31.00	69.00

TABLE 3. Base Composition of DNA from XO, XX, XY, and XXY Flies from Stocks of *Drosophila melanogaster*

Karyotype of DNA analyzed	No. of Determinations	Base Composition, Per Cent					G + C, Per Cent	Het, Per Cent
		Adenine	Guanine	Cytosine	Thymine			
XO	9	$30.4 \pm 0.6$	$20.0 \pm 0.7$	$19.1 \pm 0.7$	$30.5 \pm 0.9$		$39.1 \pm 1.3$	21.2
XX	15	$28.4 \pm 0.1$	$19.1 \pm 0.3$	$21.0 \pm 0.4$	$31.5 \pm 0.2$		$40.1 \pm 0.3$	22.4
XY	23	$29.1 \pm 0.3$	$18.2 \pm 0.2$	$20.4 \pm 0.3$	$32.3 \pm 0.4$		$38.6 \pm 0.3$	30.8
<u>XXY</u>	18	$30.0 \pm 0.3$	$21.0 \pm 0.5$	$19.0 \pm 0.3$	$30.0 \pm 0.3$		$40.0 \pm 0.5$	31.0



(per cent *eu*), expressed in the same terms as used for total heterochromatic GC, or

$$\Sigma(\text{GC}) = (\text{het GC})(\text{per cent het}) + (\text{eu GC})(\text{per cent eu}) \quad (1)$$

It is sometimes assumed, however, that heterochromatin is more dense and contains more DNA per unit volume than euchromatin. If this is true, the error of omitting a factor for density of DNA in Equation 1 would introduce a bias tending to reduce the observable differences in base composition between any two karyotypes, since our estimate on the amount of heterochromatic DNA would be low.

If eu- and heterochromatin contain DNA with essentially the same base composition, then  $\Sigma(\text{GC})\text{XO} = \Sigma(\text{GC})\text{XY} = \Sigma(\text{GC})\text{XXY}$ . On the other hand, if there is a real difference in the GC composition between euchromatin and heterochromatin,  $\text{het GC} = \text{eu GC} \pm \Delta(\text{GC})$ , and the change in  $\Sigma\text{GC}$  composition introduced by the difference in amount of heterochromatin would be the per cent difference in the heterochromatic mass of the two karyotypes times the  $\Delta(\text{GC})$ , or

$$\begin{aligned} \Sigma(\text{GC}) \text{ karyotype } A - \\ \Sigma(\text{GC}) \text{ karyotype } B = \\ (\text{per cent het } A - \\ \text{per cent het } B) (\Delta\text{GC}) \quad (2) \end{aligned}$$

and substituting values from Table 2 yields

$$\begin{aligned} \Sigma(\text{GC})\text{XXY} - \Sigma(\text{GC})\text{XO} &= 9.8\% (\Delta\text{GC}) \\ \Sigma(\text{GC})\text{XY} - \Sigma(\text{GC})\text{XO} &= 9.6\% (\Delta\text{GC}) \\ \Sigma(\text{GC})\text{XY} - \Sigma(\text{GC})\text{XX} &= 8.4\% (\Delta\text{GC}) \end{aligned}$$

Since the experimental error in most base analyses is  $\pm 2$  per cent, we can determine that a difference in GC content between heterochromatin and euchromatin of 20.4 per cent would be apparent in the comparison between XO and XXY flies. Our analyses have been refined so

that an error no greater than  $\pm 1$  per cent is expected, and we may therefore state that a 10.2 per cent change in GC content would be detected.

Results of the analyses of DNA extracted from the four types of flies described, using a modification of the method of Mead, are summarized in Table 3. No significant differences in GC values were obtained. The grand mean of GC content for all measurements made is 39.7 per cent and the average deviation from this mean was 0.7 per cent for the various karyotypes tested. The *t*-test evaluation of the mean GC content for the  $\text{XXY} - \text{XO}$  (0.9 per cent) and the  $\text{XY} - \text{XO}$  (0.7 per cent) reveals no significant difference ( $p = 0.05$ ) in GC content.

If for purposes of discussion we take the observed difference of 0.9 per cent between the GC values of the  $\text{XXY}$  flies and XO flies to determine the  $\overline{\text{GC}}$  difference between euchromatin and heterochromatin that this would indicate, we find that the  $\Delta\text{GC} = 9.2$  per cent (using Equation 2), and heterochromatic GC would have to be  $40 \pm 6.3$  per cent (using Equation 1). We can consequently conclude from our observed values of base composition of  $\text{XXY}$  and XO flies that in *Drosophila*, heterochromatin cannot be more than 66.3 per cent A-T when euchromatin is 57.1 per cent A-T.

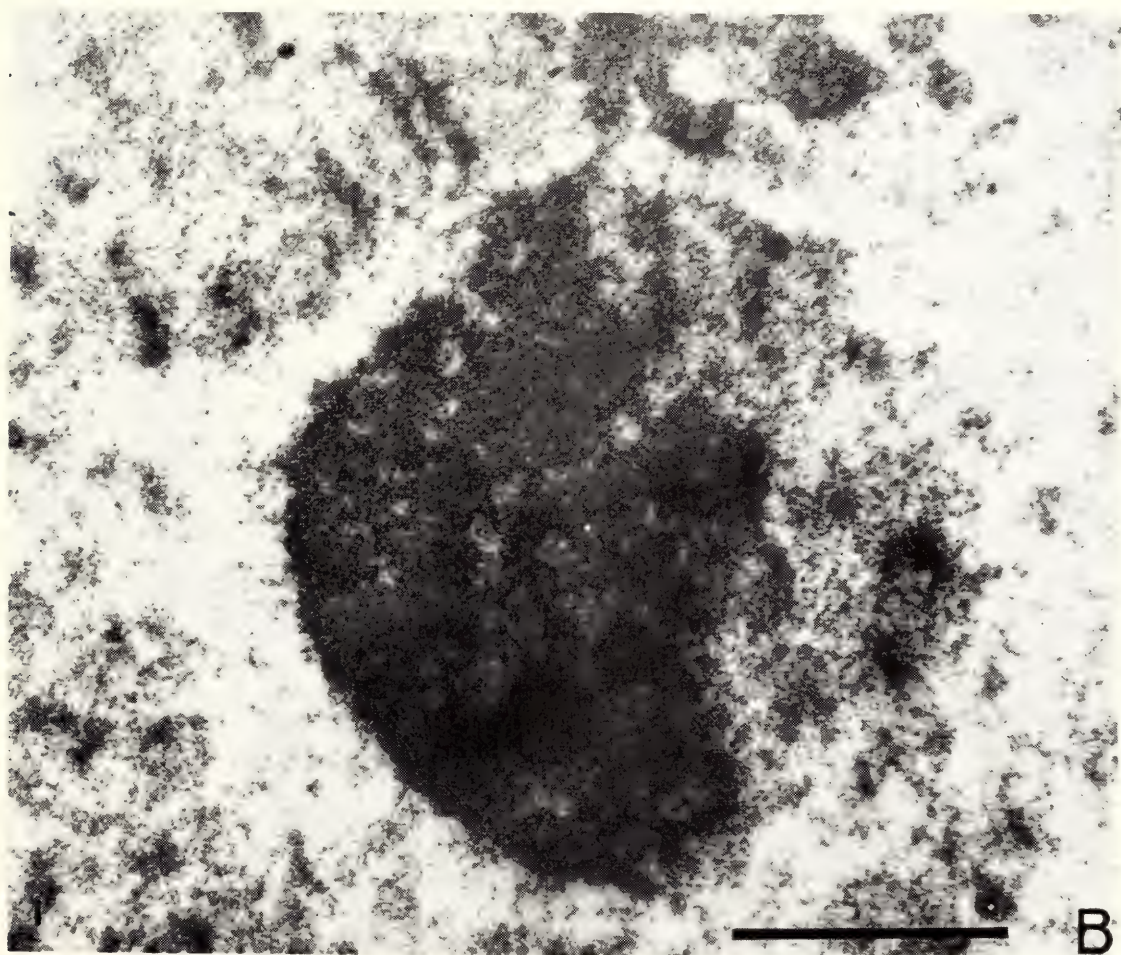
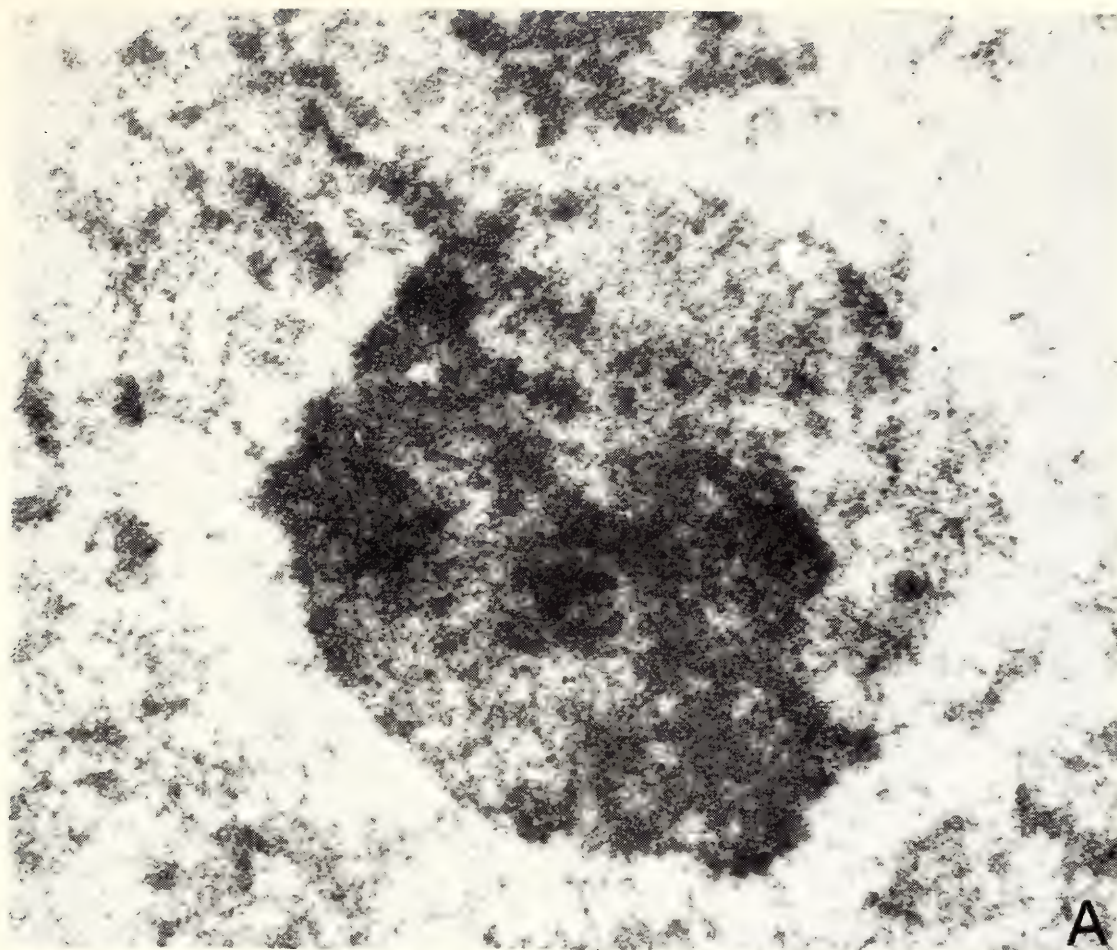
These rather extensive analyses of base composition of DNAs of various classes of *Drosophila* containing different amounts of heterochromatin show that large differences in base composition (such as a high preponderance of A-T) are not characteristic of the heterochromatin of *D. melanogaster*. In fact, the guanine + cytosine composition of heterochromatin does not differ by more than about 10 per cent from that of the euchromatin.

## BIBLIOGRAPHY

- Das, C. C., B. P. Kaufmann, and H. Gay, Autoradiographic evidence of synthesis of an arginine-rich histone during spermiogenesis in *Drosophila melanogaster*, *Nature*, 204, 1008-1009, 1964.
- Gay, H., New evidence on chromosome structure and function (abstract), *Science*, 146, 425, 1964; see also Das, C. C., Maruyama, K.; Sparvoli, E.
- Kaufmann, B. P., see Das, C. C., Maruyama, K.; Sparvoli, E.
- Maruyama, K., H. Gay, and B. P. Kaufmann, The nature of the wall between generative and vegetative nuclei in the pollen grain of *Tradescantia paludosa*, *Am. J. Botany*, 52, 607-610, 1965.
- Sparvoli, E., H. Gay, and B. P. Kaufmann, Open-face epoxy embedding of single cells for ultrathin sections, *Stain Technol.*, 40, 83-88, 1965.
- Sparvoli, E., H. Gay, and B. P. Kaufmann, Number and pattern of association of chromonemata in the chromosomes of *Tradescantia*, *Chromosoma*, 16, 415-435, 1965.



Plate 1. Two transverse serial sections through a salivary-gland chromosome from a third-instar larva of *D. melanogaster*, fixed in 2% buffered osmium tetroxide, pH 7.0. Complete series of 12 sections shows that plane of sectioning has passed successively through an interband region, a band, and the next interband; *A* and *B* represent 6th and 7th sections in the series with *B* traversing the dense-band region. Solid line indicates 1  $\mu$ .





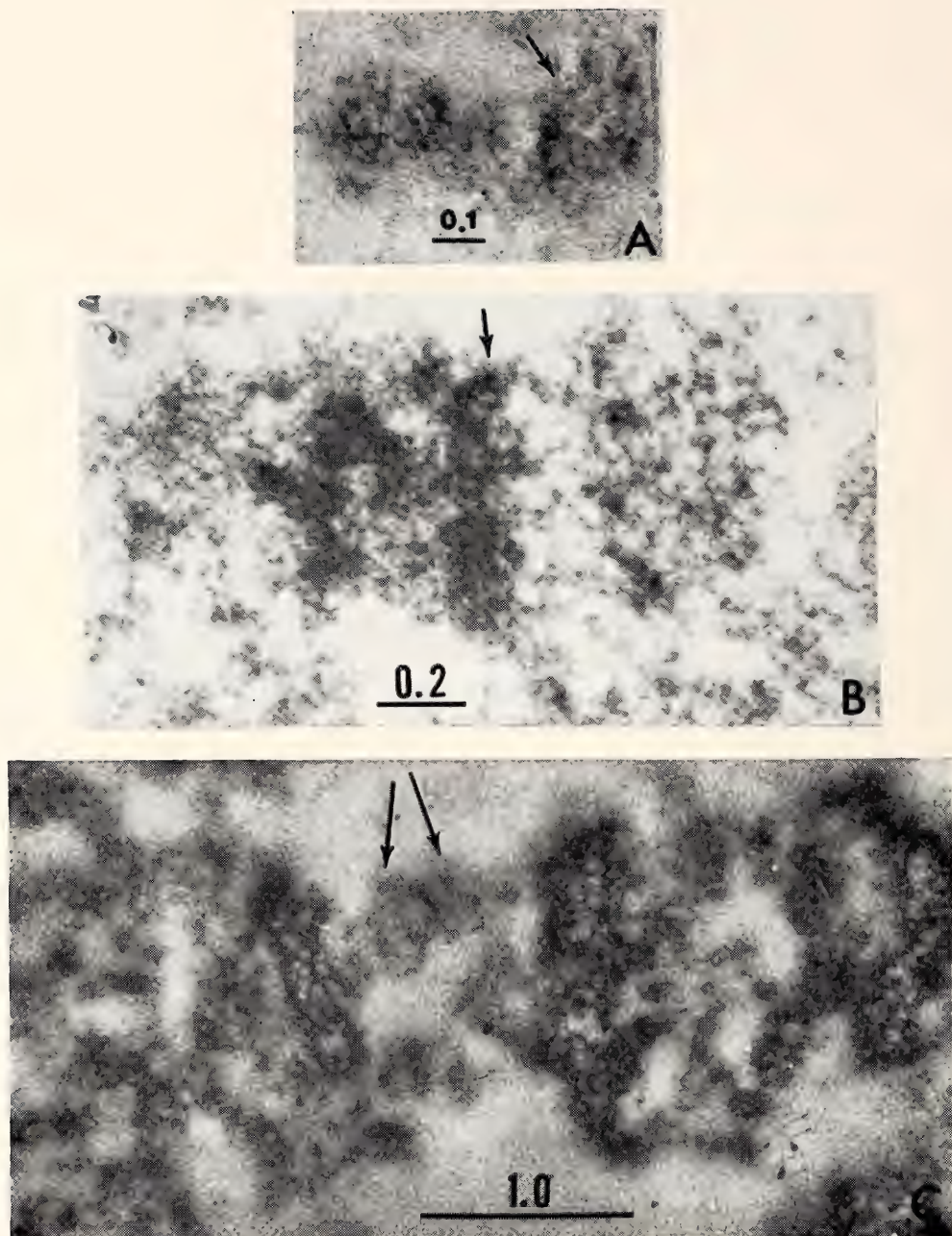


Plate 2. Banding pattern within chromonemata of the *Drosophila* salivary glands from first-, second-, and third-instar larvae. Arrows indicate bands; solid lines indicate  $\mu$  values.

A. Chromosome from a first-instar salivary gland fixed in Ernst's fluid. At this stage fine bands appear to be made up of subchromonemata.

B. Chromosome from a second-instar salivary-gland nucleus fixed in 2% buffered osmium tetroxide. Band formation across entire width of chromosome begins to appear.

C. Clearly defined chromonemata within chromosome of a third-instar salivary gland, fixed in Ernst's fluid; a fine banding pattern is demonstrated.



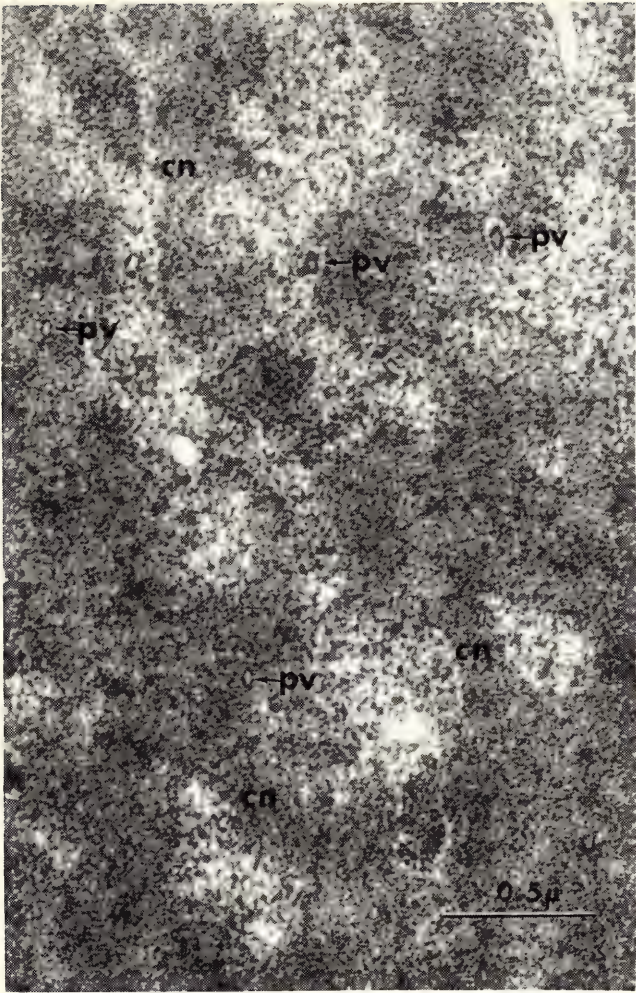


Plate 3. Part of an early telophase nucleus from a *Tradescantia* staminate-hair cell fixed in 1% buffered osmium tetroxide, pH 7.4, with postfixation treatment in uranyl acetate. Some of the pv are surrounded by a clear zone, others are not; pv = perichromatin vesicles, cn = chromonemata.

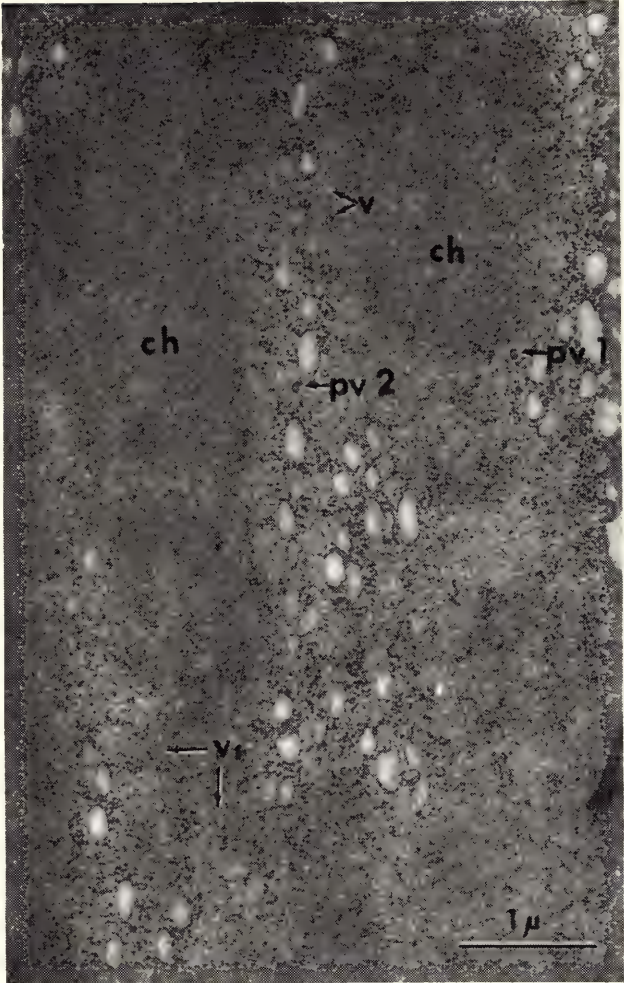


Plate 4. Small part of a late anaphase nucleus fixed in 1% osmium tetroxide buffered at pH 7.4 and posttreated with uranyl acetate. The late anaphase is shown in entirety in Fig. 4 of *Year Book 63*, following p. 614; pv 1 = pv associated with the chromosome (ch); pv 2 = pv lying in the cytoplasm between two chromosomes and very close to vesicles of the ER, which are in process of nuclear membrane formation; v = vesicles of uncertain origin; v<sub>1</sub> = similar to v but clearly associated with chromatin.



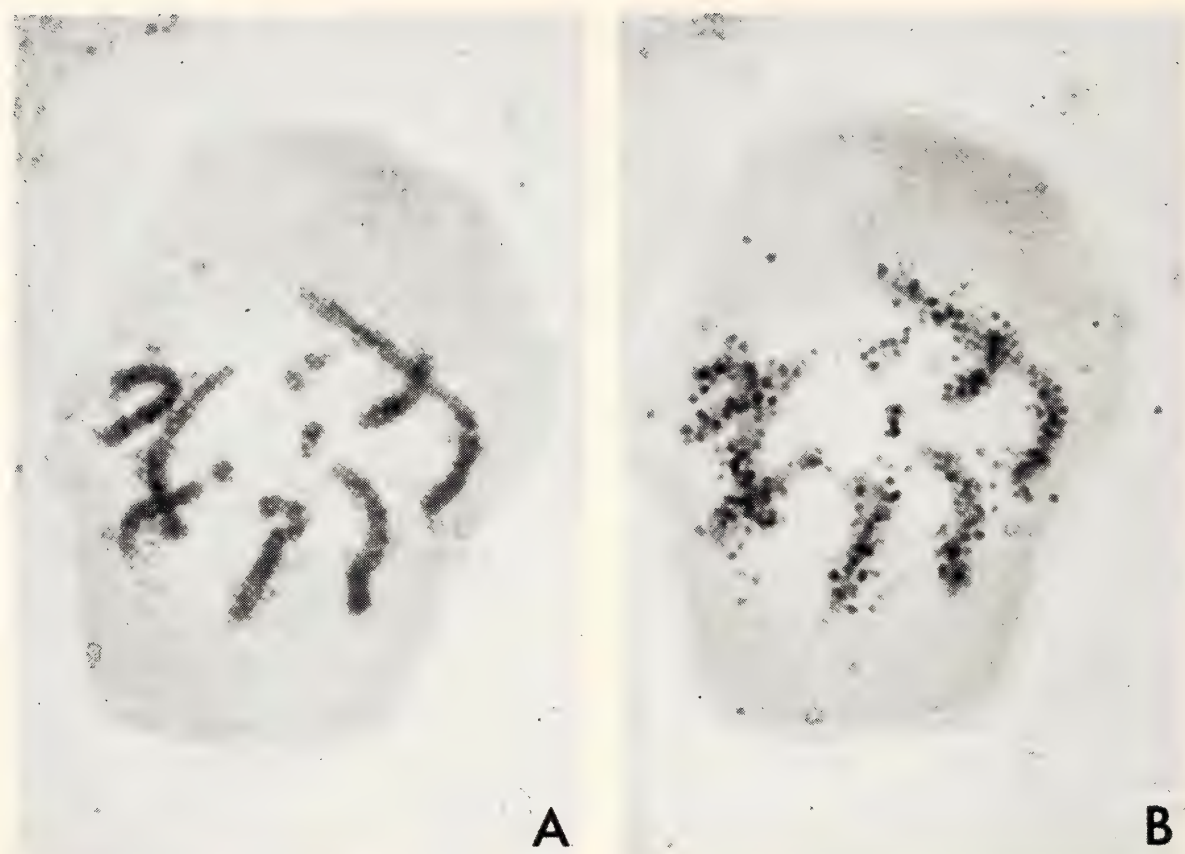


Plate 5. First anaphase chromosomes showing silver grains distributed throughout the chromosome. *A*, Focus on the chromosomal level; *B*, focus on the overlying silver grains.



Plate 6. *A*, Third prophase chromosomes after labeling with  $H^3$ -thymidine revealing in more detail segregation of label that occurred in the second division; *B*, diagram of label distribution.  $A_1 A_2 A_3 A_4$  show a twin exchange.  $A_5 A_6 A_7 A_8$  show twin isolabeling in short arm and one occurrence of single isolabeling in long arm.





# Bibliography

July 1, 1964–June 30, 1965

## PUBLICATIONS OF THE INSTITUTION

*Year Book 63, 1963–1964.* Octavo, xi + 73 + 661 pp., 33 plates, 293 figs. Dec. 1964.

609. Shepard, Anna O., *Ceramics for the Archaeologist*. 5th printing, Washington, D.C., Kirby Lithographic Co., Sept. 1965.

624. Roberts, Richard B., ed., *Studies of Macromolecular Biosynthesis*. Octavo, xiii + 702 pp. Illus. Colored frontispiece. Baltimore, Md., Garamond/Pridemark Press, Aug. 1964.

*Drosophila Guide: Introduction to the Genetics and Cytology of Drosophila melanogaster*. 7th edition, 4th printing, M. Demerec and B. P. Kaufmann, in collaboration with Jennie S. Buchanan (curator), Agnes C. Fisher (editor), and Henry H. Jones (photographer). Octavo, iii + 44 pp. 14 figs. Aug. 1965.

## PUBLICATIONS BY THE PRESIDENT

Caryl P. Haskins

Report of the President. *Carnegie Institution of Washington Year Book 63*, pp. 1–73, 5 plates. Carnegie Institution of Washington, Washington, D. C., Dec. 1964. Reprinted under title "The Changing Environments of Science," *Daedalus, Journal of the American Academy of Arts and Sciences*, summer 1965, pp. 682–712. Excerpts reprinted under title "The Evolution of Science," *Science*, Vol. 148, No. 3671, May 1965, p. 37.

Preface to *Studies of Macromolecular Biosynthesis*, Richard B. Roberts, ed., pp. iii–vi. Carnegie Institution of Washington Publication 624. Carnegie Institution of Washington, Washington, D. C., Aug. 1964.

Science in Red China: the enigmatic dragon (excerpt from *The Scientific Revolution and World Politics*), *Air Force and Space Digest*, Vol. 47, No. 8, Aug. 1964, pp. 60–63.

Contemporary science and American policy (excerpt from Walter E. Edge Lectures at Princeton Univ., Mar. 1964), "Men With Ideas," *International Science and Technology*, Sept. 1964, p. 100.

Some thoughts on our scientific revolution (Commencement address given at the University of Delaware, June 1965), *Four Significant Addresses Given at the University of Delaware in the Academic Year 1964–1965. The Scientific Revolution and World Politics* (see *Year Book 63*, p. 615), translated into Japanese by Morinosuke Kajima. Kajima Institute Publishing Co., Ltd., 1965.

With Roy M. Whelden, "Queenlessness," worker sibship, and colony versus population structure in the Formicid genus *Rhytidoponera*, *Psyche*, Vol. 72, No. 1, Mar. 1965, pp. 87–112.

With Edna F. Haskins, Notes on the biology and social behavior of *Myrmecia inquilina*, the only known myrmecine social parasite, *Insectes Sociaux*, Vol. 11, No. 3, 1964, pp. 267–282.

## PUBLICATION BY THE EXECUTIVE OFFICER

Edward A. Ackerman

California State Development Program. Progress report and summary interpretation of phase I studies. 39 pp., 31 illus., 8 tables. Department of Finance, State Office of Planning, Sacramento, Calif., Feb. 1965.





# Report of the Executive Committee

*To the Trustees of the Carnegie Institution of Washington*

Gentlemen: In accordance with the provisions of the By-Laws, the Executive Committee submits this report to the Annual Meeting of the Board of Trustees.

During the fiscal year ending June 30, 1965, the Executive Committee held four meetings. Printed accounts of these meetings have been or will be mailed to each Trustee.

The estimate of expenditures for the fiscal year beginning July 1, 1965, has been reviewed by the Executive Committee.

The terms of office of the Chairmen of all Committees of the Board expire on May 7, 1965. The terms of the following members of Committees also expire on May 7, 1965:

*Executive Committee*

Robert A. Lovett  
James N. White

*Retirement Committee*

Omar N. Bradley  
Henry S. Morgan

*Finance Committee*

Richard S. Perkins  
Elihu Root, Jr.  
James N. White

*Nominating Committee*

Charles P. Taft

HENRY S. MORGAN, *Chairman*

*May 7, 1965*





# *Report of Auditors*

LYBRAND, ROSS BROS. & MONTGOMERY

To the Auditing Committee of Carnegie Institution of Washington:

We have examined the statement of assets, liabilities and fund balances of Carnegie Institution of Washington as of June 30, 1965, and the related summary statement of changes in funds for the year then ended and the supporting exhibits and schedules, which have been prepared on the general basis of cash receipts and disbursements and accordingly do not reflect accrued income, accounts payable nor provision for depreciation. Our examination was made in accordance with generally accepted auditing standards, and accordingly included confirmation from the custodian of securities owned at June 30, 1965, and such tests of the accounting records and such other auditing procedures as we considered necessary in the circumstances. We previously examined and reported upon the financial statements of the Institution for the year ended June 30, 1964.

In our opinion, the accompanying financial statements and supporting exhibits and schedules present fairly the assets, liabilities and fund balances of Carnegie Institution of Washington at June 30, 1965 and 1964, and the changes in funds for the year ended June 30, 1965, on the basis described above consistently applied.

LYBRAND, ROSS BROS. & MONTGOMERY

Washington, D. C.  
August 6, 1965



STATEMENT A      ASSETS, LIABILITIES, AND FUND BALANCES  
JUNE 30, 1965 AND 1964

	June 30	
	<u>1965</u>	<u>1964*</u>
ASSETS		
Cash . . . . .	\$ 796,075.17	\$ 1,029,415.87
Advances . . . . .	44,239.59	32,419.60
Investments, Schedule 2:**		
Savings account . . . . .	591,277.86	1,467,277.86
Mortgage . . . . .	22,893.74	24,832.19
Governmental obligations . . . . .	8,294,830.90	4,796,803.27
Nongovernmental bonds . . . . .	38,754,878.48	35,972,475.22
Corporate stocks . . . . .	28,488,461.76	29,627,959.68
Land (at cost) . . . . .	362,147.71	312,647.71
Buildings and equipment (at cost) . . . . .	5,993,736.61	5,839,977.33
Prepaid insurance . . . . .	27,283.08	30,286.22
	<hr/>	<hr/>
Total Assets . . . . .	\$83,375,824.90	\$79,134,094.95
	<hr/>	<hr/>
LIABILITIES AND FUNDS		
Liabilities:		
Income taxes, etc., withheld . . . . .	\$ 6,411.37	\$ 11,216.05
	<hr/>	<hr/>
Funds:		
Operating Funds, Exhibit 1 . . . . .	\$ 1,466,308.04	\$ 1,398,333.47
Restricted Grants, Exhibit 2 . . . . .	153,086.94	95,596.65
Endowment and Special Funds, Exhibit 3 . . . . .	75,394,134.23	71,476,323.74
Land, Buildings, and Equipment Fund, Exhibit 4 . . . . .	6,355,884.32	6,152,625.04
	<hr/>	<hr/>
Total Funds . . . . .	\$83,369,413.53	\$79,122,878.90
	<hr/>	<hr/>
Total Liabilities and Funds . . . . .	\$83,375,824.90	\$79,134,094.95
	<hr/>	<hr/>

\*Assets for the fiscal year ended June 30, 1964, have been reclassified to conform with the current year's presentation.

\*\*Approximate market value at June 30, 1965: \$105,577,591.

STATEMENT B

SUMMARY STATEMENT OF CHANGES IN FUNDS

FOR THE YEAR ENDED JUNE 30, 1965

	Operating Funds (Exhibit 1)	Restricted Grants (Exhibit 2)	Endowment & Special Funds (Exhibit 3)	Land, Buildings, & Equipment (Exhibit 4)	Total
Balance July 1, 1964.....	\$ 1,398,333.47	\$ 95,596.65	\$ 71,476,323.74	\$ 6,152,625.04	\$ 79,122,878.90
Additions:					
Realized capital gain, net .....	.....	.....	\$ 3,812,937.63	.....	\$ 3,812,937.63
Investment income .....	.....	.....	3,721,583.79	.....	3,721,583.79
Restricted grants .....	.....	\$ 519,712.86	.....	.....	519,712.86
Sales of publications .....	.....	.....	16,703.88	.....	16,703.88
Other income and gifts .....	.....	.....	41,524.81	.....	41,524.81
Expenditures capitalized					
Current year .....	.....	.....	.....	\$ 222,129.65	222,129.65
Prior year .....	.....	.....	.....	62.54	62.54
By transfer					
Appropriations, July 1, 1964, to June 30, 1965 .....	\$ 3,662,852.00	.....	(3,662,852.00)	.....	.....
Bush Gift .....	6,718.17	.....	(6,718.17)	.....	.....
Bush Trust .....	5,369.45	.....	(5,369.45)	.....	.....
	\$ 3,674,939.62	\$ 519,712.86	\$ 3,917,810.49	\$ 222,192.19	\$ 8,334,655.16
Deductions:					
Expenditures .....	\$ 3,606,965.05	\$ 462,222.57	.....	.....	\$ 4,069,187.62
Disposition of equipment .....	.....	.....	.....	\$ 18,932.91	18,932.91
	\$ 3,606,965.05	\$ 462,222.57	.....	\$ 18,932.91	\$ 4,088,120.53
Net change during year .....	\$ 67,974.57	\$ 57,490.29	\$ 3,917,810.49	\$ 203,259.28	\$ 4,246,534.63
Balance June 30, 1965 .....	\$ 1,466,308.04	\$ 153,086.94	\$ 75,394,134.23	\$ 6,355,884.32	\$ 83,369,413.53



## EXHIBIT 1

CHANGES IN OPERATING FUNDS  
FOR THE YEAR ENDED JUNE 30, 1965

Balance July 1, 1964 .....		\$1,398,333.47
<u>Additions, Statement B:</u>		
Transfers		
Appropriations, July 1, 1964, to		
June 30, 1965, Exhibit 3 .....	\$3,662,852.00	
Bush Gift .....	6,718.17	
Bush Trust .....	5,369.45	3,674,939.62
		<hr/>
Total Available for Expenditure ...		\$5,073,273.09
 <u>Expenditures:</u>		
Salaries .....	\$1,862,198.93	
Employee benefits .....	331,527.05	
Laboratory .....	324,680.03	
Operating .....	204,911.43	
Equipment .....	195,797.34	
Fellowship program .....	194,067.04	
Building .....	100,697.79	
Financial advisory services .....	76,749.49	
Travel .....	71,915.22	
Publications .....	70,616.18	
Consulting fees, insurance .....	41,831.38	
Taxes .....	40,359.01	
Awards .....	38,098.90	
Rent .....	26,195.00	
Shop .....	20,134.96	
Dormitory .....	7,185.30	
		<hr/>
Total Expenditures .....		3,606,965.05
		<hr/>
Balance June 30, 1965 .....		\$1,466,308.04
		<hr/>

EXHIBIT 2

CHANGES IN RESTRICTED GRANTS

FOR THE YEAR ENDED JUNE 30, 1965

	Balance		Expenditures & Transfers			Balance	
	July 1, 1964	Grants	Salaries	Other		June 30, 1965	
American Cancer Society . . . . .	. . . . .	\$ 500.00	. . . . .	\$ 334.97	\$	165.03	
American Geophysical Union . . . . .	. . . . .	7,000.00	\$ 7,000.00	. . . . .	. . . . .	. . . . .	
Anonymous . . . . .	\$14,500.00	. . . . .	. . . . .	. . . . .	. . . . .	14,500.00	
Carnegie Corporation of New York . . . . .	36,502.21	95,000.00	. . . . .	45,625.92	. . . . .	85,876.29	
Arthur L. Day Library . . . . .	7,457.16	3,938.00	. . . . .	10,671.51	. . . . .	723.65	
Holt, Rinehart & Winston, Inc. . . . .	1,880.00	2,000.00	. . . . .	1,517.80	. . . . .	2,362.20	
International Council of Scientific Unions . . . . .	. . . . .	2,000.00	. . . . .	2,000.00	. . . . .	. . . . .	
Charles F. Kettering Foundation . . . . .	15,500.00	. . . . .	. . . . .	13,749.97	. . . . .	1,750.03	
National Science Foundation . . . . .	19,437.81	343,000.00	. . . . .	327,765.46	. . . . .	34,672.35	
Office of Naval Research . . . . .	. . . . .	414.30	. . . . .	414.30	. . . . .	. . . . .	
Organogenesis Conference . . . . .	. . . . .	13,511.56	. . . . .	13,511.56	. . . . .	. . . . .	
U. S. Public Health Service . . . . .	319.47	52,349.00	23,437.50	16,193.58	. . . . .	13,037.39	
Total . . . . .	\$95,596.65	\$519,712.86	\$30,437.50	\$431,785.07		\$153,086.94	



EXHIBIT 3

CHANGES IN ENDOWMENT AND SPECIAL FUNDS  
FOR THE YEAR ENDED JUNE 30, 1965

	Balance July 1, 1964	Realized Capital Gain, net	Investment Income	Other Income	Appropriations	Transfers	Balance June 30, 1965
<u>Endowment Fund:</u>							
Gifts							
Andrew Carnegie	\$22,000,000.00	.....	.....	.....	.....	.....	\$22,000,000.00
Carnegie Corporation of New York	10,000,000.00	.....	.....	.....	.....	.....	10,000,000.00
Realized capital gain, net	27,350,488.78	\$3,194,304.81	.....	.....	.....	.....	30,544,793.59
Unrestricted Capital Fund							
Gifts	71,527.81	.....	.....	\$ 6,700.01	.....	.....	78,227.82
Realized capital gain, net	4,455,936.50	583,476.56	.....	.....	.....	\$ 97,149.50	5,136,562.56
Income							
Andrew Carnegie, Reserve	2,500,000.00	.....	.....	.....	.....	.....	2,500,000.00
Other	604,201.60	.....	.....	34,824.80	.....	(100,197.11)	538,829.29
Working Capital Fund							
Income	3,753,800.79	.....	\$3,687,094.20	16,703.88	\$3,619,808.00	3,047.61	3,840,838.48
<u>Special Funds:</u>							
Bush Gift	3,707.54	2,116.16	2,141.47	.....	1,247.00	(6,718.17)	.....
Bush Trust	3,461.29	1,466.72	1,605.44	.....	1,164.00	(5,369.45)	.....
Colburn	197,811.27	9,553.76	9,302.41	.....	30,172.00	.....	186,495.44
Hale Relief	6,673.87	345.88	336.78	.....	187.00	.....	7,169.53
Harkavy	8,645.06	416.98	406.00	.....	171.00	.....	9,297.04
Teeple	17,518.00	930.86	906.37	.....	408.00	.....	18,947.23
Wood	502,551.23	20,325.90	19,791.12	.....	9,695.00	.....	532,973.25
Total	\$71,476,323.74	\$3,812,937.63	\$3,721,583.79	\$58,228.69	\$3,662,852.00	(\$ 12,087.62)	\$75,394,134.23

CHANGES IN LAND, BUILDINGS, AND EQUIPMENT FUND  
FOR THE YEAR ENDED JUNE 30, 1965

Classification of June 30, 1965 Balance								
	Balance July 1, 1964	Expenditures*	Deductions	Balance June 30, 1965	Land	Buildings	Library	Equipment
Departmental Research Operations:								
Department of Plant Biology								
Stanford, California.....	\$ 203,890.99	\$ 10,505.32	.....	\$ 214,396.31	.....	\$ 75,802.76	\$ 35,230.34	\$ 103,363.21
Geophysical Laboratory								
Washington, D. C. ....	702,060.87	55,966.42	\$13,987.53	744,039.76	\$ 22,907.27	147,476.52	85,729.66	487,926.31
Mount Wilson Observatory								
Pasadena, California .....	1,737,099.13	6,676.56	.....	1,743,775.69	27,278.87	288,211.32	102,172.12	1,326,113.38
Department of Terrestrial Magnetism								
Washington, D. C. ....	1,066,769.99	45,949.35	3,339.13	1,109,380.21	74,449.98	326,631.31	60,665.96	647,632.96
Department of Embryology								
Baltimore, Maryland .....	237,190.67	34,362.52	.....	271,553.19	.....	.....	19,929.09	251,624.10
Total Departmental Research Operations .....	\$3,947,011.65	\$153,460.17	\$17,326.66	\$4,083,145.16	\$124,636.12	\$ 838,121.91	\$303,727.17	\$2,816,659.96
Genetics Research Units								
Long Island, N. Y., and								
Ann Arbor, Michigan .....	1,261,579.95	10,241.36	1,606.25	1,270,215.06	31,925.54	964,465.47	105,065.38	168,758.67
Office of Administration								
Washington, D. C. ....	944,033.44	58,490.66	.....	1,002,524.10	205,586.05	689,943.49	.....	106,994.56
Total .....	\$6,152,625.04	\$222,192.19	\$18,932.91	\$6,355,884.32	\$362,147.71	\$2,492,530.87	\$408,792.55	\$3,092,413.19
*Current expenditures for equipment								
Operating Funds .....		\$195,797.34						
Restricted Grants .....		4,832.31						
Expenditures capitalized								
Current year .....		21,500.00						
Prior year .....		62.54						
Total .....		\$222,192.19						



SCHEDULE 1

BUDGET SUMMARY OF OPERATING FUNDS  
FOR THE YEAR ENDED JUNE 30, 1965

Disposition of Total Appropriations									
	Unexpended Appropriations					Reserved for Liabilities			
	Unexpended Appropriations July 1, 1964	Budget Approp- riation for Fiscal Year Ended June 30, 1965	Transfers and Allotments	Total Appropriations	Total Expenditures	Transferred to Unallo- cated Appro- priations Fund	Unallocated Appropriations Fund	Commit- ments and	
								Unallocated	
								Appropriations	
Departmental Research Operations:									
Department of Plant Biology	\$ 6,817.62	\$ 151,145.00	\$ 4,400.00	\$ 162,362.62	\$ 148,570.80	\$ 8,604.89	\$ 5,186.93		
Geophysical Laboratory	35,635.88	502,400.00	43,958.34	581,994.22	529,344.14	520.61	52,129.47		
Mt. Wilson Observatory	74,353.93	561,200.00	4,887.11	640,441.04	565,530.52	23,687.46	51,223.06		
Department of Terrestrial Magnetism	92,798.52	562,000.00	34,211.98	689,010.50	590,002.41	16,518.56	82,489.53		
Department of Embryology	13,136.42	458,780.00	.....	471,916.42	422,396.02	19,459.71	30,060.69		
Total Departmental Research Operations	\$ 222,742.37	\$ 2,235,525.00	\$ 87,457.43	\$ 2,545,724.80	\$ 2,255,843.89	\$ 68,791.23	\$ 221,089.68		
Nondepartmental Research Operations:									
Genetics Research Units	\$ 1,624.07	\$ 136,480.00	\$ 2,250.00	\$ 140,354.07	\$ 128,233.28	\$ 8,024.64	\$ 4,096.15		
Fellowship program	178,659.09	150,000.00	.....	328,659.09	194,067.04	130,225.35	4,366.70		
Research projects, etc.	94,561.88	50,750.00	52,139.78	197,451.66	88,253.20	3,161.27	106,037.19		
Total Nondepartmental Research Operations	\$ 274,845.04	\$ 337,230.00	\$ 54,389.78	\$ 666,464.82	\$ 410,553.52	\$ 141,411.26	\$ 114,500.04		
Administration	3,343.06	309,100.00	43,574.62	356,017.68	350,640.84	.....	5,376.84		
Contingent operating fund	115,894.36	215,000.00	(182,121.55)	148,772.81	.....	148,772.81	.....		
Employee benefits	219,929.14	351,704.00	35,523.94	607,157.08	331,527.05	7,974.91	267,655.12		
Financial advisory services	14,894.34	76,000.00	1,175.78	92,070.12	76,749.49	.....	15,320.63		
General publications	45,163.63	30,000.00	.....	75,163.63	43,750.09	4,331.45	27,082.09		
Consulting fees, insurance, taxes	127.01	96,000.00	.....	96,127.01	82,190.39	10,419.35	3,517.27		
Total	\$ 896,938.95	\$ 3,650,559.00	\$ 40,000.00	\$ 4,587,497.95	\$ 3,551,255.27	\$ 381,701.01	\$ 654,541.67		
Special funds	126,251.98	12,293.00	2,087.62	140,632.60	55,709.78	.....	84,922.82		
Unallocated appropriations fund	375,142.54	.....	(30,000.00)	345,142.54	.....	(381,701.01)	726,843.55		
Total	\$ 1,398,333.47	\$ 3,662,852.00	\$ 12,087.62	\$ 5,073,273.09	\$ 3,606,965.05	.....	\$ 1,466,308.04		

SCHEDULE 2

INVESTMENTS, JUNE 30, 1965  
AND INTEREST AND DIVIDENDS INCOME RECEIVED DURING YEAR

	Percentage of Total Investments			
	Approximate Market Value		Approximate Market Value	
	Book Value		Book Value	Income Received
<u>Savings Account:</u>				
The New York Bank for Savings .....	\$ 591,277.86		\$ 591,278.00	.78 .56 \$ 39,067.66
<u>Mortgage:</u>				
Alfred D. & Harriet D. Hershey .....	\$ 22,893.74		\$ 22,894.00	.03 .02 \$ 1,317.39
<u>Bonds:</u>				
Federal agencies and U. S. Government .....	\$ 8,294,830.90		\$ 8,310,644.00	10.89 7.87 \$ 268,110.29
Foreign and International Bank .....	6,581,802.18		6,539,238.00	8.64 6.19 275,540.88
Public utilities .....	8,808,927.64		8,364,748.00	11.57 7.92 366,165.06
Communication .....	3,442,959.97		3,120,000.00	4.52 2.96 126,928.10
Railroad .....	367,977.67		332,793.00	.48 .32 16,088.89
Industrial and miscellaneous .....	19,553,211.02		19,490,943.00	25.68 18.46 803,584.79
Total Bonds .....	\$47,049,709.38		\$ 46,158,366.00	61.78 43.72 \$1,856,418.01*
<u>Stocks:</u>				
Preferred .....	\$ 1,356,239.80		\$ 1,272,050.00	1.78 1.20 \$ 67,425.00
Common .....	27,132,221.96		57,533,003.00	35.63 54.50 1,757,355.73
Total Stocks .....	\$28,488,461.76		\$ 58,805,053.00	37.41 55.70 \$1,824,780.73
Total .....	\$76,152,342.74		\$105,577,591.00	100.00 100.00 \$3,721,583.79

\*After deducting bond premium amortization of \$9,207.35.



# SCHEDULE OF INVESTMENTS

<u>Principal Amount</u>	<u>Description</u>	<u>Matu- rity</u>	<u>Book Value</u>	<u>Approximate Market Value</u>
Savings Account				
\$ 591,277.86	The New York Bank for Savings . . . . .	...	\$ 591,277.86	\$ 591,278
Mortgage				
\$ 22,893.74	Alfred D. Hershey and Harriet D. Hershey, 5½s . . . . .	1974	\$ 22,893.74	\$ 22,894
Federal Agencies and United States Government Bonds				
\$ 400,000	Federal Farm Loan Consolidated, 4¾s . . . . .	1969	\$ 394,000.00	\$ 399,500
285,000	Federal Farm Loan Consolidated, 4½s . . . . .	1970	284,330.96	285,713
1,025,000	Federal National Mortgage Association, 4½s . . . . .	1970	1,015,070.31	1,010,906
465,000	Federal National Mortgage Association, 4½s . . . . .	1971	465,686.94	458,606
400,000	Federal National Mortgage Association, 4½s . . . . .	1970	394,500.00	403,500
500,000	Federal National Mortgage Association, 5½s . . . . .	1972	498,125.00	518,750
2,638,000	United States of America, Treasury Bonds, 4s . . . . .	1969	2,633,978.62	2,629,756
780,000	United States of America, Treasury Bonds, 4s . . . . .	1970	780,000.00	775,613
720,000	United States of America, Treasury Bonds, 4s . . . . .	1971	714,984.38	714,600
1,120,000	United States of America, Treasury Bonds, 4½s . . . . .	1973	1,114,154.69	1,113,700
\$8,333,000	Total Federal Agencies and United States Government Bonds		\$8,294,830.90	\$8,310,644
Foreign and International Bank Bonds				
\$ 700,000	Alberta Government Telephone Commission, Deb., 4¾s . . . . .	1989	\$ 700,000.00	\$ 700,000
750,000	Alcan Aluminum Corporation, Prom. Note, 4¾s . . . . .	1984	750,000.00	750,000
489,000	Aluminium Co. of Canada, Ltd., S. F. Deb., 4½s . . . . .	1980	496,018.84	481,665
146,000	Australia (Commonwealth of), 4½s . . . . .	1971	143,810.00	143,993
119,000	Australia (Commonwealth of), 5s . . . . .	1972	119,000.00	117,959
483,000	Australia (Commonwealth of), 5½s . . . . .	1982	485,576.09	478,170
750,000	Bell Telephone Co. of Canada, 1st Mtg. Series "X", 4¾s . . . . .	1988	747,300.00	753,750
250,000	British Columbia Power Commission, S. F. Deb. Series "L", 4¾s . . . . .	1987	245,000.00	238,125
750,000	Industrial Acceptance Corp., Ltd., Sec. Note Series "Z", 5¼s . . . . .	1982	750,000.00	759,375
125,000	Intl. Bank for Reconstruction & Development, 3s . . . . .	1976	125,000.00	109,688

SCHEDULE OF INVESTMENTS—Continued

<u>Principal Amount</u>	<u>Description</u>	<u>Matu- rity</u>	<u>Book Value</u>	<u>Approximate Market Value</u>
Foreign and International Bank Bonds—continued				
\$ 125,000	Intl. Bank for Reconstruction & Development, 3 $\frac{3}{8}$ s . . . . .	1975	\$ 123,125.00	\$ 113,750
250,000	Intl. Bank for Reconstruction & Development, 4 $\frac{1}{2}$ s . . . . .	1977	250,000.00	248,750
150,000	Noranda Mines Ltd., S. F. Deb., 4 $\frac{3}{4}$ s . .	1968	150,349.75	135,563
810,000	Quebec Hydro-Electric Commission, S. F. Deb., 5s . . . . .	1988	795,825.00	805,950
200,000	Shawinigan Water & Power Co., 1st Mtg. & Collat. Tr. S. F. Series "M", 3s . .	1971	202,160.00	182,500
500,000	Toronto (Municipality of Metropolitan), S. F. Deb., 5s . . . . .	1979	498,637.50	520,000
<hr/>				
\$6,597,000	Total Foreign and International Bank Bonds . . . . .		\$6,581,802.18	\$6,539,238
<hr/>				
Public Utility Bonds				
\$ 125,000	Columbia Gas System, Inc., Series "B", 3s . . . . .	1975	\$ 126,326.53	\$ 109,375
250,000	Columbia Gas System, Inc., Series "F", 3 $\frac{7}{8}$ s . . . . .	1981	245,937.50	228,750
237,000	Columbus & Southern Ohio Electric Co., 1st Mtg., 3 $\frac{1}{4}$ s . . . . .	1970	240,439.29	221,595
300,000	Commonwealth Edison Co., 1st Mtg. Series "R", 3 $\frac{1}{2}$ s . . . . .	1986	300,552.80	261,000
300,000	Consolidated Edison Co. of N. Y., 1st & Ref. Mtg. Series "L", 3 $\frac{5}{8}$ s . . .	1986	302,762.47	264,000
300,000	Consolidated Edison Co. of N. Y., 1st & Ref. Mtg. Series "N", 5s . . . .	1987	301,728.04	312,000
150,000	Consumers Power Co., 1st Mtg., 4s . .	1986	151,027.74	138,750
55,000	Consumers Power Co., 1st Mtg., 4 $\frac{3}{4}$ s .	1987	55,259.34	56,100
300,000	Florida Power Corporation, 1st Mtg., 3 $\frac{7}{8}$ s . . . . .	1986	301,546.15	273,000
500,000	Illinois Power Co., 1st Mtg., 3 $\frac{3}{4}$ s . . . .	1986	497,937.50	446,250
200,000	Minnesota Power & Light Co., 1st Mtg., 3 $\frac{1}{8}$ s . . . . .	1975	201,616.41	176,000
250,000	Niagara Mohawk Power Corp., Gen. Mtg., 3 $\frac{5}{8}$ s . . . . .	1986	252,335.66	219,375
400,000	Niagara Mohawk Power Corp., Gen. Mtg., 4 $\frac{7}{8}$ s . . . . .	1987	402,578.55	412,000
100,000	Ohio Power Co., 1st Mtg., 3 $\frac{1}{4}$ s . . . . .	1968	101,500.00	96,125
200,000	Pacific Gas & Electric Co., 1st & Ref. Mtg. Series "X", 3 $\frac{1}{8}$ s . . . . .	1984	201,108.26	165,000
300,000	Pacific Gas & Electric Co., 1st & Ref. Mtg. Series "Y", 3 $\frac{3}{8}$ s . . . . .	1987	304,901.01	251,250
250,000	Pacific Gas & Electric Co., 1st & Ref. Mtg. Series "BB", 5s . . . . .	1989	251,463.82	258,750
250,000	Pacific Power & Light Co., 1st Mtg., 4 $\frac{3}{8}$ s . . . . .	1986	252,513.31	239,375
500,000	Philadelphia Electric Co., 1st & Ref. Mtg., 4 $\frac{5}{8}$ s . . . . .	1987	500,000.00	507,500



SCHEDULE OF INVESTMENTS—Continued

Principal Amount	Description	Matu- rity	Book Value	Approximate Market Value
Public Utility Bonds— continued				
\$ 236,000	Potomac Electric Power Co., Deb., 4 $\frac{5}{8}$ s	1982	\$ 240,119.56	\$ 238,360
200,000	Public Service Co. of Indiana, 1st Mtg. Series "F", 3 $\frac{1}{8}$ s . . . . .	1975	201,726.83	177,000
400,000	Public Service Co. of Indiana, 1st Mtg. Series "L", 4 $\frac{7}{8}$ s . . . . .	1987	400,000.00	415,000
500,000	Public Service Electric & Gas Co., 1st & Ref. Mtg., 4 $\frac{7}{8}$ s . . . . .	1987	503,513.41	515,000
250,000	Southern California Edison Co., 1st & Ref. Mtg. Series "G", 3 $\frac{5}{8}$ s . . . . .	1981	247,765.00	221,250
250,000	Southern California Edison Co., 1st & Ref. Mtg. Series "H", 4 $\frac{1}{4}$ s . . . . .	1982	251,250.04	253,125
200,000	Southern California Edison Co., 1st & Ref. Mtg. Series "J", 4 $\frac{7}{8}$ s . . . . .	1982	201,491.85	204,000
500,000	Tennessee Gas Transmission, 5s . . . .	1982	504,250.00	497,500
229,000	Tennessee Gas Transmission, 1st Mtg. Pipe Line, 5 $\frac{1}{4}$ s . . . . .	1977	229,000.00	233,580
500,000	Union Electric Co., 1st Mtg., 3 $\frac{3}{4}$ s . . . .	1986	500,056.47	446,250
235,000	Virginia Electric & Power Co., 1st & Ref. Mtg. Series "M", 4 $\frac{1}{8}$ s . . . . .	1986	238,220.10	221,488
300,000	Washington Water Power Co., 1st Mtg., 4 $\frac{7}{8}$ s . . . . .	1987	300,000.00	306,000
<u>\$8,767,000</u>	Total Public Utility Bonds . . . . .		<u>\$8,808,927.64</u>	<u>\$8,364,748</u>
Communication Bonds				
\$ 350,000	American Telephone & Telegraph Company, 3 $\frac{1}{4}$ s . . . . .	1984	\$ 357,428.56	\$ 294,000
800,000	American Telephone & Telegraph Company, Deb., 3 $\frac{7}{8}$ s . . . . .	1990	815,551.60	726,000
500,000	American Telephone & Telegraph Company, Deb., 4 $\frac{3}{8}$ s . . . . .	1985	504,016.68	495,000
400,000	Illinois Bell Telephone Co., 1st Mtg. Series "E", 4 $\frac{1}{4}$ s . . . . .	1988	403,832.84	387,000
200,000	Mountain States Telephone & Telegraph Co., Deb., 3 $\frac{1}{8}$ s . . . . .	1978	200,560.00	173,000
100,000	New York Telephone Co., Ref. Mtg. Series "E", 3 $\frac{1}{8}$ s . . . . .	1978	100,591.67	86,750
200,000	Pacific Telephone & Telegraph Co., Deb., 3 $\frac{1}{4}$ s . . . . .	1978	201,765.82	178,750
300,000	Pacific Telephone & Telegraph Co., Deb., 4 $\frac{3}{8}$ s . . . . .	1988	305,108.42	294,000
250,000	Southern Bell Telephone & Telegraph Co., Deb., 4s . . . . .	1983	250,854.38	235,000
300,000	Southwestern Bell Telephone Co., Deb., 3 $\frac{1}{8}$ s . . . . .	1983	303,250.00	250,500
<u>\$3,400,000</u>	Total Communication Bonds . . . . .		<u>\$3,442,959.97</u>	<u>\$3,120,000</u>
Railroad Bonds				
\$ 100,000	Chesapeake & Ohio Railway Co., Gen. Mtg., 4 $\frac{1}{2}$ s . . . . .	1992	\$ 99,500.00	\$ 98,500

SCHEDULE OF INVESTMENTS--Continued

<u>Principal Amount</u>	<u>Description</u>	<u>Matu- rity</u>	<u>Book Value</u>	<u>Approximate Market Value</u>
<u>Railroad Bonds--continued</u>				
\$267,000	Fort Worth & Denver Railway Co., 1st Mtg., 4 $\frac{3}{8}$ s Guar. ....	1982	\$268,477.67	\$234,293
<u>\$367,000</u>	<u>Total Railroad Bonds .....</u>		<u>\$367,977.67</u>	<u>\$332,793</u>
<u>Industrial and Miscellaneous Bonds</u>				
\$242,000	Aluminum Co. of America, S. F. Deb., 4 $\frac{1}{4}$ s .....	1982	\$242,000.00	\$234,740
262,500	Bethlehem Steel Corporation, Sub. Deb., 4 $\frac{1}{2}$ s .....	1990	183,637.50	260,859
550,000	C. I. T. Financial Corp., Deb., 4 $\frac{3}{4}$ s ...	1970	536,937.50	552,750
750,000	Colonial Pipeline Co., Sec. Note Series "A", 4 $\frac{3}{4}$ s .....	1990	750,000.00	753,750
400,000	Commercial Credit Co., Note, 3 $\frac{5}{8}$ s ...	1976	404,970.00	364,000
700,000	Commercial Credit Co., Note, 4 $\frac{3}{4}$ s ...	1982	700,000.00	696,500
105,000	Corn Products Co., Sub. Deb., 4 $\frac{5}{8}$ s ...	1983	108,890.23	106,050
425,000	Crown Zellerbach Corp., Prom. Note, 4 $\frac{1}{8}$ s .....	1981	425,000.00	411,188
611,000	Erie Mining Company, 1st Mtg. Series "B", 4 $\frac{1}{2}$ s .....	1983	593,207.68	597,253
500,000	F M C Corp., S. F. Deb., 3.80s .....	1981	500,000.00	460,000
151,000	First National City Bank, Capital Conv. Notes, 4s .....	1990	151,000.00	155,530
258,000	Four Corners Pipe Line Co., Sec. Note, 5s .....	1982	258,000.00	263,160
500,000	General Electric Credit Corp. (N. Y.), Sub. Note, 4 $\frac{3}{4}$ s .....	1987	500,000.00	493,750
500,000	General Electric Credit Corp. (N. Y.), Prom. Note, 5s .....	1975	500,000.00	510,000
200,000	General Motors Acceptance Corp., Deb., 3 $\frac{1}{2}$ s .....	1972	201,227.34	187,000
480,000	General Motors Acceptance Corp., Deb., 4s .....	1979	435,037.50	451,200
200,000	General Motors Acceptance Corp., Deb., 5s .....	1977	195,000.00	205,250
200,000	General Motors Acceptance Corp., Deb., 5s .....	1981	199,000.00	206,000
150,000	General Portland Cement Co., Conv. Sub. Deb., 5s .....	1977	154,500.00	148,500
509,409	Instlcorp, Inc., Collat. Tr. Note, Series A-16 .....	1991	492,392.99	514,503
428,528.35	Instlcorp, Inc., Collat. Tr. Note, Series A-19 .....	1991	414,349.07	430,671
251,176.68	Instlcorp, Inc., Collat. Tr. Note, Series A-21 .....	1991	242,385.53	252,432
298,317.63	Instlcorp, Inc., Collat. Tr. Note, Series A-23 .....	1991	293,485.04	299,809
965,391.14	Instlcorp, Inc., Collat. Tr. Note, Series A-36 .....	1992	925,964.15	941,256
400,000	Intl. Harvester Credit Corp., Deb., 4 $\frac{5}{8}$ s	1979	398,000.00	400,000
270,000	Kaiser Aluminum & Chemical Corp., 1st Mtg., 5 $\frac{1}{2}$ s .....	1987	270,000.00	276,075



SCHEDULE OF INVESTMENTS—Continued

Principal Amount	Description	Matu- rity	Book Value	Approximate Market Value
Industrial and Miscellaneous Bonds —continued				
\$ 700,000	Kresge (S. S.) Company, Prom. Note, 4 $\frac{7}{8}$ s .....	1983	\$ 700,000.00	\$ 700,000
200,000	Montgomery Ward Credit Corp., Deb., 4 $\frac{7}{8}$ s .....	1980	199,000.00	201,000
95,000	National Dairy Products Corp., Deb., 2 $\frac{3}{4}$ s .....	1970	94,950.74	87,400
400,000	Pan American World Airways, Inc., Conv. Sub. Deb., 4 $\frac{7}{8}$ s .....	1979	785,020.00	736,000
218,000	Scovill Mfg. Co., Deb., 4 $\frac{3}{4}$ s .....	1982	214,730.00	216,910
525,000	Sears Roebuck Acceptance Corp., Sub. Deb., 4 $\frac{5}{8}$ s .....	1977	511,505.00	521,063
1,000,000	Shell Funding Corporation, Collat. Tr. Bonds Series "B", 4 $\frac{3}{4}$ s .....	1985	1,000,000.00	1,000,000
300,000	Sinclair Oil Corporation, Conv. Sub. Deb., 4 $\frac{3}{8}$ s .....	1986	315,054.10	316,500
250,000	Spiegel, Inc., Deb., 5s .....	1987	250,000.00	251,563
492,000	Statewide Stations Inc., Sec. Note 4 $\frac{5}{8}$ s .	1994	492,000.00	485,850
300,000	Superior Oil Company (Calif.), Deb., 3 $\frac{3}{4}$ s .....	1981	300,000.00	276,750
215,000	Talcott (James ) Inc., Senior Note, 5 $\frac{1}{2}$ s	1980	212,850.00	221,450
700,000	Texas Gulf Sulphur Co., Prom. Note, 4.7s .....	1989	700,000.00	693,000
250,000	Tidewater Oil Company, S. F. Deb., 3 $\frac{1}{2}$ s .....	1986	250,000.00	216,875
711,799.01	Trailer Train Co., 4 $\frac{7}{8}$ s .....	1976	711,799.01	711,799
390,000	Tremarco Corporation, 1st Mtg. Series "E", 5s .....	1983	390,000.00	397,800
700,000	United Air Lines, Inc., 5s .....	1984	700,000.00	700,000
400,000	Westinghouse Electric Corp., Deb., 2 $\frac{5}{8}$ s	1971	400,510.14	358,000
250,000	Whirlpool Corporation, S. F. Deb., 3 $\frac{1}{2}$ s.	1980	250,000.00	223,438
500,000	Woolworth (F. W.) Company, Prom. Note, 5s .....	1982	500,000.00	516,250
315,000	Xerox Corporation, Conv. Sub. Deb., 4s .....	1984	500,807.50	487,069
<hr/> \$19,219,121.81	Total Industrial and Miscellaneous Bonds .....		<hr/> \$19,553,211.02	<hr/> \$19,490,943
<hr/> \$46,683,121.81	Bonds, Funds Invested .....		<hr/> \$47,049,709.38	<hr/> \$46,158,366

SCHEDULE OF INVESTMENTS—Continued

<u>Number of Shares</u>	<u>Description</u>	<u>Book Value</u>	<u>Approximate Market Value</u>
Preferred Stocks			
1,500	Appalachian Power Co., 4½% Cum. Pref. . . . .	\$ 159,000.00	\$ 141,750
3,800	Carrier Corporation, 4½% Cum. Pref. . . . .	197,931.28	185,250
1,900	Consolidated Edison Co. of N. Y., \$5.00 Cum. Pref. . . . .	202,815.00	199,025
2,000	Niagara Mohawk Power Corp., 3.6% Cum. Pref. . . . .	207,990.00	151,000
1,300	Ohio Power Co., 4½% Cum. Pref. . . . .	144,630.02	123,825
3,100	United States Steel Corporation, 7% Cum. Pre. . . . .	443,873.50	471,200
13,600	Total Preferred Stocks . . . . .	\$1,356,239.80	\$1,272,050
Common Stocks			
28,100	Aluminium, Ltd. . . . .	\$ 825,815.21	\$ 755,188
12,800	American Cyanamid Co. . . . .	850,430.03	916,800
21,861	American Electric Power Co., Inc. . . . .	135,613.53	931,825
24,700	American Smelting & Refining Company . . . . .	1,360,570.39	1,241,175
41,314	American Telephone & Telegraph Company . . . . .	1,097,438.59	2,783,531
7,000	Armco Steel Corporation . . . . .	290,041.87	464,625
16,000	Armstrong Cork Company . . . . .	131,908.39	1,104,000
10,000	Atchison, Topeka & Santa Fe Railway Co. . . . .	166,235.85	313,750
15,600	Burlington Industries, Inc. . . . .	494,681.48	1,010,100
24,000	Caterpillar Tractor Co. . . . .	97,534.09	1,032,000
11,000	Celanese Corp. of America . . . . .	568,604.02	860,750
15,000	Chicago Pneumatic Tool Co. . . . .	601,964.31	545,625
19,600	Coca-Cola Company (The) . . . . .	628,984.09	1,506,750
18,000	Continental Oil Company (Del.) . . . . .	146,960.65	1,311,750
2,500	Corning Glass Works . . . . .	59,631.83	469,063
15,000	Crown Zellerbach Corp. . . . .	839,257.85	791,250
3,100	E. I. du Pont de Nemours & Co. . . . .	465,161.33	730,050
19,718	Eastman Kodak Company . . . . .	109,798.57	1,572,511
9,500	Falconbridge Nickel Mines, Ltd. . . . .	550,837.50	863,883
12,000	Federated Department Stores, Inc. . . . .	582,805.81	868,500
15,104	First National City Bank . . . . .	348,278.77	817,504
9,000	Florida Power & Light Co. . . . .	111,572.19	664,875
19,400	Ford Motor Company . . . . .	577,047.36	1,020,925
30,000	General Electric Company . . . . .	711,024.99	2,876,250
35,156	General Motors Corporation . . . . .	1,124,435.30	3,361,793
16,500	Gillette Company . . . . .	401,418.90	546,563
21,712	Goodyear Tire & Rubber Company . . . . .	488,401.64	1,085,600
20,006	Gulf Oil Corporation . . . . .	154,333.51	1,097,829
14,000	Household Finance Corp. . . . .	659,231.85	840,000
8,875	International Business Machines Corp. . . . .	120,760.13	4,064,750
13,800	International Nickel Co. of Canada, Ltd. . . . .	379,279.52	1,155,750
17,000	Kellogg Company . . . . .	332,482.68	833,000
15,100	Kennecott Copper Corporation . . . . .	1,196,127.94	1,532,650
15,000	May Department Stores Company . . . . .	859,378.02	886,875
13,000	Mead Corporation . . . . .	614,427.23	526,500
15,000	Merck & Co., Inc. . . . .	107,286.55	815,625
40,000	Niagara Mohawk Power Corp. . . . .	863,803.67	1,070,000
9,000	Northwest Bancorporation . . . . .	231,895.01	418,500
34,000	Ohio Edison Co. . . . .	587,855.31	1,011,500
16,400	Panhandle Eastern Pipe Line Co. . . . .	431,553.54	635,500
5,000	Philip Morris Incorporated . . . . .	493,240.88	417,500



SCHEDULE OF INVESTMENTS--Continued

<u>Number of Shares</u>	<u>Description</u>	<u>Book Value</u>	<u>Approximate Market Value</u>
<u>Common Stocks--continued</u>			
7,500	Revere Copper & Brass Inc. ....	\$ 327,497.32	\$ 330,000
25,400	Royal Dutch Petroleum Co. ....	759,558.24	965,200
4,600	Sears, Roebuck and Co. ....	207,078.03	313,375
15,100	Socony Mobil Oil Company, Inc. ....	1,077,572.43	1,255,188
22,000	Standard Oil Co. (New Jersey) ....	555,503.23	1,721,500
27,500	Stevens (J. P.) & Company ....	707,606.34	1,306,250
24,190	Texaco Inc. ....	249,172.89	1,874,725
7,600	Texas Utilities Co. ....	104,621.78	469,300
19,000	Travelers Insurance Co. ....	357,962.28	722,000
7,200	United Air Lines, Inc. ....	551,656.36	504,000
14,000	United Gas Corp. ....	516,981.45	481,250
28,400	U. S. Plywood Corp. ....	697,928.16	1,107,600
16,000	Virginia Electric & Power Co. ....	220,973.07	730,000
<hr/>		<hr/>	<hr/>
928,336	Total Common Stocks ....	\$27,132,221.96	\$ 57,533,003
<hr/>		<hr/>	<hr/>
	Common and Preferred Stocks, Funds		
	Invested ....	\$28,488,461.76	\$ 58,805,053
		<hr/>	<hr/>
	Aggregate Investments ....	\$76,152,342.74	\$105,577,591
		<hr/>	<hr/>

SUMMARY OF INVESTMENT TRANSACTIONS  
FOR THE YEAR ENDED JUNE 30, 1965

Cash awaiting investment, July 1, 1964 ..... \$ 82,490.69

Sales and Redemptions

	Capital		
	Gain	Loss	Book Value
Savings account . . . . .	.....	.....	\$ 1,026,000.00
Mortgage . . . . .	.....	.....	1,938.45
Bonds . . . . .	\$ 13,477.03	\$ 623.33	3,233,008.55
Preferred stocks . . . . .	.....	.....	183,637.50
Common stocks . . . . .	3,883,112.52	83,028.59	6,180,669.36
	<u>\$3,896,589.55</u>	<u>\$ 83,651.92</u>	<u>\$10,625,253.86</u>
Realized capital gain, net Statement B . . . . .	.....	3,812,937.63	\$ 3,812,937.63
	<u>\$3,896,589.55</u>	<u>\$3,896,589.55</u>	

Total Sales and Redemptions . . . . .	14,438,191.49
Income applied to amortization of bond premium . . . . .	9,207.35
Market value of stock dividend . . . . .	788.45
Cash transferred for investment . . . . .	500,000.00
	<u>.....</u>
Total . . . . .	\$15,030,677.98

Acquisitions

Savings account . . . . .	\$ 150,000.00
Bonds . . . . .	9,522,646.79
Common stock . . . . .	5,224,808.94
	<u>.....</u>
Total Acquisitions . . . . .	14,897,455.73
	<u>.....</u>
Cash awaiting investment, June 30, 1965 . . . . .	\$ 133,222.25
	<u>.....</u>





# *Abstract of Minutes*

## *of the Sixty-Seventh Meeting of the Board of Trustees*

The annual meeting of the Board of Trustees was held in the Board Room of the Administration Building on Friday, May 7, 1965. Chairman Barklie McKee Henry called the meeting to order.

The following Trustees were present: Amory H. Bradford, Vannevar Bush, Crawford H. Greenewalt, Caryl P. Haskins, Barklie McKee Henry, Alfred L. Loomis, Robert A. Lovett, Garrison Norton, Richard S. Perkins, Elihu Root, Jr., William W. Rubey, Frank Stanton, Charles P. Taft, and James N. White.

The minutes of the Sixty-Sixth meeting were approved.

The Chairman notified the Trustees of the death of Robert E. Wilson. Dr. Bush spoke of the Trustees' high esteem for Dr. Wilson, and of his many contributions to the Institution. Dr. Bush proposed the following resolution, which the Trustees adopted unanimously:

*Be It Resolved*, That the Trustees of the Carnegie Institution of Washington desire to record their deep sense of loss at the death of their distinguished fellow member, Robert E. Wilson.

*And Be It Further Resolved*, That this resolution be entered on the Minutes of the Institution and a copy be sent to Mrs. Wilson.

Charles Hard Townes was elected a member of the Board of Trustees.

James N. White was elected Chairman of the Board for a term ending in 1968.

The following were elected for one-year terms: Henry S. Morgan as Chairman of the Executive Committee, Richard S. Perkins as Chairman of the Finance Committee, Keith S. McHugh as Chairman of the Nominating Committee and as Chairman of the Auditing Committee, and Omar N. Bradley as Chairman of the Retirement Committee.

Vacancies in standing committees, with terms ending in 1968, were filled as follows: Robert A. Lovett and William I. Myers were elected members of the Executive Committee, Crawford H. Greenewalt was elected a member of the Finance Committee, Barklie McKee Henry was elected a member of the Nominating Committee, and Frank Stanton was elected a member of the Retirement Committee.

After the election, Mr. White took over the Chairmanship of the Board of Trustees and conducted the remainder of the meeting.

The reports of the Executive Committee, the Finance Committee, the Auditor, the Auditing Committee, and the Retirement Committee were accepted.

To provide for the operation of the Institution for the fiscal year beginning July 1, 1965, and upon recommendation of the Executive Committee, the sum of \$3,925,716 was appropriated, the appropriation to be made specifically in the amount of \$3,893,717 from the Working Capital Fund, \$9,291 from the Colburn Fund, \$3,373 from the Hale Fund, \$397 from the Harkavy Fund, \$862 from the Teeple Fund, and \$18,076 from the Harry Oscar Wood Fund.

The annual report of the President was accepted.





# Articles of Incorporation

*Public No. 260. An Act to incorporate the Carnegie Institution of Washington*

*Be it enacted by the Senate and House of Representatives of the United States of America in Congress assembled,* That the persons following, being persons who are now trustees of the Carnegie Institution, namely, Alexander Agassiz, John S. Billings, John L. Cadwalader, Cleveland H. Dodge, William N. Frew, Lyman J. Gage, Daniel C. Gilman, John Hay, Henry L. Higginson, William Wirt Howe, Charles L. Hutchinson, Samuel P. Langley, William Lindsay, Seth Low, Wayne MacVeagh, Darius O. Mills, S. Weir Mitchell, William W. Morrow, Ethan A. Hitchcock, Elihu Root, John C. Spooner, Andrew D. White, Charles D. Walcott, Carroll D. Wright, their associates and successors, duly chosen, are hereby incorporated and declared to be a body corporate by the name of the Carnegie Institution of Washington and by that name shall be known and have perpetual succession, with the powers, limitations, and restrictions herein contained.

*Sec. 2.* That the objects of the corporation shall be to encourage, in the broadest and most liberal manner, investigation, research, and discovery, and the application of knowledge to the improvement of mankind; and in particular—

(a) To conduct, endow, and assist investigation in any department of science, literature, or art, and to this end to cooperate with governments, universities, colleges, technical schools, learned societies, and individuals.

(b) To appoint committees of experts to direct special lines of research.

(c) To publish and distribute documents.

(d) To conduct lectures, hold meetings, and acquire and maintain a library.

(e) To purchase such property, real or personal, and construct such building or buildings as may be necessary to carry on the work of the corporation.

(f) In general, to do and perform all things necessary to promote the objects of the institution, with full power, however, to the trustees hereinafter appointed and their successors from time to time to modify the conditions and regulations under which the work shall be carried on, so as to secure the application of the funds in the manner best adapted to the conditions of the time, provided that the objects of the corporation shall at all times be among the foregoing or kindred thereto.

*Sec. 3.* That the direction and management of the affairs of the corporation and the control and disposal of its property and funds shall be vested in a board of trustees, twenty-two in number, to be composed of the following individuals: Alexander Agassiz, John S. Billings, John L. Cadwalader, Cleveland H. Dodge, William N. Frew, Lyman J. Gage, Daniel C. Gilman, John Hay, Henry L. Higginson, William Wirt Howe, Charles L. Hutchinson, *Samuel P. Langley*, William Lindsay, Seth Low, Wayne MacVeagh, Darius O. Mills, S. Weir Mitchell, William W. Morrow, *Ethan A. Hitchcock*, Elihu Root, John C. Spooner,



Andrew D. White, Charles D. Walcott, Carroll D. Wright, who shall constitute the first board of trustees. The board of trustees shall have power from time to time to increase its membership to not more than twenty-seven members. Vacancies occasioned by death, resignation, or otherwise shall be filled by the remaining trustees in such manner as the by-laws shall prescribe; and the persons so elected shall thereupon become trustees and also members of the said corporation. The principal place of business of the said corporation shall be the city of Washington, in the District of Columbia.

*Sec. 4.* That such board of trustees shall be entitled to take, hold, and administer the securities, funds, and property so transferred by said Andrew Carnegie to the trustees of the Carnegie Institution and such other funds or property as may at any time be given, devised, or bequeathed to them, or to such corporation, for the purposes of the trust; and with full power from time to time to adopt a common seal, to appoint such officers, members of the board of trustees or otherwise, and such employees as may be deemed necessary in carrying on the business of the corporation, at such salaries or with such remuneration as they may deem proper; and with full power to adopt by-laws from time to time and such rules or regulations as may be necessary to secure the safe and convenient transaction of the business of the corporation; and with full power and discretion to deal with and expend the income of the corporation in such manner as in their judgment will best promote the objects herein set forth and in general to have and use all powers and authority necessary to promote such objects and carry out the purposes of the donor. The said trustees shall have further power from time to time to hold as investments the securities hereinabove referred to so transferred by Andrew Carnegie, and any property which has been or may be transferred to them or such corporation by Andrew Carnegie or by any other person, persons, or corporation, and to invest any sums or amounts from time to time in such securities and such form and manner as are permitted to trustees or to charitable or literary corporations for investment, according to the laws of the States of New York, Pennsylvania, or Massachusetts, or in such securities as are authorized for investment by the said deed of trust so executed by Andrew Carnegie, or by any deed of gift or last will and testament to be hereafter made or executed.

*Sec. 5.* That the said corporation may take and hold any additional donations, grants, devises, or bequests which may be made in further support of the purposes of the said corporation, and may include in the expenses thereof the personal expenses which the trustees may incur in attending meetings or otherwise in carrying out the business of the trust, but the services of the trustees as such shall be gratuitous.

*Sec. 6.* That as soon as may be possible after the passage of this Act a meeting of the trustees hereinbefore named shall be called by Daniel C. Gilman, John S. Billings, Charles D. Walcott, S. Weir Mitchell, John Hay, Elihu Root, and Carroll D. Wright, or any four of them, at the city of Washington, in the District of Columbia, by notice served in person or by mail addressed to each trustee at his place of residence; and the said trustees, or a majority thereof, being assembled, shall organize and proceed to adopt by-laws, to elect officers and appoint committees, and generally to organize the said corporation; and said trustees herein named, on behalf of the corporation hereby incorporated, shall thereupon receive, take over, and enter into possession, custody, and management of all property, real or personal, of the corporation heretofore known as the Carnegie Institution, incorporated, as hereinbefore set forth under "An Act to establish a Code of Law for the District of Columbia, January fourth, nineteen hundred and two," and to all its rights, contracts, claims, and property of any kind or nature; and the several officers of such corporation, or any other person having charge of any of the securities, funds, real or personal, books, or property thereof, shall, on demand, deliver the same to the said trustees appointed by this Act or to the persons appointed by them to receive the same; and the trustees of the existing corporation and the trustees herein named shall and may take such other steps as shall be necessary to carry out the purposes of this Act.

*Sec. 7.* That the rights of the creditors of the said existing corporation known as the

Carnegie Institution shall not in any manner be impaired by the passage of this Act, or the transfer of the property hereinbefore mentioned, nor shall any liability or obligation for the payment of any sums due or to become due, or any claim or demand, in any manner or for any cause existing against the said existing corporation, be released or impaired; but such corporation hereby incorporated is declared to succeed to the obligations and liabilities and to be held liable to pay and discharge all of the debts, liabilities, and contracts of the said corporation so existing to the same effect as if such new corporation had itself incurred the obligation or liability to pay such debt or damages, and no such action or proceeding before any court or tribunal shall be deemed to have abated or been discontinued by reason of the passage of this Act.

*Sec. 8.* That Congress may from time to time alter, repeal, or modify this Act of incorporation, but no contract or individual right made or acquired shall thereby be divested or impaired.

*Sec. 9.* That this Act shall take effect immediately.

*Approved, April 28, 1904*





# By-Laws of the Institution

*Adopted December 13, 1904. Amended December 13, 1910, December 13, 1912, December 10, 1937, December 15, 1939, December 13, 1940, December 18, 1942, December 12, 1947, December 10, 1954, October 24, 1957, May 8, 1959, May 13, 1960, May 10, 1963, and May 15, 1964.*

## ARTICLE I

### *The Trustees*

1. The Board of Trustees shall consist of twenty-four members with power to increase its membership to not more than twenty-seven members. The Trustees shall hold office continuously and not for a stated term.

2. In case any Trustee shall fail to attend three successive annual meetings of the Board he shall thereupon cease to be a Trustee.

3. No Trustee shall receive any compensation for his services as such.

4. All vacancies in the Board of Trustees shall be filled by the Trustees by ballot at an annual meeting, but no person shall be declared elected unless he receives the votes of two-thirds of the Trustees present.

5. If, at any time during an emergency period, there be no surviving Trustee capable of acting, the President, the Director of each existing Department, and the Executive Officer, or such of them as shall then be surviving and capable of acting, shall constitute a Board of Trustees *pro tem*, with full powers under the provisions of the Articles of Incorporation and these By-Laws. Should neither the President, nor any such Director, nor the Executive Officer be capable of acting, the senior surviving Staff Member of each existing Department shall be a Trustee *pro tem* with full powers of a Trustee under the Articles of Incorporation and these By-Laws. It shall be incumbent on the Trustees *pro tem* to reconstitute the Board with permanent members within a reasonable time after the emergency has passed, at which time the Trustees *pro tem* shall cease to hold office. A list of Staff Member seniority, as designated annually by the President, shall be kept in the Institution's records.

## ARTICLE II

### *Officers of the Board*

1. The officers of the Board shall be a Chairman of the Board, a Vice-Chairman, and a Secretary, who shall be elected by the Trustees, from the members of the Board, by ballot to serve for a term of three years. All vacancies shall be filled by the Board for the unexpired term; provided, however, that the Executive Committee shall have power to fill a vacancy in the office of Secretary to serve until the next meeting of the Board of Trustees.

2. The Chairman shall preside at all meetings and shall have the usual powers of a presiding officer.

3. The Vice-Chairman, in the absence or disability of the Chairman, shall perform the duties of the Chairman.

4. The Secretary shall issue notices of meetings of the Board, record its transactions, and conduct that part of the correspondence relating to the Board and to his duties.



## ARTICLE III

*Executive Administration**The President*

1. There shall be a President who shall be elected by ballot by, and hold office during the pleasure of, the Board, who shall be the chief executive officer of the Institution. The President, subject to the control of the Board and the Executive Committee, shall have general charge of all matters of administration and supervision of all arrangements for research and other work undertaken by the Institution or with its funds. He shall prepare and submit to the Board of Trustees and to the Executive Committee plans and suggestions for the work of the Institution, shall conduct its general correspondence and the correspondence with applicants for grants and with the special advisers of the Committee, and shall present his recommendations in each case to the Executive Committee for decision. All proposals and requests for grants shall be referred to the President for consideration and report. He shall have power to remove, appoint, and, within the scope of funds made available by the Trustees, provide for compensation of subordinate employees and to fix the compensation of such employees within the limits of a maximum rate of compensation to be established from time to time by the Executive Committee. He shall be *ex officio* a member of the Executive Committee.

2. He shall be the legal custodian of the seal and of all property of the Institution whose custody is not otherwise provided for. He shall sign and execute on behalf of the corporation all contracts and instruments necessary in authorized administrative and research matters and affix the corporate seal thereto when necessary, and may delegate the performance of such acts and other administrative duties in his absence to the Executive Officer. He may execute all other contracts, deeds, and instruments on behalf of the corporation and affix the seal thereto when expressly authorized by the Board of Trustees or Executive Committee. He may, within the limits of his own authorization, delegate to the Executive Officer authority to act as custodian of and affix the corporate seal. He shall be responsible for the expenditure and disbursement of all funds of the Institution in accordance with the directions of the Board and of the Executive Committee, and shall keep accurate accounts of all receipts and disbursements. Following approval by the Executive Committee he shall transmit to the Board of Trustees before its annual meeting a written report of the operations and business of the Institution for the preceding fiscal year with his recommendations for work and appropriations for the succeeding fiscal year.

3. He shall attend all meetings of the Board of Trustees.

4. There shall be an officer designated Executive Officer who shall be appointed by and hold office at the pleasure of the President, subject to the approval of the Executive Committee. His duties shall be to assist and act for the President as the latter may duly authorize and direct.

5. The President shall retire from office at the end of the fiscal year in which he becomes sixty-five years of age.

## ARTICLE IV

*Meetings and Voting*

1. The annual meeting of the Board of Trustees shall be held in the City of Washington, in the District of Columbia, in May of each year on a date fixed by the Executive Committee, or at such other time or such other place as may be designated by the Executive Committee, or if not so designated prior to May 1 of such year, by the Chairman of the Board of Trustees, or if he is absent or is unable or refuses to act, by any Trustee with the written consent of the majority of the Trustees then holding office.

2. Special meetings of the Board of Trustees may be called, and the time and place of meeting designated, by the Chairman, or by the Executive Committee, or by any Trustee

with the written consent of the majority of the Trustees then holding office. Upon the written request of seven members of the Board, the Chairman shall call a special meeting.

3. Notices of meetings shall be given ten days prior to the date thereof. Notice may be given to any Trustee personally, or by mail or by telegram sent to the usual address of such Trustee. Notices of adjourned meetings need not be given except when the adjournment is for ten days or more.

4. The presence of a majority of the Trustees holding office shall constitute a quorum for the transaction of business at any meeting. An act of the majority of the Trustees present at a meeting at which a quorum is present shall be the act of the Board except as otherwise provided in these By-Laws. If, at a duly called meeting, less than a quorum is present, a majority of those present may adjourn the meeting from time to time until a quorum is present. Trustees present at a duly called or held meeting at which a quorum is present may continue to do business until adjournment notwithstanding the withdrawal of enough Trustees to leave less than a quorum.

5. The transactions of any meeting, however called and noticed, shall be as valid as though carried out at a meeting duly held after regular call and notice, if a quorum is present and if, either before or after the meeting, each of the Trustees not present in person signs a written waiver of notice, or consent to the holding of such meeting, or approval of the minutes thereof. All such waivers, consents, or approvals shall be filed with the corporate records or made a part of the minutes of the meeting.

6. Any action which, under law or these By-Laws, is authorized to be taken at a meeting of the Board of Trustees may be taken without a meeting if authorized in a document or documents in writing signed by all the Trustees then holding office and filed with the Secretary.

7. During an emergency period the term "Trustees holding office" shall, for purposes of this Article, mean the surviving members of the Board who have not been rendered incapable of acting for any reason including difficulty of transportation to a place of meeting or of communication with other surviving members of the Board.

## ARTICLE V

### *Committees*

1. There shall be the following standing Committees, *viz.* an Executive Committee, a Finance Committee, an Auditing Committee, a Nominating Committee, and a Retirement Committee.

2. All vacancies occurring in the Executive Committee, the Finance Committee, the Auditing Committee, the Nominating Committee, and the Retirement Committee shall be filled by the Trustees at the next regular meeting. In case of vacancy in the Finance Committee, the Auditing Committee, the Nominating Committee, or the Retirement Committee, upon request of the remaining members of such committee, the Executive Committee may fill such vacancy by appointment until the next meeting of the Board of Trustees.

3. The terms of all officers and of all members of committees, as provided for herein, shall continue until their successors are elected or appointed.

### *Executive Committee*

4. The Executive Committee shall consist of the Chairman, Vice-Chairman, and Secretary of the Board of Trustees, the President of the Institution *ex officio*, and, in addition, not less than five or more than eight trustees to be elected by the Board by ballot for a term of three years, who shall be eligible for re-election. Any member elected to fill a vacancy shall serve for the remainder of his predecessor's term.

5. The Executive Committee shall, when the Board is not in session and has not given specific directions, have general control of the administration of the affairs of the corporation and general supervision of all arrangements for administration, research, and other matters undertaken or promoted by the Institution. It shall also submit to the Board of Trustees a



printed or typewritten report of each of its meetings, and at the annual meeting shall submit to the Board a report for publication.

6. The Executive Committee shall have power to authorize the purchase, sale, exchange, or transfer of real estate.

#### *Finance Committee*

7. The Finance Committee shall consist of not less than five and not more than six members to be elected by the Board of Trustees by ballot for a term of three years, who shall be eligible for re-election.

8. The Finance Committee shall have custody of the securities of the corporation and general charge of its investments and invested funds, including its investments and invested funds as trustee of any retirement plan for the Institution's staff members and employees, and shall care for and dispose of the same subject to the directions of the Board of Trustees. It shall have power to authorize the purchase, sale, exchange, or transfer of securities and to delegate this power. It shall consider and recommend to the Board from time to time such measures as in its opinion will promote the financial interests of the Institution and of the trust fund under any retirement plan for the Institution's staff members and employees, and shall make a report at each meeting of the Board.

#### *Auditing Committee*

9. The Auditing Committee shall consist of three members to be elected by the Board of Trustees by ballot for a term of three years.

10. Before each annual meeting of the Board of Trustees, the Auditing Committee shall cause the accounts of the Institution for the preceding fiscal year to be audited by public accountants. The accountants shall report to the Committee, and the Committee shall present said report at the ensuing annual meeting of the Board with such recommendations as the Committee may deem appropriate.

#### *Nominating Committee*

11. The Nominating Committee shall consist of the Chairman of the Board of Trustees *ex officio* and, in addition, three trustees to be elected by the Board by ballot for a term of three years, who shall not be eligible for re-election until after the lapse of one year. Any member elected to fill a vacancy shall serve for the remainder of his predecessor's term, provided that of the Nominating Committee first elected after adoption of this By-Law one member shall serve for one year, one member shall serve for two years, and one member shall serve for three years, the Committee to determine the respective terms by lot.

12. Sixty days prior to an annual meeting of the Board the Nominating Committee shall notify the Trustees by mail of the vacancies to be filled in membership of the Board. Each Trustee may submit nominations for such vacancies. Nominations so submitted shall be considered by the Nominating Committee, and ten days prior to the annual meeting the Nominating Committee shall submit to members of the Board by mail a list of the persons so nominated, with its recommendations for filling existing vacancies on the Board and its Standing Committees. No other nominations shall be received by the Board at the annual meeting except with the unanimous consent of the Trustees present.

#### *Retirement Committee*

13. The Retirement Committee shall consist of three members to be elected by the Board of Trustees by ballot for a term of three years, who shall be eligible for re-election, and the Chairman of the Finance Committee *ex officio*. Any member elected to fill a vacancy shall serve for the remainder of his predecessor's term.

14. The Retirement Committee shall, subject to the directions of the Board of Trustees, be responsible for the maintenance of a retirement plan for staff members and employees

of the Institution and act for the Institution in its capacity as trustee under any such plan, except that any matter relating to investments under any such plan shall be the responsibility of the Finance Committee subject to the directions of the Board of Trustees. The Committee shall submit a report to the Board at the annual meeting of the Board.

ARTICLE VI  
*Financial Administration*

1. No expenditure shall be authorized or made except in pursuance of a previous appropriation by the Board of Trustees, or as provided in Article V, paragraph 8, hereof.
2. The fiscal year of the Institution shall commence on the first day of July in each year.
3. The Executive Committee shall submit to the annual meeting of the Board a full statement of the finances and work of the Institution for the preceding fiscal year and a detailed estimate of the expenditures of the succeeding fiscal year.
4. The Board of Trustees, at the annual meeting in each year, shall make general appropriations for the ensuing fiscal year; but nothing contained herein shall prevent the Board of Trustees from making special appropriations at any meeting.
5. The Executive Committee shall have general charge and control of all appropriations made by the Board. Following the annual meeting, the Executive Committee may allocate these appropriations for the succeeding fiscal year. The Committee shall have full authority to reallocate available funds, as needed, and to transfer balances.
6. The securities of the Institution and evidences of property, and funds invested and to be invested, shall be deposited in such safe depository or in the custody of such trust company and under such safeguards as the Finance Committee shall designate, subject to directions of the Board of Trustees. Income of the Institution available for expenditure shall be deposited in such banks or depositories as may from time to time be designated by the Executive Committee.
7. Any trust company entrusted with the custody of securities by the Finance Committee may, by resolution of the Board of Trustees, be made Fiscal Agent of the Institution, upon an agreed compensation, for the transaction of the business coming within the authority of the Finance Committee.

ARTICLE VII  
*Amendment of By-Laws*

1. These by-laws may be amended at any annual or special meeting of the Board of Trustees by a two-thirds vote of the members present, provided written notice of the proposed amendment shall have been served personally upon, or mailed to the usual address of, each member of the Board twenty days prior to the meeting.





# *Index of Names*

Numbers in italic type refer to the Report of the President.

- Abbott, James E., 516  
Abelson, Philip H., *34, 39, 40, 41*, 59, 63, 64, 65, 235, 250  
    publications, 243, 247  
    report of Director, Geophysical Laboratory, 63–237  
    studies, 218–223, 223–232  
Ackerman, Edward A., viii, *63*  
    publication, 553  
Agassiz, Alexander, xi, 577  
Agriculture, U.S. Department of, *46*, 406 ff., 316, 345  
Ajdukovic, I. A., 446, 515  
    studies, 511–512  
Aldrich, L. T., vi, 347, 349  
    publications, 243, 347  
    studies, 165–177, 257–273, 286–296  
Allan, Frank D., 515  
Allen, G., 250  
Aller, Lawrence H., publication, 53, 54  
    studies, 40–41  
Allerhand, A., studies, 210–212  
Anderson, Carl D., 3  
Anderson, Christopher, 8, 57  
    studies, 17  
Anderson, Fred, 58  
Anderson, Joan M., 365, 372, 373  
    publication, 435  
Anderson, Kurt, 57  
Anzoleaga, Rodolfo, 286, 350  
Aparicio, Pablo, 351  
Appleman, D. E., 205, 207, 213  
Aries, James, 57  
Arp, Halton C., vi, 35, 56  
    publication, 53  
    studies, 23–24, 25, 31–32, 34  
Arpigny, Claude, publication, 53  
Ator, C., 351  
Axelrod, D., 345, 350  
    publication, 347  
    studies, 317–333  
Baade, Walter, publication, 53  
Babcock, Harold D., 57  
Babcock, Horace W., vi, 3, 7, 53, 56  
    report of Director, Mount Wilson and Palomar  
    Observatories, 5–52  
Bailey, D. Kenneth, 250  
    publication, 246  
Baker, Dennis, 57  
Baker, E. W., 212  
Baldwin, George J., xi  
Barbour, Thomas, xi  
Barnhart, Paul F., 58  
Bartelmez, W., 511  
    publication, 514  
Barton, Mary N., 516  
Baschek, Bodo, 53  
Batten, C. A., 250  
Bauer, Ailene J., *61*  
Baum, Ester Bru 56, 57  
Baum, William A., vi, 43, 44, 47, 50, 52, 56, 353, 356, 359, 360  
    publications, 53, 347  
    studies, 15, 17, 31, 45–46  
Beach, L., 350  
Beck, Felix, 515  
    publications, 514  
Becklin, Eric, 26  
Beermann, W., 446  
Bell, James F., xi  
Bell, Peter M., *35*, 67, 68, 236, 237, 250  
    studies, 120–123, 139–141, 141–144, 150–153, 197–199  
Bendich, A., 350



- Berkebile, Wilma J., 58  
 Berwald, Yoheved, 446, 515  
     studies, 470  
 Billings, John S., xi, 577  
 Bishop, David W., vii, 444, 446, 500, 515  
     studies, 495-496  
 Björkman, Olle, 44, 45, 368, 369, 370, 415, 436, 437  
     publication, 435  
     studies, 415-416, 416-420, 420-424  
 Blackwell, James, 516  
 Blackwell, Paul, 516  
 Blakeé, Lawrence E., 57  
 Bleich, H. H., 52  
 Blinks, Lawrence R., 380,  
     publication, 435  
 Bliss, Robert Woods, xi  
 Boardman, N. Keith, 365, 372, 373  
     publication, 435  
 Bocskay, Elizabeth M., 535  
 Boettinger, George, 516  
 Boise, James W., viii  
 Bolton, Ellis T., vi, 45, 251, 349, 521, 526  
     publication, 347  
     studies, 313-345  
 Botanical Congress, 10th International  
     (Edinburgh), 236, 369-370  
 Böving, Bent G., vii, 515  
     studies, 504-506  
 Bowen, Ira S., vi, 32, 5, 56  
     publications, 53, 54  
     studies, 47  
 Boyce, Peter B., 38  
 Boyd, Francis R., Jr., 35, 67, 142, 236, 238, 250, 326  
     studies, 117-120  
 Bracken, P. A., studies, 308  
 Bradford, Amory H., iv, v, 575  
 Bradford, Lindsay, xi  
 Bradley, Omar N., iv, v, 555, 575  
 Brett, P. Robin, 250  
     publications, 245  
 Briggs, Winslow, 367  
     studies, 406-412  
 Bril, Cornelis, 44, 365, 436, 437  
     studies, 370-373, 373-374, 374-379  
 Britten, Roy J., vi, 45, 349  
     publication, 347  
     studies, 313-345  
 Brookhart, M. S., 212  
 Brookings, Robert S., xi  
 Brown, A., 250  
 Brown, Donald D., vii, 446, 515  
     publications, 514  
     studies, 446-452  
 Brown, Jeanette S., vii, 44, 365, 436, 437  
     studies, 373-374, 374-379,  
 Brown, Louis, vi, 349  
     studies, 310-313  
 Brueckel, Frank J., 57  
     studies, 24  
 Bruinsma, Jan A., 58  
 Bruinsma, Maria J., 58  
 Buchanan, Jennie S., 535  
 Bullen, K. E., 350  
     publications, 347  
 Bumba, V., 6, 7, 8  
     publications, 53, 54  
 Burchard, W. K., 351  
 Burd, Sylvia, 57  
 Burgi, Elizabeth, vii, 520, 535  
     publication, 534  
     studies, 520  
 Burke, Bernard F., vi, 349  
     publication, 348  
     studies, 300-307  
 Burnham, Charles W., 68, 238, 250  
     publication, 243  
     studies, 200-207  
 Burr, Henry, 470, 516  
 Bush, Vannevar, iv, xi, 60, 345, 575  
 Butler, R. L., 250  
 Buuren, Hendrika E. van, 58  
 Buuren, John E. van, 58  
 Buynitzky, S. J., 350  
 Byers, Thomas J., 349  
 Cabre, R., S.J., 350  
     studies, 273-286  
 Cadwalader, John L., xi, 577  
 Caherty, F. J., 351  
 California Institute of Technology, 3, 26  
 Cameron, R. M., 8  
 Campbell, William W., xi  
 Canter, Dorothy, 351  
 Careaga, J., 350  
     studies, 273-286  
 Carnegie, Andrew, 370, 578,  
 Carty, John J., xi  
 Casanova, Manuel, 58  
 Casaverde, M., 350  
     studies, 309-310  
 Challacombe, Eileen I., 57  
 Chamberlin, M., 350  
 Chambers, Robert J., studies, 39  
 Chang, Joseph S., 437  
 Chase, John, 516  
 Chayes, Felix, 39, 40, 65, 67, 77 f., 135, 236, 238, 250  
     publications, 243, 245, 247  
     studies, 153-165  
 Christ, Hans A., 349  
     studies, 310-313  
 Clausen, Jens C., 369, 370, 415, 436, 437  
     publications, 435  
     studies, 431-435  
 Cleary, William I., 516  
 Cole, Whitefoord R., xi  
 Connes, Pierre, studies, 42  
 Conti, Peter S., 57  
     publications, 53  
     studies, 11, 14-15, 16-17, 20, 24  
 Cortez, Rolando H., 58

- Coslet, J. George, 515  
 Couch, Hugh T., 58  
 Cowie, Dean B., vi, 45, 349  
   publications, 348, 534  
   studies, 313-345  
 Cragg, Thomas A., 6, 57  
 Craig, James Roland, 250  
 Crotty, Daniel L., 56, 58  
   studies, 52  
 Czaplicki, Helen S., 58  
 Czyzak, Stanley, studies, 40-41
- Dallwitz, W. B., 82  
 Daly, M. F., 351  
 Danziger, Ivan J., 57  
   studies, 11, 13-15, 20, 24  
 Danziger, Rowena, 57  
 Das, C. C., 546  
   publication, 551  
 Davern, C. I., 520  
   publication, 534  
 Davis, Brian T. C., 67, 250, 347  
   studies, 120-123, 123-126  
 Davis, Gordon L., 65, 236, 242, 250, 294, 347  
   publications, 243, 348  
   studies, 165-177, 286-296  
 Dawid, Igor, 51, 443, 445, 448, 449, 452, 515  
   studies, 465-469  
 Day, Floyd E., 57  
 DeHaan, Robert L., vii, 445, 446, 472, 512, 515  
   publication, 514  
   studies, 471-477, 511-512  
 DeHuff, Kenneth E., 58  
 Dekaban, A. S., 511  
   publication, 514  
 DeLanney, Louis E., 515  
 Delano, Frederic A., xi  
 Denis, Herman, 443, 446, 515  
   studies, 452-465, 466  
 Dennison, Edwin W., vi, 47, 49, 56  
 Deutsch, Armin J., vi, 8, 53, 56  
   publications, 53  
   studies, 11, 16-17, 39  
 Dillin, D., 351  
 Divine, T. Neil, studies, 37  
 Djavadi, G. R., 515  
 Doak, J. B., 350  
 Dodge, Cleveland H., xi  
 Dodge, William E., xi, 577  
 Doermann, A. H., 523  
 Dollase, W. A., 205  
 Donnay, Gabrielle, 69, 239, 250  
   publications, 244, 245  
   studies, 207-209, 209-210, 210-212, 212-215  
 Donnay, J. D. H., 209, 239, 250  
   publications, 244, 245  
   studies, 207-209, 209, 210-215  
 Donner, Martin W., 446, 515  
   publications, 514  
   studies, 506-510  
 Douglas, Nina, 516  
 Dove, William N., 351
- Duncan, William H., 516
- Ebert, James D., vii, 50, 51, 52, 56, 63, 444, 446,  
   471, 486, 487, 515  
   publications, 514, 515  
   report of Director, Department of Em-  
   bryology, 443-514  
   studies, 483-486  
 Ebstein, Bonnie Sue, 512  
 Ecklund, E. T., 306, 350  
 Eckstein, Peter, 446, 515  
 Edgar, Robert, 523  
 Edwards, Ernest W., 516  
 Eggen, Olin J., 17, 56  
   publications, 54  
   studies, 10-11, 21  
 Ehring, Ruth, 520, 535  
   studies, 523-524  
 Eldredge, Marylee H., 437  
 Ellison, Eleanor G., 58  
 Emerson, Robert, 367, 403  
   publication, 435  
 Emmel, John F., 437  
 England, Joseph L., 35, 67, 238, 250, 326  
   studies, 117-120, 197-199  
 Engstrom, Ralph, 361  
 Ephrussi, Boris, 445, 511  
 Etheart, J. F., 250
- Fado, Raymond, 516  
 Fawcett, J. Jeffrey, publications, 243  
 Fejfar, Adolph, 414, 437  
 Fenkert, Rolf P., 57  
 Fenner, Charles P., xi  
 Ferguson, Homer L., xi  
 Ferguson, M., 250  
 Fernandez, L., S.J., 350  
 Fisher, Agnes C., 535  
 Fisher, George Wescott, 250  
 Fleischer, E. B., 214  
 Flexner, J. B., 345  
   publications, 348  
 Flexner, L. B., ix, 345, 515  
   publication, 348  
 Flexner, Simon, xi  
 Forbes, W. Cameron, xi  
 Forbush, Scott E., vi, 35, 349  
   publications, 348  
   studies, 307-309, 309-310  
 Ford, W. Kent, Jr., vi, 345, 349, 357, 359, 360,  
   361  
   publication, 348  
   studies, 15, 45-46  
 Fork, David C. vii, 43, 365, 366, 367, 378, 379,  
   436, 437  
   publications, 435  
   studies, 381-390, 390-395, 406-412, 416-420  
 Forrestal, James, xi  
 Forsbacka, Allen, 351  
 Forsey, A. L., 250  
 Forward, Kay, 540, 547



- Frankel, Fred R., 524, 526  
 French, C. Stacy, vii, 63, 370, 437  
   publications, 435, 436  
   report of Director, Department of Plant  
     Biology, 365-435  
   studies, 414-415  
 Frew, William N., xi, 577  
 Fudali, R. F., 82
- Gabrielson, Fanny G., 58  
 Gage, Lyman J., xi, 577  
 Gajardo, E., 350  
 Galbraith, Joan D., viii  
 Garde, Wilbur F., 516  
 Gardner, Ernst, studies, 510-511  
   publication, 514  
 Garrels, R. M., 413  
   publication, 435  
 Garrett, P. S., 250  
 Garver, L. C., 250  
 Gast, Paul W., 347  
   publication, 245  
 Gates, Howard S., 57  
   studies, 35  
 Gaustad, John E., 57  
 Gawrys, S., 351  
 Gay, Helen, vii  
   publications, 551  
   report of Cytogenetics Laboratory, 539-  
     550  
 Gehrels, T., studies, 42  
 Gelderman, Albert, 53, 341, 345, 350  
 Geological Survey, U.S., 68, 82, 172  
 Georgen, Robert D., 58  
 Giesecke, A. A., Jr., 350  
   studies, 309-310  
 Gifford, Walter S., iv, v  
 Gilbert, Carl J., iv, v  
 Gilbert, Cass, xi  
 Gillett, Frederick H., xi  
 Gilman, Daniel Coit, xi, 577  
 Goedheer, Joop C., 398  
 Goldberg, Edward, 49, 520, 535  
   studies, 524  
 Gortt, Norman R., 516  
 Gratton, L., studies, 39  
 Green, R., 349  
 Greenewalt, Crawford H., iv, v, 575  
 Greenstein, Jesse L., iv, 3, 28, 56  
   publications, 54, 55, 56  
   studies, 10-12, 13, 39  
 Grill, Richard D., 516  
 Griswold, William R., 365, 415, 437  
 Gunn, James E., 57  
   studies, 37  
 Gurdon, John B., 446, 515  
   publication, 514
- Haber, L. J., 351  
 Hales, A. L., 350  
 Hall, John S., 353  
   publication, 347  
 Hallberg, R. L., 515  
 Hancock, Eugene L., 58  
 Hansen, Edward C., 84, 116, 250  
 Hare, P. Edgar, 41, 65, 236, 239, 250  
   studies, 223-232, 232-235  
 Hargett, Charles E., 516  
 Haro, G., 29, 53  
 Harper, Ernest, 516  
 Harris, J. W. S., 446, 509, 511, 516  
 Hart, P. J., 350  
 Hart, Richard W., 437  
 Hart, Roger, 250  
 Hart, Stanley R., vi, 38, 39, 272, 349  
   publications, 348  
   studies, 286-296, 296-300  
 Hartmann, Olaf, vi, 349  
   studies, 309-310  
 Harvey, Jack, 57  
 Haskins, Caryl P., iv, v, viii, 52, 575  
   publication, 553  
   Report of the President, 1-63  
 Haslan, Eugene, 34  
 Hauschka, S. D., 515  
   studies, 470  
 Haxo, Francis T., 380,  
   publication, 435  
 Hay, John, xi, 577  
 Hays, J. F., 35, 68, 250  
   studies, 141-144  
 Helfer, H. L., 39  
 Henard, Kenneth R., viii  
 Henderson, Mark D., 58  
 Henry, Barklie McKee, iv, v, 575  
 Herbert, Floyd, 57  
 Herbert, N. C., 413  
 Hernandez, Frank, 58  
 Herrick, Myron T., xi  
 Hershey, Alfred D., vii, 48, 49, 56, 63, 336, 345,  
   535  
   publications, 348, 534  
   report of Director, Genetics Research Unit,  
     519-534  
   studies, 519-521  
 Hertig, Arthur T., 515  
 Herzog, Emil, 57  
   publications, 54  
   studies, 34  
 Hett, Victor A., 58  
 Heuser, Chester H., 59, 515  
 Hewitt, Abram S., xi  
 Hicks, Shirley, 516  
 Hicks, Virginia, 516  
 Hiesey, William M., vii, 368, 369, 437  
   publications, 436  
   studies, 420-424, 425-427, 427-429, 429-431  
 Higginson, Henry L., xi, 577  
 Hill, Byron, 58  
 Hill, E. K., 351  
 Hill, Ruth, 523  
 Hitchcock, Ethan A., xi, 577  
 Hitchcock, Henry, xi

Hoering, Thomas C., 40, 41, 63, 64, 65, 236, 250  
    publications, 243  
    studies, 215–218, 218–223  
Hoffman, R. A., studies, 308  
Hoffmaster, R., 351  
Holloway, Helen D., 58  
Hoover, Alan, 351  
Hoover, Herbert, xi, 57  
Hopson, C. A., 291  
    publications, 247, 348  
    studies, 171–174, 174–176  
Hornblower, Marshall, viii  
Houten, C. J. van, 42  
Howard, Robert F., vi, 6, 7, 8, 57  
    publications, 53, 54  
    studies, 44  
Howe, William Wirt, xi, 577  
Hoyer, Bill, 345, 350, 443, 466  
    publication, 348  
    studies, 317–333  
Hubbard, Jeannie, 516  
Huffaker, E. C., 250  
Hutchinson, Charles L., xi, 577  
  
Imlay, Marjorie E., 235, 250  
Ingamells, C. O., 150  
Ingraham, Laura, 520, 535  
    studies, 520–521  
Irwin, John B., 50, 58  
    publications, 54  
  
Jacobson, T. V., publication, 54, 56  
    studies, 13  
James, D. E., 349  
James, Odette, 250  
Jeffrey, Doris, 58  
Jermann, David C., 58  
Jessup, Walter A., xi  
Jewett, Frank B., xi  
Johnson, Donald E., 58  
Johnson, Kurt, 516  
Johnson, Melvin W., 58  
Johnson, P. A., 350  
Johnston, G. J., 351  
Johnston, Henry Freeborn, 59, 60  
Jordan, Eddie, 516  
Joy, Alfred H., 57  
    publication, 54  
  
Kaighn, M. Edward, 51, 444, 445, 446, 515  
    publications, 514  
    studies, 483–486  
Kamen, M. D., 42, 43, 44  
Kamitsuki, A., 349  
Karpowicz, Maria, 57  
    publication, 54, 56  
    studies, 28, 34, 35  
Katem, Basil, 57  
    studies, 23  
Kato, Yoshiko, 349  
Katz, Margaret, 57  
Kaufmann, Berwind P., 539, 540  
    publications, 551  
    studies, 548–550  
Kearns, Charles E., 58  
    publication, 54  
Keeley, Douglas, 30, 57  
Keenan, Philip C., publication, 54  
    studies, 38–39  
Keller, Geoffrey, 361  
Kerby, Elaine C., 516  
Kimmel, C. B., 515  
    studies, 487–494  
Kissell, K. E., 350  
Kleczek, J., 8  
    publication, 53, 54  
Kloetzel, John A., 516  
Knight, Wiley, Jr., 437  
Koch, Robert, H., studies, 40  
Kocher, G. E., studies, 43  
Kocher-Becker, Ursula,  
    publication, 514  
    studies, 482  
Kocmaneck, J. F., 250  
Konigsberg, Irwin R., vii, 52, 444, 445, 446, 483,  
    486, 515  
    publications, 514  
    studies, 469–470  
Kormann, Leo, 516  
Kostowiecki, M., 516  
Kouchkovsky, Yaroslav de, 366, 367, 378, 389,  
    436, 437  
    publications, 435  
    studies, 397–398  
Kovar, Robert, 57  
Kowal, Charles T., 57  
    publication, 54  
    studies, 34, 35  
Kowalik, Jan, 437  
Kraft, Robert P., vi, 57  
    publications, 54  
    studies, 17, 18, 46  
Krogh, T. E., 347, 349  
    studies, 286–296  
Kuhi, Leonard, 57  
    publication, 54  
    studies, 18, 20  
Kulangara, A. C., 516  
Kullerud, Gunnar, 38, 63, 64, 236, 240, 250  
    publications, 243, 248  
    studies, 177–188, 188–192, 192–193, 193–197,  
    197–199  
Kupres, Francis J., 469, 516  
Kushiro, Ikuo, 67, 237, 250  
    studies, 89–94, 100–103, 103–109, 109–112,  
    112–117  
  
Landsman, Shirley G., 437  
Lane, Harold, 361  
Langley, Samuel P., xi, 577  
Laniz, Ruperto, 413  
Lara, J. Luz, 58  
Large, Fred, 58



- Larimer, J., 250  
 Lasker, Barry M., 57  
     studies, 42  
 Lawrence, Ernest O., xi  
 Lawrence, Mark, 437  
 L'Ecuyer, J., studies, 40  
 Ledinko, Nada, 527  
     publication, 534  
 Lee, E. K., publications, 54, 56  
     studies, 13  
 Lee, Mary, 540  
 Legum, Elizabeth, 516  
 Leighton, Robert B., vi, 3, 6, 22, 57  
     publication, 54  
     studies, 25, 48  
 LeMaitre, R. W., 82  
 Leone, J. A., 214  
 Libby, Paul R., studies, 497-503  
 Lichtenstein, Edna G., 516  
 Lieberman, Melvyn, 446, 472, 515  
     publications, 514  
     studies, 475  
 Lincoln, Thomas L., 53, 341, 345, 350  
 Lindbergh, Charles A., xi  
 Lindsay, William, xi, 577  
 Lindsley, Donald H., 68, 119, 203, 236, 250  
     studies, 144-150  
 Lin Ho, 351  
 Little, C. A., 350  
 Littna, Elizabeth, 516  
 Locanthi, Dorothy D., 57  
     studies, 12, 39  
 Lodge, Henry Cabot, xi  
 Lomnitz, Cinna, vi, 349  
 Loomis, Alfred L., iv, v, 575  
 Lorenz, Ernest, 57  
 Lorz, J. G., 351  
 Lothrop, Samuel Kirkland, 59, 60  
 Lovett, Robert, A., iv, v, 555, 575  
 Low, Frank J., 38  
 Low, Seth, xi, 577  
 Lowell Observatory, 33  
 Lowen, A. Louise, 57  
 Lutz, H. J., 250  
 Luyten, W. J., 29  
     studies, 18, 42  
 Lyons, W. H., 250
- Macdonald, G. A., 82  
 MacGregor, Ian D., 67, 250  
     studies, 126-139  
 MacVeagh, Wayne, xi, 577  
 Marshall, R. E., 446, 516  
 Martin, C. B., Jr., 446, 515  
     publications, 514, 515  
     studies, 506-510  
 Martin, Malcolm, 345, 350  
     studies, 317-333  
 Marton, L. L., 353  
     publication, 347  
 Martz, Dowell E., 25-26
- Matson, Dennis, 10  
 Matthews, Thomas A., 30, 5, 27, 43  
     publication, 54  
     studies, 26  
 Mazza, Raymond, 351  
 McCarthy, Brian J., 348, 443, 521, 526  
     studies, 466  
 McClintock, Barbara, vii, 50, 55, 56, 63, 519, 535  
     studies, 527-534  
 McClunin, O. R., 250  
 McConnell, Anne, 61, 62, 58  
 McCord, Thomas, 10  
 McGaughey, Harry S., Jr., 446, 506, 516  
     publication, 514  
 McGee, James D., ix, 45, 47, 356, 359  
     studies, 17, 46  
 McHugh, Keith S., iv, v, 575  
 McIntyre, L. C., 313  
 McNamara, D. H., studies, 45  
 Mellon, Andrew W., xi  
 Merriam, John Campbell, xi  
 Mihalas, Dimitri, publications, 55  
 Miles, Mary Jane, 235  
 Miller, J. S., studies, 40  
 Miller, Margaret Carnegie, iv, v  
 Miller, Roswell, xi  
 Miller, William C., 25, 34, 57  
     publications, 55  
 Mills, Darius O., xi, 577  
 Milner, Harold W., vii, 57, 58, 368, 370, 437  
     publications, 436  
     studies, 425-427  
 Minkowski, Rudolph, 7, 30, 5  
     publications, 54, 55  
 Mitchell, S. Weir, xi, 577  
 Mitchell, Walter E., studies, 44  
 Mitterer, R. M., 250  
 Moberly, Betty J., 540  
 Moffett, Benjamin C., Jr., 516  
 Moh, Günter, 250  
 Montague, Andrew J., xi  
 Moore, Joseph C., 361  
 Morehead, Allen, 361  
 Morey, George W., 36, 58, 59, 66, 241  
     publication, 244  
 Morgan, Henry S., iv, v, 555, 575  
 Morgan, William W., 43  
     publication, 54  
 Morowitz, Harold, 336  
 Morrow, William W., xi, 577  
 Mosig, Gisela, 49, 520, 523, 524, 526, 535  
     studies, 521-523  
 Mossor, D. E., 351  
 Mudd, Seeley G., iv, v  
 Muecke, E. C., publication, 514  
 Mulders, Gerald, 361  
 Müller, Alexander, 403, 437  
 Mullin, K., 351  
 Münch, Guido, vi, 9, 45, 57  
     publications, 55, 56  
     studies, 22, 24, 38, 48, 49

- Murray, Bruce C., 10, 50  
     publication, 55  
     studies, 44  
 Musselman, Arlyne, 495, 516  
 Mutschler, Leah M., 58  
 Myers, William I., iv, v, 575  
 Mylonas, George P., 57  
  
 Naldrett, Anthony J., 38, 63, 209, 236, 250  
     studies, 177–188  
 Nation, Bula H., 58  
 National Bureau of Standards, 33  
 National Geographic Society, 34  
 National Radio Astronomy Observatory, 26, 32, 38  
 Naval Observatory, U.S., 33  
 Neill, Catherine A., 446, 516  
 Nelson, Sharon, 515  
 Neugebauer, G., 9, 22  
     studies, 25  
 Newman, John B., 208  
 Newton, Mildred, 58  
 Nichol, Richard, 57  
 Nicholls, G. D., 82  
 Nichols, Richard F. F., viii  
 Nicholson, Frank, 437  
     studies, 429–431  
 Nicolaysen, L. O., 171  
 Nobs, Malcolm A., vii, 369, 437  
     studies, 420–424, 427–429  
 Nordsieck, Kenneth, 57  
 Norton, Garrison, iv, v, 575  
  
 O'Dell, Charles R., 25  
 O'Hara, M. J., 294  
 Ohmoto, H., 350  
 Okada, Tokindo, 445, 446, 515  
     studies, 486  
 Oke, J. Beverly, 49, 57  
     publications, 53, 55  
     studies, 11, 12, 13, 14, 20, 24, 27, 29, 30, 36  
 Olmstead, Alfred H., 58  
 O'Rahilly, Ronan, 446, 511, 516  
     publication, 514  
     studies, 510–511  
 Orozco, Edward T., 250  
 Osborn, William Church, xi  
 Osterbrock, D. E., 52  
     studies, 40  
  
 Pabst, A., 211  
 Padget, Dorcas H., 446, 516  
 Papaconstantinou, John, 446, 516  
     studies, 482  
 Parker, P. L., publications, 243, 244  
 Parker, Robert, 52  
     studies, 41–42  
 Parkinson, Wilfred C., 59, 60  
 Parmelee, James, xi  
 Parsons, Wm. Barclay, xi  
 Paton, Stewart, xi  
 Patton, Donald J., viii  
  
 Pazdernik, John, 516  
 Peacor, D. R., 204  
 Peck, Eleanor F., viii  
 Peoples, J. A., Jr., 235  
 Peoples, Rowena E., 235  
 Pepper, George W., xi  
 Perkins, Richard S., iv, v, 555, 575  
 Perreault, William J., 540  
     studies, 548–550  
 Pershing, John J., xi  
 Peterson, Bruce, 57  
 Peterson, V., studies, 12, 37  
 Petrologists' Club, 237  
 Peveling, Elisabeth, 539  
     studies, 540–542  
 Picken, Kathe A., 437  
     studies, 429–431  
 Poe, G. R., 350  
 Pohn, Howard A., 45  
     publication, 55  
 Pollock, Harry E. D., ix  
 Prentis, Henning W., Jr., xi  
 Presnall, Dean Carl, 250  
 Prewitt, C. T., 204  
 Pritchett, Henry S., xi  
 Proctor, Margaret J., 516  
 Proskouriakoff, Tatiana, viii  
 Prothro, L. J., 350  
 Purgathofer, Alois Th., vi, 349, 357, 359, 360, 361  
     studies, 15, 45–46  
  
 Quade, E., 351  
 Quilligan, Edward J., 446, 516  
     studies, 509  
 Quinn, Robert D., 58  
  
 Rama, S. N. I., 349  
     publication, 348  
 Ramirez-Toledano, Oscar, 515  
 Ramsey, Elizabeth M., vii, 63, 446, 511, 515  
     publications, 514, 515  
     studies, 506–510  
 Randall, John, 351  
 Rawles, Mary E., vii, 515  
     studies, 481–482  
 Reeves, G., studies, 35  
 Regulski, Ted C., 58  
 Rentschler, Gordon S., xi  
 Reporter, Minocher C., 51, 445, 446, 471, 515  
     publications, 515  
     studies, 444  
 Rever, Arthur G., 516  
 Reynolds, Samuel R. M., 515  
 Ribbens, Rudolf E., 47, 58  
 Ridgway, Stuart L., 57  
     studies, 49  
 Ried, August, 44, 367, 368, 382, 403, 437  
     publication, 435  
     studies, 399–406  
 Righini, G., 8  
     publication, 53, 55



- Riley, Malcolm S., 57  
 Rinehart, C., 351  
 Ringwood, A. E., 238, 250  
     publications, 243  
 Roberts, Philip, 57  
 Roberts, Richard B., vi, 52, 349  
     publications, 348, 349, 553  
     studies, 313-345  
 Rockefeller, David, xi  
 Roddy, John, 351  
 Roddy, M., 351  
 Rodriguez B., A., 350  
 Roeder, E., 289  
     publication, 348  
 Rood, H. J., studies, 44  
 Roosen-Runge, Edward C., 446, 516  
 Root, Elihu, xi, 577  
 Root, Elihu, Jr., iv, v, 555, 575  
 Roseboom, E. H., 67  
     studies, 139-141  
 Rosen, Frederick, 516  
 Rosenquist, Glenn C., 445, 446, 510, 511, 515  
     publication, 515  
     studies, 472, 477-481  
 Rosenthal, Miriam D., 512  
 Rosenwald, Julius, xi  
 Rowe, F. A., 250  
 Roy, Robert F., 68, 250  
     studies, 150-153  
 Rubenstein, Irwin, 521  
 Rubey, William W., iv, 575  
 Rubin, Harry, 483  
 Rubin, Vera C., vi, 349, 360, 361  
 Rule, Bruce H., 32, 47, 49, 50, 52, 56, 57  
 Russell, Helen E., 351  
 Ryerson, Martin A., xi
- Saa, G., S. J., 350  
 Sachs, Robert, 516  
 Sacks, I. Selwyn, vi, 349  
     publications, 348  
     studies, 273-286  
 St. John, William D., 58  
 Salgueiro, R., 350  
 Sandage, Allan R., vi, 8, 30, 31, 3, 5, 10, 27, 34,  
     36, 40, 44, 53, 57  
     publications, 54, 55  
     studies, 22, 23, 26, 28, 29-30  
 Sanger, Glen, 58  
 Sargent, Wallace L. W., 30  
 Scargle, Jeffrey, 57  
     studies, 22  
 Schaefer, Henry F., 58  
 Schairer, J. Frank, 63, 67, 84, 136, 236, 238,  
     241, 250  
     publications, 246  
     studies, 69-82, 95-100, 100-103, 123-126  
 Schmidt, Maarten, vi, 8, 30, 5, 27, 29, 37, 43,  
     57  
     publications, 54, 55  
     studies, 28, 30
- Schmucker, Ulrich, vi, 349  
     studies, 309-310  
 Schrank, Winslow, 516  
 Schuetz, Marlin N., 58  
 Seemann, M., 351  
 Sensenig, E. C., 446, 516  
 Severn, C. B., 516  
 Shafa, F., 515  
 Shaw, H. R., 89  
 Sheahan, M. T., 351  
 Sheeley, Neil R., 57  
 Shepard, Anna O., viii  
     publication, 553  
 Shepley, Henry R., xi  
 Shields, Allan Oakley, 437  
 Shipley, E. J., 250  
 Shirey, John E., 58  
 Shirley, John, 58  
 Shirven, A., 350  
 Shuey, Elizabeth M., 58  
 Simmons, Gene, 35, 68  
     studies, 141-144  
 Singer, A. David, 235, 250  
 Sinton, William M., 38  
 Skalka, Anna Marie, 49, 50, 520, 526, 535  
     studies, 526-527  
 Skumanich, Andrew, publications, 55, 56  
     studies, 15  
 Smith, Benny W., 58  
 Smith, Bessie, 516  
 Smith, James H. C., 368, 437  
     studies, 412-414  
 Smith, J. R., 186  
 Smith, J. V., 119  
 Smith, Mervyn, 520, 526, 535  
     studies, 524-526  
 Smith, Sara F., 7  
     publication, 53, 55  
 Smith, T. Jefferson, vi, 349  
     publications, 348  
     studies, 257-273  
 Smith, Theobald, xi  
 Soeder, Carl J., 403  
     publication, 435  
 Sparvoli, Elio, 540, 543  
     publications, 551  
     studies, 544-546  
 Speicher, G. E., 250  
 Spencer, A. B., 82  
 Spoehr, H. A., 43, 57  
 Spooner, John C., xi, 577  
 Stanton, Frank, iv, v, 2, 575  
 Stawikowski, Antoni, 57  
     publication, 55  
 Steiger, Rudolf Heinrich, 65, 242, 250, 295, 347  
     publications, 246  
     studies, 165-177  
 Steinhart, John S., vi, 38, 39 347, 349  
     publications, 348  
     studies, 257-273, 296-300  
 Stoeckly, Robert, 57  
     studies, 11, 17

- Storey, William Benson, xi  
 Storm, C. B., studies, 212–215  
 Stott, Pauline M., 51, 444, 516  
   studies, 483–486  
 Stoudenheimer, E. G., 361  
 Straus, W. L., Jr., 516  
 Strong, Richard P., xi  
 Stryker, Lucile B., 61, 235  
 Sugiura, Masahisa, 309  
 Sumner, Roger, 349  
   studies, 273–286  
 Supper, Charles, 200, 202, 205  
 Suyehiro, S., 37, 347, 349  
   publication, 348  
   studies, 273–286  
 Suzuki, Ziro, 281, 347, 350  
   publication, 348  
 Swantkowski, S., 351  
 Swope, Henrietta H., 57  
   publication, 53, 55  
   studies, 31  
 Szafranski, P., 45, 350  
   studies, 313–345
- Taft, Charles P., iv, v, 555, 575  
 Taft, William H., xi  
 Tammann, Gustav A., 31, 57  
   publications, 55  
   studies, 40  
 Taylor, Albert E., 535  
 Thackeray, A. D., 24  
 Thayer, William S., xi  
 Thomas, Dolores M., 250  
 Thomas, Gloria, 437  
 Thomas, J. R., 250  
 Thompson, J. E., 82  
 Tiedemann, Heinz, 446, 515  
   publication, 514, 515  
   studies, 482–483  
 Tiedemann, Hildegard, publication, 514, 515  
   studies 482,  
 Tifft, William G., 36  
 Tilley, C. E., ix, 63, 67, 94, 235, 236, 241, 242, 250  
   studies, 69–82, 95–100  
 Tilton, George R., 65, 236, 237, 242, 250, 347  
   publications, 245, 247, 348  
   studies, 165–177, 286–296  
 Timms, D., 171  
 Title, Alan M., 57  
 Townes, Charles Hard, iv, 62, 575  
 Trächslin, W., 350  
   studies, 310–313  
 Trafton, Laurence M., 9, 57  
   publication, 55  
 Traxler, Benjamin B., 58  
 Trebst, A., 385  
 Treible, Kathryn E., 535  
 Trippe, Juan T., iv, v  
 Truesdale, R. L., 250  
 Tulinsky, A., 212, 213  
 Turner, Kenneth C., vi, 349  
   publication, 348  
   studies, 300–307  
 Tuton, Gary M., 58  
 Tuve, Merle A., vi, 29, 33, 34, 215, 271, 349, 353, 360  
   publications, 347, 348  
   report of Chairman, Committee on Image Tubes for Telescopes, 353–361  
   report of Director, Department of Terrestrial Magnetism, 253–346  
   studies, 273–286, 300–307
- Ulrich, B., 25  
 Urbach, Wolfgang, 43, 365, 366, 367, 436, 437  
   publication, 435  
   studies, 374–379, 381–390, 390–395, 416–420  
 Utter, Merwyn G., 6, 57  
   publication, 55
- Van Hook, William C., 58  
 Varsavsky, C., 350  
   studies, 300–307  
 Vaughan, Arthur H., Jr., 57  
   studies, 22, 24–25, 48  
 Vega, Rolando, 58  
 Velde, Bruce, 238, 250  
   publications, 243, 247, 248  
 Velde, D., 250  
   studies, 155–159, 160–161  
 Veron, Philippe, 30, 5, 34, 43, 57  
   publications, 55  
   studies, 26, 29,  
 Viazov, Oleg E., 446, 516  
 Vidaver, William E., 366, 368, 437  
   publication, 436  
   studies, 379–381, 395–397
- Wadsworth, James W., xi  
 Wagner, Manfred, 50, 58  
 Walburn, Marjorie H., viii  
 Walcott, Charles D., xi, 577, 578  
 Walcott, Frederic C., xi  
 Walcott, Henry P., xi  
 Walker, M. F., 22  
 Wallace, Betty A., 58  
 Wallerstein, George, 57  
   publication, 53, 55  
   studies, 14, 16, 39  
 Waring, M. J., 45, 350  
   publication, 348  
   studies, 313–345  
 Waters, A. C., 291  
   studies, 171–174  
 Webb, J. P., 350  
 Weber, Carl, 446, 515  
 Weber, Gus, 58  
 Wedum, Bernice G., 516  
 Weed, Lewis H., xi  
 Welch, William H., xi



- Westphal, James A., 10  
 publication, 55
- White, Andrew D., xi, 577, 578
- White, Edward D., xi
- White, Henry, xi
- White, James N., iv, v, 555, 575
- Whiteoak, John B., 57  
 studies, 20, 42
- Wickersham, George W., xi
- Willey, Robert L., 9-10, 57  
 publications, 55, 56
- Williams, Isabel P., 516
- Wilson, A. G., studies, 43
- Wilson, Carole E., 535
- Wilson, Olin C., vi, 3, 25, 40, 57  
 publications, 54, 56  
 studies, 15, 16, 17
- Wilson, Ralph W., 58
- Wilson, Robert E., xi, 575
- Wing, Robert, studies, 14
- Wiseman, J. D. H., 177
- Wiser, John L., 516
- Wisotzki, Ann, 516
- Woerden, Hugo van, 57  
 publication, 56  
 studies, 25
- Wolfowitz, Paul D., 535
- Womack, Frances C., 523
- Woodward, Robert Simpson, xi
- Wright, Carroll D., xi, 577, 578
- Wright, K. O., publication, 56  
 studies, 13
- Wright, R. R., studies, 44
- Wyller, Arne A., publication, 56  
 studies, 12-13
- Wyndham, John D., 30, 5, 32, 43  
 publication, 55, 56  
 studies, 26
- Yamaguchi, M., 293, 296, 347, 350  
 studies, 286-296
- Yarus, Michael, 523
- Yates, J., 351
- Yoder, Hatten S., Jr., 36, 63, 67, 103, 186, 210,  
 235, 237, 240, 241, 242, 250, 294, 351  
 publications, 243, 248  
 studies, 69-82, 82-89, 89-94, 95-100, 192-193
- Yoss, Kenneth M., studies, 39
- Youle, Merry, 516
- Younkin, Robert L., publications, 55, 56  
 studies, 44-45
- Yund, R. A., publication, 245
- Zies, Emanuel G., 153, 250  
 publications, 243
- Zirin, Harold, vi, 8, 56, 57  
 publications, 54, 56  
 studies, 22, 48, 53
- Zwaan, J., 516
- Zwicky, Fritz, vi, 63, 57  
 publications, 56  
 studies, 28, 32, 34, 35, 36











